

The Rise and Fall of the Ediacaran Biota

Edited by
P. Vickers-Rich and P. Komarower



Geological Society
Special Publication 286



The Rise and Fall

Geological
Society
Special
Publication
286

Edited by



the
Geological
Society

The Rise and Fall of the Ediacaran Biota

Edited by
P. Vickers-Rich and P. Komarower

The Proterozoic and early Phanerozoic was a time punctuated by a series of significant events in Earth history. Glaciations of global scale wracked the planet, interfingering with dramatic changes in oceanic and atmospheric chemistry and marked changes in continental configuration. It was during these dynamic and 'weedy' times that metazoans first appeared. Their subsequent diversification culminated in the appearance of hard tissue skeletons and deep 'farming' of the marine substrate in late Proterozoic and first few millions of years of the Phanerozoic. The papers in this book deal specifically with the precise timing of physical events and teasing out of the effects which these changing environments,



climates, global chemistry and palaeogeography had on the development and diversification of animals, resulting in the spectacular Ediacaran/Vendian faunas of the late Precambrian.

Visit our online bookshop: <http://www.geolsoc.org.uk/bookshop>

Geological Society web site: <http://www.geolsoc.org.uk>



Cover illustration:

Yorgia rising – an imaginative vista by Melbourne artist Peter Trusler of the White Sea cliffs of northern Russia. *Yorgia* is one of the oldest animals on Earth, an Ediacaran, common in the Vendian sequences of the Russian north, which left traces of movement and detailed imprints of its anatomy in the shallow marine muds more than 550 million years ago.



The
Geological
Society

Edited by
P. Vickers-Rich and P. Komarower

Geological
Society
Special
Publication
286



Geological Society
Special Publication 286



The Rise and Fall of the Ediacaran Biota

Edited by
P. Vickers-Rich and P. Komarower



The Rise and Fall of the Ediacaran Biota

The Geological Society of London
Books Editorial Committee

Chief Editor

BOB PANKHURST (UK)

Society Books Editors

JOHN GREGORY (UK)

JIM GRIFFITHS (UK)

JOHN HOWE (UK)

PHIL LEAT (UK)

NICK ROBINS (UK)

JONATHAN TURNER (UK)

Society Books Advisors

MIKE BROWN (USA)

ERIC BUFFETAUT (France)

JONATHAN CRAIG (Italy)

RETO GIERÉ (Germany)

TOM MCCANN (Germany)

DOUG STEAD (Canada)

RANDELL STEPHENSON (The Netherlands)

IUGS/GSL publishing agreement

This volume is published under an agreement between the International Union of Geological Sciences and the Geological Society of London and arises from IGCP Program 493, *The Rise and Fall of the Vendian Biota*.

GSL is the publisher of choice for books related to IUGS activities, and the IUGS receives a royalty for all books published under this agreement.

Books published under this agreement are subject to the Society's standard rigorous proposal and manuscript review procedures.

It is recommended that reference to all or part of this book should be made in one of the following ways:

VICKERS-RICH, P. & KOMAROWER, P. (eds) 2007. *The Rise and Fall of the Ediacaran Biota*. Geological Society, London, Special Publications, **286**.

RAUB, T. D., EVANS, D. A. D. & SMIRNOV, A. V. 2007. Siliciclastic prelude to Elatina-Nuccaleena deglaciation: lithostratigraphy and rock magnetism of the base Ediacaran system. In: VICKERS-RICH, P. & KOMAROWER, P. (eds) *The Rise and Fall of the Ediacaran Biota*. Geological Society, London, Special Publications, **286**, 53–76.

GEOLOGICAL SOCIETY SPECIAL PUBLICATION NO. 286

The Rise and Fall of the Ediacaran Biota

EDITED BY

PATRICIA VICKERS-RICH

and

PATRICIA KOMAROWER

Monash University, Melbourne, Australia

2007

Published by
The Geological Society
London

THE GEOLOGICAL SOCIETY

The Geological Society of London (GSL) was founded in 1807. It is the oldest national geological society in the world and the largest in Europe. It was incorporated under Royal Charter in 1825 and is Registered Charity 210161.

The Society is the UK national learned and professional society for geology with a worldwide Fellowship (FGS) of over 9000. The Society has the power to confer Chartered status on suitably qualified Fellows, and about 2000 of the Fellowship carry the title (CGeol). Chartered Geologists may also obtain the equivalent European title, European Geologist (EurGeol). One fifth of the Society's fellowship resides outside the UK. To find out more about the Society, log on to www.geolsoc.org.uk.

The Geological Society Publishing House (Bath, UK) produces the Society's international journals and books, and acts as European distributor for selected publications of the American Association of Petroleum Geologists (AAPG), the Indonesian Petroleum Association (IPA), the Geological Society of America (GSA), the Society for Sedimentary Geology (SEPM) and the Geologists' Association (GA). Joint marketing agreements ensure that GSL Fellows may purchase these societies' publications at a discount. The Society's online bookshop (accessible from www.geolsoc.org.uk) offers secure book purchasing with your credit or debit card.

To find out about joining the Society and benefiting from substantial discounts on publications of GSL and other societies worldwide, consult www.geolsoc.org.uk, or contact the Fellowship Department at: The Geological Society, Burlington House, Piccadilly, London W1J 0BG; Tel. +44 (0)20 7434 9944; Fax +44 (0)20 7439 8975; E-mail: enquiries@geolsoc.org.uk.

For information about the Society's meetings, consult *Events* on www.geolsoc.org.uk. To find out more about the Society's Corporate Affiliates Scheme, write to enquiries@geolsoc.org.uk.

Published by The Geological Society from:

The Geological Society Publishing House, Unit 7, Brassmill Enterprise Centre, Brassmill Lane, Bath BA1 3JN, UK

(Orders: Tel. +44 (0)1225 445046, Fax +44 (0)1225 442836)

Online bookshop: www.geolsoc.org.uk/bookshop

The publishers make no representation, express or implied, with regard to the accuracy of the information contained in this book and cannot accept any legal responsibility for any errors or omissions that may be made.

© The Geological Society of London 2007. All rights reserved. No reproduction, copy or transmission of this publication may be made without written permission. No paragraph of this publication may be reproduced, copied or transmitted save with the provisions of the Copyright Licensing Agency, 90 Tottenham Court Road, London W1P 9HE. Users registered with the Copyright Clearance Center, 27 Congress Street, Salem, MA 01970, USA: the item-fee code for this publication is 0305-8719/07/\$15.00.

British Library Cataloguing in Publication Data

A catalogue record for this book is available from the British Library.

ISBN: 978-1-86239-233-5

Typeset by Techset Composition Ltd, Salisbury, UK

Printed by Cromwell Press, Trowbridge, UK

Distributors

North America

For trade and institutional orders:

The Geological Society, c/o AIDC, 82 Winter Sport Lane, Williston, VT 05495, USA

Orders: Tel. +1 800-972-9892
Fax +1 802-864-7626
E-mail: gsl.orders@aidcvt.com

For individual and corporate orders:

AAPG Bookstore, PO Box 979, Tulsa, OK 74101-0979, USA

Orders: Tel. +1 918-584-2555
Fax +1 918-560-2652
E-mail: bookstore@aapg.org
Website <http://bookstore.aapg.org>

India

Affiliated East-West Press Private Ltd, Marketing Division, G-1/16 Ansari Road, Darya Ganj, New Delhi 110 002, India

Orders: Tel. +91 11 2327-9113/2326-4180
Fax +91 11 2326-0538
E-mail: affiliat@vsnl.com

Contents

Preface	vii
General geology	
ACEÑOLAZA, G. & ACEÑOLAZA, F. Insights in the Neoproterozoic–Early Cambrian transition of NW Argentina: facies, environments and fossils in the proto-margin of western Gondwana	1
CHUMAKOV, N. M. Climates and climate zonality of the Vendian: geological evidence	15
KATSUTA, N., TOJO, B., TAKANO, M., YOSHIOKA, H., KAWAKAMI, S., OHNO, T. & KUMAZAWA, M. Non-destructive method to detect the cycle of lamination in sedimentary rocks: rhythmite sequence in Neoproterozoic Cap carbonates	27
LINDEMANN, U. Ediacaran rocks from the Cadomian basement of the Saxo-Thuringian Zone (NE Bohemian Massif, Germany): age constraints, geotectonic setting and basin development	35
RAUB, T. D., EVANS, D. A. D. & SMIRNOV, A. V. Siliciclastic prelude to Elatina–Nuccaleena deglaciation: lithostratigraphy and rock magnetism of the base of the Ediacaran system	53
TEWARI, V. C. The rise and decline of the Ediacaran biota: palaeobiological and stable isotopic evidence from the NW and NE Lesser Himalaya, India	77
TOJO, B., KATSUTA, N., TAKANO, M., KAWAKAMI, S. & OHNO, T. Calcite–dolomite cycles in the Neoproterozoic Cap carbonates, Otavi Group, Namibia	103
Correlation and naming	
GREY, K. & CALVER, C. R. Correlating the Ediacaran of Australia	115
JENKINS, R. J. F. ‘Ediacaran’ as a name for the newly designated terminal Proterozoic period	137
Micropalaeontology	
BRAUN, A., CHEN, J., WALOSZEK, D. & MAAS, A. First Early Cambrian Radiolaria	143
LI, C.-W., CHEN, J.-Y., LIPPS, J. H., GAO, F., CHI, H.-M. & WU, H.-J. Ciliated protozoans from the Precambrian Doushantuo Formation, Wengan, South China	151
Ediacarans	
FEDONKIN, M. A., SIMONETTA, A. & IVANTSOV, A. Y. New data on <i>Kimberella</i> , the Vendian mollusc-like organism (White Sea region, Russia): palaeoecological and evolutionary implications	157
TRUSLER, P., STILWELL, J. & VICKERS-RICH, P. Comment: future research directions for further analysis of <i>Kimberella</i>	181
FEDONKIN, M. A. & IVANTSOV, A. Y. <i>Ventogyrus</i> , a possible siphonophore-like trilobozoan coelenterate from the Vendian Sequence (late Neoproterozoic), northern Russia	187
JENKINS, R. J. F. & NEDIN, C. The provenance and palaeobiology of a new multi-vened, chambered frondose organism from the Ediacaran (later Neoproterozoic) of South Australia	195
JENSEN, S., PALACIOS, T. & MARTÍ MUS, M. A brief review of the fossil record of the Ediacaran–Cambrian transition in the area of Montes de Toledo-Guadalupe, Spain	223
LAFLAMME, M., NARBONNE, G. M., GREENTREE, C. & ANDERSON, M. M. Morphology and taphonomy of an Ediacaran frond: <i>Charnia</i> from the Avalon Peninsula of Newfoundland	237
LEONOV, M. V. Comparative taphonomy of Vendian genera <i>Beltanelloides</i> and <i>Nemiana</i> : taxonomy and lifestyle	259
LEONOV, M. V. & RAGOZINA, A. L. Upper Vendian assemblages of carbonaceous micro- and macrofossils in the White Sea Region: systematic and biostratigraphic aspects	269
MACGABHANN, B. A., MURRAY, J. & NICHOLAS, C. <i>Ediacaria booleyi</i> : weeded from the Garden of Ediacara?	277

MACGABHANN, B. A. Discoidal fossils of the Ediacaran biota: a review of current understanding	297
MAITHY, P. K. & KUMAR, G. Biota in the terminal Proterozoic successions on the Indian subcontinent: a review	315
SEREZHNIKOVA, E. A. Vendian <i>Hiemalora</i> from Arctic Siberia reinterpreted as holdfasts of benthic organisms	331
Body plans	
SAVAZZI, E. A new reconstruction of <i>Protolyellia</i> (Early Cambrian psammocoral)	339
SPERLING, E. A., PISANI, D. & PETERSON, K. J. Poriferan paraphyly and its implications for Precambrian palaeobiology	355
VALENTINE, J. W. Seeing ghosts: Neoproterozoic bilaterian body plans	369
Functional morphology	
ANTCLIFFE, J. B. & BRASIER, M. D. Towards a morphospace for the Ediacara biota	377
SEILACHER, A. The nature of vendobionts	387
TOJO, B., SAITO, R., KAWAKAMI, S. & OHNO, T. Theoretical morphology of quilt structures in Ediacaran fossils	399
Precambrian–Cambrian transition	
DZIK, J. The Verdun Syndrome: simultaneous origin of protective armour and infaunal shelters at the Precambrian–Cambrian transition	405
PARKHAEV, P. Y. The Cambrian ‘basement’ of gastropod evolution	415
Short papers	
BRAUN, A., CHEN, J.-Y., WALOSZEK, D. & MAAS, A. Siliceous microfossils and biosiliceous sedimentation in the lowermost Cambrian of China	423
GEHLING, J. G. Fleshing out the Ediacaran period	425
HERMANN, T. N. & PODKOVRVYROV, V. N. <i>Rugosoopsis</i> : a new group of Upper Riphean animals	429
JAFARI, S. M., SHEMIRANI, A. & HAMDI, B. Microstratigraphy of the Late Ediacaran to the Ordovician in NW Iran (Takab area)	433
MAHESHWARI, A., SIAL, A. N. & MATHUR, S. C. $\delta^{13}\text{C}$ stratigraphy of the Birmania Basin, Rajasthan, India: implications for the Vendian–Cambrian transition	439
TURNER, S. & VICKERS-RICH, P. Sprigg, Glaessner and Wade and the discovery and international recognition of the Ediacaran fauna	443
VICKERS-RICH, P. Saline giants, cold cradles and global playgrounds of Neoproterozoic Earth: the origin of the Animalia	447
Index	449

Preface

The Proterozoic and early Phanerozoic, especially the time from Neoproterozoic to Early Palaeozoic, was punctuated by a series of significant events in Earth history. Glaciations of global scale wracked the Earth and interfingered with dramatic changes in the chemistry of oceans and atmosphere, marked shifts in continental configuration. It was during these dynamic and ‘weedy’ times that metazoans first appeared and increased in diversity, culminating in the appearance of a variety of hard tissue skeletons and deep ‘farming’ of the marine substrate, which marked the end of the Proterozoic and the first few millions of years of the Phanerozoic.

UNESCO International Geological Correlation Project 493 has been concerned with the precise timing of such Neoproterozoic events, teasing out the effects which these changing environments, climates, global chemistry and palaeogeography had on the development and diversification of animals, culminating in the spectacular Ediacaran/Vendian faunas of the late Precambrian, best represented along the Winter Coast of the White Sea in Russia, the Flinders Ranges of South Australia, the deserts of southern Namibia and the coastal outcrops of Newfoundland.

This project has aimed, from the beginning, to locate and document additional material from areas with a sparse Ediacaran biotic record (South America in particular), which though rare, have marked palaeobiogeographic and evolutionary interest. IGCP493 has also hosted studies that closely compared settings of these Ediacaran metazoans (using sedimentology, carbon and oxygen isotope signatures, palaeogeographic positioning). And, as part of this, IGCP493 has attempted to bring together in field and laboratory, as well as in targeted symposia, researchers with diverse backgrounds to work together in attempting to understand the physical settings in which biological events took place.

Two symposia are of importance for IGCP493, one in Prato, Italy in 2004 held in concert with the International Geological Congress in Florence and a second in Kyoto, Japan in early 2006. Papers that resulted from each of these symposia constitute this volume. The collection of papers comprising this Special Publication of the Geological Society of London is the result of these two interdisciplinary symposia.

This Special Publication of the Geological Society of London is divided into several sections: general geology, stratigraphy, magnetostratigraphy,

and the stable isotope record; correlation and basis of the name Ediacaran; micropalaeontology; characterization of the Ediacaran biota; the nature of body plans; functional morphology; and the nature of the Neoproterozoic-Cambrian transition. Abstracts of some papers presented at each of these meetings that were not developed further are available on line at: <http://www.geolsoc.org.uk/SUP18273>. A hardcopy can be obtained from the Society Library.

We are indebted to many people for help in producing this volume. We have asked much from the authors and reviewers, and have been blessed with endless patience on their part. Thanks are due to the authors for the papers they contributed, and the reviewers for their assessment of the papers. Among the reviewers, Sören Jensen deserves special mention for his generous, and rapid, response to multiple requests. We also thank F. & G. Aceñolaza, P. Betts, A. Braun, D. Collins, D. Condon, M. Fedonkin, L. Frakes, J. Gehling, D. Gray, K. Grey, K. H. Hoffmann, R. Jenkins, B. MacGabhann, M. Laffamme, C. Li, A. Martin, M. Moczydlowska, G. Narbonne, T. Ohno, P. Parkhaev, W. Preiss, E. Savazzi, G. Schneider, A. Seilacher, E. Serezhnikova, R. Squire, J. Stilwell, W. Sun, C. Tassell, S. Turner and S. Xiao.

We would like to thank Tom Rich (Museum Victoria, Melbourne) and Mary Walters (Monash University, Melbourne) for assistance with manuscript revision and proofreading, Draga Gelt (Monash University) for assisting with numerous illustrations and providing graphic advice and Steven Morton for assistance with photographs. We would also like to thank the School of Geosciences at Monash University for providing facilities and significant funding which made the production of this volume possible, especially for the salaries of the editors! Thanks are due to staff at the Prato Centre of Monash University in Prato (especially Cecilia Hewlitt and Prof. Bill Kent), Italy, and to Kyoto University and staff at the Kyoto University Museum (especially Prof. Terufumi Ohno) for providing the venues and assistance during the two symposia and facilitating as the magnet allowing presentation and preparation of these papers. UNESCO’s International Geological Correlation Program provided support for IGCP493, the umbrella for both symposia, and their funding support was critical to the hosting of the symposia and the production of this volume—both the international and the

Australian programmes. The Japan Society of the Promotion of Science Fellowship to PVR (October 2005–February 2006) was of great assistance in providing undisturbed time needed for editing and writing that led to this volume.

We are tremendously indebted to the Geological Society of London, with special thanks to Angharad Hills, for the offer to publish this collection of

papers dedicated to the understanding of Neoproterozoic Earth and the origin and early evolution of the Metazoa.

PATRICIA VICKERS-RICH

PATRICIA KOMAROWER



The authors are grateful for support from the UNESCO International Geological Correlation Program, Project 493, The Rise and Fall of the Vendian Biota, coordinated by Mikhail Fedonkin, Patricia Vickers-Rich and Jim Gehling (2003-2007).

Insights in the Neoproterozoic–Early Cambrian transition of NW Argentina: facies, environments and fossils in the proto-margin of western Gondwana

G. ACEÑOLAZA & F. ACEÑOLAZA

Instituto Superior de Correlación Geológica (Consejo Nacional de Investigaciones Científicas y Técnicas, Universidad Nacional de Tucumán), Miguel Lillo 205, 4000 San Miguel de Tucumán, Argentina (e-mail: insugeo@csnat.unt.edu.ar)

Abstract: In NW Argentina, over 3000 metres of highly tectonized and metamorphosed siliciclastics of the Puncoviscana Formation underlie the more fossiliferous Cambro–Ordovician strata of the Mesón and Santa Victoria groups. Historically regarded as the non-fossiliferous ‘basal Precambrian shield’ of the region, its age was later found to be in part Phanerozoic, with the discovery of Early Cambrian trace fossils, and more recently refined with geochronological data. Widespread siliciclastic deposits characterize this sequence. A review of trace fossils in the Puncoviscana Formation has added new taxa. Trace fossil assemblages denote? geographical belts, indicating shallower marine conditions to the east (*Nereites* association) and deeper to the west (*Oldhamia* association). Such assemblages related to the palaeomorphology of the basin also represent different temporal levels, and in so doing reflect the overall evolution of the Puncoviscana Sea through time. The use of taxa that characterize Siberian stages in order to date parts of the Puncoviscana Formation should be abandoned as Siberian stages are defined by a specific set of fossils that are absent in the strata of NW Argentina. Thus, careful systematic studies and re-evaluation of the strata and fauna in the Puncoviscana Basin are the only way to improve understanding of the Neoproterozoic–Cambrian transition in the Andean margin of South America.

The Neoproterozoic–Early Cambrian transition records some of the most important events in the evolution of the Earth, from a major plate-tectonic reconfiguration (Scotese & McKerrow 1990; Bengtson 1994), to the diversification of metazoans (Glaessner 1984; Fedonkin 1990; Narbonne 1998; Narbonne & Gehling 2003), the end of the ‘Snowball’ glaciations (Hoffman *et al.* 1998) and profound changes in the isotopic composition of seawater (Kaufman & Knoll 1995; Eriksson *et al.* 1998). These remarkable events triggered major evolutionary biotic evolution.

More than one hundred years of research resulted in the definition of the base of the Phanerozoic at Fortune Head, Newfoundland, Canada (Gradstein *et al.* 2004 with references). Analysis of the discussions held over the last 30 years clearly highlights that most debates concerning this boundary and others, involved data from North America, Africa, Asia and Australia, but lacked information from the Neoproterozoic–Early Cambrian sequences of South America (Glaessner 1984; Fedonkin 1987, 1994). Thus further research is required on the sedimentary and metamorphic rocks of this region.

The Neoproterozoic–Early Cambrian sequence in the central Andean Basin of South America is best exposed in northwestern Argentina, where it

is dominated by thick, heterogeneous slightly metamorphosed and predominantly siliciclastic successions of the Puncoviscana Formation. This unit represents the regional basement (Turner 1960; Aceñolaza & Toselli 1981; Omarini *et al.* 1999a), but its stratigraphy has been obscured by several deformational events. The strata of the Puncoviscana Formation represent multiple sedimentary environments (Jezek 1990; Aceñolaza & Aceñolaza 2003). As a consequence, lithological correlation, dating and precise identification of sequences in the Puncoviscana basin are highly problematic, with the only clear data points provided by trace fossils and rare geochronological input. Based on these studies, it is clear that at least part of the Puncoviscana Formation is Early Cambrian in age (Aceñolaza *et al.* 1999; Omarini *et al.* 1999b with references) (Figs 1–4).

Corsetti & Hagadorn (2000) noted that the ability to correlate and refer sequences from one part of the globe to another is the key to understanding those biological changes across the Neoproterozoic–Cambrian transition. New palaeontological data, complemented with isotopic stratigraphy carried out on the highly deformed sequences of northern Argentina, are dependable tools for correlating strata at an intra- and inter-basinal level (e.g. Knoll & Walter 1992; Grotzinger

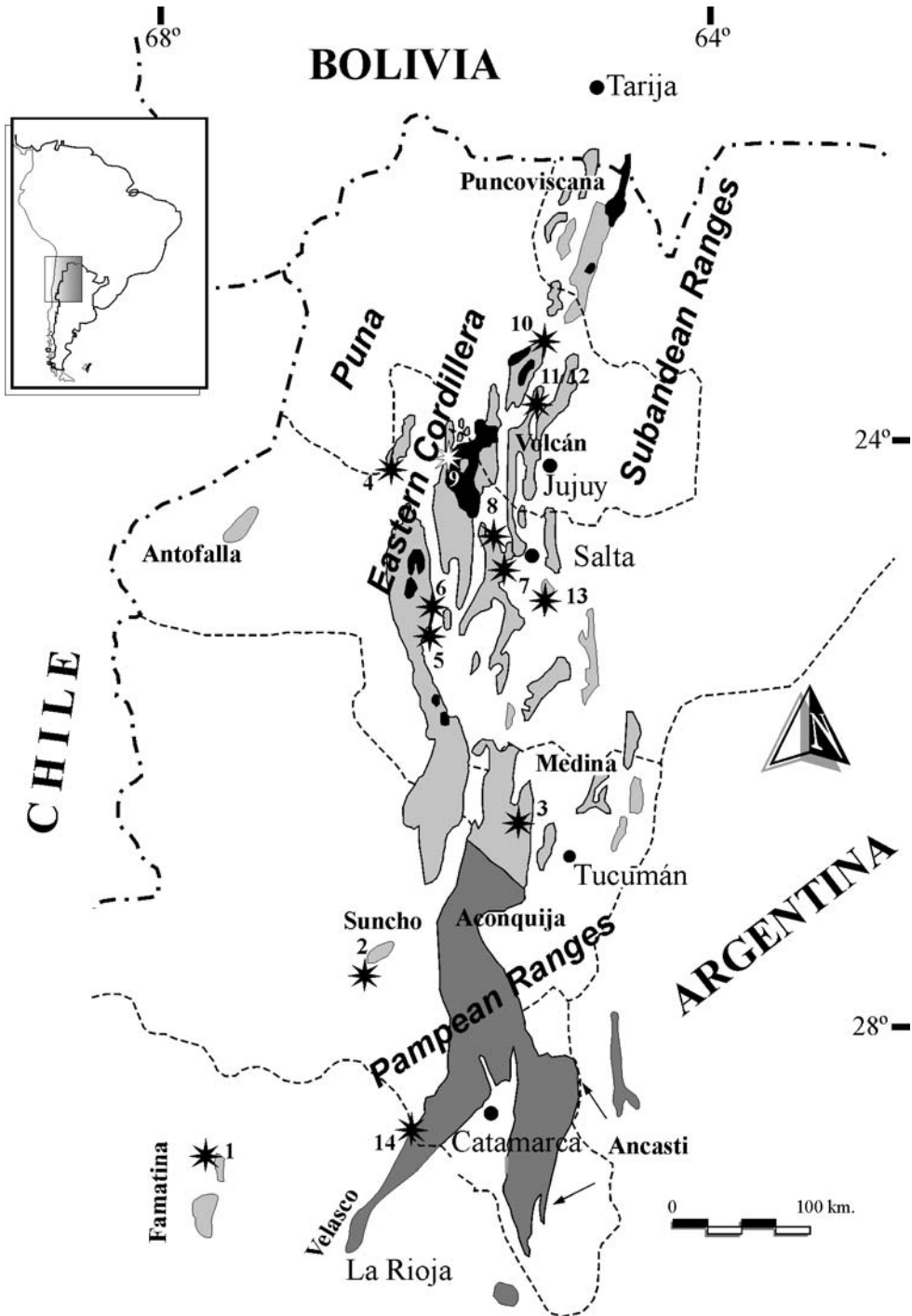


Fig. 1. Outcrops of the Puncoviscana Formation and equivalent units in NW Argentina with fossiliferous localities highlighted (*). Light grey: Puncoviscana *s.l.*; dark grey: low and mid grade metamorphic rocks derived from Puncoviscana *s.l.* Localities: 1, Angulos; 2, Suncho; 3, Choromoro; 4, San Antonio de Los Cobres; 5, Cachi; 6, Payogasta; 7/8, Quebrada del Toro; 9, Abra Blanca/Muñano; 10, Coraya; 11, Purmamarca; 12, Lipán; 13, Los Guachos; 14, La Cébila.

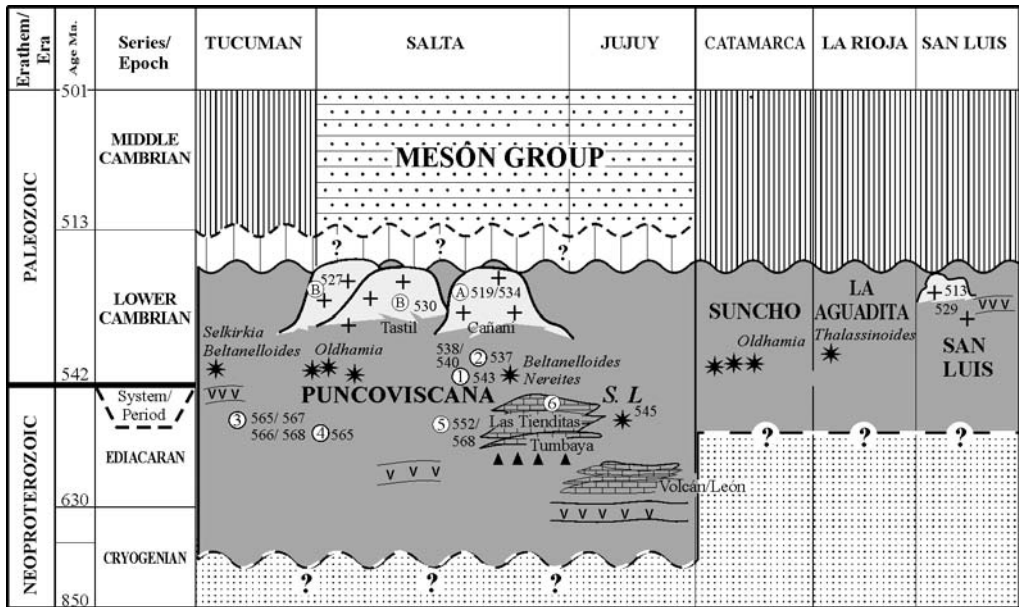


Fig. 2. Stratigraphy of the Puncoviscana Formation *s.l.* with intrusives, sediments and discordances. Radiometric dates are on plutons and metamorphic rocks. A; Cañaní Granite; B; Tastil Granite; 1, Don Bartolo; 2, Quebrada del Toro; 3, Choromoro; 4, San Javier; 5, Cuesta del Obispo; 6, Purmamarca.

et al. 1995; Sial *et al.* 2001; Aceñolaza 2004; García Bellido & Aceñolaza 2005).

This contribution summarizes the current knowledge of the Neoproterozoic–Early Cambrian transition in the Central Andean Basin: the Puncoviscana Formation and related units. It focuses on NW Argentina, where exposures are best developed, and the only region where enough data is available to allow a well-defined lithostratigraphic framework centred on the Proterozoic–Phanerozoic transition.

The Neoproterozoic–Early Cambrian in the South American Central Andean Basin

The sedimentary basement of the Central Andean Basin is best represented by the Puncoviscana Formation *s.l.*, which crops out from Tarija in the southern part of Bolivia (=San Cristobal Formation), to Tucumán in northern Argentina. Even though there are a variety of facies and lithologies, the entire region appears to be part of the same Neoproterozoic–Early Cambrian belt, that continues southwards into the Sierras Pampeanas and northern Patagonia (Turner 1976; Caminos 1979; Ramos 1999; González *et al.* 2002; Sato *et al.* 2002; Schwartz & Gromet 2004) (Fig. 1). An even larger extension has been also proposed, from the highlands of Perú (Díaz Martínez 1996)

to Antarctica, on the basis of lithology and trace fossil content (Tessensohn 1982; Jezek *et al.* 1985). Low-grade metamorphic basins of this type are also recorded eastwards in Australia, as part of a major structural unit, resulting from the break-up of Rodinia (Moore 1991; Ross 1991; Storey *et al.* 1992; Rowell *et al.* 1993).

In Argentina, the northern outcrops are dominated by very low- to low-grade metasedimentary rocks, whereas southwards gneisses and migmatites are more common, all having been affected by Middle Cambrian to Early Ordovician plutonism (Rapela *et al.* 1992, 1998; Keppie & Bahlburg 1999). Ramos (1999) noted that there is no consensus in interpretation of the tectonic setting of the Puncoviscana Basin. Ideas range from: it being a passive margin (Jezek *et al.* 1985; Jezek 1990); to a closing ocean with collision and subduction (Ramos 1988); rifting processes (Omarini & Sureda 1993; Suárez Soruco 1989, 2000; Aceñolaza & Alonso 2001); a foreland basin (Kraemer *et al.* 1995; Keppie & Bahlburg 1999); or even part of an island arc (Omarini *et al.* 1999).

In addition, a spectrum of environmental settings has been identified in the Puncoviscana Formation, with an eastern ‘Nereites belt’ characterized by a particular trace fossil associated with current-rippled sandstones, turbidites and conglomerates from a shallower setting; and a western ‘Oldhamia belt’, with relatively deeper-water facies associated with turbidites, shales and

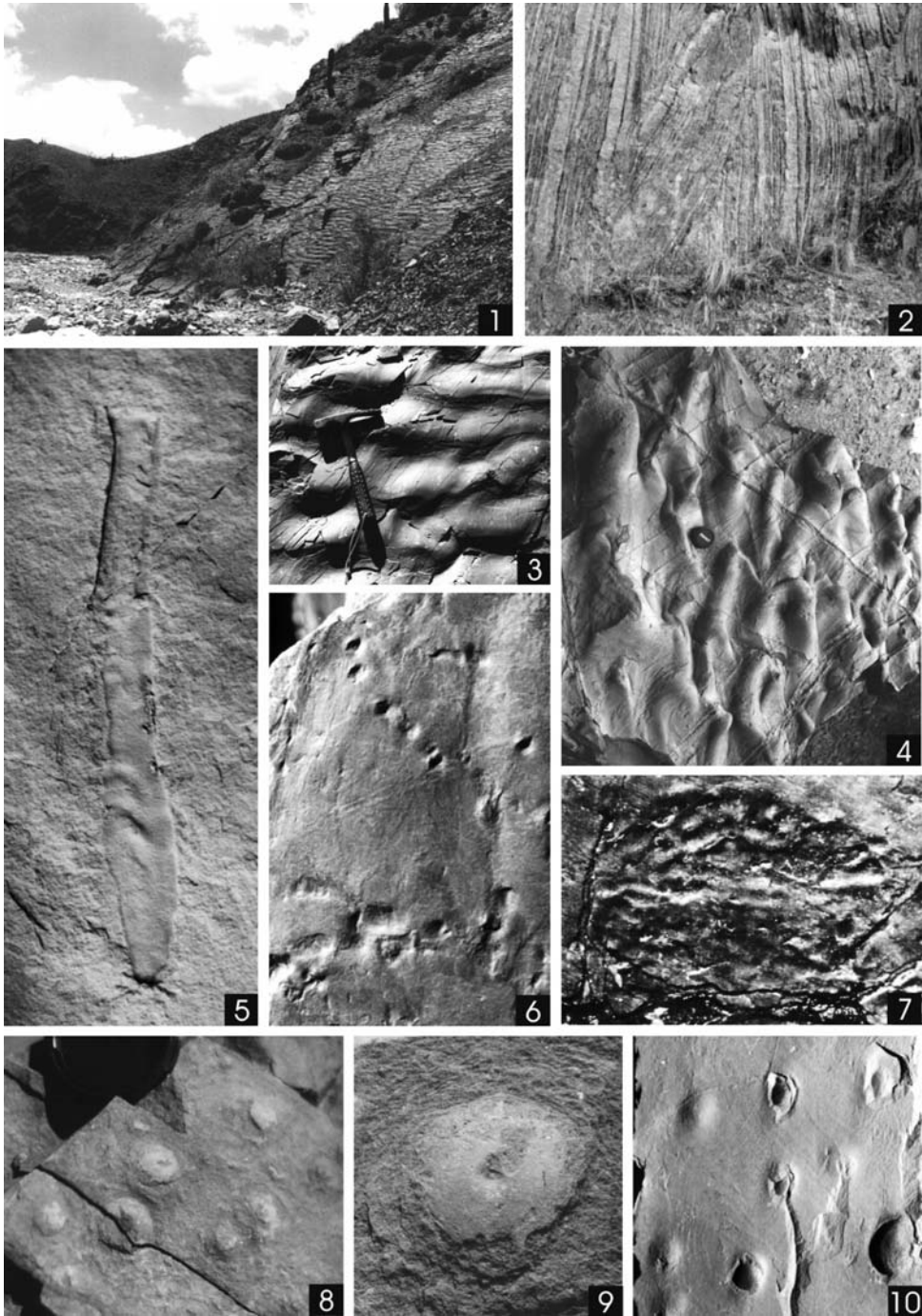


Fig. 3. Outcrops displaying sedimentary rocks and deformation structures, soft-bodied fossils and enigmatic material from the Puncoviscana Formation in northwest Argentina. (1) Rippled surface at Escoipe; Salta Province; (2) Tight folded succession at El Alisal, Quebrada del Toro, Salta Province; (3) Current-rippled surface at Purmamarca, Jujuy Province; (4) Flute marks on sole of sandstones of the Puncoviscana Formation at Escoipe, Salta Province. (5) *Selkirkia* sp. from Choromoro, Tucumán Province ($\times 0.5$). (6, 7, 10) Enigmatic material present in the slates and sandstones of the Puncoviscana Formation from Tucumán Province (6×0.2 ; 7×0.35 ; 10×0.2). (8, 9) *Beltanelloides* sp. from Purmamarca, Jujuy Province (8×0.5 ; 9×1.3).

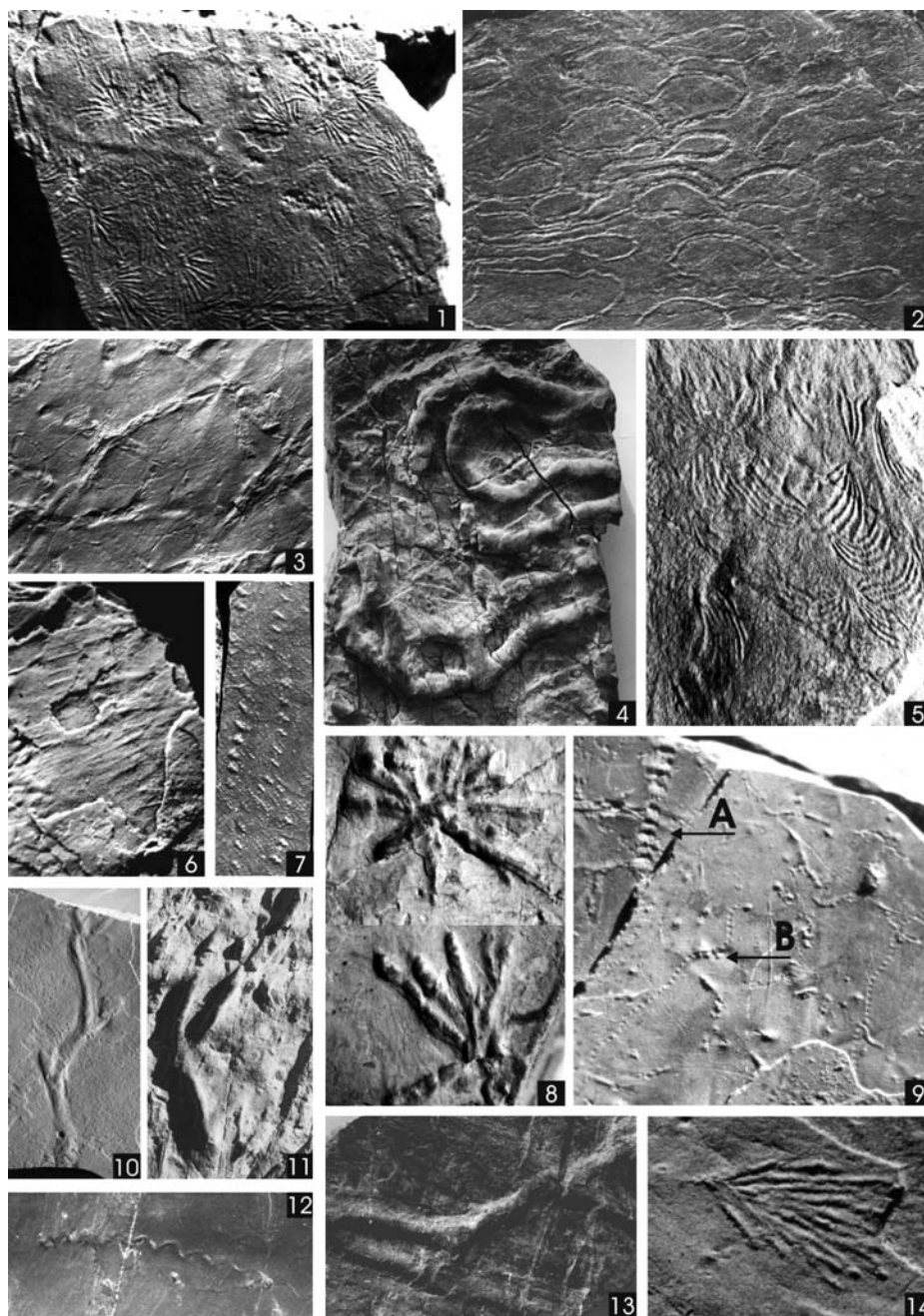


Fig. 4. Selected trace fossils from the Puncoviscana Formation and equivalent units in northwest Argentina. (1) *Oldhamia radiata* from San Antonio de los Cobres, Salta Province ($\times 1.5$); (2) *Nereites saltensis* from Salta Province ($\times 0.15$; non-*Psammichnites saltensis* in Seilacher *et al.* 2005); (3) *Palaeophycus* isp. associated with *Helminthoidichnites tenuis* from Quebrada del Toro, Salta Province ($\times 0.4$); (4) *Helminthoraphe* isp. ($\times 0.2$); (5) *Oldhamia curvata* from Quebrada del Toro, Salta Province ($\times 0.6$); (6) *Monomorphichnus lineatus* from El Alisal, Salta Province ($\times 2.5$); (7) *Tasmanadia cachii* from Cachi, Salta Province ($\times 0.5$); (8) *Glockerichnus* sp. ($\times 1.5$); (9) A: *Neonereites biserialis* ($\times 0.5$). B: *N. uniserialis* ($\times 0.5$) from Salta Province; (10) *Treptichnus* cf. *aequalternus* from Choromoro, Tucumán Province ($\times 0.8$); (11, 13) cf. *Thalassinoides* isp. from San Antonio de Los Cobres, Salta province (11 $\times 0.3$; 13 $\times 0.5$); (12) *Cochlichnus anguineus* from the Quebrada del Toro, Salta Province ($\times 0.45$); (14) *Oldhamia flabellata* from San Antonio de Los Cobres, Salta Province ($\times 0.9$).

pelagic clays (Salfity *et al.* 1975; Jezek *et al.* 1985; Jezek 1986, 1990; Willner 1990; Durand & Aceñolaza 1990; Durand 1993; Aceñolaza & Aceñolaza 2001). Neither belts is characterized by archetypal ichnofacies. Contrary to recent suggestions by Buatois & Mángano (2003*b*), neither Jezek (1990) nor Aceñolaza *et al.* (1999) documented an exclusive deep water setting for the Puncoviscana Formation. Locally, turbidites and sandstones are associated with limestone units (e.g. Volcán and Las Tienditas Fm), whose depositional setting is contentious; they have been interpreted as olistostromal or autochthonous deposits on submarine swells (e.g. Jezek 1986). Aceñolaza (2005) noted that limestones, conglomerates and shales, to mention only some facies represented in the unit, do not form under the same palaeoenvironmental conditions. The Puncoviscana Formation is considered to be a continental margin wedge succession that was deposited during Neoproterozoic–Cambrian times, consisting mostly of shelf, shelf-edge and slope deposits, with a general deepening trend towards the west (Borrello 1969; Aceñolaza *et al.* 1999; Aceñolaza & Alonso 2001 with references).

The facies complexity with tectonically-obscured relationships makes interpretation of the stratigraphic succession difficult (Mon & Hong 1996). In addition, the existence of igneous material interbedded in the Puncoviscana Formation at several localities in Salta and Jujuy (Toselli & Aceñolaza 1984; Chayle & Coria 1987; Manca *et al.* 1987; Toselli & Rossi 1990; Coria *et al.* 1990; Omarini *et al.* 1993) records eruptive events that occurred during the deposition of the unit. Unfortunately, dates for these different magmatic rocks are controversial, highlighting the need of more detailed geochemical investigation (see Omarini *et al.* 1999).

Several attempts have been made to order the sequences in the Puncoviscana Basin (Salfity *et al.* 1975; Baldis & Omarini 1984; Moya 1998), but most of the studies are local to the Valle de Lerma in Salta Province and should not be applied to the basin as a whole.

The Puncoviscana Formation of NW Argentina

The Puncoviscana Formation was originally described by Turner (1960), in the Sierra de Santa Victoria, northern Salta Province. This study described more than 2000 metres of unfossiliferous shales and sandstones, and was later extended to similar strata underlying the highly fossiliferous Cambro-Ordovician rocks.

Even though the term of Puncoviscana Formation (*s.l.*) in northern Argentina has been applied to the Neoproterozoic–Lower Cambrian metasedimentary basin in the region, several other questions and inconsistencies arise as detailed work proceeds (Aceñolaza *et al.* 1999; Durand & Aceñolaza 1990; Ramos 1999; Sial *et al.* 2001; Buatois & Mángano 2003*a, b*) (Fig. 2).

Taking into account that the highly deformed siliciclastic rocks of the type area are depleted of biogenic structure and fossils, and that similar sequences located to the south and west (e.g. Valle de Lerma, San Antonio de los Cobres in Salta and Choromoro in Tucumán), contain fossils, correlation is rather complex. Any correlation must be based on detailed and precisely located information. Lithology changes laterally and rapidly, with common interbeds of conglomerates, limestones and vulcanites; their stratigraphic position is unclear due to the strong deformation of the whole complex. The mentioned differences, far from contributing to a clear understanding of the unit, only increase the complexity of this regional Neoproterozoic–Cambrian transition panorama further.

Omarini (1983), Omarini & Baldis (1984) and Jezek (1986) discussed sedimentary characters of the Puncoviscana Basin, distinguishing lithological types based on texture and internal structures: (a) coarse-grained flysch-like turbiditic sandstones; (b) thick and monotonous sequences of argillites, siltstones, and sandstones; (c) minor diamictites and polymictic conglomerates; and (d) isolated shallow water micritic limestones, reflecting a wide spectrum of sedimentary settings for the Puncoviscana Basin.

In addition, Omarini *et al.* (1999) distinguished at least three episodes within the succession: a basal sequence formed primarily by immature epiclastic sediments associated with ultra-potassic dykes (with interbedded mantle-related volcanic flows); shelf deposits with near-shore sandstones (associated with alkalic and tholeiitic lavas); and an upper sequence with flysch-like, siliciclastic deeper water facies (associated to minor pyroclastites, volcanic layers, breccias and granites). Jezek (1990) provided a detailed sedimentological analysis of the Puncoviscana Formation in Tucumán and Salta provinces, distinguishing several sedimentary facies: Facies 1: ‘conglomerate facies’ described from various localities in Salta Province, are characterized by pebbly sandstones/mudstones and organized/disorganized conglomerates representing different detritic flows in the basin; Facies 2: ‘proximal facies’ characterized by dominance of psammites, representing braided river channels, common in Tucumán Province; Facies 3: ‘intermediate’ with mid- to outer fan

prograding lobes including a wide spectrum of sedimentary structures; Facies 4: ‘distal facies’ with low density and low-velocity turbidites; and Facies 5: dominated by hemipelagic slates. Trace fossils and wrinkle structures are common in facies 2, 3, 4; and all are well represented in the northern sector of the Puncoviscana Basin.

Interbedded dark grey limestone facies are known to occur in the region, with notable outcrops at Volcán, León, Tumbaya (Jujuy) and Las Tienditas (Salta). Recent study of these carbonate bodies (Toselli *et al.* 2005) indicate similar $\delta^{13}\text{C}$ signatures for Las Tienditas and Tumbaya limestones and dolomites, with -1.33 to 2.28% PDB for the latter ones; whereas Volcán and León carbonates display higher values, between -6.11 to 4.58% PDB, probably representing older ages (possibly Sturtian?). Toselli *et al.* (2005) note the possibility that the Las Tienditas and Tumbaya limestones may represent ‘cap-carbonates’, highlighting that in the latter locality dolomites are deposited above basalt. In both localities, underlying strata have been considered as likely glacial (Sial *et al.* 2001; Toselli *et al.* 2005).

Volcanic rocks associated with these carbonate-rich bodies are subalkaline basalts, transitional basalts and alkaline basalts associated with minor dacites and leucitites, either intruding or as lava flows in the sequence. These have been interpreted as a product of rifting associated with the formation of the Puncoviscana Basin, evolving into a passive margin volcanism and a magmatic arc environment (Omarini & Sureda 1999; Omarini *et al.* 1999).

The regional metamorphism which affected the sequences of the Puncoviscana Basin has been referred to the anchizone with a maximum depth of 6 km, developed between Tucumán Province southwards to the Sierras Pampeanas of Catamarca, La Rioja, Córdoba and San Luis (Toselli 1990; Willner 1990). Contact metamorphism with development of hornfels has been described in different areas of the basin, along edges of plutons intruding the Puncoviscana Formation in Salta and Jujuy, at Cañaní, Tipayoc, Fundición, Santa Rosa de Tastil and Cachi (Kilmurray *et al.* 1974; Toselli 1990; Lork *et al.* 1990; Rossi *et al.* 1992; Omarini *et al.* 1999).

Fossils and age

The Puncoviscana Formation *s.l.* contains diverse trace fossils, with a variety of ichnotaxa that provide insights into the biota that produced them and ecology of the Puncoviscana Sea in late Neoproterozoic–Cambrian times. Body fossils are rare, with only two undoubted entries after 30

years of palaeontological research (Aceñolaza 2004, and this paper) (Figs 3 & 4).

Preservation varies from good to fairly good, depending on lithology. Tectonism has played a primary role in preservation. It is almost impossible to distinguish any biological signature where cleavage strongly superimposes primary bedding. Ichnofossils occur throughout the basin, except in the northernmost outcrops, where tight folds and the near-absence of traces precludes dating and correlation of strata. Body fossils are located within the shallower eastern belt (‘*Nereites* belt’ of Aceñolaza & Durand 1973, 1986; Aceñolaza 1990), which implies better environmental conditions and preservation patterns for organisms in these facies.

Trace fossils

More than twenty localities in Jujuy, Salta, Tucumán, Catamarca and La Rioja provinces have yielded a moderately diverse ichnofauna, with locomotion traces, feeding and grazing furrows, trails and tracks, denoting significant biological activity in the Puncoviscana Sea during the Neoproterozoic–Early Cambrian (Fig. 1). The fossils that occur in sediments deposited during this time include several whose taxonomic validity is debated, so the status of several trace fossils described previously have been subject to re-evaluation (i.e. Aceñolaza & Aceñolaza 2001, 2003). Abundance of trace fossils varies, according to facies, and the fossils themselves do not represent typical ichnofacies. The entire sequence in NW Argentina has undergone metamorphism and coeval deformation.

A summary of the ichnofauna is mentioned below, with comments on the taxonomy where possible. Early attempts, with different goals, have been published before (Buatois & Mángano 2003a, b), with assignments broadly recognized but not universally accepted (Aceñolaza & Aceñolaza 2001, 2003; Aceñolaza 2005).

The Puncoviscana ichnofauna includes: *Archaeonassa fossulata*, *Asaphoidichnus* sp., *Cochlichnus anguineus*, *Didymaulichnus lyelli*, *Dimorphichnus obliquus*, *Diplichnites* sp., *Glockerichnus* sp., *Helminthoraphe* sp., *Helminthopsis abeli*, *H. tenuis*, *Helminthoidichnites tenuis*, *Monomorphichnus lineatus*, *M. isp.*, cf. *Multipodichnus*, *Nereites saltensis* (non-*Psammichnites saltensis* of Seilacher *et al.* 2005; Aceñolaza & Aceñolaza 2006), *Neonereites uniserialis*, *N. biserialis*, *Oldhamia alata*, *O. antiqua*, *O. curvata*, *O. flabellata*, *O. geniculata*, *O. radiata*, cf. *Thalassinoides* isp., *Palaeophycus tubularis*, *Palaeophycus* isp., *Protichnites* isp., *Protovirgularia* isp., *Tasmanadia cachii*, *Treptichnus* isp., *Treptichnus* cf. *aequalternus* and *T. pollardi*, and a variety of undetermined arthropod-related scratch marks and isolated

imprints (Durand & Aceñolaza 1990; Aceñolaza *et al.* 1999; Aceñolaza & Tortello 2003; Buatois & Mángano 2003a, b; Aceñolaza 2004; Seilacher *et al.* 2005).

The poorly preserved material assigned to *Circulichnis montanus* (Buatois & Mángano 2003a) displays ambiguous morphological characters and lacks diagnostic characters, precluding precise taxonomic assignment. Even though the ichnogenus *Treptichnus* is recognized in the unit (Aceñolaza & Alonso 2001; Aceñolaza 2004), the taxonomic status of *Phycodes/Treptichnus/Trichophycus* is still a matter of debate, and the taxonomy of these three forms should take into account early interpretations of open burrows or feeding structures (Erdoğan *et al.* 2004).

The presence of large-sized, irregular, three-dimensional burrow systems with few dichotomous bifurcations allows the identification of possible trapping or farming networks in the bases of sandstone layers associated with turbidites in San Antonio de Los Cobres (Salta Province). These networks are comparable to *Thalassinoides* isp., where as individual burrows can be identified as large-sized *Palaeophycus tubularis* (Figs 4, 11–13). Branching can be falsely assumed when in reality the traces are superimposed or crossing traces, but undoubted dichotomizations were recorded after a detailed pattern analysis of a single surface of over 20 square metres at one locality. The strata at San Antonio de los Cobres are characterized by a slightly-reworked sedimentary fabric, with a low overall degree of bioturbation restricted to the sandstone–mudstone interval (Durand & Aceñolaza 1990; Buatois & Mángano 2003b). These traces may represent an early attempt to develop possible trapping methods as feeding strategies. Traces penetrate the substratum up to 8 cm, a remarkable depth when compared to the associated traces restricted to the upper few millimetres (*Cochlichnus*, *Oldhamia*, *Helminthopsis*, *Diplichnites* and small *Palaeophycus*).

In general, the ichnological record preserved in the Puncoviscana Formation includes diverse ethological variants, ranging from grazing to feeding and locomotion structures possibly made by vermiform organisms and arthropods. The possible presence of trapping structures in the locality of San Antonio de los Cobres reflects a particular feeding strategy not recorded before in the Early Cambrian of South America.

Body fossils

As stated by Fedonkin (1992), the systematic position of Ediacaran metazoans is controversial. Several interpretations have been presented on their relationships. Glaessner (1984) placed

Precambrian animals in a framework of Phanerozoic invertebrates, but Seilacher (1984, 1989) stressed the uniqueness of Precambrian organisms with no modern analogues. Fedonkin (1983, 1985, 1987) supported a different taxonomic arrangement for Precambrian metazoans based on body plans and further suggested that the metazoan fossil record of the Late Proterozoic, with its much lower diversity than today might be, a preservational artefact (Fendonkin 1992).

Aside from the relatively good record of trace fossils, two undoubted body fossils have been recognized in the Puncoviscana Formation after almost 30 years of palaeontological research: *Selkirkia* sp. (= *Sphenothallus?* sp., in Aceñolaza 2004) occurs in outcrops near Choromoro village in Tucumán Province (García Bellido & Aceñolaza 2005), and well preserved samples of *Beltanelloides* sp., were recovered at Purmamarca village in Jujuy Province. Early references to '*Beltanelliformis*, *Sekwia* and *Nemiana*' have been re-assigned to *Beltanelloides* sp., following the detailed revision of Leonov (2007) (Aceñolaza *et al.* 1999, 2005, with references).

Other biologically induced structures

The knowledge of Neoproterozoic–Early Phanerozoic siliciclastic environments and their biological signature has dramatically increased during the last fifteen years. The Puncoviscana Formation displays some unique surface morphologies that were historically referred as to wrinkle structures associated to certain lithofacies (i.e. Durand *et al.* 1994; Aceñolaza *et al.* 1999 with references). During the 1990s, these structures were re-evaluated as microbial mat-related structures, following ideas of Seilacher & Pflüger (1994), Seilacher (1999), Noffke *et al.* (2001, 2002) and Pflüger (1999). In the case of the Puncoviscana Formation, Omarini *et al.* (1999) were the first to propose these ideas, followed by Buatois *et al.* (2000), Aceñolaza & Aceñolaza (2001, 2003) and Aceñolaza (2004), supporting a microbial mat-related lifestyle of the fauna.

The age of Puncoviscana

So far, the only reliable chronological indicators in the Puncoviscana Basin are the Early Cambrian fossils restricted to certain strata, as well as some limited geochronological data (for summaries, see Aceñolaza & Durand 1986; Do Campo 1999; Omarini *et al.* 1999; Sureda *et al.* 1999). Lork *et al.* (1990) noted a 530 to 560 Ma date for detritic zircons in the Puncoviscana Formation, and Bachmann *et al.* (1987) presented 536 ± 7 Ma and 534 ± 9 Ma dates for plutonic bodies intruding

Puncoviscana Formation, therefore as a minimum date. In addition, Adams *et al.* (1990) recorded metamorphic events between 530 to 540 million years ago, where as Cordani *et al.* (1990) suggested an age ranging from 520 to 538 million years ago, all pointing to a Neoproterozoic–Early Cambrian age for the sedimentation and metamorphism of the unit. Assuming C-isotope stratigraphy is a powerful temporal tool in Precambrian stratigraphy, especially for sediments lacking recognizable fossils (Kaufman 1988), the recent record of a strong C-isotope peak in the upper part of Las Tienditas Formation suggests a Proterozoic–Phanerozoic datum in the upper part of this calcareous unit in the Puncoviscana Formation *s.l.* (Sial *et al.* 2001; Toselli *et al.* 2005). In addition, recent work on these limestone units of Salta and Jujuy (Toselli *et al.* 2005) suggests that possible Sturtian sequences with ‘cap-carbonates’ at Las Tienditas and Tumbaya, supporting early and ignored interpretations of glacial-related sediments associated to the Puncoviscana Formation (Loss & Giordana 1952) (Fig. 2). This, however, needs a more precise age control.

Final remarks and conclusions

Despite the many stratigraphic studies of the rock units representing the Neoproterozoic–Cambrian transition in Argentina, general use of any of the defined units for the whole sedimentary succession will remain problematic until a framework is better understood. Presently, the terms Puncoviscana Basin, Puncoviscana Complex or Puncoviscana Formation *s.l.* are recommended for use in NW Argentina, where no other formal designation has been presented. The sparse fossil record, its uniqueness and its style of preservation, with the complicated structural history of the region, present a complex scenario for the Neoproterozoic–Early Cambrian in the South American Central Andean Basin.

Distinctive facies within this basin, including limestones and conglomerates, should be noted under their original designation (i.e. Volcán Formation, Las Tienditas Formation, El Coro Member, etc.), and the use of the Lerma Group (Salfty *et al.* 1975) should be restricted to the Valle de Lerma in Salta Province.

New palaeontological finds and new geochronological dating are the most reliable sources that provide a more accurate age definition and better correlation of rock units discussed in this paper. The Early Cambrian trace fossils and body fossils are clearly restricted to certain lithologies within the basin, and the geochronological data points to a Neoproterozoic–Early Cambrian age. Until

now, there are no definite indicators, neither palaeontological nor isotopic, that allow a sharper chronological dating of the unit.

The lack of distinct or reference fossil remains (macro- and micro-) in the Neoproterozoic/Cambrian transition interval in the Early Palaeozoic Central Andean Basin, does not allow a biozonation to be defined, allowing correlation to other reference sections (Newfoundland, Siberia, Baltica or China). As recently stated by García Bellido and Aceñolaza (2005), miscorrelation by previous workers occurred because of forcing of unreliable data into a chronological system (systemic divisions, stages, biozones, etc.).

The detailed chronostratigraphic and biostratigraphic correlation of the Puncoviscana rock sequence to the Siberian section is not really possible at present due of the lack of palaeontological data that characterize biostratigraphic subdivisions in the Argentine strata. Linkage of the Neoproterozoic–Early Cambrian strata of NW Argentina to other reference sections around the world must be carried out carefully. A global chronostratigraphy for the lowermost Cambrian has been discussed often (Landing 1992). Interregional correlation based on fossiliferous data at a stage-level (Nemakit–Daldynian, Atdabanian, etc.) is highly speculative in NW Argentina, and names are irrelevant because of the lack of index fossils in the Andean Margin of South America. As noted by Landing (1992), Siberian stages reflect a long-term evolutionary development and immigration of species and communities that define a warm-water faunal province for the Siberian Basin: a very different setting that that of the Argentine sequences and other reference sections around the world (i.e. Avalon).

Early records of *Beltanelliformis*, *Sekwia* and *Nemiana* in the Puncoviscana Formation should be synonymized with *Beltanelloides* sp., and a new fossiliferous locality noted in the province of Jujuy. Material there is preserved in highly tectonized sandstones and shales, that crop out near the village of Purmamarca (Jujuy Province), and yield well-preserved samples of *Beltanelloides* sp. (an element that characterizes Vendian (Ediacaran age) biota of Siberia and those of similar age from other regions of the world (Figs 3, 8–9)).

The presence of microbially-induced structures, mostly restricted to finer-grained lithologies in the Puncoviscana Formation, stresses the importance of sediment binding in the earliest Cambrian, prior to the general substrate revolution (matgrounds being replaced by mixgrounds).

The occurrence of dichotomous traces assigned to cf. *Thalassinoides* network systems in the sediments of San Antonio de los Cobres (Salta Province), adds an interesting new feeding strategy in

the Early Cambrian on the seafloor of the Puncoviscana Sea, with possible primitive trapping structures not previously reported in this unit.

Further efforts are necessary to integrate structural, geochemical, sedimentological and palaeontological data known from the Puncoviscana Formation. Systematic studies and re-evaluation of published material from the in the Puncoviscana Basin, are the only way to obtain reliable data for an in-depth understanding of the Neoproterozoic–Cambrian transition in the Andean margin of South America.

Authors are indebted to M. Fedonkin and P. Vickers-Rich whose expertise in the Neoproterozoic–Cambrian transition provided new insights into the faunas and ecology of the Puncoviscana Basin. We thank A. Toselli, J. Rossi (Tucumán), R. Alonso, C. Moya (Salta), A. Sial and V. Ferreira (Brazil) for the valuable discussions. E. Gómez Hasselrot and D. Ruiz Holgado kindly did the line-drawings. We also thank the reviewers, R. Jenkins and A. Seilacher.

References

- ACEÑOLAZA, F. G. & ALONSO, R. 2001. Incoasociaciones en la transición Precámbrico/Cámbrico en el noroeste de Argentina. *Journal of Iberian Geology*, **27**, 11–22.
- ACEÑOLAZA, F. G. & DURAND, F. R. 1973. Trazas fósiles del basamento cristalino del noroeste argentino. *Boletín de la Asociación Geológica de Córdoba*, **1**, 45–52.
- ACEÑOLAZA, F. G. & DURAND, F. R. 1986. Upper Precambrian—Lower Cambrian biota from the northwest of Argentina. *Geological Magazine*, **123**, 367–375.
- ACEÑOLAZA, F. G. & TOSELLI, A. J. 1981. *Geología del Noroeste Argentino*. Publicación 1287, Facultad de Ciencias Naturales e Instituto Miguel Lillo, Universidad Nacional de Tucumán.
- ACEÑOLAZA, F. G., ACEÑOLAZA, G. F. & ESTEBAN, S. B. 1999. Bioestratigrafía de la Formación Puncoviscana y unidades equivalentes en el NOA. *Relatorio del 14 Congreso Geológico Argentino*, **1**, 91–114.
- ACEÑOLAZA, G. F., FEDONKIN, M., ACEÑOLAZA, F. & VICKERS-RICH, P. 2005. The Ediacaran/Early Cambrian transition in northwest Argentina: new paleontological evidence along the proto-margin of Gondwana. *II International Symposium on Neoproterozoic—Early Paleozoic events in southwestern Gondwana*. Windhoek, 2–4.
- ACEÑOLAZA, G. F. 2004. Precambrian–Cambrian ichnofossils, an enigmatic ‘annelid tube’ and microbial activity in the Puncoviscana Formation (La Higuera; Tucumán Province, NW Argentina). *Geobios*, **37**, 127–133.
- ACEÑOLAZA, G. F. 2005. The Cambrian System in Northwestern Argentina: stratigraphical and palaeontological framework. Reply. *Geologica Acta*, **3**, 73–77. Barcelona.
- ACEÑOLAZA, G. F. & ACEÑOLAZA, F. G. 2001. Ichnofossils and microbial activity in the Precambrian/Cambrian transition of northwestern Argentina. *Palaeoworld*, **13**, 241–244.
- ACEÑOLAZA, G. F. & ACEÑOLAZA, F. G. 2003. Trace fossils, microbial mats and sedimentary structures in the Puncoviscana Formation of northwestern Argentina (Neoproterozoic—Lower Cambrian): their record on a varied spectrum of palaeoenvironmental settings. In: FRIMMEL, H. (ed.) *III International Colloquium Vendian-Cambrian of W-Gondwana*. Program and extended abstracts, 4–6.
- ACEÑOLAZA, G. F. & ACEÑOLAZA, F. G. 2006. *Nereites saltensis* (Trace fossil): A taxonomical reevaluation of type and additional material from the Puncoviscana Formation of NW Argentina (Ediacaran—Early Cambrian). *V South American Symposium on Isotope Geology, Short Papers*, 218–220.
- ACEÑOLAZA, G. F. & TORTELLO, M. F. 2003. El Alisal: a new locality with trace fossils of the Puncoviscana Formation (late Precambrian—early Cambrian) in Salta province, Argentina. *Geologica Acta*, **1**, 95–102.
- ADAMS, C., MILLER, H. & TOSELLI, A. 1990. Nuevas edades de metamorfismo por el método K-Ar de la Formación Puncoviscana y equivalentes, NW de Argentina. In: ACEÑOLAZA, F. G., MILLER, H. & TOSELLI, A. J. (eds) *El Ciclo Pampeano en el Noroeste Argentino*. *INSUGEO Serie Correlación Geológica*, **4**, 199–208.
- BACHMANN, G., GRAUERT, B., KRAMM, U., LORK, A. & MILLER, H. 1987. El magmatismo Cámbrico Medio—Cámbrico Superior en el basamento del noroeste Argentino: investigaciones isotópicas y geocronológicas sobre los granitoides de los complejos intrusivos Santa Rosa de Tastil y Cañaní. *10 Congreso Geológico Argentino*, **4**, 125–127.
- BALDIS, B. & OMARINI, R. 1984. El grupo Lerma (Precámbrico—Cámbrico) en la comarca central Salteña y su posición en el borde Pacífico Americano. *Actas 9º Congreso Geológico Argentino*, **1**, 64–78.
- BENGTSON, S. 1994. (ed.) *Early Life on Earth*. Nobel Symposium, 84. Columbia University Press, New York.
- BORRELLO, A. V. 1969. Los geosinclinales de la Argentina. *Dirección Nacional de Geología y Minería. Anales*, **14**, 1–188.
- BUATOIS, L. A. & MÁNGANO, M. G. 2003a. La icnofauna de la Formación Puncoviscana en el noroeste argentino: Implicancias en la colonización de fondos oceánicos y reconstrucción de paleoambientes y paleoecosistemas de la transición Precámbrica—Cámbrica. *Ameghiniana*, **40**, 103–117.
- BUATOIS, L. A. & MÁNGANO, M. G. 2003b. Early colonization of the deep sea: Ichnologic evidence of deep-marine benthic ecology from the Early Cambrian of northwest Argentina. *Palaios*, **18**, 572–581.
- BUATOIS, L. A., MÁNGANO, M. G., ACEÑOLAZA, F. G. & ESTEBAN, S. B. 2000. The Puncoviscana ichnofauna of northwest Argentina: a glimpse into the ecology of the Precambrian—Cambrian transition. In: ACEÑOLAZA, G. F. & PERALTA, S. (eds) *Cambrian from the Southern Edge*, *INSUGEO Miscelánea*, **6**, 82–84.
- CAMINOS, R. 1979. Sierras Pampeanas Noroccidentales. Salta, Tucumán, Catamarca, La Rioja y San Juan. In: TURNER, J. C. (ed.) *2 Simposio de Geología Regional*

- Argentina. *Academia Nacional de Ciencias*, **1**, 225–291.
- CHAYLE, W. & CORIA, B. 1987. Vulcanitas básicas a ultrabásicas y mesosilícicas de la Formación Puncoviscana en el área del cerro Alto de Minas, Departamento Tilcara-Jujuy, Argentina. *10 Congreso Geológico Argentino*, **2**, 296–298.
- CORDANI, U., OMARINI, R., VANCINI, K. & PETRONILHO, L. 1990. Geocronología Rb/Sr y K/Ar del complejo granítico Santa Rosa de Tastil y de la Formación Puncoviscana, Salta, Argentina. *11 Congreso Geológico Argentino*, **2**, 239–242.
- CORIA, B., MANCA, N. & CHAYLE, W. 1990. Registros volcánicos en la Formación Puncoviscana. *Serie Correlación Geológica*, **4**, 53–60.
- CORSETTI, F. & HAGADORN, J. 2000. Precambrian–Cambrian transition: Death Valley, United States. *Geology*, **28**, 299–302.
- DÍAZ MARTÍNEZ, E. 1996. Paleozoico Inferior del Altiplano Norte de Bolivia. *12 Congreso Geológico de Bolivia, Tarija*, 131–135.
- DO CAMPO, M. 1999. Metamorfismo del basamento en la Cordillera Oriental y borde oriental de la Puna. In: GONZÁLEZ BONORINO, G., OMARINI, R. & VIRAMONTE, J. (eds) Geología del Noroeste Argentino. *14 Congreso Geológico Argentino*, **1**, 41–51.
- DURAND, F. R. 1993. Las icnofacies del basamento del Noroeste Argentino: significado cronológico e implicancias paleogeográficas. *12 Congreso Geológico Argentino*, **2**, 260–267.
- DURAND, F. R. & ACEÑOLAZA, F. G. 1990. Caracteres biofaunísticos, paleoecológicos y paleogeográficos de la Formación Puncoviscana (Precámbrico Superior—Cámbrico Inferior) del Noroeste Argentino. In: ACEÑOLAZA, F. G., MILLER, H. & TOSELLI, A. J. (eds) El ciclo Pampeano en el Noroeste Argentino. *INSUGEO, Serie de Correlación Geológica*, **4**, 71–112.
- DURAND, F. R., LECH, R. R. & TORTELLO, M. F. 1994. Nuevas evidencias paleontológicas en el basamento Precámbrico–Cámbrico del noroeste Argentino. *Acta Geológica Leopoldensia*, **39**, 691–701.
- ERDOGAN, B., UCHMAN, A., GÜNGÖR, T. & ÖZGÜL, N. 2004. Lithostratigraphy of the Lower Cambrian metaclastics and their age based on trace fossils in the Sandıklı region, Southwestern Turkey. *Geobios*, **37**, 346–360.
- ERIKSSON, P. G., CONDIE, K. C., TIRSGAARD, H., MUELLER, W. U., ALTERMANN, W., MIALI, A. D., ASPLER, L. B., CATUNEAU, O. & CHIARENZELLI, J. R. ET AL. 1998. Precambrian clastic sedimentation systems. *Sedimentary Geology*, **120**, 5–53.
- FEDONKIN, M. A. 1983. The Organic world of the Vendian. *Itoq Nauki i tekhniki VINITI Akademii Nauk SSSR, Series Stratigraphy and Paleontology*, **12**, 1–128.
- FEDONKIN, M. A. 1985. Non-skeletal fauna of the Vendian: Promorphological analysis. In: SOKOLOV, B. & IWANOWSKI, A. (eds) *The Vendian System, Paleontology*. Springer **1**, 10–60.
- FEDONKIN, M. A. 1987. Non-skeletal fauna of the Vendian and its place in the evolution of metazoans. *Trudy paleontologicheskogo Instituta Akademii Nauk SSSR*, **226**.
- FEDONKIN, M. A. 1990. Systematic description of Vendian Metazoa. In: SOKOLOV, B. S. & IVANOVSKIJ, A. B. (eds) *The Vendian System: Paleontology*. Springer, Berlin, **1**, 71–120.
- FEDONKIN, M. A. 1992. Vendian faunas and the early evolution of Metazoa. In: LIPPS, J. & STIGNOR, P. (eds) *Origin and Evolution of the Metazoa*. Plenum Press, New York, 87–129.
- FEDONKIN, M. A. 1994. Vendian body fossils and trace fossils. In: BENGTON, S. (ed.) *Early life on Earth*. Nobel Symposium, **84**. Columbia University Press, New York, 370–388.
- GARCÍA BELLIDO, D. & ACEÑOLAZA, G. F. 2005. Organismos de cuerpo blando en los estratos Cámbricos del noroeste Argentino. *16 Congreso Geológico Argentino*, La Plata.
- GLAESSNER, M. F. 1984. *The Dawn of Animal Life: a Biohistorical Study*. Cambridge University Press, Cambridge.
- GONZÁLEZ, P., POIRÉ, D. & VARELA, R. 2002. Hallazgo de trazas fósiles en la Formación El Jagüelito y su relación con la edad de las metasedimentitas, Macizo Nordpatagónico Oriental, provincia de Río Negro. *Revista de la Asociación Geológica Argentina*, **57**, 35–44.
- GRADSTEIN, F., OGG, J., SMITH, A. & BLEEKER, W. 2004. A new Geologic Time Scale, with special reference to Precambrian and Neogene. *Episodes*, **27**, 83–100.
- GROTZINGER, J., BOWRING, S., SAYLOR, B. & KAUFMAN, A. 1995. Biostratigraphic and Geochronologic constraints on early animal evolution. *Science*, **270**, 549–704.
- HOFFMAN, P., KAUFMAN, A., ALVERSON, P. & SCHRAG, D. 1998. A Neoproterozoic Snowball Earth. *Science*, **281**, 1342–1346.
- JEZEK, P. 1986. *Petrographie und facies der Puncoviscana Formation, einer turbidischen folge im Jungprä Kambrium und Unter Kambrium Nordwest Argentiniens*. Ph.D. Thesis, Wilhelms Universität, Münster, Germany.
- JEZEK, P. 1990. Análisis sedimentológico de la Formación Puncoviscana entre Tucumán y Salta. In: ACEÑOLAZA, F., MILLER, H. & TOSELLI, A. J. (eds) El ciclo Pampeano en el Noroeste Argentino. *INSUGEO, Serie Correlación Geológica*, **4**, 9–36.
- JEZEK, P., WILLNER, A. P., ACEÑOLAZA, F. G. & MILLER, H. 1985. The Puncoviscana trough—a large basin of Late Precambrian to Early Cambrian age on the Pacific edge of the Brazilian shield. *Geologische Rundschau*, **47**, 573–584.
- KAUFMAN, A. J. 1988. Neoproterozoic chemostratigraphy: key events in earth history ordered by detailed intra and inter-basinal correlation. *Sociedade Brasileira de Geología, Belo Horizonte*, 1–2.
- KAUFMAN, A. & KNOLL, A. 1995. Neoproterozoic variations in carbon isotopic composition of seawater: Stratigraphic and biogeochemical implications. *Precambrian Research*, **73**, 27–49.
- KEPPIE, J. D. & BAHLBURG, H. 1999. Puncoviscana Formation of northwestern and central Argentina: Passive margin or foreland basin deposit? In: RAMOS, V. & KEPPIE, J. (eds) *Laurentia–Gondwana*

- connections before Pangea. *Geological Society of America*, Special Paper, **336**, 139–143.
- KILMURRAY, J. O., MERODIO, J. & RAPELA, C. 1974. Las metamorfitas cordieríticas del área estación Incahuasi—Santa Rosa de Tastil, Provincia de Salta: rasgos petrológicos y geoquímicos. *Revista de la Asociación Geológica Argentina*, **29**, 425–442.
- KNOLL, A. & WALTER, M. 1992. Latest Proterozoic stratigraphy and earth history. *Nature*, **356**, 673–678.
- KRAEMER, ESCAYOLA, M. P. & MARTINO, R. D. 1995. Hipótesis sobre la evolución tectónica neoproterozoica de las Sierras Pampeanas de Córdoba (30°40'–32°40'), Argentina. *Revista de la Asociación Geológica Argentina*, **50**, 47–59.
- LANDING, E. 1992. Precambrian—Cambrian boundary GASP, SE Newfoundland, Biostratigraphy and Geochronology. In: ODIN, G. S. (ed.) *Phanerozoic Time Scale*. Bulletin of the Liaison and Informations, IUGS Subcommission for Geochronology, **11**, 6–8.
- LEONOV, M. V. & RAGOZINA, A. L. 2007. Upper Vendian assemblages of carbonaceous micro- and macrofossils in the White Sea Region: systematic and biostratigraphic aspects. In: VICKERS-RICH, P. & KOMAROWER, P. (eds) *The Rise and Fall of the Ediacaran Biota*. Geological Society, London, Special Publications, **286**, 269–276.
- LORK, A., MILLER, H., KRAMM, U. & GRAUERT, B. 1990. Sistemática U/Pb de zircons detríticos de la Formación Puncoviscana y su significado para la edad máxima de la sedimentación en la Sierra de Cachi (Provincia de Salta), Argentina. In: ACEÑOLAZA, F. G., MILLER, H. & TOSELLI, A. J. (eds) *El Ciclo Pampeano en el Noroeste Argentino*. *INSUGEO, Serie Correlación Geológica*, **4**, 199–208.
- LOSS, R. & GIORDANA, A. 1952. Osservazioni sul Proterozoico di Jujuy. *Atlas di la Società Italiana di Scienze Naturali*. Milano, 1–46.
- MANCA, N., CORIA, B., BARBER, E. & PEREZ, W. A. 1987. Episodios magmáticos de los ciclos Pampeano y Famatiniano en el Río Yacoraité, Provincia de Jujuy. *10 Congreso Geológico Argentino*, **4**, 299–301.
- MON, R. & HONG, F. 1996. Estructura del basamento proterozoico y paleozoico inferior del norte argentino. *Revista de la Asociación Geológica Argentina*, **51**, 3–14.
- MOORE, E. M. 1991. Southwest US East Antarctic (SWEAT) connection: a hypothesis. *Geology*, **5**, 425–428.
- MOYA, M. C. 1998. El Paleozoico inferior de la Sierra de Mojotoro, Salta-Jujuy. *Revista de la Asociación Geológica Argentina*, **53**, 219–238.
- NARBONNE, G. 1998. The Ediacara Biota: a terminal Proterozoic experiment in the evolution of life. *Geological Society of America Today*, **8**, 1–6.
- NARBONNE, G. & GEHLING, J. 2003. Life after snowball: the oldest complex Ediacaran fossils. *Geology*, **31**, 27–30.
- NOFFKE, N., GERDES, G., KLENKE, T. & KRUMBEIN, W. 2001. Microbially induced sedimentary structures—a new category within the classification of primary sedimentary structures. *Journal of Sedimentary Research*, **17**, 649–656.
- NOFFKE, N., KNOLL, A. & GROTZINGER, J. P. 2002. Sedimentary controls on the formation and preservation of microbial mats in siliciclastic deposits: a case study from the Upper Neoproterozoic Nama Group, Namibia. *Palaaios*, **17**, 533–544.
- OMARINI, R. 1983. *Caracterización litológica, diferenciación y génesis de la Formación Puncoviscana entre el Valle de Lerma y la Faja Eruptiva de La Puna*. Ph.D. Thesis, Universidad Nacional de Salta, 1–202.
- OMARINI, R. & BALDIS, B. 1984. Sedimentología y mecanismos deposicionales de la Formación Puncoviscana (Grupo Lerma, Precámbrico—Cámbrico) del Noroeste Argentino. *9 Congreso Geológico Argentino*, **1**, 384–398.
- OMARINI, R. & SUREDA, R. 1993. Evolución geodinámica y configuración paleogeográfica en los Andes centrales del Proterozoico superior al Paleozoico inferior: Modelos alternativos y problemas. *12 Congreso Geológico Argentino*, **3**, 291–308.
- OMARINI, R. & SUREDA, R. 1999. Evolución geodinámica. In: GONZÁLEZ BONORINO, G., OMARINI, R. & VIRAMONTE, J. (eds) *Geología del Noroeste Argentino Relatorio 14 Congreso Geológico Argentino*, **1**, 115–121.
- OMARINI, R., ALONSO, R. N. & MARCUZZI, J. J. 1993. Hallazgo de vulcanitas en la Formación Puncoviscana, Puna Argentina. *Revista de la Asociación Geológica Argentina*, **48**, 179–183.
- OMARINI, R., SUREDA, R., TOSELLI, A. & ROSSI, J. 1999a. Magmatismo. In: GONZÁLEZ BONORINO, G., OMARINI, R. & VIRAMONTE, J. (eds) *Geología del Noroeste Argentino Relatorio 14 Congreso Geológico Argentino*, **1**, 29–40.
- OMARINI, R. H., SUREDA, R. J., GÖTZE, H. J., SEILACHER, A. & PFLÜGER, F. 1999b. Puncoviscana folded belt in northwestern Argentina: testimony of Late Proterozoic Rodinia fragmentation and pre-Gondwana collisional episodes. *International Journal of Earth Sciences (Geologische Rundschau)*, **88**, 76–97.
- PFLÜGER, F. 1999. Matground structures and redox facies. *Palaaios*, **14**, 25–39.
- RAMOS, V. 1988. Tectonics of the Late Proterozoic—Early Paleozoic: a collisional history of southern South America. *Episodes*, **11**, 168–174.
- RAMOS, V. 1999. Rasgos estructurales del territorio Argentino. In: CAMINOS, R. (ed.) *Geología Argentina, Instituto de Geología y Recursos Minerales, SEGEMAR*. Anales, **29**, 715–784.
- RAPELA, C., CORIA, B., TOSELLI, A. & SAAVEDRA, J. 1992. El magmatismo del paleozoico inferior en el sudoeste de Gondwana. In: GUTIÉRREZ-MARCO, J. C., SAAVEDRA, J. & RÁBANO, I. (eds) *Paleozoico Inferior de Iberoamérica. Publicación Especial Universidad de Extremadura*, 21–68.
- RAPELA, C., PANKHURST, R., CASQUET, C., BALDO, E., SAAVEDRA, J. & GALINDO, E. 1998. The Pampean orogeny of the southern proto-Andes: Cambrian continental collision in the Sierras de Córdoba. In: PANKHURST, R. & RAPELA, C. (eds) *The Proto-Andean Margin of Gondwana*. Geological Society of London, Special Publications, **142**, 181–217.
- ROSS, R. J. 1991. Tectonic setting in the Windermere Supergroup: The continental perspective. *Geology*, **19**, 1125–1128.

- ROSSI, J., TOSELLI, A. & DURAND, F. 1992. Metamorfismo de baja presión, su relación con el desarrollo de la cuenca Puncoviscana. Plutonismo y régimen tectónico Argentina. *Estudios Geológicos*, **48**, 279–287.
- ROWELL, A. J., REES, M., DUEBENDORFER, E., WAN SCHMUS, W., WALLIN, E. & SMITH, E. 1993. An active Neoproterozoic margin: evidence from the Skelton Glacier area, Transantarctic Mountains. *Journal of the Geological Society of London*, **150**, 321–343.
- SALFITY, J., OMARINI, R., BALDIS, B. & GUTIÉRREZ, W. 1975. Consideraciones sobre la evolución geológica del Precámbrico y Paleozoico del Norte Argentino. *Actas 2 Congreso Iberoamericano Geología Económica, Buenos Aires*, **4**, 341–343.
- SATO, A. M., GONZÁLEZ, P. & LLAMBÍAS, E. J. 2002. The Ordovician of Sierra de San Luis: Famatinian magmatic arc and low to high-grade metamorphism. In: ACEÑOLAZA, F. G. (ed.), Aspects on the Ordovician System of Argentina. *INSUGEO, Serie Correlación Geológica*, **16**, 327–346.
- SCHWARTZ, J. J. & GROMET, L. P. 2004. Provenance of a late Proterozoic—early Cambrian basin, Sierras de Córdoba, Argentina. *Precambrian Research*, **129**, 1–21.
- SCOTSESE, C. & MCKERROW, W. 1990. Revised world maps and introduction. In: MCKERROW, W. & SCOTSESE, C. (eds) Palaeozoic Palaeogeography and Biogeography. *Geological Society Memoir*, **12**, 1–21.
- SEILACHER, A. 1984. Late Precambrian and early Cambrian metazoan: preservational or real extinction? In: HOLLAND, H. & TRENDALL, A. (eds) *Patterns of Change in Earth Evolution* (Dahlem Konferenzen 1984), Springer, Berlin, 159–168.
- SEILACHER, A. 1989. Vendozoa: Organismic construction in the Proterozoic biosphere. *Lethaia*, **22**, 229–239.
- SEILACHER, A. 1999. Biomat-related lifestyles in the Precambrian. *Palaios*, **14**, 86–93.
- SEILACHER, A. & PFLÜGER, F. 1994. From biomats to benthic agriculture: a biohistoric revolution. In: KRUMBEIN, W., PATERSON, D. & STAL, J. (eds) Biostabilization of sediments. *BIS Odemburg*, 97–105.
- SEILACHER, A., BUATOIS, L. & MÁNGANO, M. G. 2005. Trace fossils in the Ediacaran–Cambrian transition: Behavioral diversification, ecological turnover and environmental shift. *Palaeogeography, Palaeoclimatology, Palaeoecology*, **227**, 323–356.
- SIAL, A. N., FERREIRA, V. P., TOSELLI, A. J., ACEÑOLAZA, F. G., PIMENTEL, M. M., PARADA, M. A. & ALONSO, R. N. 2001. C and Sr isotopic evolution of the Carbonate sequence in NW Argentina: implications for a probable Precambrian–Cambrian transition. *Carbonates and Evaporites*, **16**, 141–152.
- STOREY, B., ALABASTER, T., MACDONALD, D., PANKHURST, R. & DALZIEL, I. 1992. Upper Proterozoic rift-related rocks in the Pensacola Mountains, Antarctica: precursors to supercontinent breakup? *Tectonics*, **11**, 1392–1405.
- SUÁREZ SORUCO, R. 1989. Desarrollo tectonosedimentario del Paleozoico inferior de Bolivia. *Información Geológica UAFT. Simposio Bodas de Oro de la Universidad Tomás Frías, Potosí*, **2**, 1–11.
- SUÁREZ SORUCO, R. 2000. Compendio de Geología de Bolivia. *Revista Técnica de YFPB*, **18**, 1–144.
- SUREDA, R., OMARINI, R. H. & ALONSO, R. 1999. El Ciclo Pannotiano, la perspectiva histórica y las nuevas definiciones. In: GONZÁLEZ BONORINO, G., OMARINI, R. & VIRAMONTE, J. (eds) *Geología del Noroeste Argentino. 14 Congreso Geológico Argentino*, **1**, 21–27.
- TESSENHORN, F. 1982. Significance of late Precambrian turbidite sequences bordering the East Antarctic shield. Proceedings Symposium on Precambrian Problems, Copenhagen. *Geologische Rundschau*, **71**, 361–369.
- TOSELLI, A. J. 1990. Metamorfismo del Ciclo Pampeano. In: ACEÑOLAZA, F. G., MILLER, H. & TOSELLI, A. J. (eds) El Ciclo Pampeano en el Noroeste Argentino. *INSUGEO, Serie de Correlación Geológica*, **4**, 181–197.
- TOSELLI, A. J. & ACEÑOLAZA, F. G. 1984. Presencia de eruptivas basálticas en los afloramientos de la Formación Puncoviscana en Coraya, depto. Humahuaca, Jujuy. *Revista de la Asociación Geológica Argentina*, **39**, 158–159.
- TOSELLI, A. J. & ROSSI, J. 1990. Plutonismo en la Formación Puncoviscana. In: ACEÑOLAZA, F. G., MILLER, H. & TOSELLI, A. J. (eds) El Ciclo Pampeano en el Noroeste Argentino. *INSUGEO, Serie de Correlación Geológica*, **4**, 221–227.
- TOSELLI, A. J., ACEÑOLAZA, F. G., SIAL, A. N., ROSSI, J. N. & FERREIRA, V. P. 2005. Los carbonatos de la Formación Puncoviscana s.l.: correlación quimioestratigráfica e interpretación geológica. *16 Congreso Geológico Argentino*, **2**, 327–333.
- TURNER, J. C. M. 1960. Estratigrafía de la Sierra de Santa Victoria y adyacencias. *Boletín de la Academia Nacional de Ciencias, Córdoba*, **41**, 163–196.
- TURNER, J. C. M. 1976. Cordillera Oriental. In: LEANZA, A. F. (ed.) *Geología Regional Argentina. Publicación Especial Academia Nacional de Ciencias en Córdoba*, 117–142.
- WILLNER, A. 1990. División tectonometamórfica del basamento del Noroeste Argentino. In: ACEÑOLAZA, F. G., MILLER, H. & TOSELLI, A. J. (eds) El Ciclo Pampeano en el Noroeste Argentino. *INSUGEO, Serie Correlación Geológica*, **4**, 113–159.

Climates and climate zonality of the Vendian: geological evidence

N. M. CHUMAKOV

*Geological Institute, Russian Academy of Sciences, 7 Pyzhevsky pereulok,
119017 Moscow, Russia (e-mail: chumakov@ginras.ru)*

Abstract: In view of the difficulties of stratigraphic correlation, the absence of being able to position continents reliably, the scarcity of climate indicators, and the fact that Vendian sequence crops out over a wide area and can be far apart, it has only so far been possible to identify the most general climatic features for three Vendian units. Late Vendian (Nemakit–Daldyn), and possibly Early Tommotian (Early Cambrian), time was characterized by a glacial climate with pronounced climatic zonation. It appears that there were northern and southern cold zones and a low-latitude, possibly mid-latitude warmer zones. Throughout the time the Middle Vendian sequence was being deposited (Redkino–Kotlin), a warm, possibly arid zone was characteristic of low and mid-palaeolatitudes. In southern high latitudes, there is evidence of a warm humid climate at some periods during this time. The Early Vendian (Laplandian or Varangian) time was characterized by a glacial climate. Some palaeocontinental reconstructions based on magnetism suggest that these glaciations affected high, middle and most of the low latitudes, extending to the palaeoequator. The timing of glacial events in the late Neoproterozoic and their extent across the globe and severity is a topic of great debate at the moment—some researchers suggesting glaciations that lasted for millions of years that locked the entire Earth in solid ice ('Snowball Earth'). Others suggest that some ice-free oceans were present even during the most severe of glacial events and certainly some geological evidence seem to fit this latter hypothesis well.

Direct application of palaeoclimatic reconstruction methods developed for the Phanerozoic (Semikhatov & Chumakov 2004), in the Vendian is hampered by several difficulties. The first arises as a result of the lack of resolution of chronostratigraphy when compared with the precision of the Phanerozoic schemes. In some of the best understood sequences the late Neoproterozoic has been divided into up to five widely correlative units based on trace fossils, microfossils, metazoans, radiometric dates, stable isotope signatures and characteristic glacial horizons (Knoll 2000; Walter *et al.* 2000). But in many Vendian sections world-wide, the set of stratigraphic data is insufficient to allow recognition and broad correlation. On the global scale, only three units in time equivalent sequences can currently be distinguished and correlated.

The second difficulty in studying Vendian palaeoclimates arises from the lack of general agreement on continental reconstructions, with available reconstructions differing greatly. It would be of great value, as has been suggested by many researchers, to cross-check reconstructions arrived at by use of palaeomagnetic evidence, with palaeoclimatic indicators (Khain & Yasamanov 1987; Smith 2001; amongst many others).

The third difficulty affecting the reconstruction of Precambrian climatic zones is that, with increased age, the number of lithological and palaeontological climate indicators vanish and geochemical indicators decrease, through alteration, recycling and thus resetting of the 'climate-signal'. The principle lithological indicators useful for Vendian/Ediacaran palaeoclimate reconstruction are tillites,

evaporites (gypsum and salts) and carbonate platform sediments. Red beds, especially those lacking carbonate cement, are more ambiguous in their climate signal (unless, of course, there are additional indicators: mineralogical, structural, etc.). Indicators of humidity levels are particularly scarce in the Vendian. Bauxites occur only in exceptional cases and their origin is frequently unclear. Grey, terrigenous rocks are generally not reliable as indicators of humid conditions, though some researchers have invoked such. Grey colour is often of secondary origin in these ancient rocks. So, in practice, palaeoclimatic reconstructions are mainly based on indicators such as tillites, evaporites and carbonate platforms. This can lead to an exaggerated estimate of glacial and arid zone distribution at the expense of humid zones. Bio-lithological indicators are primarily limited to the occurrence of stromatolitic reefs, which occur occasionally as thick sequences, indicative of a warmer climate.

Finally, present-day outcrop areas of Late Precambrian deposits are separated by considerable distance. This also limits the accuracy of reconstructions.

These restrictions allow only the most general conclusions on global climates of the Vendian to be drawn.

Stratigraphic and palaeogeographic framework

The stratigraphic distribution of climatic indicators in some of the key sections of the Vendian System on five continents is summarized in Figure 1.

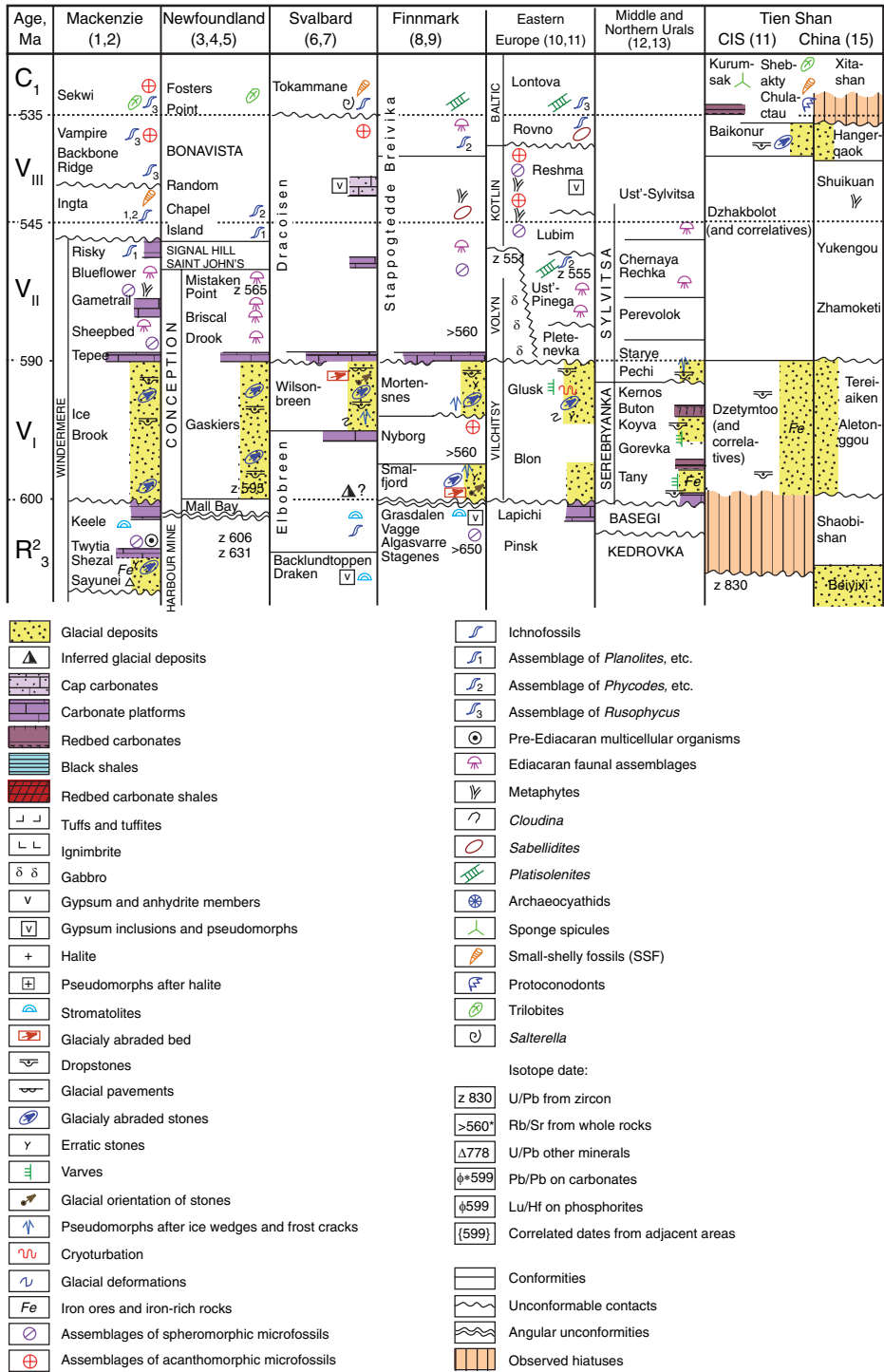


Fig. 1. Attempt at correlation of glacial horizons and other climatic indicators in key sections of the Vendian. The names of supergroups, groups, and subgroups are in capital letters, and those of formations and smaller stratigraphic units are in lower case. V_I, V_{II}, and V_{III} denote the 'Early,' 'Middle,' and 'Late Vendian'—informal units used in this paper. References: 1, Narbonne & Aitken 1995; 2, Walter *et al.* 2000; 3, Myrow 1995; 4, Myrow & Kaufman 1999; 5, Narbonne & Gehling 2003; 6, Chumakov 1978*b*; 7, Harland *et al.* 1993; 8, Vidal 1981; 9, Gorokhov *et al.* 2001; 10,

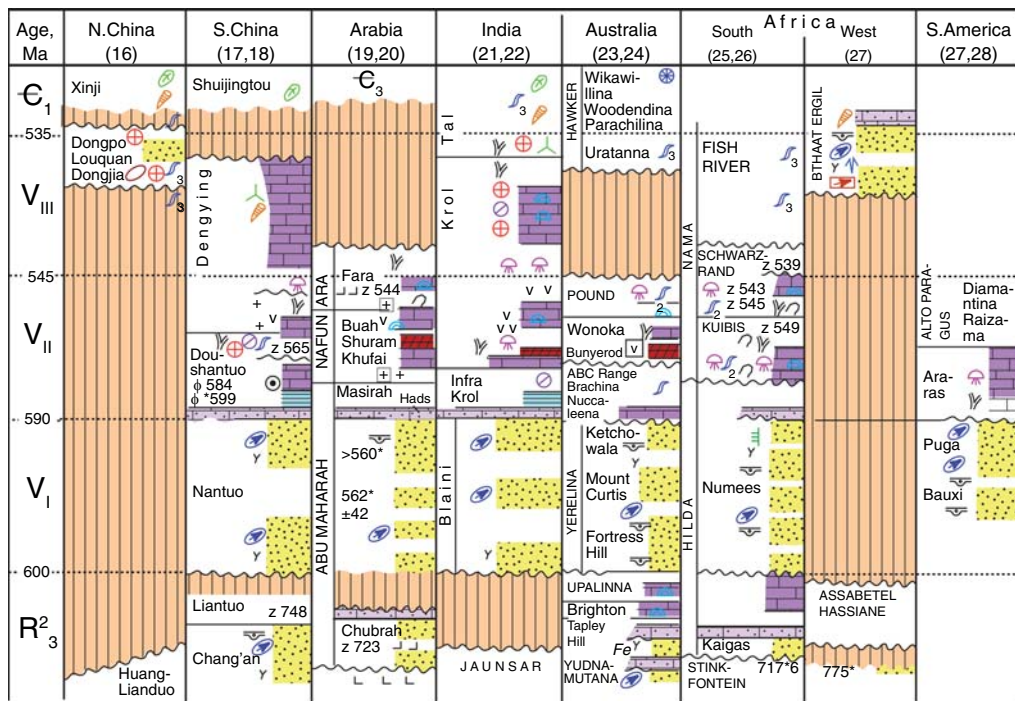


Fig. 1. (Continued) Aksenov 1990; 11, Vidal & Moczydłowska 1995; Martin *et al.* 2000; 12, Bekker 1992; 13, Chumakov 1998; 14, Kiselev & Korolev 1981; 15, Hambrey *et al.* 1981; 16, Bobrov 1965; Chumakov 1993; Pokrovsky *et al.* 2005. 17, Wang *et al.* 1998; 18, Zhang *et al.* 1998; Barfod *et al.* 2002; Condon *et al.* 2005; Yin *et al.* 2005; 19, Brasier & McCarron 2000; 20, Leather *et al.* 2002; 21, Tiwari & Knoll 1994; 22, Tiwari 1999; 23, Preiss 2000; 24, Walter 2000; Calver 2000; 25, Germs 1995; 26, Walter *et al.* 2000; 27, Trompette 1994, 1996; 28, Alvarenga & Trompette 1998, 1992.

Suggested correlations between Vendian and Ediacaran Systems are shown in Table 1. Based on the distribution of Small Shelly Fossils (SSF) and other metazoans, multicellular algae, trace fossils and microfossils, glacial horizons and radiometric dating, it is possible to define three divisions of the Vendian, which are loosely referred to here as 'Early,' 'Middle,' and 'Late' Vendian and are designated V_I , V_{II} , and V_{III} in Figure 1. The Early Vendian contains one or, in some regions, two glacial horizons (one at the base—Lower Blon' Subformation, Smalfjord Formation etc.; another at the top—Glusk and Mortensnes formations, etc.), and is characterized by a significant negative $\delta^{13}C$ at the base and the top. New data provide some evidence of correlation of the upper glacial formations of the Lower Vendian with the Gaskiers Formation of Newfoundland, dated at *c.* 580 Ma (Knoll *et al.* 2004). The base of lower glacial formations of the Lower Vendian may be correlated to the base of the glacial Nantuo Formation *sensu stricto* (age between 635 and 663 Ma; Zhou *et al.* 2004; Condon *et al.* 2005) or to the base of Nantuo Formation *sensu*

lato (including Gucheng Formation; Evans 2000) of age >663 Ma (Zhou *et al.* 2004). The Middle Vendian contains primitive ichnofossils, specific assemblages of acanthomorphic acritarch, metaphyts and Ediacaran metazoans and is radiometrically dated at between 580 Ma and *c.* 545 Ma (Semikhatov 2000). The Late Vendian is characterized by the Nemakit–Daldyn assemblage of small shell fossils, complex ichnofossils, at the top by a significant negative $\delta^{13}C$ and glacial horizons in some regions, along with radiometric dates between 545 and 535 Ma (Semikhatov 2000).

Early, Middle and Late Vendian correspond, on the Russian Platform, to: (a) the Laplandian glacial horizon (comprising the Glusk and Blon' formations); (b) the Redkino and Kotlin horizons; and (c) the Rovno horizon of B. S. Sokolov (1998). In Siberia, a likely stratigraphic correlative of the Rovno horizon is the Nemakit–Daldyn stage. Outside Russia, these three parts of the Vendian are usually referred to as Varangerian (comprising Smalfjord, Nyborg and Mortensnes formations), Ediacaran, and pre-Tommotian Cambrian.

Table 1. Accepted correlation between Vendian and Ediacaran Systems

		Vendian System Sokolov 1998 (with some additions)	Ediacaran System Knoll <i>et al.</i> 2004	
Lower Cambrian	Tommotian Stage \approx 535 Ma		Lower Cambrian 543 Ma	
	V _{III}	Nemakit-Daldyn Stage		
Vendian System	V _{II}	Kotlin Horizon Redkino Horizon	Ediacaran System 620 Ma	Gaskiers Glaciation
	V _I	Laplandian Horizon (Varangerian)	Glusk Fm. (Mortensnes Fm.) Upper Blon' Subfm. (Nyborg Fm.) Lower Blon' Subfm. (Smalfjord Fm.)	
		>635– <660/ >660 Ma		
Upper Riphean			Cryogenian	

Thus, the intervals for which Vendian palaeoclimatic reconstructions might be possible are comparable in duration to long stages in the Phanerozoic (V_{III}) or to the longest Phanerozoic periods (V_I).

The use of palaeogeography as a basis for palaeoclimatic reconstruction is more complex than it might seem (Chumakov 1992; Kirschvink 1992a; Scotese & McKerrow 1990; Dalziel *et al.* 1994; Young 1995; Mossakovsky *et al.* 1996; Piper 2000; Scotese 2000; Dalziel & Soper 2001; Smith 2001; Kheraskova *et al.* 2003; Smith & Pickering 2003; and many others). Many of these reconstructions are similar with regard to the positioning of the main continents, but differ significantly with respect to location of microcontinents. This situation reflects the vigorous effort being made to refine such reconstructions—and, indeed, many of these are beginning to converge. In this paper, the palaeoclimatic schemes are based on the palaeogeographic reconstructions proposed by Smith & Pickering (2003) for the Early Vendian (600 Ma), and on tentative ones proposed by Smith (2001) for the Middle Vendian (580 Ma) and the earliest Cambrian Period (540 Ma). Following recommendations of the International Stratigraphic Commission, Smith assigned the Nemakit–Daldyn stage to the earliest Cambrian. In this paper and in Russia generally, this stage is regarded as Late Vendian. Smith's reconstructions were based on the most reliable palaeomagnetic and palaeotectonic data available at the time of publication, placing early Vendian tillites in high and middle latitudes. This may not now always be the case. In

this paper, Smith's reconstructions are used with insignificant changes, as explained below.

Climatic zonation of the Late Vendian (Nemakit–Daldyn, 'V_{III}')

Climatic indicators of the V_{III} (Fig. 1) were plotted on Smith's (2001) palaeogeographical reconstruction for 540 Ma. These indicators suggest the existence of three roughly east-westerly trending climatic zones during the Late Vendian (possibly earliest Cambrian): two zones of cold climate (northern and southern), delimited by glacial deposits, and a third zone with evidence of a warm, locally arid zone (Fig. 2c). The northern zone includes glacial deposits deposited near end of Vendian time on the Tarim and North China blocks (Hambrey *et al.* 1981; Yin & Guan 1999). A glacially-striated basement occurs locally in sequences on the North China block beneath glacial deposits (Guan *et al.* 1986). According to Smith's (2001) reconstruction, at the peak of this glaciation, terrestrial ice sheets in the northern hemisphere could have reached a palaeolatitude of 45° north. The southern cold zone, developed during Early Cambrian or Late Vendian times, is exemplified by glacial deposits in north and west Africa (West African Glacial Horizon—Chumakov 1993; Bertrand–Sarfati *et al.* 1995; Trompette 1997), which may have been limited to the high southern palaeolatitudes (approximately 75° S). The original geographical positions of Late Vendian glacial deposits in Kazakhstan and Tien

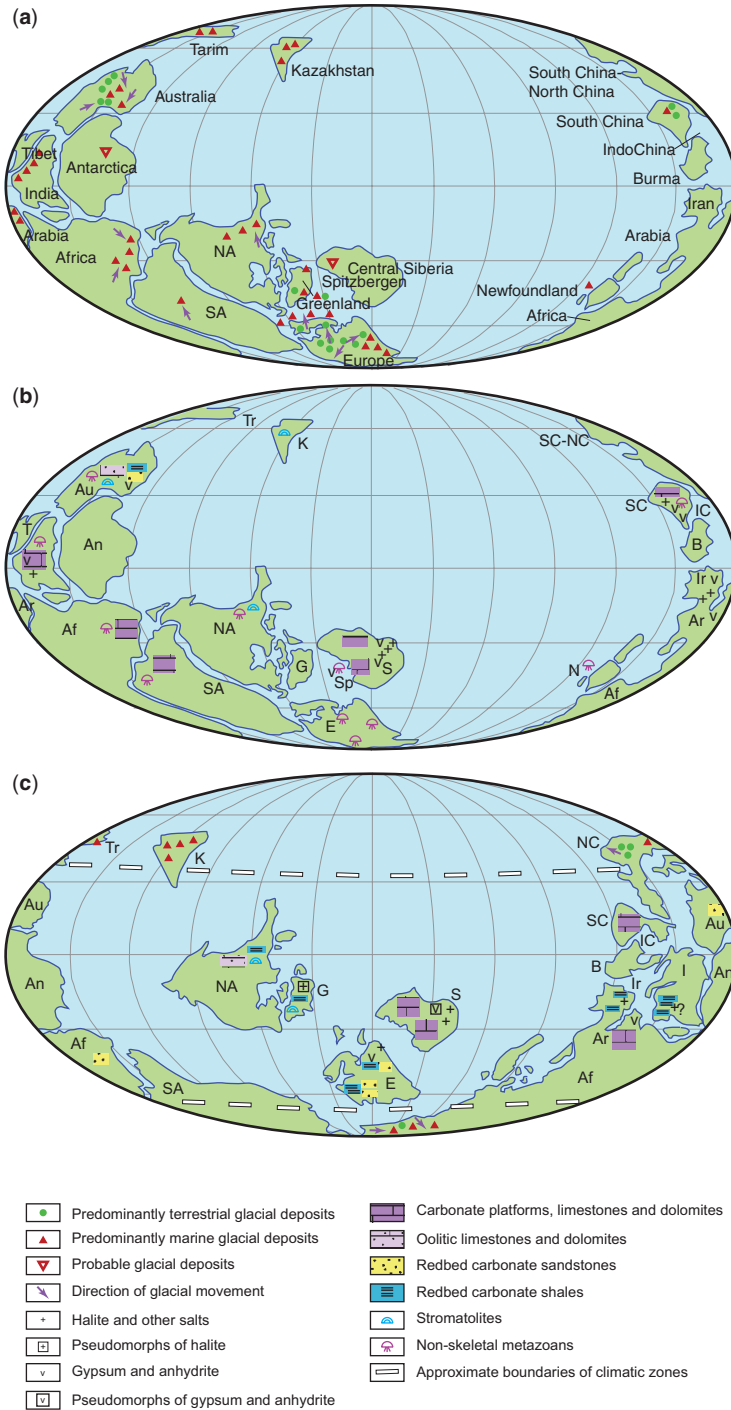


Fig. 2. Schemes of the Vendian zonation (palaeogeographic basis is modified after Smith (2001) and Smith & Pickering (2003): **(a)** Early Vendian (Laplandian or Varangian time); **(b)** Middle Vendian (Redkino–Kotlin time); **(c)** End of the Vendian –? beginning of the Early Cambrian (Nemakit–Daldyn, ? early Tommotian time). Au, Australia; An, Antarctica; Ar, Arabia; Af, Africa; B, Burma; G, Greenland; E, North-eastern Europe; I, India; IC, Indo-China; Ir, Iran; K, Kazakhstan blocks; N, Newfoundland; S, Central Siberia; NA, North America; NC, North China; T, Tibet; Tr, Tarim; Sp, Spitsbergen; SA, South America; SC, South China.

Shan (Baikonur Glacial Horizon—Chumakov 1978) are not well defined. Smith (2001) associated these tectonic blocks with the Siberian block, all located in low latitudes of the southern hemisphere. Considering the similarity of Vendian to Cambrian sequences (in particular their glacial deposits) of the Tien Shan, Kazakh blocks, Tarim blocks, and taking into account minimal subsequent movement, it seems most logical that the Kazakh, Tien Shan and Tarim blocks were relatively close to each other in the northern hemisphere. This positioning of the Kazakh, Tien Shan and Tarim blocks is more consistent with the tectonic ideas about make-up of the Central Asian fold belt (Mossakovsky *et al.* 1996; Kheraskova *et al.* 2003). Separating the cold zones during Nemakit–Daldyn time, was a warmer belt in which predominantly stromatolitic and oncolitic carbonate platforms were forming (northwestern North America, Siberia, Arabia and South China). Much of this zone was arid, as indicated by extensive deposits of salt, gypsum and anhydrite in Siberia (Zharkov 1981; Khomentovsky 1990), Arabia (Brasier *et al.* 2000; Walter *et al.* 2000), Iran and northwestern India (Strauss *et al.* 2001). Sabkha-type gypsum-bearing deposits and imprints of salt and gypsum crystals and anhydrite nodules are known outside these basins as well. All attest to a warm to hot arid climate in low and some middle latitudes in Nemakit–Daldyn time. Carbonate red beds of this age are known from South Africa (Germs 1995) and Australia (Walter *et al.* 1995). Non-carbonate red beds, showing evidence of aridity gypsification, halite films and desiccation cracks (Aksenov 1990) occur in the Reshma Formation in the East European Craton and in north India (Tiwari 1999; Kumar *et al.* 2000). These terrigenous red beds, including carbonate-bearing sediments, were deposited at midlatitudes between cold and warm zones and may have formed in semi-arid climate. According to the reconstruction used in this paper, the southernmost occurrence of polymict red bed lay at palaeolatitude of 60° south (Suvorovo Formation in the southwestern Ukraine). All of the above data give some support for the cold zone of the southern hemisphere being restricted to high latitudes, with the midlatitudes hosting a semi-arid or arid belt. Of course, all of these reconstructions depend heavily on precise dating of the sediments so that climatic events are contemporaneous and at the moment there is lively discussion and disagreement that may lead to quite different conclusions in the future.

Analysis of the palaeoclimatic reconstruction for the Nemakit–Daldyn stage leads to three essential conclusions. First, the latitudinal positions of two

cold and warm climatic belts are consistent with the principal climatic trends on Earth and, hence, Smith's (2001) palaeoclimatic reconstruction at the moment appears consistent with observed palaeoclimatic indicator distribution. The second conclusion is no less important: the climate during the Late Vendian times was glacial. The existence of an extensive Late Vendian glaciation is consistent with a large negative anomaly of $\delta^{13}\text{C}$ at the Vendian–Cambrian boundary (Knoll 2000) and deposition of cap carbonates signalling the end of the glaciation (Kazakhstan and Tien Shan: Chumakov 1978, 1992; West Africa: Trompette 1997). Lastly, the climatic zoning at the end of the Vendian was asymmetrical, a pattern similar to such zonation during Phanerozoic glacial episodes.

Climatic zonation of the Middle Vendian (Kotlin–Redkino; Ediacaran; 'V_{II}')

Smith's reconstructions for the Middle Vendian (Fig. 2b) are consistent with the distribution of carbonate platforms at low and middle latitudes (deposits currently found in Australia, Kazakhstan, North India, Arabia, South Africa, South America, Siberia and South China). Deposition of salts and gypsum in North India, Siberia, South China and in the region of the present-day Persian Gulf testifies to the wide distribution of arid environments within this climatic zone. The evaporite basins of the south Siberia and Iranian–Arabian regions are of enormous proportions. The latter probably included northwestern Hindustan. To the south of this warm zone, in high latitudes in the East European craton and in the Cis-Ural region, the sediments that accumulated in the seas invading the shallow Valdai Basin were dominated by bluish-grey, fine-grained, thin-bedded clays and siltstones, some enriched in organic matter, which preserved the characteristic Ediacaran metazoans along with metaphytes. In the marginal parts of the Valdai Basin, fine-grained and thin-bedded rocks graded into coarser grained non-carbonate, variegated red beds containing an admixture of kaolinite; indicative of erosion under humid conditions. This suggests that the land adjacent to the Valdai Basin was under the regime of a warm and humid climate. Thus, the climate in the high latitudes during the Middle Vendian times was humid and relatively warm, consistent with the lack of glacial indicators preserved in Middle Vendian deposits.

Climatic zonation of the Early Vendian (Laplandian or Varangian, 'V_I')

Evidence of glaciation is widespread in Lower Vendian deposits. There are two glacial units in

the Lower Vendian: one in the lower part and one in the upper part (Fig. 1). These lower glacial unit occurs on many large continents, and on some microcontinents as well. These units are located on the northeastern European craton with adjacent orogenic zones (Chumakov 1990, 1992; Harland *et al.* 1993), South Africa (Germs 1995), the Lesser Himalayas (Tiwari & Knoll 1994; Kumar *et al.* 2000), Australia (Preiss 1987, 2000; Walter 2000), and South China (Wang *et al.* 1998), as well as some other regions (Figs 1, 2a). In addition to those mentioned above, there are numerous occurrences of Lower Vendian diamictites whose age or origin is not well constrained (for a review see Evans 2000). The diversity of published continental reconstructions suggest that many of these glacial deposits were formed at low latitudes, some on the Equator. Such a wide latitudinal distribution indicates a profound glacial climate at beginning of the Early Vendian. Non-glacial facies of this time have not been identified. They may have been removed by the glacio-eustatic subaerial exposure of the continental shelves and inland basins.

This rock-record points to a severe glacial event on Earth at the beginning of the Early Vendian. Some authors supposed that this glaciation was global (Harland 1964; ‘Snowball Earth’ of Kirschvink 1992*b*; Hoffman & Schrag 2002 and others). Although there are currently no compelling counter-arguments against the ‘Snowball Earth’ hypothesis, which suggests that the entire Earth was covered by ice—serious doubts as to its validity do exist. There are a number of reasons for these doubts.

1. There are numerous indications of frequent glacial oscillations within the Lower Vendian and Upper Riphean sequences (Chumakov 1992, 1998, 2004; Condon *et al.* 2002; Hambrey *et al.* 1981; Leather *et al.* 2002 etc.). Typical examples are the glacial sequences of Belarus (Chumakov 1992) and of the Middle and South Urals (Chumakov 1998). The Vil’chitsy Group of Belarus consists of two units; the lower Blon’ Formation and the unconformably overlying Glusck Formation (Fig. 3). The Blon’ Formation is composed of glacial sediments at the base and interglacial sandstones and sandy dolomites in its upper part. In the most complete sections, the Glusck Formation includes three till members separated by varved clays with dropstones, and by well sorted, likely fluvial and aeolian sands with thin clay intercalations, rare ripple marks, and desiccation cracks (Fig. 3b). The uppermost layers of interglacial members reveal glacial deformations. Each till member has an intricate structure and consists

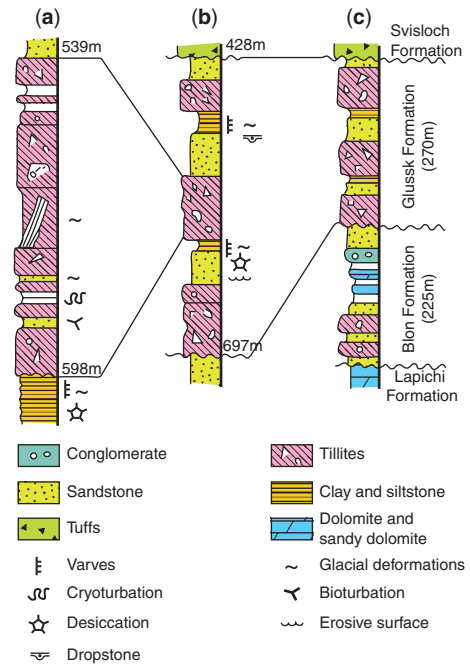


Fig. 3. Cyclic structure of the glacial Vil’chitsy Group in the Vil’chitsy drill hole, Lower Vendian sequence, Belarus: (a) middle member of the Glusck Formation; (b) Glusck Formation; (c) Vil’chitsy Group.

of several layers of differing composition and facies, usually separated from each other by thin-bedded clay with glacial deformations (Fig. 3a). This complicated structure of the Vil’chitsy Group is related to the number glacial oscillations of different scale. The Vil’chitsy Group is much thicker than all Pleistocene glacial sequences at platforms and is similar to Permian glacial sequences. It is difficult therefore to suggest that the Vil’chitsy Group was deposited during deglaciation of ice sheet only, as suggested by some authors. Another typical example of glacial oscillations occurs in the Lower Member of the Kurgashlya Formation. This member consists of an alternation of tillites, cap dolomites and laminated siltstones containing dropstones (Fig. 4). The ‘Snowball Earth’ requires the stable existence of each global ice cover for several million years. A marked increase in the heat balance of the planet’s surface would be required for the termination of each glaciation. Mechanisms for such dramatic, multiple and rapid warming are unknown and unlikely.

2. Numerical simulations of glacial events carried out for the Late Proterozoic (Jenkins & Frakes 1998; Poulsen *et al.* 2002; Poulsen 2003 and

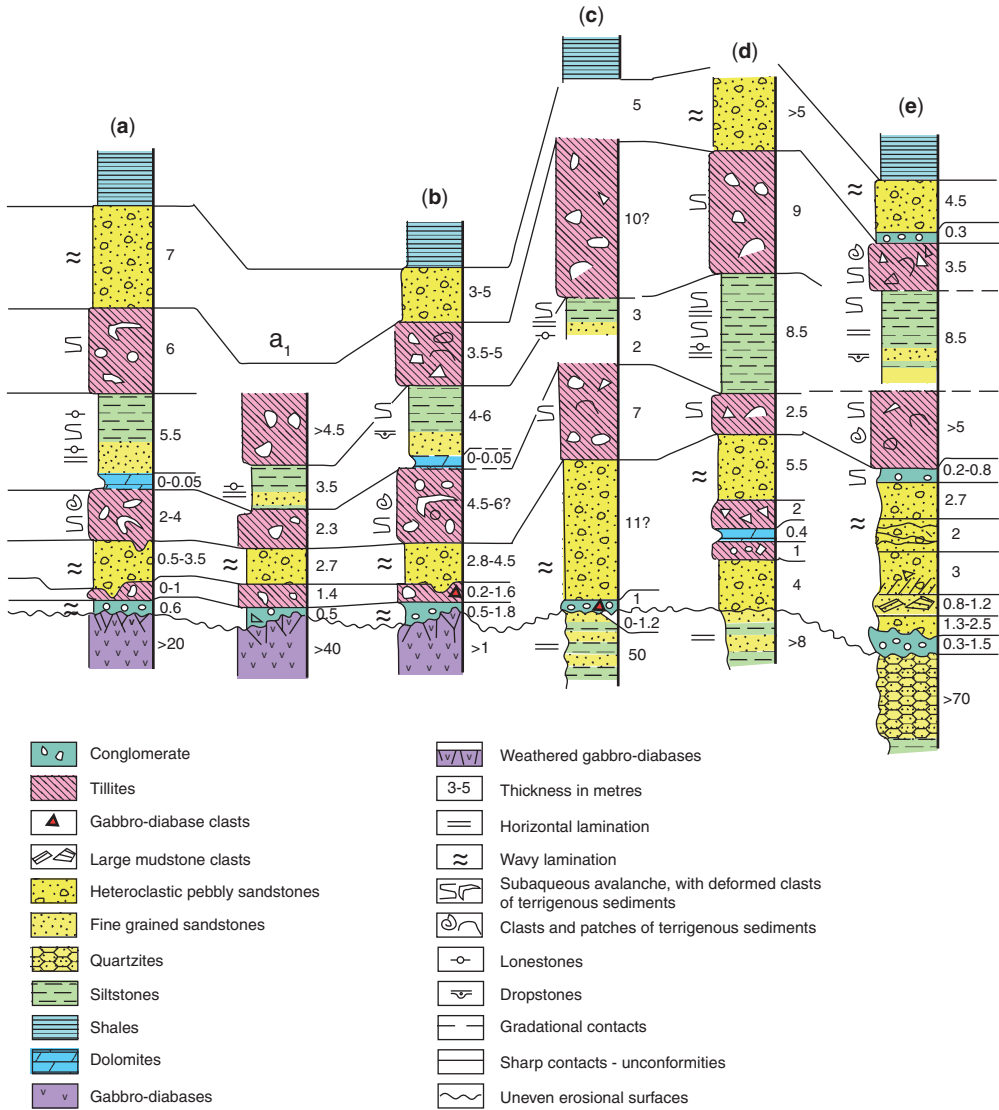


Fig. 4. Cyclic structure of the glacial Lower Member of Kurgashly Formation, Lower Vendian sequence, Belaya River, South Ural. Sections: (a) Krivaya Luka, ridge; (a₁) Krivaya Luka river cuts; (b) 2 km up-stream of Krivaya Luka; (c) 1.5 km NE of Muradymovo village; (d) left side of Belaya River 1.5 km down-stream of Aps Shak brook; (e) at mouth of Aps Shak brook.

- others) do not support long, uninterrupted total glaciations, such as that required by the ‘Snowball Earth’ hypothesis.
3. Fossils and biomarkers of phototrophism in glacial deposits provide clear evidence for the continuous existence of phytoplankton and, hence, photosynthesis in the late Precambrian (Fedonkin 2003, and references therein), suggesting that the world ocean was not

completely covered by thick ice as required by the ‘Snowball Earth’ hypothesis.

4. New data suggest the possibility of underestimating palaeomagnetic latitudes determined from sedimentary rocks, particularly red beds. Original palaeomagnetic directions on Palaeogene red beds of Central Asia were underestimated by 20°–30° due to secondary flattening of the natural remanent magnetism

- (NRM) vector (Bazhenov & Mikolaichuk 2002). The possibility of secondary flattening of the NRM in the much older Upper Precambrian sedimentary rocks (in Yrelina Subgroup of Australia, for example) is a real concern due to solution, loss and redistribution of material in the rocks and the reorientation of some clastic grains through long exposure to static load metamorphism (Kholodov 1994).
5. A necessary condition for a 'Snowball Earth' is the tropical position of most continents (Schrug *et al.* 2002). At the same time, according to most reconstructions of continental positions published in recent years, significant landmasses were located in high and middle latitudes during the Vendian (e.g. Scotese & McKerrow 1990; Dalziel 1997; Piper 2000; Scotese 2000; Powell *et al.* 2001—used by Hoffman & Schrag 2002; Dalziel & Soper 2001; Smith 2001; Kheraskova *et al.* 2003; Smith & Pickering 2003).
 6. The presence of cap carbonates atop glacial deposits and the occurrence of banded iron formations associated with these sequences is viewed in the 'Snowball Earth' hypothesis as a result of global events related to rapid deglaciation (Hoffman & Schrag 2002). However, even though cap carbonates occurred widely, they do not necessarily occur globally. Cap carbonates are shallow-water, post-glacial sediments demonstrating regional facies changes. The South Australian Nuccaleena Formation, a typical cap carbonate that occurs over a large area, consists of paralic and shallow-water, nearshore dolomites, which grade laterally into shales and sandstones that were deposited in a more open basin (Preiss 1987). Rapid replacement of cap carbonates by sandstones along strike is observable in the Kurgashly Formation of the South Urals (Fig. 4) and in some other regions. In the South (Fig. 4) and Middle Urals, Spitsbergen and in some glacial sequences elsewhere, thin carbonate beds are found within marine glacial deposits. The regional nature of Late Precambrian banded iron formations and manganese occurrences associated with glacial deposits is even more obvious (Chumakov 1992; Young 2002). Almost all occurrences of these ores are confined to volcanic areas, partly those of rift origin: Tien Shan (Dzholdoshev 1964), SW and South Africa (Martin 1965), northwestern Canada (Yeo 1981), Brazil (Ferran 1982), Middle Urals (Chumakov 1992). In some cases, iron-rich rocks and iron ores occur between marine glacial strata (the Tien Shan and Urals) or form the matrix of these strata: the Tien Shan and Canada (Dzholdoshev

1964; Eisbacher 1981; Yeo 1981). These data have led researchers studying Fe and Mn occurrences in glacial sequences to the conclusion that such metals precipitated locally from volcanic fluids in a zone containing a mixture of fresh glacial water and seawater.

Conclusion

Palaeoclimatic reconstructions indicate that, during Vendian time, there were at least two main intervals of glacial climate (V_I and V_{III}), with a non-glacial interval between (V_{II}). This alternation was responsible for the reorganization of climatic zonality, and it changed environments from warm to cold and back, which most certainly would have had significant effects on the biosphere. The Early Vendian 'Snowball Earth' hypothesis needs further critical consideration. At the moment, geological data favours a 'Slushball Earth' hypothesis for this period (Poulsen 2003; Poulsen *et al.* 2002).

The investigations were supported by Project No 05-05-64949 of the Russian Fund of Base Investigations and Programme 18 of Presidium RAS. I appreciate the suggestions by L. A. Frakes and the second anonymous reviewer. This paper was written as a part of UNESCO IGCP493.

References

- AKSENOV, E. M. 1990. The Vendian of the East European platform. In: SOKOLOV, B. S. & FEDONKIN, M. A. (eds) *The Vendian System. Vol. 2. Regional Geology. Processes*. Springer-Verlag, Berlin, 1–37.
- ALVARENGA, C. J. S. & TROMPETTE, R. 1992. Glacially influenced sedimentation in the Later Proterozoic of the Paraguay belt (Mato Grosso, Brazil). *Palaeogeography, Palaeoclimatology, Palaeoecology*, **92**, 85–105.
- BARFOD, G. H., ALBAREDE, F., KNOLL, A. H., XIAO, S. H., TELOUK, P., FREI, R. & BAKER, J. 2002. New Lu–Hf and Pb–Pb age constraints on the earliest animal fossils. *Earth and Planetary Science Letters*, **201**, 203–212.
- BAZHENOV, M. L. & MIKOLAICHUK, A. V. 2002. Paleomagnetism of Palaeogene basalts from the Tien Shan, Kyrgyzstan: rigid Eurasia and dipole geomagnetic field. *Earth and Planetary Science Letters*, **195**, 155–166.
- BEKKER, Yu. R. 1992. The Oldest Ediacaran biota of the Urals (in Russian). *Izvestiya Akademiyies Nauk SSSR, Series Geological*, **6**, 16–24.
- BERTRAND-SARFATI, J., MOUSSINE-POUCHKINE, A., AMARD, B. & AHMED, A. K. 1995. 1st Ediacaran fauna found in Western Africa and evidence for an Early Cambrian glaciation. *Geology*, **23**, 133–136.
- BRASIER, M. D., MCCARRON, G. & TUCKER, R. 2000. New U–Pb zircon dates for the Neoproterozoic Ghubrah glaciation and for the top of the Huqf Supergroup, Oman. *Geology*, **28**, 175–178.

- CHUMAKOV, N. M. 1978. *Dokembriiskie tillity i tilloidy* (Precambrian tillites and tilloids). Moscow, Nauka. [In Russian].
- CHUMAKOV, N. M. 1990. Laplandian glacial horizon and its equivalents. In: SOKOLOV, B. S. & FEDONKIN, M. A. (eds) *The Vendian System. Vol. 2. Regional Geology. Processes*. Springer-Verlag, Berlin, 191–225.
- CHUMAKOV, N. M. 1992. *The problems of old glaciations (pre-Pleistocene glaciogeology in the USSR)*. Harwood Academic Publishers, Pennsylvania.
- CHUMAKOV, N. M. 1993. Riphean Middle Siberian glacial horizon. *Stratigraphy and Geological Correlation*, **1**, No 1, 17–28.
- CHUMAKOV, N. M. 1998. The key section of Vendian glacial deposits in the South Urals (Kurgashly Formation, Krivolukhsy graben). In: KNIPPER, A. L., KURENKOV, C. A. & SEMIKHATOV, M. A. (eds) *Ural: fundamental'nye problemy geodinamiki i stratigrafii* (*The Urals: Fundamental Problems of Geodynamics and Stratigraphy*). Nauka, Moscow, 138–153.
- CHUMAKOV, N. M. 2004. Trends in global climatic changes inferred from geological date. *Stratigraphy and Geological Correlations*, **12**, 117–138.
- CONDON, D. J., PRAVE, A. R. & BENN, D. I. 2002. Neoproterozoic glacial-rainout intervals: observations and implications. *Geology*, **30**, 35–38.
- CONDON, D. J., ZHU, M., BOWRING, S., WONG, W., YANG, A. & JIN, Y. 2005. U–Pb ages from the Neoproterozoic Doushantuo formation, China. *Science*, **308**, 95–98.
- DALZIEL, I. W. D. 1997. Neoproterozoic–Paleozoic geography and tectonics: Review, hypothesis, environmental speculation. *Geological Society of America Bulletin*, **109**, 16–42.
- DALZIEL, I. W. D. & SOPER, N. J. 2001. Neoproterozoic extension on the Scottish Promontory of Laurentia: Paleogeographic and tectonic implications. *Journal of Geology*, **109**, 299–317.
- DALZIEL, I. W. D., SALDA, L. H. D. & GAHAGAN, L. M. 1994. Paleozoic Laurentia–Gondwana interaction and the origin of the Appalachian–Andian mountain system. *Geological Society of America Bulletin*, **106**, 243–252.
- DZHOLDOSHEV, B. 1964. Stratigraphy of the Dzhetyntoo Formation within the Dzhetyntskoe Iron Deposit, Tien Shan (In Russian). In: ANONYM (ed.) *Voprosy stratigrafii dokembriya i nizhnego paleozoya Kirgizii* (*Issues of Precambrian and Lower Paleozoic stratigraphy of Kirghizia*). Frunze, Izdatel'stvo Acad. Nauk Kirgizskoy SSR, 23–33.
- EISBACHER, G. H. 1981. Late Precambrian tillites of the northern Yukon–Northwest Territories region, Canada. In: HAMBREY, M. J., HARLAND, W. B. & CHUMAKOV, N. M. (eds) *Earth's Pre-Pleistocene Glacial Record*. Cambridge University Press, Cambridge, 724–727.
- EVANS, D. A. D. 2000. Stratigraphic, geochronological, and palaeomagnetic constraints upon the Neoproterozoic climatic paradox. *American Journal of Science*, **300**, 347–433.
- FEDONKIN, M. 2003. The origin of the Metazoa in the light of the Proterozoic fossil record. *Paleontological Research*, **7**, No 1, 9–41.
- FERRAN, AXEL DE 1982. Vue d'ensemble sur les minéralisations sédimentaires du Tardi-Proterozoïque brésilien. *Chronique de la Recherche Minière*, **466**, 5–39.
- GERMS, G. J. B. 1995. The Neoproterozoic of southwestern Africa, with emphasis on platform stratigraphy and paleontology. *Precambrian Research*, **73**, 137–151.
- GOROKHOV, I. M., SIEDLECKA, A., ROBERTS, D. ET AL. 2001. Rb–Sr dating of diagenetic illite in Neoproterozoic shales, Varangian Peninsula, North Norway. *Geological Magazine*, **138**, 541–562.
- GUAN, B., RUITANG, W. U., HAMBREY, M. J. & WUCHEN, G. 1986. Glacial sediments and erosional pavements near the Cambrian–Precambrian boundary in western Henan Province, China. *Journal of Geological Society, London*, **143**, 311–323.
- HAMBREY, M. J., HARLAND, W. B., CHUMAKOV, N. M. ET AL. (eds) 1981. *Earth's Pre-Pleistocene Glacial Record*. Cambridge University Press, Cambridge.
- HARLAND, W. B. 1964. Critical evidence for a great infra-Cambrian glaciation. *Geologische Rundschau*, **54**, 45–91.
- HARLAND, W. B., HAMBREY, M. J. & WADDAMS, P. 1993. Vendian geology of Svalbard. *Norsk Polar Institut Skrifter*, **193**.
- HOFFMAN, P. F. & SCHRAG, D. P. 2002. The Snowball Earth hypothesis: testing the limits of global change. *Terra Nova*, **14**, 129–155.
- JENKINS, G. S. & FRAKES, L. A. 1998. GCM sensitivity test using increased rotation rate, reduced solar forcing and orography to examine low latitude glaciation in the Neoproterozoic. *Geophysical Research Letters*, **25**, 3525–3528.
- KHAIN, V. E. & YASAMANOV, N. A. 1987. The paradox of Late Proterozoic glaciations and continental drift (in Russian). *Vestnik Moskovskogo Universiteta, Seriya 4 Geologiya*, **1**, 15–25.
- KHERASKOVA, T. N., DIDENKO, A. N., BUSH, V. A., VOLOZH & YU, A. 2003. The Vendian–Early Paleozoic history of continental margin of Eastern Paleogondwana, Paleasian Ocean, and Central Asian Foldbelt. *Russian Journal of Earth Sciences*, **5**, No 3, 165–184.
- KHOLODOV, V. N. 1994. The L. I. Salop–G. Gilluli curve: A reality or an artifact? *Lithology and Mineral Resources*, **2**, 49–65.
- KHOMENTOVSKY, V. 1990. The Vendian of the Siberian platform. In: SOKOLOV, B. S. & FEDONKIN, M. A. (eds) *The Vendian System. Vol. 2. Regional Geology. Processes*. Springer-Verlag, Berlin, 102–183.
- KIRSCHVINK, J. A. 1992a. Paleogeographic Model for Vendian and Cambrian Time. In: SCHOPF, J. W. & KLEIN, C. (eds) *The Proterozoic Biosphere*. Cambridge University Press, New York, 567–582.
- KIRSCHVINK, J. A. 1992b. Late Proterozoic Low-Latitude Global Glaciation: the Snowball Earth. In: SCHOPF, J. W. & KLEIN, C. (eds) *The Proterozoic Biosphere*. Cambridge University Press, New York, 51–52.
- KISELEV, V. V. & KOROLEV, V. G. 1981. *Paleotektonika dokembriya i nizhnego paleozoya Tyan'-Shanya* (*Precambrian and Lower Paleozoic Paleotectonics of the Tien Shan*). Frunze, Ilim.
- KNOLL, A. H. 2000. Learning to tell Neoproterozoic time. *Precambrian Research*, **100**, 3–20.

- KNOLL, A.H., WALTER, M. R., NARBONNE, G. M. & CHRISTIE-BLICK, N. 2004. A new period for the Geologic Time Scale. *Science*, **305**, 621–622.
- KUMAR, G., SHANKER, R., MATHUR, V. K., & MAITHY, P. K. 2000. Maldeota Section, Mussoorie Syncline, Krol Belt, Lesser Himalaya, India: A Candidate for Global Stratotype Section and Point for Terminal Proterozoic System. In: ANONYM (ed.) *Terminal Proterozoic System*. Subcommittee on terminal Proterozoic System, 9–19.
- LEATHER, J., ALLEN, P. A., BRASIER, M. D. & COZZI, A. 2002. Neoproterozoic snowball earth under scrutiny: Evidence from the Fig glaciation of Oman. *Journal of Geology*, **30**, 891–894.
- MARTIN, H. 1965. *The Precambrian Geology of South West Africa and Namaqualand*. Cape Town University Press, Cape Town.
- MARTIN, M. W., GRAZHDANKIN, D. V., BOWRING, S. A. ET AL. 2000. Age of Neoproterozoic bilaterian body and trace fossils, White Sea, Russia: implication for Metazoan evolution. *Science*, **288**, 841–845.
- MOSSAKOVSKY, A. A., PUSHCHAROVSKY, Y. M. & RUZHENTSEV, S. V. 1996. Spatiotemporal relationships of structures of the Pacific and Indo-Atlantic types in the Late Precambrian and Vendian (in Russian). *Doklady Akademiy Nauk*, **350**, 799–802.
- MYROW, P. M. 1995. Neoproterozoic rocks of the Newfoundland Avalon Zone. *Precambrian Research*, **73**, 123–136.
- MYROW, P. M. & KAUFMAN, A. J. 1999. A newly discovered cap carbonate above Varangian-age glacial deposits in Newfoundland, Canada. *Journal of Sedimentary Research*, **69**, 784–793.
- NARBONNE, G. M. & AITKEN, J. D. 1995. Neoproterozoic of the Mackenzie Mountains, northwestern Canada. *Precambrian Research*, **73**, 101–121.
- NARBONNE, G. M. & GEHLING, J. G. 2003. Life after snowball: the oldest complex Ediacaran fossils. *Geology*, **31**, 27–30.
- PIPER, J. D. A. 2000. The Neoproterozoic Supercontinent: Rodinia or Paleopangaea? *Earth and Planetary Science Letters*, **176**, 131–146.
- POKROVSKII, B. G., MELEZHNIK, V. A. & BUYAKAITE, M. I. 2006. C, O, Sr, S isotopic compositions in late Precambrian rocks of the Patom Complex, central Siberia: Communication 1. Results, isotope stratigraphy, and dating problems. *Lithology and Mineral Resources*, **41**, 450–474.
- POULSEN, C. J. 2003. Absence of a runaway ice-albedo feedback in the Neoproterozoic. *Geology*, **31**, 473–476.
- POULSEN, C. J., PIERREHUMBERT, R. T. & JACOB, R. L. 2002. Impact of oceanic dynamics on the simulation of the Neoproterozoic “snowball Earth”. *Geophysics Research Letters*, **28**, 1575–1578.
- POWELL, C. McA., PISAREVSKY, S. A. & WINGATE, M. T. D. 2001. An animated history of Rodinia. *Geological Society Australia Abstracts*, **65**, 85–87.
- PREISS, W. V. (Compiler) 1987. The Adelaide Geosyncline—Late Proterozoic stratigraphy, sedimentation, palaeontology and tectonics. *Bulletin Geological Survey of South Australia*, **53**.
- PREISS, W. V. 2000. The Adelaide Geosyncline of South Australia and its significance in Neoproterozoic continental reconstruction. *Precambrian Research*, **100**, 21–63.
- SCHRAG, D. P., BERNER, R. A., HOFFMAN, P. F. & HALVERSON, G. P. 2002. On the initiation of a snowball Earth. *Geochemistry, Geophysics, Geosystems*, **3**, 1–21.
- SCOTSE, C. R. 2000. Paleomap project 2000. <<http://www.scotese.com>>
- SCOTSE, C. R. & MCKERROW, W. S. 1990. Revised world maps and introduction. *Paleozoic Palaeogeography and Biogeography*, Geological Society, London, *Memoir*, **12**, 1–21.
- SEMIKHATOV, M. A. 2000. Refining radiometric ages for the lower boundaries of the Upper Riphean, Vendian, Upper Vendian, and Cambrian. In: ANONYM (ed.) *Dopolneniya k stratigraficheskomu kodeksu Rossii (Supplements to the Stratigraphic Code of Russia)*, Supplement 4. St. Petersburg, ВСЕГЕИ (All-Russian Geological Institute), 95–107.
- SEMIKHATOV, M. A. & CHUMAKOV, N. M. (eds) 2004. *Klimat v epokhi krupnykh biosfernykh perestroek (Climate in Epochs of Major Biospheric Reorganization)*. Nauka, Moscow.
- SMITH, A. G. 2001. Palaeomagnetically and tectonically based global maps for Vendian to Mid-Ordovician time. In: ZURAVLEV, A. Yu & RIDING, R. (eds) *The Ecology of the Cambrian Radiation*. Columbia University Press, New York, 11–46.
- SMITH, A. G. & PICKERING, K. T. 2003. Oceanic gateways as a critical factor to initiate icehouse Earth. *Journal of Geological Society, London*, **160**, 337–340.
- SOKOLOV, B. S. 1998. *Ocherki stanovleniya venda (Essays on the Advent of the Vendian System)*. Moscow, KMK Ltd.
- STRAUSS, H., BANERJEE, D. M. & KUMAR, V. 2001. The sulfur isotopic composition of Neoproterozoic to early Cambrian seawater—evidence from the cyclic Hanseran evaporites, NW India. *Chemical Geology*, **175**, 17–28.
- TIWARI, M. 1999. Organic-walled microfossils from the Chert-Phosphorite Member, Tal Formation, Precambrian–Cambrian Boundary, India. *Precambrian Research*, **97**, 99–113.
- TEWARI, M. & KNOLL, A. 1994. Large acanthomorphic acritarchs from the Infrakrol Formation of the Lesser Himalaya and their stratigraphic significance. *Journal of Himalayan Geology*, **5**, 193–201.
- TROMPETTE, R. 1996. Temporal relationship between cratonization and glaciation: The Vendian-early Cambrian glaciation in Western Gondwana. *Palaeogeography, Palaeoclimatology, Palaeoecology*, **123**, 373–383.
- TROMPETTE, R. 1997. Neoproterozoic (~600 Ma) aggregation of Western Gondwana: a tentative scenario. *Precambrian Research*, **82**, 101–112.
- VIDAL, G. 1981. Micropaleontology and biostratigraphy of the Upper Proterozoic and Lower Cambrian sequences in East Finnmark, northern Norway. *Norges Geologiske Undersokelse Bulletin*, **53**, 362.
- VIDAL, G. & MOCZYDŁOWSKA, M. 1995. The Neoproterozoic of Baltica—stratigraphy, paleobiology and general geological evolution. *Precambrian Research*, **73**, 197–216.
- WALTER, M. R., VEEVERS, J. J., CALVER, C. R. & GREY, K. 1995. Neoproterozoic stratigraphy of the

- Centralian Superbasin, Australia. *Precambrian Research*, **73**, 173–195.
- WALTER, M. R., VEEVERS, J. J., CALVER, C. R., GORJAN, P. & HILL, A. C. 2000. Dating the 840–544 Ma Neoproterozoic interval by isotopes of strontium, carbon, and sulfur in seawater, and some interpretative models. *Precambrian Research*, **100**, 371–433.
- WANG, X., ERDTMANN, B., XIAOHONG, C. & XIAODONG, M. 1998. Integrated sequence-, bio- and chemo- stratigraphy of the terminal Proterozoic to Lowermost Cambrian “black rock series” from central South China. *Episodes*, **21**, 3, 178–189.
- YEO, G. M. 1981. The Late Proterozoic Rapitan Glaciation in the Northern Cordillera. *Geological Survey of Canada, Paper* **81–10**, 25–46.
- YIN, L. M. & GUAN, B. D. 1999. Organic-walled microfossils of Neoproterozoic Dongjia, Lushan Country, Henan Province, North China. *Precambrian Research*, **94**, 121–137.
- YOUNG, G. M. 1995. Are Neoproterozoic glacial deposits preserved on the margins of Laurentia related to the fragmentation of two supercontinents? *Geology*, **23**, 153–156.
- YOUNG, G. M. 2002. Stratigraphic and tectonic settings of Proterozoic glaciogenic rocks and banded iron-formations: relevance to the snowball Earth debate. *Journal of African Earth Sciences*, **35**, 451–466.
- ZHANG, Y., YIN, L., XIAO, S. & KNOLL, A. H. 1998. Permineralised fossils from the terminal Proterozoic Doushantou Formation South China. *Paleontological Society Memoirs*, **72**, 52.
- ZHARKOV, M. A. 1981. *History of Paleozoic Salt accumulation*. Springer-Verlag, Berlin.
- ZHOU, CH., TUCKER, R., XIAO, SH., PENG, ZH., YUAN, X. & CHEN, ZH. 2004. New constraints on the age of Neoproterozoic glaciations in South China. *Geology*, **32**, 437–440.

Non-destructive method to detect the cycle of lamination in sedimentary rocks: rhythmite sequence in Neoproterozoic Cap carbonates

N. KATSUTA¹, B. TOJO², M. TAKANO¹, H. YOSHIOKA³, S. KAWAKAMI²,
T. OHNO⁴ & M. KUMAZAWA¹

¹*Graduate School of Environmental Studies, Nagoya University, Furo-cho, Chikusa-ku, Nagoya 464–8601, Japan (e-mail: katsuta@eps.nagoya-u.ac.jp)*

²*Faculty of Education, Gifu University, 1–1 Yanagido, Gifu 501–1193, Japan*

³*Institute for Geo-Resources and Environment, National Institute of Advanced Industrial Science and Technology, Central 7, 1–1–1 Higashi, Tsukuba, 305–8567, Japan*

⁴*The Kyoto University Museum, Kyoto University, Yoshida Honmachi, Sakyo-ku, Kyoto 606–8501, Japan*

Abstract: Environmental changes were flagged by lamination within Precambrian sedimentary rocks sequences using a high-resolution method. A continuous sample was collected and embedded in epoxy resin to form sample plates in order to investigate 2D laminations on sample surfaces. Elemental distributions in laminated samples were determined and recorded as XRF profiles, using the scanning X-ray analytical microscope (SXAM) and an image processing lamination tracer.

These methods were used to study a rhythmite sequence at the base of a Neoproterozoic cap carbonates, which immediately overlies glacial deposits in Namibia, to determine profiles of Si, Ca, Mn, Ti, Fe, and Sr. At the base and top of each interval, the concentrations of six elements were relatively constant. In the middle of the interval, Ca–Sr and Mn, which reflect presence of calcite and dolomite respectively, fluctuated. This reflects seventeen cycles. The cyclic fluctuations of Ca–Sr and Mn were interpreted as calcite–dolomite cycles. Strontium also recorded two cycles. Furthermore, the fluctuations of Ca–Sr and Mn in calcite–dolomite cycles were laterally traceable. Possibly, these calcite–dolomite cycles were deposited synchronously and regionally. New methods allow the extraction of data that record cyclic- and event-phenomena from long sequences of laminated sedimentary rocks; this is not isolated to the Neoproterozoic but also throughout Earth's history.

Neoproterozoic glaciogenic deposits are distributed globally, and according to relatively recent palaeomagnetic data, some appear to have been deposited in low latitudes (Kirschvink 1992; Hoffman & Schrag 2002). Low-latitude ice sheets indicate global glaciation and perhaps, a 'Snowball Earth' (Kirschvink 1992; Hoffman *et al.* 1998). The unified scenario of the 'Snowball Earth' hypothesis can attempt to explain low-latitude glacial deposits, banded iron formation and negative carbon isotope excursions (Kirschvink 1992; Hoffman *et al.* 1998; Hoffman & Schrag 2002).

The carbonate (cap carbonate), which typically precipitates in low latitudes and in warm water, was deposited atop Neoproterozoic glacial deposits. The 'Snowball Earth' hypothesis explains these postglacial cap carbonates as documentation of the recovery phase from an ice-covered episode to that of an interglacial period, which experienced

extreme greenhouse conditions (Hoffman *et al.* 1998). Thus, the cap carbonates are regarded as geological evidence for decoding the behaviour of the Earth system in extreme cold and warm conditions.

The Neoproterozoic global glacial periods are recognized to have occurred at least two times (e.g. Kennedy *et al.* 1998) or perhaps several times (e.g. Kaufman *et al.* 1997). The Rasthof cap carbonate in Namibia, which overlies the oldest, perhaps Sturtian glaciogenic deposits, is well laminated (Hoffman 2002). However, in the past there have been no suitable methodologies for high-resolution analyses of these laminations in long and broadly distributed sedimentary samples. Here, we report a newly developed methodology used to detect the cycles in laminated sedimentary rocks and its application to analysis of the rhythmite sequence in the basal unit of the Rasthof cap carbonates.

Methodology for the analysis of laminated sedimentary rocks

Sample

The Rasthof cap carbonate sequence overlies glacio-genic deposits in the Chuos Formation, within the Otavi Group which crops out in NW Namibia (Hoffmann & Prave 1996). The Otavi Group contains two discrete glacial units—the Chuos Formation, interpreted as Sturtian in age (~760–700 Ma), and the Ghaub Formation, interpreted as Varangian (~620–550 Ma) (Hoffmann & Prave 1996). The Chuos Formation lies unconformably on felsic ash flows, with a U–Pb zircon age of 746 ± 2 Ma (Hoffman *et al.* 1996). Palaeomagnetic data from the eastern part of the Congo Craton (Meert *et al.* 1995; Meert & Van der Voo 1996) indicate that the Otavi Group lay at *c.* 12°S palaeolatitude at 743 ± 30 Ma and *c.* 39°S palaeolatitude at 547 ± 4 Ma. Thus, the Rasthof cap carbonate is thought to have been deposited in a low-latitude palaeocean.

The section under analysis consists of dark grey rhythmite in the basal unit of the Rasthof Formation, characterized by abiotic, mm-scale laminations (Hoffman 2002). Stratigraphy and geochemical studies indicate that the rhythmite section consists of three separate intervals (Yoshioka *et al.* 2003). The second interval (interval II) of this sequence can be further divided into seventeen sub-units that have been interpreted as calcite–dolomite cycles (Tojo *et al.* 2007).

Sampling methods and sample preparation

A continuous sample, named K₁, was collected, which included a complete 14.2 m rhythmite unit on the *Khowarib Schlucht* tributary of the Hoanib River (Yoshioka *et al.* 2003; Tojo *et al.* 2006). Additionally, in order to examine the regional distribution of the calcite–dolomite cycles, we collected several metre long continuous samples, K₂, at about 0.25 km SSW from K₁; K₃, about 1.25 km SSW; K₄, about 0.5 km NNE; and W₁, about 10 km NNE (Tojo *et al.* 2006).

In order to study the cap carbonate in detail, we developed a method to cut out a continuous rock samples without loss from the outcrop, which dips *c.* 90°, using a cutter (TS400, STIHL Ltd) with a diamond cutting wheel (Fig. 1; Kumazawa *et al.* 2002; Yoshioka *et al.* 2003). We positioned the cutter on a mobile stage that could slide along normal to the bedding plane. We cut two 5 cm deep and one 7 cm deep grooves, which were 3 cm apart, and carefully collected two sets of continuous samples for both non-destructive and destructive analyses using wide flat chisels and hammers.

In the laboratory, the samples were shaped into plates about 40 cm × 20 cm, with a thickness of

3 cm for 2D investigation on the sample surface. We reproduced the bed order by sequentially placing the rock specimens into a plastic box. Epoxy resin containing cherty pebbles was poured into the plastic box and cured. The sample surface was polished with abrasive of #600 to #800 size. By using this procedure, we obtained a number of plastic sample plates, in which the unweathered sub-surface of the carbonate rhythmite could be studied (Fig. 2c). Cherty pebbles should be used for the carbonate sample and marble pebbles for the banded iron formation and banded chert samples. The pebble serves to absorb the heat generated by mixing the resin and the hardening agent and also to save on the amount of epoxy resin needed.

XRF images obtained with the scanning X-ray analytical microscope

The scanning X-ray analytical microscope (SXAM; XGT-2000V, Horiba, Japan) is a type of XRF analyser (Fig. 2a), and it can determine elemental distribution images on a sample surface (Hosokawa *et al.* 1997; Michibayashi *et al.* 1999; Togami *et al.* 2000). The high-intensity continuous X-ray (Rh anode, 50 kV, 1 mA), when focused into a beam 100 μm in diameter with an X-ray guide tube (XGT), can scan a sample surface on a PC controllable X–Y stage. XRF from the sample surface can be detected with an hp-Si detector of an energy-dispersion spectrometer and the transmitted X-rays are measured with the NaI scintillation detector. The XRF images of thirty-one elements and a transmitted X-ray image are simultaneously analysed.

An advantage of SXAM is that the sample can be analysed in ambient atmosphere (Fig. 2a). The SXAM is an extremely effective tool for examining elemental distribution of a large number of samples. However, it has some difficulty analysing for elements lighter than magnesium, because of the absorptions of soft XRF by both the air between the sample, chamber and the thin resin film of the X-ray window.

The sample plate area of 400 × 200 mm² was analysed on an image of 512 × 256 pixels, resulting in a spatial resolution of 0.8 × 0.8 mm². The time duration for analysing an area of 400 × 200 mm² (Fig. 2b) was about 1 day. The XRF images (Fig. 2c) for six elements (Si, Ca, Mn, Ti, Fe, and Sr) were produced for a 14.2 m long rhythmite sequence in the basal unit of the Rasthof cap carbonate (Fig. 2c).

Conversion of XRF images to elemental profiles

The XRF images of the six elements for each sample plate were converted into a set of 1D profiles using an

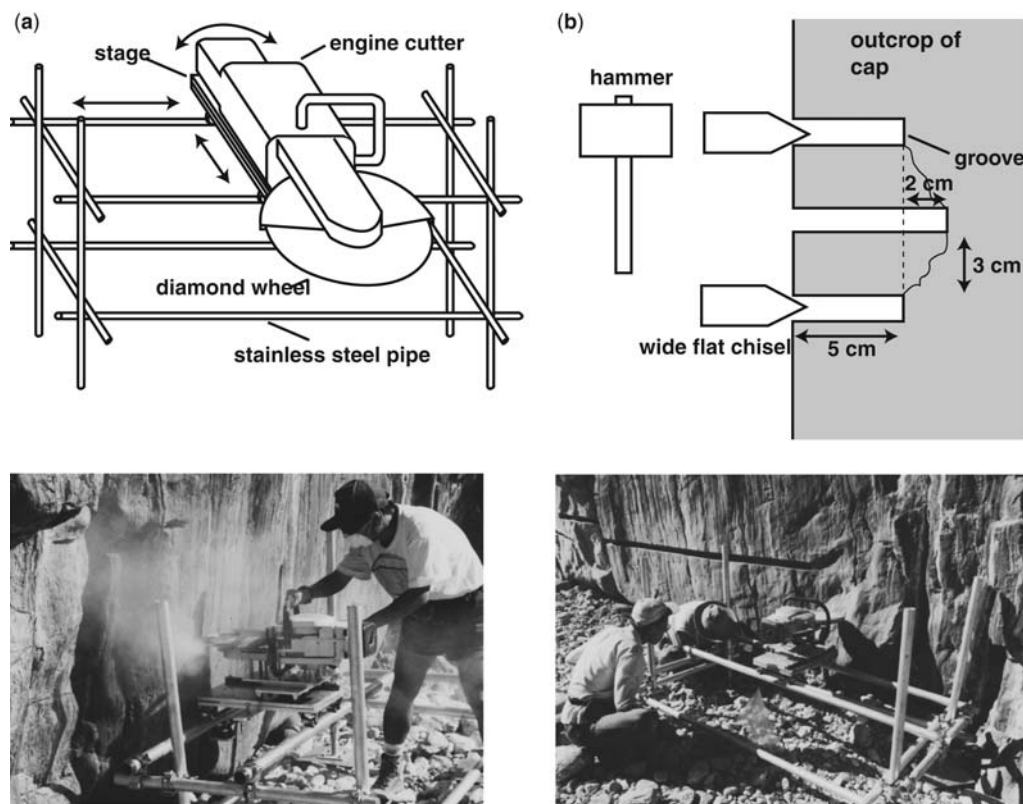


Fig. 1. (a) Schematic sketch of the engine cutter with a diamond-cutting wheel mounted on a mobile stage. The stage can be slid crosswise on stainless steel pipes. The engine cutter is rotatable on the stage; (b) Schematic cross-sectional sketch of the grooves in the outcrop of the Rasthof cap carbonate. The grooves were cut in the normal direction of the cap carbonate, which dips *c.* 90°; (c) Photograph of continuous sampling of the Rasthof cap carbonate; (d) Photograph after collecting continuous samples. This figure has been modified from Kumazawa *et al.* (2002).

image processing lamination tracer (Katsuta *et al.* 2003). The lamination tracer is an image processing technique employed to extract 1D sequential profiles from a variety of 2D measurements on the cross sections of deformed, laminated sedimentary rocks containing many defects. We developed an algorithm for the lamination tracer and constructed a computer code. The algorithm for the lamination tracer is as follows:

The bedding planes (laminae) viewed in the cross section of sedimentary rocks represent isochronous lines. To detect these lines automatically, we introduced an 'isochron function'. This is a 2D function and its value defines the relative time for any point on a 2D measured image. Any points on the same contour line of the isochron functions are, therefore, isochronous.

If the lamination is not deformed, the isochron function forms a monotonously increasing plane, where the strike is parallel to the lamination of the material. In this case, the contour lines of the function are parallel to each other as well as to

the lamination. If the lamination is deformed, the isochron function can be modified from an evenly increasing one to a curved plane one. In order to determine the isochronous functions for the deformed lamina, it is necessary to investigate the direction of the maximum slope of the lamination as well as maximum rate of change in curvature. This is calculated by using the first and second partial derivative coefficients. Through this procedure, the tilting direction of an isochron at every data point can be calculated. A function normal to this direction can be calculated; the sequential integration of this, plus the isochron function for the non-deformed lamina, will yield the isochron function for the case of deformed lamination. Moreover, the 'noise' components of the slope map are eliminated by the weighted Fourier transform filter. Once the isochron function is determined for a measured image by the lamination tracer, the average operation along the isochronous lines will yield a 1D sequential profile with a high spatial resolution and accuracy.

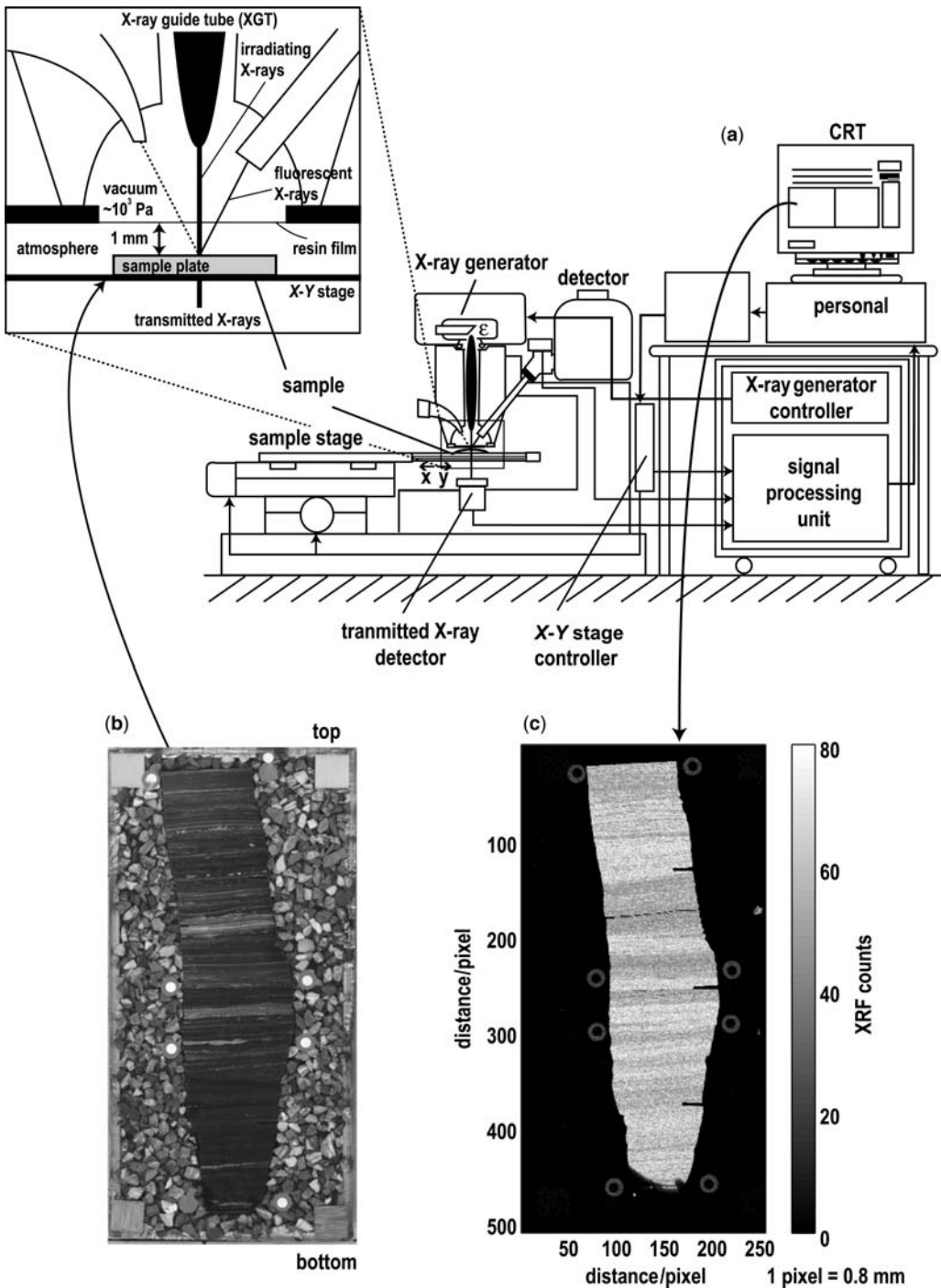


Fig. 2. (a) Schematic sketches of scanning X-ray analytical microscope; (b) Photograph of the sample plate with a size of 40 cm × 20 cm. The black sample and its surrounds are cap carbonate and epoxy resin containing cherty pebble, respectively; (c) XRF image of Ca abundance on the surface of (b) acquired by (a). The image size is 512 × 256 pixels wide with a spatial resolution of 0.8 mm/pixel.

This algorithm is discussed in detail by Katsuta *et al.* (2003). The computational program that has been coded in MATLAB version 5.3 is available at <http://www.iamg.org/>

1D—elemental profiles acquired by lamination tracer

Figure 3a demonstrates how the lamination tracer was used to obtain an Fe image of the rhythmite in the Rasthof cap carbonate. The Fe image was acquired by SXAM with a spatial resolution of 0.1 mm/pixel for an area of $5.12 \times 4.32 \text{ cm}^2$ in the test case. In the figure, the thin lines are the isochronous lines calculated by the lamination tracer. It should be noted that these isochronous lines faithfully trace the actual lamination of the cap carbonate. Figure 3b is a 1D profile obtained by averaging the data measured in the horizontal direction. This profile shows a small standard deviation

(indicated by the grey curve). However, because the laminae are not parallel to the horizontal line, the average value contains information of non-isochronous nature; and therefore, the peaks are obscured. Figure 3c is a 1D profile obtained along the measured line marked by the narrow rectangle. Although the profile contains many peaks, it is accompanied with a large standard deviation and thus has low reliability. Figure 3d is the 1D profile obtained by averaging the 2D data along the isochrons determined by the lamination tracer. This curve has both clear peaks and a very small standard deviation, which indicates that the treatment of the data with the lamination tracer yields highly significant and reliable data.

Using the same method, we carried out a six-element distribution analysis with a spatial resolution of 0.8 mm for the 14.2 m long rhythmite sequence sample taken from the Rasthof cap carbonates in Namibia (Fig. 4).

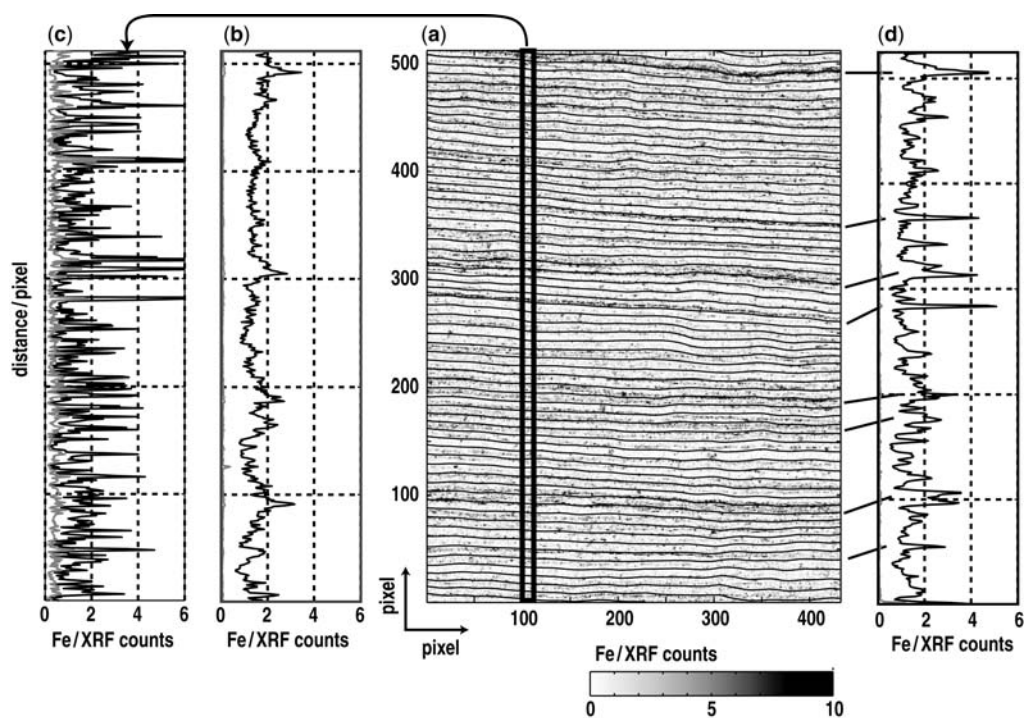


Fig. 3. An example of the conversion of a 2D image to 1D profiles of Fe abundance in a cap carbonate from the Rasthof Formation in Namibia. (a) Fe image acquired by SXAM. This image is 512×432 pixels with a spatial resolution of 0.1 mm/pixel. The black lines plotted on the image are the isochronous lines calculated by the lamination tracer. Note that the isochronous lines trace the original lamination of the cap carbonate very well; (b) Fe profile (black line) obtained by averaging (a) simply in the horizontal direction and its standard deviation (grey line); (c) Fe profile (black line) obtained by the measurement along the line marked by the narrow rectangle in (a) and its standard deviation (grey line); (d) Fe profile (black line) averaged along the isochronous lines and its standard deviation (grey line).

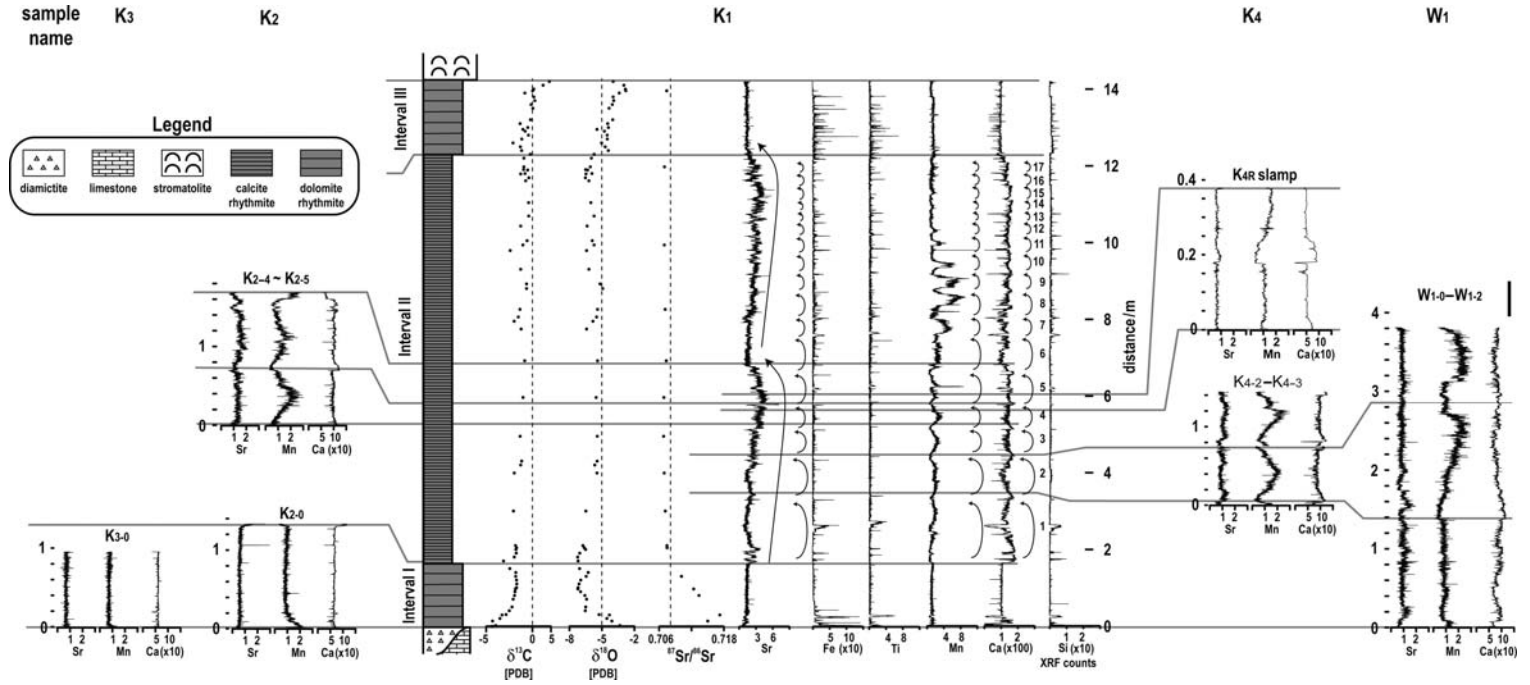


Fig. 4. Profiles of six major elements (Si, Ca, Ti, Mn, Fe, and Sr) and three stable isotopes (C, O, and Sr) obtained from Yoshioka *et al.* (2007) in the rhythmite sequence that lies in the basal unit of the Rasthof cap carbonate in Namibia. K_1 – K_4 and W_1 correspond to the sample names of Tojo *et al.* (2007). The numbers in the Ca profile of K_1 indicate the number of calcite–dolomite cycles and correspond to the subscript number of each sample— K_{2-4} and W_1 .

Application to the Rasthof rhythmite sequence

We obtained about 14.2 m long elemental profiles of Si, Ca, Ti, Mn, Fe, and Sr with a spatial resolution of 0.8 mm from the locality K₁ (Fig. 4). Moreover, we obtained the elemental profiles of Ca, Mn, and Sr in the correlative section of interval I, and each calcite–dolomite cycle in the four investigated sections (Fig. 4).

In intervals I and III, these six elements demonstrated no clear fluctuation patterns, although the C, O and Sr isotopic ratios varied rapidly (Yoshioka *et al.* 2003). The peaks characterized by Si, Ti and Fe corresponded to presence of clay minerals, which were identified by the X-ray diffraction patterns in the remaining carbonate samples where acid preparation (Tojo *et al.* 2007). Intervals I and III consist mostly of dolomite (average: 98%, Yoshioka *et al.* 2003). Thus, the concentration of Ca and Mn reflects the dolomite ($\text{Ca}_{0.5}\text{Mg}_{0.5}\text{CO}_3$) content and the manganese substitution for cations in dolomite. In interval I, the C isotopic ratio increased rapidly, whereas both the O and Sr isotopic ratios decreased just as rapidly (Yoshioka *et al.* 2003). In interval III, the C and O isotopic ratios increased. The Sr ratios also increased and approached higher values in the stromatolitic unit (Yoshioka *et al.* 2003).

In the intermediate interval II, where the C, O and Sr isotopic ratios were relatively constant (Yoshioka *et al.* 2003), the intensity of Ca–Sr and Mn showed a negative correlation and seventeen periodical variations with a scale of tens of centimetres to several metres (Fig. 4). Interval II consists mainly of calcite (average: 74%, Yoshioka *et al.* 2003). In one cycle of the periodical variations of the Ca and Mn intensities, tagged the calcite–dolomite cycle, the ratio of calcite (CaCO_3) to dolomite ($\text{Ca}_{0.5}\text{Mg}_{0.5}\text{CO}_3$) gradually decreased, then gradually increased. The calcite–dolomite cycles consist of fine laminated layers of a micrometre to millimetre scale. The concentration of Sr, which substituted for other cations in calcite, shows two cyclic variations with a scale of about 5 m, gradually increasing and then rapidly decreasing (Fig. 4). Additionally, the Ti and Fe peaks, which characterize the clay layers, always occur at the boundary of each calcite–dolomite cycle (Tojo *et al.* 2007).

The same elemental variation patterns of the K₁ calcite–dolomite cycles were observed in the other sections (Fig. 4). In particular, the same trends were found to be reproducible in W₁, tens of kilometres apart from K₁. Accordingly, the K₁ calcite–dolomite cycles are distributed regionally, as shown by the stratigraphical study (Tojo *et al.* 2006). The interpretation of the elemental variations in the calcite–dolomite cycle is given by Tojo *et al.* (2006).

Conclusions

Continuous collection was made of firm, laminated Precambrian sedimentary rocks using an engine cutter. The sample slabs (or plates) were embedded in epoxy resin and standardized in shape, then polished, so providing an analytical surface, allowing systematic production of 2D images of various sorts, e.g. RGB, XRF, and X-ray CT images (Kumazawa *et al.* 2002). Use of the lamination tracer made it possible to acquire 1D elemental profiles with a high spatial resolution from the XRF images by employing the SXAM and the lamination tracer. Then, applying integrated methods to the Rasthof rhythmite sequence overlying the Chuos glaciogenic deposits, we succeeded in obtaining elemental profiles for Si, Ca, Ti, Mn, Fe and Sr with a spatial resolution of 0.8 mm.

The intermediate unit of the rhythmite sequence contains seventeen periodical variations of calcite and dolomite with a scale of tens of centimetres to several metres. These had characteristic Ca, Mn and Sr signatures. Additionally, Sr, which is present in calcite, demonstrated two cyclic variations with a scale of about 5 m. The elemental variations in the cap carbonates possibly suggest that the environmental variations may have occurred during the recovery to a warmer interglacial period from a ‘Snowball Earth’ glacial. These newly developed high-resolution methods used in this study can be useful tools to detect environmental variations in the Precambrian evidenced in laminated sedimentary rocks.

We express our cordial thanks to P. Hoffman, Professor of Harvard University, for his support and positive discussions and Gabi Schneider, Director of the Geological Survey of Namibia, for her kind permission and support for our research activities in Namibia. We also thank T. Okaniwa, Nagoya University, for sampling a continuous Rasthof cap carbonate; Y. Okuda, Gifu University, for examining the elemental distribution of the Rasthof cap carbonate; and T. Masuda and K. Suzuki, Instrument Development Center of School of Science, Nagoya University, for fabricating a mobile stage for mounting the engine cutter. A part of this study was supported by the Decoding Earth Evolution Program (DEEP), a Grant-in-Aid for Scientific Research on Priority Areas (No. 07238104). We thank our reviewers: G. Schneider and an anonymous reviewer. We would also like to acknowledge Pat Vickers-Rich (editor), Professor of Monash University and Patricia Komarower, Research Assistant of Monash University, for editing the text.

References

- HOFFMAN, P. F. 2002. Carbonates bounding glacial deposits: evidence for Snowball Earth episodes and greenhouse aftermaths in the Neoproterozoic Otavi Group of northern Namibia. *International Association*

- of *Sedimentologists Field Excursion Guidebook, Auckland Park, South Africa*, 1–39.
- HOFFMAN, P. F. & SCHRAG, D. P. 2002. The snowball Earth hypothesis: testing the limits of global change. *Terra Nova*, **14**, 129–155.
- HOFFMAN, P. F., HAWKINS, D. P., ISACHSEN, C. E. & BOWRING, S. A. 1996. Precise U–Pb zircon ages for early Damaran magmatism in the Summas Mountains and Welwitschia Inlier, northern Damara belt, Namibia. *Communications of the Geological Survey of Namibia*, **11**, 47–52.
- HOFFMAN, P. F., KAUFMAN A. J., HALVERSON, G. P. & SCHRAG, D. P. 1998. A Neoproterozoic snowball Earth. *Science*, **281**, 1342–1346.
- HOFFMANN, K.-H. & PRAVE, A. R. 1996. A preliminary note on a revised subdivision and regional correlation of the Otavi Group based on the glaciogenic diamictites and associated cap dolostones. *Communications of the Geological Survey of Namibia*, **11**, 77–82.
- HOSOKAWA, Y., OZAWA, S., NAKAZAWA, H. & NAKAYAMA, Y. 1997. An X-ray guide tube and a desk-top scanning X-ray analytical microscope. *X-ray Spectrometry*, **26**, 380–387.
- KATSUTA, N., TAKANO, M., OKANIWA, T. & KUMAZAWA, M. 2003. Image processing to extract sequential profiles with high spatial resolution from the 2D map of deformed laminated patterns. *Computers & Geosciences*, **29**, 725–740.
- KAUFMAN, A. J., KNOLL, A. H. & NARBONNE, G. M. 1997. Isotopes, ice ages, and terminal Proterozoic earth history. *Proceedings of the National Academy of Sciences*, **94**, 6600–6605.
- KENNEDY, M. J., RUNNEGAR, B., PRAVE, A. R., HOFFMANN, K.-H. & ARTHUR, M. A. 1998. Two or four Neoproterozoic glaciations? *Geology*, **26**, 1059–1063.
- KIRSCHVINK, J. L. 1992. Late Proterozoic low-latitude global glaciation: the Snowball Earth. In: SCHOPF, J. W. & KLEIN, C. (eds) *The Proterozoic Biosphere*. Cambridge University Press, Cambridge, 51–52.
- KUMAZAWA, M., ITO, T. & YOSHIDA, S. 2002. *Decoding the Earth's Evolution*. University of Tokyo (in Japanese).
- MEERT, J. G. & VAN DER VOO, R. 1996. Paleomagnetic and $^{40}\text{Ar}/^{39}\text{Ar}$ study of the Sinyai dolerite, Kenya: implications for Gondwana assembly. *Journal of Geology*, **104**, 131–142.
- MEERT, J. G., VAN DER VOO, R. & AYUB, S. 1995. Paleomagnetic investigation of the Neoproterozoic Gagwe lavas and Mbozi complex, Tanzania and the assembly of Gondwana. *Precambrian Research*, **74**, 225–244.
- MICHIBAYASHI, K., TOGAMI, S., TAKANO, M., KUMAZAWA, M. & KAGEYAMA, T. 1999. Application of scanning X-ray analytical microscope to the petrographic characterization of a ductile shear zone: an alternative method to image microstructures. *Tectonophysics*, **310**, 55–67.
- TOJO, B., KATSUTA, N., TAKANO, M., KAWAKAMI, S. & OHNO, T. 2007. Calcite–dolomite cycles in the Neoproterozoic Cap carbonates, Otavi Group, Namibia. In: VICKERS-RICH, P. & KOMAROWER, P. (eds) *The Rise and Fall of the Ediacaran Biota*. Geological Society, London, Special Publications, **286**, 103–113.
- TOGAMI, S., TAKANO, M., KUMAZAWA, M. & MICHIBAYASHI, K. 2000. An algorithm for the transformation of XRF images into mineral-distribution maps. *Canadian Mineralogist*, **38**, 1283–1294.
- YOSHIOKA, H., ASAHARA, Y., TOJO, B. & KAWAKAMI, S. 2003. Systematic variations in C, O, and Sr isotopes and elemental concentrations in Neoproterozoic carbonates in Namibia: implications for a glacial to interglacial transition. *Precambrian Research*, **124**, 69–85.

Ediacaran rocks from the Cadomian basement of the Saxo-Thuringian Zone (NE Bohemian Massif, Germany): age constraints, geotectonic setting and basin development

U. LINNEMANN

Staatliche Naturhistorische Sammlungen Dresden, Museum für Mineralogie und Geologie, Königsbrücker Landstrasse 159, D-01109 Dresden, Germany
(e-mail: ulf.linnemann@snsd.smwk.sachsen.de)

Abstract: This paper is focused on a compilation of known data from the low-grade metamorphosed rocks of the Ediacaran period in the German part of the Saxo-Thuringian Zone at the northeastern margin of the Bohemian Massif. The geotectonic setting during the formation of Ediacaran rock units is characterized by Cadomian orogenic processes from c. 650–540 Ma at the periphery of the West African Craton. The basin development during that time is characterized by the formation of a Cadomian backarc basin with a passive margin, and the outboard sitting Cadomian magmatic arc originated at c. 570–560 Ma. This arc-marginal basin system was formed on stretched continental crust in a strike-slip regime and reflects an active-margin setting in a style similar to the recent West Pacific. The backarc basin was closed between c. 560–540 Ma by the collision of the Cadomian magmatic arc with the cratonic hinterland: this resulted in the closure of the backarc basin and the formation of a Cadomian retroarc basin. Collision of an oceanic ridge with the Cadomian Orogenic Belt led to a slab break-off of the subducted oceanic plate resulting in an extreme heat flow, and a magmatic and anatectic event culminating at c. 540 Ma that was responsible for the intrusion of voluminous granitoid plutons.

Ediacaran rock complexes in Germany are restricted to the Saxo-Thuringian Zone in the Bohemian Massif, which represents the largest and most important basement inlier of the Central European Variscides (Fig. 1). Low-grade Ediacaran metamorphic rocks occur mainly in the Saxo-Thuringian Zone (Germany) and the Tepla-Barrandian Unit (Czech Republic) (Fig. 2). This paper presents a review on the weakly metamorphosed Ediacaran to Early Cambrian rocks of the Saxo-Thuringian Zone. These rocks units are affected by the tectonometamorphic overprint of the Late Neoproterozoic–Early Cambrian Cadomian and the Late Devonian–Early Carboniferous orogenies. In some areas of the Saxo-Thuringian Zone, such as the Erzgebirge Mountains, some of the rocks display a high-grade metamorphic overprint. These rocks are not discussed in this paper.

Cadomian orogenic processes comprise a series of complex sedimentary, magmatic, and tectonometamorphic events that spanned the period from the mid-Neoproterozoic (c. 650 Ma) to the earliest Cambrian (c. 540 Ma) (e.g. Linnemann *et al.* 2000; Nance *et al.* 2002). Rock units formed by the Cadomian orogeny are generally referred to as ‘Cadomian basement’. Due to very similar contemporaneous orogenic processes in the Avalonian microplate, the collective term ‘Avalonian-Cadomian’ orogeny has often been used in the modern literature (e.g. Dörr

et al. 2004). Peri-Gondwanan terranes, microcontinents and crustal units in Europe and in North Africa are affected by the Cadomian orogeny (e.g. Murphy *et al.* 2004). Related orogenic events, such as the Avalonian orogeny, are known in the Appalachians (eastern US and Atlantic Canada), and from the non-Laurentian part of Ireland and the British Isles (e.g. Nance & Murphy 1996). Baltica escaped the Avalonian-Cadomian orogenic activity, although the ‘Cadomian affinity’ of the late Precambrian orogenic events in the Urals and in the Timanides on the periphery of Baltica was recognized (Roberts & Siedlecka 2002; Glasmacher *et al.* 2004).

The Cadomian orogeny was first defined in the North Armorican Massif in France on the basis of the unconformity that separates deformed Precambrian rock units from their Early Palaeozoic (Cambro-Ordovician) overstep sequence (Bunel 1835; Dufrenoy 1838; Barrois 1899; Kerforne 1901). ‘Cadomus’ is an old Latin term for the modern city of Caen and is the source of the name of the orogeny. The term ‘discordance cadomienne’ was first used by Bertrand (1921). The best illustration of the unconformity in Rocreux (Normandy) was published by Graindor (1957). In Central and Western Europe the unconformity is commonly referred to as the ‘Cadomian unconformity’. It is possible that the youngest metasedimentary rocks

affected by the Cadomian deformation are earliest Cambrian in age. Many geologists assume that the final stages of Cadomian orogenesis were spatially diachronous, lasting from the latest Neoproterozoic to the earliest Cambrian. From this viewpoint the term 'Cadomian basement' includes Neoproterozoic (Ediacaran) to Early Cambrian sedimentary, igneous and metamorphic complexes. The stratigraphic range of the involved rock complexes changes from region to region.

In some publications, the term 'Pan-African orogeny' is used in the same sense as Cadomian orogeny, because both events were related to the Gondwana supercontinent in the late Precambrian and occurred more or less in the same time interval. The main difference between the Cadomian and Pan-African orogenic events is their position within the configuration of the Gondwana supercontinent in Neoproterozoic time. The crustal units affected by the Pan-African orogeny are located between the cratons assembling Gondwana and reflect continent–continent collision, at least in most cases (e.g. compilation of Windley 1996). In contrast, the Cadomian orogen or, alternatively, the Avalonian-Cadomian orogenic belt is a peripheral orogen at the edge of the Gondwanan supercontinent and was characterized by orogenic processes similar to those presently observable in the Andes and the Cordilleran chains of the American continents and in the West Pacific Region (Murphy & Nance 1991; Nance & Murphy 1994; Buschmann 1995; Linnemann *et al.* 2000; Nance *et al.* 2002; Linnemann *et al.* 2004).

Provenance studies including: (1) U/Pb-ages of detrital zircon grains from sedimentary rocks and inherited zircons from igneous rocks; (2) Nd–Sr–Pb isotope; and (3) palaeomagnetic and palaeobiogeographic data, suggest that the origin of the Cadomian basement of Central and Western Europe was at the periphery of the West African craton of Gondwana (e.g. Linnemann *et al.* 2004; Murphy *et al.* 2004).

Remnants of the old cratonic basement derived from the cratonic source areas are represented by the Icartian basement (2.01–2.06 Ga) in the Armorican massif, and the Svetlik gneiss (2.05–2.1 Ga) and the Dobra gneiss (1.38 Ga) in the Bohemian Massif. In view of the occurrence of these rock complexes, and many Archaean and Palaeoproterozoic detrital zircons in Neoproterozoic sedimentary rocks, it seems that most of the Cadomian basement had developed on a stretched and thinned old cratonic crust, from which cratonic material was available for erosion and deposition into basins and also for the incorporation of large blocks from the basement into the Cadomian orogen.

Nance *et al.* (2002) proposed a Cordilleran model for the evolution of the Neoproterozoic to

Cambro-Ordovician rock complexes in Avalonia that was a part of the 'Avalonian-Cadomian orogenic belt' on the periphery of the Gondwana supercontinent during the Neoproterozoic and the Early Palaeozoic. This model uses the North American plate at Baja California as a modern analogue to explain the plate-tectonic setting, including terrane accretion, subduction-related processes, ridge-trench collision and rifting.

The impact of the Variscan orogeny during the closure of the Rheic Ocean in Devonian and Carboniferous times resulted in a penetrative overprinting and recrystallization of the Cadomian basement rocks and of their structures in many areas during Pangea amalgamation. Therefore, this compilation is focused on the Saxo-Thuringian Zone at the periphery of the Bohemian Massif, which is less affected by younger orogenies. This zone contains a number of the best-preserved and most representative Ediacaran rock complexes in the Cadomian basement of Central Europe.

The Precambrian of the Bohemian Massif

The Bohemian Massif is bounded to the north and the NE by the Mid-German Crystalline zone, which most likely represents the suture formed during the closure of the Rheic Ocean in the Late Devonian to Early Carboniferous period. To the south and SE the Bohemian Massif is covered by the Meso-Cenozoic orocline of the Alps and the Carpathians. Steeply dipping faults in the SW, such as the Franconian Line and the Danube Fault, divide the basement rocks from Mesozoic platform sediments and the Alpine molasses (Fig. 1).

The Bohemian Massif represents the most prominent inlier of basement rocks in Central Europe that underwent a long geological history from Cadomian orogenic processes to the core of the Variscan Orogen in the Central European Variscides. Some of the marginal units and inliers contain very weak metamorphosed and deformed Ediacaran to Palaeozoic rock complexes. Good examples are the western and northern parts of the Saxo-Thuringian Zone and the Tepla-Barrandian Unit (Fig. 1).

The Bohemian Massif is generally interpreted as a part of Armorica (Van der Voo 1979). Tait *et al.* (1997, 2000) suggested that Armorica drifted across the Rheic Ocean during Ordovician to Devonian times. In contrast, the interpretation of palaeobiogeographical, geochronological, geochemical and sedimentological data led to the conclusion that Armorica never left Gondwana mainland in pre-Pangean time (Robardet 2002; Linnemann *et al.* 2004). The Cadomian basement of the Armorican Massif, the French Central

Massif and the Bohemian Massif, excepting the Brunovistulian in the Moravo-Silesian Zone, is summarized as 'Cadomia' (Nance & Murphy 1996; Murphy *et al.* 2004). Studies of U/Pb-ages from detrital zircon grains have suggested that the Saxo-Thuringian Zone, the Tepla-Barrandian Unit and the Moldanubian Zone of the Bohemian Massif show a West African provenance (Linnemann *et al.* 2000, 2004; Gehmlich 2003; Tichomir-owa 2003; Drost *et al.* 2004). These units are believed to be a part of Cadomia *sensu* Murphy *et al.* (2004). One old basement sliver from the Cadomia part of the Bohemian Massif is represented by the *c.* 2.1 Ma old Svetlik gneiss (Wendt *et al.* 1993), which probably was a part of the West African Craton.

According to Finger *et al.* (2000) the Brunovistulian in the Moravo-Silesian Zone may represent a part of Avalonia. For that part in the Bohemian Massif, an Amazonian provenance is suggested at the base of the age cluster of magmatic and inherited zircon grains (Friedl *et al.* 2000). A cratonic inlier related to Avalonia is represented by the 1.38 Ma old Dobra gneiss (Gebauer & Friedl 1994; Friedl *et al.* 2004).

Ediacaran rock units of the Saxo-Thuringian Zone

The Saxo-Thuringian Zone was defined by Kossmat (1927) and is situated in the northeast region of the Bohemian Massif (Fig. 1). To the north, the Saxo-Thuringian Zone is separated by the Mid-German Crystalline Zone from the Rheno-Hercynian Zone (Fig. 2). The bounding element to the SW is the Franconian Line, which is a relatively young fault system originated during Mesozoic to Cenozoic reactivation of the crust. A continuation of the Saxo-Thuringian Zone to the west, up into the northern parts of the Black Forest and the Vosges, is suggested by many authors. To the south, the fault system representing the boundary to the Moldanubian zone is mostly hidden by Tertiary sediments of the Ohre Graben. In its eastern part the Saxo-Thuringian Zone continues into the eastern part of the Sudetes (Fig. 2).

Important and dominant structures of the Saxo-Thuringian Zone are represented by the Schwarzburg, North Saxon, Berga and Lausitz Antiforms, the Torgau-Doberlug and the Ziegenrück-Teuschnitz Synclines and the Elbe Zone (Fig. 2).

Zircon dating has shown that Ediacaran rocks in the Cadomian Basement of the Saxo-Thuringian Zone are generally not older than *c.* 570 Ma (Linnemann *et al.* 2000, 2004). The sections are rootless in the lower part and fault-bounded. Older Precambrian basement rocks are not known. In the upper

part, Ediacaran rocks, except for the Schwarzburg antiform, are unconformably overlain by Cambro-Ordovician sedimentary rocks. This unconformity in the Saxo-Thuringian Zone is interpreted as the Cadomian unconformity, and was first recognized in the drill core of the deep drilling 5507/77 near Gera (Linnemann & Buschmann 1995*a, b*). In that core, steeply dipping Ediacaran rocks of the Leipzig Formation are overlain by sub-horizontal Early Ordovician quartzites (Linnemann & Buschmann 1995*a*). Later, the unconformity between Late Ediacaran sediments of the Rothstein Formation and Lower Cambrian sedimentary rocks is described from the drill core 1614/79 from the Torgau-Doberlug Syncline (Buschmann *et al.* 2006).

The Ediacaran rocks and the rest of the Cadomian basement are divided into an internal and an external domain (Figs 2 & 3). The external zone is composed of Ediacaran volcano-sedimentary units (Rothstein Formation in the Torgau-Doberlug Syncline and Altenfeld Formation in the NW part of the Schwarzburg Antiform). Both are characterized by massive black chert units (Figs 3, 5*a*), and are assumed to be originated in a backarc setting (Buschmann 1995; Linnemann *et al.* 2000). The sediments include dark-grey to black distal turbidites, with greywacke and mudstone bedsets. The Rothstein Formation is overlain by Lower to Middle Cambrian sediments, whereas the Altenfeld Formation is covered by Lower Ordovician siliciclastics. In contrast to the internal domain, no extensive plutonism is known at *c.* 540 Ma in the external domain. Only one very small granitoid body of uncertain age, represented by the Milchberg Granite, was intruded into the Altenfeld Formation. Another important part of the external domain is the Vesser complex, which is Middle to Upper Cambrian in age. This unique complex is characterized by mid-ocean ridge-related rocks (Bankwitz *et al.* 1992).

The boundary between the external and the internal domains is represented by the Blumenau Shear Zone, dividing the Schwarzburg Antiform into a NW and a SE region (Fig. 2). In this paper, the Blumenau Shear Zone is interpreted as a structural feature that most probably formed during the Cadomian Orogeny, during the transition between backarc basin and retroarc basin (Fig. 10). During Variscan orogenic processes, the Blumenau Shear Zone was reactivated into a sinistral shear zone (Heuse *et al.* 2001).

The internal domain of the Saxo-Thuringian Zone contains sedimentary units from two different Ediacaran basin types. It is characterized by voluminous Cadomian plutons intruded at *c.* 540–530 Ma, and a very thick and widespread Ordovician overstep sequence. Cambrian deposits are very rare

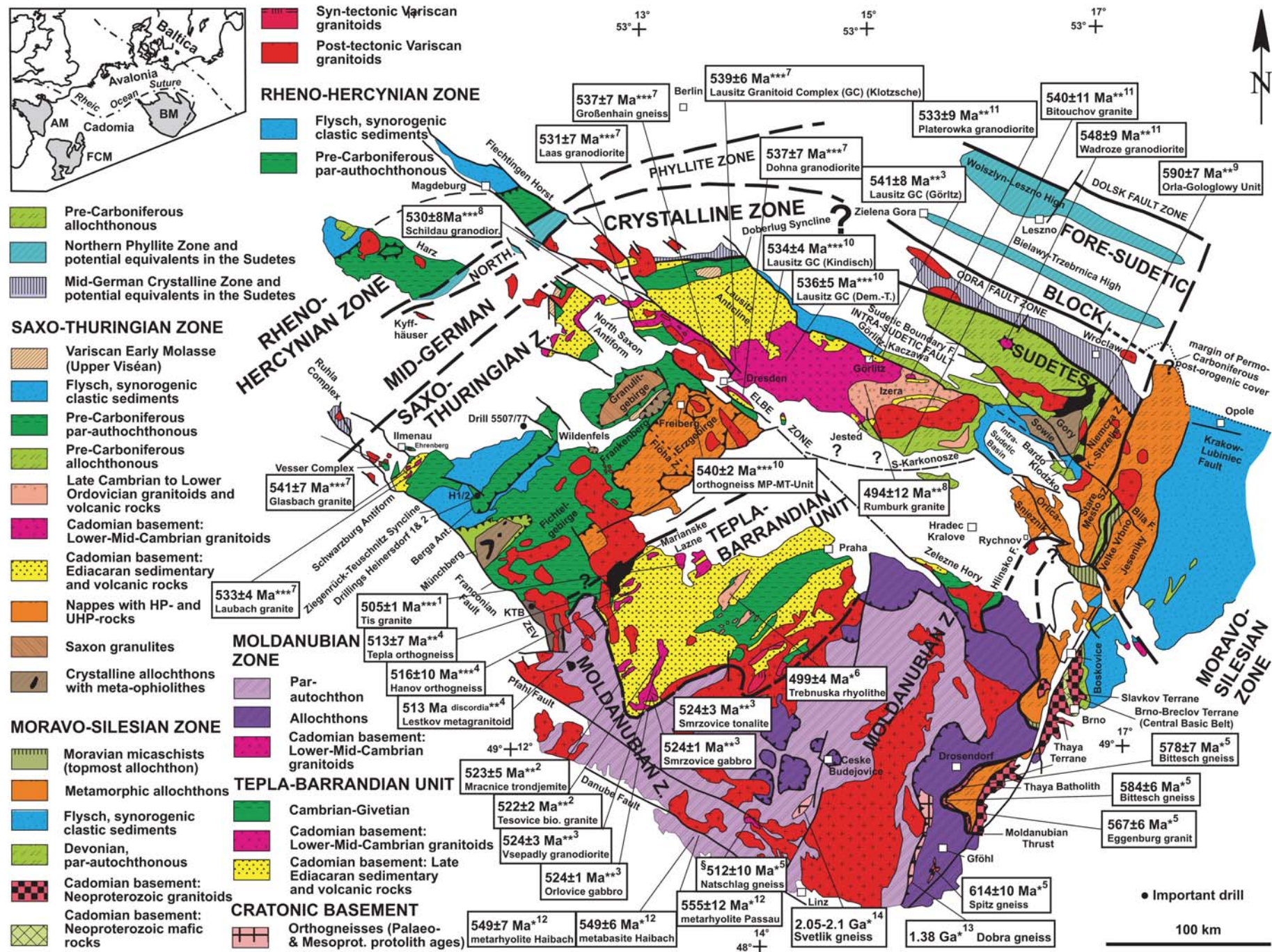


Fig. 1. Geological map of the Bohemian Massif showing the Cadomian orogenic imprints and cratonic slivers in the Variscan basement, the published ages of plutons and volcanic rocks related to pre-Cadomian, Cadomian and Cambro-Ordovician geotectonic processes and the opening of the Rheic Ocean (modified after Linnemann & Schauer 1999; Kozdroj *et al.* 2001; Franke & Zelaźniewicz 2002). Sources of geochronological data: 1, Venera *et al.* 2000; 2, Zulauf *et al.* 1997; 3, Dörr *et al.* 2002; 4, Dörr *et al.* 1998; 5, Friedl *et al.* 2004; 6, Drost *et al.* 2004; 7, Linnemann *et al.* 2000; 8, Hammer *et al.* 1999; 9, Mazur *et al.* 2004; 10, Tichomirowa 2003; 11, Zelaźniewicz *et al.* 2004; 12, Teipel *et al.* 2004; 13, Gebauer and Friedl 1994; 14, Wendt *et al.* 1993. (*, U/Pb-SHRIMP; **, U/Pb TIMS; ***, Pb/Pb TIMS; §, age of the youngest concordant zircon of the Natschlag gneiss; Lausitz GC, Lausitz Granitoid Complex). Inset: Location of the prominent massifs of Cadomia containing Ediacaran rocks: BM, Bohemian Massif; AM, Armorican Massif; FCM, French Central Massif.

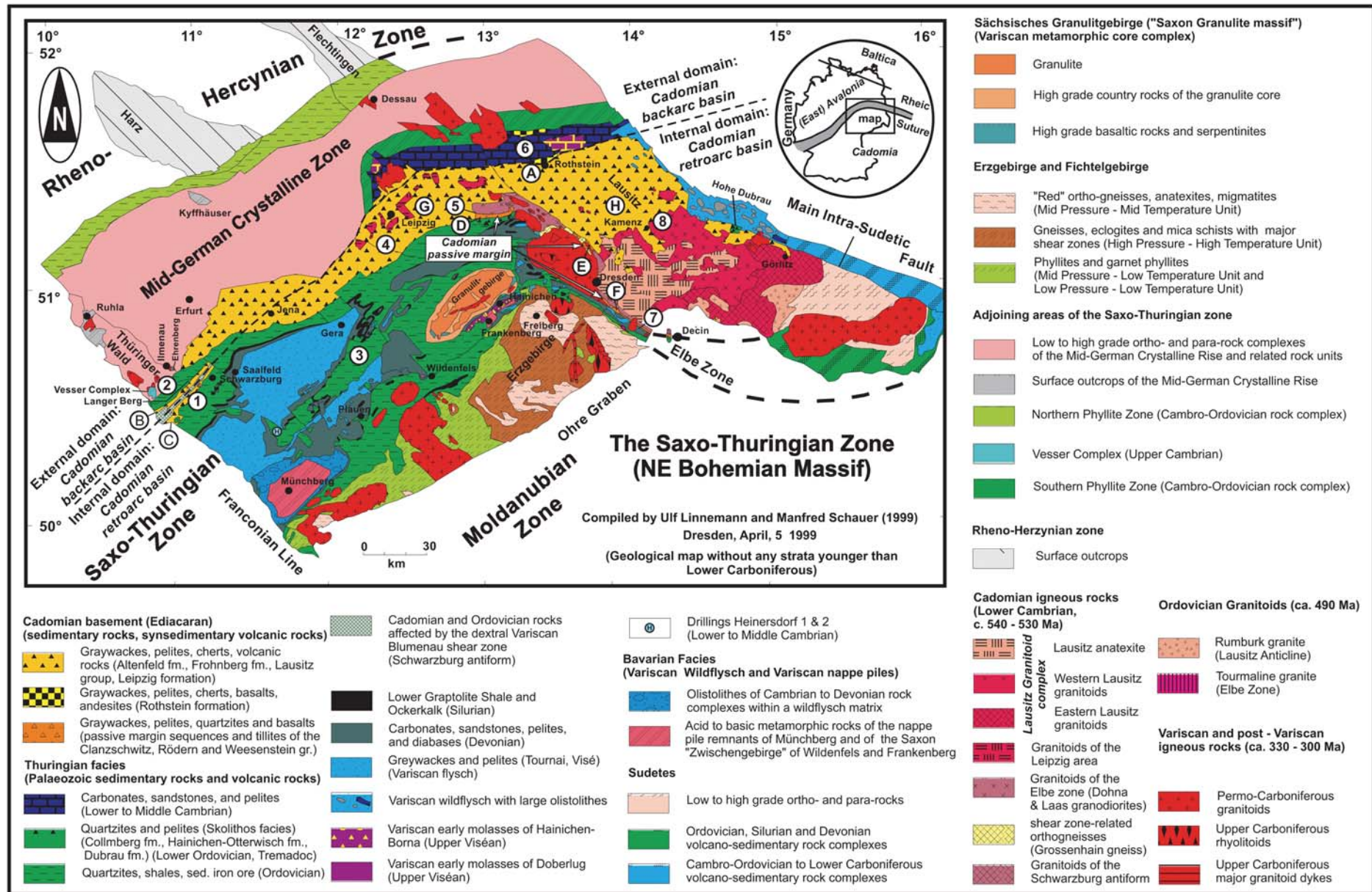


Fig. 2. Geological map of the Saxo-Thuringian Zone in the NE part of the Bohemian Massif, showing Lower Carboniferous and older strata only, and the principal distribution of fragments from different stages of Cadomian basin development (modified from Linnemann & Schauer 1999; Linnemann & Romer 2002). Tectonostratigraphic units: 1, Schwarzburg Antiform (SE-part); 2, Schwarzburg Antiform (NW-part); 3, Berga Antiform; 4, North Saxon Antiform (Leipzig area); 5, North Saxon Antiform (Clanzschwitz area); 6, Torgau-Doberlug Syncline; 7, Elbe Zone; 8, Lausitz Antiform. Neoproterozoic volcano-sedimentary complexes: (A) Rothstein formation; (B) Altenfeld formation; (C) Frohnberg formation; (D) Clanzschwitz group; (E) Rödern group; (F) Weesenstein group; (G) Leipzig formation; (H) Lausitz group.

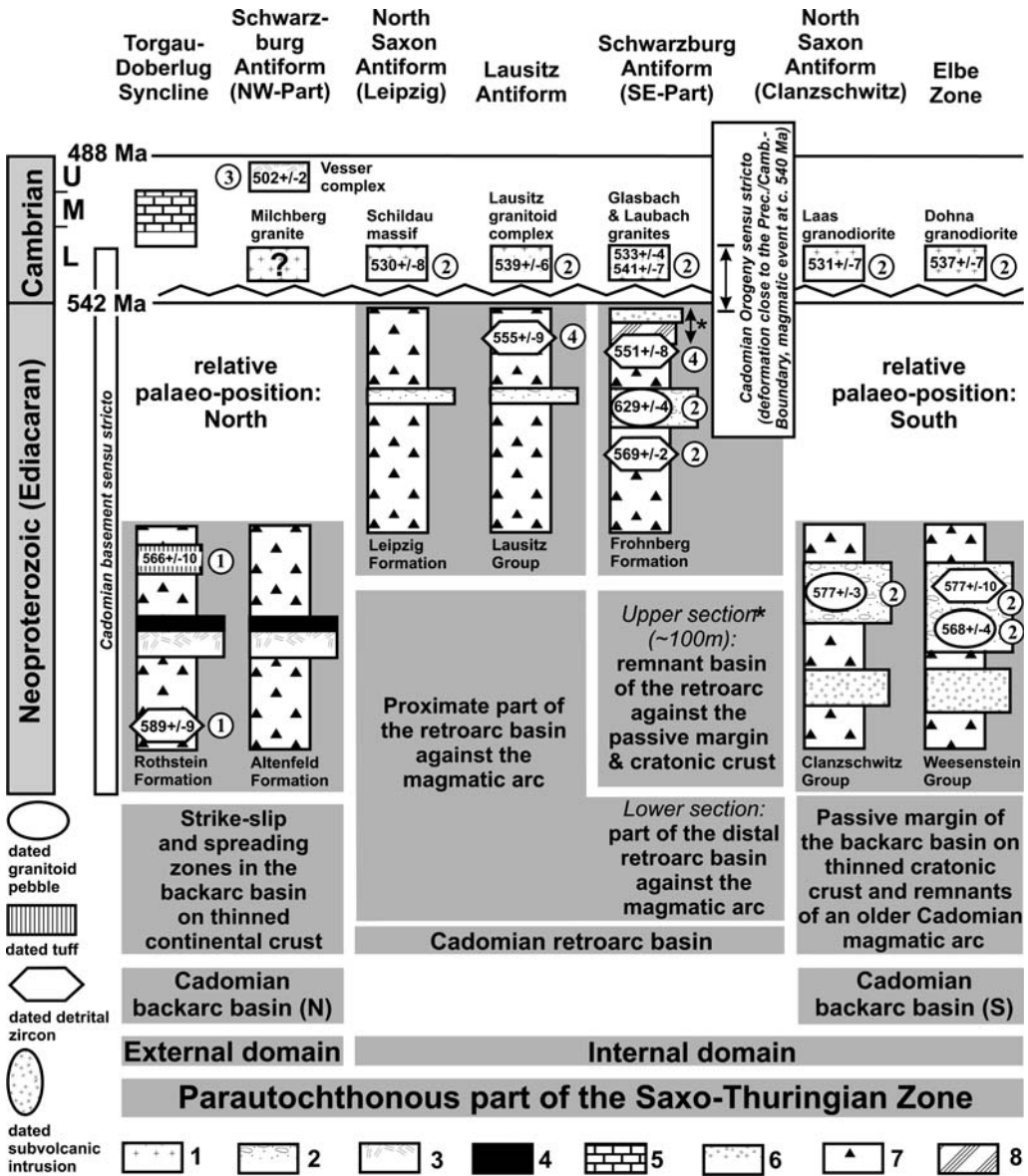


Fig. 3. Generalized lithosections, geotectonic setting and published geochronological data of the Cadomian basement and parts of its Cambrian overstep sequence in the Saxo-Thuringian Zone. Legend: 1, Cadomian granitoids of the magmatic event at c. 540 Ma; 2, Ediacaran diamictites; 3, igneous rocks and meta-sediments of the Upper Cambrian Vesser complex (predominantly mafic rocks); 4, Ediacaran hydrothermal cherts; 5, Lower to Middle Cambrian sediments; 6, conglomerates, quartzites and quartzitic shales of the Purpurberg Quartzite in the Weesenstein Group, and its equivalent in the Clanzschwitz group; 7, greywackes and mudstones; 8, predominantly mudstones. Sources of geochronological data (encircled numerals): 1, SHRIMP U/Pb (Buschmann *et al.* 2001); 2, TIMS Pb/Pb (Linnemann *et al.* 2000); 3, TIMS U/Pb (Kemnitz *et al.* 2002); 4, SHRIMP U/Pb (Linnemann *et al.* 2004).

and restricted to the drillings Heinersdorf 1 and 2 in the Berga Antiform. In addition, Cambrian rocks became known from large olistoliths in a Lower Carboniferous flysch matrix in the Görlitz Synform.

One basin type in the internal domain is represented by passive margin sequences characterized by high mature quartzites, sandstones and quartz-rich shales deposited in a shallow marine

environment (Figs 2 & 10). The most prominent deposit of this type is represented by the Purpurberg Quartzite in the lower part of the Weesenstein Group (Fig. 4). A facies analysis of the Purpurberg

Quartzite has shown that this deposit displays a fan shape, an upward increase in bed thickness, and sedimentary structures typical of shallow water deposits, such as cross-bedding and ripple-marks

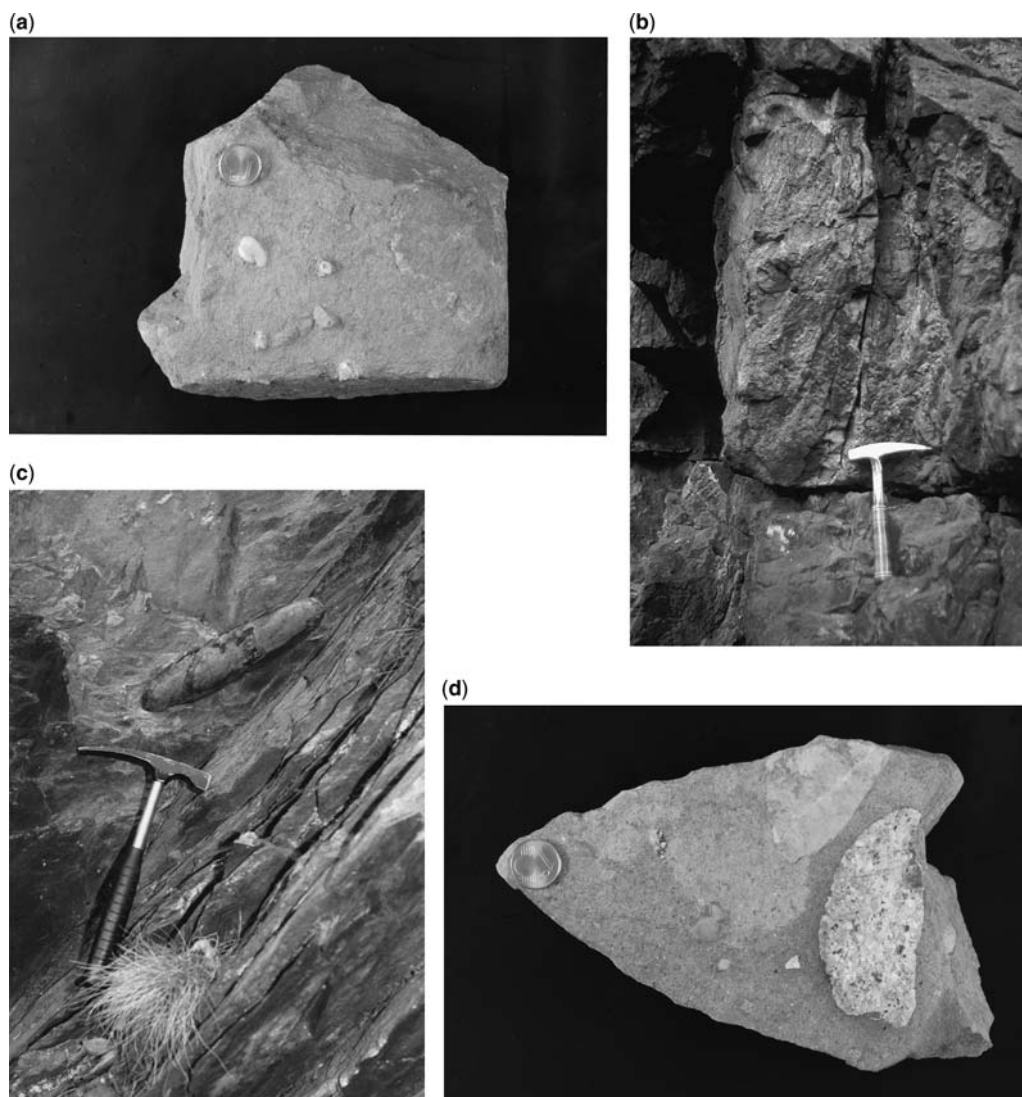


Fig. 4. Photographs of Ediacaran rocks in the Cadomian backarc basin (Saxo-Thuringian Zone, Bohemian Massif): (a) Hand specimen of a diamictite of possible glaciomarine origin with out-weathered fragments from the upper Weesenstein Group (Ediacaran, *c.* 570 Ma, Weesenstein Group, 100 m to the east of the Weesenstein Railway Station, Cadomian basement of the Elbe zone); (b), Steeply dipping bed of the Purpurberg quartzite with internal cross bedding and ripple marks. The quartzite occurs in the lower part of the Weesenstein Group, which represents the passive margin of the Cadomian backarc basin (Ediacaran, *c.* 570 Ma, Weesenstein Group, Purpurberg near Niederseidewitz, Cadomian basement of the Elbe zone); (c) Stretched granitoid pebble from a diamictite in the upper part of the Weesenstein Group. The pebbly mudstone facies of the Weesenstein Group is interpreted to be in part glaciomarine (Ediacaran, *c.* 570 Ma, Weesenstein group, 100 m to the east of the Weesenstein Railway Station, Cadomian basement of the Elbe zone); (d) Polished hand specimen of a diamictite of possible glaciomarine origin from the upper Weesenstein Group (Ediacaran, *c.* 570 Ma, Weesenstein Group, 100 m to the east of the Weesenstein Railway Station, Cadomian basement of the Elbe zone).

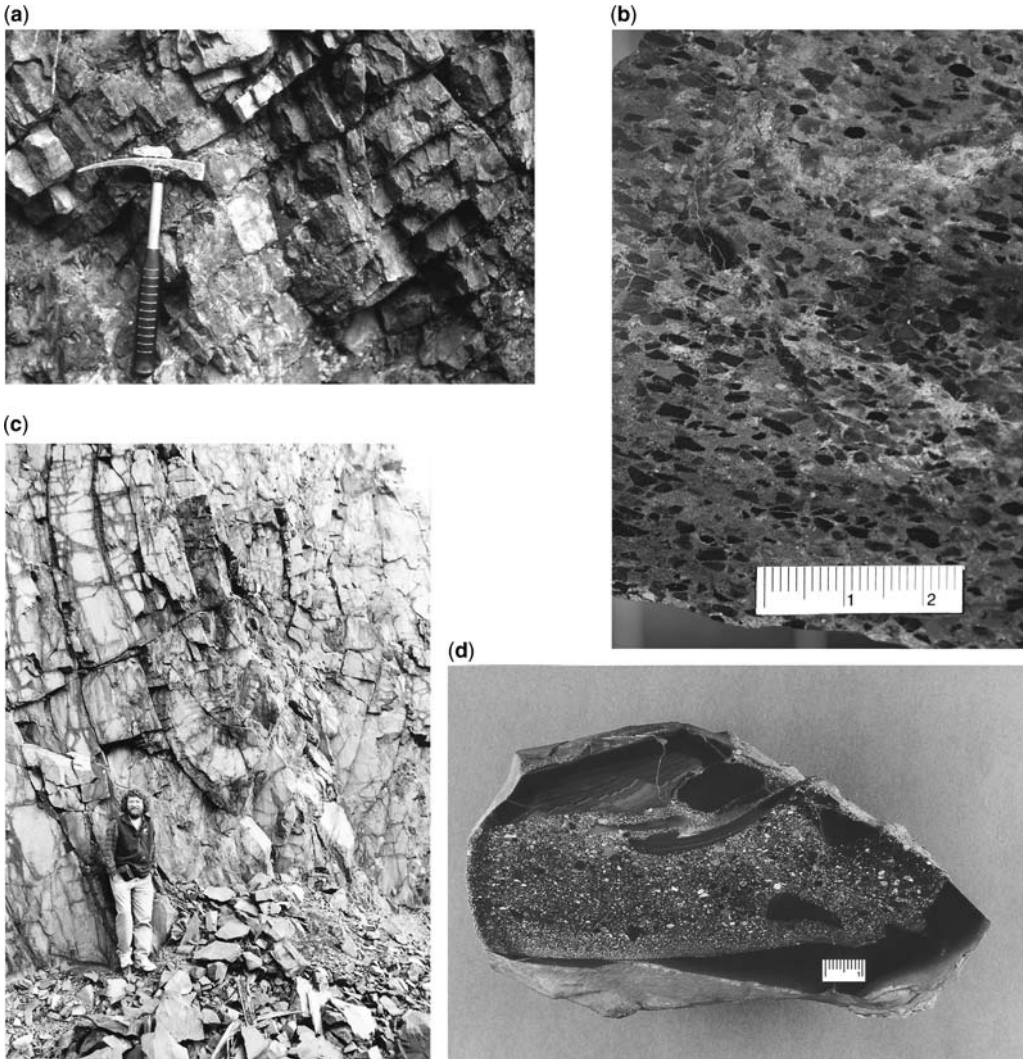


Fig. 5. Photographs of Ediacaran rocks in the Cadomian retroarc basin (Saxo-Thuringian Zone, Bohemian Massif): (a) Black cherts at the Rothstein Rock originated close to spreading zones in the Cadomian backarc basin (Ediacaran, c. 566 Ma, Rothstein Formation, Cadomian basement of the Torgau-Doberlug Syncline); (b) Microconglomerate with clasts of cherts and felsic rocks of the Lausitz Group, demonstrating the re-deposition of the black cherts and arc volcanics during the formation of the Cadomian retroarc basin (Ediacaran, c. 555–540 Ma, Lausitz Group, Petershain near Kamenz, Cadomian basement of the Lausitz Antiform); (c) Isoclinally folded greywacke turbidites of the Lausitz Group (Ediacaran, c. 555–540 Ma, Lausitz Group, Butterberg Quarry near Bernsdorf, Cadomian basement of the Lausitz Antiform); (d) Specimen from a seismically induced debris flow. The conglomeratic matrix includes fragments of seismites (upper left), mudclasts and black chert fragments (Ediacaran, c. 555–540 Ma, Lausitz Group, Wetterberg Quarry near Ebersbach, Cadomian basement of the Lausitz Antiform).

(Fig. 4) (Linnemann 1991). In this paper, the depositional environment is interpreted as a deltaic deposit resulting from a drop in sea level. A stratigraphic equivalent of the Purpurberg Quartzite occurs in the Clanzschwitz Group (North Saxon Antiform). Other parts of the Weesenstein and Clanzschwitz

Groups are also related to passive margin deposits, with quartz-rich mud- and siltstones.

In the upper part of the Weesenstein and the Clanzschwitz Groups, diamictites and layers with isolated pebbles occur that could be glaciomarine in origin (Fig. 5) (Linnemann & Romer 2002).

This is yet to be confirmed as tectonometamorphic overprinting may have obscured diagnostic criteria, such as dropstones or striated pebbles. The main argument for a glaciomarine origin of the diamictites of the Weesenstein and the Clanzschwitz Groups is based on the drastic sea level fall in the lower part of the section, which is represented by the deposition of the Purpurberg Quartzite. Further, the diamictites are distributed over long distances, and not interfingered with turbidites. It is, therefore, unlikely that the diamictites are debris flows, which are commonly intercalated with turbidites.

The second basin type in the internal domain is represented by the Lausitz Group (Lausitz Antiform), the Leipzig Formation (Northsaxon Antiform) and the Frohnberg Formation (SE region of the Schwarzburg Antiform). All three units are characterized by monotonous and flysch-like sections of proximal to distal, dark-grey to black turbidites, composed of greywacke and mudstone units (Figs 5 & 6). The presence of seismites indicates an active tectonic setting during basin formation (Fig. 5). Further, intercalations of conglomerates containing fragments of black chert and other debris from older Neoproterozoic sediments and igneous rocks occur (Fig. 5). Especially, the abundant occurrence of black chert fragments in the greywackes and conglomerates (Fig. 5) suggests that deposits from the Cadomian backarc basin of the external zone became eroded, recycled and redeposited in a Cadomian retroarc basin, from which the remnants are represented by the Lausitz Group, and the Leipzig and the Frohnberg Formations (Fig. 10).

The turbidites of the Lausitz Group often show typical groove and tool marks at their base (Fig. 6). In some layers, scours and remnants of microbial mats ('elephant skin') can be observed (Fig. 6). The latter is sometimes deformed by chevron marks caused by passing tools or slumps (Fig. 6). Early diagenetic concretions of calc-silica rock occur in places (Fig. 7). These often contain a fragment of mudstone in the centre, suggesting that the activity of microorganisms in the mudstone fragment may be responsible for the formation of the concretions. In one case, hemispherical bodies on the surface of a mudstone bed were found, and interpreted to be of organic origin (Fig. 8). Similar organic structures have been described in the Ediacaran sediments of the Longmyndian Supergroup in Shropshire (UK) (McIlroy *et al.* 2005).

SHRIMP-U/Pb dating of detrital zircon grains has shown that the Lausitz Group and the Frohnberg Formation are younger than 555 ± 9 Ma and 551 ± 8 Ma, respectively (Fig. 3) (Linnemann *et al.* 2004). In general, all Ediacaran sections in the Cadomian basement of the Saxo-Thuringian

Zone seem to be rootless. An underlying cratonic basement is not known. But all Nd-model ages of Late Neoproterozoic sediments in the Cadomian basement are very old and range between 1.3–1.9 Ga (Linnemann & Romer 2002). These data show clearly that the source area of the Neoproterozoic sediments was dominated by old cratonic crust.

All the Ediacaran sedimentary sequences of the Cadomian basement in the Saxo-Thuringian Zone were intruded by Early Cambrian post-kinematic granitoid plutons in a time interval of *c.* 540–530 Ma (Tichomirowa 2003; Gehmlich 2003; Linnemann *et al.* 2000). These plutonic rocks are composed of granites, syeno- and monzogranites, granodiorites and tonalites (Hammer 1996). Most of the plutons are granodiorites.

Ediacaran sedimentary rocks in the Cadomian basement of the Saxo-Thuringian Zone are overlain unconformably by Lower Palaeozoic sediments (Cadomian Unconformity), except in the SE part of the Schwarzburg Antiform (see below). Transgression and the development of Lower to Middle Cambrian overstep sequences, including the deposition of conglomerates, carbonates, siliciclastics, and red beds, with a depositional gap during the lowermost Cambrian (*c.* 540–530 Ma), represent the first post-Cadomian sedimentary sequence (Buschmann *et al.* 2006). A second remarkable and widespread gap in sedimentation occurred during the Upper Cambrian (*c.* 500–490 Ma). Exceptionally, the Vesser Complex is composed predominantly of Mid- to Upper Cambrian MOR-related magmatic rocks and metasediments (Bankwitz *et al.* 1992; Kemnitz *et al.* 2002).

Ediacaran rocks of the Cadomian backarc basin

There are a number of key features in the Saxo-Thuringian Zone and adjoining crustal units of the Bohemian Massif, relating to the origin of Ediacaran rocks and the modelling of the Cadomian Orogeny. Firstly, the recycling of old cratonic crust is documented by: (1) the occurrence of large quantities of Archaean and Palaeoproterozoic zircons (Linnemann *et al.* 2000, 2004; Drost *et al.* 2004), and (2) the Nd-model ages of Late Neoproterozoic to Cambro-Ordovician sediments ranging from *c.* 1.5–2.1 Ga (Linnemann & Romer 2002; Drost *et al.* 2004). Secondly, large sedimentary basins opened up during Ediacaran time at *c.* 570 Ma with simultaneous magmatic arc activity (Linnemann *et al.* 2000). Thirdly, the deformation of most of the sedimentary basins, close to the magmatic event at *c.* 540 Ma, is documented in the

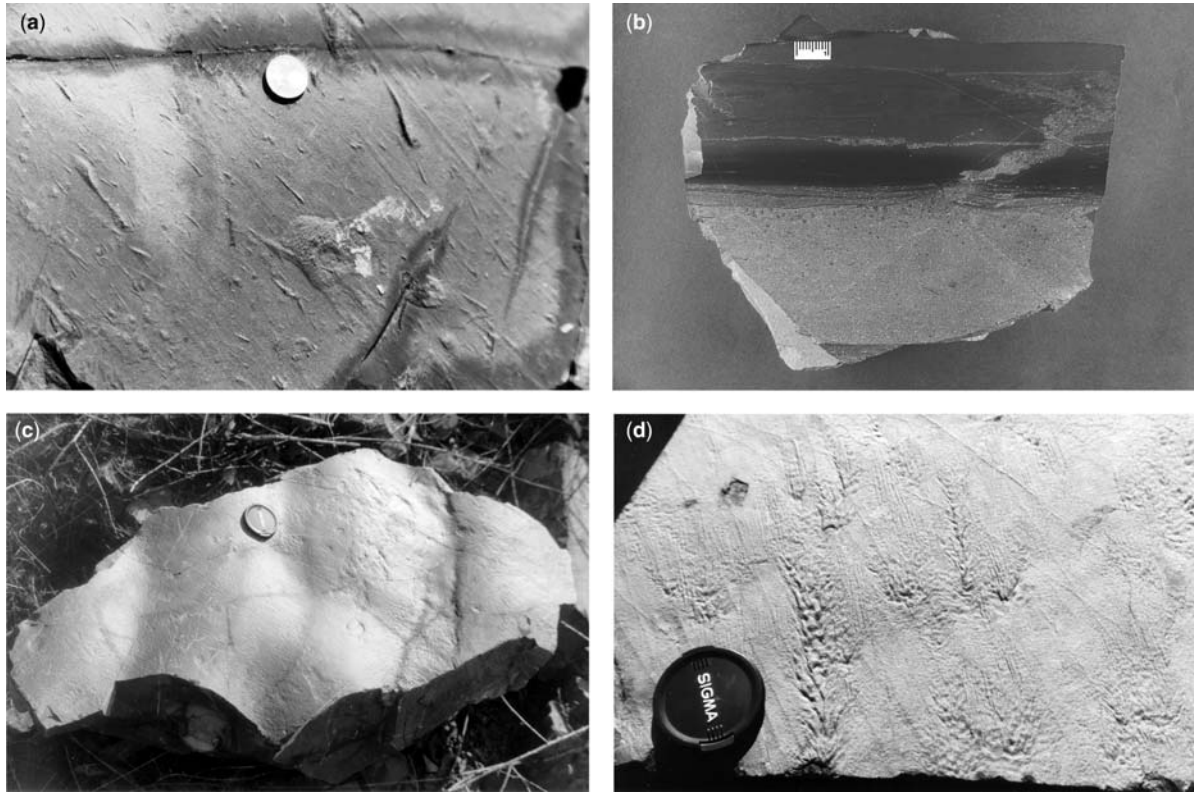


Fig. 6. Photographs of bed surfaces from Ediacaran sediments in the Cadomian retroarc basin (Saxo-Thuringian zone, Bohemian Massif): **(a)** Tool and groove marks at the base of a slab from a greywacke turbidite of the Lausitz Group (Ediacaran, *c.* 555–540 Ma, Lausitz Group, Butterberg Quarry near Bernsdorf, Cadomian basement of the Lausitz Antiform); **(b)** Water escape structure at the top of the a-interval of a greywacke turbidite of the Lausitz Group demonstrating rapid sedimentation in the Cadomian retroarc basin (Ediacaran, *c.* 555–540 Ma, Lausitz Group, Wetterberg Quarry near Ebersbach, Cadomian basement of the Lausitz Antiform); **(c)** Rough surface on a wavy greywacke bed interpreted as microbial mat (‘elephant skin’) (Ediacaran, *c.* 555–540 Ma, Lausitz Group, Butterberg Quarry near Bernsdorf, Cadomian basement of the Lausitz Antiform); **(d)** Structures on a greywacke bed interpreted as microbial mat deformed by slumping or a passing tool (chevron mark) (Ediacaran, *c.* 555–540 Ma, Lausitz Group, Butterberg Quarry near Bernsdorf, Cadomian basement of the Lausitz Antiform).

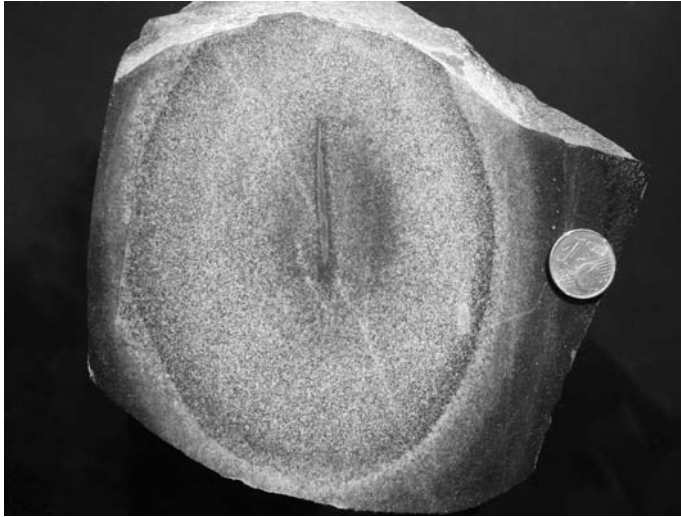


Fig. 7. Polished hand specimen of an early-diagenetic concretion with a mud clast in the centre. The concretion consists of calc-silicate rock and is developed in the greywacke layer of a turbidite (Ediacaran, c. 555–540 Ma, Lausitz Group, Butterberg Quarry near Bernsdorf, Cadomian basement of the Lausitz Antiform).



Fig. 8. Hemispherical bodies on the surface of a mudstone bed interpreted to be of organic origin (Ediacaran, c. 555–540 Ma, Lausitz Group, quarry Butterberg near Bernsdorf, Cadomian basement of the Lausitz Antiform).

intrusion of voluminous granitoid plutons. There is no noticeable tectonic thickening of the crust (Linnemann *et al.* 2000). Cadomian orogenic processes in the Saxo-Thuringian Zone are bracketed between c. 570–540 Ma (Linnemann *et al.* 2000). But there are also numerous detrital zircons from Ediacaran sediments in the range of c. 600–650 Ma, which most probably were also related to Cadomian orogenic processes (Linnemann *et al.* 2004). Lastly the record of detrital and inherited zircons points to a West African provenance for the Saxo-Thuringian Zone (Fig. 11) (Drost *et al.* 2004; Linnemann *et al.* 2004).

The oldest rocks in the Saxo-Thuringian Zone are sediments aged at c. 570 Ma (Linnemann *et al.* 2000). The general setting of these Late Neoproterozoic deposits in the Saxo-Thuringian Zone is interpreted in terms of a backarc basin generated on thinned continental crust, and flanked by a magmatic arc and a cratonic source (Fig. 9) (Linnemann *et al.* 2000; Buschmann *et al.* 2001). The existence of the latter is represented by: (1) Nd-model ages of Late Neoproterozoic to Cambro-Ordovician sediments in the range of c. 1.5–2.1 Ga (Linnemann & Romer 2002); (2) pre-Neoproterozoic detrital and inherited zircons, most of which are Palaeoproterozoic (Linnemann *et al.* 2004); and (3) passive margin sequences like the Weesenstein and Clanzschwitz Groups are extremely enriched in cratonic detrital zircons and characterized by the occurrence of highly mature sediments like the Purpurberg Quartzite (Linnemann 1991; Linnemann *et al.* 2004). Significant traces of the magmatic

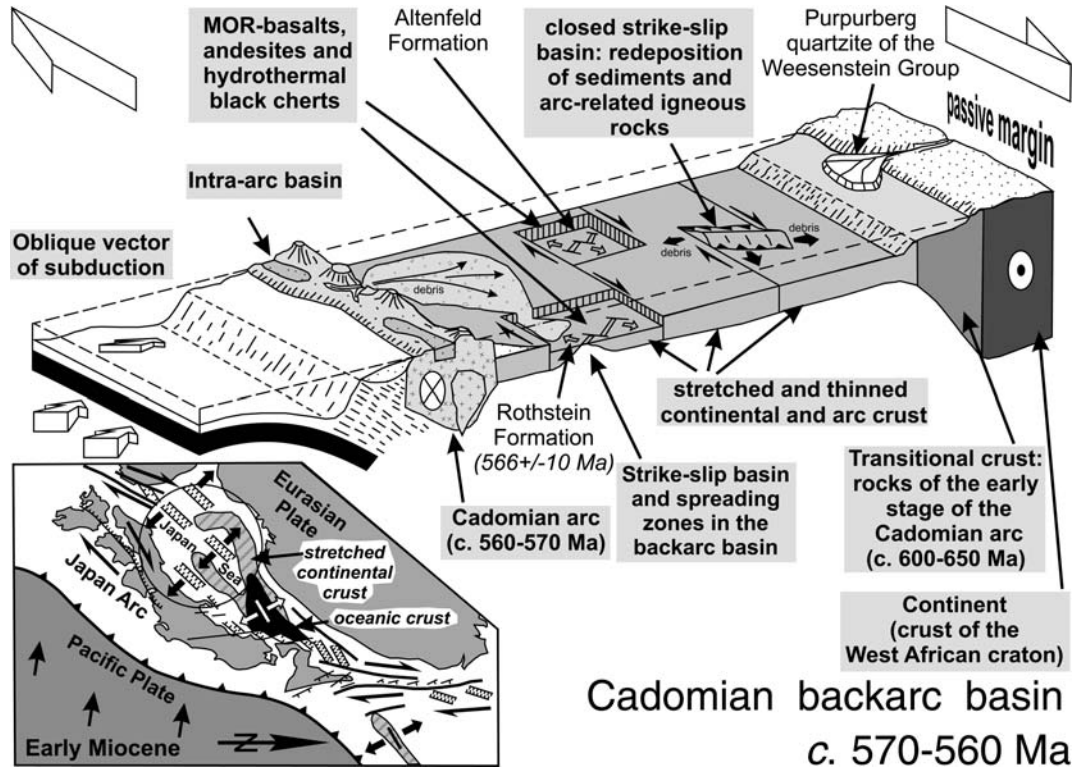


Fig. 9. Model of the geotectonic setting of Ediacaran rocks and development of the Cadomian backarc basin at c. 570–560 Ma derived from data of the Saxo-Thuringian Zone (Bohemian Massif). Not to scale. Please note: The basin consists of a continentward passive margin characterized by a stretched continental crust, accumulation of predominantly arc-derived debris, spreading zones with MORB-related rocks and the formation of hydrothermal black cherts (examples: Altenfeld Formation in the NW part of the Schwarzburg Antiform and the Rothstein Formation). Inset shows the sketch of an analogue plate tectonic configuration from the opening of the Japan Sea in the Western Pacific region during the Early Miocene (after Jolivet *et al.* 1992). Please note: The backarc basin of the Japan Sea is developed in large parts on stretched continental crust.

Cadomian retroarc basin c. 560-540 Ma

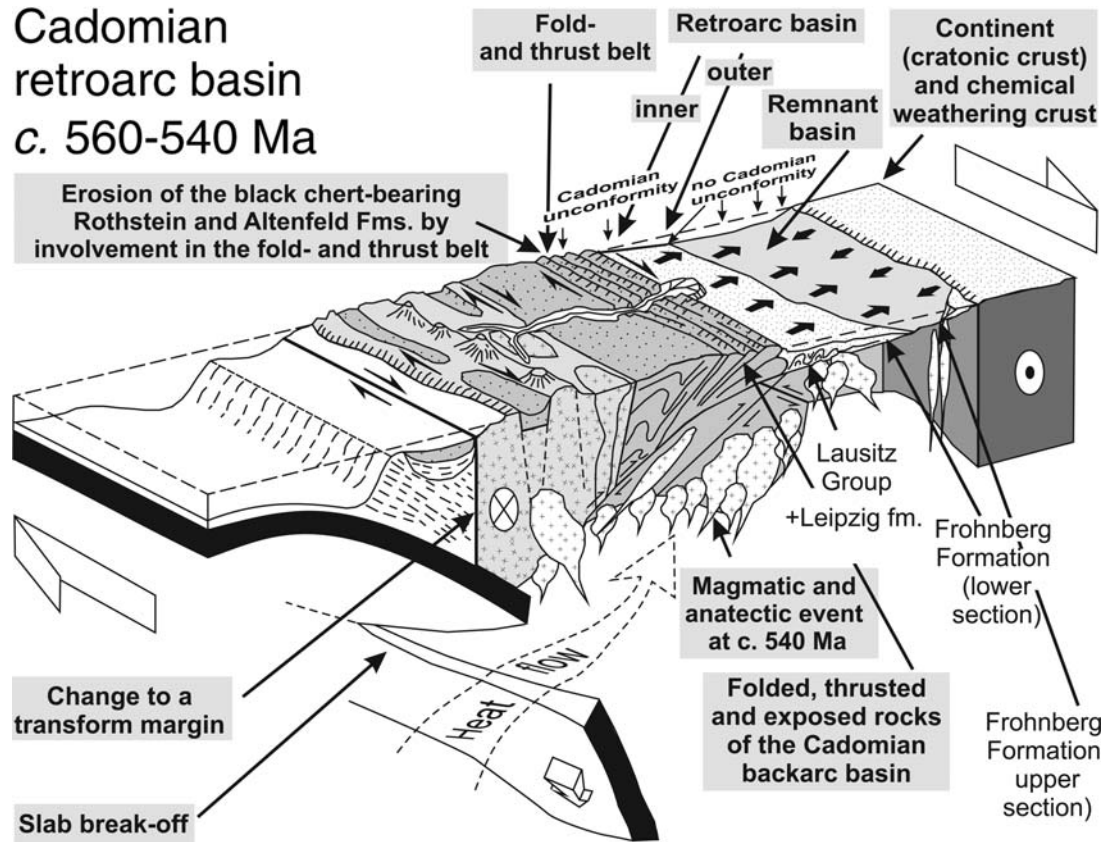


Fig. 10. Model of the geotectonic setting of Ediacaran rocks and the Cadomian retroarc basin at c. 560–540 Ma derived from data of the Saxo-Thuringian Zone (Bohemian Massif). Not to scale. Please note: There is no Cadomian unconformity in the continent-directed outer margin of the retroarc basin, because the Ediacaran sediments are not affected by any deformation (example: upper section of the Frohnberg Formation in the SE part of the Schwarzburg Antiform). In contrast, closer to the fold and thrust belt in the inner part of the retroarc basin, the sediments are deformed and, consequently, there is an unconformity observable between Neoproterozoic retroarc sediments and overstepping Cambro-Ordovician strata (example: Cadomian unconformities at the top of the Lausitz Group and the Leipzig Formation).

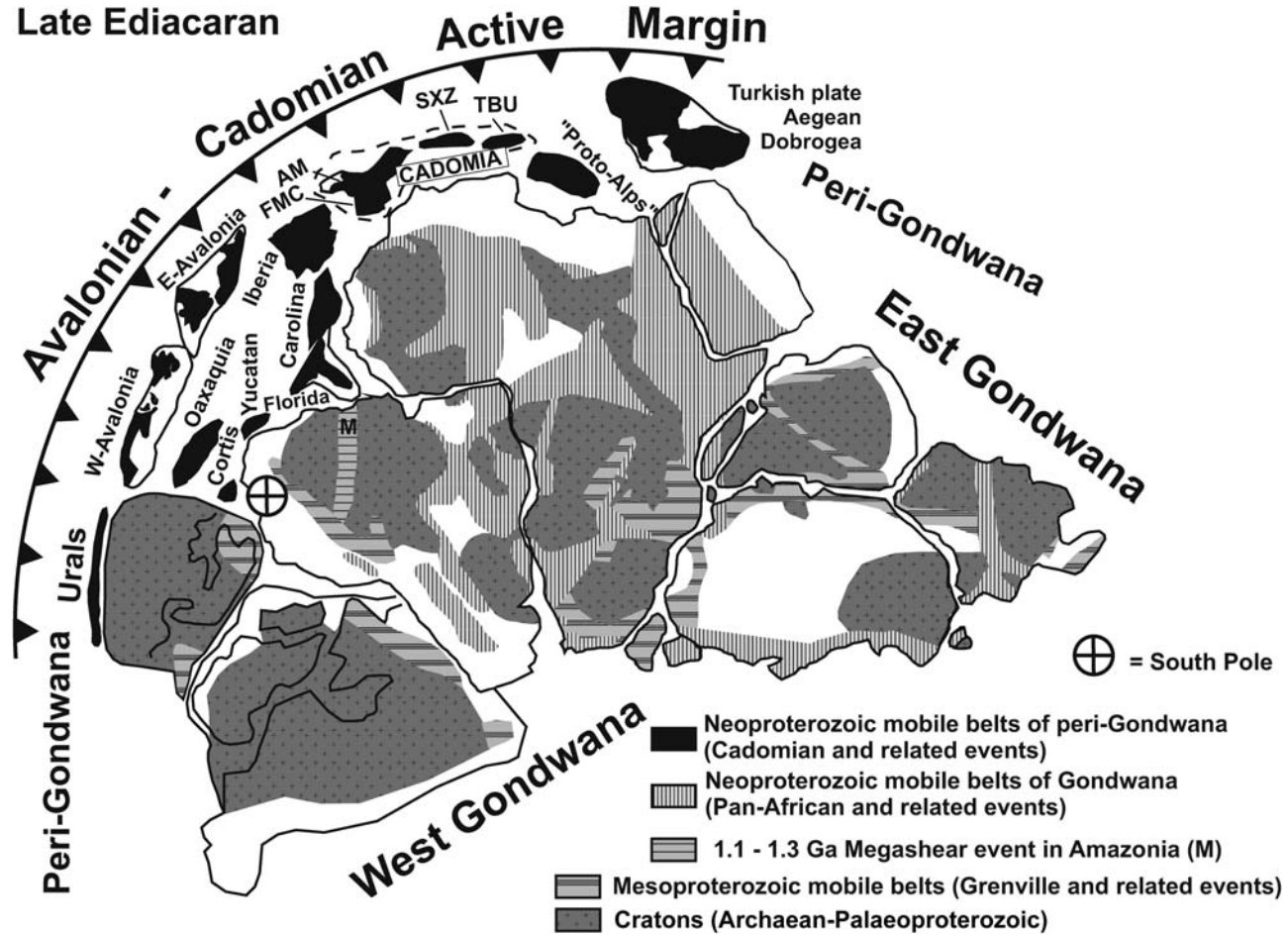


Fig. 11. Palaeogeography of the Cadomian—Avalonian active margin and related prominent peri-Gondwanan terranes at c. 580–560 Ma (modified after Nance & Murphy 1994, 1996; Linnemann *et al.* 2000; Murphy *et al.* 2004; Linnemann & Romer 2002; Nance *et al.* 2004; Linnemann *et al.* 2004); palaeogeography of the Gondwanan continental plates after Unrug (1996). AM, Armorican Massif; FMC, French Central Massif; SXZ, Saxo-Thuringian zone (Bohemian Massif); TBU, Tepla-Barrandian unit (Bohemian Massif).

arc are represented by geochemical signatures of Late Neoproterozoic sediments, pointing to deposition in a continental arc setting (Buschmann 1995; Linnemann & Romer 2002; Drost *et al.* 2004). These sedimentary rocks show a felsic provenance, suggesting that the Cadomian arc was developed on a relatively thick arc root.

The main activity of the arc magmatism must be placed at *c.* 560–580 Ma. This is the age of the majority of detrital zircons in Ediacaran sediments (Linnemann *et al.* 2004).

Backarc spreading is best documented in the magmatism and hydrothermal activity of the Rothstein Formation (Fig. 9) (Buschmann 1995). The geochemistry of the volcanic rocks is diverse, comprising a suite of E-type MOR metabasalts to metaandesites, calc-alkaline metabasalts, and subordinate alkaline metabasalts. Effusive alkaline metabasalts form mini-pillow sequences, E-type MOR metabasalts pillow sequences, calc-alkaline metabasalts and metaandesites sills and dykes. The eruption modes, characterized by the formation of pillow sequences and sill emplacements in unconsolidated sediments, point to seafloor-spreading processes in thinned continental crust. Further, the presence of seafloor-spreading processes is supported by relics of hydrothermal activity in volcanic and sediment-hosted submarine environments (e.g. black cherts). The cherts reflect discharges of silica-rich hydrothermal fluids. The basin formation of the Rothstein Formation is attributed to submarine pull-apart processes in a strike-slip dominated active continental margin environment. Strike-slip motions resulted in re-sedimentation of unconsolidated sediments (Buschmann 1995). Seafloor spreading and hydrothermal activity point to the development of an oceanic substratum in a continental-margin back-arc facies. The sedimentation age of the Rothstein Formation was determined by SHRIMP U/Pb dating of zircons from a submarine tuff, and gave an age of 566 ± 10 Ma (Buschmann *et al.* 2001). The Altenfeld Formation, in the NW part of the Schwarzburg antiform, is characterized by the occurrence of black chert deposits and mafic igneous rocks. Therefore, the Altenfeld Formation is interpreted in this study to be an equivalent of the Rothstein Formation, indicating the same geotectonic setting.

The passive margin sequences of the Weesenstein and Clanzschwitz Groups were most probably deposited at approximately the same time as the Rothstein and the Altenfeld Formations. A model for the Cadomian backarc basin in the Saxo-Thuringian Zone can be reconstructed, based on the isochronous origin of passive margin sequences (Weesenstein and Clanzschwitz Groups) and the inner parts of the backarc basin

(Rothstein and Altenfeld Formations) (Fig. 9). The passive margin sequences of the Weesenstein and Clanzschwitz Groups occur in the southern flank of that area in the Saxo-Thuringian Zone, in which only weakly metamorphosed Late Ediacaran rock units are present (Fig. 2). On the opposite side of this area, in the external domain of the Saxo-Thuringian Zone, the Rothstein and Altenfeld Formations are located. This geographical situation is interpreted to be a result of the palaeoposition of the rock units in their original setting during Ediacaran time. There is strong evidence that the inner part of the Cadomian backarc basin in the Saxo-Thuringian zone is preserved in the external zone to the north, and its passive margin sequences are positioned to the south (Fig. 2).

Dating of granitoid pebbles from the Weesenstein and Clanzschwitz Groups, with ages at 577 ± 3 Ma and 568 ± 4 Ma (Linnemann *et al.* 2000), demonstrates the rapid exhumation of these granitoids in the source area. The rapid exhumation of *c.* 570 Ma old granitoid pebbles (Linnemann *et al.* 2000) and their deposition together with intraformational sediments in Ediacaran sediments (Linnemann 1991), and the style of the magmatism in the Rothstein Formation (Buschmann 1995) suggest that intense strike-slip processes took place during the history of the backarc basin. Local sub-basins, which opened in the backarc basin in a strike-slip-regime, may also have contributed sediments, including material derived from the underlying stretched crust. Comparing this with a similar situation in Avalonia, Nance and Murphy (1994) proposed a model assuming the oblique vector of subduction beneath the arc leading to strike-slip motions in the backarc basin. The model of backarc spreading, oblique running subduction, and resulting effects is shown in Figure 9. The geotectonic setting is comparable to a modern equivalent in the Western Pacific (inset, in Fig. 9).

Ediacaran rocks of the Cadomian retroarc basin

Most of the well-preserved Ediacaran sedimentary rocks in the Saxo-Thuringian Zone belong to the Lausitz Group (Lausitz Antiform), Leipzig Formation (North Saxon Antiform) and Frohnberg Formation (SE part of the Schwarzburg Antiform). These units are characterized by monotonous series of dark-grey greywacke turbidites, with intercalation of conglomerates and microconglomerates. The latter often show fragments of granitoids, metasediments and black cherts. The flysch-like character and abundant chert fragments, both in the conglomerates and in the sandy grain fraction,

show that these sedimentary complexes differ very much from backarc basin deposits.

The primary and massive deposits of black cherts are a distinct feature of the Rothstein and Altenfeld Formations from the Cadomian backarc basin. Because of the frequent occurrence of black chert fragments, it is suggested in this paper that the Lausitz Group and the Leipzig and Frohnberg Formations consist mostly of debris derived from reworked parts of the backarc basin.

In view of their spatial distribution, the Lausitz Group, and the Leipzig and Frohnberg Formations are positioned between the deposits from the inner backarc basin in the north (Rothstein and Altenfeld Formations) and the passive margin deposits to the south (Weesenstein and Clanzschwitz Groups).

Because of the occurrence of chert fragments in the monotonous turbidites and conglomerates, there is strong evidence that: (1) the Lausitz Group and the Leipzig/Frohnberg Formations are significantly younger than the deposits of the Cadomian backarc basin; and (2) that these sedimentary units are composed mostly of the eroded material derived from the deposits of the backarc basin. SHRIMP-U/Pb dating of detrital zircon grains in the Lausitz Group and the Frohnberg Formation has shown that these deposits are younger than 555 ± 9 Ma and 551 ± 8 Ma, respectively (Fig. 3) (Linnemann *et al.* 2004). Further, in these sequences, primary sedimentary structures occur such as water escape structures, soft pebbles and seismites: these are typical of rapid sedimentation and seismic vibrancies (Figs 5, 6) (Linnemann 2003). Because of age constraints and basin history, the Lausitz Group and the Leipzig/Frohnberg Formations are interpreted as parts of a Cadomian retroarc basin or foreland basin, respectively (Fig. 10). The retroarc basin was formed during the collision of the Cadomian magmatic arc with the West African Craton, and the closure of the backarc basin. The inner part of the retroarc basin was folded and thrust, whereas the outer part was not deformed. Consequently, the more northern Lausitz Group and Leipzig Formation were deformed before the magmatic event at *c.* 540 Ma occurred (Linnemann *et al.* 2000). An angular Cadomian Unconformity between Ediacaran rocks and Cambro-Ordovician deposits can be observed (Linnemann & Buschmann 1995*a, b*). In contrast, there is no evidence for of a Cadomian deformation of the Frohnberg Formation in the SE part of the Schwarzbürg Antiform. Therefore, in our interpretation, the Frohnberg Formation was originated more distally from the fold and thrust belt that was feeding the assumed Cadomian retroarc basin. This part of the sedimentary system escaped the Cadomian deformation (Fig. 10). The palaeogeographic position of the Frohnberg Formation is proximal to the

cratonic hinterland, whereas the folded and thrust sediments of the Lausitz Group and the Leipzig Formation are more distal to the craton, and more proximal to the colliding arc (Fig. 10).

The lower part of the Frohnberg Formation is composed of thick-bedded greywacke turbidites and some conglomeratic layers of a deeper marine basin. In contrast the *c.* 100 m thick upper part of the Frohnberg Formation displays features of deposition in a shallower basin: this is documented by: (1) rare findings of hummocky cross-stratification in sandstones; (2) the occurrence of laminated mudstones reflecting a muddy coast; and (3) a topmost upward-thickening bed set of quartzite layers (former sandstone bed sets). The latter show a much higher maturity than the greywackes from the lower part of the section (Linnemann 2003). These characteristics of the Frohnberg Formation show that the retroarc basin ended at the top of the lower part of the Frohnberg formation. The deposition of sediments in the upper part of the Frohnberg formation was probably controlled by shallower sedimentation in a remnant basin, which was placed in front of the outer retroarc deposits (Fig. 10). The uppermost quartzite bed of the section is often referred to as 'Basisquarzit' (=basal quartzite) in the traditional German literature. This quartzite layer represents the youngest Ediacaran sediment in the pile of sediments, because it is the final bed of a continuous thickening-upward section in the remnant basin. The traditional German name 'Basisquarzit' is confusing, because in former time the quartzite was believed to be the base of the Cambrian. This interpretation was done without any palaeontological or geochronological data.

The Cadomian retroarc basin and the related remnant basin were short-lived depositional systems. The age of these sediments is bracketed between *c.* 555–540 Ma. The Precambrian-Cambrian boundary dated at 542 Ma (Bowring *et al.* 2003) has not been observed in the Saxo-Thuringian Zone.

The deposits of the backarc and retroarc basins were both intruded by voluminous granitoid plutons (e.g. the Lausitz Granitoid Complex (539 ± 6 Ma), the Glasbach Granite (533 ± 4 Ma), the Laubach granite (541 ± 7 Ma), the Schildau Massif (530 ± 8 Ma), the Laas Granodiorite (531 ± 7 Ma) and the Dohna Granodiorite (537 ± 7 Ma) (Linnemann *et al.* 2000)). These granitoids are anatectic, and show a large amount of inherited zircons with the same ages as the zircon populations from the Late Neoproterozoic sediments (Linnemann *et al.* 2000, 2004; Gehmlich 2003; Tichomirowa 2003). Most of these granitoids were derived from molten Ediacaran sedimentary rocks. This interpretation is supported by

geochemical data and greywacke xenoliths in the granitoids, which range from granites and granodiorites to rare tonalites (Hammer 1996). The magmatic and anatectic event at *c.* 540 Ma is expressed by the intrusion of granodiorites (Linnemann *et al.* 2000). The intense heat flow and the lack of evidence of a much-thickened crust, allows only two explanations: (1) slab break-off; or (2) delamination of the crust. The latter is restricted to orogens resulting from continent-continent collision and the formation of a thick orogenic root. The slab break-off of the subducted oceanic plate is typical of active margin settings: in view of the known data, this is a more likely case for the Cadomian orogenic processes (Fig. 10).

All the processes resulting from the activity of the Cadomian magmatic arc (the opening of the Cadomian backarc basin (*c.* 560–570 Ma), its closure by the arc-continent collision resulting in the formation of a retroarc basin (>*c.* 560 Ma and <*c.* 540 Ma) and the magmatic/anatectic event at *c.* 540 Ma) can be attributed to Cadomian orogenic processes, which formed a part of the Cadomian orogen at the margin of the West African Craton (Fig. 11). This is the geotectonic framework within which the Ediacaran rock units of the Saxo-Thuringian Zone originated.

Conclusions

Available data and field observations allow the reconstruction the geotectonic setting during the Ediacaran period and Early Cambrian in the Saxo-Thuringian Zone (NE Bohemian Massif, Germany):

- Ediacaran rocks of the Saxo-Thuringian Zone were formed in an active margin setting during Cadomian orogenic processes on the periphery of the West African Craton (peri-Gondwana).
- Ediacaran rocks of the Saxo-Thuringian Zone are younger than *c.* 570 Ma.
- Activity of the Cadomian magmatic arc starts in a Cordilleran-type margin setting at *c.* 600–650 Ma, as shown by detrital and inherited zircons in younger Ediacaran rocks.
- A Cadomian backarc basin with a passive margin and the outboard sitting Cadomian magmatic arc commenced at *c.* 570–560 Ma on stretched continental crust in a strike-slip regime.
- There is some evidence, but no certain proof, for a local glaciation during the deposition of the passive margin sequence in the backarc basin.
- The Cadomian magmatic arc collided with the cratonic hinterland, resulting in the closure of the backarc basin and the formation of a

Cadomian retroarc basin between *c.* 555 Ma and *c.* 540 Ma.

- Mat grounds ('elephant skin') and hemispherical bodies, interpreted to be of organic origin, were observed in the retroarc basin.
- Slab break-off of the subducted oceanic plate caused a magmatic/anatectic event culminating in the earliest Cambrian at *c.* 540 Ma.

D. Gray (Melbourne University) and R. Squire (Monash University) are thanked for their critical reviews. The author also thanks very much P. Vickers-Rich and P. Komarower (Monash University) for editorial assistance.

References

- BANKWITZ, P., BANKWITZ, E., KRAMER, W. & PIN, C. 1992. Early Paleozoic bimodal volcanism in the Vesser area, Thuringian Forest, eastern Germany. *Zentralblatt für Geologie und Paläontologie*, **1**, 1113–1132.
- BARROIS, C. 1899. Sketch of the Geology of Brittany. *Proceedings of the Geologists' Association*, **16**, 101.
- BERTRAND, L. 1921. *Histoire de la Formation du Sous-sol de la France. Les Anciennes Mers de la France et leurs Dépôts*. Flammarion, Paris.
- BOWRING, S. A., RAMEZANI, J. & GROTZINGER, J. P. 2003. High-precision U–Pb geochronology and the Cambrian-Precambrian boundary. *In: NUNA Conference 2003, New frontiers in the fourth dimension: Generation, calibration and application of geological time scales, Mont Tremblant, Québec, March 15–18, 2003*. Geological Association of Canada.
- BUNEL, H. 1835. Observations sur les terrains intermédiaires du Calvados. *Mémoires de la Société Linnéenne de Normandie*, **5**, 99–100.
- BUSCHMANN, B. 1995. *Geotectonic facies analysis of the Rothstein Formation (Neoproterozoic, Saxothuringian Zone, Germany)*. (Unveröffentlichte Dissertation), Bergakademie Freiberg, Freiberg.
- BUSCHMANN, B., NASDALA, L., JONAS, P., LINNEMANN, U. & GEHMLICH, M. 2001. SHRIMP U–Pb dating of tuff-derived and detrital zircons from Cadomian marginal basin fragments (Neoproterozoic) in the northeastern Saxothuringian Zone (Germany). *Neues Jahrbuch für Geologie und Paläontologie, Monatshefte*, **2001**, 321–342.
- BUSCHMANN, B., ELICKI, O. & JONAS, P. 2006. The Cadomian unconformity in the Saxo-Thuringian Zone, Germany: palaeogeographic affinities of Ediacaran (terminal Neoproterozoic) and Cambrian strata. *Precambrian Research*, **147**, 387–403.
- DÖRR, W., FIALA, J., VEJNAR, Z. & ZULAUF, G. 1998. U–Pb zircon ages and structural development of meta-granitoids of the Teplá crystalline complex: evidence for pervasive Cambrian plutonism within the Bohemian massif (Czech Republic). *Geologische Rundschau*, **87**, 135–149.
- DÖRR, W., ZULAUF, G., FIALA, J., FRANKE, W. & VEJNAR, Z. 2002. Neoproterozoic to Early Cambrian

- history of an active plate margin in the Teplá-Barrandian unit—a correlation of U–Pb isotopic-dilution-TIMS ages (Bohemia, Czech Republic). *Tectonophysics*, **352**, 65–85.
- DÖRR, W., FINGER, F., LINNEMANN, U. & ZULAUF, G. 2004. The Avalonian–Cadomian Belt and related peri-Gondwanan terranes. *International Journal of Earth Sciences (Geologische Rundschau)*, **93**, 657–658.
- DROST, K., LINNEMANN, U., MCNAUGHTON, N., FATKA, O., KRAFT, P., GEHMLICH, M., TONK, C. & MAREK, J. 2004. New data on the Neoproterozoic — Cambrian geotectonic setting of the Teplá-Barrandian volcano-sedimentary successions: geochemistry, U–Pb zircon ages, and provenance (Bohemian Massif, Czech Republic). *International Journal of Earth Sciences (Geologische Rundschau)*, **93**, 742–757.
- DUFRENOY, P. A. 1838. Mémoire sur l'âge et la composition des terrains de transition de l'Ouest de la France. *Annales des Mines*, **3**, 91–100.
- FINGER, F., HANS, P., PIN, C., VON QUAD, A. & STIRRER, H. P. 2000. The Brunovistulian: Avalonian Precambrian sequence at the eastern end of the Central European Variscides. In: FRANKE, W., HAAK, U., ONCKEN, O. & TANNER, D. (eds) *Orogenic Processes: Quantification and Modelling in the Variscan Belt*. Geological Society, London, Special Publications, **179**, 103–112.
- FRANKE, W. & ŻELAZNIEWICZ, A. 2002. Structure and evolution of the Bohemian arc. *Geological Society, London, Special Publications*, **201**, 279–293.
- FRIEDL, G., FINGER, F., MCNAUGHTON, N. J. & FLETCHER, I. R. 2000. Deducing the ancestry of terranes: SHRIMP evidence for South America-derived Gondwana fragments in Central Europe. *Geology*, **28**, 1035–1038.
- FRIEDL, G., FINGER, F., PAQUETTE, J. L., VON QUAD, A., MCNAUGHTON, N. J. & FLETCHER, I. R. 2004. Pre-Variscan geological events in the Austrian part of the Bohemian Massif deduced from U–Pb zircon ages. *International Journal of Earth Sciences (Geologische Rundschau)*, **93**, 802–823.
- GEBAUER, D. & FRIEDL, G. 1994. A 1.38 Ga protolith age for the Dobra orthogneiss (Moldanubian Zone of the Southern Bohemian Massif, NE-Austria): Evidence from ion-microprobe (SHRIMP) dating of zircon. Abstract. *Journal of the Czech Geological Society*, **39/1**, 34–35.
- GEHMLICH, M. 2003. Die Cadomiden und Varisziden des Saxothuringischen Terranes—Geochronologie magmatischer Ereignisse. *Freiberger Forschungshefte*, **2003**, 1–129.
- GLASMACHER, U. A., BAUER, W., CLAUER, N. & PUCHKOV, V. N. 2004. Neoproterozoic metamorphism and deformation at the southeastern margin of the East European Craton, Uralides, Russia. *International Journal of Earth Sciences (Geologische Rundschau)*, **93**, 921–944.
- GRAINDOR, M. J. 1957. Le Briovérien dans le Nord-Est du Massif Armoricain. *Mémoires pour servir à l'explication de la Carte Géologique Détaillée de la France*, Paris.
- HAMMER, J. 1996. Geochemie und Petrogenese der cadomischen und spätvariszischen Granitoide der Lausitz. *Freiberger Forschungshefte*, **C 463**, 107.
- HAMMER, J., EIDAM, J., RÖBER, B. & EHLING, B.-C. 1999. Prävariszischer und variszischer granitoider Magmatismus am NE-Rand des Böhmisches Maasivs—Geochemie und Petrogenese. *Zeitschrift für Geologische Wissenschaften*, **27**, 401–415.
- HEUSE, T., KRONER, U. & BARTL, S. 2001. Tektono- und lithostratigraphische Kartierungskriterien für den Zentralteil des Schwarzburger Sattels. *Geowissenschaftliche Mitteilungen von Thüringen*, **9**, 107–124.
- JOLIVET, L. M., FOURNIER, P., HUCHNON, V. S., ROZHDESTVENSKIY, K. F. S. & OSCORBIN, L. S. 1992. Cenozoic intracontinental dextral motion in the Okhotsk-Japan Sea region. *Tectonics*, **11**, 968–977.
- KEMNITZ, H., ROMER, R. L. & ONCKEN, O. 2002. Gondwana breakup and the northern margin of the Saxothuringian belt (Variscides of Central Europe). *Geologische Rundschau*, **91**, 246–259.
- KERFORNE, F. 1901. Discordance du Cambrien sur le Précambrien, près de Rennes. *Bulletin de la Société Géologique de France*, **4**, 2587–2590.
- KOSSMAT, F. 1927. Gliederung des varistischen Gebirgsbaues. *Abhandlungen des Sächsischen Geologischen Landesamtes*, **1**, 1–39.
- KOZDRÓJ, W., KRENTZ, O. & OPLETAL, M. E. 2001. *Geological Map Lausitz-Jizera-Karkonosze (without Cenozoic sediments), 1:100 000, and Comments*. Warsaw, Państwowy Instytut Geologiczny, **64**.
- LINNEMANN, U. 1991. Glazieostatisch kontrollierte Sedimentationsprozesse im Oberen Proterozoikum der Elbezone (Weesensteiner Gruppe/Sachsen). *Zentralblatt für Geologie und Paläontologie*, **I(12)**, 2907–2934.
- LINNEMANN, U. 2003. Sedimentation und geotektonischer Rahmen der Beckenentwicklung im Saxothuringikum (Neoproterozoikum-Unterkarbon). In: LINNEMANN, U. (ed.) *Das Saxothuringikum-Abriss der Präkambrischen und Paläozoischen Geologie von Sachsen und Thüringen*. Geologica Saxonica, **48/49**, 71–110.
- LINNEMANN, U. & BUSCHMANN, B. 1995a. Der Nachweis der cadomischen Diskordanz in einer Tiefenbohrung bei Gera und deren Bedeutung für das proterozoisch-paläozoische Standardprofil im Schwarzburger Antiklinorium. *Geowissenschaftliche Mitteilungen von Thüringen*, **3**, 1–11.
- LINNEMANN, U. & BUSCHMANN, B. 1995b. Die cadomische Diskordanz im Saxothuringikum (oberkambrisch-tremadocische overlap-Sequenzen). *Zeitschrift für Geologische Wissenschaften*, **23**, 707–727.
- LINNEMANN, U. & ROMER, R. L. 2002. The Cadomian orogeny in Saxo-Thuringia, Germany: geochemical and Nd–Sr–Pb isotopic characterization of marginal basins with constraints to geotectonic setting and provenance. *Tectonophysics*, **352**, 33–64.
- LINNEMANN, U. & SCHAUER, M. 1999. Die Entstehung der Elbezone vor dem Hintergrund der cadomischen und variszischen Geschichte des saxothuringischen Terranes. *Zeitschrift für Geologische Wissenschaften*, **27**, 529–561.
- LINNEMANN, U., GEHMLICH, M., TICHOMIROVA, M., BUSCHMANN, B., NASDALA, L., JONAS, P., LÜTZER, H. & BOMBACK, K. 2000. From Cadomian

- subduction to Early Paleozoic rifting: the evolution of Saxo-Thuringia at the margin of Gondwana in the light of single zircon geochronology and basin development (Central European Variscides, Germany). *Geological Society, London, Special Publication*, **179**, 131–153.
- LINNEMANN, U., MCNAUGHTON, N. J., ROMER, R. L., GEHMLICH, M., DROST, K. & TONK, C. 2004. West African provenance for Saxo-Thuringia (Bohemian Massif): Did Armorica ever leave pre-Pangean Gondwana?—U/Pb-SHRIMP zircon evidence and the Nd-isotopic record. *International Journal of Earth Sciences*, **93**, 683–705.
- MAZUR, S., TURNIAK, K. & BRÖCKER, M. 2004. Neoproterozoic and Cambro-Ordovician magmatism in the Variscan Klodzko Metamorphic Complex (West Sudetes, Poland): new insights from U/Pb zircon dating. *International Journal of Earth Sciences (Geologische Rundschau)*, **93**, 758–772.
- MCILROY, D., CRIMES, T. P. & PAULEY, J. C. 2005. Fossils and matgrounds from the Neoproterozoic Longmyndian Supergroup, Shropshire, UK. *Geological Magazine*, **142**, 441–455.
- MURPHY, J. B. & NANCE, R. D. 1991. Supercontinent model for the contrasting character of Late Proterozoic orogenic belts. *Geology*, **19**, 469–472.
- MURPHY, J. B., PISAREVSKY, S. A., NANCE, R. D. & KEPPIE, J. D. 2004. Neoproterozoic Early Paleozoic evolution of peri-Gondwanan terranes: implications for Laurentia–Gondwana connections. *International Journal of Earth Sciences (Geologische Rundschau)*, **93**, 659–682.
- NANCE, R. D. & MURPHY, J. B. 1994. Contrasting basement isotopic signatures and the palinspastic restoration of peripheral orogens: Example from the Neoproterozoic Avalonian-Cadomian belt. *Geology*, **22**, 617–620.
- NANCE, R. D. & MURPHY, J. B. 1996. Basement isotopic signatures and Neoproterozoic paleogeography of Avalonian-Cadomian and related terranes in the circum-North Atlantic. In: NANCE, R. D. & THOMPSON, M. D. (eds) *Avalonian and Related Peri-Gondwanan Terranes of the Circum-North Atlantic*. Geological Society of America Special Paper, **304**, 333–346.
- NANCE, R. D., MURPHY, J. B. & KEPPIE, J. D. 2002. A Cordilleran model for the evolution of Avalonia. *Tectonophysics*, **352**, 11–31.
- ROBARDET, M. 2002. Alternative approach to the Variscan Belt in southwestern Europe: Preorogenic paleobiogeographical constraints. In: MARTINEZ CATALAN, J. R., HATCHER, R. D. J., ARENAS, R. & DIAZ GARCIA, F. (eds) *Variscan-Appalachian Dynamics: The Building of the Late Paleozoic Basement*. Geological Society of America Special Paper, **364**, Boulder, 1–15.
- ROBERTS, D. & SIEDLECKA, A. 2002. Timanian orogenic deformation along the northwestern margin of Baltica, Northwest Russia and Northeast Norway, and Avalonian-Cadomian connections. *Tectonophysics*, **352**, 169–184.
- TAIT, J. A., BACHTADSE, V., FRANKE, W. & SOFFEL, H. C. 1997. Geodynamic evolution of the European Variscan fold belt: paleomagnetic and geological constraints. *Geologische Rundschau*, **86**, 585–598.
- TAIT, J., SCHÄTZ, M., BACHTADSE, V. & SOFFEL, H. C. 2000. Palaeomagnetism and Palaeozoic palaeogeography of Gondwana and European terranes. In: FRANKE, W., HAAK, V., ONCKEN, O. & TANNER, D. (eds) *Orogenic Processes: Quantification and Modelling in the Variscan Belt*. The Geological Society, London, Special Publications, **179**, 21–34.
- TEIPEL, U., EICHHORN, R., LOTH, G., ROHRMÜLLER, J., HÖLL, R. & KENNEDY, A. 2004. U–Pb SHRIMP and Nd isotopic data from the western Bohemian Massif (Bayerischer Wald, Germany): Implications for Upper Vendian and Lower Ordovician magmatism. *International Journal of Earth Sciences (Geologische Rundschau)*, **93**, 782–801.
- TICHOMIROVA, M. 2003. Die Gneise des Erzgebirges—hochmetamorphe Äquivalente von neoproterozoisch-frühpaläozoischen Grauwacken und Granitoiden der Cadomiden. *Freiberger Forschungshefte*, **C 495**, 1–222.
- UNRUG, R. 1996. *Geodynamic Map of Gondwana Supercontinent Assembly*. 1:10 000 000. Council for Geosciences, Bureau de Recherches Géologiques et Minières, Orléans.
- VAN DER VOO, R. 1979. Paleozoic assembly of Pangea: a new plate tectonic model for the Taconic, Caledonian and Hercynian orogenies. *EOS Transactions of the American Geophysical Union*, **60**, 241.
- VENERA, Z., SCHULMANN, K. & KRÖNER, A. 2000. Intrusion within a transitional tectonic domain: the Cistá granodiorite (Bohemian Massif)—structure and rheological modelling. *Journal of Structural Geology*, **22**, 1437–1454.
- WINDLEY, B. F. 1996. *The Evolving Continents*. Wiley & Sons, 3rd Edition.
- WENDT, J. I., KRÖNER, A., FIALA, J. & TODT, W. 1993. Evidence from zircon dating for existence of approximately 2.1 Ga old crystalline basement in southern Bohemia, Czech Republic. *Geologische Rundschau*, **82**, 42–50.
- ŽELAŽNIEWICZ, A., DÖRR, W., BYLINA, P. ET AL. 2004. The eastern continuation of the Cadomian orogen: U–Pb zircon evidence from Saxo-Thuringian granitoids in south-western Poland and the northern Czech Republic. *International Journal of Earth Sciences (Geologische Rundschau)*, **93**, 773–781.
- ZULAUF, G., DÖRR, W., FIALA, J. & VEJNAR, Z. 1997. Late Cadomian crustal tilting and Cambrian transtension in the Teplá-Barrandian unit (Bohemian Massif, Central European Variscides). *International Journal of Earth Sciences (Geologische Rundschau)*, **86**, 571–584.

Siliciclastic prelude to Elatina–Nuccaleena deglaciation: lithostratigraphy and rock magnetism of the base of the Ediacaran system

T. D. RAUB, D. A. D. EVANS & A. V. SMIRNOV

Department of Geology and Geophysics, Yale University, New Haven, CT 06520-8109 USA (e-mail: timothy.raub@yale.edu)

Abstract: The basal Ediacaran global boundary stratotype section and point (GSSP) horizon beneath Nuccaleena Formation cap dolostone in South Australia's central Flinders Ranges South Australia coincides with an interpreted unconformity preceding deglacial transgression. Detailed lithostratigraphy of three sections across the base of the Ediacaran System at its type area reveals contrasting character of the Elatina Formation—Nuccaleena Formation transition across c. 9 km of exposure, changing the interpretive context of the GSSP.

We suggest that a locally pervasive, incisive flaser-bedded sandstone exposed between Elatina diamictites and Nuccaleena cap dolostone lies above an unconformity that correlates with the defined base of Wilpena Group, reflecting onset of terminal Elatina 'Snowball Earth' deglaciation and dynamic interplay between eustatic sea level change and isostatic rebound. Nuccaleena cap dolostone is sedimentologically mixed and conformable with underlying siliciclastics at Elatina Creek; hence the recently defined Ediacaran GSSP horizon, at the base of solid cap carbonate at Enorama Creek, lies in continuous section and not at an unconformity.

Nuccaleena Formation cap dolostone contains pervasive terrigenous debris, including apparently detrital hematite. While magnetite and/or maghemite is produced in abundance upon heating of the cap carbonate above c. 400°C, and we cannot exclude secondary origin of any Nuccaleena magnetite, Nuccaleena Formation cap dolostone should preserve primary magnetization.

Cap carbonates overlying late Neoproterozoic glacial rocks in Australia, and presumed correlative supraglacial carbonates around the world, are considered to record the aftermath of a glaciation of Marinoan age (widely termed 'Marinoan glaciation' e.g. Kennedy 1996; Kennedy *et al.* 1998; Evans 2000; Hoffman & Schrag 2002; here termed 'Elatina glaciation' to emphasize region-specific, and not necessarily globally-generalizable implications, for 'Snowball Earth' climate dynamics). In South Australia's Adelaide Rift Complex, the type-Marinoan Series (Preiss 1987, 1993, 2000) includes ferric siliciclastic units correlated to Elatina Formation, which variably exhibit undeniably glaciogenic facies (Lemon & Gostin 1990) deposited at low palaeolatitude (Embleton & Williams 1986; Sumner *et al.* 1987; Schmidt *et al.* 1991; Schmidt & Williams 1995; Sohl *et al.* 1999).

Although Lemon & Gostin (1990) considered all Elatina Formation in central Flinders Ranges as deposited following peak glaciation, subsequent development of 'hard' (e.g. Hoffman *et al.* 1998; Hoffman & Schrag 2002; Goodman & Pierrehumbert 2003; Halverson *et al.* 2004; Bodiselitch *et al.* 2005; Hoffman *et al.* 2005; Kasemann *et al.* 2005; Pollard & Kasting 2005; Pierrehumbert 2005) and 'soft' (e.g. Kirschvink 1992; Hyde *et al.* 2000; Kennedy *et al.* 2001) 'Snowball

Earth' hypotheses offer considerable interpretive flexibility for assigning stratigraphic intervals of either monotonic or alternating waxing and waning to the Elatina ice age. Frequently, terminal Elatina deglaciation is hypothesized to begin during a depositional hiatus between the Elatina Formation and the overlying Nuccaleena Formation, at a level where siliciclastics traditionally assigned to Elatina Formation and equivalents in central Flinders Ranges contact 'cap' dolostone of Nuccaleena Formation (e.g. Christie-Blick *et al.* 1995; Kennedy 1996; implied as the base of the cap carbonate transgressive system tract by Knoll *et al.* 2004; Knoll *et al.* 2006; though Hoffman 2005 and Nogueira *et al.* 2003 interpret minimal hiatus beneath cap carbonates in Namibia and Brazil, respectively). For extended discussion of Elatina Formation, Nuccaleena Formation, and hypothesized correlative lithofacies outside central Flinders Ranges, see Preiss (1992), Preiss *et al.* (1998) and Preiss (2000).

The first part of this paper modifies this definition by placing the basal Nuccaleena Formation sequence boundary within siliciclastics that has been traditionally assigned to the Elatina Formation beneath Nuccaleena Formation cap dolostone, an interpretation permitted, though not explicated, by Lemon & Gostin (1990). The threefold division and basinal correlation of Elatina Formation by

those authors, modified and extended by Preiss (1992, 2000) and Preiss *et al.* (1998) may readily fit the observations described here if this basal Nuccaleena Formation siliciclastic facies is unique, or if it correlates with Sealcliff sandstone. This siliciclastic unit may also correlate with uppermost Reynella siltstone or uppermost Ketchowla siltstone, if deposition persisted in the Oraparinna diapir salt-withdrawal syncline during erosion or non-deposition of coeval strata in the type-areas of those members. This condition is required in order to permit observed unconformity of Wilpena Group atop Elatina Formation equivalents in those locations. All three possibilities are discussed later; with the first two preferred over the third.

Nuccaleena Formation cap dolostone

Throughout Adelaide Rift Complex, Nuccaleena Formation is reported to show several contact relations with underlying siliciclastics. As summarized by Preiss (1987, 1992, 2000) and Preiss *et al.* (1998), the Umberatana Group—Wilpena Group boundary is a fundamental erosional surface, and the bedding of basal Wilpena Group Nuccaleena Formation or Brachina Formation equivalents is frequently low-angle discordant and only locally concordant with Elatina-correlative siliciclastics. Where concordant, the basal Nuccaleena contact is generally sharp, often recessive, and in places disconformable above an uppermost-Elatina pebble-bearing lag deposit. Lemon & Gostin (1990) interpret rare, calcareous-weathering Elatina horizons within centimetres of basal Nuccaleena Formation cap dolostone at the Enorama Creek GSSP as an exceptional ‘gradational’ (more accurately, mixed) formational transition. Subsequent workers tend to favour invoking Nuccaleena-age diagenetic carbonate fronts invading downward through pre-deposited siliciclastics to create layering at this particular outcrop (N. Christie-Blick and J. Gehling, pers. comm. 2004).

In light of the global expression of late Neoproterozoic ‘Snowball Earth’ cap carbonates, these collective indications of unconformity at the base of Nuccaleena Formation cap dolostone were used to construct a close approximation of a globally synchronous surface, thereby defining the Ediacaran Period GSSP at the base of solid cap carbonate in Enorama Creek, central Flinders Ranges, South Australia (Christie-Blick *et al.* 1995; Knoll *et al.* 2004; Knoll *et al.* 2006). Observations described in this paper demonstrate that, at least in the GSSP-hosting Oraparinna diapir salt-withdrawal syncline, the unconformity more accurately lies within defined Elatina Formation; and Nuccaleena Formation (basal Wilpena Group) must be

redefined downward to contain initial siliciclastic lithofacies. The Enorama Creek GSSP horizon, consequently, need not be considered controversial for occupying an assumed unconformable surface.

Generally, Nuccaleena Formation cap dolostone varies in thickness and continuity of character. Where dominated by nearly continuous, low-angle to parallel-bedded peloidal dolomicrite in central Flinders Ranges, Nuccaleena Formation cap dolostone is everywhere at least 75 cm thick and ranges to approximately 10 metres, averaging about 3–4 m. Discontinuous expression of carbonate spans *c.* 50 m near Leigh Creek (Preiss 1987). The typical <10 m thick Nuccaleena Formation cap dolostone of central Flinders Ranges conveniently corresponds to the best-understood outcrop belt of demonstrably glaciogene, underlying Elatina facies, which has received focus in early studies, particularly that of Lemon & Gostin (1990). For that reason, although further complications of the Elatina–Nuccaleena transition interval across the basin may be anticipated or unresolved, this paper restricts focus to three sections in a continuous outcrop belt along the western homocline of the central Flinders zone in order to reassess the Elatina terminal-deglacial palaeoenvironment.

Palaeomagnetism

Palaeomagnetic studies of presumed Marinoan cap carbonates in Western Australia (Li 2000), Brazil (Trindade *et al.* 2003), and Oman (Kilner *et al.* 2005) have reported various patterns of geomagnetic reversal within directly-measured or composite lithostratigraphic sections. Limited rock-magnetic data and scanning electron microscope (SEM) imaging of Brazilian cap carbonates are interpreted to document detrital magnetite and detrital hematite as dual carriers of ancient magnetization (Font *et al.* 2005). The unexpectedly long duration of deposition that is seemingly required to account for numerous geomagnetic polarity reversals in cap carbonate calls into question most models of rapid Snowball deglaciation, or at least casts aspersions on the primary nature of those magnetizations or the interpretation of those rock magnetic data. This report details rock-magnetic and environmental-SEM petrographic analyses of iron-bearing phases contained in Nuccaleena Formation cap dolostone in order to establish hematite as the predicted primary character of that unit’s magnetization.

Regional geology

Elatina–Nuccaleena contact may be traced along a nearly continuous outcrop belt north from

Bunyeroo Gorge, past the area of Trezona Bore, a distance of *c.* 20 km entirely within Flinders Ranges National Park in the vicinity of the Heysen Trail (Oraparinna 1:100 000 mapsheet; Wilpena 1:63 360 mapsheet; Flinders Ranges National Park mapsheet, Callen & Reid 1994). NW-, W-, and SW-dipping sections are best exposed in minor and major intermittent-stream drainages incising the neotectonically active (Celerier *et al.* 2005) western margin of Flinders Ranges. The strike of this belt is nearly parallel to the north–south trend of Torrens Hinge Zone, a post-Elatina structure roughly delineating the late Ediacaran depositional shoreline (Fig. 1). During Elatina glaciation, subaerial facies (Williams & Tonkin 1985) are preserved *c.* 70 km west of the modern location of Torrens Hinge Zone at the latitude of the outcrop belt of this paper, and submarine facies are also preserved west of the trace of Torrens Hinge Zone.

Sections detailed here are from Elatina Creek, Enorama Creek (Ediacaran GSSP), and composite from several ravine drainages draining easterly hills and plains close to the immediate southeast of Trezona Bore (Fig. 1, Table 1). The section at Trezona Bore was considered as an alternative candidate for the Ediacaran GSSP (discussion can be found in reports of the International Commission on Stratigraphy's Terminal Proterozoic Subcommission, at <http://www.stratigraphy.org/precambrian/tpz.htm>). The section at Elatina Creek is informally considered, and in this report formally suggested, as a parastratotype that is better suited than Enorama Creek for continuous exposure and scientific sampling (K. Anderson, N. Bailey, and J. Gehling, pers. comm. 2004).

With isopachs influenced by multiple episodes of rifting beginning *c.* 175 million years before deposition of Nuccaleena Formation and with migrating loci of prolonged diapirism influencing accommodation space, this central zone of the Adelaide Rift Complex does not follow simple rules of basin architecture (Lemon & Gostin 1990; Preiss 1990, 2000). Elatina Creek and Enorama Creek sections are roughly equidistant and distal to the main exposed body of Oraparinna diapir; Trezona Bore section is relatively proximal to the northern arm of Oraparinna diapir, termed, wholly or partly, 'Enorama diapir' in some publications, e.g. Lemon (2000) and Knoll *et al.* (2006) (Fig. 1).

Although Cambrian rifting and Cambrian–Ordovician intrusive orogenesis are restricted to southern and eastern Adelaide Rift Complex (eastern Mount Lofty Ranges) (Preiss 2000), cleavage and general indicators of that thermal event extend somewhat further from the locus of magmatism. However, the central Flinders zone has experienced only low-grade Phanerozoic regional

metamorphism. The SE-dipping, frontal thrust associated with medium-grade Delamerian deformation is *c.* 50 km south of Elatina Creek section (Marshak & Flottman 1996). Although the northern and central Flinders zone may have experienced late Palaeozoic to Mesozoic block tectonism (folded Triassic coal measures are exposed at Leigh Creek to the north of the sections described, and near Quorn to the south), open folding in the central zone is considered syn- and shortly post-Cambrian in age. Gently dipping Mesozoic strata flank both margins of Flinders Ranges; these likely have been disturbed only by Cenozoic neotectonic deformation.

Lithostratigraphy

Enorama Creek, GSSP

Although Elatina Formation may be mapped in subcrop and float on the broad plain between Enorama Creek and Brachina Gorge road and geological trail, it is dominantly covered by streambed gravel and canyon-wall colluvium near to Enorama Creek. During numerous visits to the site, we have observed upper Elatina diamictite intervals emerge from and disappear beneath migrating boulders in the creek (Fig. 2a). These diamictite beds, which vary in matrix colour from moderate red 5R 4/6 to dark reddish brown 10R 3/4, include outsized boulders of quartzite, andesite, basalt, specularite, and granite in fine-grained matrix.

A singular exception is one bed which contains a *c.* 70 cm wide by *c.* 20 cm thick raft of yellow-weathering, planar-laminated pink sandstone (Fig. 2a). Lemon & Gostin (1990) invoke reworking of prior Elatina glacial deposits for most, if not all, deposition of upper Elatina diamictite and indeed, a similar sandstone bed crops out near the bottom of the Elatina section at Elatina Creek, some 4 km south of Enorama Creek. For this and other reasons, Elatina Formation diamictite provenance is generally considered, at least in part, locally sourced.

At least two metres of cobble-bearing, fine-grained, massive diamictite are probably perpetually exposed as a sloping creek wall closely below the Ediacaran GSSP. The diamictite appears less conglomeratic upward and undergoes a transition into a relatively resistant, coarse-grained, greyish red 10R 4/2, convolute-laminated, flaser-bedded arkose (hereafter, 'red sheet sandstone'). The red sheet sandstone is unquestionably distinct from, and erosive into, the immediately underlying massive siltstone, and at outcrop scale the loading surface is easily defined (Fig. 2a, b).

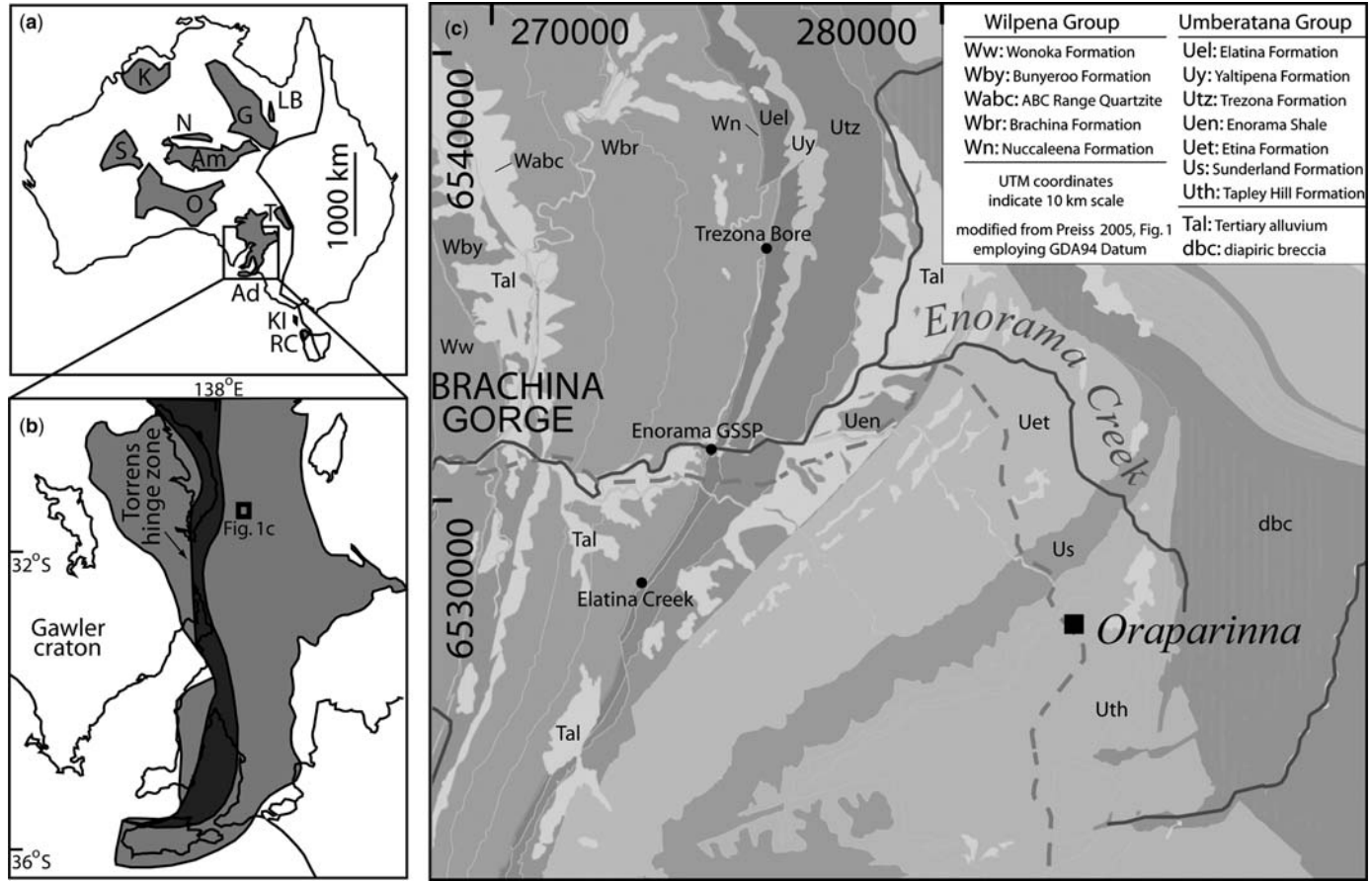


Fig. 1. Regional geology. Modified from the inset map of Preiss (2005), from 1:250 000 Parachilna geologic mapsheet. (a) Approximate outcrop limits of Australia’s Neoproterozoic basinal blocks. K, Kimberley; S, Savory; N, Ngalia; Am, Amadeus; G, Georgina; LB, Little Burke outlier; O, Officer; Ad, Adelaide; T, Torrowangee; KI, King Island; RC, Rocky Cape; (b) Close-up of Adelaide Rift Complex, exposed in Flinders fold belt. Torrens hinge zone approximates the mid- to late-Ediacaran shoreline of the eastern edge of Gawler craton. (c) An *c.* 50 km² area of the central Flinders zone discussed in this report. Three sections at Elatina Creek, Enorama Creek, and near Trezona Bore expose Elatina–Nuccaleena contact with varying character. Oraparinna diapir and its northern arm (Enorama diapir) are inferred to be active during early Elatina time because of the corresponding isograds of its fringing reefs, including Trezona Formation to the west, and preservation of a locally-restricted, basal Elatina glacial unit in the same sink (Lemon & Gostin 1990; Sohl *et al.* 1999). All sites are in Flinders Ranges National Park. Access to Enorama Creek via public road and *c.* 200 m trail. Access to Elatina Creek via *c.* 2 km hike or gated park-service road. Access to Trezona Bore via *c.* 6 km hike or gated park-service road.

Table 1. *Sample information*

Site	Northing	Easting	Sample No.	Position	Technique	Details
Trezona Bore	6535080	276050	TBNU 28	Carbonate interbed in lower Brachina shale, c. 75 cm above base	Thermosusceptibility	Run 1: peak temperatures 321°C, 691°C Run 2: peak temperatures 459°C, 557°C, 584°C, 636°C, 673°C, 710°C
Enorama Creek	6231050	274750	TBlag1	Nuccaleena, basal c. 5 cm	eSEM	Not figured
			GSSP 31			
Elatina Creek	6528200	273000	GSSP 30	Nuccaleena, 1.7 m above base	Hysteresis	
			NUEL 131	Carbonate interbed in Brachina shale, 5.91 m above Nuccaleena base	IRM acquisition	
			NUEL 123	Nuccaleena, 4.16 m above base	IRM acquisition	
			NUEL 57	Nuccaleena, 1.98 m above base	eSEM	
			NUEL 16	Nuccaleena, 47 cm above base	Hysteresis	
			NUEL 148	Nuccaleena, 29 cm above base	IRM acquisition	
Bunyeroo Creek	6522500	274000	NUEL 147	Nuccaleena, 25 cm above base	IRM acquisition	
			SCN 4	Nuccaleena, 5.67 m above base	IRM acquisition	
			SCE 3	red sheet sandstone, 9.54 m below contact	IRM acquisition	

*Position to nearest 50 m, AGD84. eSEM (see Fig. 6). thermosusceptibility, hysteresis, IRM acquisition, (see Fig. 7).

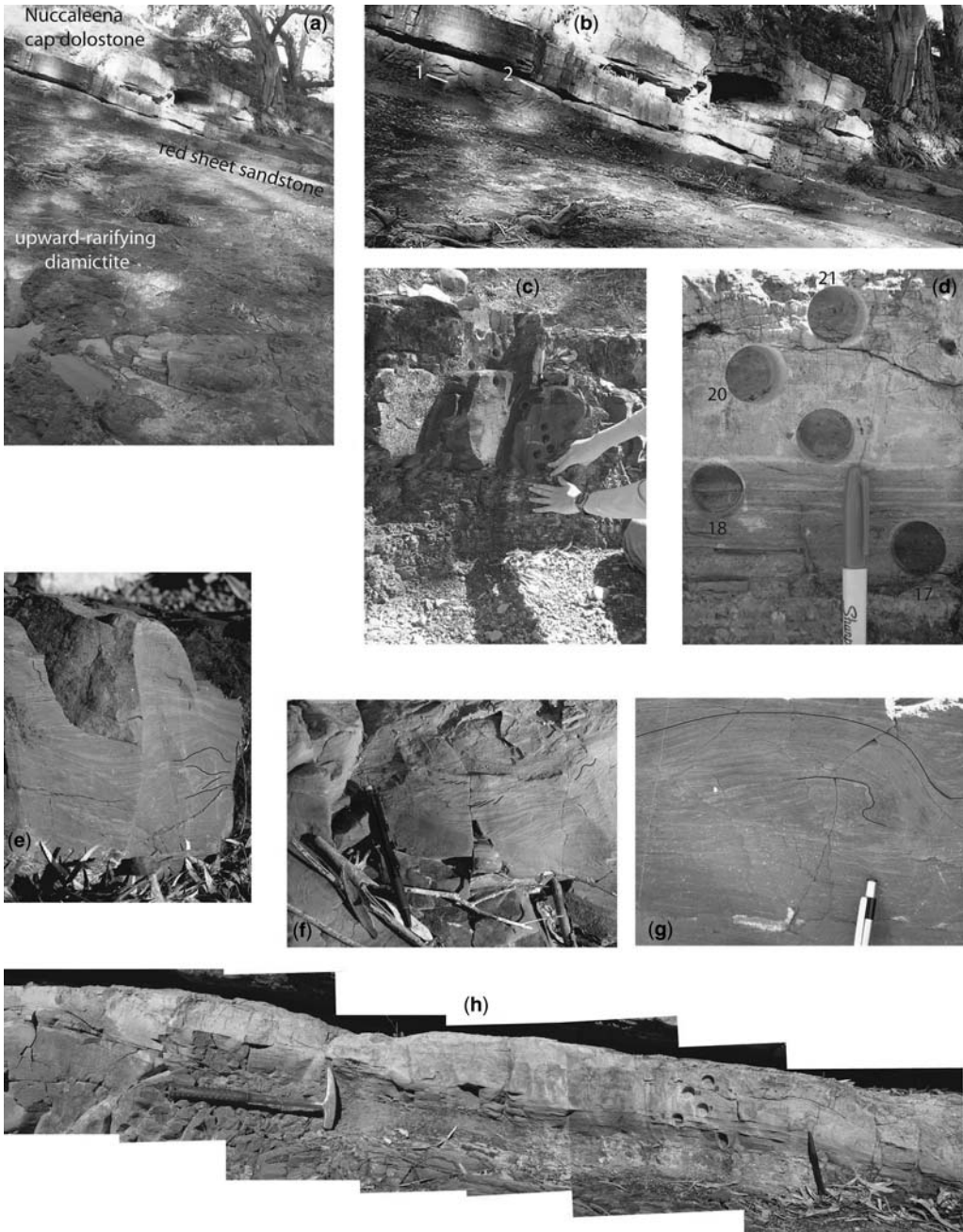


Fig. 2. Enorama Creek GSSP. Key facies and contact relations through Elatina-Nuccaleena transition at Enorama Creek GSSP. (a) Eastward view from the base of continuous exposure, 2003. Note pink, laminated sandstone raft as diamictite clast in foreground. Diamictite becomes less conglomeratic upward, and is incised by a red sheet sandstone (resistant ledge, above label, beneath Nuccaleena hillside outcrop). Much of the foreground is covered and uncovered episodically by torrent-swept streambed boulders. (b) Closer view of Elatina–Nuccaleena contact. White bar labelled ‘1’ marks approximate base of the red sheet sandstone, which cuts downward into Elatina diamictite closely creekward. White bar labelled ‘2’ marks basal Nuccaleena Formation cap dolostone contact, which disappears into the re-entrant upslope. Red sheet sandstone continues to thicken off-picture, up-slope. No fault is

However at hammer-scale, cleavage in the lower part of the sheet sandstone (later, reassigned to basal Nuccaleena Formation) and transposed nubbins weathering texture in the topmost siltstone of Elatina Formation interfere and often make precise placement of a contact difficult (Fig. 2c). Over a zone of several centimetres upward, however, cross- and convolute-bedded lamination (Fig. 2e, f, g) in the sheet sandstone disappears. Hypothesizing remaining, mean planar flaser fabric of the red sheet sandstone as palaeohorizontal, the unit could incise underlying massive diamictite by *c.* 46 cm, have *c.* 11 cm top-surface relief, and vary between *c.* 55 cm and *c.* 110 cm thick over an exposure scale of *c.* 4.8 m (Figs 2a, b).

In a detrital zircon study, Gehrels *et al.* (1996) dated fifty zircon crystals, presumably from this sheet sandstone unit and locality. Dominated by *c.* 1630–1570 Ma grains, the age spectrum of the Elatina red sheet sandstone could be sourced from the Nuyts volcanics and St Peters Suite, and the Hiltaba Suite, respectively, of adjacent Gawler Craton to the west. Alternative, east-derived sources from Curnamona Province or from southern Flinders inliers are also possible. If sourced from Gawler Craton, heavy mineral stringers throughout Elatina Formation might represent detrital input from Middleback Iron Formation, close to Torrens Hinge Zone and slightly south of due west from Enorama Creek. Noting contrast, then, with the mixed or local (diapir and underlying Elatina Formation) dominated provenance of Elatina diamictite, the depositional environment appears to have changed, at least itinerantly, across the uppermost Elatina diamictite to sheet sandstone transition to record locally voluminous input from continental sources.

Where bed top relief is greatest in the red sheet sandstone, near the creek bed, the unit encloses a

laterally discontinuous, *c.* 6 cm thick mudstone lens and is depositionally overlain by similar, greyish brown 5R 3/2, rare pebble-bearing, rubbly-weathering mudstone. Multiple calcareous-weathering horizons laminate an uppermost, coarser, redder interval of the mudstone unit immediately beneath solid Nuccaleena Formation cap dolostone, which displays sharp, centimetric-undulatory contact with Elatina Formation (Fig. 2h here; fig. 5e of Lemon & Gostin 1990). These calcareous horizons are conservatively assumed to represent Nuccaleena-age diagenetic fronts invading topmost Elatina siltstone. Palaeomagnetic drill holes that are now partly obliterated by the GSSP golden spike demonstrated horizontal continuity and sharp margins of these layers into the outcrop (Fig. 2d).

Where red sheet sandstone is thickest, however, the rubbly mudstone, siltstone, and mixed-calcareous-weathering interval is attenuated or even unexpressed, and the solid Nuccaleena Formation cap dolostone closely overlies the red sheet sandstone, with a *c.* 1–10 cm re-entrant masking the contact (Fig. 2b). Chalky-weathering carbonate may be dug out of this crevasse, suggesting a correlation with the mixed-calcareous-weathering interval exposed further down the creek slope. Even so, the thickness of calcareous-weathering siltstone filling relief atop the red sheet sandstone appears to vary by a factor of *c.* 2 across the span of exposure (see schematic lithostratigraphic sections and sequence-stratigraphic summary, Fig. 3).

Bed 1 of solid Nuccaleena Formation cap dolostone at Enorama Creek is recrystallized and undulose at low amplitude. Centimetric, spar-filled sheet cracks are common. Ensuing beds are buff-weathering (greyish orange 10 TR 7/4), pale red

Fig. 2. (Continued) evident near the site of dramatic downcutting of the red sheet sandstone, in the sandstone, the underlying diamictite, or in the smooth-weathered units occupying the re-entrant, when viewed with a flashlight. (c) Lower contact of red sheet sandstone into non-conglomeratic Elatina siltstone. While sandstone cleavage tends to interfere with loading-induced nubbins weathering-style of underlying siltstone, presence/absence of heavy-mineral lamination is the useful diagnostic. Contact between left thumb and right forefinger. Palaeomagnetic samples drilled in both units. (d) The Basal Ediacaran GSSP 'Golden Spike' interval. Samples #17–21 of TDR's collection. Formal placement of the Cryogenian–Ediacaran Period 'unconformity' between samples 20 and 21. Note three-dimensional, sharply defined, calcareous-weathering horizons extending downward, even into sample 17. While interpretation as post-depositional diagenetic fronts is plausible and conservative here at Enorama Creek, similar features are undeniably primary sedimentary just *c.* 2 km to the south, at Elatina Creek. (e) Undulose to planar-lamination surrounding disrupted (bifurcated) lamination at lower right, in red sheet sandstone unit. Bordering construction lines. (f) Climbing and starved ripples amidst otherwise planar-laminated flaser-bedded siltstone. Change in attitude of exposure across line from upper left to lower right. (g) Convolute bedding includes overturned laminae and near-vertical exposure. Altogether, indications in the red sheet sandstone range from high to low flow regime, and appear to permit both sudden depositional episodes and prolonged deposition. Though strange in the context of Enorama Creek alone, these different aspects are sensible in context of similar units at Trezona Bore to the north and Elatina Creek to the south. (h) Elatina–Nuccaleena contact just before it disappears into re-entrant. Note attenuation of supra-red sheet sandstone calcareous-weathering mudstone-and-siltstone unit upward and to the left.

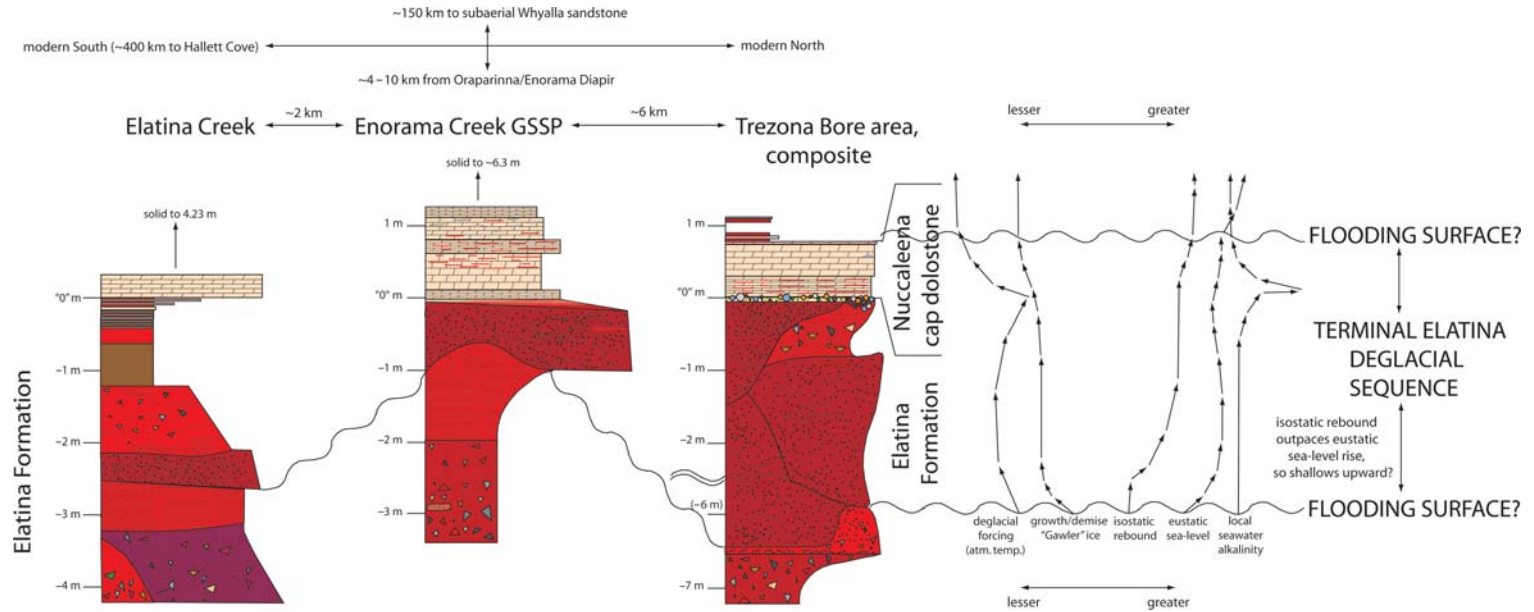


Fig. 3. Nuccaleena Formation Terminal Elatina Deglacial Correlation Scheme. Schematic lithostratigraphic profiles of Elatina–Nuccaleena transition intervals at Elatina Creek, Enorama Creek, and in the Trezona Bore area. Note that at Trezona Bore, only profiles on the right and left sides of the cartoon section are directly observed. All other relations are inferred or required by the observation that all sections in the area possess at least one red sheet sandstone bed (some expose three nested sandstones) and both sections examined in detail possess a basal Nuccaleena lag, assumed to represent a locally persistent time-horizon, possibly an exposure or a flooding surface. Five physical variables probably sufficient to model predicted litho/sequence-stratigraphic outcomes of Elatina deglaciation are listed, with highly speculative senses of growth/diminution. It is not clear whether solid Nuccaleena Formation cap dolostone deepened or shallowed through its interval of deposition. Though conventionally regarded as a flooding-surface at the base of a transgressive system tract, onset of Nuccaleena Formation cap dolostone may reflect some nontrivial combination of senses of change in these five variables, or of interaction with a dynamic chemocline (Hoffman 2005). We preserve the notion of basal Nuccaleena flooding by appealing to isostatic rebound to dominate the siliciclastic portion of the terminal Elatina deglacial sequence, and eustatic sea level rise to dominate the carbonate portion. Alternative explanations are suggested in the text.

10 R 6/2-coloured, medium-fine grained, low-angle cross-laminated peloidal dolomicrites. The abundance of sheet cracks (thin, discontinuous red silt horizons, and oversteepened, centimetric peloidal antiforms) decreases upsection. Outcrop-scale stylolite horizons of low tortuosity are episodic throughout the *c.* 5.8 m of Nuccaleena Formation cap dolostone exposed at Enorama Creek (total thickness *c.* 6.3 m, with an obscure interval disrupted by the root system of a large eucalyptus tree). These might reflect Delamerian attenuation of the section; however they could also mark primary or early diagenetic dissolution surfaces.

Full lithostratigraphy of Nuccaleena Formation cap dolostone is left for future description; this report focuses on the Elatina-Nuccaleena contact interval (except where basic description of stratigraphically-higher Nuccaleena Formation cap dolostone is appropriate to provide context for rock magnetic results).

Elatina Creek

While Elatina Creek section of Elatina Formation is potentially attenuated by faulting mid-unit, the upper portion is coherent (Fig. 4a). Fine-matrix, massive red diamictite indistinguishable from the lowest unit described above at Enorama Creek hosts outsized boulders and is incised by dark reddish brown 10 R 3/4, medium-grained, matrix-supported, cobble-bearing channelized diamictite, in turn topped by pebble- to cobble-bearing, fine-grained, massive diamictite. A red sheet sandstone unit (Fig. 4a), ranging from *c.* 37 cm to >50 cm thick, incises conglomeratic Elatina Formation by at least *c.* 3 cm over an outcrop scale of *c.* 6 m (small-scale faults cut the unit and make determination of incision relief somewhat ambiguous). The sheet sandstone does preserve at least 10 cm of relief on its top surface, in which red, laminated siltstone is preserved and presumed to mark palaeohorizontal.

Although the flaser-bedding is not as apparent at Elatina Creek as at Enorama Creek, this unit is continuously traceable (excepting intermittent alluvial cover) for *c.* 2 km north to Enorama Creek and likely reflects the same depositional era as the zircon-bearing red sheet sandstone unit described in the previous subsection. The same lithology appears *c.* 6 km north of Enorama Creek (next subsection), and later we suggest the base of this red sheet sandstone unit, best exposed at Elatina Creek, marks a regionally-extensive sequence boundary extending upward through ultimate deglaciation of the Elatina Snowball ice age.

At Elatina Creek, the red sheet sandstone unit is depositionally overlain by *c.* 60 cm of fine-grained, sparse pebble-conglomerate, which grades into *c.* 80 cm of rubbly-weathering, non-conglomeratic

mudstone. Unique among sections we have observed in Flinders Ranges, Elatina Creek section exposes a continuous stratigraphic profile across the Elatina-Nuccaleena transition, and it is strikingly conformable (Fig. 3). Within *c.* 55 cm of solid Nuccaleena Formation cap dolostone, rubbly-weathering, non-conglomeratic mudstone begins to pick up coarser siliciclastic grains and becomes increasingly laminated, presenting a calcareous weathering profile mixed at centimetre-scale with intermittent, fine-grained siliciclastics.

Within decimetres of the contact, these mixed units gain lateral persistence and display unequivocal loading structures: red silt flames asymmetrically downward into calcareous-weathering, buff silt (Fig. 4b, d). This relation seems consistent with depositional origin as centimetric siliciclastic debris flows overriding unconsolidated, partly calcareous ooze. In this framework, palaeocurrents would have been generally toward either the NE or SW (asymmetric structures verge both directions). Although the calcareous-weathering beds only rarely yield identifiable primary carbonate petrographic textures, the density distinction evident in the inverted flame outcrop texture of some calcareous-siliciclastic doublets requires distinct bulk sedimentary compositions.

Fraction of calcareous-weathering lithology increases dramatically upward, and calcareous beds become compositionally unequivocal within *c.* 22 cm of the basal Nuccaleena contact, especially at creek level, where at least two beds of carbonate interfinger with red siltstone (Fig. 4c) preceding outcrop of recrystallized carbonate in 'bed 1' of Nuccaleena Formation cap dolostone. Continuous exposure may be dug out of the creek bed, and both *c.* 3 cm thick carbonate beds are sharply surrounded by unbroken red siltstone.

As at Enorama Creek GSSP, bed 2 and all ensuing beds in the *c.* 4.2 m thick, continuous outcrop of Nuccaleena Formation cap dolostone are cross-laminated at low-angle, comprising sub-millimetre to *c.* 2 mm peloids generally evident in weathered outcrop but rarely in thin-section, and sometimes inversely graded. Spar-filled sheet cracks and centimetric, oversteepened, sharp-crested peloidal antiforms are present in the lower part of the section.

Laterally extensive and vertically continuous, fresh exposure of uppermost Elatina Formation and most of Nuccaleena Formation at Elatina Creek renders this site as an exceptional section for study of the GSSP interval. Precise placement of the GSSP is nontrivial since, in contrast with the section at Enorama Creek, the basal Nuccaleena contact at Elatina Creek is convincingly conformable. In spirit, the Ediacaran Period at Elatina

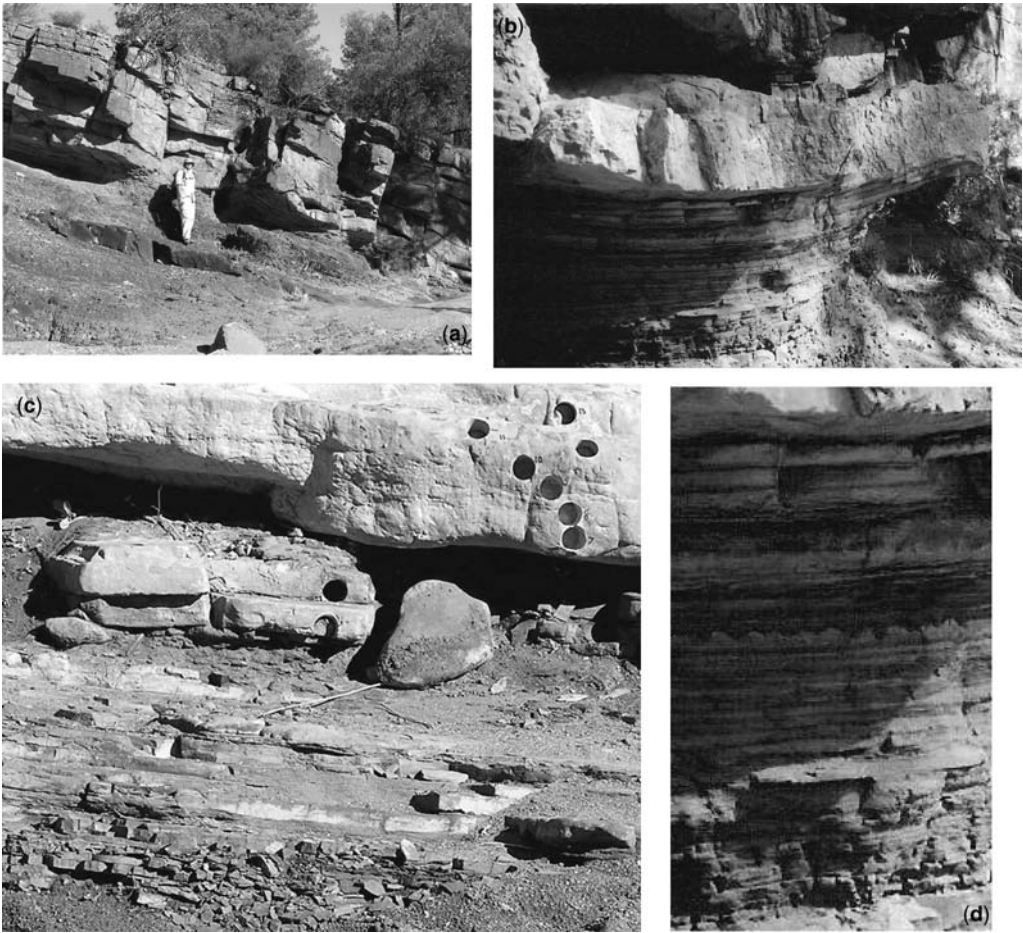


Fig. 4. Elatina Creek. (a) Cliffy exposure of proposed Ediacaran parastratotype. Creek runs left to right in foreground. Geologist Ryan Petterson, *c.* 1.8 m, for scale, standing on top surface of red sheet sandstone. (b) Mixed siliciclastic-carbonate interval of deglacial sequence, here assigned to lower Nuccaleena Formation. Carbonate-in just below shadow inflection; undulose current-loading of siltstone onto carbonate (ooze?) most prominent in middle bed. Two of the three topmost carbonate beds, separated by fine layers of siltstone, are present in creek bed, *c.* 5 m to right. They clearly underlie disrupted carbonate forming a 'keystone' block in bed 1, associated with a strange 'tepid' structure, above shadow at head level in (a). (c) Creek bed exposure of the simplest-correlated 'GSSP' level, at the base of solid carbonate bed 1 (nearly continuous exposure in re-entrant visible with a flashlight). (d) Close-up, Elatina–Nuccaleena transition.

Creek begins at the base of bed 1 of solid Nuccaleena Formation cap dolostone, a recrystallized carbonate bed *c.* 20–40 cm thick in the creek bed. Independent relative chronological (e.g. magnetostratigraphic) investigation might verify or deny that simplest correlation.

Arguably, continuous deposition at Elatina Creek extends downward to the incisive surface at the base of the red sheet sandstone unit of upper Elatina Formation. Because of the three to five-fold expansion and clear continuity of this section relative to that at Enorama Creek, we suggest the Elatina Creek site

be considered a basal Ediacaran parastratotype, in the mode adopted by the International Commission on Stratigraphy for augmentary sections (Ain Settara and Elles) near the Cretaceous–Paleocene boundary GSSP at El Kef, Tunisia (e.g. Remane & Adatte 2002). Elatina Creek is accessible either by *c.* 2 km hike south from the Elatina Formation parking area of the Brachina Gorge Geological Trail, or by four wheel-drive accessible fire road, following the Heysen trail and navigable past normally-locked gates by prior arrangement with park authorities.

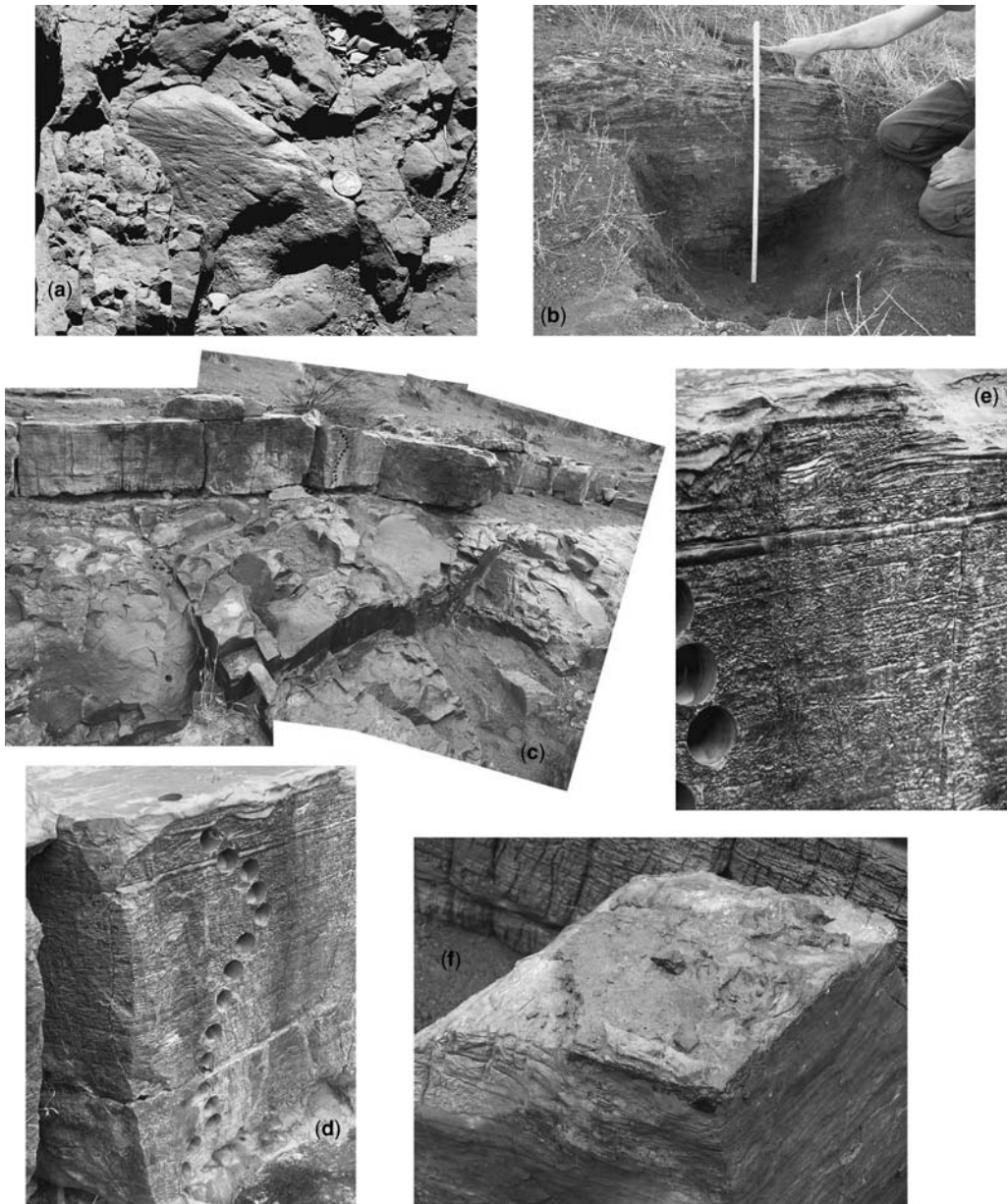


Fig. 5. Trezona Bore area. (a) Multiple sets of presumably glacial striations on a diapir-derived (?) basic volcanic clast above red sheet sandstone and highest successful palaeomagnetic site of Sohl *et al.* (1999), in sparse diamictite interval below cover including subcrop of cap carbonate. (b) c. 75 cm highly-weathered Nuccaleena Formation cap dolostone dug out of cover at top of Sohl *et al.*'s magnetostratigraphic section. The carbonate sits directly atop a grit-to-pebble layer, which sits above non-conglomeratic siltstone (only c. 8 cm dug out). (c) Best-exposed Nuccaleena section in area, up hillside gully to north of Sohl *et al.*'s (1999) section. (d) Full thickness of cap carbonate at magnetostratigraphic section, note spackly-weathering micrite layer at top, and thinner analogues lower in section. (e) Close-up of spackly-weathering micrite v. low-angle cross-bedded peloidal dolomicrite. Apparent foresets in middle of view, below level of label. (f) Loose block, up-ended, exposes Nuccaleena Formation cap dolostone cementation of supra-red sheet sandstone pebble lag. The same basal cap carbonate lag lies c. 2 m higher than the top of a single red, sheet sandstone bed at Sohl *et al.*'s (1999) section, close to the south.

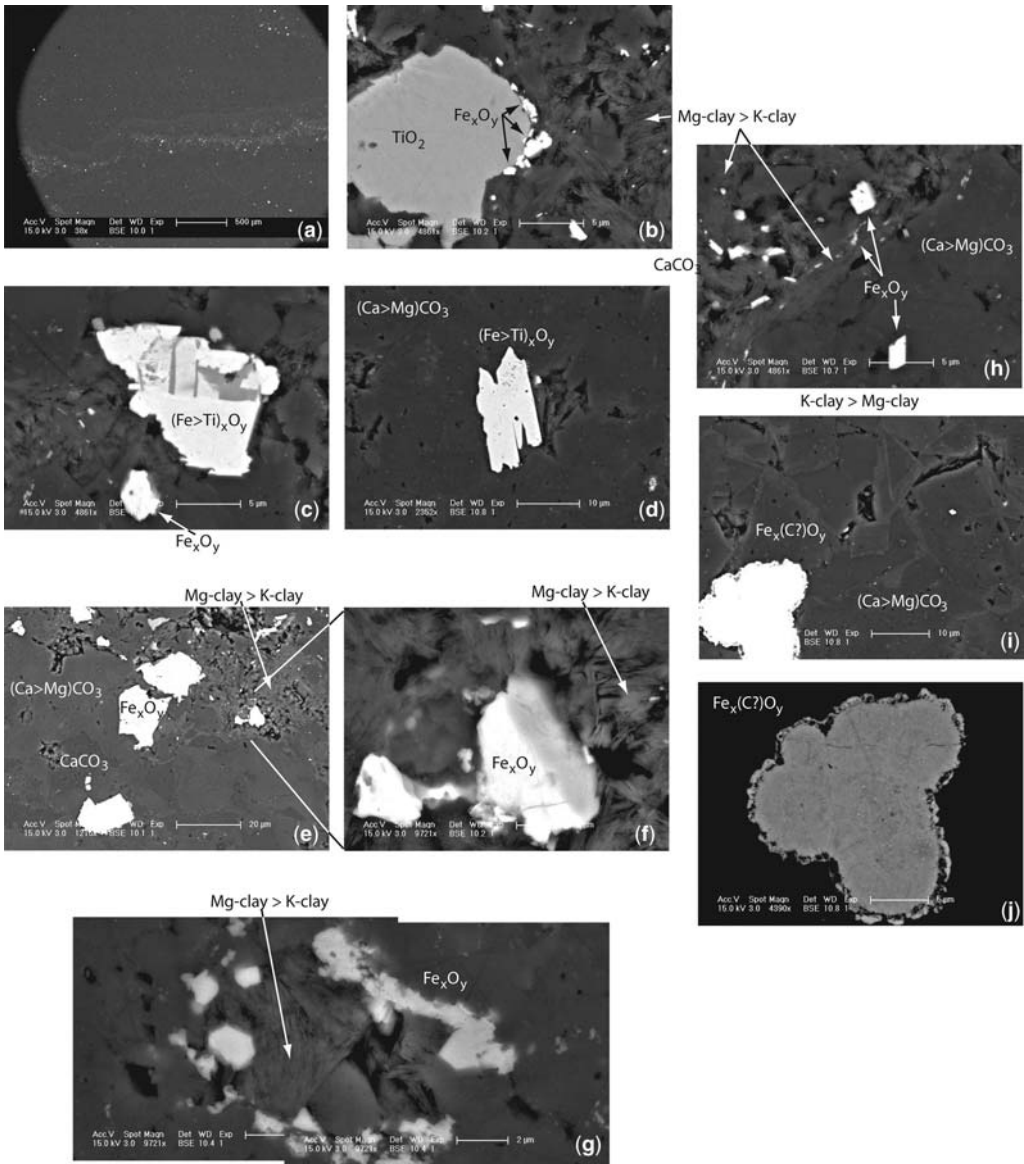


Fig. 6. eSEM petrography of terrigenous and carbonate cap constituents. Stratigraphic up is topward in all. Qualitative chemistry by EDS analysis, spectra not shown. (a) Heavy minerals often concentrated in undulose, subhorizontal layers, but also dispersed throughout carbonate-dominated portions of specimen. (b) Sub-micron iron oxide agglomerates clustered on clay-ward rim of rutile grain. Carbonate encroaches close to the other sides of this rutile. (c) Large, chemically zoned, Ti-bearing iron oxide; smaller iron oxide; and very small (EDS-unresolvable) iron oxide crystals near clay floc, sandwiched between dolomite crystal networks. (d) Platy Ti-bearing iron oxide adjacent to small pocket of clay, otherwise isolated in region of dolomite rhombs. (e) Irregular iron oxide grains and clay sector amidst mixed Mg-rich and Mg-poor dolomite, and calcite rhombs. (f) Magnified sector of e. (g) Clusters of putatively single domain-sized iron oxide crystals surrounding clay floc, in otherwise carbonate-dominated sector. (h) Smallest iron oxides appear to follow fabric of clay floc. (i) and (j) Single occurrence of botryoidal iron oxide (?). Preferred interpretation as a relict, microbially bound macropeloid/macro-oid, with bio-induced rim precipitate. Since specimen was carbon-coated, it is possible the relict mineral is siderite or iron (oxyhydr)oxide.

Trezona Bore

About 6 km north of Enorama Creek, along a continuous but progressively shallowing homocline, the Heysen trail and an associated, gate-accessed 4WD track reach Trezona Bore amid mixed Brachina Formation sandstones and siltstones. Gentle undulation of regional folds shallows the westward dip of units to the east of Trezona Bore, so that Elatina and Nuccaleena formations are exposed mostly as dip-slope geomorphology and occasionally in creek cross-section over several kilometres to the south along strike. The Terminal Proterozoic Subcommittee considered Trezona Bore as well as Enorama Creek and a third section, outside Flinders Ranges National Park as candidate GSSP locations (Knoll *et al.* 2006).

Sohl *et al.* (1999) report the best-constrained magnetostratigraphy of Elatina Formation from one of these creek sections, containing at least six reversals defined between sites that are separated by decimetres to metres of stratigraphic height. Noting the site-based sampling strategy employed and the regional heterogeneity and impersistence of glacial lithofacies, Sohl *et al.* (1999) stipulate 'six' as a minimum estimate for the number of geomagnetic reversals spanning Elatina deposition.

The topmost polarity zone in the Trezona Bore area section of Sohl *et al.* (1999) preserves a NE, shallow-down palaeomagnetic remanence direction; it is represented by two sites within a *c.* 2 m thick, red, sheet sandstone bed. Atop this bed, striated cobble-bearing, massive diamictite is poorly exposed (Fig. 5a), and *c.* 1 m higher, *c.* 10 cm of peloidal dolostone crops out of shale-fragmentary regolith. It is possible to excavate the regolith to a depth of *c.* 50 cm, which exposes a full thickness of *c.* 75 centimetres of shallowly-dipping cap carbonate sitting directly atop a poorly-consolidated pebble gravel (Fig. 5b), underlain *in-situ* by red, non-conglomeratic siltstone.

The Nuccaleena Formation cap dolostone outcrop disappears beneath fragmentary shale regolith along strike to the east. The resistant red sandstone in uppermost Elatina Formation, however, is readily traceable for a kilometre to the south and some distance, uphill, to the north and east. Over this distance, some dozen creeks expose it in profile; and variously one, two, or three distinct, red sheet sandstones are nested, with occasionally high-amplitude erosive contact.

The lithostratigraphic section figured from the Trezona Bore area (Fig. 3) includes not only the units atop Sohl *et al.*'s (1999) Elatina Formation magnetostratigraphy, but also a composite from sections in the deepest five creek beds south of that and (with digital pictures, Fig. 5) a section along a steep gully dissecting the backside of a

hill only *c.* 400 m south of Trezona Bore. That creek cuts, at elevation *c.* 440 m, abruptly downward through Nuccaleena Formation cap dolostone (which is exposed in profile along strike over tens of metres and for about 1 m as clean, top-surface dip slope, due to the high topographic relief against easily-weathered, overlying Brachina siltstones).

Here, as immediately above the magnetostratigraphic section of Sohl *et al.* (1999), the solid Nuccaleena Formation cap dolostone is *c.* 75 cm thick (Fig. 5c). It is entirely peloidal cross-laminated except in its bottom *c.* 3 cm, in which carbonate of enigmatic origin cements a pebble to cobble-sized, heterolithic gravel lag sitting atop red sheet sandstone (Fig. 5d). Although eroded to a re-entrant at immediate creek level, vantage may be gained into the recess, and it is clear that the pebbles contained in basal Nuccaleena Formation cap dolostone directly load atop red sheet sandstone, the section lacking any intervening silt.

This is a basal disconformity to the letter of formal Ediacaran GSSP definition. Solid Nuccaleena Formation cap dolostone is essentially unbroken by thin siltstone horizons, in contrast to the sections at Elatina and Enorama creeks. A prominent spar-filled sheet crack occurs *c.* 50 cm above dolostone base (Fig. 5e); and solid carbonate is terminated by a *c.* 2 cm thick, non-peloidal-expressing, spackly-weathering bed of micrite (Fig. 5f). Two similar, but thinner, apparently micritic beds punctuate the solid dolostone near its half-thickness and toward its top (Fig. 5c, e). At least two more, thin, micritic carbonate beds are mixed with dominant siltstone in the ensuing *c.* 1 m, below continuous outcrop of Brachina Formation siliciclastics.

Downward in this gully from the Elatina–Nuccaleena contact, two red sandstone units are present; the higher incises the lower by at least *c.* 2 m on an outcrop scale. The bottom contact of the lower sheet sandstone unit cuts fine-matrix, heterolithic, boulder diamictite, which is the lowest traceable Elatina unit before outcrop disappears beneath alluvium.

We suspect, then, that the red sheet sandstone unit discussed at length in the Elatina Creek and Enorama Creek subsections represents multiple events of deposition, or else multiple events of erosion punctuating prolonged deposition of clastic, monolithic debris. Alternatively, a single red sheet sandstone bed might be deposited catastrophically, as during a jökulhlaup sourced beneath a waning Elatina ice sheet on Gawler Craton; and each section received detritus from a different number of such events. Preiss (2000), however, questions whether there ever was a low-altitude, continental ice sheet on Gawler Craton during Marinoan time.

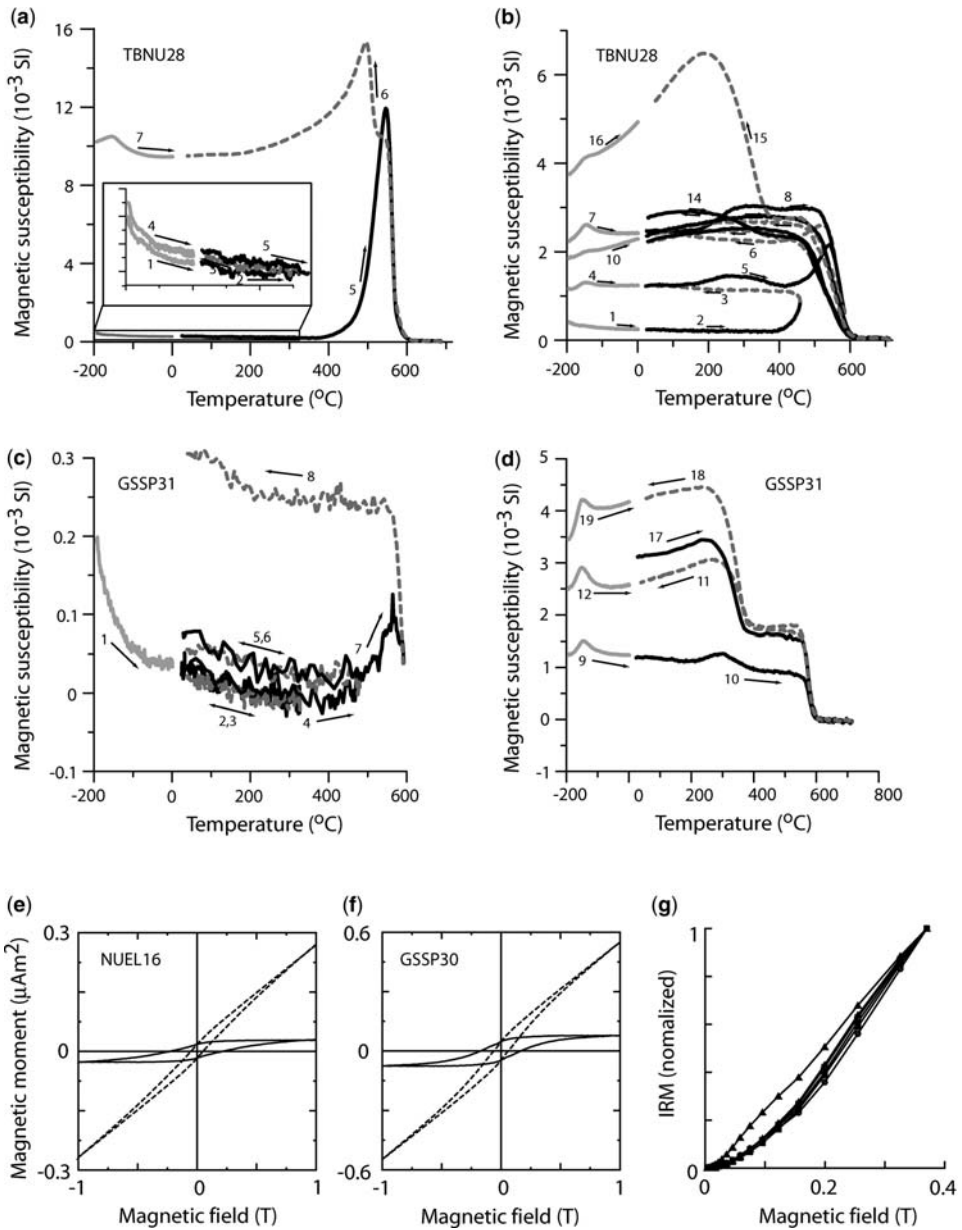


Fig. 7. Rock Magnetism. For thermosusceptibility experiments, arrows indicate heating/cooling and consecutive order. Some intermediate cycles not shown. (a) Initial warming from liquid nitrogen temperature dominated by paramagnetic signal, possible hint of Verwey transition. Reversible heating and cooling through 300°C. Dramatic formation of magnetite above 400°C. Above Curie temperature of magnetite, further creation of low-Ti magnetite. Verwey transition now associated with one (or both) phases on final warming run. (b) Same sample as (a), but to different temperatures. Highly labile (reactive below *c.* 200°C magnetite/titano(?)magnetite formed just above 400°C, associated with broadened Verwey transition which is accentuated by further reaction to *c.* 560°C but destroyed by reaction to *c.* 600°C. Broad, low-unblocking temperature phase (Mn-ferrite?) only created upon heating to *c.* 670°C. (c) and (d) Different specimen, nearly the same behaviour and inferred reaction products. (e) and (f) unsaturated (at 1.5 T) magnetic hysteresis loops on Nucleaena Formation cap dolostone samples; wasp-waistedness indicates mixture of high- and low-coercivity components. (g) Low-field IRM-acquisition curves for five samples of Nucleaena Formation cap dolostone and one of upper-Elatina red sheet sandstone. All appear dominated by the same magnetic phase, but the sandstone and the most tectonized dolostone show enhanced mixture of a low-coercivity phase.

Certainly, only two red sheet sandstone intervals are nested in the Trezona Bore gully, while up to three are expressed in west-draining creeks c. 800 m to the south, and four may be recorded atop a nearby summit to the north. Only one event (or uninterrupted interval of sheet sand deposition) is evident at Elatina Creek, while the mudstone enclave within the red sheet sandstone at Enorama Creek could permissibly argue for two events, or a sand hiatus within one prolonged depositional interval.

Summary

In a salt-withdrawal syncline actively accommodating sediment load in the central Flinders zone during Elatina glaciation, the Nuccaleena cap dolostone at Elatina Creek shows mixed conformable contact with underlying non-conglomeratic siltstones traditionally assigned to Elatina Formation. The nearest unconformable surface lies metres below the base of solid cap dolostone, beneath a thin interval of flaser-bedded, red sandstone. Along strike to the north, an identical lithofacies incises massive Elatina Formation diamictite at Enorama Creek GSSP, and is closely overlain by Nuccaleena Formation cap dolostone, with an intervening, thin interval of variable calcareous-weathering, non-conglomeratic siltstone. Still further north along strike, anomalously thin Nuccaleena Formation cap dolostone near Trezona Bore cements a gravel lag sitting variably above mostly non-conglomeratic siltstone or flaser-bedded, red sandstone. The 'red sheet sandstone' lithofacies near Trezona Bore consists of multiple depositional episodes, and at least three beds are nested, with occasionally high amplitude basal relief, sometimes bracketing pockets of bedded or massive diamictite. The base of the lowest red sheet sandstone closely beneath cap dolostone most accurately represents the basal Nuccaleena Formation (and Wilpena Group) sequence boundary.

Sedimentological interpretation

Our preferred interpretation of the uppermost Elatina-Nuccaleena package begins with Elatina boulder-diamictite sedimentation. This might define an era of net glacial advance (potential stadial/interstadial cycles aside); it might represent syn-Snowball sedimentation, if specific global climate dynamism were assumed or permitted at Elatina palaeolatitude (e.g. Warren *et al.* 2002; Goodman & Pierrehumbert 2003; Pollard & Kasting 2005); or it might represent a prolonged era of net glacial retreat (Lemon & Gostin 1990; Preiss *et al.* 1998), possibly associated with sea

ice-bound oases occupying tropical embayments in the early stages of global deglaciation (Halverson *et al.* 2004). There is no easy intersection of the simple Snowball Earth theory with the timescale implied for mixed diamictic/nonconglomeratic siliciclastic deposition by six geomagnetic reversals (Sohl *et al.* 1999); but various authors have shown that the boundary conditions and dynamics of both hard and soft Snowball worlds are sufficiently malleable that neither hypothesis need seem disproved on the basis of those reversals alone (e.g. Pierrehumbert 2005; Pollard & Kasting 2005; and see Hoffman & Schrag 1998). A comprehensive sequence-stratigraphic framework for Elatina Formation remains elusive (despite preliminary suggestions of such a scheme in, e.g. Preiss *et al.* 1998), so all possibilities are currently permitted.

Nuccaleena Formation cap dolostone is not similarly permissive. Absence of dropstones in Nuccaleena Formation cap dolostone requires absence of ice-rafted debris and implies considerable waning, if not total disappearance, of tropical (whether or not Gawler Craton) ice sheets and/or (i.e. Adelaide Rift Complex) ice shelves. All other Nuccaleena inferences are, to date, model-dependent. For instance, major antiformal structures of enigmatic origin have been hypothesized as mega-teepee's (James *et al.* 2001), which could indicate exposure towards upper Nuccaleena Formation cap dolostone (Plummer 1979; Williams 1979). The same features might be referable to the 'megaripple' hypothesis (Allen & Hoffman 2005) developed for other Australian and Laurentian cap carbonates, and interpreted to require deep water. Mixed, variable transition of Nuccaleena Formation cap dolostone into Brachina shale is generally considered as a high stand systems tract, in part by assuming the presence or absence of laminated ribbon carbonates is controlled by carbonate compensation depth (e.g. Kennedy 1996).

In the rock magnetics section below, we note that Nuccaleena Formation cap dolostone pervasively contains terrigenous debris, especially detrital (titano)hematite and rutile, potassic and magnesium clays, and quartz, even in intervals macroscopically free of silt horizons. It is not clear whether trace apatite (not figured) is of detrital or diagenetic origin. Nuccaleena Formation cap dolostone seems, then, not to necessarily represent background flux of alkalinity otherwise suppressed by siliciclastic input (for one relevant discussion of mixed shale and carbonate sedimentation, see Chetel *et al.* (2005). Instead, we favour Nuccaleena Formation cap dolostone marking overwhelming flux of alkalinity introduced *de novo* near its base and waning gradually near its top (where calcite compensation depth (CCD) may certainly have effect). Shale input to the Adelaidean depocentre

may have been shut down during Nuccaleena deposition—or at least diminished during lower Nuccaleena deposition and disappeared during upper Nuccaleena deposition—or alternatively, deposition rate of Nuccaleena Formation cap dolostone might be so high as to dominate normal shale input in the lower half of the unit, and swamp it outright in its upper interval.

Regardless, it is stressed that the influx of alkalinity to the Adelaidean depocentre cannot represent initial sedimentation accompanying onset of terminal deglaciation. Elatina Creek preserves silt turbidites encroaching on incipient carbonate oozes at the beginning of Nuccaleena age. These silt turbidites are the energetic gradational superiors to rubbly mudstone that filled palaeorelief atop sheet sand beds marking (episodic or protracted) influx of coarse debris from Gawler Craton. The erosional event that preceded or accompanied initial deposition of these red sheet sands marks the oldest recognizable boundary delimiting a terminal deglacial sequence (widely regarded as a transgressive system tract) including Nuccaleena Formation cap dolostone from earlier, possibly pre- or syn-Elatina glacial deposits (Fig. 3).

This scheme seems to account for the Trezona Bore area disconformity expressed by a gravel lag atop red sheet sandstone and calcified by basal Nuccaleena Formation cap dolostone only if the siliciclastic portion of the Elatina–Nuccaleena terminal deglacial sequence were confined to an era of post-glacial isostatic rebound outpacing glacio-eustatic sea-level rise. Since Elatina red sheet sandstone is non-conglomeratic, the lag must be a post-sheet sand depositional event. The lag sits directly atop the second of two sheet sands in our Trezona Bore section but atop poorly conglomeratic siltstone filling red sheet sandstone palaeorelief at the Sohl *et al.* (1999) Trezona Bore section. It conveniently, therefore, might represent melt water-emplaced debris derived locally from northern Oraparinna/Enorama diapir, largely winnowed and deflated by diapir rebound (during the era of uppermost Elatina mixed siltstone-carbonate and/or lowermost Nuccaleena deposition, prior to transgression during lower or upper Nuccaleena time).

Finally, we note non-unique coherence of our model with some published interpretations of the presumed Nuccaleena-correlative carbonate unit in the Marinoan type section at Hallett Cove, south of Adelaide. Here, non-conglomeratic ‘Seacliff’ sandstone overlies the basal Wilpena Group sequence boundary and spans a thick stratigraphic interval between sparsely conglomeratic beds and a several metre-thick interval of mixed dolostone and siliciclastics (e.g. Christie-Blick *et al.* 1995).

Along the length of the Torrens Hinge Zone, Seacliff sandstone occupies various positions and

displays various compositions (Preiss 1993), so its presentation at Hallett Cove should not be taken as generally representative. At Hallett Cove, however, the first appearance of cap carbonate is as decimetre-scale beds with purportedly concordant lower contacts but reworked top surfaces (unpublished theses of E. M. Alexander and I. A. Dyson; e.g. citation of the former in Lemon & Gostin 1990). Sandstone between these interbeds is hummocky cross-stratified and presumably responsible for high-energy scouring of each thin carbonate interbed (Dyson 1992). Only the highest carbonate bed, *c.* 1 m thick, is uninterrupted and unscoured at its top.

Although Hallett Cove is sufficiently distant from the central Flinders zone to permit several model-driven relative age relations between Nuccaleena outcrops of the two areas, simple lithostratigraphic correlation is now possible by considering the Elatina Creek section. The Hallett Cove mixed carbonate-siliciclastic interval is certainly more clearly expressed than at Elatina Creek, and it is thicker (*c.* 6 m versus *c.* 55 cm). Solid, overlying cap carbonate at Hallett Cove is, however, attenuated relative to Elatina Creek (*c.* 1 m v. 4.2 m). Accepting the widespread assumption that top-Nuccaleena transition to ribbon carbonate is CCD-controlled amid a high stand systems tract, Hallett Cove must occupy a deeper-water setting than Elatina Creek, if deposition rates of solid carbonate are broadly similar.

This is plausible given Elatina Creek’s proximity to presumed-emergent Oraparinna diapir, and several consequences seem implied by accepting the water-depth interpretation of the preceding paragraph. First, expansion of the Hallett Cove sub-cap mixed interval over the same interval at Elatina Creek would appear to favour upwelling rather than surface origin for cap-controlling alkalinity, if mixed siliciclastic-carbonate deposition rate is approximately equal at the two locations. Upwelling origin of alkalinity for cap carbonates (Grotzinger & Knoll 1995) is not simply compatible with interpretations of other aspects of cap carbonate sedimentology (Higgins & Schrag 2003; Shields 2005); but when considered in isolation of those arguments, the two Adelaidean sections with obvious mixed siliciclastic prelude to cap carbonate deposition seem to permit that possibility.

Alternatively, postglacial, craton-derived sedimentation might precede the first appearance of cap carbonate if the time interval spanning basal Nuccaleena Formation siliciclastics represents the timescale of ocean buffering prior to build up of excess alkalinity (Hoffman *et al.* 1998; Higgins & Schrag 2003). Basal Nuccaleena Formation siliciclastic input might reflect local (tropical) deglaciation, as envisioned by Halverson *et al.* (2004)

while Nuccaleena Formation cap dolostone is synchronous with rapid global deglaciation.

Further elaboration of, and discrimination between, these hypotheses ought to be testable if basin-wide application of magnetic stratigraphy (or of any independent chronometer) seems robust—a scenario for which we lay a foundation in the remaining sections.

Rock magnetism

Cap carbonate coloration has largely driven regional, continental, and global correlation of associated Neoproterozoic ice ages; yet the origin of the (frequent, though not ubiquitous) ‘pinkness’ in cap units such as Nuccaleena Formation cap dolostone is not understood. Four scenarios are possible: (1) cap pinkness results from detrital iron oxides of sundry origin (eroded igneous, metamorphic, or second-cycle sedimentary, or biogenic/bioinduced in the aftermath of glaciation); (2) cap pinkness results from secondary iron oxide pigmentation—accompanying oxidation of organic matter originally present in caps but remineralized in the earliest diagenetic window, or accompanying chemical oceanographic changes during late diagenesis, post-lithification; (3) cap pinkness is a consequence of unique carbonate composition (e.g. Mn-rich dolomite) and is unrelated to iron-cycling; and (4) cap pinkness is a recent feature essentially induced by arid surficial weathering. This study favours a combination of the first and second hypotheses at the expense of the third, because terrigenous debris is ubiquitous in Nuccaleena Formation cap carbonate by direct observation and by rock-magnetic inference. The fourth is suggestively discounted, because recently pink cap dolostones have been described in quarry outcrop of a humid climate (Nogueira *et al.* 2003) and in Cenozoic mountaintop outcrop of a subalpine, temperate climate (Lorentz *et al.* 2004).

Environmental scanning electron microscopy and electron diffraction spectroscopy

Analyses of Nuccaleena Formation cap dolostone samples from the Elatina Creek and Trezona Bore sections reveal multiple non-carbonate phases, by rough order of abundance:

- (1) equant iron oxide grains *c.* 0.1–100 microns in diameter, mode (O)10 microns;
- (2) equant, low-Ti iron oxide grains *c.* 0.1–100 microns in diameter, mode (O)10 microns;
- (3) nearly stoichiometric iron oxide grains \ll 0.1 microns in diameter;
- (4) Mg-clay;
- (5) euhedral to subhedral rutile;

- (6) well-rounded quartz;
- (7) K-clay;
- (8) subhedral to rounded apatite;
- (9) relatively rare assemblages (REE-phosphate; botryoidal iron oxide or carbonate; zircon).

In Nuccaleena Formation cap dolostone, component-1 and -2 iron oxides, component-5 rutile, and component-6 quartz are ubiquitously rimmed by or adjacent to clays (Fig. 6b–h). Component-1 iron oxides are commonly concentrated in slightly undulose, bedding-parallel zones, without obvious grading (Fig. 6a). These zones are slightly undulose even when clearly not associated with stylolites. Supra-stylolite gangue might thicken in troughs and thin toward crests; but we have studied too few examples to generalize confidently. Nonetheless, Nuccaleena Formation cap dolostone clearly contains bedded iron oxides associated with other terrigenous mineral grains. If hematite or maghemite, these grains are expected to be of mostly single-domain size and therefore capable of recording a stable magnetization on geological timescales.

The smallest of the iron oxide size fraction observed (component-3) would also verge into the pseudo-single domain and single domain fields of magnetite. This crystal population is relatively scarce, though potential detection-limit imaging bias exists given the greater size and hence dominant conductivity/contrast of component-1 and -2 grains.

Component-3 iron oxide sometimes appears as ‘salted, cloudy’ sectors of clay platelets (Fig. 6e, h) and rarely, non-clay carbonate matrix (Fig. 6i).

Matrix carbonate textures are post-depositionally recrystallized; peloid margins, where visible in thick-section, are invisible under the eSEM. Small (mode *c.* 200 microns) dolomite rhombs dominate Nuccaleena Formation cap dolostone but vary size over of an order of magnitude. Low-Mn dolomite crystals are a minor component, and basal Trezona Bore carbonate (not figured) is more frequently zoned (calcite rims) than mid-Elatina Creek cap carbonate (rare, slightly zoned sector in Fig. 6i).

All Nuccaleena dolostone samples preserve occasional calcite rhombs mixed among dolomite rhombs, and also localize calcite to post-depositional textures, including subvertical, mildly tortuous zones. These calcite ‘pipes’ frequently crosscut macroscopic peloid lamination, and they sometimes feed, and are also often sourced by, calcite spar-filled sheet cracks. Rarely, a calcite pipe is upward-truncated by depositional peloid laminae. These pipes are interpreted as fluid escape structures active syn-depositionally and related to sheet crack growth and fill. Although recrystallization into pervasive rhomb fabric and calcification of some

rhombs certainly may have occurred long after Nuccaleena Formation cap dolostone was deposited, as calcite also appears to track these depositional sheet crack and pipe features, an early diagenetic origin can not be discounted.

Temperature dependence of magnetic susceptibility

Temperature dependences of low-field magnetic susceptibility, $k(T)$, were measured on two Nuccaleena samples (macroscopically non-silty dolostone *c.* 2.5 m into solid cap carbonate at Enorama Creek GSSP; and spackly-weathering micrite, Brachina Formation interbed above solid dolostone at our Trezona Bore section; Table 1).

Changes in $k(T)$ during warming from -192°C to room temperature in ambient atmosphere and cycling between room temperature and peak temperatures up to *c.* 720°C in flowing argon were measured using an AGICO KLY 4S magnetic susceptibility meter equipped with a high-temperature furnace and a cryostat. Repeated low-temperature warming runs, and successive heating-and-cooling runs to progressively higher peak temperatures were employed to document the temperature range and product character of the irreversible chemical reaction within cap dolostone more precisely, beginning between *c.* 330°C and 440°C (Fig. 7a, b, c).

For both samples, an inverse logarithmic decay of susceptibility, with a steep lowest-temperature tail, is observed during the initial warming-from-low-temperature run. Such behaviour suggests that magnetism of fresh Nuccaleena Formation cap dolostone is dominated by paramagnetic minerals (e.g. clays). A broad peak at *c.* -153°C on these low-temperature $k(T)$ curves, associated with the Verwey transition (Verwey 1939) is hinted at by the initial Trezona Bore run, but not by the fresh Enorama Creek sample. Both samples, once thermally-altered by heating them to various temperatures, show Verwey transitions of varying definition, indicating the creation of near-stoichiometric magnetite.

No other magnetic transitions (such as hematite's Morin transition at *c.* -15°C [Morin 1950]) are observed. If hematite is present in either sample, it is also nonstoichiometric, or else smaller than *c.* 0.1 micron (Bando *et al.* 1965). eSEM analysis rules out the latter option.

When heated in argon, both samples show essentially reversible susceptibility at a *c.* 320°C peak temperature step. Elevated return susceptibility from *c.* 440°C and new presence of a broadened Verwey transition in the ensuing low-temperature warming run of Trezona Bore Nuccaleena document the onset of chemical reaction in that temperature interval. Steep susceptibility decrease in the

c. 560°C – 590°C range indicates presence of substantial magnetite by that point of the experiment, but absence of a well-expressed Hopkinson peak suggests that the magnetite is not single-domain (e.g. Dunlop 1974).

Further heating does not show a hematite signal (Néel temperature at *c.* 690°C), though cooling from peak temperatures above *c.* 580°C accentuates the near-stoichiometric magnetite signal (unblocking temperatures) and also creates at least one other phase, which ultimately stabilizes with distributed unblocking temperatures *c.* 250°C – 400°C . We suspect this last phase is a manganese ferrite, which manifests similar behaviour during thermomagnetic analyses of synthetic and natural siderites (Isambert *et al.* 2003). The third local susceptibility maxima present on some runs, with peak susceptibility in the low 500°C s, may be a metastable phase involved with the creation of the low-temperature ferrite.

Altogether, these changes suggest thermal lability of carbonate, including Mn-dolomite, in Nuccaleena Formation cap dolostone, with respect to an iron-bearing phase that is also initially present and labile. Magnetite may be created *de novo* from trace Fe-bearing carbonate (thus far unidentified by eSEM/EDS, although see unusual, interpreted microbialite phase, Fig. 7i, j) or from minor clay fractions in bulk Nuccaleena Formation cap dolostone, but almost surely, hematite and/or maghemite, if originally present in the rock, partly or wholly convert to magnetite beginning at *c.* 350°C . Carbon dioxide evolved from Nuccaleena Formation cap carbonate itself is likely the other major reactant, as carbonates undergo decarbonation reactions ('calcination' in the metallurgical literature, regardless of carbonate composition) between room temperature and *c.* 450°C , with reaction rates fixed by strong grain-size and weaker oxygen fugacity dependences (e.g. French & Rosenberg 1965).

As results of these experiments, we infer that magnetite, present in trace quantities of some pristine Nuccaleena Formation cap dolostone, should not contribute significantly to natural remanent magnetization; and is of generally <500 nm grain size (below the threshold of eSEM resolution). As eSEM imaging documents a significant clay component, yet ferromagnetic susceptibility does not show significant change across magnetite-evolving clay reaction temperatures (*c.* 120°C – 170°C), it is likely that Nuccaleena Formation cap dolostone has been heated, *in situ*, to peak temperatures in or exceeding that range during its geological history. Any iron-bearing clay originally present has probably inverted, producing magnetite of ancient but secondary age (possibly evident in Fig. 7h, i). Such a thermal effect is plausible since



Fig. 8. Palaeomagnetic at the Ediacaran GSSP. Rock magnetic experiments described here seem to assure a detrital palaeomagnetic signal in Nuccaleena Formation cap dolostone, with or without overprinting by Ediacaran early diagenesis. Other studies document one, four, and one magnetic reversal during deposition of Walsh, Mirassol d'Oeste, and Hadash cap carbonates, potential 'Marinoan' correlative units to Nuccaleena Formation cap dolostone. If you were to wear 'magnetic goggles', the GSSP magnetic fingerprint might look something like this. White indicates 'reversed' polarity, directed SW and shallow upward, black indicates 'normal' polarity, directed NE and shallow downward, following polarity character and assignment of Sohl *et al.* (1999) for underlying Elatina Formation. Higher resolution sampling and pursuit of direct field tests of magnetization should better constrain the fidelity and interpretation of this signal.

the Ediacaran–Cambrian section above Nuccaleena Formation cap dolostone spans *c.* 3.5 km, of likely high geothermal gradient during Delamerian orogenesis.

Similarly, however, the change from reversible to irreversible susceptibility tracks between heating-to and cooling-from peak temperature runs beginning at *c.* 350°C establishes that as a maximum palaeothermometer constraint, if the phase reacting above 350°C is itself a primary component (Hrouda *et al.* 2003). Since the initial low-temperature experiments show only minor stoichiometric magnetite, and since the bulk susceptibility of unheated sample is low, hematite and/or maghemite are likely reactants during carbon dioxide volatilization. Continued production of magnetite from hematite and/or maghemite above 350°C possibly reflects kinetic limitation by the hematite and/or maghemite phase.

Magnetic hysteresis properties

Room-temperature hysteresis loops were collected using a Princeton Measurement vibrating sample magnetometer at the Institute of Rock magnetism (University of Minnesota) and a Princeton Measurement alternating gradient force magnetometer at the University of Rochester. Isothermal remanent magnetization (IRM) acquisition was performed on a 2G Enterprises™ DC-SQUID magnetometer in line with horizontal and vertical solenoids custom-built at California Institute of Technology, charged by a 2G capacitor relay box and modulated by custom-built transformer boxes.

Hysteresis loops on Nuccaleena Formation cap dolostone from *c.* 40 cm into the cap section at Elatina Creek, at a level where silt is still episodically visible to the naked eye, and from *c.* 2.1 m into the cap at Enorama Creek GSSP, where silt has mostly disappeared, are unsaturated at peak fields of *c.* 1.5 T (Fig. 7e, f). Consistent with initial low-temperature susceptibility experiments, both loops require significant paramagnetic corrections, indicating appreciable clay content. Upon correction, both samples exhibit wasp-waisted hysteresis (Fig. 7e, f), documenting presence of both a low-coercivity phase (like magnetite or maghemite) and a high-coercivity phase (goethite or hematite) in a ratio of at most 1:100 by saturation magnetization-corrected volume, respectively (Roberts *et al.* 1995; Tauxe *et al.* 1996).

IRM acquisition curves were measured for five Nuccaleena samples from various stratigraphic levels (Table 1) and for one upper Elatina, red sheet sandstone sample (collected from a section not otherwise described in this report—Bunyerook Creek, at the southern margin of the continuous outcrop belt which includes Elatina Creek, Enorama Creek, and Trezona Bore).

All five cap carbonate curves cluster tightly and are dominated by a high-coercivity phase that is far from saturated at 370 mT (Fig. 7 g), the maximum field available using our equipment. The high-field slopes of remanence acquisition are higher than expected for goethite, marking hematite as the dominant high-coercivity phase (France & Oldfield 2000). The red sheet sandstone also yields a magnetically hard IRM acquisition spectrum, but one clearly mixed with a broad fraction of low-coercivity grains, probably clay-associated magnetite. Interestingly, the magnetically softest of the tightly clustered cap carbonate group is the single cap carbonate sample that also comes from Bunyerook Creek, a section which is strongly tectonized and somewhat weathered with respect to the others. Of all Nuccaleena sections reported here, our secondary magnetite hypothesis described above would predict most secondary magnetite at Bunyerook Creek.

Since eSEM imaging documents bedding-parallel layers of abundant iron oxide grains larger than the single-domain stability field of magnetite, all rock magnetic experiments described herein point to hematite as the dominant ancient carrier of detrital magnetization. Since hematite is documented as a detrital component carrying primary magnetization in underlying Elatina Formation and overlying Brachina siltstone, and since abundant hematite may be sourced from Palaeoproterozoic banded iron formations or Mesoproterozoic hydrothermal breccia deposits exposed on Gawler craton, we interpret detrital hematite to dominate Nuccaleena natural remanence and plausibly preserve primary magnetization.

Since thermomagnetic evolution experiments establish *c.* 330°C as a maximum estimate for peak palaeotemperature, any Ediacaran hematite magnetization will be preserved to the present unless chemically altered. At present, we cannot distinguish hematite pigments, possibly formed on the surface of detrital hematite grains while Nuccaleena Formation cap dolostone was still in the diagenetic window, from exclusively detrital hematite. Delamerian and younger pigments are largely ruled out, as they would coat quartz and carbonate grains as well as opaque crystals. Therefore magnetite remanence, if extractable during demagnetization, should be largely secondary, and higher unblocking-temperature phases should be purely detrital or a mixture of detrital and early diagenetic magnetization.

Discussion

For any rock of this assemblage, laboratory characterization of that compound remanence can be challenging. Alternating field demagnetization cannot

isolate characteristic magnetization alone, since goethite and hematite both will be unaffected. As documented in the thermosusceptibility section above, however, wholly thermal demagnetization is likely to destroy the very particles carrying primary remanence, and create new ferromagnetic grains locking in laboratory remanences with blocking temperatures appropriate to the oxygen fugacity of the demagnetizing furnace. It might be difficult to distinguish this laboratory magnetite remanence from that carried by geologic, secondary magnetite in a cap carbonate.

Context

Some of these concerns are voiced by Font *et al.* (2005), who undertake a similar SEM–rock magnetics study on Mirassol d’Oeste cap dolostone in Brazil. We confirm their findings: that pink cap dolostones contain micron-diameter iron oxide grains with bedded texture, most likely hematite because of high coercivity; that irreversible chemical reactions occur upon heating; and that clay is closely associated with iron-bearing phases, on the scale of an EDS analysis (see their fig. 9).

The conclusion applied to the Mirassol d’Oeste cap (that magnetite is a likely detrital magnetization carrier) is not shared. It seems difficult to rule out secondary origin of magnetite without independent palaeothermometry. With this minor exception, we replicate the findings of Font *et al.* (2005) and augment them by applying thermal-dependence of susceptibility reversibility as a palaeothermometer for low-grade burial metamorphism of Nuccaleena Formation cap carbonate; by documenting at least two distinct thermal reaction products in flowing argon atmosphere; and by determining the temperature ranges of those reactions.

Li (2000) presaged both petrophysical studies by noting thin, red silt stringers common in Walsh cap carbonate samples from Western Australia’s Kimberley region and suggesting that detrital hematite accounts for Marinoan cap ‘pinkness.’ His findings are supported by the documenting here of detrital hematite grains in unerring association with clay floes as well as commonly with detrital quartz and rutile, in cap carbonate facies where no red silt is apparent to the naked eye. It is suggested that the *c.* 300°C instability (sample explosions in the furnace; acquisition of anomalous magnetizations) Li (2000) noted in *c.* 50% of samples, and the similar instability previously reported to account for unsuccessful palaeomagnetic investigation of Nuccaleena Formation (Sohl *et al.* 1999, supplementary data) are due to ferric reduction (and possibly re-oxidation) accompanying carbon dioxide devolatilization of carbonate samples in that temperature range.

Kilner *et al.* (2005) figure orthogonal demagnetization vector diagrams that unblock by *c.* 600°C or by *c.* 690°C. Without knowing the lithologic identity of those specimens, and in the absence of other petrographic or rock-magnetic data published to-date from Oman’s Hadash cap, it is difficult to assess the extent to which these interpretations apply to that study.

Several hybrid demagnetization strategies have been attempted here, designed to isolate carriers of each natural- or laboratory-induced remanence, on Nuccaleena Formation cap dolostone, with varying success (Fig. 8). If direct field tests of Nuccaleena magnetization were to demonstrate ancient origin of a particular component, considerable light would be shed on the robustness of that and other palaeomagnetic results from cap carbonates worldwide.

Conclusions

Nuccaleena Formation cap dolostone was deposited in varying thickness along strike of a single outcrop belt during the terminal phase of Elatina–Nuccaleena deglaciation. This terminal deglaciation began amid widespread erosion, and accommodation space preserved on the flank of a salt diapir or in deep-water settings recorded siliciclastic input of pulsed or prolonged character, with accompanying or episodic episodes of renewed erosion during deposition of ‘red sheet sandstone’. These erosive episodes might have occupied intervals when ongoing isostatic rebound temporarily outpaced eustatic transgression. Later influx of alkalinity is separable from physical onset of ultimate deglaciation, and it may have been sourced by deep water upwelling, in the simplest lithostratigraphic correlation scheme presented here.

The Ediacaran GSSP is not marked at the basal Wilpena Group unconformity, as intended, but fully *c.* $\frac{1}{3}$ of the way through the terminal deglacial sequence at the very sections in Flinders Ranges showing clearest evidence for low-palaeolatitude Elatina glaciation.

Terrigenous input continued to those sections during deposition of Nuccaleena Formation cap carbonate, possibly decoupled from shale input. Detrital hematite is expected to record a faithful, stable magnetization in Nuccaleena Formation cap dolostone and other ‘pink’ cap carbonates, but elucidation of detrital versus early diagenetic magnetizations will be challenging for conventional palaeomagnetic laboratory techniques.

The authors acknowledge support from the Australian Research Council through its Research Centres Program, the David and Lucile Packard Foundation, and the National Science Foundation Graduate Research Fellowship Program. Critical reviews by W. Preiss and P. Betts

and informal reviews by A. Maloof, B. Kopp, and E. Sperling greatly improved the manuscript. Discussions in the field with T. Prave, N. Christie-Blick, J. Gehling, R. Petterson, and B. Wernicke; and out of it with D. Kent, R. Trindade, P. Hoffman, A. Kosterov, and M. Kennedy improved the authors' understanding of complications and caveats. Field work in Flinders Ranges National Park was particularly facilitated by K. Anderson, N. di Preu, and P. Canty of Parks and Wildlife South Australia, by R. Coulthard and P. Coulthard of the Flinders Ranges Aboriginal Heritage Consultative Committee Inc; and by able field assistantship from C. Izard and I. Howley. This paper is publication #390 of the Tectonics Special Research Centre and a contribution to International Geological Correlation Program (IGCP) 493 and 512.

References

- ALLEN, P. A. & HOFFMAN, P. F. 2005. Extreme winds and waves in the aftermath of a Neoproterozoic glaciation. *Nature*, **433**, 123–127.
- BANDO, Y., KIYAMA, M., YAMAMOTO, N., TAKADA, T., SHINJO, T. & TAKAKI, H. 1965. Magnetic properties of alpha-Fe₂O₃ fine particles. *Journal of the Physical Society of Japan*, **20**, 2086.
- BODISELITSCH, B., KOEBERL, C., MASTER, S. & REIMOLD, W. U. 2005. Estimating intensity and duration of Neoproterozoic snowball glaciations from Ir anomalies. *Science*, **308**, 239–242.
- CALLEN, R. A. & REID, P. W. 1994. Geology of the Flinders Ranges National Park. *South Australia Geological Survey. Special Map*, 1:75 000.
- CELERIER, J., SANDIFORD, M., HANSEN, D. L. & QUIGLEY, M. 2005. Modes of active intraplate deformation, Flinders Ranges, Australia. *Tectonics*, **24**, Art. No. TC6006. DOI: 10.1029/2004TC001679, 2005.
- CHETEL, L. M., SIMO, J. A. & SINGER, B. S. 2005. 40-Ar/39-Ar geochronology and provenance of detrital K-feldspars, Ordovician, Upper Mississippi Valley. *Sedimentary Geology*, **182**, 163–181.
- CHRISTIE-BLICK, N., DYSON, I. A. & VON DER BORCH, C. C. 1995. Sequence stratigraphy and the interpretation of Neoproterozoic Earth history. *Precambrian Research*, **73**, 3–26.
- DUNLOP, D. J. 1974. Thermal enhancement of magnetic susceptibility. *Journal of Geophysics*, **40**, 439–451.
- DYSON, I. A. 1992. Stratigraphic nomenclature and sequence stratigraphy of the lower Wilpena Group, Adelaide Geosyncline; the Sandison Subgroup. *Quarterly Geological Notes of the Geological Survey of South Australia*, **122**, 2–13.
- EMBLETON, B. J. J. & WILLIAMS, G. E. 1986. Low paleolatitude of deposition for Late Precambrian periglacial varvites in South Australia—Implications for paleoclimatology. *Earth and Planetary Science Letters*, **79**, 419–430.
- EVANS, D. A. D. 2000. Stratigraphic, geochronological, and paleomagnetic constraints upon the Neoproterozoic climatic paradox. *American Journal of Science*, **300**, 347–433.
- FONT, E., TRINDADE, R. I. F. & NÉDÉLEC, A. 2005. Detrital remanent magnetization in haematite-bearing Neoproterozoic Puga cap dolostone, Amazon craton: a rock magnetic and SEM study. *Geophysical Journal International*, **163**, 491–500.
- FRANCE, D. E. & OLDFIELD, F. 2000. Identifying goethite and hematite from rock magnetic measurements of soils and sediments. *Journal of Geophysical Research*, **105**, 2781–2795.
- FRENCH, B. M. & ROSENBERG, P. E. 1965. Siderite (FeCO₃)—thermal decomposition in equilibrium with graphite. *Science*, **147**, 1283.
- GEHRELS, G. E., BUTLER, R. F. & BAZARD, D. R. 1996. Detrital zircon geochronology of the Alexander terrane, southeastern Alaska. *Geological Society of America Bulletin*, **108**, 722–734.
- GOODMAN, J. C. & PIERREHUMBERT, R. T. 2003. Glacial flow of floating marine ice in 'Snowball Earth.' *Journal of Geophysical Research*, **108**, Art. No. 3308. DOI: 10.1029/2002JC001471, 2003.
- GROTZINGER, J. P. & KNOLL, A. H. 1995. Anomalous carbonate precipitates: Is the Precambrian the key to the Permian? *Palaaios*, **10**, 578–596.
- HALVERSON, G. P., MALOOF, A. C. & HOFFMAN, P. F. 2004. The Marinoan glaciation (Neoproterozoic) in northeast Svalbard. *Basin Research*, **16**, 297–324.
- HIGGINS, J. A. & SCHRAG, D. P. 2003. Aftermath of a snowball Earth. *Geochemistry, Geophysics, Geosystems*, **4**, Art. No. 1028. DOI: 10.1029/2002GC000403.
- HOFFMAN, P. F. 2005. 28th DeBeers Alex Du Toit Memorial Lecture: On Cryogenian (Neoproterozoic) ice-sheet dynamics and the limitations of the glacial sedimentary record. *South African Journal of Geology*, **108**, 557–577.
- HOFFMAN, P. F. & SCHRAG, D. P. 2002. The snowball Earth hypothesis: testing the limits of global change. *Terra Nova*, **14**, 129–155.
- HOFFMAN, P. F., KAUFMAN, A. J., HALVERSON, G. P. & SCHRAG, D. P. 1998. A Neoproterozoic snowball Earth. *Science*, **281**, 1342–1346.
- HROUDA, F., MÜLLER, P. & HANÁK, J. 2003. Repeated progressive heating in susceptibility vs. temperature investigation: a new palaeotemperature indicator? *Physics and Chemistry of the Earth*, **28**, 653–657.
- HYDE, W. T., CROWLEY, T. J., BAUM, S. K. & PELTIER, W. R. 2000. Neoproterozoic 'Snowball Earth' simulations with a coupled climate/ice-sheet model. *Nature*, **405**, 425–429.
- ISAMBERT, A., VALET, J. P., GLOTER, A. & GUYOT, F. 2003. Stable Mn-magnetite derived from Mn-siderite by heating in air. *Journal of Geophysical Research*, **108**, Art. No. 2283. DOI: 10.1029/2002JB002099, 2003.
- JAMES, N. P., NARBONNE, G. M. & KYSER, T. K. 2001. Late Neoproterozoic cap carbonates: Mackenzie Mountains, northwestern Canada: precipitation and global glacial meltdown. *Canadian Journal of Earth Sciences*, **38**, 1229–1262.
- KASEMANN, S. A., HAWKESWORTH, C. J., PRAVE, A. R., FALLICK, A. E. & PEARSON, P. N. 2005. Boron and calcium isotope composition in Neoproterozoic carbonate rocks from Namibia: evidence for extreme environmental change. *Earth and Planetary Science Letters*, **231**, 73–86.
- KENNEDY, M. J. 1996. Stratigraphy, sedimentology, and isotopic geochemistry of Australian Neoproterozoic

- postglacial cap dolostones: Deglaciation, δC -13 excursions, and carbonate precipitation. *Journal of Sedimentary Research*, **66**, 1050–1064.
- KENNEDY, M. J., RUNNEGAR, B., PRAVE, A. R., HOFFMANN, K. H. & ARTHUR, M. A. 1998. Two or four Neoproterozoic glaciations? *Geology*, **26**, 1059–1063.
- KENNEDY, M. J., CHRISTIE-BLICK, N. & PRAVE, A. R. 2001. Carbon isotopic composition of Neoproterozoic glacial carbonates as a test of paleoceanographic models for snowball Earth phenomena. *Geology*, **29**, 1135–1138.
- KILNER, B., MAC NIOCAILL, C. & BRASIER, M. 2005. Low-latitude glaciation in the Neoproterozoic of Oman. *Geology*, **33**, 413–416.
- KIRSCHVINK, J. L. 1992. Late Proterozoic Low-Latitude Global Glaciation: The Snowball Earth. In: SCHOPF, J. W., KLEIN, C. & DES MARAIS, D. (eds) *The Proterozoic Biosphere: A Multidisciplinary Study*. Cambridge University Press, 51–52.
- KNOLL, A. H., WALTER, M. R., NARBONNE, G. M. & CHRISTIE-BLICK, N. 2004. A new period for the geologic time scale. *Science*, **305**, 621–622.
- KNOLL, A. H., WALTER, M. R., NARBONNE, G. M. & CHRISTIE-BLICK, N. 2006. The Ediacaran Period: a new addition to the geologic time scale. *Lethaia*, **39**, 13–30.
- LEMON, N. M. 2000. A Precambrian fringing stromatolite reef complex, Flinders Ranges, South Australia. *Precambrian Research*, **100**, 109–120.
- LEMON, N. M. & GOSTIN, V. A. 1990. Glacigenic sediments of the late Proterozoic Elatina Formation and equivalents, Adelaide Geosyncline, South Australia. In: JAGO, J. B. & MOORE, P. S. (eds) *The Evolution of a Late Precambrian–Early Palaeozoic Rift Complex: The Adelaide Geosyncline*. Geological Society of Australia Special Publication, **16**, 149–163.
- LI, Z. X. 2000. New palaeomagnetic results from the ‘cap dolomite’ of the Neoproterozoic Walsh Tillite, north-western Australia. *Precambrian Research*, **100**, 359–370.
- LORENTZ, N. J., CORSETTI, F. A. & LINK, P. K. 2004. Seafloor precipitates and C-isotope stratigraphy from the Neoproterozoic Scout Mountain Member of the Pocatello Formation, southeast Idaho: implications for Neoproterozoic earth system behavior. *Precambrian Research*, **130**, 57–70.
- MARSHAK, S. & FLOTTMANN, T. 1987. Structure and origin of the Fleurieu and Nackara arcs in the Flinders fold-thrust belt, south Australia: Salient and recess development in the Delamerian Orogen. *Journal of Structural Geology*, **18**, 891–908.
- MORIN, F. J. 1950. Magnetic susceptibility of $\alpha\text{Fe}_2\text{O}_3$ and $\alpha\text{Fe}_2\text{O}_3$ with added titanium. *Physical Reviews*, **78**, 819–820.
- NOGUEIRA, A. C. R., RICCOMINI, C., SIAL, A. N., MOURA, C. A. V. & FAIRCHILD, T. R. 2003. Soft-sediment deformation at the base of the Neoproterozoic Puga cap carbonate (southwestern Amazon Craton, Brazil): confirmation of rapid icehouse-greenhouse transition in snowball earth. *Geology*, **31**, 613–616.
- PIERREHUMBERT, R. T. 2005. Climate dynamics of a ‘hard’ snowball Earth. *Journal of Geophysical Research*, **110**, Art. No. D01111. DOI: 10.1029/2004JD005162.
- PLUMMER, P. S. 1979. Note on the palaeoenvironmental significance of the Nuccaleena Formation (upper Precambrian), central Flinders Ranges, South Australia. *Journal of the Geological Society of Australia*, **25**, 395–402.
- POLLARD, D. & KASTING, J. F. 2005. Snowball Earth: a thin-ice solution with flowing sea glaciers. *Journal of Geophysical Research*, **110**, Art. No. C07010. DOI: 10.1029/2004JC002525.
- PREISS, W. V. 1987. The Adelaide Geosyncline—late Proterozoic stratigraphy, sedimentation, palaeontology and tectonics. *Geological Survey of South Australia, Bulletin*, **53**.
- PREISS, W. V. 1990. A stratigraphic and tectonic overview of the Adelaide Geosyncline, South Australia. In: JAGO, J. B. & MOORE, P. S. (eds) *The Evolution of a Late Precambrian–Early Palaeozoic Rift Complex: The Adelaide Geosyncline*. Geological Society of Australia Special Publication, **16**, 1–33.
- PREISS, W. V. 1992. The Ketchowla Siltstone and Stratigraphy of the Marinoan Glacial Yereлина Subgroup. *Quarterly Geological Notes of the Geological Survey of South Australia*, **121**, 7–15.
- PREISS, W. V. 1993. Neoproterozoic. In: DREXEL, J. F., PREISS, W. V. & PARKER, A. J. (eds) *The Geology of South Australia. Vol. 1, The Precambrian*. Geological Survey of South Australia, Bulletin, **54**, 171–202.
- PREISS, W. V. 2000. The Adelaide Geosyncline of South Australia and its significance in Neoproterozoic continental reconstruction. *Precambrian Research*, **100**, 21–63.
- PREISS, W. V. 2005. Global stratotype for the Ediacaran System and Period—the golden spike has been placed in South Australia. *MESA Journal*, **37**, 20–25.
- PREISS, W. V., DYSON, I. A., REID, P. W. & COWLEY, W. M. 1998. Revision of lithostratigraphic classification of the Umberatana Group. *MESA Journal*, **9**, 36–42.
- REMANE, J. & ADATTE, T. 2002. Foreword. *Palaeogeography, Palaeoclimatology, Palaeoecology*, **178**, 137.
- ROBERTS, A. P., CUI, Y. L. & VEROSUB, K. L. 1995. Wasp-waisted hysteresis loops—mineral magnetic characteristics and discrimination of components in mixed magnetic systems. *Journal of Geophysical Research*, **100**, 17909–17924.
- SCHMIDT, P. W. & WILLIAMS, G. E. 1995. The Neoproterozoic climatic paradox; equatorial palaeolatitude for Marinoan Glaciation near sea level in South Australia. *Earth and Planetary Science Letters*, **134**, 107–124.
- SCHMIDT, P. W., WILLIAMS, G. E. & EMBLETON, B. J. J. 1991. Low palaeolatitude of late Proterozoic glaciation; early timing of remanence in haematite of the Elatina Formation, South Australia. *Earth and Planetary Science Letters*, **105**, 355–367.
- SHIELDS, G. A. 2005. Neoproterozoic cap carbonates: a critical appraisal of existing models and the plume-world hypothesis. *Terra Nova*, **17**, 299–310.
- SOHL, L. E., CHRISTIE-BLICK, N. & KENT, D. V. 1999. Paleomagnetic polarity reversals in Marinoan (ca. 600 Ma) glacial deposits of Australia; implications for the

- duration of low-latitude glaciation in Neoproterozoic time, *Geological Society of America Bulletin*, **111**, 1120–1139.
- SUMNER, D. Y., KIRSCHVINK, J. L. & RUNNEGAR, B. N. 1987. Soft-sediment paleomagnetic field tests of late Precambrian glaciogenic sediments. *EOS, Transactions of the American Geophysical Union*, **68**, 1251.
- TAUXE, L., MULLENDER, T. A. T. & PICK, T. 1996. Potbellies, wasp-waists, and superparamagnetism in magnetic hysteresis. *Journal of Geophysical Research*, **101**, 571–583.
- TRINDADE, R. I. F., FONT, E., D'AGRELLA-FILHO, M. S., NOGUEIRA, A. C. R. & RICCOMINI, C. 2003. Low-latitude and multiple geomagnetic reversals in the Neoproterozoic Puga cap carbonate, Amazon craton. *Terra Nova*, **15**, 441–446.
- VERWEY, E. J. W. 1939. Electron conduction of magnetite (Fe_3O_4) and its transition point at low temperatures. *Nature*, **144**, 327–328.
- WARREN, S. G., BRANDT, R. E., GRENFELL, T. C. & MCKAY, C. P. 2002. Snowball Earth: ice thickness on the tropical ocean. *Journal of Geophysical Research*, **108**, Art. No. 31. DOI: 10.1029/2001JC001123.
- WILLIAMS, G. E. 1979. Sedimentology, stable-isotope geochemistry and palaeoenvironment of dolostones capping late Precambrian glacial sequences in Australia. *Journal of the Geological Society of Australia*, **26**, 377–386.
- WILLIAMS, G. E. & TONKIN, D. G. 1985. Periglacial structures and palaeoclimatic significance of a late Precambrian block field in the Cattle Grid copper mine, Mount Gunson, South Australia. *Australian Journal of Earth Sciences*, **32**, 287–300.

The rise and decline of the Ediacaran biota: palaeobiological and stable isotopic evidence from the NW and NE Lesser Himalaya, India

V. C. TEWARI

Wadia Institute of Himalayan Geology, 33, General Mahadeo Singh Road, Dehradun—248001, Uttarakhand, India (e-mail: vctewari@rediffmail.com)

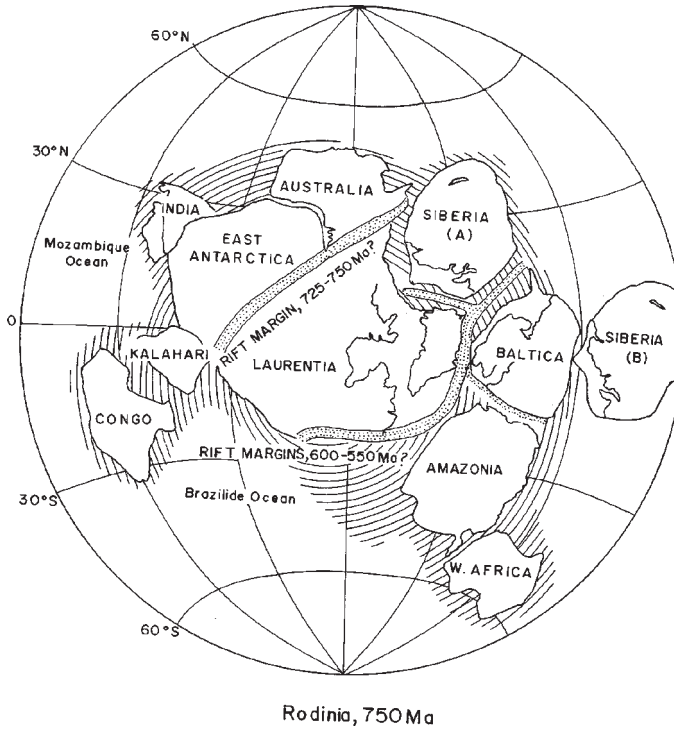
Abstract: Sediments of Ediacaran age have recently been recognized in the Krol Belt (NW Lesser Himalaya, India) with the discovery of pre-Ediacaran and Ediacaran biotas, carbon isotopic excursions matching the global curve and evidence for one Neoproterozoic glacial event. Other data include evidence for termination of the Krol algal-stromatolitic carbonate cycle in Late Proterozoic and deposition of phosphorite, phosphatic stromatolites similar to Tommotian taxa, and diversification of Small Shelly Fossils (SSF) of Tommotian/Meischucunian Zone 1 in Lower Tal Formation. Recently, Riphean–Ediacaran organic-walled microfossils, stromatolites and sponge spicules (monaxon) have been recovered. The link between the decrease in microbial-induced carbonate sedimentation and the decline of large Riphean stromatolites is recorded in the inner sedimentary belt (Deoban–Gangolihat). The first appearance of complex organic-walled microfossils and acanthomorphic acritarchs is recorded in the Blaini–Infrakrol sediments along with possible Ediacaran soft-bodied metazoans and metaphytes in the Krol Formation. In India, the Late Proterozoic base occurs at the bottom of a pink, microbial limestone in the Blaini Formation, and the Precambrian–Cambrian boundary occurs somewhere in the Lower Tal Formation. Ediacaran metazoans occur above glacial deposits assigned to the Varangian/Marinoan/Blainian and below the first occurrence of SSF (Meischucunian zone I), in the lowermost Cambrian.

Hoffman *et al.* (1998) proposed the term ‘Snowball Earth’ to describe the concept of Neoproterozoic low latitude glaciation. They suggested that oceans became completely frozen. However, not all researchers would agree (e.g. Etienne *et al.* 2006), and others suggest that some ocean waters were free of ice, and that primary biological productivity may have collapsed during this period (e.g. Hyde *et al.* 2000). Indeed, some even infer that continental ice cover was thin and patchy (e.g. Powell *et al.* 1993). Palaeomagnetic data also supports the view that some Neoproterozoic sequences on different continents accumulated at low palaeolatitudes, for instance in Australia (Chumakov & Elston 1989; Brookfield 1994). They also emphasized that if glacial deposits were not present in the Late Proterozoic sections, there would be no reason to question the validity of the low palaeomagnetic inclinations and palaeolatitudes of accumulation.

Jenkins (1981) proposed the concept of an Ediacarian Period as the terminal Precambrian subdivision. This time period was finally officially termed the ‘Ediacaran’ in 2004 (Gradstein *et al.* 2004). The Ediacaran stratotype occurs in the Flinders Ranges of South Australia. The Ediacaran Period corresponds to the Vendian Period in the Russian Platform. A supercontinent, Rodinia, including most of the continental crust may have

existed at the end of the Mesoproterozoic (1000 Ma) up until around 750 Ma. During the Neoproterozoic, Gondwana consisted of two separate plates: the Eastern (Australia–Antarctica–India) and Western (Africa–South America) plates. These plates collided during the Cambro-Ordovician Pan African orogenies, to which the coeval Ross (Antarctica) and Delamerian (Australia) events are related (Dalziel *et al.* 2000). In South Australia, the Flinders Ranges host the Adelaidean–Cambrian sequence. The Wilpena Pound Quartzite, well known for its Ediacaran metazoan fossils, underlies the Lower Cambrian archaeocyathan-bearing limestones.

The presence of Ediacaran metazoans and carbonate stromatolitic platform sedimentation has been reported from the Krol Group of the NW Lesser Himalaya in India. In the Tethys Himalaya, the Phe Formation of Zaskar Range consists of Late Proterozoic–Cambrian carbonate platform deposits (Tewari 1998*b*). The SE coast of present day India was probably connected with East Antarctica at this time (Fig. 1). The Himalayan Cambrian sedimentary succession closely resembles the deposits of the Pacific margin of Antarctica and Australia. Cambrian sequences of northern Victoria Land (Antarctica) and South Australia, both part of Gondwana, have been correlated with the coeval Tethys Himalayan sequence. The Tethyan Early



Rodinia, 750 Ma

Fig. 1. Rodinia supercontinent (after Powell 1996; Yoshida & Arima 2000).

Cambrian sequence of the Zanskar Range is furthermore linked with the Shackleton Limestone Group of Antarctica and Normanville Group of Southern Australia (Casnedi 2002).

The Terminal Proterozoic–Cambrian sequences in the Himalaya are referred to as Blaini–Krol–Tal groups in the Krol belt of Lesser Himalaya (Figs 2 & 3), the Macchal–Lolab groups in Kashmir, the Batal–Kunzam La formations in Spiti, the Martoli Group in Kumaon and Buxa–Miri groups in the NE Lesser Himalaya (Tewari 1998a, b, c, 2002a, b, 2003). Sedimentation in the Lesser Himalaya was terminated by the Pan African Orogeny in the Late Cambrian. The Ediacaran biota recorded in these sequences includes stromatolites, cyanobacteria, acritarchs, algae, sponges and other metazoans, metaphytes (vendotaenids) from the Krol Belt of the Himachal and Uttaranchal Lesser Himalaya (Tewari 1989, 1993, 1994, 1996, 1998a, b, 1999a, b, 2001a, b, 2002a, b, 2003, 2004b; Mathur & Shanker 1989; Shanker *et al.* 1997; Kumar *et al.* 1997, 2000; Tewari *et al.* 2000).

The Deoban–Jaunsar groups in the Lesser Himalaya represents pre–Ediacaran carbonate–siliciclastic sedimentation, and a Mesoproterozoic age is strongly supported by the presence of Early to Late Riphean stromatolite assemblages, and associated microbiota (Table 1).

The stromatolite assemblage characteristic of the Deoban–Gangolihat dolomite includes *Kussiella kussiensi*, *Colonnella columnaris*, *Conophyton garganicum* in the lower part, *Baicalia chandakia*, *Jacutophyton* sp., *Baicalia nova*, *Tungussia* sp. in the middle part and *Jurusania–Gymnosolen–Minjaria–Inzeria* assemblage in the upper part of the sequence (Valdiya 1969, 1980; Tewari 1989, 1996; Fig. 5). Cyanobacteria found in the Deoban Chert include *Huronispora psilata*, *Glenobotrydion aenigmatis*, *Myxococcoides minor*, *Oscillatorioopsis*, *Obruchevella*, *Siphonophycus* and *Kildinosphaera* (Tewari 1989, 2003). Biodiversity of stromatolites and microbiota declined at the end of the Mesoproterozoic. The Jaunsar clastic facies contains no preservation of trace fossils or soft-bodied metazoans. The unconformably overlying Blaini Formation is a glacial unit. The pink cap microbial carbonate of the Blaini Formation may represent the base of the Late Proterozoic (base of the Ediacaran) where simple acritarchs such as the Sphaeromorphida and stratified stromatolites occur.

Rodinia began to fragment around 750 Ma, and East Gondwana (India, Australia and Antarctica) separated from West Laurentia. Baltica, Africa and South America were positioned on the other side of Rodinia. Neoproterozoic rifting, breakup of Rodinia and fragmentation of Gondwana, low-latitude

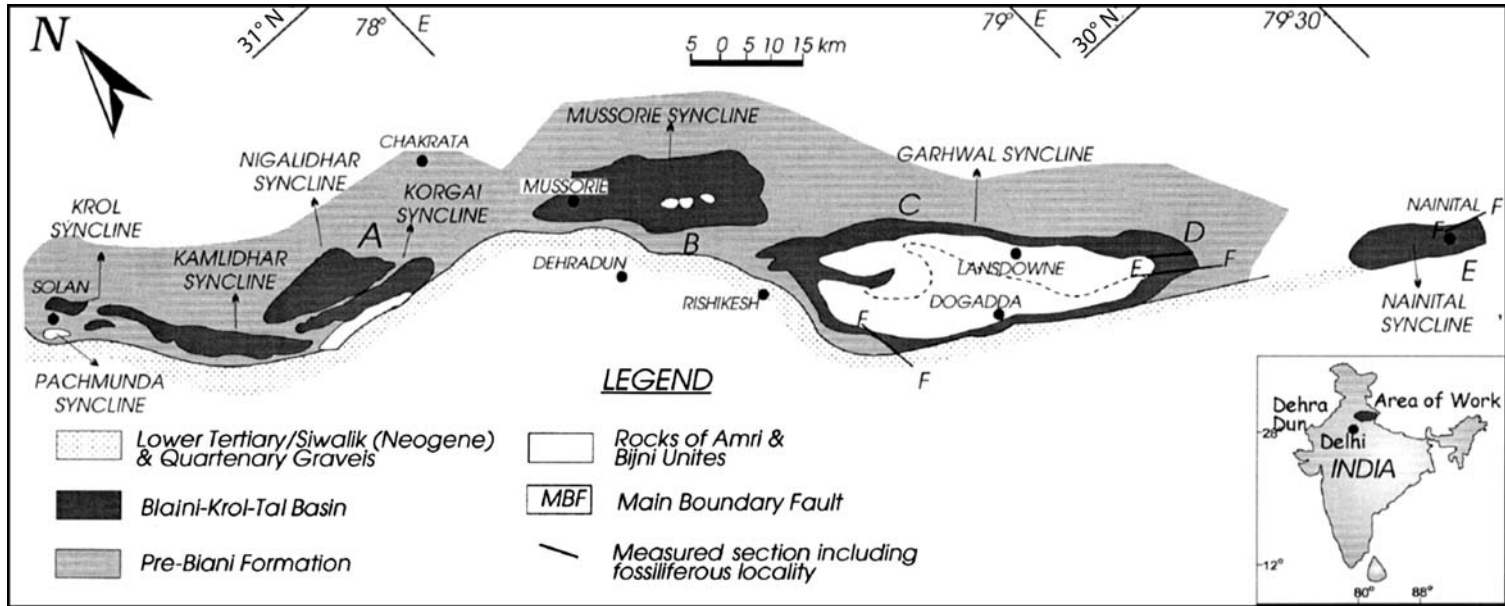


Fig. 2. Geological map of the Blaini-Krol-Tal basin, Lesser Himalaya, India (after Geological Survey of India).

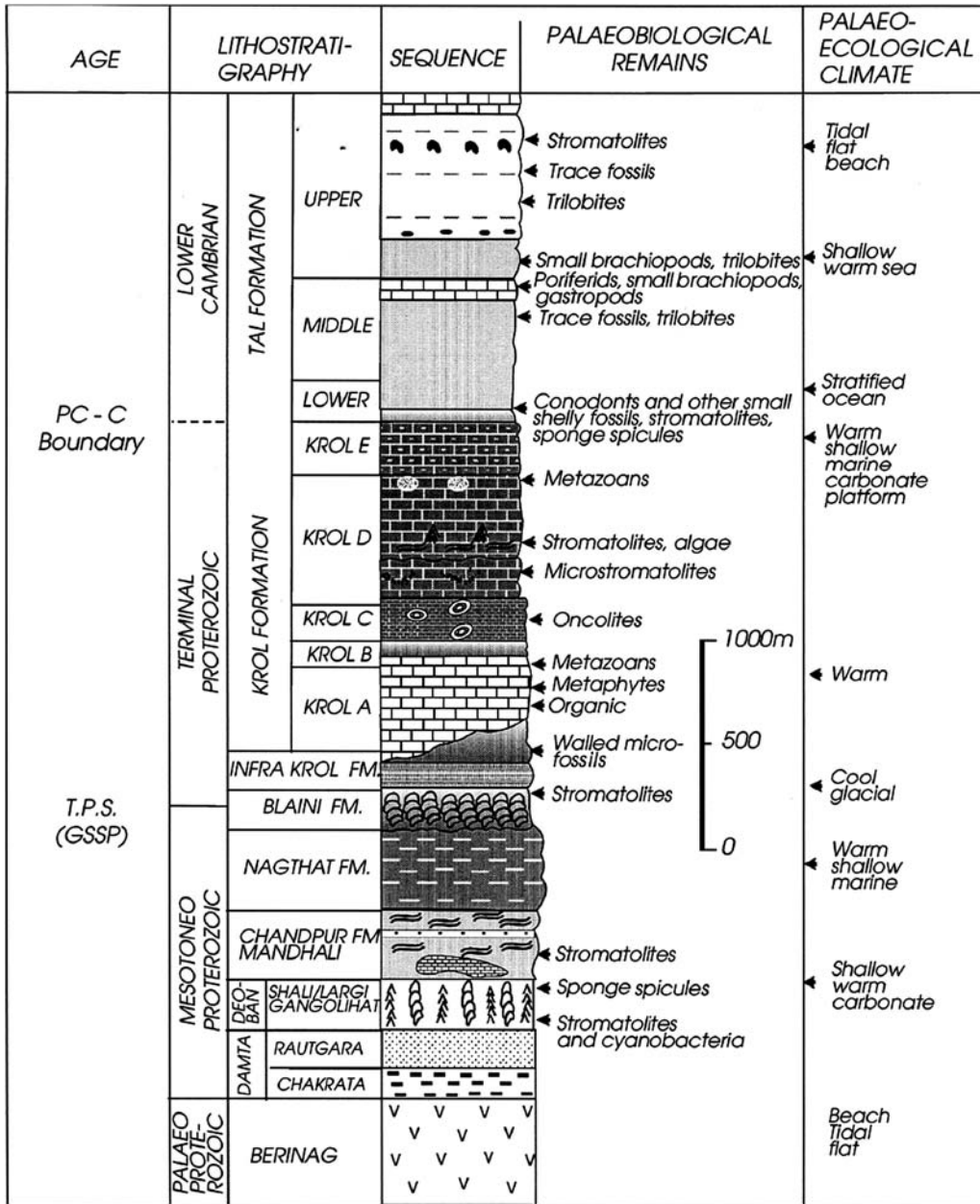


Fig. 3. Lithostratigraphic column, palaeobiological remains and palaeoclimatic events in the Lesser Himalaya, India.

glaciation and global warming events have all been recorded from the Lesser Himalaya of India. Carbon and oxygen isotopic variation and chemostratigraphy of the Blaini-Krol-Tal succession strongly suggests that the Lower Tal Formation ($\delta^{13}C = -4\text{‰}$ PDB) is of Late Neoproterozoic to Cambrian age. In contrast, sediments of the Krol belt in the

Lesser Himalaya are characterized by positive $\delta^{13}C$ values (+1 to 6‰ PDB). The presence of multicellular fossils in the Upper Krol is consistent with a possible increase in atmospheric oxygen.

The base of the Late Proterozoic in the Lesser Himalaya occurs in the Blaini Formation. A pink cap carbonate in the Blaini Formation registers a

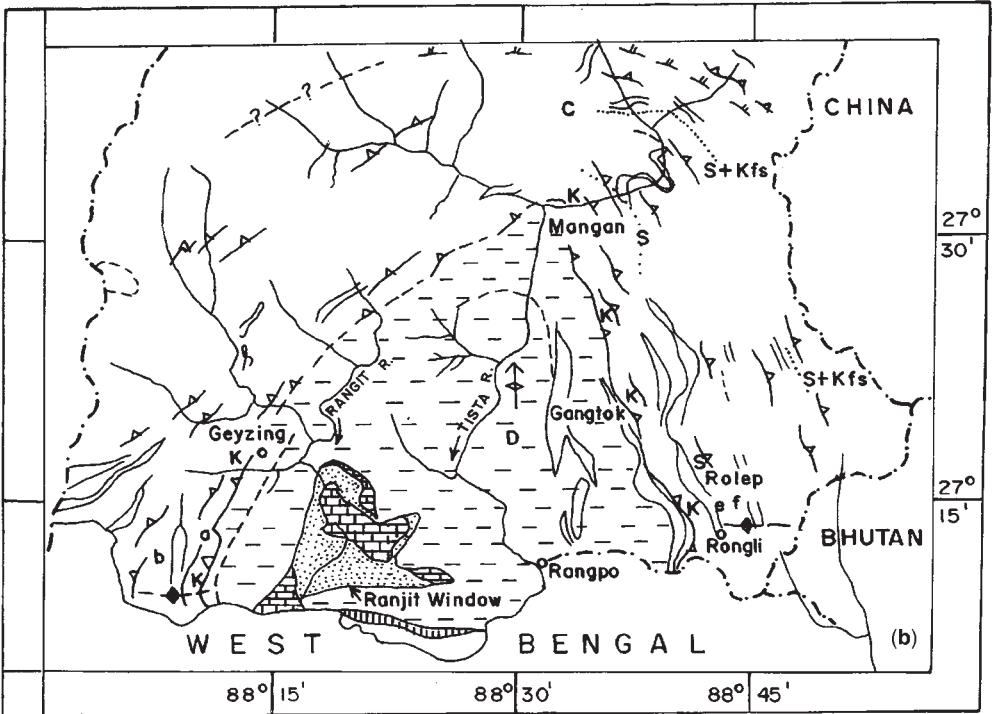
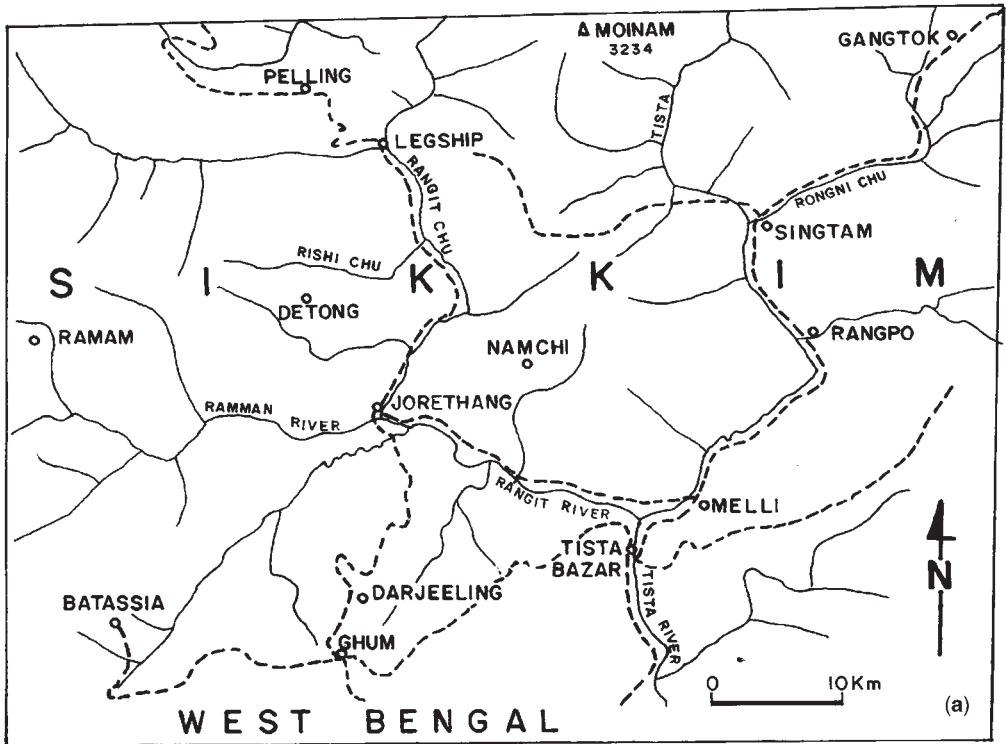


Fig. 4. Location and geological map of the Ranjit Window (RW), Sikkim, NE Lesser Himalaya, India.

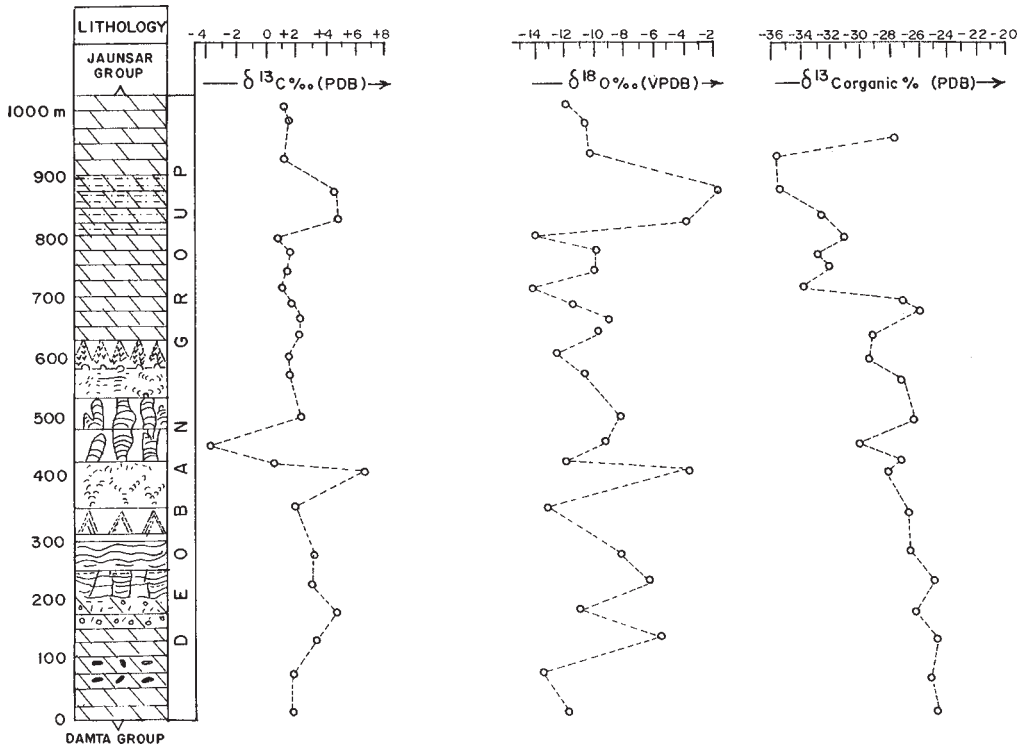


Fig. 5. Carbon isotope chemostratigraphy of the Deoban Group (Meso-Neoproterozoic) Garhwal, Lesser Himalaya, India.

negative $\delta^{13}\text{C}$ value (-3‰ PDB) and caps glacial sediments that are possibly representative of the Varanger glacial event. Comparison of the available carbon and oxygen isotope curves from other regions of Eastern Gondwana and South China, parts of Siberia and North Africa suggests that the Neoproterozoic–Early Cambrian chemostratigraphy is consistent in isotopic variation, with carbon isotopic signatures similar between Neoproterozoic sediments of the Bambui Group, Central Brazil and the Krol Formation of the Lesser Himalaya, India. In the northeastern Lesser Himalaya of India, the Neoproterozoic sedimentary successions show well developed carbonates, the Buxa Dolomite, with positive C-isotope ratios ($\delta^{13}\text{C} = +3.7$ to $+5.4\text{‰}$ PDB). The O-isotopic data also demonstrate $\delta^{18}\text{O}$ values fluctuating within a narrow range between -8.9 and -7.2‰ PDB corresponding with global Late Proterozoic C-isotopic evolution, followed by oscillations during the Precambrian–Cambrian transition in the Lesser Himalaya of Eastern Gondwana.

The break-up of Rodinia, East Gondwana and the Lesser Himalayas

The Rodinia supercontinent (Fig. 1) began to fracture around 750 Ma. East Gondwana (India, Australia and Antarctica) separated from West Laurentia (Powell *et al.* 1993). Baltica, Africa and South America occupied the other side of Rodinia. However, the existence of a Neoproterozoic supercontinent Rodinia is still hypothetical (Yoshida & Arima 2000) and recent geochronological and palaeomagnetic records of South America and Africa show that these cratonic fragments may not have been part of Rodinia (Cordani *et al.* 2003). The Neoproterozoic evidence for the rifting apart of Rodinia and the fragmentation of Gondwana low-latitude glaciation and global warming events have been recorded from the Lesser Himalaya of India (Tewari 2002a). Carbon and oxygen isotopic variation and chemostratigraphy of the Lesser Himalayan carbonate formations evidently reflect global palaeoclimatic and palaeobiological events (Tewari 2001a, b, c, 2002a, b, 2003, 2004b; Figs 6,

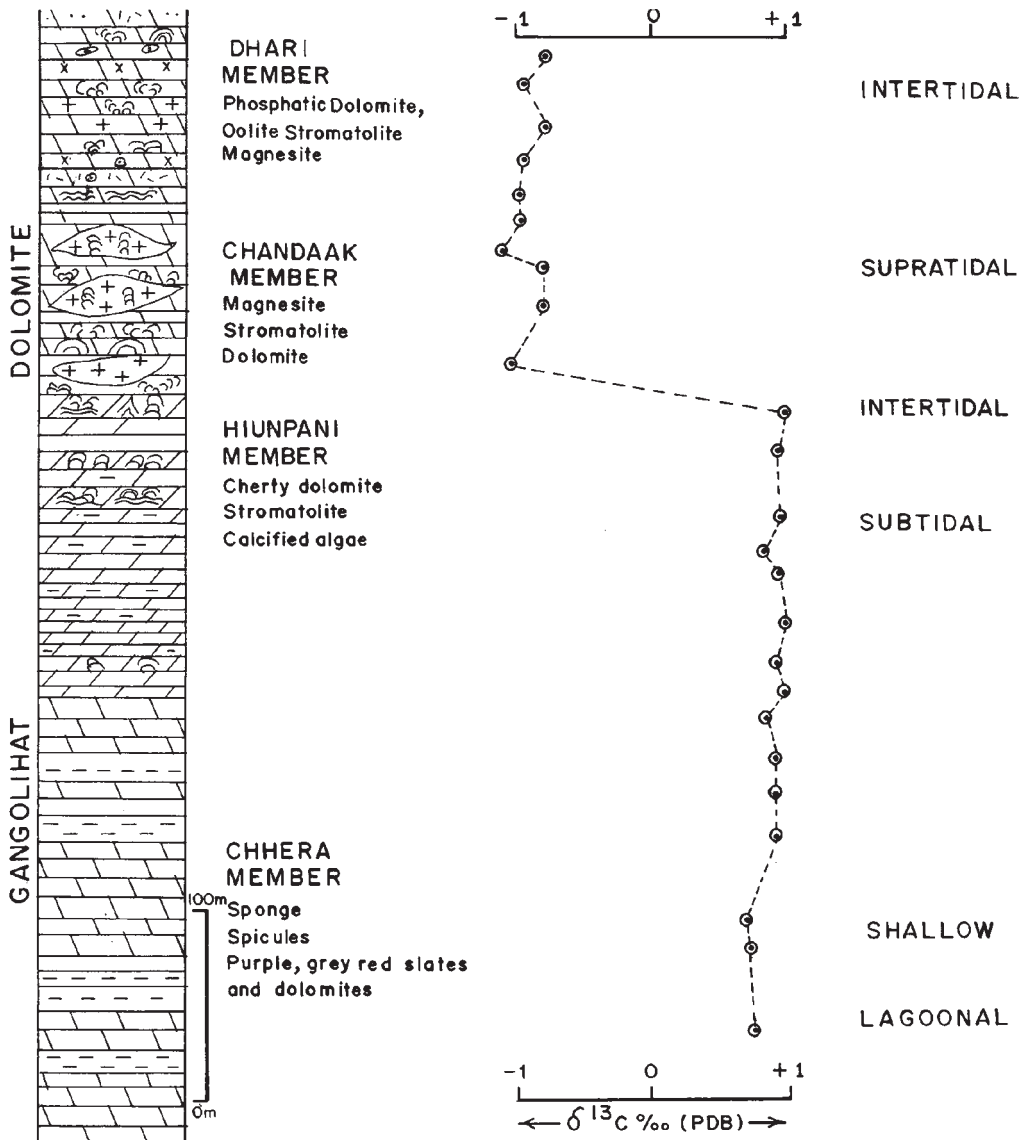


Fig. 6. Carbon isotope chemostratigraphy of the Gangolihat Dolomite (Meso-Neoproterozoic), Kumaun, Lesser Himalaya, India.

7 and 8). The concept of using C-isotope variation as a global correlator is based upon the assumption that C-isotopic ratios fluctuate in response to changes in the net rate of organic burial, climate variations and availability of atmospheric oxygen.

Terminal Proterozoic glacial deposits have been recorded from most continents, suggesting that palaeoclimatic change on Earth over the last

650 Ma is directly related to atmospheric CO₂ fluctuations (Jacobson & Kaufman 1999; Tewari 2001a, 2003). The 'Snowball Earth' model suggests that during global glaciation there may be a short-lived change in the C-isotopic ratios of the ocean because of elimination of marine life (not all researchers ascribe to this model, (e.g. Etienne *et al.* 2006). Hence, the $\delta^{13}\text{C}$ in marine carbonates

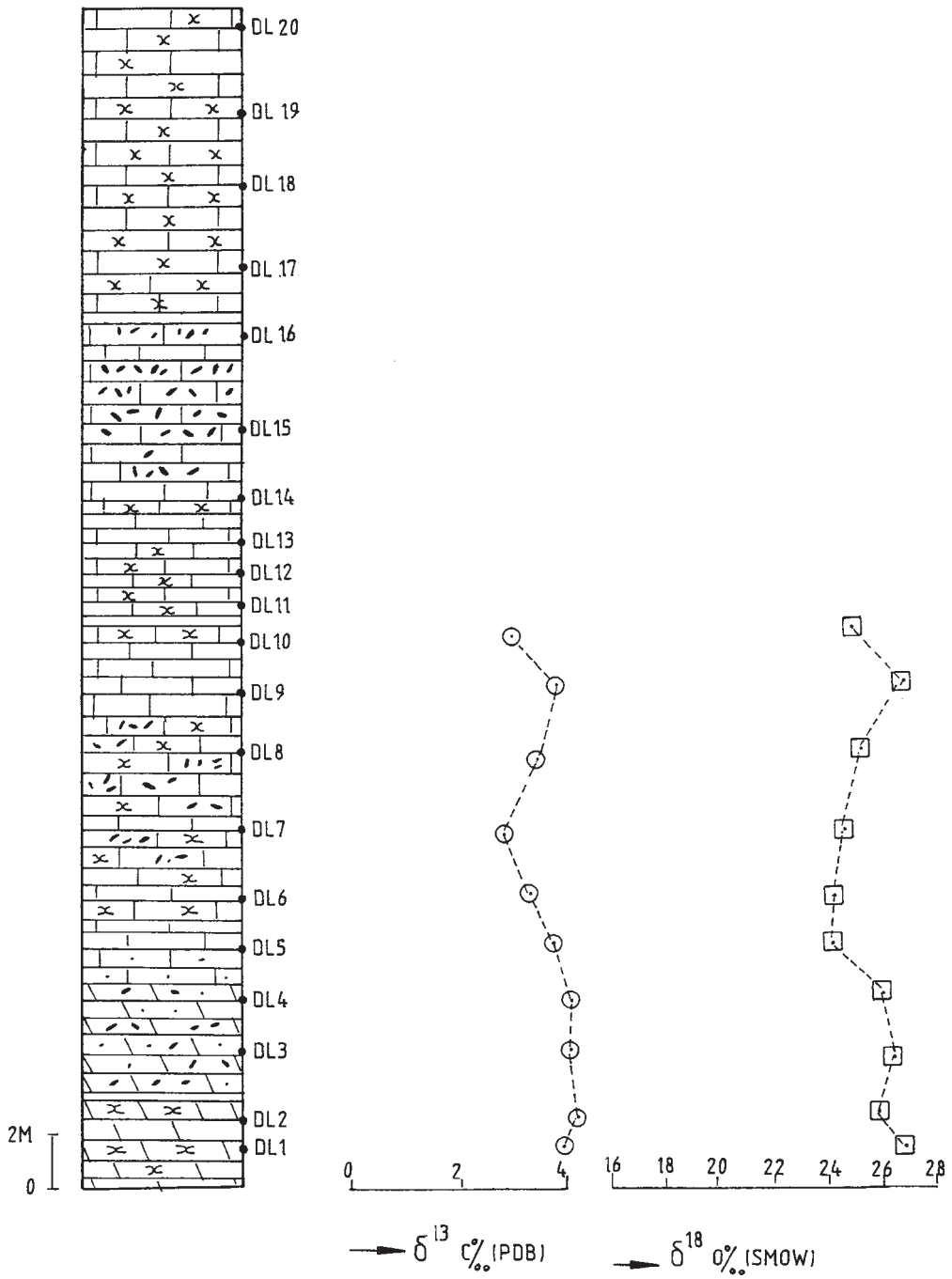


Fig. 7. C-isotope chemostratigraphy of the Uttarkashi Limestone, Garhwal, Lesser Himalaya, India.

will drastically decrease to $-6 \pm 1\%$ (PDB) (Jacobsen 2001). The deglaciation event is recorded in the C-isotope variation from a pink cap carbonate indicating the end of the Terminal Proterozoic glaciation (Tewari 2001a, 2003). Kaufman *et al.* (1997) reported $\delta^{13}\text{C}$ values in cap carbonates varying globally from 0 to -5% PDB. The $\delta^{13}\text{C}$ values of the pink Blaini Limestone also vary from 0 to 3% PDB, consistent with the global record. Major palaeoclimatic changes, carbon isotopic fluctuations, biotic extinction-evolutionary events, sea level changes during the Late Proterozoic that are recorded from the Lesser Himalaya, India, are discussed in some detail in this paper.

Secular variations in carbon isotopes, palaeobiological and biogeochemical cycles

Palaeobiological activities on Earth started around 3800 million years ago with carbon as the main element in organic matter (Schidlowski *et al.* 1975; Eichmann & Schidlowski 1975). The ratio of stable C-isotopes reflects the effect of biological activity in the carbon cycle. Isotopic fractionation of *c.* 25% between the two carbon species (terrestrial or carbonate carbon, and organic or reduced carbon) has been recorded from rocks *c.* 3500 Ma old (Eichmann & Schidlowski 1975; Schidlowski *et al.* 1975, 1983). Carbon isotope stratigraphies of Proterozoic and Early Cambrian sequences have been established in recent years from many different parts of the world (e.g. Knoll *et al.* 1995; Santos *et al.* 2000). Carbon isotope excursions through the Neoproterozoic and across the Precambrian–Cambrian boundary have been interpreted to explain evolutionary diversification and extinction events, palaeoenvironmental and palaeoceanic conditions, changes in sea water chemistry and extraterrestrial impacts, and have been used to set up a chemostratigraphy for this time period (see reviews of Brasier *et al.* 1990, 1996; Brasier 1992; Knoll *et al.* 1995; Ripperdan 1994; Tucker 1986).

Ediacaran carbon-isotope chemostratigraphy and trace element geochemistry of the Blaini–Krol–Tal sequence, Lesser Himalaya

The Neoproterozoic is characterized by global occurrence of thick tidal flat carbonate-siliciclastic sequences and glacial cycles. Carbon and oxygen isotopic variations in these sequences have been used as palaeoclimatic indicators. Neoproterozoic carbonates have been studied worldwide for

variations in oxygen and carbon isotope ratios, with special reference to inorganic and organic carbon reservoirs (Schidlowski *et al.* 1976; Aharon *et al.* 1987; Brasier *et al.* 1996; Kaufmann & Knoll 1995; Hoffman *et al.* 1998; Tewari 1991, 1997; Kumar & Tewari 1995). Low (-3% to -5%) $\delta^{13}\text{C}$ PDB values have been reported from reddish-pinkish dolomites (cap carbonates) associated with Neoproterozoic deglaciation around the globe, including the Blaini Formation (Bhattacharya *et al.* 1997; Tewari 1999a, b; Kumar *et al.* 2000; Santos *et al.* 2000; Alvarenga *et al.* 2003).

The carbon isotope chemostratigraphy of the Blaini pink microbial/stromatolitic cap carbonate shows negative values ($\delta^{13}\text{C} -2.7\%$ PDB), and the overlying Krol carbonates indicate very high positive values ($+6\%$ PDB, Fig. 9, Tewari 1991; Kumar & Tewari 1995). Isotopically heavy carbonates ($\delta^{13}\text{C} +6.6\%$ PDB) were deposited in the Upper Krol D stromatolitic facies representing enhanced organic burial. This strong positive isotopic shift is followed by a decrease in $\delta^{13}\text{C}$ from $+2\%$ to *c.* 0% in Krol E carbonates. There is a negative shift in $\delta^{13}\text{C}$ (-2.2% to -4% PDB) just below the Lower Cambrian (Fig. 9). These $\delta^{13}\text{C}$ records are in concert with global isotopic variations in Neoproterozoic–Early Cambrian oceans of the world (Tewari 1998c). Bhattacharya *et al.* (1997) have also reported four depletions in $\delta^{13}\text{C}$ values from Mussoorie and Garhwal synclines. However, only two peaks are of global significance, the first corresponding to what appears to be the end of the Varanger glaciation of Late Neoproterozoic age. The Blaini pink limestone in the Nainital syncline also shows depleted $\delta^{13}\text{C}$ values ($\delta^{13}\text{C} = -2.2\%$ PDB). The oxygen isotopes ($\delta^{18}\text{O} +20.1$ to 28.6% SMOW) of the Upper Krol carbonates indicate high oxygen levels associated with possible Ediacaran diversification (Fig. 9). Major Neoproterozoic and Cambrian palaeoclimatic events, isotopic fluctuations and biotic evolution recorded in Lesser Himalaya are summarized in Table 2.

Carbon, oxygen and strontium isotopes, trace and rare earth element data are known from the Dhanaulti–Durmala section of the Mussoorie Syncline (Fig. 2; Table 3). The Precambrian–Cambrian boundary has been placed in the Lower Tal Formation (Aharon *et al.* 1987; Shanker & Mathur 1992; Tewari 1984, 1996, 1999a). The contact between the uppermost Krol Formation (Krol E) and the lower Tal Formation (chert-phosphorite member) is well exposed at Durmala Phosphorite Mine, where phosphorite is being commercially mined. An Early Cambrian stromatolite assemblage including *Collumnaefacta vulgaris*, *Boxonia gracilis*, *Colleniella*, *Aldania mussoorica*

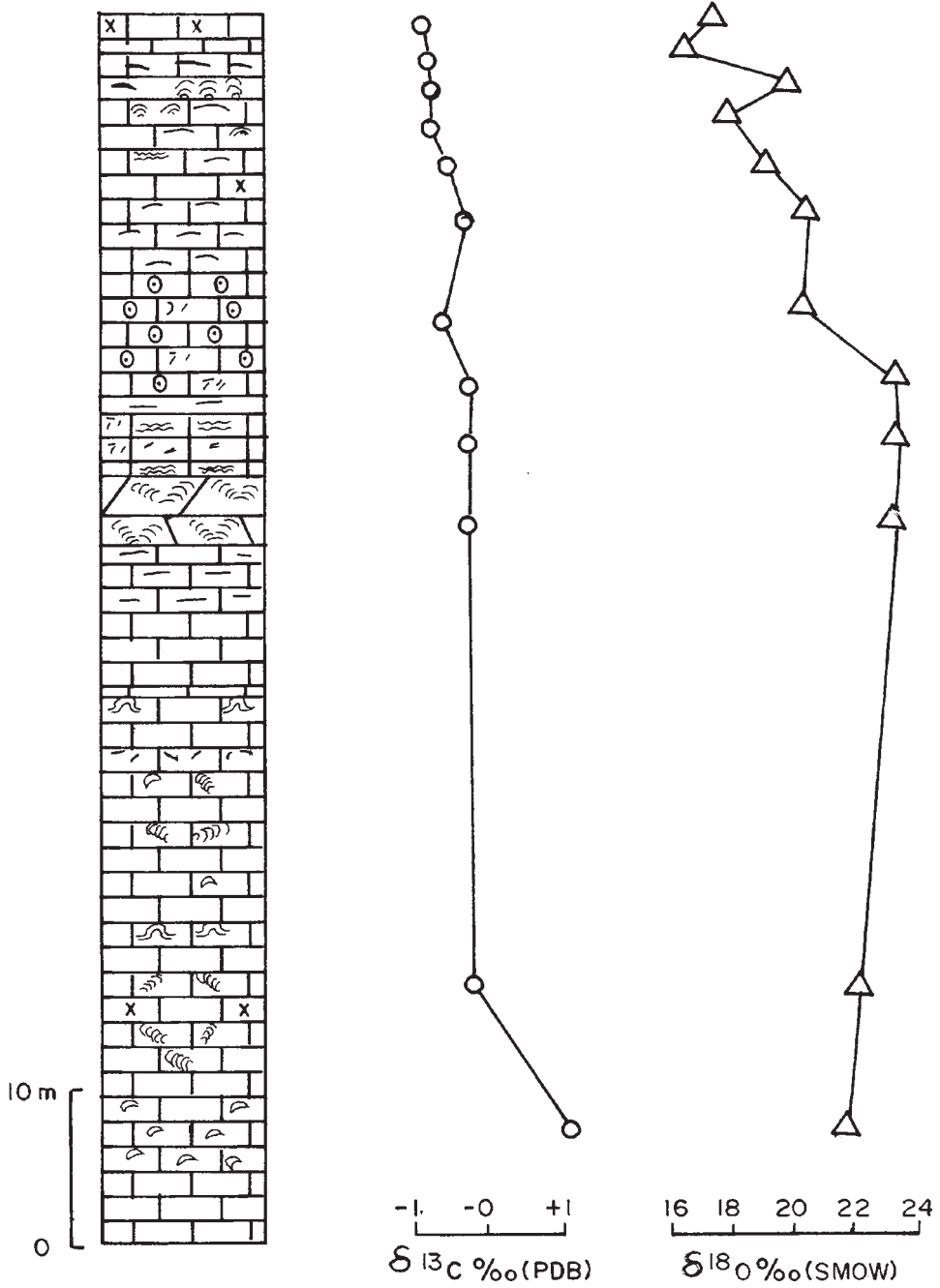


Fig. 8. C-isotope chemostratigraphy of the Lameri Limestone, Garhwal, Lesser Himalaya, India.

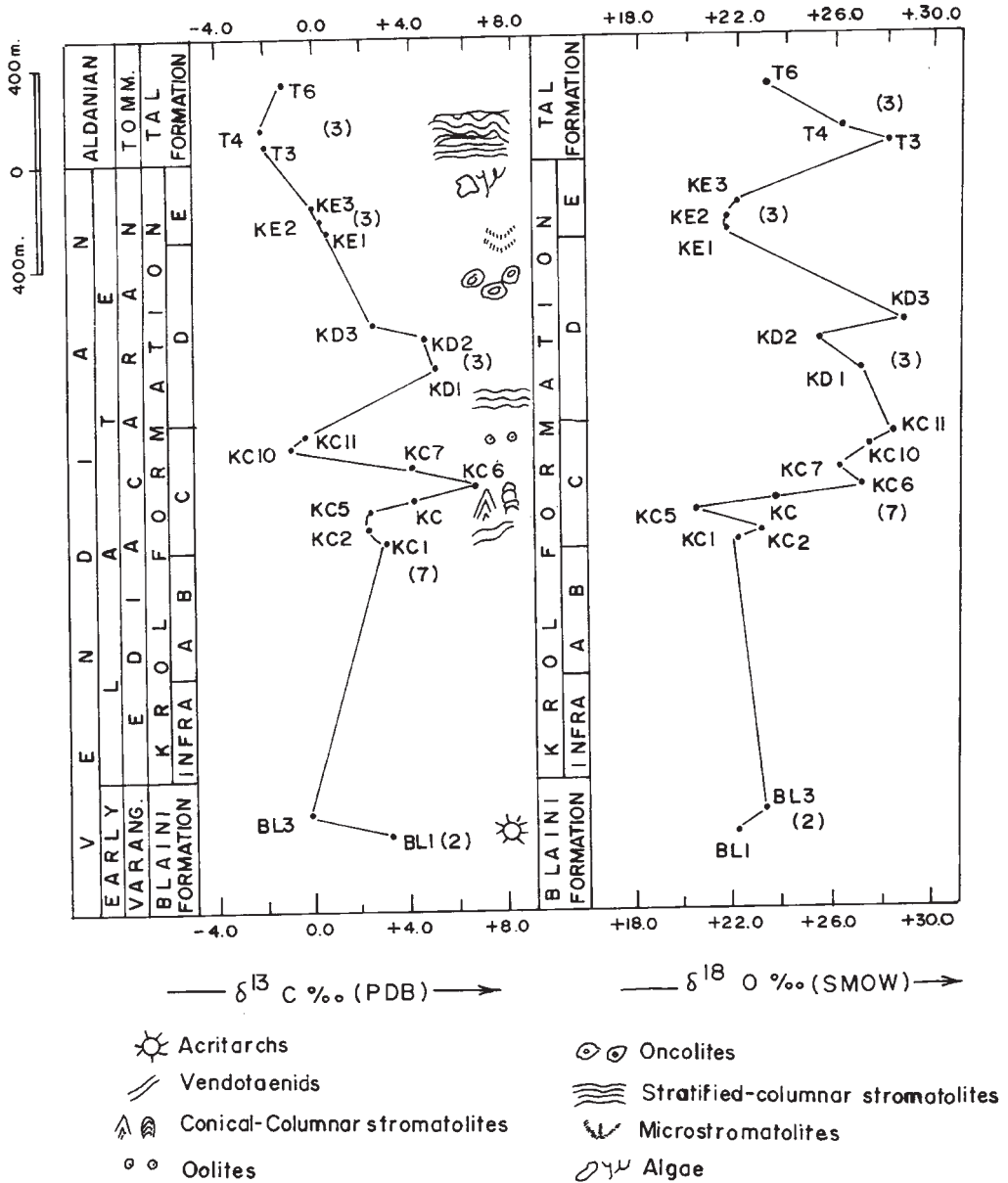


Fig. 9. C-isotope chemostratigraphy of the Blaini–Krol–Tal (Terminal Proterozoic–Lower Cambrian) succession of the Lesser Himalaya, India.

and oncolites are recorded from this locality (Tewari 1984, 1989, 1993, 1996). Small Shelly Fossils of Tommotian (Early Cambrian) age are also reported from phosphatic deposits in the Lower Tal Formation (Brasier & Singh 1989; Brasier *et al.* 1996). Laser Raman spectroscopy of the Mussoorie Tal Phosphorite indicates the presence of amino acids.

The underlying Krol carbonates are tidal flat deposits including stromatolites, and fenestral facies are well developed (Tewari 1984, 2001a, 2002a, b). Carbon, oxygen and strontium isotope data from the Krol Tal carbonates in the Mussoorie syncline are summarized in Table 4. Stable isotope values range from -2.9 to +6.5‰ PDB for $\delta^{13}\text{C}$ and +20.1 to +28.6‰ SMOW for $\delta^{18}\text{O}$

Table 1. C- and O-isotope analyses for Deoban carbonates

Sample No.	Description of sample	$\delta^{13}\text{C}\%_{\text{CPDB}}$	$\delta^{18}\text{O}\%_{\text{CSMOW}}$
25. D25	Light grey laminated dolomite (altitude 10 000 feet)	1.1	19.1
24. D24	Light grey laminated dolomite (altitude 10 000 feet)	1.4	20.6
23. D23	Light grey dolomite (altitude 9000 feet)	1.1	20.9
22. D22	Finely laminated calcareous silty layers	4.3	29.4
21. D21	Alternating thin dolomite and silty layers	4.8	27.3
20. D20	Light grey dolomite after 100 feet interval	0.9	16.8
19. D19	Light grey dolomite after 100 feet interval	1.3	21.1
18. D18	Light grey dolomite after 100 feet interval	1.2	21.0
17. D17	Light grey dolomite after 100 feet interval	0.9	16.8
16. D16	Light grey dolomite after 100 feet interval	1.5	19.6
15. D15	Light grey dolomite after 100 feet interval	2.1	21.9
14. D14	Light grey dolomite foot path to Deoban summit	2.0	21.1
13. D13	Dark bluish grey dolomite with elongated conical <i>Georginia</i> sp. and <i>Conophyton</i> sp. structures	1.4	18.5
12. D12	Dark bluish grey dolomite with <i>Tungussia</i> sp	1.4	20.4
11. D11	Dark bluish grey dolomite with <i>Jurusania</i> sp. and <i>Minjaria</i> sp. biostrome, 100 m below Deoban Forest Rest House (DFRH)	2.0	22.6
10. D10	Dark bluish grey dolomite with <i>Jurusania</i> sp. and <i>Minjaria</i> sp. biostrome, 100 m below DFRH	-3.7	21.5
9. D9	Dark black (organic) silty shale (similar to D8)	0.3	18.9
8. D8	Greyish black shale with <i>Chuarina circularis</i> megascopic acritarch between stromatolitic buildups, 500 m west of DFRH. Locality as D7	6.6	27.2
7. D7	Dark bluish dolomite with <i>Baicalia nova</i> biostrome, 500 m west of DFRH (altitude 9232 feet)	1.7	17.8
6. D6	Light grey dolomite with <i>Stratifera</i> sp. 1 km from bifurcation	3.0	22.7
5. D5	Light grey dolomite with large <i>Kussiella kussiensis</i> biostrome and small <i>Conophyton</i> sp. biostrome, DFRH road, 100 m from bifurcation	2.9	24.5
4. D4	Oolitic-intraclastic, coated carbonate grains near bifurcation to Deoban Forest Rest House (DFRH) mule path, Deoban 3 km	4.6	19.9
3. D3	Dark bluish (organic) cherty laminated dolomite (microbiota-bearing), Chakrata-Deoban road, 1.3 km	3.2	25.4
2. D2	Dark bluish dolomite with chert lenses and layers (microbiota), Chakrata-Deoban road, 1.2 km	1.8	17.3
1. D1	Grey dolomite, lowermost Deoban road section 1 km near the contact with Chakrata slates (Damta Group)	1.4	19.2

Table 2. Major palaeoclimatic and biotic changes across Neoproterozoic-Cambrian Transition in the Lesser Himalaya, India (Tewari 2001a)

Age/Stage	Period	Climate	$\delta^{13}\text{C}$ values	Fossils
Cambrian	Talian	Warm	Changing (-ve to +ve)	Brachiopods, trilobites, trace fossils, small shelly fossils, sponge spicules, stromatolite
Ediacaran	Krolian	Warm	Positive	Ediacaran, vendotaenilids, algae and stromatolites
Varangian	Blainian	Glacial	Negative (lighter)	Acritarchs, microbialites
Riphean-Early Vendian	Deobanian	Warm	Positive (heavier)	Predominantly stromatolites, cyanobacteria, organic walled microfossils, sponge spicules, epiphyton algae

Table 3. $\delta^{13}C$, $\delta^{18}O$ and Sr-Isotope data of Krol–Tal carbonates from the Mussoorie Syncline, Uttaranchal

Sample	Lithological units	Rock type	$\delta^{13}C\text{‰}_{PDB}$	$\delta^{18}O\text{‰}_{SMOW}$	$^{87}Sr/^{86}Sr$
T6	Tal	Oncolitic	−1.2	23.1	N.D.
T4	Tal	Stromatolitic	−2.5	27.3	0.7092
T3	Tal	Phosphatic & dolomite	−2.9	27.8	0.7098
KE3	Krol E	Shaly dolomite	0.1	21.9	N.D.
KE2	Krol E	Shaly dolomite	0.0	21.8	0.7151
KE1	Krol E	Shaly dolomite	0.5	22.2	0.7151
KD3	Krol D	Shaly dolomite (micritic)	2.4	28.6	0.7094
KD2	Krol D	Microbial mat dolomite	4.6	25.8	0.7091
KD1	Krol D	Shaly dolomite	4.8	28.5	0.7091
KC11	Krol C	Shaly dolomite	0.3	28.2	N.D.
KC10	Krol C	Cherty dolomite	1.0	27.3	N.D.
KC7	Krol C	Cherty dolomite	2.9	26.0	N.D.
KC6.1	Krol C	Oolitic dolomite	2.4	24.3	0.7110
KC6	Krol C	Cherty banded limestone	6.5	27.4	0.7094
KC5.1	Krol C	Oolitic limestone	2.4	24.5	0.7104
KC5	Krol C	Fine grained limestone	2.2	20.4	N.D.
KC	Krol C	Bhatta limestone (micritic)	2.1	20.1	0.7088
KC2	Krol C	Oolitic limestone	2.1	23.2	0.7122
KC1	Krol C	Brecciated limestone	2.8	21.9	N.D.
BL3	Blaini	Pink dolomite (fine grained)	−0.4	23.3	N.D.
BL1	Blaini	Pink laminated dolomite	2.9	22.1	N.D.

N.D. not determined.

respectively; $\delta^{13}C$ values are generally positive for Krol C and D, carbonates reaching a $\delta^{13}C$ maximum of 6.5‰ PDB. Krol E carbonates have near zero $\delta^{13}C$ values. Tal carbonates show negative $\delta^{13}C$ values with a $\delta^{13}C$ minimum of −2.9‰ PDB. The petrographic study of these carbonates indicates that they preserve primary fabric-like oolites, microbial laminites and micrite. The isotopic signatures are considered unaltered and primary (Aharon *et al.* 1987). Hence, the positive $\delta^{13}C$ values relative to PDB represent high rates of organic carbon burial whereas negative $\delta^{13}C$ values and $\delta^{13}C$ maxima of 6.5‰ PDB for Krol D dolomite represent increased organic carbon burial. Conversely, ^{13}C minima of −2.9‰ PDB of Lower Tal Formation indicate low rate of organic carbon burial. Possible Ediacaran metazoans and metapytes are recorded in the Krol Formation (Tewari 1993, 1998b, 2001a, 2002b).

$^{87}Sr/^{86}Sr$ data in the Krol sequence vary from 0.7088 to 0.7151 (Table 4). The lowest value of 0.7088 was obtained from the Middle Krol C limestone. Krol C is a cement grade limestone in the Mussoorie Syncline, which has a Sr content of 659 ppm. Veizer *et al.* (1983) and Burns *et al.* (1994) have shown that the seawater $^{87}Sr/^{86}Sr$ value was *c.* 0.707, during what appears to be the Varanger glaciation, and rapidly rose to 0.709 during Late Ediacaran (to near present day sea water value). The Sr-isotope value of 0.7088 for

the Upper Krol carbonates of the Mussoorie syncline may be taken as a near pristine sea water value, confirming that Late Proterozoic sea water values reached to *c.* 0.709 and corroborating with the earlier findings (Veizer *et al.* 1983; Burns *et al.* 1994; Aharon & Liew 1992). According to Aharon & Liew (1992), the high Sr-isotope value of >0.7095 for Krol and Tal carbonate may be due to exchanges with crustal fluids.

Trace element abundances of Blaini–Krol–Tal carbonate rocks are shown in Table 4. All samples from Krol E have high concentration of transition metals (Co, Ni, Cu and Zn), lithophile elements (Cs, Rb, Ba and Pb) and high field strength-cations (Y, Th, U, Zr and Nb), but are depleted in vanadium (Table 5). The strontium content is high for the Lower Tal carbonates. Major oxides, trace elements, and rare earth concentrations are summarized in Table 3.

Oxides include Al_2O_3 , which varies from 0.01% to 0.72%, K_2O which varies from 0.01% to 0.017, SiO_2 which varies from 0.02% to 1%, and 74.5% in the black chert straddling the Precambrian–Cambrian boundary. CaO varies from 30.56% to 31.0% in the uppermost Krol and is 9.6% in Lower Tal. MgO varies from 20.97% to 21.0% (0.84% in lower Tal). Na_2O varies from 0.033% to 0.34% (0.03% in Lower Tal). Fe_2O_3 (total) varies from 0.042% to 0.16% (10% in Lower Tal). P_2O_5 varies from 0.015% to 0.039% (4.0% in Lower

Table 4. Trace element distribution in Blaini–Krol–Tal carbonates of the Mussoorie Syncline

Sample No.	Cu (ppm)	Ni (ppm)	Pb (ppm)	Zn (ppm)	Co (ppm)	Cr (ppm)	Ba (ppm)	Sr (ppm)	V (ppm)	U (ppm)
GC3	11	<5	12	18	5	73	239	74	36	20
GC2	7	<5	10	14	5	59	228	72	37	17
GC1	10	<5	10	19	5	68	191	73	37	16
KP3	18	28	<5	<5	<5	328	133	50	115	20
KP1	20	38	<5	43	<5	331	146	28	111	19
TIM	19	76	23	<5	10	114	1654	12	240	56
KCM	42	52	30	66	18	105	292	39	142	20
KT2	47	16	8	51	16	106	437	66	352	19
KT1	52	88	15	55	18	102	430	69	304	19
TC2	21	29	13	44	15	106	362	45	76	16
TC1	14	9	<5	20	5	82	238	60	39	16
TD2	50	205	21	34	23	112	1878	61	478	42
TD1	45	92	22	16	5	112	223	722	585	103
TD1	45	247	23	89	15	105	1609	25	274	62
MP2	98	5	29	82	5	628	981	78	958	20
MP1	10	14	<5	7	<5	<5	1496	291	49	19
KER1	13	<5	<5	23	<5	31	501	63	34	12
VKD2	<5	<5	<5	<5	<5	11	17	36	<10	17
KD1	15	<5	<5	22	<5	17	4419	253	15	17
KC9	12	<5	<5	13	<5	92	273	40	126	19
KC8	13	<5	14	13	<5	89	254	39	113	15
KC6	<5	<5	<5	<5	<5	23	11	78	<10	17
KC3	<5	<5	<5	14	<5	12	32	64	<10	22
KC1	7	<5	<5	6	<5	141	24	45	<10	15
KB4	50	16	14	270	8	94	220	24	55	15
KB2	5	5	5	17	5	36	70	58	13	13
KB1	6	5	5	17	5	27	91	55	17	20

Table 5. REE, Y, Sc and Th distribution in the Blaini and Krol carbonates of the Mussoorie Syncline

REE (ppm)	KD1	VKD2	KC1	KC6	KC9	KC8	KC3	KB1	KB2	KB4
La	<5	<5	<5	<5	70	70	<5	10	9	30
Ce	<10	<10	<10	<10	105	103	<10	17	13	57
Pr	<10	<10	<10	<10	14	11	<10	<10	<10	<10
Nd	<10	<10	<10	<10	45	46	<10	<10	<10	20
Sm	<10	<10	<10	<10	11	10	<10	<10	<10	<10
Eu	<10	<1	<1	<1	<1	<1	<1	<1	<1	1.2
Gd	<10	<10	<10	<10	<10	<10	<10	<10	<10	<10
Tb	<5	<5	<5	<5	<5	<5	<5	<5	<5	<5
Dy	<2	<2	<2	<2	5	4	<2	<2	<2	6.5
Ho	<2	<2	<2	<2	<2	<2	<2	<2	<2	<2
Er	<3	<3	<3	<3	4	3.5	<3	<3	<3	<3
Tm	<2	<2	<2	<2	<2	<2	<2	<2	<2	<2
Yb	2.3	<1	<1	<1	2.8	2.7	<1	1.0	<1	3.3
Lu	<1	<1	<1	<1	<1	<1	<1	<1	<1	<1
Y	8.3	2.5	3.2	<1	24	22.3	<1	8	7	30
Sc	<1	<1	<1	<1	13.5	13.7	<1	2.8	2.0	7.9
Th	<10	<10	<10	<0	25	22	<10	<10	<10	13

Tal). TiO₂ varies from 0.001% to 0.022% (0.008% in Lower Tal). MnO varies from 0.004% to 0.035% (0.44% in Lower Tal) (Tables 6 and 7).

Carbon and oxygen isotope chemostratigraphy and palaeobiology of the Buxa Dolomite, NE Lesser Himalaya

Acharyya (1974) subdivided the Buxa Group into two units in the type area based on carbonate content and colour. Namely: (1) the lower Sinchula Formation overlain by (2) the Jainti Formation. The Buxa Group is exposed in Nakshal Khola and in the Jaldhaka river section in the easternmost part of

the Darjeeling foothills, eastern Himalaya (Fig. 4). It is also recognized in the Sikkim Himalaya in the Ranjit Window (Raina 1976; Tewari 2004a). In western Arunachal, the Buxa Group is subdivided into two units separated by a pebbly diamictite bed (Shergaon pebble bed). However, the tectonostratigraphic position of the Buxa Group is still not certain in the Arunachal Lesser Himalaya. (Tandon *et al.* 1979; Tewari 1998a, b, 2002a, b, 2003).

The base of this Late Proterozoic carbonate sequence is represented by glaciomarine-fluvial diamictite-pebble beds. Other sedimentary facies include microbial buildups, oncolites, oolites, fenestral-textured sediments and microstromatolites, suggestive of shallow marine tidal flat

Table 6. REE distribution in Lower Tal (Precambrian–Cambrian boundary) Formation, Mussoorie Syncline

REE (ppm)	TD-1	TD-1	TD-2	TC-2	TC-1	KT-2	MP-2
La	101	53	43	46	40	37	48
Ce	65	85	72	89	79	64	61
Pr	<10	<10	<10	<10	<10	<10	<10
Nd	69	40	31	31	24	31	38
Sm	<10	<10	<10	<10	<10	<10	<10
Eu	3.2	1.1	1.2	1.1	1.0	1.1	2.3
Gd	14	<10	<10	<10	<10	<10	<10
Tb	<5	<5	<5	<5	<5	<5	<5
Dy	17	5	5	6	5	5	10
Ho	3.5	<2	<2	<2	<2	<2	<2
Er	11	4	5	5	4	5	5
Tm	<2	3	2	<2	<2	3	2
Yb	8.6	4.5	4.5	3.8	2.8	3.3	6.8
Lu	<1	<1	<1	<1	<1	<1	<1
Y	242	29	31	29	28	29	105
Sc	<1	15	13	11	6	13	4
Th	<10	21	19	21	18	17	10

Table 7. REE distribution in Lower Tal Formation, Mussoorie Syncline

S. No.	Sample No.	La	Ce	Pr	Nd	Sm	Eu	Gd	Tb	Dy	Ho	Er	Tm	Yb	Lu	Y	Sc	Th
1	KER-1	14	26	<10	12	<10	<1	<10	<5	2	<2	<3	<2	1.6	<1	14.6	4.6	<10
2	GC-1	<10	17	<10	<10	<10	<1	<10	<5	<2	<2	<3	<2	<1	<1	6.6	1.3	<10
3	GC-2	10	16	<10	<10	<10	<1	<10	<5	<2	<2	<3	<2	<1	<1	6.5	1.3	<10
4	GC-3	11	20	<10	<10	<10	<1	<10	<5	<2	<2	<3	<2	1.2	<1	7.6	1.6	<10
5	MP-1	11	17	<10	<10	<10	1.7	<10	<5	2	<2	<3	<2	1.1	<1	8.7	1	<10
6	KCM	53	86	<10	40	<10	1.3	11	<5	7	<2	4	<2	4.1	<1	32	17.8	24
7	KT-1	36	66	<10	26	<10	1.0	<10	<5	5	<2	4	<2	3.7	<1	30	13.2	17
8	TIM	42	81	<10	32	<10	1.0	<10	<5	4	<2	4	<2	4.5	<1	26	9.7	16
9	KP-3	12	16	<10	10	<10	1.0	<10	<5	5	<2	<3	<2	1.8	<1	36	1.7	<10
10	KP-1	<10	<10	<10	10	<10	<1	<10	<5	<2	<2	<3	<2	<1	<1	13.6	1.5	<10

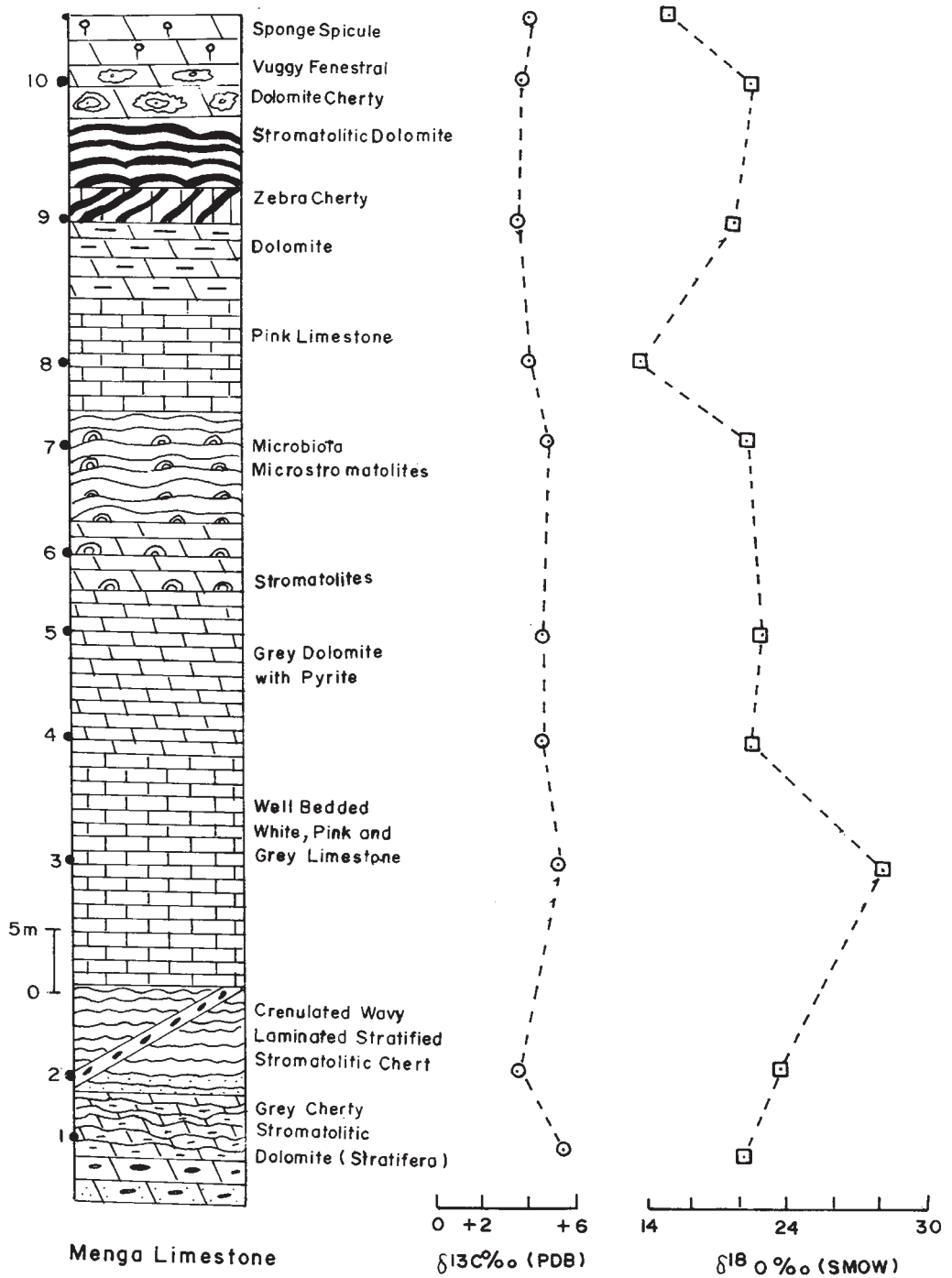


Fig. 10. C-isotope chemostratigraphy of the Menga (Buxa) Limestone (Terminal Proterozoic), Arunachal, Lesser Himalaya, Northeastern Himalaya (East Gondwana).

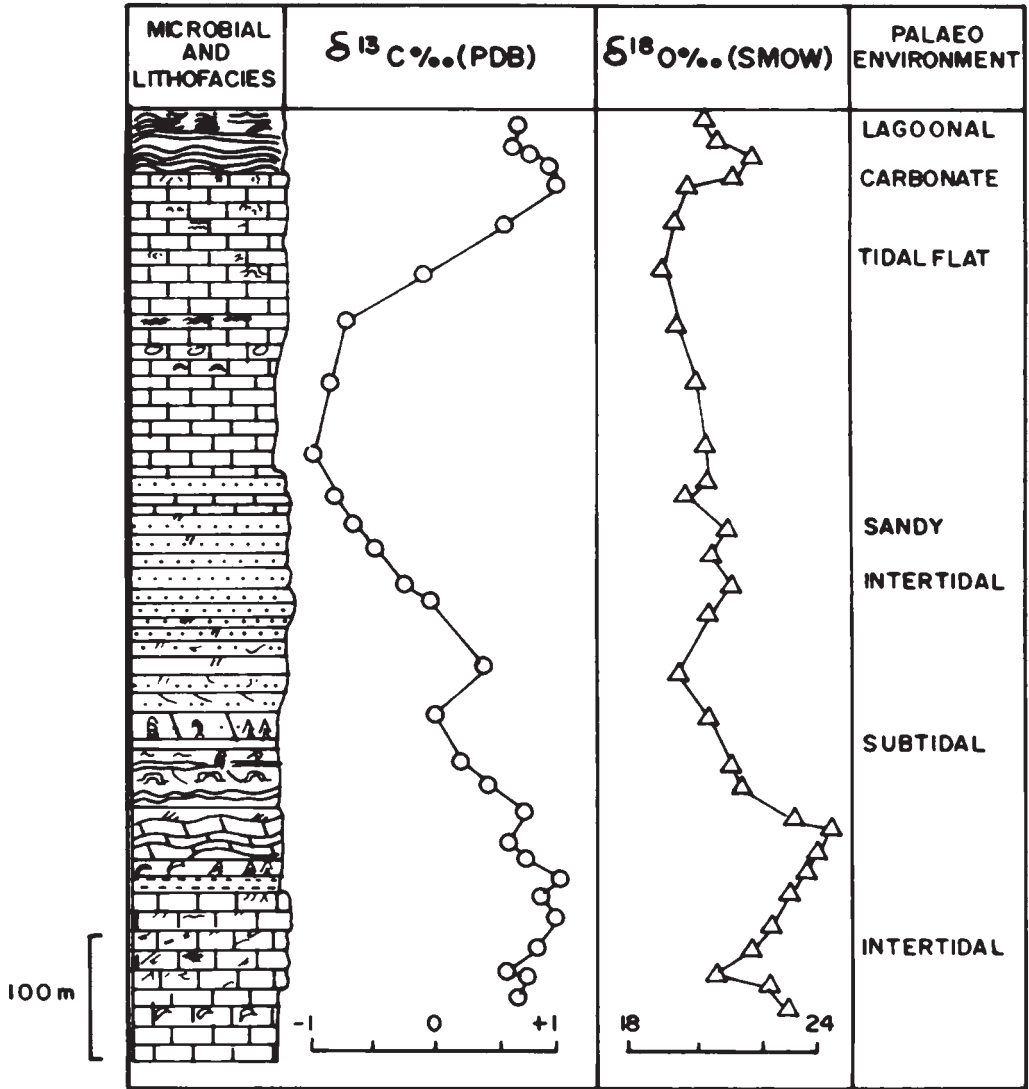


Fig. 11. C-isotope chemostratigraphy of the Buxa Dolomite, Ranjit Window (Meso-Neoproterozoic), Sikkim, NE Lesser Himalaya, Northeastern Himalaya (East Gondwana).

depositional environments for the Chillipam, Rupa, Dedza, Menga and Panging limestones. Acharyya (1974) interpreted the Buxa Dolomite as shallow subtidal to intertidal deposits. Fossils include organic-walled microfossils, vase-shaped microfossils and micro metazoans, in addition to stromatolites, all suggestive of a Late Proterozoic age (Figs 13 and 14). Positive C-isotopic values (+3.7 to +5.4‰ PDB) of the Buxa Limestone (Fig. 10) relate to known global palaeobiological events. High positive values of $\delta^{13}\text{C}$ from +2.8‰ PDB to +4.2‰ PDB characterize the Chillipam Dolomite

and the Dedza Dolomite in the West Kameng of the Arunachal Lesser Himalaya ($\delta^{13}\text{C} = +5.8\text{‰ PDB}$). Additional microbiota have been recorded from the Subansiri area of the Arunachal Lesser Himalaya (Tewari 2005).

The stable carbon and oxygen isotope data from the Buxa Dolomite (Meso-Neoproterozoic) cropping out in the Ranjit river valley, western Sikkim, NE Lesser Himalaya, India (Figs 4 and 11). The Buxa Dolomite comprises stromatolitic dolomite, cherty dolomite, intraclastic-oolitic dolomite, and minor siliciclastic sediments (Fig. 11).

The stromatolite assemblage and the recently discovered microbiota from the Buxa Dolomite in Ranjit window, Sikkim Lesser Himalaya suggest a Meso-Neoproterozoic age (Tewari 2003, 2004a, b). The $\delta^{13}\text{C}$ (PDB) varies in a narrow range from -1.4‰ to $+1.0\text{‰}$. (Fig. 11) Oxygen isotope values grade from 19‰ to 23.9‰ ($\delta^{18}\text{O}$ SMOW). The lower part of the Buxa Dolomite showing a mostly positive trend may be the result of an increased rate of organic matter burial in a shallow carbonate platform. The $\delta^{13}\text{C}$ and $\delta^{18}\text{O}$ values of the Buxa Dolomite are summarized in Table 8.

The recorded stromatolite assemblage includes: *Kussiella kussiensis*, *Clonnella columnaris*, *Conophyton gargaricum*, *Baicalia* sp., *Tungussia* sp., *Jurusania* sp., *Gymnosolen* sp., *Minjaria* sp., *Kalpanaella* n. sp., *Nucliella*, *Colleniella*, *Conistratiferia*, *Aldania* sp. and *Collumnaefacta* sp. (Tewari 2004a). The microbial assemblage from cherts includes *Obruchevella* sp., *Eomycetopsis* sp., *Myxococcoides* sp., *Huronispora* sp., *Melanocyrium* sp. etc (Tewari 2004b).

Based on isotope data combined with sedimentological and palaeobiological data, the Buxa Dolomite appears to have been deposited on a carbonate

platform, well connected with the ocean, the environment favourable for the formation of microbialites and cyanobacterial microbial mats, indicating that the environment of deposition was shallow marine (peritidal/subtidal to intertidal).

Discussion and conclusions

The Ediacaran radiation of metazoan and metaphytic multicellular life seems to have occurred after a change from ‘Snowball Earth’ to global warming in the Neoproterozoic period (Fig. 12). A major global decline of Mesoproterozoic stromatolites, planktonic acritarchs and other prokaryotic biota has been recorded on Earth, related to Neoproterozoic glaciation (Hoffman *et al.* 1998; Tewari 1993). Radiation of new acanthomorphic acritarchs, stromatolites, multicellular brown algae, vendotaenids, *Tyrosotaenia*, *Krolotaenia* and Ediacaran metazoans like *Cyclomedusa*, *Charniodiscus*, *Dickinsonia*, *Spriggina* and *Pteridinium* was recorded widely, and possibly in the Krol Group of the Lesser Himalaya (Fig. 3) (Knoll & Walter 1992; Kaufman & Knoll 1995; Mathur & Shanker 1989; Shanker *et al.* 1997; Tewari 1993, 1999a, b; Kaufman *et al.* 1997). Ediacaran animals originated prior to the main Varanger glaciation and diversified. The Cambrian explosion of shelled organisms is recorded in the Tal Group of rocks of the Lesser Himalaya (Fig. 12) and in the Tethyan sequences of Spiti-Zaskar and Uttaranchal Himalaya (Kumar *et al.* 1997; Tewari 1998b). Tewari (2001b) has reported Late Proterozoic organisms and microstromatolites in the Menga (Buxa) Limestone of the northeastern Himalaya. In this sequence, there is a well-developed diamictite, stromatolitic carbonate sequence (Buxa Dolomite/Chillipam Formation) exposed in the West Kameng district of the Arunachal Lesser Himalaya, similar to the Blaini diamictite and Krol Formation in sedimentary facies and microbial buildups (Tewari 2003). The Precambrian–Cambrian boundary may exist in this section (Tewari 1998a).

The Buxa Dolomite of the Northeastern Himalaya of Bhutan, Sikkim, Darjeeling and Arunachal Pradesh has been traditionally correlated with the Mesoproterozoic (Riphean) Shali–Deoban–Gangolihat carbonate belt of the NW Himalaya, on the basis of lithological similarities and stromatolite content (Valdiya 1969, 1980; Tewari 2003). Acharyya (1974), to the contrary, considered the Buxa Dolomite to be older than Late Palaeozoic but younger than the Shali–Deoban stromatolitic carbonates. This paper suggests correlation of Buxa, Chillipam and Dedza dolomites of the northeast Himalaya to the Late Neoproterozoic on the basis of microstromatolites/stromatolites,

Table 8. $\delta^{13}\text{C}_{\text{PDB}}$ and $\delta^{18}\text{O}_{\text{PDB}}$ of the Buxa Dolomite, Ranjit Window, Sikkim, NE Lesser Himalaya

Sample	$\delta^{18}\text{O}_{\text{SMOW}}$	$\delta^{18}\text{O}_{\text{‰PDB}}$	$\delta^{13}\text{C}_{\text{‰PDB}}$
TR30	19.7	-10.8	-0.1
TR29	20.1	-10.5	-0.9
TR28	21.8	-8.7	-0.1
TR27	21.1	-9.5	0.1
TR26	19.4	-11.1	0.4
TR24	19.0	-11.5	-0.1
TR23	19.5	-11.1	-0.1
TR22	20.6	-10.0	0.1
TR20	22.8	-7.9	-0.9
TR19	20.6	-10.0	-1.4
TR18	19.8	-10.8	-0.9
TR17	21.8	-8.8	-0.8
TR16	21.4	-9.2	-0.7
TR15	21.6	-9.0	-0.7
TR13	19.5	-11.1	0.3
TR12	20.9	-9.7	-0.4
TR11	21.8	-8.8	0.1
TR10	22.9	-7.7	0.6
TR9	23.9	-6.7	0.5
TR8	23.9	-6.8	0.6
TR7	23.5	-7.1	0.9
TR6	23.4	-7.3	0.9
TR5	22.6	-8.0	1.0
TR4	22.2	-8.4	1.0
TR3	20.8	-9.7	0.5
TR2	22.8	-7.8	0.7
TR1	23.0	-7.6	0.7

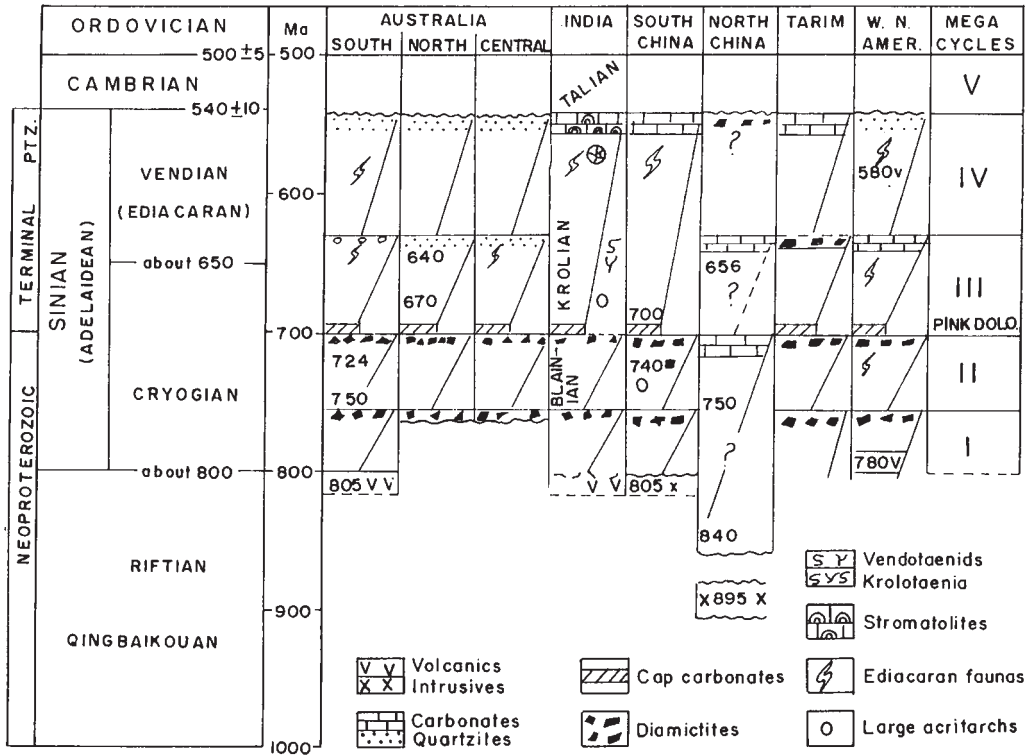


Fig. 12. Global correlation of the Blainian-Krolian and Talian (Neoproterozoic to Lower Cambrian) stages of the Lesser Himalaya, India, East Gondwana, (after Brookfield 1994 with slight modification).

microbiota and carbon isotope stratigraphy (Tewari & Sial 2003, 2004). Recently discovered microbialites, organic walled microfossils, sponge spicules and extensive carbonates (Tewari 2001a, b, c, 2002a, 2003, 2004a) (Fig. 10) from the Mengamara section in Subansiri Valley indicate a Late Proterozoic age for this sequence. Ten representative samples (MM1 to MM10, Fig. 10) of dolomite were analysed for C- and O-isotopes. The C-isotopic ratios are significantly positive and quite consistent with $\delta^{13}\text{C}$ (carbonate carbon) values varying from +3.7 to +5.4‰ PDB. $\delta^{18}\text{O}$ values fluctuate between -8.9 and -7.2‰ PDB. The consistency of the carbon isotopic record from the Buxa Dolomite indicates that the isotopic data are representative and the signatures are unaltered. The significantly positive C-isotopic results are in concert with global Late Proterozoic isotopic patterns (Aharon *et al.* 1987; Kumar & Tewari 1995; Tewari 1991, 1997, 1998c, 2001a, 2002a; Tewari & Sial 2004; Bhattacharya *et al.* 1996). A close relationship of $\delta^{13}\text{C}$ enriched carbonate rocks with peaks in stromatolite diversity and

biomass can be attributed to the enhanced bioproductivity.

The Late Proterozoic–Early Cambrian sequence of the Uttaranchal Central Lesser Himalaya has been studied in detail for C-isotope chemostratigraphy (Aharon *et al.* 1987; Tewari 1991, 1997, 2001a, b; Kumar & Tewari 1995; Tewari & Sial 2004; Bhattacharya *et al.* 1996)—the first such attempt in the northeastern Himalaya. The Buxa Dolomite positive isotopic excursions are strikingly similar to those of the Krol Formation (Krolian) of the Uttaranchal (Central Lesser) Himalaya. It is interesting that the Doushantuo carbonates of the Yangtze Platform, Southern China (Shen & Schidlowski 2000) display high positive $\delta^{13}\text{C}$ values similar to the Krol–Buxa belt. The Krol–Buxa–Doushantuo carbonates were deposited after a Neoproterozoic glaciation (Tewari 2001b, c, 2002a, 2003) and have very similar sedimentary facies, biota, and carbon-isotope chemostratigraphy (Tewari 2001a, b, 2002). The Lesser Himalayan sequences of India show similar palaeobiological and stable isotopic patterns to other Ediacaran

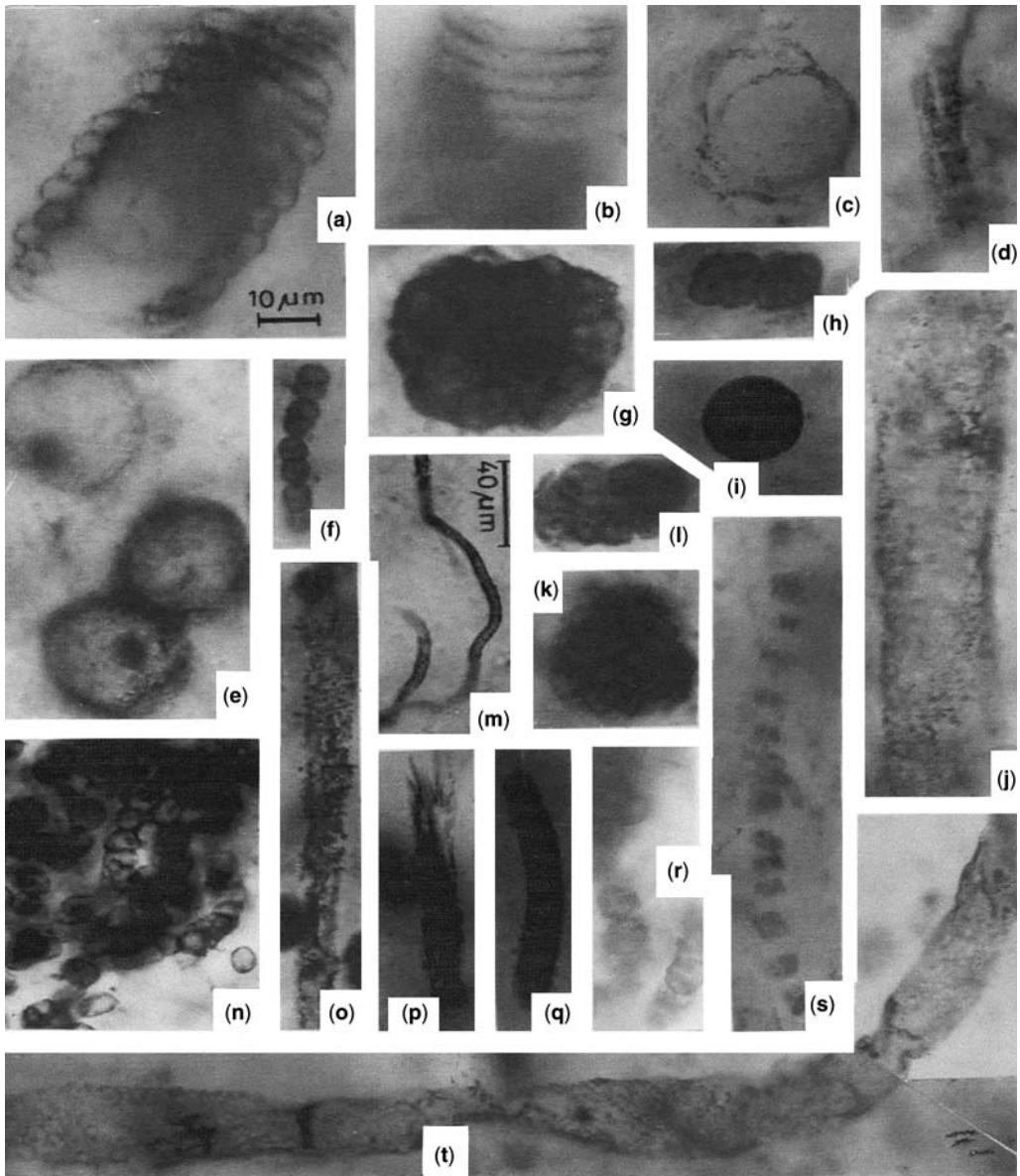


Fig. 13. Neoproterozoic microfossils from the Buxa Dolomite, NE Himalaya. (a–b) *Obruchevella parva* Reitlinger 1959, BSIP Slide No. 13; (c) *Volyniella valdaica* (Shepeleva 1967), BSIP Slide No. 13; (d) *Palaeolyngbya catenata* Hermann 1974, *emend* Butterfield *et al.* 1994, BSIP Slide No. 13; (e) *Glenobotrydion aenigmatis* Schopf 1968, BSIP Slide No. 13; (f) *Vetronostocale equale* sp. nov., BSIP Slide No. 13; (g) *Palaeoanacystes suktenensis* Zhang 1984, BSIP Slide No. 13; (h and i) *Paratetraphycus giganteus* Zhang 1984, BSIP Slide No. 13; (j) *Oscillatorioopsis robusta* Mendelson & Schopf 1980, BSIP Slide No. 13; (k) *Syphonophycus typicum* Hermann 1974, BSIP Slide No. 11; (m) *Myxococcooides minor* Schopf 1968, BSIP Slide No. 13; (n) *Eosynechococcus rugosum* (Maithy) Hofmann & Jackson 1994, BSIP Slide No. 13; (o) *Siphonophycus rugosum* (Maithy) Hofmann & Jackson 1994, BSIP Slide No. 13; (p) *Polythrycooides lineatus* German 1974 *emend* Timofeev *et al.* 1976, BSIP Slide No. 13; (q and r) *Vetronostocale amoenum* Schopf and Blacic, *emend* Xu & Awramik 2001, BSIP Slide No. 13; (s) *Oscillatorioopsis breviconvexa* Schopf & Blacic 1971, BSIP Slide No. 13; (t) *Oscillatorioopsis rhomboidalis* Sivertseva 1989, BSIP Slide No. 13.

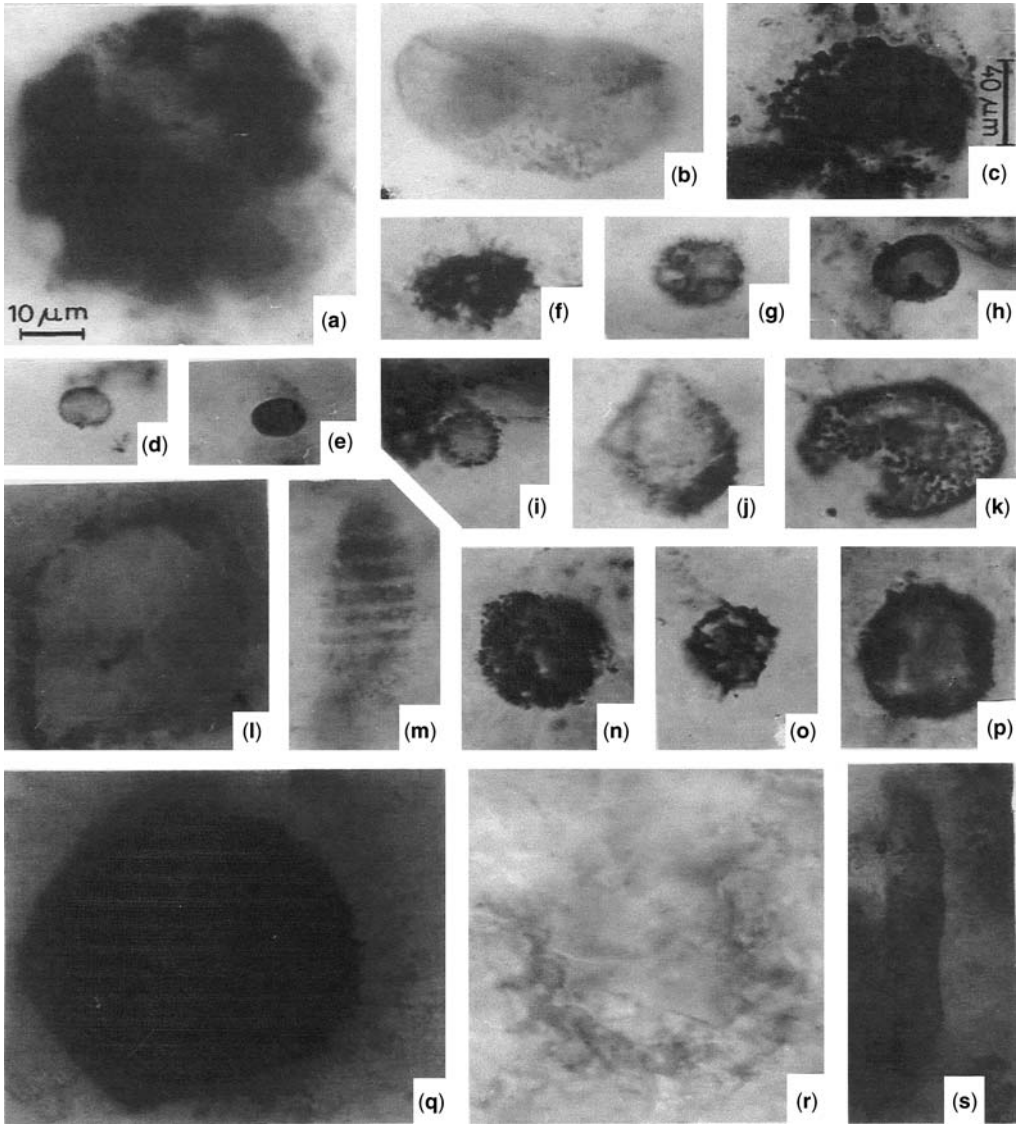


Fig. 14. Neoproterozoic microfossils from the Buxa Dolomite, NE Himalaya. (a) *Trachyhystrichosphaera aimica* Hermann 1981, BSIP Slide No. 13; (b) *Lophosphaeridium rarum* Timofeev 1959, BSIP Slide No. 13; (c) *Vandalosphaeridium reticulatum* Vidal 1981, BSIP Slide No. 13; (d) *Margominuscula rugosa* Naumova 1960, BSIP Slide No. 13; (e) *Margominuscula simplex* Pychova 1973, BSIP Slide No. 13; (f) *Archaeohystrichosphaeridium semireticulatum* Timofeev 1959, BSIP Slide No. 13; (g) *Micrhystridium lanatum* Volkova 1969, BSIP Slide No. 13; (h) *Granomarginata vetula* Saluja *et al.* 1972, BSIP Slide No. 13; (i) *Micrhystridium ampliatum* Wang 1985, BSIP Slide No. 13; (j) *Melanocyrrillum hexodiadema* (Bloesser) *cf. Angochitina milanensis*, BSIP Slide No. 13; (k) *Lophosphaeridium jansoniusii* Saluja *et al.* 1971b, BSIP Slide No. 13; (l) *Leiosphaeridia visingsa* Zang *in* Zang & Walter 1995, BSIP Slide No. 13; (m) *Navifusa segmentatus* Prasad & Asher 2001, BSIP Slide No. 13; (n) *Trachysphaeridium robustum* Yin & Li 1978, BSIP Slide No. 13; (o) *Archaeohystrichosphaeridium cellulare* Timofeev 1959, BSIP Slide No. 13; (p) *Polythrycoides lineatus* German 1974 *emend.* Timofeev *et al.* 1976, BSIP Slide No. 13; (q) *Vetronostocale amoenum* Schopf and Blacic, *emend.* Xu & Awramik 2001, BSIP Slide No. 13; (r) *Vetronostocale amoenum* Schopf & Blacic, *emend.* Xu & Awramik 2001, BSIP Slide No. 13; (s) *Oscillatorioopsis brevicconvexa* Schopf & Blacic 1971, BSIP Slide No. 13.

sequences; further detailed investigation shows promise of correlation worldwide.

I am thankful to M. Schidlowski, Biogeochemistry Department at Max Planck Institute für Chemie, Mainz, Germany and A. N. Sial, NEG-LABISE, Pernambuco University, Recife, Brazil for carbon isotopic analysis of the carbonates and discussions. Professors R. J. F. Jenkins, University of Adelaide, Australia, S. Turner, Monash University, and M. Yoshida, Gondwana Institute of Geology and Environment, Hashimoto, Japan are thanked for critical reviews of the manuscript and valuable suggestions. The author is grateful to P. Vickers-Rich (Australia), M. Fedonkin (Russia), J. Gehling Project leaders of I.G.C.P.-493 for discussions on Ediacaran and Vendian biota. M. Tucker, University of Durham, England is thanked for discussions in the field. K. S. Valdiya, Chairman and B. R. Arora, Director, Wadia Institute of Himalayan Geology, Dehradun, India provided facilities and permission to publish the paper. This is a contribution to the I.G.C.P. Project 493 on 'Rise and Fall of the Vendian Biota'. G. Chauhan ably typed the article.

References

- ACHARYYA, S. K. 1974. Stratigraphy and sedimentation of the Buxa Group, Eastern Himalaya. *Himalayan Geology*, **4**, 102–116.
- AHARON, P. & LIEW, T. C. 1992. An assessment of the Precambrian/Cambrian transition events on the basis of Carbon isotope records. In: SCHIDLOWSKI, M. ET AL. (eds) *Early Organic Evolution—Implication for Mineral and Energy Resources*. Springer-Verlag, Berlin-Heidelberg, 212–223.
- AHARON, P., SCHIDLOWSKI, M. & SINGH, I. B. 1987. Chronostratigraphic carbon isotopic record of the Lesser Himalaya. *Nature*, **327**, 699–702.
- ALVARENGA, C. J. S., SANTOS, R. V., DANTAS, E. L., BROD, E. R. & GIOIA, S. M. C. L. 2003. C, O and Sr isotope in the cap carbonate sequence overlying Sturtian–Rapitan and Varanger–Marinoan glacial events in Brazil. *IV South American Symposium on Isotope Geology, Salvador-BA Brazil*, 313–316.
- BHATTACHARYA, S. K., JANI, R. A., MATHUR, V. K., ABSAR, A., BODAS, M. S., KUMAR, G. & SHANKER, R. 1997. Stable carbon and Oxygen isotopic changes and rare earth elements across Precambrian–Cambrian boundary Lesser Himalaya. *Geological Survey of India Special Publication*, **21**, 225–231.
- BRASIER, M. D. 1992. Palaeoceanography and changes in the biological cycling of phosphorus across the Precambrian–Cambrian boundary. In: LIPPS, J. L. & SIGNOR, P. W. (eds) *Origin and Early Evolution of the Metazoa*. Plenum Press, New York, 483–515.
- BRASIER, M. D. & SINGH, P. 1989. Microfossils and Precambrian–Cambrian boundary stratigraphy at Maldeota, Lesser Himalaya. *Geological Magazine*, **127**, 319–332.
- BRASIER, M. D., MAGARITZ, M., CORFIELD, R., LUO, H., WU, X., LIN, O. & JIANG, Z. ET AL. 1990. The carbon and oxygen isotope record in the Precambrian–Cambrian boundary interval in China and Iran and their correlation. *Geological Magazine*, **127**, 319–332.
- BRASIER, M. D., SHIELD, G., KULESHOV, V. N. & ZHEGALLO, E. H. 1996. Integrated chemo and biostratigraphic calibrations of early animal evolution: Neoproterozoic–Early Cambrian of southwest Mongolia. *Geological Magazine*, **133**, 445–485.
- BROOKFIELD, M. E. 1994. Problems in applying preservation, facies and sequence models to Sinian (Neoproterozoic) glacial sequences in Australia and Asia. *Precambrian Research*, **70**, 113–143.
- BURNS, S. J., HAUDERNSCHILD, U. & MATTER, A. 1994. The strontium isotopic composition of carbonates from the Late Precambrian (ca. 560–540 Ma) Haqf Group of Oman. *Chemical Geology*, **111**, 269–282.
- BUTTERFIELD, N. J., KNOLL, A. H. & SWETT, K. 1994. Palaeobiology of the Neoproterozoic Svanbergfjellet formation, Spitsbergen. *Fossils and Strata*, **34**, 1–84.
- CASNEDE, R. 2002. Cambrian evolution of the Pacific Gondwana margin (Antarctica, South Australia, North India). *Memorie della Società Geologica Italiana*, **57**, 239–248.
- CHUMAKOV, N. M. & ELSTON, D. P. 1989. The paradox of late Proterozoic glaciation at low latitudes. *Episodes*, **12**, 115–120.
- CORDANI, U. G., D'AGRELLA-FILHO, M. S., BRITONEVES, B. B. & TRINDADE, R. I. F. 2003. Tearing up Rodinia, the Neoproterozoic palaeogeography of South American Cratonic fragments. *Terra Nova*, **15**, 350–359.
- DALZIEL, I. W. D., MOSHER, S. & GAHAGAN, M. L. 2000. Laurentia–Kalahari collision and assembly of Rodinia. *Journal of Geology*, **108**, 493–513.
- EICHMAN, R. & SCHIDLOWSKI, M. 1975. Isotopic fractionation between coexisting carbonate pairs in Precambrian sediments. *Geochimica et Cosmochimica Acta*, **39**, 585–595.
- ETIENNE, J. L., ALLEN, P., LE GUERROUÉ, E. & RIEU, R. 2006. 'Snowball Earth' 2006 Abstract Volume. 'Snowball Earth' Symposium, Swiss National Science Foundation, Ascona.
- GRADSTEIN, F., OGG, J. & SMITH, A. 2004. *A Geological Time Scale*. Cambridge University Press, Cambridge.
- HERMANN, T. N. 1974. Nakhodka Massovykh Skopleniyi Trikhomov v Rifeei. In: TIMOFEEV, B. V. (ed.) *Mikro-fossilii Proterozoya i rannego Palaeozoa SSSR*, 6–10 [In Russian].
- HERMANN, T. N. 1981. Nakhodi nitchaykh vodorosely vmiroyedikh Skay Suite Vrkhnego do kembriya (Occurrence of filamentous algae from the Miroedikha Formation of Upper Precambrian). *Paleontologicheskii Zhurnal*, **14**, 118–112 [In Russian].
- HOFFMAN, P. F., KAUFMAN, A. J., HALVERSON, G. P. & SCHRAG, D. P. 1998. A Neoproterozoic 'Snowball Earth'. *Science*, **281**, 1342–1346.
- HOFMANN, H. J. & JACKSON, G. D. 1994. Shale facies microfossils from the Proterozoic, Bylot Supergroup, Baffin Island, Canada. *Memoirs of the Palaeontological Society Canada*, **37**, 1–35.
- HYDE, W. T., CROWLEY, T. J., BAUM, S. K. & PELTIER, W. R. 2000. Neoproterozoic snowball earth simulations with a coupled climate/ice sheet model. *Nature*, **405**, 425–429.

- JACOBSON, S. B. & KAUFMAN, A. J. 1999. The Sr, C and O isotopic evolution of Neoproterozoic sea water. *Chemical Geology*, **161**, 37–57.
- JENKINS, R. J. F. 1981. The concept of the Ediacaran Period and its stratigraphic significance in Australia. *Transactions of the Royal Society of South Australia*, **105**, 179–194.
- KAUFMAN, A. J. & KNOLL, A. H. 1995. Neoproterozoic variations in the carbon isotopic composition of seawater: stratigraphic and biogeochemical implications. *Precambrian Research*, **73**, 27–49.
- KAUFMAN, A. J., KNOLL, A. H. & NARBONNE, G. M. 1997. Isotopes, ice ages and Terminal Proterozoic earth history. *Proceedings of the National Academy of Science*, **94**, 6600–6605.
- KNOLL, A. H. & WALTER, M. R. 1992. Latest Proterozoic stratigraphy and Earth history. *Nature*, **356**, 673–678.
- KNOLL, A. H., KAUFMAN, A. J. & SEMIKHATOV, M. A. 1995. The carbon isotopic composition of Proterozoic carbonates: Riphean successions from Northeastern Siberia (Anabar massif, Turukhansk Uplift). *American Journal of Science*, **295**, 823–850.
- KUMAR, B. & TEWARI, V. C., 1995. Carbon and Oxygen isotope trends in Late Precambrian–Cambrian carbonates from the Lesser Himalaya, India. *Current Science*, **69**, 929–931.
- KUMAR, G., SHANKER, R., MAITHY, P. K., MATHUR, V. K. & BHATTACHARYYA, S. K. 1997. Terminal Proterozoic–Cambrian sequences in India—A review with special reference to Precambrian–Cambrian boundary. *The Palaeobotanist*, **46**, 19–31.
- KUMAR, G., SHANKER, R., MATHUR, V. K. & MAITHY, P. K. 2000. Maldeota section, Mussoorie Syncline, Krol belt, Lesser Himalaya, India. A candidate for global stratotype section and point for terminal Proterozoic system. *Geological Science Journal*, **21**, 1–10.
- MATHUR, V. K. & SHANKER, R. 1989. First record of Ediacaran fossils from the Krol Formation, Nainital Syncline. *Journal of the Geological Society of India*, **34**, 245–254.
- MENDELSON, C. V. & SCHOPF, J. W. 1982. Proterozoic microfossils from Sukhaya-Tunguska Shorika and Yudoma formations of Siberian platform. *Journal of Paleontology*, **56**, 43–83.
- NAUMOVA, S. N. 1960. Spore and pollen assemblages in the Riphean and lower Cambrian deposits of USSR. *Proceedings of the International Geological Congress, Session XXI*, **8**, 109–117. Nauka, Moscow [In Russian].
- POWELL, C., MCA LI, Z. X., MC ELHINNY, M. W., MEERT, J. G. & PARK, J. K. 1993. Palaeomagnetic constraints on timing of the Neoproterozoic break up of Rodinia and the Cambrian formation of Gondwana. *Geology*, **21**, 889–892.
- PRASAD, B. & ASHER, R. 2001. Acritarch biostratigraphy and lithostratigraphic classification of Proterozoic and Lower Palaeozoic Sediments (Pre-Unconformity sequence) of Ganga basin, India. *Palaeontographica Indica*, **5**, 1–153.
- PYCHOVA, N. G. 1973. Acritarchs of Precambrian sections of southern Ural, Siberia, Eastern European Platform and their significance. In: Microfossils of the oldest deposits. VOZHENNIKOVA, T. V. & TIMOFEEV, B. V. (eds) *Proceedings of the International Palynological Congress, Session III*, Nauka, Moscow, 5–17 [with summaries in English].
- RAINA, V. K. 1976. The Ranjit tectonic window: stratigraphy, structure and tectonic interpretation and its bearing on the regional stratigraphy. *Geological Survey of India Miscellaneous Publication*, **41**, 36–42.
- REITLINGER, E. A. 1959. Atlas of microscopic fossils and problematics of ancient strata of Siberia. *Trudy Geologicheskogo Instituta Akademii Nauk SSSR*, **25**, 1–63.
- RIPPERDAN, R. L. 1994. Global variations in carbon isotope composition during the latest Neoproterozoic and earliest Cambrian. *Annual Review of Earth and Planetary Science*, **22**, 385–417.
- SALUJA, S. K., REHMAN, K. & RAWAT, M. S. 1971. Fossil palynomorphs from the Vindhya of Rajasthan. *Review of Palaeobotany and Palynology*, **2**, 65–83.
- SANTOS, R. V., ALVARENGA, C. J. S., DE DARDENNE, M. A. & SIAL, A. N. 2000. Carbon and Oxygen isotope profiles across Meso-Neoproterozoic limestones from Central Brazil: Bambui and Paranao groups. *Precambrian Research*, **104**, 107–122.
- SCHIDLowski, M., EICHMANN, R. & JUNGE, C. E. 1975. Precambrian sedimentary carbonates: carbon and oxygen isotope geochemistry and implications for the terrestrial oxygen budget. *Precambrian Research*, **2**, 1–69.
- SCHIDLowski, M., EICHMANN, R. & JUNGE, C. E. 1976. Carbon isotope geochemistry of the Precambrian Lomgundi carbonate province. *Geochimica et Cosmochimica Acta*, **40**, 449–455.
- SCHIDLowski, M., HAYS, J. M. & KAPLAN, I. R. 1983. Isotopic inferences of ancient biochemistries: Carbon, Sulfur, Hydrogen and Nitrogen. In: SCHOPF, J. W. (ed.) *Earth's Earliest Biosphere: Its Origin and Evolution*. Princeton University Press, 27–39.
- SCHOPF, J. W. 1968. Microflora of the Bitter Springs Formation, late Precambrian, Central Australia. *Journal of Paleontology*, **42**, 651–688.
- SCHOPF, J. W. & BLACIC, J. M. 1971. New microfossils from the Bitter Spring Formation (Late Precambrian) of North Central Amadeus Basin, Australia. *Journal of Paleontology*, **45**, 925–960.
- SHANKAR, R. & MATHUR, V. K. 1992. The Precambrian–Cambrian sequence in Krol belt and additional Ediacaran fossils. In: VENKATACHALA, B. S., JAIN, K. P. & AWARTHY, N. (eds) *Proceedings of the Birbal Sahni Birth Centenary Paleobotanical Conference*. *Geophytology*, **22**, 27–39.
- SHANKER, R., MATHUR, V. K., KUMAR, G. & SRIVASTAVA, M. C. 1997. Additional Ediacaran biota from the Krol Group, Lesser Himalaya, India and their significance. *Geoscience Journal*, **18**, 79–94.
- SHEPELEVA, E. D. 1974. Stratigraphic subdivisions of Venedian deposits of the Central Russian platform from acritarchs. *Izvestiya Akademii Nauk SSSR, Novosobrisk*, **81**, 13–23 [In Russian].
- SHUKLA, M., TEWARI, V. C., BABU, R. & SHARMA, A. 2006. Microfossils from the Neoproterozoic Buxa Dolomite, West Siang District, Arunachal Lesser Himalaya, India and their significance. *Journal of the Geological Society of India*, **51**, 57–73.
- SHEN, YANAN & SCHIDLowski, M. 2000. New C isotope stratigraphy from southwest China:

- Implications for the placement of the Precambrian–Cambrian boundary on the Yangtze platform and global correlations, *Geology*, **28**, 623–626.
- TANDON, S. K., NANDA, A. C. & SINGH, T. 1979. The Miri rocks of the eastern Himalaya, stratigraphic and ichnological considerations. In: VERMA, P. K. (ed.) *Metamorphic Rocks Sequences of the Eastern Himalaya*, K. P. Bagchi and Co., Calcutta, 85–99.
- TEWARI, V. C. 1984. Stromatolites and Precambrian and Lower Cambrian biostratigraphy of the Lesser Himalaya, India. *Proceedings of the Fifth Indian Geophytological Conference*, Palaeobotanical Society, 1983, *Special Publication*, 71–91.
- TEWARI, V. C. 1989. Upper Proterozoic–Lower Cambrian stromatolites and Indian Stratigraphy. *Himalayan Geology*, **13**, 143–180.
- TEWARI, V. C. 1991. The carbon and oxygen isotope trend of the Deoban-Blaini-Krol-Tal microbial carbonate from the Lesser Himalaya, India. *Geoscience Journal*, **12**, 13–16.
- TEWARI, V. C. 1993. Precambrian and Lower Cambrian stromatolites of the Lesser Himalaya, India. *Geophytology*, **23**, 19–39.
- TEWARI, V. C. 1994. Sedimentology of the rocks of Deoban basin, Dhuraphat area, Saryu Valley, Eastern Kumaon, Lesser Himalaya. *Geoscience Journal*, **15**, 117–162.
- TEWARI, V. C. 1996. Discovery of pre Ediacaran acritarch *Chuarina circularis* (Walcott 1899, Vidal & Ford 1985) from the Deoban Mountains, Lesser Himalaya, India. *Geoscience Journal*, **17**, 25–39.
- TEWARI, V. C. 1997. Carbon and oxygen isotope stratigraphy of the Deoban Group (Mesoproterozoic), Garhwal lesser Himalaya. *Geoscience Journal*, **18**, 95–101.
- TEWARI, V. C. 1998a. Prospects of delineating Terminal Proterozoic and Precambrian–Cambrian boundary in the Northeastern Himalaya. *Geoscience Journal*, **19**, 19–23.
- TEWARI, V. C. 1998b. Regional correlation of the Lesser Himalayan and Tethyan basin sediments of Kali Valley, Indo-Nepal area. *Journal of Nepal Geological Society*, **18**, 37–57.
- TEWARI, V. C. 1998c. Lower Cambrian carbon isotope evidence of photosynthesis from Krol-Tal carbonates of the Lesser Himalaya and global stratification in early Cambrian oceans. *Mineralogical Magazine*, **62A**, 1506.
- TEWARI, V. C. 1999a. Candidate GSSP for the initial boundary of the Terminal Proterozoic. Blaini Formation (Baliana Group), Mussoorie Syncline Lesser Himalaya, India. *Terminal Proterozoic System, 12th Circular, May 1999. I.U.G.S. Subcommittee on the Terminal Proterozoic System*, 17–24.
- TEWARI, V. C. 1999b. Vendotaenids: Earliest megascopic multicellular algae on Earth. *Geoscience Journal*, **20**, 77–85.
- TEWARI, V. C. 2001a. Neoproterozoic glaciation in the Uttaranchal Lesser Himalaya and the global. Palaeoclimatic change. National Symposium on the Role of Earth Science in Integrated Development and related Societal Issues, *Geological Survey of India Special Publication*, **65**, 49–56.
- TEWARI, V. C. 2001b. Discovery and Sedimentology of microstromatolites from Menga Limestone (Neoproterozoic/Vendian). Upper Subansiri district, Arunachal Pradesh, Northeastern Himalaya, India. *Current Science*, **80**, 1440–1444.
- TEWARI, V. C. 2001c. *Origins of Life in the Universe and earliest Prokaryotic Micro-organisms on Earth*. CHELA FLORES, J. (ed.) Kluwer Publishers, Netherland, 251–254.
- TEWARI, V. C. 2002a. Lesser Himalayan stratigraphy, sedimentation and correlation from Uttaranchal to Arunachal. In: CHARU, C. & SHARMA, A. K. (eds) *Aspects of Geology and Environment of the Himalaya*. Gyanodaya Prakashan, Nainital, India, 63–88.
- TEWARI, V. C. 2002b. Proterozoic–Cambrian sedimentation and associated natural resources of Uttaranchal. *Proceedings of the National Workshop on Natural Wealth of Uttaranchal*. Technology Publishers, Dehradun, 189–222.
- TEWARI, V. C. 2003. Sedimentology, palaeobiology and stable isotope chemostratigraphy of the Terminal Neoproterozoic Buxa Dolomite, Arunachal Pradesh NE Lesser Himalaya. *Journal of Himalayan Geology*, **24**, 1–18.
- TEWARI, V. C. 2004a. Palaeobiology and biosedimentology of the stromatolitic Buxa Dolomite, Ranjit window, Sikkim, NE, Lesser Himalaya, India. Kluwer Academic Publishers, Netherland, 249–250.
- TEWARI, V. C. 2004b. Microbial diversity in Meso-Neoproterozoic formations, with particular reference to the Himalaya. In: SECKBACH, J. (ed.) *Origins*. Kluwer Academic Publishers, Netherlands, 515–528.
- TEWARI, V. C. 2005. Vendian (Ediacaran) biota from the Lesser Himalaya, India and Southern China with special reference to early evolution of life on Earth. *14th International Conference on the Origin of Life*, Beijing, China, 143–144. Tsinghua University.
- TIMOFEEV, B. V. 1959. Ancient flora of Baltic region and its stratigraphic significance. *VNIGRI, Trudy*, **129**, 1–320 [in Russian].
- TIMOFEEV, B. V., HARMANN, T. N. & MIKHAILOVA, N. S. 1976. *Microphytofossils of the Precambrian, Cambrian and Ordovician*. Academy of Sciences, USSR. Nauka, Leningrad [In Russian].
- TIWARI, M., PANT, C. C. & TEWARI, V. C. 2000. Neoproterozoic sponge spicules and organic walled microfossils from the Gangolihat Dolomite, Lesser Himalaya, India. *Current Science*, **79**, 651–654.
- TUCKER, M. E. 1986. Carbon isotope excursions in Precambrian/Cambrian boundary beds, Morocco. *Nature*, **319**, 48–50.
- VALDIYA, K. S. 1969. Stromatolites of the Lesser Himalayan carbonate formations and the Vindhyan. *Journal of Geological Society of India*, **10**, 1–25.
- VALDIYA, K. S. 1980. *Geology of Kumaun Lesser Himalaya*. Wadia Institute of Himalayan Geology, Dehradun.
- VEIZER, J., COMPSTEN, W., CLAUER, N. & SCHIDLowski, M. 1983. $^{87}\text{Sr}/^{86}\text{Sr}$ in Late Proterozoic carbonates: evidence for a 'Mantle' event at ≈ 900 Ma ago. *Geochimica et Cosmochimica Acta*, **47**, 295–302.
- VIDAL, G. 1981. Micropalaeontology and biostratigraphy of the Upper Proterozoic and Lower Cambrian sequences in East Finnmark, northern Norway. *Norges Geologiske Undersøkelse, Bulletin*, **362**, 1–53.

- VOLKOVA, N. A. 1969. Acritarchs of the north west Russian platform. In: ROZANOV, V. V., MISSARZHEVSKII, N. A., VOLKOVA, L. G. ET AL. (eds) *Tommotian Stage and the Cambrian Lower Boundary Problem*. Nauka, Moscow, 224–235.
- WANG, F. X. 1985. Middle–Upper Proterozoic and Lowest Phanerozoic Microfossil assemblage from south west China and contiguous area. *Precambrian Research*, **29**, 33–43.
- XU, Z. L. & AWRAMIK, S. M. 2001. New organisms from the Gaoyuzhuang Formation of Northern Taihang Mountain, China. *Acta Botanica Sinica*, **43**, 295–311.
- YIN, L. 1987. Microbiotas of latest Precambrian sequence in China. In: Nanjing Institute of Geology Palaeontology (ed.) *Stratigraphy and Palaeontology of Systemic Boundaries in China: Precambrian–Cambrian Boundary (I)*. Nanjing University Press, Nanjing, 415–494.
- YOSHIDA, M. & ARIMA, M. 2000. Assembly and breakup of super continent and global environmental change (IGCP-368). *Japan contribution to the IGCP, Annual Report*, 1–8.
- ZHANG, Z. 1984. Microfossil flora from the late Sinian, Doushantuo Formation, Hubei Province, China. In: XIE, L. & ZHANG, J. (eds) *Scientific Papers on Geology for International Exchange*. Beijing, Geological Publishing House, 129–137 [In Chinese].
- ZHANG, W. & WALTER, M. R. 1995. Late Proterozoic and Early Cambrian microfossils and biostratigraphy, Amadeus Basin, Central Australia. *Memoirs of the Association of Australasian Palaeontologists*, **12**, 1–132.

Calcite–dolomite cycles in the Neoproterozoic Cap carbonates, Otavi Group, Namibia

B. TOJO¹, N. KATSUTA², M. TAKANO², S. KAWAKAMI¹ & T. OHNO³

¹*Faculty of Education, Gifu University, 1-1 Yanagito, Gifu City 501-1193, Japan
(e-mail: btojo227@cc.gifu-u.ac.jp)*

²*Graduate School of Environmental Studies, Nagoya University, Japan*

³*The Kyoto University Museum, Kyoto University, Japan*

Abstract: The lower cap carbonate (Rasthof Formation) overlies Neoproterozoic glacial deposits (Chuosi Formation) and is exposed in the Khowarib-Warmquelle area in Northern Namibia. The basal 14.2 m part of the Rasthof Formation (total about 220 m) consists of the carbonate rhythmite. The rhythmite part of the Rasthof Formation contains 1 m cycles of dark- and light-coloured rhythmites. Alizarin-red staining of thin sections and elemental mapping of polished samples indicate that the dark-coloured parts are rich in calcite, whereas the light-coloured parts are dolomite-rich. On a 1 cm scale, a reddish clay layer is intercalated in each calcite rich dark-coloured rhythmite part. These cycles of reddish clays as well as some associated major turbidites can be well correlated between columns up to about 20 km distance. Furthermore, at one locality (K4), rip-up clasts occur in a turbidite bed. Their lithology consists of dark- and light-coloured rhythmite and a reddish clay layer and can be judged to have been derived from underlying horizons. Because the clasts are elastically deformed, it is strongly suggested that the difference in lithology observed within the basal part of the Rasthof Formation existed when clasts were ripped-up shortly after sedimentation. This suggests that the cycle involving dolomite is syndimentary, and not a diagenetic feature. Direct precipitation of dolomite does not occur in present day open marine seawater. Hurtgen *et al.* (2002) suggest that seawater was depleted in sulphate after Neoproterozoic glaciation. It is proposed here that some possible depositional models of cycles that consist of calcite-rich and dolomite-rich parts as well as reddish clay beds in rhythmites of the Rasthof cap carbonate.

The Neoproterozoic is a remarkable era in the history of the Earth because of low latitude glaciations and the emergence of the Metazoa. The era is characterized by geological phenomena of controversial nature: global distribution of glacial deposits, negative excursion of carbon isotopes, deposition of banded iron formations and thick carbonates that cover the glacial deposits. The ‘Snowball Earth’ hypothesis emerged as a solution for the enigma of these Neoproterozoic geological phenomena (Kirschvink 1992; Hoffman *et al.* 1998). Associated with the ‘Snowball Earth’ hypothesis, some scenarios have been suggested to explain the emergence of the Metazoa at this time, for example, increasing pO₂ after the glaciation, or increasing evolutionary rate within small communities in isolated refuges during the global glaciation. Researchers dealing with the Neoproterozoic glaciations expect that the deeper insights into the glaciation events of the time may provide a sounder basis for understanding the emergence of the Metazoa.

Neoproterozoic successions bearing glacial deposits are distributed globally (Hambrey & Harland 1981; Evans 2000). The Otavi Group is one of the most famous of these Neoproterozoic successions. It is rich in carbonates, and Hoffman *et al.*

(1998) revived the ‘Snowball Earth’ hypothesis with carbon isotope studies of the carbonates of this group. Following Hoffman *et al.* (1998), many researchers turned their attention to the Otavi Group in an attempt to understand the Neoproterozoic glacial episodes. Carbonates that cover these glacial deposits are called ‘cap carbonates’ and are regarded as the important keys to understanding the Neoproterozoic glaciations. In Namibia, glacial deposits are known at two different stratigraphic horizons (Hoffmann & Prave 1996). This paper examines the cyclic fluctuations of calcite–dolomite composition in the lower cap carbonate sequence (Rasthof Formation), which covers the lowermost glacial deposits (Chuosi Formation), correlated with the Sturtian glaciation. Here it is reported that the calcite–dolomite cycles in the Rasthof Formation are primary, and not diagenetic features, based on field, petrological and chemical analysis of the rocks reflecting these cycles.

In the modern sea, dolomite is rarely precipitated, although it is far more common than calcite in the Precambrian strata. Today dolomite is formed as a product of diagenesis. The lack of good modern analogues for understanding ancient dolomite formation led to the notion of the

'dolomite problem' (e.g. Zenger 1972; Tucker 1990). In the modern sea, sulphate impedes dolomite precipitation (Tucker 1990). Seawater depleted in sulphate (brought about by the reducing environment that would have existed under a global ice cap) may have promoted dolomite precipitation (Hurtgen *et al.* 2002). The calcite–dolomite cycle in the Rasthof Formation is, therefore, an interesting sequence to study in order to understand ocean chemistry of the Neoproterozoic and its fluctuations.

Neoproterozoic glacial deposits

One of the most important problems concerning the Neoproterozoic glaciations is just how many glaciation events occurred. It is generally assumed there are at least two groups of Neoproterozoic glacial deposits that exhibit similar geological and geochemical characteristics (Kennedy *et al.* 1998). The younger group is often termed the Marinoan glaciation, the older the Sturtian. Geochemical studies suggest there are at least four $\delta^{13}\text{C}$ excursions in the Neoproterozoic (Kaufman *et al.* 1997), which indicate at least four glacial events. In addition, there are some reliable age constraints for Neoproterozoic glacial deposits, for example, the 713 Ma Gubrah Member (Oman) (Allen *et al.* 2002), the 635 Ma Ghaub Formation (Namibia) (Hoffmann *et al.* 2004), and the 580 Ma Gaskiers Formation (Newfoundland) (Bowring *et al.* 2003).

In northern Namibia, the Otavi Group, which was deposited on the margin of the Congo Craton, contains two glacial horizons, each overlain by a cap carbonate. The lower glacial deposit is the Chuos Formation. A reliable maximum age constraint for the Chuos Formation is 746 ± 2 Ma (U–Pb zircon), based on studies of felsic volcanic rocks of the Naauwpoort Formation (Hoffman *et al.* 1996). The lower cap carbonate, which lies atop the Chuos Formation, is the Rasthof Formation. The upper glacial deposit is the Ghaub Formation. Mafic lava flows and thin felsic ash beds are interbedded within the Ghaub Formation and provide a date of 635.5 ± 1.2 Ma (U–Pb zircon) (Hoffmann *et al.* 2004). The upper cap carbonate is the Maieberg Formation. Both cap carbonates contain, at their bases and just above the glacial sediments, a considerable amount of dolomite associated with negative carbon isotope excursions (Hoffman *et al.* 1998; Halverson *et al.* 2002; Yoshioka *et al.* 2003).

Rasthof Formation

Rasthof Cap carbonate sequence

The Rasthof Formation overlies the Chuos diamictite (the Chuos Formation) and is typically a light

grey-coloured carbonate with a thickness of 200–240 m, in the Khwarib-Warmquelle area of northern Namibia (Fig. 1). The Otavi Group is well exposed around this region. At several outcrops we measured columnar sections and collected samples for chemical profiling (Fig. 2).

The basal 14.2 m thick part of the formation consists of thinly laminated carbonate rhythmites, overlain by stromatolite-rich sediments. In the rhythmite-bearing part of the formation, the thickness of the lamination varies from a scale of mm down to 100 μm . A number of thin, massive carbonate layers occur among the rhythmites, some of which show grading in grain size or/and colour, the thickness of these layers ranging from 1–30 cm. Some thick layers show grading and contain rip-up clasts. These features indicate that these layers are turbidites. The rhythmites are overlain by a stromatolitic part. In general, stromatolites are dome-like in structure, with thick layers at the top and thinner layers in the steep furrows on both sides of the crest. To the contrary, stromatolites in the Rasthof Formation are constructed of nearly parallel lamina, and there are numerous brecciated horizons.

$\delta^{13}\text{C}$ values

The rhythmite section located at the base of the Rasthof Formation, with about 14.2 m thickness, is the main target of this study. Several columnar sections of this part of the Formation around Khwarib-Warmquelle region were measured and recorded in detail (Fig. 3). The K1 section (Fig. 3a) exhibits the best exposure and was sampled for the geochemical studies by Yoshioka *et al.* (2003) as well as in this present study. Yoshioka *et al.* (2003) divided this section into three intervals, based on stable isotope signature. In interval I (base of the rhythmites to 1.5 m) $\delta^{13}\text{C}$ values [PDB] increased from -5 to -2 per mm upwards. In the interval II (1.5 m to 12 m) the value remained nearly constant at -2 to -1 per mm. In interval III (12 m to the top of the rhythmites) the value increased from -1 to $+5$ per mm. Each interval exhibits different sedimentary features.

Field observations

In interval I, the basal part of the section contains three massive layers: a calcite-rich layer, a dolomite-rich layer, and a clay-rich layer, in ascending order. Each is about 5 cm thick. Above these layers, the interval I consists of light grey, finely laminated rhythmites; the thickness of the lamination ranges from 100 μm to 1 mm. The rhythmites consist of dolomite and this part of the

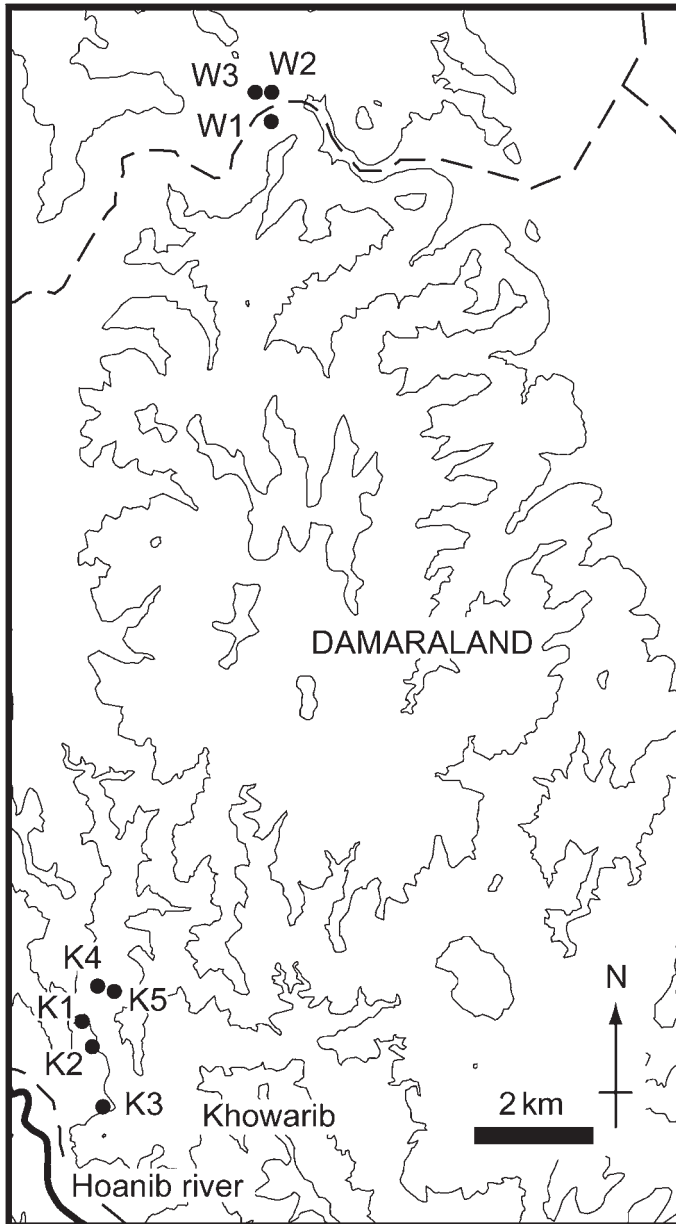


Fig. 1. Area studied in Northern Namibia. W1 to W3: localities of measured columnar sections near Warmquelle in the north. K1 to K5: localities of measured columnar sections near Khovarib. Columnar sections are shown in Figure 2.

section is almost free of turbidites. The $\delta^{13}\text{C}$ value is about -5 per mil at the base of the massive layers, gradually increasing to about -2 per mil in the rhythmite part of the interval I.

In interval II, the colour of the rhythmite changes cyclically from dark to light colours

(Fig. 3). The rhythmite contains intercalations of thin turbidites. The dark part of interval II consists of calcite-rich carbonate, and the light-coloured is made up of rhythmites rich in dolomite. The rhythmites in interval I consist mostly of dolomite, and their colour is slightly green, but the light-colour

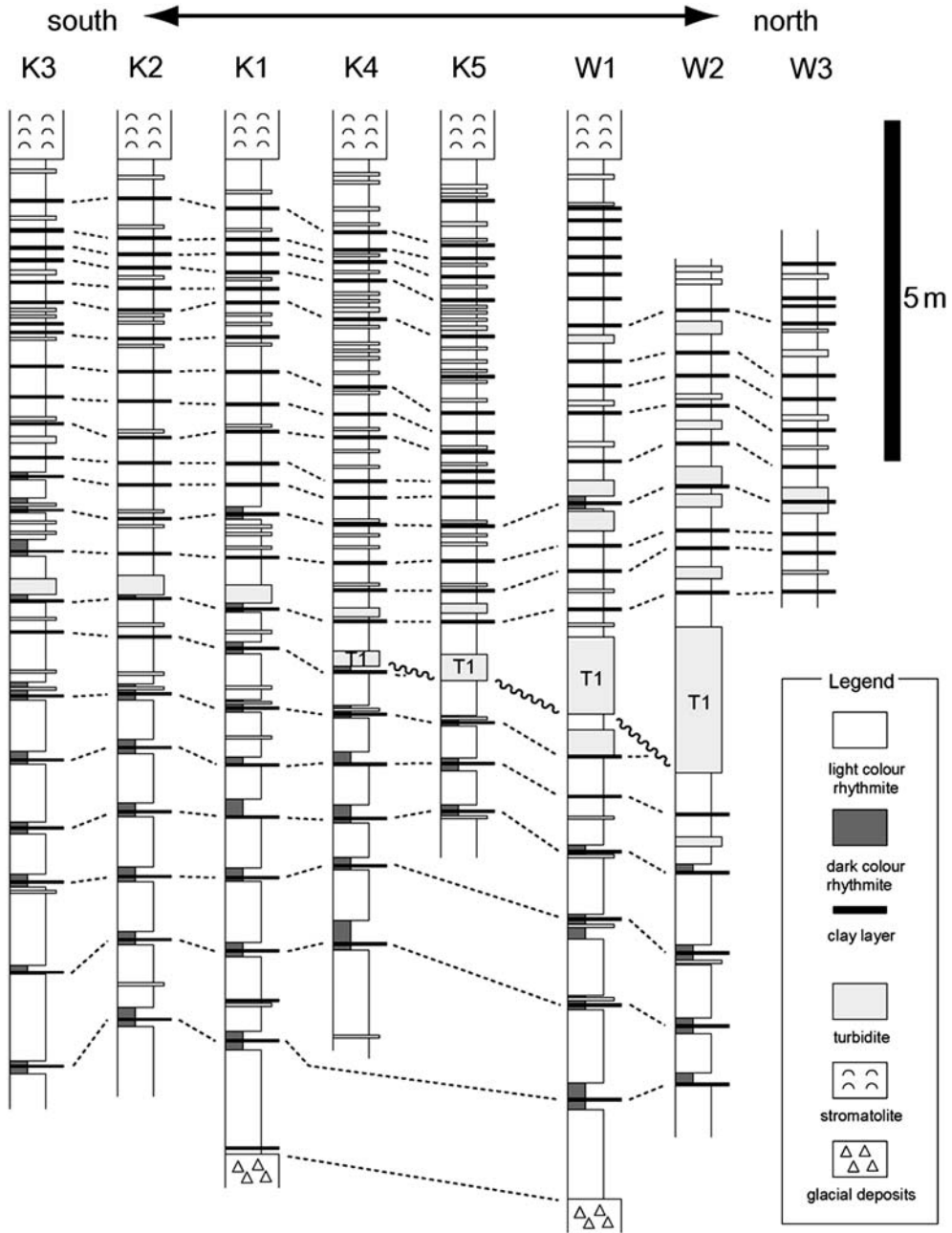


Fig. 2. Columnar sections. Correlation is indicated by thin dotted tie lines. The cycle of dark- and light-coloured rhythmites in the lower part of the columns constitute especially good marker beds. The clay layers are always associated with dark-coloured rhythmite in interval II.

dolomitic rhythmites in interval II contain some calcite and are yellow to brown. Each dark part contains a reddish clay layer of about 1 cm thickness (Fig. 4e). In the lower part of interval II, clay layers always accompany the dark-coloured

rhythmites (Fig. 2). In interval III, clay layers are thin and irregular.

The thickness of the dark band, as well as the colour contrast of the rhythmite cycles, decreases upwards. The thin turbidite layers are only a few

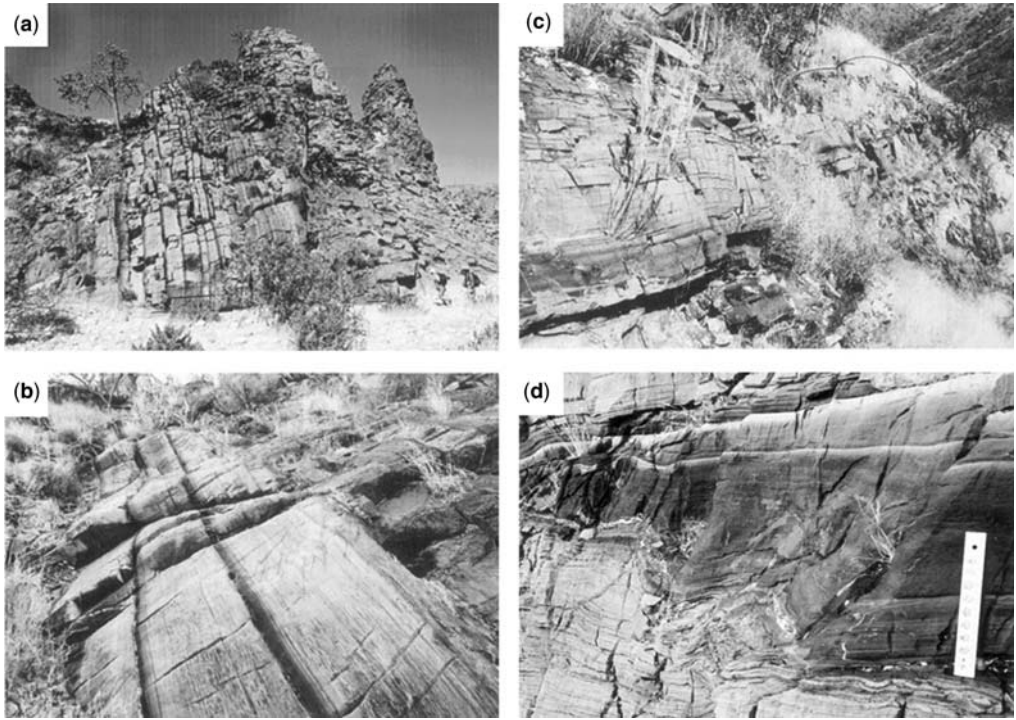


Fig. 3. Photographs of the outcrops. (a) Locality K1 (Khowarib area), where a 14.2 m long set of continuous section was recovered and used for a chemical profiling study. Beds are tilted almost vertically (older to the left). Dark bands are clearly evident; (b) Locality K4 (Khowarib area). Photograph depicts the lower part of the interval II with conspicuous cycles of dark-coloured, calcitic bands alternating with light-coloured dolomitic bands; (c) Locality W1 (Warmquelle area). The basal part of the interval II. Also in the area near Warmquelle, rhythmites contain dark-coloured calcitic bands; (d) Locality W1 (Warmquelle area). The middle part of the interval II exposes the dark-coloured calcitic band.

centimetres in thickness. The thick turbidites are about 10 cm in thickness and exhibit colour grading (Fig. 4f). Turbidites of *c.* 0.5 to 1 m thickness contain rip-up clasts occasionally. In this interval, $\delta^{13}\text{C}$ values are nearly constant around -2 to -1 per mil.

In interval III, the rhythmites exhibit rather thick and undulating lamination, and consist of pure dolomite. Their colour is light grey and blue. Laminations contain clay and hematite. This interval contains massive turbidites, but their thickness is generally thinner than those in interval II. In this interval, $\delta^{13}\text{C}$ values increase from -1 to $+5$ per mil upsection.

Columnar sections were measured in the Khowarib-Warmquelle area, with particular emphasis on the rhythmite part of the Rasthof Formation (Fig. 2). The same set of dark- and light-coloured carbonate rhythmites and thin reddish clay layers, as well as some turbidite layers, can be correlated with the measured columnar sections up to a distance of 20 km away from the K1.

Thin section data

In thin sections, calcite and dolomite were distinguished by using alizarin red. The rhythmites of interval I consist of micritic dolomite layers and fine clay layers (Fig. 4b). The thickness of the lamina is about $100\ \mu\text{m}$ to 1 mm. Clay galls occur as spherical clusters, containing micritic dolomite grains in some horizons. These clusters could have been flocculated by the mixing of freshwater and seawater.

Carbonates in the dark bands of interval II consist of brick-shaped calcite crystals (Fig. 4a). Lamination of these rhythmites reflects the structure of these crystals. Thickness of the lamination is about $100\ \mu\text{m}$. The light-coloured carbonates in interval II consist of, in addition to brick shaped calcites, micritic dolomite inclusions (Fig. 4c). The thickness of the lamination is thicker than that of the dark-coloured rhythmites.

Carbonate rhythmites in interval III consist of dolomite and clay (Fig. 4d). Dolomite crystals

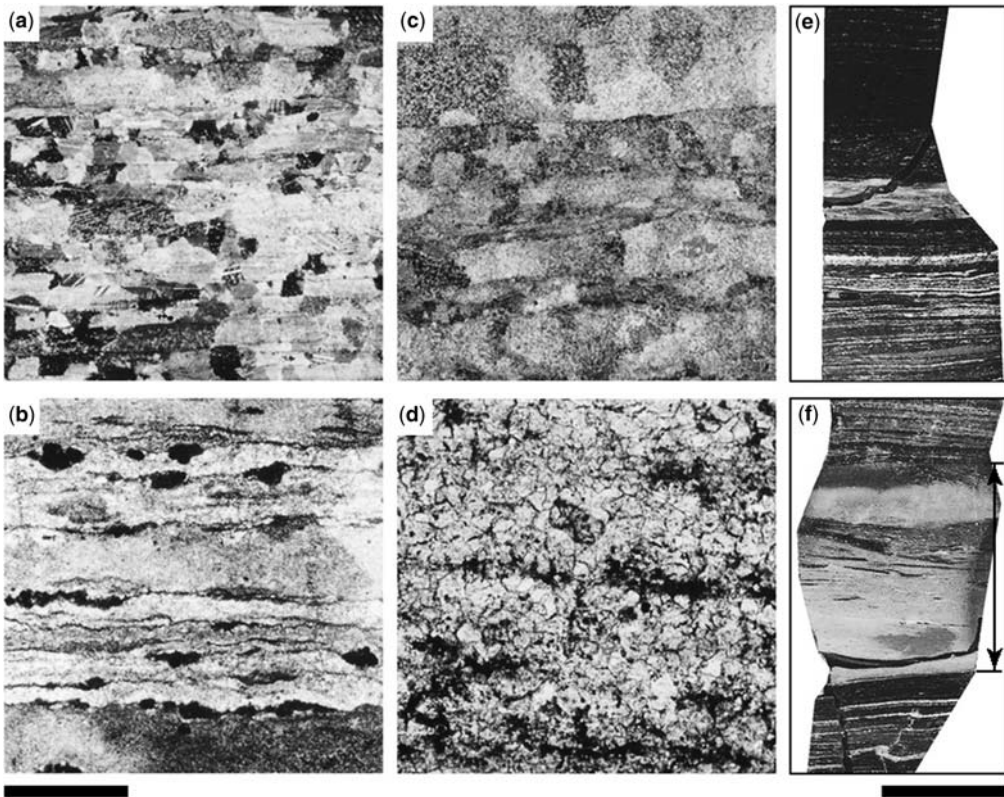


Fig. 4. Thin sections and polished slabs. Specimens collected at K1 locality. Lower left scale bar is 1 mm long and for Figure 4a–d. Lower right scale bar is 3 cm long and for Figure 4e–f. (a) Thin section of dark-coloured rhythmite from the interval II (under crossed nicols). Brick-shaped calcite grains are arranged with their long axes parallel to the bedding (horizontal in the photomicrograph), forming fine lamination. Dark and very fine clay particles are arranged into lamina. One such lamina is sub-horizontal and 2/3 of the height from the base of the micrograph on the right hand side. (b) Thin section of the specimen from Interval I (open nicol). Micritic dolomite (white to grey) matrix and dark-coloured clay particles arranged in lamina are visible. Larger dark spots along the clay lamina are spherical clay particles. (c) Thin section of a light-coloured rhythmite in the interval II (crossed nicols). Within the large ‘bricks’ of calcite crystals, dark, micritic dolomite grains are scattered, most easily discernible near the upper left-hand corner. Clay particles form thin dark laminations. (d) Thin section of the dolomitic part from the interval III. Coarse dolomite crystals and clay laminations, with the most conspicuous one running horizontally near the middle of the height of the photographs, are visible. (e) Clay layer in the interval II, about 1 cm thick and intercalated in dark-coloured calcitic rhythmite. Such clay layers intercalate in each dark rhythmite in the interval II. In the lower part of the photograph, fine laminae of dolomite are visible. (f) Turbidite layer in carbonate rhythmites in the interval II, grading from light to dark colour. The upper 1/3 shows an apparent secondary grading from light to dark colour.

are coarser than those in intervals I and II. Laminations are also thicker than those in intervals I, II, and undulating. Goethite occurs in the dark clay lamina.

Chemical profiles

Element mapping using XRF was carried out of the rhythmite part of the Rasthof Formation. At the K1 locality, a continuous series of samples from the entire rhythmite unit of 14.2 m were collected and

embedded in epoxy resin in order to produce slabs that could be polished. These were analysed using a scanning XRF analytical microscope (SXAM). The element mapping images were processed by ‘lamination tracer algorithm’ (Katsuta *et al.* 2005) to obtain chemical profiles of the section. Furthermore at the K2-4, and W1 localities a part of the rhythmite unit was chemically profiled using the same method (Fig. 5).

Characteristics of the chemical profiles obtained for the Rasthof rhythmites mirror the lithology.

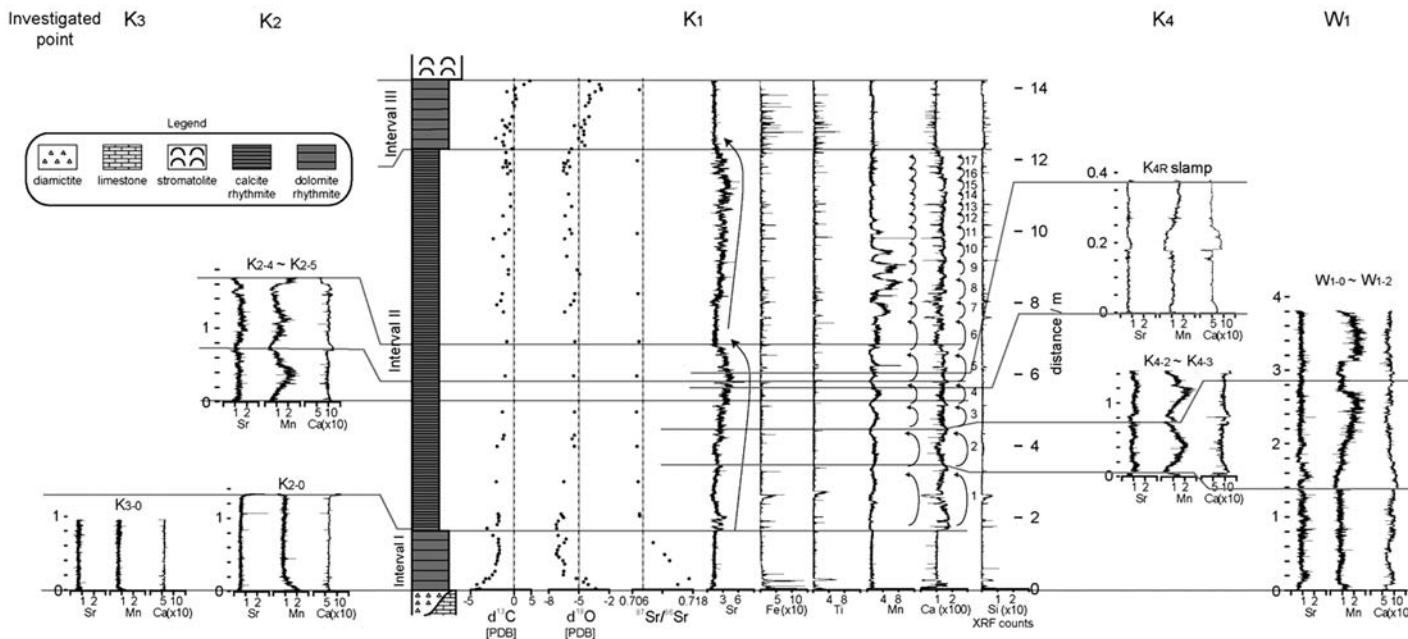


Fig. 5. Chemical profiles. Element mapping using XRF was carried out for the rhythmite part of Rasthof Formation at K1 locality with the spatial resolution of about 0.8 mm. The obtained element mapping images were processed by the 'lamination tracer algorithm' (Katsuta *et al.* 2005) to obtain this chemical profiles. Ca intensity fluctuates in interval II related to dark- and light-coloured cycles.

The moderate and constant Ca intensity, of about 100 XRF counts, in intervals I and III, correlates well with the relative dominance of dolomite over calcite. In interval II, the Ca profile exhibits a metre-scale cyclic fluctuation. Higher Ca intensity corresponds to the dark bands with high calcite content, and a lower intensity relates to the light-coloured bands, with relatively high dolomite content. Fe and Si peaks correspond to the reddish clay layers, defining the boundaries of cycles.

Mn and Sr profiles exhibit unique fluctuations in interval II. Their content is low in the clay layer, whereas higher in the carbonate-rich layer. The metre-scale cyclic fluctuations in the Mn profile correlate with the calcite–dolomite cycles in interval II. The Mn profile has a negative correlation with the Ca profile, and Mn seems associated with the dolomite. On the other hand, the Sr profile has some correlation with the Ca profile. In addition to metre-scale fluctuation, the Sr profile shows a 5 m-order fluctuation.

Rip-up clasts in turbidites

During the field survey, we made an interesting observation on outcrop K4. A 30 cm thick turbidite layer (T1) contains dark-coloured rip-up clasts as well as red and light-coloured clasts (Fig. 6). These clasts show elastic deformation, which indicates that they are derived from unconsolidated layers when they were ripped up.

Figure 6 shows typical rip-up clasts in the upper part of the bed. The elastically deformed dark block has fine laminations and intercalation with a thin, reddish clay layer. Thin fragments of light-coloured layers were also observed. Therefore, the clasts seem to have not fully been consolidated when they were incorporated into the turbidite. The dark and light layers in the rip-up clasts correspond to the calcitic and dolomitic parts of interval II, respectively and suggest that the calcite–dolomite cycles in interval II were already formed before the later deposition of the turbidite (T1).

Discussion

Synsedimentary dolomites

In interval II, the dark- and light-coloured carbonates form cycles, which can be correlated between localities over at least 20 km distance in the Khowarib-Barmquelle area. Observation in the field, as well as on stained thin sections, and chemical profiling of the rhythmites demonstrate that the rhythmic change in colour reflects the cyclic change of carbonate mineral compositions.

The basal rhythmite of the Rasthof Formation contains turbidite layers of about 1 to 30 cm in thickness. Some of them exhibit colour grading. The rip-up clasts within a 30 cm thick turbidite at the K4 locality exhibit elastic deformation and consist of dark-coloured and light-coloured rhythmite and reddish clay layers (typically observed in the sequence above and below the clasts horizon). The elastic deformation of the rip-up clasts suggests that the characteristic features of the calcite–dolomite cycles observed in interval II existed as primary, synsedimentary structures when the carbonate was unconsolidated and before the formation of rip-up clasts.

Model for synsedimentary dolomite formation

The existence of dolomite in sediment which is still elastic suggests that the dolomite has been formed either through sea floor dolomitization in the very early stage of diagenesis, or, has been formed as a primary precipitate from the seawater. In recent environments, the former can occur the interface where freshwater and seawater intermix. However, the depth of deposition of the rhythmites in the Rasthof Formation is estimated to have formed below storm wave base. Sea-level rise that occurred during deglaciation in the Neoproterozoic is estimated to be of a significant magnitude (Hoffman *et al.* 1998; Hoffman & Schrag 2002). Deep marine rhythmite formation is not concordant with the freshwater mixing required for primary dolomitization and thus, because the dolomite at the base of the Rasthof Formation appears to be a primary, synsedimentary precipitate, there must be another explanation for its presence.

Direct precipitation of dolomite does not occur in the present open oceans, because of the inhibiting effect of sulphate in the seawater. If sulphate is depleted up to 5% of the present concentration, dolomite precipitation may occur directly from seawater (Tucker 1990). Hurtgen *et al.* (2002) suggested that Neoproterozoic seawater was depleted in sulphate nearly 5% of the present concentration during meltdown of the 'Snowball Earth' condition, based on the sulphur isotope data from the Otavi Group. Dolomite in interval I in the basal part of the Rasthof cap carbonate may have been directly deposited within such sulphate depleted seawater. However, the residence time of Mg^{2+} is 1.3×10^7 years (Broecker & Peng 1982). The 'Snowball Earth' hypothesis implies about the same time scale for the duration of the glaciation. Thus seawater immediately after the glaciation should have contained only a small amount of dissolved Mg^{2+} . The dolomite precipitation,

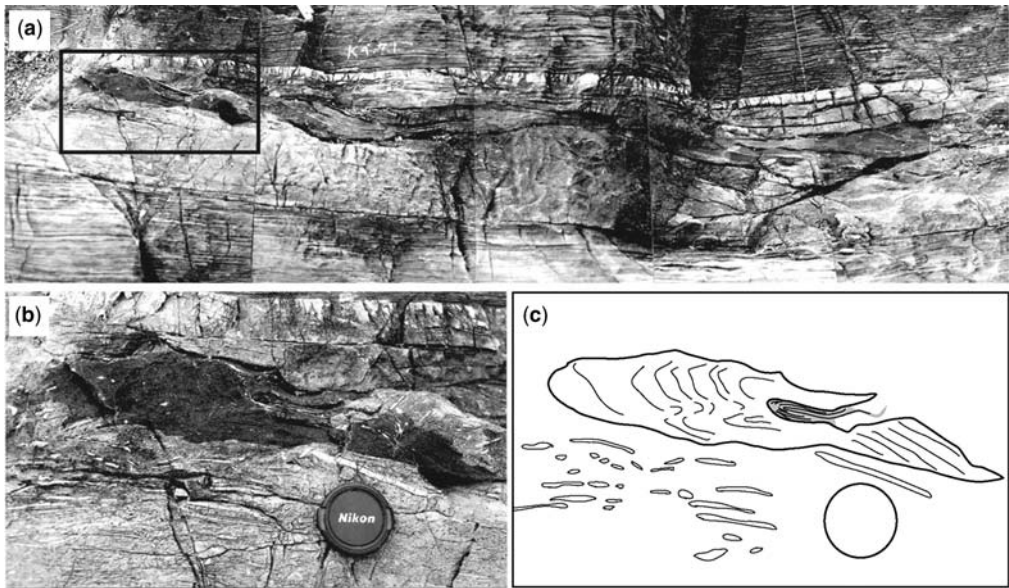


Fig. 6. Rip-up clasts within a 30 cm thick turbidite layer (T1). Dark-coloured rip-up clasts, as well as red and light-coloured clasts, in outcrop. (a) T1 turbidite layer intercalates within the rhythmites. The massive turbidite lies nearly horizontal and occupies the middle part of the composite photographs. (b) Enlarged photograph (b) of the part marked with a frame in (a) and (c) outline drawing of the rip up clasts (c) visible on the enlarged photograph (b). Scale is 5 cm in diameter for (b) and (c). Elastic deformation is easily to be observed, which is reproduced on (c). Large fragment of an elastically deformed clast with clear deformation of calcitic lamina. An intercalated reddish clay layer also demonstrates strong elastic deformation and acute folded, is denoted with grey tone in (c). Thin, light-coloured, dolomitic fragments are apparent near the lower left corner of parts (b) and (c).

therefore, likely ceased when the dissolved Mg^{2+} was rapidly exhausted. The end of dolomite precipitation coincides with the boundary between intervals I and II. But this will not immediately lead to the precipitation of calcite because sulphate inhibition.

After the end of the glacial events, the supply of Mg^{2+} may have resumed with the recovery of fresh-water inflow from the land. River water would have been the main source of Mg^{2+} , supplying about 5.3×10^{12} moles of Mg^{2+} per year to seawater in today's oceans (Edmond *et al.* 1979). This may have contributed to formation of the dolomite in interval II. However, it seems that there was a fluctuation in Mg^{2+} supply, indicated by the alternating precipitation of dolomite and calcite in this interval. Because the ratio of Mg^{2+}/Ca^{2+} contained in river water is <0.4 , this will have been rapidly consumed by dolomite precipitation in ocean water. If the flux of Mg^{2+} was insufficient, then dolomite precipitation would have ceased and been followed by calcite precipitation. The fluctuation of Mg^{2+} supply may be brought about in two ways: fluctuation in volume and rate of river inflow or fluctuation of sea level. During the time of high river water inflow, the rich supply of Mg^{2+} will

promote dolomite precipitation. To the contrary, during times of low river water influx, Mg^{2+} will be consumed prior to reaching a site of precipitation, so resulting in the calcite formation. Sea level change will influence the distance from land where dolomite can be formed. During a sea level high stand, the distance between the site of precipitation and the shoreline may increase and the inflowing Mg^{2+} may be consumed before reaching precipitation site; then calcite instead of dolomite will be deposited. On the other hand, when sea level is low, the site of precipitation will be close to the shoreline and increased Mg^{2+} supply promotes the precipitation of dolomite. In both cases, the fluctuation of Mg^{2+} supply apparently caused the cyclic formation of dolomite in interval II. It is concordant with the fact that calcite-rich rhythmites, which should be precipitated at the time of low river inflow or when the distance of the site from the shoreline is greater, contain less abundant clastic material.

Reddish clay layers in the calcite-rich rhythmites of interval II can be widely correlated between the many localities in our study area. Similar clay layers intercalated within carbonates are also known from sediments deposited during

the Paleocene–Eocene Thermal Maximum (PETM) event. At that time, the postulated rapid release of a large amount of carbon in the form of methane appears to have brought about deep-sea acidification and led to the dissolution of carbonates, leaving clay layers behind as residuals. At the end of Snowball Earth conditions, Hoffman *et al.* (1998) estimated that it is likely that 250 000 gigatons of carbon were released in the form of CO₂. Such huge amounts of released CO₂ could have brought about rapid acidification of the oceans, similar to the Phanerozoic PETM. It is, therefore, an interesting theme for future investigation; if the reddish clay layers of interval II are truly linked with the release of CO₂ at the end of the ‘Snowball Earth’ condition. If the clay layer is evidence of ocean acidification after the Neoproterozoic glaciations, this most certainly would have influenced the marine biosphere. Neoproterozoic glaciation influenced evolution of life not only physically (temperature), but also chemically (pH).

Conclusions

The basal rhythmite of Rasthof Formation contains cycles of dark- and light-coloured rhythmites. Alizarin red staining of thin sections and elemental mapping of polished samples indicate that the dark-coloured part of these sediments is rich in calcite, whereas the light-coloured parts are dolomite-rich with a weak calcite signal. Reddish clay layers are intercalated in each calcite-rich, dark-coloured rhythmite layer. These cycles, as major turbidites, can be well correlated between sections up to 20 km apart. Rip-up clasts of dark- and light-coloured rhythmites and reddish clay layers exhibiting elastic deformation preserved in a turbidite at K4 suggest a synsedimentary, not a diagenetic origin.

The authors greatly thank P. Hoffman and G. P. Halverson for field guidance and help for sampling. The authors also express our cordial thanks to Gabi Schneider, Director of the Geological Survey of Namibia, for her kind permission and support for our research activities in Namibia. We thank M. Kumazawa, H. Yoshioka and T. Okaniwa, for their support in the research and sampling. This work was supported by the ‘Decoding the Earth Evolution’ Program.

References

- ALLEN, P. A., BOWRING, S. A., LEATHER, J., BRASIER, M., COZZI, A., GROTZINGER, J. P., MCCARRON, G. & AMTHOR, J. 2002. Chronology of Neoproterozoic glaciations: New insights from Oman. *16th International Sedimentological Congress Abstract Volume*. Johannesburg, International Association of Sedimentologists, 7–8.
- BOWRING, S., MYROW, P., LANDING, E., RAMEZANI, J. & GROTZINGER, J. 2003. Geochronological constraints on terminal Neoproterozoic events and the rise of metazoans. *Geophysical Research Abstracts*, **5**, 13219.
- BROECKER, W. S. & PENG, T.-H. 1982. *Tracers in the Sea*. Columbia University, Palisades, New York.
- EDMOND, J. M., MEASURES, C., MCDUFF, R. E., CHAN, L. H., COLLIER, R., GRANT, B., GORDON, L. I. & CORLISS, J. B. 1979. Ridge Crest hydrothermal activity and the balances of the major and minor elements in the ocean: the Galapagos data. *Earth and Planetary Science Letters*, **46**, 1–18.
- EVANS, D. A. D. 2000. Stratigraphic, geochronological, and paleomagnetic constraints upon the Neoproterozoic climatic paradox. *American Journal of Science*, **300**, 347–433.
- HALVERSON, G. P., HOFFMAN, P. F., SCHRAG, D. P. & KAUFMAN, A. J. 2002. A major perturbation of the carbon cycle before the Ghaub glaciation (Neoproterozoic) in Namibia: prelude to Snowball Earth? *Geochemistry Geophysics Geosystems*, **3**, 1035.
- HAMBREY, M. J. & HARLAND, W. B. 1981. *Earth's Pre-Pleistocene Glacial Record*. Cambridge University Press, Cambridge.
- HOFFMANN, K.-H. & PRAVE, A. R. 1996. A preliminary note on a revised subdivision and regional correlation of the Otavi Group based on glaciogenic diamictites and associated cap dolostones. *Geological Survey of Namibia Communications*, **11**, 77–82.
- HOFFMANN, K.-H., CONDON, D. J., BOWRING, S. A. & CROWLEY, J. L. 2004. U–Pb zircon date from the Neoproterozoic Chaub Formation, Namibia: Constraints on Marinoan glaciation. *Geology*, **32**, 817–820.
- HOFFMAN, P. F., HAWKINS, D. P., ISACHSEN, C. E. & BOWRING, S. A. 1996. Precise U–Pb zircon ages for early Damaran magmatism in the Summas Mountains and Welwitschia Inlier, northern Damara belt, Namibia. *Geological Survey of Namibia Communications*, **11**, 47–52.
- HOFFMAN, P. F., KAUFMAN, A. J., HALVERSON, G. P. & SCHRAG, D. P. 1998. A Neoproterozoic snowball Earth. *Science*, **281**, 1342–1346.
- HOFFMAN, P. F. & SCHRAG, D. P. 2002. The snowball Earth hypothesis: testing the limits of global change. *Terra Nova*, **14**, 129–155.
- HURTGEN, M. T., ARTHUR, M. A., SUITS, N. S. & KAUFMAN, A. J. 2002. The sulphur isotopic composition of Neoproterozoic seawater sulphate: implications for a snowball Earth? *Earth and Planetary Science Letters*, **203**, 413–429.
- KATSUTA, N., TOJO, B., KAWAKAMI, S., TAKANO, M., OHNO, T. & KUMAZAWA, M. 2005. A method to detect rhythm of lamination in Precambrian sedimentary rocks: evidences for environmental variation during a glacial to interglacial period in Neoproterozoic. *IGCP493 Prato Meeting Extended Abstract*.
- KAUFMAN, A. J., KNOLL, A. H. & NARBONNE, G. M. 1997. Isotopes, ice ages, and terminal Proterozoic

- earth history. *Proceedings of the National Academy of Science USA*, **94**, 6600–6605.
- KENNEDY, M. J., RUNNEGAR, B., PRAVE, A. R., HOFFMANN, K.-H. & ARTHUR, M. A. 1998. Two or four Neoproterozoic glaciations? *Geology*, **26**, 1059–1063.
- KIRSCHVINK, J. K. 1992. Late Proterozoic low-latitude global glaciation: the snowball earth. In: SCHOPF, J. W. & KLEIN, C. (eds) *The Proterozoic Biosphere*. Cambridge University Press, Cambridge, 51–52.
- TUCKER, M. 1990. Dolomites and dolomitization models. In: TUCKER, M. E. & WRIGHT, V. P. (eds) *Carbonate Sedimentology*. Blackwell Scientific Publication, London, 365–396.
- YOSHIOKA, H., ASAHARA, Y., TOJO, B. & KAWAKAMI, S. 2003. Systematic variations in C, O, and Sr isotopes and elemental concentrations in Neoproterozoic carbonates in Namibia: implications for a glacial to interglacial transition. *Precambrian Geology*, **124**, 69–85.
- ZENGER, D. H. 1972. Dolomitization and uniformitarianism. *Journal of Geological Education*, **20**, 107–124.

Correlating the Ediacaran of Australia

K. GREY¹ & C. R. CALVER²

¹*Geological Survey of Western Australia, 100 Plain Street, East Perth, Western Australia 6004, Australia; Research Associate, School of Earth and Planetary Sciences, Macquarie University, New South Wales, 2109, Australia; Honorary Research Associate, School of Geosciences, Monash University, Melbourne, Victoria, 3800, Australia (e-mail: kath.grey@doir.wa.gov.au)*

²*Mineral Resources Tasmania, PO Box 56, Rosny Park, Tasmania 7018, Australia*

Abstract: Now that a Global Stratotype Section and Point (GSSP) has been ratified and a new system defined for the terminal Proterozoic era, the Ediacaran, the next step is to develop global correlations and to further subdivide this system. Means of correlating and subdividing older parts of the Proterozoic era are also needed. This is not a simple task. Phanerozoic correlations depend on biostratigraphic zonation made possible by biodiversity, supported by geochronology. Proterozoic biotas are more restricted, geochronological data is often sparse, and although rapid and significant carbon isotope excursions are present through some time intervals, the curve is essentially quiescent and of limited utility at other times. Nevertheless, a foundation for Ediacaran acritarch biostratigraphy has now been established in Australia and linked to the carbon-isotope curve using sample splits. In conjunction with other correlation techniques, this has allowed the development of a continent-wide correlation scheme. The Australian Ediacaran experience suggests that an integrated approach offers the best way forward for Proterozoic subdivision. However, it raises issues about some aspects of Neoproterozoic correlation; in particular, it indicates that reliance on a two-main-glaciations model may be over simplistic.

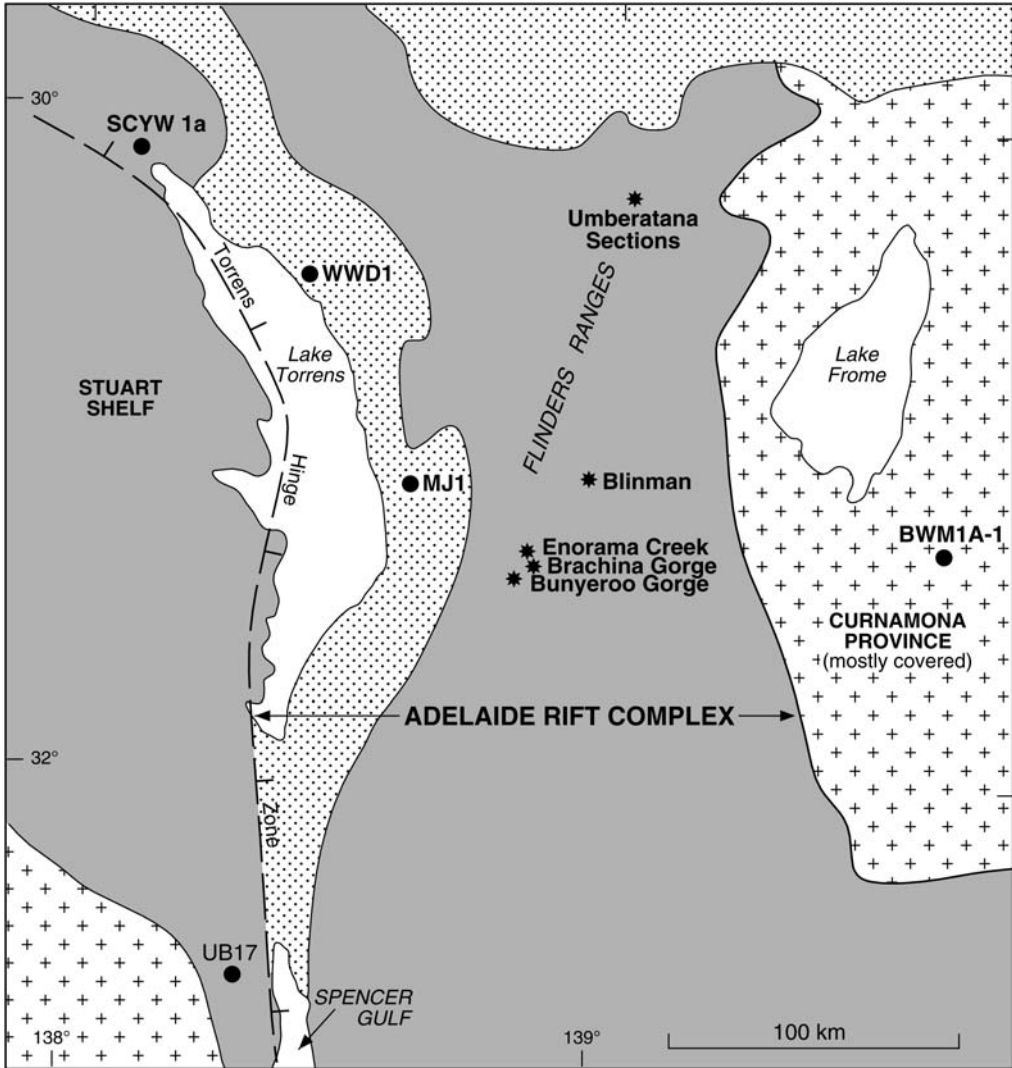
In 2004, the International Union of Geological Sciences (IUGS) defined a Global Stratotype Section and Point (GSSP) for the Ediacaran System and Period (Gradstein *et al.* 2004; Knoll *et al.* 2004) with the boundary at the base of the Nuccaleena Formation ('cap carbonate') in Enorama Creek, Flinders Ranges at 31° 19' 53.8"S, 138° 38' 00.4"E (Fig. 1) (Gehling 2004). A near-continuous section crops out in the Flinders Ranges, with constituent stratigraphic units well exposed in gorge sections. Detailed lithostratigraphy and local and regional correlations are firmly established through many years of study and extensive regional mapping (Preiss 1987, 2000; Gehling 2000, 2004). Correlations are traceable from the type sections, via other measured Flinders Ranges sections, to continuously cored drill holes *c.* 100 km NW on the Stuart Shelf (Figs 1, 2) then westward to continuously-cored Officer Basin drill holes and NW to the Amadeus Basin and other areas of the Centralian Superbasin (Figs 1, 3, 4) (Preiss 2000; Walter *et al.* 2000; Morton & Drexel 1997; Grey 2005). Correlation utilizes lithostratigraphy, seismic interpretation, sequence stratigraphy, event stratigraphy (the recognition of key markers such as glaciations and the time-synchronous Acraman impact ejecta layer), isotope chemostratigraphy and biostratigraphy.

Australian Ediacaran correlations are based on integrated techniques that produce consistent results, and Australia-wide correlations (Fig. 5) can be viewed with considerable confidence.

In 1991, a rigorous sampling program was begun to try to establish an Ediacaran acritarch biostratigraphy based on palynology of continuously cored drill holes (Figs 1–4). A zonation has been constructed for the lower and middle Ediacaran System (Grey *et al.* 2003; Grey 2005) and studies continue on poorly documented parts of the succession. High thermal maturity limits the development of an acritarch biostratigraphy for the Ediacaran type section, but this paper summarizes how the Officer Basin scheme can be tied to the type section through the integrated approach outlined above (where there is a comprehensive palynological record). Acritarchs show good potential for Neoproterozoic subdivision and have promise for the development of a global correlation scheme (Grey 2005).

Geological setting, lithostratigraphy and age

The well-exposed, nearly continuous Ediacaran succession of the Adelaide Rift Complex (Figs 1, 2) (Preiss 1987, 2000) contains the GSSP and global



- Neoproterozoic successions
- Post-Cambrian Basin
- Mesoproterozoic Craton
- Sampled drill hole
- Field section

Fig. 1. Location map showing Adelaide Rift Complex, position of the Ediacaran Global Stratotype Section and Point (GSSP) at Enorama Creek, and key sections and drill holes studied (after Grey 2005).

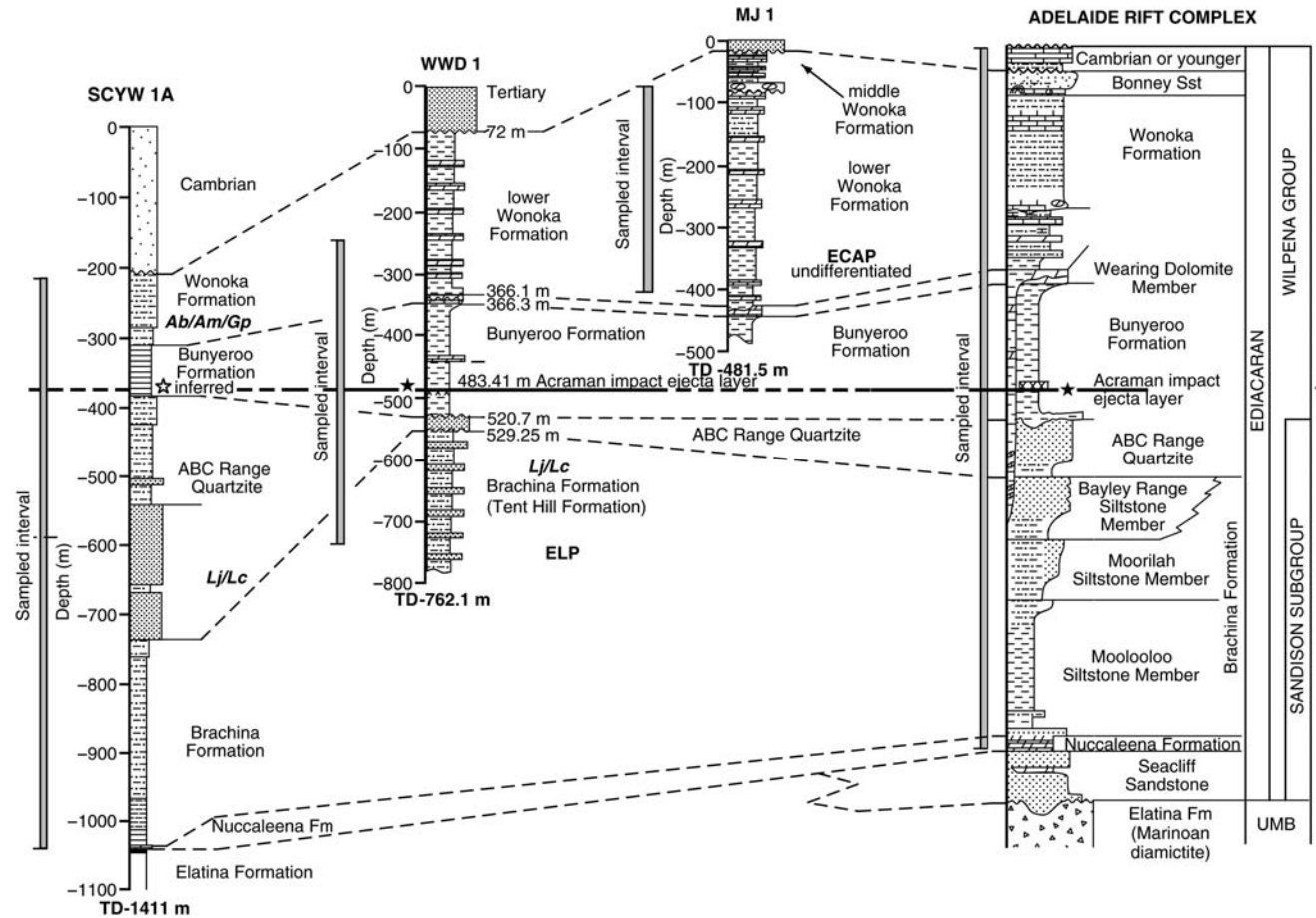


Fig. 2. Correlation of generalized section for the Ediacaran in the Adelaide Rift Complex with drill holes on the Stuart Shelf, showing stratigraphic position of the Marinoan glaciogenic sediments, the actual or inferred position of the Acraman impact ejecta layer and correlations using acritarch zones (after Grey 2005). Lj/Lc, *Leiosphaeridia jacutica/Leiosphaeridia crassa* Assemblage Zone; Ab/Am/Gp, *Appendisphaera barbata/Alicesphaeridium Medusoidum/Gyalosphaeridium pulchrum* Assemblage Zone; ELP, Ediacaran Leiosphere palynoflora; ECAP, Ediacaran Complex Acritarch-dominated palynoflora; UMB, Umberatana Group; WeDM, Wearing Dolomite Member; TD, total depth.

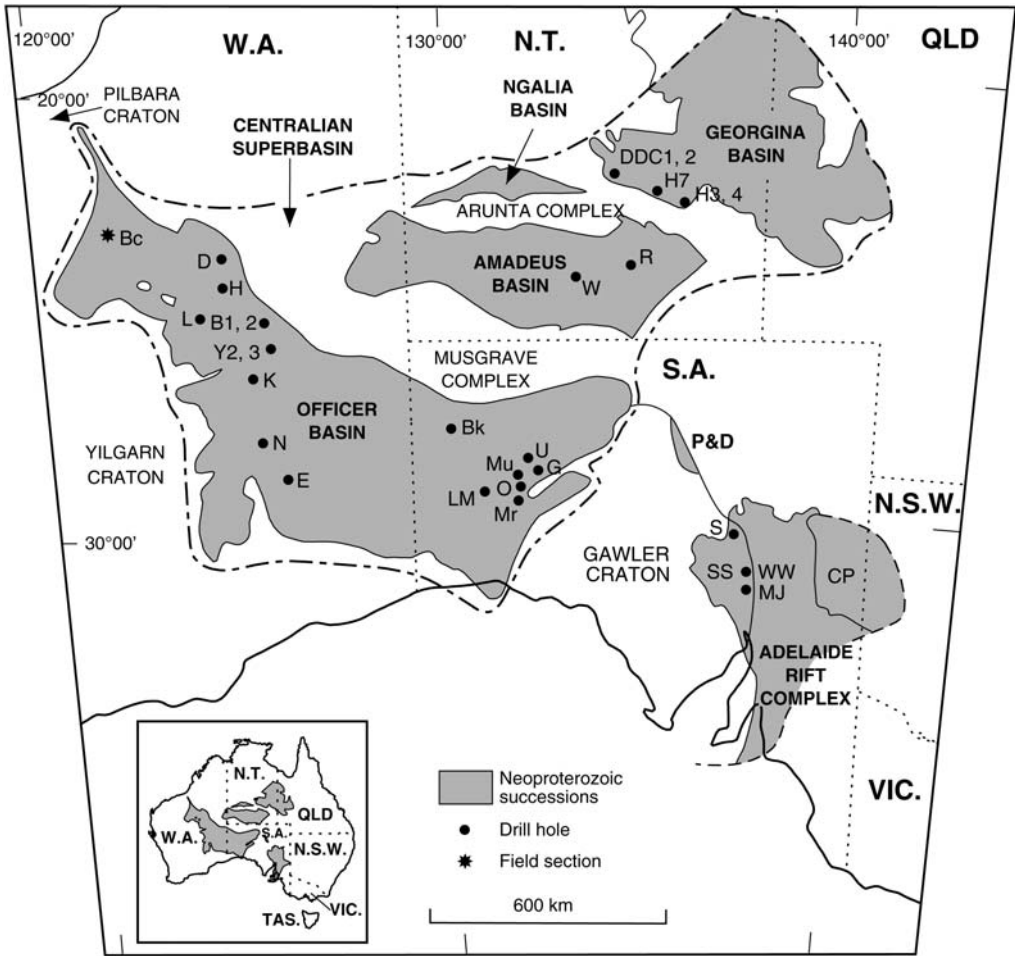
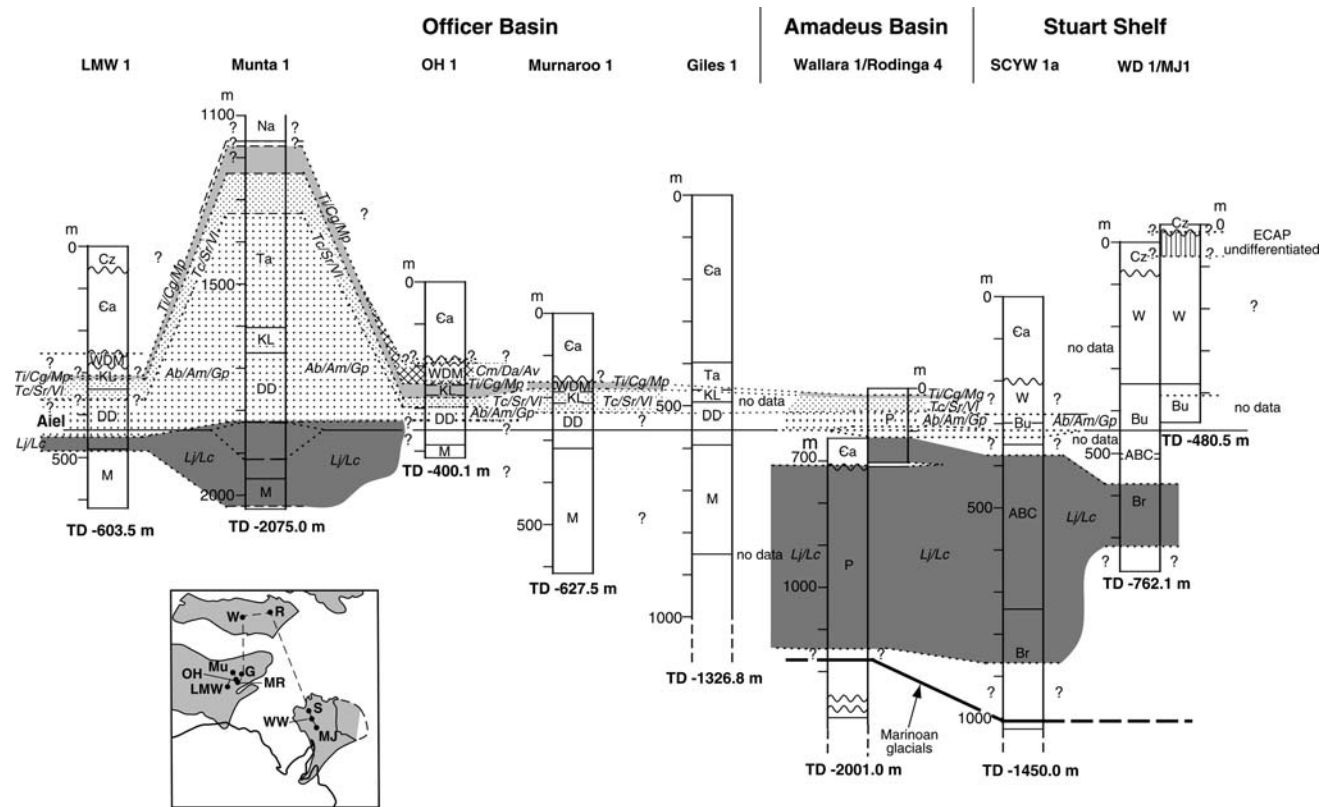


Fig. 3. Location map for the Centralian Superbasin and Adelaide Rift Complex (dot and dash outline), showing constituent structural basins (shaded) and key drill holes studied (after Grey 2005). CP, Curnamona Province; P&D, Peake and Denison Inliers; SS, Stuart Shelf; Drill holes (solid circles): B1, 2, Browne 1 & 2; Bk, Birksgate 1; D, Dragoon 1; DDC1 and DDC2, Centamin Mount Skinner 1 & 2; G, Giles 1; H, Hussar 1; H3, H4 & H7, Huckitta 3, 4, & 7; K, Kanpa 1A; L, Lancer 1; LM, Lake Maurice West 1; MJ, Mount James 1; Mr, Murnaroo 1; Mu, Munta 1; N, NJD 1; O, Observatory Hill 1; R, Rodinga 4; S, SCYW 1a; U, Ungoolya 1; W, Wallara 1; WW, WWD 1; Y2, 3, Yowalga 2 & 3.

stratotype for the Ediacaran System (Gehling 2004). Stratigraphic terminology is based mainly on Preiss (1987, 2000), who set forth earlier proposals relating to system terminology (Termier & Termier 1960; Jenkins 1981; Cloud & Glaessner 1982). The Ediacaran System in the Adelaide Rift Complex consists of the Wilpena Group, which comprises two major upward-coarsening, transgressive–regressive cycles, the first extending from the Nuccaleena Formation to the top of the ABC Range Quartzite and the second including the Bunyeroo and Wonoka formations and the Pound

Subgroup. Palaeogeographic time-slice reconstructions (Preiss 1987) indicate mainly intracratonic deposition, with an ocean basin to the SE, and a possible deep ocean to the north during Wonoka time.

In the Officer Basin, the Wilpena Group equivalent consists of the Lake Maurice and Ungoolya groups (Tarlina Sandstone, Meramangye and Murnaroo formations and Dey Dey Mudstone, Karlaya Limestone, Tanana Formation, including the Wilari Dolomite Member, Munyarai and Narana formations, and Punkerri Sandstone). In the Amadeus Basin, the Wilpena Group equivalent



EDIIACARAN CORRELATION

Fig. 4. Acritarch zonation for drill holes in the Officer Basin (Lake Maurice West 1, Munta 1, Observatory Hill 1, Murnaroo 1, and Giles 1), the Amadeus Basin (Wallara 1 and Rodinga 4) and the Adelaide Rift Complex (SCYW1a, WWD 1 and MJ1). ABC, ABC Range Quartzite; Br, Brachina Formation; Bu, Bunyeroo Formation; Cz, Cenozoic; DD, Dey Dey Mudstone; KL, Karlaya Limestone; M, Murnaroo Formation; Na, Narana Formation; P, Pertatataka Formation; Ta, Tanana Formation; W, Wonoka Formation; WDM, Wilari Dolomite Member; ε, Cambrian. Lj/Lc, *Leiosphaeridia jacutica/Leiosphaeridia crassa* Assemblage Zone; Ab/Am/Vp, *Appendisphaera barbata/Alicesphaeridium medusoidum/Gyalosphaeridium pulchrum* Assemblage Zone; Tc/Sr/Vl, *Tanarium conoideum/Schizofusa risoria/Variomargosphaeridium litoschum* Assemblage Zone; Ti/Cg/Mp, *Tanarium irregulare/Ceratosphaeridium glaberosum/Multifronsphaeridium pelorium* Assemblage Zone; Cm/Da/Av, *Ceratosphaeridium mirabile/Distosphaera australis/Apodastoides verobturatus* Assemblage Zone; ECAP, Ediacaran Complex Acritarch-dominated palynoflora; ELP, Ediacaran Leiosphere-dominated palynoflora. Also shown are the position of Marinoan glaciogene sediments, the actual or inferred position of the Acraman impact ejecta layer, and the first recorded appearance of acanthomorph acritarchs (after Grey 2005).

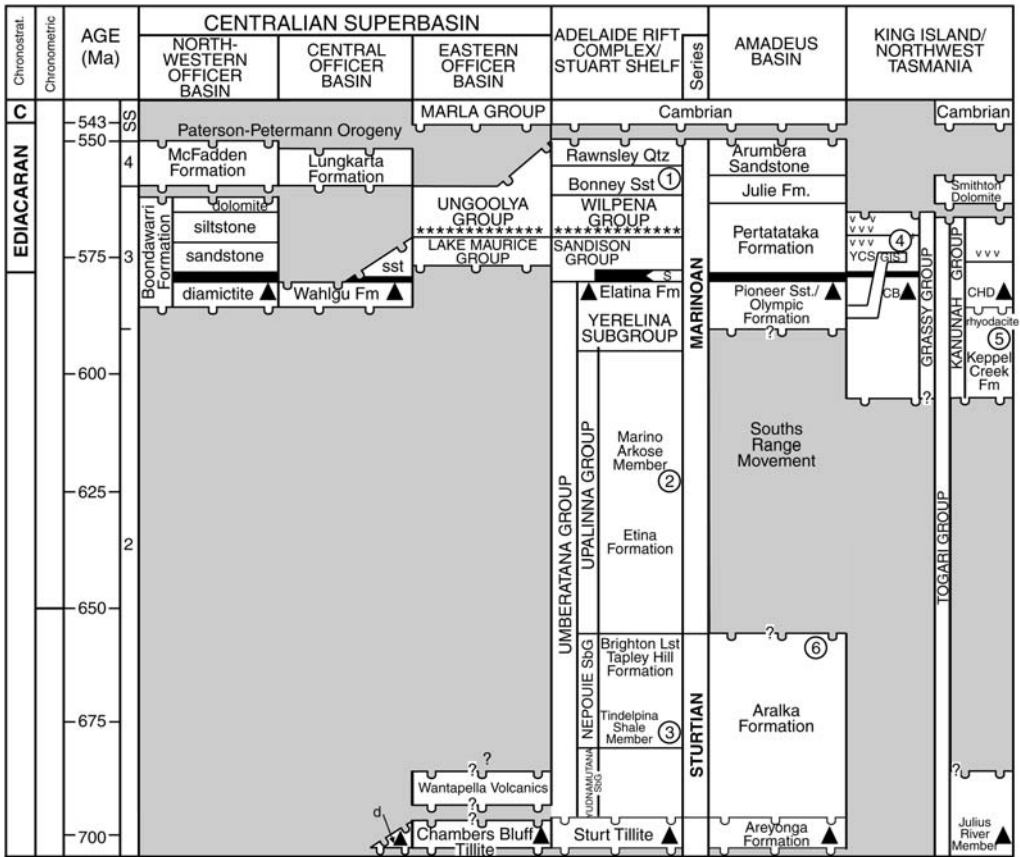


Fig. 5. Generalized time-space diagram for the Ediacaran of Australia showing correlations between tectonic units derived by use of integrated techniques (after Grey 2005) with key tie points based on biostratigraphy and isotope chemostratigraphy. CB, Cottons Breccia; CHD, Croles Hill Diamictite; GDS, Gairdner Dyke Swarm; GIS, Grimes Intrusive Suite; YCS, Yarra Creek Shale. Diamictite is represented by a triangle, Acraman impact ejecta layer is shown by asterisks and cap carbonate by solid black lines. Numbers in circle represents the appropriate age; i.e. 1, detrital zircon age of 556 ± 24 Ma in Bonney Sandstone (see Preiss 2000); 2, detrital zircon age of 657 ± 17 Ma in Marino Arkose (see Preiss 2000); 3, Re–Os age of 643.0 ± 2.4 Ma in Tindelpina Shale (Kendall *et al.* 2005). 4, U–Pb zircon age of 575 ± 3 Ma on intrusive sill in Yarra Creek Shale (Calver *et al.* 2004); 5, U–Pb zircon age of 582 ± 4 Ma on rhyodacite below Croles Hill Diamictite (Calver *et al.* 2004); 6, Re–Os age of 657 ± 5.4 Ma on Aralka Formation (Kendall *et al.* 2005).

comprises the uppermost Pioneer Sandstone, the Pertatataka and Julie formations and the Arumbera Sandstone.

Adelaide Rift Complex and Stuart Shelf

Widespread diamicrites and glacial outwash units, the Elatina Formation and correlatives, such as the Perpuarta Tillite and the Seaciff Sandstone, mark the Marinoan glaciation in the Adelaide Rift Complex. Glacial units crop out throughout the Flinders Ranges, and are present in Stuart Shelf drill holes, such as SCYW 1a (Preiss 1987, 2000; Dyson 1992a), WWD 1 and MJ 1 (Zang 1977).

The basal Wilpena Group represents a rapid post-glacial transgression widening an earlier rift basin to form a shallow carbonate shelf sea over the central Flinders Ranges area (Preiss 1987). The Ediacaran System GSSP, at the base of the ‘cap carbonate’ Nuccaleena Formation, coincides with the base of the Wilpena Group (Preiss 2000).

The Nuccaleena Formation conformably overlies the UMBERATANA Group in the central Flinders Ranges near the type section, but is disconformable elsewhere. It extends to SCYW 1a on the Stuart Shelf. Despite some facies variation, the formation is mostly a typical ‘cap dolostone’ overlying glaciogenic sediments (Williams 1979; Dyson 1992b).

It consists of 10–60 m of pink or yellow laminated micritic dolomite, overlain by *c.* 60 m of purple shale with rare dolostone lenses, deposited in a middle- to outer-shelf environment below wave base and probably representing a transgressive systems tract (Dyson 1992*b*).

The gradational boundary between the Nuccaleena and overlying Brachina formations marks the base of a transgressive-regressive cycle up to 2200 m thick (Haines 1990). The Brachina Formation is one of the most widespread formations in the Adelaide Rift Complex (Preiss 1987), with well-exposed sections in the Flinders Ranges gorges, and is present in SCYW 1a and WWD 1 on the Stuart Shelf. It consists mainly of red-brown or olive-green, thinly laminated siltstone and interbedded flaggy, medium-grained, thinly bedded sandstone and contains fine-grained sandstone 'event beds' up to 1 m thick (Dyson & von der Borch 1986). As subsidence continued, extensive red-brown, finely laminated mud and silt were deposited, marking the maximum post-glacial transgression. The formation reflects an upwards-shallowing sea, and includes sediments deposited below storm wave base to those laid down in a tidally influenced shallow-marine environment. It forms part of a highstand systems tract that accumulated as an eastward-prograding clinoform (Dyson & von der Borch 1986; Preiss 1987; Dyson 1992*b*). A moderately high-energy regime is indicated for sediments making up the formation with benthic microbial-mat remnants indicating periods of quieter deposition (Calver 2000).

The boundary with the overlying ABC Range Quartzite is gradational and deposition continued as a series of eastward-prograding deltal fronts derived from the Gawler Craton. The ABC Range Quartzite represents a regressive phase that terminated post-glacial marine transgression (Preiss 2000). The formation is >2000 m thick near the Torrens Hinge Zone, but thins rapidly eastward, where it is commonly *c.* 500 m thick. In the Flinders Ranges, it consists mainly of pinkish-grey, fine- to medium-grained quartzite with minor greenish-grey, micaceous siltstone partings. In the more proximal SCYW 1a section, it consists of fine- to medium-grained, cross-bedded quartz arenite, passing upward into interbedded, dominantly grey-green, siltstone, shale, and cross-bedded sandstone. The palaeoenvironment represented by these sediments varied from shallow marine to tidal flat, with intermittent subaerial exposure and fluvial or very shallow marine conditions.

The boundary with the overlying Bunyerroo Formation is a persistent erosional horizon (in some areas the ABC Range Quartzite is unconformably overlain by Cambrian formations) marking the beginning of a second, rapid transgression, which

deposited fine-grained siliciclastic sediment up to 700 m thick in the type section but thinning northward over the Stuart Shelf (Preiss 1987, 2000). The Bunyerroo Formation is only 70 m thick in SCYW 1a (Figs 2, 4), where it consists of red shale with rare, green, dolomitic mudstone bands. Incomplete sections are present in WWD 1 and MJ 1 (Zang 1977) (Fig. 2). For the most part, the Bunyerroo Formation comprises a monotonous succession of maroon, silty shale, although a dark grey pyritic interval occurs near the base and there are interbeds of greenish siltstone, grey dolomite and lenses of dark grey limestone (Preiss 1987). Deposition began in a localized fluvial or shallow marine environment, at or near fair-weather wave base, and was followed by rapid transgression to a sediment-starved depositional environment of quiet, deep water, below wave base (Preiss 1987; Haines 1990).

A distinctive band of clasts derived from the Gawler Range Volcanics, the Acraman impact ejecta layer, lies about 80 m above the base of the Bunyerroo Formation. The layer is a thin (*c.* 40 cm in the Flinders Ranges), persistent horizon of coarse, feldspathic detritus containing quartz crystals with planar deformation features (PDFs) and is likely the result of a *c.* 4.7 km diameter bolide which impacted near Lake Acraman in the Gawler Craton (Fig. 1) (Gostin *et al.* 1986; Williams 1986; Williams *et al.* 1996; Wallace *et al.* 1996; Williams & Wallace 2003). The debris layer covered an area *c.* 1000 km in diameter, and forms a synchronous marker horizon present in the Flinders Ranges and Officer Basin (Fig. 4). It was identified in WWD 1 (Fig. 2) on the Stuart Shelf (Gostin *et al.* 1986, Wallace *et al.* 1990*a*), but has not yet been located in SCYW 1a, although its approximate position is indicated by the first appearance of shattered crystals in palynological preparations (Hill *et al.* 2004; Grey 2005). Its position in Stuart Shelf and Officer Basin drill holes is characterized by an iridium anomaly (Wallace *et al.* 1990*b*, 1996) and a coeval negative $\delta^{13}\text{C}_{\text{organic}}$ isotope anomaly (Calver & Lindsay 1998; Grey *et al.* 2003).

The contact between the Bunyerroo and Wonoka formations is the base of the Wearing Dolomite Member (Haines 1990; Calver 1995). It is gradational in SCYW 1a (Calver 1995) but may be disconformable in WWD 1 and MJ 1 (Zang 1997). The Wonoka Formation is widely distributed in the Adelaide Rift Complex, but only the basal part is present in SCYW 1a (Calver 1995). The formation is *c.* 500 m thick in the type section but elsewhere reaches about 700 m (Preiss 1987). Generally, it consists of a broadly shallowing-upward succession of mixed siliciclastic and carbonate rocks (Haines 1987, 1988, 1990; Calver & Lindsay 1998) that indicate continuation of quiet water, fine-grained

sedimentation. There was a gradual shallowing upwards from a condensed marine section and maximum flooding surface in the Wearing Dolomite Member (Dyson 1992*b*) to a shallow-water, prograding tidal flat in the overlying Bonney Sandstone. The middle Wonoka Formation is marked by deeply incised canyons (von der Borch *et al.* 1982, 1985; Eickhoff *et al.* 1988; Christie-Blick *et al.* 1990, 1995; Dyson 1992*a*). To the NE, thick, basinal sediments (the Billy Springs beds) indicate a rapidly subsiding trough.

The Patsy Hill Member, a carbonate at the base of the overlying Bonney Sandstone, is 16 m thick in Bunyeroo Gorge, but it thickens northwards and eastwards to at least 80 m (Haines 1990; Reid & Preiss 1999; Preiss 2000). It is dominated by coarsening upward cycles of grey and black limestone, and contains oolitic grainstone, fine-grained limestone, and small stromatolitic bioherms (Walter *et al.* 1979; Grey & Corkeron 1998). It represents a return to shallow lagoonal conditions. The remaining Bonney Formation consists of cyclic, mostly red, fine to medium-grained silty sandstone and siltstone indicating a mainly fluvial and tidal deltaic environment (Preiss 2000). The Ediacara Member of the overlying Rawnsley Quartzite contains the Ediacara fauna, which was deposited in shallow marine conditions indicating renewed transgression and progradation.

Officer Basin succession

The Officer Basin spans the Western and South Australian border (Fig. 3) and separate stratigraphies have been used in the two states (Fig. 5). The basin is *c.* 1400 km long and contains up to 7 km of Proterozoic sediments, in places overlain by Palaeozoic, Mesozoic, and Cenozoic sediments. There is an extensive Cryogenian succession in the western Officer Basin, and some areas with Marinoan glacial deposits, but Ediacaran rocks (Boondawari Formation and Disappointment Group) are restricted primarily to the NW (Jackson & van de Graaff 1981; Williams 1992; Grey *et al.* 2005; Grey 2005). In the eastern Officer Basin, the Ediacaran succession is thicker and more extensive. Data have been recovered mostly from exploratory drill holes and seismic interpretation (Figs 1, 3, 4) (Lindsay 1995; Lindsay & Reine 1995; Zang 1995; Morton & Drexel 1997; Grey 2005).

There is a lacuna of at least 20 million years between the Cryogenian and Ediacaran successions in the eastern Officer Basin (Gravestock 1997). In the east of the basin, the Chambers Bluff Tillite and overlying Wantapella Volcanics are probably Sturtian in age, although evidence for this is sparse (Preiss 1993; Morton 1997). Diamictite is present in several places in the western Officer

Basin, although the age and correlation of some units is uncertain. From stratigraphic data, the Lupton and Turkey Hill formations are probably Marinoan in age (Jackson & van de Graaff 1981; Grey *et al.* 1999). The Lupton Formation diamictite varies from 175 m to 250 m thick, and the Turkey Hill Formation is several hundred metres thick, but neither has a cap carbonate. The Wahlgu Formation (*c.* 165 m thick) consists of diamictite and a thin cap carbonate (*c.* 15 cm thick) and, in Empress 1 and 1A, it is overlain by an unnamed sandstone unit (Stevens & Apak 1999; Grey *et al.* 1999, 2005). Only diamictite (122.2 m thick) was intercepted in Lancer 1 (Haines *et al.* 2004). Correlation between the Wahlgu, Lupton and Turkey Hill formations is uncertain because of lithological differences (Grey *et al.* 2005), but, the Wahlgu Formation can be correlated with the Elatina and Nuccaleena formations (Grey *et al.* 1999, 2005) and with part of the Boondawari Formation (Williams 1992; Walter *et al.* 1994). The poorly exposed Boondawari Formation consists of consists of a lower diamictite unit, a middle sandstone-dominated unit, and an upper argillite and carbonate unit, and may reach 800 m thickness. A thin, red, micritic dolomite in the middle of the formation underlies the upper siltstone and appears to correlate with cap carbonates in other basins (Walter *et al.* 1994). The top of the formation is a thin-bedded, grey and pink dolomite, containing oolites, pisolites, stromatolites, and local halite casts. It is probably equivalent to the Patsy Hill Member of the Bonney Sandstone in the Adelaide Rift Complex and the Julie Formation in the Amadeus Basin (Walter *et al.* 1994). The Boondawari Formation probably corresponds to a large proportion of the Ediacaran succession elsewhere in Australia.

No Marinoan diamictite has been identified in the eastern Officer Basin, but Calver and Lindsay (1998) correlated the Lake Maurice Group with the lower Wilpena Group of the Adelaide Rift Complex based on lithological comparisons and similarities in the $\delta^{13}\text{C}_{\text{organic}}$ curve. The Tarlina Sandstone, Meramangye Formation, and Murnaroo Formation were correlated with the Sealiff Sandstone, Brachina Formation and ABC Range Quartzite respectively (Morton 1997). The Lake Maurice Group is a post-glacial transgressive–regressive cycle consisting of lowstand fluvial conglomerates, which grade upward into transgressive to highstand siltstones and silty mudstones and then into a regressive system tract of shore face and estuarine–fluvial sediments.

The overlying Ungoolya Group correlates with the upper Wilpena Group of the Adelaide Rift Complex (Fig. 5). The Dey Dey Mudstone overlies the Murnaroo Formation either conformably or unconformably, and the formation is widely

distributed in the eastern Officer Basin. It may be up to 900 m thick in the trough areas. It consists mainly of red-brown and grey-green silty mudstone (Morton 1997). The basal conglomerate was probably deposited in a fluvial environment, but the unit was mostly deposited in predominantly deep-water (below wave base) environment in a prodelta to shelf setting with a reduced sediment supply (Arouri *et al.* 2000).

In the eastern Officer Basin, the Acraman impact ejecta layer (Fig. 1) is present in the lower Dey Dey Mudstone in several drill holes (Gostin *et al.* 1986, 1989; Wallace *et al.* 1989, 1990a, b, c, 1996; Hill *et al.* 2004). It is a thin, distinctive horizon of medium to coarse sand-sized acid volcanic clasts with a thin, pale-green alteration halo, and is marked by a high iridium anomaly, quartz crystals with planar deformation features (PDFs), and devitrified melt particles as in the Flinders Ranges. It also coincides with a negative $\delta^{13}\text{C}_{\text{organic}}$ excursion (Calver 1995, 2000; Calver & Lindsay 1998).

The contact between the Dey Dey Mudstone and overlying Karlaya Limestone is conformable and transitional. The limestone is between 13 m and 66 m thick and is predominantly micritic with thin silty mudstone interbeds (Morton 1997). Limestone intraclasts indicate a subtidal shelf environment, probably below fair-weather wave base, forming part of a subtidal to neritic transgressive systems tract (Zang 1995; Calver & Lindsay 1998; Arouri *et al.* 2000). The lower Karlaya Limestone indicates a low energy carbonate slope and the upper part, a shoal water carbonate shelf that concluded deposition of the 'first slope-apron'. Near the top of the formation, silty slope carbonates indicate subsidence and the beginning of the next cycle of slope-apron formation.

The Tanana Formation unconformably overlies the Karlaya Limestone (Morton 1997). It is a widely distributed formation that is 523 m thick in the type section in Munta 1. It is thinner on the platform, where it is commonly represented only by the thin Wilari Dolomite Member (up to c. 60 m thick), probably equivalent to the uppermost Tanana Formation (Grey 2005). The Tanana Formation comprises limestone, calcareous siltstone, and minor sandstone. The siltstone or silty mudstone is massive to laminated, occasionally cross-bedded or slump cross-bedded (Morton 1997). The upper Tanana Formation comprises red-brown and grey-green siltstone interbedded with thin sandstone; cross bedding and erosional surfaces are common (Morton 1997). Most of the Tanana Formation was deposited in a prodelta- and distal-delta front to shelf setting (Morton 1997). The Wilari Dolomite Member contains fractures and intraclasts that suggest formation in an intertidal to upper subtidal shelf setting (Morton 1997). Arouri *et al.* (2000)

identified four slope-aprons separated by carbonate shelves in the underlying part of the Ungoolya Group, and the Wilari Dolomite Member may represent the base of a fifth slope-apron cycle that over-lapped a more extensive area than previous cycles. It is probably a correlative of the basal Bonney Sandstone and the Julie Formation.

The Munyarai Formation conformably overlies the Tanana Formation, and is up to 450 m thick, although the formation is missing in many areas (either not present or eroded by canyon cutting). The formation comprises grey- to dark-grey calcareous siltstone with thin limestone interbeds in the lower part. It is massive to laminated with graded bedding (Morton 1997). It was deposited in a prodelta to shelf environment and is probably partly equivalent to 'slope-apron 5' of Arouri *et al.* (2000).

The Narana Formation infills canyons incised into the lower Ungoolya Group and in some areas cuts down as far as the lower Dey Dey Mudstone. The formation ranges in thickness from 8 m to 328 m and seismic evidence suggests it may be as thick as 1500 m (Morton 1997). The Narana Formation comprises conglomerate, sandstone, dark grey silty mudstone, and silty limestone in varying proportions in different areas (Morton 1997). Its lower part consists of debris flow deposits grading upwards into tidal flat deposits. The upper part is a turbidite succession deposited as a submarine fan that shallows upwards to a marine shelf limestone and mudstone (Morton 1997). The upper unit was interpreted as a transgressive to highstand sequence tract (Zang 1995).

The Punkerri Sandstone is one of the few outcropping units, although it has not been recognized in drill holes, and it extends into Western Australia. It is >1200 m thick in the type section and has two subdivisions. The lower part is a purple- or red-brown, medium grained flaggy quartzose sandstone with some feldspar and biotite, and the upper part is red and white, medium-grained feldspathic sandstone and some quartzose sandstone with interbedded red sandstone and siltstone. The lower Punkerri Sandstone contains scour casts, ripple marks, pellets, and siltstone flakes. Cross bedding, siltstone clasts, and quartz pebbles occur in the upper unit (Morton 1997). Neither the lower nor the upper contact is exposed, but they are inferred to be regional unconformities. The Punkerri Sandstone is a tidally influenced, shallow-marine sandstone similar to the Pound Subgroup and contains poorly preserved Ediacara Member assemblage fossils (Jenkins & Gehling 1978). Unconformably overlying stratigraphic units are assigned to the Cambrian Marla Group and are not differentiated here. In the western Officer Basin, two younger sandstone units, the McFadden and Lungkarta

formations are possibly Punkerri Sandstone equivalents (Grey *et al.* 2005).

Amadeus Basin succession

The Amadeus Basin is about 800 km long and about 300 km wide (Fig. 3). It was probably much more extensive, particularly during early depositional stages, its present shape being the result of tectonism (Lindsay & Korsch 1991; Walter *et al.* 1995). Sedimentation in the basin began in the middle Neoproterozoic (*c.* 850 Ma) and continued to the Late Devonian. Drill holes Wallara 1 and Rodinga 4 (Figs 3, 4) provide an almost continuous Ediacaran section from the Pioneer Sandstone, through the Pertatataka Formation, to just below the Julie Formation (Fig. 5).

The sediments deposited during the Marinoan glaciation consist of the Olympic Formation and its lateral equivalents, the Pioneer Sandstone, and Boord Formation. The base of the cap carbonate above the Pioneer Sandstone corresponds to the base of the Ediacaran System. The Olympic Formation is often poorly exposed and is characterized by rapid and variable facies changes. It is mostly a reddish diamictite, containing striated and faceted clasts and dropstones. It infills pre-existing basin topography, and ranges from 0 to 300 m in thickness. The Pioneer Sandstone consists of sandstone and conglomerate, is about 170 m thick, and is probably a glacial outwash fan. In places, it rests with inferred unconformity on the Cryogenian succession; elsewhere, it conformably overlies or interfingers with the Olympic Formation. The glacial units form a lowstand systems tract at the base of a transgressive cycle (Lindsay & Korsch 1991).

The lower boundary of the cap carbonate is abrupt, and in places is an erosional disconformity. It consists of a dolostone that exhibits considerable variation in lithology and includes maroon shale, interbedded dolomitic sandstone dolostone and dark-grey shale passing up into pale yellow dolomite. In some areas, it is pinkish grey with lenses of red chert in the lower part and contains small stromatolitic bioherms (Walter *et al.* 1979). The cap dolostone was interpreted as a transgressive systems tract deposited under a deepening water body that was starved of siliciclastic input and was mostly below wave base (Kennedy 1993, 1996; Calver 1995; Calver & Lindsay 1998).

The Pertatataka Formation unconformably overlies the cap dolostone and is at least 570 m thick. Lateral equivalents include the Winnall beds and Gaylad Sandstone (Calver 1995). Sedimentation was initially from the south, but the centre of deposition then shifted and was concentrated in northern sub-basins and troughs, with only limited sedimentation on the southern platform. The Pertatataka

Formation consists mainly of grey-green and purple-brown laminated micaceous siltstone and shale with thin interbeds of sandstone and limestone. In places it contains glauconite and clay pellets. To the NE, a sandstone-dominated unit, the Cyclops Member, lies about one third of the way up the Pertatataka Formation and is a probable correlative of the ABC Range Quartzite. The Pertatataka Formation is predominantly marine and forms part of the upward-shallowing succession that includes the Julie Formation. Deposition began with a abrupt deepening of the basin. Most of the formation represents a highstand systems tract deposited as a shallowing-upward shelfal pelagic and turbiditic unit (Calver 1995; Calver & Lindsay 1998). The Winnall beds comprise siltstone, sandstone, pebbly sandstone, dolomite, and limestone, and are estimated to be *c.* 2500 m thick.

The overlying Julie Formation is widely distributed in the northeastern part of the basin, but is absent south of the central ridge. The formation base is an abrupt but conformable contact with the Pertatataka Formation. Thickness varies mostly from 90 to 150 m, but reaches 550 m in some areas. The formation consists mainly of carbonate, but contains shaly and sandy limestone, as well as siltstone with lenses of sandstone and ooid grainstone (Calver 1995). Much of the formation consists of shallowing-upward cycles or parasequences that consist of an erosional base overlain by thinly bedded quartz sandstone, then by dolograins and dolomitic chert nodules. The Julie Formation is the upper part of an upward shallowing succession which began at the base of the Pertatataka Formation. Lithologies are characteristic of a shallow marine environment with oolitic platform carbonates, and a partial evaporitic environment.

The Arumbera Sandstone overlies the Julie Formation and is a thick clastic succession that onlapped from steep-sided, rapidly subsiding NE sub-basins and was sourced from the SW. It consists of red-brown and white sandstone and minor siltstone, shale, conglomerate and carbonate. Thickness varies, but may reach up to 2000 m in deeper depocenters. Four lithological units (Arumbera 1–4) are present. Tracks and trails are common in Arumbera 3, a dark red-brown siltstone and shale with minor sandstone and dolomite, leading McLroy *et al.* (1997) to recognize the Arumbera 2 and 3 contact as a truncational nonconformity that coincides with the Proterozoic–Cambrian boundary and Petermann Orogeny. However, sedimentation was probably continuous in some depocentres. In places, the formation shows progressive onlap indicating a sea-level rise. The formation was deposited in a shallow marine and deltaic or coastal-plain setting with a

sediment supply derived from the southwest and carried by heavily laden, braided streams (Lindsay 1987). The four lithological units form two large-scale shallowing-upward cycles, each consisting of storm deposits passing into prodelta sediments and finally into thick delta or coastal plain sandstone (Lindsay 1987). The Arumbera Sandstone is unconformably overlain by various Cambrian formations, although sedimentation was probably continuous into the early Phanerozoic in deeper depocentres (Lindsay 1987). The succession was later folded during the Delamerian and Alice Springs orogenies (*c.* 515 Ma and *c.* 320 Ma respectively).

Review of correlation methods and results

Throughout much of the Neoproterozoic, Australia was dominated by two major depositional regimes, the Adelaide Rift Complex and the Centralian Superbasin (Preiss 1987, 2000; Walter *et al.* 1995). Today, the remnants of these tectonic units occupy over a third of the Australian continent, and their original extent was probably much greater (Fig. 2). Correlation between tectonic units presents a major challenge because of the lack of geochronological dating, but by using a combination of the techniques described below, a framework has now been established (Fig. 5) that exhibits a high degree of internal consistency (Preiss 1987, 2000; Walter *et al.* 1994, 1995, 2000; Calver 2000; Morton & Drexel 1977; Calver & Lindsay 1998; Grey 2005).

Geochronology

There are few geochronological constraints on the Ediacaran System of Australia because a lack of suitable volcanic units limits dating on individual units. Preiss (2000) assessed existing dates for the whole of the Neoproterozoic succession in the Adelaide Rift Complex, including those determined by studies of detrital zircons. Several reliable ages are available for the interval preceding the Sturtian glaciation (part of the Cryogenian), and they suggest that the Sturtian glaciation in Australia probably took place about 700 Ma ago (Preiss 2000; Grey *et al.* 2005). One of the most definitive of these is a U–Pb sensitive high-resolution ion microprobe (SHRIMP) zircon age of 777 ± 7 Ma on the Boucaut Volcanics of the basal Burra Group (Preiss 2000). A detrital zircon U–Pb SHRIMP age of 725 ± 11 Ma from the upper Kanpa Formation in Empress 1A, *c.* 75 m below the eroded top of Buldya Group (Nelson 2002), gives a maximum age for the hiatus equivalent to

the glaciation in this part of the Officer Basin. By inference, the Sturtian glaciation must be considerably younger than this, both because the zircons have been redeposited and because of the thickness of the overlying succession. Further analyses are currently in progress.

Few direct dates are available for the post-Sturtian part of the Australian succession. In the Adelaide Rift Complex, dating based mainly on Rb–Sr isochrons from sedimentary rocks remains equivocal, although a sedimentary zircon grain of 657 ± 17 Ma places a maximum age on the Marino Arkose Member and overlying sediments, including the Marinoan glacials (Preiss 1987, 2000). Re–Os dating of the Tindelpina Shale member just above the Sturtian glacials, and from the Aralka Formation in Wallara 1, Amadeus Basin, has given ages of 643 ± 2 Ma and 657 ± 5 Ma, respectively (Kendall *et al.* 2005).

The age of the Marinoan glaciation remains uncertain. An age of between 590–610 Ma for the glacial interval was originally inferred by correlation with Canadian and South African successions (Walter *et al.* 2000), but this age is no longer consistent with dates on many presumed Marinoan glacial successions outside Australia. Recent U–Pb SHRIMP zircon dating on volcanic horizons associated with diamictite in NW Tasmania and cap carbonate and diamictite on nearby King Island has magnified the disparities (Calver *et al.* 2004). These suggest that the glaciation is younger than 582 ± 4 Ma and older than 575 ± 3 Ma. The diamictites are probable correlatives of the Elatina Formation (Calver & Walter 2000). Consequently, an age of *c.* 580 Ma (similar to that of the Gaskiers Formation and Squantum Tillite of North America) is possible for the type Marinoan glaciation. However, putative correlatives of the Marinoan glacials have been dated at *c.* 635 Ma in both Namibia (Hoffmann *et al.* 2004) and south China (Condon *et al.* 2005).

Most Rb–Sr ages on the Ediacaran succession in both the Adelaide Rift Complex and Centralian Superbasin are poorly constrained (Gravestock *et al.* 1997; Preiss 2000). However, Preiss (2000) considered a Model 3 Rb–Sr whole rock isochron of 588 ± 35 Ma from the Bunyerroo Formation in SCYW 1a to be a reliable indicator of depositional age because it was from fine-grained shale containing a low proportion of detrital silicate minerals. This date is from samples several hundred metres above the Nuccaleena Formation and close to the inferred level of the Acraman impact ejecta layer in SCYW 1a (Hill *et al.* 2004). There is no precise dating for the Acraman impact, because only zircon source ages (Mesoproterozoic Gawler Range Volcanics ages of 1575 ± 11 Ma) were obtained from ejecta clasts (Wallace *et al.* 1996). The impact was possibly *c.* 570 Ma.

A single detrital zircon grain from the Bonney Sandstone, dated at 556 ± 24 Ma, may record penecontemporaneous volcanism and provide a maximum age for the Ediacara Member assemblage in the Rawnsley Quartzite (Preiss 2000). This is consistent with the timing of the first appearance of bilaterians elsewhere in the world, and the *c.* 543 Ma age of the Proterozoic–Cambrian boundary inferred by correlation with Canadian successions, and constraints on the boundary age in Namibia (Grotzinger *et al.* 1995).

Sequence stratigraphy and seismic interpretation

Christie-Blick *et al.* (1990, 1995) identified a series of sequence boundaries in outcrop in the Adelaide Rift Complex. Sukanta *et al.* (1991) studied seismic reflectors and sequence boundaries in the Officer Basin and proposed correlations between the Adelaide Rift Complex and Officer basins, later modified by Calver (1995) (Fig. 6). Seismic and well-log data in the eastern Officer Basin were subjected to more detailed interpretation by Zang (1995), Lindsay (1995), Lindsay & Reine (1995), Morton & Drexel (1997), and Calver & Lindsay (1998). Further refinement of sequence stratigraphic interpretations of the Adelaide Rift Complex followed (Preiss 2000, Table 2; Gehling 2000). Preiss recognized two major sequence sets and eight sequences, whereas Gehling recognized only seven sequences, including the interval from the Nuccaleena Formation to the top of the ABC Range Quartzite in a single sequence. In similar studies in the Officer Basin, Zang (1995) also recognized eight sequences, with later modifications (Lindsay 1995; Morton & Drexel 1997; Lindsay & Calver 1998; Arouri *et al.* 2000). Sea-level curves from the two successions show good correspondence. Consequently, subsurface relationships between stratigraphic units are well understood.

Sequence Boundary 1 at the base of the Nuccaleena Formation correlates with Reflector G at the base of the Tarlina Sandstone, Sequence boundary 2 at the top of the ABC Range Quartzite with Reflector F₆ at the top of the Murnaroo Formation, and Sequence boundary 3 at the base of the Wonoka Formation with Reflector F₅ at the base of the Karlaya Limestone (Figs 5, 6; Preiss 1993; Calver & Lindsay 1998). Correlations above this are less certain. Sequence boundary 4 in the Wonoka Formation is a canyon-cutting unconformity that may correlate with a similar canyon-cutting unconformity (Reflector F) in the Officer Basin. Reflectors 8 and E are probably the Cambrian unconformity.

In the Amadeus Basin, Lindsay & Korsch (1991) recognized the Pertatataka Formation as a single

transgressive–regressive cycle, with a second cycle in the lower Arumbera Sandstone.

Event stratigraphy

Three significant Ediacaran events indicate correlation across Australia and could be used for broader correlations. These are the Marinoan glaciation, the Acraman impact and the appearance of bilaterian metazoa. As discussed above, the younger of the two widespread glacial episodes in Australia appears synchronous, although its synchronicity with glacial episodes on other continents is less certain. The Acraman ejecta layer provides a time-synchronous horizon across a wide area of Australia, but could provide a global marker through the recognition of an associated iridium anomaly (Gostin *et al.* 1989) and negative anomaly in the $\delta^{13}\text{C}$ curve (Calver & Lindsay 1998; Grey *et al.* 2003). The first appearance of the Ediacara biota in Australia also appears to be a synchronous event, although it is not the first appearance of members of the Ediacaran fauna globally. Changes in other environmental parameters must have affected the Ediacaran biosphere, but at present, none can be shown to be widespread.

Isotope chemostratigraphy

Isotopes of carbon and strontium are well documented for the Ediacaran System in Australia (Williams 1979; Pell *et al.* 1993; Calver 1995, 1998, 2000; Calver & Lindsay 1998) and allow correlation with reference curves in other parts of the globe (Walter *et al.* 2000).

Because of a dearth of carbonates in the studied sections, a continuous carbon isotope curve has been obtained mainly from the sedimentary organic carbon of marine shale, although this has been tied to the carbonate curve wherever feasible (Fig. 7). Organic carbon is depleted in $\delta^{13}\text{C}$ by around 30‰ relative to primary marine carbonate: its isotopic composition reflecting the strong negative fractionation associated with photosynthetic carbon fixation and various relatively small shifts associated with post-burial processes. Organic carbon is generally, therefore, considered a less reliable chemostratigraphic signal carrier than carbonate (Hayes *et al.* 1983; Popp *et al.* 1989). Nevertheless, it has yielded coherent and consistent results from our Ediacaran successions (Calver 1995; Calver & Lindsay 1998; Calver 2000). Treatment of organic carbon results is outlined in Calver (2000). The shifts in $\delta^{13}\text{C}_{\text{organic}}$ caused by regional variation in thermal maturation were quantified using kerogen H/C ratios, to allow an integrated (organic + carbonate) signal to be produced for each section. The upper Ediacaran sandstones of the

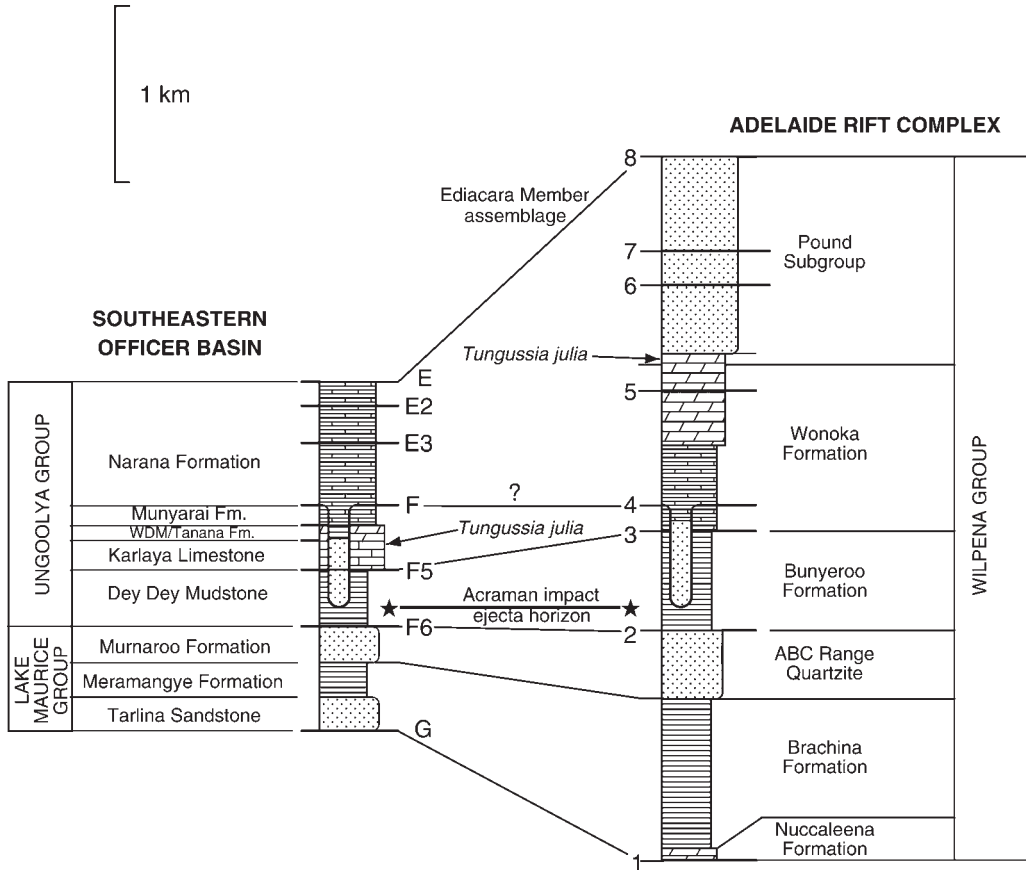


Fig. 6. Generalized stratigraphic correlation between the Adelaide Rift Complex and Officer Basin (after Calver 1995; Grey 2005). Numbers in Adelaide Rift Complex column are depositional sequence boundaries (after Christie-Blick *et al.* 1990); those in the Officer Basin are seismic sequence boundaries (after Sukanta *et al.* 1991). Scale is indicative only.

Pound Subgroup and Arumbera Sandstone are not amenable to C and Sr chemostratigraphic study, and the isotope data, therefore, cover the lower and middle parts of the Ediacaran System, mainly in the Officer and Amadeus Basins and the Adelaide Rift Complex (Fig. 6). Isotope-stratigraphic data have also been obtained from Ediacaran successions in the Georgina and Northwestern basins (Calver 1995; Walter *et al.* 1994, 1995), the Kimberley area (Kennedy 1996) and Tasmania (Calver 1998; Calver & Walter 2000).

Strontium isotopic compositions of marine carbonates are particularly sensitive to diagenetic alteration, and sufficiently well preserved carbonates (typically limestone with strontium content of 1000 ppm or more) have only been found at a few horizons. However, the seawater $^{87}\text{Sr}/^{86}\text{Sr}$ ratio is believed to have increased steeply and monotonically

through at least the earlier part of the Ediacaran System (Walter *et al.* 2000), so these results, though few, are potentially very useful in constraining relative ages (Fig. 7).

The 'cap carbonates' that flag the base of the Ediacaran System in most places are characterized by relatively depleted $\delta^{13}\text{C}_{\text{carbonate}}$ (-1 to -4‰ ; Williams 1979) that tend to decrease up-section (Kennedy 1996; Calver 2000). This pattern is seen in the Adelaide Rift Complex (Nuccaleena Formation), in the Amadeus Basin and on King Island (Calver & Walter 2000). Above the cap carbonate, the curve defined by organic carbon shows an apparently rapid rise to relatively enriched values (equivalent to $\delta^{13}\text{C}_{\text{carbonate}}$ of $+3$ to $+5\text{‰}$) that persist through most of the Brachina Formation (Adelaide Rift Complex) and lower half of the Peratatata Formation (Amadeus Basin). The upper

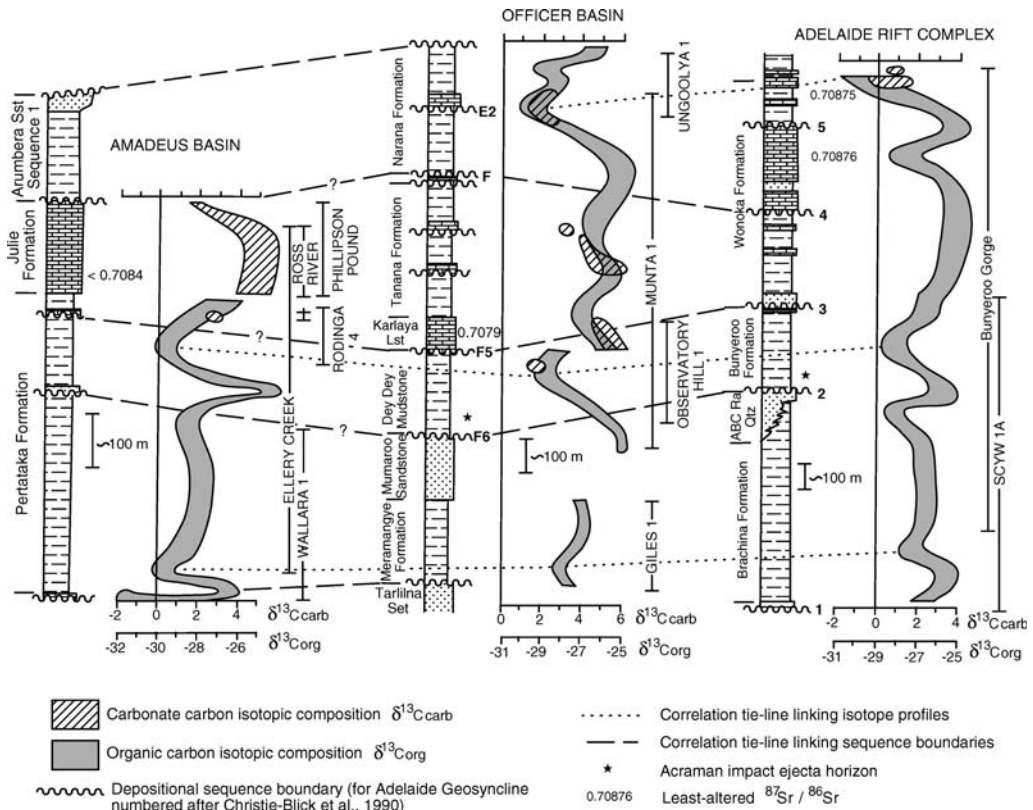


Fig. 7. Generalized carbon isotope trends for lower to middle Ediacaran sections in the Amadeus Basin, Officer Basin and Adelaide Rift Complex, with selected, least-altered $^{87}\text{Sr}/^{86}\text{Sr}$ values. Also shown are major sequence boundaries and suggested correlations (see text). Outcrop sections and drill holes sampled are indicated to the right of the profiles. Anomalously ^{13}C -depleted carbonates of the Wonoka Formation (Adelaide Rift Complex) and just below sequence boundary F (Officer Basin) not shown. Based on the following total numbers of isotopic analyses: 238 (Amadeus basin), 165 (Officer Basin), 158 (Adelaide Geosyncline) (after Calver & Lindsay 1998).

part of the Pertataka Formation, the Bunyeroo Formation (Adelaide Rift Complex), and the Dey Dey Mudstone (Officer Basin) all show a negative excursion in organic carbon isotope compositions, the nadir being variable from place to place, and equivalent to $\delta^{13}\text{C}_{\text{carbonate}}$ of -1 to $+2\text{‰}$. The commencement of this negative excursion is located stratigraphically at or just below the Acraman impact ejecta layer in the Adelaide Rift Complex and Officer Basin (Fig. 7), and the nadir and subsequent rise are associated with the first appearance of the spiny acritarch flora in the Officer and Amadeus basins (see below).

Higher up, there is a return to more strongly enriched values ($\delta^{13}\text{C}_{\text{carbonate}}$ $+4$ to $+6\text{‰}$), recorded in the Karlaya Limestone, Tanana Formation and Wilari Dolomite Member (Officer Basin) and the Julie Formation (Amadeus Basin). The Karlaya Limestone has a little-altered

$^{87}\text{Sr}/^{86}\text{Sr}$ ratio of 0.7079; that of the Julie Formation is 0.7084 but is probably somewhat altered and therefore higher than the original value. The broadly equivalent, deep-water carbonate facies of the lower and middle Wonoka Formation in the Adelaide Rift Complex (both above and below the canyon unconformity) are characterized by strongly $\delta^{13}\text{C}$ -depleted carbonates (-6 to -10‰ ; Pell *et al.* 1993; Calver 2000). These are mostly below the lowest value, -5‰ , considered possible for normal marine carbonates, even though textural and geochemical evidence does not suggest strong diagenetic alteration. By contrast, accompanying organic carbon isotopic compositions are relatively enriched and consistent with normal (shallow-marine) carbonates of around $+5\text{‰}$. Probably little-altered $^{87}\text{Sr}/^{86}\text{Sr}$ from the middle Wonoka Formation (above the canyon unconformity) is 0.7087, suggesting this level is

younger than the Karlaya and Julie formations and probably the Tanana Formation (0.7085) but older than the Narana Formation (0.7089). Strontium isotopes are therefore consistent with correlation of the canyon unconformities in the Officer Basin and the Adelaide Rift Complex (Calver & Lindsay 1998).

In the Officer Basin, strongly ^{13}C -depleted carbonate similar to that of the Wonoka Formation is restricted to a thin unit at the top of the Tanana Formation, just below the canyon unconformity in drill hole Munta-1. Acritarch evidence suggests this unit is a (deeper-water) equivalent of the Wilari Dolomite Member, a correlation permitted by the isotope evidence if deeper basinal waters were strongly depleted in ^{13}C relative to shallow waters, as proposed by Calver (2000) for the Wonoka Formation.

Calver (2000) suggested the strongly ^{13}C -depleted carbonates of the lower and middle Wonoka Formation might have been precipitated from the lower layer of a salinity-stratified, restricted basin (consistent with the Messinian-type desiccation model proposed for the origin of the canyons: von der Borch *et al.* 1989; Christie-Blick *et al.* 1990). Carbon isotope patterns for this interval in the Adelaide Rift Complex and Officer Basin may, therefore, be independent of the global curve. However, similarly ^{13}C -depleted carbonates are now known from Ediacaran sections on other continents (including the upper Doushantuo Formation of south China and the Nafun Group of Oman) and have been correlated with the Wonoka Formation, requiring a marked global negative excursion (or widespread oceanic stratification) in the middle Ediacaran System (Condon *et al.* 2005). The negative excursion in the upper Doushantuo Formation is older than 551 Ma (Condon *et al.* 2005).

The least altered of the shallow-marine carbonates of the Patsy Hill Member of the basal Bonney Sandstone are $+2.5\text{‰}$ in $\delta^{13}\text{C}$ and 0.7088 in $^{87}\text{Sr}/^{86}\text{Sr}$ at Bunyerroo Gorge near the type section, and probably correlate with isotopically similar, minor carbonates of the Narana Formation in the Officer Basin. Higher up, organic carbon in shale of the uppermost Narana Formation in Ungoolya-1 shows an upward trend to heavier values. North of Bunyerroo Gorge, the Patsy Hill Member thickens and includes carbonates up to $+6\text{‰}$ (Pell *et al.* 1993). The Billy Springs Formation in the northern Adelaide Rift Complex also includes enriched ($+6\text{‰}$) carbonates (Pell *et al.* 1993); this unit is younger than the Wonoka Formation but its age relative to the Patsy Hill Member is uncertain.

In the Georgina Basin, carbon isotope trends are consistent with correlation of the Elyuah and Grant

Bluff formations with the lower part of the Pertataka Formation, in agreement with lithostratigraphy, and the lower part of the dolomitic Elkeria Formation with the Julie Formation (Walter *et al.* 1995). Carbon isotopes and broad lithostratigraphic correlation also suggests the carbonates in the upper part of the Boondawari Formation, northwestern Officer Basin, may be equivalent to the Julie Formation, though this must be regarded as tentative without corroborative evidence (Walter *et al.* 1994). In the Kimberley region, the cap carbonates overlying the Walsh, Landrigan and Moonlight Valley tillites are all probably correlative with each other and with the Nuccaleena Formation cap carbonate on the basis of $\delta^{13}\text{C}_{\text{carbonate}}$ and lithology. A distinctly younger, glaciogenic diamictite within the Egan Formation is enclosed by shallow marine carbonates (Corkeron and George 2001) with a generally moderately enriched carbon isotopic compositions (0 to $+3\text{‰}$), but with a negative excursion immediately above the diamictite (Corkeron 2002). This pattern cannot be uniquely located within the more complete C isotope curves from the other basins, but stromatolite biostratigraphy indicates a mid-Ediacaran age (Grey & Corkeron 1998).

The base of the Ediacaran System in Tasmania lies within a succession dominated by mafic rift volcanics and volcanoclastics, known as the Grassly Group on King Island and the Kanunnah Subgroup in NW Tasmania (Calver 1998; Calver & Walter 2000). The Kanunnah Subgroup is overlain by the 1.5 km thick Smithton Dolomite which is thought to be middle to possibly late Ediacaran in age, as little-altered $^{87}\text{Sr}/^{86}\text{Sr}$ ratios range from 0.7079 near the base to 0.7085, 1 km above the base, which is a similar range to the Karlaya Limestone—Tanana Formation interval in the Officer Basin (Calver 1998).

Palaeontology

The Australian Ediacaran System contains several taxa of stromatolites, trace fossils and the Ediacara fauna itself, some of which are useful for correlation. Additionally, a number of dubiofossils and pseudofossils have been reported, particularly from the Bunyerroo and Wonoka formations, and these may prove to be significant as studies progress.

The stromatolite *Elleria minuta* is widespread in the cap carbonate of the Pioneer Sandstone (Walter *et al.* 1989) in the Amadeus Basin, and is probably also present in the cap carbonate at the top of the Wahlgu Formation (Grey *et al.* 1999, 2005).

Bunyerichnus dalgarnoi Glaessner 1969 from the Brachina Formation is a rhythmical marking interpreted as a tool marking made by tethered

structure moving in small jumps in an arcuate manner over the substrate (Jenkins 1995). Reports of *Chuarina* sp. and *Tawuia* sp. in the ABC Range Quartzite in drill holes MRD 1 and BLD 3 and the Wonoka Formation in MJ 1 by Zang (1997) are questionable and are probably mainly shale pellets. Stromatolites have been reported from the middle Wonoka Formation (Haines 1990), but mostly remain unidentified, except for a poorly preserved *Linella* f. indet. in the north of the rift complex (Preiss 1987). A little higher in the formation, a series of curved, dark, banded structures that form widening swaths on bedding planes was interpreted as a meandering trace fossil (Jenkins 1995), although Haines (1990) considered these structures to be of algal origin. Rare discoid structures, dimple marks, and a possible frondose structures have been reported from near the top of the Wonoka Formation (Jenkins 1995), but they are poorly preserved and have not been systematically evaluated. A possible fossil, shaped like a palm leaf, occurs at about the same stratigraphic horizon, and may be of algal origin (Haines 1990; Jenkins 1995).

The carbonate at the base of the overlying Bonney Sandstone contains small bioherms of *Tungussia julia* (Walter *et al.* 1979). This form is also present in the Julie Formation of the Amadeus Basin, the Elkeru Formation of the Georgina Basin and the Egan Formation of the central Kimberley glaciogenic successions (Grey & Corkeron 1998), and Wilari Dolomite Member in the Officer Basin (Grey 2005). Stromatolites are present at about same stratigraphic level in the Boondawari Formation (Walter *et al.* 1994), but all three forms *Eleonora boondawarica*, *Acaciella savoryensis* and Stromatolite form 1, are known only from this formation, so currently are not of biostratigraphic value.

Unequivocal metazoan trace fossils such as burrows and body fossils have not been reported from horizons lower than the overlying Bonney Sandstone and its equivalents in Australia (Jenkins 1995).

Acritarch biostratigraphy

More than 1000 samples from 10 key drill holes provide a reasonably continuous record of acritarch distributions at 10–20 m intervals, and allow correlation between the Adelaide Rift Complex, Stuart Shelf and eastern Officer and Amadeus basins (Grey *et al.* 2003; Grey 2005). Acritarch assemblages in the middle Ediacaran System are taxonomically diverse, morphologically complex and show unmistakable patterns of secular variation. These characteristics have led to the development of a zonal scheme at levels of precision equivalent

to those of the Phanerozoic record. The zones are independent of taphonomic and palaeoenvironmental influences, and are demonstrably independent of lithology, lithostratigraphy and sequence stratigraphy. Acritarch distributions can be tied to the isotope curves discussed above, because results for both studies are based on splits of the same samples.

Only a few lithologies in the Adelaide Rift Complex and adjacent Curnamona Craton and Stuart Shelf were suitable for palynological sampling. Samples from Bunyeroo and Brachina Gorges and drill holes in the Curnamona Craton and southern Stuart Shelf showed thermal maturity levels too high for the preservation of identifiable organic-walled microfossils. However, thermal maturity levels are lower in the northern Stuart Shelf in drill holes SCYW 1a, WWD 1 and MJ 1 (Damassa & Knoll 1986; Zang 1997; Grey 2005) and sufficient palynomorphs were extracted to tie these drill holes to the exceptionally well-preserved and near-continuous Officer Basin record, and to the Amadeus Basin (Figs 2, 4).

Assemblages older than the Marinoan glaciations are well represented in Western Australian drill holes, although there are some large gaps, most notably through the time of the Sturtian and Marinoan glaciations and the interval in between. Samples immediately above the Marinoan glaciation are barren, but a benthic mat and leiosphere assemblage quickly re-established itself and proliferated as sea level rose. Assemblages recorded in sediments spanning the first sea-level transgression and part of the second transgression consist of pre-glacial species and differ little from those recorded globally back to *c.* 1200 Ma, except that there are fewer species (Fig. 8). No new, rapidly diversifying species with different ecological niches, as predicted by the Snowball Earth model, have been observed (Grey 2005). There is a later marked change in phytoplankton assemblages, when more than 50 species of large, complex acanthomorph (spiny) acritarchs appear for the first time (Fig. 8). These differ from previously-recorded morphotypes in the earlier fossil record in having a very thin, translucent wall and highly complex processes, and some may resemble the resting cysts of modern dinoflagellates, although the absence of a cingulum and tabulation precludes their inclusion in this group. They may well represent a new, short-lived group of green algae. The change from the older, leiosphere-dominated palynoflora to the younger, acanthomorph-dominated palynoflora is abrupt, and is apparently synchronous in all drill holes studied (Fig. 4). The coincidence between the first appearance of the acanthomorph palynoflora, a $\delta^{13}\text{C}$ organic carbon excursion (Calver & Lindsay 1998), and the ejecta layer

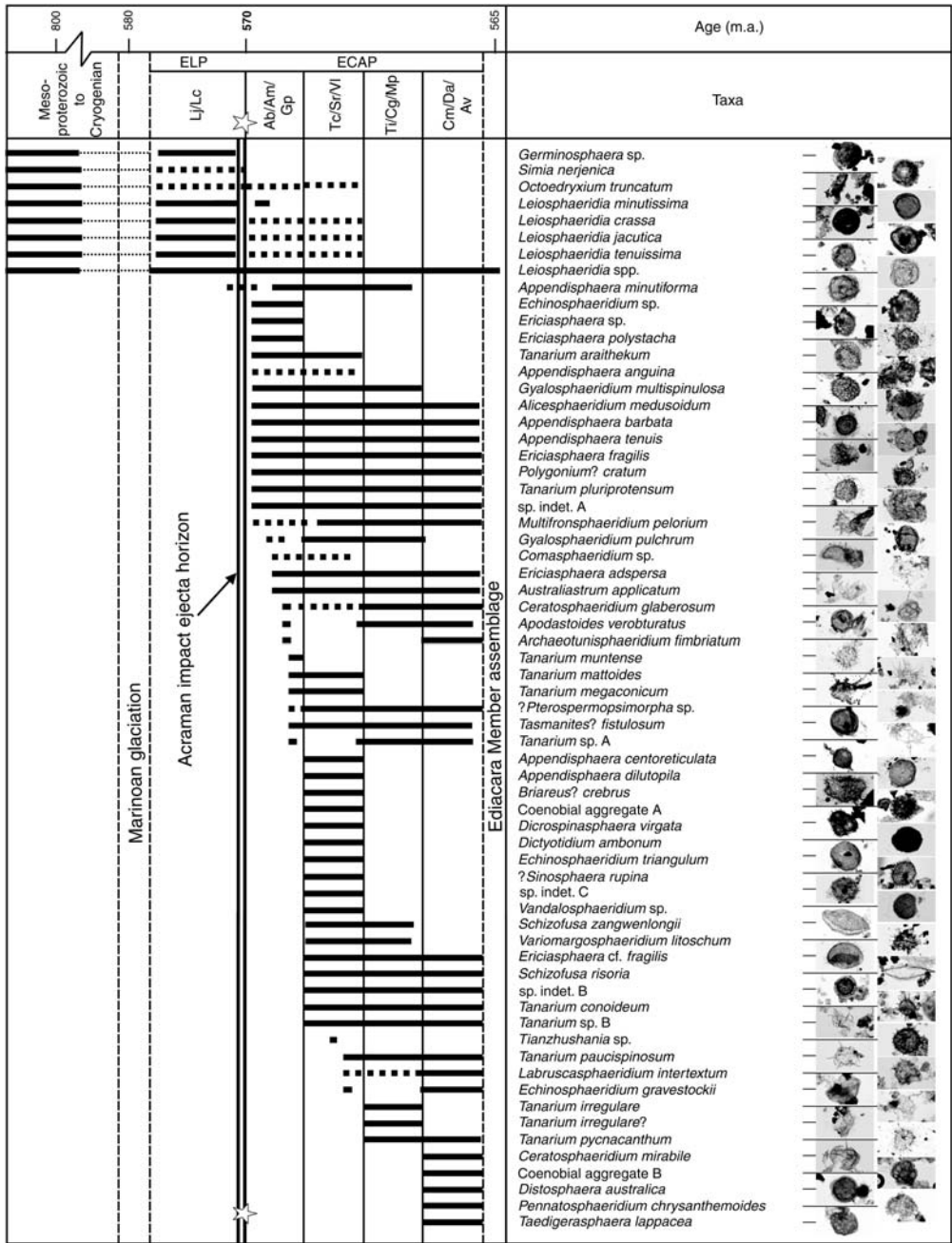


Fig. 8. Composite zonation scheme for the Ediacaran of Australia (after Grey 2005) with illustrations of selected species. Distributions are plotted by zone, which is the highest degree of refinement currently possible. Note the profound change that occurs at the boundary between the ELP and ECAP (double line), and the rapid increase in numbers of acanthomorph acritarchs following the Acraman impact event. Lj/Lc, *Leiosphaeridia jacutica*/*Leiosphaeridia crassa* Assemblage Zone; Ab/Am/Gp, *Appendisphaera barbata*/*Alicesphaeridium medusoidum*/*Gyalosphaeridium pulchrum* Assemblage Zone; Tc/Sr/Vl, *Tanarium conoideum*/*Schizofusa risoria*/*Variomargosphaeridium litoschum* Assemblage Zone; Ti/Cg/Mp, *Tanarium irregulare*/*Ceratosphaeridium glaberosum*/*Multifronsphaeridium pelorium* Assemblage Zone; Cm/Da/Av, *Ceratosphaeridium mirabile*/*Distosphaera australica*/*Apodastoides verobuturatus* Assemblage Zone; ECAP, Ediacaran Complex Acritarch-dominated palynoflora; ELP, Ediacaran Leiosphere-dominated palynoflora.

formed by the Acraman impact, and the possible significance of these observations were discussed by Grey *et al.* (2003) and Grey (2005).

Two palynofloras were recognized: the Ediacaran Leiosphere Palynoflora (ELP), consisting of a single biozone: the *Leiosphaeridia jacutica*–*Leiosphaeridia crassa* Assemblage Zone, and the Ediacaran Complex Acanthomorph Palynoflora (ECAP), comprising four zones (in ascending order): the *Appendisphaera barbata*–*Alicesphaeridium medusoidum*–*Gyalosphaeridium pulchrum* Assemblage Zone (Ab–Am–Gp); the *Tanarium conoideum*–*Schizofusa risoria*–*Variomargosphaeridium litoschum* Assemblage Zone (Tc–Sr–Vl); *Tanarium irregulare*–*Ceratospaeridium glaberosum*–*Multifronsphaeridium pelorium* Assemblage Zone (Ti–Cg–Mp); and the *Ceratospaeridium mirabile*–*Distosphaera australica*–*Apodastoides verobturatus* Assemblage Zone (Cm–Da–Av). Zones were described in detail by Grey (2005), and follow up studies of Murnaroo 1 have confirmed the distributions and indicated that higher resolution subdivisions may be possible (Willman *et al.* 2006).

Correlations between individual drill holes from the Stuart Shelf and Officer basins show a high degree of consistency, and similar patterns are present in the Amadeus Basin. Although the Adelaide Rift Complex succession lacks a palynological record, it represents a well-exposed, well-documented reference section that can be tied to the Stuart Shelf section, and thence by palynostratigraphy to drill core sections in the adjacent Officer Basin (Figs 2, 4). Some minor inconsistencies remain to be resolved, for instance, the base of the Tc–Sr–Vl zone in Munta 1 is uncertain and the present first record of *Tanarium conoideum* in this drill hole is anomalously high with respect to correlation based on isotope chemostratigraphy and sequence stratigraphy. Such anomalies will probably be resolved as work progresses.

The presence of certain acritarch species in probably coeval successions in Australia, Siberia, China, and northern Europe, suggests that the proposed zonation has good potential for global application, and that biostratigraphic principles and methodology can be applied to the Neoproterozoic era. Palynostratigraphy is still preliminary, but represents a significant advance in Neoproterozoic biostratigraphic studies, and should provide an important tool for future stratigraphic correlation.

Conclusions

The Australian Ediacaran System correlations suffer from a lack of numerical age constraints, but correlations are possible using an integrated approach combining lithostratigraphy, event stratigraphy,

sequence stratigraphy, seismic interpretation, isotope chemostratigraphy and biostratigraphy. By using this approach, the GSSP and associated sections in the Flinders Ranges can be tied to successions across much of Australia. The consistent patterns that emerge strengthen the case for an integrated approach. Detailed stable isotope correlations have much to offer for correlation, but the curves must be firmly anchored by other data in order to prevent matching repeated sections of the curve. Biostratigraphy is an effective correlation tool in the late Neoproterozoic, but Neoproterozoic palynology is only at the stage attained by Phanerozoic palynology about forty years ago. A basic framework has been recognized, but there is scope for refinement. Future studies need to apply palynological biostratigraphy globally. It is important that further attempts be made to improve the subdivision of the Ediacaran System and Period. If the Elatina Formation is a correlative of the Nantuo Tillite, and the system extends from this age to 543 Ma, the base of the Cambrian, then the Ediacaran is 92 Ma long, nearly as long as the Cambrian and Ordovician combined. The current disparity in ages between the two glaciations, both perceived as so-called Marinoan glaciations, raises some interesting issues with regard to the number of glaciations and the severity of 'Snowball Earth', which will only be resolved when better dating is available.

K. Grey publishes with permission of the Director of the Geological Survey of Australia. C. Calver publishes with permission of the Director, Mineral Resources Tasmania. Early studies were carried out while both authors were holders of Australian Postgraduate Research Awards. This paper is a contribution to International Geological Correlation Programs 440 (Assembly and Break-Up of Rodinia), 493 (The Rise and Fall of the Vendian Biota) and the International Working Group on the Subdivision of the Ediacaran. The authors thank the reviewers M. Moczyłowska-Vidal and T. Ohno.

References

- AROURI, K., CONAGHAN, P. J., WALTER, M. R., BISCHOFF, G. C. & GREY, K. 2000. Reconnaissance sedimentology and hydrocarbon biomarkers of Ediacarian microbial mats and acritarchs, lower Ungoolya Group, Officer Basin. *Precambrian Research*, **100**, 235–281.
- CALVER, C. R. 1995. *Ediacarian Isotope Stratigraphy of Australia*. PhD Thesis, Macquarie University.
- CALVER, C. R. 1998. Isotope stratigraphy of the Neoproterozoic Togari Group, Tasmania. *Australian Journal of Earth Sciences*, **45**, 865–874.
- CALVER, C. R. 2000. Isotope stratigraphy of the Ediacarian (Neoproterozoic III) of the Adelaide Rift Complex, Australia, and the overprint of water column stratification. *Precambrian Research*, **100**, 121–150.

- CALVER, C. R. & LINDSAY, J. F. 1998. Ediacarian sequence and isotope stratigraphy of the Officer Basin, South Australia. *Australian Journal of Earth Sciences*, **45**, 513–532.
- CALVER, C. R. & WALTER, M. R. 2000. The late Neoproterozoic Grassy Group of King Island, Tasmania: correlation and palaeogeographic significance. *Precambrian Research*, **100**, 299–312.
- CALVER, C. R., BLACK, L. P., EVERARD, J. L. & SEYMOUR, D. B. 2004. U–Pb zircon age constraints on late Neoproterozoic glaciation in Tasmania. *Geology*, **32**, 893–896.
- CHRISTIE-BLICK, N., VON DER BORCH, C. C. & DI BONA, P. A. 1990. Working hypothesis for the origin of the Wonoka canyons (Neoproterozoic), South Australia. *American Journal of Science*, **290A**, 295–332.
- CHRISTIE-BLICK, N., DYSON, I. A. & VON DER BORCH, C. C. 1995. Sequence stratigraphy and the interpretation of Neoproterozoic earth history. *Precambrian Research*, **73**, 3–26.
- CLOUD, P. E. & GLAESSNER, M. F. 1982. The Ediacarian Period and System: Metazoa inherit the Earth. *Science*, **217**, 783–792.
- CONDON, D., ZHU, M., BOWRING, S., WANG, W., YANG, A. & JIN, Y. 2005. U–Pb ages from the Neoproterozoic Doushantuo Formation, China. *Science*, **308**, 95–98.
- CORKERON, M. 2002. *Neoproterozoic glacial events in the Kimberley Region, Western Australia: sedimentology and regional correlation in the context of continental- and global-scale Neoproterozoic glaciation*. PhD thesis, University of Western Australia.
- CORKERON, M. L. & GEORGE, A. D. 2001. Glacial incursion on a Neoproterozoic carbonate platform in the Kimberley region, Australia. *Geological Society of America Bulletin*, **113**, 1121–1132.
- DAMASSA, S. P. & KNOLL, A. H. 1986. Micropalaeontology of the late Proterozoic Arcoona Quartzite Member of the Tent Hill Formation, Stuart Shelf, South Australia. *Alcheringa*, **10**, 417–430.
- DYSON, I. A. 1992a. Stratigraphy of the Neoproterozoic Tent Hill Formation and Simmens Quartzite at South Tent Hill on the Stuart Shelf, South Australia. *Transactions of the Royal Society of South Australia*, **120**, 117–129.
- DYSON, I. A. 1992b. Stratigraphic nomenclature of the lower Wilpena Group, Adelaide Geosyncline: the Sandison Subgroup. *South Australia Geological Survey Quarterly Geological Notes*, **122**, 2–13.
- DYSON, I. A. & VON DER BORCH, C. C. 1986. A field guide to the geology of the late Precambrian Wilpena Group, Hallett Cove, South Australia. In: PARKER, A. J., *One Day Geological Excursions of the Adelaide Region* (ed.) Geological Society of Australia (South Australian Division), Adelaide, 17–40.
- EICKHOFF, K. H., VON DER BORCH, C. C. & GRADY, A. E. 1988. Proterozoic canyons of the Flinders Ranges, South Australia: submarine canyons or drowned river valleys? *Sedimentary Geology*, **58**, 217–235.
- GEHLING, J. G. 2000. Environmental interpretation and a sequence stratigraphic framework for the terminal Proterozoic Ediacara Member within the Rawnsley Quartzite, South Australia. *Precambrian Research*, **100**, 65–95.
- GEHLING, J. G. 2004. *Field guide to the Ediacaran—Cambrian of the Flinders Ranges, South Australia, IGCP 493*. South Australian Museum, Adelaide.
- GOSTIN, V. A., HAINES, P. W., JENKINS, R. J. F., COMPSTON, W. & WILLIAMS, I. S. 1986. Impact ejecta horizon within late Precambrian shales, Adelaide Geosyncline, South Australia. *Science*, **233**, 198–200.
- GOSTIN, V. A., KEAYS, R. R. & WALLACE, M. W. 1989. Iridium anomaly from the Acraman impact ejecta horizon: impacts can produce sedimentary iridium peaks. *Nature*, **340**, 542–544.
- GRADSTEIN, F., OGG, J. & SMITH, A. 2004. *A Geological Time Scale*. Cambridge University Press, Cambridge.
- GRAVESTOCK, D. I. 1997. Chapter 5: Geological setting and structural history. In: MORTON, V. & DREXEL, J. F. (eds) *Petroleum Geology of South Australia, Volume 3: Officer Basin*. South Australia Department of Mines and Energy Resources Report Book **97/19**, 35–451.
- GRAVESTOCK, D. I., MORTON, J. G. G. & ZANG, W. L. 1997. Chapter 7: Biostratigraphy and correlation. In: MORTON, V. & DREXEL, J. F. (eds) *Petroleum Geology of South Australia, Volume 3: Officer Basin*. South Australia Department of Mines and Energy Resources Report Book **97/19**, 87–97.
- GREY, K. 2005. Ediacaran palynology of Australia. *Association of Australasian Palaeontologists Memoir*, **31**, 1–439.
- GREY, K. & CORKERON, M. 1998. Late Neoproterozoic stromatolites in glaciogenic successions of the Kimberley region, Western Australia: evidence for a younger Marinoan glaciation. *Precambrian Research*, **92**, 65–87.
- GREY, K., APAK, S. N., EYLES, C., EYLES, N., STEVENS, M. K. & CARLSEN, G. M. 1999. Neoproterozoic glaciogenic successions, western Officer Basin. *Western Australia. Geological Survey of Western Australia Annual Review 1998–99*, 74–80.
- GREY, K., WALTER, M. R. & CALVER, C. R. 2003. Neoproterozoic biotic diversification: Snowball Earth or aftermath of the Acraman impact? *Geology*, **31**, 459–462, & Data Repository item 2003061.
- GREY, K., HOCKING, R. M., STEVENS, M. K., BAGAS, L., CARLSEN, G. M., IRIMIES, F., PIRAJNO, F., HAINES, P. W. & APAK, S. N. 2005. Lithostratigraphic nomenclature of the Officer Basin and correlative parts of the Paterson Orogen, Western Australia. *Geological Survey of Western Australia Report*, **93**.
- GROTZINGER, J. P., BOWRING, S. A., SAYLOR, B. Z. & KAUFMAN, A. J. 1995. Biostratigraphic and geochronological constraints on early animal evolution. *Science*, **270**, 598–604.
- HAINES, P. W. 1987. *Carbonate shelf and basin sedimentation, late Proterozoic Wonoka Formation, South Australia*. PhD thesis, University of Adelaide.
- HAINES, P. W. 1988. Storm-dominated mixed carbonate/siliciclastic shelf sequence displaying cycles of hummocky cross-stratification, Late Proterozoic Wonoka Formation, South Australia. *Sedimentary Geology*, **58**, 237–254.
- HAINES, P. W. 1990. A late Proterozoic storm-dominated carbonate shelf sequence: the Wonoka Formation in the central and southern Flinders Ranges, South Australia. In: JAGO, J. B. & MOORE, P. S. (eds) *The*

- evolution of a Late Precambrian–Early Palaeozoic rift complex: Adelaide Geosyncline*. Geological Society of Australia Special Publication **16**, 177–198.
- HAINES, P. W., MORY, A. J., STEVENS, M. K. & GHORI, K. A. R. 2004. GSWA Lancer 1 well completion report (basic data), Officer and Gunbarrel basins, Western Australia. *Geological Survey of Western Australia Record* **2004/10**.
- HAYES, J. M., KAPLAN, I. R. & WEDEKING, K. W. 1983. Chapter 5. Precambrian organic geochemistry, preservation of the record. In: SCHOPF, J. W. (ed.) *Earth's Earliest Biosphere: its Origin and Evolution*. Princeton University Press, Princeton, 93–134.
- HILL, A. C., GREY, K., GOSTIN, V. A. & WEBSTER, L. J. 2004. New records of Late Neoproterozoic Acraman ejecta in the Officer Basin. *Australian Journal of Earth Sciences*, **51**, 47–51.
- HOFFMAN, K. -H., CONDON, D. J., BOWRING, S. A. & CROWLEY, J. L. 2004. U–Pb zircon date from the Neoproterozoic Ghaub Formation, Namibia: Constraints on Marinoan glaciation. *Geology*, **32**, 817–820.
- JACKSON, M. J. & VAN DE GRAAFF, W. J. E. 1981. Geology of the Officer Basin, Western Australia. *Australia Bureau of Mineral Resources Bulletin*, **206**.
- JENKINS, R. J. F. 1981. The concept of an 'Ediacaran Period' and its stratigraphic significance in Australia. *Transactions of the Royal Society of South Australia*, **105**, 179–194.
- JENKINS, R. J. F. 1995. The problems and potential of using animal fossils and trace fossils in terminal Proterozoic biostratigraphy. *Precambrian Research*, **73**, 51–69.
- JENKINS, R. J. F. & GEHLING, J. G. 1978. A review of the frond-like fossils of the Ediacara assemblage. *Records of the South Australian Museum*, **17**, 347–359.
- KENDALL, B. S., CREASER, R. A. & SELBY, D. 2005. Re–Os depositional ages for Neoproterozoic post-glacial black shales in Australia: evidence for diachronous Neoproterozoic glaciations. *Geological Society of America, Abstracts with Programs*, 16–6, **37**, 7, 42.
- KENNEDY, M. J. 1993. The Undoolya Sequence: Late Proterozoic salt influenced deposition, Amadeus Basin, central Australia. *Australian Journal of Earth Sciences*, **40**, 217–228.
- KENNEDY, M. J. 1996. Stratigraphy, sedimentology, and isotopic geochemistry of Australian Neoproterozoic postglacial cap dolostones: deglaciation, $\delta^{13}\text{C}$ excursions, and carbonate precipitation. *Journal of Sedimentary Research*, **66**, 1050–1064.
- KNOLL, A. H., WALTER, M. R., NARBONNE, G. M. & CHRISTIE-BLICK, N. 2004. A new period for the geologic time scale. *Science*, **305**, 621–622.
- LINDSAY, J. F. 1987. Sequence stratigraphy and depositional controls in Late Proterozoic–early Cambrian sediments of the Amadeus Basin, central Australia. *American Association of Petroleum Geologists, Bulletin*, **71**, 1387–1403.
- LINDSAY, J. F. 1995. *Geological Atlas of the Officer Basin South Australia*. Australian Geological Survey Organisation and Mines and Energy Department, South Australia.
- LINDSAY, J. F. & KORSCH, R. J. 1991. The evolution of the Amadeus Basin, central Australia. In: KORSCH, R. J. & KENNARD, J. M. (eds) *Geological and Geophysical Studies in the Amadeus Basin Central Australia*. Australian Bureau of Mineral Resources, Bulletin, **236**, 7–32, Australian Government Publishing Service, Canberra.
- LINDSAY, J. F. & REINE, K. 1995. Well-log data, Officer Basin, South Australia. *Australian Geological Survey Organisation, Record*, **1995/2**.
- MCILROY, D., JENKINS, R. J. F. & WALTER, M. R. 1997. The nature of the Proterozoic–Cambrian transition in the northern Amadeus Basin, central Australia. *Precambrian Research*, **86**, 93–113.
- MORTON, J. G. G. 1997. Chapter 6: Lithostratigraphy and environments of deposition. In: MORTON, J. G. G. & DREXEL, J. F. (eds) *Petroleum Geology of South Australia, Volume 3: Officer Basin*. South Australia Department of Mines and Energy Resources Report Book **97/19**, 47–86.
- MORTON, J. G. G. & DREXEL, J. F. (eds) 1997. *Petroleum Geology of South Australia, Volume 3: Officer Basin*. South Australia Department of Mines and Energy Resources Report Book **97/19**.
- NELSON, D. R. 2002. 154667: sandstone, Empress 1A. In: *Compilation of Geochronology Data*. October 2004 update, Western Australia Geological Survey (CD data compilation).
- PELL, S. D., MCKIRDY, D. M., JANSYN, J. & JENKINS, R. J. F. 1993. Ediacaran carbon isotope stratigraphy of South Australia—an initial study. *Transactions of the Royal Society of South Australia*, **117**, 153–161.
- POPP, B. N., TAKIGIKU, R., HAYES, J. M., LOUDA, J. W. & BAKER, E. W. 1989. The post-Paleozoic chronology and mechanism of ^{13}C depletion in primary marine organic matter. *American Journal of Science*, **289**, 436–454.
- PREISS, W. V. 1987. (compiler) *The Adelaide Geosyncline—Late Proterozoic Stratigraphy, Sedimentation, Palaeontology and Tectonics*. South Australia Geological Survey, Bulletin **53**.
- PREISS, W. V. 1993. (compiler) Neoproterozoic. In: DREXEL, J. F., PREISS, W. V. & PARKER, A. J. (eds) *The Geology of South Australia. Volume 1. The Precambrian*. South Australia Geological Survey, Bulletin, **54**, 171–203.
- PREISS, W. V. 2000. The Adelaide Geosyncline of South Australia and its significance in Neoproterozoic continental reconstruction. *Precambrian Research*, **100**, 21–63.
- REID, P. W. & PREISS, W. V. 1999. *Parachilna map sheet (second edition)*. South Australia Geological Survey, Geological Atlas 1:250 000 Series, Sheet **SH54-13**.
- STEVENS, M. K. & APAK, S. N. 1999. (compilers) Empress 1 and 1A Well Completion Report, Yowalga Sub-basin, Officer Basin, Western Australia. *Western Australia Geological Survey Record* **1999/4**.
- SUKANTA, U., THOMAS, B., VON DER BORCH, C. C. & GATEHOUSE, C. G. 1991. Sequence stratigraphic studies and canyon formation, South Australia. *Petroleum Exploration Society of Australia Journal* **19**, 68–73.
- TERMIER, H. & TERMIER, G. 1960. L'Ediacarien, premier étage paléontologique. *Revue générale des Sciences pures et appliquées et Bulletin de*

- l'Association Française pour l'Avancement des Sciences*, **67**, 79–87.
- VON DER BORCH, C. C., SMIT, R. & GRADY, A. E. 1982. Late Proterozoic submarine canyons of Adelaide Geosyncline, South Australia. *Bulletin of the American Association of Petroleum Geologists*, **66**, 332–347.
- VON DER BORCH, C. C., GRADY, A. E., ALDAM, R., MILLER, D., NEUMANN, R., ROVIRA, A. & EICKHOFF, K. 1985. A large-scale meandering submarine canyon: outcrop example from late Proterozoic Adelaide Geosyncline, South Australia. *Sedimentology*, **32**, 507–518.
- WALLACE, M. W., GOSTIN, V. A. & KEAYS, R. R. 1989. Discovery of the Acraman impact ejecta blanket in the Officer Basin and its stratigraphic significance. *Australian Journal of Earth Sciences*, **36**, 585–587.
- WALLACE, M. W., WILLIAMS, G. E., GOSTIN, V. A. & KEAYS, R. R. 1990a. The Late Proterozoic Acraman impact—towards an understanding of impact events in the sedimentary record. *Mines and Energy Review, South Australia*, **57**, 29–35.
- WALLACE, M. W., GOSTIN, V. A. & KEAYS, R. R. 1990b. Acraman impact ejecta and host shales—evidence for low-temperature mobilization of iridium and other platinumoids. *Geology*, **18**, 132–135.
- WALLACE, M. W., GOSTIN, V. A. & KEAYS, R. R. 1990c. Spherules and shard-like clasts from the Late Proterozoic Acraman impact ejecta horizon, South Australia. *Meteoritics*, **25**, 161–165.
- WALLACE, M. W., GOSTIN, V. A. & KEAYS, R. R. 1996. Sedimentology of the Neoproterozoic Acraman impact-ejecta horizon, South Australia. *AGSO Journal of Australian Geology and Geophysics*, **16**, 443–451.
- WALTER, M. R., KRYLOV, I. N. & PREISS, W. V. 1979. Stromatolites from Adelaidean (Late Proterozoic) sequences in central and South Australia. *Alcheringa*, **3**, 287–305.
- WALTER, M. R., GREY, K., WILLIAMS, I. R. & CALVER, C. 1994. Stratigraphy of the Neoproterozoic to early Palaeozoic Savory Basin, Western Australia, and correlation with the Amadeus and Officer Basins. *Australian Journal of Earth Sciences*, **41**, 533–546.
- WALTER, M. R., VEEVERS, J. J., CALVER, C. R. & GREY, K. 1995. Neoproterozoic Stratigraphy of the Centralian Superbasin, Australia. *Precambrian Research*, **73**, 173–196.
- WALTER, M. R., VEEVERS, J. J., CALVER, C. R., GORJAN, P. & HILL, A. C. 2000. Dating the 840–544 Ma Neoproterozoic interval by isotopes of strontium, carbon, and sulfur in seawater, and some interpretative models. *Precambrian Research*, **100**, 371–433.
- WILLIAMS, G. E. 1979. Sedimentology, stable-isotope geochemistry and palaeoenvironment of dolostones capping late Precambrian glacial sequences in Australia. *Journal of the Geological Society of Australia*, **26**, 377–386.
- WILLIAMS, G. E. 1986. The Acraman impact structure: source of ejecta in late Precambrian shales, South Australia. *Science*, **233**, 200–203.
- WILLIAMS, G. E. & WALLACE, M. W. 2003. The Acraman asteroid impact, South Australia: magnitude and implications for the late Vendian environment. *Journal of the Geological Society, London*, **160**, 545–554.
- WILLIAMS, G. E., SCHMIDT, P. W. & BOYD, D. M. 1996. Magnetic signature and morphology of the Acraman impact structure, South Australia. *AGSO Journal of Australian Geology and Geophysics*, **16**, 431–442.
- WILLIAMS, I. R. 1992. Geology of the Savory Basin, Western Australia. *Western Australia Geological Survey, Bulletin*, **141**.
- WILLMAN, S., MOCZYDIOWSKA, M. & GREY, K. 2006. Neoproterozoic (Ediacaran) diversification of acritarchs—A new record from the Murnaroo 1 drillcore, Officer Basin, Australia. *Review of Palaeobotany and Palynology*, **139**, 17–39.
- ZANG, W. 1995. Early Neoproterozoic sequence stratigraphy and acritarch biostratigraphy, eastern Officer Basin, South Australia. *Precambrian Research*, **74**, 119–175.
- ZANG, W. 1997. Megascopic carbonaceous *Chuaria* and *Tawuia* from the late Neoproterozoic in South Australia. *MESA Journal*, **4**, 37–41.

'Ediacaran' as a name for the newly designated terminal Proterozoic period

R. J. F. JENKINS

South Australian Museum, North Terrace, Adelaide, South Australia, 5000
(e-mail: Jenkins.Richard@saugov.sa.gov.au)

Abstract: The 'International Geological Commission on Stratigraphy Working Group on the Terminal Proterozoic Period' held a series of ballots to vote for criteria identifying the new Period. These included establishing the international site and direct locality for the 'Global Stratotype Section and Point' (GSSP), as well as its stratigraphic level and the official name of the new period. Information included in the present note was submitted for circulation to members of the voting committee in April 2003 for their consideration on the occasion of the formal vote to ratify the name, and was a successful proposal for the designation 'Ediacaran'.

The name Ediacara is historically established as an alliteration of the Aboriginal reference to an ephemeral lake recorded on the first geological map of the Flinders Ranges, and subsequently transmitted through references in Parliament, historical pastoral runs (named properties), and the surveying of a new mining town. During this history its application moved some 60 km south. The name refers to a place of water, possibly in the context of ancestral time. Aspects of the subsequent history of concepts embraced in the original presentation are included.

This note includes information presented in support of the name 'Ediacaran' for the newly designated Period (Gradstein *et al.* 2004; Knoll *et al.* 2004a, b, 2006). It was submitted to the 'International Commission on Stratigraphy Working Group for a Terminal Proterozoic Period' for consideration on the occasion of their formal vote for the name of the new Period, mid-2003.

'Ediacaran' was originally nominated for a potential Late Proterozoic period by Harland & Herod (1975). The name has long been associated with the Ediacara Hills of the western Flinders Ranges, where the distinctive 'Ediacara' fauna (assemblage of soft-bodied fossil remains) was discovered in the mid 1940s. The term 'Ediacaran' has come to be rather loosely promoted in recent literature but, in the sense of Harland & Herod (1975) and the manner in which the writer uses it, refers specifically to a nominated interval of geological time associated with a type section in the central Flinders Ranges (Jenkins 1981, 1984a, 1995; Preiss 1987, 2005). Against this background, two important issues are highlighted:

First, the nominated Ediacaran of Harland & Herod (1975) was considered to have a base at *c.* 650 ± Ma, and by implication, corresponded with the Nuccaleena Formation. The lower boundary favoured by Jenkins (1981) is the base of the Wearing Dolomite Member of the Wonoka Formation (Fig. 1). The older part of the underlying Bunyeroo Formation includes isolated clasts, perhaps introduced by ice rafting. In terms of

homotaxial stratigraphy, the Bunyeroo Formation likely corresponds to the Mortensnes Tillite of the Vestertana Group, Finnmark, northern Norway.

The Wonoka Formation itself is closely correlative with subsurface strata in the Officer Basin (to the NW), which indicate a diverse radiation of process-bearing acritarchs (Grey 2005). According to Grey (2005), this radiation shows only moderate similarity to Ediacaran process-bearing acantomorphic acritarchs known in China. However, an alternative school of thought supports the view that parts of the Australian palynofloral radiation are represented in phosphorites and cherts of the Doushantuo Formation, south China, where they responded to phases of warming following the close of the Nantuo glaciation.

Hoffmann *et al.* (2004) presented a U–Pb zircon concordia intercept age of 635.5 ± 1.2 Ma for a tuff within a dropstone unit of the Ghaub Formation, central Namibia. The essentially coeval similar age of 635.23 ± 1.5 Ma reported by Condon *et al.* (2005) for the lower part of the Doushantuo Formation provides a close 'fix' on the post Ghaub–Nantuo global warming. As well, a SHRIMP U–Pb zircon age of 628.3 ± 5.8 Ma has been obtained from the lower Doushantuo Formation (Yin *et al.* 2005). For reasons of palaeoclimatic evidence, and biostratigraphic information, such as outlined in Grey *et al.* (2003), the Ediacaran GSSP was placed at the base of the Nuccaleena Formation, which overlies the glacial Elatina Formation. This level is *c.* 1.4 km stratigraphically lower

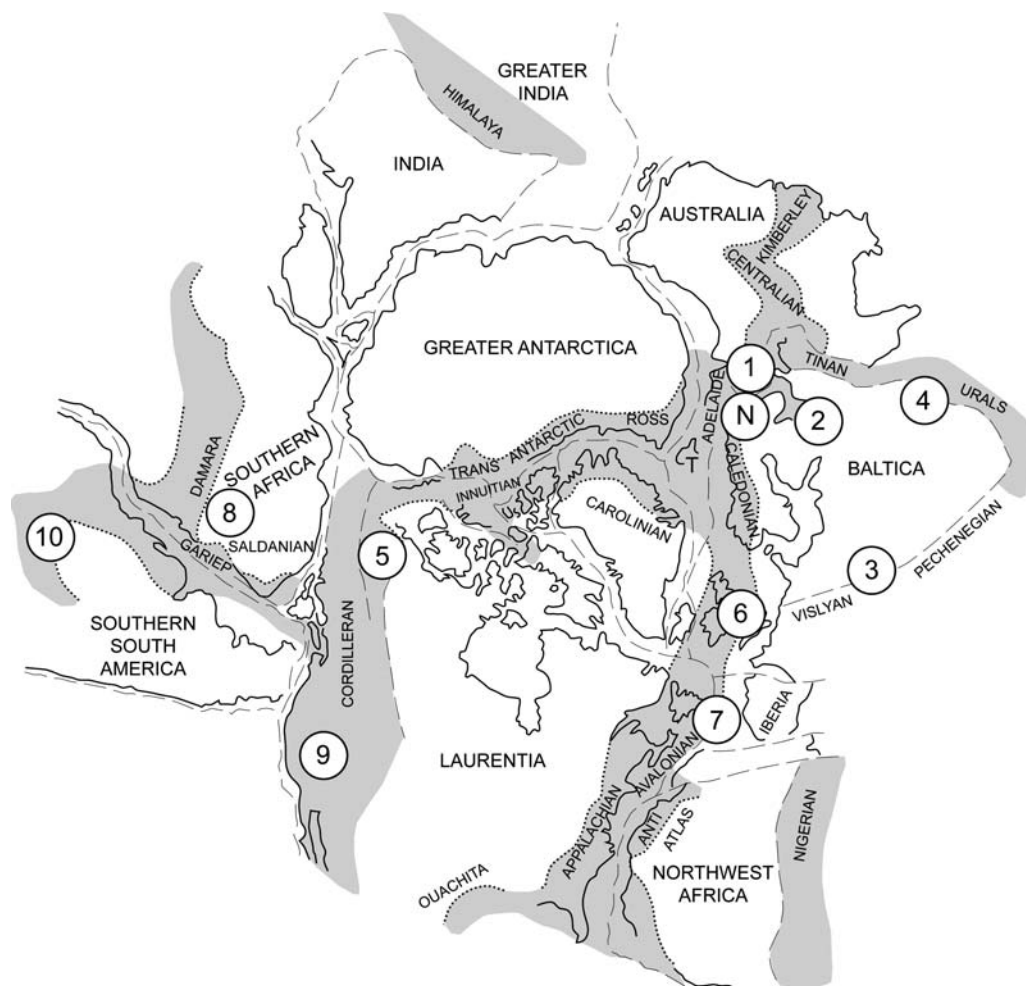


Fig. 2. Suggested jigsaw juxtaposition of modern continental outlines constituting the heartland of the supercontinent of Rodinia during the late Ediacaran Period. Continents and active mobile belts of the time (hatched) are named. The construct places the similar geologies of the Ediacaran of north Norway, N, and the Flinders Ranges, I, in close proximity, and the comparable late Ediacaran stratigraphies of the Flinders Ranges and the Onega Peninsula on the White Sea adjacent. The Proterozoic part of Tasmania, T, sometimes described in the late nineteenth century as the most metalliferous piece of crust on Earth, lies precisely at the triple junction of three great rift systems. The construct also satisfies Waggoner's (1999) finding that the soft-bodied biotas of the Ediacaran comprise three main associations of component taxa. These are, with indicated notation: first association: 1, the Flinders Range; 2, White Sea; 3, Podolia; 4, Urals; 5, NW Canada; second association: 6, Charnwood and 7, Newfoundland; third association: 8, SW North America and 10, South America. Other weaker associations show in Waggoner's data set, but as the component taxa are so poorly defined little reliance can be accorded. The construct implies that several parts of Africa were not then united as in the present continent. Break-up of Australia, Norway and the Ross Orogen probably commenced in the mid- to late-Botomian around 518 ± 2 Ma ('age' of the Cymric Vale mélange in Jenkins *et al.* 2002.) Continental projections are after Smith *et al.* (1981).

in the Ediacaran stratotypic section than the base of the Wonoka Formation. In the SE sector of the Adelaide Rift Complex, a cumulative thickness of strata exceeding 8800 m is present between the Nuccaleena Formation and the base of the Wonoka

Formation, surely representing a depositional time-span approaching several tens of millions of years. The Elatina Formation likely corresponds to the Smalfjord Formation of northern Norway in terms of homotaxial stratigraphy (Fig. 1). The possibility

that the Flinders Ranges and Finnmark were located in close proximity during the Ediacaran is explored in Figure 2.

Jenkins (1981) suggested such a period with an Australian stratotype, and the age of the older boundary for the Ediacaran was thought to be close to 640 Ma. Dating based on Sr–Rb whole-rock analyses for the Adelaide Rift Complex has proven controversial (e.g. Preiss 1987), and as yet, extraction of zircon from latest Proterozoic tuffs for U–Pb ages has been unsuccessful. However, a few detrital zircons, which are probably of volcanogenic origin, have been detected through bulk screening with the Canberra-based SHRIMPs (Sensitive High Resolution Ion MicroProbes). Work in progress suggests that caution should be exercised when considering the accuracy of such numerical ages until fuller analyses are made. Nevertheless, two zircons from sandstones that lie below the glaciogenic Elatina Formation, and the nominated GSSP boundary marked by the Nuca-leena Formation, indicate a maximum age for the sediment of about 650 Ma (Ireland *et al.* 1998). This age is for the Marino Arkose south of Adelaide at a level approximately 200 metres stratigraphically below the Elatina Formation. A more rigorous constraint is provided by the SHRIMP zircon age close to the 658 Ma Fanning & Link (2006) find for the upper part of the Merinjina Formation, the highest ‘tillitic’ interval of the ‘Sturtian’ glacial cycle in the northern Flinders Ranges. This level is some 3150 metres stratigraphically below the local equivalent of the Ediacaran GSSP boundary.

Of note, a small number of detrital zircons from the Bonney Sandstone of the Pound Subgroup limit the maximum age of sedimentation to around 600 Ma. The Bonney Sandstone includes well defined, but rare, simple surface trace fossils, and in its upper part, rather small (1–1.5 cm) round markings of the sort included in ‘*Aspidella*’ (e.g. Jenkins 1995). Preiss (2000) indicates a U–Pb zircon SHRIMP dating of a single zircon crystal from an unknown level in the Bonney Sandstone as 556 ± 24 Ma. The earliest U–Pb zircon SHRIMP dating for the basal Cambrian is the 538.2 ± 1.5 Ma ($^{206}\text{Pb}/^{238}\text{U}$) for Bed 5 in the Meishucunian of south China given by Jenkins *et al.* (2002). This is a limiting minimum age for the top of the Ediacaran using SHRIMP technology, which may have differing uncertainties from the frequently cited Pb/Pb and concordia intercept ages incorporating particular common lead corrections.

Presupposing that different episodes of glaciation during the later Neoproterozoic are coeval, the oldest sediment markings or permineralized remains attributed to ‘metazoans’ are probably dated a little over 580 Ma to perhaps *c.* 600 Ma. The earliest known remains of large structurally ‘complex’

fossils known from the Ediacaran are dated at *c.* 575 Ma (Condon *et al.* 2005; Narbonne 2005; Droser *et al.* 2006).

Another point of interest is the true etymology of the name ‘Ediacara’. Early historical documentation for the Flinders Ranges region indicates that Ediacara is a synonym for the similar sounding ‘Idiyakra’ or ‘Ideyaker’, representing an aboriginal name subsequently applied to a pastoral area. During the 1880s, the present area of the Ediacara Hills was embraced by copper mining leases broadly connected to mines near Beltana, about 26 km to the east. In order to facilitate the listing of a new mining company on the London Stock Exchange, a township was gazetted in the area of the later recognized fossiliferous beds and named ‘Ediacara’ in 1887–1888. The town was surveyed in 1891 and inhabited for about a dozen years. It is clear that the miners observed the fossils because many flagstones they used for flooring or as fire-hearths show unusual and fine examples of the large discoidal fossil remains suggesting their deliberate collection for curiosity value.

An extended etymology of the name, more precise than the preceding outline, is given below. The aboriginal name ‘Ediacara’ or ‘Idiyakra’ (Freeling 1860, in an instruction dated 1859) is indicated on an early map of the Flinders Ranges as ‘L(ake) Ideyaker’ (Selwyn 1860), the site of Goyder’s (1860) Lake ‘Weatherstone’. Goyder (1860) referred to a dray route through ‘Myrtle Spring, Idiyakra and Mirrabuckina’. Ideyaka Hill and the adjacent Lake Watherston were embraced in the ‘Ideyaker Pastoral Run’ of G. Tinline and A. B. Murray in 1866 (Manning 1990). The adjacent ‘Ediacara Pastoral Run’, with the greater part of its elongate north–south axis bordering the north eastern shore of Lake Torrens, was held by W. C. Burkitt from 1871, and the homestead ‘Old Ediacara’, now in ruin, came to be established on the southern part of his run. The mining field gazetted as Ediacara in 1887–1888 evidently derived its name from the adjacent pastoral run and is located some 21 km SSE of the ‘Old Ediacara’ ruin.

Located 41 km NW of Copley, the rather remote, ephemeral Lake Watherston forms a shallow bowl, which appears to have been called ‘Idiyakra’ or ‘Ideyaker’ by aboriginal inhabitants. Information from an aboriginal person in the Flinders Ranges, suggests that a better alternative for an earlier translation of the name (Jenkins 1984b) is an alliteration of ‘idni-’ for ‘round about’ (e.g. subsurface water) or ‘out of the way’ (Shürmann 1844), or perhaps ‘indi-’, meaning something far away or belonging to the distant past, or even the source of a river (Reed 1967); and ‘jakara’ for ‘spring of water’ (Cooper 1969). At least fourteen dams or wells have been developed within a

10 km radius of the site in historical times, so such a 'naming' seems appropriate.

In conclusion, the name 'Ediacaran' has now been used for more than a quarter of a century as the name for an informal period preceding the Cambrian, and for the greater part of this time has been linked to a stratotype located in the central Flinders Ranges. The name 'Idiyakra' or 'Ediacara' is of aboriginal origin and can be traced back to at least 1859 or a little earlier, when the first white pastoralists took up lands in the far northwestern Flinders Ranges. Its etymology links it to a place where water is, or was present close by, either in the sense of the present or extending distantly into past wetter times. As water is synonymous with life in the harsh, arid lands of Australia, it is a fitting name for a time when the first megascopic marine animals evolved. As the records of early surveyors and State Parliamentary records demonstrate, the ending of the name sounded as a 'kra', 'ker' or 'ka', and hence the appropriate name of the period is 'Ediacaran'.

Bill Watt and Maria Vassalla of the Geographical Names Advisory Committee, South Australia, assisted in tracing the history of pastoral holdings. The author would like to thank the two reviewers, S. Jensen and A. Martin.

References

- CONDON, D., ZHU, M., BOWRING, S., WANG, W., YANG, A. & JIN, Y. 2005. U–Pb ages from the Neoproterozoic Doushantuo Formation, China. *Science*, **308**, 95–98.
- COOPER, H. M. 1969. *Australian Aboriginal Words*. South Australian Museum, Adelaide.
- DROSER, M. L., GEHLING, J. G. & JENSEN, S. R. 2006. Assemblage palaeoecology of the Ediacara biota: The unabridged edition? *Palaeogeography, Palaeoclimatology, Palaeoecology*, **232**, 131–147.
- FANNING, C. M. & LINK, P. 2006. Constraints on the timing of the Sturtian glaciation from southern Australia; i.e. for the true sturtian. *Geological Society of America Abstracts with Programs*, **38**, 115.
- FREELING, A. H. 1860. Instructions to Mr. Goyder, 10th October 1859. *Proceedings of the Parliament of South Australia*, **1860**, No. 41.
- GOYDER, G. W. 1860. Report from Mr. G. W. Goyder relative to the progress of the work of triangulation and well sinking in the far north. *Proceedings of the Parliament of South Australia*, **1860**, No. 177.
- GRADSTEIN, F., OGG, J. & SMITH, A. 2004. *A Geologic Timescale 2004*. Cambridge University Press, Cambridge.
- GREY, K. 2005. Ediacaran palynology of Australia. *Association of Australasian Palaeontologists Memoir*, **31**, 1–439.
- GREY, K., WALTER, M. R. & CALVER, C. R. 2003. Neoproterozoic biotic diversification: Snowball Earth or aftermath of the Acraman impact? *Geology*, **31**, 459–462.
- HARLAND, W. B. & HEROD, K. N. 1975. Glaciation through time. In: WRIGHT, A. E. & MOSELY, F. (eds) *Ice Ages: Ancient and Modern*. *Geological Journal Special Issue*, **6**. Seel House Press, Liverpool, 189–126.
- HOFFMANN, K. H., CONDON, D. J., BOWRING, S. A. & CROWLEY, J. L. 2004. U–Pb zircon date from the Neoproterozoic Ghaub Formation, Namibia: Constraints on Marinoan glaciation. *Geology*, **32**, 817–820.
- IRELAND, T. R., FLOTTMANN, T., FANNING, C. M., GIBSON, G. M. & PREISS, W. V. 1998. Development of the early Paleozoic Pacific margin of Gondwana from detrital-zircon ages across the Delamerian orogen. *Geology*, **26**, 243–246.
- JENKINS, R. J. F. 1981. The concept of an 'Ediacaran Period' and its stratigraphic significance in Australia. *Transactions of the Royal Society of South Australia*, **105**, 179–194.
- JENKINS, R. J. F. 1984a. Ediacaran events: boundary relationships, correlation of key sections especially in 'America'. *Geological Magazine*, **121**, 635–643.
- JENKINS, R. J. F. 1984b. Interpreting the oldest fossil cnidarians. Proceedings of the 4th International Symposium on Fossil Cnidaria. *Palaeontographica Americana*, **54**, 95–104.
- JENKINS, R. J. F. 1995. The problems and potential of using animal fossils and trace fossils in terminal Proterozoic biostratigraphy. *Precambrian Research*, **73**, 51–69.
- JENKINS, R. J. F., COOPER, J. A. & COMPSTON, W. 2002. Age and biostratigraphy of Early Cambrian tuffs from SE Australia and southern China. *Journal of the Geological Society*, London, **159**, 645–658.
- KNOLL, A. H., WALTER, M. R., NARBONNE, G. M. & CHRISTIE-BRICK, N. 2004a. Three 'first places' for Ediacaran Period. *Episodes*, **27**, 222.
- KNOLL, A. H., WALTER, M., NARBONNE, G. M. & CHRISTIE-BLICK, N. 2004b. A new Period for the geological time scale. *Science*, **305**, 621–622.
- KNOLL, A. H., WALTER, M., NARBONNE, G. M. & CHRISTIE-BLICK, N. 2006. The Ediacaran Period: A new addition to the geological time scale. *Lethaia*, **39**, 13–30.
- MANNING, G. H. 1990. *Manning's Place Names of South Australia*. Published by author, Adelaide.
- NARBONNE, G. M. 2005. The Ediacara biota: Neoproterozoic origin of animals and their ecosystems. *Annual Review of Earth and Planetary Sciences*, **33**, 421–442.
- PREISS, W. V. 1987 (Compiler). The Adelaide Geosyncline—Late Proterozoic stratigraphy, palaeontology and tectonics. *Geological Survey of South Australia Bulletin*, **53**.
- PREISS, W. V. 2000. The Adelaide Geosyncline of South Australia and significance in Neoproterozoic continental reconstruction. *Precambrian Research*, **100**, 21–63.
- PREISS, W. V. 2005. Global stratotype for the Ediacaran system and Period - the golden Spike has been placed in South Australia. *MESA Journal*, **37**, 20–25.
- REED, A. W. 1967. *Aboriginal Place Names and their Meanings*. A. H. & A. W. Reed, Sydney.
- SELWYN, A. R. C. 1860. Geological notes of a journey in South Australia from Cape Jervis to Mount Serle.

- Proceedings of the Parliament of South Australia*, **1860**, No. 20.
- SIEDLECKA, A. 1994. Field guide to the workshop in eastern Finnmark, north Norway, 1–8 August 1994. *Geological Survey of Norway*, Report no. **94.065**.
- SIEDLECKA, A. & ROBERTS, D. 1992. The bedrock geology of Varanger Peninsula, Finnmark, north Norway: an excursion guide. *Norges Geologiske Undersøkelse*, **5**.
- SHÜRMANN, C. W. 1844. *A Vocabulary of the Parnkalla Language*. George Dehane, Adelaide.
- SMITH, A. G., HURLEY, A. M. & BRIDEN, J. C. 1981. *Phanerozoic Paleogeographic World Maps*. Cambridge University Press, Cambridge.
- WAGGONER, B. 1999. Biogeographic analysis of the Ediacara biota: A conflict with paleotectonic reconstructions. *Paleobiology*, **25**, 44–458.
- YIN, C. Y., TANG, F., LIU, Y. *ET AL.* 2005. U–Pb zircon age from the base of the Ediacaran Doushantuo Formation in the Yangtze Gorges, South China: constraint on the age of the Marinoan Glaciation. *Episodes*, **28**, 48–49.

First Early Cambrian Radiolaria

A. BRAUN¹, J. CHEN², D. WALOSZEK³ & A. MAAS³

¹*Institute of Palaeontology, University of Bonn, Nussallee 8, D-53115 Bonn, Germany (e-mail: braun@uni-bonn.de)*

²*Nanjing Institute of Geology and Palaeontology, Academia Sinica, 39 Beijingdonglu Street, Nanjing 210008, Peoples Republic of China*

³*Section for Biosystematic Documentation, University of Ulm, Helmholtzstrasse 20, D-98081 Ulm, Germany*

Abstract: Radiolarian skeletons are known from a limestone concretion collected from a black shale succession and from black cherts of the Yangtze Platform, China. Both occurrences are of earliest Cambrian age. The findings, reported in this paper, represent the oldest known fossil Radiolaria. Their spherical skeletons display a morphology typical of spherical radiolarians from Ordovician and younger faunas. This occurrence of radiolarians with radial symmetry and, most probably, a planktonic lifestyle can now be traced back into the earliest Cambrian. Thus, radiolarians have been part of the early oceanic plankton and likely played a significant role in the silica cycle of the oceans along with siliceous sponges.

Apart from their natural beauty, radiolarians are an important constituent of today's oceanic plankton and one of the major groups of organisms utilizing opaline silica to form their skeletons (Anderson 1983). They significantly influence the oceanic silica cycle, and their skeletons contributed to oceanic sediments and siliceous sedimentary rocks since, at least, the Ordovician (Grunau 1965; Danelian 1999). The last decades have seen a significant increase in the practical value of radiolarians for biostratigraphy and palaeoceanography for all periods from the Cambrian onwards (Vishnevskaya *et al.* 2000; De Wever *et al.* 2001).

Although it has frequently been postulated that radiolarians are a very old group of protists (Campbell 1954), extending back into the Precambrian, very little is known about their origin and early history during Precambrian and Cambrian times. Finds of skeletons in rocks of 'Precambrian' age have been reported (Cayeux 1894; David *et al.* 1896), but have either been disputed or revised in terms of age or are not fully accepted as radiolarian remains because of poor preservation (Deflandre 1949). From the biological side, and based mostly on softpart characteristics and cytology, several contradictory statements as to the origin and ancestry of the radiolarians have been made (Chatton 1934; Dogel 1950; Hollande *et al.* 1970; Strelkov *et al.* 1974; Petrushevskaya 1977). In addition, molecular data are currently being obtained specifically for radiolarian groups (Amaral-Zettler *et al.* 1997). Considerations on the timing of eukaryote groups based on molecular data point to an origin

of the Radiolaria approximately 1 billion years ago (Knoll 1992; Blair Hedges *et al.* 2001); these data are currently not supported by fossil evidence. The fossil record of well-preserved radiolarian skeletons goes back reliably only to the Middle Cambrian (Won *et al.* 1999). A report of Early Cambrian radiolarians from the Altai-Sayan region (Nazarov 1973) was based on spherical bodies in thin section, the radiolarian nature of which remains disputable. Late Cambrian and Early Ordovician faunas have been described by Kozur *et al.* (1996) and Dong *et al.* (1997).

The well-preserved skeletons from the earliest Cambrian of China described herein, therefore, are of importance both with respect to existing data on early radiolarian evolution, and with regard to the more general discussion on the development of faunal communities around the Precambrian–Cambrian boundary.

Localities

Hetang Formation, Xintangwu, Jianshan County, W. Zhejiang Province

A few radiolarian skeletons have been recovered from large carbonate concretions occurring within a black shale succession (the 'Hetang' Formation; see Zhu *et al.* 2000; cf. Fig. 1b). Spicules of siliceous sponges, small shelly fossils (SSF) and indeterminate bivalved arthropod shields have been found in the residues associated with radiolarian fragments

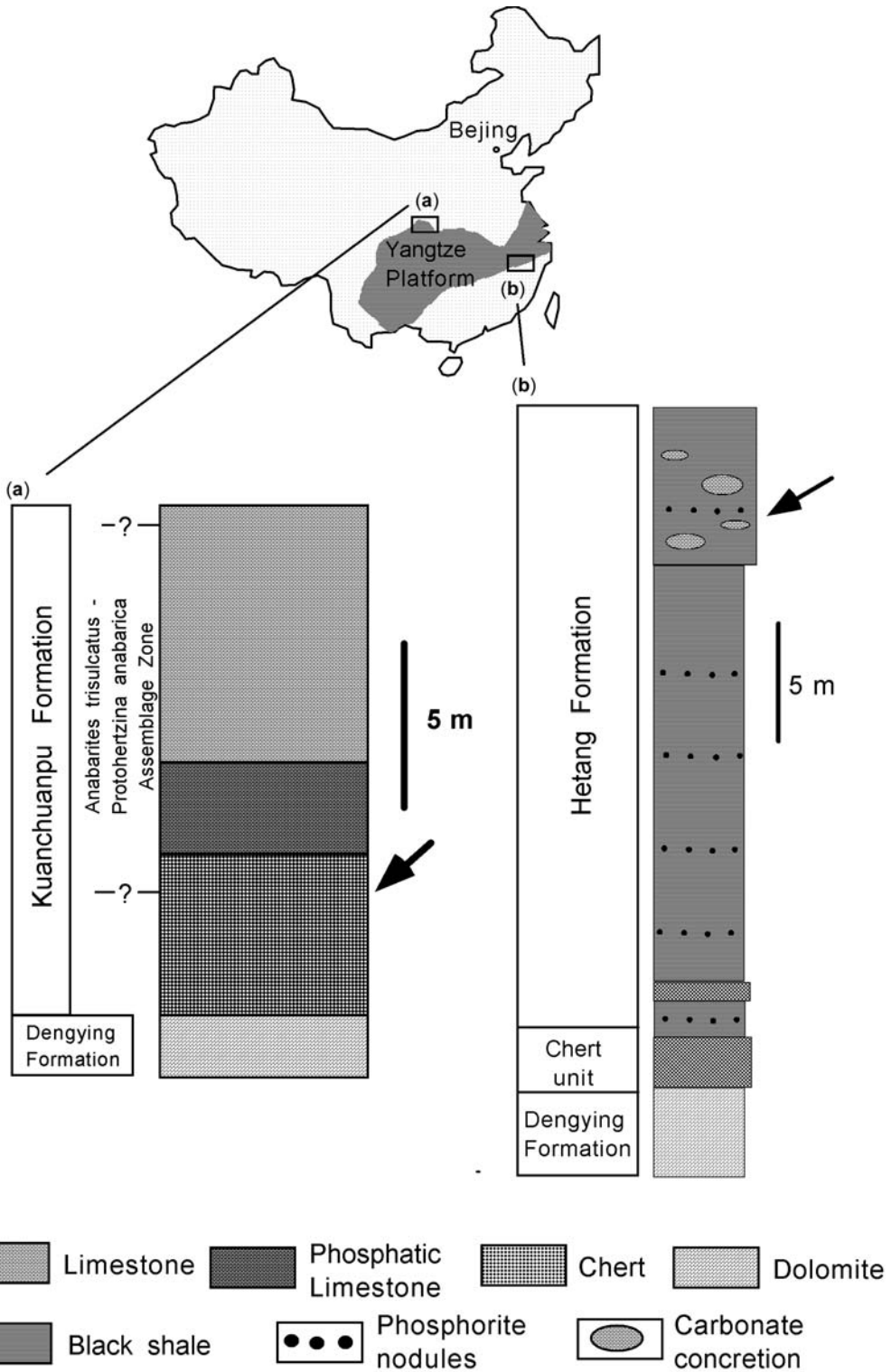


Fig. 1. Sample location areas on the Yangtze Plate, China and stratigraphic columns. Arrows point to radiolarian-bearing horizons. (a) Stratigraphic column of the Kuanchuanpu Formation at Shizonggou, near Kuanchuanpu, Ningqian County (Shaanxi Province). (b) Stratigraphic column of the Hetang Formation at Xintangwu, Jianshan County, W. Zhejiang Province.

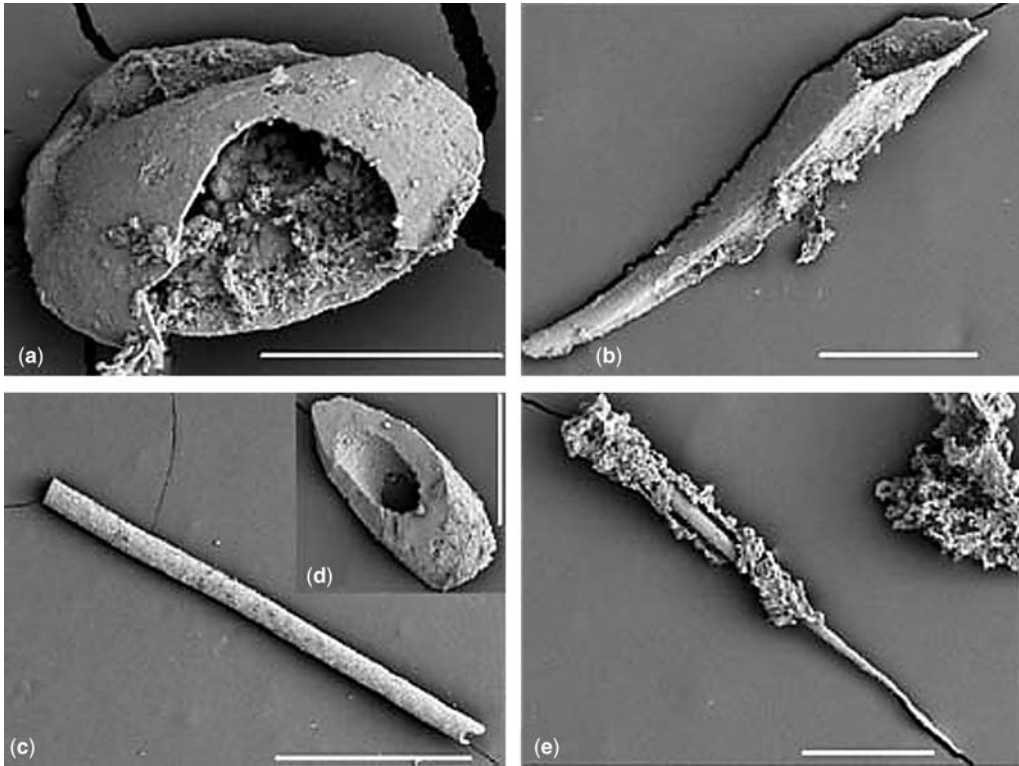


Fig. 2. Microfossils from the radiolarian-bearing residue of the Xintangwu carbonate concretion. (a) undetermined bivalved arthropod shield. (b) *Protohertzina* sp. (c, d, e) Spicules of siliceous sponges, with open (d) and diagenetically filled (e) central canal. Lower Cambrian, Meishucunian Stage, *Anabarites-Protohertzina* zone, Xintangwu, western Zhejiang, China. Length of the scale bars: 100 μm .

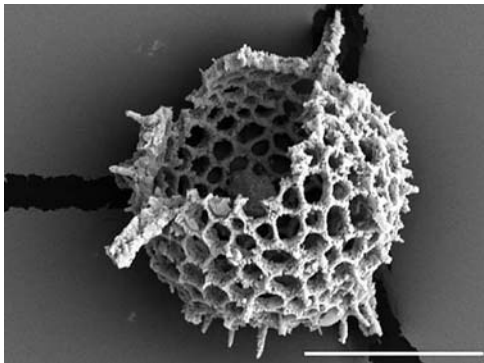


Fig. 3. Spherical radiolarian skeleton possessing a lattice sphere and spines of different orders of magnitude. Lower Cambrian, Meishucunian Stage, *Anabarites-Protohertzina* zone, Xintangwu, western Zhejiang, China. Length of the scale bar: 100 μm .

(cf. Fig. 2a–e). Compared to the sponge spicules, radiolarians are very rare.

The age of the occurrence is provided by the small shelly fossils *Anabarites trisulcatus* and *Protohertzina* sp. (= *Anabarites-Protohertzina* Zone, Meishucunian Stage; earliest Cambrian, cf. Zhu *et al.* 2000). The lithological association in the area is interpreted as basinal and oceanic. However, compared to the widespread, completely carbonate-free shales of the Hetang Formation, the rock sequence at Xintangwu appears to have been deposited in a shallower environment, probably in a slope or marginal platform setting. This is evidenced by the immediately-underlying stromatolitic succession and the higher carbonate content in concretions and layers of the Hetang Formation itself. Besides dark, bituminous carbonates, the black shales at Xintangwu contain small amounts of black cherts and phosphatic concretions. Cherts, as well as phosphatic concretions, have been sampled for radiolarians but, as yet, without success.

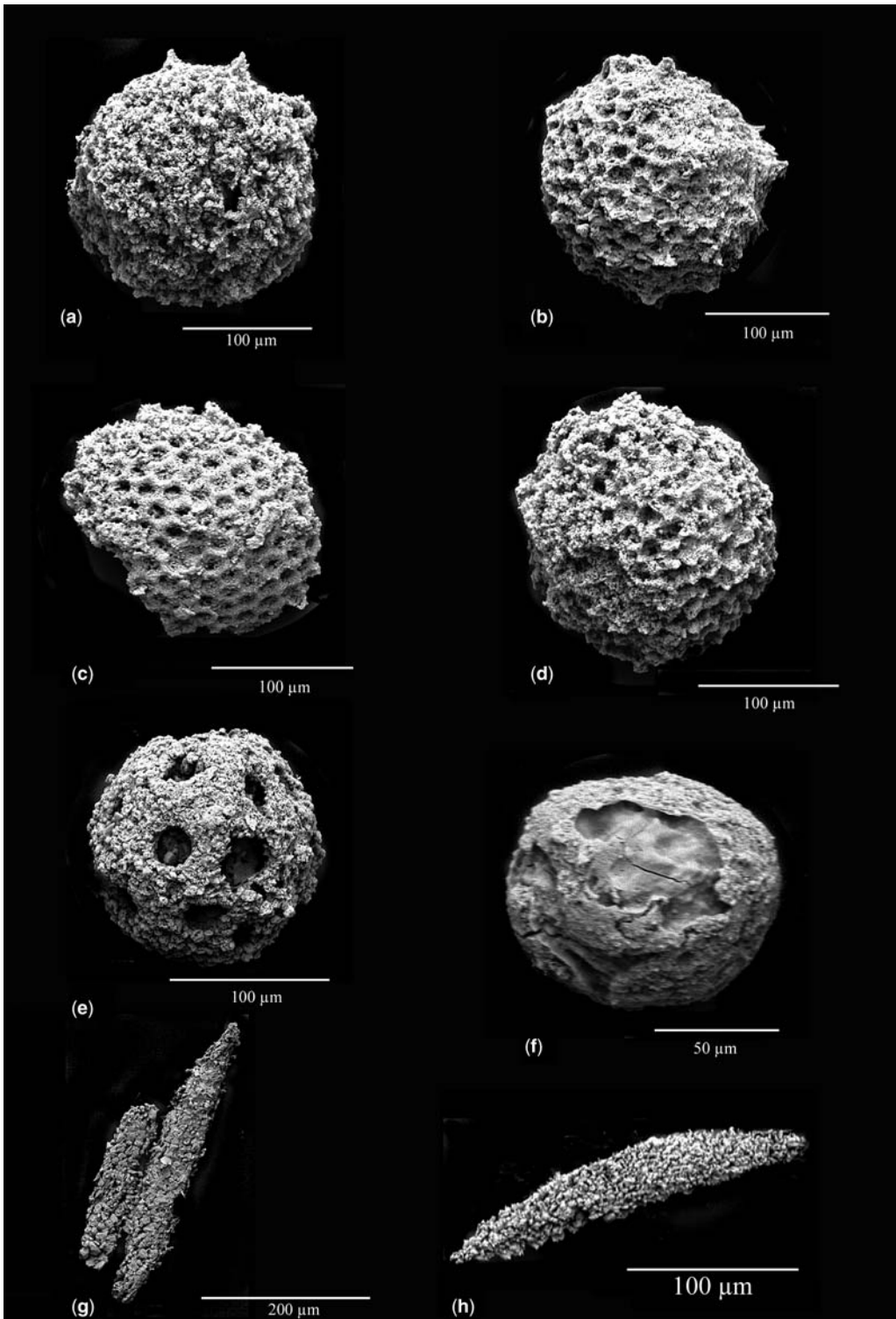


Fig. 4. Siliceous microfossils from HF acid residues of black cherts, locality Ningqiang, S. Shaanxi, Kuanchuanpu Formation. (a, b, c, d) Spherical radiolarian skeletons with lattice spheres (b, c, d) and short, triangular spines (a). Residue and matrix of the rock is strongly dominated by monaxon sponge spicules (g, h), along with silica spherules, probably representing radiolarian Steinkerns (e, f).

*Kuanchuanpu Formation, Ningqian,
S. Shaanxi Province*

Radiolarian skeletons have been recovered from a sequence of black cherts underlying phosphatic carbonate beds, the latter containing *Olivoides* and the embryonic series described by Zhao & Bengtson (1999). The area is situated near the northern rim of the Yangtze Platform (cf. Fig. 1a). Its lithologies are generally interpreted as being of shallow shelf origin. However, the lithologies at Ningqian lack any sediments and structures indicative of such shallow water origin. Black cherts and phosphatic limestones, lacking autochthonous fauna, seem to indicate a deeper water setting, at least at this locality. Details of lithology and the bathymetry of Ningqian are currently being investigated by the authors. The chert samples did not yet yield any microfossils other than sponge spicules and radiolarians. As the first Early Cambrian small shelly fossils (*Anabarites trisulcatus* and *Protoherzina*) occur in the lowermost bed of phosphatic carbonate above the sample horizon (see profile in Zhao & Bengtson 1999), it cannot be stated with certainty whether the radiolarians are of latest Precambrian or earliest Cambrian age.

Material and methods

Xintangwu concretion

Besides several lattice fragments, one well preserved and fairly complete specimen has been found in a sample of 1 kg of carbonate rock after digestion in 10% acetic acid (cf. Fig. 3). Preservation of radiolarians in calcareous concretions within clay-dominated sediments has been repeatedly recovered from sedimentary successions of different ages (Blome & Albert 1985). Early carbonate precipitation protected the radiolarian skeletons from early diagenetic dissolution, which is otherwise common in clay-rich sediments (Riedel 1959). Co-existence of radiolarians and sponge spicules has been observed in many other radiolarian occurrences, and the preservation of radiolarians has been attributed to the presence of sponge spicules (Fortey & Holdsworth 1972).

Because of the significance of the finds, special attention has been paid to the question of whether or not the skeleton fragments are original to the rocks dissolved. The following observations suggest that the resulting fossils are original:

- (1) the sorted material contains not only a fairly complete skeleton, but also several fragments of lattice spheres;
- (2) the external appearance and crystallinity of the siliceous remnants of the limestone sample is the same between sponge spicules and radiolarians;

- (3) the lithology and fossil content of the sample (bituminous carbonate concretion in a black shale containing abundant siliceous sponge spicules) is exactly the kind of lithological and diagenetic facies commonly containing radiolarians from other periods, especially in the Palaeozoic (e.g. Holdsworth 1966).

The material was processed and the residue sieved and picked by an experienced laboratory technician in clean and new sieves, which had not been used in any kind of radiolarian preparation before.

Ningqian chert

Four lattice spheres (cf. Fig. 4a–d) that were preserved well-enough to permit further investigations have been found in addition to monaxon siliceous sponge spicules (cf. Fig. 4g, h) and spherical bodies, most probably representing siliceous Steinkerns of Radiolaria (cf. Fig. 4e–f). Pieces of the black chert have been etched with diluted (10%) HF acid, as described for younger radiolarian-bearing rocks by Pessagno and Newport (1972) and Braun (1990). Abundance of siliceous microfossils (predominantly sponge spicules) and the regular, dm-scale bedding suggests that the cherts are biosiliceous sediments, much like the bedded radiolarian cherts of the Palaeozoic age.

Morphological characteristics of the Radiolaria

The skeletons from the two localities are very similar to each other in external aspect. They possess a lattice sphere with a diameter of slightly more than 150 μm . The Xintangwu specimen displays two sets of spines, the larger seemingly bladed, the smaller needle-like. Only one specimen from the Ningqian cherts has fragmentary, small spines of equal size left on the surface of the lattice sphere. The lattice pores are similar in size and rounded polygonal in outline. We found no internal structures, such as an internal spicule or additional internal spheres in our material, but this may well be attributed to the diagenetic silica filling and does not suggest original absence of internal structures. We have avoided treating the specimens systematically, because the few specimens found are too incompletely preserved for closer systematic assignment. A systematic study must await additional material.

Discussion

Spherical shape and the regular, two-dimensional lattice of our radiolarian skeletons are unlike the irregular spongy framework, present in well-preserved radiolarian faunas from the Middle and Late Cambrian of Australia and China, which have

been found in carbonate lithologies of shallower water environments. (Dong *et al.* 1997; Won *et al.* 1999). They show neither a needle-like morphology nor a spicular construction mode postulated to be characteristic for ancestral radiolarians (Archaeospirocularia, cf. Petrushevskaya 1977; Dumitrica *et al.* 2000). In addition, there is no sign of polarity. Polarity in the architecture of many Palaeozoic radiolarians has been interpreted as a morphological expression of a sessile life habit before a benthos-plankton transition. All such presumed or predicted ancestral characteristics are completely missing in the Early Cambrian skeletons described here. Instead, the overall morphology is decidedly more similar to that of younger Palaeozoic radiolarians from the Ordovician (Dunham *et al.* 1976) or younger faunas dominated by spherical entactinids, which commonly occur in a similar kind of oceanic sedimentary environment (black shales with carbonate and/or phosphatic concretions).

Our finds indicate that by the Early Cambrian, radiolarians living in an oceanic setting had already developed advanced skeletal architecture with several sets of spines, a lattice sphere and radial symmetry. Lattice sphere, spines and radial symmetry are adaptations to a planktonic mode of life in radiolarians and so even this early, radiolarians seem to have been adapted morphologically to a planktonic mode of life in the oceans. Our finds support the idea that spherical radiolarians are a very ancient morphology among radiolarians (Kling 1978).

Early development and composition of plankton communities

Radiolarians are now known to be constituents of zooplankton communities and as part of the oceanic food chain in the earliest Cambrian. The composition and biodiversity of oceanic plankton, at the time of the Early Cambrian 'bioradiation' (Butterfield 1997), is usually considered to be dominated by acritarchs (Vidal *et al.* 1983). To that group we can now add the radiolarians. The occurrence of radiolarians in rocks of black shale and black bedded chert lithologies as early as earliest Cambrian corresponds well with the connection of radiolarian occurrences and anoxic to dysoxic oceanographic conditions ('events') observed during later time periods (Thurrow 1988; Erbacher & Thurrow 1997). At Xintangwu, anoxic/dysoxic conditions followed blooms of phytoplankton, as indicated by the carbonaceous and highly bituminous black shale lithology and by biodiverse phytoplankton discovered in thin sections of phosphorite concretions and cherts (Braun *et al.* 2003). The hypothesis of an origin of a planktic mode of life as a kind of 'evasive action' during times of poor

bottom oxygenation during such anoxic events (Tappan & Loeblich 1973; Leckie 1989) gains further support from this ancient co-occurrence.

Geological implications

Of the siliceous planktonic organisms known to play an important role in the silica cycle of the oceans, at least since the Cretaceous (Heath 1974), radiolarians are currently the only major group recognized from fossils at the beginning of the Cambrian. Based on the rare skeleton findings reported herein, however, nothing can be said about how important their role was in biomass and silica cycling. However, our findings do indicate, that by the Early Cambrian siliceous zooplankton were contributing to the oceanic silica balance in addition to the siliceous sponges (Bengtson 1986). The latter are common and sometimes present in rock forming amounts within chert sequences spanning the Precambrian/Cambrian boundary (Braun *et al.* 2004). Should the Neoproterozoic series of siliceous shales and bedded cherts, underlying the Cambrian in many places of the Yangtze Platform, turn out to be radiolarian-rich sedimentary rocks (in the field, they are indistinguishable from bedded radiolarian cherts) this would introduce significant constraints for the palaeo geochemistry of the oceans. We did not find traces of radiolarian skeletons during our processing in a first test series of these siliceous rocks, but this could be due to the strong recrystallization of the chert matrix in the area sampled (southern Shaanxi Province). Exploration for more evidence of Radiolaria and biosiliceous sedimentation will be conducted in the basal facies of the Neoproterozoic of the Yangtze Platform.

We thank the reviewers K. Gray and P. Parkhaev.

References

- AMARAL-ZETTLER, L. A., SOGIN, M. L. & CARON, D. A. 1997. Phylogenetic relationships between the Acantharea and the Polycystinea: a molecular perspective on Haeckel's Radiolaria. *Proceedings of the National Academy of Sciences*, **94**, 11411–11416.
- ANDERSON, O. R. 1983. *Radiolaria*. Springer, New York.
- BENGTSON, S. 1986. Siliceous microfossils from the Upper Cambrian of Queensland. *Alcheringa*, **10**, 195–216.
- BLAIR HEDGES, S., CHEN, H., KUMAR, S., WANG, D. Y. C., THOMPSON, A. S. & WATANABE, H. 2001. A genomic timescale for the origin of eukaryotes. *BMC Evolutionary Biology*, **1**, 4.
- BLOME, C. D. & ALBERT, N. R. 1985. Carbonate concretions: an ideal sedimentary host for microfossils. *Geology*, **13**, 121–215.
- BRAUN, A. 1990. Radiolarien aus dem Unter-Karbon Deutschlands. *Courier Forschungsinstitut Senckenberg*, **133**, 1–177.

- BRAUN, A. & CHEN, J. 2003. Plankton from Early Cambrian black shale series on the Yangtze Platform, and its influences on lithologies. *Progress in Natural Sciences*, **13**, 777–782.
- BRAUN, A., CHEN, J., WALOSZEK, D. & MAAS, A. 2004. Siliceous microfossils and biosiliceous sedimentation in the Lowermost Cambrian of China. Monash Science Centre, Melbourne (extended abstract).
- BUTTERFIELD, N. J. 1997. Plankton ecology and the Proterozoic–Phanerozoic transition: *Paleobiology*, **23**, 247–262.
- CAMPBELL, A. S. 1954. Radiolaria. In: MOORE, R. C. (ed.) *Treatise on Invertebrate Paleontology. Part D—Protista 3*, Geology Society of America and The University of Kansas, D11–D163.
- CAYEUX, L. 1894. Les preuves de l'existence d'organismes dans le terrain précambrien. Première note sur les Radiolaires précambriens. *Société Géologique de France, Bulletin. Séries 3*, 197–228.
- CHATTON, E. 1934. L'origine péridinienne des Radiolaires et l'interprétation parasitaire de l'anisosporegnèse. *Comptes Rendus de l'Académie des Sciences*, **198**, 309–312.
- DANELIAN, T. 1999. Taxonomic study of Ordovician (Llanvirn–Caradoc) Radiolaria from the Southern Uplands (Scotland, UK). *Geodiversitas*, **21**, 625–635.
- DAVID, T. W. & HOWCHIN, W. 1896. Note on the occurrence of casts of Radiolaria in Pre-Cambrian (?) rocks, South Australia. *Proceedings of the Linnean Society of New South Wales*, **XXI**, 571–583.
- DEFLANDRE, G. 1949. Les soi-disant radiolaires du Précambrien de Bretagne et la question de l'existence de radiolaires embryonnaires fossils. *Bulletin de la Société Zoologique de France*, **74**, 351–352.
- DE WEVER, P., DUMITRICA, P., CAULET, J.-P., NIGRINI, C. & CARIDROIT, M. 2001. *Radiolarians in the Sedimentary Record*. Gordon & Breach, London.
- DOGEL, V. A. 1950. New data on the phylogeny of Radiolaria. *Zoologicheskii Zhurnal*, **29**, 562–565.
- DONG, X., KNOLL, A. H. & LIPPS, J. H. 1997. Late Cambrian Radiolaria from Hunan China. *Journal of Paleontology*, **71**, 753–758.
- DUMITRICA, P., CARIDROIT, M. & DE WEVER, P. 2000. Archaeospicularia, ordre nouveau de radiolaires: une nouvelle étape pour la classification des radiolaires du Paléozoïque inférieur. *Comptes Rendus de l'Académie des Sciences (Paris)*, Série II, **330**, 563–569.
- DUNHAM, J. B. & MURPHY, M. A. 1976. An occurrence of well preserved Radiolaria from the Upper Ordovician (Caradocian), Eureka county, Nevada. *Journal of Paleontology*, **50**, 882–887.
- ERBACHER, J. & THUROW, J. 1997. Influence of anoxic events on the evolution of mid-Cretaceous Radiolaria in the North Atlantic and western Tethys. *Marine Micropaleontology*, **30**, 139–158.
- FORTEY, R. A. & HOLDSWORTH, B. K. 1972. The oldest known well preserved Radiolaria. *Bolletino della Società Paleontologica Italiana*, **10**, 35–41.
- GRUNAU, H. R. 1965. Radiolarian cherts and associated rocks in space and time. *Eclogae Geologicae Helveticae*, **58**, 157–208.
- HEATH, G. R. 1974. Dissolved silica and deep-sea sediments. In: HAY, W. W. (ed.) *Studies in Paleontology*. Society of Economic Paleontology and Mineralogy Special Publication, **20**, 77–93.
- HOLDSWORTH, B. K. 1966. Radiolaria from the Namurian of Derbyshire. *Paleontology*, **9**, 319–329.
- HOLLANDE, A., CACHON, J. & CACHON, M. 1970. La signification de la membrane capsulaire des Radiolaires et ses rapports avec le plasmalemma et les membranes de reticulum endoplasmique. Affinités Radiolaires, Heliozoaires et Peridiniens. *Protistologica*, **6**, 311–318.
- KLING, S. A. 1978. Radiolaria. In: HAQ, B. U. & BOERSMA, A. (eds) *Introduction to Marine Micropaleontology*. Elsevier, New York, 203–244.
- KNOLL, A. 1992. The early evolution of eucaryotes: a geological perspective. *Science*, **256**, 622–627.
- KOZUR, H. W., MOSTLER, H. & REPETSKI, J. E. 1996. Well preserved Tremadocian primitive radiolarian from the Windfall Formation of the Antelope range, Eureka County, Nevada, USA. *Geologisch-Paläontologische Mitteilungen der Universität Innsbruck*, **21**, 245–271.
- LECKIE, R. M. 1989. An oceanographic model for the early history of planktonic Foraminifera. *Palaeogeography, Palaeoclimatology, Palaeoecology*, **73**, 107–138.
- NAZAROV, B. B. 1973. Radiolaria from Lower Cambrian horizons. *Trudi Instituta Geologii, Akademia Nauk SSSR*, **49**, 5–13.
- PESSAGNO, E. A. & NEWPORT, R. L. 1972. A technique for extracting Radiolaria from Radiolarian cherts. *Micropaleontology*, **18**, 231–234.
- PETRUSHEVSKAYA, M. 1977. On the origin of Radiolaria. *Zoologicheskii Zhurnal*, **56**, 1448–1458.
- RIEDEL, W. R. 1959. Siliceous organic remains in pelagic sediments. In: IRELAND, H. A. (ed.) *Silica in Sediments*. Society of Economic Paleontologists and Mineralogists, Special Publication, **7**, 80–91.
- STRELKOV, A. A. & RESHETNYAK, V. V. 1974. Radiolaria Acantharia. In: *Chemisoradioecology of Pelagics and Benthics*. Naukova Dumka, Kiev, 95–188.
- TAPPAN, H. & LOEBLICH, A. R. 1973. Evolution of the oceanic plankton. *Earth Science Reviews*, **9**, 207–240.
- THUROW, J. 1988. Radiolarians of Turonian bituminous carbonates (transgressive sequences of Northwest African Coastal Basins). In: SCHMIDT-EFFING, R. & BRAUN, A. (eds) *First International Conference on Radiolaria (Eurorad V)*, Abstracts: *Geologica et Palaeontologica*, **22**, 210.
- VIDAL, G. A. H. & KNOLL, A. H. 1983. Proterozoic plankton. *Geological Society of America, Memoir*, **161**, 265–277.
- VISHNEVSKAYA, V. S. & KOSTYUCHENKO, A. S. 2000. The evolution of radiolarian biodiversity. *Paleontologicheskii Zhurnal*, **34**, 124–130.
- WON, M.-Z. & BELOW, R. 1999. Cambrian Radiolaria from the Georgina basin, Queensland, Australia. *Micropaleontology*, **45**, 325–363.
- ZHAO, Y. & BENGSTON, S. 1999. Embryonic and post-embryonic development of the early Cambrian cnidarian *Olivoooides. Lethaia*, **32**, 181–195.
- ZHU, M., ZHANG, J., STEINER, M., LI, G. & YANG, A. 2000. *Sino-German Cooperative Program. Programme and Excursion Guide*. Nanjing Institute of Geology and Paleontology, Academia Sinica.

Ciliated protozoans from the Precambrian Doushantuo Formation, Wengan, South China

C.-W. LI¹, J.-Y. CHEN², J. H. LIPPS³, F. GAO^{2,4}, H.-M. CHI² & H.-J. WU¹

¹*Department of Life Sciences, National Tsing Hua University, Hsinchu, Taiwan, China (e-mail: lslcw@life.nthu.edu.tw)*

²*Nanjing Institute of Geology and Palaeontology, Nanjing 210008, China*

³*Divisions of Biology, California Institute of Technology, Pasadena, CA 91125, USA*

⁴*Department of Integrative Biology, Museum of Paleontology, University of California, Berkeley, CA 94720, USA*

Abstract: Ciliates, a major eukaryotic crown-group lineage with thousands of living species, are poorly represented in the fossil record. Ciliate biomarkers are known from the Precambrian, but only one group, the tintinnids, have an extensive fossil record dating back to the Ordovician. Thus, the occurrence of probable ciliate body fossils in Neoproterozoic rocks confirms their earlier appearance, so far inferred only from molecular sequence data and biomarkers. In this paper, we describe those fossils from the 580 million year old Precambrian Doushantuo phosphates, Guizhou, South China. Three new monospecific genera (100 µm to 200 µm in size) are represented by three-dimensional specimens with exceptionally well-preserved cell bodies including cilia, cytostome and tentacles. Two possess loricas and are referred to the tintinnids. The third has numerous tentacles, an apical cytostome and somatic cilia; it is interpreted as an ancestral early suctorian ciliate. These fossils indicate that the origin and evolutionary differentiation and specialization of ciliates took place before or along with the radiation of other crown-group eukaryotes, including metazoans.

The phylum Ciliophora (ciliates) undoubtedly had a deep Precambrian origin (Wright & Lynn 1997) and is a very diverse group (comprising over 7000 described extant species) that is widely distributed (fresh and marine waters, parasitic, and edaphic habitats). However, among the unicellular protozoans (Sleigh 1988), few of these fossilize. The fossils are mostly external skeletons (loricas), except for a few specimens preserved as body fossils in much younger amber, phosphates, chert or bituminous shale (Tappan 1993). Loricas occur in several groups of ciliates, but most commonly in tintinnids. Thus the tintinnids have the most extensive fossil record in the Ciliophora starting in the Ordovician and persisting discontinuously to the Recent (Tappan 1993), where they may be quite diverse and abundant in many marine situations (Dolan *et al.* 2002). Tintinnid fossils were also reported previously from the Precambrian (1000 Ma) of Checkoslovakia (Kosheva 1987), but these objects are unlike any other ciliates, including tintinnids. In contrast to modern tintinnid loricas, which are mostly organic with agglutinated particles covering them, most fossils are chiefly calcareous (Tappan 1993). Ciliates also produce tetrahymenol, a specific biomarker for those ciliates that feed predominately on bacteria (Harvey &

McMans 1991). Tetrahymenol is likely reduced to gammacerane in sediments, which is found in Precambrian sedimentary rocks of the Chuar Group, some 850 Ma (Summons *et al.* 1988).

Here we report single-celled, ciliated organisms from the 580 Ma phosphate deposits called the Wengan Phosphate Member of the Neoproterozoic Doushantuo Formation, at Wengan, central Guizhou (South China). Three new monospecific genera of ciliates, *Eotintinnopsis*, *Wujiangella* and *Yonyangella*, are described. Two of them are preserved with an outer cover comparable to the extant tintinnids, while the third possesses a soft body with tentacles. All three preserve the details of cell-body anatomy including ciliature, cytostome and tentacles. These findings shed light on our understanding of the evolutionary patterns in the ciliates.

The Doushantuo Formation is a shallow transgressive marine phosphate sequence capping the top of the glacial deposits known as the Nantuo Formation (Chen *et al.* 2002). The Doushantuo Formation is divided into five lithological units: the Lower Dolomite (8.0 m), Lower Phosphate (17.5 m), Middle Dolomite (3.5 m), Wengan Phosphate (7.4 m), and Top Phosphate beds (7.6 m). The Wengan Phosphate bed is a transgressive

sequence bearing extremely well-preserved fossils. The fossils include filamentous bacteria, seaweeds, fungi, metazoan embryos, and adult forms of sponges, cnidarians and bilaterians (Li *et al.* 1998; Xiao *et al.* 1998, 2000; Chen *et al.* 2000, 2002, 2004; Yuan *et al.* 2005). Most of them are phosphatized, either as a part of phosphatic intraclasts 1–5 mm in size or as reworked intraclasts within the matrix. Most developing eggs are preserved in three-dimensions with fine details of cellular structure visible in them; these indicate a very early phosphatization before the egg's compaction, or even before blastomeres and the blastomere's nucleus collapsed.

The Wengan Phosphate contains abundant acritarchs of varied preservation (Yin 1997; Yuan *et al.* 2002). Some of these acritarchs have fine spines that might be confused with the ciliates. However, these fossils lack defined body ciliature and other cytoplasmic structures characteristic of the ciliates. In contrast to the simple depressed 'escape hole' in the acritarchs (Yuan *et al.* 2002), the feeding apparatus in these Precambrian ciliates are much more complicated and shows striking similarities with the extant ciliates.

All three monospecific ciliates are identified from thin sections, which were prepared from the organic-rich black phosphate beds of the Wengan Member. Sections were ground to a thickness of *c.* 70 μm and all the specimens were documented with a series of photos taken at different planes of focus. Comparison study and automontage analysis of the images taken at successive focal planes will provide us with 3D information about the ciliates. The images for the present study were obtained by microscope under direct transmitted or differential interference contrast light.

The two tintinnids from the late Precambrian Wengan Phosphates are not only represented by their loricas but also by the cell body with ciliature and feeding apparatus. The lorica in *Eotintinnopsis* (Fig. 1a) is globular-shaped with a small apertural opening, about 100 μm in diameter. The thin wall consists of a dark organic single layer as in extant tintinnids. The cell body partially protrudes from the aperture, having at least six strongly developed arms with feathery tentacle-like membranelles, 20 μm long and 1.5 μm wide (Fig. 1b). The membranelle is actually a bundle of fused cilia, and usually 16–24 membranelles form a spiraling whorl surrounding the adoral region in living tintinnids. Within the lorica, the cell body continuously extends aborally from aperture to form a conical structure with a stalk-like peduncle attaching to the lorica. Our observation of the sectioned specimen suggests that the wall of the lorica was phosphatized in a very early diagenetic stage even before matrix dewatering. The dewatering has

caused the shrinkage of the matrix filling, thus leading to the formation of a fissure cavity along the inner surface of the lorica. The fissure cavity was later filled by silicated cement. The central adoral region of this cell body may have been ground away during preparation. Therefore a rounded cavity interpreted as a probable prostomial cavity is exposed. A three-dimensional model of this organism is shown in Figure 1c.

The goblet-shaped lorica (Figs 1d and 2a) in *Wujiangella* (about 215 μm long and 150 μm wide) has an apertural shelf that tilts aborally toward a narrow aperture opening at the center of the lorica aperture (Fig. 2a). The aboral end of the lorica appears to be flared and opens externally. The relatively thick wall consists of two organic and agglutinated layers separated with an open space between the two layers (Fig. 2a). Above the shelf, the cell body (155 μm long, 140 μm wide) has at least 35 membranelles (Fig. 1g, 20 μm long, 1.5 μm wide) surrounding the adoral region and numerous cilia (Fig. 1h, 40–50 μm long, 0.5 μm wide) on the rest of its surface. The adoral region represents a depressed, sub-rounded area about 100 μm in diameter (Fig. 1d). In the depressed center of the adoral region is a distinct feeding organelle consisting of a cytostome and a cytopharynx (Fig. 1d and e). Some short cilia can be discerned in the cytostome by differential interference contrast microscopy (Fig. 1e). A three-dimensional model of *Wujiangella* is shown in Figure 1f.

Yonyangella has a subspherical oval cell body, 180 μm long and 150 μm wide, and its surface is densely covered with cilia (20 μm long, 0.5 μm wide). In addition, it has an apical cytostome, and at least 10 tentacle-like structures, each about 15 μm long and 3 μm wide. These structures resemble feeding tentacles in extant suctorians, especially in three ways:

- (1) they are straight;
- (2) they have a distinct wall comparable to a ring of microtubules; and
- (3) they have apical swellings that might represent haptocysts (Fig. 2b–d), which are unique organelles of the suctorians for contacting and paralyzing the prey (Corliss 1979; Harrison & Corliss 1991). The feeding tentacles with haptocysts are a typical feature in suctorians and therefore we interpret *Yonyangella* as a suctorian. Its suctorian affinity is also supported by the presence of a stalk at the aboral end of the cell body for attaching to substrata. Unlike the extant suctorians that are cilia-less (in adult stage) and polystomatic, *Yonyangella* was covered densely with cilia and all the feeding tentacles shared a common mouth-opening at the apical end of

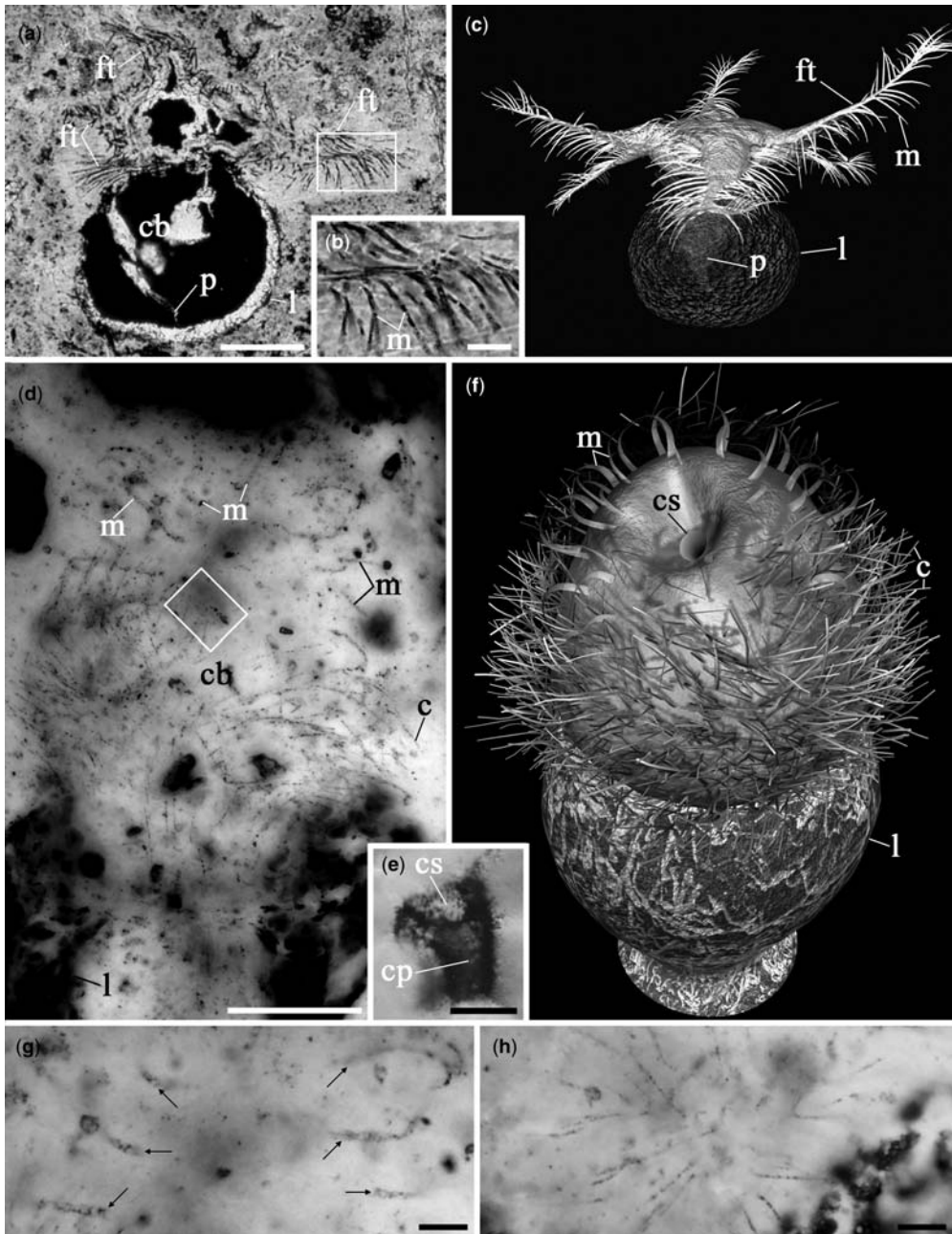


Fig. 1. (a–c) *Eotintinnopsis pinniforma* gen. et sp. nov. (a) A longitudinal section of the holotype, showing the organic lorica (l) and the cell body (cb) with feathery tentacle-like membranelles (ft) and the stalk-like peduncle (p). The membranelles (m) in the frame are magnified in (b). Scale bar: 50 μm in (a) and 10 μm in (b). (c) A reconstruction of this new ciliate. (d–h) *Wujiangella beidoushanese* gen. et sp. nov. (d) An automontage image processed by the software, Image-Pro Plus, which combining 12 successive digital images taken at different focal planes (4 μm apart) of the holotype, showing the organic lorica (l) and the cell body (cb) with somatic cilia (c) and membranelles (m) surrounding the adoral region. Scale bar, 50 μm . The depressed center of the adoral region is framed and focused in deeper plane (e), showing the cytotome (cs) and the cytopharynx (cp) in differential interference contrast microscopy. Scale bar, 10 μm . (f) A reconstruction of this new ciliate. (g) Higher magnification showing 6 membranelles (arrows). Scale bar, 10 μm . (h) Higher magnification showing somatic cilia. Scale bar, 10 μm .

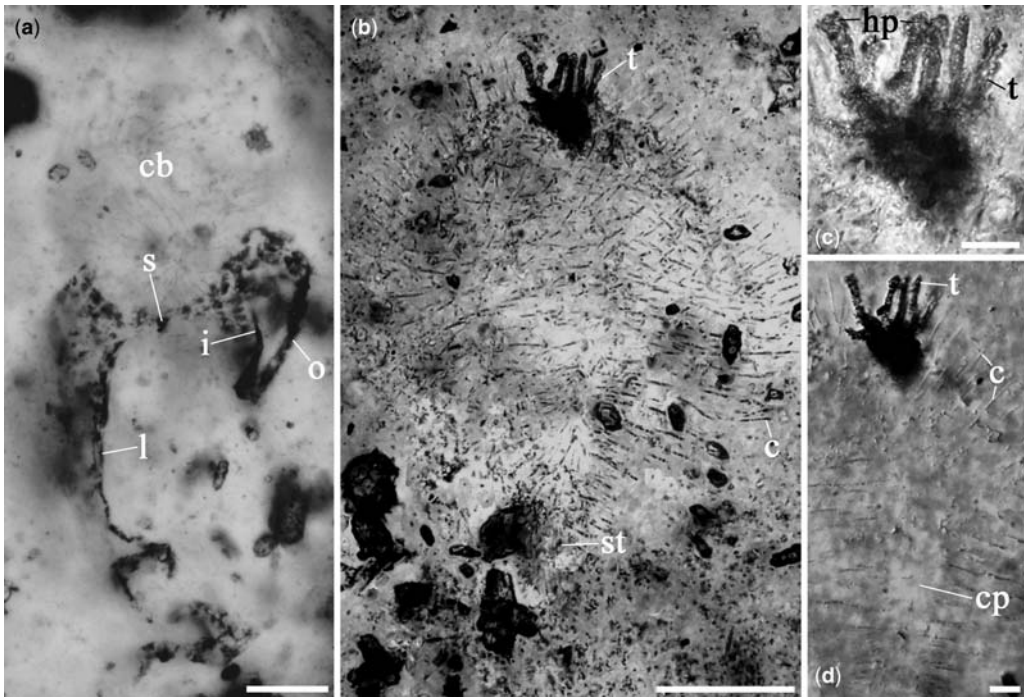


Fig. 2. (a) Complete cell body (cb) and lorica (l) of *Wujiangella beidoushanes*, showing outer layer (o), inner layer (i), and the apertural shelf (s) of the lorica. Scale bar: 50 μm . (b–d) *Yonyangella ovalis* gen. et sp. nov. (b) An automontage image combining 12 successive images of the holotype, showing its stalk (st), cilia (c), and feeding tentacles (t). Scale bar: 50 μm . (c) High magnification of the feeding tentacles (an automontage image combining 5 successive images), showing the apical haptocysts (hp). Scale bar: 10 μm . (d) Differential interference contrast microscopy showing the cytopharynx (cp) underneath the complex of feeding tentacles (t). Scale bar: 10 μm .

the cell instead of polystomy with feeding tentacles in the crown of the suctorians. Interior to the cytostome is a long duct interpreted as cytopharynx (about 75 μm long and 15 μm wide) that extends axially and aborally with a blind end (Fig. 2d).

Ecology

Ciliates occupy nearly every marine environment known. They are most abundant where their food is plentiful (Dolan *et al.* 2002) and that would be in regions of nearshore eutrophic or offshore upwelling regions. Tintinnids live dominantly in upper levels of water column of both offshore, nearshore and shallow embayments and estuaries. Likewise the suctorians attach to substrata and shallow waters are known habitats (Coppellotti & Matarazzo 2000). Deeper-water suctorians are not yet known. The Precambrian tintinnids, together with the suctorians *Yonyangella* and the other fossils from the Wengan Phosphorite, suggest that the ciliates

described here lived in shallow waters not far from a coast line.

Affinity and evolutionary significance

The ciliate affinities of the three organisms are supported by several characters: the presence of cilia or compound ciliary organelles and the presence of a distinct cytostome, (which is associated with the depression and membranelles in *Wujiangella* and with feeding tentacles in *Yonyangella*). As in most of the extant ciliates, the cytostome in both *Wujiangella* and *Yonyangella* possesses a distinct duct-like structure called a 'cytopharynx' that extends from cytostome deep into the cytoplasm. The cytostome in *Eotintinnopsis*, however, lies in a deep preoral cavity and is surrounded by feathery ciliary membranelles protruding from the lorica.

Yonyangella displays a close relationship to prostomian ciliates with apical (or near apical) cytostomes and a near-spherical cell body. The order Prostomatida has been considered as the recent representative of the primitive ciliates from

which the main lines of ciliates including suctorians may have arose (Sleigh 1988), although recent molecular evidence (Wright & Lynn 1997) indicates that they diverged early but did not give rise to other lineages. The relationship of suctorians with other ciliate groups, because of the presence of several unusual characters including tentacles (with haptocysts), stalk and cilia-less in the suctorians, suggests that they too are specialized ciliates at the tip of their own evolutionary branch. The fossil ciliate *Yonyangella* described here, with the presence of the usual combination of suctorian characters (tentacles with haptocysts and a stalk) with prostomian characters (an apical cytostome and somatic cilia), indicates that the suctorian lineage, or one similar to it morphologically, was developed 580 Ma.

The tintinnid affinity of *Eotintinnopsis* and *Wujiangella* is supported by presence of an external cover and apically-located ciliature, which are widely accepted as the most prominent characteristics of the tintinnid ciliates. In addition, feathery membranelles in *Eotintinnopsis* are a distinct character for some tintinnids. Tintinnids are generally regarded as a derived Spirotrich ciliate and one of the last lineages to have evolved (Sleigh 1988; Wright & Lynn 1997).

The fossils reported here confirm that ciliates were highly diversified by the later Neoproterozoic. Because both tintinnids and suctorians are highly derived and terminal clades among modern ciliates, ciliate classes and orders may well have diverged well before the time that metazoans and other eukaryotes appeared about 600 Ma. Indeed the presence of ciliate biomarkers at 850 Ma indicates that the group had a much longer history, dating back to perhaps 1200 Ma when other eukaryotes also diversified (Javaux *et al.* 2001). In addition, these fossils in Neoproterozoic rocks that also contain metazoans may support the hypothesis that the radiation of metazoans was induced by an environmental factor that affected all levels of biological organization.

Systematic palaeontology

Phylum Ciliophora
Class Polyhymenophorea
Order Tintinnida

Genus *Eotintinnopsis* gen. nov.

Type species. *Eotintinnopsis pinniforma* gen. et sp. nov.

Etymology. The generic name is a compound of the living *Tintinnopsis* with a prefix of *eo-* (Gr. primitive or earliest).

Diagnosis. Organic globular lorica (100 μm diameter) with narrow aperture opening. Thin wall

consisting of single layer. Cell body partially protrudes anteriorly from the aperture, having at least six strongly developed arms with feathery tentacle-like membranelles, 20 μm long and 1.5 μm wide. It was conic-shaped, tapering toward base of the lorica to form a stalk-like peduncle.

Remarks. *Eotintinnopsis* is similar to the extant ciliate *Tintinnopsis* (Coppellotti & Matarazzo 2000) in several features, including long feather-like membranelles on adoral region, globular lorica, and an elongated cell-body with a peduncle at posterior end for attachment to the lorica.

Eotintinnopsis pinniforma gen. et sp. nov.
(Fig. 1a–c)

Holotype. A complete cell body with an organic lorica.

Etymology. The specific name refers to its feather-like membranelles (L., *pinniformis*, feather-like).

Diagnosis. Same as in the generic diagnosis.

Genus *Wujiangella* gen. nov.

Type species. *Wujiangella beidoushanese* gen. et sp. nov.

Etymology. The generic name refers to the Wujiang River, near the fossil locality.

Diagnosis. Goblet-shaped lorica having an aperture shelf with an opening at centre relatively thick wall consisting of two, organic agglutinated layers separated with an open space between the two layers. Main part of cell body sitting above the shelf, 155 μm long and 140 μm wide. A slight depressed adoral region rounded and bearing feeding tentacles (numerous membranelles), each 20 μm long and 1.5 μm wide. Somatic cilia, 40–50 μm long and 0.5 μm wide. Cytostome lying at centre of adoral region and deeply situated. A cytopharynx extended anteriorly from cytostome.

Remarks. This new genus is characterized by having a large shallow depression of adoral region, which lies ventrally on aperture surface. The lorica bears an aperture shelf and small opening at central of aperture. In addition to feeding tentacles within the adoral region there are densely arranged somatic cilia in the remainder of the cell surface.

Wujiangella beidoushanese gen. et sp. nov.
(Figs 1d–h, 2a)

Holotype. A complete cell body with an organic lorica.

Etymology. Specific name refers to the Beidou Mountain, near fossil locality.

Diagnosis. Same as in the generic diagnosis.

Class Kinotofragminophora

Order Suctorida

Genus *Yonyangella* gen. nov.*Type species. Yonyangella ovalis* gen. et sp. nov.*Etymology.* The generic name refers to Yonyan, a county-town of Wengan, near fossil locality.*Diagnosis.* Oval cell body elongated, 180 μm long and 150 μm wide. Surface densely ciliated, each cilium 20 μm long and 0.5 μm wide. An apical cytostome about 75 μm long, 15 μm wide; a stalk at aboral end. At least 10 tentacle-like structures lying on distal margin of cytostome, each tentacle 15 μm long and 3 μm wide.*Remarks.* This primitive suctorian ciliate *Yonyangella* differs from most of the extant suctorians by having cilia and a cytostome. Several features including ciliature and an apical cytostome however resemble *Actinobolina*. The present genus differs from the later form by their tentacles, which are fewer in number and larger in diameter, lying at distal margin of cytostome.*Yonyangella ovalis* gen. et sp. nov.

(Fig. 2b–d)

Etymology. Specific name refers to its egg-like shape (*L. ovalis*, egg-shaped).*Holotype.* A complete cell body.*Diagnosis.* Same as in the generic diagnosis

Supported by National Science Council (Taiwan, China) and Chinese Academy of Science Grant KZCX3-SW-141 and National Science Foundation of China (2006CB806400). Thanks are also due to two anonymous reviewers for comments that improved the manuscript. All the fossil material has been deposited at the Early Life Research Centre (Nanjing Institute of Geology and Palaeontology), Chengjiang, China.

References

- CHEN, J.-Y., OLIVERI, P., LI, C. W., ZHOK, G. Q., GAO, F., HAGADORM, J. W., PETERSON, K. J. & DAVIDSON, E. H. 2000. Precambrian animal diversity: Putative phosphatized embryos from the Doushantuo Formation of China. *Proceedings of the National Academy of Sciences U.S.A.*, **97**, 4457–4462.
- CHEN, J.-Y., OLIVERI, P., GAO, F., DORNBOSS, S. Q., LI, C. W., BOTTJER, D. J. & DAVIDSON, E. H. 2002. Precambrian animal life: Probable developmental and adult cnidarian forms from southwest China. *Developmental Biology*, **248**, 182–196.
- CHEN, J.-Y., BOTTJER, D. J., OLIVERI, P., DORNBOSS, S. Q., GAO, F., RUFFINS, S., CHI, H., LI, C. W. & DAVIDSON, E. H. 2004. Small bilaterian fossils from 40 to 55 million years before the Cambrian. *Science*, **305**, 218–222.
- COPPELLOTTI, O. & MATARAZZO, P. 2000. Ciliate colonization of artificial substrates in the Lagoon of Venice. *Journal of the Marine Biological Association of the United Kingdom*, **80**, 419–427.
- CORLISS, J. O. 1979. *The Ciliated Protozoa*. 2nd edn, Pergamon Press.
- DOLAN, J. R., CLAUSTRÉ, H., CARLOTTI, F., PLOUNÉVEZ, S. & MOUTIN, T. 2002. Microzooplankton diversity: relationships of tintinnid ciliates with resources, competitors and predators from the Atlantic Coast of Morocco to the Eastern Mediterranean. *Deep-Sea Research (Part I, Oceanographic Research Papers)* **49**, 1217–1232.
- HARRISON, F. W. & CORLISS, J. O. 1991. *Microscopic Anatomy of Invertebrates (1): Protozoa*. Wiley-Liss, New York.
- HARVEY, H. R. & MCMANUS, G. B. 1991. Marine ciliates as a widespread source of tetrahymanol and hopan-3-beta-ol in sediments. *Geochimica et Cosmochimica Acta*, **55**, 3387–3390.
- JAVAUX, E. J., KNOLL, A. H. & WALTER, M. R. 2001. Morphological and ecological complexity in early eukaryotic ecosystems. *Nature*, **412**, 66–69.
- KOSHEVOU, V. V. 1987. *Izvestiya Veshich Ycheniye Zavedeniya, Geologiyai Pazvedka*, **2**, 20.
- LI, C.-W., CHEN, J.-Y. & HUA, T.-E. 1998. Precambrian sponges with cellular structures. *Science*, **279**, 879–882.
- SLEIGH, M. A. 1988. *Protozoa and Other Protists*. Edward Arnold Publishers, London.
- SUMMONS, R. E., BRASSELL, S. C., EGLINTON, G., EVANS, E., HORODYSKI, R. J., ROBINSON, N. & WARD, D. M. 1988. Distinctive hydrocarbon biomarkers from fossiliferous sediment of the Late Proterozoic Walcott Member, Chuar Group, Grand Canyon, Arizona. *Geochimica et Cosmochimica Acta*, **52**, 2625–2637.
- TAPPAN, H. 1993. Tintinnids. In: LIPPS, J. H. (ed.) *Fossil Prokaryotes and Protists*. Blackwell Scientific Publications, Oxford, 285–303.
- WRIGHT, A. D. G. & LYNN, D. H. 1997. Maximum ages of ciliate lineages estimated using a small subunit rRNA molecular clock: Crown eukaryotes date back to the Paleoproterozoic. *Archiv Protistenkd*, **148**, 329–341.
- XIAO, S., ZHANG, Y. & KNOLL, A. H. 1998. Three-dimensional preservation of algae and animal embryos on a Neoproterozoic phosphorite. *Nature*, **391**, 553–558.
- XIAO, S., YUAN, X. & KNOLL, A. H. 2000. Eumetazoan fossils in terminal Proterozoic phosphorites? *Proceedings of the National Academy of Sciences U.S.A.*, **97**, 13684–13689.
- YIN, L. 1997. Precambrian–Cambrian transitional acritarch biostratigraphy of the Yangtze Platform. *Bulletin of National Museum of Natural Science (Taipei)*, **10**, 217–231.
- YUAN, X., XIAO, S. & TAYLOR, T. N. 2005. Lichen-like symbiosis 600 million years ago. *Science*, **308**, 1017–1020.
- YUAN, X.-L., XIAO, S.-H., YIN, L.-M., KNOLL, A. H., ZHOU, C.-M. & MU, X.-N. 2002. *Doushantuo Fossils: Life on the Eve of Animal Radiation*. The University of Science and Technology of China Press, Hefei [in Chinese, with English summary].

New data on *Kimberella*, the Vendian mollusc-like organism (White Sea region, Russia): palaeoecological and evolutionary implications

M. A. FEDONKIN^{1,3}, A. SIMONETTA² & A. Y. IVANTSOV¹

¹*Paleontological Institute, Russian Academy of Sciences, Profsoyuznaya ul., 123, Moscow, 117997 Russia (e-mail: mfedon@paleo.ru)*

²*Dipartimento di Biologia Animale e Genetica 'Leo Pardi', Università degli studi di Firenze, via Romana 17, 50125 Florence, Italy*

³*Honorary Research Fellow, School of Geosciences, Monash University, Melbourne, Victoria 3800, Australia*

Abstract: The taphonomic varieties of over 800 specimens of *Kimberella* (collected from the Vendian rocks of the White Sea region) provide new evidence of the animal's anatomy such as: shell morphology, proboscis, mantle, possibly respiratory folds and possibly musculature, stomach and glands. Feeding tracks, crawling trails and, presumably, escape structures preserved along with the body imprint provide insights on the mode of locomotion and feeding of this animal. The shield-like dorsal shell reached up to 15 cm in length, 5–7 cm in width, and 3–4 cm in height. The shell was stiff but flexible. Evidence of dorso-ventral musculature and fine transverse ventral musculature suggests arrangement in a metameric pattern. Locomotion may have been by means of peristaltic waves, both within the sediment and over the surface of the sea floor, by means of a foot resembling that of monoplacophorans. Respiration may have been through a circumpedal folded strip (possibly an extension of the mantle). Feeding was accomplished by a retractable proboscis bearing terminal hook-like organs and provided with a pair of structures interpreted here as glands. Whilst feeding, *Kimberella* moved backwards. The structural complexity of *Kimberella* poses questions about the time of origin of the triploblastic metazoans.

The Late Precambrian *Kimberella quadrata* Glaessner & Wade, 1966 was originally described from the late Precambrian Pound Quartzite of Ediacara Hills, South Australia. Originally considered as a problematic fossil, possibly belonging to the Siphonophora (Glaessner, in Glaessner & Daily 1959), *Kimberella* was then reconstructed as a medusa of uncertain affinities (Glaessner & Wade 1966). Known from a few specimens, it was later interpreted as a cnidarian pelagic medusa, closely related to extant cubozoans or box jellies (Wade 1972). Later authors have reconstructed *Kimberella* as an animal similar to extant chirodropid cubozoans or sea wasps (Glaessner 1984; Jenkins 1984, 1992; Gehling 1991). Thus reconstructed, *Kimberella* has been used as one of the best examples of a metazoan lineage crossing the Precambrian-Cambrian boundary with essentially no morphological change up to the present day. It has been cited as one of the most convincing counterexamples against hypotheses grouping all Vendian macrofossils in non-metazoan higher taxa (*sensu* Seilacher 1992). The acceptance of *Kimberella* as an essentially modern cubozoan also had major palaeoecological implications: living chirodropids are fast-swimming predators

with powerful venom, and *Kimberella* thus has also been reconstructed by some as a coelenterate predator (Jenkins 1992).

New fossil material from the Vendian of the White Sea region forced reinterpretation of *Kimberella* as a mollusc-like animal (Fedonkin & Waggoner 1997) with a high dorsal, non-mineralized shell and an animal capable of active locomotion. The radioisotope U–Pb age 555.3 ± 0.3 Ma of a zircon from a volcanic ash bed in the Vendian marine siliciclastic rocks inside the stratigraphic range of *Kimberella* in the Winter Coast of the White Sea region was, therefore, assumed as the minimum age for the oldest triploblastic invertebrates (Martin *et al.* 2000). This is the oldest calibration point of molecular clocks for the Precambrian bilaterians. Co-occurrence of the body fossils and trace fossils produced by *Kimberella* revealed the mode of feeding and locomotion of this animal (Ivantsov & Fedonkin 2001; Fedonkin 2001, 2003; Gehling *et al.* 2005).

In this paper we describe a new fossil collection of unique preservation, which sheds light on the previously unknown aspects of morphology, anatomy and lifestyle of *Kimberella*.

Stratigraphic setting

Over 800 specimens of *Kimberella* have been excavated from the Vendian siliciclastic rocks in the White Sea region, northern Russia during the last few years. Major fossil localities were discovered in the deposits exposed in the valleys of rivers of the Onega Peninsula (Suzma, Karakhta, and Solza rivers) and on Zimny Bereg (Winter Coast) of the White Sea. Most of the collection described here has been systematically excavated by the field teams led by A. Ivantsov. Some specimens were found in the core of boreholes. All the fossils are preserved on the soles of the fine-grain sandstones or mudstone beds intercalated with the clay lamina within the Verkhovka, Zimmie Gory and Yorga formations of the Vendian. Stratigraphy and the sedimentology of the fossiliferous deposits have been described by Grazhdankin (2003). These sedimentary successions were formed in off-shore shallow water marine conditions under influence of a vast deltaic system, which prograded towards the SW from the Kanin–Timan fold-and-thrust belt. The stratigraphic range of *Kimberella* exceeds the radiometrically dated time interval 555–558 Ma based on ages determined on zircons from the volcanic ash beds (Martin *et al.* 2000; Grazhdankin 2003).

Taphonomy and ecology

Environmental conditions of the deltaic platform of the Vendian Basin were characterized by sporadic turbid flows initiated by seasonal precipitation, snow melt or storm events. These ‘density currents’ produced deep erosion that modified bottom relief and sporadically brought about catastrophic sedimentation, burying entire benthic populations *in situ*. Preservation of *Kimberella* on the sand-clay interface is often associated with the imprints of bacterial mats (‘elephant skin structure’ and other kinds of shagreen surfaces) and abundant benthic algae such as the filamentous *Striatella* and the net-like *Orbisiana* (Grazhdankin & Ivantsov 1996). This indicates that *Kimberella* preferred calm, well-aerated conditions of shallow marine habitats, well inside the photic zone where benthic photosynthesis could be quite effective. These conditions seem to have existed long enough to allow epibenthic communities to form and reach maturity. This assumption can be substantiated by the usual association of *Kimberella* with other benthic organisms, such as the vagile bilaterians *Yorgia*, *Dickinsonia* and *Andiva*, discoidal *Tribrachidium* and frond-like *Charniodiscus*. The co-occurrence of individuals of different species with body sizes ranging from 0.2 to 50 cm in length in their life

positions, and often associated with traces of their activity on the vast bedding planes, appears to represent actual community structure.

We conclude that the depth of *Kimberella*'s habitats ranged from the uppermost subtidal zone down to a depth of tens of metres. That most of the fossiliferous sediments seem to be formed below the storm wave base does not necessarily reflect a great depth in a broad, shallow marine basin. The habitat would probably have provided a reasonably high primary production due to the availability of dissolved mineral nutrients eroded from a nearby subaerial landmass. This conclusion is supported by the fact that the Vendian metazoan fossil assemblages had a very high density, comparable to that of the recent populations living in shallow marine environments. Sedentary benthic species such as *Nemiana* and the burrowing organisms that produced the traces *Skolithos*, may reach 100 and 400 individuals per square decimetre. In the Solza River basin, A. Ivantsov was able to trace one fossiliferous layer whose surface was completely processed by grazing *Kimberella* for a few hundred metres laterally. This fossiliferous bedding plane bears both the trace fossils and numerous body imprints of small individuals (<1 cm long), perhaps reflecting initial colonization of an open habitat by newly hatched *Kimberella*.

The taphonomic variability of *Kimberella* is very high. Preservational diversity allows detailed reconstruction of the external morphology and even the internal anatomy, as well as locomotion and feeding styles. Several preservation modes of the soft body imprints of *Kimberella* occur in addition to the imprints of separate shells, feeding tracks, crawling trails and perhaps escape structures. This rich taphonomic spectrum for a single species of metazoan seems to have formed under influence of a variety of factors: (1) *Kimberella*'s anatomical and morphological complexity preserved at different stages of development, from juveniles to adults; (2) a relatively high diversity of the habitat occupied by the animal; and (3) variations in the properties of the fossiliferous rocks. The case of *Kimberella* demonstrates the immense value of large fossil collections, systematically sampled from different localities and a variety of sedimentary facies that represent a wide spectrum of palaeoenvironments.

Most specimens of *Kimberella* seem to preserve the relative positions that they occupied in life on the sea bottom. These organisms were unable to move quickly enough to escape rapid burial in sand. The initial disturbance of their surroundings caused these animals to retract all soft parts under a shell, thus initially protecting them from fouling. Very few specimens preserve what appear to be

soft tissues spreading beyond the shell edge. This behaviour could certainly have helped them to survive episodic turbidity currents or storm events, but did not prevent death in the case of catastrophic sedimentation. Some individuals, usually relatively small ones, are preserved at the end of their feeding tracks or crawling trails. Of particular interest are the fossil crawling trails that cross the grazing marks of the animal as it presumably tried to escape the accumulating sediment. Such fossils reflect the dynamics of benthic life of *Kimberella*. Most of this latter category of fossils is represented by small juveniles commonly preserved in the laminated siltstone that do not bear any features of sudden rapid sedimentation. Slow sedimentation did not kill some larger individuals, but in this circumstance some juveniles failed to escape even though they were able to move a few centimetres through the water-saturated sediment.

Many specimens show an anterior elongated structure, here interpreted as a proboscis, and a pair of basal miniature structures that may represent two pharyngeal glands. These features as well as the imprints of a dorsal surface of the shell with a peculiar ornamentation are illustrated here for the first time. In many cases the surface of the fossil retains not only the external appearance of the organisms, but also overprints of internal anatomical structures. The overprinting phenomena have been reported before in other Vendian metazoan fossils, as in the case of the diverticula of the gut of the segmented bilaterians *Dickinsonia*, *Yorgia* and others (Jenkins 1996; Dzik & Ivantsov 2002; Ivantsov *et al.* 2004). The body fossils of *Kimberella* also provide a number of examples of overprinting, particularly of the gut and musculature. The ventral surface of the soft body is often well-preserved, in spite of *post mortem* deformations related to the decomposition of the tissues as well as to the compaction, dewatering and other diagenetic changes of the sediment.

A critical role in the preservation of the soft-body imprints and bioturbations may have been played by the mucus secreted by *Kimberella* while it was alive. Animal mucus (a complex glycoprotein mixture) could act as glue that cemented the underlying mud. If we assume that it was secreted by a dying animal and that it was immediately attacked by bacteria living in the sediment, such a mucus-clayey mixture may have produced a kind of biofilm that was cohesive and elastic enough to remain intact during the post-mortal deformations. The taphonomic process that ended in the fossilization of the soft parts can be reconstructed as follows: (1) fast sedimentation covers the animal resting on the surface of the muddy bottom; (2) formation of a mucus-clayey film under the foot of animal; (3) the soft mud from below moves

upward replacing the space occupied by the decomposing soft body under the shell; (4) the cohesive film on the mud surface meets resistant structures (such as internal organs) that leave imprints over the mucous film; and (5) full decomposition of the shell and its collapse. Rapid mineralization of the sediment immediately above the decaying animal due to bacterial interaction with the decay products might have played a significant role in the formation of the body fossils of *Kimberella* as well. This phenomenon is described by the 'death mask' taphonomic model that is applicable to some Ediacara organisms (Gehling 1999). The presence of a clay layer below the fossil imprint is indicative of a prolonged period of very slow sedimentation, which allowed establishment of the microbial films and bacterial mats. These were likely the feeding substrate and acted as a taphonomic factor. In addition, clay effectively decreases permeability of the sediment, thus increasing the rate of fossilization due to early diagenetic mineralization. The properties of the substrate on which *Kimberella* lived can be deduced to some extent based on the preservation style of the finest scratch marks, which could have been preserved only in case of cohesive sediment. Some casts of the pits in the feeding tracks may be interpreted as biofilm tears.

Kimberella is always preserved in negative hyporelief, that is by depressions of various depth on the sole of the competent bed (sandstone or mudstone). This kind of preservation puts *Kimberella* in a category of 'resistant' fossil *sensu* Wade (1968), implying that the original structure was comparatively firm in order to retain its shape in spite of decomposition and compaction of the sediment. However, no direct signs of biomineralization have been found. There is now evidence of pyritization, common to most specimens, related to the *post mortem* taphonomic processes, in particular, to the activity of the sulphate reducing bacteria. Our field observations indicate that the amount of pyrite precipitated is roughly directly proportional to the body size of *Kimberella*, and in reverse to permeability of the sediment.

Fossil material is of *Kimberella quadrata* (Glaessner & Wade 1966); Vendian sequence deposits (Ediacaran in age), White Sea Region, Russia. All figured specimens are accompanied by the museum catalogue numbers of the Vendian Collection, Laboratory of Precambrian Organisms, Paleontological Institute (PIN), Russian Academy of Sciences, Moscow. Most of the figured specimens are latex casts pulled from the actual fossils preserved as impressions into the sole of the overlying sandstone layer, negative hyporelief. For photography the latex casts are coated with ammonium chloride, which helps to reveal fine morphological detail. Pictures of the rock specimens are indicated

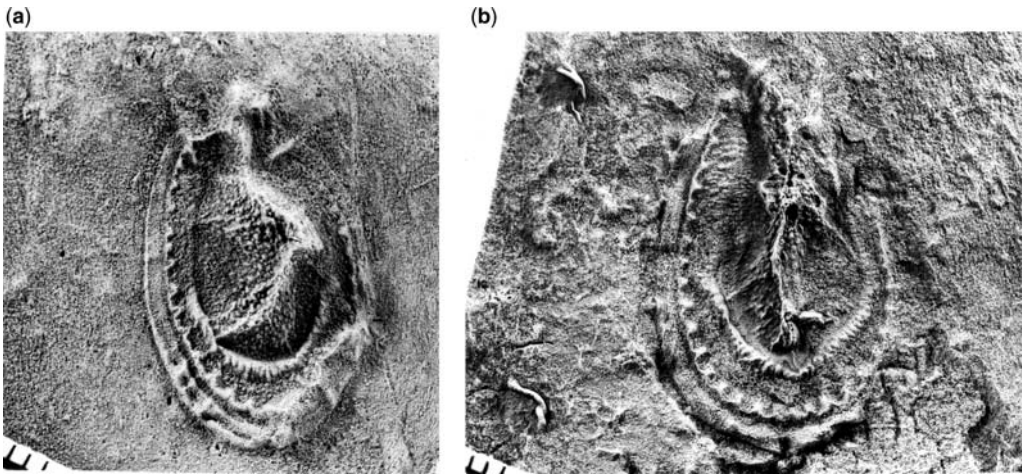


Fig. 1. (a) PIN 3993–5573. (b) PIN 3993–5575. Latex peel of bed sole. Scale in mm. Overall shape of the fossil showing oral (narrow) end and aboral (wide) end, smooth external outline of the foot (left side of both specimens) and distorted shell above.

in the captions (Figs 4, 11, 13a, 19a, b). All photographs are provided with a millimetre-scale bar.

These >800 specimens are all collected from the Ust'-Pinega Formation (Upper Vendian sequence) in the southeastern White Sea Region, Arkhangel'sk District, Russia. Major fossil localities occur between Medvezhy Creek and the Yorga River along the Winter Coast of the White Sea, about 100 km north of Arkhangel'sk City, and from outcrops in the valleys of Suzma, Solza and Karakhta rivers, Summer Coast, on the northeastern Onega Peninsula.

Geographic position is indicated by the first four digits of the specimen numbers: 3993, Winter Coast, White Sea; 3992, Suzma River; 4853, Solza River; 4852, Karakhta River; all the last three localities are on the northeastern Onega Peninsula, Summer Coast, White Sea.

Morphology of *Kimberella*

Most of the body fossils are oval-shaped, bilaterally symmetrical imprints, with several zones arranged concentrically. The length of the fossils ranges from 2–3 mm to 150 mm. The large number of specimens available may be arranged as a growth series and allows observation of the effect of taphonomic phenomena, which is informative of both external morphology and internal anatomy. Extensive use of latex replicas in the study of these fossils helped to reveal fine detail, in particular, of the smallest individuals. It is convenient to use neutral descriptive terms for characters of the body fossils and later offer interpretation of these features.

Shell

The rounded, broader end of the fossil is here considered as the posterior (aboral) end of the organism (Fig. 1a, b). In most of the specimens, it is well-preserved. The anterior (oral) end tends to be narrower than the posterior (aboral). Termination of the oral end is rather variable and may depend on its lesser mechanical durability. The best-preserved specimens demonstrate that the anterior part was a narrow, tapering structure that resembles a hood, with a clear, bilobate fore end, present even in the juveniles (Figs 2, 5a–b, e, 7b).

The high, dorsal shell has an elongated oval, shield-like outline, which ranges from nearly



Fig. 2. PIN 3993-5590. Latex peel of bed sole. One of the smallest specimens still identifiable as *Kimberella*. Almost discoidal shape can be partially explained by the flattening in the course of decomposition.



Fig. 3. PIN 3993-5084. Latex peel of bed sole. Scale in cm. Such large individuals are usually characterized by their slender outline, deep medial depression and well-preserved imprints of the soft parts. However, large fossils normally do not show any remnants of the shell.

round in many of the small specimens to a much more elongated structure in larger individuals. However, some very small individuals are often strongly elongated, and it is suggested here that these individuals represent a phase when the formation of the shell had not yet begun or was just incipient. In this state, individuals were able to contract or extend themselves to a greater extent than adults. The tallest zone of the shell is bordered by a flatter limb. The hood-like structure on the narrow anterior end is often visible in the relatively larger specimens (Fig. 5a, b) and weakly developed in the smallest (Fig. 5c). The outer surface of the dorsal side of the smaller specimens is covered with numerous round protuberances, uniformly spaced over the major part of the shell. In the smallest specimens, these protuberances are all approximately the same size (Fig. 5c, d). In larger shells, the size of the protuberances decreases towards the periphery (Fig. 5a–b, e). The nature of the



Fig. 4. PIN 3993-5607. Rock specimen of small individual. Regular shape of deep medial invagination with some traces of segmentation may represent the internal structure such as a simple gut (well preserved in the specimens shown below).

protuberances is not clear although there are some possible interpretations: the protuberances might be simple outgrowths marking the shell surface or, alternatively, they may represent separate initial nodules of shell formation. In connection with the latter hypothesis, an analogy of the formation of small, separate platelets in the development of late metatrochophores of some molluscs is suggested. These platelets later fuse into larger plates (as in *Chiton*), or disappear in others (some adult Solenogastres such as *Neomenia*). Alternatively, these protuberances might be the bases for fine mineral spines, such as those in recent *Patella lusitanica* (Archeogastropoda, Prosobranchia).

In many small specimens the peripheral shelf of the shell bears numerous, radially oriented, short ribs that are regularly spaced (Fig. 5c, d). Both protuberances and the ribs are clearly visible, even in the smallest specimens, although fewer in number (Fig. 6a). However, in some well-preserved specimens the peripheral shelf with the ribs is covered by what appears to be soft tissue (Fig. 5a–b, e). This tissue is interpreted as an edge of the mantle by analogy with modern molluscs (for instance, many prosobranchs and pulmonates) whose mantle may spread over the outer surface of the shell.

The taphonomic varieties of the shell imprints clearly demonstrate that the shell was stiff, but thin and flexible, particularly in juveniles (Fig. 6b). In the smallest specimens, the shell is almost flat, being deformed in the course of

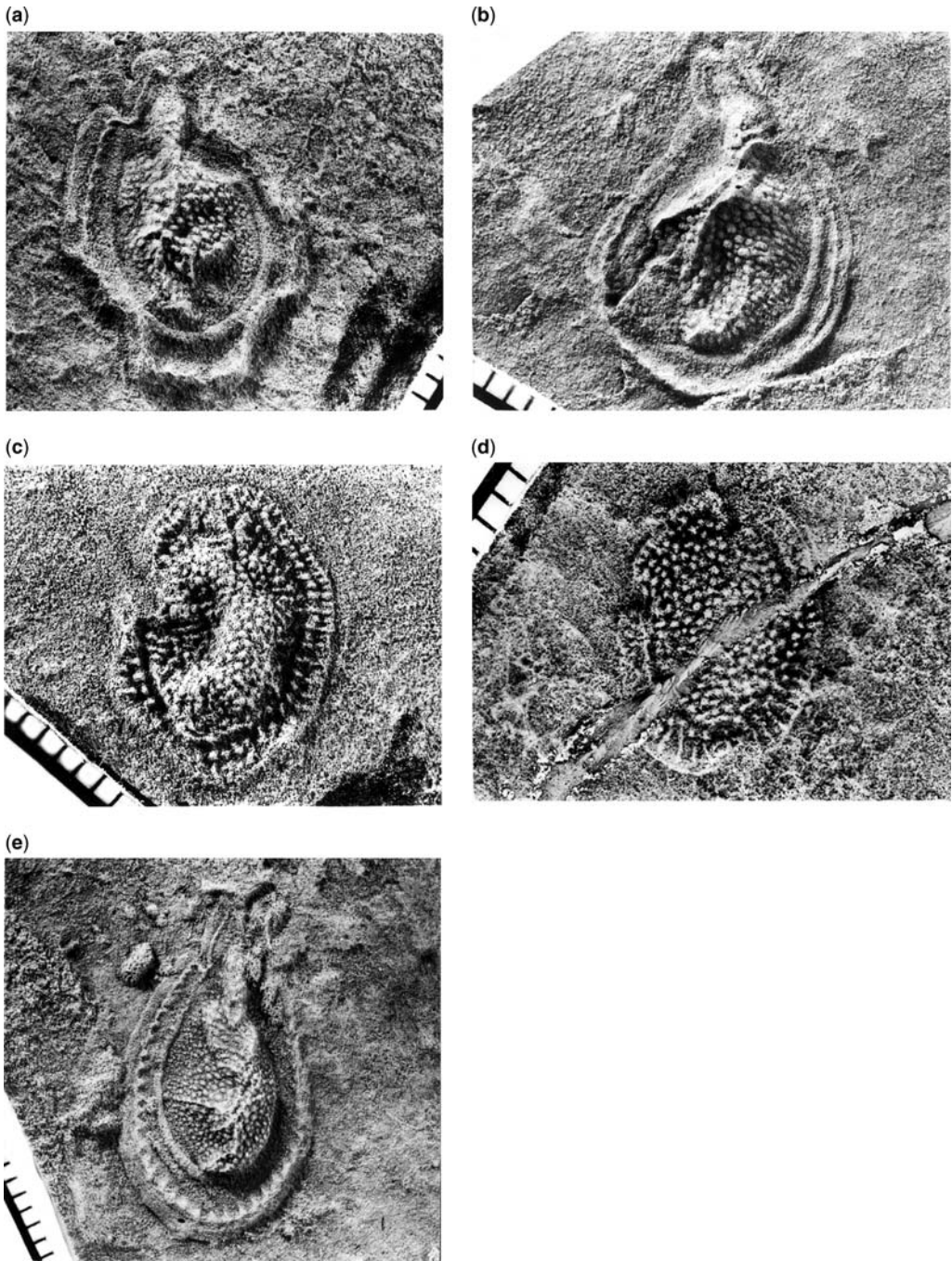


Fig. 5. (a) PIN 3993-5570. (b) PIN 3993-5585. (c) PIN 3993-5609. (d) PIN 3993-5599. (e) PIN 3993-5604. Latex peels of bed sole. External surface of the shell demonstrates its characteristic knobby relief (covered with protuberances). Anterior, hood-like bilateral elongation is well expressed in larger specimens (Fig. 5a, b) and hardly developed in very small individuals (Fig. 5c) in spite of outstanding preservation of shell dorsal surface detail. No obvious growth zonation can be seen in the shell structure.

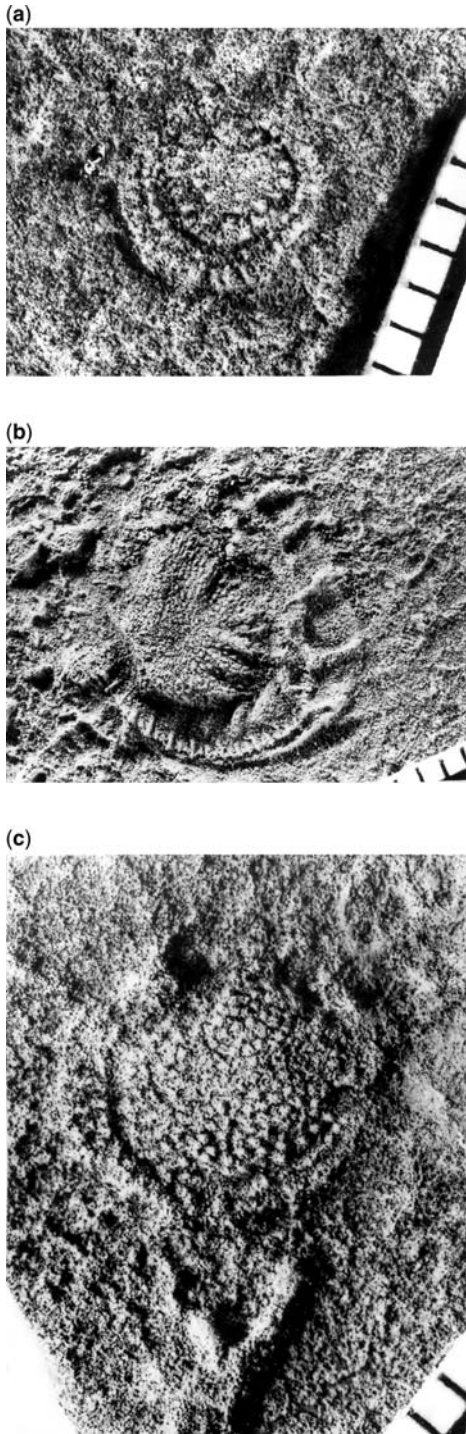


Fig. 6. (a) PIN 4852-94. (b) PIN 4852-93. (c) PIN 3993-5564. Latex peel of bed sole. External surface of the shell in small individuals. Mode of deformation indicates the thin and flexible shell wall.

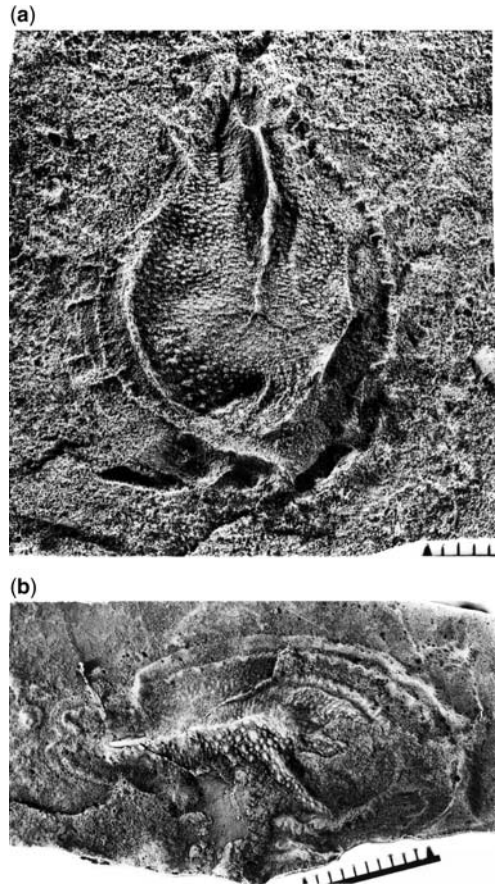


Fig. 7. (a) PIN 4852-265. (b) PIN 3993-5554. Latex peel of bed sole. Mode of post mortem deformation of the shell. Oral end of organism with bilobate outline is well preserved and clearly visible in Figure 7b.

sediment compaction and organic decomposition (Fig. 6a, c). The fact that the vast majority of specimens did not preserve a shell indicates that it was rather fragile and could be subjected to fast microbial decomposition (in case of its organic composition) or chemical dissolution (in case of biomineralization) after death. Having in mind that the Vendian palaeobasins of the Russian platform lay well beyond the carbonate belt of the planet, one can assume that the biomineralization of the shell, if any, could hardly have been considerable. A sharp longitudinal folding of some deformed shells (Figs 5b, 7a), as well as broken fragments of the shell (Fig. 7b), demonstrate that the thickness of the shell in the individuals 30–40 mm long did not exceed 0.3 mm. The shell was apparently purely organic and became more rigid with growth, explaining why the larger

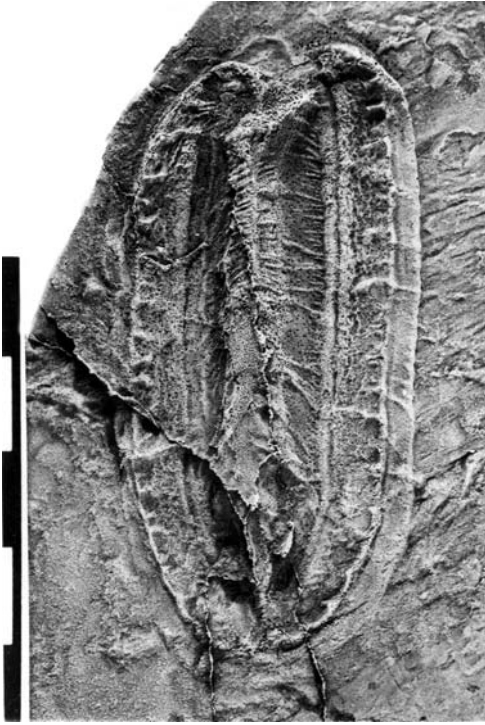


Fig. 8. PIN 3993-5136. Latex peel of bed sole. Scale in cm. In spite of heavy vertical deformation of the soft tissues of a relatively large individual, its axis remains straight. Oral (upper) end is commonly more deformed than the aboral, even in large individuals.

specimens are normally straight and seldom show lateral bending. If such bending does occur, it may be due to deformations of the non-lithified sediment in late diagenesis after full decomposition of all tissues including the shell material (Figs 3, 8). As indicated above, the smaller individuals do demonstrate some lateral bending, which is quite rare for the larger individuals (Fig. 9a, b). This may indicate some flexibility of the shell during its early development.

The cast of the internal surface of the shell can be seen in some specimens in which the shell is partially preserved (Figs 1a–b, 7b, 10a–d). The internal impression of the shell is comparatively smooth in the upper part showing, in some specimens, fine transverse striations (Figs 1b, 10a, d) that perhaps related to muscle scars of the possible dorso-ventral musculature. More prominent but no less enigmatic, structures are preserved in specimens shown in the figure 1a, b. These structures occur around the periphery of the shell, close to the shelf: distinct, short, linear imprints that are oriented radially and lie lying very close to each other (almost fused at their proximal ends). One interpretation of these structures, which resemble rather deep and regularly spaced imprints on the internal side of the shell, is that they represent the attachment points (muscle scars) of the musculature of the foot retractors, similar in position and outline to such muscle scars of the Palaeozoic *Pilina*, a monoplacophoran.

The absence of any growth zonation in the shell structure suggests that the shell of *Kimberella* was the homologue of the periostracum of later Mollusca.

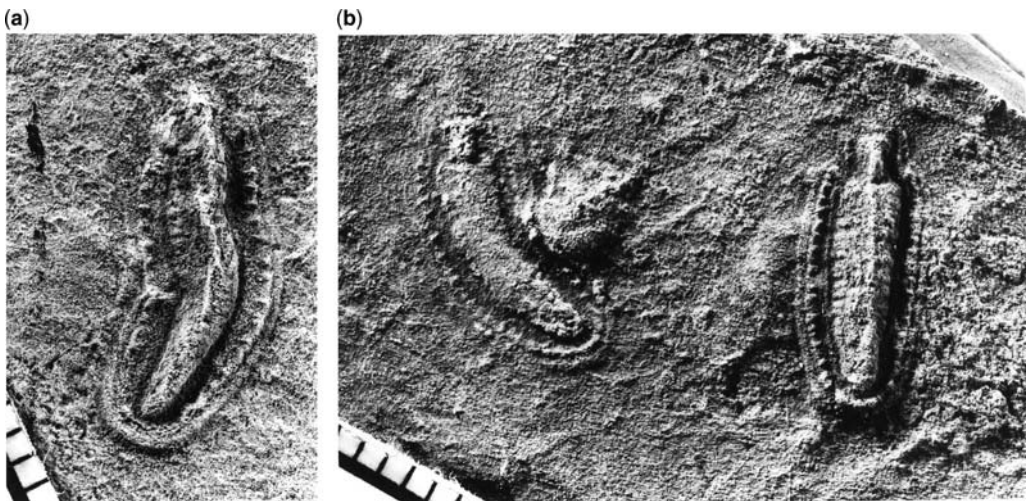


Fig. 9. (a) PIN 3993-5605. (b) PIN 3993-5533. Latex peel of bed sole. Examples of lateral bending of the body in small individuals.

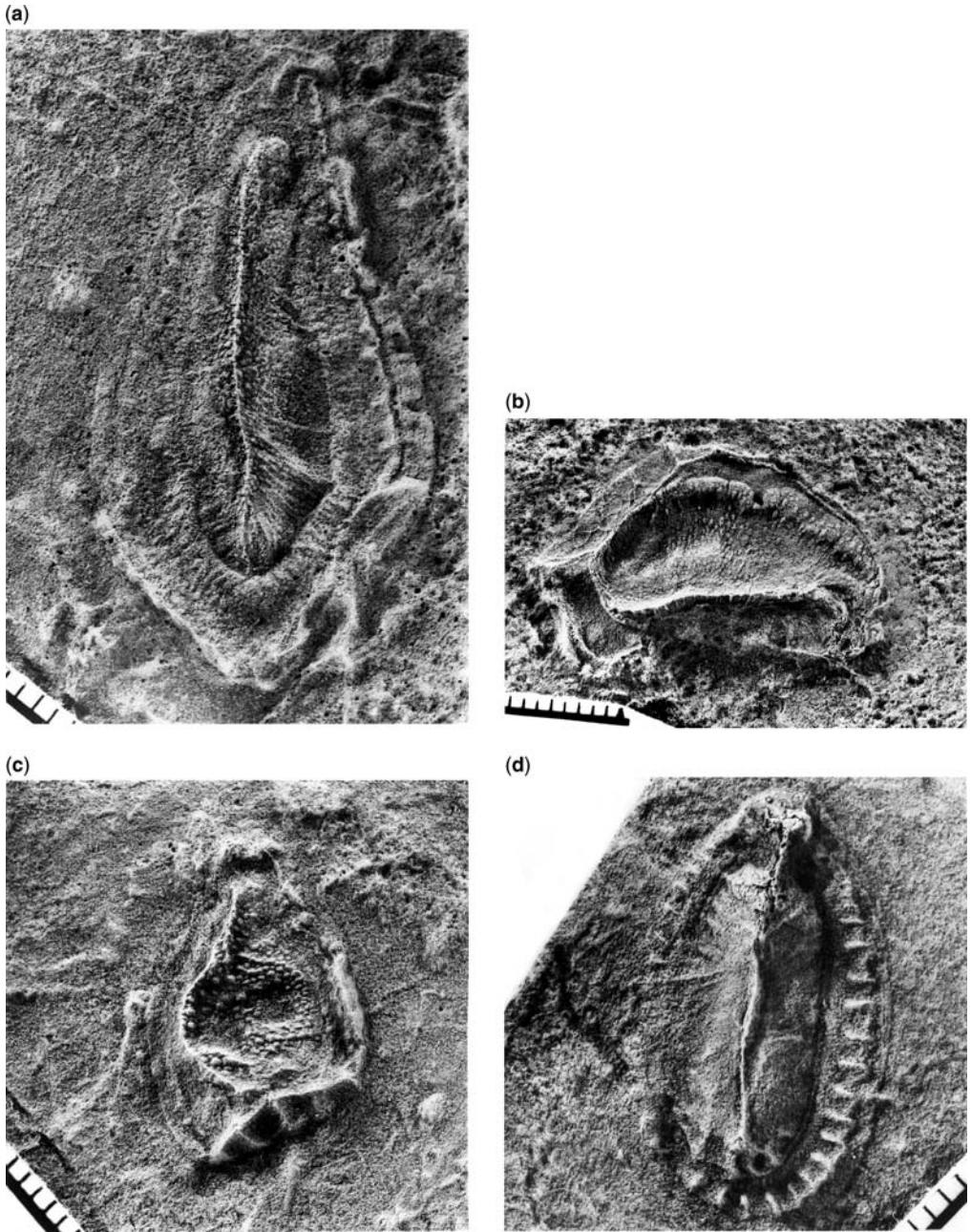


Fig. 10. (a) PIN 3993-6501. (b) PIN 3993-5608. (c) PIN 3993-5574. (d) PIN 3993-5581. Latex peel of bed sole. Specimens showing imprints of some internal surface structures. Transverse ridges on the surface of the latex peels (Figs 10a, d) could reflect the position of the muscle scars and metameric arrangement of the muscle myomers, but could be due to simple deformation or other causes. Degree of flexibility of the shell can be seen in Figure 10c showing overfolding of aboral end of the shell.



Fig. 11. PIN 3993-4004. Rock specimen. Scale in cm. One of the largest individuals ever found. Lower portion is cut off by a sand-fill of the syneresis crack. This strongly asymmetric fossil is interpreted as a ventral impression, with the left half well-preserved, while most of the right half appears to have disappeared into a slit due to the collapse of deep invagination during the post mortem taphonomic process inside the sediment. The left side is remarkably smooth with very fine, oblique furrows which course from the medial furrow to the 'crenulated zone' and cut the proximal ridge. Like transverse wrinkles, these oblique furrows seem to be related to the structures, which were close to the ventral surface. The proximal ridge is interpreted here as an outline of a completely contracted foot.

Soft parts

Although the external morphology of the soft parts is usually best preserved in large specimens, details of internal anatomy are commonly preserved in the smaller fossils. The preservation of the latter can be explained by the increased chance of overprinting of the internal structures through thin external tissues. Oval imprints of the soft body are usually preserved as concentric zones, showing different relief and modes of deformation.

Anterior end. New material shows that the anterior end of the soft body had a rather complex structure. All features do not appear in every specimen, but some clearly demonstrate that at least part of the anterior end was protrusible; although the extent of such protrusion may be only indirectly inferred from the scratches the animal was apparently capable of producing on the bacterial mat upon which it fed. Again, as clearly seen in some specimens, this anterior organ housed a pharynx provided with paired sac-like structures, which may have been pharyngeal glands (comparable with those found in many extant molluscs). As many otherwise well-preserved specimens, especially larger ones, do not show any evidence of these structures it is presumed that the protrusible organ could be retracted completely under the mantle and shell (see discussion below).

Inner zone. The inner zone (bounded by a narrow proximal ridge) is flat and smooth in non-deformed individuals (Figs 11, 12), and it must be the imprint of the ventral side of the organism. However, quite often, the inner zone shows a variety of deformations, such as numerous transverse wrinkles or lobes, and some longitudinal markings. The inner zone also reflects vertical deformation: most of the imprints have longitudinal invagination that may be deep enough to involve, in some cases, most of the inner zone (Fig. 3). This invagination may be caused both by the contraction of dorso-ventral muscles when the foot was retracted and by the encroachment of the clay following the decay of the inner organs. The depth of the medial invagination can reach 20 mm in the largest fossils. In a number of cases, particularly in the large specimens, the walls of such deep invagination join, producing a slightly curved longitudinal furrow (Fig. 13a). This phenomenon may have been caused by a side tilt of the laterally collapsed shell and specimens could give a false impression on the width of the ventral side. Some specimens show one side preserved in full while another is almost completely folded in by the collapsed invagination (Figs 11, 13b). The inner zone is interpreted here as a contracted foot.

Proximal ridge. The circular, proximal ridge present in many specimens is here considered as the margin of a contracted and, to some extent, an invaginated foot. It can thus be compared to the appearance of the contracted foot in Placophora and Monoplacophora.

Axial structure. In small specimens, the longitudinal invagination often has a rather regular, cigar-like shape with a round rear end and a tapering anterior one (Fig. 14a). Very often, a rather regular annulation or segmentation can be observed (Fig. 14b–d). This cigar-like depression is interpreted here as an imprint of a voluminous gut, not differentiated into distinct stomach and intestine, which has a well-developed musculature arranged as segmental rings.

Arrow-like structure. The anterior part of the longitudinal depression ends with an arrow-like structure (Fig. 15a–d). This structure joins with what we have considered to be the imprint of the main portion of the gut, the connection is not terminal but rather shifted somewhat backward (Fig. 15e) and has a swelling near the place of connection (Fig. 15f). The arrow-like structure is interpreted as either a feeding organ, which was a retractable proboscis, or invertible pharynx that had at its proximal end a pair of lateral pharyngeal glands. In many small specimens, this structure could extend well beyond the anterior end of the shell (see Fig. 15 g–i). In most specimens, the terminal part of the proboscis is bent or retracted. In one specimen, this proboscis has a terminal structure, which resembles the imprint of a funnel-like

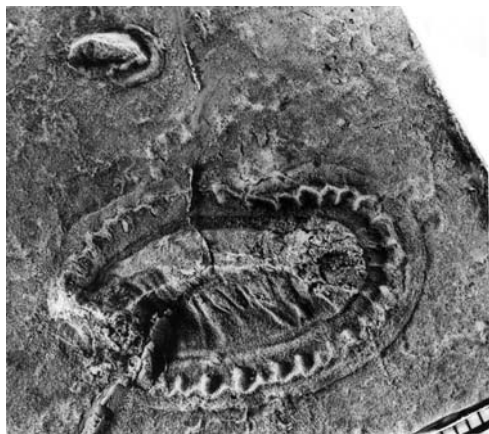


Fig. 12. PIN 3993-4006. Latex peel of bed sole. Scale in mm. Medium-sized individual with well preserved aboral end on the right and distorted oral side on the left. Smooth external band could be an imprint of the foot. The folds (crenulae) have notably irregular size.

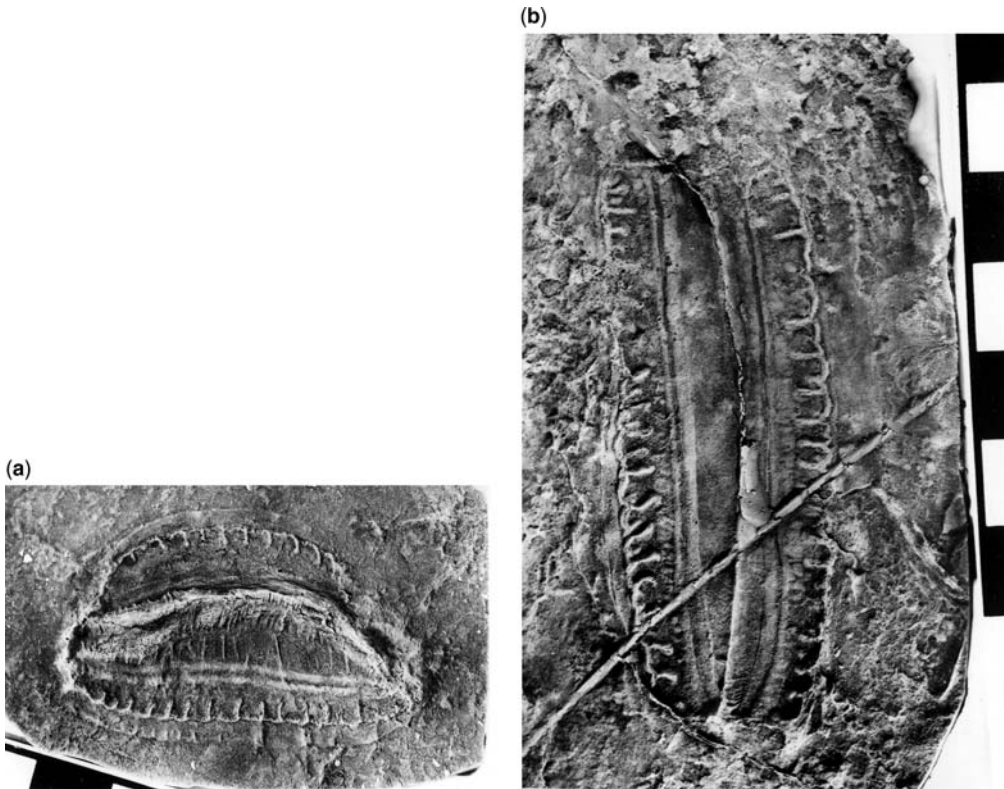


Fig. 13. (a) PIN 3993-5551. (b) PIN 3993-5552. Latex peels of bed sole. Scale in cm. Rather common asymmetry of *Kimberella* fossils (see also Fig. 11) interpreted as brought about by deep invagination of the ventral part upward under the shell during the decomposition process and subsequent collapse of the slit while the high narrow shell tilted aside.

organ provided with several uniform teeth or digits, at least seven are plainly visible (Fig. 15j).

Axial band. A number of specimens demonstrate a prominent axial band of a uniform width that connects the base of the arrow-like structure, presumed proboscis or pharynx, with the rear end of the longitudinal depression, interpreted here as a stomach. This band is even visible on the surface covered with the transverse wrinkles (Fig. 16a), but it is preserved much better on the smooth surface of the longitudinal depression (Figs 19b, 14d, 16b). The axial band may have some relation to the rear terminal wrinkles well-preserved in some specimens (Figs 15j, 16a), but any plausible interpretation can be suggested.

Lobes. A few specimens show a clear division of the inner zone into large lobes, bilaterally arranged (Fig. 17a, b, see also the specimen Fig. 1d in Fedonkin and Waggoner 1997). These lobes are interpreted here as an expression of internal metameric structure which, however, does not

embrace the external morphology. Two possible interpretation of these lobes are suggested: (1) an overprint of a voluminous, somewhat segmented stomach; or (2) a reflection of myomeres of a dorso-ventral muscle system. In *Kimberella* the dorso-ventral musculature could be used for the following functions: (1) locomotion in synergy with the transverse pedal muscles; (2) to flatten the body and so to press the body liquids into the crenula and foot and expand them when the animal was stationary: the degree of their contraction could impinge on the shape of the gut. In this case, the metameric arrangement of this musculature in *Kimberella* could be reflected in the fossil morphology.

Transverse wrinkles. Far more common are relatively thin, regular transverse wrinkles that cover the inner zone but do not cross the proximal ridge (Figs 15j, 16a, 18a). There are at least three kinds of such wrinkles. In some specimens they are almost invisible in the axial region and deepen towards the periphery of the inner zone (Figs 15j, 17b). A second type of finer wrinkles can be

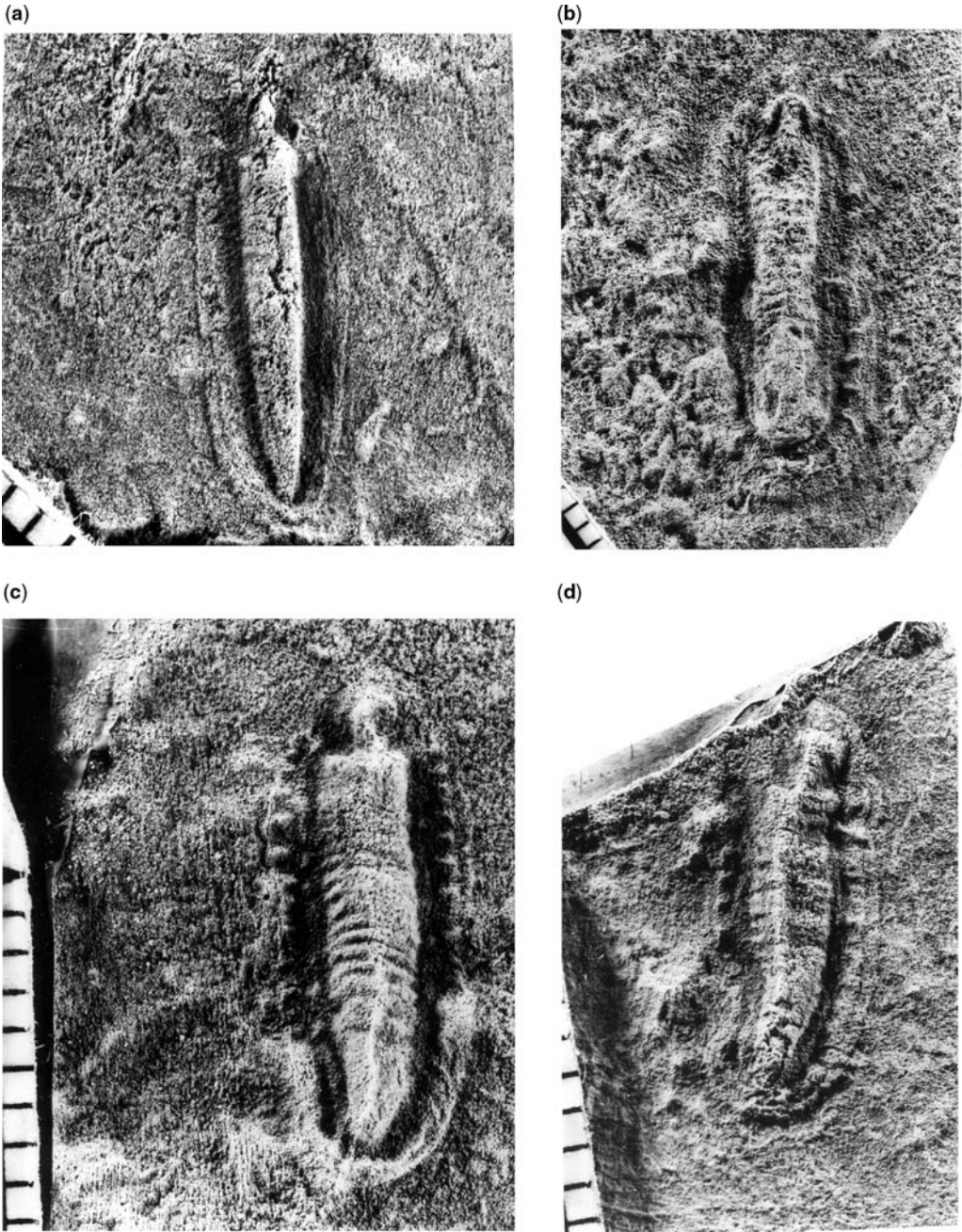


Fig. 14. (a) PIN 3993-5607. (b) PIN 4853-372. (c) PIN 3993-5536. (d) PIN 3993-5583. Latex peels of bed sole. Various types of preservation of a 'cigar-shaped' axial structure (interpreted as a straight, voluminous gut). It is suggested that this feature can be observed only in small individuals because it could be printed through the thin layer of the ventral musculature below. Regular annulations of this structure are visible in Figure 14c and partially preserved in other specimens (Figs 14b, d)—perhaps segmentation reflective of gut musculature.

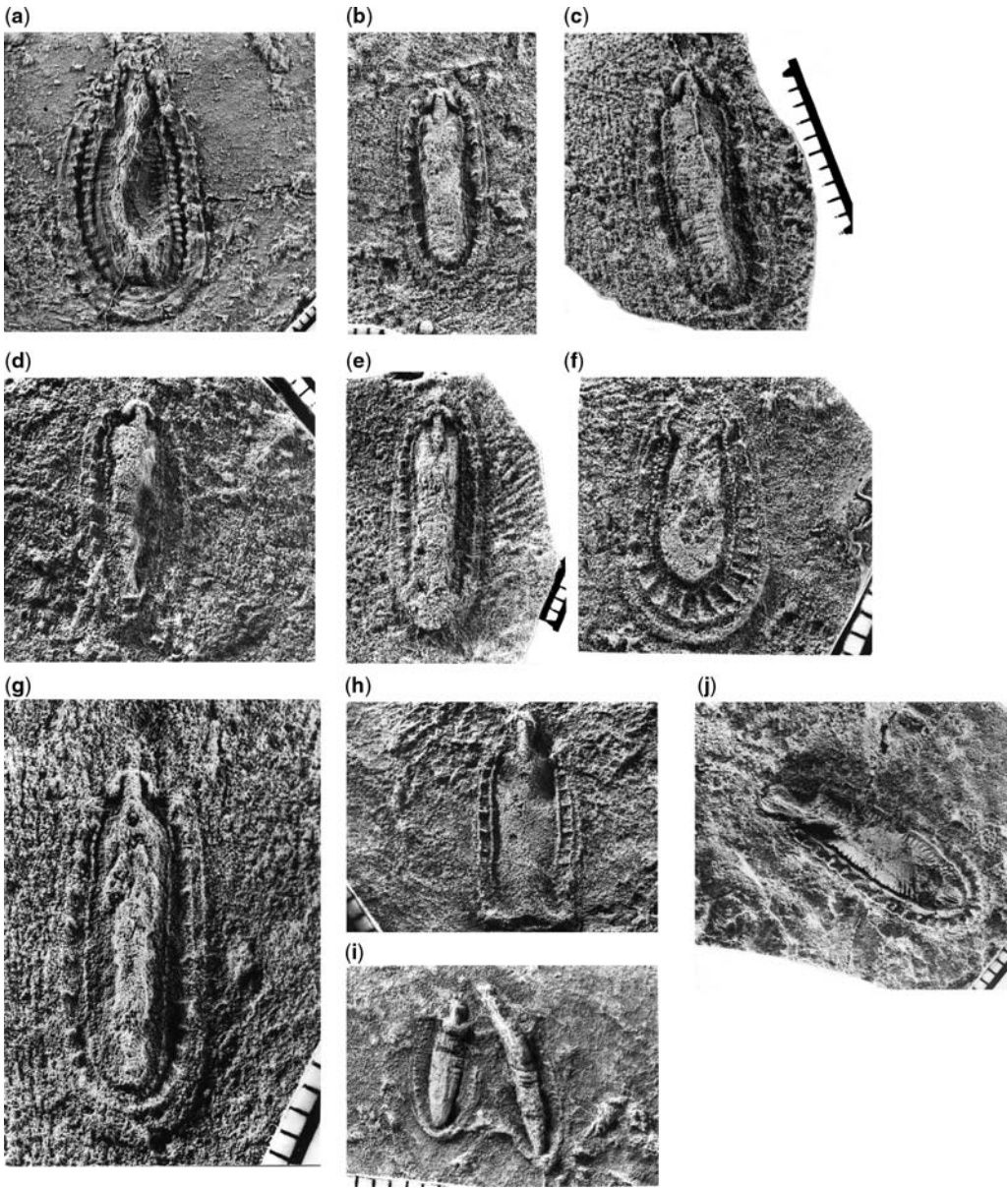


Fig. 15. (a) PIN 3993-5253. (b) PIN 4853-314. (c) PIN 4853-364. (d) PIN 4853-369. (e) PIN 4853-161. (f) PIN 4853-375. (g) PIN 4853-361. (h) PIN 3993-5596. (i) PIN 3933-5594. (j) PIN 3933-5565. Latex peels of bed sole. Arrow-shaped structure on the oral end of the body is interpreted here as a proboscis or extendable feeding structure bearing two lateral bag-like structures oriented oblique to the proboscis. The proboscis can extend beyond the oral end of the body. The fossils demonstrate different degrees of extension of the proboscis/feeding structure (Fig. 15i). The base of the proboscis is situated at the anterior-dorsal side of the gut and surrounded by the swelling (Fig. 15e, h) that may correspond to the massive retractive musculature of the proboscis. Lateral bag-like structures are interpreted here as paired glands.

traced across the inner zone (Fig. 18b). And in some specimens the wrinkles of the second kind cross with short transverse wrinkles that occupy predominantly the axial zone (Figs 16a, 18a). One cannot

exclude the possibility that some wrinkles may be the result of post mortem shrinking of the body, but it is unlikely that this can be the cause of all wrinkles, as they appear too regular in size and

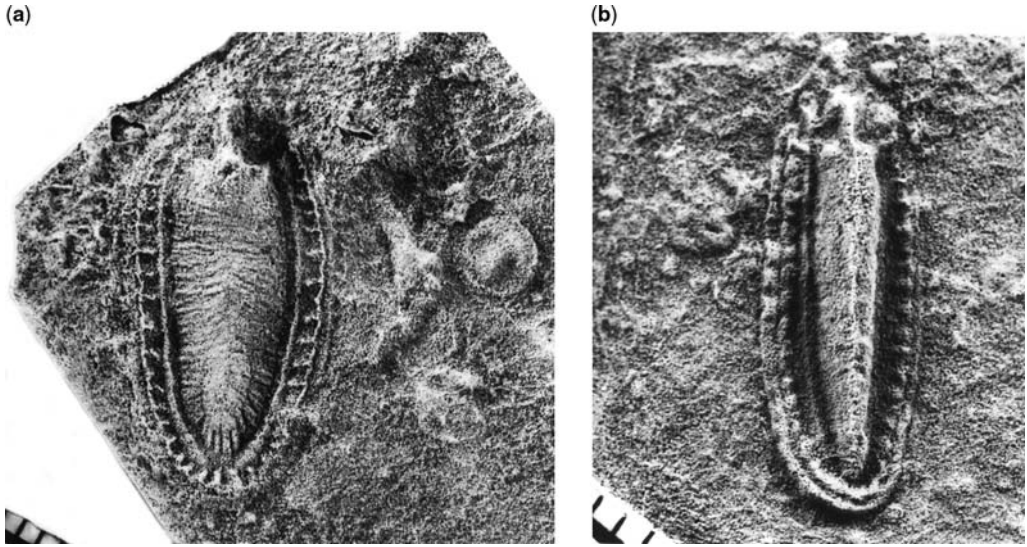


Fig. 16. (a) PIN 3993-5598. (b) PIN 3993-5540. Latex peels of bed sole. Axial band (also visible in Figs 9b and 14d) may be related to the dorsal surface of the gut but, as to the functional meaning of this structure, we cannot give a plausible interpretation at this point.

distribution. More likely, the transverse wrinkles are the result of the post mortem contraction of transverse pedal muscles. A similar arrangement of the uniform transverse muscle fibres is a common feature of the large molluscs. As for the lateral, slightly more widely and regularly spaced wrinkles (Figs 15j, 17b), we suggest that these are

diverticulae of a voluminous gut (compare with the structure of the stomach in living solenogaster *Proneomenia*).

Crenulated zone. The crenulation observed on the periphery of the oval imprint of *Kimberella* is interpreted here as a thin, lateral extension of

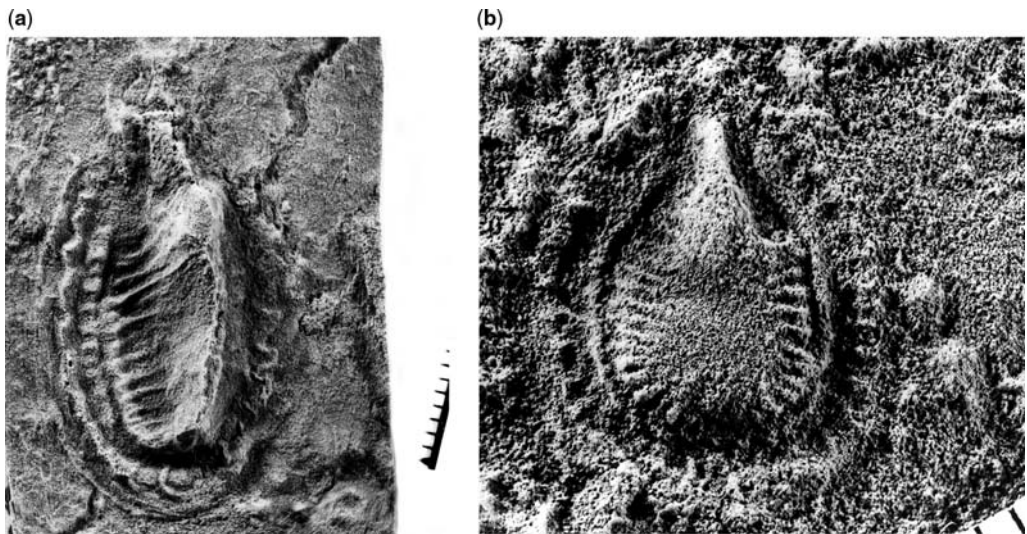


Fig. 17. (a) PIN 3993-5586. (b) PIN 3993-5542. Latex peel of bed sole. Both in medium-sized specimens and in the smallest, the regular segmentation could represent the myomeres of dorsal-ventral musculature. An alternative interpretation of the bilaterally arranged ridges in Figure 17b would be numerous lateral diverticulae of a large gut (such diverticulae are common for the straight gut of *Proneomenia*, *Solenogastra*).

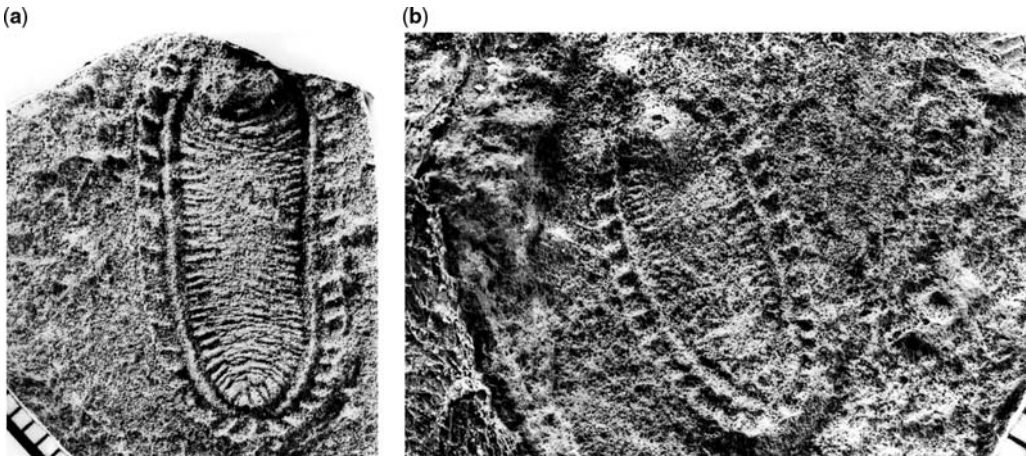


Fig. 18. (a) PIN 3993-5563. (b) PIN 3993-5502. Latex peels of bed sole. Fine transverse wrinkles in these specimens and in a number of other ones (e.g. Figs 15j, 16a) are interpreted as transverse ventral musculature.

body (Figs 11, 13a) (probably morphologically a part of the lower surface of the mantle) at its junction with the lateral side of the animal. This structure was regularly folded when retracted under the shell. This organ is likely to have had a function of respiration and thus be considered a possible predecessor of the ctenidia. The reconstruction of this structure as a folded band, rather than a circumpedal series of lappets, is supported by the following observations: (1) the crenulae never overlap each other, as would be expected in the case of free lappets; (2) adjacent crenulae may have rather different sizes as measured parallel to axis (Fig. 13b); and (3) regular preservation of the crenulae suggests that these structures were rather thick and dense (possibly due to folding).

The number of the crenulae is more or less constant, about 34 to 36, both in small (juvenile) and in the largest individuals. The width of the crenula measured parallel to the axis of the body is about 1 mm in individuals about 15 mm long, and reaches 5–6 mm in the forms that reach 80–100 mm in length. In the well-preserved specimens the distal side of the crenulated zone is straight. The crenulae are usually regular in size and spacing, but their size and shape may vary due to deformation, and in a few specimens a crenula may be twice as broad as the next one. Some crenulae tend to fold into two smaller ones; others show just small inward indentation of the distal side.

Some recent gastropods have a foot with a multifolded thin edge, actively used for swimming, notably by certain unshelled opisthobranchs, such as *Oscanius* and *Akera* (Morton 1988). A similar morphology is characteristic of

some large flatworms, for example, the freshwater *Baikaloplana valida* that can reach over 10 cm in length (Porfirieva 1977). The crenulated band of *Kimberella*, by analogy with these living flatworms and molluscs, appears to be able to create a kind of running wave. This wave might improve the respiration of the animal by ventilating the mantle space under the shell. There is no evidence of gills in *Kimberella*, while the large surface of the multifolded crenulated zone could effectively perform the respiration function. In support of this interpretation, both monoplacophorans and limpets are noted to have developed respiratory and/or ventilatory organs arranged in a circle around the foot, in about the same position as the crenulation of *Kimberella*. The running wave might have assisted the locomotion of the animal over the bottom surface (gliding rather than crawling).

The more or less regular size of the crenulae observed in the fossil *Kimberella* may have been caused by compact folding of the thin peripheral parts of the crenulated organ during retraction of the foot and crenulated organ under the shell. Most, if not all, fossil *Kimberella* show the soft parts retracted under the unfavourable conditions of burial in life position. Thus, under the shell the folds might have had S-shape character in lateral view. When expanded beyond the shell, the edge of the crenulated organ might become less folded. In the best-preserved specimens, the crenulae form a full oval all way around the mantle cavity.

Growth pattern. Comparison of complete specimens showing both the imprints of the soft body

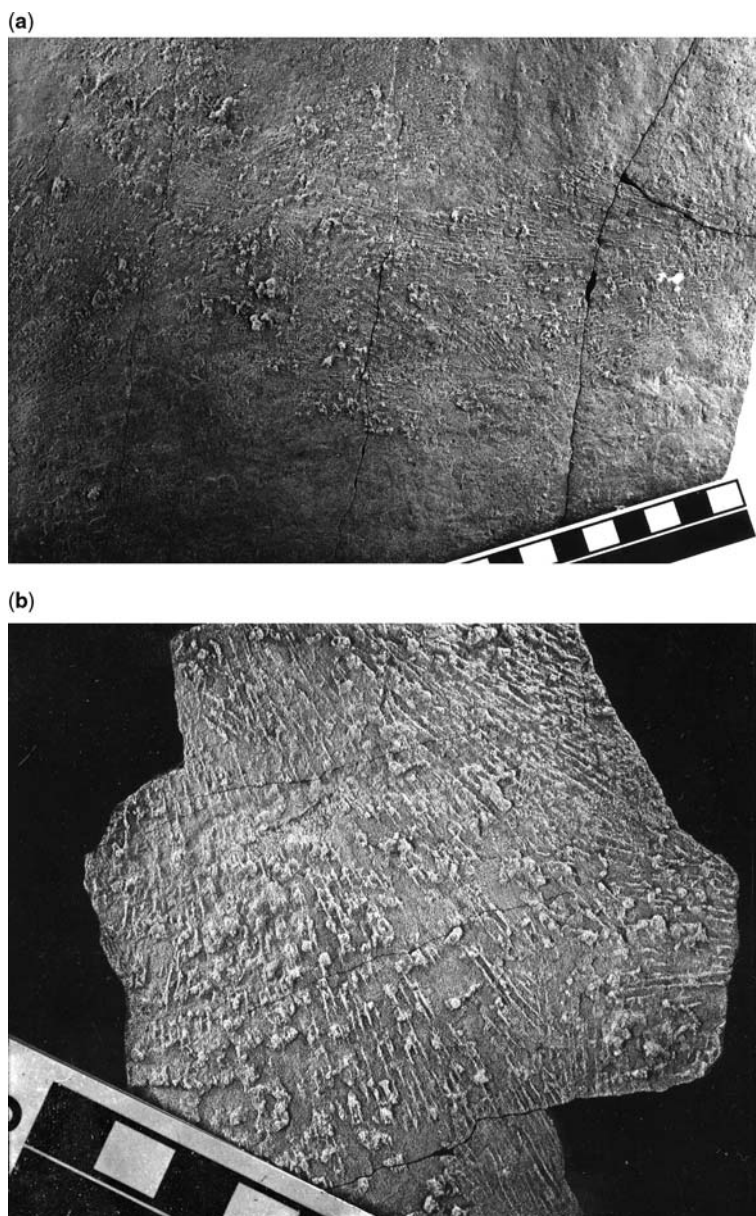


Fig. 19. (a) PIN 4853-334. (b) PIN 3993-4074. Rock samples, sole of the sandstone beds. Scale in cm. Grazing tracks produced by *Kimberella* often have a fan-like pattern (Fig. 19a) indicating the ability of feeding organ to extend for about 2 cm (Fig. 19b) and to exploit a considerable area of the bottom surface from one resting position of the animal. After grazing, *Kimberella* moved aborally and continued grazing over the next sector, thus not moving over already-exploited territory. The high intensity of grazing is mirrored by the overprinting of many layers of tracks that cross each other. The detailed and sharply-defined shape of the paired scratch grooves is indicative of a capacity of the sediment to preserve such tracks produced by hard parts embedded in the feeding organ. Small round bodies scattered over the grazed area (but not seen beyond it) have been interpreted as faecal pellets of the grazer. Alternative interpretation: these round structures represent the sand casts of the prey organisms pulled out by *Kimberella* from the muddy sediment.

and shell indicate that the growth of *Kimberella* was gradual. Proportions of the smallest and largest specimens are rather similar. The presence in the collection of rather broad, elongated individuals can be variously explained: taphonomic causes, morphological variability, sexual dimorphism and even the co-existence of different species. There is no evidence of discrete size classes or that growth was limited or indeterminate. There is no evidence of metamorphosis or other radical anatomical changes within the observed size range. If such a metamorphosis occurred, it must have occurred at a stage earlier than any of those represented. Maximum size in particular fossil assemblages may be related to the time available to grow before the deadly burial by the catastrophic sedimentation. The large number of relatively small individuals preserved can be explained by a high reproductive rate and dominating juvenile mortality as well as, possibly, by a greater chance of the largest individuals escaping from the sediment after fast sedimentation.

Grazing tracks

The sets of the miniature sand casts of the linear depressions have been first documented on the lower bedding surface of Precambrian quartzite within the Ediacara Member of the Rawnsley Quartzite in South Australia (Glaessner & Wade 1966). These structures were tentatively interpreted as the imprints of spicules. Later, these fossils were reinterpreted as the scratch marks produced by the feet of unknown arthropods, which were not depicted by Jenkins (1992). These enigmatic structures were found to show some similarity to features of a large meanderform grazing trace fossil recovered from peritidal carbonates of probable Late Cambrian age in Saudi Arabia (Gehling *et al.* 1995). Judging from the size of the individual meander loops of this Cambrian trail (that is over 50 cm), the body size of the animal was inferred to reach a metre in length.

New fossil material recovered from the Vendian rocks of the White Sea (Ivantsov & Fedonkin 2001; Fedonkin 2003) and Ediacaran rocks of South Australia (Gehling *et al.* 2005) demonstrated no meandering loops associated with the scratches, but instead rather fan-shaped clusters of these 'paired scratches'. This observation excluded interpretation of these scratches as the traces left by a radula in its classical sense. Another misconception was the idea that, in the process of grazing, the trace maker was crawling over a previously formed set of scratches and expanded the fan span. To explain why the previous scratches were not destroyed, the authors postulated the

presence of a microbial mat at the sediment surface. Indeed, the sediments bound by the biofilms or bacterial mats seemed to be widespread during the Proterozoic until the time of active bioturbation at the very end of the Vendian through the Early Palaeozoic.

In the course of extensive excavations on the Winter Coast of the White Sea, large bedding plane surfaces were exposed. Particularly abundant scratch marks have been documented on the lower surface of the laminated, fine-grained sandstones underlain by clays. These sediments represent the distal part of a suspension flow fan that accumulated on a flat, muddy seafloor in relatively deep conditions of the subtidal zone below the wave base. One particular sandstone bed contains thousands of the sets of these scratches, so that it is difficult to distinguish the individual fans (Fig. 19a, b). The parallel position of each pair of the scratches demonstrates that the hard parts on the end of the feeding structure resembled hook-like teeth, similar to the only pair of teeth in some *Solenogastra*, such as *Alexandromenia valida* (Grassé 1960). The absence of other trace fossils on the same bedding plane indicate that in particular environments, *Kimberella* was the dominant grazer, able to regulate the growth of the benthic primary producer over a vast space.

The morphological features of these structures, the fan-like patterns of their arrangement and mode of their distribution in the bedding plane as well as direct association with body fossils of *Kimberella* allow us to interpret these fossils as the grazing structures produced by means of a rather long proboscis bearing a pair of thin hook-like organs (Ivantsov & Fedonkin 2001; Fedonkin 2003). Preservation of the body imprints at the end of the cascades of the similarly oriented fan-like sets of the scratch marks (Fig. 20a, b) indicates that during the feeding process, the animal periodically moved backward. Grazing over the large area by means of the proboscis requires some adaptations allowing sufficient stabilisation of the body on the surface. This function could be performed by a large foot that spread widely and attached the animal to the bottom surface.

An alternative suggestion has been made by A. Ivantsov, who suggests that instead of an elongate proboscis, there could have been a rather wide feeding organ, which could spread like a fan. Equipped with numerous teeth this organ scratched a large surface area of the sea floor in one simultaneous sweep collecting food particles (algae, protozoans or meiofauna) from the surface or from the uppermost zone of the sediment. However, mechanical constraints and the absence

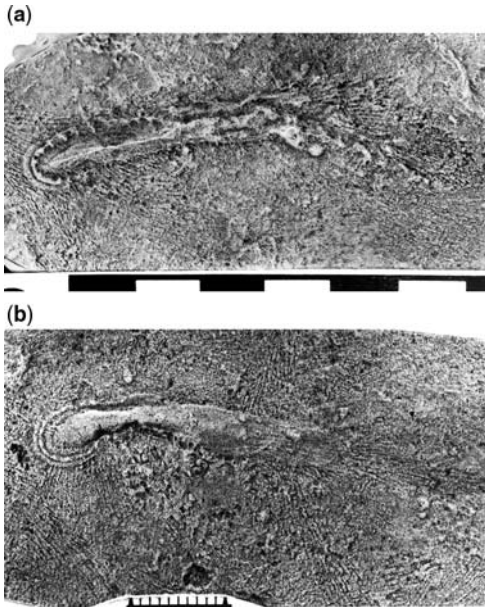


Fig. 20. (a) PIN 4853-334. (b) PIN 4853-318. Latex peels of bed sole. The specimens demonstrate the transition from the grazing phase (marked by the scratches on the right in both pictures) to the locomotion, likely brought about by the disturbance related to the sedimentation event. Traces of the final movement of *Kimberella*, it is suggested, were produced under the sand event bed, which entrapped and killed the organisms.

of morphological evidence do not allow us to accept this model.

Feeding

Kimberella was a selective predator or grazer and not a deposit feeder. This conclusion is based on the form of its feeding tracks and the absence, in spite of the large number of specimens, of any evidence of associated faecal cord or large pellets that are common for the non-selective mud-eaters. Scratch marks are often associated with numerous round bodies preserved in a positive relief on the sole of the bed. These bodies up to 3 mm across might correspond to the large objects (prey?) that *Kimberella* was able to pull out of the sediment by its proboscis. The shallow water habitats of *Kimberella* and its common association with the remains of microalgae and with the structures interpreted as a bacterial mat may indicate that this organism had some preferred grazing areas (Gehling *et al.* 2005). One cannot exclude that *Kimberella* may even have penetrated to tidal flats and semi-isolated lagoons. The evidence of the giant Late Cambrian trail *Climactichnites*, produced



Fig. 21. PIN 4853-5, 11, 12. Latex peels of bed sole. Scale in cm. Three small (juvenile?) individuals, which have produced long burrows under a thin layer of sand in a failed attempt to escape. The burrows are preserved in the negative hyporelief on the sole of the entombing sand layer. Note, that the locomotion trail is narrower than the shell imprint.

by a problematic soft-bodied invertebrate crawling on tidal flats (Yochelson & Fedonkin 1993) demonstrates that metazoan colonization of the subaerial environment began much earlier than it was previously thought. *Kimberella* was adapted to feeding on the algal or bacterial mats and could well enter the shallowest parts of the subtidal zone and even the littoral zone. In the conditions of the very short trophic chains typical for the Vendian (Fedonkin 1987), *Kimberella* seems to occupy the topmost position of the trophic pyramid.

Locomotion trails

The vast majority of the trace fossils produced by *Kimberella* are related to its grazing activity. The mode of feeding and crawling backwards help to

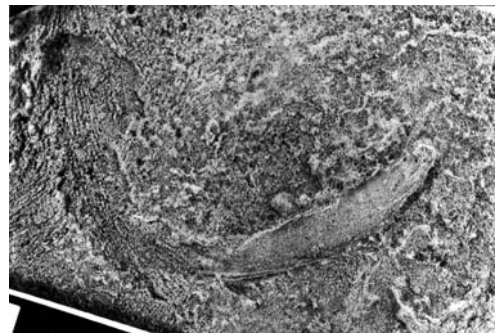


Fig. 22. PIN 4853-316. Latex peel of bed sole. Scale in cm. Smooth part of the locomotion trail seems to represent the successful escape of *Kimberella* from the incoming event sand bed.

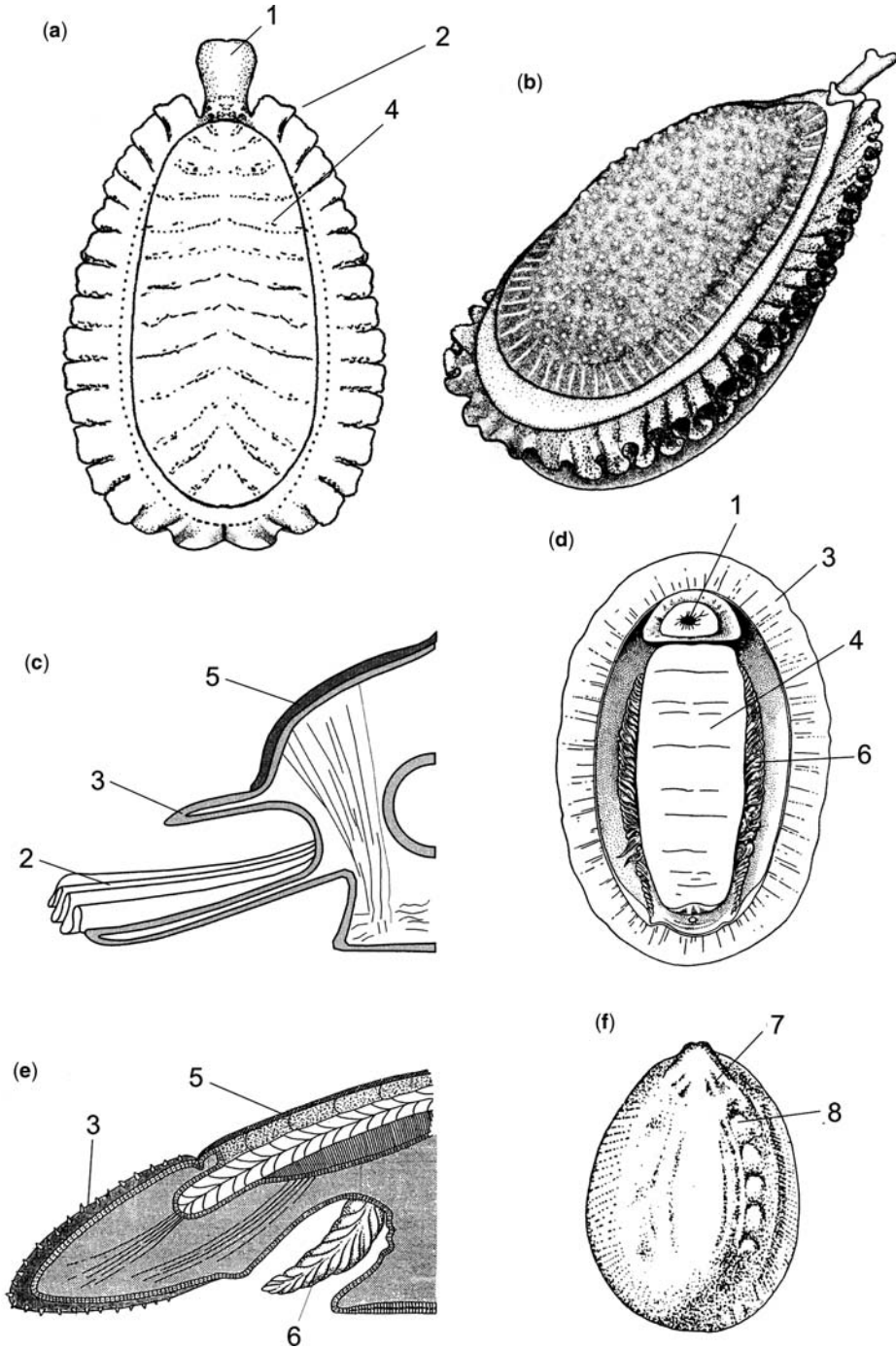


Fig. 23. (a) Reconstruction in ventral view of *Kimberella quadrata* with foot partly retracted. (b) Reconstruction in dorsal-oblique view of *Kimberella*. (c) Diagrammatic section of the reconstruction proposed for *Kimberella*. (d) Ventral view of *Chiton* for comparison with proposed interpretation of *Kimberella*. (e) Semi-diagrammatic section of a living *Chiton* (Mollusca, Placophora) for comparison with c). (f) Dorsal view of the shell of *Biopulvina* (Mollusca, Monoplacophora): the traces of the insertions of the dorso-pedal muscles are clearly visible. 1, proboscis and mouth; 2, crenula; 3, extension of the mantle beyond the shell; 4, foot; 5, shell (note that in *Kimberella* only of the periostracum); 6, ctenidia; 7, traces of the insertion of muscles related with the buccal apparatus; 8, traces of the insertions of the dorso-pedal muscles.

understand why the locomotion trails are so rare: the trails have been erased by the grazing activity. However, a few specimens demonstrate directly the ability to crawl through the sediment and escape from it after the burial (Figs 21, 22). These trails are preserved in the negative relief on the sole of thin sandstone beds. The thin layer of the sediment, that buried the animals alive, was water-saturated and this allowed them to crawl and even escape. These trails represent the roof of the tunnel and often have fine longitudinal markings produced by the miniature knobs of the outer sculpture of the shell.

Discussion and conclusions

Study of the large sample of *Kimberella* specimens recovered from the White Sea region of Russia allow us to make the following conclusions concerning the grade of organization and ecology of *Kimberella* as well as its taxonomic positions within the bilaterians.

The dorsal shield of *Kimberella* appears to correspond with the periostracum of Mollusca, especially that of the monoplacophorans (Fig. 23). The metamerism that appears on its inner surface in some specimens may well be imprints of segmented dorso-pedal muscles, comparable with the muscles in monoplacophorans and chitonids (metameric muscles occur also in the forepart of the body of some Caudofoveata). The remarkable frilled fringe preserved on most specimens seems to correspond with the fringe of ctenidia. However, when fully extended it would appear as a flat, extremely thin lamella, while the folded arrangement may have been produced when the flange was partly retracted. It is also possible that it was permanently folded when inside the shell in order to increase the respiratory surface without the need to extend much beyond the border of the shell. A true circulatory system may have been absent in *Kimberella*, but instead there may have been a meshwork of lacunae. It seems most probable that the extension of the foot, crenulae and proboscis was achieved by hydrostatic pressure. All molluscs have an open circulatory system so an open coelom is suggested for *Kimberella*. Extension and retraction of the foot, respiration fringe and proboscis, as well as obvious elongation and contraction of the body, are indicative of an extensive and complex system of lacunae filled with the coelomic fluids. Coelom, thought to have evolved originally as a hydrostatic skeleton, must have reached the molluscan level of organization before the Cambrian radiation of the phylum.

The fact that the respiratory folds extended well beyond the foot and the shell may have been due to

two factors: (1) as this structure had not yet developed into fringed ctenidia, the inefficient circulatory lacunae required a great respiratory surface; and (2) the absence of efficient predators did not require the protection of the respiratory surface (the shell having the function of an insertion surface for metameric muscles). The fact that the ctenidia of monoplacophorans are structurally rather different from those of typical molluscs may support the idea that ctenidia evolved in molluscs independently at least two times. The respiratory fringe of *Kimberella* can be considered as an evolutionary predecessor of the ctenidia, which developed later via structural differentiation of the fringe.

The presence of a true foot, possibly comparable in structure with that of monoplacophorans, gives an additional insight on the level of organisation achieved by the bilaterians prior to the Cambrian. During locomotion, that the foot was rather narrow and elongated can be deduced from the structure of the trails left by the moving animals. In the grazing phase, function of the foot may have required it to spread well beyond the shell to provide additional attachment to the substrate while the proboscis was raking the food from the uppermost layer of the microbial mat.

Not all the characters observed in the fossils receive an indisputable interpretation here. Thus, the prominent circumnodal band close to the basis of the respiratory flange may be gonads, nervous tracts or a very large blood lacuna.

The case of *Kimberella* demonstrates that true mineralized shells, so common for the most of the molluscs in the Phanerozoic, were preceded (and that may be common for all shell bearing phyla), by the organic dorsal structures covered by or impregnated with the microsclerites so common in later strata. True shells were likely to have developed by fusion of such microsclerites.

No specimens of *Kimberella* have been found undergoing any kind of asexual reproduction such as fission or budding; it seems, therefore, that it must have reproduced sexually. The wide geographic occurrence of the species indicate an effective mechanism of dispersal that must have been a planktonic larval strategy, as the structure of even the most juvenile specimens found is that of an animal of limited mobility. There is no indication of seasonal reproduction because the size of the body fossils in the majority of the habitats represents the whole range of growth.

The presence of a fundamentally mollusc-like architecture in animals belonging to a typical Ediacaran faunal assemblage leads to search for corresponding ecological niches and habitats in the late Precambrian ecosystems. There is no evidence that *Kimberella* was a macropredator. Evidence of predation in the Vendian is quite rare.

The reconstruction of *Kimberella* as a micropredator feeding on the protozoans or meiofaunal metazoans living by the sediment-water interface cannot be ruled out. Feeding on algae seems less probable. Most recent marine herbivores are derived from microphages, detritivores or predators, and have a post-Paleozoic origin (Vermeij & Lindberg 2000). Besides, contrary to digestion of proteins, that of cellulose requires a more complex set of enzymes.

Some implications of the molluscan nature of *Kimberella* require further mention. If *Kimberella* is assumed to be a true mollusc, then this implies that it possessed a trochophore, a spiral segmentation and this, in turn, requires that: (1) the Trochophorata are a really monophyletic assemblage (discarding for the time being the argument by Nielsen (1995) about trochophore and pseudotrochophore) or (2) the Trochophorata are a merely polyphyletic group. If we assume (1), then almost all living phyla must have begun to differentiate well before *Kimberella*, long before commonly assumed.

The study of the world's richest collections of *Kimberella* provides strong evidence for the existence of a morphologically complex, heterotrophic, triploblastic invertebrate in late Neoproterozoic marine ecosystems. If *Kimberella* was a mollusc, it implies that the Protostomata and Deuterostomata lineages must have diverged early, in pre-Ediacaran times: a model which is consistent with those molecular clock models that place the origin of the metazoans further back in time (Wray *et al.* 1996; Bromham *et al.* 1998; Wang *et al.* 1999; Hedges *et al.* 2004; Pisani *et al.* 2004; Bromham 2006) and not just an integral part of the Cambrian 'explosion' (Conway Morris 1997; Aris-Brosou & Yang 2003; Peterson *et al.* 2004; Peterson & Butterfield 2005).

The authors are grateful to J. Gehling, E. Yochelson and B. Waggoner for the stimulating discussion and to A. Mazin, who has made most of the photographs. This study is supported by the Russian Fund for Basic Research (Grant 05-05-64825) and by the President of the Russian Federation (Grant 2899.2006.5), and Program 18 of the Russian Academy of Sciences. Fieldwork in the White Sea Region of Russia was supported by the National Geographic Society. Thanks are also due to Monash University for providing funding for MAF as a Scientist in Residence during 2002–2003 and to J. Stilwell, P. Trusler, P. Vickers-Rich and one anonymous reviewer for providing valuable comments on the manuscript. This study has been carried out as part of UNESCO IGCP Project 493.

References

ARIS-BROUSOU, S. & YANG, Z. 2003. Bayesian models of episodic evolution support a late Precambrian explo-

- sive diversification of the Metazoa. *Molecular Biology and Evolution*, **20**, 1947–1954.
- BROMHAM, L. 2006. Molecular dates for the Cambrian explosion: is the light at the end of the tunnel an oncoming train? *Palaentologia Electronica*, **9**(1).
- BROMHAM, L., RAMBAUT, A., FORTEY, R., COOPER, A. & PENNY, D. 1998. Testing the Cambrian explosion hypothesis by using a molecular dating technique. *Proceedings of the National Academy of Sciences of the United States of America*, **95**, 12386–12389.
- CONWAY MORRIS, S. 1997. Molecular clocks: defusing the Cambrian 'explosion'? *Current Biology*, **7**, 71–74.
- DZIK, J. & IVANTSOV, A. YU. 1999. An asymmetric segmented organism from the Vendian of Russia and the status of the Dipleurozoa. *Historical Biology*, **13**, 255–268.
- DZIK, J. & IVANTSOV, A. YU. 2002. Internal anatomy of a new Precambrian dickinsoniid dipleurozoan from northern Russia. *Neues Jahrbuch für Geologie und Paläontologie Monatshefte*, **7**, 385–396.
- FEDONKIN, M. A. 1987. Non-skeletal Fauna of the Vendian and Its Place in the Evolution of Metazoa (Besskeletnaja fauna vendi i eyo mesto v evoljutsii metazoa). Moscow, Nauka. *Transactions of the Paleontological Institute*, **227**, 1–176. [in Russian].
- FEDONKIN, M. A. 2001. Glimpse into 600 million years deep. *Science in Russia*, **6**, 4–15.
- FEDONKIN, M. A. 2003. The origin of the Metazoa in the light of the Proterozoic fossil record. *Paleontological Research*, **7**, 9–41.
- FEDONKIN, M. A. & WAGGONER, B. M. 1997. The Vendian fossil *Kimberella*: The oldest mollusk. *Nature*, **388**, 868–871.
- GEHLING, J. G. 1991. The case of Ediacaran fossil roots to the metazoan tree. In: RADHAKRISHNA, B. P. (ed.) *The World of Martin F. Glaessner*. Geological Society of India, Bangalore. Geological Society of India Memoir, **20**, 181–224.
- GEHLING, J. G. 1999. Microbial mats in terminal Proterozoic siliciclastics: Ediacaran death masks. *Palaos*, **14**, 40–57.
- GEHLING, J. G., DROSER, M. L., JENSEN, S. R. & RUNNEGAR, B. N. 2005. Ediacara organisms: relating form to function. In: BRIGGS, D. E. G. (ed.) *Evolving Form and Function: Fossils and Development*. A Special Publication of the Peabody Museum of Natural History, Yale University, New Haven, Connecticut, 43–66.
- GEHLING, J. G., RUNNEGAR, B. & SEILACHER, A. 1995. Rasping marks of large metazoan grazers, terminal Proterozoic of Australia and Late Cambrian of Saudi Arabia. In: HINE, C. & HALLEY, R. B. (eds) *Linked Earth Systems*, SEPM, Tulsa, OK 57–58.
- GLAESSNER, M. F. 1984. *The Dawn of Animal Life*. Cambridge University Press, Cambridge.
- GLAESSNER, M. F. & DAILY, B. 1959. The geology and Late Precambrian fauna of the Ediacara fossil reserve. *Records of the South Australian Museum*, **13**, 369–401.
- GLAESSNER, M. F. & WADE, M. 1966. The late Precambrian fossils from Ediacara, South Australia. *Palaentologia*, **9**, 599–628.

- GRASSÉ, P. 1960. *Traité de Zoologie. Tome V: Méta-zoaires (suite). Fasc. 2 Bryozoaires, Mollusques: apla-, poly-, mono-placophores, bivalves.*
- GRAZHDANKIN, D. V. 2003. [Structure and depositional environment of the Vendian Complex in the Southeast White Sea area]. Stroenie i uslovia osadkonakopleniia vendskogo kompleksa v iugo-vostochnom Belomorie. *Stratigrafiia. Geologicheskaiia korreliatsiia*, **11**, 3–24 [in Russian; English translation published by Nauka/Interperiodica International Academic Publishing Company in *Stratigraphy and Geological Correlation*, **11**, 313–331].
- GRAZHDANKIN, D. V. & IVANTSOV, A. Yu. 1996. Reconstruction of biotopes of ancient Metazoa of the late Vendian White Sea biota. *Paleontological Journal*, **30**, 676–680.
- HEDGES, S. B., BLAIR, J. E., VENTURI, M. L. & SHOE, J. L. 2004. A molecular timescale of eukaryote evolution and the rise of complex multicellular life. *BMC Evolutionary Biology*, **4**, 1–9.
- IVANTSOV, A. YU. & FEDONKIN, M. A. 2001. Locomotion trails of the Vendian invertebrates preserved with the producer's body fossils, White Sea, Russia. North American Paleontological Convention, Abstracts with Program, Berkeley, *PaleoBios*, **21**, 72.
- IVANTSOV, A. YU., MALAKHOVSKAYA, Ya. E. & SEREZHNIKOVA, E. A. 2004. Some problematics from the Vendian deposits of South-East White Sea Region. *Paleontologicheskii Zhurnal*, **1**, 3–9.
- JENKINS, R. J. F. 1984. Interpreting the oldest fossil cnidarians. *Palaeontographica Americana*, **54**, 95–104.
- JENKINS, R. J. F. 1992. Functional and ecological aspects of Ediacaran assemblages. In: LIPPS, J. H. & SIGNOR, P. W. (eds) *Origin and Early Evolution of the Metazoa*. Plenum Press, New York, 131–176.
- JENKINS, R. J. F. 1996. Aspects of the geological setting and palaeobiology of the Ediacara assemblage. In: DAVIES, M., TWIDALE, C. R. & TYLER, M. J. (eds) *Natural History of the Flinders Ranges*. Royal Society of South Australia, 33–45.
- MARTIN, M. W., GRAZHDANKIN, D. V., BOWRING, S. A., EVANS, D. A. D., FEDONKIN, M. A. & KIRSCHVINK, J. L. 2000. Age of Neoproterozoic bilaterian body and trace fossils, White Sea, Russia: Implications for metazoan evolution. *Science*, **288**, 841–845.
- MORTON, J. E. 1988. The pallial cavity. In: TRUEMAN, E. R. & CLARKE, M. R. (eds) *The Mollusca*. Volume 11, Form and Function. Academic Press, 253–286.
- PORFIRIEVA, N. A. 1977. *Planarians of Lake Baikal*. Nauka, Novosibirsk. [in Russian]
- NIELSEN, C. 1995. *Animal Evolution: Interrelationships of the living Phyla*. Oxford University Press, New York.
- PETERSON, K. J., LYONS, J. B., NOWAK, K. S., TAKACS, C. M., WARGO, M. J. & MCPEEK, M. A. 2004. Estimating metazoan divergence time with a molecular clock. *Proceedings of the National Academy of Sciences of the United States of America*, **101**, 6536–6541.
- PETERSON, K. J. & BUTTERFIELD, N. J. 2005. Origin of the Eumetazoa: Testing ecological predictions of molecular clocks against the Proterozoic fossil record. *Proceedings of the National Academy of Sciences of the United States of America*, **102**, 9547–9652.
- PISANI, D., POLING, L. L., LYONS-WEILER, M. & HEDGES, S. B. 2004. The colonization of land by animals: molecular phylogeny and divergence times among arthropods. *BMC Evolutionary Biology*, **2**, 1–10.
- SEILACHER, A. 1992. Vendobionta and Psammocorallia: lost constructions of Precambrian evolution. *Journal of the Geological Society of London*, **149**, 607–613.
- VERMEIJ, G. J. & LINDBERG, D. R., 2000. Delayed herbivory and the assembly of marine benthic ecosystems. *Paleobiology*, **26**, 419–430.
- WADE, M. 1968. Preservation of soft-bodied animals in Precambrian sandstones at Ediacara, South Australia. *Lethaia*, **1**, 238–267.
- WADE, M. 1972. Hydrozoa and Scyphozoa and other medusoids from the Precambrian Ediacara fauna, South Australia. *Palaeontology*, **15**, 197–225.
- WANG, D. Y. C., KUMAR, C. & HEDGES, S. B. 1999. Divergence time estimates for the early history of animal phyla and the origin of plants, animals and fungi. *Proceedings of the Royal Society of London Series B*, **268**, 163–171.
- WRAY, G. A., LEVINTON, J. S. & SHAPIRO, L. H. 1996. Precambrian divergences among metazoan phyla. *Science*, **274**, 568–573.
- YOCHELSON, E. L. & FEDONKIN, M. A. 1993. Paleobiology of *Climactichnites*, an Enigmatic Late Cambrian Fossil. *Smithsonian Contribution to Paleobiology*, **74**, 1–74.

Comment: future research directions for further analysis of *Kimberella*

P. TRUSLER, J. STILWELL & P. VICKERS-RICH

School of Geosciences, Monash University, Clayton Campus, Victoria 3800, Australia (e-mail: Pat.Rich@sci.monash.edu.au)

For meaningful future research directions, the following should be taken into consideration.

- (1) Detailed analysis of the influence of taphonomy—all those factors that affected the form of the living organism from the time it died until it was collected as a fossil. Detailed models need to be proposed and supported, specimen by specimen (Figs 1–3).
- (2) Detailed descriptions need to be presented to explain the processes that led to the preservation of the organism and features described need to be in concert with the depositional model. For example, it is important to make clear whether one is observing a dorsal or a ventral preservation and reasons given for that interpretation. It also needs to be justified that observations are of the sole or of the top of beds, and if ventral and internal features of an organism are ‘underprinted’ on a dorsal surface of the deceased organism.
- (3) Detailed considerations of the structures proposed for a given taxon be evaluated in light of the possible association/relationship available for similar, contemporaneous material. These should be *Brachina* (Wade 1972) and *Solza* (Ivantsov *et al.* 2004) in the case of *Kimberella* (Glaessner & Wade 1996). This will allow the distinction of real biological entities from taphomorphs produced from the same taxon.

- (4) When diagnosing any fossil taxon, in addition to comparing its morphology with a range of known taxa (such as *Kimberella* with monoplacophorans or other molluscs) (Fig. 2), one must keep in mind: (1) the concepts of analogy versus homology; and (2) the problems that arise when a three-dimensional organism is preserved in a deformed state (in particular when three dimensions are preserved as two). If comparisons are made to particular modern taxa, it would be helpful to include detailed illustrations of those taxa and the morphological characters under discussion.

Historically, the assignment of *Kimberella* and its traces (*Radulichnus* (Fedonkin & Waggoner 1997)) to many different phyla serves to highlight the intrinsic and problematic issue of pattern recognition in the analysis of Precambrian soft-bodied fossils. Without detailed anatomical consideration of the above-mentioned factors and rigour taken to override the psychological influence of ‘seeing familiar morphology’, the reconstruction of three-dimensional form from essentially two-dimensional patterns is tenuous. This is why it is critical that for each interpretation, data upon which this interpretation is based and the reasoning behind that interpretation, must be presented in detail.

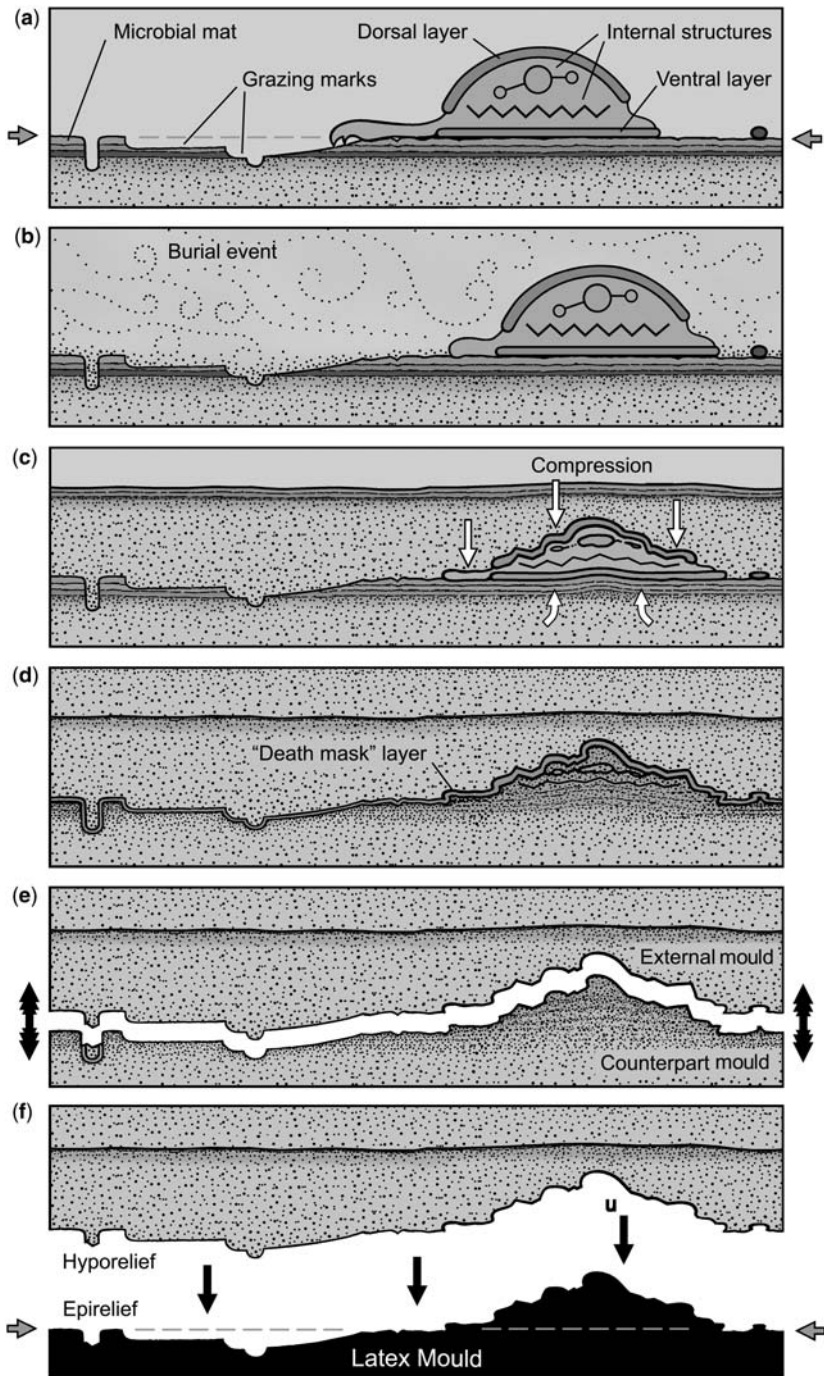


Fig. 1. Reconstruction of steps in the process of fossilization of *Kimberella* resulting in the final taphomorphology of the fossil (P. Trusler).

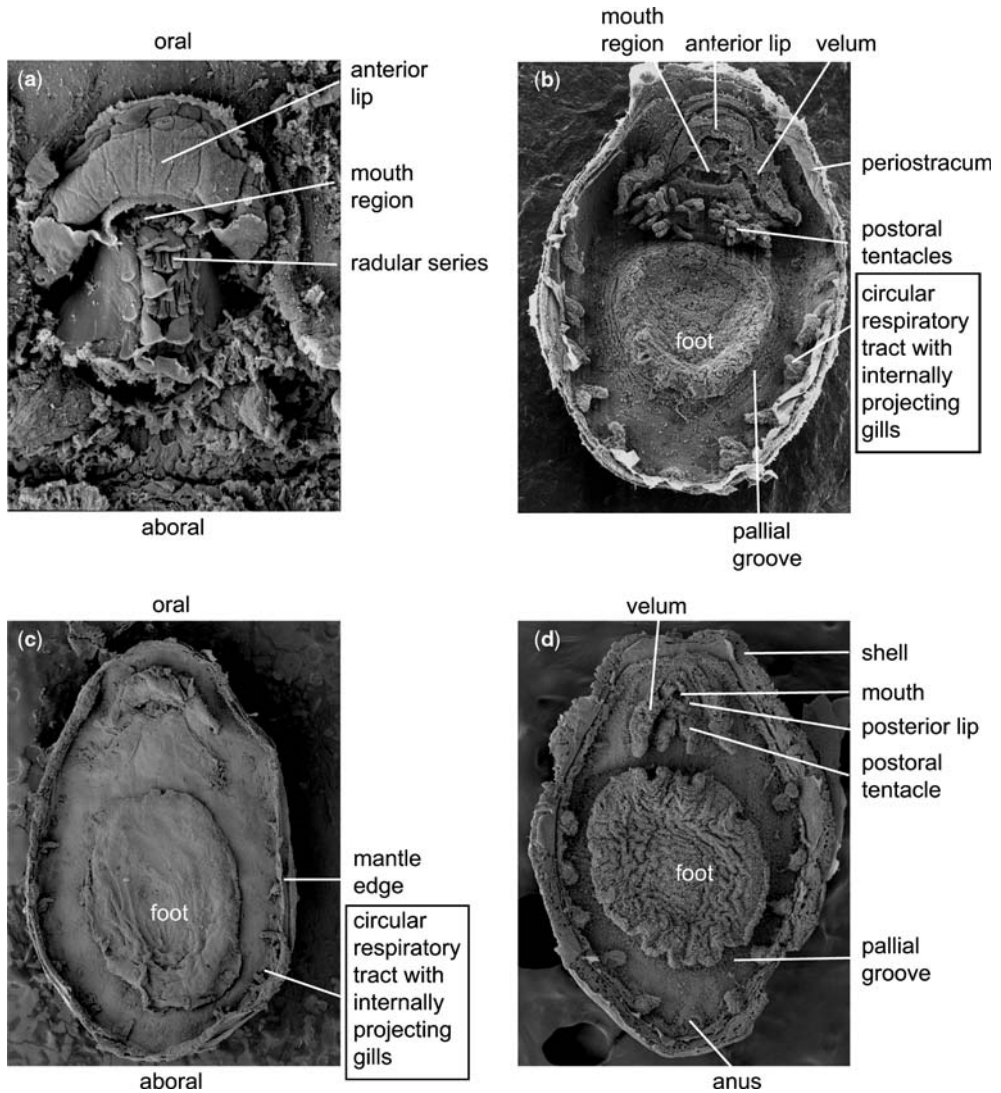


Fig. 2. Living monoplacophorans. Figure 2 (a–d), ventral SEM views of extant species of the macro-invertebrate Class Monoplacophora (Mollusca), all critical-point dried specimens, photographs courtesy of Dr A. Warén, Swedish Museum of Natural History, Stockholm, Sweden. (a) Greatly magnified view of the mouth region of the neopilinid *Rokopella euglypha* (Dautzenberg & Fischer 1897) with radula partially everted, live specimen from seamounts south of the Azores, from a depth of 1200–1600 m, $\times 200$; (b) Recent species *Laevipilina rolani* Warén and Bouchet 1990, from 1000 m depth on the Galicia Bank, off northwestern Spain, ventral view of critical point dried body of 1.4 mm length illustrating internal soft parts and part ventrally exposed part of shell, $\times 50$; (c) Living specimen of *Rokopella oligotropha* Rokop 1972, from 6000 m depth off the northern coast of Hawaii, depicting complete ventral view of specimen. Note the relatively small size of the vela and very small gills compared with the size of the animal, $\times 35$; (d) Recent species *Veleropilina* sp., specimen collected from off the southern point of Baja California, Mexico, at 1950 m depth from mineral particles on a submarine volcano, critical-point dried complete body 1.2 mm, illustrating soft parts and somewhat eroded edge of shell, $\times 55$. It could be that the structure interpreted by Fedonkin *et al.* (2007) as the crenulated zone is actually more analogous to the tubular respiratory system in the monoplacophorans rather than a folded soft tissue (as mentioned in their paper).

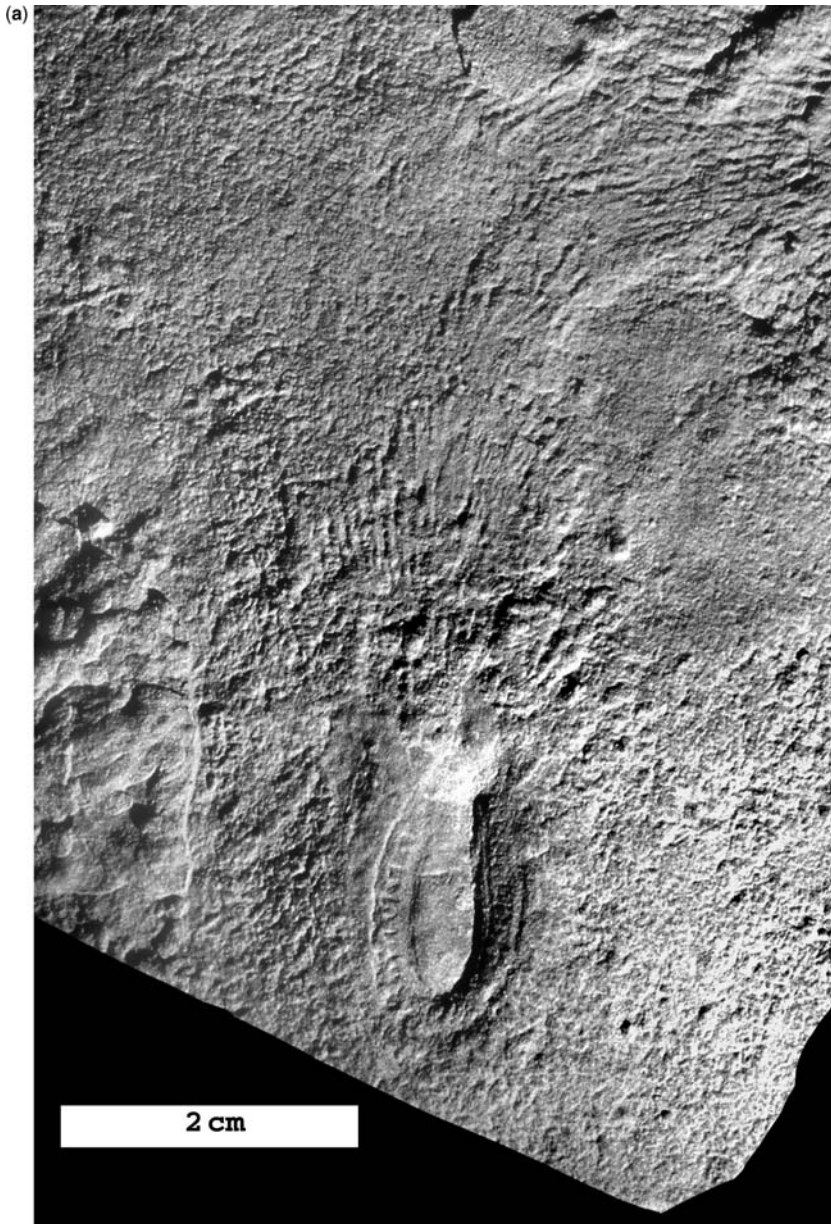


Fig. 3. Preserved morphology of *Kimberella*, body fossil and traces, indicating analogous (but not necessarily homologous) structure of the ‘crenulate’ zone to that of the tubular respiratory system of monoplacophorans (see Fig. 2) and detail of one set of traces (noted before by A. Ivantsov, pers. com.). Such traces may indicate that, instead of an elongate proboscis bearing only a pair of resistant structures, *Kimberella* may have possessed a much more complex ‘radular’ morphology, again analogous to that present in monoplacophorans (see Fig. 2), which did not require a lengthy extension of the feeding organ. In fact, it may well be that the feeding structure was entirely beneath the organism or only slightly extended when it ‘farmed’ the microbial mat and its contents, and only protruded beyond the main body in death when compressed. (a) Specimen of *Kimberella quadrata* from the White Sea region, northern Russia in the collections of the Paleontological Institute, Russian Academy of Sciences, Moscow and (b) detailed interpretation by P. Trusler.

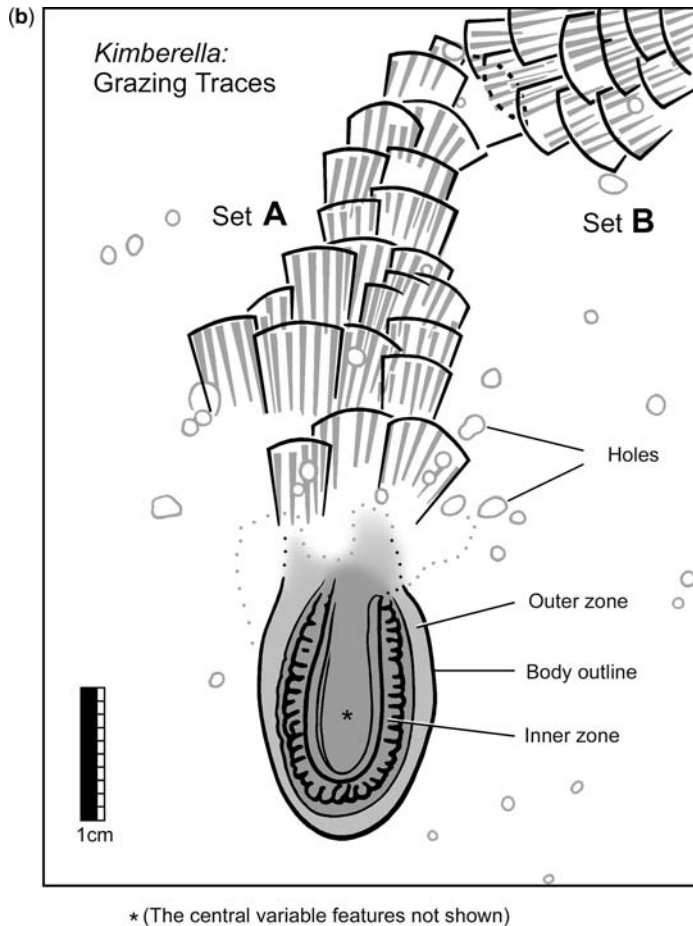


Fig. 3. Continued

References

- DAUTZENBERG, P. & FISCHER, H. 1897. Dragages effectués par l'Hirondelle et la Princesse Alice 1888–1895. *Memoires de la Société Zoologique de France*, **10**, 139–234.
- FEDONKIN, M. A. & WAGGONER, B. M. 1997. The Late Precambrian fossil *Kimberella* is a mollusc-like bilaterian organism. *Nature*, **388**, 868–871.
- FEDONKIN, M. A., SIMONETTA, A. & IVANTSOV, A. Y. 2007. New data on *Kimberella*, the Vendian mollusc-like organism (White Sea region, Russia): palaeoecological and evolutionary implications. In: VICKERS-RICH, P. & KOMAROWER, P. (eds) *The Rise and Fall of the Ediacaran Biota*. Geological Society, London, Special Publications, **286**, 157–180.
- IVANTSOV, A. Y., MALAKHOVSKAYA, Y. E. & SEREZHNIKOVA, E. A. 2004. Some problematic fossils from the Vendian of the southeastern White Sea Region. *Paleontological Journal*, **38**, 1–9.
- ROKOP, F. J. 1972. A new species of monoplacophoran from the abyssal north Pacific. *Veliger*, **15**, 91–95.
- WADE, M. J. 1972. *Hydrozoa* and *Scyphozoa* and other medusoids from the Precambrian Ediacara fauna; South Australia. *Palaeontology*, **15**, 197–255.
- WARÉN, A. & BOUCHET, P. 1990. *Laevipilina rolani*, a new monoplacophoran from off Southwestern Europe. *Journal of Molluscan Studies*, **56**, 449–553.

Ventogyrus, a possible siphonophore-like trilobozoan coelenterate from the Vendian Sequence (late Neoproterozoic), northern Russia

M. A. FEDONKIN & A. Y. IVANTSOV

Paleontological Institute, Russian Academy of Sciences, Profsoyuznaya ul. 123, Moscow, Russia 117997 (e-mail: mfedon@paleo.ru)

Abstract: Complex internal anatomy is documented for the first time in a Neoproterozoic soft-bodied invertebrate. New data suggests that *Ventogyrus*, originally described as a sessile, boat-shaped form belonging to the enigmatic Neoproterozoic group Petalonamae, is actually composed of three, identical modules, arranged around an axial rod. Each module has one longitudinal and numerous transverse septa, which delimit chambers of decreasing size from one end to the other. Three distinct longitudinal channels with alternating lateral branches make up an internal network, perhaps a circulatory system. *Ventogyrus* is a most unusual form, particularly in the quality of its three dimensional preservation of a complex internal structure and a three-fold symmetry, a symmetry shared by many Ediacarans.

Ediacaran metazoans of the late Neoproterozoic are attracting growing attention as key evidence of an early radiation of the Metazoa. Different specialists consider many, if not all, of these fossilized remains are representatives of a totally extinct group while others suggest that at least some Ediacarans gave rise to living groups (Glaessner 1984; Seilacher 1989, 1992; Gehling 1991; Jenkins 1992; Runnegar & Fedonkin 1992; Fedonkin

1992, 2003; Fedonkin & Waggoner 1997; Dzik 2003). The perplexing issue remains—what are the exact relationships between these enigmatic Ediacaran organisms and to which known groups might they belong? Current studies are underway in a variety of fields—comparative anatomy, molecular and developmental biology (Lipps *et al.* 1998; Ayala *et al.* 1998; Valentine 2004; Valentine *et al.* 1999; Peterson & Butterfield 2005).

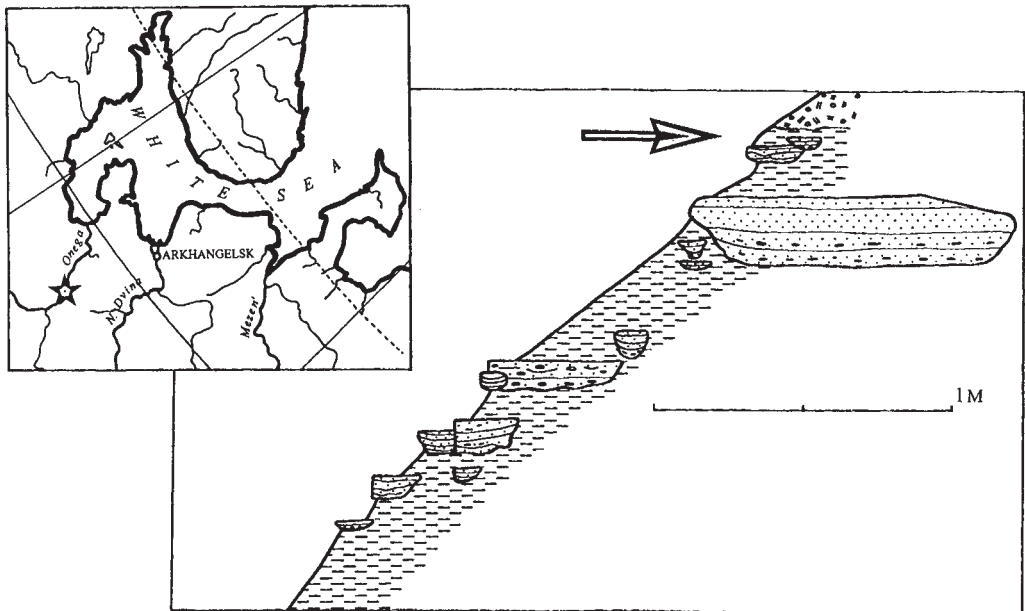


Fig. 1. Location of *Ventogyrus* fossil locality (starred) and geological setting of the outcrop on the Onega River. Sandstone lenses are shown in cross-section.

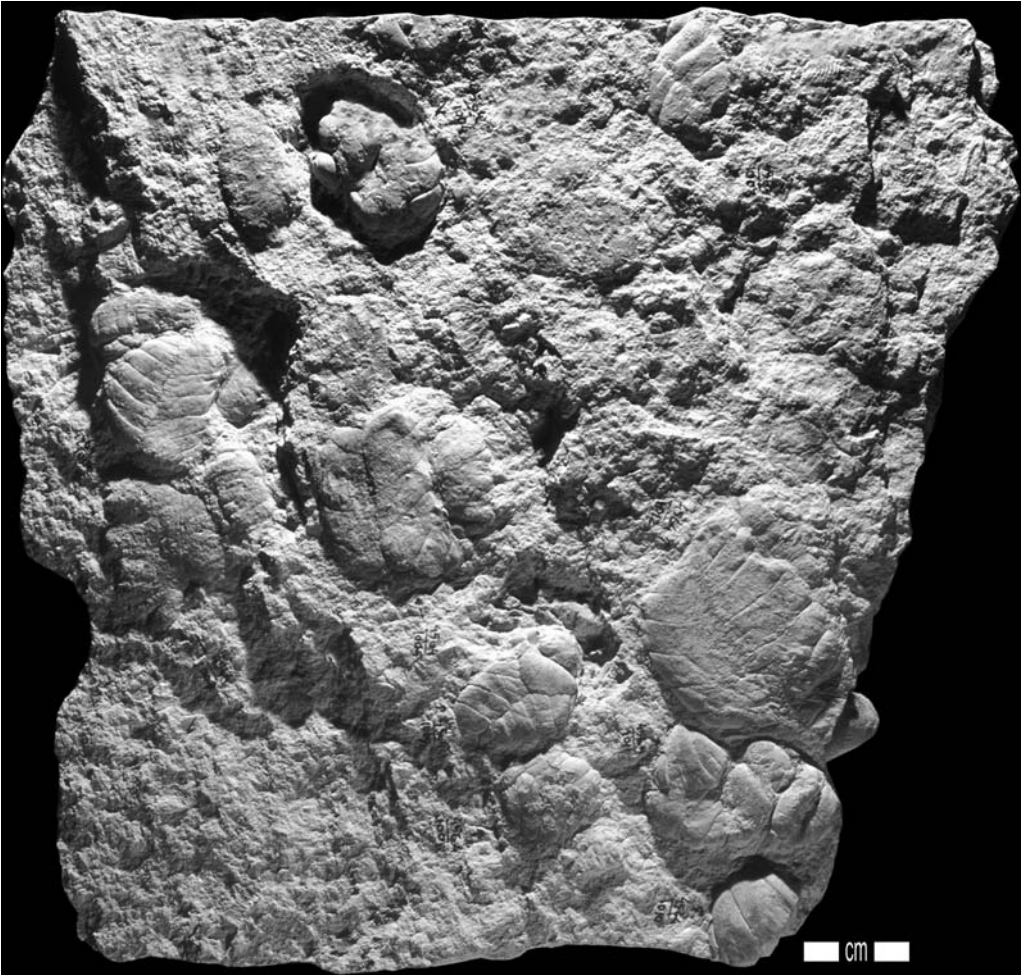


Fig. 2. *Ventogyrus chistyakovi*, Paleontological Institute, Russian Academy of Science, Moscow PIN No 4564/1006-1014, light from the top, internal cast of several modules, Yarnema, Onega Peninsula, White Sea region, northern Russia (F. Coffa).

Of the more than 200 species of Ediacaran metazoan fossils described to date, only a few show any details of their internal anatomy. *Ventogyrus chistyakovi* (Ivantsov & Grazhdankin 1997) is exceptional because abundant fossils are preserved in three dimensions. Complex casts record imprints of this form's internal structure in a fine-grained sandstone. The fossils occur in the lower part of the Ust'-Pinega Formation, a part of the Vendian sequence, which crops out along the Winter Coast of the White Sea in Russia's north, to the west of Arkhangel'sk (Chistyakov *et al.* 1984; Ivantsov & Grazhdankin 1997; Fedonkin *et al.* 1999).

Originally *Ventogyrus* was interpreted as a solitary, sessile, immobile organism, reaching up to 60 mm wide \times 120 mm long and 40 mm high,

thought to have been buried in life position. The supposed boat-like shape of this organism was structurally supported by a single, longitudinal septum with additional septa branching off it, with several orders of branching. These septa surrounded regular chambers that decreased in volume with increasing distance from the central axis. One unique, unpaired chamber occurs at one end of the structure. The impression of a thin layer of enclosing tissue is preserved as an external cast, and the branching channels of an internal tubular system are preserved in exquisite detail (Ivantsov & Grazhdankin 1997).

The construction in *Ventogyrus* (one longitudinal septum, with numerous transverse septa surrounding chambers) was originally supposed to

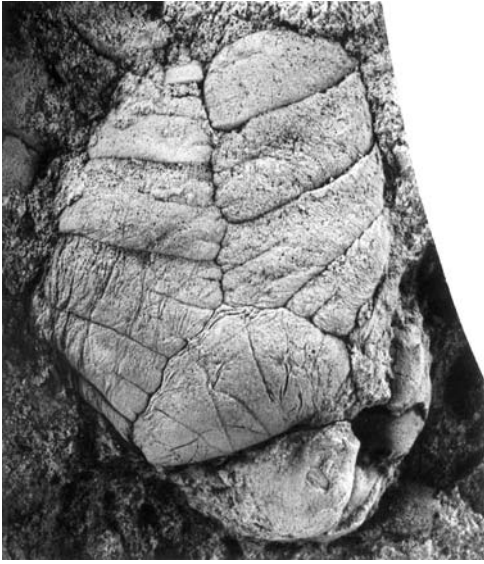


Fig. 3. *Ventogyrus chistakovi*, PIN No. 4564/1009, internal cast of module with well-preserved basal chamber. Yarnema, Onega Peninsula, White Sea region, northern Russia (M. Leonov).

be an architecture shared with other members of the Petalonamae, in particular with *Pteridinium*. *Ventogyrus* was thus assigned to the family Pteridinidae of Richter (1955). The taxonomic status and true nature of this group remains today uncertain and is the centre of much ongoing discussion. In fact, the Phylum Petalonamae may well be a

heterogeneous group, not a natural or homologous phylogenetic grouping.

The questioning of the assignment of *Ventogyrus* to the Petalonamae arose when specimens in this genus with unusual preservation were collected by the authors from a new locality on the Onega River in 1997–1999 (Fig. 1). The fossil assemblage at this locality includes complex casts of *Ventogyrus* (Figs 2–7), numerous tubular forms called *Calyptrina*, rare forms that show similarity to *Podolimirus*, *Swartpuntia* and a few other new taxa, including a conulariid-like fossil *Vendoconularia* with three-fold symmetry (Ivantsov & Fedonkin 2002). *Calyptrina* itself was originally described based on specimens recovered in a drill core from the Ust'-Pinega Formation on the northern Russian Platform (Sokolov 1968), later found elsewhere in the lower part of the Upper Vendian sequence (Gnilovskaya 1996; Sokolov 1997). *Podolimirus* was originally described from deposits near the base of the Vendian sequence in outcrops along the Dniester River of the Ukraine (Fedonkin in Velikanov *et al.* 1983). *Swartpuntia*, on the other hand, was known from the uppermost part of the Neoproterozoic section in Namibia (Narbonne *et al.* 1997).

This new find is of significant importance, because a few specimens are preserved with their axes oriented vertically within a small sand channel. These specimens broke apart along their median septa, and reveal a far more complex internal construction than was previously known (Fig. 4). Three, not one, major longitudinal septa connected the outer wall with an axial rod (Fig. 7). The overall form of the organism was

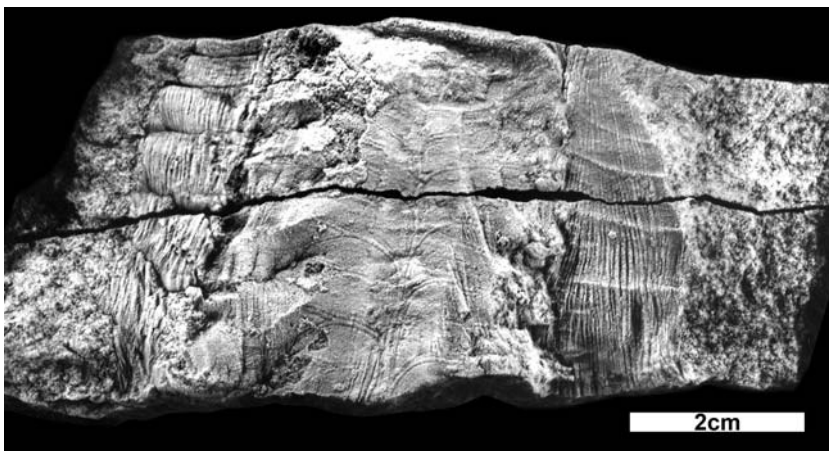


Fig. 4. *Ventogyrus chistakovi*, PIN No. 4564/1025, details of internal anatomy including the branching channel system in the middle part. The imprint was situated vertically in the host rock. Onega Peninsula, White Sea region, northern Russia (M. Leonov).

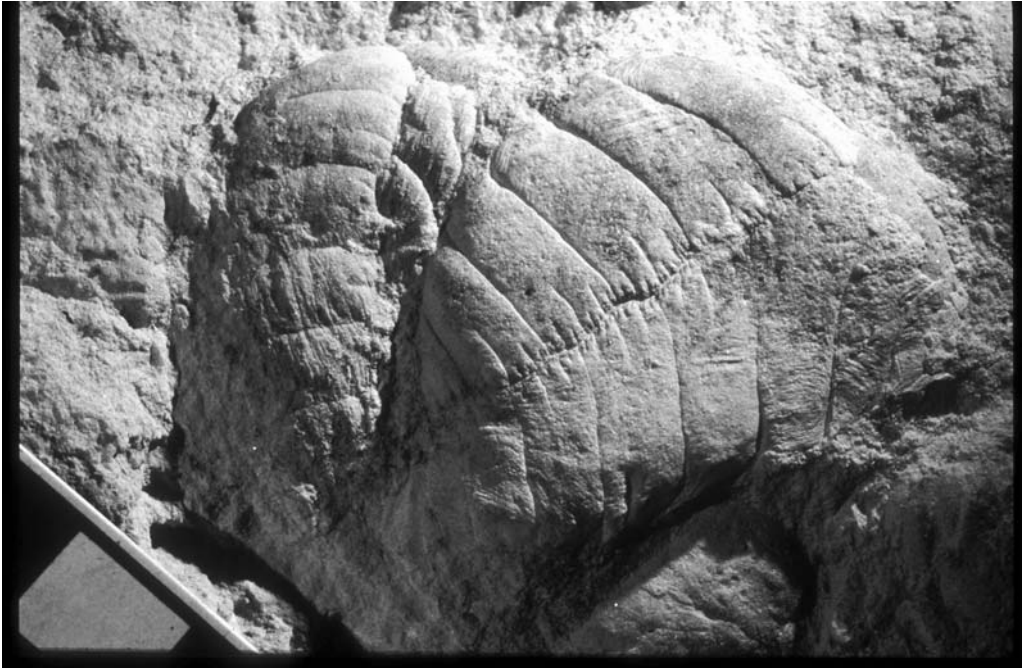


Fig. 5. *Ventogyrus chistakovi*, PIN No. 4564/1006, internal cast of two modules joined by their lateral and apical parts. The module on the left is strongly deformed but one can see its medial furrow and alternating position of the lobes. Yarnema, Onega Peninsula, White Sea region, northern Russia.

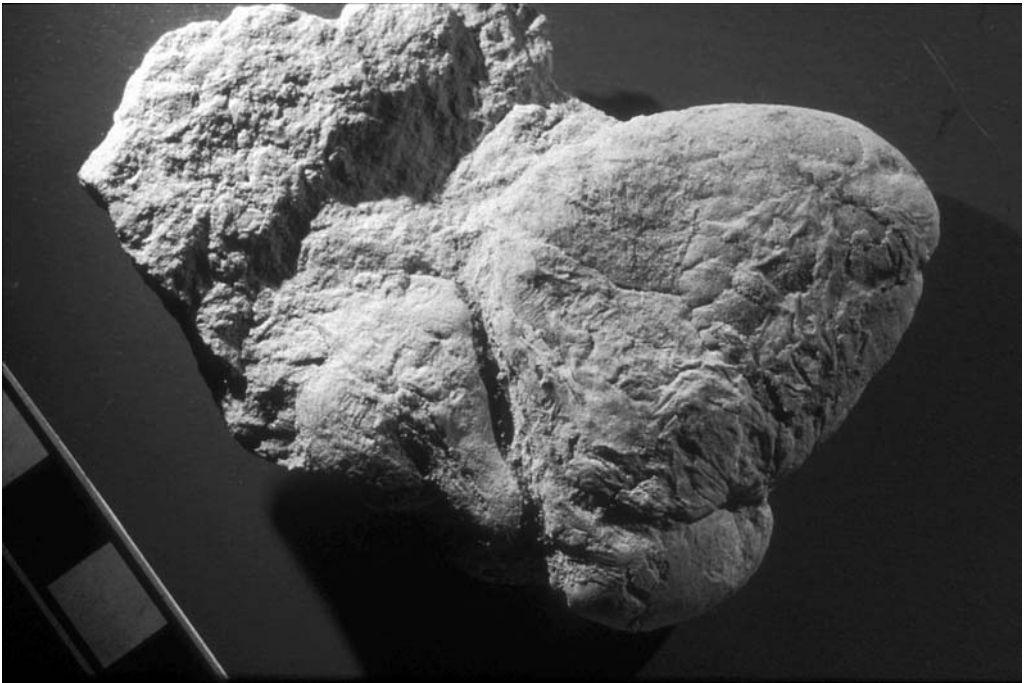


Fig. 6. *Ventogyrus chistakovi*, PIN No. 4564/1026, complex cast showing the external surface of the egg-shape body and the internal casts of the chambers (in the middle). Yarnema, Onega Peninsula, White Sea region, northern Russia.

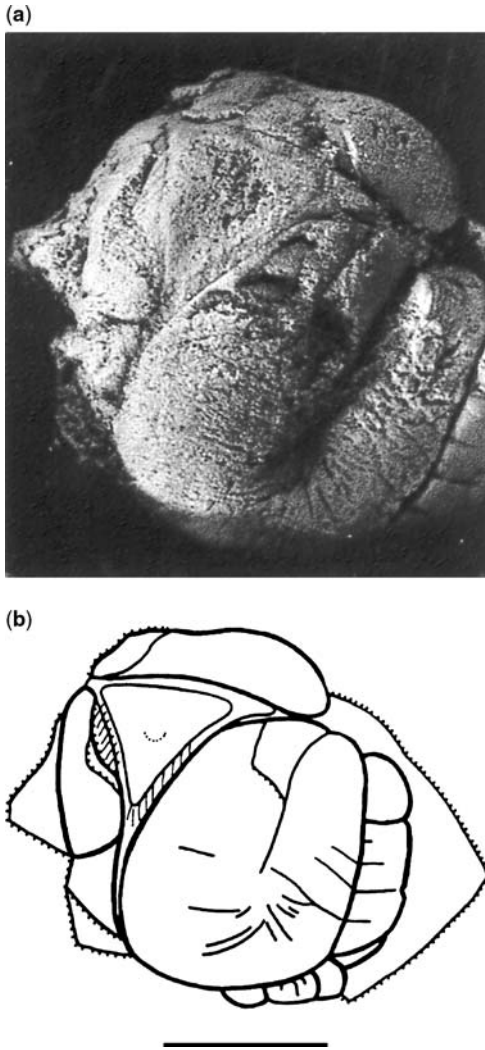


Fig. 7. *Ventogyrus chistyakovi*, (a) PIN No. 4564/1014, light from the top left, fragment of an internal cast viewed from its basal end; triangular base of a possible axial rod bordered by the three basal chambers variously deformed; (b) line drawing based on the photograph (scale: 1 cm).

not, indeed, boat-shaped, but instead more egg-shaped (Ivantsov 2001). The internal space was clearly divided into three distinct modules. The body was covered by thin integument which can sometime be preserved as an external cast (Fig. 6).

In the course of original study, fine linear structures were identified on what was thought to be the body surface of *Ventogyrus* (Ivantsov & Grazhdankin 1997). These structures have now been interpreted as likely part of a circulatory system, which

occurred beneath a thin membrane covering the body. New material clearly illustrates that these structures make up a complex internal system, consisting of at least three major channels (or tubes) that course along the axial rod (Figs 4, 8d). Each of the major channels branches laterally, originating from the axis in alternating order—the ‘symmetry of gliding reflection’ possessed by many of the Ediacarans. Lateral branches of the channels bifurcate a few times distally in a regular fashion. The width of these channels decrease step-wise at each branching point as they course away from the midline towards the periphery. This channel system spreads over the surfaces of the septa. The distal ends of channel branches intersect the transverse septa at points where these transverse septa meet the medial septum.

The complex system of septa certainly produced a stiffened organism. Additional rigidity of the entire body of *Ventogyrus* could have been provided by the content of the chambers themselves. Those could have been filled with body fluids or gas. *Ventogyrus* certainly exhibits a wide range of body deformation, and the fact that the chambers and module as a whole are preserved only when filled with sand supports the view that there was no cellular material or tissue inside the chambers.

If the chambers were filled with gas, it might have produced a strong positive buoyancy of such an egg-shaped organism. Such buoyancy could have allowed the organism to float or at least maintain a position in the water column above the sea floor. The bipolar structure of *Ventogyrus* may reflect an environmental gradient and suggest a vertical orientation of the body axis in life. Rare specimens which preserve the basal side of the body demonstrate the presence of a triangular cross-section of what appears to be an axial rod with a circular structure at its centre (Fig. 7a, b). We suggest that this round structure could represent the site where a stem could have attached, either to tether *Ventogyrus* to the bottom or to act as a stabilizer similar to such a structure known in recent floating cnidarian siphonophorans (Fig. 8). So far, however, no such stem has been found directly attached to the *Ventogyrus*. Numerous tubular and globular fossils (sand casts) associated with *Ventogyrus* may be parts of the same organism, but the more evidence must be obtained in the course of further field work to clarify such interpretations. Some researchers have suggested an alternative hypothesis—*Ventogyrus* reconstructed as an egg-shaped ctenophoran (Dzik 2003) floating with its wider end up (Ivantsov 2003).

Ventogyrus is best preserved in the submarine channel deposits, emplaced when storm or seasonal input brought about downslope avalanches, cut into the offshore platform and marine slope settings. It is

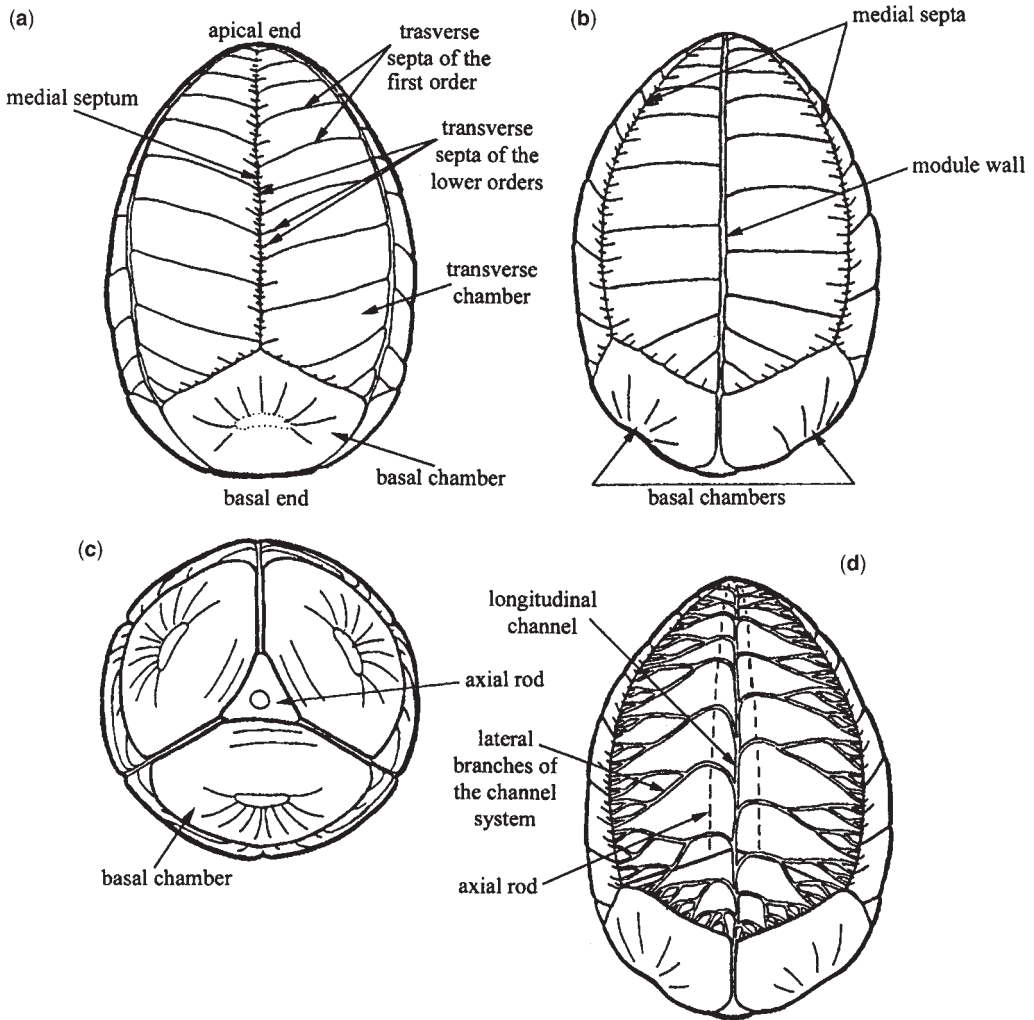


Fig. 8. Reconstruction of the internal anatomy of *Ventogyrus* with the cover tissue removed. (a) side views with one medial septum and a basal chamber in view; (b) side view of the same body rotated 60 degrees around the axis; (c) basal view; (d) view in the same position as (b), with two sectors of adjacent modules removed, morphology of one of three identical channel systems (after Ivantsov 2003).

rarely preserved in sediments that were deposited outside of these channels. The most abundant accumulation occurs well above the base of these channels, indicating that they were deposited within the sediments that were moving down the slope and not bottom dwellers that were suddenly overwhelmed by the sand avalanche. But, once again, further collection, careful mapping of the occurrence and association with other taxa need to be carried out before establishing the mode of life of this unusual organism.

At this point, too, it is difficult to relate the detail of the preserved material to any extent group.

Ventogyrus possesses a unique body plan, rather different from Phanerozoic organisms, but consistent with that of some other Ediacaran-Early Cambrian metazoans. The three-fold symmetry that so commonly makes its appearance in forms such as *Albumares*, *Anfesta*, *Tribrachidium*, *Pteridinium* and *Hallidaya* is a linkage between all of these taxa and the reason the Class Trilobozoa was erected originally (Fedonkin, 1990, 3–120.). Such organisms may, in fact, be part of a high-ranking taxon that was replaced by the ‘new kids on the block’, which developed in the early part of the Phanerozoic, as metazoans gained hard

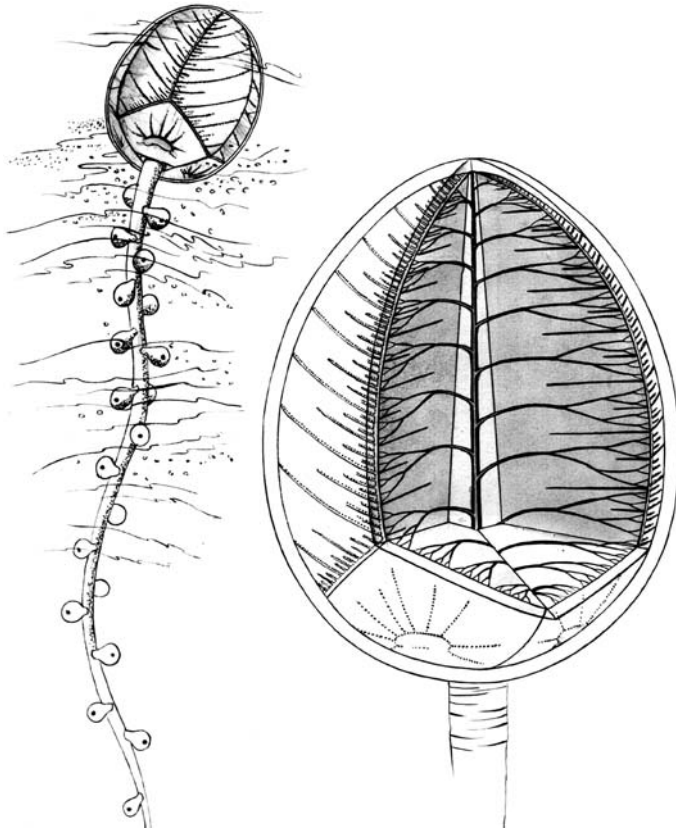


Fig. 9. Reconstruction of *Ventogyrus* as a siphonophore-like coelenterate.

mineralized parts, the ability to burrow deeply and exploit effectively the food resources of the ocean and in doing so changed the world forever.

Comparison of soft body fossils (both casts and molds) of Ediacarans with skeletal remains of Cambrian organisms encounters some difficulties when one attempts to determine phylogenetic ties between the metazoans of these two periods. In the case of *Ventogyrus* there is remarkable similarity of its axial rod with three major septa and similar structures found in Early Cambrian anabaritids—phosphatic conical fossils bearing outer septa, e.g. *Selindeochrea ternaria* or *Anabarites tricarinatus* (Missarzhevsky 1989; Rozanov & Zhuravlev 1992) and structures which certainly represent internal skeletons.

Ventogyrus has such outstanding preservation of its detailed architecture that it needs considerably more attention—both in the field and in the laboratory—for it holds great promise for giving an in-depth understanding of at least one high-rank taxon of the Ediacaran organisms.

The project was supported by the Russian Fund for Basic Research (Grant No. 96-05-64806 and 99-05-64547) and by the National Geographic Society (Grant 6015-97). We are grateful to E. A. Vysotsky for his help in the field, A. V. Mazin, M. V. Leonov and F. Coffa for photography, N. V. Bochkareva and S. V. Rozhnov (Jr.) for technical assistance at the Paleontological Institute (Moscow), to D. H. Erwin, J. G. Gehling, L. Gershwin, J. H. Lipps, A. Seilacher and B. S. Sokolov for fruitful discussions. We also thank the reviewers J. Stilwell and P. Vickers-Rich.

References

- AYALA, F. J., RZHETSKY, A. & AYALA, F. J. 1998. Origin of the metazoan phyla: Molecular clocks confirm paleontological estimates. *Proceedings of the National Academy of Science*, **95**, 606–611.
- CHISTYAKOV, V. G., KALMYKOVA, N. A., NESSOV, L. A. & SUSLOV, G. A. 1984. On the presence of the Vendian deposits in the mid-stream of Onega River and on the possible existence of tunicates (Tunicata: Chordata)

- in the Precambrian. *Vestnik of the Leningrad State University*, **6**, 11–19 [in Russian with English summary].
- DZIK, J. 2003. Anatomical information content in the Ediacaran fossils and their possible zoological affinities. *Integrative Comparative Biology*, **43**, 114–126.
- FEDONKIN, M. A. 1990. Non-skeletal fauna of the Vendian: promorphological analysis. In: SOKOLOV, B. S. & IWANOWSKI, A. B. (eds) *The Vendian System. 1. Paleontology*, Springer-Verlag, Berlin, 7–120, 132–137.
- FEDONKIN, M. A. 1992. Vendian faunas and the early evolution of Metazoa. In: LIPPS, J. H. & SIGNOR, P. W. (eds) *Origin and Early Evolution of the Metazoa*, Plenum Press, New York, 87–129.
- FEDONKIN, M. A. 2003. The origin of the Metazoa in light of the Proterozoic fossil record. *Paleontological Research*, **7**, 9–41.
- FEDONKIN, M. A. & WAGGONER, B. M. 1997. The late Precambrian fossil *Kimberella* is a mollusk-like bilaterian organism. *Nature*, **388**, 868–871.
- FEDONKIN, M. A., IVANTSOV, A. Y. & GRAZHDANKIN, D. V. 1999. Biostratigraphic potential of the Vendian fauna. In: *Stratigraphy, Paleontology, and Perspectives for Oil of the Riphean and Vendian of East Part of the East-European Platform, Proceedings*, Pt. 1 7–11, Pt. 2, 77–78 [in Russian].
- GEHLING, J. G. 1991. The case for Ediacaran fossil roots to the Metazoan tree. In: RADHAKRISHNA, B. P. (ed.) *The World of Martin Glaessner*. Geological Society of India Memoir, **20**, 181–224.
- GLAESSNER, M. F. 1984. *The Dawn of Animal Life—A Biohistorical Study*. Cambridge University Press, Cambridge.
- GNILOVSKAYA, M. B. 1996. New saarinnids from the Vendian of the Russian Platform. *Doklady Rossiiskoi Akademii Nauk*, **348**, 89–93.
- IVANTSOV, A. Y. 2001. Dependence of reconstructions on the preservation character of the Ediacaran organisms. In: PONOMARENKO, A. G., ROZANOV, A. Y. & FEDONKIN, M. A. (eds) *Ecosystem Restructurings and Evolution of Biosphere*. Moscow, Paleontological Institute RAS, **4**, 64–67 [in Russian].
- IVANTSOV, A. Y. 2003. Vendian organisms are identified by the imprints. *Priroda*, **10**, 3–9 [in Russian].
- IVANTSOV, A. Y. & GRAZHDANKIN, D. V. 1997. A new representative of the Petalonamae from the Upper Vendian of the Arkhangelsk Region. *Paleontological Journal*, **31**, 1–16.
- IVANTSOV, A. Y. & FEDONKIN, M. A. 2002. Conulariid-like fossil from the Vendian of Russia: a metazoan clade across the Proterozoic/Palaeozoic boundary. *Palaentology*, **45**, 1219–1229.
- JENKINS, R. J. F. 1992. Functional and ecological aspects of Ediacaran Assemblages. In: LIPPS, J. H. & SIGNOR, P. W. (eds) *Origin and Early Evolution of the Metazoa*. Plenum Press, New York, 131–176.
- LIPPS, J. H., COLLINS, A. G. & FEDONKIN, M. A. 1998. Evolution of biological complexity: Evidence from geology, paleontology and molecular biology. In: HOOVER, R. B. (ed.) *Instruments, Methods, and Missions for Astrobiology*. Proceedings of the International Society for Optical Engineering, **3441**, 138–148.
- MISSARZHEVSKY, V. V. 1989. Oldest skeletal fossils and stratigraphy of Precambrian and Cambrian boundary beds. *Transactions of the Geological Institute, USSR Academy of Sciences*, **443**, 1–237 [in Russian].
- NARBONNE, G. M., SAYLOR, B. Z. & GROTZINGER, J. P. 1997. The youngest Ediacaran fossils from Southern Africa. *Journal of Paleontology*, **7**, 953–967.
- PETERSON, K. J. & BUTTERFIELD, N. J. 2005. Origin of the Eumetazoa: Testing ecological predictions of molecular clocks against the Proterozoic fossil record. Proceedings of the National Academy of Sciences, **102**, 9547–9552.
- RICHTER, R. 1955. Die ältesten Fossilien Sud-Afrikas. *Senckenbergiana Lethaea*, **36**, 243–289.
- ROZANOV, A. Yu. & ZHURAVLEV, A. Yu. 1992. The Lower Cambrian fossil record of the Soviet Union. In: LIPPS, J. H. & SIGNOR, P. W. *Origin and Early Evolution of the Metazoa*. Plenum Press, New York, 205–282.
- RUNNEGAR, B. N. & FEDONKIN, M. A. 1992. Proterozoic metazoan body fossils. In: SCHOPF, J. W. & KLEIN, C. (eds) *The Proterozoic Biosphere. A Multidisciplinary Study*. Cambridge University Press, New York, 369–388.
- SEILACHER, A. 1989. Vendozoa: Organismic construction in the Proterozoic biosphere. *Lethaia*, **22**, 229–239.
- SEILACHER, A. 1992. Vendobionta and Psammocorallia: Lost construction of Precambrian evolution. *Journal of the Geological Society of London*, **149**, 607–613.
- SOKOLOV, B. S. 1968. Vendian and Early Cambrian Sabelliditidae (Pogonophora) of the USSR. *Proceedings of the 23rd International Geological Congress*, 79–86.
- SOKOLOV, B. S. 1997. *Essays on the Advent of the Vendian System*. KMK Scientific Press, Moscow [in Russian with English summary].
- SOKOLOV, B. S. & IWANOWSKI, A. B. 1990. *The Vendian System. Volume 1*. Springer Verlag, Heidelberg.
- VALENTINE, J. W. 2004. *On the Origin of Phyla*. University of Chicago Press, Chicago.
- VALENTINE, J. W., JABLONSKI, D. & ERWIN, D.H. 1999. Fossils, molecules and embryos: New perspectives on the Cambrian Explosion. *Development*, **126**, 851–859.
- VELIKANOV, V. A., ASEVA, E. A. & FEDONKIN, M. A. 1983. *The Vendian of the Ukraine*. Naukova Dumka, Kiev [in Russian].

The provenance and palaeobiology of a new multi-vened, chambered frondose organism from the Ediacaran (later Neoproterozoic) of South Australia

R. J. F. JENKINS¹ & C. NEDIN²

¹Science Centre, South Australian Museum, North Terrace, Adelaide, SA 5000, Australia
(e-mail: Jenkins.Richard@saugov.sa.gov.au)

²Department of Industry, Tourism and Resources, GPO Box 9839,
Canberra ACT 2601, Australia

Abstract: The new, large, frondose and stalked, Ediacaran (late Neoproterozoic) ‘petalonamid’ *Pambikalbae hasenohrae* gen. et sp. nov. is preserved in a three-dimensional manner within sandy channel fills occurring directly below the Ediacara Member of the Rawnsley Quartzite on the ‘Nilpena’ pastoral property at a western outlier of the Flinders Ranges, South Australia. *Pambikalbae hasenohrae* was made up of numerous chambered vanes supported by a tapering axial stem and an anchoring stalk. Chambers forming the vanes were commonly infilled with sediment, though variably flattened; groups of vanes representing individual specimens can extend as much as c. 3.7 cm deep through the hosting sandstone matrix. Several series of chambers present in each vane abut at zigzag sutures. *Pambikalbae* is clearly not a cnidarian sea pen, but nevertheless exhibits characteristics suggestive of an evolutionary grade comparable to that of known modern cnidarian divisions. Though the serial geometric configuration of its thin integument seems ideally suited to house symbiotic microbial photoautotrophs, our appraisal of the palaeoecology of *Pambikalbae* is supportive of its being a heterotrophic suspension feeder. *Pambikalbae* may plausibly be a highly derived hydrozoan, part of the ancestral stock of the Siphonophorida, or a sister group to the early Chondrophorina.

The realization that the majority of discoidal remains in Ediacaran biotas are either the basal aspects of anemone-like forms or actually holdfasts of frondose organisms, and not cnidarian medusae (Glaessner 1959; Seilacher 1984, 1989, 1992; Jenkins 1989, 1992, 1996; McMenamin & McMenamin 1990; Narbonne 1998; Preiss 1999; Gehling *et al.* 2000; Steiner & Reitner 2001), necessitates a profound reappraisal of the composition of early metazoan communities. Frondose fossils are the longest studied of any Ediacaran remains, but, despite this, their affinities and biology are amongst the most controversial (Seilacher 1984, 1989, 1992; Fedonkin 1985*a, b*, 1990; Jenkins 1985, 1995; McMenamin & McMenamin 1990; Runnegar 1991, 1995; Fedonkin & Runnegar 1992*a, b*; Conway Morris 1992, 1993*a, b*; Narbonne *et al.* 1997; Narbonne 1998; Dzik 1999, 2002; Narbonne & Gehling 2003; Laflamme *et al.* 2004; Narbonne 2005). This paper describes a new, spectacular, frondose fossil, *Pambikalbae hasenohrae* gen. et sp. nov. preserved in channel sandstones low in the Rawnsley Quartzite in a western outlier of the Flinders Ranges on the ‘Nilpena’ pastoral property (Fig. 1).

An observant amateur, Pamela Hasenhor, drew R.J.F.J.’s attention to fossiliferous exposures in

the area, though Wade (1970) had made an earlier investigation. Lithologies present resemble those at the nearby Ediacara Range, where the fossils have been greatly depleted by long-term collecting.

Geological setting

The late Neoproterozoic soft-bodied Ediacara ‘fauna’ or assemblage has previously been considered as occurring in a mainly recessive stratigraphic interval present in the lower to mid-part of the Rawnsley Quartzite of the Pound Subgroup (Wade 1968, 1970, 1971) described as the Ediacara Member (Jenkins *et al.* 1983; Gehling 1987, 1988, 1999, 2000; Jenkins 1992; 1995, 1996; Preiss 1999). Recent investigations in the western Flinders Ranges indicate that this notion embraces a considerable oversimplification, and three separate faunal levels, sequential in age, are presently identified. Each of these faunal levels holds potential promise for intercontinental biostratigraphic correlation (cf. Jenkins 1995; Nedin & Jenkins 1998) and their individual placement can be established within different sequence stratigraphic cycles or distinct parts of such cycles. A new formal stratigraphic nomenclature for relevant parts of the succession is proposed below.

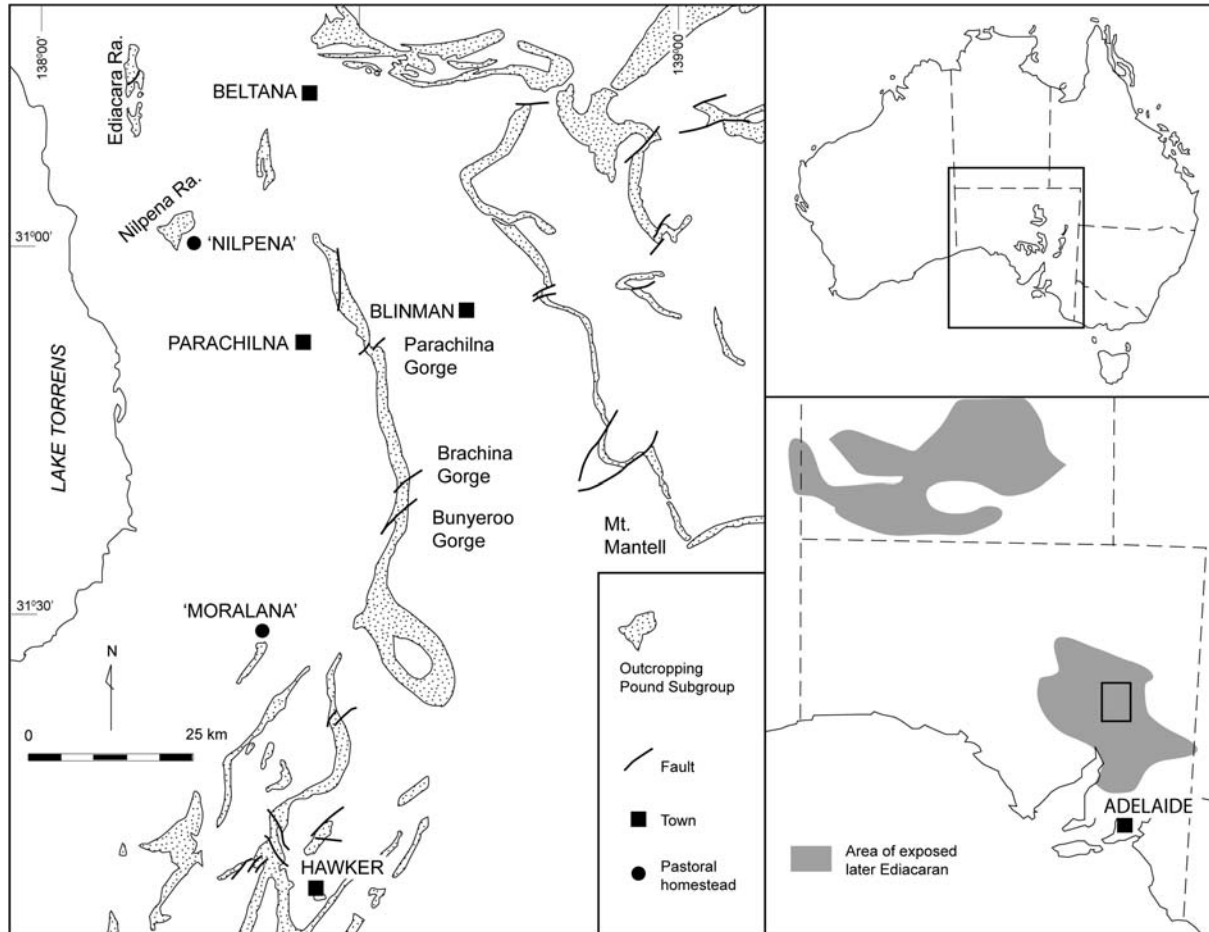


Fig. 1. Locality map for sites of interest in the Flinders Ranges, South Australia. Brachina Gorge is the site of the Global Stratotype Section and Point (GSSP) designated by the International Union of Geological Sciences for the new Ediacaran Period and System.

Transition between Bonney Sandstone and Rawnsley Quartzite

It is recognized that the abrupt change between the maroon-brown Bonney Sandstone and the more boldly outcropping white sandstones or quartzites of the Chase Quartzite Member (Reid & Preiss 1999; Preiss 1999; Gehling 2000) of the Rawnsley Quartzite validly marks a meaningful boundary between these two formations (Fig. 2). The uppermost Bonney Sandstone commonly comprises poorly bedded or wavy-bedded, maroon-brown, sandy siltstones and interbeds of brown sandstone with common polygonal mudcracks on upper surfaces. These lithologies are interpreted as indicating quiet water suspension deposition of silt in a terrigenous, interfluvial, flood plain setting, with episodic sheet flooding and subsequent exposure and desiccation.

Chase Quartzite Member of Rawnsley Quartzite

Within the southern and middle Flinders Ranges the sharp lower boundary of the Chase Quartzite Member (Fig. 2, MEMBER '1') chiefly represents a marine flooding surface with flaggy, granule-

bearing, ripple-bedded, shoreline sandstones above (e.g. Gehling 2000). These grade upwards into thicker bedded, white weathering, feldspathic sandstones with abundant 'dish' structures and sub-polygonal ridges resembling the 'gamma-petee' structures which Reineck *et al.* (1990) attributed to lateral overthrusting of microbial bound sediment laminae due to interstitial crystal growth in a super-saturated/evaporitic upper tidal setting (Gehling 1999, 2000). We concur with Gehling (2000) that deposition occurred in a tidal setting. Near the pastoral homestead 'Moralana', the Chase Quartzite Member measures some 90 m thick and has a thick upper component of sandstone with dish-structures and petee-ridges below a thin development of the fossiliferous Ediacara Member. Though parts of the Chase Quartzite Member commonly include flaggy sand beds, which mould smooth clay partings, such as those that characterize the higher fossiliferous Ediacara Member, few possible indications of animal fossils have been found. A delicate tracery of the kind referred to as 'old elephant skin' structure (Narbonne 1998), attributed to cyanobacterial films or mats (Gehling 1988, 1999; Hagadorn & Bottjer 1997; Gehling *et al.* 2000), commonly marks surfaces.

Breakfast Time Creek Member of Rawnsley Quartzite, new member

Locally, the Chase Quartzite Member is sharply incised by channels containing thin (0–3 m thick) basal sandstones with mud-clast conglomerates, and maroon-brown laminated siltstones which grade upwards into an interval consisting of flaggy, fossiliferous sandstone beds. Uncommon casts of tool marks at the base of these flags are orientated in a variety of directions. Top surfaces show 'rib and furrow' markings, indicating interfering oscillatory currents. These characteristics conform closely to those, which Grey & Benton (1982) and Seilacher (1982) indicated as diagnostic for storm beds or tempestites. Cleaner sandstones with abundant mudcracks on upper surfaces predominate in the upper parts of the cycle. Impurities in the sandstones cause them to weather to a distinctive, dark red-brown colour with abundant black manganese-stainings. These channel deposits reach a local thickness of about 34 m and are formally nominated here as the Breakfast Time Creek Member of the Rawnsley Quartzite (Fig. 2, '2'). The associated fossil remains comprise the 'Rangeid-Hiemalora' assemblage (Zone) of Jenkins (1995). Clustered, bag-shaped structures recently found in the older part of one of these channels resemble the *in situ* 'colonies' of *Ernieta* known from the Kliphoeck Member of the Dabis Formation in the Nama

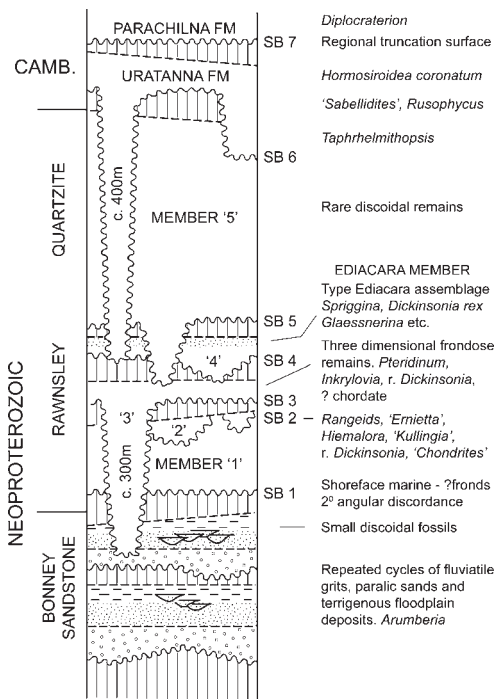


Fig. 2. Stratigraphic diagram of the late-older Ediacaran cambrian sequence in the Flinders Ranges of South Australia.

Group of Namibia (e.g. Jenkins 1992, fig. 7; Dzik 1999, figs 1d, 3).

The type section of the Breakfast Time Creek Member is located in the east-dipping fill of a large channel, and the section runs NE–SW. This location was sited by satellite coordinates using a new instrument owned by an electronics engineer (WGS 84 standard). The coordinates have been registered with the Australian Stratigraphy Sub-commission for inclusion in the Australian Stratigraphic Units Database with restricted permission for access. The thickness at the type section is measured as close to 34 metres.

Winnowie Member of Rawnsley Quartzite, new member

Both the older fossiliferous channels and the Chase Quartzite Member may be truncated or deeply incised by thick bedded to massive white quartzites and mud-clast conglomerates comprising ‘nested’ channel deposits. R. Fargher of Parachilna has located distinctive associated faunal remains preserved in a three-dimensional manner in a lensoid transgressive phase towards the top of one of these nested channel fills. These channel deposits often form prominent, blocky outcrops with grey-weathering quartzites demonstrating curved fractures and common moulds of twisted or torn scraps of organic tissues. Other flaggy sandstones can also be present. The equivalent channel deposits present at the southern end of Ediacara Range were described by Wade (1971, p. 183) as occurring 7 m to ‘no more than 18 m below the main fossiliferous unit’ (or Ediacara Member *sensu* Jenkins *et al.* 1983), and known to include *Pteridinium* cf. *simplex* (= *Pteridinium carolinaense*), other frondose remains and *Chondroplon bilobatum*. The erosive base of these channels (e.g. Gehling 1987, 2000), downcutting some 90 m in the southeastern part of Ediacara Range, likely reflects a low-stand of sea level. This 90 m thick suite of channel deposits and its lateral equivalents are recognized formally as the Winnowie Member of the Rawnsley Quartzite (Fig. 2, ‘3’). In the ‘Nilpena’ area, the base of this member may erode down c. 300 m through the Chase Quartzite Member (and the channelized member with *Rangea*) and locally forms deep incisions, well below the top of the Bonney Sandstone.

Faunal elements in these channel sandstones are remarkable for their three-dimensional mode of preservation (‘Nama’ preservation of Narbonne 2005, see also below) and include examples of *Charnia* cf. *masoni*, with the holdfast disc on a bedding sole and the stem and fusiform, chambered frond projecting obliquely upwards into individual event beds (Nedin & Jenkins 1998). Other identified

faunal remains include *Pteridinium carolinaense*, cf. *Inkrylovia*, ‘*Cyclomedusa plana*’, and rare *Dickinsonia costata*. Trace fossils are relatively uncommon, mainly *Planolites*.

The base of the Zimneygory Formation in the White Sea Zimney Gory section, northern Russia, hosts a megascopic biota similar to the classical Ediacara Assemblage of the Flinders Ranges, and is dated utilizing U–Pb zircon concordia intercepts at 555.3 ± 0.3 Ma (Martin *et al.* 2000). Grazhdan-kin (2004, figs 1 and 2) reported a technically unpublished U–Pb zircon age of 558 ± 1 Ma (2σ), for the base of the Verkhovka Formation, which directly underlies the Zimneygory Formation. These ages both reduce to equivalents c. 553 Ma with a change in spike calibration and use of a newly determined ^{235}U decay constant (W. Compton, Australian National University, pers. comm., 2006). On the basis of faunal content, the Winnowie Member correlates approximately with the mid Verkhovka Formation, now indicated at c. 553 Ma.

The type section of the Winnowie Member is located on the SE sector of the large syncline extending through the Ediacara Range, and is placed by the satellite coordinates as 138 08.688 E, 30 49.740 S, (base) and 138 08.564 E, 30 49.733 S (top). The member is 48 m thick at the type section, and is named for the nearby historical dwelling ‘Winnowie Hut’.

Pambikalbae hasenohrae occurs in current-deposited, sheet sands of a channel, and in similar beds towards the top of a thick interval of clean sands filling another large channel scour in the ‘Nilpena’ area.

Ediacara Member of the Rawnsley Quartzite

The base of the Ediacara Member is defined as the erosive, locally downcutting surface between the medium-bedded channel sandstones described above, and the succeeding white-weathering shaley beds (Jenkins *et al.* 1983), which grade upward into flaggy fossiliferous strata (Fig. 2, ‘4’). Evidently, the deeply weathered and leached white shaley beds were formerly a ‘black-shale’ facies, deposited in shallow estuarine embayments under conditions of partial anoxia during an early stage of transgression linked to the deposition of the Ediacara Member. Speckles of red oxide are interpreted as representing weathered pyrite. The member is characterized by its own distinctive faunal association (Jenkins 1992, 1996; Droser *et al.* 2005, 2006). Mid parts of the lower cycle of the Ediacara Member at ‘Nilpena’ include several thin quartzite beds, which preserve numerous remains of *Dickinsonia costata*, probably deposited as a result of local density currents. The abundantly fossiliferous overlying sandstones are ripple-bedded, and it is suggested that near-shore

wave action is responsible for such ripple forms, contrary to previous interpretations. The lower fossiliferous cycle of the member is topped by a narrow interval (several metres) with mud cracks in flaggy sandstones indicative of local emergence. Above this, a second relatively thin flaggy fossiliferous interval is succeeded by medium-bedded fossil-bearing sandstones characterized by large dune forms (Facies 'D' of Jenkins *et al.* 1983; this alphabetical designation does not correspond to that of Gehling 2000). Facies 'D' represents sediments deposited in an upper shoreface setting, and grades up into current-swept, thin-bedded sandstones. Massive bedded channel sandstones characterize the 'upper member' of the Rawnsley Quartzite and become prevalent at about this level.

The presence of three distinctive faunal associations over an apparent vertical stratigraphic interval of as little as *c.* 90 m is an indication that the disjunctive sedimentary cycles represented in this part of the older Rawnsley Quartzite reflect significant condensation, probably manifest principally at the deeply incised surfaces. Gehling (2000) does not recognize separate faunal associations, but it is suggested that taxa unique to each assemblage can be recognized, and sharp changes in the abundance of those species do occur. Each assemblage is considered separated temporally from the next by an erosive surface. Perhaps in the central Flinders Ranges, only the correlative conformities are represented. Alternatively, the earlier fossiliferous cycles may have simply been eroded away completely, or are not locally fossiliferous and have gone unrecognized.

Frondose remains are relatively uncommon in all three assemblages, perhaps because the fossiliferous wave-rippled sandstones were deposited in environments not conducive to their preservation. The fronds likely extended into the water and thus had a different preservational potential to that of their resilient holdfasts, already buried at the time of death (Jenkins 1989, 1992, 1996; Narbonne 2005). Because the integument of the free-living animals, such as the dickinsoniids was 'leather-like' (Seilacher 1989), they were preserved in a manner different from that of the fronds (Wade 1968), and obviously different from trace fossils (see also Fedonkin & Runnegar 1992*b*; Crimes & Fedonkin 1996; Droser *et al.* 2005; Narbonne 2005). Thus it is difficult to assess the original abundance of forms in the communities from counts of the fossil remains present.

Repositories

All studied materials are held in the palaeontology collection of the South Australian Museum and are indicated by register numbers prefixed 'SAM'.

Preservation

Previous studies of the Ediacara assemblage in the Flinders Ranges indicate that the majority of the fossil remains are preserved as low relief markings on the soles of sand beds, which are now resistant sandstone or quartzite. Organisms that had a relatively tough or resilient integument, such as *Dickinsonia*, *Spriggina*, *Parvancorina*, *Tribrachidium*, and *Rugoconites*, tended to support the sand that buried them, so that the interlocking of the sand grains on compaction and subsequent early cementation formed a 'hollow' external mould of the upper surface of their body (Wade 1968; Gehling 1987, 1988, 1991, 1999; Runnegar 1991; Fedonkin & Runnegar 1992*a*; Gehling *et al.* 2000). The primary cementing agent was apparently a fine film of pyrite constituting a 'death-mask' (Gehling 1999).

Other organisms, like *Charniodiscus*, began to decompose soon after burial, and Wade (1968) considered that sand subsiding through their disintegrating tissues settled into an under-mould of the body formed on the thixotropic silts which comprised the substrate at the time the organism came to rest on the bottom (e.g. Gehling 1999, 2000). A taphonomic study of the preservational potential of modern soft-bodied metazoans utilizing freezing of the water-saturated sediment as a means of simulating lithification (Norris 1989) had substantially confirmed Wade's observation.

The flat shapes of most local Ediacaran fossil remains led some workers to conclude that the original organisms were foliate or sheet-like (Raff & Raff 1970; Cloud 1976; Runnegar 1982*a, b*, 1991, 1995; Seilacher 1984, 1989, 1992). While this was probably true for a few forms (e.g. some rare medusiform structures), it seems far from likely for most of the Ediacaran organisms. Where the preserving sands happen to have buried resilient bodies lying on thick, soft clays, deep three-dimensional moulds have resulted, and it is apparent that the more common flat imprints are an artefact of compaction of a 'heavy' sand cover (Gehling 1987, 1988, 1991, 1999; Jenkins 1992, 1995, 1996; Gehling *et al.* 2000). Broad animals, such as the dickinsoniids, were particularly prone to such flattening (e.g. Dzik 2002), and the 5% or so individuals of *Dickinsonia costata* seen compressed into asymmetrical shapes provide an indication that after burial, fluid was squeezed from the organism and the upper and lower tissue layers of the body tended to slide over one another so that the axial line displaced towards one side (Jenkins 1992, 1996).

Retallack (1994) compared the preservation of Ediacaran forms with flattened fossil plant stems and woody logs (mainly Palaeozoic) enveloped by sand and compressed through substantial burial

loading, and also studied Late Carboniferous jellyfish occurring in siderite nodules. Steiner & Reitner (2001) reported Ediacaran fossils from northern Russia to include thin, carbonized layers such as those that commonly accompany plant compressions. In the South Australian material, any such partings have apparently been oxidized, and preservation is apparently due to closely appressed surfaces formed by aligned grains in direct contact, an indication that the tissue layer was thin and membranous, not comprising some substantive cellulose-like substance. This alignment of grains in opposition is not consistent with the idea of Crimes & Fedonkin (1996) that certain forms grew by migration of naked protoplasm through pore spaces. There is abundant evidence of overfolding (Seilacher 1992, fig. 3), creasing and wrinkling (Cloud 1976) or stretching (Runnegar 1982a, fig. 1a) of the integument of some Ediacaran forms (e.g. *Pteridinium*), prior to burial, thus demonstrating that the tissues in these taxa were supple. It appears that the fossil imprints were formed at early stages of burial because they may be cross-cut by fluidized sand injected into fractures as a result of soft-sediment slumping (Wade 1968, fig. 17) or transected by synaeresis cracks (Glaessner 1969, fig. 1e). Gehling (1999; Gehling *et al.* 2000) and others, suggest the possibility that the fixative properties of the sediments in moulding the remains were substantially increased by a high interstitial content of microbial filaments rendering a jelly-like thixotropy. The copious secretion of sticky mucilage by dying or moribund medusoids may similarly act to bind adjacent sediment (L. A. Gerswin, UC Berkeley, pers. comm., 1997).

A chance rock-fall in the high western Flinders Ranges exposed well-preserved counterpart surfaces of large discoidal remains. The several layers of grits and sands incorporated between the enveloping surface moulds of the organism disclose that the preservation is not of a single flattened film (such as a diaphanous 'medusa'), but of a hollow body whose internal spaces were at least partly filled with sediment prior to flattening of the structure during its burial. In the harsh climates which have prevailed in the arid area of Ediacara Range and Nilpena, lower surfaces of the resilient sandstone flags become case-hardened (processes of late Tertiary silicification may be involved), preserving the markings on them, but immediately adjacent tissues were moulded in clay-rich silts and sands that have commonly fretted and crumbled away. Rarely, the actual silt-rich parting 0.1–2.0 mm thick is seen adhering to the fossiliferous undersurface of a sandstone slab. Thus, the simple disc-shaped impressions of one tissue layer usually collected may be an artefact resulting from loss of significant parts of the actual preserved

fossil specimens during the processes of their exhumation and subsequent exposure. The common practice of proposing binomial designations to many of the more 'simple' concentric circular markings commonly observed is not conducive either to a fuller understanding of their biogenic placement or indeed, even justification that some of these forms truly represent organic remains (e.g. Gehling *et al.* 2000; Jensen *et al.* 2002).

The forms *Rangea*, *Pteridinium*, *Ernietta*, *Nasepia* and *Swartpuntia*, occurring in the latest Neoproterozoic Nama System of Namibia, are also preserved in a three-dimensional manner (Richter 1955; Germs 1968, 1973; Pflug 1970a, b, 1972; Jenkins 1985, 1992, 1996; Narbonne *et al.* 1997; Dzik 1999, 2002; Grazhdankin & Seilacher 2002; Narbonne 2005). These forms commonly occur in relatively homogeneous, medium grained, feldspathic sandstones and are seen as leaf- or bag-shaped, film-like partings or compressions, which form curved shapes within the rock matrix. Commonly, several leaf-like forms are conjoined or lie side-by-side so that one foliate element has some random orientation in the rock matrix, and another originating along a suture curves out into the rock in a different direction (Richter 1955; Jenkins 1985, fig. II; Crimes & Fedonkin 1996, pl. 2, fig. c, f). The foliate elements may also overlap, folding over or 'closing' around envelopes of sediment (Jenkins 1985, fig. 1G; Narbonne *et al.* 1997, figs 6, 7, 9; Narbonne 2005). In *Pteridinium*, *Ernietta* and *Swartpuntia* the foliate structures are formed by elongate tubes arranged in a regular array and may be intimately penetrated and moulded by the now lithified sands of the rock matrix (e.g. Narbonne *et al.* 1997, fig. 9.4). Twisted and deformed specimens of *Pteridinium* occur in relatively homogeneous sandstone beds, which probably originated from a process of mass movement, such as a density current, or slumped after deposition (Crimes & Fedonkin 1996, p. 324). On the other hand, Grazhdankin & Seilacher (2002) suggest that some deformed and strangely intertwined examples of *Pteridinium* might have been in life position, where they were buried more or less intact in sand, a view with which we concur, because, in the field, crossbedding can be seen in the fill between individual vanes. Preservation of *Rangea* and *Pteridinium* in sandstones occurring in the Flinders Ranges is analogous to that of the African material.

The nature of three-dimensional preservation of all known specimens of *Pambikalbae hasenohrae* closely resembles that of *Rangea*, *Pteridinium* and *Swartpuntia*. The examples of fronds apparently laid over flat during burial and their preservation is similar. The large block including the holotype of *Pambikalbae* (Figs 3a, b, 4a–c, 5a, b) shows

conspicuous hummocky laminations, with several micro-fault displacements. Crossbedding indicates that the flattened, best-preserved frond probably lies on the sole of the flag (Figs 3a, b, 5a). Other frondose elements present show curved, three-dimensional shapes and lie in the general plane of the internal lamination of the matrix (Figs 4b, 6c), except for one ‘vane’ of the paratype SAM P35065, which curves upwards relative to the bedding plane (Fig. 5b) as is commonly seen in many examples of *Pteridinium*. A composite mould (McAlester 1962; Wade 1968; Gehling 1988) has formed between the tapering stem and overlapping frondose elements (Figs 3a, b). The large stalk attributed to *Pambikalbae* (SAM P35067) forms a curved shape extending through

a block of weathered sandstone (Fig. 6e). It appears to comprise a counterpart cast and mould (Wade 1968; Gehling 1988) formed by the sand that filled spaces in the basal parts of overlapping fronds with the internal hollow of the stalk appressing closely against the sand mould of its external surface. Part of another comparable stem extends from the base of the paratype frond SAM P35065 (Fig. 5a).

One or two frondose structures, occurring higher in the rock than the holotype specimen composite mould (SAM P35063) and almost precisely overlapping it, reflect curved longitudinal shapes or possible sand-infillings in line with the stem of the flattened frond (Figs 3a, 4a, b). It was not immediately obvious if these additional frondose

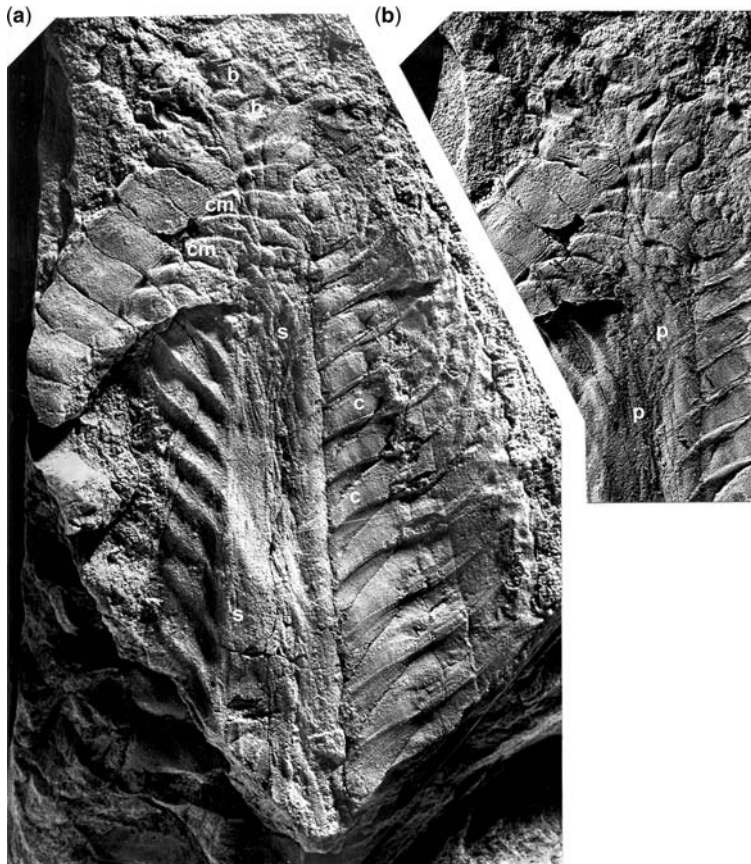


Fig. 3. *Pambikalbae hasenohrae* gen. et sp. nov., SAM P35063, holotype, distal part of frond; Late Neoproterozoic, Winnowie Member, Rawnsley Quartzite; ‘Nilpena’, Flinders Ranges, South Australia. (a) overall aspect with compression of stem (s), indication of faint secondary cross-structure (c) on inner ‘chambers’ of right vane, area of sharp composite moulding of chambers on superimposed vanes (cm) and inflated or bulbous distal ‘chambers’ (b) visible; part of frond illustrated c. 15.5 cm long. (b) distal part of same in different lighting with fine wrinkles or creases marking apparently membranous integument of ‘chambers’ of vane on left side, note criss-cross pattern (p) formed by several vanes collapsed on to and composite moulded against stem compression; scale as for Figure 3a.

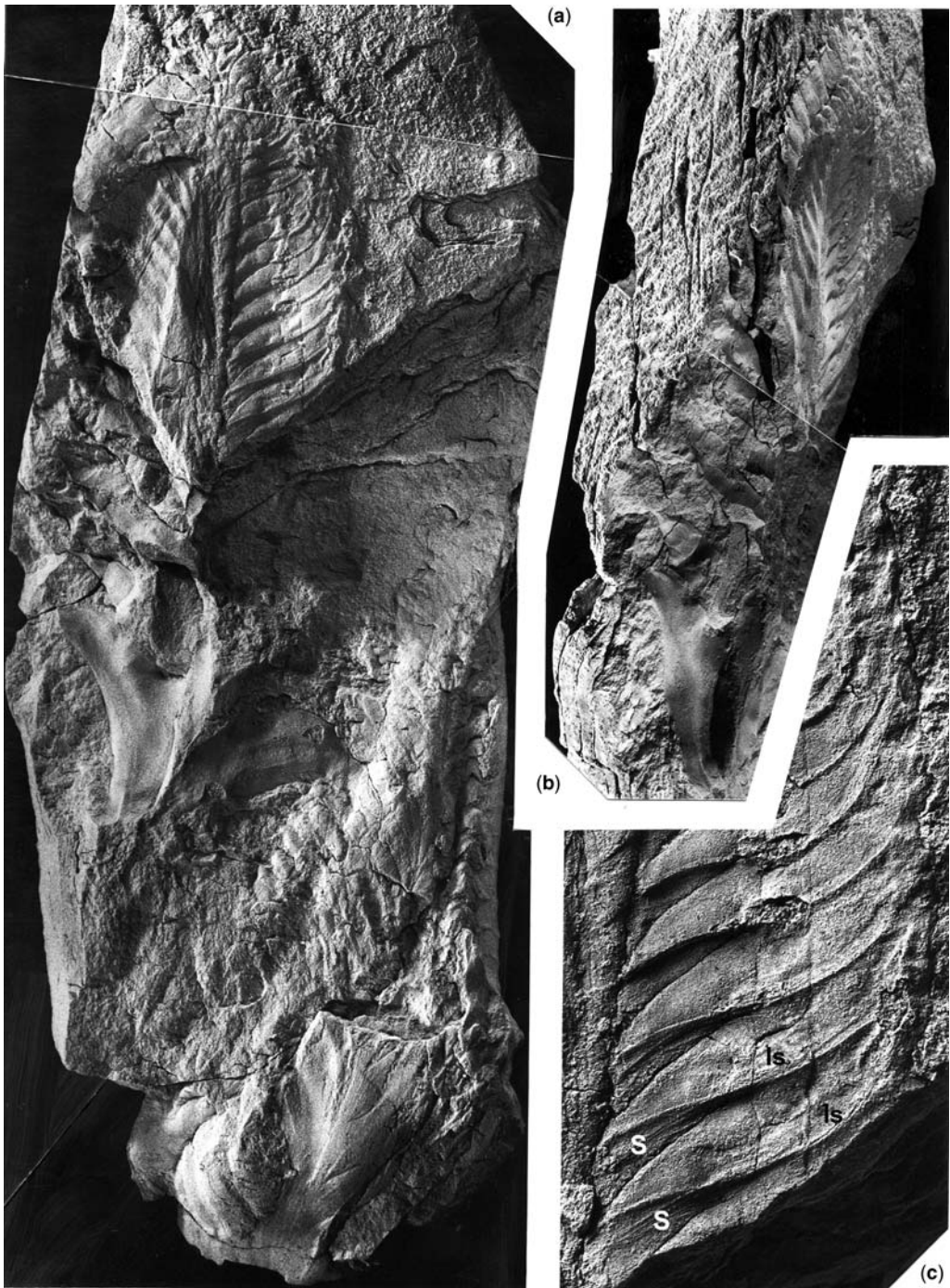


Fig. 4. *Pambikalbae hasenohrae* gen. et sp. nov. (a) SAM P35063, holotype upper left, and SAM P35064, paratype, lower left, on lower aspect of same block of sandstone; visible parts of hosting flag 45 cm long. (b–c) SAM P35063; (b) view of upper left side of hosting sandstone block illustrating parts of holotype interlayered and/or interpenetrating the matrix, the bedding of which is indicated by shadowed vertical cracks mainly on left side of photograph; scale similar to Figure 5a. (c) part of right vane, mid area of frond of holotype, with compressions of possible stolons (s) and slightly zigzag longitudinal sutural traces (ls); illustrated part 12 cm long.

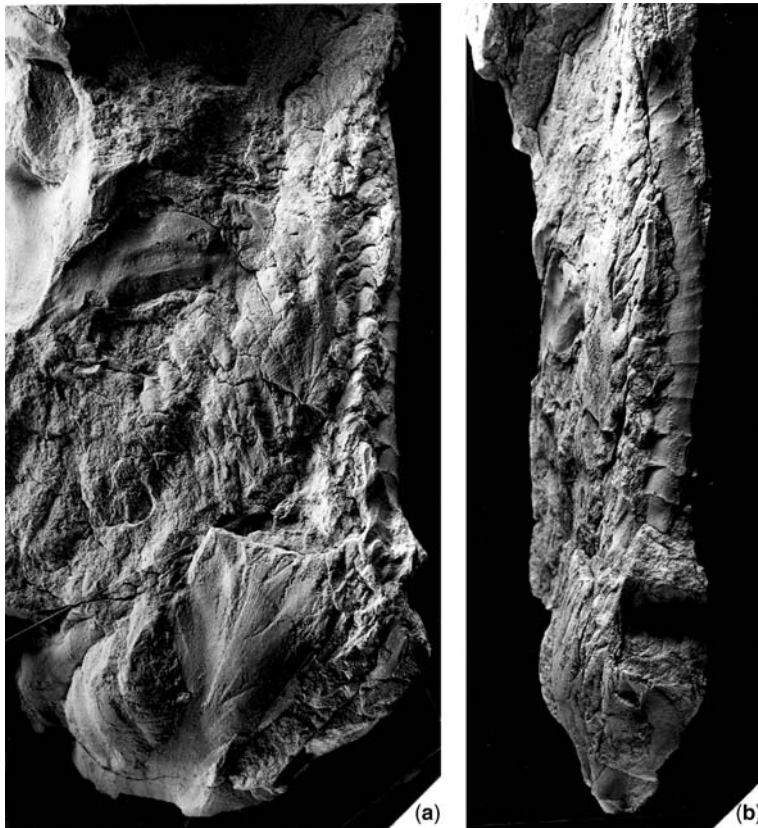


Fig. 5. *Pambikalbae hasenohrae* gen. et sp. nov., SAM P35064, paratype, base and mid parts of frond. (a) overall aspect viewing lower side of compression representing internal mould and composite moulds with suggestion of alternate or sympodial arrangement of 'chambers' near or at mid-line, and some evident secondary cross-structure on 'chambers' at left of base and at right-centre of image; preserved parts of specimen 28 cm long. (b) view of same from right side of hosting sandstone slab showing one vane with strongly developed interchamberal sutures projecting more or less vertically (to right) up through the matrix in the manner commonly evident in specimens of *Pteridinium*; scale similar to Figure 5a.

structures belonged to the holotype or had been juxtaposed accidentally above it. Despite the possibility of some damage to the specimen, a split was made along part of the bedding of the rock in order to resolve this question. This showed that towards the midline of the form, inner chambers of a vane positioned *c.* 1.4 cm higher in the rock curve sharply downwards to meet the stem of the flattened (holotype) frond. Hence, all the structures in proximity to the holotype almost certainly belong to a single individual, which displays a three-dimensional stacked structure or array of parts extending as much as *c.* 3.7 cm deep through the matrix. Some of the fronds or vanes represented have hollow internal spaces packed with sand or are separated by centimetric thicknesses of sand (now lithified), which show both fine, internal lamination and small scale crossbedding. Thus, the

burial of the specimen could not have been instantaneous, but took place progressively as each lamina of sand was deposited, and perhaps represents a time interval spanning some minutes, hours or possibly longer. The hydrodynamic energy associated with the current was sufficient to pack sand into the many hollow spaces.

The paratype SAM P35064 demonstrates complex overlapping of frondose elements partly separated by envelopes of sand (Fig. 5a, b), but the close juxtaposition of the several foliate structures and near register of their base and terminations lends weight to the consideration that they may all be parts of one individual.

The frondose structures of *Pambikalbae* each comprise a series of large tubular elements or chambers that may complexly overlap, forming composite moulds (Figs 3a, b, 4c). The tubular structures are

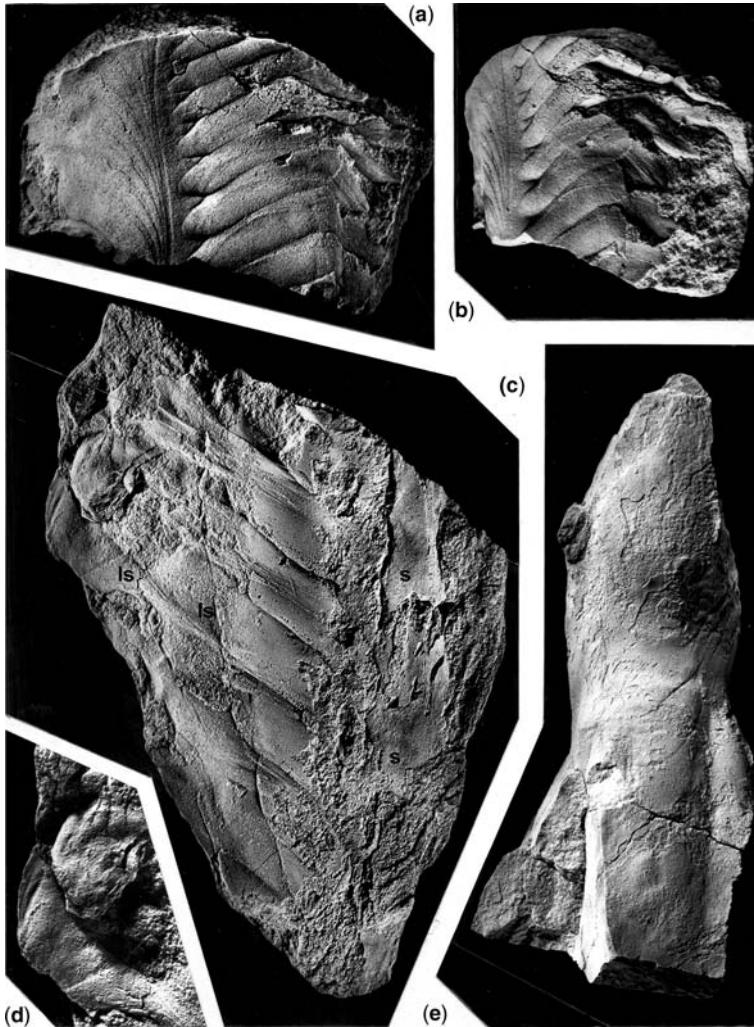


Fig. 6. *Pambikalbae hasenohrae* gen. et sp. nov. (a–b), SAM P35066. (a) internal mould showing axial part of the mid-frond; vertical line of axis 7 cm. (b) same rotated, showing complexity of ‘side’ region in which partings representing an apparently membranous integument forming the ‘floor’ of individual ‘chambers’ extend about 3 cm through the hosting sandstone matrix; vertical line of axis (left of image) 7 cm. (c–d) SAM P35065; (c) internal mould of basal part of frond lying in plane of (wavy) bedding, stem (s), longitudinally sutures (ls) extend approximately through mid-vane; maximum length of rock specimen 25.5 cm. (d) lateral ‘terminations’ of ‘chambers’ of vane with various evident cross grooves or wrinkles; visible part 5.5 cm vertically (in plane of page). (e) SAM P35067, stem preserved as an internal mould ‘in the round’ with oblique grooves evidently representing composite moulds of septal tissues demarking poorly preserved overlapping ‘chambers’; hosting rock 24 cm vertically.

commonly infilled with sand resembling closely appressed butchers’ sausages squeezed against flat surfaces.

The sediments including the holotype likely reflect deposition by a storm-generated waning density current, but the included fossil remains were very likely rooted at their place of life and were simply bent over and aligned with the current.

The matrix of the block including the holotype is a relatively well sorted, but slightly impure, fine-grained sandstone with numerous clay-rich partings including some fine mica. Paratype SAM P35065 is presented within a comparable, but fractionally coarser grained sandstone, and paratypes SAM P35066 and P35067 are both preserved in medium-grained arkosic sandstones.

Systematic palaeontology

Phylum ?CNIDARIA Hatschek, 1888

Class ?HYDROZOA Owen, 1843

Genus *PAMBIKALBAE* nov.

Etymology. Named for *pambi*, a small bag or purse (in reference to the chambers), and *kalbi*, leaf, in the Parnkalla language of the Kujani aboriginal tribe who inhabited the area of the fossil find.

Diagnosis. As for type species.

Pambikalbae hasenohrae sp. nov.

Figures 3–7

Etymology. For Mrs. Pamela Hasenohr who discovered the fossil site.

Diagnosis. Broad, fusiform body comprising multiple vanes conjoined to a tapering axial stem, but sometimes overlapping stem and seemingly meeting at a sinusoidal median groove; stem passing into a broad attachment stalk; vanes showing strong sinusoidal primary furrows reflecting an architecture of three evident serial series of chambers which commonly contain a sediment infill, chambers offset at zigzag sutures, inner series comparatively wide, mid series forming a narrow band, outer series approach breadth of inner set; transverse, more or less faint, serial secondary structure resembling that in *Charnia*.

Dimensions. Body of holotype, SAM P 35063 in excess of 29 cm long and estimated as at least 13 cm wide, stem 2.6 cm wide at about middle of length; paratype SAM P35065 estimated as at least 20 cm wide; paratype SAM P35067 showing stem 6.6 cm wide.

Remarks. Full specific characteristics are outlined in the main text of this study. In general, *P. hasenohrae* is broader than described species of *Charnia* and differs in tending to show only a faint hint of secondary structure transverse to the primary 'branches'; it further differs from *Charnia masoni* in its more tapered overall shape, in the maintenance of relatively wide primary elements towards the distal tips of the vanes or in not showing tertiary grooves. The zigzag sutures evident in the vanes of *Pambikalbae* are unknown in *Charnia*.

Description and interpretation

The morphology of this organism can be divided into two major parts: (1) a broad, tapering axial stem, which extends into a relatively wide basal stalk, and (2) the overlapping, rather broad, foliate, frondose elements. Although there is evidence of at least one of the single 'fronds' being approximately bisymmetrical, it is useful to

describe one 'half' frond extending either side from its join with the stem or the median line as a 'vane'. The composite outline of the overlapping, compressed vanes forms a subovate, fusiform shape tapering somewhat towards free end, which is moderately acute to broadly obtuse and nearly rounded, depending on the degree of distortion (Fig. 3a, b). The number of vanes present in the complete frondose structure is unclear, but the holotype shows evidence of as many as nine vanes, and up to six are recognizable in paratype SAM P35064.

The vanes of *Pambikalbae* have a relatively complex, metameric structure comprising regularly arranged 'tubes' or sub-rectilinear, hollow, elongate box-shaped structures or 'chambers' arranged serially (side by side). The imprints of the membranes, which formed the 'tubes', show fine striations or creases. The frequent distortion, stretching or collapse evident in respect of all the tissues indicates that they were entirely soft, flexible and elastic, and the very faint and delicate imprints of structures on some specimens (Figs 3b, 5a) further suggest that the integument could have been more or less diaphanous.

In the holotype, the tapering axis is outlined partly by the moulding of its infilling sand against the sand fill of the chambers of one vane (right side of Fig. 3a, b), and partly by composite moulding against the termination of wedge-shaped plugs of sand filling chambers of the vane lying on the opposite side. The stem is compressed to a 2.5 cm width near the 'middle' of the preserved frondose structure, and a c. 1.1 cm width near its distal termination. Close examination of the surface of the stem compression indicates that not only is it significantly overlapped by the internal parts of the vanes that lie flat on either side of it, but an eccentrically-positioned zone of thin ridges of sand and patches of criss-crossing furrows suggest that several other vanes collapsed and were compressed into an elongate bundle against the axial element. These vanes either did not include sediment infills or contained only narrow trails of sand. Towards the distal tip of the frondose structure, a substantial portion of a partly collapsed vane has folded flat to overlap the more extended vane on the left side of the axis; the two have become composite moulded so that the collapsed vane has left a serial series of strongly curved imprints which impress the overlapped vane and parts of the mould of the stem.

The structure of the frondose elements is probably made to seem more complex than it really is by the complex counterpart moulding of the sand infillings against adjacent vanes. This makes the presumption that only one layer of chambers or 'tubes' is directly involved with the construction of each vane. The two structures which are at first obvious on one of these counterpart impressions

(e.g. the right side of the holotype frond) are the serial 'wall' sutures between the chambers (Fig. 3a, b), and ridges representing composite moulds of the series of wall sutures of the chambers of the presumably oppressed adjacent vane, where the sand infill of the 'tubes' of this vane have broken away. The wall sutures and the counterpart moulds of the sutures of the adjacent vane form reflexed or sigmoidal curves extending away from the stem towards the free margin of the vane, with the straighter parts of these curves inclined at commonly 45° to 80° relative to the axis of the complete frondose structure. The chambers appear to be blind-ended where they attach to the stem, which they seem simply to abut (SAM P35063) or somewhat overlap, forming scalloped shapes (SAM P35065, P35066; Fig. 6a, c). The tubes of one vane are set along the stem at half an intercept difference from those of the next adjacent vane. Walls of the chambers tend to be rather regularly marked by narrow bands of striations or narrow bands of fibre-like markings made by stringers of very fine sand (Fig. 4c). These striations may represent the collapsed or compressed walls of the chambers of an adjacent vane or, alternatively, collapsed stolon-like tubes with a resistive, fibrous integument, perhaps the most likely notion with respect to the holotype. The chambers vary from about 0.4 cm to 2.2 cm in width (measured approximately parallel to the long axis of the frondose structure), and vary serially in width along the vanes, narrowing towards the distal extremity of the organism.

At about half the breadth of individual vanes, two faint longitudinal grooves are present (Figs 4c & 6c). On close examination of especially well preserved areas, it is evident that these lines mark membranes which divide an inner series of chambers from a narrow medial series of box-shaped structures and thence an external series of longer chambers that form the free edge of the vane. The medial chambers are spaced half an intercept from the inner series, and the outer series are again offset by the same amount. The paratype specimens SAM P35064, P35065 and P35066 all show evidence of these longitudinal structures and pieces of the infilling of adjacent chambers broken away from them; it is apparent that while small parts of these chamber-terminating membranes may lie nearly vertical relative to the surfaces of vanes, in other instances they form oblique configurations, perhaps as a result of distortion. Paratype SAM P35066 is broken in such a way as to show a cross-section of the inner chambers of a vane, and this indicates that the vanes were not at all leaf-like in life, but that their true 'thickness' could have been up to four times the intercept distance between the chambers. Thus, rather than

being tube-like or subquadrate in section during life, the chambers formed a 'stack' of wide, subhorizontal spaces, rather like the juxtaposed, open-plan floors of a high-rise building (presuming that in the live animal the whole frondose structure projected upwards).

The lateral terminations of the outer series of the chambers of the vanes appear poorly preserved. In the holotype, a small curved ridge (or dilation) is associated with the ends of the chambers on the left side, and where one of the overfolded vanes forms a composite mould, narrow subtriangular pits mark the ends of its chambers. Overall, the ends of the chambers seem to have been less resilient than the tissues of the remainder of the vane. Since sand readily entered the chambers during burial of the organism, it seems likely they had a terminal opening. The thickening of the sand infillings near the termination may indicate a rather fragile hood around the aperture. Chambers at the distal tip of the vanes seem to widen and dilate distally, in one instance forming an expanded round shape.

A small, preserved part of SAM P35064 shows two vanes joined medially to form one entire frond, with a sympodial arrangement or alternate positioning of the inner chambers of the vanes at the midline (Fig. 5a). At least one other vane seems to have overlapped the 'frontal' side of the two contiguous vanes, also joining to the midline. Where part of this possibly overlapping vane joins the stem region, several of its chambers show conspicuous transverse ribbing, resembling the transverse markings on the 'branches' of *Charnia* Ford 1958. Low angled lighting reveals that the chambers of other parts of the vanes of this paratype, and lateral parts of the vanes of the holotype and paratype SAM P35065, show indications of metameric transverse markings spaced at intervals of 3–6 mm (Fig. 6d).

The overall disposition of the vanes around the axial stem is not completely clear. On one side of the stem (what we term the 'frontal' side), the vanes seem to have formed entire sheets or 'fronds' with chambers in sympodial arrangements along the midline. At least in the more 'internally' sited 'fronds', the inner series of chambers forming them extended or curved still deeper into the whole frondose structure to join the stem. However, in paratype SAM P35064 the infilling of the chambers of one 'externally' situated vane seems to abut or overlap the surface of an entire frond. In the holotype, vanes seem to both join the sides of and complexly overlap the 'reverse' side of the stem; several may have joined one rather narrow strip of the stem. Paratypes SAM P35065 and P35066 seem to show vanes joining or overlapping relatively wide strips of the stem. It is more or

less clear that in life the stem was largely hidden by its conjoining vanes.

The attachment stalk of *Pambikalbae* was apparently hollow and evidently quite broad (Fig. 6e). Adjacent to the stalk of paratype SAM P35064 are several foliaceous structures separated by or including envelopes of sand, and giving evidence of the chambered construction that characterizes vanes. The curving shapes of these structures seem to indicate their origin from or near the stalk, but it cannot be determined if they actually were parts of the more complete individuals, or were a separate frondose structure with other tissues 'accidentally' appressed against them. The structural similarities of these juxtaposed elements suggest that they all joined, or at least that individuals lived in a tight cluster.

Reconstruction

Since vanes or fronds more or less completely enclosed the axial stem, there can be little doubt

that the whole frondose structure projected into the water column from its presumed anchorage and this is the attitude shown in the reconstructions presented in Figure 7. There is considerable uncertainty as to how auxiliary fronds and extraneous tissues may have related as a whole structure. None of the specimens collected seems to show evidence of any long-distance transport, and there is no evidence that the organism was contractile.

Considerations on biological relationships and function

In its disposition of frondose elements or vanes about a stem, *Pambikalbae* shows an organizational grade close to cnidarians and perhaps pennatulaceans. However, there is no evidence of polyp-like elements in the fossil material. Could it be a plant? The apparent flexibility of all the tissues and the manner in which some vanes seem to have collapsed away to almost nothing is more reminiscent of an animal with a collagen-based integument

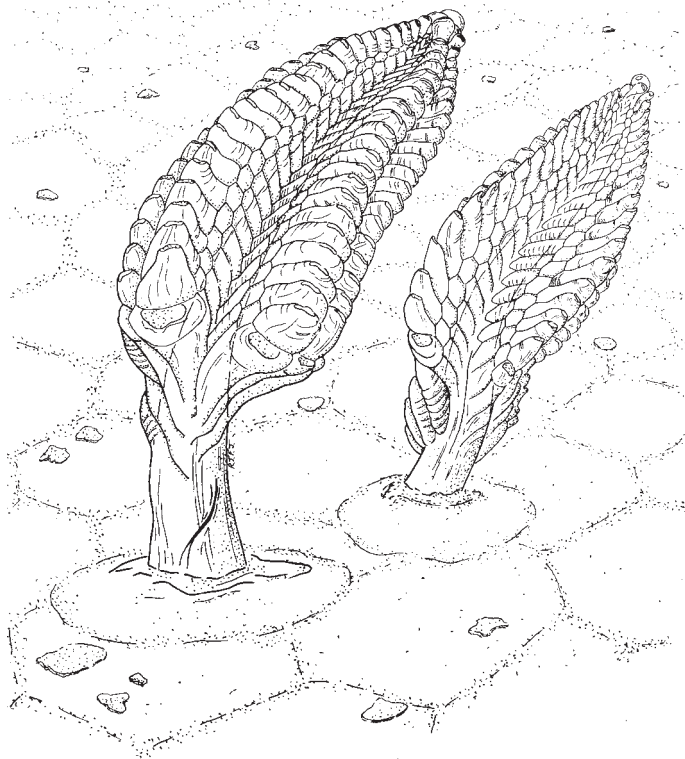


Fig. 7. Reconstructions of *Pambikalbae hasenohrae* anchored in a field of interference ripples, with stray mud flakes. The two interpretations reflect slightly different concepts, that on the left indicating the axial stem enveloped by serial 'chambers' comprising the 'vanes' and that on the right with a 'track' along the stem exposed. Specimens indicate either possibility. The live organism stood about 30–40 cm tall.

rather than a cellulose-based one, but indeed some metazoans, such as tunicates, possess flexible cellulose-based construction.

The regular chambered construction of *Pambikalbae* supports its placement with members of the Ediacaran biota, and is particularly suggestive of an affinity with such forms as *Ernietta*, *Pteridinium*, *Phyllozoon*, *Inkrylovia*, *Ventogyrus*, *Swartpuntia* and possibly *Valdainia*. *Pambikalbae* is also broadly similar in form to the small, frondose structures reported by Jensen *et al.* (1998) in the Early Cambrian of the Uratanna Formation, in the Flinders Ranges. *Ernietta* and *Swartpuntia* occur in Namibia and in the terminal Proterozoic of Nevada (Runnegar *et al.* 1995; Waggoner & Hagadorn 1997; Hagadorn & Waggoner 2000). The time range of *Swartpuntia* extends up into the Early Cambrian in neighbouring southeastern California (Hagadorn *et al.* 2000). The comparable taxon *Pteridinium* is also found in Namibia, on the far north of the Russian Platform and in the Ukraine, southern Australia, northwestern Canada and in North Carolina, USA (e.g. Narbonne *et al.* 1997; Weaver *et al.* 2006). *Phyllozoon* occurs in the Neoproterozoic of the Flinders Ranges. *Inkrylovia*, *Ventogyrus* and *Valdainia* are all reported from the northern Russian Platform, but the first is also known from northwest Canada (Hofmann 1981). Pflug (1970a) linked his new phylum 'Petalonamae' to specimens, which Jenkins (1985, p. 351) refers to *Ernietta*.

Ernietta was bag-shaped and composed of several rings of 'tubes' (Jenkins *et al.* 1981, figs 5, 6; Dzik 1999). On the lower aspect of the 'bag', which was likely attached to or partly buried in the substrate, rows of 'tubes' met at a basal zigzag suture; one row of tubules was offset half an intercept relative to the other (e.g. Dzik 1999, fig. 3; Grazhdankin & Seilacher 2002, fig. 9c, e). Approximately half-way up the sides of the 'bag', another suture terminated the lower rings of tubes, and other rings of tubes completed what appears to be the upper part of the structure. These tubes terminated in tapered conical projections in the Nevada material according to B. Runnegar (pers. comm., 1997), but an alternative possibility is that V-shaped portions of sediment project in-between tubes bending into the matrix. Such projections have not been observed in Namibian material, in which, admittedly, the upper tissues uncommonly present seem to be contorted and crumpled. The intercept width between the tubes tends to remain regular, but the cross partitions between the 'walls' of the bag appear as though they were capable of considerable distension. *Ernietta* is commonly preserved in life position with its interior cavity and the 'tubes' packed with sediment (Jenkins *et al.* 1981; Jenkins

1985, fig. 1; 1992, fig. 7; Dzik 1999, fig. 1d). The sac-shaped forms reported herein from the Breakfast Time Greek Member at Nilpena seem to show faint indications of the parallel sutures between the presumed tubes, but no indication of a basal zigzag suture or 'line of budding'.

The several known species of *Pteridinium* comprised three elongate vanes, which joined at a common axis (Fig. 8a). There is limited evidence for each vane consisting of two rows of 'tubes' joined 'back-to-back' but with one row offset half an intercept relative to the other. Where the vanes joined, their tubes were similarly offset, thus forming a zigzag suture (Fig. 8b). The whole fusiform frond was quite flexible, being completely overfolded in slumped beds (the 'winnowed' specimens of Grazhdankin & Seilacher 2002), but the inner parts of the tubes were relatively stiff or resilient and their outer-parts much more membranous and subject to creasing. Fedonkin (1985a) has observed a specimen extending upright through a bed in northern Russia. This orientation may perhaps have come about accidentally due to thixotropic movement of the sediment. No stalk or stem of *Pteridinium* has been observed.

Swartpuntia, first described comprehensively by Narbonne *et al.* (1997; see also Narbonne 1998) from the uppermost Neoproterozoic section of the Nama Group, was constructed of multiple vanes joining a central stem extending from a stalk. From the published illustrations (Narbonne *et al.* 1997), it is possible to infer that as many as five separate vanes were disposed about the stem. Similar to *Pambikalbae*, an inner series of 'lobate projections' lying close to or overlapping the stem and perhaps representing deflated or collapsed chambers, pass into the narrow, 'imbricate', parallel tubes that formed the wider part of the vanes. These tubes are gently recurved or form weakly sigmoidal lines. Such a level of similarity between *Pambikalbae* and *Swartpuntia* and the likelihood of their near concordance in age, surely supports the possibility that they may be closely related, or had a similar lifestyle.

Ventogyrus chistyakovi is described as having the shape of a small boat with a zigzag axis corresponding to the keel-line and sand-infilled 'elements' (chambers) extending away from it at a high angle. Other, shorter second, third, fourth and sometimes fifth order furrows extend away from the central zigzag suture (Ivantsov & Grazhdankin 1997). Of considerable interest, fine parallel striae mark parts of the moulds of the tissues of the chambers and casts of a fan-like array of branching ducts form an 'internal structure' extending lengthwise through the lateral 'elements'. Later study has shown that examples of *Ventogyrus* occurring in a cluster of three nodules were

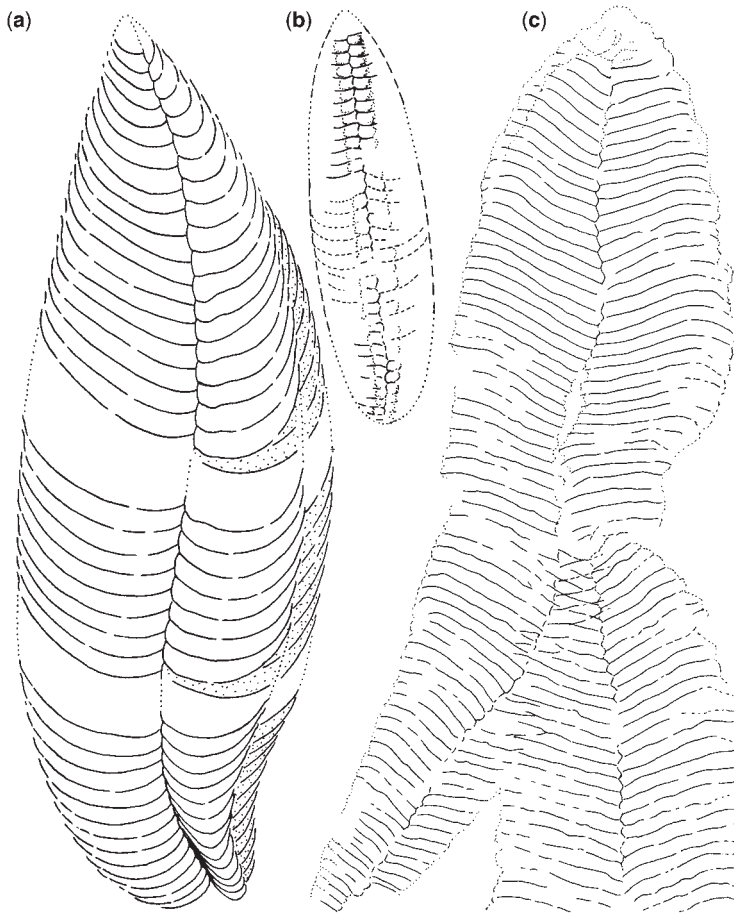


Fig. 8. (a) Reconstruction of *Pteridinium carolinaense* based on material collected from the Winnowie Member, and showing three 'vanes' joined at a median axis. Exposed part of third 'vane' stippled. (b) Compressed 'immature' of presumably the same taxon seen as a very rare element in the Ediacara Member. (c) Type specimens of *Phyllozoon hanseni*, one of the reasonably common elements in the Ediacara Member, with interference pattern formed by composite moulding of resistive walls between the tubules comprising the fronds. Longest frond SAM P19508 (holotype) 18 cm long, Fig. 8a same scale.

originally described as a single organism (Fedonkin & Ivantsov 2007 and references therein).

Other forms which need further comparison with *Pambikalbae* include *Phyllozoon*, a more or less bisymmetrical leaf-shaped structure also composed of serial 'tubes' which met at a zigzag central suture (Fig. 8c). There seems to have been only one layer of tubes forming the 'vanes' of the frond and the integument was relatively 'stiff' or resilient. Numerous individuals are commonly scattered over bedding planes, sometimes overlapping. Such an accidental overlap is incorrectly sketched by Seilacher (1989, fig. 2) and interpreted by him as a join between the fronds. Close inspection reveals the composite moulding of the resilient

'ribs' of the two juxtaposed fronds. The fronds exhibit obvious polarity and their common association with the wide, flattened, tube-like structure which Glaessner (1969) described as a trace fossil designated 'Form D' (e.g. Runnegar 1994, fig. 3) seems too frequent to be due to chance alone. It is possible that this 'tube' constituted a stolon to which the fronds were joined at the narrowly subdivided end (Jenkins 1992). *Valdainia* is a compressed frond with a zigzag suture; the divisions of the vanes show the serial regularity of other members of the 'Petalonamae'.

The foliaceous or frondose taxa, which might have been included in the 'Petalonamae', share the following characteristics: the construction of

the 'body', fronds or vanes consisted of serial rows of 'tubes' or elongate chambers present either in a single 'layer' or several conjoined 'layers'; at least one major join between several series of chambers formed a zigzag suture with one array of chambers abutting the other at half an intercept offset; and all or most forms were likely benthonic, favouring marine shelf settings. Three-dimensional preservation occurs most often in massive sandstones and, as the tubular structure is commonly seen packed with sand, tubes may have had openings to the external environment. The expected placement of these openings (such as at the free edges of the fronds or vanes) seems to have been constructed of fragile tissues and the actual openings themselves have not been observed. *Ernietta* and *Pambikalbae* apparently had membranes which 'blocked' or constricted rows of tubes or chambers that abutted longitudinally; the tubes were of millimetric diameter in most taxa, but centimetric in *Pambikalbae*, which resembles *Swartpuntia* in possessing an axial stem.

Pambikalbae and *Rangea* may have some characteristics in common—multiple foliaceous fronds arranged about an axial stem and anchoring stalk (e.g. Jenkins 1985). The fronds of *Rangea* were also formed by serial elements originating in an alternating manner along the midline, and the edges of the fronds were fragile. *Rangea* is commonly preserved in a three-dimensional manner (Narbonne 2004, 2005), as are the monospecific taxa *Bomakellia* and *Mialsemia*, from northern Russia. Do the similarities between *Rangea* and *Pambikalbae* also reflect close affinity or are they a product of convergence? Of 15 specimens of *Rangea* showing a three-dimensional preservation (Jenkins 1985, p. 342), none seem to show fronds with elongate, hollow tubes packed with sediment. Rather, the fronds seem to include 'branch'-like elements, which further subdivide in an intricate alternating manner. The branches apparently had the capacity to rotate or fold; in compression they are intimately appressed against the interbranch sutures of the neighbouring frond. Thus, close comparison does not presently suggest a near relationship between *Rangea* and *Pambikalbae*, but their similar gross organization does indicate a comparable evolutionary grade ultimately derived from an earlier ancestor.

Size is not a question in Dzik's (2002) referral of *Rangea* and other 'petalonamids' to the Ctenophora. There are examples of comb jellies reaching up to 60 cm to 1.5 m in length (Haeflinger 1974). However, pelagic members of this phylum are extremely fragile, which renders them both susceptible to renting by storms or damage during capture. An early form of cell determinism during the first cell divisions of the embryo, or 'germ mosaic',

causes the adult to lack regenerative capacity. Thus, at first glance, this would not seem likely to be part of a stock tending to prosper in a regime of strong currents, and with their thick mesogloea jelly split into symmetrical halves by a slit-like central enteron, it seems unlikely that sand could intimately penetrate the entire structure during processes of fossilization. Dzik (2002) considered early benthonic ctenophores may have had a much more robust construction, a position which we cannot refute. Nonetheless, the supposed homology between the 'polyp leaves' of 'petalonamids' and the comb rows of ctenophores is unlikely, as individual polyp leaves are 10–12 cm long in large specimens of *Charniodiscus*, while the individual combs of comb-jellies are comprised of fused cilia. Moreover, the tubules or chambers of some petalonamids seem to have no evident analogue in the Ctenophora.

What was the possible relationship between *Pambikalbae* and *Charnia*, especially in view of the enigmatic secondary structures, which mark parts of the chambers of the first? Close examination of the holotype of *Pambikalbae* and SAM P35064 in very low angle lighting reveals a variety of 'cross-wrinkles' set at about the angle of the secondary divisions of *Charnia*. These 'cross-wrinkles' vary from striae set at millimetric to sub-millimetric spacings, to the faintest of serial ridges repeated at intervals of about 2–3 mm (Figs 3a, 5a). In oblique lighting, similar faint cross grooves, set at a spacing of 3–6 mm, are seen obliquely positioned over the outer parts of the lateral chambers of paratype SAM P35065 (Fig. 6d). The alternating arrangement of major divisions of *Charnia* fronds and their strangely inflated shape indicated by moulds (e.g. Jenkins 1985, Fig. 7b) are similar to these elements in *Pambikalbae*. Steiner & Reitner (2001) document the same morphology in material from northern Russia, and additionally show that the integument of these Russian organisms is represented by a compressed and carbonized film. Fedonkin (1983, 1985a) has observed specimens of *Charnia* from the Khatyspyt Formation of the Olenek Uplift, preserved in a three-dimensional manner, with imprints of overlapping fronds that can be exposed by peeling away bedding lamellae. In an illustration of one specimen such as this (Fedonkin 1985a, pl. 13, fig. 3), part of a frond seems to be marked by faint oblique ridges that evidently represent a composite mould of the 'branches' of an overlapping frond; this is very like the composite moulding present in the holotype of *Pambikalbae*. However, the Australian material of *Charnia* provides evidence that the serial secondary (crosswise) divisions of the branches were apparently small, hollow chambers, which became infilled with sediment. Thus, while the similarities

between *Pambikalbae* and *Charnia* are suggestive of affinity, their fronds show important constructional differences.

Seilacher's ideas (1984, 1989) that the majority of known Ediacaran body-fossil remains belong in the 'Vendozoa' or the notion (Seilacher 1992; Buss & Seilacher 1994) of their representing two major taxonomic entities, the 'Vendobionta' and the 'Psammocorallia' are well reviewed by Crimes & Fedonkin (1996) and Narbonne *et al.* (1997) (for viewpoints at variance with Seilacher, see Gehling 1991; Runnegar 1991, 1994, 1995; Conway Morris 1992, 1993a, b). A restricted interpretation of the 'Vendobionta' might place all late Precambrian frondose remains within this division (e.g. Narbonne *et al.* 1997), a notion lent tangential support by the suggestion of Glaessner (1984, pp. 57, 87) and Runnegar (1991, p. 76) that the supposed sea-pen-like taxa *Glaessnerina* Germs, 1973 and *Charnia* could be synonymous.

Of two specimens of *Glaessnerina grandis* Glaessner & Wade, 1966, known from Ediacara Range, both are positive hyporelief casts exhibiting the 'frontal' side of the 'frond'. One specimen in Bunyeroo Gorge, referable to this taxon, shows a prominent axial stem. Other recently located material includes a large 'frond' in excess of 73 cm long, preserved compressed, yet in a three-dimensional manner, with smaller and larger segments of the counterpart, a second adjacent specimen on the same rock flag and its counterpart, a separate incompletely preserved part of a large frond, and part of yet another large frond, including the mould of a short convex portion of an axial stem. These new specimens indicate that this taxon had a particularly complex construction. The rather broad (?tapering) stem is evident on only one or two specimens. The 'fronds' themselves were not integral structures or single sheet-like layers of tissue, but were formed by separate 'branches' or large leaf-shaped elements arranged in overlapping series and preserved with thin layers or wedges of sand up to a few millimetres thick spacing the moulds of the tissues of each 'leaf' from its neighbour. Evidently, the leaves were broad, perhaps rather more than a third as wide as long. A long, tapering part attached them to one side of the stem at widely-spaced intervals equal to about half the length of each individual leaf in series, and another series of leaves on the opposite side of the mid-line of the stem was attached at the mid-intercept spacing of the first series. The margins of individual leaves are incompletely preserved but seem to have formed strong sigmoidal curves. On one margin of each leaf about one third of the width of the leaf was marked by deep 'grooves' or sutures separating a row of up to 16 or more serial elements, each

perhaps four times longer than wide and commonly showing some curvature. These serial divisions are sometimes preserved by an infilling body of sand forming internal moulds and thus seem to have been hollow originally.

In our view, the marginal divisions of the leaves could have been sites of polyps (e.g. Jenkins 1996, fig. 4.1), and as the individual leaves in series were widely separated, free circulation of water was possible for feeding and respiration. However, no polyp impressions have been found with certainty.

When the whole organism came to rest on the substrate, possibly undergoing contraction immediately prior to its burial, various leaves forming the 'frond' likely were compressed in juxtaposition to form complicated, composite moulds as their more resistive elements pressed together and through different layers of tissue. The resultant conspicuous 'ribbing' related to the compaction of the secondary divisions is typically more or less parallel with, or at a slight angle to the mid-line of the whole 'frond'.

The separation of the individual 'branches' of *Glaessnerina*, their general leaf-like form, and the occurrence of 'hollow' divisions on one margin of each leaf are all characteristics shared with living pennatulaceans. In contradistinction, there seems to be no evidence that the primary divisions of *Charnia* were constructed of a broad, smooth leaf-like part or any indication that they were clearly separate. Moreover, the secondary divisions marking the branches of *Charnia* can decrease in width towards the midline of the frond (Fedonkin 1985a, pl. 13, fig. 3), making it unlikely that they represent serially-budded polyps (arising in sequence on the terminal parts of the branches). The sometimes well marked, oblique tertiary structure has been interpreted as indicating the presence of polyps (Glaessner 1984, pp. 57, 87), but this is now not likely because of evident similarities between *Charnia* and *Pambikalbae*. Thus, it is possible to maintain that there is *not* an obvious relationship between *Charnia* and *Glaessnerina* and the gross geometric resemblance between these forms (Glaessner 1984; Runnegar 1991; Laflamme *et al.* 2007) is not compelling evidence of their structural homology.

Overfolded specimens of *Charniodiscus* indicate that each frond was a single, leaf-shaped entity (Jenkins & Gehling 1978; Jenkins 1992). Three-dimensional compressions of the holdfast are discussed above, and the specimen illustrated by Runnegar (1991, fig. 4c) is likely the imprint of the upper surface of such an anchoring device.

The holotype of *Charniodiscus oppositus* Jenkins & Gehling, 1978 is preserved in three-dimensions and shows the linked 'branches' markedly inflated, with grooves between (ridges in the

preserved external mould; Jenkins & Gehling 1978, fig. 6). No fine sutures indicative of subdividing membranes are evident. Rather, each 'branch' supported a foliate, half-leaf-shaped element, which projected out from the frond towards the surrounding water, and on burial was folded back against the frond, either compressed lying towards the distal end of the frond, or rotated 180° and lying towards the proximal direction (e.g. Glaessner & Wade 1966). In a specimen recently recovered from Bunyeroo Gorge in the Flinders Ranges, some of these 'polyp-leaves' are well displayed, either bent back towards the stalk end of the frond, or partly folded on themselves. They show wide, oblique secondary divisions (spaced at *c.* 15–29 mm) marked by transverse structures resembling the polyp anthosteles of some modern sea pens. However, their arrangement is unique because the 'polyp-leaves' evidently formed a kind of hood or cover (wide enough to fold partly back on itself) and the polyps may be reconstructed as standing in numerous diagonal rows on the upper side of each leaf (Jenkins 1996, fig. 3). During feeding, the muscular polyp-leaves may have folded outward and downward so that the many rows of polyps could project into the water to catch micro-organisms with their tentacles. The polyp-leaves of even small individuals of *Charniodiscus* (*c.* 10–12 cm tall) projected 3–4 mm out from the surface of the frond, and in large individuals (*c.* >1 m tall) extended some 2.5–3 cm out from the surface. This separation could clearly have enhanced the circulation of adjacent waters necessary for efficient feeding and respiration. At times of current influence or perhaps emergence, contraction of the polyps was possibly followed by polyp-leaves folding up over to cover them, so that they would have been contained in a closed pocket. The lips of the 'leathery' covers may have tightly appressed against the sides of the frond to keep out sand or prevent dehydration. Specimens of *Charniodiscus* may show wrinkling and folding, perhaps as a result of partial decomposition prior to burial and the fixative processes which resulted in their casting and composite moulding. There is evidence of a ribbon of supportive tissue underling the basal line of each polyp-leaf. The probability that the close-spaced, short imprints commonly marking stems or stalks represent spicules has been investigated to the limits of preservation the material permits (Jenkins & Gehling 1978).

While *Pambikalbae*, *Glaessnerina* and *Charniodiscus* show obvious similarities in their gross morphology, closer study reveals marked differences. *Pambikalbae* does not exhibit the conspicuous structures interpreted as polyp anthosteles in *Glaessnerina*, and the latter does not reveal the

sutural membranes indicative of a chambered construction. Similarly, the single foliate frond of *Charniodiscus* seems to form an integral element with the stem (cf. Laflamme *et al.* 2004) and not consist of chambered vanes abutting sutures. Moreover, its tissues seem to have been fleshy, and while it might well have had a hydrostatic skeleton pressured by water filling pervasive canals (certainly the stalk appears to have been hollow), there is no evidence in the *c.* 100 specimens known that the fronds included tubular or box-shaped spaces which became packed with sand. Furthermore, 'polyp-leaves' are not apparent in *Pambikalbae*, nor are the imprints that might be attributed to spicules.

The possibility of some considerable separation of the branches and the converse compressive overlap of the 'polyp anthosteles' in *Glaessnerina*, and the distinctive 'polyp-leaves' of *Charniodiscus* (e.g. Jenkins 1996) obviate Seilacher's (1989, p. 231) suggestions that these genera were 'leaf-like structures without branch separation which would have been necessary to let the filter currents past the polyps' and that 'it would be difficult to identify the places of the individual polyps'.

The preceding discussion highlights the gross similarities between Ediacaran frondose fossils, but also points out structural differences that may indicate deep separations at high systematic levels (cf. Laflamme *et al.* 2007). At present, the significance of these differences is unclear. There is little doubt that the bizarre, tubular- or box-like construction has major systematic importance, and the designation 'Petalonamae' holds priority and is potentially available (Ivantsov & Grazhdankin 1997; Narbonne 2004, 2005; Narbonne *et al.* 1997). The taxa which might belong to this division are *Ernietta*, *Pteridinium*, *Phyllozoon*, *Inkrylovia*, *Ventogyrus*, *Swartpuntia* and *Pambikalbae*, plus (with less certainty) *Charnia* and possibly *Valdania*. *Rangea* shows an enigmatic similarity to *Pambikalbae*, but there seems to be no convincing indication that it was constructed of tubes or chambers. In this it approaches a second significant division, which includes forms that show possible evidence of polyps, but no suggestion of the tubular construction of the 'Petalonamae'; this section embraces *Glaessnerina* and *Charniodiscus*, and possibly the Russian form *Vaizitsinia*. *Thaumaptilon*, from the Middle Cambrian of British Columbia, also resembles this group; it apparently lacks a membranous edge to the frond and lacks obvious preserved polyp leaves, but possesses a more elongate holdfast. The small, round markings on the surface of the frond and patches of the stem of *Thaumaptilon* are interpreted as probable siphonozooids rather than the autozooids as interpreted by Conway Morris (1993a). The grade of

organization of these forms is consistent with that of the Cnidaria and more particularly pennatulaceans, specifically the probable presence of zooids (e.g. Jenkins 1992, 1995; Conway Morris 1993a), evidence for a system of internal canals (Conway Morris 1993b) and overall shape. While mere resemblance is not proof of affinity, it is a primary yardstick of biological classification. *Thaumaptilon* broadly resembles *Charniodiscus* and the possible indication of zooids in either is consistent with their designation within the cnidarian Anthozoa. Thus, there seems no particular reason to exclude this second major clade from the Cnidaria unless proof of some difference is ultimately unearthed. Deep divergences between major polypoid cnidarian clades suggested by molecular data (Bridge *et al.* 1995) may well portend early morphological diversity such as might be reflected in their older fossil record. The mosaic of similarities and differences members of the 'Petalonamae,' including *Pambikalbae*, show to the more or less coeval sea-pen-like taxa certainly enhance the kind of morphological spectrum expected to accompany a primal cnidarian radiation.

The complex chambering of the 'Petalonamae' poses a question as to their functioning and mode of life in respect of this adaptation. Their common manner of three-dimensional preservation may be an indication that their tissues were in some way especially resilient, perhaps toughened by an abundant connective compound, or perhaps more likely, chitinous material. This is lent support by the occurrence of little deformed specimens of *Swartpuntia* in association with mud-flake conglomerates that presumably reflect energetic transport (Narbonne *et al.* 1997). Hence, the chambered construction of the 'Petalonamae' could have functioned principally in the role of mechanical support rather than more dynamic processes related to feeding or ingestion of nutrients.

If the 'Petalonamae' harboured photosynthetic symbionts, then it might be expected that their preferred life habit was one of shallow, clean, clear waters. However, lithologies preserving the organisms suggest that they tended to live offshore or in channels, where there may have been some attenuation of light levels. The matrix of many of the remains includes an admixture of clay or silt that helped form the 'moulding sand' (Milner *et al.* 1962, pp. 576–577; Jenkins 1985) that was probably important in their preservation. The silt suggests turbid water, not a favoured characteristic in the environment of organisms dependent on photosymbionts. The propensity of some 'Petalonamae' to be preserved in channel deposits or even to have colonised current-scoured pot holes (*Ventogyrus*, see Ivantsov & Grazhdankin 1997) further explains their requirement for a tough integument

as a necessity to withstand buffeting by sediment-charged, storm currents (see Fedonkin & Ivantsov 2007).

Gentle movement of currents along such surge channels during fair conditions likely carried a rain of fine detrital food particles released by inshore wave-winnowing of sandy sediments known to have included abundant decaying remains (those that formed the characteristic, abundant shallow-water fossil assemblages). Perhaps the chambers of *Pambikalbae* were carpeted with flagellate cells similar to the choanocytes of sponges, or otherwise bore bands of cilia that helped waft in suspended food particles. One appraisal is that the 'Petalonamae' may have had an oxidative metabolism with their tubes/chambers connected to the surrounding waters, and they were possibly heterotrophic suspension feeders. The possibility that the tubes or chambers actually housed polypoid zooids interconnected by thin stolons can not be ruled out, though the mathematical regularity of *Ernietta* which seems to have some 64 tubes in each cirlet comprising the body irrespective of the size of the individuals, poses major questions as to how the zooids could have reproduced with such precision, and the manner in which the complete structure increased in size. Moreover, if the interpretation of Runnegar (pers. comm., 1997) that the tubules of *Ernietta* terminate in conical projections is correct, no obvious peripheral apertures are apparent for the extension of the polypoid feeding device. Narbonne *et al.* (1997) suggested that the open ends of the tubes of a sand infilled specimen of *Swartpuntia* were either original or due to damage by storm action, and described the serrated segment terminations of other specimens as surrounded by a smooth groove along the entire margin of the petaloid, implying that the tubes were closed at their ends.

Even more bizarre is the possibility that members of the 'Petalonamae' either tended to 'ingest' sediment while still alive, or were packed with sand so near to death that their tissues did not lose any of their vital resilience (e.g. Jenkins *et al.* 1981, p. 75; Seilacher 1992; Buss & Seilacher 1994; Crimes & Fedonkin 1996; Narbonne *et al.* 1997; Grazhdankin & Seilacher 2002). Thus, colonies of complete individuals of *Ernietta* evidently preserved in life position have the body spaces packed with fine sand and even show discontinuities in the sediments forming the clastic infill of the central space (Jenkins *et al.* 1981, figs 5b, c). If the organisms died during their infilling or had a large amount of sediment suddenly dumped upon them, then surely their tissues would have collapsed flat; the inference is that the organism's structure was sufficiently robust to maintain its gross shape even as the creature was intimately permeated

with sand over some finite interval of time (minutes? days?). This trait seemingly militates against the presence of corporal zooids within the tubes. The idea of growth of protoplasm through interstices between sediment grains (Crimes & Fedonkin 1996) is not supported to the extent that *Ernietta* is preserved by direct contact moulding of grains, and its internal fill shows miniature erosive unconformities indicating its interior space was truly a confined hollow, and filled subsequently by the entry of current-transported sediment.

The likelihood that *Pteridinium simplex* lived partially buried in the substrate (Grazhdankin & Seilacher 2002) is lent support by study of the site Seilacher (1992) investigated on Farm Aar (the Aarhaus site) in Namibia. The numerous associated individuals present at one level in medium bedded sandstone (Saylor *et al.* 1995) are mostly aligned as though orientated by the current (e.g. Jenkins 1985, fig. 1e), but almost all are positioned with the convex aspect of the joined vanes downward in the 'virgin' association of Grazhdankin & Seilacher 2002. Moreover, some long examples show curious snake-like bends or kinks, which would surely have resulted in juxtaposition of specimens if their placement were simply due to chance. Instead, they evidently represent a life assemblage, the two lower vanes of each formed into a shape like a canoe (Grazhdankin & Seilacher 2002), which was partly filled with sand, but still with the encircling free margins projecting above the substrate. Thus, the projecting margins were probably subject to abrasion and imperfectly preserved, or not evident at all. The level filling of the enveloping sand (Crimes & Fedonkin 1996) can be attributed to the equal upward accumulation of sediment settling from currents varying in strength and direction (as tidal sands are sometimes seen to bury moribund anemones); this fill rarely shows small-scale cross-bedding. For the most part, the ends of the fronds also curved upwards above the substrate and are rarely observed. Broken beds reveal that the central medial ('third') vane also projected upwards and probably through the substrate almost like a longitudinal sail. The alignment of the fronds then becomes a necessity for growth as the ends of the creatures prolonged between their neighbouring fellows Fedonkin (2000) has reconstructed *Pteridinium* as an elongated tubular organism that had three longitudinal 'septa', very similar to the body plan of *Ventogyrus*. The evidence of interpenetration of specimens considered by Grazhdankin & Seilacher (2002) to indicate growth of individuals through sediment is open to interpretation. One of us (RJJ) has observed two individual (calcareous) bivalve shells at right angles in an event bed with a thick valve cleanly cutting a lighter one, clearly an example of post

mortem impact, suggestive of the old hack of using a gun to fire a straw through a barn door. Whether or not *Pteridinium* had to be buried before a growing one worked its way through the dead and decaying integument of another is a further issue. Ivantsov & Grazhdankin (1997) present analogous information for the life orientation of *Ventogyrus*, with its remarkable colonisation of the successive sediment levels filling potholes.

The robust or leather-like (Seilacher 1992) consistency of some members of the 'Petalonamae' mitigates against their being of syncytial grade (tissue comprising multinucleate protoplasm) as posed by Runnegar (1995), and if, as he considers, they were of 'algal' rather than animal affinities, how could their habits of living partly buried or colonisation of channels and/or pot holes favour photosynthesis?

Vanes of some members of the 'Petalonamae' incorporated resistive but flexible material; the 'stiff' septa forming the walls of the tubes in *Phyllozoon* are one example (Jenkins 1992; Runnegar 1995). The characteristics of this material on preservation simulate the same geometry as the chambered structures which represent the identified chondrophores *Ovatoscutum*, and *Chondroplon*. Hofmann's (1981) interpretation of the latter as a deformed *Dickinsonia* completely failed to appreciate the resilience of *Chondroplon* implied by the broad, radiating folds, which deform its centre (Wade 1971) or its unique marginal lappets. For comparable reasons it is probable that a 'chitinoïd' stiffening was present in some of the 'Petalonamae'.

Living relatives?

Possible tunicate affinities have been suggested for several Neoproterozoic forms, with the sac-shaped *Yarnemia* (in Chistyakov *et al.* 1984) from the middle Onega River, and also *Inkrylovia*, interpreted to form a broadly hollow bag (Chistyakov *et al.* 1984; Fedonkin 1990). The characteristics of colonial tunicates, including a tough but flexible integument composed of tunicin, the metamerism associated with replication of the body parts, the occurrence of stolons and the overall size of the colonies, provide a possible basis for comparison with the 'Petalonamae'. The large chambers forming the 'vanes' of *Pambikalbae* are wide enough to have housed the barrel-shaped, ciliated branchial chamber that is diagnostic of the tunicates, but while fine mouldings reflect their membranous construction, no indication of any branchial apparatus is evident. It is perhaps noteworthy that in the pelagic salps, the gill apparatus

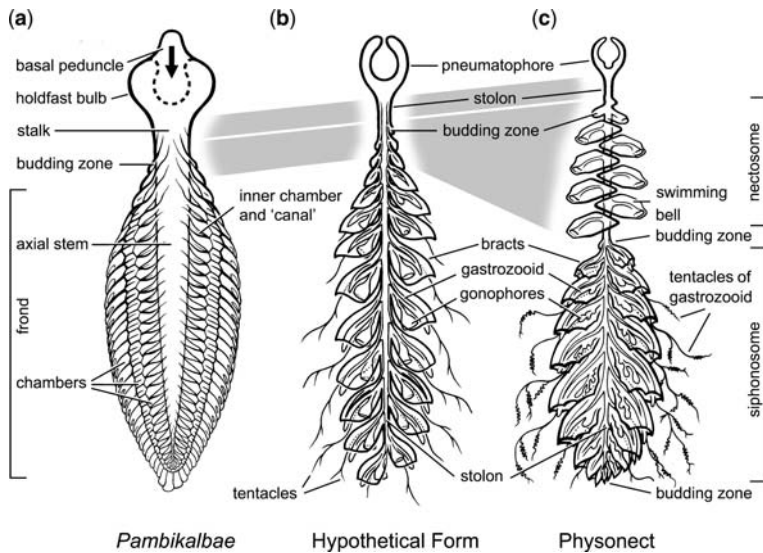


Fig. 9. Comparison between an 'inverted' *Pambikalbae*. (a), a hypothetical ancestral 'calycophore' siphonophore in which the swimming bell (nectophore) has yet to evolve (b), and a generalized modern physonect (c). The frondose fossil animal represented might well have adapted the holdfast to a pneumatophore by simple invagination of the basal peduncle and development of gas secreting cells. The gross homology of the 'colony' is indicated. Modern calycophores have a swimming bell, but have apparently 'lost' the pneumatophore. The further point of comparison is that in *Pambikalbae*, the 'vanes' are comprised of three serial rows of chambers, and in calycophore and physonect siphonophores, the serial 'persons' arrayed along the stem are tripartite, consisting of a more or less enveloping passive bract, a feeding gastrozoid, and the reproductive gonophore which doubles as a swimming bell.

is reduced to a pair of slits on either side of a sloping bar and the potential for this device to be preserved is minimal.

There are at least superficial similarities between the strangely flattened 'horizontal' chambers of *Pambikalbae* and the compressed swimming-bells and cormidia variously crowding the trailing stolon-like coenosarc of the pelagic cnidarian calycophore and physophorid Siphonophorida (Fig. 9). These fragile nectonic creatures comprise either an upper swimming-bell or compound swimming-bells, or a gas-filled primary float or pneumatophore, and a succeeding coenosarc or extensile hollow stem of varying length from which numerous medusa-buds or cormidia ('persons' in earlier works) arise asexually (Fig. 9b, c). The cormidia develop at one or several growth loci (Hyman 1940; Totton 1954; 1965).

The widened chambers of *Pambikalbae* show enigmatic structural parallelisms with the extraordinary compound cormidia and eudoxids (separate free living cormidia) of some calycophores. In these compound elements, several medusa-buds or individuals may insert one within the other to become inextricably interlocking, a circumstance at least reminiscent of the distinctive longitudinal suturing of the 'vanes' of *Pambikalbae* and its

internal transverse partitioning of the chambers. Walls in the calycophores and physophorids tend to be muscular and, unlike other hydrozoans, have thick developments of mesogloea, which makes the elements relatively resistive, in contrast with their fragile, stolon-like or membranous connections to the coenosarc. The narrow ribbon-like line extending through the 'horizontal' walls of the chambers of *Pambikalbae* is similar to the 'principle radial canal' which links all of the cormidia of a compound medusa-bud back to its attachment stolon. The branched, stolon-like tubules in *Ventogyrus* might be considered as having functioned in a comparative role. Both single swimming-bells and compound elements in the living animals may show unusual ribs, grooves and sutures; for example the nectophores of *Halistemma striata* show serial side ribs.

Totton (1954, 1965) considered the pneumatophore, stem (coenosarc) and distal gastrozoid of the physonects as representing the primary oozoid. The stem of *Pambikalbae* might also be considered as representing a primary oozoid (as it is in pennatulaceans) and its 'vanes' to be formed of compound 'cormidia' at least analogous to those in siphonophorids (9a–c). Presuming that *Pambikalbae* had a discoidal holdfast as occurs in

its assumed fossil allies, perhaps such a structure became secondarily modified as the physophorid pneumatophore by simple invagination of its base, evolution of a gas gland and some chitinous stiffening of the inner gas vesicle (Figs 9a, b, 10a, b). It is noteworthy that the pneumatophore has no mesogloea, but possesses simple two-layered walls which are highly muscular (Hyman 1940, p. 469) as also might be expected for a holdfast. The gastrovascular cavity of the pneumatophore passes directly into the central hollow of the stem, and the sand infilling comprising internal moulds of Ediacaran discoidal holdfasts and stems of frondose remains indicates both that the holdfasts were hollow and that this cavity was in open connection with a wide hollow extending through the stalk and stem.

Runnegar (1995) cautioned that there is a danger of overlooking true fossil representatives of the primary stock of major clades because the expected character states of crown-group members may not be present. Thus, the probably benthonic *Pambikalbae* is certainly distant from the living Siphonophorida, but shows several analogous characteristics and a general organizational grade consistent with it potentially representing a highly derived member of the cnidarian class Hydrozoa. Perhaps *Pambikalbae* and some of its near allies are an evolutionary plesion broadly related to the stem stock of the siphonophorids, which may have had a benthonic origin in the Neoproterozoic and secondarily evolved a float, a more fragile colony

and specialized adaptations related to their becoming pelagic (Fig. 9).

The question as to whether any of the other known Ediacaran frondose remains may represent hydrozoans (Glaessner 1979, 1984; Boynton & Ford 1995) and indeed the reality of any zoological affinities between suggested members of the 'Petalonamae' remains opaque in-so-far as the state of knowledge of most is relatively incomplete. The sympodial growth of the 'branches' in *Rangea*, *Bradgatia* Boynton & Ford 1995, and the spindle-shaped fossils in southeastern Newfoundland may be compared with modern hydroid colonies such as *Halecium*, but by no means compel a hydrozoan placement. *Rangea* certainly had a central oozoidal stem or polypoid-like *Pambikalbae* and multiple foliate fronds. An alternative possible interpretation of the branching elements in *Rangea* is as relatively elaborate gonodendra, with the major and subsidiary series of branches signalling different developmental maturity, or somewhat less likely, physically separate male and female gonodendra. The fine third order structure of the branches (Jenkins 1985, figs 4a, 5) could just possibly be an actual indication of the gonophores. In some siphonophorids the tentacles bear the nematocysts on small serial tentilla and when these are strongly withdrawn the coils form little, serial, knob-like projections at the sides of the clumped structure, a configuration somewhat resembling the third order structure on the branches of *Rangea*.

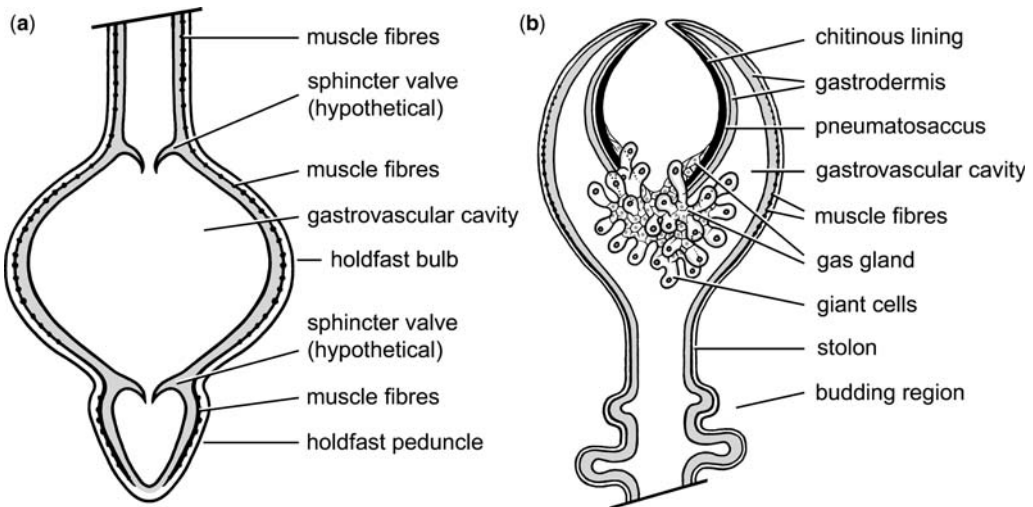


Fig. 10. Comparison between the holdfast of an Ediacaran frondose fossil as hypothesized from characteristics of preserved material (a), and the 'float' or pneumatophore of a physonect siphonophore (b) (adapted after Hyman 1940, p. 472), exploring the possibility of their homologous construction. Of particular note, both have muscle fibres in the wall of the bulb, a necessary adaptive characteristic for a holdfast, and the pneumatophore may have a chitinous lining, a possible synapomorphy in relation to the stiff material making some frondose fossil remains (e.g. *Phyllozoon*).

On the other hand, considering that *Pambikalbae* shows striking similarities to several other coeval fossil forms, its possible placement relative to any modern division can hardly be argued in isolation. What, then, of its evident alliance with *Swartpuntia*, which in turn is apparently a near relative of *Pteridinium*? It is noteworthy that an aspect of the geometric construction of *Swartpuntia*, the way in which the tubes forming the vanes parallel the inferred proximal margin of the later (Narbonne *et al.* 1997, figs 6, 7, 9.1) and directly intersect the remaining margins, sometimes widening slightly and curving inwards near the distal (medial) tip of the frond, resembles the disposition of the comparable elements in the unique South Australian specimen of *Chondroplon*, which is preserved in an identical manner. Both occur in near association with *Pteridinium carolinaense* and in broad terms, must be of similar age. *Chondroplon* apparently lacks the elaboration of the medial axis evident in *Swartpuntia* and the end with the widened chambers shows a deep inflection. *Swartpuntia* and *Chondroplon* were evidently similar in their stiff or resilient integument.

If *Chondroplon* is truly a chondrophore as posed by Wade (1971), then by comparison with the ontogeny of living examples, the central chamber of the 'float' formed first and the subsequent (narrowing chambers) progressively added in a concentric manner towards the free margin, and indeed decrease to only fractions of a millimetre in width at the youngest formed pole. It needs to be clearly stated that unlike '*Kullingia*', which Jensen *et al.* (2002) consider as a marks made by a tethered and ribbed strand twisting about in currents, *Chondroplon* is not a scratch circle and shows both complicated moulding of the ends of chambers and radial flexure attributed to a stiff integument (Wade 1971). Intuitively it might be expected that the manner of increase in the tubes in the vanes of *Swartpuntia* was exactly the reverse, that is, the new elements grew sequentially at the 'distal' tip of the frond. But what if this was not true and the apparently membranous fragile tissues at the 'proximal' end of the frond (Narbonne *et al.* 1997, figs 6, 7, 9.1) formed the actual site of increase?

Exactly the same question may be posed for *Pteridinium carolinaense* where specimens from Ediacara indicate that the tubes were shorter and narrower at the blunt or rounded end of the frond and comparatively wide at the more pointed (? 'distal') tip. Likewise, in *Phyllozoon* the part of the frond that might be interpreted as 'basal' or proximal has the narrowest and shortest tubes consistent with their being relatively immature. In *Pambikalbae* it is again the 'distal' end of the frond which shows the most highly ordered metamerism, while on the stalk and basal or proximal

part of the stem incompletely defined 'chambers' are marked by grooves with an irregular geometry, bulges or 'branches' with poorly defined cross structure and virtually shapeless or irregular foliaceous outgrowths. Are these evidence of growing tissues incompletely organized into the rhythmical metameric format of the more mature distal frond? A valid question is whether any living Cnidaria show such a retrograde pattern of growth, and immediate examples occur within the Siphonophorids where new nectophores bud off the proximal end of the coenosarc in the physophorids and a budding zone at the join of the siphosome (trailing coenosarc with secondary cormidia) with the nectosome or first definitive nectophores gives rise to the cormidia in both the physophorids and calycophores (e.g. Totton 1965). Additional budding zones may also be present.

Chondroplon provides a bridging morphotype between the characteristic fusiform bipolar organization evident in various genera of the 'Petalonanae' or 'Vendobionta' and the concentric, but still approximately bisymmetrical geometry of both the presumed Ediacaran chondrophore *Ovatoscutum*, and the living *Verella*, in which the vertically orientated, chitin-supported sail (see Kaestner 1967, fig. 4.42) is at least the analogue of one of multiple vanes of the frond or the 'third' vane of *Pteridinium*.

These observations pose a basis for a new morphostructural interpretation of the 'Petalonanae', not as a hollow translucent device to house symbiotic photoautotrophs, and not forming tubes or chambers to house enigmatic zooids, but as a resistive and likely chitinous tubular or chambered endoskeleton made by communal hydrozoans phylogenetically near the ancestors of the Chondrophorina. As in the living animals, the endoskeleton could have been secreted by an aboral ectodermal invagination of the communal coenosarc.

As primarily simple diploblasts without the supportive advantage of the 'stiff' mesoglea present in the Anthozoa, the constructional fragility of poly-poid hydrozoans greatly limits their potential for size increase in energetic environments. This is overcome to an extent by their tendency to secrete a chitinous periderm, which forms a tubular support enclosing the stolons and cups or bells housing the polyps or hydranths, as in the extant *Gymnoblantina*. The Hydroactinidae make a chitinous or calcareous mat from a periderm of tangled hydrorhizae. By the process of invaginating the secretory membrane of their basal coenosarc the Chondrophorina are able to completely envelope their hollow, chambered chitinous skeleton or 'support', which constitutes the gas-filled float. However, there is no *a priori* reason why the forms that first evolved the capacity to secrete an internal chambered device should have been

pelagic, and its potential benefit in enabling early hydrozoans to reach large colony-size and exploit the inner neritic realm of the terminal Proterozoic is readily apparent. The imbricate series of tubes forming individual vanes of the supportive endoskeleton would have similar stiffening properties to flat cardboard sandwiching a plicate medial sheet, and the occurrence of multiple vanes extending from a common axis evidently served to increase the surface area of the whole colony. Presumably the stalk and stem in essence comprised a single 'giant' polyp.

This model is useful in explaining the peculiar modes of life of some 'Petalonamae' as the living coenosarc and myriad supported polyps enveloped a 'dead' chitinous frame, which could become progressively buried in the substrate. The coenosarc would presumably die on the buried parts, but free margins of vanes extending above into the water may have been maintained in growth as they supported live tissue and hydranths. A difficulty with this hypothesis lies in the extraordinary near-mathematical constancy of the number of tubules in each sheath of *Ernietta*; because the construction is in essence bisymmetrical, it follows the tubules must form an even number to generate a closed circlet, but what characteristic in a 'primitive' invertebrate could control their fixed number?

Without more definitive evidence of the problematic placement of the frondose Neoproterozoic forms relative to the Hydrozoa or Anthozoa, Glaessner (1979) chose to maintain his several newly-erected family divisions within the informal section 'Petalonamae'. Noting that the division of the 'Petalonamae' was first used by Pflug (1970a, p. 228) with reference to synonyms of *Ernietta*, which is surely among the most aberrant of all Neoproterozoic foliate remains, Jenkins (1985) promoted the 'order' Rangeomorpha Pflug, 1972, as a section of the subclass Octocorallia. The striking and (in the sense of fossil remains) singular characteristics of *Pambikalbae* and its potential identification as a hydrozoan lead us to nominate it to a separate section, *Pambikalbiidae* fam. nov., assigned to the new order Palaeophorina, which may possibly be considered as part of an early hydrozoan radiation that evolved structural traits showing some analogies with, or broadly foreshadowing either the Siphonophorida or Chondrophorina.

The extraordinary diversity present among modern cnidarians and likelihood that numerous past clades within this phylum have become extinct over the geological ages, as is true for most kinds of multicellular life, hardly makes the exercise of suggesting a possible classification for *Pambikalbae* one of artificial 'shoehorning' into the Hydrozoa. This classification is not 'proved', but appeals to the time honoured approach of comparative

morphology as providing a philosophical basis for arguing the ancestry or subsequent diversification of taxa. In respect of this, morphological traits are unable to be detected in *Pambikalbae* that place it outside the known variability of the Cnidaria, notwithstanding that other problematic fossil remains of similar age, to which it may or may not be directly related, can not presently be confined to any modern phylum with a level of certainty. Thus, we do not view *Pambikalbae* as lending support to Seilacher's (1992) Kingdom 'Vendozoa', which is defined to include the characteristics of the present form, nor particular merit in the notion that organisms of essentially cnidarian grade should have evolved twice over (e.g. Gould 1998; McMenamin 1998), separated by the arbitrary historical dichotomy of the Neoproterozoic/Phanerozoic transition. The Cambrian similarly contains highly derived cnidarians (Conway Morris 1993b) as well as representatives of the sister phylum Ctenophora showing considerable evolutionary divergence (Conway Morris & Collins 1996; Dzik 2002). The possibility that several of the earliest phyla had overlapping characteristics or generated highly convergent morphologies, is in essence an expected consequence near the rootstock of major radiations. In soft-bodied remains these subtleties of overlap and convergence will be further mantled by the vagaries of preservation, including accidental retention of particular body parts, and the bias of the observer.

Molecular sequence data for ribosomal RNA provides indications that the Cnidaria are among the most primitive of the metazoans and that their ancestry is appreciably deeper in time than the diversification of the 'deuterostome' and 'protostome' phyla whose early history is shown directly by body fossil remains or inferred from trace fossils to be embodied in the terminal Proterozoic/older Cambrian evolutionary 'explosion' (Lake 1990; Adoutte & Philippe 1993; Conway Morris 1993a, b; Halanych *et al.* 1995). Studies of the homology of the relatively diverse homeobox genes now known in hydrozoans and anthozoans also supports the archaic evolutionary placement of the Cnidaria, either as the rootstock of higher animals (Finnerty & Martindale 1997; Valentine 2001), or as a sister clade to the form which provided the monophyletic origins of the articulates and vertebrates (Carroll *et al.* 2001, Peterson *et al.* 2005; Sempere *et al.* 2006).

References

- ADOUTTE, A. & PHILIPPE, H. 1993. The major lines of metazoan evolution: Summary of transitional evidence and lessons from ribosomal RNA sequence analysis. In: PICHON, Y. (ed.) *Comparative Molecular Neurobiology*. Birkhäuser Verlag, Basel, 1–30.

- BOYNTON, H. E. & FORD, T. D. 1995. Ediacaran fossils from the Precambrian (Charnian Supergroup) of Charnwood Forest, Leicestershire, England. *Mercian Geologist*, **13**, 165–182.
- BRIDGE, D., CUNNINGHAM, C. W., DESALLE, R. & BUSS, L. W. 1995. Class-level relationships in the Phylum Cnidaria: Molecular and morphological evidence. *Molecular Biology and Evolution*, **12**, 679–689.
- BUSS, L. W. & SEILACHER, A. 1994. The Phylum Vendobionta: a sister group to the Eumetazoa? *Paleobiology*, **20**, 1–4.
- CARROLL, S. B., GRENIER, J. K. & WEATHERBEE, S. D. 2001. *From DNA to diversity: molecular genetics and the evolution of animal design*. Blackwell Science, Malden, Mass.
- CHISTYAKOV, V. G., KALMYKOVA, N. A., NESOV, L. A. & SUSLOV, G. A. 1984. On the presence of Vendian deposits in the Middle Onega and on the possible presence of Tunicata: Chordata. *Vestnik Leningradskogo Universiteta Geologiya Geografiya*, **6**, 11–18 [in Russian].
- CLOUD, P. 1976. Beginnings of biospheric evolution and their biochemical consequences. *Paleobiology*, **2**, 351–387.
- CONWAY MORRIS, S. 1992. Burgess Shale-type faunas in the context of the 'Cambrian explosion': a review. *Journal of the Geological Society, London*, **149**, 631–636.
- CONWAY MORRIS, S. 1993a. Ediacaran survivors in Burgess Shale-type faunas of North America. *Palaeontology*, **36**, 593–636.
- CONWAY MORRIS, S. 1993b. The fossil record and the early evolution of the metazoa. *Nature*, **361**, 219–225.
- CONWAY MORRIS, S. & COLLINS, D. H. 1996. Middle Cambrian ctenophores from the Stephen Formation, British Columbia, Canada. *Philosophical Transactions of the Royal Society, Biological Sciences*, **351**, 279–308.
- CRIMES, T. P. & FEDONKIN, M. A. 1996. Biotic changes in platformal communities across the Precambrian-Phanerozoic boundary. *Rivista Italiana di Paleontologia e Stratigrafia*, **102**, 317–332.
- DZIK, J. 1999. Organic membranous skeletons of the Precambrian metazoans from Namibia. *Geology*, **27**, 519–522.
- DZIK, J. 2002. Possible ctenophoran affinities of the Precambrian 'sea-pen' *Rangia*. *Journal of Morphology*, **252**, 315–334.
- DROSER, M. L., GEHLING, J. G. & JENSEN, S. R. 2005. Ediacaran trace fossils: true and false. In: BRIGGS, D. E. G. (ed.) *Evolving form and function: Proceedings of a Symposium Honouring Adolf Seilacher for his Contributions to Paleontology, in Celebration of his 80th Birthday*. Special Publication of the Peabody Museum of Natural History, Connecticut, Yale University, New Haven, 125–138.
- DROSER, M. L., GEHLING, J. G. & JENSEN, S. R. 2006. Assemblage palaeoecology of the Ediacara biota: The unabridged edition. *Palaeogeography, Palaeoecology, Palaeoecology*, **232**, 131–147.
- FEDONKIN, M. A. 1983. [Non-skeletal fauna of the Podolian Dniester basin]. In: VELIKANOV, V. A., ARSAYEVA, E. A. & FEDONKIN, M. A. (eds) *Vendian of the Ukraine*. Naukova Dumka, Kiev, 128–139 [in Russian].
- FEDONKIN, M. A. 1985a. The non skeletal fauna of the Vendian: a promorphological analysis. In: SOKOLOV, B. S. & IVANOVSKIY, A. B. (eds) *Vedskaya Sistema I*. Nauka, Moscow, 10–69 [in Russian, English translation published by Springer-Verlag, Berlin, 1990, 7–70].
- FEDONKIN, M. A. 1985b. Precambrian metazoans: the problems of preservation, systematics and evolution. *Philosophical Transactions of the Royal Society of London B*, **311**, 27–45.
- FEDONKIN, M. A. 1990. Systematic description of Vendian metazoa. In: SOKOLOV, B. S. & IWANOWSKI, A. B. (eds) *The Vendian System, Vol. 1 Paleontology*. Springer-Verlag, Berlin, 71–120.
- FEDONKIN, M. A. 2000. Cold dawn of animal life. *Priroda*, **9**, 3–11 [in Russian].
- FEDONKIN, M. A. & IVANTSOV, A. Y. 2007. *Ventogyrus*, a possible siphonophore-like trilobozoan coelenterate from the Vendian sequence (late Neoproterozoic), northern Russia. In: VICKERS-RICH, P. & KOMAROWER, P. L. (eds) *The Rise and Fall of the Ediacaran Biota*. Geological Society, London, Special Publications, **286**, 187–194.
- FEDONKIN, M. A. & RUNNEGAR, B. N. 1992a. Proterozoic metazoan body fossils. In: SCHOPF, J. W. & KLEIN, C. (eds) *The Proterozoic Biosphere: An Interdisciplinary Study*. University of Cambridge Press, New York, 369–388.
- FEDONKIN, M. A. & RUNNEGAR, B. N. 1992b. Proterozoic metazoan trace fossils. In: SCHOPF, J. W. & KLEIN, C. (eds) *The Proterozoic Biosphere: An Interdisciplinary Study*. University of Cambridge Press, New York, 389–395.
- FINNERTY, J. R. & MARTINDALE, M. Q. 1997. Homeoboxes in sea anemones (Cnidaria; Anthozoa): A PCR-based survey of *Nematostella vectensis* and *Metridium senile*. *Biological Bulletin*, **193**, 62–76.
- FORD, T. D. 1958. Precambrian fossils from Charnwood Forest. *Proceedings of the Yorkshire Geological Society*, **31**, 211–217.
- GEHLING, J. G. 1987. Earliest known echinoderm—a new Ediacaran fossil from the Pound Subgroup of South Australia. *Alcheringa*, **11**, 337–345.
- GEHLING, J. G. 1988. A cnidarian of actinian-grade from the Ediacaran Pound Subgroup, South Australia. *Alcheringa*, **12**, 299–314.
- GEHLING, J. G. 1991. The case for Ediacaran fossil roots to the metazoan tree. *Memoirs of the Geological Society of India*, **20**, 181–224.
- GEHLING, J. G. 1999. Microbial mats in terminal Proterozoic siliciclastics: Ediacaran death masks. *Palaios*, **14**, 40–57.
- GEHLING, J. G. 2000. Environmental interpretation and a sequence stratigraphic framework for the terminal Proterozoic Ediacara Member within the Rawnsley Quartzite, south Australia. *Precambrian Research*, **100**, 65–95.
- GEHLING, J. G., NARBONNE, G. M. & ANDERSON, M. M. 2000. The first named Ediacaran body fossil: *Aspidella terranova* Billings 1872. *Palaeontology*, **43**, 427–456.
- GEHLING, J. G., DROSER, M. L., JENSEN, S. & RUNNEGAR, B. N. 2005. Ediacaran organisms: relating form

- to function. In: BRIGGS, D. E. G. (ed.) *Evolving form and function: Fossils and development: Proceedings of a symposium honouring Adolph Seilacher for his contributions to paleontology in celebration of his 80th birthday*. Peabody Museum of Natural History, Yale University, New Haven, 1–25.
- GERMS, G. J. B. 1968. Discovery of a new fossil in the Nama System, South West Africa. *Nature*, **219**, 53–54.
- GERMS, G. J. B. 1973. A reinterpretation of *Rangea schneiderhoehni* and the discovery of a related new fossil from the Nama Group, South West Africa. *Lethaia*, **6**, 1–10.
- GLAESSNER, M. F. 1959. Precambrian Coelenterata from Australia, Africa and England. *Nature*, **183**, 1472–1473.
- GLAESSNER, M. F. 1969. Trace fossils from the Precambrian and basal Cambrian. *Lethaia*, **2**, 369–393.
- GLAESSNER, M. F. 1979. Precambrian, Introduction Fossilization (Taphonomy) Biogeography and Biostratigraphy. In: ROBINSON, R. A. & TEICHERT, C. (eds) *Treatise on Invertebrate Paleontology, Part A. Geological Society of America and University of Kansas Press, Lawrence, Kansas, A79–A118*.
- GLAESSNER, M. F. 1984. *The Dawn of Animal Life: A Biohistorical Study*. Cambridge University Press, Cambridge.
- GLAESSNER, M. F. & WADE, M. 1966. The late Precambrian fossils from Ediacara, South Australia. *Palaeontology*, **9**, 599–628.
- GOULD, S. J. 1998. On embryos and ancestors. *Natural History*, **107**, 20–22, 58–65.
- GRAZHDANKIN, D. 2004. Patterns of distribution in the Ediacaran biotas: facies versus biogeography and evolution. *Paleobiology*, **30**, 203–221.
- GRAZHDANKIN, D. & SEILACHER, A. 2002. Underground Vendobionta from Namibia. *Palaeontology*, **45**, 57–78.
- GREY, D. I. & BENTON, M. J. 1982. Multidirectional palaeocurrents as indicators of shelf storm beds. In: EISELE, G. & SEILACHER, A. (eds) *Cyclic and Event Stratification*, Springer-Verlag, Berlin, 350–353.
- HAEFLINGER, H. R. 1974. Phylum: Acnidaria. In: GRZIMEK, H. C. (ed.) *Grzimek's Animal Life Encyclopedia*, Van Nostrand Reinhold, New York, 255–268.
- HAGADORN, J. W. & BOTTJER, D. T. 1997. Microbial carpeting of ancient siliciclastic seafloors: aid to preservation of early metazoan biosedimentary structures. *Geological Society of America, Abstracts with Programs*, **29**, A193.
- HAGADORN, J. W. & WAGGONER, B. M. 2000. Ediacaran fossils from the south—western Great Basin, United States. *Journal of Paleontology*, **74**, 349–359.
- HAGADORN, J. W., FEDO, C. M. & WAGGONER, B. M. 2000. Early Cambrian Ediacaran—type fossils from California. *Journal of Paleontology*, **74**, 731–740.
- HALANYCH, K. M., BACHELLER, J. D., AGUINALDO, A. M. A., LIRA, S. M., HILLIS, D. M. & LAKE, J. A. 1995. Evidence from 18S Ribosomal DNA that the lophophorates are protostome animals. *Science*, **267**, 1641–1642.
- HATSCHKE, B. 1888. *Lehrbuch der Zoologie. Eine morphologische Übersicht der Tierreiches zur Einführung in das studium dieser Wissenschaft. Erste Lieferung*. Jena, Fisher.
- HOFMANN, H. J. 1981. First record of a Late Proterozoic faunal assemblage in the North American Cordillera. *Lethaia*, **14**, 303–310.
- HYMAN, L. H. 1940. *The Invertebrates: Protozoa through Ctenophora*. 1st edn McGraw-Hill, New York.
- IVANTSOV, A. Y. & GRAZHDANKIN, D. V. 1997. A new representative of the Petalonamae from the Upper Vendian of the Arkhangelsk Region. *Palaeontological Journal*, **31**, 1–16.
- JENKINS, R. J. F. 1985. The enigmatic Ediacaran (Late Precambrian) genus *Rangea* and related forms. *Paleobiology*, **11**, 336–355.
- JENKINS, R. J. F. 1989. The 'supposed terminal Precambrian extinction event' in relation to the Cnidaria. *Memoirs of the Association of Australasian Palaeontologists*, **8**, 307–317.
- JENKINS, R. J. F. 1992. Functional and ecological aspects of Ediacaran assemblages. In: LIPPS, J. H. & SIGNOR, P. W. (eds) *Origin and Early Evolution of the Metazoa*. Plenum Press, New York, 131–176.
- JENKINS, R. J. F. 1995. The problems and potential of using animal fossils and trace fossils in terminal Proterozoic biostratigraphy. *Precambrian Research*, **73**, 51–69.
- JENKINS, R. J. F. 1996. Aspects of the geological setting and palaeobiology of the Ediacara assemblage. In: DAVIES, M., TWIDALE, C. R. & TYLER, M. J. *Natural History of the Flinders Ranges*. Royal Society of South Australia, 33–45.
- JENKINS, R. J. F. & GEHLING, J. G. 1978. A review of the frond-like fossils of the Ediacara assemblage. *Records of the South Australian Museum*, **17**, 347–359.
- JENKINS, R. J. F., PLUMBER, P. S. & MORIARTY, K. C. 1981. Late Precambrian pseudofossils from the Flinders Ranges, South Australia. *Transactions of the Royal Society of South Australia*, **105**, 67–83.
- JENKINS, R. J. F., FORD, C. H. & GEHLING, J. G. 1983. The Ediacara Member of the Rawnley Quartzite: the context of the Ediacara assemblage (late Precambrian, Flinders Ranges). *Journal of the Geological Society of Australia*, **30**, 101–119.
- JENKINS, R. J. F., COOPER, J. A. & COMPSTON, W. 2002. Age and biostratigraphy of Early Cambrian tuffs from SE Australia and southern China. *Journal of the Geological Society*, **159**, 645–658.
- JENSEN, S., GEHLING, J. G. & DROSER, M. L. 1998. Ediacara-type fossils in Cambrian sediments. *Nature*, **393**, 567–569.
- JENSEN, S., GEHLING, J. G., DROSER, M. L. & GRANT, S. W. F. 2002. A scratch circle origin for the medusoid fossil *Kullingia*. *Lethaia*, **35**, 291–299.
- KAESTNER, A. 1967. *Invertebrate Zoology. Vol. 1*. Interscience Publishers, New York.
- LAFLAMME, M., NARBONNE, G. M. & ANDERSON, M. M. 2004. Morphometric analysis of the Ediacaran frond *Charniodiscus* from the Mistaken Point formation, Newfoundland. *Journal of Paleontology*, **78**, 827–837.
- LAFLAMME, M., NARBONNE, G. M., GREENTREE, C. & ANDERSON, M. M. 2007. Morphology and taphonomy of an Ediacaran frond: *Charnia* from the Avalon Peninsula, of Newfoundland. In: VICKERS-RICH, P. & KOMAROWER, P. (eds) *The Rise and Fall of the Ediacaran Biota*. Geological Society, London, Special Publications, **286**, 237–258.

- LAKE, J. A. 1990. Origin of the metazoa. *Proceedings of the National Academy of Science*, **87**, 763–766.
- MARTIN, M. W., GRAZHDANKIN, D. V., BOWRING, S. A., EVANS, D. A. D., FEDONKIN, M. A. & KIRSCHVINK, J. L. 2000. Age of Neoproterozoic bilaterian body and trace fossils, White Sea, Russia: Implications for metazoan evolution. *Science*, **288**, 841–845.
- MCALISTER, A. L. 1962. Mode of preservation in early Palaeozoic pelecypods and its morphological and ecological significance. *Journal of Paleontology*, **36**, 67–93.
- MCMENAMIN, M. A. S. 1998. *The Garden of Ediacara: Discovering the First Complex Life*. Columbia University Press, New York.
- MCMENAMIN, M. A. S. & MCMENAMIN, D. L. S. 1990. *The Emergence of Animals*. Columbia University Press, New York.
- MILNER, H. B., WARD, A. M. & HIGHAM, F. 1962. *Sedimentary Petrography. Vol. 2. Principles and Applications*. George Allen & Unwin, London.
- NARBONNE, G. M. 1998. The Ediacara biota: A terminal Neoproterozoic experiment in the evolution of life. *GSA Today*, **8**, 1–6.
- NARBONNE, G. M. 2004. Modular construction of early Ediacaran complex life forms. *Science*, **305**, 1141–1144.
- NARBONNE, G. M. 2005. The Ediacara biota: Neoproterozoic origin of animals and their ecosystems. *Annual Reviews of Earth and Planetary Science*, **33**, 421–442.
- NARBONNE, G. M. & GEHLING, J. G. 2003. Life after snowball: The oldest complex Ediacaran fossils. *Geology*, **31**, 27–30.
- NARBONNE, G. M., DALRYMPLE, R. W. & MACNAUGHTON, R. B. 1997. Deep-water microbialites and Ediacara-type fossils from northwestern Canada. *Geological Society of America, Abstracts with Programs*, **29**, A–193.
- NARBONNE, G. M., SAYLOR, B. Z. & GROTZINGER, J. P. 1997. The youngest Ediacaran fossils from southern Africa. *Journal of Paleontology*, **71**, 953–967.
- NEDIN, C. & JENKINS, R. F. J. 1998. First occurrence of the Ediacaran fossil *Charnia* from the southern hemisphere. *Alcheringa*, **22**, 315–316.
- NORRIS, R. D. 1989. Cnidarian taphonomy and affinities of the Ediacaran biota. *Lethaia*, **22**, 381–393.
- OWEN, R. 1843. *Lectures on the Comparative Anatomy and Physiology of the Invertebrate Animals Delivered at the Royal College of Surgeons in 1843*. Longman, Brown, Green and Longman, London.
- PETERSON, K. J., MCPEEK, M. A. & EVANS, D. A. D. 2005. Tempo and mode of early animal evolution: inferences from rocks, HOX, and molecular clocks. In: VRBA, E. S. & ELDRIDGE, N. (eds) *Macroevolution. Diversity, Disparity, Contingency*. Paleontological Society, Lawrence, Kansas, 36–55.
- PFLUG, H. D. 1970a. Zur Fauna der Nama-Schichten in Südwest-Afrika. I. Pteridinia, bau und systematische Zugehörigkeit. *Palaeontographica Abteilung A.*, **134**, 226–262.
- PFLUG, H. D. 1970b. Zur Fauna der Nama-Schichten in Südwest-Afrika. II. Rangidae, bau und systematische Zugehörigkeit. *Palaeontographica Abteilung A.*, **135**, 198–231.
- PFLUG, H. D. 1972. Systematic der jung-präkambrischen Petalonamae Pflug 1970. *Paläontologische Zeitschrift*, **46**, 56–67.
- PREISS, W. V. 1987. (compiler) The Adelaide Geosyncline—Late Proterozoic stratigraphy, palaeontology and tectonics. *Geological Survey of South Australia Bulletin*, **53**.
- PREISS, W. V. 1999. *PARACHILNA South Australia 1:250 000 Geological Series—Explanatory Notes—Sh54–13 International Index* (2nd edn). Primary Industries and Resources South Australia, Adelaide.
- RAFF, R. A. & RAFF, E. C. 1970. Respiratory mechanisms and the metazoan fossil record. *Nature*, **228**, 1003–1005.
- REID, P. & PREISS, W. V. 1999. PARACHILNA map sheet. *South Australia. Geological Survey Geological Atlas 1:250 000 Series*, sheet SH54-13.
- REINECK, H. E., GERDES, G., CLAES, M., DUNAJTSCHIK, K., REIGE, H. & KRUMBEIN, W. E. 1990. Microbial modification of sedimentary surface structures. 254–276. In: HELING, D., ROTHE, P., FÖRSTER, V. & STOFFERS, P. (eds) *Sediments and Environmental Geochemistry*. Springer-Verlag, Berlin.
- RETALLACK, G. J. 1994. Were the Ediacaran fossils lichens? *Paleobiology*, **20**, 523–544.
- RICHTER, R. 1955. Die ältesten Fossilien Süd-Afrikas. *Senckenbergiana Lethaea*, **36**, 243–289.
- RUNNEGAR, B. 1982a. Oxygen requirements, biology and phylogenetic significance of the late Precambrian worm *Dickinsonia*, and the evolution of the burrowing habit. *Alcheringa*, **6**, 223–239.
- RUNNEGAR, B. 1982b. The Cambrian Explosion: animals or fossils? *Journal of the Geological Society of America*, **15**, 683.
- RUNNEGAR, B. 1991. Oxygen and the early evolution of the Metazoa. In: BRYANT, C. (ed.) *Animal Life Without Oxygen*. Chapman Hall, London, 65–87.
- RUNNEGAR, B. 1994. Proterozoic eukaryotes: Evidence from biology and geology. In: BENGSTON, S. (ed.) *Early Life on Earth. Nobel Symposium No. 84*. Columbia University Press, New York, 287–297.
- RUNNEGAR, B. 1995. Vendobionta or Metazoa? Developments in understanding the Ediacara 'fauna'. *Neues Jahrbuch für Geologie und Paläontologie*, **195**, 303–318.
- RUNNEGAR, B., GEHLING, J. G., HORODYSKI, R. J., JENSEN, S. & KNAUTH, L. P. 1995. Base of the Sauk sequence is a global event that lies just above the Precambrian-Cambrian boundary. *Geological Society of America, Abstracts with Programs*, **27**, A–330.
- SAYLOR, B. Z., GROTZINGER, J. P. & GERMS, G. J. B. 1995. Sequence stratigraphy and sedimentology of the Neoproterozoic Kuibis and Schwarzrand Subgroups (Nama Group) southwest Namibia. *Precambrian Research*, **73**, 153–171.
- SEILACHER, A. 1982. Distinctive features of sandy tempestites. In: EINSELE, G. & SEILACHER, A. (eds) *Cyclic and Event Stratification*. Springer-Verlag, Berlin, 333–349.
- SEILACHER, A. 1984. Late Precambrian and Early Cambrian Metazoa: preservational or real extinctions? In: HOLLAND, H. D. & TRENDALL, A. F. (eds)

- Patterns of Change in Earth Evolution*. Springer-Verlag, Berlin, 159–168.
- SEILACHER, A. 1989. Vendozoa: organismic construction in the Proterozoic biosphere. *Lethaia*, **22**, 229–239.
- SEILACHER, A. 1992. Vendobionta and Psammocoralia: lost construction of Precambrian evolution. *Journal of the Geological Society of London*, **149**, 607–613.
- SEMPERE, L. F., COLE, C. N., MCPEEK, M. A. & PETERSON, K. J. 2006. The phylogenetic distribution of metazoan micro RNAs: Insights into evolutionary complexity and constraint. *Journal of the Experimental Zoology*, **306B**, 575–588.
- STEINER, M. & REITNER, J. 2001. Evidence of organic structures in Ediacara-type fossils and associated microbial mats. *Geology*, **29**, 1119–1122.
- TOTTON, A. K. 1954. Siphonophora of the Indian Ocean together with systematic and biological notes on related specimens from other oceans. *Discovery Report*, **27**, 1–16.
- TOTTON, A. K. 1965. *A Synopsis of the Siphonophora*. British Museum (Natural History), London.
- VALENTINE, J. W. 2001. How were vendobiont bodies patterned? *Paleobiology*, **27**, 425–428.
- WADE, M. 1968. Preservation of soft-bodied animals in Precambrian sandstones at Ediacara, South Australia. *Lethaia*, **1**, 238–267.
- WADE, M. 1970. The stratigraphic distribution of the Ediacara fauna in Australia. *Transactions of the Royal Society of South Australia*, **94**, 87–104.
- WADE, M. 1971. Bilateral Precambrian chondrophores from the Ediacara fauna, South Australia. *Proceedings of the Royal Society of Victoria*, **84**, 183–188.
- WAGGONER, B. M. & HAGADORN, J. W. 1997. Ediacara fossils from western North America: Stratigraphy and paleogeographic implications. *Geological Society of America, Abstracts with Programs*, **29**(6), A–30.
- WEAVER, P. G., MCMENAMIN, M. A. S. & TACKER, R. C. 2006. Paleoenvironmental and paleobiogeographic implications of a new Ediacaran body fossil from the Neoproterozoic Carolina Terrane, Stanly County, North Carolina. *Precambrian Research*, **150**, 123–135.

A brief review of the fossil record of the Ediacaran–Cambrian transition in the area of Montes de Toledo–Guadalupe, Spain

S. JENSEN, T. PALACIOS & M. MARTÍ MUS

*Area de Paleontología, Facultad de Ciencias, Universidad de Extremadura,
E-06071 Badajoz, Spain (e-mail: soren@unex.es)*

Abstract: The area of western Montes de Toledo to Guadalupe boasts a thick succession of mainly siliciclastic sediment spanning terminal Ediacaran to lower Cambrian strata as indicated by a relatively sparse but diverse palaeontological record. A terminal Ediacaran age is based on the occurrence of *Cloudina* in platform carbonates of the lower part of the Ibor group and in correlative levels of olistostromes at the base of the Río Huso group. Higher in the Río Huso group are found trace fossils which indicate a Cambrian age, notably *Treptichnus bifurcus*, which overlaps the local stratigraphic range of macroscopic carbonaceous disc-shaped fossils identified as *Beltanelliformis*. Strata underlying the Río Huso group contain treptichnids. The fossil record of the terminal Ediacaran–Lower Cambrian of this area is in part comparable to *Cloudina*-bearing sediments from other regions, in particular Namibia, where treptichnid trace fossils also overlap the range of *Cloudina*. The possibility of a wider biostratigraphic significance of this should be further tested, including its relation to the base of the Cambrian.

Ediacaran to Cambrian strata crop out over a large area broadly encompassed by Coimbra, Salamanca, Ciudad Real, and Badajoz in central and western Iberia, within the Central Iberian Zone of the classical subdivision of the Iberian Massif (e.g. Vidal *et al.* 1994a; Valladares *et al.* 2002; Rodríguez Alonso *et al.* 2004). Of particular interest to the discussion of terminal Ediacaran palaeontology and biostratigraphy are strata exposed in anticlinal systems spanning the western end of the Montes de Toledo to the area of Guadalupe (Fig. 1). In most areas of Spain, the Ediacaran–Cambrian transition is represented by a major break in sedimentation (e.g. Liñán *et al.* 2002), whereas palaeontological data suggest that the sediments preserved in the Valdelacasa and Ibor anticlines represent essentially uninterrupted deposition. Brasier *et al.* (1979) noted that sections along a dismantled railway running parallel to river Huso in the area of La Nava de Ricomalillo contained fossils of a mixed Ediacaran–Cambrian character; Cambrian-type trace fossils such as *Treptichnus* and *Monomorphichnus*, occurring with disc-shaped carbonaceous compressions similar to *Chuarina* and *Beltanelliformis*, taxa not generally known from the Cambrian. The subsequent discovery (Palacios 1989) and identification (e.g. Vidal *et al.* 1994a) of *Cloudina* from sediments in this region provided further support for the transitional nature of the strata.

Here the current knowledge of the Ediacaran to Cambrian transition in this area is summarized and new data from ongoing studies is provided. The Spanish sequence is compared to other areas

containing terminal Ediacaran strata and the possible biostratigraphical implications are discussed.

Geological setting and lithostratigraphic nomenclature

Terminal Ediacaran to Lower Cambrian strata in the area of western Montes de Toledo to Guadalupe are preserved in broadly NW–SE trending Hercynian folds (Fig. 1). The extent of pre-Hercynian deformation generally decreases up-section, suggesting a transition from a syntectonic to a post-tectonic regime was recorded during the final phase of the Cadomian Orogeny (Vidal *et al.* 1999; Palacios *et al.* 2002). Deposition is thought to have occurred in pull-apart basins under extensional tectonics, with the development of an immature passive margin (Vidal *et al.* 1994a; Valladares *et al.* 2002; see Rodríguez Alonso *et al.* 2004 for alternative interpretations). The least deformed, and most complete exposure, is found along the NE flanks of both anticlines. Exposure is primarily along rivers, road cuts and railway cuttings. Estimates of the exact thickness of the sequences vary greatly as a consequence of conflicting structural interpretations (e.g. Vidal *et al.* 1994a; Santamaría 1995). As a consequence of such problems, an extensive, largely informal, and often poorly defined lithostratigraphic nomenclature exists, as well as differing opinion on the temporal relations of these units. For summaries and different views on these problems see San José *et al.* (1990), Vidal *et al.* (1994a, b), and Valladares *et al.* (2002).

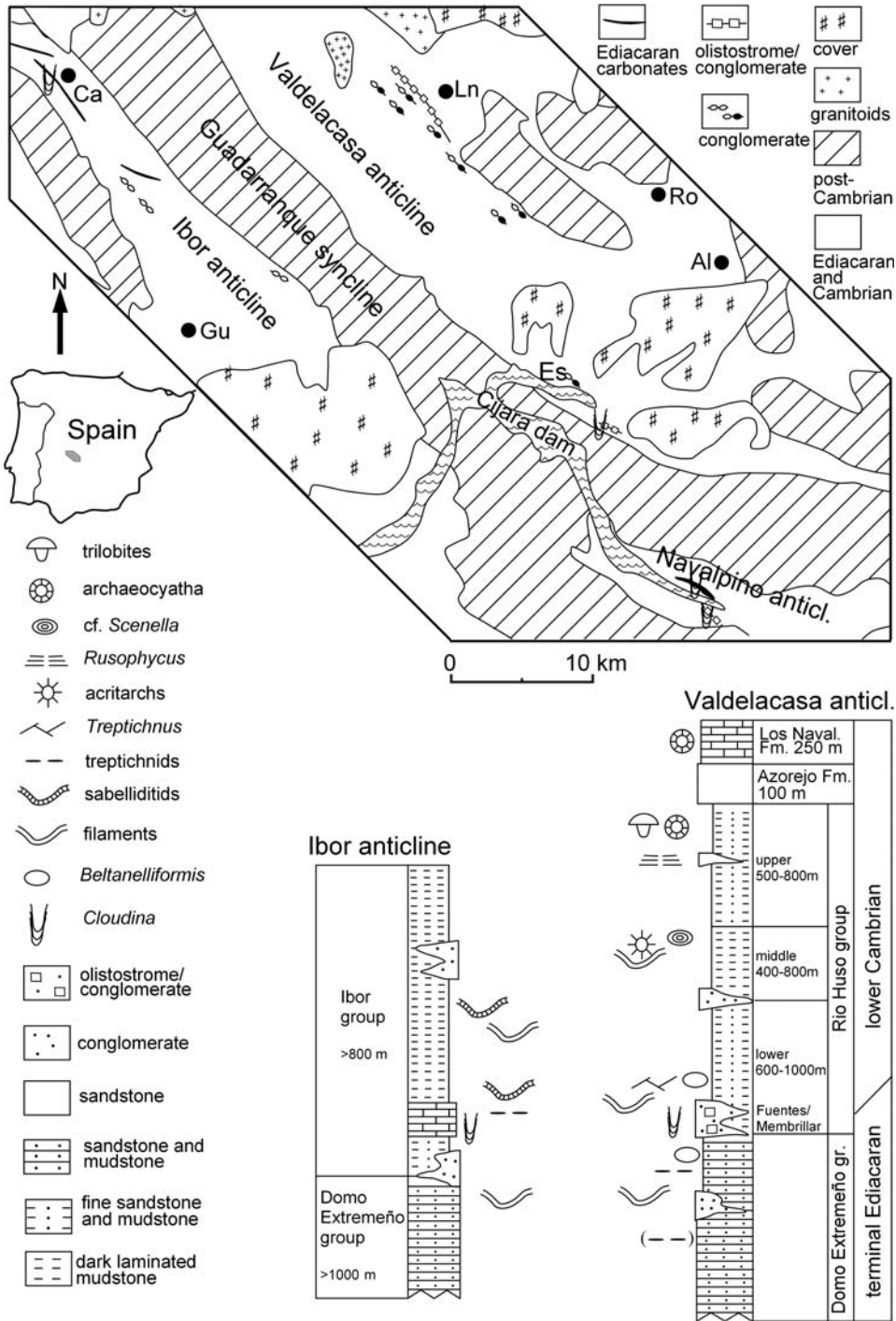


Fig. 1. Geological setting and simplified stratigraphic columns for the Ediacaran–Cambrian transition in the Ibor and Valdelacasa anticlines. Plotted are the first and common occurrences of selected fossils. Alignment of columns assumes coeval occurrences of *Cloudina* (see text for discussion), except for this no detailed correlation is implied. Stratigraphic columns modified from Vidal *et al.* (1999). Al, Los Alares; Ca, Castañar de Ibor; Es, Estenilla section; Gu, Guadalupe; Ln, La Nava de Ricomalillo; Ro, Robledo del Buey.

Here we use the nomenclature of Vidal *et al.* (1994a and 1999), who recognize the Domo Extremeño, Ibor and Río Huso groups. Of the widely used classical terminology, the Domo Extremeño group corresponds to the lower Alcludian and the Ibor and Río Huso groups to the upper Alcludian (but see Vidal *et al.* 1994a, b, for different definitions of the upper Alcludian). The Río Huso group broadly corresponds to the Pusa Shale or Pusa formation of various authors.

The Domo Extremeño group consists of a thick package of sandstones and siltstones, often of greywacke character, containing well-developed turbidites but also strata interpreted as storm deposits, especially towards the top of the sequence (e.g. Palacios 1989; Santamaría 1995; Valladares *et al.* 2000). Conglomeratic intervals have generally been interpreted as representing distributary channels on a slope (e.g. Valladares *et al.* 2000). This paper is concerned only with the upper part of the Domo Extremeño group. In the southern area of the Valdelacasa anticline, Palacios (1989) erected the Estenilla and Cijara formations. These units were also applied to the area of La Nava de Ricomalillo (Palacios 1989; Vidal *et al.* 1994a; Gámez Vintaned 1996). However, the recognition of the Estenilla Formation in this area is now considered problematic.

The Ibor group of the Ibor anticline is dominated by dark, finely-laminated to microlaminated siltstones, mudstones and shale. In the lower part, there is one, or possibly several, carbonate levels (e.g. Cuvelier *et al.* 1982; García-Hidalgo 1985), up to 200 m thick, which locally yield *Cloudina* as accumulations in storm beds (Vidal *et al.* 1994a; Fernandez Remolar 2001; Fig. 1). These carbonates have been interpreted as formed on a rimmed carbonate platform with oolitic shoals, opening to the NE (Calvet & Salas 1988). The Ibor group, with similar occurrences of *Cloudina*, can be traced SE to the Navalpino anticline (Vidal *et al.* 1994a; López Diaz 1994; fig. 1). Especially in the upper part of the Ibor group there are rich accumulations of diverse filamentous organisms (Hufnagel 1969), including sabelliditids (Vidal *et al.* 1994a).

The Río Huso group of the Valdelacasa anticline can be broadly divided into three units (see Palacios & Vidal 1996; Vidal *et al.* 1999). It consists of siltstones and fine, impure sandstones with dark finely laminated siltstones and shales, particularly common in the middle unit. In the middle of the Río Huso group there are phosphate-rich intervals. At the base of the Río Huso group conglomeratic levels occur that in many places are developed as megabreccias with chaotic masses of carbonates (Moreno 1975; Vidal *et al.* 1994b). Similar beds can be traced in a discontinuous band, and with

considerable lateral variability, for a great distance along the Valdelacasa anticline. A well-known example is the Membrillar Olistostrome (e.g. Santamaría & Pardo 1994), which has yielded *Cloudina* (Palacios 1989; Vidal *et al.* 1994a). In the area of La Nava de Ricomalillo comparable units are known as the Fuentes Olistostrome or Fuentes Member (Moreno 1975; Santamaría & Remacha 1994). Conglomeratic levels are found also higher in the Río Huso group (e.g. Santamaría 1995). Overall, the Río Huso and Ibor groups represent shallowing compared to the Domo Extremeño group and have been interpreted to largely be shelf deposits, essentially below wave base, and including periods of poor circulation leading to low oxygen levels (Vidal *et al.* 1994a). Strata of the Domo Extremeño, Ibor and Río Huso groups have been interpreted within a sequence stratigraphic framework by Valladares *et al.* (2000, 2002).

What has not been fully resolved, and fundamental to establishing a stratigraphic framework for the area, is the temporal relationship of the Río Huso and Ibor groups and the significance of the carbonate-bearing olistostromic levels. One school of thought considers the Ibor and Río Huso groups to largely follow in temporal succession (e.g. Álvarez Nava *et al.* 1988; Santamaría 1995; Valladares *et al.* 2002). In this view, the Fuentes Olistostrome marks a period of erosion explaining the absence of the Ibor group in the Valdelacasa anticline. An alternative view, and the one favoured here, is that the rocks of the Ibor and Río Huso groups are more or less contemporaneous, and that sedimentary differences reflect lateral facies changes (Vidal *et al.* 1994a). In this model, the olistostromes represent material shed from the carbonate platform into a more basinal setting, and the supposed local evidence of angular unconformity with underlying rocks of the Domo Extremeño group are the result of drag-folds (see Vidal *et al.* 1994a). Valladares *et al.* (2000) interpreted correlative levels as a type 1 sequence boundary, representing a distal expression of a relative drop in sea level, mentioning evidence for subaerial exposure in the form of blocks with signs of palaeokarst, though we are not aware of the documentation for this. On the other hand, Vidal *et al.* (1994a) reported soft sediment injection in micritic limestone boulders incorporated in the Membrillar Olistostrome. An interesting question requiring further study is: does the olistostrome level correlate with erosion in more shallow-water settings or does it merely represent increased instability perhaps related to tectonic activity? Supporting the latter interpretation there are numerous levels within the Domo Extremeño, Río Huso and Ibor groups with evidence of depositional instability in the form of

large-scale slumps. In any case, fossil evidence is incompatible with a break in sedimentation for more than a few million years.

Trace fossils

Trace fossils from the area of La Nava de Ricomalillo were first described in detail by Brasier *et al.* (1979), based on material from the river Huso section. This included the recognition of trace fossils comparable to *Treptichnus*, as well as *Monomorphichnus* low in the section. Numerous additional taxa were listed by Palacios (1989), and Gámez Vintaned (1996). Gámez Vintaned (1996) listed 28 ichnotaxa from the upper Domo Extremeño and Río Huso groups in the Río Huso section, but the majority of these remain undescribed; some of the listed taxa were figured and discussed by Vidal *et al.* (1994a) including *Phycodes* aff. *pedum* and *Belorhaphé* sp. García-Hidalgo (1993) and Fernández Remolar *et al.* (2005) reported *Palaeophycus* sp., *Hormosiroidea* sp., *Belorhaphé?* sp. and *Phycodes?* sp., from a siliciclastic interval within carbonates of the Ibor group. Vidal *et al.* (1994b) described simple trace fossils from 'lower Alcludian' strata but it is possible that at least some of these are better explained by three-dimensionally preserved tubular organisms (Jensen *et al.* 2005). In the following, selected trace fossils are discussed in more detail.

Treptichnus and *treptichnids*

Treptichnids are complex trace fossils consisting of successive curved probes that opened onto the sea floor. Depending on the arrangement of the probes, various ichnospecies can be identified, including *Treptichnus bifurcus* and *Treptichnus pedum* (see Jensen 1997). Identical or comparable trace fossils have also been described from the Cambrian as *Hormosiroidea* and *Tuberculichnus* (e.g. Paczesna 1996). As discussed by Uchmann (1995, 1998) the continued use of *Hormosiroidea* and *Tuberculichnus* may be unsuitable. Gámez Vintaned (1996) reported *Phycodes pedum* and *Treptichnus bifurcus* occurring about 400 m above the Fuentes Olistostrome in the Río Huso section (though the exact distance is unknown due to faulted contacts). Vidal *et al.* (1994a) described material from the same level as *Phycodes* aff. *pedum*. This is apparently the same general level from which Brasier *et al.* (1979) reported *Phycodes pedum* and *Treptichnus*-like material. New material that can be identified as *Treptichnus bifurcus* occurs at a probably lower stratigraphical level in a nearby section close to road between La Nava de Ricomalillo and La Estrella, near the intersection of Río Huso and Arroyo de Cubilar

(Fig. 2a). Together with these, are found rows of pits (Fig. 2f) of a type commonly reported as *Hormosiroidea* (e.g. Crimes & Anderson 1985), which may be a preservational variation of *Treptichnus*. *Treptichnus*-type trace fossils have been described from siliciclastics of the carbonate-bearing interval of the Ibor group (García-Hidalgo 1993; Fernández Remolar *et al.* 2005, plate 2:2). Treptichnids occur in the Cijara Formation, which is stratigraphically subjacent (Palacios 1989; Vidal *et al.* 1994b) to the Membrillar olistostrome. These consist of rows of short vertical broken probes or elongate, almond-shaped elements (Fig. 2b). Similar trace fossils have been identified as *Tuberculichnus* (e.g. Paczesna 1996). Following Jensen *et al.* (2000) this type of trace fossils can be referred to as treptichnids. Vidal *et al.* (1994a) identified *Phycodes* aff. *pedum* from the upper part of the Domo Extremeño group, in the area of La Nava de Ricomalillo. Tectonic modification of simple trace fossils has to be considered for this rather poorly preserved material, but the identification as treptichnids is reasonable. Trace fossils with a gentle zigzag shape have been found in Arroyo de Cubilar, also in the area of La Nava de Ricomalillo, several hundred meters (precise stratigraphic distance is unknown at this time) down-section from the Fuentes level (Fig. 2d). These probably are treptichnids in *Plangtichnus*-style preservation (see Maples & Archer 1987); reports of *Belorhaphé* from the lower part of the Río Huso group (see Vidal *et al.* 1994a, fig. 15g) may be another example of the same preservational style of treptichnids. Even further down-section, along Arroyo de Cubilar, possible rows of short elongate burrow segments are known (Fig. 2c). Finally, trace fossils with closely spaced oblique 'probes' occur a few hundred metres below the Fuentes level (Fig. 2e). Although these trace fossils resemble *Treptichnus pedum*, a tectonic origin cannot be excluded for the 'probes' at this time.

Arthropod-type trace fossils

Brasier *et al.* (1979) reported *Monomorphichnus* in the Río Huso section from beds with 'Chuaría', as well as from 100 m below the main *Chuaría* beds (according to Vidal *et al.* 1994a, p. 745–746, the stratigraphic level of the presumably lower occurrence is uncertain). *Monomorphichnus lineatus* was described by Vidal *et al.* (1994a) from the lower part of the Río Huso group. The *Dimorphichnus* of Vidal *et al.* (1994a, fig. 15e) is likely to be a treptichnid. The first bilobed arthropod-type trace fossils appear in the upper part of the Río Huso group in the area of Los Alares in the form of large, but shallow, paired lobes probably representing *Rusophycus bonnarensis*.

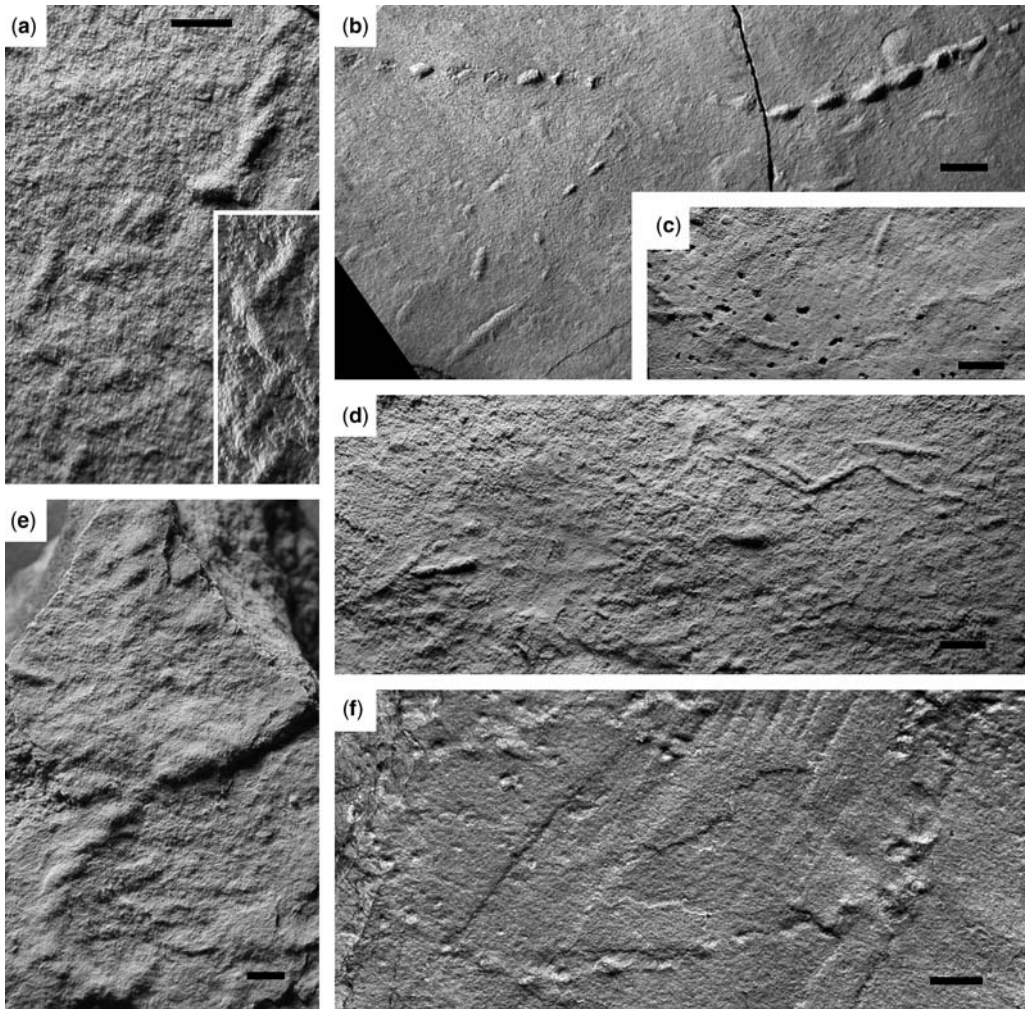


Fig. 2. Treptichnids and related trace fossils. All in sole view. (a) *Treptichnus bifurcus* from lower part of lower unit of Río Huso group, exposure close to road between La Nava de Ricomalillo and La Estrella, near intersection of Río Huso and Arroyo de Cubilar. Inset shows section with zigzag development in different lighting. Scale bar = 2 mm. UEXP682Hu2:003. (b) Treptichnids on the sole of sandstone bed developed as aligned almond-shaped pods. Probes in upper left side of figure with fractured surface indicate vertical probes. Upper part of Domo Extremeño group (Cijara Formation), close to intersection of Estenilla River and Cijara Dam. A field photograph of this specimen was published by Vidal (1998, fig. 11). Scale bar = 7 mm. UEXP708Es1:004. (c) Probable treptichnid (compare with (b)) from the upper part of the Domo Extremeño group in section along Arroyo del Cubilar, area of La Nava de Ricomalillo. Scale bar = 6 mm. UEXP682Cu1:001. (d) Possible treptichnids from the upper part of Domo Extremeño group (Cijara Formation) in section along Arroyo del Cubilar, area of La Nava de Ricomalillo. Scale bar = 4 mm. UEXP682Cu2:001. (e) Possible *Treptichnus pedum* from the upper part of the Domo Extremeño group. From section along road CM-411 close to intersection with the Río Huso. Scale bar = 2 mm. UEXP682Fe2:002. (f) Treptichnid developed as rows of pods in places showing fractured surface of vertical elements. On same slab as specimen in (a). Scale bar = 4 mm.

Psammichnitids

Spectacular *Psammichnites gigas* occur in the upper unit of the Río Huso group in the southeastern end

of the Valdelacasa anticline, and in various modes of preservation (Moreno *et al.* 1976; Seilacher 1997). The occurrence of *P. gigas* approximately coincides with the first *Rusophycus* (see Fig. 1).

Carbonaceous compressions

Filamentous or globular carbonaceous compressions occur in all three groups. The diversity of these fossils in the sections in the Ibor and Valdelacasa areas remains largely unstudied; for the purpose of this paper two major morphotypes are distinguished.

Beltanelliformis

Disc-shaped compressions, which likely represent originally more or less globular organisms, occur in the Río Huso group and the upper part of the Domo Extremeño group (Brasier *et al.* 1979; Vidal *et al.* 1994a). The discs, often showing evidence of compactional folding, are found as dense aggregates, chains and isolated specimens (Fig. 3). The problems involved in the naming and interpretation of such morphologically simple structures have been discussed by Brasier *et al.* (1979), Vidal *et al.* (1994a) and Xiao *et al.* (2002). Because of the consistent morphology these are all included in the same form taxon, *Beltanelliformis*, following what appears to be the current preference (see Xiao *et al.* 2002).

Ring-like structures on bed soles of the Domo Extremeño group have been identified as *Nimbia*

occlusa (Vidal *et al.* 1994a, fig. 15f), but their relationship to other occurrences of *Nimbia* is inconclusive. Two possible explanations are suggested for this type of structure in the Domo Extremeño group. They could represent isolated loops of trace fossils or three-dimensionally preserved filaments (see Fig. 4d). Alternatively they could be a preservational form of large *Beltanelliformis*, with which they share a similar outline.

Filaments

Filamentous fossils are found throughout the Domo Extremeño, Río Huso and Ibor groups (Figs 4, 5, 6). These probably represent a variety of organisms, some of which were originally tubular, and are found in different styles of preservation. Some are preserved as flattened carbonized ribbons (Fig. 5), and some as thin films without obvious carbonaceous material (Fig. 4b, c). In the Ibor group, forms with coarse (Fig. 6a, b) or fine (Fig. 6c, d) transverse wrinkles are found, apparently representing various types of sabelliditids (Contreras Sanchez *et al.* 2006). Specimens from the upper part of the Ibor group have been identified as *Sabellidites* sp. (Vidal *et al.* 1994a) and *Sabellidites camabriensis* (Vidal *et al.* 1999). This material is currently under study.

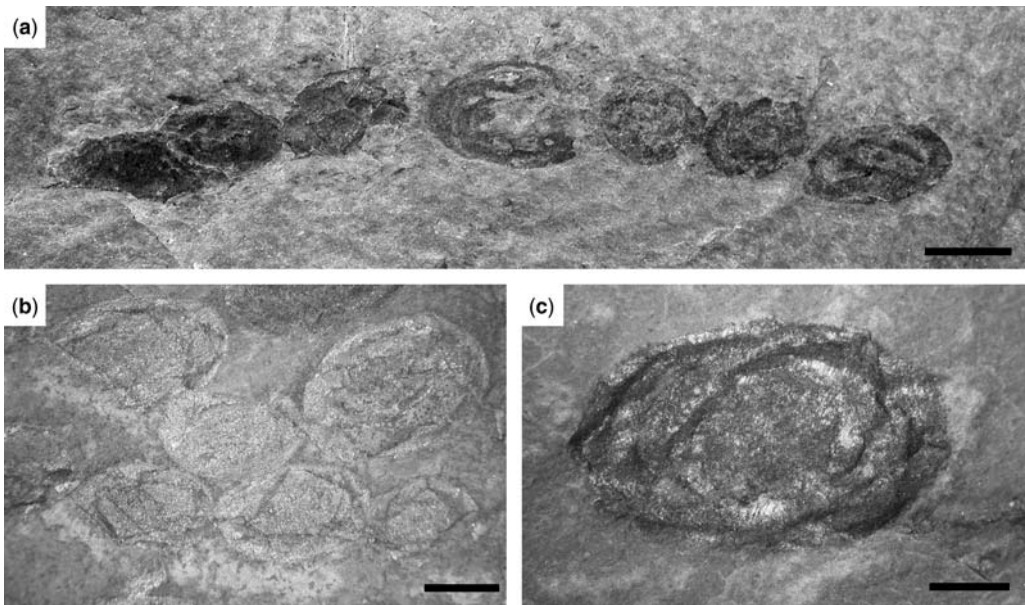


Fig. 3. Carbonaceous compressions identified as *Beltanelliformis*, from lower part of lower unit, Río Huso group, along railway section, area of La Nava de Ricomalillo. (a) Specimens aligned in row. Scale bar = 5 mm. UEXP682Fe1:002. (b) Partly pyritized specimens showing compactional folding. Scale bar = 3 mm. UEXP682Fe1:001. (c) Large specimen with compactional folding. Scale bar = 2 mm. UEXP682Fe1:003.

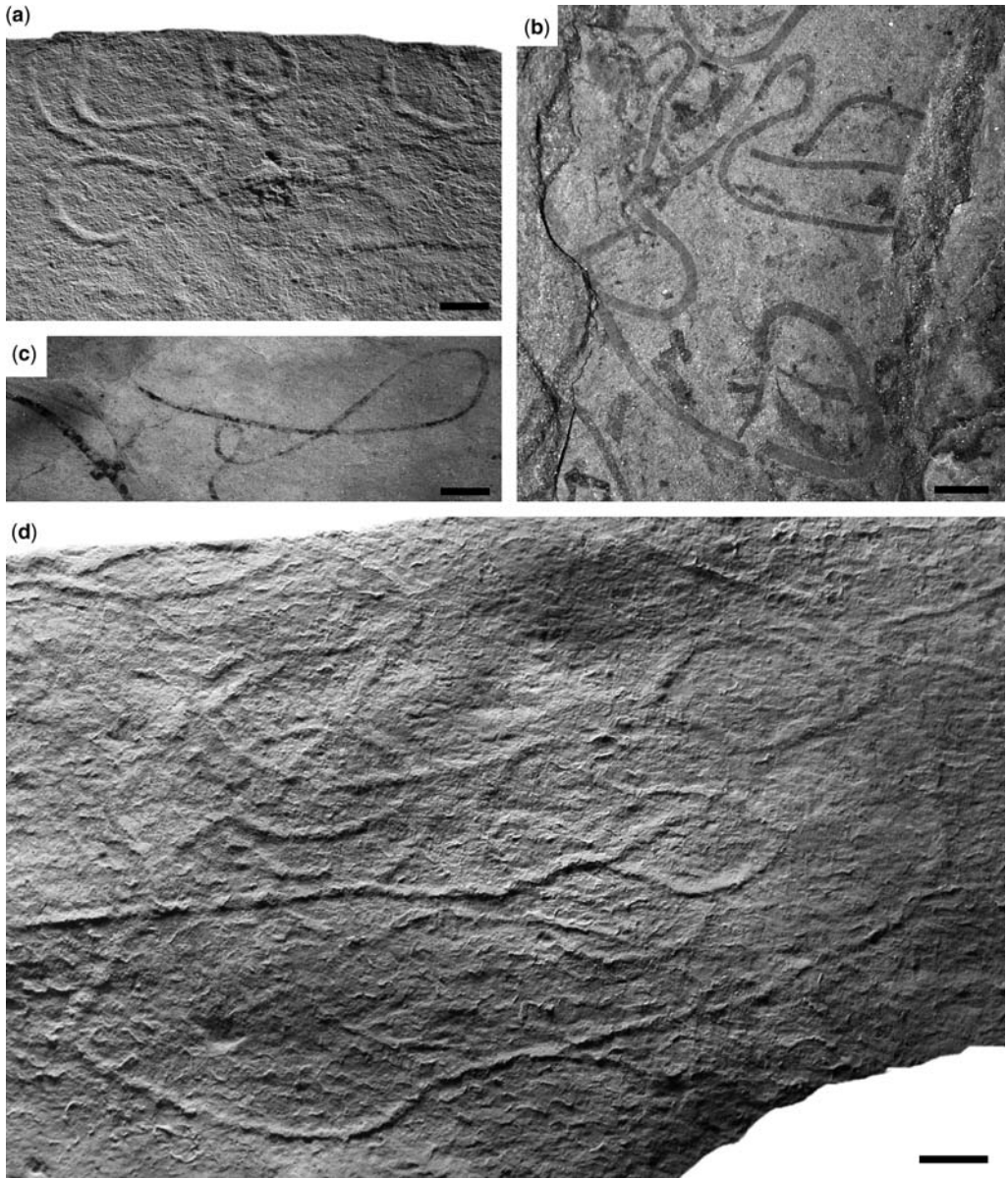


Fig. 4. Filamentous organisms in different styles of preservation. **(a)** Specimen from the upper part of the Domo Extremeño group previously figured by Vidal *et al.* (1994b, fig. 3b) and originally interpreted as trace fossil. Preserved as a shallow furrow. Light from lower right. Scale bar = 5 mm. **(b)** Filaments from the Ibor group in the area of Guadalupe, preserved as thin dark films. Notice the presence of gentle, curved portions as well as sharp angles. These filaments have a weakly developed transverse wrinkling (not easily seen in photograph) and may represent sabelliditids. Scale bar = 5 mm. UEXP707Pm1:005. **(c)** Looping filaments preserved as dark film. Road between Navatrasierra and La Calera. Scale bar = 5 mm. UEXP681Ca1:072. **(d)** Upper surface of sandstone with numerous specimens preserved as raised ridges. These may be trace fossils or three-dimensionally-preserved filamentous organisms. Notice what appear to be circular elements. It has not been possible to conclude if these are loops within the filament or individual structures. Upper part of Domo Extremeño group, section along the Río Huso, close to intersection with road CM-411. Scale bar = 10 mm. UEXP682Hu1:001.

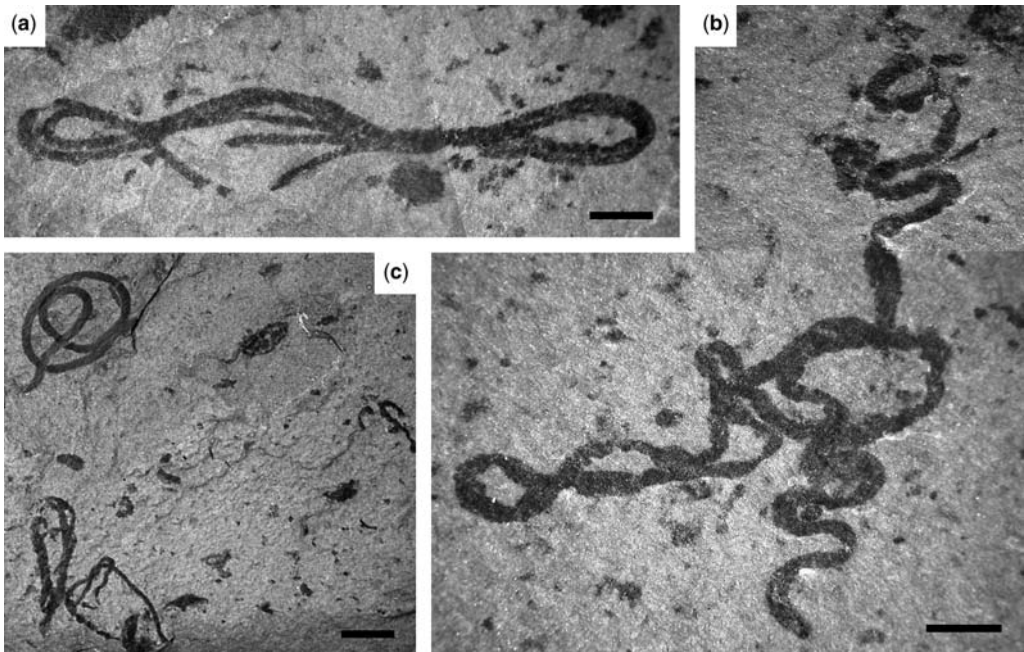


Fig. 5. Filamentous organisms from upper part of the Río Huso group close to La Nava de Ricomalillo. (a) Specimen fraying into multiple strands. Scale bar = 2 mm. UEXP682Nr1:035. (b) Long, in part, sinusoidal filament. Similar forms from China have recently been re-interpreted as possible faecal strands (Steiner *et al.* 2005). Scale bar = 5 mm. UEXP682Nr1:036. (c). Smoothly curved specimen in upper left corner and several irregular strands. Scale bar = 2 mm. UEXP682Nr1:037.

A noteworthy discovery from this area is that the same organisms that are typically preserved as filaments can also be preserved as grooves and ridges along bedding-planes (Jensen *et al.* 2005). This leaves open to question the interpretation of some of the structures from the Domo Extremeño group that previously have interpreted as simple bedding-plane trace fossils (see Fig. 4 and Vidal *et al.* 1994b), and may have wider implications for the Ediacaran trace fossil record. A detailed study of this problem will be presented elsewhere.

Skeletal fossils

The weakly mineralized tubular fossil *Cloudina* (Fig. 7a) was first figured from central Spain by Palacios (1989) and subsequently identified as *Cloudina hartmannae* (see Vidal *et al.* 1994a). The geographic distribution of *Cloudina* in central Spain has been discussed by Vidal *et al.* (1994a). Cortijo *et al.* (2006) presented new data on Spanish *Cloudina* including specimens with dichotomous branching and a probable new species of *Cloudina*.

The Río Huso group in the Valdelacasa anticline contains small shelly fossils (e.g. Vidal *et al.* 1999;

Fernández Remolar 2001; Palacios *et al.* 2002) that so far remain largely undescribed, and therefore published identifications should be considered preliminary. The upper part of the middle unit of the Río Huso group at La Nava de Ricomalillo contains newly-discovered large, cap-shaped fossils (Fig. 7b), which have been tentatively identified as *Scenella* (Palacios *et al.* 2002). The upper unit of the Río Huso group in the area of Robledo del Buey contains trilobites, archaeocyathids and cancellorids (Vidal *et al.* 1999; Palacios *et al.* 2002; Fig. 7c). Vidal *et al.* (1999) reported the occurrence of *Anabarella* sp. cf. *A. plana* from mudstones with abundant phosphate nodules from the Alcudia valley in strata correlatable with the Río Huso group.

Organic-walled microfossils

The upper part of the Domo Extremeño group and the lower part of the Ibor and Río Huso groups yield abundant but biostratigraphically undiagnostic microfossils attributed to *Sphaerocongregus variabilis* and *Palaeogomphosphaeria cauriensis* (Palacios 1989). The only age-diagnostic microfossils to date, from this area, is the occurrence of the

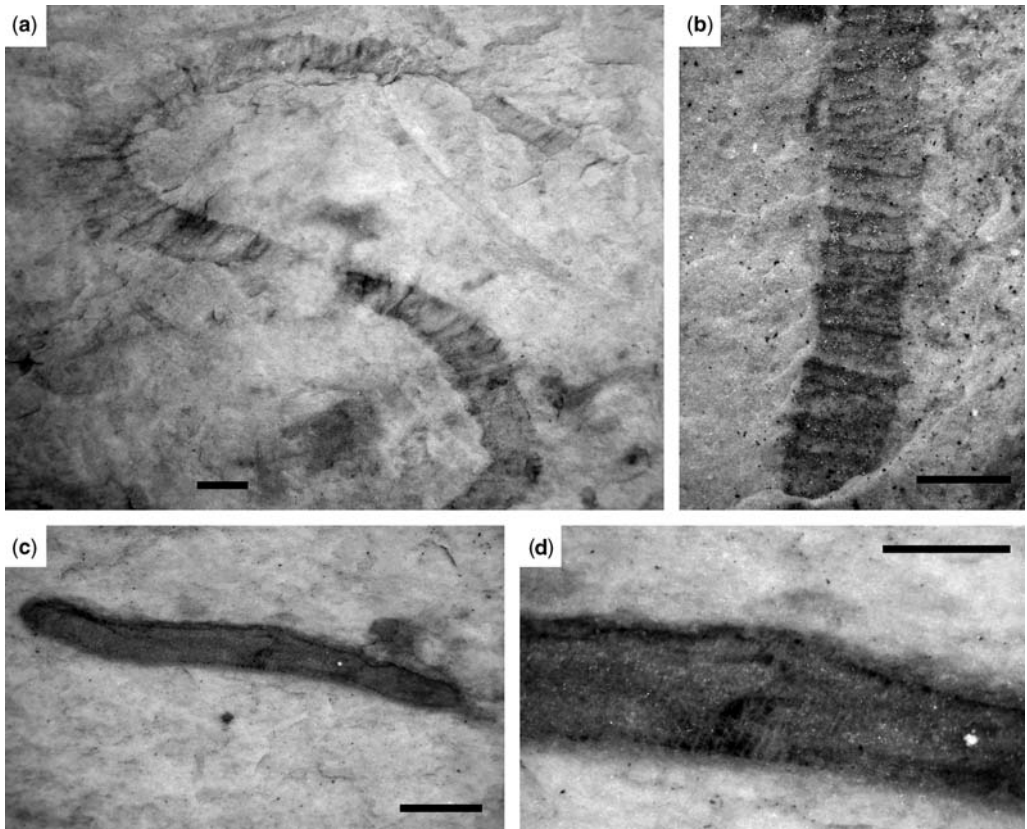


Fig. 6. Sabelliditids from the upper part of the Ibor group in section along road from La Calera to Navatrassiera. (a) Specimen with poorly preserved, widely spaced transverse structures. Scale bar = 1 mm. UEXP681Ca1:066. (b) Fragment of similar but better-preserved specimen. Scale bar = 1 mm. UEXP681Ca1:001. (c) Small specimen (?fragment) with fine transverse wrinkles best seen in the mid-section. Scale bar = 1 mm. UEXP681Ca1:071. (d) Close-up of specimen in (c). Scale bar = 0.5 mm.

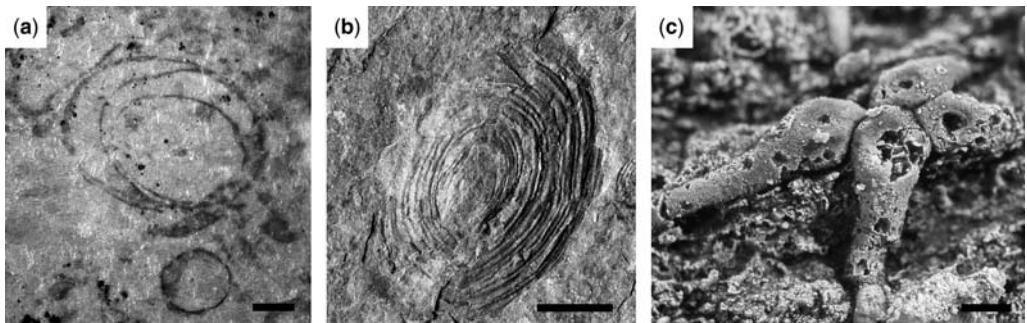


Fig. 7. Skeletal fossils from the Ibor and Río Huso groups. (a) *Cloudina* sp. from carbonates of the Navalpino anticline. Scale bar = 0.2 mm UEXP734Um1:001. (b) Internal mould of cap-shaped fossil comparable to *Scenella*. Top of middle unit, section close to La Nava de Ricomalillo. Scale bar = 5 mm. UEXP682Nr1:014. (c) Latex cast of mould of chancellorid from archaeocyath-bearing mudstone. Upper unit of Río Huso group, close to Robledo del Buey. Scale bar = 5 mm. UEXP683Rb1:011.

acritarch *Comasphaeridium velvetum* in the upper part of the middle unit of the Río Huso group (Fig. 1), suggesting correlation to the *Asteridium tornatum-Comasphaeridium velvetum* Zone on the East European Platform (Palacios *et al.* 2002).

Ediacaran—Lower Cambrian biostratigraphy of the Ibor and Río Huso groups

The presence of *Cloudina* strongly indicates a terminal Ediacaran age for the lower part of the Ibor group. Several studies have found the stratigraphic range of *Cloudina* to be restricted to the terminal Ediacaran, for which it may be an index fossil (Grant 1990; Conway Morris *et al.* 1990). In Namibia, *Cloudina* ranges from about 550 to 543 Ma (Grotzinger *et al.* 1995). In Oman, the upper limit of the range of *Cloudina* in the Ara Formation (see Conway Morris *et al.* 1990) approximately coincides with a pronounced negative carbon isotope excursion and with a U–Pb zircon date of 542.0 ± 0.3 Ma (Amthor *et al.* 2003). Thus, current data gives a range of *Cloudina* from c. 550 to 542 Ma, putting the upper range close to the currently accepted age for the base of the Cambrian. In the absence of contrary evidence, the Spanish *Cloudina* is considered to be latest Ediacaran. *Cloudina* is known from the lower part of the carbonate bearing unit in Castañar de Ibor and the area of Villarte de los Montes. However, the upper limit of the range of *Cloudina* within the carbonate-bearing unit of the Ibor Group remains to be established and it is unclear if the distribution of *Cloudina* overlaps with the treptichnids reported by García-Hidalgo (1993) and Fernández Remolar *et al.* (2005). Sabelliditids occur above *Cloudina* in the Ibor group. At the present state of investigation they do not provide further stratigraphic resolution but are consistent with a latest Ediacaran to earliest Cambrian age.

The base of the Cambrian in Spanish sections is currently defined on the first occurrence of a *Monomorphichnus lineatus-Treptichnus pedum* assemblage (Gámez Vintaned 1996); in the Valdelacasa anticline it is located low in the Río Huso group (e.g. Gámez Vintaned 1996). However, the precise location of the Ediacaran–Cambrian boundary within the Valdelacasa anticline is problematic because of the small number of outcrops suitable for the recovery of discrete trace fossils. Also of importance in positioning the Ediacaran–Cambrian boundary is the interpretation of the olistostromic beds. In the model favoured here, the olistostromic level is essentially coeval with the platform carbonates of the Ibor group, and therefore of Ediacaran age, whereas in the vertical stacking model the olistostromic level could be Ediacaran or Cambrian.

Valladares *et al.* (2006) suggested that the olistostromic level sits on a sequence boundary that correspond to a globally recognized drop in sea-level close to the Ediacaran–Cambrian boundary, but as mentioned above, the published evidence for this sequence boundary is considered here to be debatable. It is proposed that the Ediacaran–Cambrian boundary lies somewhere between the Fuentes olistostrome and the occurrence of *Treptichnus pedum* in Río Huso railway section. The new material of *Treptichnus bifurcus* occurring between these two stratigraphic levels, supports this proposal. Treptichnids occur in the upper part of the Domo Extremeño group of the Valdelacasa anticline, a considerable distance below the lowest *Treptichnus pedum* or *Treptichnus bifurcus* (Palacios 1989; Vidal *et al.* 1994a) in strata that are probably of Ediacaran age. Skeletal fossils, including trilobites and archaeocyaths, as well as trace fossils and acritarchs demonstrate that the upper part of the Río Huso group is moderately high lower Cambrian.

Discussion

Almost 30 years after the paper by Brasier *et al.* (1979) was published, palaeontological studies of the Ediacaran–Cambrian sediments in the Montes de Toledo–Guadalupe region remain preliminary, and there are yet unsettled stratigraphical problems. Nevertheless, the emerging picture raises potentially important questions that have bearing on latest Ediacaran biostratigraphy. There are recent reports of time-significant associations of Ediacaran-type fossils (Waggoner 1999, 2003; Gehling & Narbonne 2002). Of these, the youngest is the Nama association (found in Namibia, British Columbia, Canada, the Mojave Desert, and south China), characterized by the appearance of the first mineralised animals, notably *Cloudina*, as well as a low diversity of Ediacara-type fossils, such as *Ernieetta* and *Swartpuntia*. In Namibia, treptichnids occur along with *Cloudina* in the upper range of the latter (Jensen *et al.* 2000). A feature linking Namibia and Spain is therefore the presence of treptichnid trace fossils overlapping the range of *Cloudina* (Jensen *et al.* 2000). Jensen (2003) proposed a latest Ediacaran trace fossil zone containing the first complex trace fossils, largely based on material from Namibia, but also on material from Spain. Several factors need be considered when interpreting the overlapping range of treptichnids and *Cloudina*, including palaeogeographic and facies controls (Grazhdankin 2004). Waggoner (2003, p. 109) noted that *Cloudina*-bearing sediments occurred in regions that were centred on the Equator. The Spanish region was not included in

the analysis of Waggoner (2003), but moderately low terminal Ediacaran—early Cambrian palaeolatitudes are probable for Spain. For example, Gubanov (2002) noted close similarities between Spanish and Siberian early Cambrian molluscs. The relation of treptichnids to *Treptichnus* also needs to be clarified. Are these taxa identical, but simply different in preservation, or are the early treptichnids comparable, but simpler, trace fossils (see Jensen *et al.* 2000)? Finally, the relation between the zone of overlap of *Cloudina* and treptichnids and the base of the Cambrian (as defined on trace fossils in Newfoundland, Narbonne *et al.* 1987) needs to be considered. South China, western USA and Canada are obvious areas in which to further examine this relationship.

Conclusions

The following points are discussed in this paper:

- As previously pointed out (Brasier *et al.* 1979), sections in the area of Montes de Toledo—Guadalupe show stratigraphic overlap of fossils having Ediacaran and Cambrian aspects.
- A terminal Ediacaran age is indicated by the presence of *Cloudina* in the lower half of the Ibor group, and in probably correlative levels at the base of the Río Huso group.
- Undoubted *Treptichnus* occur somewhat above the *Cloudina*-bearing levels in the lower unit of the Río Huso group and overlap the range of the macroscopic carbonized discoidal fossil *Beltanelliformis*.
- The stratigraphic range of treptichnid trace fossils overlaps with that of *Cloudina*.
- Filamentous organisms occur throughout the interval encompassing the Ediacaran–Cambrian boundary, and include sabelliditids in the Ibor group.
- The palaeontological record of the Spanish sections is in part comparable to that of the upper part of the Nama group in Namibia, where there is also an overlap in the range of treptichnids and *Cloudina* below the first undoubted *Treptichnus pedum*.
- This zone of overlap of *Cloudina* and treptichnids may prove to be stratigraphically significant. The exact position of this zone relative to the base of the Cambrian system merits further attention.

We gratefully acknowledge funding from the Spanish Ministry of Education and Sciences (MEC) through Programa Ramon y Cajal and projects MAT-2000-0142-P4 and CGL-2004-02967/BTE (co-financed by FEDER). This paper benefited from the editorial assistance of P. Komarower and P. Vickers-Rich. We thank

J. Gehling and G. Acenolaza for their reviews of the manuscript. Figured material is housed in the collections of Area de Paleontología, Universidad de Extremadura, Badajoz.

References

- ÁLVAREZ NAVA, H., GARCÍA CASQUERO, J. L., GIL TOJA, A. *ET AL.* 1988. Unidades litesstratigráficas de los materiales Precámbrico-Cámbrico en la mitad suroriental de la Zona Centro-Ibérica. *Comunicaciones, II Congreso Geológico de España*, **1**, 19–22.
- AMTHOR, J. E., GROTZINGER, J. P., SCHRÖDER, S., BOWRING, S. A., RAMEZANI, J., MARTIN, M. W. & MATTER, A. 2003. Extinction of *Cloudina* and *Namacalathus* at the Precambrian–Cambrian boundary in Oman. *Geology*, **31**, 431–434.
- BRASIER, M. D., PEREJÓN, A. & SAN JOSÉ, M. A. 1979. Discovery of an important fossiliferous Precambrian–Cambrian sequence in Spain. *Estudios Geológicos*, **35**, 379–383.
- CALVET, F. & SALAS, R. 1988. Tipos de plataformas carbonatadas del Precámbrico terminal de la Zona Centro-Ibérica. *Comunicaciones, II Congreso Geológico de España*, **1**, 59–62.
- CONTRERAS SANCHEZ, M. M., JENSEN, S. & PALACIOS, T. 2006. Sabelliditidos y vendoténidos del Anticlinal de Ibor (Zona Centroibérica). *XXII Jornadas de la Sociedad Española de Paleontología, Resúmenes*, 101–103.
- CONWAY MORRIS, S., MATTES, B. W. & CHEN, M. 1990. The early skeletal organism *Cloudina*: new occurrences from Oman and possibly China. *American Journal of Science*, **290**–A, 245–260.
- CORTIJO, I., PALACIOS, T., JENSEN, S. & MARTÍ MUS, M. 2006. Nuevos datos sobre los cloudínidos de España. *XXII Jornadas de la Sociedad Española de Paleontología, Resúmenes*, 103–105.
- CRIMES, T. P. & ANDERSON, M. A. 1985. Trace fossils from the Late Precambrian—Early Cambrian strata of southeastern Newfoundland (Canada): temporal and environmental implications. *Journal of Paleontology*, **59**, 310–343.
- CUVELIER, N., KIRCH, P., WEMPE, H., WEYER, H.-J. & WALTER, R. 1982. La geología del Anticlinal de Ibor en la región de Navalvillar de Ibor. *Münstersche Forschungen zur Geologie und Paläontologie*, **56**, 29–44.
- FERNÁNDEZ REMOLAR, D. C. 2001. Latest Neoproterozoic to Middle Cambrian body fossil record in Spain (exclusive of trilobites and archaeocyaths) and their stratigraphic significance. *Geologiska Föreningens i Stockholm Förhandlingar*, **123**, 73–80.
- FERNÁNDEZ REMOLAR, D. C., GARCÍA-HIDALGO, J. F. & MORENO-EIRIS, E. 2005. Interés del registro de los primeros organismos en el Arcaico y Proterozoico. *Boletín de la Real Sociedad Española de Historia Natural, Sección Geológica*, **100**, 177–209.
- GÁMEZ VINTANED, J. A. 1996. The Río Huso section. *II Field Conference of the Cambrian stage subdivision working groups, Field trip guide and Abstracts*, 28–31.
- GÁMEZ-VINTANED, J. A. & LIÑÁN, E. 1995. Trace fossil biostratigraphy of the late Neoproterozoic—early

- Cambrian of Iberia. In: RODRIGUEZ ALONSO, M. D. & GONZALO CORRAL, J. C. (eds) *XIII Reunión de Geología del Oeste Peninsular*. Annual IGCP Project-319 Meeting: 19–30 de Septiembre de 1995. Sigüo, S. L., Salamanca, p. 73.
- GARCÍA-HIDALGO, J. F. 1985. Estratigrafía y sedimentología del Alcudiense superior en los anticlinorios de Ibor y Navezuelas–Robledollano. *Seminarios de Estratigrafía, Serie Monografías*, **12**.
- GARCÍA-HIDALGO, J. F. 1993. Las pistas fósiles del Alcudiense superior en el anticlinal de Ibor. consideraciones cronoestratigráficas. *Geogaceta*, **13**, 33–35.
- GEHLING, J. G. & NARBONNE, G. M. 2002. Zonation of the terminal Proterozoic (Ediacaran). *Geological Society of Australia Abstracts*, **68**, 63–64.
- GRANT, S. W. F. 1990. Shell structure and distribution of *Cloudina*, a potential index fossil for the terminal Proterozoic. *American Journal of Science*, **290**–A, 261–294.
- GRAZHDANKIN, D. 2004. Patterns of distribution in the Ediacaran biotas: facies versus biogeography and evolution. *Paleobiology*, **30**, 203–221.
- GROTZINGER, J., BOWRING, S. A., SAYLOR, B. Z. & KAUFMAN, A. J. 1995. Biostratigraphic and geochronologic constraints on early animal evolution. *Science*, **270**, 598–604.
- GUBANOV, A. P. 2002. Early Cambrian palaeogeography and the probable Iberia–Siberia connection. *Tectonophysics*, **352**, 153–168.
- HUFNAGEL, H. 1969. Paläobotanische untersuchungen in Kambrium von Spanien. Dissertation, Julius-Maximilians-Universität. Würzburg.
- JENSEN, S. 1997. Trace fossils from the Lower Cambrian Mickwitzia sandstone, south–central Sweden. *Fossils and Strata*, **42**, 1–110.
- JENSEN, S. 2003. The Proterozoic and Earliest Cambrian trace fossil record: patterns, problems and perspectives. *Integrative and Comparative Biology*, **43**, 219–228.
- JENSEN, S., SAYLOR, B. Z., GEHLING, J. G. & GERMS, G. J. B. 2000. Complex trace fossils from the terminal Proterozoic of Namibia. *Geology*, **28**, 143–146.
- JENSEN, S., PALACIOS, T. & MARTÍ MUS, M. 2005. Megascopic filamentous organisms preserved as grooves and ridges in Ediacaran siliciclastics. *Paleobios*, **25**, 65–66.
- LIÑÁN, E., GOZALO, R., PALACIOS, T., GÁMEZ VINTANED, J. A., UGIDOS, J. M. & MAYORAL, E. 2002. Cambrian. In: GIBBONS, W. & MORENO, M. J. (eds) *The Geology of Spain*, 17–29. Geological Society, London.
- LÓPEZ DIAZ, F. 1994. Estratigrafía de los materiales anterordovícicos del anticlinal de Navalpino (Zona Centro-Ibérica). *Revista de la Sociedad Geológica de España*, **7**, 31–45.
- MAPLES, C. G. & ARCHER, A. W. 1987. Redescription of early Pennsylvanian trace —fossil holotypes from the nonmarine Hindostan Whetstone beds of Indiana. *Journal of Paleontology*, **61**, 890–897.
- MORENO, F. 1975. Olistostromas, fanglomerados y ‘slump folds’. Distribución de facies en las series tránsito Precámbrico–Cámbrico en el anticlinal de Valdelacasa (Provincias de Toledo, Cáceres y Ciudad Real). *Estudios Geológicos*, **31**, 249–260.
- MORENO, F., VEGAS, R. & MARCOS, A. 1976. Sobre la edad de las series Ordovícicas y Cambricas relacionadas con la discordancia ‘Sárdica’ en el anticlinal de Valdelacasa (Montes de Toledo, España). *Breviora Geológica Astúrica*, **20**, 8–15.
- NARBONNE, G. M., MYROW, P. M., LANDING, E. & ANDERSON, M. M. 1987. A candidate stratotype for the Precambrian–Cambrian boundary, Fortune Head, Burin Peninsula, southeastern Newfoundland. *Canadian Journal of Earth Sciences*, **24**, 1277–1293.
- PACZESNA, J. 1996. The Vendian and Cambrian ichno-coenoses from the Polish part of the East-European platform. *Prace Panstwowego Instytutu Geologicznego*, **152**, 1–77.
- PALACIOS, T. 1989. Microfósiles de pared orgánica del Proterozoico superior (Región central de la Península Ibérica). *Memorias del Museo Paleontológico de la Universidad de Zaragoza*, **3**(2), 1–91.
- PALACIOS, T. & VIDAL, G. 1996. El Neoproterozoico Superior–Cámbrico inferior del centro de España. *Comunicaciones, XII Jornadas de Paleontología*, 170–179.
- PALACIOS, T., EGUÍLUZ, L. & MARTÍ, M. 2002. New paleontological and structural data from the Upper Vendian–Lower Cambrian of Valdelacasa Anticline (Central Spain). *VIII Conference of the Cambrian Stage Subdivision working group, Programme and Abstracts*, 31.
- RODRÍGUEZ ALONSO, M. A., DÍEZ BALDA, M. A., PEREJÓN, A. ET AL. 2004. La secuencia litoestratigráfica del Neoproterozoico–Cámbrico inferior. In: VERA, J. A. (ed.) *Geología de España*, 78–81.
- SAN JOSÉ, M. A., DE PIEREN, A. P., GARCÍA-HIDALGO, F. J., VILAS, L., HERRANZ, P., PELÁEZ, J. R. & PEREJÓN, A. 1990. Ante-Ordovician. In: DALLMEYER, R. D. & MARTINEZ GARCIA, E. (eds) *Pre-Mesozoic Geology of Iberia*, 147–159.
- SANTAMARÍA, J. 1995. *Los yacimientos de fosfato sedimentario en el límite Precámbrico–Cámbrico del anticlinal de Valdelacasa (Zona Centro-Ibérica)*. PhD thesis, Universitat Autònoma de Barcelona.
- SANTAMARÍA, J. & PARDO, M. V. 1994. Las megabrechas del Membrillar y su relación con el sustrato. Precámbrico–Cámbrico de la zona Centro-Ibérica. *Geogaceta*, **15**, 10–13.
- SANTAMARÍA, J. & REMACHA, E. 1994. Variaciones laterales del ‘Nivel de Fuentes’, Precámbrico–Cámbrico de la zona Centro-Ibérica. *Geogaceta*, **15**, 14–16.
- SEILACHER, A. 1997. *Fossil Art. An exhibition of the Geologisches Institut Tuebingen University*. The Royal Tyrrell Museum of Paleontology, Drumheller.
- STEINER, M., ZHU, M. Y., ZHAO, Y. L. & ERDTMANN, B.-D. 2005. Lower Cambrian Burgess Shale-type fossil associations of South China. *Paleogeography, Palaeoclimatology, Palaeoecology*, **220**, 129–152.
- UCHMANN, A. 1995. Taxonomy and palaeoecology of flysch trace fossils: the Marnoso-arenacea Formation and associated facies (Miocene, Northern Apennines, Italy). *Beringeria*, **15**, 1–115.
- UCHMAN, A. 1998. Taxonomy and ethology of flysch trace fossils: revision of the Marian Książkiewicz collection and studies of complementary material.

- Annales Societatis Geologorum Poloniae*, **68**, 105–218.
- VALLADARES, M. I., BARBA, P., UGIDOS, J. M., COLMENERO, J. R. & ARMENTEROS, I. 2000. Upper Neoproterozoic–Lower Cambrian sedimentary successions in the Central Iberian Zone (Spain): sequence stratigraphy, petrology and chemostratigraphy. Implications for other European zones. *International Journal of Earth Sciences*, **89**, 2–20.
- VALLADARES, M. I., BARBA, P. & UGIDOS, J. M. 2002. Precambrian. In: GIBBONS, W. & MORENO, M. J. (eds) *The Geology of Spain*, 8–16. Geological Society, London.
- VALLADARES, M. I., UGIDOS, J. M., BARBA, P., FALLICK, A. E. & ELLAM, R. M. 2006. Oxygen, carbon and strontium isotope records of Ediacaran carbonates in Central Iberia (Spain). *Precambrian Research*, **147**, 354–365.
- VIDAL, G. 1998. Proterozoic and Cambrian bioevents. *Revista Española de Paleontología, numero extr. Homenaje al Prof. Gonzalo Vidal*, 11–16.
- VIDAL, G., PALACIOS, T., DIEZ BALDA, M. A., GÁMEZ VINTANED, J. A. & GRANT, S. W. F. 1994a. Neoproterozoic–early Cambrian geology and palaeontology of Iberia. *Geological Magazine*, **131**, 729–765.
- VIDAL, G., JENSEN, S. & PALACIOS, T. 1994b. Neoproterozoic (Vendian) ichnofossils from the Lower Alcuadian strata in central Spain. *Geological Magazine*, **131**, 169–179.
- VIDAL, G., PALACIOS, T., MOCZYDŁOWSKA, M. & GUBANOV, A. P. 1999. Age constraint from small shelly fossils on the early Cambrian terminal Cadomian Phase in Iberia. *GFF*, **121**, 137–143.
- WAGGONER, B. 1999. Biogeographic analyses of the Ediacara biota: a conflict with paleotectonic reconstructions. *Paleobiology*, **25**, 440–458.
- WAGGONER, B. 2003. The Ediacaran biota in space and time. *Integrative and Comparative Biology*, **32**, 104–113.
- XIAO, S., YUAN, X., STEINER, M. & KNOLL, A. H. 2002. Macroscopic carbonaceous compressions in a terminal Proterozoic shale: a systematic reassessment of the Miaohu biota, south China. *Journal of Paleontology*, **76**, 347–376.

Morphology and taphonomy of an Ediacaran frond: *Charnia* from the Avalon Peninsula of Newfoundland

M. LAFLAMME¹, G. M. NARBONNE¹, C. GREENTREE² & M. M. ANDERSON³

¹*Department of Geological Sciences and Geological Engineering, Queen's University, Kingston, Ontario, Canada K7L 3N6 (e-mail: laflamme@geoladm.geol.queensu.ca)*

²*1-249 Macdonnell Street, Kingston, Ontario K7L 4C4*

³*53 Sterling Crescent, St. John's Newfoundland A1A 4J9*

Abstract: The Ediacaran frond *Charnia*, known mainly from fragmentary leaf-like fronds from around the world, is represented by completely preserved specimens with holdfasts in the Mistaken Point biota of Newfoundland. Previous reconstructions of *Charnia* from two-dimensional impressions were significantly oversimplified, resulting in three-dimensional reconstructions which highlighted a sheet-like morphology. Overlapping relationships and internal structures are rarely (if ever) preserved, and only through detailed photography together with both landmark and traditional morphometric analyses of numerous complete *Charnia* specimens can the preservational biases be removed. *Charnia* is reinterpreted here as having a series of individual overlapping primary branches attached to an internal central stalk, and with individual branches constrained by an internal, organic skeleton and/or attachments between adjacent branches. Three species, *C. masoni* Ford 1958, *C. wardi* Narbonne & Gehling 2003, and *C. antecedens* sp. nov. can be distinguished on the basis of length/width ratios and the degree of attachment of adjacent branches. Morphological, taphonomical, and ecological studies at Mistaken Point imply that *Charnia* was a sessile, epibenthic frond that fed from suspension in this deep-water volcanoclastic setting. Evolution of more rigorous connections between the primary branches allowed *Charnia* to migrate into more turbulent, shallower-water habitats by the late Ediacaran.

Charnia Ford, 1958 is a cosmopolitan Ediacaran frond first described from Charnwood Forest, England (Ford 1958, 1962, 1963, 1999; Boynton & Ford 1995), and subsequently was documented from the White Sea of Russia (Fedonkin 1985, 1992; Grazhdankin 2004), north-eastern Siberia (Fedonkin 1985), Ediacara in South Australia (Nedin & Jenkins 1998), and from the Mistaken Point Formation in Newfoundland (Fig. 1; Anderson 1978; Conway Morris 1989; Jenkins 1992; Narbonne *et al.* 2001; Clapham & Narbonne 2002; Narbonne & Gehling 2003; Clapham *et al.* 2003; Narbonne *et al.* 2005). Original descriptions of *Charnia*, interpreted from the well-preserved type specimen from Charnwood Forest, England (fig. 2; Ford 1958), highlight the relatively simple repeating pattern of both the primary branches and secondary modular elements, in addition to the overall sheet-like morphology. Ford (1958) also erected the taxon *Charniodiscus* Ford, 1958, which consisted of a disc-like organism with a rough-surfaced central boss surrounded by multiple concentric rings, and in some earlier figures showed the *Charnia* frond and the *Charniodiscus* anchoring disc as elements of the same organism or colony (Ford 1958, 1962). Later work (Ford 1963) revealed that the holotype of *Charniodiscus* was attached to a

foliate structure with fine detail that differed significantly from the holotype of *Charnia*. Jenkins & Gehling (1978) distinguished *Charnia* and *Charniodiscus* on the basis of the small-scale branching pattern in their respective fronds, a view that has been supported by virtually all subsequent workers (see review in Laflamme *et al.* 2004). In the Treatise, Glaessner (1979) defined *Charnia* as having 'Narrow petaloids with sinuous median line and sharply defined primary grooves forming acute angles with corresponding secondary grooves and branches; these are therefore in almost transverse position on the petaloids'.

Complete specimens of *Charnia* with its basal attachment bulb also preserved are exceedingly rare, with mostly fragmentary specimens described from outside Newfoundland, hindering attempts to deduce the taxonomy and biology of *Charnia*. Eastern Newfoundland is unique in producing thousands of complete fronds, including hundreds of *Charnia* specimens (Narbonne *et al.* 2001; Clapham *et al.* 2003). This paper utilizes the large number of complete specimens of *Charnia* available in the Avalon Peninsula of Newfoundland (Fig. 1) to determine the growth patterns, inter- and intraspecific variability, and evolutionary patterns of *Charnia*.

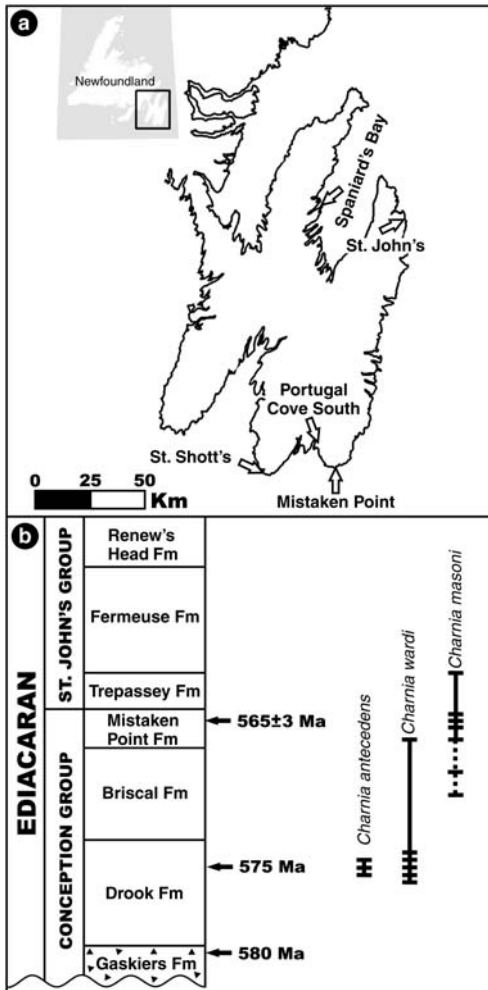


Fig. 1. Geographic and stratigraphic distribution of *Charnia* Ford, 1958. (a) Location map of Avalon Peninsula of Newfoundland Canada. (b) Composite stratigraphic section, indicating stratigraphic ranges of *C. masoni*, *C. wardi*, and *C. antecessens*. U–Pb dates from Dunning *in* Benus (1988) and Bowring *et al.* (2003).

Geographic and stratigraphic setting

The fossiliferous strata from the Avalon Zone of Newfoundland, Canada (Fig. 1a) occur in the western part of Avalonia, representing a string of microcontinental volcanic arcs that originally emplaced off the northwestern coast of Amazonia during the terminal Proterozoic (Murphy *et al.* 2002). The close proximity of the Mistaken Point assemblage to the eastern Avalonia Ediacara Biota of Charmwood Forest, England, is

supported by both biogeographic analyses and tectonic reconstructions (Waggoner 1999; Murphy *et al.* 2002). The Ediacara Biota at Mistaken Point was first reported by Anderson and Misra (1968) and Misra (1969) and subsequently documented by numerous authors. Available U–Pb dates on volcanics associated with the Mistaken Point fossil assemblage range between 575 and 565 Ma (Dunning *in* Benus 1988; Bowring *et al.* 2003), thus predating most other known Ediacara assemblages (Martin *et al.* 2000; Condon *et al.* 2005; Narbonne 2005).

Charnia ranges through much of the stratigraphic succession hosting the Avalonian assemblage, with specimens from the Drook, Briscal, Mistaken Point, and Trepassey formations, spanning upwards of 2.5 km of section of the Conception and St John's Groups and representing more than 10 million years (Fig. 1b). Sedimentological studies of the area imply that the fossil localities represent deposits in deep water axial and slope environments, well below storm wave-base (Misra 1971, 1981; Benus 1988; Narbonne *et al.* 2001; Wood *et al.* 2003; Narbonne *et al.* 2005). The Conception Group is dominated by fine- to medium-grained turbidites interspersed with thin interturbidite siltstone beds which contain the fossil horizons (Wood *et al.* 2003). Interturbidite fossil beds are numerous throughout the Avalonian strata, and are commonly blanketed by a veneer of volcanic ash, which accelerated lithification and preserved the fossil fronds in positive epirelief on the upper surfaces of fine-grained siltstone bedding planes (Narbonne 2005). The volcanic ash restricts preservation of features to those present on the upper surface of the organism, while the thickness and coarseness of the fallout ash is responsible for the varying quality and amount of epirelief of each individual specimen (Narbonne 2005). Microbial mats preserved as 'old elephant skin' wrinkles on the fossil-bearing surfaces initiated mineral encrustation of the organic material and cemented the surrounding sediment resulting in preservational 'death masks' (cf. Gehling 1999). Strata throughout the Avalon Peninsula have been subject to tectonic deformation, resulting in a significant (<40%) shortening, perpendicular to cleavage, of all fossil specimens, thus altering the shape and orientation of all structures measured from the surfaces (Seilacher 1999; Wood *et al.* 2003; Laflamme *et al.* 2004). This deformation can be corrected by applying photographic or mathematical corrections termed 'retrodeformation' (see Wood *et al.* 2003 for rationale and the formulas used in the morphological correction). All measurements presented in this paper have been retrodeformed.

Traditional interpretations of the morphology of *Charnia*

Original descriptions of *Charnia* are based on the exquisitely-preserved holotype of *C. masoni* from Charnwood Forest, England (Ford 1958). This specimen is characterized by an ovate (or lance-shaped) to strongly parallel frond which tapers abruptly at the distal tip and is composed of a series of sigmoidal to rectangular primary branches (Fig. 2). The central axis of the frond consists of a zigzag central midline resulting from the alternation of the primary branches on either side of the central axis. Branch width and length tend to increase proximally, with the smallest (and assumed youngest) branches located at the distal tip. Each primary branch is composed of several

secondary modular elements (Fig. 2), which vary in size and shape along the length of each branch. Well-preserved specimens of *Charnia* exhibit curved tertiary divisions within the secondary modular elements (Fig. 2). In *C. wardi*, these third-order divisions can be shown to represent the edges of rangeomorph elements similar to those illustrated by Narbonne (2004). Narbonne (2004, 2005) and Brasier and Antcliffe (2004) followed Jenkins (1985) in regarding *Charnia masoni* as a rangeomorph, but further study of exceptionally-preserved specimens from Charnwood Forest (Brasier & Antcliffe 2004; Brasier *et al.* 2005) and northern Russia (Grazhdankin 2004) is necessary to confirm or refute this hypothesis. The holotype slab from Charnwood Forest is broken just above the base of the frond.

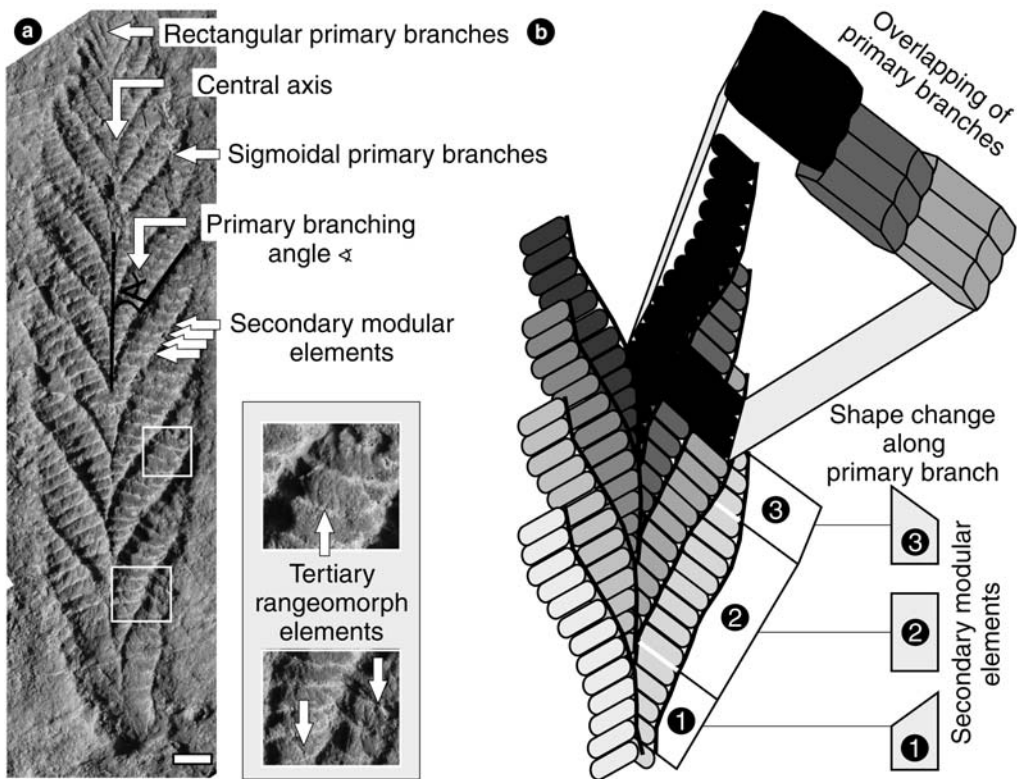


Fig. 2. *Charnia masoni*. (a) Labeled type specimen of *C. masoni* from Charnwood Forest, England, displaying the fractal, third-order microstructure present in each secondary modular element. Multiple tertiary rangeomorph elements are present within each secondary modular element. (b) Hypothetical reconstruction of *C. masoni* demonstrating the overlying relationships between adjacent primary branches. The corresponding shape of each secondary modular element is delineated by the proximity and amount of overlapping contributed by surrounding modular elements. Labels (1, 2 and 3) represent proximal, central, and distal regions of the primary branches respectively. Specimen A whitened with ammonium chloride. Scale bar 1 cm.

Landmark morphometric analysis

Previous attempts to couple traditional taxonomic work with mathematical (morphometric) descriptions were effective at Mistaken Point, and readily allowed for the segregation of characters which varied with growth versus those which represented true taxonomic differences between two morphologically similar species of *Charniodiscus* (Laflamme *et al.* 2004). However, since much of the species variation in *Charnia* is restricted to microstructural details, poorly described by distance measurements (Fig. 2), and since taphonomic characters of the volcanic ash limit the preservation of the most distal branches and secondary modular elements, the overall morphology of *Charnia* from the Avalon is difficult to investigate using traditional morphometric techniques. Recent advances in the field of landmark morphometrics has resulted in robust quantitative means of describing shapes independent of size, translation, rotation or scaling (Bookstein 1991), and may be used to quantify morphological changes in shapes. Although traditional and landmark morphometrics may not be applicable for defining the overall morphology of *Charnia*, these mathematical techniques can be applied to define the shape changes between the secondary modular elements, and possibly elucidate the origin of these shape changes.

By selecting points in two or three dimensional space that correspond to the position of a particular character on an object of interest (Lele & Richtsmeier 2001), landmarks outline or define the form in question and allow for comparisons of shape between different samples. The covariance between landmark sets can be identified and highlighted through various multivariate statistical analyses, such as principal components analysis (PCA). The goal is to isolate purely shape-driven changes between similar forms.

Morphological relationships between various components of the *Charnia* morphotype suggest a more complex external form than has been previously diagnosed for this genus. The morphological variation in the shape of the secondary modular elements, in addition to the appearance of an overlying relationship between adjacent primary branches, is ideally suited for a landmark morphometric analysis. By removing the influence of growth and size of the shape component, it is possible to compare how each secondary modular element is influenced by its neighbouring elements.

The relatively simple shape of the secondary modular elements in *Charnia masoni* can easily be defined by four unique landmarks, which provide an adequate representation of the entire secondary modular element (Fig. 3a). The restriction to traditional (Lele & Richtsmeier 2001) or Type 1

(Bookstein 1991) landmarks corresponding to biologically significant structures that represent a point in space at which three structures meet (Bookstein 1991; Lele & Richtsmeier 2001) reduce the amount of subjectivity introduced into the analysis. The chosen landmarks are structurally homologous and represent structurally similar features present on all branches analysed.

Four landmarks were placed on every complete secondary modular element from the second to the sixth primary branch of the right side of the holotype of *Charnia masoni* from Charnwood Forest. The incomplete preservation of the secondary elements on the left side of the holotype, in addition to the poor preservation of the distal branches above the sixth primary branch, restricted the analysis to the selected branches. Distal secondary modular elements (the last few secondary modular elements from region 3 in Fig. 2b) along the chosen primary branches were also excluded due to incomplete preservation. Landmarks were collected from high quality digital photographs and digitised using TPSDIGW32.EXE (by F. James Rohlf. Version 1.40; <http://life.bio.sunysb.edu/morph/>). In order to reduce human error, all landmarks were chosen and digitized by ML. Digitized landmarks were collected in a landmark coordinate matrix and converted into corresponding vectors of all possible pair-wise distances therefore restricting information to shape coordinates. Shape coordinates were transformed into Procrustes coordinates by setting the centroid location (average location of all landmarks) of each sample to the centre of a Cartesian graph (0,0), therefore removing the influence of translation on the data. Size or scale was removed by calculating the centroid size, which corresponds to the square root of the summed squared distances of each landmark from the centroid, and by rescaling the centroid size to 1.0 by dividing all landmark location by the original centroid size. Finally, rotating the rescaled forms to an optimal overlap of all landmarks by minimizing the summed squared distances between each corresponding landmark and the reference form, which is an average of all specimens, removed the influence of rotation on the data. This final step resulted in a Procrustes alignment and was performed with the 'CoorDGen6' program designed by David S. Sheets (<http://www2.canisius.edu/~sheets/morphsoft.html>).

Once the coordinate matrix has been converted into a Procrustes coordinates matrix, it is possible to analyse the relationship between landmarks and samples through standard multivariate statistics such as principal components analysis, which allows for multiple landmark configurations to be compared between multiple samples. PCA is a statistical means of comparing multivariate data by constructing principal components (or eigenvectors),

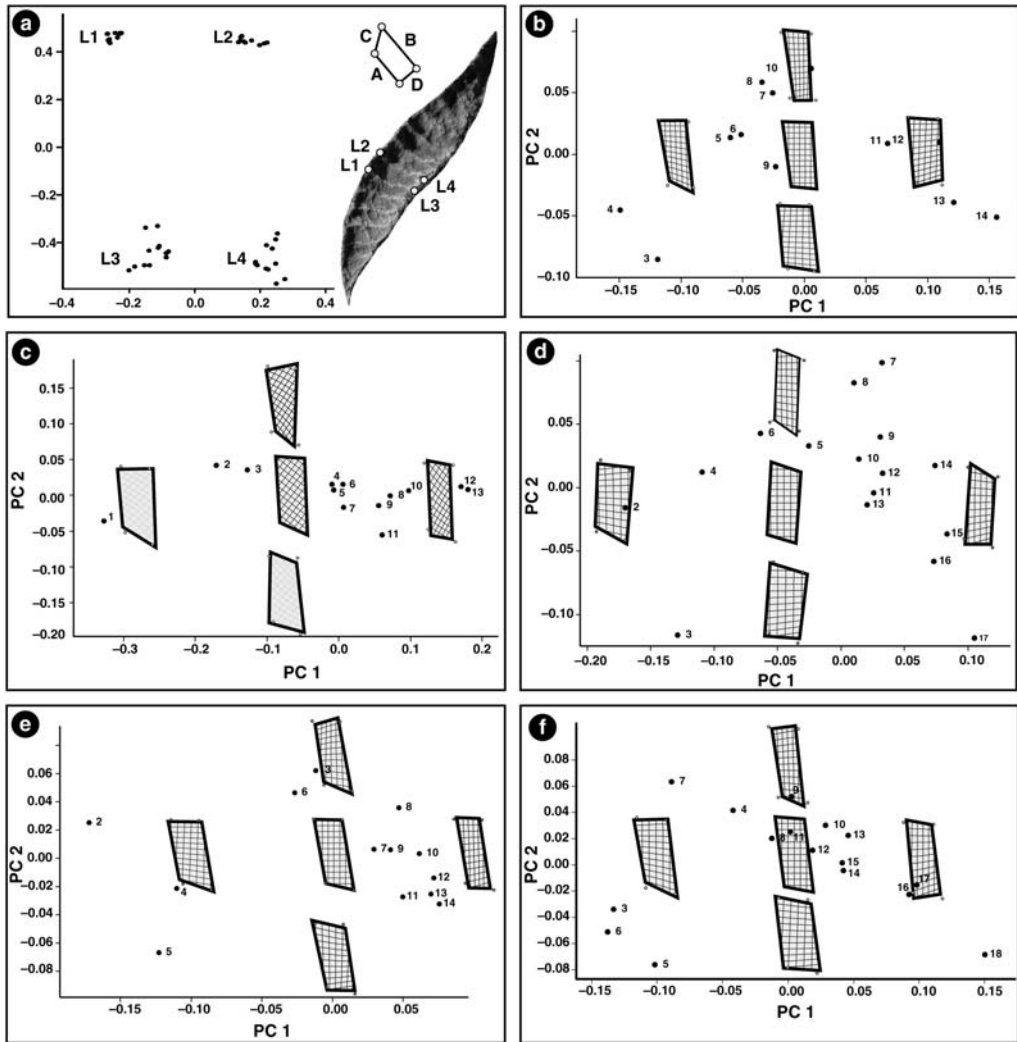


Fig. 3. Landmark morphometric analysis of the holotype of *Charnia masoni*. (a) Distribution of all four landmarks of each well-preserved secondary modular element from the second primary branch. Notice the high degree of precision surrounding landmarks 1 and 2. (b–f) Principal components analysis of the landmark analysis of the second to sixth primary branches of the holotype of *C. masoni*. Sub-rectangular to trapezoidal forms within the graphs represent the shape of the secondary modular elements without the influence of size, rotation, or translation. Notice the trend of shorter L1–L3 (a) distances in the proximal secondary elements followed by a more equidistant L1–L3 v. L2–L4 (a v. b) distances in the more central secondary modular elements, and finishing with a shorter L2–L4 (b) distance in the distal secondary modular elements. This trend continues until the secondary modular element is completely covered by an adjacent primary branch. Numbered data points from 1 (proximal to the stalk) up to 18 (distal).

which are mutually orthogonal vectors that explain the greatest amount of variance found within the data. PCA groups similar landmark arrangements (shapes) together while distancing different shape configurations from each other. Traditionally, landmark morphometrics is used to distinguish shape differences between species, but this analysis applied landmark morphometrics to shape changes

within a seemingly repeatable set of landmarks in order to distinguish shape changes within sections of a single specimen. PCA allows for the partitioning of morphological variation into components that independently describe shape variation (Strauss & Bookstein 1982; Somers 1986; James & McCulloch 1990; Cadima & Jolliffe 1996). The data reconfigured into partial Procrustes was

analysed with PCAGen6 N (<http://www2.canisius.edu/~sheets/morphsoft.html>), which performed a PCA analysis on each branch independently in order to demonstrate the variation in form of the secondary modular elements along the primary branches of *C. masoni*.

The first set of interpretations drawn from the landmark analysis is the degree of variance within each individual landmark. As seen in Figure 3a, the spread of landmarks 3 and 4 is much greater than the spread surrounding landmarks 1 and 2. Since landmark identification of these points is similar, this variation implies deformation of the terminations of the secondary lobes and, therefore, a translation of the landmarks out of their 'normal' positions. If this hypothesis is correct, the relatively tight landmark arrangement for landmarks 1 and 2 may suggest that the only true shape variation of the secondary modular elements can be explained with a translation of only two landmarks, and with most of the translation restricted to the 'Y' axis (Fig. 3a). This hypothesis is further substantiated by the repeatable and predictable shape changes of the secondary lobes along the primary branches. As demonstrated in Figures 3b–f, the proximal modular elements (region 1 in Fig. 2b) along all five primary branches are characterized by smaller L1–L3 landmark distances (distance A in Fig. 3a), while the central secondary lobes (region 2 in Fig. 2b) are more uniform in L1–L3 v. L2–L4 distances (distances A and B in 3a), whereas the terminal secondary lobes (region 3 in Fig. 2b) have a distinctively smaller L2–L4 landmark distance (distance B in 3a). This is in stark contrast to the L1–L2 (distance C in 3a) or L3–L4 (distance D in 3a) distances, which are uniform in shape distances throughout the entire length of the primary branches. This suggests that there is a semi-rectangular shape for each secondary lobe, and that the trapezoidal or rhombic shape classically associated with the secondary lobes of *Charnia* is a taphonomic response to overlying from adjacent primary branches. The translation and predictability of the landmarks represent an artificial termination of the secondary lobes due to imbrication or overlapping from adjacent primary branches. This hypothesis suggests that the true termination of the secondary lobe is located beneath the overlying adjacent primary branch, and that this overlapping relationship accounts for the shape of the secondary lobes in *Charnia*.

Taphonomy of Newfoundland *Charnia*

The *Charnia* forms from Mistaken Point and the surrounding Avalonian localities are morphologically diverse, but as most specimens are

taphomorphs of the well-known species of *Charnia masoni* (Fig. 4) or *Charnia wardi* (Fig. 5), the true taxonomic diversity is likely quite limited. The shapes of the specimens vary greatly as an expression of taphonomy on the classical *C. masoni* morphoshape. Due to local differences in ash thickness and tectonic deformation of the beds containing the fossils, the morphological expression of the classical *C. masoni* morphoshape greatly varies between localities. The soft-bodied nature of *Charnia* and the apparent flexibility of the primary and secondary branches contributed to the morphological disparity between specimens.

The selective nature of the preserving ash restricts preservation of features present on the upper surface of the organism at the interface between the underlying sediment and the overlying fallout ash (Narbonne 2005). Even small amounts of ash that reached the substrate prior to felling of the organism resulted in poor preservation of morphological traits, a process that was largely responsible for the decrease in resolution distally from the holdfast to the tip of the frond (Seilacher 1992; Wood *et al.* 2003; Laflamme *et al.* 2004). The thickness and coarseness of the fallout ash responsible for the preservation of all Ediacaran fossils at Mistaken Point also dictates the overall external morphology and epirelief of each individual specimen (Narbonne *et al.* 2001). Stalks and finer microstructural details that are well preserved in specimens of *C. wardi* are invariably associated with a thin, fine fallout ash (Fig. 5a–f), and are typically absent or difficult to see in specimens preserved beneath thicker, medium- to coarse-grained volcanic tuffs (Fig. 5g–h). However, the cylindrical, three-dimensional morphology of *C. wardi* is best seen in thick coarse ash (Fig. 5g–h) since thinner, finer fallout ash was more prone to compaction than the coarser-grained tuffs (Narbonne & Gehling 2003).

It is evident that taphonomy played a major role in controlling the preservational form of *Charnia* specimens from Newfoundland and presumably elsewhere. Three distinct morphological forms are readily recognized even when taphonomic variation is taken into account. The nature of these species, one of which is new, and their relationships to previously described taxa are discussed at the end of this paper (see Systematic palaeontology).

Taphomorphology of *Charnia*

Taphonomic processes responsible for the preservation of soft-bodied Ediacara Biota govern the final morphology of the fossils found (Jenkins 1985; Gehling 1991; Narbonne *et al.* 1997; Narbonne 2005; Grazhdankin & Seilacher 2005).

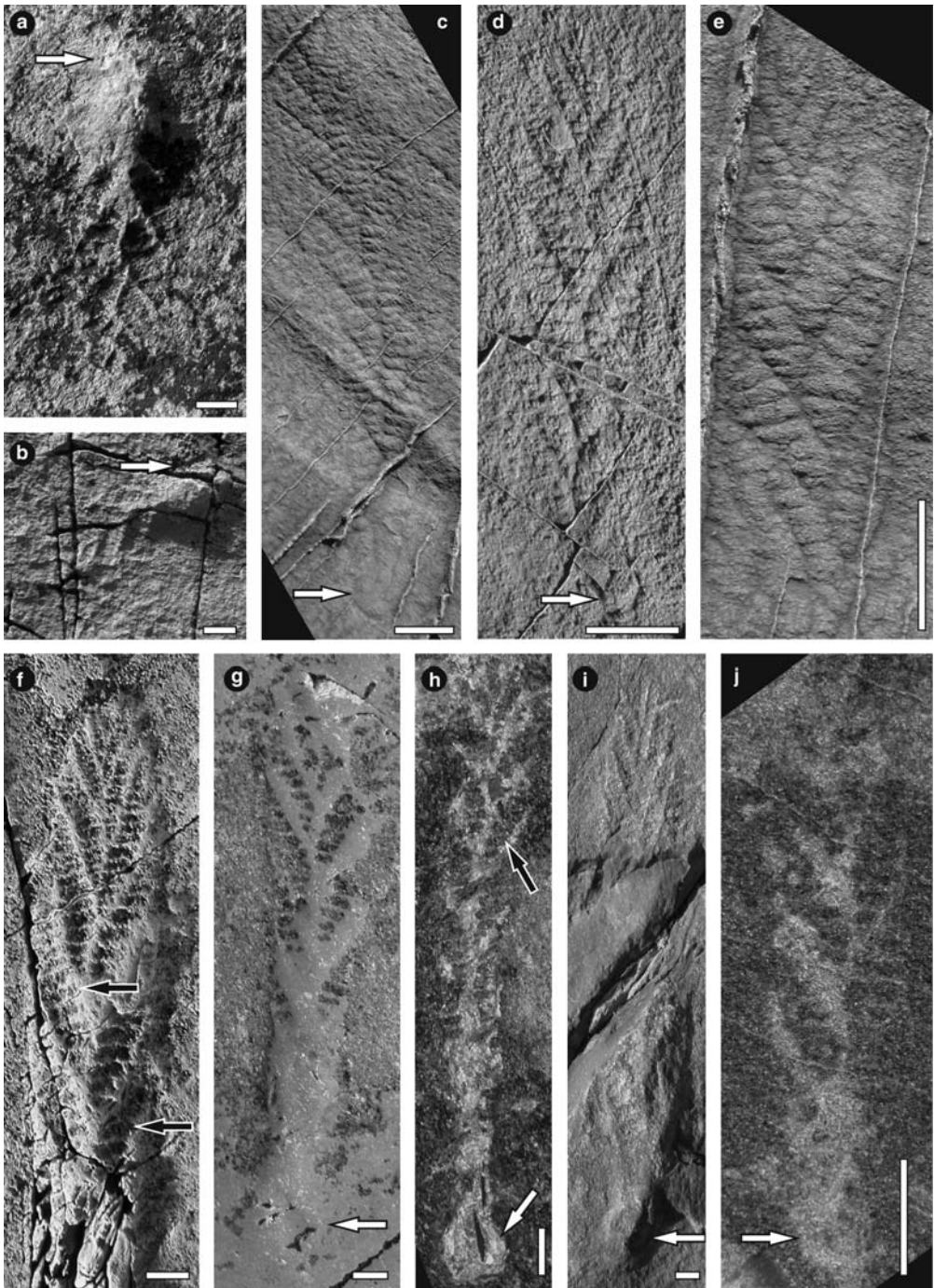


Fig. 4. *Charnia masoni* preserved in positive epirelief on the upper bedding plane surfaces. (a–b) Juvenile specimens of *C. masoni* displaying basal attachment disc from the ‘E’ surface of the Mistaken Point Formation (Landing *et al.* 1988). (c–e) Latex moulds whitened with ammonium chloride of *C. masoni* from Sword Point of the Mistaken Point Formation. (c) and (d) displaying basal attachment disc. (f) *C. masoni* from a loose block believed to be from Long Beach of the Mistaken Point Formation. Specimen whitened with ammonium chloride. (g–i) *C. masoni* from Long Beach of the Mistaken Point Formation, displaying basal attachment discs. (j) *C. masoni* from Lower Mistaken Point from the Mistaken Point Formation. White arrows indicating basal anchoring discs, black arrows indicating possible tertiary divisions. All scale bars 1 cm.

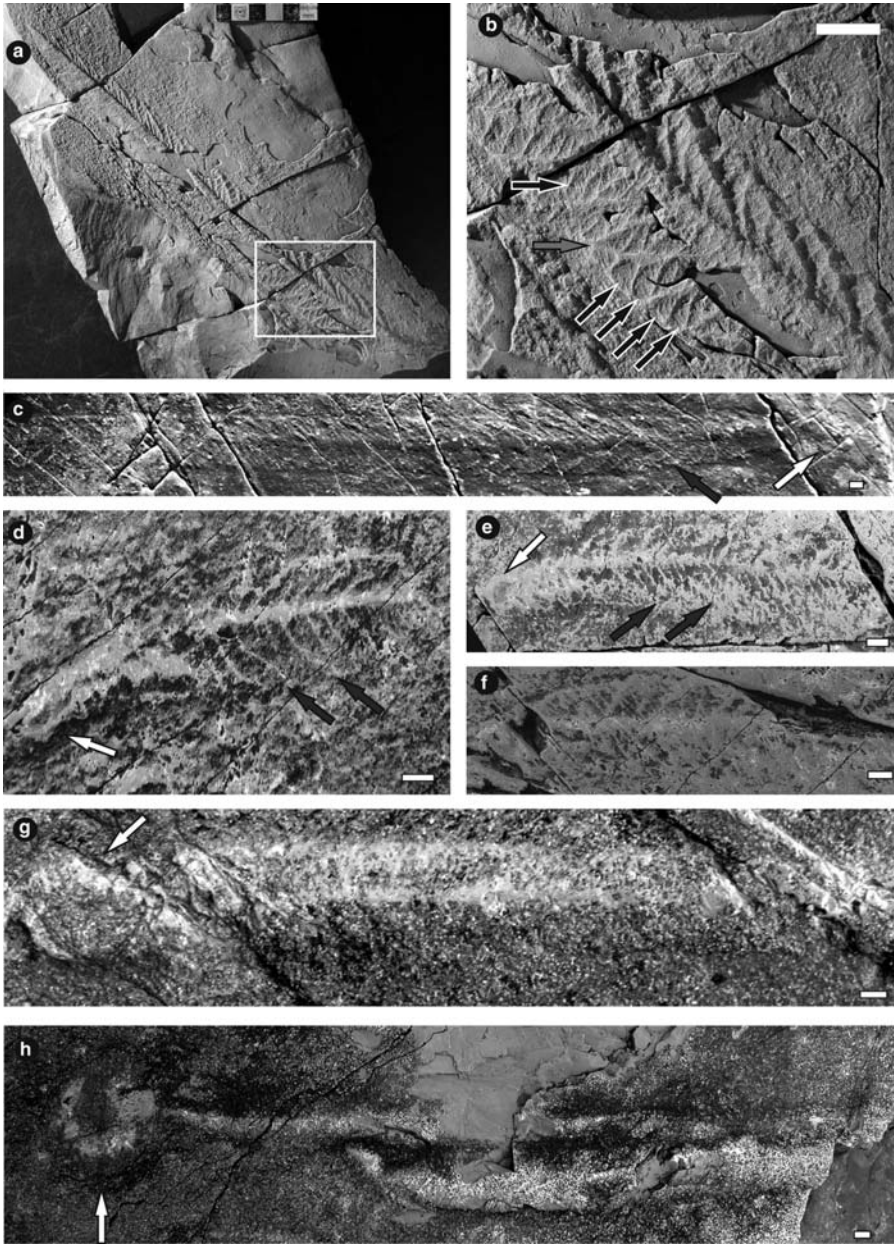


Fig. 5. *Charnia wardi* preserved in positive epirelief on the upper bedding plane surfaces. (a) Type specimen of *C. wardi* from the Drook Formation displaying the prominent central ridge and repeatable *Charnia* branching pattern. (b) enlarged view of the area indicated in A displaying the rangeomorph elements (grey arrows) restricted to one per secondary modular element and also demonstrating the rare longer and acutely angled primary branches (termed bundles; white arrows). (c) *C. wardi* from the Drook Formation. (d–f) *C. wardi* from the Mistaken Point Formation. Specimens at this horizon are significantly smaller than those from older formations. d–e displaying basal anchoring disc (white arrows). (g–h) Poorly preserved specimens of *C. wardi* from the Drook Formation, preserved under thick, coarser grained volcanic tuffs and with large basal anchoring disc (white arrow, only visible in upper frond). (h) Two specimens of *C. wardi* in close proximity to one another. White arrows indicate basal anchoring discs, black arrows indicate tertiary divisions, and grey arrows indicate branch bundling. All scale bars 1 cm.

Understanding the effects of these processes allows more accurate interpretation of the original morphology of the fossil. As the Ediacara Biota was smothered beneath volcanic ash (Conception-style preservation of Narbonne 2005) or cast beneath beds of sandstone with the chemical assistance of microbial mats (Flinders- or Fermeuse-style preservation of Narbonne 2005), the overall morphology of the preserved organisms has been restricted to near two dimensional impressions that remained after fossilization. Morphological reconstruction of three-dimensional forms from impressions has always been difficult when interpreting Ediacaran fossils (Narbonne *et al.* 1997; Gehling *et al.* 2000; Grazhdankin & Seilacher 2002; Dzik 2002), and has commonly resulted in oversimplification of the real external morphology. Overlapping relationships and internal structures are rarely preserved, resulting in three-dimensional reconstructions highlighting sheet-like morphologies. Internal features, such as strengthening structures (non-mineralized organic skeletons), may be difficult to interpret from well-preserved specimens displaying only the external form (Narbonne 2004). This seems particularly true of *Charnia*, which originally may have been nearly cylindrical and in which all the elements have been superimposed onto a two dimensional sheet. The following section will explore the 'taphomorphology', or the altered morphology remaining after preservation, of *Charnia* in order to reconstruct the original three-dimensional configuration.

Several specimens of *Charnia* from Mistaken Point and Spaniard's Bay display significant variation in the angle of primary branching (Table 1), a predictable shape-change of the secondary modular elements within each primary branch (Fig. 3), and a variable central zigzagging midline (compare specimens from Figs 4–6). These traits suggest that *Charnia* represents a series of independent, overlapping, primary branches, which result in the taphonomic expression of a complete, unsegregated sheet.

Each individual primary branch is overlapped by a second branch located on the opposite side of the midline, resulting in the covering of proximal secondary modular elements (region 1 in Fig. 2b) and therefore smaller L1–L3 landmark distances (distance A in Fig. 3a) for these secondary lobes. As each primary branch alternates and overlaps along the midline, the taphonomic response is a zigzagging central furrow. Furthermore, each primary branch is also overlapped by an adjacent primary branch as the distal tip is tucked in underneath the overlying branch (region 3 in Fig. 2b), resulting in smaller L2–L4 landmark distances (distance B in Fig. 3a) for these secondary modular elements. This hypothesis suggests that the outer rim/margin present in *Charnia* most

likely represents the natural termination of the distal tip of a branch, as it is tucked in underneath the overlying branch (region 3 in Fig. 2b), and does not represent a true distal boundary. In contrast, the secondary modular elements located along the middle of each primary branch (region 2 in Fig. 2b) are characterized by a more rectangular shape, which consists of somewhat equidistant L1–L3/ L2–L4 landmark distances, resulting from the limited amount of overlapping from adjacent primary branches. The secondary modular elements in region 2 (of Fig. 2b) may best represent the true shape of each individual secondary modular element due to the limited amount of overlap from adjacent primary branches. The distal primary branches located near the tip of the frond (rectangular primary branches, Fig. 2a) are significantly more rectangular in shape and lack the characteristic sigmoidal shape (sigmoidal primary branches, Fig. 2a), resulting from the limited amount of overlap with adjoining primary branches.

The overall alternating branching pattern, which has come to represent *Charnia*, varies little, despite the numerous specimens present at Mistaken Point (Fig. 4). In *C. masoni*, the proximal secondary lobes (region 1 in Fig. 2b) are acutely angled as a direct response to the acute angle of the primary branches. After the initial acute branching, the primary branches continue to curve until a maximal branching angle is reached (between 19°–37°, Table 1). At this point the secondary modular elements are located at right angles to the base of the primary branches (region 2 in Fig. 2b). At the distal tip of each primary branch, the secondary modular element branching angle becomes acute as the primary branch dips underneath the distal tips of the overriding branch (region 3 in Fig. 2b). In *C. masoni*, these branches are strictly parallel and errors in overlapping are virtually non-existent, requiring that each primary branch be attached to an internal central stalk at the proximal branching site and also anchored at the distal tip by an internal outer margin (Narbonne 2004, Fig. 3d) or that each primary branch was joined to adjoining primary branches by flexible soft tissue.

The secondary modular elements vary between a pill-shaped to a more rectangular- or straight-sided shaped secondary modular element. This variation in the shape of the secondary modular elements is directly linked to the soft-bodied nature of *Charnia*. If secondary elements were compressed laterally either during death or preservation, the original box-shaped secondary elements could have been modified into a pill-shaped element. This variation in shape cannot represent a taxonomic variation because both types of modular elements are preserved on the same specimen, and commonly on the same primary branch.

Table 1. Distance measurements, number of primary and secondary branches, and the primary branching angle of *Charnia* from Mistaken Point Newfoundland. All measurements have been retrodeformed to adjust for tectonic shortening

Specimen	Morphotype	# Primary	# Secondary	Length (cm)	Width (cm)	L/W ratio	Angle range	Mean
<i>Charnia masoni</i>								
Sword Point 1	Ovate	11	14	13.1	4.0	3.2	20–32	26
Sword Point 2	Ovate	9	13	15.1	5.8	2.6	25–40	29
Sword Point 3	Ovate	9	11	10.6	4.2	2.5	27–35	30
Sword Point 4	Ovate	13	13	23.9	6.6	3.6	17–29	21
Sword Point 5	Ovate	13	14	25.7	5.2	4.9	18–32	24
Sword Point 6	Ovate	11	12	11.9	3.3	3.6	26–42	31
Sword Point 7	Ovate	11	13	18.9	3.9	4.9	17–42	30
Sword Point 8	Ovate	11	13	14.4	3.0	4.8	22–43	31
Sword Point 9	Ovate	9	11	7.3	2.5	2.9	26–40	30
Sword Point 10	Ovate	11	14	21.1	4.6	4.6	20–33	26
	Average	11	13	16.2	4.3	3.8	22–37	28
Lower Mistaken Point 1	Parallel	8	8	6.0	1.2	5.2	23–29	25
Long Beach 1	Parallel	7	11	14.6	3.5	4.2	23–33	27
Long Beach 2	Parallel	8	9	13.0	2.3	5.6	16–35	26
Long Beach 3	Parallel	11	10	16.9	3.8	4.4	13–29	24
	Average	9	10	12.6	2.7	4.8	19–31	26
<i>Charnia wardi</i>								
Lower Mistaken Point 2	Short	28	10	23.9 +	4.6	N/A*	Reg/Bdl 42–64/26–36	Reg/Bdl 53/29
Lower Mistaken Point 3	Short	23	8	11.0 +	2.8	N/A*	49–86/22–37	65/31
Lower Mistaken Point 4	Short	28	11	20.9 +	5.3	N/A*	43–74/21–35	58/26
Lower Mistaken Point 5	Short	19	9	17.3 +	5.7	N/A*	45–88/29–39	62/33
Lower Mistaken Point 6	Short	28	12	12.9 +	3.4	N/A*	42–58/23–30	48/27
	Average	25	10	N/A*	4.3	N/A*	44–74/24–35	57/29
ROM 54349	long	>60	12	61.6 +	4.4	N/A*	39–64/21–31	49/26
ROM 38628	long	>30	12?	30.2 +	3.0	N/A*	35–63/16–32	46/24
Drook 1	long	N/A*	N/A*	49.7	2.7	18.4	N/A*	N/A*
Drook 2	long	N/A*	N/A*	36.6	2.3	15.9	N/A*	N/A*
Drook 3	long	N/A*	N/A*	48.3	3.8	12.7	N/A*	N/A*
Drook 4	long	N/A*	N/A*	42.2	3.2	13.2	N/A*	N/A*
Drook 5	long	N/A*	N/A*	37.9	3.9	9.7	N/A*	N/A*
Drook 6	long	N/A*	N/A*	45.2	2.8	16.1	N/A*	N/A*
Drook 7	long	N/A*	N/A*	77.9	2.8	27.8	N/A*	N/A*
Drook 8	long	N/A*	N/A*	77.4	2.9	26.7	N/A*	N/A*
Drook 9	long	N/A*	N/A*	65.7	5.2	12.6	N/A*	N/A*
	Average	N/A*	N/A*	53.4	3.4	17.0	N/A*	N/A*
<i>Charnia antecedens</i>								
ROM 54348		8	N/A*	19.6	4.1	4.8	13–36	19
Drook 10		9	10	25.5	5.1	5.0	15–31	23
	Average	8.5	10	22.5	4.6	4.9	13–33	21

N/A*, elements of the frond that were poorly-preserved and could not be counted/measured.
 Reg/Bdl, the differences in branching angles between regular and bundled branches.
 +, minimal distance measurements from incomplete specimens.

The width of the frond and the number of secondary modular elements in *Charnia masoni* from Mistaken Point varies considerably between specimens, resulting in specimens that vary from the traditional ovate shape (Fig. 4a–e, i–j) to those that appear more parallel-sided (Fig. 4f–h). Specimens with a more parallel-sided appearance typically exhibit a larger frond length v. width ratio (Fig. 4f–h; Table 1) and fewer secondary modular elements per primary branch when compared with the ovate form (Table 1). Furthermore, the parallel-sided morphs of *C. masoni* do not exhibit the underlying of the distal tip of the primary branch typically visible in the ovate forms of *C. masoni* and the average angle at which the primary branches diverge from the central stalk is more acute (Table 1). A final character of interest is the apparent sharp edge, almost resembling an outer rim, which constrains the distal tips of the primary branches in the parallel-sided form, but which is absent from the well-preserved ovate form.

Taphonomy is most likely responsible for the parallel-sided and ovate morphs, although the morphological shape variation between the two morphotypes is possibly ontogenetic or based on branching angles (Fig. 7b–c). The sharp termination of the distal region of each primary branch in the parallel-sided morph of *C. masoni*, in addition to the absence of the overlapping of the distal secondary modular elements (region 3 in Fig. 2b) and the apparent shape and size variation of these same distal elements is suggestive that the distal secondary lobes were not preserved (Fig. 7c). For proper preservation of Ediacara Biota at Mistaken Point, the organism must have been trapped between the muddy substrate and the overlying veneer of volcanic ash. It is probable that, as *Charnia* was felled and then covered by fallout ash, the distal tips of the primary branches were curved upwards and therefore were jutting outside of the veneer of ash required for proper preservation (Fig. 7c). This resulted in a sharp outer margin in the parallel-sided morph of *Charnia*, and may explain both the size and shape variations in the distal modular elements. The taphonomic margin produced by trapping volcanic ash between the distal tips of the primary branches and the underlying muddy substrate distorts the familiar ovate shape of *Charnia*, and should not be used as a taxonomic means of distinguishing between species of *Charnia*. Therefore, it is important to stress that the frond widths presented in this paper represent minimum distances, especially when comparing the parallel-sided taphomorphs to other specimens from around the world.

The type specimen of *C. masoni* from Charnwood Forest is broken just above its base, but several specimens of *Charnia masoni* from Mistaken

Point exhibit holdfast discs (Fig. 4a–d, g–j). The presence of a holdfast disc is consistent with the view that *Charnia* was an erect frond similar in function to other stalked Ediacaran organisms.

As with *C. masoni*, *C. wardi* is composed of several primary branches, which are overlapped by adjacent primary branches at the proximal anchoring site, and are tucked under adjacent branches at the distal tip, resulting in the appearance of a complete, unsegregated sheet. Primary branches are typically rectangular or sigmoidal throughout their length, although certain rare branches are more acutely angled than their surrounding primary branches, producing 'bundling' of the branches (Fig. 5b; Table 1). Branch bundling results in a greater exposure of the secondary modular elements that make up the displaced branch, although it also results in an increased amount of overlap with adjacent branches, therefore reducing the exposure/preservation of the overridden branches. This taphonomic character explains irregularities in the outer margin of the frond, which represent the distal termination of each individual branch, and not a true physical character. Unlike *Charniodiscus*, which has a definitive outer rim or margin of soft tissue, the outer margin of *Charnia* is irregular as the distal tip of each independent branch is tucked under adjacent branches.

The oldest specimens of *C. wardi* from the Drook Formation (Figs 1, 5a–c, g–h) are up to an order of magnitude longer (longest specimens up to 185 cm) than the youngest specimens of the basal Mistaken Point Formation. (between 11 and 23.9 cm, averaging 17.2 cm; Table 1), however none of the specimens from the basal Mistaken Point Formation are complete (Fig. 5d–f). Both the Drook and the Lower Mistaken Point specimens exhibit similar frond widths (averaging 43 mm and 34 mm respectively; Table 1), and share the characteristic branch bundling, central midline, primary branch shape, and secondary modular elements.

C. wardi is thought to be composed of a series of alternating primary branches which cross-over on either side of the central stalk, thus sometimes obscuring the preservation of the stalk. In areas where the preservation of the primary branches crossing over the stalk is best, the branch overlapping results in a zigzagging central midline characteristic of *Charnia*. The most parsimonious explanation for the varying morphology of the central stalk is that the support structure which serves as a basal anchoring site for each primary branch lies internally. In cases where the primary branches are well preserved and cross over the centre of the frond, the midline is obscured or missing, whereas in examples where central midline is well defined, the primary branches are

poorly preserved. It is believed that the presence of a straight, central stalk results from composite moulding of the internal stalk onto the surface expression of the primary branches, and explains how the primary branches cross over the central stalk in some specimens (Narbonne & Gehling 2003).

Due to the coarseness of the volcanic tuff that blanketed specimens from the Drook (Fig. 1), the original 3D morphology was better preserved when compared to the easily compressible, fine-grained volcanic ash which is typical of the remainder of the Mistaken Point assemblage. The high relief (sometimes up to 10 mm) of the specimens from the Drook Formation, suggests that the original 3D morphology of *C. wardi* was more cylindrical than sheet-like in shape.

The type specimen of *Charnia wardi* consists exclusively of the distal tip of the frond, but many other specimens preserve disc-like holdfasts on their proximal end. Although most specimens (e.g. Fig. 5c) preserve basal holdfasts, which appear smaller than would be expected for an Ediacaran frond of this size (Peterson *et al.* 2003), additional specimens of *C. wardi* exhibit larger discs (Fig. 5h–i). It seems likely that the apparent scarcity of holdfast discs and the small size of many of the ones that are preserved reflects the fact that the *Charnia* holdfast was largely buried in the substrate, and would have resulted in the poor expression of the basal anchoring disc (Narbonne & Gehling 2003) whereas the majority of the *Charniodiscus* holdfasts at Mistaken Point rested on the substrate (Seilacher 1992, 1999; Laflamme *et al.* 2004).

Unlike the typical, repeatable branching pattern that typifies *C. masoni* and *C. wardi*, several specimens from the Drook Formation of Mistaken Point (Fig. 6) and the Mistaken Point Formation from the Bonavista Peninsula (O'Brien & King 2004) of Newfoundland, and possibly from the Rawnsley Quartzite, Flinders Ranges, South Australia (Nedin & Jenkins 1998), display a disorganized branching pattern sufficiently distinct from *C. masoni* to warrant the definition of a new species of *Charnia*. *Charnia antecessens* n. sp. is characterized by severe shape variation within the primary branches, interpreted to be a result of disproportioned overlapping from adjacent branches, which had the effect of producing a disorganized rather than the highly repetitive shape that is typical of other *Charnia* species (Fig. 6, see grey arrows). This disproportioned overlapping of the primary branches may have resulted from poor (or nonexistent) anchoring of the distal tips of the primary branches with the internal marginal rim or with the central stalk. The rectangular distal termination of the primary branches (Fig. 6a–c) is a direct and predictable result of the *Charnia* branching pattern

once untucked from the overlying primary branch (region 3 in Fig. 2b). The taphonomic sigmoidal shape of a primary branch of *Charnia* is lost once the distal tip is exposed from beneath the overriding branch. The acutely angled secondary modular elements of *C. antecessens* are similar to the most proximal secondary modular elements (region 1 of Fig. 2b) of *C. masoni*, and may be a result of the very acute primary branching angles, which are on average more acutely angled than in *C. masoni* (Table 1). Unlike *C. masoni*, primary branches in *C. antecessens* retain the initial branching angle and only rarely change orientation at the distal tip. Through both quantitative and qualitative analysis of several complete specimens of *Charnia* from Mistaken Point and Spaniard's Bay Newfoundland, it is possible to decouple the influence of taphonomy from the morphological shape remaining after fossilization, and use differences in morphological responses to taphonomy in order to elucidate new species.

Life habits of *Charnia*

Infaunal v. epifaunal

Charnia was originally interpreted as a sessile benthic, epifaunal organism with an elevated frond that extended upward into the water column (Ford 1958), a view that has been supported by virtually all subsequent workers (e.g. Jenkins & Gehling 1978; Glaessner 1979; Fedonkin 1992; Jenkins 1992; Runnegar & Fedonkin 1992). Recently, the apparent absence of a basal holdfast in many specimens outside of Avalonia (and the presence of peculiar truncated laminae in the sediment encasing a three-dimensional cast of *Charnia masoni* from the White Sea) led Grazhdankin (2004) and Grazhdankin & Seilacher (2005) to suggest an infaunal lifestyle for White Sea and Newfoundland *Charnia*, similar to the lifestyle they envision for *Pteridinium* and *Rangia* (Grazhdankin & Seilacher 2002, 2005). In contrast with the White Sea, no infaunal organisms or burrows have been found in the Conception Group. The White Sea specimens described by Grazhdankin (2004) have not been studied, but all evidence from the Avalonian specimens of *Charnia* supports the traditional view that they represent sessile fronds that were elevated above the sea floor. Support is as follows:

(1) Preservation beneath ash—As with all other fossils and taxa in the Conception Group, Avalonian specimens of *Charnia* are preserved exclusively at the interface between the underlying mudstone and the overlying volcanic ash-fall tuff. Quality of preservation commonly decreases with distance from the holdfast, implying that minute

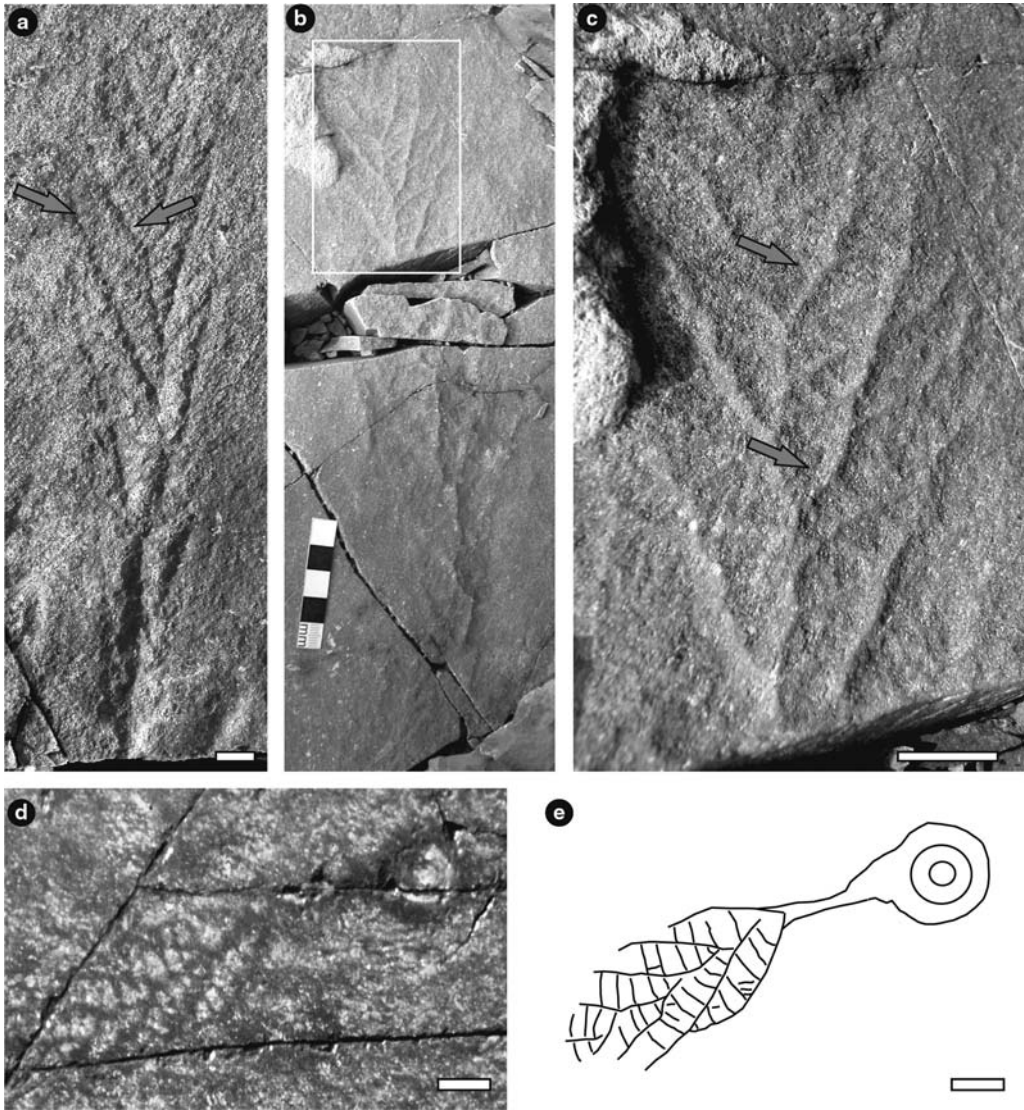


Fig. 6. *Charnia antecedens* n. sp. from the Drook Formation. (a–c) and *Charnia* sp. displaying prominent stem and holdfast from the Briscal Formation (d–e). (a) Holotype of *C. antecedens* n. sp. ROM 54348. Arrows indicate defects in the traditional *Charnia* branching pattern resulting from overlap with adjacent primary branches. (b) *C. antecedens* n. sp. with close-up in (c). Notice that the branches overlap the central axis, forming a zigzagging pattern. Arrows indicate defects in the traditional *Charnia* branching pattern resulting from overlap with adjacent primary branches. (d) Frond with well defined stem and composed of *Charnia*-like primary and secondary branching patterns indistinguishable from *C. masoni*. Prominent stem may represent poorly preserved or lost basal primary branches. (e) Line drawing of D. All scale bars 1 cm.

quantities of ash were increasingly likely to be present beneath the frond distally from the holdfast (see above). These taphonomic aspects are consistent with preservation as an ‘Ediacaran Pompeii’ beneath volcanic ash falls (Seilacher 1992;

Narbonne 2005), but are difficult to envision for an infaunal organism or colony. Specimens preserved in their entirety were either already dead on the sea floor or were recumbent and covered immediately by the ash, whereas more

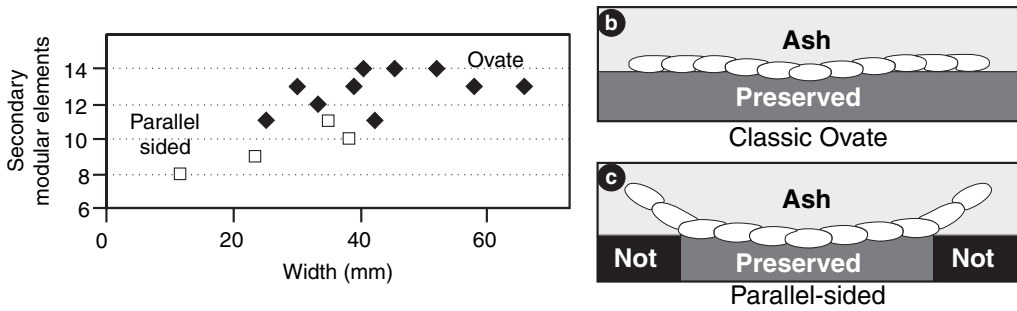


Fig. 7. (a) Traditional morphometric analysis of *Charnia masoni* from the Mistaken Point Formation. White filled squares represent the parallel-sided morph of *C. masoni*, whereas the black diamonds represent the ovate morph. Growth trend lines are similar and the increased number of secondary modular elements with width represent a taphonomic response due to preferential ash preservation. (b–c) Interpretive figure displaying (b) complete preservation of ovate frond and (c) incomplete preservation of distal tips of primary branches resulting in the preservation of a parallel-sided frond shape.

upright specimens are now represented only by the abundant discs, some of which exhibit partial stem impressions (Wood *et al.* 2003).

(2) Fossil orientations—All frondose taxa on every fossiliferous bedding plane in the Portugal Cove South-Mistaken Point area show strong unimodal current orientations that reflect contour-parallel or rarely down-slope currents (Seilacher 1999; Wood *et al.* 2003). Orientations of specimens of *Charnia* on each surface are indistinguishable from those of the other frondose taxa on the same bedding surface, with a strong preferred orientation down current with basal holdfasts serving as anchors. These current orientations would be expected if *Charnia* was an elevated frond like *Charniodiscus*, but would be difficult to explain if *Charnia* was infaunal.

(3) Tiering—Mistaken Point communities show a pronounced tiering of fossils on each bedding surface which is strikingly similar to that observed in communities of filter-feeding animals throughout the Phanerozoic (Clapham & Narbonne 2002). Specimens of *Charnia* occur in all three tiers, but adult specimens are especially common in the middle and upper tiers with the longest specimens dominating the uppermost tier (Clapham & Narbonne 2002). This style of tiering is typical of epifaunal suspension-feeding organisms (Ausich & Bottjer 1982, 2001); tiering of infauna did not begin until the middle or late Palaeozoic and is in any case dissimilar to that shown by *Charnia* and other Mistaken Point taxa (Droser & Bottjer 1993).

Feeding

Several different feeding strategies have been suggested for members of the Ediacara Biota,

including photo- or chemoautotrophy (McMenamin 1986), absorbing dissolved nutrients directly from seawater (Seilacher 1989), and suspension feeding (Jenkins & Gehling 1978; Clapham & Narbonne 2002; Laflamme *et al.* 2004). Phototrophic feeding strategies can be dismissed for the Mistaken Point Ediacara Biota since the accumulation of kilometres of metre-thick turbidites, the complete absence of any shallow-water sedimentary features such as storm beds, Hummocky Cross-Stratification and Swaley Cross-Stratification (HCS-SCS), or exposure features such as desiccation cracks, all suggest that these organisms were living in deep-water ecosystems well below the euphotic zone and storm wave base (Wood *et al.* 2003). Chemoautotrophy is also a tenuous proposition due to the rarity of sulphides or carbonates typical of hydrogen sulphide or methane seeps (Little *et al.* 1998). The tiering structure described from the Mistaken Point communities (Clapham & Narbonne 2002) differs from that exhibited by marine phototrophic communities (which grow preferentially towards the surface and, therefore, are largely unconstrained by height above the sea bottom; Foster 1975) and from chemosynthetic communities (which have less need for modern style tiering), and is strikingly similar to that of epifaunal suspension-feeding organisms (Clapham & Narbonne 2002). The distinction between absorbing dissolved nutrients directly from seawater and suspension filter feeding is difficult to distinguish since both models explain the strong tiering component of the Mistaken Point assemblages (Clapham & Narbonne 2002) and the proportion of regular, irregular and aggregated lateral distributions (Clapham *et al.* 2003).

If the frond leaf is correctly interpreted as a nutrient-gathering structure, the presence of an inferred internal stalk in lieu of a simple stem in

Charnia masoni, *C. wardi*, and *C. antecessens* would have allowed these organisms to feed along the entire length of the frond and resulted in the frondose branching elements being attached directly to the basal anchoring structure (Clapham & Narbonne 2002). *C. wardi* demonstrates clear evidence of an internal central stalk (Fig. 5a–f), and further support for the idea that *C. masoni* also contained an internal stalk comes from a single specimen of *Charnia* sp. from the Briscall Formation which displays both the classic *C. masoni* alternating branching structure and a stem attached to a basal anchoring disc (Fig. 6d–e). Ediacaran fronds typically exhibit a central stalk from which the primary branching units diverge (Jenkins & Gehling 1978; Glaessner 1979; Narbonne *et al.* 1997; Narbonne & Gehling 2003; Laflamme *et al.* 2004), which provided a means of supporting the frond upright in addition to a rigid branching point for further subdivision of the frond. This central stalk is commonly an extension of the stem, which joins the frond to the basal anchoring structure.

Affinities of *Charnia*

Charnia was originally interpreted as a macrophytic alga (Ford 1958), but this was immediately disputed, and this genus was subsequently regarded as a pennatulacean Cnidarian (Glaessner 1979, 1984) a lichen (Retallack 1994), a stem group of the Fungi (Peterson *et al.* 2003), a representative of an extinct high-order taxonomic group of class (Jenkins 1985) or kingdom (Seilacher 1992; McMenamin 1998) level, or any one of a variety of other explanations. As shown above, sedimentological studies implying a deep-water axial/slope environment well below storm wave base for the Mistaken Point assemblage and a community organization similar to that of Phanerozoic and modern filter-feeding animals rules out any affinities for *Charnia* that rely on photosynthesis for feeding (such as plants, algae, or lichen) and implies that an animal origin is most likely. Narbonne (2004, 2005) and Brasier & Antcliffe (2004) followed Jenkins (1985) in regarding *Charnia* as a representative of the rangeomorphs, and extinct phylum-level group of basal animals that characterized early Ediacaran communities (Narbonne 2004).

In the only treatment of the Ediacara Biota in the *Treatise of Invertebrate Paleontology* to date, Glaessner unified *Charnia*, *Charniodiscus* and *Glaessnerina* under the family Charniidae (Glaessner 1979, based on the overall frond-like morphology of all three members (Glaessner 1979). Inclusion of *Glaessnerina* in the Charniidae is clearly justified; indeed, *Glaessnerina* may well

be a junior synonym of *Charnia* (Runnegar & Fedonkin 1992; see Systematic palaeontology). The tiering structure of early Ediacaran communities (Clapham & Narbonne 2002; Laflamme *et al.* 2004) is highly suggestive that the frondose morphology represents a biological response in order to maximize food gathering, and not an evolutionary character that warrants all frondose Ediacarans to be placed within a separate and distinct clade (see also Narbonne *et al.* 1997). The tertiary rangeomorph microstructure present within *Charnia* differs significantly from the branching pattern present within *Charniodiscus*, consisting of several primary branches joined together by a single sheet, in which each branch is subdivided into several perpendicular secondary elements composed of parallel tertiary branches (Jenkins & Gehling 1978; Jenkins 1996; Laflamme *et al.* 2004). Therefore, Jenkins (1985) is followed here in excluding *Charniodiscus* from the Charniidae.

Conclusions

The abundance and taphonomic diversity of fronds from the Avalon Peninsula of Newfoundland has allowed reinterpretation of the classic Ediacaran frond *Charnia*. Numerous specimens from Avalon show that the frond was tethered to the seafloor with a spherical or bulbous holdfast, which was buried in the substrate. Descriptive, quantitative, landmark and traditional morphometric analyses imply that *C. masoni* exhibited a series of overlapping primary branches that taphonomically controlled the morphological expression of secondary-order modular elements. Individual branches appear to have been closely fixed in position, implying that *C. masoni* had either an internal organic skeleton or organic attachments between branches. *C. antecessens* n. sp. is broadly similar in morphology, but exhibits primary branches that were commonly dislodged or ripped-out of sequence, suggestive of a weaker connection with adjacent branches than is evident in *C. masoni*. *C. wardi* is interpreted as a cylindrical, rod-like frond with an internal central stalk, and branches whose attachment with each other was intermediate between the very loose organization of *C. antecessens* and the more rigorous organization of *C. masoni*.

Disorganized forms of *Charnia* (*C. wardi* and *C. antecessens*) dominate the oldest assemblages of *Charnia* in the Drook Formation (575 Ma) but are vastly overshadowed by more organized forms (*C. masoni*) in the Mistaken Point Formation (565 Ma) and Charnwood Forest, and have not been reported from younger occurrences of *Charnia* from the White Sea or Siberia (<555 Ma; Knoll *et al.* 1995; Martin *et al.* 2000; Grazhdankin

2004), which consist entirely of *C. masoni*. The ecological consequence of an increased rigidity in *Charnia* was the eventual capability to colonize shallower waters affected by wave turbulence and periodic energetic storm events. Our systematic, taphonomic and stratigraphic occurrence of *Charnia* reveals a more ecologically and evolutionally dynamic taxon than was previously recognized, and highlights the difficulties associated with interpreting a three-dimensional form from two-dimensional impressions.

Systematic palaeontology

Genus *CHARNIA* Ford, 1958

Type species. *Charnia masoni* Ford, 1958, from Charnwood Forest, England

Diagnosis (new): Parallel-sided to ovate, distally and proximally tapering frond composed of multiple, sigmoidal to rectangular primary branches alternating along a central stalk, overlapping adjacent primary branches and typically crossing over the central midline forming a zigzagging central axis. Primary branches composed of multiple secondary modular elements arranged acutely to almost perpendicularly to the primary branches. Proximal tapering of frond lacks a distinct stem. Surface expression of basal disc commonly small or missing.

Comparisons: *Charnia masoni* is similar in many respects to *Glaessnerina grandis* Glaessner & Wade, 1966. The two forms are segregated on the basis of the large angle of the secondary modular elements, which are oblique in *Glaessnerina* and may represent a taphonomic response to a soft-bodied morphology. Runnegar & Fedonkin (1992) considered *Glaessnerina* a junior synonym of *Charnia*, but Jenkins (1996) considered *Glaessnerina* a valid genus based on the apparent arrangement of the primary branches, which he considered to be a sequence of overlapping leaves. The evidence provided both in this study and independently by Jenkins (1996) and Nedin and Jenkins (1998) of the overlapping sequence of primary branches in *Charnia* further supports the synonymy of *Charnia* and *Glaessnerina* proposed by Runnegar & Fedonkin (1992).

Several of the morphological characters that were used previously to segregate *Charnia* from *Charniodiscus* have now been identified in both genera, and thus are no longer valid. The basal anchoring structure is present in both genera, albeit a larger fraction of the disc is preserved in *Charniodiscus* while a significant portion of the

disc appears to have been buried in *Charnia*. The concentric rings or raised central boss within the basal holdfast in *Charniodiscus* is absent from all studied *Charnia*. The characteristic stalk from which diverged the primary branches in *Charniodiscus* is present as an internal structure in *Charnia wardi* and inferred to be present internally within *C. masoni* and *C. antecessens*.

With the loss of several key characteristics distinguishing *Charnia* and *Charniodiscus*, the few remaining differences become pivotal in segregating both genera. The foremost differentiating character resides within the alternating branching pattern, which overlaps the central stalk, and results in a zigzag central mid line in *Charnia*. Detailed analysis of the nature of the tertiary divisions further help define the differences between *Charnia* and *Charniodiscus*: *Charnia* is characterized by highly repetitive, curved divisions that are inferred to represent rangeomorph microstructure, whereas *Charniodiscus* is composed of several primary branches from which diverge perpendicular secondary branches highlighted by tertiary branching divisions (Jenkins & Gehling 1978; Jenkins 1996; Laflamme *et al.* 2004). Finally, as demonstrated above (see 'Morphometric Analysis'), the sigmoidal taphomorphology of each primary branch due to the overlying relationship of the primary branches in *Charnia* is strikingly dissimilar to the alternating branches of *Charniodiscus*.

Species Charnia masoni Ford, 1958

Figure 4a–j

Diagnosis (new): Parallel-sided to ovate *Charnia* with broad, semicircular distal termination, zigzagging central axis and sigmoidal primary branches. Length to width ratio less than 5:1 (typically between 2:1 and 3:1). Primary branches highly acute (typically less than 30° from midline).

Description: *Charnia masoni* is characterized by a distally tapering, ovate frond with a broad, semicircular to arrow-shaped distal termination. The type specimen from Charnwood Forest is 188 mm long and 46 mm wide, consisting of 18 primary branches on either side and composed of a maximum of 22 (average 18) secondary modular elements per branch. Specimens from Mistaken Point are typically slightly smaller (Table 1), averaging 160 mm long by 41 mm wide, with fewer primary branches (max 13) and secondary modular elements (max 14). The primary branching angle (as defined by the angle between the central midline and the base of the primary branch; see Fig. 2a) is strongly acute and ranges on average between 19° and 37° (mean of 26°–28°, Table 1).

Primary branches are composed of multiple, rhombic secondary modular elements, which form acute to right angles with the base of the primary branches, and result in an almost transverse position along the entire length of the primary branches. The primary branches are strongly angled at both proximal branching site and the distal tips (which curve to run almost parallel to the central midline), resulting in a sigmoidal shape. In specimens with primary branches characterized by relatively more obtuse branching angles (greater than 30° from the central midline), the branching angle remains relatively constant throughout the entire length of the primary branch and results in rectangular primary branches when compared to the acutely angled sigmoidal branches. A distinct, zigzagging central midline is characteristic of *Charnia*. Unlike the typical sigmoidal shape of the basal primary branches (sigmoidal primary branches, Fig. 2a), the distal primary branches located near the tip of the frond are rectangular and composed of significantly smaller and rectangular rather than rhombic secondary modular elements (rectangular primary branches, Fig. 2a). The proximal secondary modular elements on each primary branch are characterized by smaller L1–L3 landmark distances (distance A in Fig. 3a) while the distal elements are defined by smaller L2–L4 landmark distances (distance B. in Fig 3a). Therefore, along a primary branch, the shape of the secondary modular elements varies from a trapezoid in the proximal region (region 1 in Fig. 2b) to a rectangle in the central region (region 2 in Fig. 2b) and finally returning to a trapezoid (albeit a mirror image to the proximal elements) as the distal region (region 3 in Fig. 2b) is overridden by another primary branch (see regional shape changes along primary branches in Fig. 2b). Primary branches extend proximally to the base of the frond into a small, typically poorly preserved or absent basal anchoring disc (Fig. 4a–d, g–j), resulting in the complete absence of a stem.

Occurrence and stratigraphic range: Oldest representatives from the Mistaken Point and Trepassy formations of Newfoundland. Additional specimens from Charnwood Forest in England and the White Sea as well as northeastern Siberia in Russia. Available U–Pb dates and chemostratigraphic correlations imply an age range 565 to <549 Ma for *Charnia masoni*.

Species *Charnia wardi* Narbonne & Gehling, 2003

Figure 5a–h

Diagnosis: (modified from Narbonne & Gehling 2003.) Very long, parallel-sided *Charnia* that

distally narrows to an acute tip, with straight central ridge or furrow. Complete specimens typically with $>10:1$ length v. width ratios. Primary branching angle typically greater than 45° (average range between 44° – 74°), with occasional acutely angled branch bundles (average range between 24° – 35°).

Description: *Charnia wardi* is a strongly elongate and tapering frond, which narrows to an acutely angled, arrowhead-shaped distal tip. A prominent central stalk (15–45 mm wide, mean 29 mm) forms a medial ridge from which and over which diverge several parallel-sided primary branches. Primary branches alternate on each side and overlap across the medial stalk, resulting in a zigzag branching pattern that locally obscures the central stalk. Most primary branches are either sigmoidal or rectangular throughout their length but taper to a point along their distal edge, and are composed of multiple (between 9 and 12) rectangular to rhombic secondary modular elements. Primary branching angle is typically greater than 45° (Table 1) from the central midline, although rare primary branches are angled more acutely (between 24° and 35° from the midline) and result in longer primary branches that cover and overlap adjacent primary branches (herein termed ‘bundles’). Displaced bundles show a rangeomorph structure (cf. Narbonne 2004) of complexly and fractally branching modules that form the edges of the curved third-order divisions (Fig. 5a–b). A taphonomically distinct outer rim represents the distal termination of each individual primary branch.

Comparison: *Charnia wardi* is unique in the genus *Charnia* in possessing a $>10:1$ length to width ratio and in attaining lengths of well over a meter. In juvenile or incomplete specimens, the presence of rare branch bundling in addition to the strongly linear shape and composite moulding of the central stalk allows for the differentiation of *C. wardi* from all other charnids. *Paracharnia dengyingensis* Sun 1986, known only from a single poorly preserved specimen from the Yangtze Gorge, China, exhibits similar length to width ratios, however, the significantly wider central stalk, which represents greater than half of the overall width, and the unusual secondary stalks which are found on each individual frondlet or petaloid leaf readily distinguish *P. dengyingensis* from *C. wardi*.

Occurrence and stratigraphic range: *Charnia wardi* is known only from the Conception Group of the Avalon Peninsula. It was first described from the upper beds of the Drook Formation (Narbonne & Gehling 2003), and the present study extends the distribution of *C. wardi* into the basal beds of the

Mistaken Point Formation to include specimens described (but not figured) as 'Charnia species B' by Clapham *et al.* (2003).

Species Charnia antecedens sp. nov.

Figure 6

?*Charnia masoni*. . . (P36574) Nedin & Jenkins, 1998, p. 315, Fig. 1

'*Charnia masoni*, ROM 54348' Narbonne & Gehling, 2003, p. 28, Fig. 2a

'*Charnia* Ford, 1958 (circled and indicated by letter C)' Clapham *et al.*, 2004, p. 1033, Fig. 2

? 'Bush-like form, possibly comparable with *Bradgatia* but showing *Charnia*-like attributes' O'Brien & King, 2004, p. 210, Pl. 5A.

Diagnosis: *Charnia* with rectangular primary branches with inconsistent width throughout their length, acutely angled secondary modular elements throughout entire length of primary branch, and 'V' shaped proximal region.

Material: Holotype (ROM 54348; Fig. 6a) from the upper part of the Drook Formation of the Conception Group of Newfoundland. Two additional specimens from the upper Drook Formation were photographed and latexed in the field.

Description: *Charnia antecedens* consists of an ovate to elliptical frond in which the primary branches are not consistent in shape throughout their length and exhibit significant tapering of the frond at the proximal anchoring region. The frond is composed of 8–10 acutely angled (average 21°) primary branches that remain relatively constant in branching angle throughout the entire length of the branch. Primary branches rectangular to trapezoidal in shape instead of the traditional sigmoidal shape of *C. masoni* branches. Distal terminations of the primary branches are rectangular rather than tapered. Primary branches consisting of approximately 10–12 secondary modular elements acutely angled with the primary branches and lying almost perpendicular to the central axis, unlike the typically right-angled branching of *C. masoni*. Anterior region strongly tapered to form a 'V' shaped proximal region. Basal anchoring disc absent or small and poorly preserved.

Comparisons: The overall morphology of *C. antecedens* is most similar to *C. masoni*. The increased amounts of imbrication of the primary branches when compared to *C. masoni*, in addition to the acute branching angle of the secondary modular elements and the 'V' shaped proximal region are all suggestive of a distinct and diagnosable difference between both species. *C. antecedens* is known mostly from early Ediacaran assemblages

whereas *C. masoni* is known mostly from younger Ediacaran assemblages, implying that the differences between these taxa are unlikely to reflect taphonomy.

Derivation of name: *antecedens*, due to the implied ancestral origin of this species.

Occurrence: Three specimens are known from the Drook Formation of the Conception Group of Newfoundland. Additional specimens of *Charnia antecedens* are known from the correlative Mistaken Point Formation from the Bonavista Peninsula (Avalon zone, Newfoundland; O'Brien & King 2004). A single specimen similar to *C. antecedens* was also described and figured as *C. masoni* from the Rawnsley Quartzite, Flinders Ranges, South Australia (Nedin & Jenkins 1998), but our examination of the additional specimens listed in their paper revealed a heterogeneous collection of discs, discs with stems and fronds that are difficult to relate to *Charnia* at the present time.

Identification Key

Charniidae:

A) Strongly linear *Charnia* with >10:1 length:width ratio. Prominent straight central stalk present and rare branch bundling

***Charnia wardi*:** Very long and tapering *Charnia* that distally narrows to the tip, with straight central ridge or furrow. Complete specimens typically with >10:1 length v. width ratios. Primary branching angle typically greater than 45° (average range between 44°–74°), with occasional acutely angled branch bundles (average range between 24°–35°).

A) Ovate to cylindrical *Charnia* with <10:1 length : width ratio. Midline zigzagging and central stalk missing. Go to B

B) *Charnia* with irregular primary branching. Primary branches rectangular and inconsistently branching. Significant increases in overlap from adjacent branches resulting in jumbled branch arrangement. Significant tapering of the proximal region of frond, resulting in 'V-shaped' proximal region.

***Charnia antecedens*:** *Charnia* with rectangular primary branches with inconsistent width shape throughout their length and acutely angled secondary modular elements throughout entire length of primary branch.

B) *Charnia* with regular and consistent branching. Primary branches sigmoidal and parallel along entire length. Go to C

C) Smaller *Charnia* (less than 200 mm in length) with fewer than 20 primary branches

***Charnia masoni*:** Cylindrical to ovate *Charnia* with broad, semicircular distal termination, zig-zagging central ridge, and sigmoidal primary branches. Length: width ratio less than 5:1 (typically between 2:1 and 3:1). Primary branches highly acute (typically less than 30° from midline).

C) Significantly larger *Charnia* (greater than 500 mm in length) with greater than 20 primary branches

Charnia grandis

Special thanks are extended to A. Decechi, R. Martindale, M. Mussa-Caleca, R. Schwartz-Narbonne, and S. Villeneuve for exceptional assistance in the field and laboratory. We thank J. G. Gehling for critical discussions and for making specimens from the South Australian Museum available for study. M. D. Brasier and J. Antcliffe introduced us to specimens at Charnwood Forest and also made useful suggestions concerning our landmark analysis of *Charnia*. We also thank D. S. Sheets for insightful discussions and guidance concerning the landmark morphometric techniques utilized in this research. Comments and reviews by R. F. Jenkins and H. J. Hofmann greatly improved the manuscript. Fieldwork in the Mistaken Point Ecological Reserve was carried out under Scientific Research Permits granted by the Parks and Natural Areas Division, Government of Newfoundland and Labrador. Research was funded by a Queen's Graduate Award, Ontario Graduate Scholarship, and a PGSD scholarship from the Natural Sciences and Engineering Research Council to Laflamme, and continual research grants from the Natural Sciences and Engineering Research Council to Narbonne. Special thanks are extended to the people of Portugal Cove South, Trepassey, and Spaniard's Bay for their constant vigilance and protection of their fossil heritage.

References

- ANDERSON, M. M. 1978. Ediacaran fauna. In: LAPEDES, D. N. (ed.) *Yearbook of Science and Technology*. New York, McGraw-Hill, 146–149.
- ANDERSON, M. M. & MISRA, S. B. 1968. Fossils found in the Pre-Cambrian Conception Group of southeastern Newfoundland. *Nature*, **220**, 680–681.
- AUSICH, W. I. & BOTTJER, D. J. 1982. Tiering in suspension-feeding communities on soft substrata throughout the Phanerozoic. *Science*, **216**, 173–174.
- AUSICH, W. I. & BOTTJER, D. J. 2001. Sessile invertebrates. In: BRIGGS, D. E. G. & CROWTHER, P. R. (eds) *Palaeobiology II*. Oxford, Blackwell Science, 384–386.
- BENUS, A. P. 1988. Sedimentological context of a deep-water Ediacaran fauna (Mistaken Point, Avalon Zone, eastern Newfoundland). In: LANDING, E., NARBONNE, G. M. & MYROW, P. (eds) *Trace Fossils, Small Shelly Fossils and the Precambrian–Cambrian Boundary*. New York State Museum and Geological Survey Bulletin, **463**, 8–9.
- BOOKSTEIN, F. L. 1991. *Morphometric Tools for Landmark Data: Geometry and Biology*. Cambridge University Press, New York.
- BOYNTON, H. E. & FORD, T. D. 1995. Ediacaran fossils from the Precambrian (Charnian Supergroup) of Charnwood Forest, Leicestershire, England. *Mercian Geologist*, **13**, 165–182.
- BOWRING, S. A., MYROW, P., LANDING, E. & RAMENZANI, J. 2003. Geochronological constraints on terminal Neoproterozoic events and the rise of Metazoans. *NASA Astrobiology Institute (NAI) General Meeting, Special Session VI: Early biosphere evolution*, Abstract **13045**, 113–114.
- BRASIER, M. & ANTCLIFFE, J. 2004. Decoding the Ediacaran enigma. *Science*, **305**, 1115–1117.
- BRASIER, M., ANTCLIFFE, J., CALLOW, R., GREEN, O., CARTY, A. & MCILROY, D. 2005. Decoding the Ediacara enigma. *49th annual meeting of the Palaeontological Association, Abstracts*, **10**.
- CADIMA, J. F. C. L. & JOLLIFFE, I. T. 1996. Size and shape related principal component analysis. *Biometrics*, **52**, 710–716.
- CLAPHAM, M. E. & NARBONNE, G. M. 2002. Ediacaran epifaunal tiering. *Geology*, **30**, 627–630.
- CLAPHAM, M. E., NARBONNE, G. M. & GEHLING, J. G. 2003. Paleoecology of the oldest-known animal communities: Ediacaran assemblages at Mistaken Point, Newfoundland. *Paleobiology*, **29**, 527–544.
- CLAPHAM, M. E., NARBONNE, G. M., GEHLING, J. G., GREENTREE, C. & ANDERSON, M. M. 2004. *Thectardis avalonensis*: A new Ediacaran fossil from the Mistaken Point Biota, Newfoundland. *Journal of Paleontology*, **78**, 1031–1036.
- CONDON, D., ZHU, M., BOWRING, S., WANG, W., YANG, A. & JIN, Y. 2005. U–Pb Ages from the Neoproterozoic Doushantuo Formation, China. *Science*, **308**, 95–98.
- CONWAY MORRIS, S. 1989. Southeastern Newfoundland and adjacent areas. In: COWIE, J. W. & BRASIER, M. D. (eds) *The Precambrian–Cambrian Boundary*. Clarendon Press, Oxford, 7–39.
- DROSER, M. L. & BOTTJER, D. J. 1993. Trends and patterns of Phanerozoic ichnofabrics. *Annual Review of Earth and Planetary Sciences*, **21**, 205–250.
- DZIK, J. 2002. Possible ctenophoran affinities of the Precambrian 'sea-pen' *Rangaea*. *Journal of Morphology*, **252**, 315–334.
- FEDONKIN, M. A. 1985. Skeleton-free fauna of the Vendian; morphological analysis. In: SOKOLOV, B. S. E. & IVANOVSKIY, A. B. (eds) *Paleontologiya; Paleontology, Venskaya Sistema; Istoriko-Geologicheskoye i Paleontologicheskoye Obosnovaniye*. Nauka, Moscow, 10–69.
- FEDONKIN, M. A. 1992. Vendian faunas and the early evolution of Metazoa. In: LIPPS, J. H. & SIGNOR, P. W. (eds) *Origin and Early Evolution of the Metazoa*. Plenum Press, New York, 87–129.
- FORD, T. D. 1958. Pre-Cambrian fossils from Charnwood Forest. *Proceedings of the Yorkshire Geological Society*, **31**, 211–217.
- FORD, T. D. 1962. The oldest fossils. *New Scientist*, **15**, 191–194.
- FORD, T. D. 1963. The Pre-cambrian fossils of Charnwood Forest. *Transactions of the Leicester Literature and Philosophical Society*, **57**, 57–62.

- FORD, T. D. 1999. The Precambrian fossils of Charnwood Forest. *Geology Today*, **15**, 230–234.
- FOSTER, M. J. 1975. Algal succession in a *Macrocystis pyrifera* forest. *Marine Biology*, **32**, 313–329.
- GEHLING, J. G. 1999. Microbial mats in terminal Proterozoic siliciclastics: Ediacaran death masks. *Palaaios*, **14**, 40–57.
- GEHLING, J. G., NARBONNE, G. M. & ANDERSON, M. M. 2000. The first named Ediacaran body fossil, *Aspidella terranovica*. *Palaeontology*, **43**, 427–456.
- GLAESSNER, M. F. 1979. Biogeography and biostratigraphy: Precambrian. In: MOORE, R. C. (founder) ROBINSON, R. A. & TEICHERT, C. (eds) KEIM, J. D., MCCORMICK, L. & WILLIAMS, R. B. (assoc. eds.) *Treatise on Invertebrate Paleontology, Part A, Introduction, Fossilization (Taphonomy), Biogeography and Biostratigraphy*. The Geological Society of America and the University of Kansas Press, Lawrence, Kansas, 79–118.
- GLAESSNER, M. F. 1984. *The Dawn of Animal Life. A Biohistorical Study*. Cambridge University Press, Cambridge.
- GLAESSNER, M. F. & WADE, M. 1966. The Late Precambrian fossils from Ediacara, South Australia. *Palaeontology*, **9**, 599–628.
- GRAZHDANKIN, D. 2004. Patterns of distribution in the Ediacaran biotas: facies versus biogeography and evolution. *Paleobiology*, **30**, 203–221.
- GRAZHDANKIN, D. & SEILACHER, A. 2002. Underground Vendobionta from Namibia. *Palaeontology*, **45**, 57–78.
- GRAZHDANKIN, D. & SEILACHER, A. 2005. A re-examination of the Nama-type Vendian organism *Rangaea schneiderhoehni*. *Geological Magazine*, **142**, 571–582.
- JAMES, F. C. & MCCULLOCH, C. E. 1990. Multivariate analysis in ecology and systematics: Panacea or Pandora's Box? *Annual Review of Ecology and Systematics*, **21**, 129–166.
- JENKINS, R. J. F. 1985. The enigmatic Ediacaran (late Precambrian) genus *Rangaea* and related forms. *Paleobiology*, **11**, 336–355.
- JENKINS, R. J. F. 1992. Functional and ecological aspects of Ediacaran assemblages. In: LIPPS, J. H. & SIGNOR, P. W. (eds) *Origin and Early Evolution of the Metazoa*. Volume 10. Topics in Geobiology. Plenum Press, 131–176.
- JENKINS, R. J. F. 1996. Aspects of the geological setting and palaeobiology of the Ediacara assemblage. In: DAVIES, M., TWIDALE, C. R. & TYLER, M. J. (eds) *Natural History of the Flinders Ranges*. Volume 7. Royal Society of South Australia. Richmond South Australia, 33–45.
- JENKINS, R. J. F. & GEHLING, J. G. 1978. A review of the frond-like fossils of the Ediacara assemblage. *Records of the South Australian Museum*, **17**, 347–359.
- KNOLL, A. H., GROTZINGER, J. P., KAUFMAN, A. J. & KOSOLOV, P. 1995. Integrated approaches to terminal Proterozoic stratigraphy: an example from the Olenek Uplift, north-eastern Siberia. *Precambrian Research*, **73**, 251–270.
- LAFLAMME, M., NARBONNE, G. M. & ANDERSON, M. M. 2004. Morphometric analysis of the Ediacaran frond *Charniodiscus* from the Mistaken Point Formation, Newfoundland. *Journal of Paleontology*, **78**, 827–837.
- LANDING, E., NARBONNE, G. M. & MYROW, G. M. 1988. *Trace Fossils, Small Shelly Fossils, and the Precambrian–Cambrian Boundary*. New York State Museum and Geological Survey Bulletin, 463.
- LELE, S. R. & RICHTSMIEIER, J. T. 2001. *An Invariant Approach To Statistical Analysis of Shapes*. Boca Raton, Chapman & Hall.
- LITTLE, C. T. S., HERRINGTON, R. J., MASLENNIKOV, V. V. & ZAYKOV, V. V. 1998. The fossil record of hydrothermal vent communities. In: MILLS, R. A. & HARRISON, K. (eds) *Modern Ocean Floor Processes and the Geological Record*. Geological Society of London Special Publications, **148**, 259–270.
- MARTIN, M. W., GRAZHDANKIN, D. V., BOWRING, S. A., EVANS, D. A. D., FEDONKIN, M. A. & KIRSCHVINK, J. L. 2000. Age of Neoproterozoic bilaterian body and trace fossils, White Sea, Russia: Implications for metazoan evolution. *Science*, **288**, 841–845.
- MCMENAMIN, M. A. S. 1986. The garden of Ediacara. *Palaaios*, **1**, 178–182.
- MCMENAMIN, M. A. S. 1998. *The Garden of Ediacara*. Columbia University Press, New York.
- MISRA, S. B. 1969. Late Precambrian (?) fossils from southeastern Newfoundland. *Geological Society of America Bulletin*, **80**, 2133–2140.
- MISRA, S. B. 1971. Stratigraphy and depositional history of late Precambrian coelenterate-bearing rocks, southeastern Newfoundland. *Geological Society of America Bulletin*, **82**, 979–987.
- MISRA, S. B. 1981. Depositional environment of the late Precambrian fossil-bearing rocks of southeastern Newfoundland, Canada. *Journal of the Geological Society of India*, **22**, 375–382.
- MURPHY, J. B., NANCE, R. D. & KEPPIE, J. D. 2002. West African proximity of the Avalon Terrane in the latest Precambrian; discussion. *Geological Society of America Bulletin*, **114**, 1049–1050.
- NARBONNE, G. M. 2004. Modular construction of early Ediacaran complex life forms. *Science*, **305**, 1141–1144.
- NARBONNE, G. M. 2005. The Ediacara biota: Neoproterozoic origin of animals and their ecosystems. *Annual Review in Earth and Planetary Sciences*, **33**, 421–442.
- NARBONNE, G. M. & GEHLING, J. G. 2003. Life after snowball: The oldest complex Ediacaran fossils. *Geology*, **31**, 27–30.
- NARBONNE, G. M., SAYLOR, B. Z. & GROTZINGER, J. P. 1997. The youngest Ediacaran fossils from Southern Africa. *Journal of Paleontology*, **71**, 953–967.
- NARBONNE, G. M., DALRYMPLE, R. W., GEHLING, J. G., WOOD, D. A., CLAPHAM, M. E. & SALA, R. A. 2001. *Neoproterozoic fossils and environments of the Avalon Peninsula, Newfoundland*. Field Trip B5, Geological Association of Canada—Mineralogical Association of Canada Joint Annual Meeting, St. John's, Newfoundland.
- NARBONNE, G. M., DALRYMPLE, R. W., LAFLAMME, M., GEHLING, J. G. & BOYCE, W. D. 2005. *Mistaken Point Biota and the Cambrian of the Avalon*. Field Trip, North American Paleontological Convention, Halifax, Nova Scotia.

- NEDIN, C. & JENKINS, R. J. F. 1998. The first occurrence of the Ediacaran fossil *Charnia* from the Southern Hemisphere. *Alcheringa*, **24**, 315–316.
- O'BRIEN, S. J. & KING, A. F., 2004. Ediacaran fossils from the Bonavista Peninsula (Avalon Zone), Newfoundland: Preliminary descriptions and implication for regional correlation. *Current Research (2004) Newfoundland and Labrador Department of Natural Resources. Geological Survey Report*, **04-1**, 203–212.
- PETERSON, K. J., WAGGONER, B. & HAGADORN, J. W. 2003. A fungal analog for Newfoundland Ediacaran fossils? *Integrated and Comparative Biology*, **43**, 127–136.
- RESTALLACK, G. J. 1994. Were the Ediacaran fossils lichens? *Paleobiology*, **20**, 523–544.
- RUNNEGAR, B. & FEDONKIN, M. A. 1992. Proterozoic metazoan body fossils In: SCHOPF, J. W. & KLEIN, C. (eds) *The Proterozoic Biosphere: A Multidisciplinary Study*. Cambridge University Press, New York, 369–388.
- SEILACHER, A. 1989. Vendozoa: Organismic construction in the Proterozoic biosphere. *Lethaia*, **22**, 229–239.
- SEILACHER, A. 1992. Vendobionta and Psammocorallia: lost constructions of Precambrian evolution. *Journal of the Geological Society of London*, **149**, 607–613.
- SEILACHER, A. 1999. Biomat-related lifestyles in the Precambrian. *Palaios*, **14**, 86–93.
- SOMERS, K. M. 1986. Multivariate allometry and removal of size with Principal Components Analysis. *Systematic Zoology*, **35**, 359–368.
- STRAUSS, R. E. & BOOKSTEIN, F. L. 1982. The Truss: body form reconstruction in morphometrics. *Systematic Zoology*, **31**, 113–135.
- SUN, W. G. 1986. Late Precambrian pennatulids (sea pens) from the Eastern Yangtze Gorge, China: *Paracharnia* a gen. nov. *Precambrian Research*, **31**, 361–375.
- WAGGONER, B. 1999. Biogeographic analysis of the Ediacara biota: A conflict with paleotectonic reconstructions. *Paleobiology*, **25**, 440–458.
- WOOD, D. A., DALRYMPLE, R. W., NARBONNE, G. M., GEHLING, J. G. & CLAPHAM, M. E. 2003. Paleoenvironmental analysis of the late Neoproterozoic Mistaken Point and Trepassey formations, southeastern Newfoundland. *Canadian Journal of Earth Sciences*, **40**, 1375–1391.

Comparative taphonomy of Vendian genera *Beltanelloides* and *Nemiana*: taxonomy and lifestyle

M. V. LEONOV

Paleontological Institute Russian Academy of Science, 117868 Profsoyuznaya Street, 123, Moscow, Russia (e-mail: maxleon@narod.ru)

Abstract: Taphonomic analysis of new material from Vendian sequences of the White Sea and southwestern Ukraine provides data for a better definition of both the widely distributed fossil taxa of *Beltanelloides* and *Nemiana*. A new type of *Beltanelloides* preservation is described, so it is now possible to attribute some sandstone imprints to this taxon. *Nemiana simplex* seems to have a lifestyle and level of body organization comparable with that of sponges. The narrow range of facies in which *Nemiana* occurs, when compared to the much broader range of *Beltanelloides*, is compelling evidence for a benthic lifestyle of *Nemiana*.

This paper clarifies the taxonomy and palaeoecology of two groups of widely distributed genera of Neoproterozoic organisms. Both genera are characterized by a simple shape, which makes comparisons and diagnosis difficult. Study of taphonomy and palaeoecology of fossils are the methods that may help us to solve some problems. Such types of investigations (Gehling 1999; Grazhdankin 2000) result in some progress in our understanding of the nature of some soft-bodied organisms. Biometric comparisons (Laflamme *et al.* 2004) also produce results that have essential significance for taxonomic comparison of Vendian fossils.

Material and methods

The basis for the study is the author's collection and observations of the range of Upper Neoproterozoic outcrops on the Eastern European Platform, studied during field trips between 2000 and 2004. Collections of the Paleontological Institute, Russian Academy of Science in Moscow were also most useful. Material was collected from the Upper Vendian sequences of Podolia and the White Sea region (Ediacaran in age), referred to the uppermost part of the Vendian sequence (Redkino and Kotlin regional stages) (Aksenov *et al.* 1978). Additionally, biometric analysis utilized images from publications (Palij 1976; Fedonkin 1985).

Collections from the type regions and from many stratigraphic levels were available, making it possible to determine taphocoenoses typical for each taxon. Some unusual forms of preservation were observed. In addition to the field studies, biometric analysis was carried out.

Beltanelloides sorichevae was first described in 1965 and further diagnosed in 1972 (Sokolov 1972). The fossils are round imprints, with very

thin concentric wrinkles around the periphery, preserved as carbonaceous films. The type material was recovered from Vendian deposits of the Onega Peninsula (White Sea area, northern Russia) and from the Odessa borehole (southern Ukraine). These remains were thought to be planktonic, colonial algae, similar in general morphology to the extent *Volvox* (Chlorophyta) (Sokolov 1965; Gnilovskaya *et al.* 1988). *Beltanelloides* may well be algal, but some forms previously included in this genus (for example, '*Beltanelloides*' from the Bernashevka Formation of Podolia, Ukraine) appear to be truly benthic organisms, possibly related to *Moraniales* (Aseeva 1988).

Nemiana simplex (Palij 1976) is a name applied to a second type of round imprints, originally described from the Upper Vendian sequence of Podolia (Ukraine) from the Redkino Regional Stage, Mogilev and Yampol formations (Palij 1976). *Nemiana* remains are also known from the Kotlin Regional Stage, Yorga Formation of the White Sea region, Russia (Fedonkin 1985), the Neoproterozoic sequence of the Wernecke Mountains, Canada (Narbonne & Hofmann 1987) ('*Beltanelliformis brunsa*' specimens on pl. 74, fig. 5–7 and pl. 75, fig. 1–8), and the Kliphhoek Member of the Neoproterozoic Dabis Formation of Namibia (Jenkins 1992). These imprints have a very well-defined shape, with high relief, preserved on the soles of sandstone beds, which can be found as single individuals or more often in dense groupings. Typically these fossils are best preserved at a clay/sandstone boundary.

Tirasiana disciformis (Palij 1976) is yet another form that is morphologically similar to *Nemiana*, but it differs in having a central peak preserved in positive hyporelief. Many examples that were originally described as *T. disciformis* on the basis of characteristics of the peripheral zone (e.g. Palij

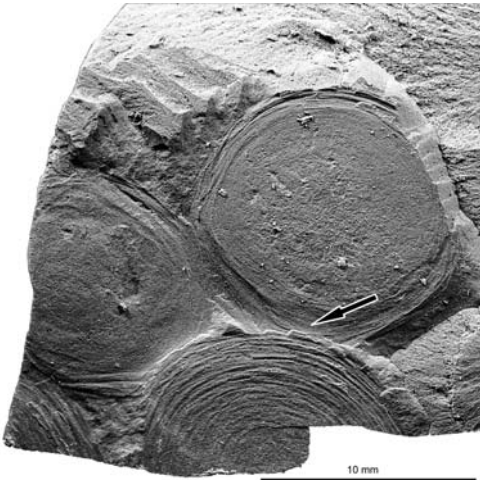


Fig. 1. PIN 5079/9 *Beltanelloides sorichevae*. Upper Vendian sequence, Redkino Regional Stage, Arkhangelsk region, Lyamtsa locality, Russia. Top surface of the split rock. Arrow marks an individual overlapping another.

1976, pl. XXIII, figs 1, 2), appear to represent a relatively large form of *Nemiana*. This idea is supported by the observation of a morphological series of *Nemiana* specimens that demonstrates that, as specimens increase in size, concentric rings can be discerned along their margins (Fig. 11; Palij 1976, pl. XXII, fig. 3).

Some researchers consider *Nemiana* a junior synonym of *Beltanelloides* and refer to these fossils as *Beltanelloides simplex* (Gureev 1988). Narbonne & Hofmann (1987) agree with this interpretation of *Beltanelliformes brunsaе* and *Nemiana simplex* noted above. They have suggested



Fig. 2. PIN 5079/13 *Beltanelloides sorichevae*. Upper Vendian sequence, Redkino Regional Stage, Arkhangelsk region, Lyamtsa locality, Russia. Top surface of the split rock. Arrow marks an individual that lies in the rock but is not seen on the break surface.

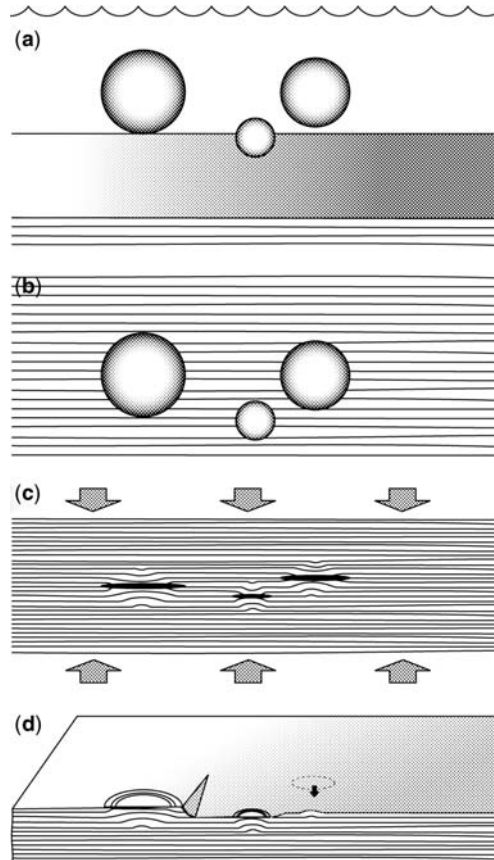


Fig. 3. Taphonomic scenario for preservation of *Beltanelloides sorichevae* (typical preservation). (a) Spherical, planktonic organisms fall to muddy seafloor. (b) Organisms buried by mud, still spherical in shape. (c) Diagenesis compacts mud. Organisms compacted to form flat imprints surrounded by organic film. Upper and lower layers of sediments deformed and fill space of inner cavity. (d) Upper and lower surfaces of organism (double-sided) leave imprints in the clay.

that the two taxa were simply different types of preservation of the same organism. Recent work, however, does not support this opinion. There are three major features of the genus *Nemiana* that are not characteristic for all other taxa, mentioned above. The first is the nature of the overall shape—hemispherical in hyporelief—of the smaller individuals (diameters of less or about 1 cm). The second feature is the nature of the marginal imprint, which rolls up towards the upper layer and then curves towards the central axis of the fossil. The third feature is nature of the distribution of specimens in dense assemblages. This new feature is specific to *Nemiana* samples from

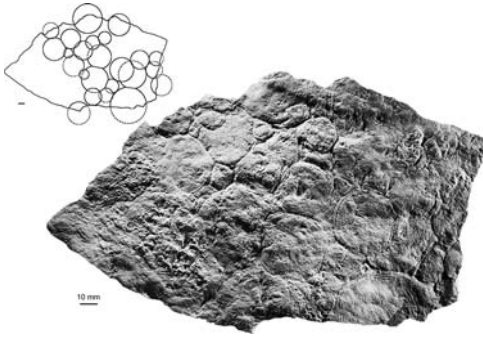


Fig. 4. PIN 5079/52. Second taphonomic scenario for preservation of *Beltanelloides* preservation. Upper Vendian Sequence, Redkino Regional Stage, Zimnie Gory Formation, Arkhangelsk region, Zimnie Gory locality, Russia. Bed sole. Note the overlaying of the clustered individuals.

the type locality in Podolia and must be included in an emended diagnosis of this taxon after revision.

All of these genera seem to be monotypic, but to which higher taxa they belong is yet to be determined.

But, first, clear criteria for generic diagnosis on the basis of detailed comparisons, noting the preservational overprints, are needed. The author supports the idea that at least two different taxa, *Beltanelloides* and *Nemiana*, should be recognized.

Taphonomic analysis

Beltanelloides sorichevae

Beltanelloides specimens from the Lyamtsa locality (southwestern Onega Peninsula) were used for study, found in the Lyamtsa Formation (assigned to the Redkino Regional Stage). The Lyamtsa Formation is characterized by thin, chocolate-brown clays with concave break surfaces, lacking visible lamination. These clays form beds up to a few dozens of centimetres that are included in a sequence of rhythmic siltstone–clay interbeds with rare sandstone beds. This complex was likely deposited in a shallow marine shelf environment, below storm wave base.

Fossils are preserved in negative relief on both the upper and lower break surfaces, thus

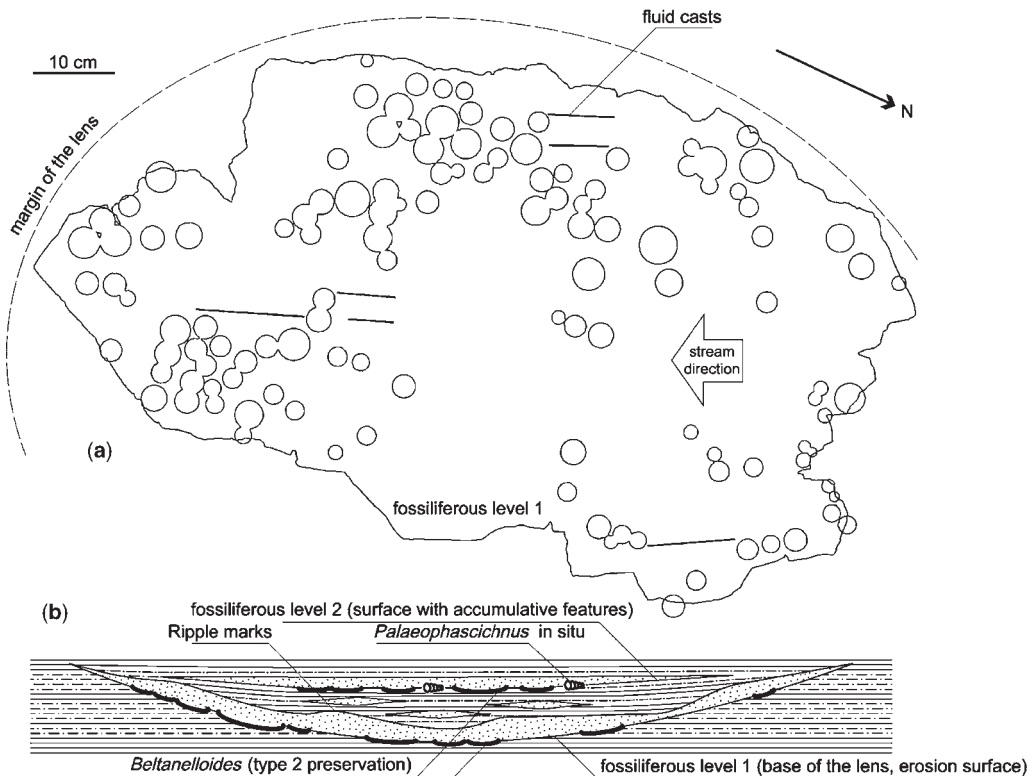


Fig. 5. PIN 5079/51. Second type of *Beltanelloides* preservation, Upper Vendian, Redkino Regional Stage, Zimnie Gory Formation, the first member, Russia, Arkhangelsk region, Zimnie Gory locality. Bed sole: (a) drawing of the bottom surface of the basal sandstone; (b) schematic cross section through the fossiliferous lens.

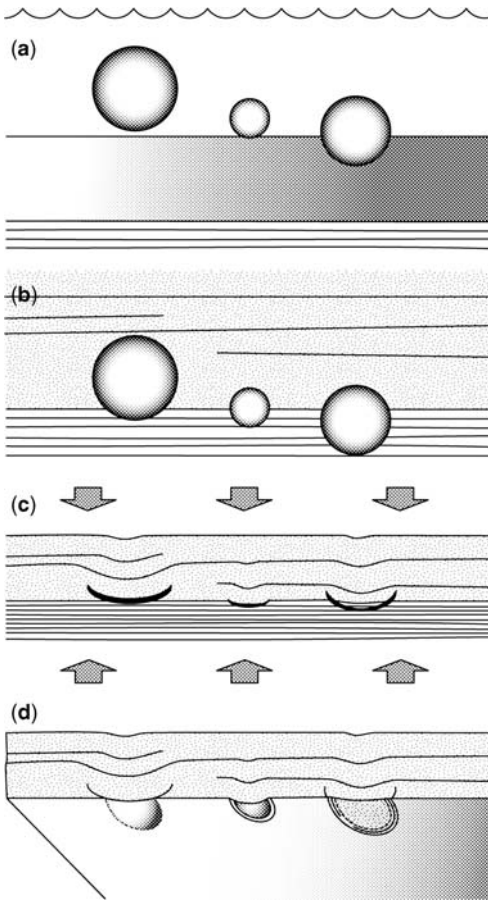


Fig. 6. Taphonomic scheme for *Beltanelloides sorichevae* (second type of preservation).

representing the upper and lower sides of the organism. There is no evidence of a carbonaceous film. An important feature is the overlying of individuals that can occur in dense clusters (Fig. 1, see arrow). This can be observed on some already published images (Sokolov 1977, p. 437, fig. a; Fedonkin 1985, Pl. FV fig. 2). *Beltanelloides* imprints can also occur on other clay surfaces in a widely spaced distribution of individuals (Fig. 2). Deformation of the clay around the individuals (marked by the arrow) that are preserved in the clays, but have not broken the surface, is visible in some specimens; these represent traces of compaction of *Beltanelloides* from its original spherical shape, within the sediment.

Some conclusions can be drawn from the above observations. Groups of *Beltanelloides* are clusters of individuals. These fossils are randomly distributed in the sediment. This certainly does not disprove their interpretation as remains of spheromorphic,

planktonic organisms. Such organisms appear to have had a thin, durable envelope surrounding less dense tissues or a cavity. A sequence of events can be suggested to explain these observations (Fig. 3): first, spherical organisms fell from the water to a muddy ocean floor. Then, these organisms were buried by mud, their form still spherical. The overlying mud, as well as the soft seafloor mud was compacted during diagenesis. At that time the organisms were compressed, forming flat imprints surrounding an organic film. Upper and lower layers of mud then filled the space occupied either by soft tissue that decayed or the inner cavities. What resulted were double-sided imprints with negative relief on the beds above and below, which may still have fragments of organic matter on their surfaces. The fossils occur not only at the boundaries of the layers. Specimens contained within the muds are more common, so the process of forming these fossils is not connected with microbial mat surfaces, as is the case for some Neoproterozoic organisms (Gehling 1999).

Another type of fossil was recovered from the Zimmie Gory locality, on the Winter Coast of the White Sea, northern Russia. These imprints were preserved in the lower member of the Zimmie Gory Formation. They occur in flat hillocks, in positive hyporelief on the bottom surfaces of the sandstones (Fig. 4). These sandstones occur as lens-shaped bodies up to 15 cm in thickness and about 1 metre wide. The lenses have an elliptical shape in plane view and cut into the underlying siltstone and clay-interbedding sequence (Fig. 5). The lower member of the Zimmie Gory Formation appears to have been deposited in a shallow marine basin that developed in valleys with low relief. The base of this sequence appears to be a flooding surface of marine transgression (Grazhdankin 2003). The lower bed within these lens-shaped bodies consists of quartzite with ripple marked top surfaces with an erosional base. The quartzites are overlain by a sandstone and siltstone interbedded unit, which may have formed as microturbidites. So the lower surface of the lenses has erosional character, but some surfaces in the lenses have accumulative character. Such event beds were likely deposited as a result of intensive local stream downcutting, with flow in the direction 120° SE, followed by relatively slow deposition that filled the downcut depression. Occurrence of ripple marks on the top surface of the basal sandstone and the presence of some benthic fossils *in situ*—such as *Palaeopascichnus* supports this interpretations. *Palaeopascichnus* are considered to be sedentary organisms, perhaps similar in morphology, if not actually related, to giant xenophaeophoran protists, which today live in biotopes that are produced by cyanobacterial biofilms (Seilacher *et al.* 2003).

The base of the lens often preserves large clusters of imprints. These organisms which produced the clusters, appear to have been buried simultaneously in one sedimentary event. It is possible to observe the absence of order in imprint distribution on the surface. In dense clusters, individuals are preserved in contact with each other or actually overlay neighbouring individuals to form a multi-layered imprint (Fig. 4). Morphology and taphonomic features of these imprints are very similar to '*Beltanelliformis brunseae*' from the Wernecke Mountains (Narbonne & Hofmann 1987, pl. 74, figs 1, 3). The following sequence is envisioned as to how this sort of accumulation occurred (Fig. 6):

- Organisms fall down to a muddy bottom from the water column. Some were buried in the mud, partially or entirely.
- As a result of some hydrodynamic event, e.g. a storm current, the thin layer of sand is deposited above the organisms and the mud. Depending on local conditions, there may have been some erosion and excavation of some levels containing the buried organisms.
- Upon sediment compaction, on the boundary between the clay and the sand, imprints formed of the lower surface of *Beltanelloides* which were immersed in the clay.
- The end result was a round, positive imprint on the undersides of sandstone beds.

Comparison of the two above-mentioned types of fossil preservation, taking into account the similar dimensions of the fossils under consideration, indicates that different sorts of sedimentary environments can make a difference in the final preservation of an organism.

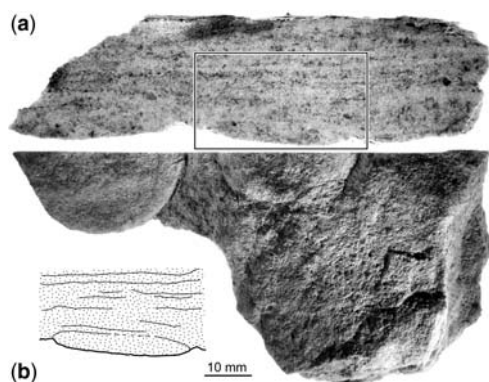


Fig. 7. PIN 3994/1013 *Nemiana simplex*. Upper Vendian sequence, Redkino Regional Stage, Mogilev Formation, Podolia, Ukraine. (a) Cross-section and bottom surface of specimen. (b) drawing of marked fragment in cross-section. Bed sole. Note the absence of deformation of layers over the fossil.

Beltanelloides imprints have a broad stratigraphic distribution, from the Lyamtsa Formation, where these fossils occur in beds of massive clays with thin interbedded layers of sandstone, into the lowermost part of the Erga Formation, where imprints occur in sandstone and mudstone interbeds. These fossils are also common at many different levels within the Redkino Series (lower part of the Upper Vendian sequence) of the Eastern European Platform (Sokolov 1973). *Beltanelloides* also occurs in many different facies, supporting the suggestion that they may have been planktonic.

Nemiana simplex

Nemiana simplex was originally described from Podolia, Ukraine, based on specimens from Novodnestrovsky Quarry. This material is from the Yampol beds of the Redkino Regional Stage. The round fossils with a simple morphology and irregular concentric wrinkles, are found on the bottom surfaces (soles) of sandstones.

Nemiana is also known from the upper part of the Vendian sequence at the Zimmie Gory and Vavilushkin Creek localities (in the Erga Formation, of the Kotlin Regional Stage), White Sea region, Russia. Fossils from there occur in sandstones that are channel fills.

The high positive hyporelief imprints with margins that disappear into the sandstone are the most common type of preservation. Such a boundary surface can be traced in cross section to the centre of the imprint, forming an incomplete, sac-like inner cast. Such structure is also characteristic for some '*Beltanelliformis brunseae*' specimens

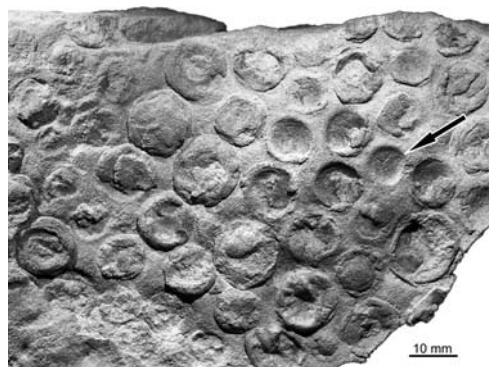


Fig. 8. PIN 3993/5611 *Nemiana simplex*. Upper Vendian sequence, Kotlin Regional Stage, Yorga Formation, third member of the first mesocycle, Arkhangelsk Region, Zimmie Gory Locality, Russia. Bed sole. Arrow marks negative imprints of the upper side of organism.

exhibiting *Nemiana*-type preservation' from the Neoproterozoic sequences of NW Canada (Narbonne & Hofmann 1987).

Sometimes the sediment that infills the casts and those that form the overlaying layer is the same, and sometimes gradational lamination in the cast is present. If the fossils have high relief, no compaction of the sediment in the fossils is visible (Fig. 9). Such is evidence that the sand fill of the inner cavity of *Nemiana* occurred before or just at the time of burial. Another type of preservation indicated that compaction has occurred. In this case, low relief casts with deep irregular wrinkles are characteristic of the fossils. A third type of preservation of *Nemiana simplex* is that of negative relief (both epi- and hyporelief) imprints of the external surface of the organism (Fig. 8). These imprints can be viewed when the cast is broken along lamination.

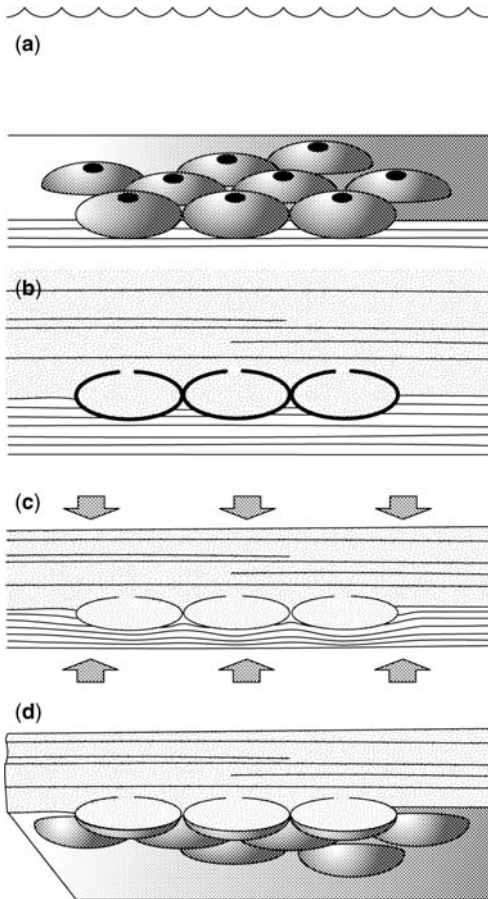


Fig. 9. Taphonomic scenario for preservation of the organism *Nemiana simplex*.

The following sequence may explain *Nemiana* type of preservation (Fig. 9):

- *Nemiana* was a benthic, sac-like organism, round in dorsal view, with an opening on the upper part of the organism. *Nemiana* would have lived on a muddy bottom, partially submerged, often living in clusters (monotaxonomic assemblages).
- Then *Nemiana* individuals were buried *in situ* by incoming sand. The event sediments immediately filled the inner cavities of the organisms.
- In the process of diagenesis, casts of the cavities became solid quite early. Fossils were compressed slightly, so the overlying layers were not deformed or pushed up and over the contours of the fossil remains.
- When found, casts of *Nemiana* occur on the bottom surfaces of sandstones.

Nemiana remains tend to occur in relatively dense groups on the surface of sandstones. In such cases all fossils occur on the same level, some individuals may be in contact along their margins. Some deformation of shape occurs, but individual

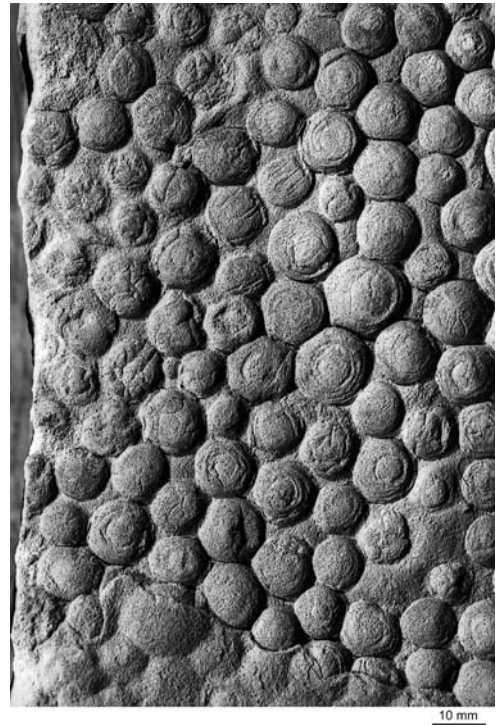


Fig. 10. PIN 3993/5610 *Nemiana simplex*. Upper Vendian sequence, Kotlin Regional Stage, Yorga Formation, third member of the first mesocycle, Archangelsk Region, Zimnie Gory Locality, Russia. Bed sole.

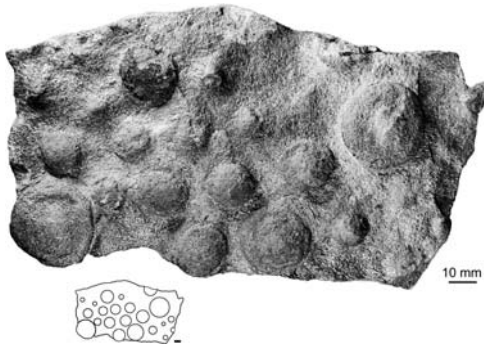


Fig. 11. *Nemiana simplex*. Upper Vendian sequence, Redkino Regional Stage, Mogilev Formation, Podolia, Ukraine. Bed sole.

remains usually retain a rounded polygonal form, similar to the regularity of ‘honeycomb’ structure (Fig. 10). It is important that such order in distribution occurs even when individuals are not in contact (Fig. 11). The distance between individuals remains uniform. It may be interpreted as evidence that *Nemiana* are the remains of benthic sedentary organisms. The absence of any indication of tentacles and the nature of the inner filling of these organisms indicate a sedentary organism. Some modern *Demospongia* are able to agglutinate the sand grains to support their inner fibrous skeleton (Reitner & Worheide 2002) and perhaps this form serves as a good analogue to *Nemiana*. Perhaps *Nemiana simplex* had a lifestyle and level of body organization comparable with that of sponges. The range of facies in which *Nemiana* occurs, when compared to the much broader range of *Beltanelloides* is compelling evidence for a benthic lifestyle of *Nemiana*.

Biometric analysis

Comparison of the distribution of *Beltanelloides* and *Nemiana* illustrate differences with regard to their distribution in the clusters on the rock surfaces. Specimens with multiple imprints of *Nemiana* from the Yampol beds of the Mogilev Formation (Novodnestrovsky Quarry, Podolia, Ukraine) and from the Yorga Formation (Zimnie Gory, White Sea Coast, Russia) were used for this comparison. *Beltanelloides* specimens are from the Lyamtsa and Zimnie Gory Formations (Lyamtsa and Zimnie Gory localities, White Sea Coast, Russia). The mean diameter of each fossil and the shortest distance between the centre of the fossil and the centre of the ‘next-door’ neighbour were measured on each of the specimens. From 20–125 imprints were measured on each specimen (on average 60).

Such measurements illustrated a significant difference between clusters of *Beltanelloides* and *Nemiana* (Fig. 12). Metric statistics (means (D, L) and standard deviations (SD, SL) of distance between imprints and diameter of specimens) do not demonstrate sufficient difference. Differences in the coefficients of variation are statistically significant for the diameter of organisms in the population and coefficients of variation for distance between them (non-metric parameters). *Nemiana* assemblages are well ordered, *Beltanelloides* more randomly distributed. Such well-ordered arrangement in *Nemiana* clusters is observed in both loose and dense distributions. This is suggestive of a sedentary form of life for *Nemiana* that were buried *in situ* contrary to the suggestions that they were allochthonous (Seilacher 1997).

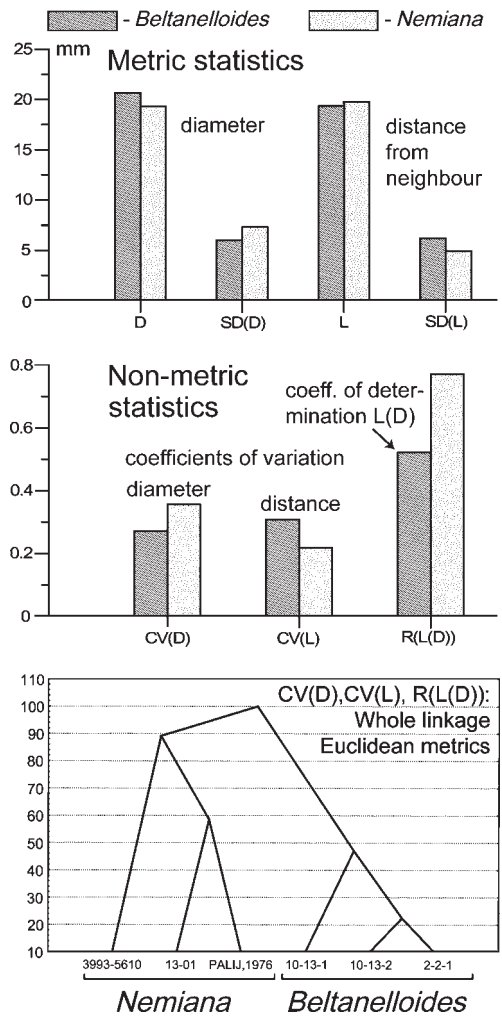


Fig. 12. Biometrical comparison of specimens with numerous *Nemiana* and *Beltanelloides* imprints.

Summary

There are two types of *Beltanelloides* preservation: (1) Double-sided imprints with negative relief and phytolite in clay; and (2) positive (in hyporelief) imprints on the bottom surface of sandstone layers.

Nemiana and *Beltanelloides* were two quite distinct groups of Ediacaran organisms with different morphologies, ecologies, and have produced quite different taphocoenoses.

Beltanelloides were planktonic forms. Fossils of these organisms occur in deposits laid down in many different environments, under both low and high-energy conditions. Fossil-bearing sediments were deposited in middle and upper sublittoral environments, both above and below storm wave base.

Nemiana was a benthic organism that occurred, for the most part, in monotonomic assemblages. It occurs in very specific types of sediments.

Beltanelloides and *Nemiana* form different types of 'death assemblages', the difference being due to their differing lifestyles. This can be documented both by taphonomic and biometric approaches. They do not occur together.

The identification of *Nemiana* and *Beltanelloides* here is quite possible where preservation is good and the samples are large. In the case of *Beltanelloides*, because of its wide geographic distribution, there is good potential for its use as a biostratigraphic tool. It occurs in the Redkino Regional Stage of the Vendian sequence. *Beltanelloides* occurrences from other stratigraphic levels, however, need to be very carefully revised. This study, along with future microstructure analyses of the carbonaceous films associated with this taxon, may lead to a thorough revision of this taxon.

The author is grateful to D. V. Grazhdankin, A. Y. Ivantsov, Y. V. Shuvalova, N. V. Bochkareva and M. A. Fedonkin (Paleontological Institute, Russian Academy of Science, Moscow) for their help with fieldwork and the study of these materials. Special thanks to A. V. Mazin for photographic images for Figs 3, 4, 7, 10, 12. This manuscript has also benefited from comments by P. Vickers-Rich and P. Komarower (Monash University, Australia), and two reviewers, B. MacGabhann and G. Acenolaza. Research was supported by a Russian Fund for Basic Research, grant (RFBR N 02-05-64658) and a Grant of the President (NSH-1790.2003.5). This study is also a part of UNESCO International Geological Correlation Project 493.

References

AKSENOV, E. M., KELLER, B. M., SOKOLOV, B. S., SOLONTSOV, L. S. & SHULGA, P. L. 1978. General

stratigraphic scheme of Upper Precambrian of Russian platform. *Proceedings of the Academy of Sciences of USSR. Series Geological*, **12**, 17–34 [in Russian].

- ASSEVA, E. A. 1988. Fossil remains of Vendian Thallophyta. In: RYABENKO, V. A., ASSEVA, E. A., FURTES, V. V. ET AL. *Biostratigraphy and Paleogeographic Reconstructions of the Precambrian of Ukraine*. Kiev, Naukova dumka, 81–92 [in Russian].
- FEDONKIN, M. A. 1985. Systematic description of Vendian Metazoa. In: SOKOLOV, B. S. & IVANOVSKY, A. B. (eds) *The Vendian System. Vol. 1. Paleontology*. Nauka, 70–106 [in Russian].
- GEHLING, J. G. 1999. Microbial mats in terminal Proterozoic siliciclastics: Ediacaran death masks. *Palaaios*, **14**, 40–57.
- GNULOVSKAYA, M. B., ISTCHENKO, A. A., KOLESNIKOV, CH. M., KORENCHUK, L. V. & UDALTSOV, A. P. 1988. *Vendotaenids of the Eastern-European Platform*. Nauka [in Russian].
- GRAZHDANKIN, D. V. 2000. The Ediacaran Genus *Inaria*: A Taphonomic/Morphodynamic analysis. *Neues Jahrbuch für Mineralogie. Geologie und Paläontologie*, **216**, 1–34.
- GRAZHDANKIN, D. V. 2003. Structure and depositional environment of the Vendian Complex in the South-eastern White Sea Area. *Stratigraphy and Geological Correlation*, **11**, 313–331.
- GUREEV, JU. A. 1988. Soft-bodied fauna of Vendian. In: RYABENKO, V. A., ASSEVA, E. A., FURTES, V. V. ET AL. *Biostratigraphy and Paleogeographic Reconstructions of the Precambrian of Ukraine*. Naukova dumka, Kiev, 81–92 [in Russian].
- JENKINS, R. J. F. 1992. Functional and Ecological Aspects of the Ediacarian Assemblages. In: LIPPS, J. H. & SIGNOR, P. W. (eds) *Origin and Early Evolution of the Metazoa*. Plenum Press, 13–176.
- LAFLAMME, M., NARBONNE, G. M. & ANDERSON, M. M. 2004. Morphometric analysis of the Ediacaran frond *Charniodiscus* from the Mistaken Point Formation, Newfoundland. *Journal of Paleontology*, **78**, 827–837.
- NARBONNE, G. M. & HOFMANN, H. J. 1987. Ediacaran biota of Wernecke Mountains, Yukon, Canada. *Palaentology*, **30**, 647–676.
- PALIJ, V. M. 1976. Remains of soft-bodied and trace fossils from deposits of Upper Precambrian and Lower Cambrian. In: RYABENKO, V. A. (ed.) *Paleontology and Stratigraphy of Upper Precambrian and Lower Paleozoic of the Southwest of Eastern-European Platform*. Naukova dumka, 63–76 [in Russian].
- REITNER, J. & WORHEIDE, G. 2002. Non-Lithistid fossil Demospongiae—Origins of their palaeobiodiversity and highlights in history of preservation. In: HOOPER, J. N. & VAN SOEST, J. N. (eds) *Systema Porifera: A Guide to the Classification of Sponges*. Kluwer Academic, New York, 52–68.
- SEILACHER, A. 1997. Sandkorallen ein ausgestorbener Lebensformtyp. *Fossilien*, **2**, 79–84.
- SEILACHER, A., GRAZHDANKIN, D. & LEGOUTA, A. 2003. Ediacaran biota: The dawn of animal life in

- the shadow of giant protists. *Palaeontological Research*, 7(1), 43–54.
- SOKOLOV, B. S. 1965. The ancient deposits of Early Cambrian and *Sabelliditides*. In: SOKOLOV, B. S. (ed.) *Symposium on Paleontology of Precambrian and Early Cambrian*. Novosibirsk, 78–92 [in Russian].
- SOKOLOV, B. S. 1972. Precambrian biosphere in the light of paleontological data. *Vestnik Akademii Nauk SSSR*, 48–54 [in Russian].
- SOKOLOV, B. S. 1973. Vendian of Northern Eurasia. In: PITHCER, M. G. (ed.) *Arctic Geology. Proceedings of the Second International Symposium on Arctic Geology*, 204–218.
- SOKOLOV, B. S. 1977. Organic world of the earth on the way to the Proterozoic differentiation. In: BELOVA, E. V. ET AL. (eds) *250 years of Russian Academy of Sciences*. Nauka, 423–444 [in Russian].

Upper Vendian assemblages of carbonaceous micro- and macrofossils in the White Sea Region: systematic and biostratigraphic aspects

M. V. LEONOV & A. L. RAGOZINA

Paleontological Institute Russian Academy of Sciences, 117868 Profsoyuznaya Street, 123, Moscow, Russia 117997 (e-mail: maxleon@narod.ru)

Abstract: Complexes of microfossils, consisting of spheromorphic acritarchs, and coccoid and filamentous cyanobacterial colonies, characterize distinct levels of the Upper Vendian sequence (Ediacaran) of the White Sea region. Three discrete assemblages of algal macrofossils have been recognized in this succession. The oldest assemblage is characteristic of the Lyamtsa Formation of Early Redkino age, the middle assemblage, the Verkhovka, Zimmegory and lowermost Yorga formations of Late Redkino age, and (provisionally) the youngest assemblage, preserved in the upper part of the Yorga Formation of Early Kotlin age. The Vendian succession studied here can be correlated with a similar succession in the Podolia region of Ukraine.

The study of terminal Neoproterozoic rocks on the Eastern European platform (Aksenov *et al.* 1978) has resulted in the recognition of two stratigraphic subdivisions of the upper part of the Vendian sequence (Ediacaran), which represent so-called 'regional stages'. These regional stages (the Redkino and Kotlin stages) can be recognized across the Eastern European Platform, from Podolia in the southwest to the White Sea Region in the north. This study presents data on the distribution of carbonaceous microfossils to assist in a more detailed correlation across this succession. Similarities of consecutive successions of cyanobacterial and algal fossils between such distant Neoproterozoic sections may be useful for more extensive global correlation using biostratigraphic methods.

Organic microfossils and cyanobacterial assemblages

Different types of organically preserved fossils characterize the Vendian succession on the Eastern European Platform. The more abundant forms are represented by organic biofilms. Numerous filamentous microfossils of cyanobacterial nature, spheromorphic acritarchs and coccoid colonial forms are preserved on the surfaces of these biofilms. The basic components of the cyanobacterial communities are members of the genus *Siphonophycus* Schopf, 1968 and *Oscillatoropsis* Schopf, 1968. The minor components include *Palaeolyngbia* Schopf, 1968 and *Polytrichoides* Hermann, 1974. Filamentous forms in the genus *Siphonophycus* Schopf, 1968 form numerous clusters on the surface of thin organic films (Fig. 1a). They are represented by thin, elastic, smoothly curved or randomly twisted,

non-branched tubular sheaths. These sheaths have a constant width. The absence of transverse cell walls in the trichome is another characteristic feature of these forms. The width of the filaments varies from 2–20 μm , the most common dimension 8–12 μm . Microfossils are similar to recent mat-producing homogniacean cyanobacteria in the genera *Microcoleus* and *Phormidium*. These forms have a wide distribution in marine and fresh waters today.

Filamentous microfossils in the genus *Oscillatoropsis* are characterized by a clearly visible cellular structure (Fig. 1b). They are found both as individuals and as fascicular clusters of filaments. The width of the sheaths varies from 4–6 to 30–40 μm . These microfossils resemble the recent cyanobacteria *Oscillatoria*.

The remains of relatively large trichomes (40–60 μm in width) are referred to the genus *Palaeolyngbia* (Schopf 1968) (Fig. 1c). Such sheaths include uniserial cell filaments. The wall of the cells does not closely adjoin the inner surfaces of the sheaths. Cells have a keg-like form and narrow at the point of contact with neighbouring cells.

Microfossils referred to genus *Ostiana* (Fig. 1d) occur in the Zimmie Gory beds of the Ust'-Pinega Formation. These forms are represented by thin organic films, $>1\text{ cm}^2$. There may be several hundred cells in a single colony. Cells have a spherical or ellipsoid form. The diameter of the cells varies from 5–18 μm . Cells occur in individual envelopes that are broader. The cells occurring in a colony have an open distribution, although sometimes (in the cases of dense clusters) the spherical shape of cells can be deformed. Recent analogues for these forms include chroococcalean cyanobacteria of the genera *Microcystis* and *Aphanothece*.

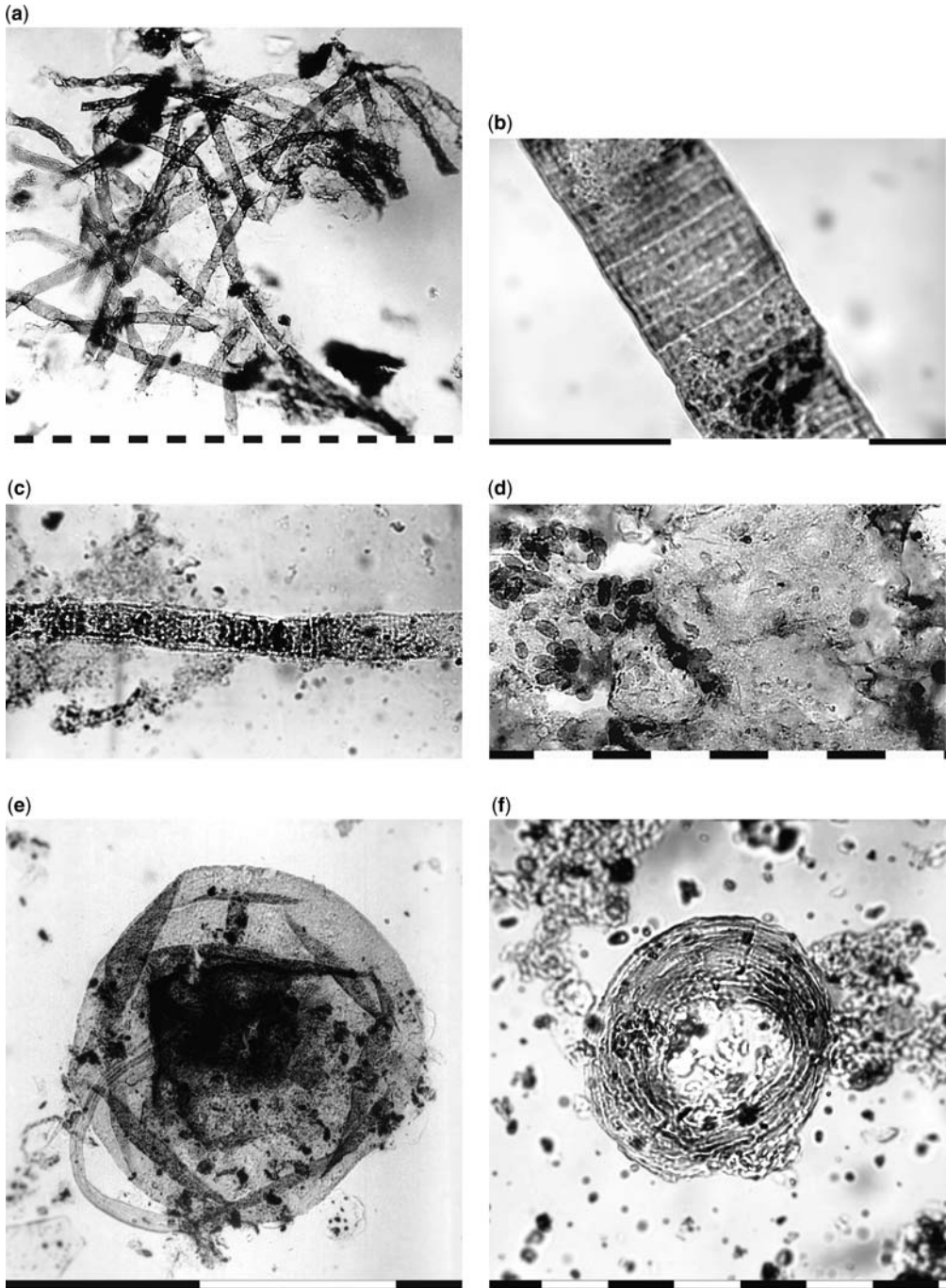


Fig. 1. Microfossils from Upper Vendian succession of the North of Arkhangelsk region. (a) *Syphonophycus* Schopf, 1968. Scale 10 μm . (b) *Oscillatotiopsis* Schopf, 1968. Scale 50 μm . (c) *Palaeolyngbia* aff. *catenata*. Scale 100 μm . (d) Fragments of the colonial microfossils *Ostiana* on the surface of the biofilms. Scale 10 μm . (e) *Leiosphaeridia minutissima*. Scale 100 μm . (f) *Volyniella valdaica*. Scale 10 μm .

Stratigraphic subdivisions (Grazhdankin 2003)		Macrophytes (Ragozina 2001; Gnilovskaya 2003; Leonov 2003)		
Vendian	Cam-brian	Rov-no	Disperse organic films of type h Disperse organic films of type l <i>Archyfasma</i> sp. Gnil., 2003 <i>Eoholynia fruticulosa</i> A. Istchenko in Gnilovskaya et al., 1988 <i>Beltanelloides sorichevae</i> Sokolov, 1965 <i>Serebrina crustacea</i> A. Istchenko, 1988 Organic films of type f <i>Eoholynia moscuensis</i> Gnil., 1975 <i>Pliitela composita</i> Aseeva, 1976	
				Kotlin
	Yorga			
	Redkino	Zimnie Gory		
		Verkhovka		
		Lyamtsa		

Fig. 2. Distribution of algal microfossils in the Upper Vendian succession of the White Sea. Taxa written in bold are significant for regional biostratigraphic correlation. Roman numbers in circles mark assemblages mentioned in text.

Two types of cyanobacterial colonies (monotaxonomic assemblages of *Ostiana* and polytaxonomic assemblages of filamentous microfossils) are known to occur in the Upper Vendian succession that crops out in the Suzda and Zimnie Gory beds of the Ust'-Pinega Formation. These two types of colonies possibly occupied different habitats in a shallow epicontinental marine basin of Late Ediacaran age.

Spheromorphic acritarchs also occur in the Zimnie Gory beds of the Ust'-Pinega Formation (Zimnie Gory locality, boreholes 1000 and 1000-1). They are represented by thin-walled forms with smooth or slightly sculptured shagrinated surfaces and few collapse folds. These forms are referred to the genus *Leiosphaeridia* (*Leiosphaeridia* minor, *L. pelicula*, *L. aperta*, *L. effusa*, *L. bituminosa*, *L. magna*, *L. minutissima* (Fig. 1e). Microfossils of the genera *Stictosphaeridium* and *Orygmato-sphaeridium* occur infrequently. *Volyniella valdaica* is another distinctive form of microfossil (Fig. 1f). These species characterize the Upper Vendian deposits (Redkino Regional Stage) of the Eastern European Platform.

Metaphyta

Macroscopic algal remains are relatively rare and concentrated in the more fine-grained members of the sequences noted above. Three assemblages of organically preserved macrofossils can be recognized at present (Fig. 2).

The first complex is typical of the lowermost Lyamtsa Formation. It includes small bush-shaped thalli of *Eoholynia fruticulosa* (Istchenko 1983) (Fig. 3e), round phytollems of *Beltanelloides sorichevae* with thin concentric wrinkles along their periphery (Fig. 3f) and relatively large, strap-like phytollems of *Archyfasma* sp. (Fig. 3a). The latter genus has a simple, ribbon-like morphology, a non-branched thallus, but tissue grade organization with thallus differentiation and a multilayered structure. Phytollems of archyfasmalean algae consist of a cortex layer with papillae and an inner layer of longitudinally oriented filaments (Gnilovskaya 2003). The level of complexity of these thalli is comparable with more highly complex living algae. Dispersed organic biofilms of types 'h' (Fig. 3c) and 'l' (Fig. 3b) (classification by Aseeva 1988a) were also found. This complex of macrofossils may be correlated with ones from the Mogilev Formation of Podolia (Ukraine) (Aseeva 1988a; Gnilovskaya et al. 1988). The stratigraphic level of this first association corresponds with the lower and middle part of the Upper Vendian Redkino Regional Stage.

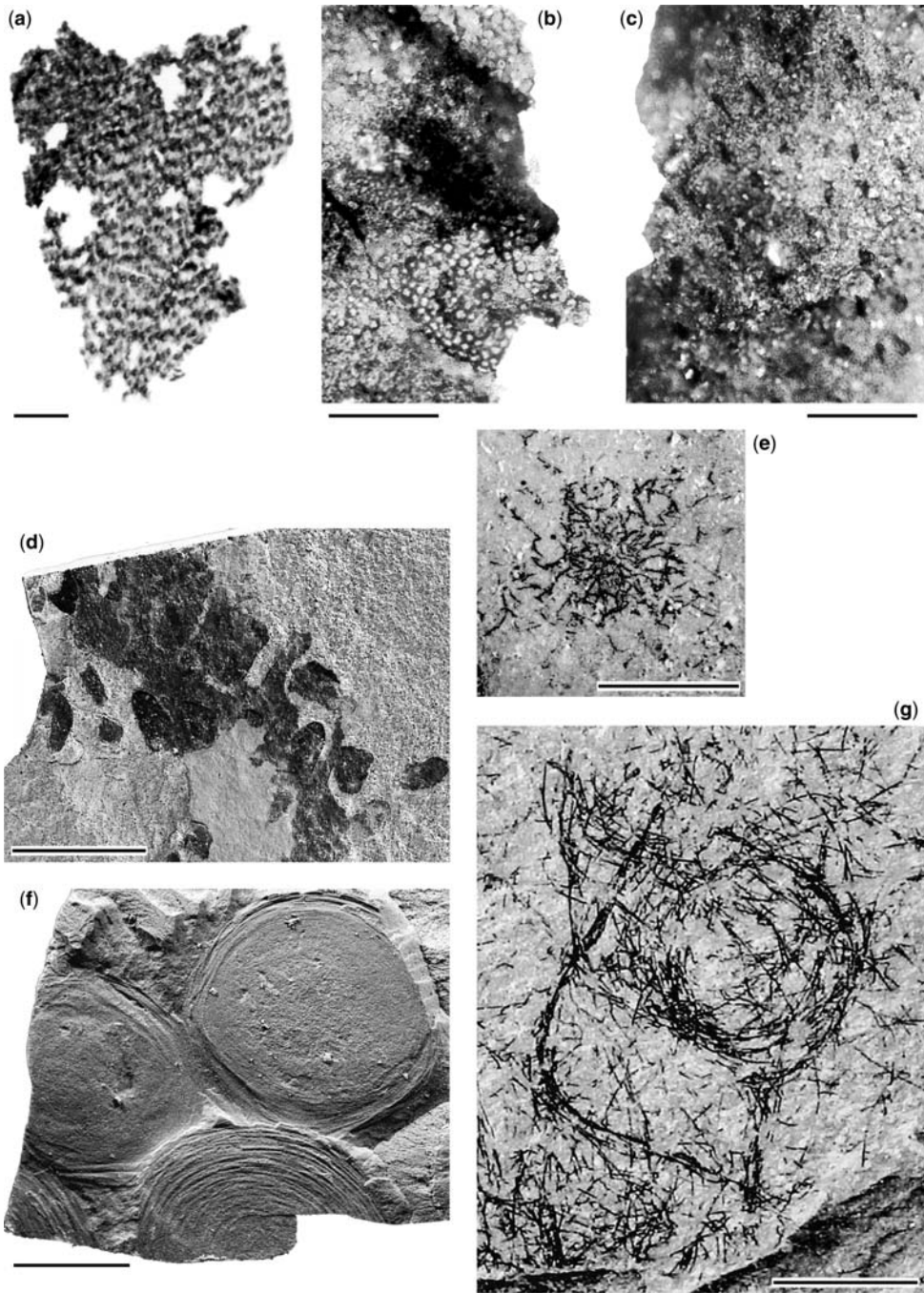


Fig. 3. Macroscopic algae from the Upper Vendian succession of the North of Arkhangelsk region. (a) *Archyfasma* sp. Fragment of macerated cortex layer of phytoleima with papillar structure, lower part of Redkino Regional Stage, Lyamtsa Formation. Scale 1 mm. (b, c) Disperse organic films—fragments of algal tissues. Lower part of Redkino Regional Stage, Lyamtsa Formation. Scale 100 μm . (b) film of type 'l'. (c) film of type 'h' (classification by Aseeva 1988a). (d) *Serebrina crustacea*, crust-like thalli on the rock surface, middle part of Redkino Regional Stage, Verkhovka Formation. Scale 10 mm. (e) *Eoholynia* cf. *fruticulosa*, lower part of Redkino Regional Stage, Lyamtsa Formation. Scale 1 mm. (f) *Beltanelloides sorichevae*, imprints of phytoleima on the rock surface, lower part of Redkino Regional Stage, Lyamtsa Formation. Scale 5 mm. (g) *Pilitella composita*, Kotlin Regional Stage, Yorga Formation. Scale 10 mm.

White Sea region		Regional Stages		Podolia	
Microfossils (Ragozina & Sivertseva, 1985, Ragozina & Leonov, 2004)	Macrophytes (Ragozina 2001, Gnilovskaya 2003, Leonov 2003)	Formations	Groups	Macrophytes (Gnilovskaya et al. 1988, Aseeva 1988)	Microfossils (Aseeva 1988)
		Mela	Kotlino Kantlovka	-	<i>Stictosphaeridium implexum</i> Tim.; <i>Bicuspidata funifirmis</i> As.; <i>Leiosphaeridia volynica</i> Tim.; <i>Cochleatina canilovica</i> ; <i>Cochleatina rara</i> (Pask.); <i>Leiosphaeridia undulata</i> Tim.; <i>Podoliella irregulare</i> Tim.; <i>Studenicia bacolica</i> As.; <i>Orygmatosphaeridium</i> sp.
<i>Oscillatoriopsis rhomboidalis</i> Shverzeva, 1985	<i>Pillitella composita</i> Aseeva, 1976	Yorga	Kotlino Nago-nyany	<i>Pillitella composita</i> As. 1976; <i>Kalusina</i> sp.; <i>Fusosquamula viasovi</i> Aseeva, 1976; <i>Vendotaenia antiqua</i> Gril., 1974	<i>Trachysphaeridium bavliense</i> (Schep.); <i>Trachysphaeridium magnum</i> (Schep.); <i>Flagellis tenuis</i> As.
<i>Oscillatorites wernadskii</i> Schep.; <i>Stratimorphis plana</i> As.; <i>Leiotrichoides</i> sp.; <i>Polytrichoides lineatus</i> Herm.; <i>Tortunema sibirica</i> Herm.; <i>Oscillatoriopsis magna</i> Tynni et Bonner; <i>Oscillatoriopsis funiformis</i> sp. nov.; <i>Palaeolyngbia</i> sp.; <i>L. culta</i> (Andr.); <i>L. magnum</i> (Schep.); <i>V. sp.</i> ; <i>Oscillatoriopsis constricta</i> T. et B.	<i>Serbrina crustacea</i> A. Istchenko in Gnilovskaya et al., 1988, <i>Eoholynia mosquensis</i> Gril., 1975	Zimnie Gory	Redkino Yaryshev	<i>Serbrina crustacea</i> A. Istchenko in Gnilovskaya et al., 1988, <i>Eoholynia</i> sp., <i>Eoholynia fruticulosa</i> A. Istchenko in Gnilovskaya et al., 1988, <i>Morania zinkovi</i> A. Istchenko in Gnilovskaya et al., 1988; <i>Ljadovites</i> A. Istchenko, 1983; <i>Beltanelloides podolicus</i> A. Istchenko in Gnilovskaya et al., 1988.	<i>Oscillatoriopsis</i> sp.; <i>Oscillatorites wernadskii</i> Schep.; <i>Palaeolyngbia catenata</i> Herm.; <i>Striatella coriacea</i> As.; <i>Polytrichoides</i> sp.; <i>Ljadovia perforata</i> As.; <i>Leiosphaeridia pruniformis</i> As.; <i>Arctocellularia</i> sp.; <i>Halythrix</i> sp.; <i>Taenitrichoides jaryshevicus</i> As.; <i>Tubulosa corrugata</i> As.; <i>Trematosphaeridium hoffdahlili</i> Tim.; <i>Nucellosphaeridium</i> sp.; <i>Leiosphaeridia jacutica</i> (Tim.);
<i>Oscillatoriopsis</i> sp., <i>Palaeolyngbia catenata</i> Herman, <i>Polytrichoides</i> sp., <i>Striatella coriacea</i> As.; <i>Symplassosphaeridium</i> sp.; <i>Leiosphaeridia gigantea</i> (Schep.); <i>Baviniella faveolata</i> Schep.; <i>Leiminuscula minuta</i> Naum.; <i>Leiotrichoides typicus</i> Herm.; <i>Leiosphaeridia effusa</i> (Schep.)		Zimnie Verkhovka			
<i>Rudnjana</i> Golub; <i>Volyniella valdaica</i> (Schep.) As.; <i>Trachysphaeridium partalum</i> (Schep.); <i>Synsphaeridium bullatum</i> Andr.; <i>Pterospermopsis</i> sp.; <i>Leiosphaeridia bitumosa</i> Tim.; <i>Stictosphaeridium pectinatum</i> Tim.; <i>Gloecospermopsis</i> sp.; <i>Leiosphaeridia pelucida</i> (Schep.); <i>Trachysphaeridium</i> Istchenko, 1988; <i>Beltanelloides bavliense</i> (Schep.); <i>Stictosphaeridium sinaptoculiferum</i> Tim.; <i>Orygmatosphaeridium sorichevae</i> Sokolov, 1965; <i>rubiginosum</i> Andr.; <i>Synsphaeridium sorediforme</i> Tim.; <i>Synsphaeridium conglutinatum</i> Tim.	disperse organic films of types "h", "l", "i"	Ljantasa	Redkino Mogilev	disperse organic films of types "g", "h", "l", "i"	<i>Rudnjana</i> Gol.; <i>Volyniella valdaica</i> (Schep.) As.; <i>Trachysphaeridium partalum</i> (Schep.); <i>Leiosphaeridia minor</i> (Schep.); <i>Leiosphaeridia pedicula</i> (Schep.); <i>Leiosphaeridia gigantea</i> (Schep.); <i>Leiosphaeridia asapha</i> (Tim.) As.; <i>Stictosphaeridium</i> sp.; <i>Leiotrichoides typicus</i> Herm.; <i>Stratimorphis rubiginosum</i> (Andr.) As.; <i>Oscillatorites wernadskii</i> Schep.; <i>Stratimorphis plana</i> As.; <i>Trachytrichoides ovalis</i> Herm.; <i>Polycavita bullata</i> (Andr.) As.; <i>Tubulosa jampolica</i> (Ass.) As.; <i>Leiosphaeridia lacata</i> (Tim.) As.; <i>Circumella mogilevica</i> As.; <i>Orygmatosphaeridium flexuosum</i> (Tim.) As.; <i>Orygmatosphaeridium unduratum</i> As.; <i>Leiotrichoides gracilis</i> Pjat.; <i>Polycavita concentrica</i> As.
			Redkino Laplandian		<i>Kladinella sinica</i> Tim., <i>Leiosphaeridia parva</i> As.

Fig. 4. Provisional chart: biostratigraphic correlation of the White Sea and Podolia Upper Vendian successions.

The second association is present at several levels on the Verkhovka Formation (Yarnema, Agma, Solza and Suzma localities) and the lower member of Zimnegory Formation (Zimnie Gory locality). The most abundant forms are rounded or ellipsoidal crust-like thalli of *Serebrina crustacea* (Istchenko 1983) (Fig. 3d). Diameters of these fossils vary from 0.9–12 mm. Bush-shaped thalli described as *Eoholynia moscuensis* Gnilovskaya, 1975 are also found. Dispersed fragments of these thalli have a close similarity to the genus *Polysphaeroides* Timofeev (Aseeva 1988b) and are also found in samples from the lower Zimnegory Formation level. Such fossils are found in several assemblages, both *in situ* and in allochthonous oryctocoenoses. The large masses of cyanobacterial biofilms with filamentous microfossils were found with allochthonous clusters of this fossil. Also phytollems of *Beltanelloides sorichevae* were observed at different levels. This association is similar to assemblages observed in the Yaryshev Formation of Podolia and the Redkino Formation of the Moscow Syncline (Gnilovskaya 1975; Istchenko 1983; Gnilovskaya *et al.* 1988), characterizing the upper part of the Redkino Regional Stage.

The third association occurs in the lower and middle mesocycles of the Yorga Formation (Zimnie Gory and Bolshaya Torozhma localities). Thin dichotomous, strap-like organic films are present. Their morphology is similar to that of some fossils in the family Vendotaeniaceae (Gnilovskaya *et al.* 1988) but this observation requires further study of microstructure for confirmation. Relatively large, bush-shaped algae, assigned to *Pilitela composita* Aseeva, 1988a (Fig. 3g) were also found at this level, forms that also characterize the Kalus beds of the Upper Vendian Nagoryany Formation of Podolia.

Summary

Almost all of the Yorga Formation (perhaps omitting the lowermost member) appears to be of early Kotlin age. This is significant because of the rich association of soft-bodied metazoans that survive into Kotlin time. It is possible now to biostratigraphically correlate between the Upper Vendian successions of Podolia (Ukraine) and the White Sea region on the basis of these macro- and microfossils (Fig. 4). It is significant that the order of appearance of macrofossil taxa is similar in regions of sufficiently different sedimentological history, often lacking corresponding facies. In future, studies of several known assemblages may allow a much more detailed biostratigraphic

subdivision of the Upper Vendian sequence, and this may have a regional or even a global application.

The research was supported by a Russian Fund for Basic Research, grant (RFBR N 02-05-64658) and a Grant from the President (NSH—1790.2003.5). Thanks are due to our reviewers, K. Grey and C.-W. Li for their constructive comments on the manuscript.

References

- AKSENOV, E. M., KELLER, B. M., SOKOLOV, B. S., SOLONTSOV, L. F. & SHULGA, P. L. 1978. General stratigraphic scheme of Upper Precambrian of Russian platform. *Proceedings of the Academy of Sciences of USSR Geological Series*, **12**, 17–34 [in Russian].
- ASEEVA, E. A. 1976. Macroscopic algae. In: RYABENKO, V. A. (ed.) *Paleontology and Stratigraphy of Upper Precambrian and Lower Paleozoic of the south-west of the Eastern European platform*. Naukova Dumka, Kiev, 56–58 [in Russian].
- ASEEVA, E. A. 1988a. Fossil remains of Vendian Thallophyta. In: *Biostratigraphy and Paleogeographic Reconstructions of the Precambrian of Ukraine*. Naukova dumka, Kiev, 81–92 [in Russian].
- ASEEVA, E. A. 1988b. Microfossils in Upper Precambrian. In: *Biostratigraphy and Paleogeographic Reconstructions of the Precambrian of Ukraine*. Naukova dumka, Kiev, 93–102 [in Russian].
- GNILOVSKAYA, M. B. 1975. New data about the nature of Vendotaenides. *Reports of the Academy of Sciences of the USSR*, **221**, 953–955 [in Russian].
- GNILOVSKAYA, M. B. 2003. About the ancient tissue organisation of the Precambrian (Vendian) algae. *Paleontological Journal*, **2**, 98–104 [in Russian].
- GNILOVSKAYA, M. B., ISTCHENKO, A. A., KOLESNIKOV, CH. M., KORENCHUK, L. V. & UDALTSOV, A. P. 1988. *Vendotaenids of the Eastern-European platform*. Nauka, 141 [in Russian].
- GRAZHDANKIN, D. V. 2003. Structure and depositional environment of the Vendian Complex in the South-eastern White Sea Area. *Stratigraphy and Geological Correlation*, **11**, 313–331.
- ISTCHENKO, A. A. 1983. To the question about stages of development of the algal flora of the south-western part of Eastern European platform. In: *Fossil fauna and flora of the Ukraine. Materials of III session of the Ukrainian Paleontological Society*. Naukova dumka, 70–75 [in Russian].
- LEONOV, M. V. 2003. Vendian cyanobacterial communities as a preservation factor of fossil eucaryotic algal remains. *Instruments, Methods and Missions for Astrobiology VI. Proceeding of SPIE*, **4939**, 47–52.
- RAGOZINA, A. L. 2001. Bush-shaped *Eoholynia* and tubular *Calyptina* in Upper Vendian of the north of Arkhangelsk region. In: *Evolution of life on the Earth. Materials of II International symposium 12–15 November 2001*, 151–154 [in Russian].
- RAGOZINA, A. L. & LEONOV, M. V. 2004. Macrophytes and organic-walled microfossils of Upper Vendian of

- south-east White Sea. In: *Biosphere Processes: Paleontology and Stratigraphy. Thesis of XLX session of Russian Paleontological Society*, 107–108 [in Russian].
- RAGOZINA, A. L. & SIVERTSEVA, I. A. 1985. Microfossils of Valday Group of North-West of Arkhangelsk region. In: SOKOLOV, B. S. & IVANOVSKIY, A. B. (eds) *Vendian System*, **1**, 139–144 [in Russian].
- SCHOPF, J. W. 1968. Microflora of the Bitter Springs Formation, late Precambrian, Central Australia. *Journal of Paleontology*, **42**, 651–688.
- SOKOLOV, B. S. 1965. The ancient deposits of lower Cambrian and sabelletids. In: *All-Union symposium on problem of Precambrian and Lower Cambrian*, 25–30 October 1965. Novosibirsk, IGG SB RAS, 78–91 [in Russian].

Ediacaria booleyi: weeded from the Garden of Ediacara?

B. A. MACGABHANN¹, J. MURRAY² & C. NICHOLAS³

¹*Department of Earth and Ocean Sciences, National University of Ireland, Galway, University Road, Galway, Ireland (e-mail: b.macgabhan1@nuigalway.ie)*

²*Department of Earth and Ocean Sciences, National University of Ireland, Galway, University Road, Galway, Ireland*

³*Department of Geology, Trinity College, University of Dublin, Dublin 2, Ireland*

Abstract: Sole markings from the Upper Cambrian Booley Bay Formation at Booley Bay, Co. Wexford, Ireland, previously described as the Ediacaran-type fossil *Ediacaria booleyi* appear to possess a number of morphological characteristics which are not consistent with assignment to the genus *Ediacaria*, nor any other known Ediacaran taxon. An inorganic origin for the structures has been proposed by several workers; we tentatively consider them to be at least in part organic, and are currently working to evaluate this hypothesis critically. If organic, the organisms must have had a density similar to that of the sediment in which they were emplaced, and to survive the transport process, they must have had a rigid integument. Neither of these properties appears to be consistent with an interpretation as an Ediacaran-type organism. We suggest here that the Booley Bay specimens should be removed from the genus *Ediacaria*. If *Ediacaria booleyi* is not related to known Ediacaran organisms, this would remove a key aspect of the argument against a mass extinction at the Precambrian/Cambrian boundary.

Theories about the demise of the Ediacaran biota have generally centred around concepts of physical or biomechanical shortcomings in the face of competition from newly evolving and diversifying metazoan phyla or an inability to adapt to changing environments in the Early Cambrian (e.g. Dzik 2005). Such ideas have led to the Ediacaran biota being described as a failed evolutionary experiment (e.g. Narbonne 1998). The general paucity of Ediacaran-type fossils in rocks of Early Cambrian and younger age seems to support this idea and has been considered indirect evidence for a Terminal Neoproterozoic mass extinction (Seilacher 1984). This event could have wiped out entire Precambrian ecosystems with trophic structures unlike any modern day marine food chains. However, evidence of Ediacaran-type organisms in rocks younger than latest Precambrian might indicate that this is not the case. The presence of fossils of Ediacaran aspect across the Precambrian–Cambrian boundary might instead suggest that these enigmatic organisms did not go extinct simultaneously in a mass extinction event, but perhaps were already in gradual decline: they simply dwindled out during the earliest Phanerozoic. Such an argument appears to be supported by just such an Ediacaran-type biota from Booley Bay in Co. Wexford, Ireland (Crimes *et al.* 1995) (Fig. 1). Dated to the latter part of the Late Cambrian by acritarch biostratigraphy (Moczydlowska & Crimes 1995), it has been remarked that this occurrence ‘may well be the

death knell for the idea that the Ediacara fauna was a failed evolutionary experiment’ (Palmer 1996, p. 114). The Booley Bay locality, in the Avalon Terrane of south-eastern Ireland, is unusual for not only its age, but also in the way fossils are preserved. Organisms appear to have been transported downslope into a deep marine environment by turbidity currents, impacted into the underlying mud, and there decayed, leaving casts which were then infilled by sand (Crimes *et al.* 1995) (Fig. 2). Similar preservation has not been observed in any other Ediacaran fossil locality to date. Given the significance of this site, a thorough reinvestigation of the sedimentology, palaeoenvironments and palaeontology has been in progress since March 2003. This paper presents initial results and sets out targets and aims currently being pursued.

Sedimentological setting

The first detailed work on the Lower Palaeozoic geology of the Booley Bay area was undertaken by Gardiner (1967), who established the stratigraphic succession. He assigned the pre-Ordovician rocks of the area to the Booley Bay Formation and recognized six distinctive lithofacies (Table 1).

The Booley Bay section is dominated by Facies C, but also contains elements of Facies A and E. Sole structures are common, and in particular Gardiner (1967) noted the presence of ‘bulbous

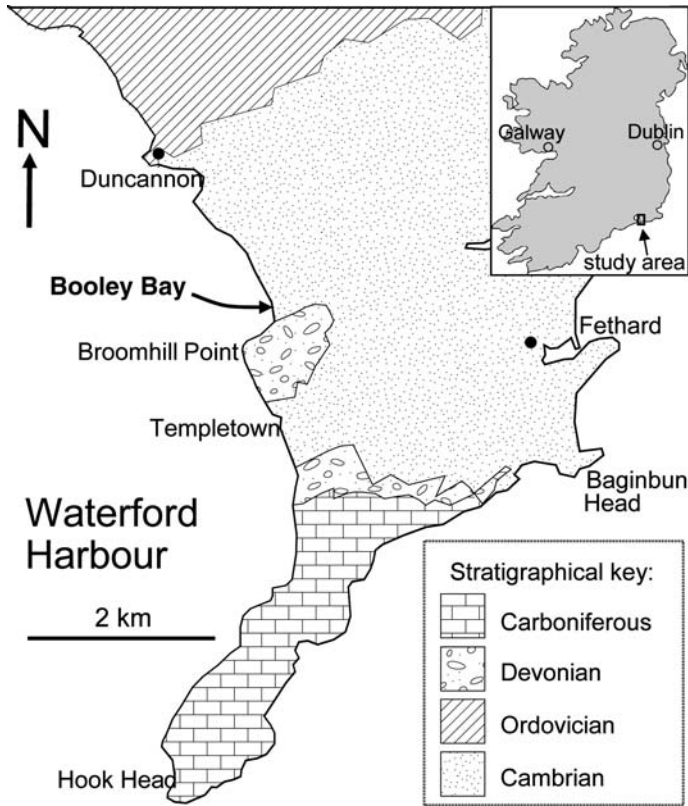


Fig. 1. Location of the study area, with regional geology.

flute moulds' and 'V-shaped flute moulds', which occurred only in Booley Bay. No body fossils were recorded from the formation. (Crimes *et al.* 1995) re-described several of these sole structures from Booley Bay as Ediacaran-type fossils. Two genera were reported, *Ediacaria* and *Nimbia*, both discoidal in shape.

The sediments in which these structures occur are thin to medium, repetitively interbedded siltstones and mudstones. Siltstone beds are generally 1–10 cm thick; mudstone beds are generally similar in thickness, but metre-scale mudstone units also occur (Facies A of Gardiner 1967). Bedding is generally tabular and laterally continuous over several tens of metres (the scale of the outcrop) and is overturned, dipping at an angle of approximately 45°, exposing the soles. The sediments were interpreted by Gardiner (1967) as distal turbidites, and all subsequent workers have closely followed this interpretation (e.g. Tietzsch-Tyler *et al.* 1994). Sole structures visible in the section include gutter casts (Fig. 3a) and flute marks (Fig. 3b), which indicate a unidirectional palaeocurrent flowing to the west. This is supported

to some extent by ripple cross-lamination (Fig. 4a). Present-day strike is approximately parallel to this direction. Hummocky-like bedding surfaces are present in some parts of the section (Fig. 4b); whilst these could be interpreted as 'hummocky cross-stratification' often associated with forming above storm wave base, there is a greater bulk of surrounding field evidence to suggest that they represent sub-critical flow in the turbidity current during emplacement. Interestingly, this flow regime is best developed in the most fossiliferous parts of the section and thus may have played a role in fossil preservation. Many beds also show evidence of liquefaction and convolution, perhaps indicating a tectonically active setting (Fig. 4c).

Structures similar to those described elsewhere (e.g. Hagadorn & Bottjer 1997; Gehling 1999) as microbially influenced sedimentary structures (for example 'wrinkle marks') are common in the section. These are currently under investigation by S. Burke and P. Orr of University College Dublin (Burke & Orr 2004, 2005), and thus will not be discussed further herein. Microbial mats have been proposed to assist in the preservation of Ediacaran

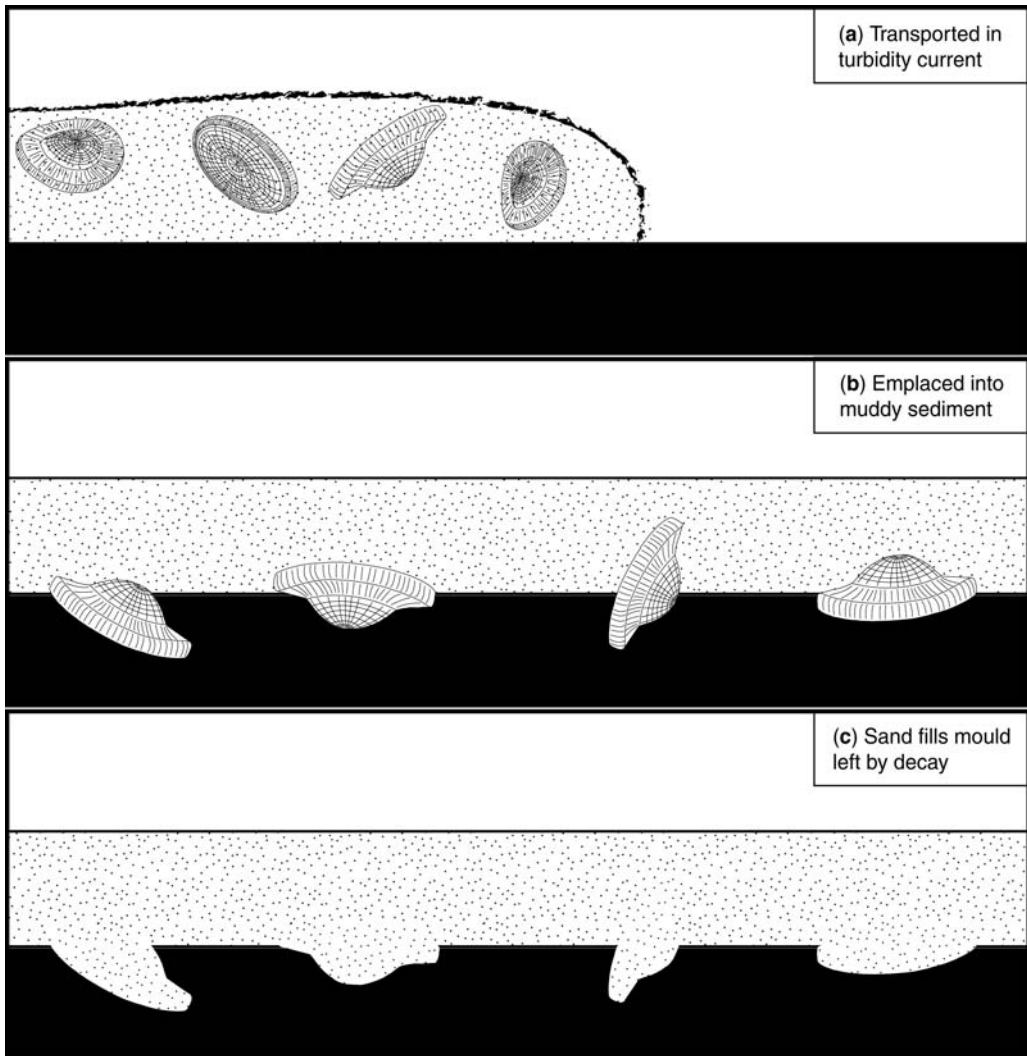


Fig. 2. Taphonomic model for *E. booleyi* proposed by Crimes *et al.* (1995).

fossils (Gehling 1999) and so their presence at Booley Bay might have facilitated Ediacaran-style preservation to occur. However, microbial binding of soft sediment may also have helped form and retain some of the clear sedimentary structures present in the section.

Ediacaria booleyi

Specimens of the discoidal Ediacaran fossil *Ediacaria* were first reported from the Booley Bay Formation at Booley Bay, SE Ireland by (Crimes *et al.* 1995); these were assigned to a new species, *E. booleyi*. As diagnosed, the new species differed quite considerably from the type species,

E. flindersi. Aside from superficial variations in external ornamentation, the specimens of *E. booleyi* were preserved as three-dimensional positive hyporelief casts on the bases of siltstone beds overlying dark mudstone layers. This led (Crimes *et al.* 1995) to propose that it must have been in possession of a rigid exoskeleton to allow appreciable sediment penetration. This presented an intriguing reconstruction and interpretation for the specimens. Perhaps here in the Late Cambrian were the last vestiges of a once widespread biota forced to live in deeper water due to competition from newly evolved metazoans exploiting shallow shelf environments. Marginalization and competitive pressure may also have been responsible for these

Table 1. *Facies elements of the Booley Bay Formation, as described by Gardiner (1967)*

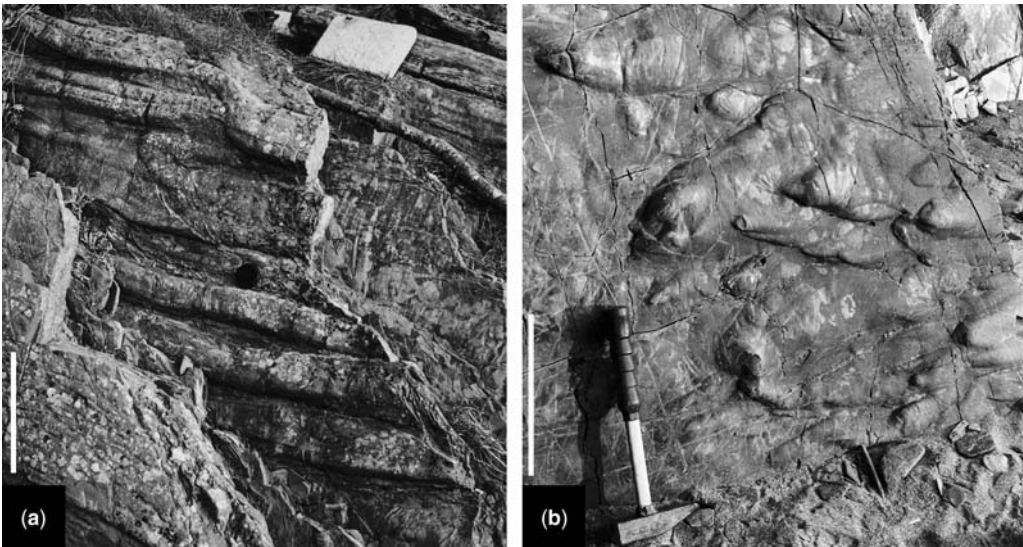
	Description
Facies A	Black shales
Facies B	Banded shales
Facies C	Siltstone-shale cycles with widespread sole structures
Facies D	Sandstone-shale cycles
Facies E	Siltstone-shale cycles with sparse sole structures
Facies F	Conglomerates

organisms constructing some form of rigid test, a characteristic rare in the Ediacaran period.

Two hundred and ten specimens on twelve different surfaces have now been examined as part of this study; isolated specimens on these surfaces have not been measured due in most cases to their inaccessible location high on steeply dipping beds. Two additional surfaces are separated from the main outcrop and may represent repetition of other stratigraphic levels: specimens on these have not been measured due to inaccessibility. It should be noted that most of these specimens were probably not observed by Crimes *et al.* (1995), who reported 27 measurable and several partial specimens on seven surfaces. We must also note that due to the fractured nature of the outcrop, collection of specimens risks severe damage: all specimens

described herein were examined (and remain) in their natural exposure.

The basic morphology of *E. booleyi* was originally reconstructed (Crimes *et al.* 1995) to be circular in overall plan, although a full circle has never yet been seen in outcrop (see below). Even specimens preserved sub-parallel with the bedding surface are preserved as a semicircle, which may cast doubt on the notion that these structures were originally totally discoidal in outline. A range of direction and angle of protrusion (these terms are clarified in Fig. 5) from the bed sole is observed in all forms. The angle of protrusion varies from 0° to about 55°, but both mean and modal values are approximately 20°. A χ^2 -test on the direction of protrusion of all 210 measured specimens (using 30° divisions), with a null hypothesis of random orientation, can be rejected at a significance level of $p < 0.01$. The vector mean of the direction of protrusion is 347.9°. This is broadly similar to palaeocurrent direction, perhaps indicating that this had a strong influence on orientation. Similar tests on the most populous surface, which has 89 measured specimens, also reject the null hypothesis of random orientation at $p < 0.01$, and produce a vector mean direction of protrusion of 345.0°. This is similar enough to the results for all measured specimens to confirm that the overall values are not an artefact of averaging over twelve different surfaces (Fig. 6). Statistical analysis and interpretation of this data is continuing. One well-exposed bedding surface in Booley Bay demonstrates clearly that in some instances these structures are

**Fig. 3.** Sole structures in the Booley Bay Formation: (a) Gutter casts; (b) Flute casts. Both scale bars 250 mm.

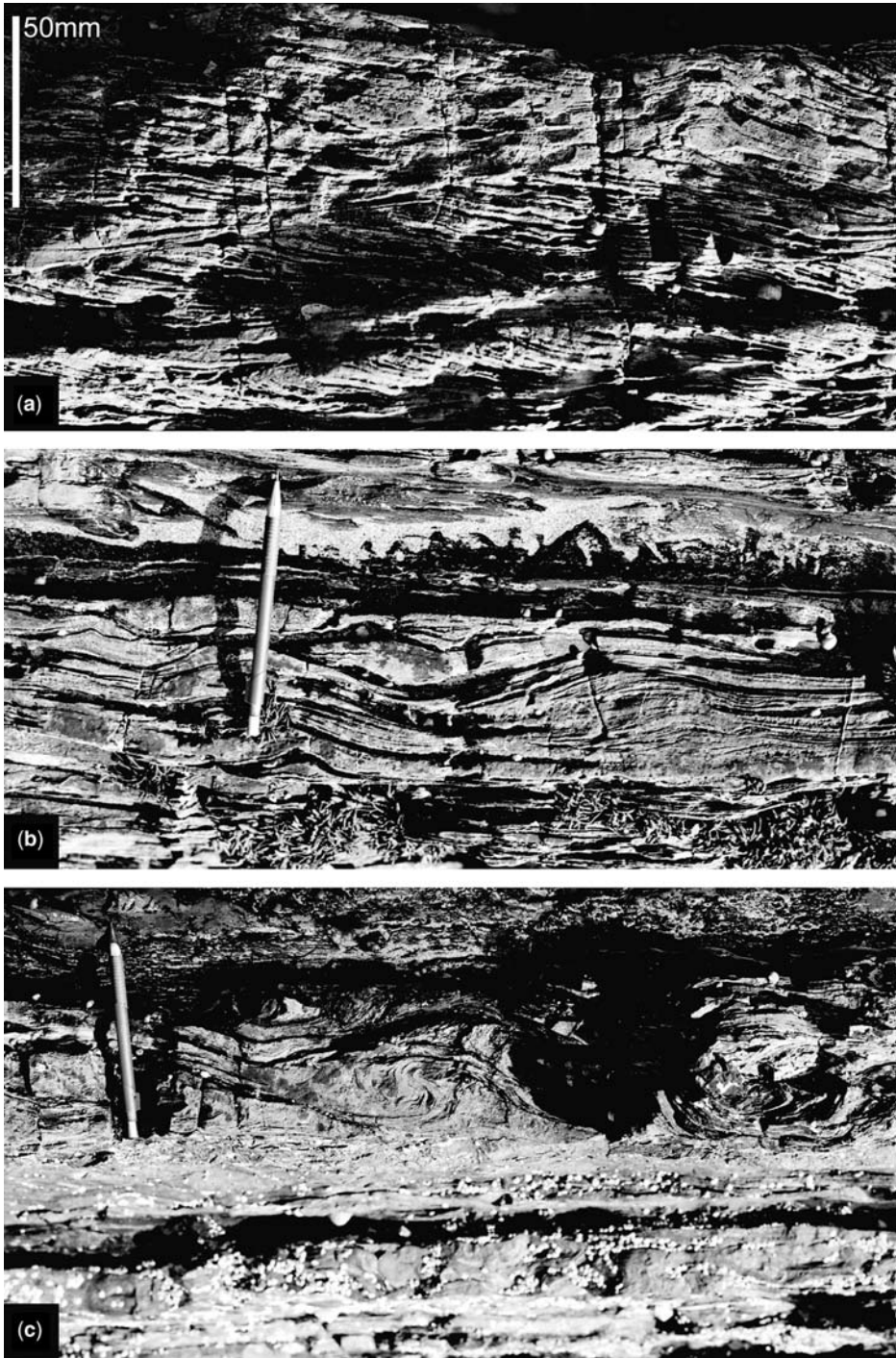


Fig. 4. Sedimentary lamination in the Booley Bay Formation: (a) Cross-lamination; (b) Hummocky-like lamination; (c) Convolute lamination. Pencil in b and c is 15 cm long. All 3 photographs have been inverted to show features in the correct stratigraphic orientation.

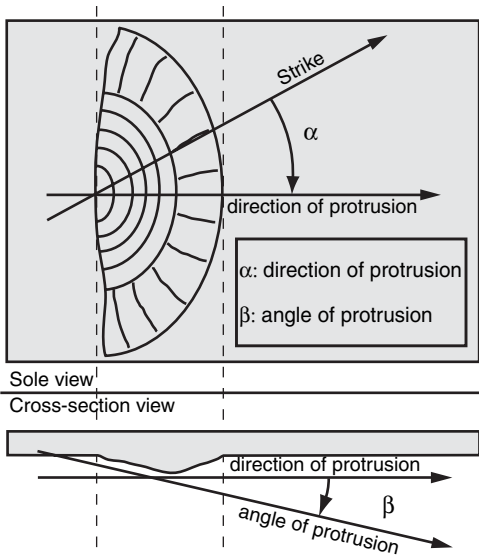


Fig. 5. Definition of terms used in the text.

grouped into palaeocurrent parallel zones or bands (Fig. 7).

In terms of size (Fig. 6), the structures range from 5–200 mm in radius. The mean radius of the measured specimens was 42 mm, with a modal value of 25 mm. Several different morphological variations are seen, which may cast doubt on the idea that the specimens referred to *E. booleyi* all belong to the same genus or species, even if these structures are biogenic. However, taphonomic preservational variation may play as large a part as original morphological disparity in distinguishing these forms. Several representative specimens are described below to illustrate these variations.

As stated above, despite initial interpretations of *E. booleyi* as being the imprints of originally disc-shaped organisms, not much more than half of each disc is ever observed in outcrop. The outer surfaces on the exposed side can be covered by a very fine concentric ornament. Depending on the original composition of the test this ornament may represent growth lamellae. Several specimens display this quite well, including the 'ventral side' holotype of Crimes *et al.* (1995, plate 6C), which has only very slight relief from the bed sole. A second specimen (Fig. 8) has a concentric ornament consisting of ridges of 1 mm in thickness, spacing and relief. It also has a raised annular band (with radius approximately half the total radius) about 1 cm thick, with crudely radial elongate depressions of thickness and relief both approximately 1 mm, spaced irregularly at about 2–3 mm intervals. One possible explanation for this form is that it may represent a 'swing mark' or 'scratch circle' (Jensen *et al.* 2002). However, in other specimens (Fig. 9),

it can be seen that the concentric ornament is not truly circular, but rather ovoid in outline. This presents obvious problems for it to have been generated by rotation of a rigid body, fixed at a central point, over the surface of the sediment, as is the case with swing marks. Elongation from tectonic strain cannot, however, be definitively ruled out at this stage. Analogue modelling is currently being undertaken by us to critically evaluate this hypothesis.

Some specimens display a combination of concentric and radial ornament, the radial aspect of which is quite variably developed. It has been suggested that forms displaying stronger concentric lamination in the centre, with radial ornament developed towards the outer edges of the discs (Fig. 10) may represent the dorsal side of specimens (Crimes *et al.* 1995, plate 3). The specimen in Figure 10a clearly shows both radial and concentric ornament, the relief of which is less than 1 mm. Spacing of the ornament is irregular, and in the case of the concentric ridges, which are less than 1 mm thick, the spacing is clearly greater parallel to, rather than perpendicular to, strike (horizontal in the photographs). Other specimens show a contradictory spacing pattern, perhaps indicating that this is an original character, rather than due to, for example, later deformation, although deformation of a soft-body is also a possibility.

Other forms display a much stronger and pervasively developed radial ornament. The specimen in Figure 11 displays quite a coarse radial ornament, which extends in an irregular fashion across the entire surface of the half disc. This appears to superimpose an underlying fainter, but conspicuous and regular, concentric ornamentation. The specimen in Figure 12 has a total radius of approximately 5 cm, with a central disc of radius approximately 1.5 cm. This central disc exhibits a faint concentric ornament of minuscule relief. An irregular, approximately radial ornament extends from the margin of the central disc to the outer margin. This is reminiscent of specimens from the Holy Cross Mountains in Poland originally described as *Medusites*, reclassified as a new genus and species *Brzechowia brzechowiensis*, and eventually redescribed as *Velumbrella czarnockii* (Stasinska 1960). Conway Morris (1993) compared these fossils with the rotascids and *Eldonia*, and all of these were included in Class Discophylla by Friend (1995). However, even in the best similar specimen from Booley Bay, only about half of the disc is preserved (poorly), and the ornament is not as regular as the structure of *Velumbrella*.

Many of the specimens examined in this study possessed essentially an inner zone dominated by a concentric ornament of fine rings, which is seen to pass abruptly into an outer area, which is flared or crudely radial (Fig. 13). This outer flared zone,

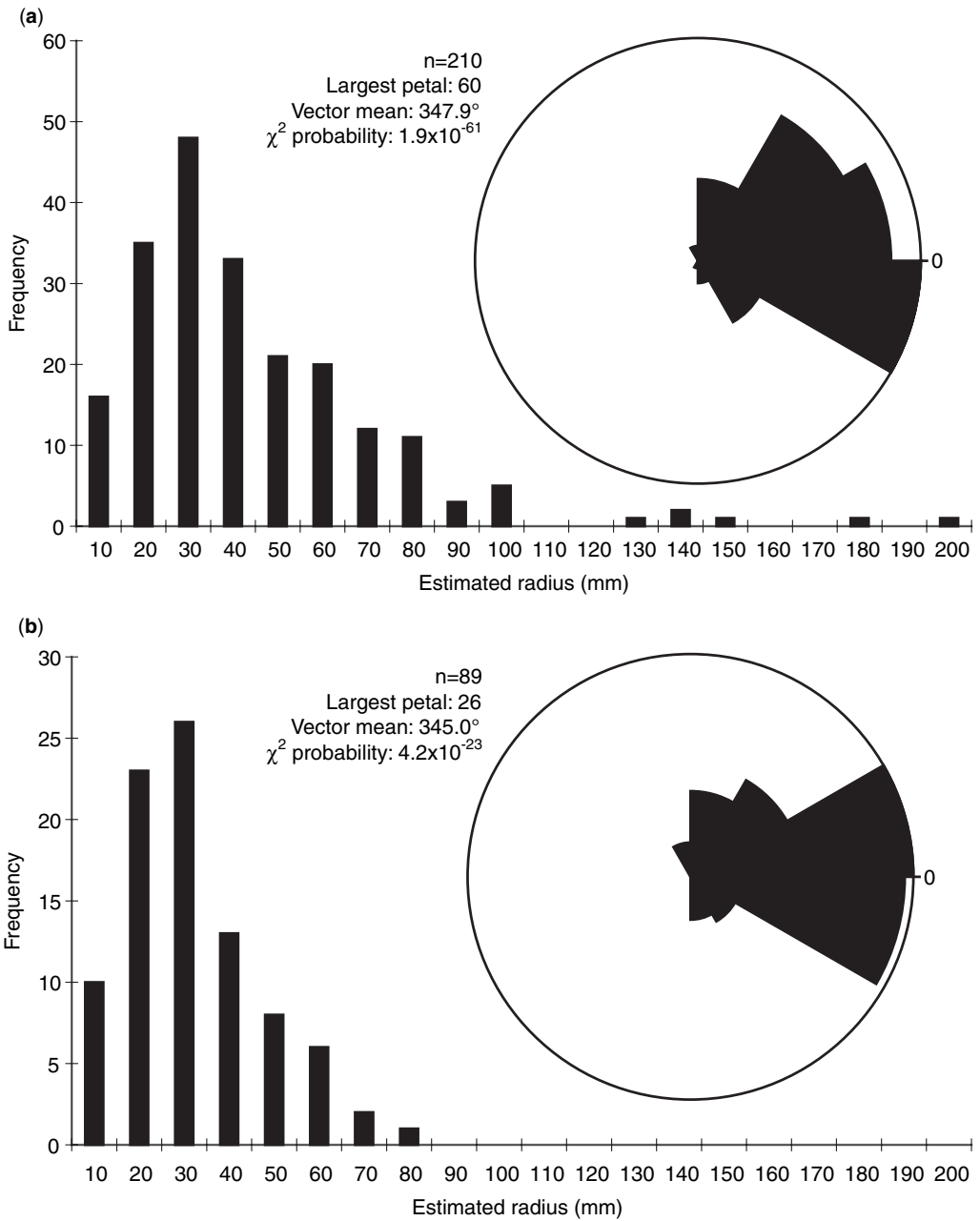


Fig. 6. Size (bar graph) and orientation (rose diagram) data for (a) all measured specimens; (b) the most populous surface. Statistical text on the figure refers to the rose diagrams.

often only very subtly developed, displays no semblance of systematic skeletal or biological organisation and it is difficult to reconcile with it being part of an outer rigid test. As common as this feature is, it was never fully incorporated in the original reconstruction by Crimes *et al.* (1995). It may represent an outer zone of soft tissue, however again this is

extremely difficult to establish. An alternative is that it may well represent drag marks of the discs drawing down onto the sediment along the leading edge. This is a possibility for the small specimen figured in Figure 13b; here the outer radial zone is seen to inflect at an angle of approximately 110–120° to the plane of the half disc. The

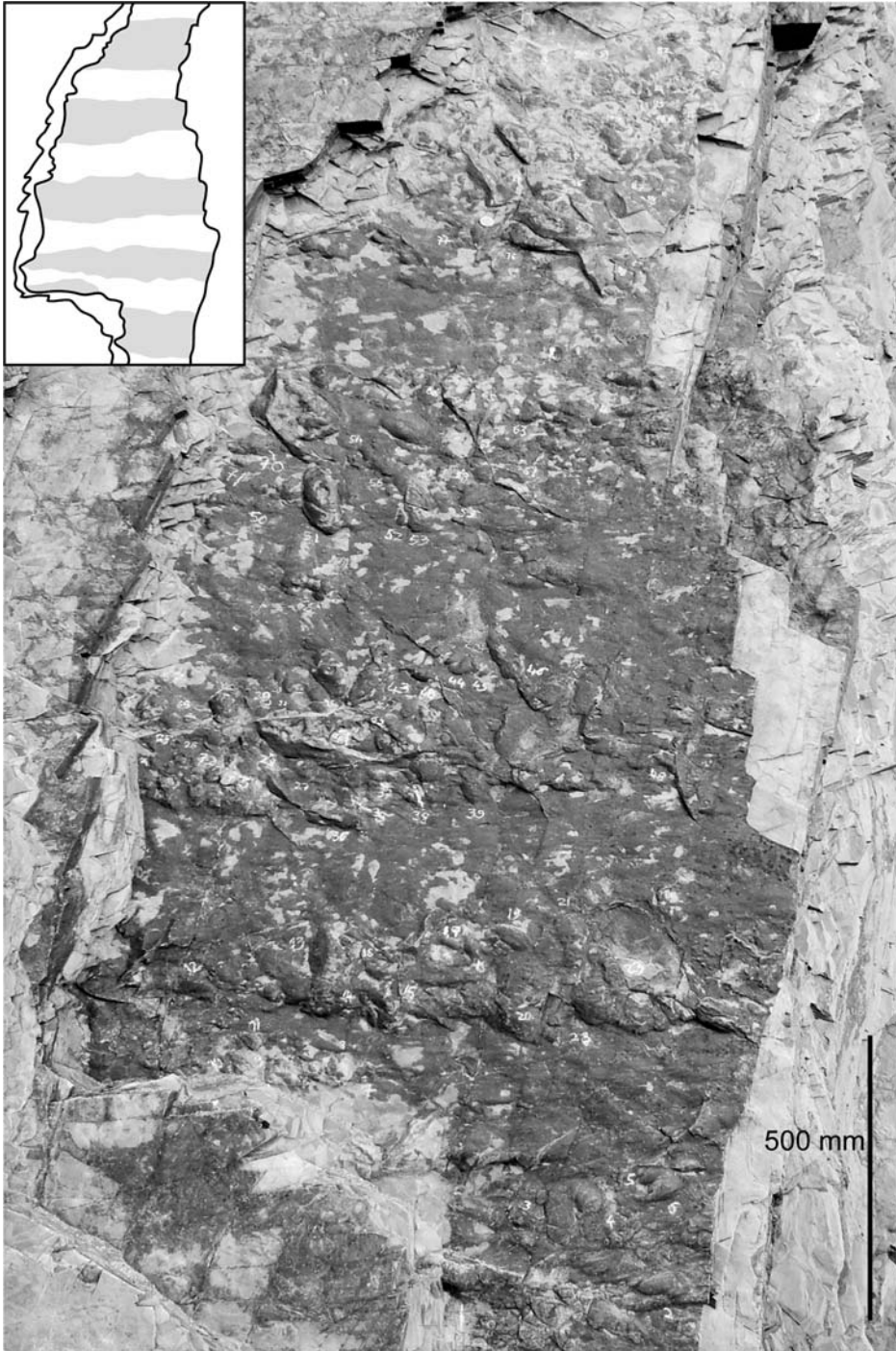


Fig. 7. Fossils in palaeocurrent parallel bands (shaded on inset) on bed sole.

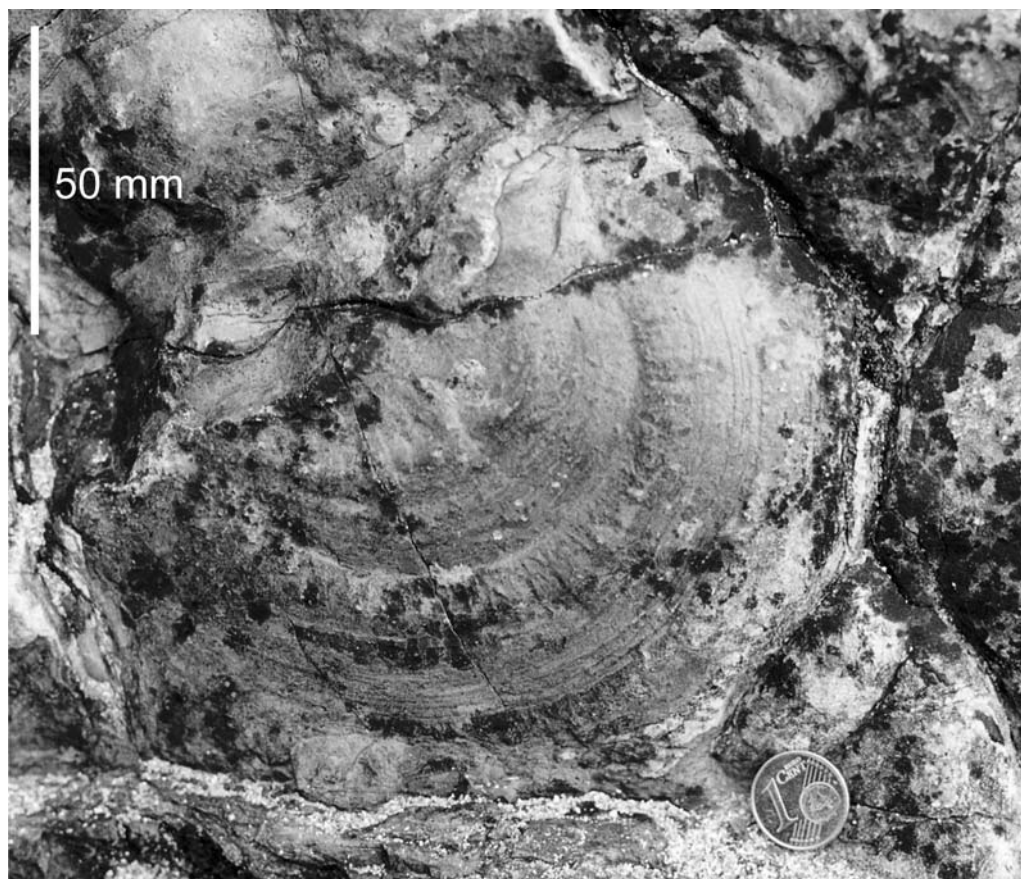


Fig. 8. Specimen exhibiting well-defined concentric structures.

specimen illustrated in Figure 13a also displays a set of curved lineations restricted to the upper portion of the visible disc, which are concentrically stacked and preserved in strong hyporelief. If considered part of the original organism then they may represent tentaculate processes along the periphery. However, they pass rapidly into a flared periphery lower down, and have not been observed in any other specimen examined to date. A more plausible explanation is that they represent systematic excavation of sorts, perhaps post mortem grazing by an unknown organism.

Other problematic structures

Smaller circular sole markings described by Crimes *et al.* (1995) as *Nimbia occlusa* Fedonkin 1980 occur on many beds at Booley Bay but are particularly common on three surfaces. These structures are circular to oval rings of diameter 2–8 mm, often with a central peak, occurring in positive hyporelief (Fig. 14). Whole and partial rings both

commonly occur. Originally interpreted by (Crimes *et al.* 1995) as the impressions of ringed discs, these have subsequently been reinterpreted as swing marks by Jensen *et al.* (2002).

Another distinctive kind of structure, which occurs in positive hyporelief in the sequence, apparently in direct association with fabrics of microbial origin, is a series of sub-parallel ridges radiating from a slope. These appear similar to structures from the Arumbera Sandstone of Central Australia described by Glaessner & Walter (1975) as the Ediacaran-type fossil '*Arumberia banksi*', which has subsequently been reported from the Urals (Bekker 1980, 1990), China (Wang *et al.* 1984), France, Newfoundland and the Channel Islands (Bland 1984), the White Sea region of Russia (Grazhdankin 2004), and Britain (Bland 1984; McIlroy *et al.* 2005). Brasier (1979), however, suggested that these were inorganic structures, and McIlroy & Walter (1997), noting similarities between forms assigned to '*Arumberia*' and flute marks generated experimentally by Allen

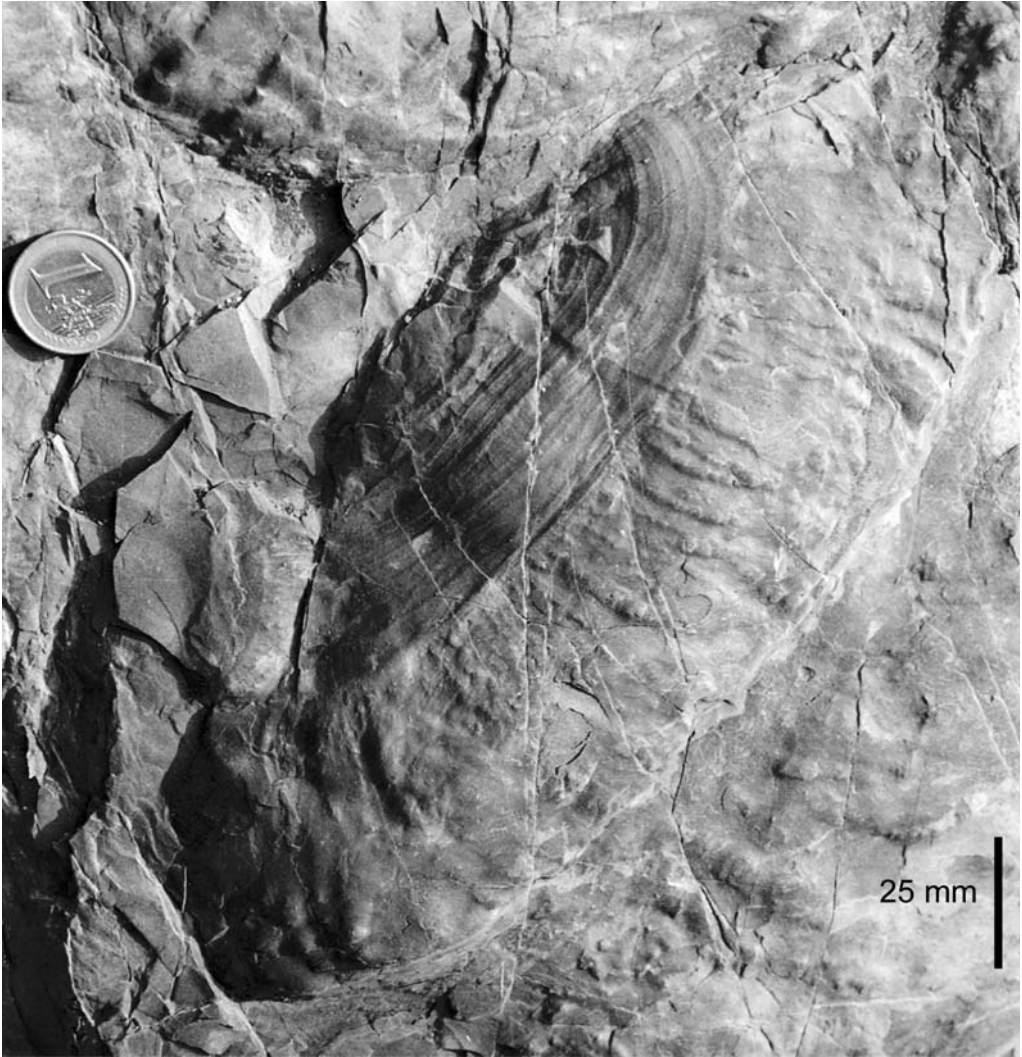


Fig. 9. Specimen with pronounced ovoid rings.

(1984), concluded that '*Arumberia*' was a microbially-influenced sedimentary structure. This has generally been accepted by other workers (e.g. Hagadorn & Bottjer 1997; Waggoner 1999; Grazhdankin 2004). Two different specimens are figured here. The first (Fig. 15a), from the Booley Bay Formation at Templetown, consists of a bulbous form approximately 10 cm in diameter in positive hyporelief, which is covered by subparallel unbranched ridges of thickness 1 mm separated by thin grooves in a regular pattern. The ridges do not extend beyond the slope; however a fainter network of curved lines is observed to extend away from the specimen. The relationship of the ridges and grooves to the palaeocurrent is unknown, as

the specimen occurs on a faulted block, and there are no other current indicators visible on the bed. The second specimen (Fig. 15b) is from Dollar Bay (immediately south of Booley Bay). An elongate (c. 20 cm) thick ridge, which is covered by a thin layer of underlying sediment, has subparallel ridges and grooves several centimetres in length extending from the slope in a linear pattern. In this specimen, the ridges and grooves are approximately parallel to palaeocurrent. The specimens resemble examples figured from Britain (Bland 1984), Australia (Glaessner & Walter 1975), and the Urals (Bekker 1980, 1990).

A further structure described in an unpublished MSc thesis (J. Vohnhof 1997) from the section at

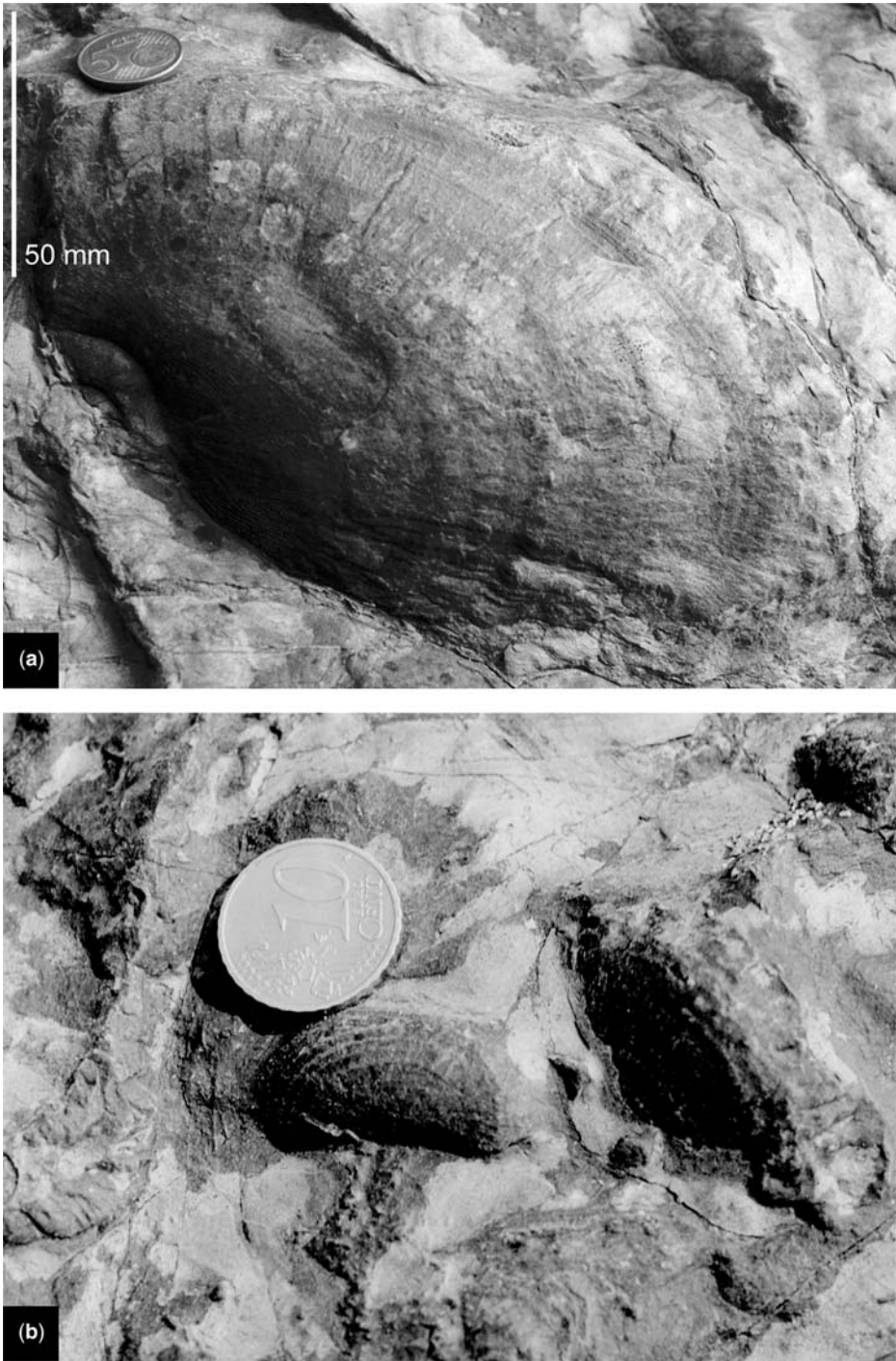


Fig. 10. Specimens of (a) large and (b) small size showing both radial and concentric ornament. Note the similarity in form despite the size difference. Coin in (b) has diameter 20 mm.

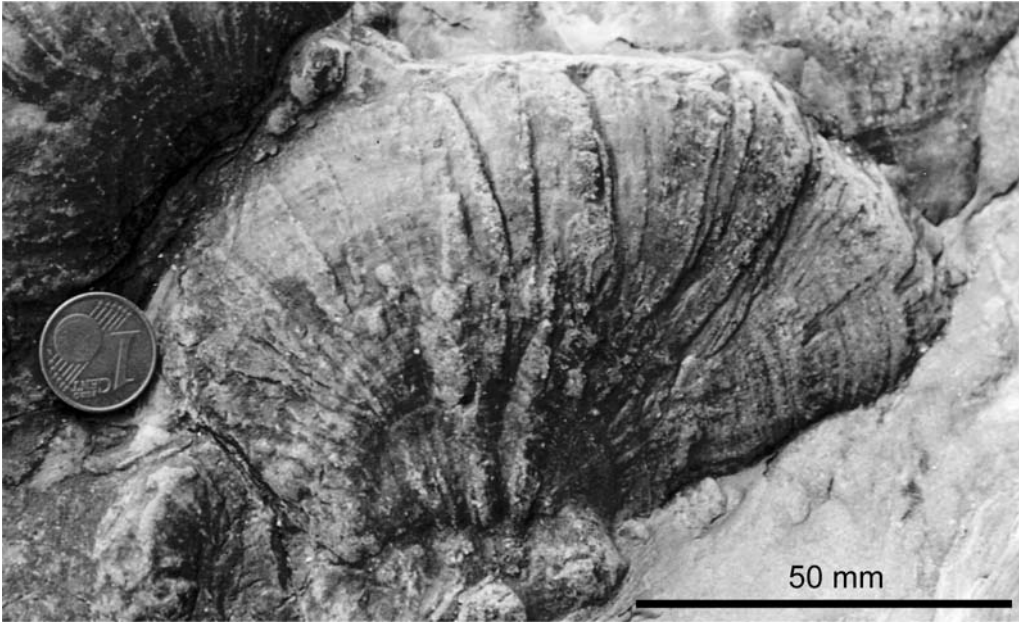


Fig. 11. Specimen showing irregular, approximately radial features and sharp regular concentric rings.

Booley Bay is a subcircular ridge in positive hyporelief, about 1 cm in diameter. The circle is not complete however, having a 2–3 mm gap on one side; the ridge on one side of this gap

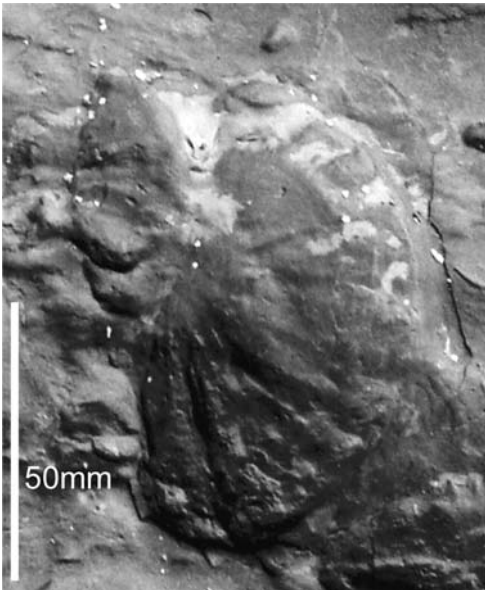


Fig. 12. Specimen with a small, flat central disc and radial marks extending to the periphery on a sloped outer area.

is orientated away from that on the other side, suggesting the beginnings of an anticlockwise-outwards spiral. The specimen in question, however, has unfortunately gone missing subsequent to collection.

Another set of problematic structures occurs in positive hyporelief on at least three beds in Booley Bay (Fig. 16a). These are elongate tubes up to 5 cm in diameter, approximately palaeocurrent parallel, striated along the outside, parallel to the sides of the structures. At first glance these resemble gutter casts, but this explanation is not tenable, as on closer examination several of the structures reverse direction (Fig. 16b). No definite interpretation can thus be suggested at this time, but a sedimentological origin appears most likely. The structures are intimately associated with a stratigraphically underlying laminated black material with a patchy surface, the laminations of which appear to be deformed to accommodate the structures. This is also of unknown origin.

The age of the Booley Bay Formation

The dating of the Booley Bay succession to the late part of the Late Cambrian is based solely on acritarch biostratigraphy undertaken by Moczydlowska & Crimes (1995). Previous palynological investigations suggested that the formation ranged in age

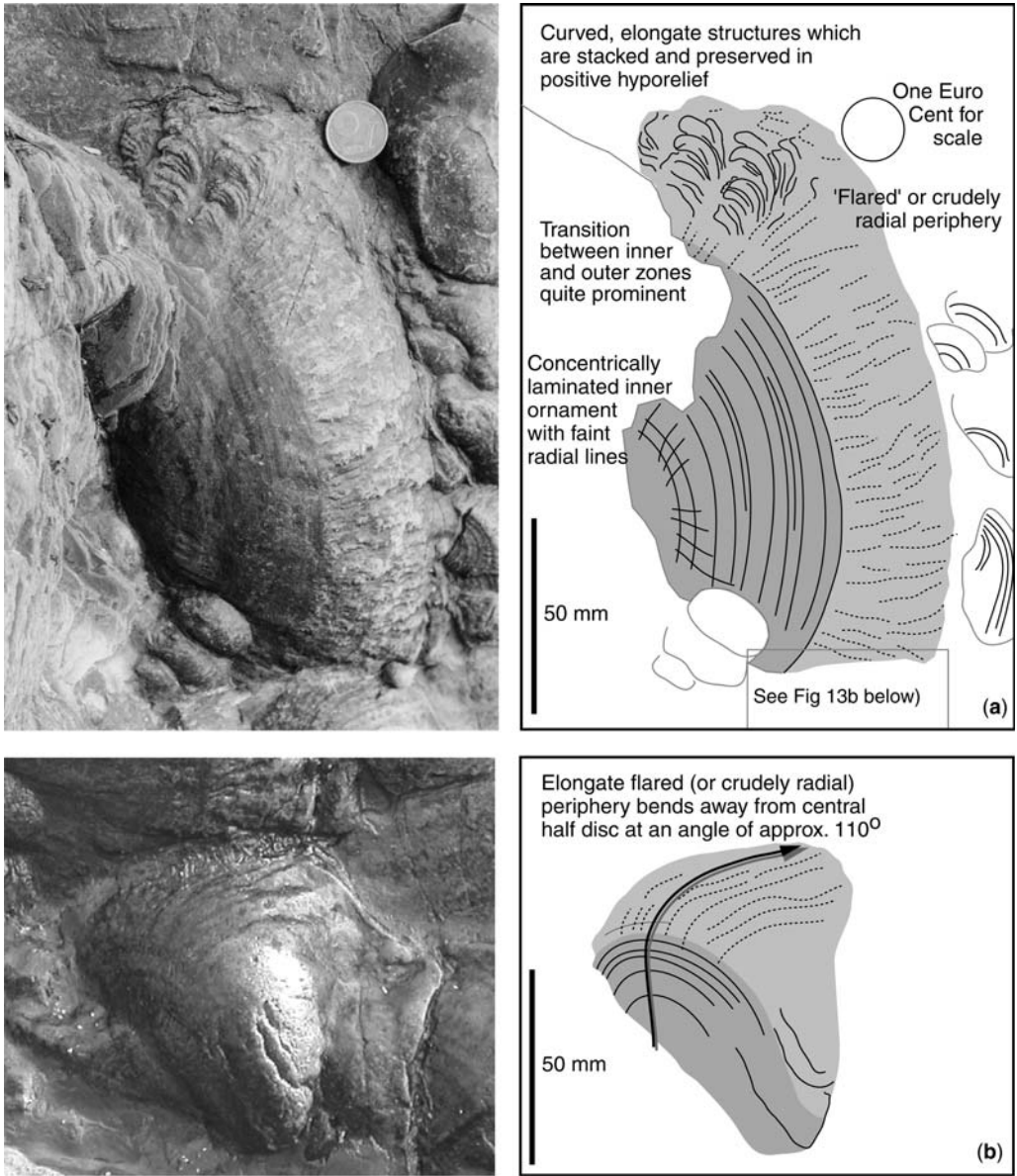


Fig. 13. Specimens showing a distinctive, crudely radial or flared periphery.

from Early Cambrian to Arenig (Gardiner & Vanguetaine 1971) or Middle Cambrian (Smith 1981). Four sample localities were collected by Moczydlowska & Crimes (1995), from which 17 acritarch species were recovered. Of these only two species, *Stellechinatum uncinatum* and *Cristallinium randomense*, have sufficiently short stratigraphic ranges to be useful for biostratigraphic

purposes and are thought to be Late Cambrian to Tremadoc in age. Attempts to better constrain the age range of the Booley Bay succession are currently underway. In the absence of volcanic ash horizons yielding zircons for radiometric dating, acritarch biostratigraphy remains the best hope of increasing the chronostratigraphic resolution of the sequence.

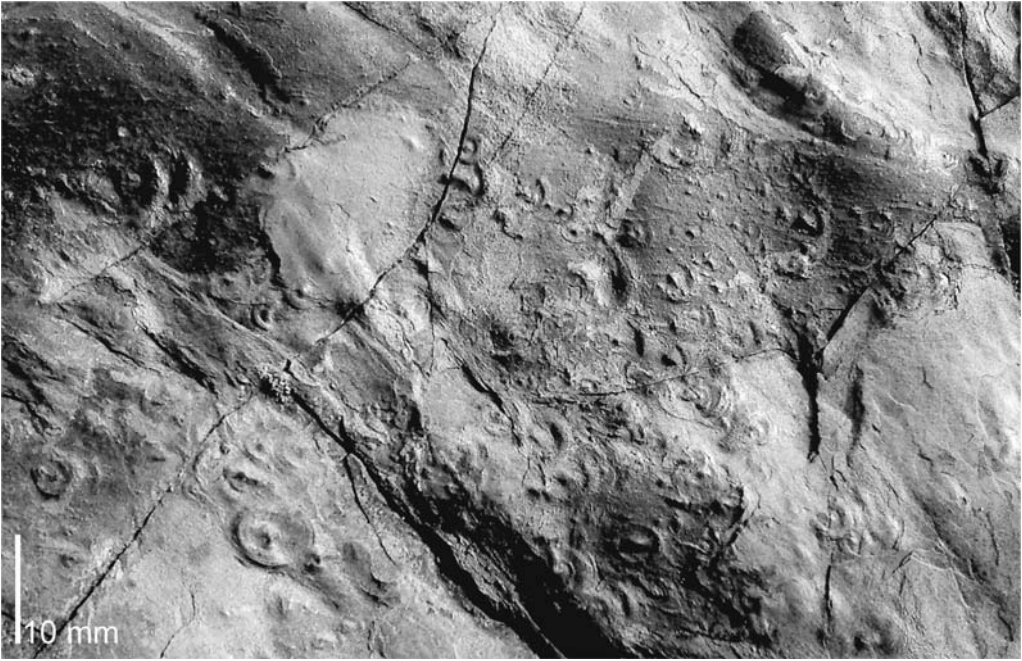


Fig. 14. Swing marks previously assigned to the Ediacaran genus *Nimbia*.

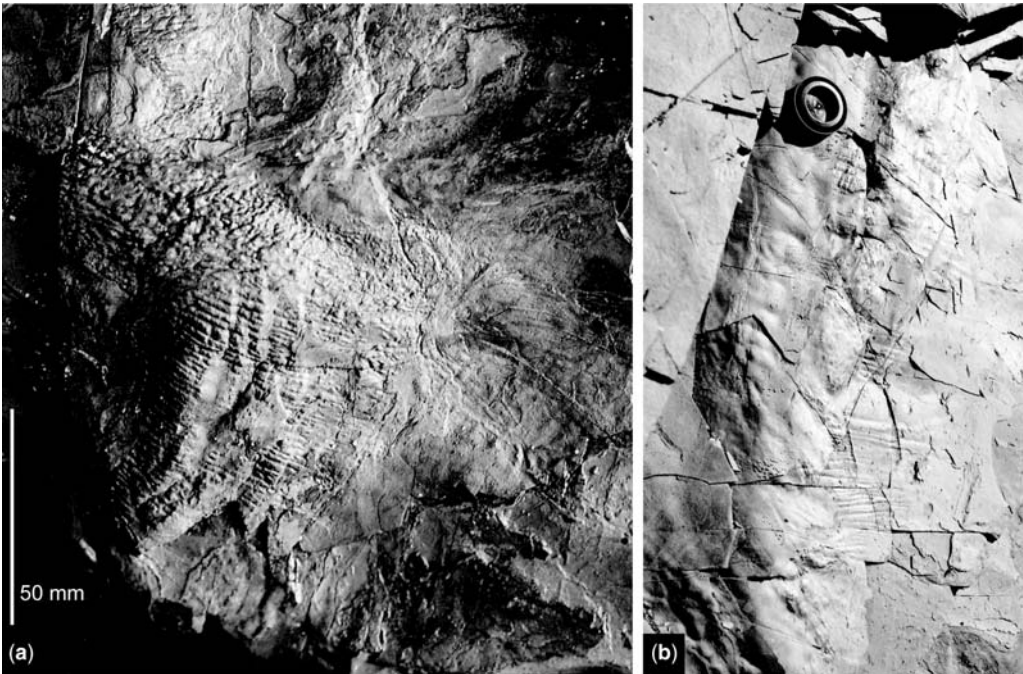


Fig. 15. Specimens of the microbially influenced sedimentary structure 'Arumberia' from the Booley Bay Formation at (a) Templetown (scale bar 50 mm) and (b) Dollar Bay (film canister lid has diameter 35 mm).

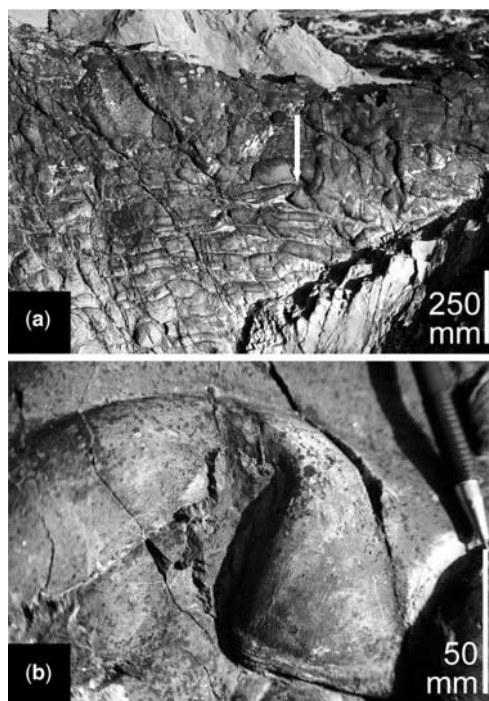


Fig. 16. Unidentified structures from Booley Bay: (a) Whole bedding surface; (b) Close-up of arched structure in (a).

Discussion

Interpretation of the Booley Bay specimens is of considerable importance to the development of models concerning the ultimate demise of the Ediacaran group as a whole. At present, there are five possible interpretations for their origin and affinity: these are listed below.

They are a species of the genus Ediacaria

Specimens of the genus *Ediacaria* have been reported from many locations worldwide, including Russia (Fedonkin 1990; Serezhnikova 2005), India (De 2003), Canada (Narbonne & Hofmann 1987; Narbonne 1994), and Australia (Sprigg 1947; Glaessner & Wade 1966; Wade 1972; Jenkins 1992, 1996), and it is regarded as a cosmopolitan taxon. The genus was initially described by Sprigg (1947), with one species, *Ediacaria flindersi*, from a small number of specimens from the Ediacara Hills, Flinders Ranges of South Australia. More extensive collections and detailed study by Glaessner & Wade (1966) and Wade (1972) assigned many new specimens to this genus, and also led to the removal of several specimens to new taxa. The genus was re-diagnosed to account

for these changes, and was described as showing a central disc and an outer ring, without any marginal flange. The central disc, which varies from two-thirds to three-quarters of the total radius, was noted to often be slightly elevated above the outer ring, but the disc was otherwise flat. Surface features were limited to concentric grooves and a sharp annular furrow (not necessarily parallel to the outer margin) on the disc, and radial furrows on the ring. The genus was also discussed by Jenkins (1992, 1996), who considered that the type specimen was damaged in such a way as to preclude full assessment of its true relationships (R. J. F. Jenkins, pers. comm., 2005). A principal question in this regard was whether the specimen may have had a stalk, and hence represents holdfast.

In a study of discoidal fossils from the Fermeuse Formation of Newfoundland, Gehling *et al.* (2000) listed *Ediacaria*, along with most other flat discoidal Ediacaran-type fossils, as synonyms of *Aspidella terranova*, and interpreted *Aspidella* as a holdfast of a larger frond-like organism. Pending further investigation of the gradation of form noted, it is suggested that their synonymy list not be formally applied as it reduces the information conveyed by the names of the fossils (see MacGabhann 2007): although Gehling *et al.* (2000) suggested assignment of specimens to one of the preservational variants noted to counter this problem, this has not been applied in practice (e.g. Hofmann & Mountjoy 2001; Pyle *et al.* 2004; Droser *et al.* 2006). In this study, we regard the genus *Ediacaria* as a form genus, diagnosed as per Wade (1972).

Crimes *et al.* (1995) diagnosed *E. booleyi* as a large, circular disc with the dorsal side divided into three concentric zones (a flat central zone, steeply sloping middle zone, and gently sloping outer flange), with additional concentric lines and numerous thin radial features, which become more prominent towards the periphery. The ventral side was described as having alternate areas of coarse and fine concentric markings, and numerous fine radial lines. Although some of the specimens described here may seem to approach the basic morphology of *Ediacaria* (i.e. an inner disc with concentric structures and outer ring with radial lines), the three-dimensional aspect of most of the Irish specimens is not seen in the type material of *Ediacaria*. Neither do the flat Irish specimens conform to that of the type; the concentric rings are far more prominent and the radial aspect of the Irish specimens is far more crude and irregular, compared to the straight, thin, regular grooves seen on some specimens of *E. flindersi*. The assignment of the Irish specimens to the genus *Ediacaria* is therefore considered highly problematic. We suggest that the Booley Bay specimens should not be assigned to this genus.

They are of Ediacaran-type, but not in the genus Ediacaria

Very few Ediacaran-type discoidal fossils (*Medusinites* and *Nemiana* for example) are found in fossil form with a significant three-dimensional aspect to their morphology preserved. Of those that are currently known, none resemble *E. booleyi*.

One of the more compelling arguments presented by Crimes *et al.* (1995) for an Ediacaran-type fossil interpretation of *E. booleyi* is the apparent lack of a convincing mouth or anus in any of the specimens. The lack of any such structures, which have not been reported in any Ediacaran-type fossil, has led to one interpretation that the organisms, at least in some cases, relied on simple diffusion of nutrients and/or oxygen across the body wall (Seilacher 1989, 1992). This has obvious limitations in the ability for the surface area of an organism to feed and support a growing internal volume and may explain why many true Ediacaran-type organisms remained quite flat and thin, often adopting a quilted constructional morphology (e.g. Seilacher 1989, 1992). The three-dimensional relief of the fossils (e.g. Figs 9–10) does not seem to be designed to maximize surface area relative to total body volume and would present a problem for a simple nutrient and/or oxygen absorbing lifestyle. This is especially important considering the largest specimen measured in the field had an estimated total diameter of nearly 40 cm; such sizes are reached by thin Ediacaran organisms including *Ediacaria* and *Dickinsonia*, but not by any forms with a strong three-dimensional aspect. The Irish specimens cannot, therefore, be interpreted in terms of the Vendobionta hypothesis of Seilacher (1992), and the lack of preserved mouth, anus or respiratory structures cannot be used as a guide to their affinities.

Alternative interpretations of Ediacaran fossils regard them as stem or crown group representatives of extant phyla (e.g. Gehling 1991) in which features such as mouths are simply not preserved. If this is the case, the occurrence of structures similar to Ediacaran-type fossils in the Cambrian may be important in terms of preservational circumstances rather than biology (Jensen *et al.* 1998), as it is of course beyond doubt that non-mineralized organisms existed in the Cambrian.

We also note that the original transport and depositional model for *E. booleyi* (as proposed by Crimes *et al.* 1995) appears to be hydrodynamically unstable, as the direction of projection of the organism out of the sediment after impact is up-current, and would maximize its hydrodynamic resistance (Fig. 17a). An interesting outcome from this observation is that it may provide an

explanation for the flared periphery to many of the specimens. The force of the current flowing against the upwardly projected rear portion of the disc and its resultant drag would force the structure to rotate slightly in the sediment. This could possibly account for the drag like marks forming the flared radial periphery to many of the specimens on the downstream side (Fig. 17b). If the structure was not securely fastened to the bottom and the current continued to flow against it, it would presumably continue to rotate before flipping free. Even to penetrate the sediment to the degree originally suggested, the density of the organism must have been at least the same as the density of the sediment into which it was emplaced. This point was alluded to by Palmer (1996). The only way to increase the density of an organism to that of the surrounding sediment is to provide it with mineralized skeletal structures. Initial analogue flume experiments that we conducted using density compensated silicon rubber replicas of the

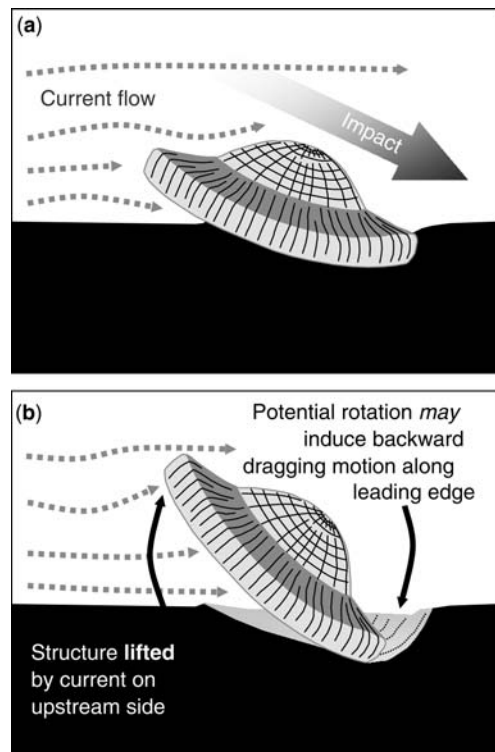


Fig. 17. Reconstruction of *E. booleyi* (modified from Crimes *et al.* 1995): (a) post-impact and (b) entrainment in the seafloor. Note how continued current action acting against the rear of the structure (projecting upstream) would eventually lift it up and possibly out of its impact position.

Crimes *et al.* (1995) reconstruction for *E. booleyi* appear to support this hypothesis. These are ongoing, and the results will be published elsewhere. In addition, the proposed taphonomic model requires the organism to have a tough integument to survive transport, coupled with some rigidity to allow appreciable sediment penetration. This component of rigidity in particular is inconsistent with an interpretation of these structures as Ediacaran-type fossils.

If an Ediacaran affinity is to be rejected for *E. booleyi* then only two plausible biogenic interpretations can be proposed for the structures.

They are body fossils, but not of true Ediacaran affinity

A radially symmetric body plan may suggest a ctenidarian affinity. The density of living medusoids (e.g. Scyphozoa medusae, or jellyfish) is close to that of seawater (1.03 g cm^{-3}). This and their nektonic habit present problems for them becoming entrained in turbidity currents. This likely also applies to other Cambrian discoidal fossils, such as the medusiform stem-group echinoderms of the Class Discophylla (Friend 1995), although there is some suggestion that discophyllans may have been benthic. An alternative is that the organism was a benthic polyp such as a solitary coral or anemone. Still, however, the problems of density and construction of an outer rigid test, enclosing the entire organism, arise. There are no modern analogues to compare with; however the Psammocorallia as defined by Seilacher (Seilacher 1992; Seilacher & Goldring 1996) do provide one possibility. These 'sand corals' are thought to have lined the inside of their enteron with sediment grains, which acted as ballast. It is possible that *E. booleyi* contained sand within its body, which could account for much of the density deficit. The concept may be useful in trying to begin to understand the taphonomy of the *E. booleyi* specimens, but as Crimes *et al.* (1995) point out, the Irish specimens bear little relation to the morphology outline in published accounts of Psammocorallia.

Many of these problems could be dismissed if the possibility is considered that the organisms were benthic, and autochthonous or preserved *in situ*. Attractive as this idea is, it does not easily explain the occurrence of the structures in regularly spaced palaeocurrent parallel bands (Fig. 7), nor how benthic organisms could be preserved on erosional turbidite soles. An interpretation of the structures as benthic organisms would require a reinterpretation of the sedimentology of the strata (long overdue), which we are currently undertaking.

They are biogenic sedimentary structures

An alternative explanation is that the structures are, in fact, trace fossils. This could explain why a full circle or disc is never observed in any of the specimens. The structures may have been made by an organism, which grazed upon the seafloor in an arcuate fashion. Also, at least one specimen (Fig. 14a) displays strong evidence for systematic excavation. Two important considerations arise when invoking a trace fossil explanation for the structures. Firstly, a range of sizes can clearly be demonstrated for similar structures (e.g. Fig. 10). Secondly, and more importantly, the structures are all approximately aligned, with the semicircular outlines directed downstream of the prevailing current direction. They are also in some instances grouped into distinct bands, which traverse bedding surfaces broadly in the direction of the palaeocurrent. This strongly suggests that the structures may have indeed been moved and aligned by current action. Alternatively, as discussed above, a swing mark origin could be invoked for several of the structures. This has yet to be fully tested.

They are simply abiogenic sedimentary structures

The variety in form, and lack of complete discoidal imprints may be considered as arguments against an organic origin, as may the lack of a sharp boundary to the structures in several cases and association with flute casts and 'Arumberia'-like structures. However, variability in form may be explained by taphonomic or original biological differences (indeed there is no reason to assume that the assemblage is necessarily monospecific or monogeneric), and the lack of complete specimens, as discussed above, may be explained by current orientation. Finally, for several specimens it is simply not the case that a sharp edge is absent: the specimen illustrated in Figure 11, for example, shows a very sharp edge truncating the ornamentation where the structure protrudes from the bed sole. Further, most of the specimens which do not show a sharp edge are those with the crudely radial structures potentially formed by current-induced rotation of the specimens, as discussed above. This would tend to obliterate sharp edges.

In any case, it is hard to understand how such consistently complex radial and concentric structures could be produced purely from a simple turbidity current, but this option cannot be ruled out at this stage.

Conclusion

Whilst we do not discount the possibility of a wholly inorganic origin for the structures described as *E. booleyi*, they are here tentatively considered at least in part biogenic. This is due to a combination of factors:

1. The range of sizes (the radius of specimens varies from *c.* 0.5 cm to *c.* 20 cm) exhibited by the different forms, while retaining reasonable constancy of structure.
2. The variance in angle of protrusion and relief (from flat to *c.* 3 cm) in forms which are otherwise morphologically similar.
3. The long axes of forms which are ovoid in outline are randomly oriented on the bedding surface.
4. The sharp boundary between the inner concentric-ornamented disc and the outer zone of radial structures.

We do not think that these structures should be assigned to the genus *Ediacaria*, and their apparently high density and rigid integument are inconsistent with their interpretation as Ediacaran-type fossils. Confirmation of this hypothesis would add considerable weight to proposals that the Ediacaran biota became extinct in a mass extinction at the end of the Ediacaran Period.

Thanks to the Project Leaders of IGCP 493, J. Gehling, P. Vickers-Rich and M. A. Fedonkin, for inviting this contribution. R. J. F. Jenkins and one anonymous reviewer are thanked for suggestions which helped us improve the paper. BAM wishes to thank G. Narbonne, A. Seilacher, S. Jensen, J. Gehling, G. Germs, and D.V. Grazhdankin for useful observations on these and other Ediacaran-type fossils; and S. Burke and P. Orr for useful debates on microbial binding of the Booley Bay sediments. The McGowan family, and J. & M. Corcoran are thanked for assistance and logistical support during fieldwork. Funding from the National University of Ireland, Galway, Millennium Research Fund is acknowledged by JM. BAM is supported by an NUIG Postgraduate Research Fellowship.

References

ALLEN, J. R. L. 1984. *Sedimentary Structures: Their Character and Physical Basis* (Unabridged one-volume edition). Elsevier, Amsterdam.

BEKKER, Y. R. 1980. A new locality with fossil fauna of the Ediacara type in the Urals. *Transactions (Doklady) of the USSR Academy of Sciences*, **254**, 235–237.

BEKKER, Y. R. 1990. Vendian Metazoa of the Urals. In: SOKOLOV, B. S. & IWANOWSKI, A. B. (eds) *The Vendian System, Vol. 1: Palaeontology* (English edition), 121–131.

BLAND, B. H. 1984. *Arumberia* Glaessner & Walter, a review of its potential for correlation in the region of

the Precambrian–Cambrian boundary. *Geological Magazine*, **121**, 625–633.

BRASIER, M. D. 1979. The Cambrian Radiation Event. In: HOUSE, M. R. (ed.) *The Origin of the Major Invertebrate Groups*. Systematics Association Special Volume, **12**, 103–159.

BURKE, S. & ORR, P. J. 2004. The evolution of ecospace utilisation in deeper marine Cambrian environments of South East Ireland. *Irish Journal of Earth Sciences*, **22**, 57.

BURKE, S. & ORR, P. J. 2005. Microbially bound substrates in Upper Cambrian deep marine settings. *Paleobios*, **25** (supplement to 2), 26.

CONWAY MORRIS, S. 1993. Ediacaran-like fossils in Cambrian Burgess Shale-type faunas of North America. *Palaeontology*, **36**, 593–635.

CRIMES, T. P., INSOLE, A. & WILLIAMS, B. P. J. 1995. A rigid-bodied Ediacaran biota from Upper Cambrian strata in Co Wexford, Eire. *Geological Journal*, **30**, 89–109.

DE, C. 2003. Possible organisms similar to Ediacaran forms from the Bhandar Group, Vindhyan Supergroup, Late Neoproterozoic of India. *Journal of Asian Earth Sciences*, **21**, 387–395.

DROSER, M. L., GEHLING, J. G. & JENSEN, S. R. 2006. Assemblage palaeoecology of the Ediacara biota: The unabridged edition? *Palaeogeography, Palaeoclimatology, Palaeoecology*, **232**, 131–147.

DZIK, J. 2005. Behavioural and anatomical unity of the earliest burrowing animals and the cause of the ‘Cambrian explosion’. *Paleobiology*, **31**, 503–521.

FEDONKIN, M. A. 1980. New Precambrian Coelenterata in the North of the Russian Platform. *Paleontological Journal*, **1980**, 1–10.

FEDONKIN, M. A. 1990. Systematic Description of Vendian Metazoa. In: SOKOLOV, B. S. & IWANOWSKI, A. B. (eds) *The Vendian System, Vol. 1: Palaeontology* (English edition), 71–120.

FRIEND, D. 1995. *Palaeobiology of Palaeozoic medusiform stem group echinoderms*. PhD Thesis, Cambridge University.

GARDINER, P. R. R. 1967. *The Geology of the Lower Palaeozoic rocks in the Duncannon area, County Wexford, Eire*. PhD Thesis, University of Dublin, Trinity College.

GARDINER, P. R. R. & VANGUESTAINE, M. 1971. Cambrian and Ordovician microfossils from south-east Ireland and their implications. *Bulletin of the Geological Survey of Ireland*, **1**, 163–210.

GEHLING, J. G. 1991. The case for Ediacaran fossil roots to the metazoan tree. *Memoirs of the Geological Society of India*, **20**, 181–224.

GEHLING, J. G. 1999. Microbial mats in terminal Proterozoic siliciclastics; Ediacaran death masks. *Palaios*, **14**, 40–57.

GEHLING, J. G., NARBONNE, G. M. & ANDERSON, M. M. 2000. The first named Ediacaran body fossil, *Aspidella terranovica*. *Palaeontology*, **43**, 427–456.

GLAESSNER, M. F. & WADE, M. 1966. The Late Precambrian fossils from Ediacara, South Australia. *Palaeontology*, **9**, 599–628.

GLAESSNER, M. F. & WALTER, M. R. 1975. New Precambrian fossils from the Arumbera Sandstone, Northern Territory, Australia. *Alcheringa*, **1**, 59–69.

- GRAZHDANKIN, D. 2004. Patterns of distribution in the Ediacaran biotas: facies versus biogeography and evolution. *Paleobiology*, **30**, 203–221.
- HAGADORN, J. W. & BOTTJER, D. J. 1997. Wrinkle structures; microbially mediated sedimentary structures common in subtidal siliciclastic settings at the Proterozoic–Phanerozoic transition. *Geology*, **25**, 1047–1050.
- HOFMANN, H. J. & MOUNTJOY, E. W. 2001. *Namacalathus-Cloudina* assemblage in Neoproterozoic Miette Group (Byng Formation), British Columbia: Canada's oldest shelly fossils. *Geology*, **29**, 1091–1094.
- JENKINS, R. J. F. 1992. Functional and ecological aspects of Ediacaran assemblages. In: LIPPS, J. H. & SIGNOR, P. W. (eds) *Origin and Early Evolution of the Metazoa*, 131–176.
- JENKINS, R. J. F. 1996. Aspects of the geological setting and palaeobiology of the Ediacara assemblage. In: DAVIES, M., TWIDALE, C. R. & TYLER, M. J. (eds) *Natural History of the Flinders Ranges*, **7**, 33–45.
- JENSEN, S., GEHLING, J. G. & DROSER, M. L. 1998. Ediacara-type fossils in Cambrian sediments. *Nature*, **393**, 567–569.
- JENSEN, S., GEHLING, J. G., DROSER, M. L. & GRANT, S. W. F. 2002. A scratch circle origin for the medusoid fossil *Kullingia*. *Lethaia*, **35**, 291–299.
- MACGABHANN, B. A. 2007. Discoidal fossils of the Ediacaran biota: a review of current understanding. In: VICKERS-RICH, P. & KOMAROWER, P. (eds) *The Rise and Fall of the Ediacaran Biota*. Geological Society London, Special Publications, **286**, 297–314.
- MCILROY, D. & WALTER, M. R. 1997. A reconsideration of the biogenicity of *Arumberia banksi* Glaessner & Walter. *Alcheringa*, **21**, 79–80.
- MCILROY, D., CRIMES, T. P. & PAULEY, J. C. 2005. Fossils and matgrounds from the Neoproterozoic Longmyndian Supergroup, Shropshire, UK. *Geological Magazine*, **142**, 441–455.
- MOCZYDLOWSKA, M. & CRIMES, T. P. 1995. Late Cambrian acritarchs and their age constraints on an Ediacaran-type fauna from the Booley-Bay Formation, Co-Wexford, Eire. *Geological Journal*, **30**, 111–128.
- NARBONNE, G. M. 1994. New Ediacaran fossils from the Mackenzie Mountains, northwestern Canada. *Journal of Paleontology*, **68**, 411–416.
- NARBONNE, G. M. 1998. The Ediacara biota: a terminal Neoproterozoic experiment in the evolution of life. *Geological Society of America Today*, **8**, 1–6.
- NARBONNE, G. M. & HOFMANN, H. J. 1987. Ediacaran Biota of the Wernecke Mountains, Yukon, Canada. *Palaeontology*, **30**, 647–676.
- PALMER, D. 1996. Ediacarans in deep water. *Nature*, **379**, 114.
- PYLE, L. J., NARBONNE, G. M., JAMES, N. P., DALRYMPLE, R. W. & KAUFMAN, A. J. 2004. Integrated Ediacaran chronostratigraphy, Wernecke Mountains, northwestern Canada. *Precambrian Research*, **132**, 1–27.
- SEILACHER, A. 1984. Late Precambrian and Early Cambrian metazoa: Preservational or real extinctions? In: HOLLAND, H. D. & TRENDALL, A. F. (eds) *Patterns of Change in Earth Evolution*, 159–168.
- SEILACHER, A. 1989. Vendozoa—Organismic construction in the Proterozoic biosphere. *Lethaia*, **22**, 229–239.
- SEILACHER, A. 1992. Vendobionta and Psammocorallia — Lost Constructions of Precambrian Evolution. *Journal of the Geological Society*, **149**, 607–613.
- SEILACHER, A. & GOLDRING, R. 1996. Class Psammocorallia (Coelenterata, Vendian Ordovician): Recognition, systematics, and distribution. *GFF*, **118**, 207–216.
- SEREZHNIKOVA, E. A. 2005. Vendian *Ediacaria* from the Zimmii Bereg locality of the White Sea: New records and new reconstructions. *Paleontological Journal*, **39**, 386–394.
- SMITH, D. G. 1981. Progress in Irish Lower Palaeozoic palynology. *Review of Palaeobotany and Palynology*, **34**, 137–148.
- SPRIGG, R. C. 1947. Early Cambrian (?) jellyfishes from the Flinders Ranges, South Australia. *Transactions of the Royal Society of South Australia*, **71**, 212–224.
- STASINSKA, A. 1960. *Velumbrella czarnockii* n. gen., n. sp.—méduse du Cambrien inférieur des Monts de Sainte-Croix. *Acta Palaeontologica Polonica*, **5**, 337–344.
- TIETZSCH-TYLER, D., SLEEMAN, A. G., BOLAND, M. A., DALY, E. P., FLEGG, A. M., O'CONNOR, P. J. & WARREN, W. P. 1994. *Geology of South Wexford: A Geological Description of South Wexford and Adjoining Parts of Waterford, Kilkenny and Carlow to accompany the Bedrock Geology*, 1:100,000 scale map series, Sheet 23, South Wexford. Dublin, Geological Survey of Ireland.
- VONHOF, J. 1997. *Aspects of the sedimentology, palaeontology, and thermal history of the Booley Bay Formation on the Hook Peninsula in SE Ireland*. Unpublished MSc thesis, University of Dublin.
- WADE, M. 1972. Hydrozoans and Scyphozoans and other medusoids from the Precambrian Ediacara fauna, South Australia. *Palaeontology*, **15**, 197–225.
- WAGGONER, B. 1999. Biogeographic analyses of the Ediacara biota; a conflict with paleotectonic reconstructions. *Paleobiology*, **25**, 440–458.
- WANG, H., LIN, B. & LIU, X. 1984. Cnidarian fossils from the Sinian System of China and their stratigraphic significance. *Palaeontographica Americana*, **54**, 136–139.

Discoidal fossils of the Ediacaran biota: a review of current understanding

B. A. MACGABHANN

*Department of Earth and Ocean Sciences, National University of Ireland Galway,
University Road, Galway, Ireland (e-mail: b.macgabhann1@nuigalway.ie)*

Abstract: Discoidal fossils, despite being the oldest, youngest, and most common elements of the Ediacaran biota, have not received their fair share of attention. Taxonomy of discoidal fossils is currently dubious, and some forms have not been properly re-examined since the initial incorrect descriptions as medusae. Attachment discs of benthic stalked forms, which adhere to microbial mats at the sediment–water interface, are unequivocally present without stalks or other upper parts in most discoidal Ediacaran assemblages. However, many discoidal assemblages are likely to have represented a heterogeneous mixture of benthic discoidal organisms, including bacterial colonies, fungi, actinian-grade cnidarians, and perhaps poriferans. Such organisms probably account for the vast majority of fossils in the Fermeuse Formation of Newfoundland and similar assemblages from Norway, England, and Wales. Discs in the underlying complex Mistaken Point assemblages, however, likely mostly represent holdfasts. Other complex assemblages, such as those of South Australia and the White Sea of Russia, unequivocally contain more than one biological construction responsible for the discoidal structures, but holdfasts likely represent a significant proportion. The disc-dominated Fermeuse assemblages and the nearby rangeomorph-dominated Mistaken Point assemblages are unlikely to merely represent different taphonomic windows on identical communities, as previously suggested, but rather reflect environmental control on both biotic composition and taphonomy.

Discoidal fossils were the first described elements of the Ediacaran biota (Billings 1872) and are by far the most abundant component. In terms of age, they are the oldest (Hofmann *et al.* 1990) and, indeed, the youngest (Crimes & McIlroy 1999; Hagadorn *et al.* 2000) Ediacaran-type fossils known. For this reason they represent, potentially, the most important constituent of the biota; however, knowledge of both disc palaeoecology and affinities does not reflect this. In particular, current understanding of disc taxonomy is rather convoluted. Indeed, one of the legacies of initial descriptions of Ediacaran discs as medusae has been a plethora of generic and specific names in the literature. Many of these were described or are known only from single (often unrepresentative, damaged or incomplete) specimens, with genera and species often distinguished by only minor differences, which may, in fact, be taphonomic artefacts or morphologically insignificant from a taxonomic perspective. It did not help that most original descriptions did not separate interpretation from observation, leaving them rather bloated with inappropriate and wildly incorrect interpretative terminology. The situation was perhaps best summarised by Runnegar and Fedonkin (1992), who noted, with reference to the genus *Ediacaria*, that ‘Many of the fossils that have been referred to *E. flindersi* do not resemble the holotype, and specimens identified as *E. flindersi* by different authors

may be totally dissimilar. This is a common situation in the literature and the result is a jumble of useless and misapplied names’ (Runnegar & Fedonkin 1992, p. 379).

In light of this, this contribution sets out to summarize our current knowledge of the Ediacaran discs, highlighting several major issues and inconsistencies, and outlining potential directions for future research.

History of research

Serious study of Ediacaran discoidal fossils began after Sprigg (Sprigg 1947, 1948, 1949) described the first-found elements in the type area in South Australia as ‘jellyfish’, and Glaessner and Wade (Glaessner 1959, 1984; Glaessner & Wade 1966; Wade 1969, 1972) more or less followed this interpretation, considering them stranded pelagic medusae. Seilacher disagreed, describing the discs as a ‘heterogeneous group of trace fossils and the remains of unidentified benthic organisms’ (Seilacher 1984, p. 163), but description of discs as ‘medusae’ continued (e.g. Sun 1986a, b). In the meantime, others had suggested that at least some discs actually represented the basal parts of frond-like taxa (e.g. *Charniodiscus concentricus* Ford, 1958), and this has been borne out by later work (e.g. Jenkins & Gehling 1978; Laflamme *et al.* 2004).

Table 1. *Principal localities of discoid Ediacaran fossils*

Location	Palaeo-continent	References
Algeria	Gondwana	Bertrand-Sarfati <i>et al.</i> 1995
Australia	Australia	Cruse & Harris 1994; Rasmussen <i>et al.</i> 2002
	Australia	Sprigg 1947, 1948, 1949; Southcott 1958; Glaessner 1959, 1984; Glaessner & Wade 1966; Wade 1972; Jenkins & Gehling 1978; Sun 1986 <i>a, b</i> ; Gehling 1987, 1988, 1991; Jenkins 1992; Gehling & Rigby 1996; Gehling <i>et al.</i> 2005; Droser <i>et al.</i> 2006
Canada	Australia	Wade 1969; Mapstone & McIlroy 2005
	Laurentia	Hofmann 1981; Hofmann <i>et al.</i> 1983, 1990; Narbonne & Hofmann 1987; Narbonne & Aitken 1990; Narbonne 1994
	Laurentia	Hofmann <i>et al.</i> 1985; Hofmann <i>et al.</i> 1991; Ferguson & Simony 1991
	Avalonia	Misra 1969; Gehling <i>et al.</i> 2000; Clapham <i>et al.</i> 2003; Laflamme <i>et al.</i> 2004, 2007; O'Brien & King 2004; Hofmann <i>et al.</i> 2005; Narbonne 2005
England	Avalonia	Ford 1958, 1963, 1999; Boynton & Ford 1995; McIlroy <i>et al.</i> 2005
India	Gondwana	De 2003; De 2006
Ireland	Avalonia	Crimes <i>et al.</i> 1995; MacGabhann <i>et al.</i> 2007
Mexico	Laurentia	McMenamin 1996
Namibia	Gondwana	Germes 1972; Crimes & Germes 1982; Hahn & Pflug 1988
Norway	Baltica	Farmer <i>et al.</i> 1992; Crimes & McIlroy 1999
Russia	Baltica	Fedonkin 1978, 1980, 1981, 1990; Martin <i>et al.</i> 2000; Serezhnikova 2005, 2007; Leonov 2007
	Baltica	Bekker 1977, 1990; Grazhdankin <i>et al.</i> 2005
	Siberia	Sokolov 1973; Sokolov & Fedonkin 1984; Vodanjuk 1989; Serezhnikova 2007
Ukraine	Baltica	Zaika-Novatskiy <i>et al.</i> 1968; Palij 1976; Palij <i>et al.</i> 1979; Fedonkin 1983
USA	Laurentia	Hagadorn <i>et al.</i> 2000; Hagadorn & Waggoner 2000

Discoidal fossils have now been described from most Ediacaran assemblages. A list of some of the more important sites, including all material referred to in the text is given in Table 1. It should be noted that this list is in no way exhaustive and, indeed, some of the material is of doubtful biogenicity.

Taphonomy of discoidal fossils

Since basic taxonomic methods and comparative morphology have proved unreliable in trying to gain a better understanding of the true nature and affinities of discoidal Ediacarans, other parameters need to be considered. An important factor in this respect is taphonomy, which must be the primary consideration in investigation of such fossils, and the context in which discoidal assemblages are viewed. Discoidal Ediacaran fossils are preserved in three main styles: these are now discussed.

Conception-style preservation

This form of preservation is currently known only from the Avalon Zone of Newfoundland, and the laterally equivalent Charnwood Forest inlier in central England. Fossils are preserved at these localities by obtrusion by volcanic ash. This ash moulded the upper surface of the organisms, and rapidly lithified, allowing the mould to be cast by sediment from the bed below, upon which the organisms had originally lived. Weathering of the ash reveals vast surfaces covered in fossils, including discoidal holdfasts and solitary discs, which are thus found as low positive epirelief casts (Narbonne 2005).

Death mask-style preservation

Many Ediacaran genera, principally bilaterally symmetrical forms like *Dickinsonia* and *Yorgia*, are found as positive epirelief casts, or negative relief moulds on bed soles (Gehling 1999;

Gehling *et al.* 2005). This particular style of preservation was, until recently, very difficult to account for. It has now been explained as being due to the influence of the microbial mats, a ubiquitous feature of Ediacaran seafloors. On burial of the organisms by event beds, anaerobic decay of the microbial mat caused the precipitation of diagenetic iron sulphide minerals in the sole of the event bed, rapidly lithifying it. This caused external moulds to form around the upper surface of the organisms, which decayed allowing sediment to cast the mould from below. This mode of preservation only occurs in organisms which were more resistant, and not instantly compacted by the rapid sedimentation (Gehling 1999; Gehling *et al.* 2005; Droser *et al.* 2006). Although in general this preservation is limited to complex fossils, some discs are preserved in this style, e.g. *Sekwia* (Hofmann 1981).

Gravity cast preservation

Most discoidal Ediacaran genera, as well as a few rare, complex forms such as *Palaeopascichnus* and *Phyllozoon*, are preserved as positive hyporelief casts on bed soles. Consensus is yet to be reached on the precise details of the taphonomy in the case of the more complex forms. Seilacher *et al.* (2003), for example, regard *Phyllozoon* as living under the mat, although Gehling (1999) regarded it as simply a less resistant form, which was easily compacted. In contrast, this particular mode of preservation is much better understood for discoidal fossils. The organisms were living partially or quasi infaunally within the upper layers of the microbial mat, and on burial, they decayed before a death mask could form. However, the microbially bound sediment was cohesive and firm enough to retain a mould of the lower surface of the organism. This was then cast from above by sediment moving under the influence of gravity. A slightly modified but essentially identical path was followed in the cases of organisms which were removed, perhaps by current action, before burial, in which case sediment cast the vacated mould at the time of sedimentation.

'Gravity cast and death mask' styles of preservation are often found to occur on the same surfaces. However, it may also be the case that no death masks are present, with all the fossils on a particular surface being gravity casts. Narbonne (2005) has labelled surfaces where both occur as 'Flinders-style' assemblages, and surfaces where only gravity casts occur as 'Fermeuse-style' assemblages. These two terms ('Flinders-style' and 'Fermeuse-style') are useful when considering entire assemblages, but the terms 'gravity cast' and 'death mask' are more appropriate when dealing with individual fossils.

Morphology of discoidal fossils

As noted above, taxonomy of discoidal fossils is currently in a state of considerable confusion, and it would, therefore, be of very limited value to simply review all the currently named genera from the literature. In fact, a far more comprehensive resurvey is required (see discussion below). An additional problem is that many descriptions, including most early work, ignored the taphonomy and did not describe the sense of relief (positive hyporelief or positive epirelief) of the fossils. However some mention of the various morphologies is necessary and the general morphological traits of some examples are summarized below and also in Figure 1.

Most discs are preserved as gravity casts, and are comparatively simple, exhibiting various combinations of radial and concentric elements, with or without a central tubercle. This ranges from the flat *Nimbia* (Fedonkin 1980, 1990), with a single ring and occasionally a central tubercle, to the slightly more convex *Tirasiana* (Palij 1976; Palij *et al.* 1979; Fedonkin 1990), with several concentric annuli surrounding a prominent tubercle, to *Spriggia* (Southcott 1958; Sun 1986a), which is flat with dense concentric ridges and grooves, to *Cyclo-medusa* (Sun 1986a), with a combination of several concentric and numerous unbranched radial grooves. Several discs, including the small and simple *Medusinites* and the largest disc *Ediacaria*, show a bipartite organization, often described as 'superimposed discs' or an 'inner disc and outer ring' (Glaessner & Wade 1966; Narbonne & Hofmann 1987). In the case of *Medusinites* the inner disc is smooth, but the outer ring may have some radial elements. *Ediacaria* commonly has concentric features on the inner disc and radial grooves on the outer ring. Although most of these exhibit only low to moderate relief, others such as *Nemiana* (Leonov 2007), which is ornamented only by simple concentric rings, are considerably more three-dimensional.

Other discs are more complex, or with more eccentric structures. *Hiemalora*, known from both positive hyporelief and positive epirelief specimens, consists of a large, smooth central disc surrounded by radial structures, variously interpreted as tentacles or rhizoids (see review in Serezhnikova 2007). *Eoporpita* consists of a small, concentric, ornamented central disc preserved in positive hyporelief, surrounded by rings of prominent tubercles, which have been suggested to represent tentacles (Wade 1972; Narbonne & Aitken 1990). *Sekwia* (found as death masks) is a simple smooth disc with a single crescentic groove (Hofmann 1981). *Mawsonites*, one of the most recognizable Ediacaran taxa and also preserved as

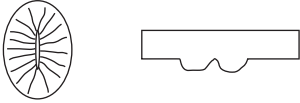
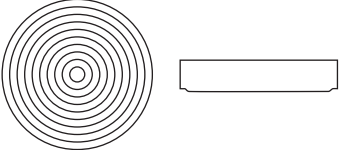

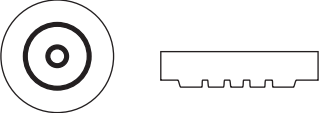
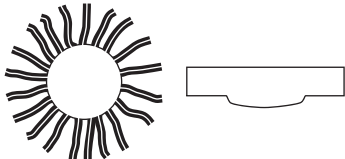
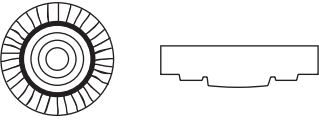
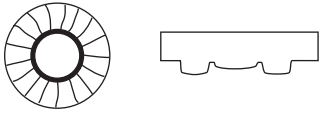
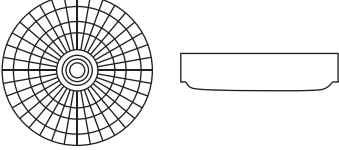

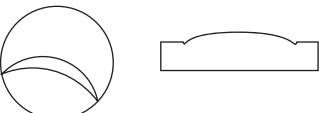
	<i>Aspidella</i> Invaginated disc with radial ribs extending from centre to margin. 2–30 mm.	Billings 1872; Gehling <i>et al.</i> 2000
	<i>Spriggia</i> Flat disc with dense concentric ridges and grooves. May also be fine radial lines extending from specimen margin. 10–80 mm.	Sprigg 1949; Southcott 1958; Sun 1986a; Gehling <i>et al.</i> 2000
	<i>Nimbia</i> Flat disc with or without central tubercle, enclosed by a single circular ridge. 4–15 mm.	Fedonkin 1980, 1990; Hofmann <i>et al.</i> 1990; Crimes & McIlroy 1999
	<i>Tirasiana</i> 2–5 concentric annuli separated by grooves, surrounding a prominent central tubercle. 10–60 mm.	Bekker 1977, 1990; Crimes & McIlroy 1999; Hagadorn <i>et al.</i> 2000
	<i>Hiemalora</i> Flat or convex central disc surrounded by irregular radial structures. 3–40 mm.	Fedonkin 1980, 1990; Vodanjuk 1989; Serezhnikova 2007
	<i>Ediacaria</i> Concentric-ornamented central disc surrounded by outer annulus, which may have thin, unbranched radial lines. ≤ 1 m.	Sprigg 1947; Glaessner & Wade 1966; Wade 1968; Fedonkin 1990; Jenkins 1992; Gehling <i>et al.</i> 2000
	<i>Medusinites</i> Smooth central disc separated from radially-ornamented outer annulus by a deep groove. 1–50 mm.	Sprigg 1947; Glaessner & Wade 1966; Fedonkin 1990; McIlroy <i>et al.</i> 2005
	<i>Cyclomedusa</i> Concentric-structured inner discs surrounded by outer area with both radial and concentric structures. 5–100 mm.	Sprigg 1947, 1949; Glaessner & Wade 1966; Wade 1972; Sun 1986a; Gehling <i>et al.</i> 2000
	<i>Nemiana</i> Highly convex disc with weak concentric ornament. 2–60 mm.	Palij 1976, 1979; Narbonne & Hofmann 1987; Leonov 2007
	<i>Sekwia</i> Convex disc with prominent crescentic groove(s). 9–33 mm.	Hofmann 1981; Narbonne & Aitken 1990

Fig. 1. Outline morphology of some common Ediacaran discs, with indication of structure, relief and key references. Sketches are approximate, and not to scale.

a gravity cast, has a central disc surrounded by rings of lobes, which increase in size outwards (Glaessner & Wade 1966). Finally, *Palaeophragmodictya* (Gehling & Rigby 1996), found in death mask preservation, has a central disc surrounded (in well preserved specimens) by an outer reticulate area, and *Inaria* (Gehling 1988) is a lobate disc (found as both death mask and gravity cast), which often shows evidence for a stalk.

Whilst the more complex discs seem to be fairly well defined, it should be stressed that the overwhelming majority of discs, including the oldest and youngest examples, belong to the morphologically simple group. The oldest discs, reported by Cruse and Harris (1994) from the Stirling Range in Australia, are concentrically arranged discs comparable to *Tirasiana* and *Cyclomedusa* on first glance, but importantly, some are preserved as positive epireliefs and thus cannot be assigned to these genera. Assemblages from strata underlying glaciogenic diamictites attributable to the Elatina glaciation, reported by Hofmann *et al.* (1990) and Bertrand-Sarfati *et al.* (1995) (note that these authors wrongly attributed this diamictite to an Early Cambrian glaciation) are also simple concentrically structured annuli and discs, similar to *Nimbia*. Younger, Cambrian-aged discs, described by Crimes & McIlroy (1999) from northern Norway, and by Hagadorn *et al.* (2000) from the southwestern United States, are again concentrically structured, and are comparable to *Nimbia* and *Tirasiana* (supposedly younger discs described by Crimes *et al.* 1995 are in fact likely to be unrelated to Ediacaran fossils; see MacGabhann *et al.* 2007).

Discoidal pseudofossils

The problem of understanding the Ediacaran discs is exacerbated by the existence of discoidal pseudofossils. The nature of Ediacaran fossils—being preserved as imprints on bed surfaces—has led to Ediacaran bed surfaces in general being examined in much more detail than typical Phanerozoic surfaces, and this has led to a plethora of published descriptions of suspect structures, not all of which seem to represent fossils (e.g. McMenamin 1996; De 2003, 2006). Often copious and highly significant phylogenetic interpretations have been based on discs, which later turn out to be something else entirely. A good example in this regard is the structure *Kullingia*. Originally described as representing a fossil chondrophorine (Føyn & Glaessner 1979; Narbonne *et al.* 1991; Jensen *et al.* 1998) (a medusoid hydrozoan of the subclass Athecatae), *Kullingia* is now known to be a swing mark, an organically generated tool mark consisting of arcuate sets of grooves cut in the sediment by current-forced

oscillation of elongate tethered benthic organisms, such as the sabelliditids (Jensen *et al.* 2002).

Other discs have been regarded as dubiofossils or inorganic structures (e.g. Hofmann 1971), such as sand volcanoes (often modified by tectonic deformation or interaction with microbial mats; Seilacher *et al.* 2005), fluid or gas escape structures, concretions or loading (Cloud 1960; Sun 1986a). While in some cases this is well justified (e.g. Cloud 1973; Sun 1986a), others have previously been interpreted as pseudofossils simply on the basis that they occurred in rocks thought to be too old to contain evidence of life. Indeed, one such case was the first named Ediacaran body fossil *Aspidella terranovica* from the Avalon Peninsula of Newfoundland, described in the late nineteenth century by Billings (1872). It was only after the discovery of much more complex undoubted fossils at Mistaken Point (Misra 1969), in strata stratigraphically beneath *Aspidella*-bearing beds, that *Aspidella* was finally confirmed as a fossil (Gehling *et al.* 2000).

The *Aspidella* controversy

Detailed examination of the *Aspidella*-bearing beds in the Fermeuse Formation of Newfoundland has revealed that the discs, previously assumed to be inorganic pseudofossils, are indeed true fossils. Rare examples of the tentaculate disc *Hiemalora*, the tri-radially symmetrical *Triforillon*, and the enigmatic serial fossil *Palaeopaschichnus* are found to occur in the section, but the vast majority of the fossils are simple discs, examples of which resemble not only the type material of *Aspidella*, but also most other Ediacaran discoidal genera (Gehling *et al.* 2000). Many of the discs were also seen to strongly resemble those known to be the basal attachment discs of known stalked frondose taxa. Furthermore, there was seen to be no clear distinction between different genera. Instead, it was proposed that the discs could be described in terms of three end-member preservational morphs of *Aspidella*, between which there exists an 'insensible gradation' (*sic*) in morphological form (Gehling *et al.* 2000). These were labelled the convex-morph (strong hyporelief, similar to *Ediacaria*), the flat-morph (low hyporelief with common concentric rings, similar to *Spriggia*), and the type morph (invaginated disc with radial ribs, similar to the type *Aspidella*). These were not distinguished as separate genera, as there was no satisfactory way to differentiate between the different forms. Observing that many Ediacaran discoidal fossils were represented within this gradation, Gehling *et al.* (2000) listed no less than twenty-four discoidal species in sixteen genera as junior synonyms of *Aspidella terranovica*. This list is reproduced in Table 2.

Table 2. Probable junior synonyms of *Aspidella*, according to Gehling *et al.* (2000)

Taxon	Author	Location	Morph
<i>Paramedusium africanum</i>	Gürich 1933	Namibia	Flat
<i>Ediacaria flindersi</i>	Sprigg 1947	South Australia	Convex
<i>Beltanella gilesi</i>	Sprigg 1947	South Australia	Convex
<i>Cyclomedusa davidi</i>	Sprigg 1947	South Australia	Convex
<i>Protodipleurosoma wardi</i>	Sprigg 1947	South Australia	Flat-type
<i>Tateana inflata</i>	Sprigg 1947	South Australia	Convex
<i>Cyclomedusa radiata</i>	Sprigg 1949	South Australia	Flat-convex
<i>Cyclomedusa gigantea</i>	Sprigg 1949	South Australia	Convex
<i>Madigania annulata</i>	Sprigg 1949	South Australia	Flat
<i>Cyclomedusa plana</i>	Glaessner & Wade 1966	South Australia	Flat
<i>Planomedusites patellaris</i>	Sokolov 1972	Ukraine	Flat
<i>Medusinites patellaris</i>	Sokolov 1972	Ukraine	Flat
<i>Tirasiana disciformis</i>	Palič 1976	Ukraine	Convex
<i>Tirasiana coniformis</i>	Palič 1976	Ukraine	Convex
<i>Tirasiana concentralis</i>	Bekker 1977	Urals	Convex
<i>Paliella patelliformis</i>	Fedonkin 1980	White Sea	Flat
<i>Protodipleurosoma rugulosum</i>	Fedonkin 1980	White Sea	Flat
<i>Cyclomedusa minima</i>	Fedonkin 1981	White Sea	Type-convex
<i>Cyclomedusa delicata</i>	Fedonkin 1981	White Sea	Flat-convex
<i>Irridinitus multiradiatus</i>	Fedonkin 1983	Ukraine	Type
<i>Spriggia wadea</i>	Sun 1986a	South Australia	Flat
<i>Vendella larini</i>	Gureev 1987	Ukraine	Type
<i>Glaessneria imperfecta</i>	Gureev 1987	Ukraine	Flat
<i>Jampolium wyrzhykowskii</i>	Gureev (in Ryabenko <i>et al.</i> 1988)	Ukraine	Flat

This was not the first time that such intergradation had been noted, or caused problems. For example, the genus *Tateana* has variously been considered a separate genus (Sprigg 1949), a junior synonym of *Ediacaria* (Harrington & Moore 1956), or a junior synonym of *Cyclomedusa* (Glaessner & Daily 1959; Sun 1986a). Jenkins (1984) however, suggested that one species of *Cyclomedusa*, *C. radiata*, did not belong to this genus, and assigned it as a junior synonym of *Tateana inflata*.

Glaessner and Wade (1966) suggested that the separation of *Spriggia* from *Cyclomedusa* was impractical due to intergrading, and Sun (1986a) similarly referred to the gradation in *Cyclomedusa* and *Spriggia* as the '*Cyclomedusa* plexus' although he considered the two genera as separate entities. Jenkins (1992) later recorded a gradation between *Cyclomedusa*, *Ediacaria* and *Spriggia* in South Australia, while Fedonkin (1990) observed that many forms assigned to *Ediacaria* intergraded with forms assigned to *Tirasiana*. Hagadorn *et al.* (2000) restated this, noting that a thorough revision of 'medusoid' taxonomy was necessary.

A. *terranovica*—a single species of organism?

One thing which Gehling *et al.* certainly did not intend by this synonymization was to imply that all Ediacaran discs belong to a single species of

organism, stating explicitly that the name carried 'no implied interpretation of the biological origins or affiliations of discs, unlike such genera as *Cyclomedusa* and *Charniodiscus*'. (Gehling *et al.* 2000, p. 446). The intention was simply to stress the fact that no consistent distinction can be made between the various discoidal structures preserved in Ediacaran assemblages and, indeed, this is, to some extent, justified. In particular, the discs of the Fermeuse Formation do exhibit the indefinable variation in form noted (personal observations). However, evidence that more than one type of organism is now included in *Aspidella* from the Fermeuse Formation of Newfoundland is plentiful.

Distribution of various morphs

The variation in form of *Aspidella* has been attributed as being due to two factors; namely the size of the discs and the clay/sand ratio of the host sediment. Gehling *et al.* (2000, text-fig. 7) presented a graph of distribution of the three end-member morphs against these two factors. The three morphs clearly fall within specific, and sometimes discrete, fields and it was proposed that this demonstrated disc preservation to be a two-variable system. It is, however, significant that, while the *Spriggia* field does not overlap the other two, the *Ediacaria* field overlaps most of the *Aspidella* field. This clearly demonstrates that a two variable system is not sufficient to

differentiate the morphs: a third factor needs to be considered in order to segregate the forms in discrete morphospace. The precise nature of this extra factor, be it intrinsic or extrinsic, is of course difficult to clearly identify; however if it was intrinsic, the most likely candidate would be biological affinity.

Ecology

Aspidella was interpreted as a holdfast based on two specimens with putative stems (Gehling *et al.* 2000), although it was stressed that this could not necessarily be extrapolated to all specimens. These specimens have since been examined by the author and also other rare stem-bearing discs observed in the Fermeuse Formation, and there is no doubt that some specimens are indeed holdfasts. Discoidal specimens from Australia and Russia have also been interpreted as holdfasts (Jenkins 1992; Serezhnikova 2005). However, the density of discs on some surfaces in the Fermeuse Formation is extremely high (Fig. 2), with up to 3000–4000 individuals per m² on some surfaces (Gehling *et al.* 2000). Such densities stand in stark contrast to those reported by Clapham *et al.* (2003) of all taxa from the stratigraphically underlying assemblages at Mistaken Point. These assemblages are preserved in Conception-style (i.e. buried by volcanic ash). Weathering of this ash reveals vast surfaces covered in complex fossils (Fig. 3), dominated by taxa belonging to the rangeomorph group (Misra 1969; Narbonne 2004, 2005). Of seven surfaces measured by Clapham and colleagues, six had densities between 7 and 40 individuals per m². The seventh, and densest surface, at Bristy Cove, was still an order of magnitude lower than the Fermeuse assemblages at 149.3 individuals per m². It should be noted, however, that this density is based on a total exposed surface area of only 0.71 m², contrasting strongly with the E surface at Mistaken Point, which has a density of 39.7 individuals per m², measured from a surface area of 103.7 m² (Clapham *et al.* 2003). The Bristy Cove density is, thus, unlikely to be statistically representative.

Clapham and colleagues also analysed the ecological structure of the Mistaken Point surfaces in detail (Clapham & Narbonne 2002; Clapham *et al.* 2003), and showed this to be strikingly similar to modern marine communities. Included in this was evidence of spatial distribution patterns for certain taxa, including frondose forms. Given the spatial distribution and relatively low population densities of frondose taxa at Mistaken Point, it would seem unlikely that a double order of magnitude increase in population to the levels seen in the Fermeuse Formation could be ecologically sustainable (see below for further discussion). Overprinting of larger specimens onto underlying laminae, which was suggested to occur by

Gehling *et al.* (2000), cannot account for more than a fraction of this difference; only a small number of specimens from each surface will overprint through, onto a small number of underlying laminae. Even if it is assumed that the extraordinarily high fossil density at Bristy Cove was representative of Mistaken Point communities, every fossil on each of 20 laminae would need to be imprinted onto a single surface to reach a density of 3000 individuals per m². A much more likely interpretation is that although some discs represent frond holdfasts, the vast majority represent other discoidal morphologies.

Mode of growth

Some of the discoidal fossils of the Fermeuse assemblages resemble stacked discs, growing larger upwards (Gehling *et al.* 2000, text-fig. 8a). Other fossils have a similar morphology, but are not quite as three-dimensional in aspect (Fig. 4). A possible interpretation of these differences is that the organisms were growing upwards to keep pace with sedimentation; where sedimentation rates were lower, fossils are less three-dimensional. Such a growth pattern has not been observed for confirmed holdfasts, indicating that these fossils may represent a different mode of growth.

Size

Discs in the Fermeuse Formation can grow quite large (Fig. 5), with some reaching *c.* 15 cm in diameter. Holdfasts of this size have not been positively identified to date; most holdfasts in the Mistaken Point assemblages would be below half this size (a similar point was made by Peterson *et al.* 2003). Limitation of such large holdfasts to the Fermeuse assemblages seems unlikely: a better interpretation may be that the larger discs represent a different construction.

Individually, perhaps none of these factors is entirely compelling but, taken in combination, they provide good evidence for the existence of several different biological constructions in the Fermeuse assemblages. This makes the synonymization of sixteen described Ediacaran genera with *Aspidella* a wholly unsatisfactory solution to the discoidal fossils issue.

Controls on composition of Avalonian assemblages

Fermeuse discs should not, however, be solely considered in isolation, but also in the context of other Avalonian biotas. Considerable differences are demonstrable between the disc dominated Fermeuse and the nearby rangeomorph dominated



Fig. 2. High density of discs in the Fermeuse Formation, Silos Cove, Ferryland. Coin (Canadian \$1) is 26 mm in diameter.



Fig. 3. Mistaken Point Biota: different taphonomic window or different organisms? Mistaken Point Formation, Mistaken Point. Coin (Canadian \$1) is 26 mm in diameter.

Mistaken Point assemblages. Three main potential explanations for these differences follow.

Age (biostratigraphic)

Since the main Fermeuse assemblages in Newfoundland are stratigraphically much younger than the Mistaken Point assemblages, differences between the two in terms of fossil content and morphology may simply be a reflection of this temporal disparity. However, the occurrence of both Fermeuse- and Mistaken Point-style assemblages

in the Trepassey Formation (which occurs stratigraphically between the two) may rule this out. This seems to be consistent with evidence from other locations with Fermeuse-style assemblages. In particular, a discoidal biota reported from the Innerelv Member of the Stappogiedde Formation in northern Norway (Farmer *et al.* 1992) occurs only 160 m stratigraphically above Mortensnes Formation (the upper of the two Varanger glacial diamictites). This is thought to be equivalent in age to the Gaskiers Formation of Newfoundland (e.g. Halverson *et al.* 2005), but in Newfoundland the stratigraphic

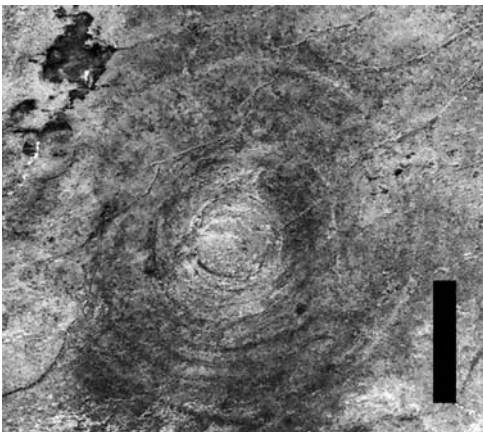


Fig. 4. Flat ‘stacked discs’ form of *Aspidella* with low relief, Fermeuse Formation, Silos Cove, Ferryland. Scale bar 20 mm.



Fig. 5. Large specimen of flat morph of *Aspidella*, Fermeuse Formation, Silos Cove, Ferryland. Scale bar 20 mm.

distance between the glacial diamictites and overlying Ediacaran fossils is 1.5 km to the oldest Mistaken Point-style assemblage in the Drook Formation (Narbonne & Gehling 2003). Fermeuse assemblages are separated from the Gaskiers by the entire thicknesses of the Drook, Briscal, and Mistaken Point formations. Even considering the potential effects of differential subsidence and sedimentation rates between the two basins, it is possible that the Norwegian discs may be much older than the lowest Fermeuse-style assemblages in Newfoundland. This is perhaps supported by the occurrence of the triradially symmetrical fossil *Triforillonia* in the Fermeuse Formation; similar fossils are elsewhere confined to the Ediacara/White Sea type assemblages, thought to be *c.* 555 Ma in age (Gehling *et al.* 2000; Martin *et al.* 2000; Narbonne 2005). Recent discoveries in the north of Newfoundland (O'Brien & King 2004) may also support this, with Mistaken Point style assemblages occurring much higher in the stratigraphic column than previously recorded on the Avalon Peninsula (Hofmann *et al.* 2005).

Preservation (taphonomic)

An alternative consideration may be that the preservation of the fossils is the key factor. The importance of taphonomic style with regard to the fossils from the Avalon Zone of Newfoundland was noted by Narbonne (2005). He observed that while the Mistaken Point assemblages were preserved in Conception-style, fossils of the stratigraphically overlying St. John's Group were preserved in Fermeuse-style (in fact, both represent the type areas for these particular styles of preservation). Noting that both styles occurred in the intervening Trepassey Formation, along with one example of three-dimensional preservation within a bed (a less significant form of preservation with regard to discoidal fossils), and that each style of preservation was associated with a very different biotic composition, Narbonne (2005) concluded that the different assemblages reflected merely different preservational windows into identical communities.

Environmental (ecological)

However, when palaeoecology is taken into consideration along with taphonomy, a different story emerges. Fossil population densities in the Fermeuse Formation are, as noted above, an order of magnitude higher than the Mistaken Point assemblages. Accepting that the different assemblages are merely different preservational windows on the identical communities means that potentially ninety five percent of the organisms originally present at Mistaken Point are not preserved. Even

assuming lower values of around 1000 individuals per m² in the Fermeuse Formation, and taking the Bristy Cove population density for the Mistaken Point assemblages, this would mean that at Bristy Cove, the preserved fossils represent only a mere fifteen percent of the organisms originally present. It is extremely difficult to envisage how this is compatible with the finely balanced ecological structure demonstrated for these surfaces by Clapham and colleagues (Clapham & Narbonne 2002; Clapham *et al.* 2003), especially if many of the discs represent holdfasts. A better interpretation may be that both the biotic composition of the assemblages and the preservation style were environmentally controlled. Fermeuse organisms may have lived only on sediment bound by a different type of microbial mat, or where sedimentation was too rapid for microbial mats to form. This may not have encouraged rapid lithification of volcanic ash if buried, preventing Fermeuse assemblages from being preserved in Mistaken Point style. Conversely, if Mistaken Point assemblage organisms could not live on Fermeuse substrates, they would not have been preserved in Fermeuse-style. This hypothesis is always going to be extremely difficult to validate, however palaeoecological segregation does appear to be consistent with the available sedimentological evidence. Fermeuse assemblages occur in the thinly bedded siltstone and mudstone dominated (and commonly slumped) slope facies of the Fermeuse Formation, whilst the Mistaken Point assemblages are restricted to the deeper basinal and lower slope facies, characterized by thickly bedded turbidites and contourites. Occurrence of both assemblages in the intervening transitional Trepassey Formation, which is dominated by mudstones and thinly bedded turbidites with some slumped beds, is not inconsistent with an environmental control interpretation (Wood *et al.* 2003). This should be testable by detailed integrated sedimentological and taphonomic analysis of the Mistaken Point, Trepassey, and Fermeuse formations: if this hypothesis is correct, Fermeuse assemblages should be limited to the shallower facies, and Mistaken Point assemblages limited to ash horizons in deeper facies. Ash horizons in the shallower facies should not preserve fossils in Mistaken Point style. The new occurrences of Ediacaran fossils on the Bonavista Peninsula of Newfoundland (O'Brien & King 2004; Hofmann *et al.* 2005), in which the typical Mistaken Point assemblages occur much higher in the stratigraphy than on the Avalon Peninsula, may be of fundamental significance in answering this particular question.

The suggestion that Fermeuse sediments were not microbially bound, despite preserving high densities of Ediacaran fossils, may cause some surprise given the degree to which the microbial mat death

mask model has been accepted. Indeed the idea that the Ediacaran was a time of 'special taphonomic conditions' has become completely entrenched in the literature. However, this over-reliance on microbial mats has disguised the fact that gravity cast preservation requires only a stiff substrate capable of holding the mould of a semi-infaunal organism until it is cast from above. Any stiff Proterozoic substrate, whether microbially bound or not, would have been sufficient to preserve organisms in this style. Droser *et al.* (2002) have shown that non-microbially bound substrates in the Early Cambrian were stiff and cohesive, and similar stiff substrates have existed, though more rarely, throughout the Phanerozoic. If the above suggestion is correct, then these stiff Phanerozoic substrates should have been able to hold moulds of bases of partially infaunal non-mineralized organisms as required, allowing their fossilization as gravity casts.

Nature of the Fermeuse discs

Accepting that the fossils of the Fermeuse assemblages are not preservational variations of the rangeomorphs and other complex organisms preserved at Mistaken Point, as demonstrated above, alternative interpretations must be sought. Peterson *et al.* (2003) have clearly outlined a compelling case for interpretation of some discs as fungi or analogous forms (note that although the tiering demonstrated by Clapham *et al.* (2003) shows the erect forms from Mistaken Point to have been partitioning a food source in the water column, a notable departure from a fungal model (Sperling & Peterson 2007) there are no such complications for the discs). Grazhdankin (2001) has also suggested that some forms may represent microbial colonies. Since growth of microbial colonies is often dependant on chemical cycles, and since both fungi and microbial colonies may have no constraints on maximum colony size, concentrically ringed and very large forms are particularly amenable to these interpretations. Further, some of the Fermeuse discs are extremely similar to discs from other localities, which have previously been interpreted as fungal or microbial: for example, Figure 4 is a disc from Silos Cove, near Ferryland, Newfoundland, which strongly resembles specimens illustrated and interpreted as 'algal colonies' by Glaessner (1969, fig. 2) from the >1 Ga Bass Formation of the Grand Canyon, Arizona, USA. Similar discs are common in the Fermeuse Formation.

The possibility that some of the discs represent poriferan-grade taxa should also not be discarded. Some of the oldest discoidal Ediacaran-type fossils known are found in the Twitya Formation of the Mackenzie Mountains, below the

Elatina-equivalent Stelfox glaciogenic diamictite (Hofmann *et al.* 1990), and are thus older than the Elatina glaciation, the end of which marks the beginning of the Ediacaran Period (Knoll *et al.* 2004). In China, the Datangpo Formation, which underlies the Elatina-equivalent Nantuo diamictite, is dated at 663 ± 4 Ma (Zhou *et al.* 2004), and the Twitya discs are likely of similar age—i.e. at least sixty million years older than any other Ediacaran fossils. Recent molecular clock dates have suggested that poriferan-grade organisms evolved around this time (Peterson & Butterfield 2005), and it might be useful to consider that this is perhaps not a coincidence. If poriferan-grade organisms were capable of being preserved in this style in the Cryogenian, there is no reason to believe they could not have been similarly preserved in the Ediacaran. The undoubted presence of crown-group sponges in *Palaeophragmodictya* (Gehling & Rigby 1996) supports this suggestion.

Another idea, which should be considered, is that some of the discs represent benthic cnidarians, in particular actinian dwelling traces, similar to the trace fossil *Bergaueria* (Alpert 1973). Thus, the discs as preserved would represent the bases of anemone-like organisms. Some specimens show possible evidence of upwards growth or movement through the sediment, which may support the idea that such organisms were present.

One potential interpretation which should however be unequivocally rejected is that any of the fossils represent any form of 'medusa'. Seilacher (1984) has outlined objections to pelagic forms being preserved on bed soles, and our work on Cambrian fossils (MacGabhann *et al.* 2007) has supported the view that low-density pelagic organisms cannot be preserved in this style. None of the fossils in the Fermeuse assemblages show any evidence of transport, and discs, which appear to be growing up through the sediment, must in any case be benthic. The idea that any of the Fermeuse specimens represent 'swing marks' should also be dismissed. *Bona fide* swing marks, such as *Kullingia*, are generally identifiable by the close spacing of ridges (in positive hyporelief) and presence of a central feature representing the attachment point of the tool. Finally, Gehling *et al.* (2000) have comprehensively dismissed the possibility of most other inorganic interpretations for the Fermeuse discs.

Nature of discs in other Ediacaran assemblages

This then leaves the issue of the discoidal fossils in other Ediacaran assemblages. Most other disc dominated assemblages—in particular those from England (McIlroy *et al.* 2005), Wales (Cope 1977),

and Finnmark (Farmer *et al.* 1992)—are likely similar in biotic composition and nature to the Fermeuse assemblages. However, most of the discs in the Mistaken Point assemblages, which are of course, preserved in Conception-style rather than as gravity casts like the Fermeuse fossils, may convincingly be interpreted as holdfasts. The same has been suggested for many Australian discs preserved as gravity casts including *Ediacaria*, but Jenkins (1992) noted that specimens comparable to *Ediacaria* reach up to one metre in diameter. Such enormous size is completely inconsistent with a holdfast interpretation, clearly indicating the presence of at least two discoidal morphologies. Russian assemblages are broadly similar to those in Australia. Interestingly, fossils preserved as gravity casts from the White Sea area have recently been assigned to *Ediacaria* and interpreted as holdfasts by Serezhnikova (2005). One unusual aspect to this interpretation is the view that the holdfasts were attached not at the sediment surface, but at a particular layer underneath the sediment–water interface; this surface is hypothesized to be a bacterial film at a boundary between liquid and microbially bound sediment. It is further speculated that organisms were preserved when their top parts were removed by storms, with the gaps then being infilled by storm-carried sediment. However this interpretation may not be consistent with the proposed nature of Ediacaran substrates, which are characterized by a sharp interface between stiff, microbially bound sediment and the overlying water column (Gehling 1999; Hagadorn & Bottjer 1999). This is clearly demonstrated for the White Sea sediments by *Dickinsonia* and *Yorgia* surface trace fossils (Ivantsov & Malakhovskaya 2002; Fedonkin 2003; Gehling *et al.* 2005), which indicate the presence of a stiff upper surface to substrates capable of holding the imprints of organisms after they had moved on. As described above, preservation of discoidal fossils as gravity casts is generally believed to be due to moulding of the lower surface of the organism on this stiff substrate.

Holdfasts? Holdfasts of what?

Finally, interpretation of discs as ‘holdfasts’ raises the interesting question of what is on the stem. In some cases attached fronds are still visible, and in the case of the Mistaken Point assemblages assignment of many solitary discs to *Charniodiscus* may not be far off the mark. Attachment discs are also associated with *Charnia* and perhaps other rangeomorphs, however these appear to have a much narrower range—both in terms of environment and age—than the discs (Narbonne 2004, 2005), and it is unlikely that rangeomorph holdfasts form a

significant component of most other discoidal assemblages. It is also entirely possible that completely unknown taxa are represented by holdfasts alone. One suggestion, which is perhaps unlikely, is the presence of true sea pens—similarities between Ediacaran forms and Phanerozoic organisms in this regard is likely due to evolutionary convergence. In defence of this statement, frondose morphology is known to have independently evolved in several unrelated Ediacaran lineages, represented for example by the taxa *Charniodiscus* (Laflamme *et al.* 2004), *Charnia* (Laflamme *et al.* 2007), *Swartpuntia* (Narbonne *et al.* 1997), and taxa (which have not been formally described) from the Mistaken Point assemblages such as the ‘Xmas tree’ (e.g. Clapham *et al.* 2003).

Taxonomy of discoidal fossils

The above discussion clearly highlights the main problem faced when trying to interpret these fossils: basic discoidal forms are geometrically and constructionally so simple that they are much more likely than other, more complex shapes, to evolve in multiple lineages. If frondose morphology can evolve independently in several unrelated groups, convergent evolution on discoidal morphology may also have been attained many times, perhaps including several extinct lineages. Further, many inorganic structures mimic biogenic forms, introducing additional complications. Thus, trying to interpret their origin is always likely to be an extremely complex problem. Integration of taphonomic and palaeoecological studies, such as the discussion above on the nature of the Fermeuse assemblage discs, is necessary to advance our knowledge of the organisms represented by the discoidal fossils.

However, the problem of disc taxonomy should not be ignored. As noted, the assignment of most discs to *Aspidella* is a rather unsatisfactory solution to the problem. Indeed, an unwelcome side effect of this has been the potential for subsequent descriptions of Ediacaran assemblages to treat the form taxon *Aspidella* as if it were a proper taxon, making no distinction between the various preservational morphs described by Gehling *et al.* (2000). This approach has the capacity to severely limit the information potential of such material. Describing all discs as *Aspidella* merely tells us there are discs present, and nothing further. Gehling *et al.* (2000, p. 446) attempted to assuage this problem by suggesting that future descriptions make reference to which preservational morph of *Aspidella* the material most closely approaches: ‘in future systematic descriptions of discoidal fossils of the *Aspidella* plexus... the commonly

used names of junior synonyms should be retained as form-genera to represent certain styles of preservation...the three end members of the *Aspidella* plexus: 'Aspidella' for invaginate morphs, 'Spriggia' for flat, annulate morphs, and 'Ediacaria' for convex morphs, represent the most parsimonious form-genera under which Ediacaran discoidal fossils can be accommodated.' Unfortunately, this has not been applied in practice (e.g. Hofmann & Mountjoy 2001; Pyle *et al.* 2004; Droser *et al.* 2006).

Conclusions and suggestions for future research

Discoidal fossils, despite their abundance in the Ediacaran biosphere, have not received their fair share of attention. Several different benthic discoidal morphologies are present in Ediacaran assemblages; no convincing cases exist for assignment of discs to pelagic 'medusae'. Attachment discs (or holdfasts) representing the basal parts of stalked forms are unequivocally present in many discoidal assemblages, but suggestions that most discs represent holdfasts are likely overstated. It is also unlikely that many holdfasts outside the Mistaken Point assemblages are attachment discs of rangeomorph taxa. The range of potential groups represented by discoidal forms is still considerable at present and may include cnidarian as well as poriferan grade organisms, whilst larger discs and concentrically ringed forms could potentially represent non-metazoan grades such as fungal or bacterial colonies. This applies to discoidal fossils from all reported Ediacaran fossil sites, but in particular the Fermeuse assemblages of Newfoundland, and similar assemblages dominated by discoidal forms. The difference between the disc-dominated Fermeuse assemblages and rangeomorph-dominated Mistaken Point assemblages in Newfoundland does not appear to be due to taphonomic style alone, but is more likely due to environmental control on the biotas. This may also have exerted an influence on taphonomy. Discoidal fossils in Australian assemblages likely represent holdfasts for the most part, although other forms are unequivocally present; the same applies to Russian assemblages.

Future research directions, which may be productive in advancing our knowledge of the Ediacaran discs, include more thorough integrated studies of the taphonomy, morphology and palaeoecology of discoidal assemblages, and a comparison of Ediacaran discs with Phanerozoic equivalents. A complete taxonomic overhaul of discoidal fossils is required: not a review from the literature, but rather a complete critical reassessment of the discs from all Ediacaran localities. It is very probably the case that due to the naming of taxa from single,

often damaged or unrepresentative specimens, the overzealous splitting of taxa in some cases, and the misuse and misapplication of names as noted by Runnegar & Fedonkin (1992), discussed above, the entire discoidal fossil taxonomy may simply have to be abandoned. Pending this revision however, future descriptions should assign fossils to whichever of the distinctive existing Ediacaran genera the material most closely approaches (see for example some of the taxa illustrated in Fig. 1), thus retaining the maximum amount of information conveyed by the names. *These disc taxa must not be used in diversity analyses, as their biological significance is not certain.* I unequivocally recommend against the establishment of new discoidal genera at present. Finally, experimental taphonomy, along the lines of Norris (1989) may also be crucial in determining the biological affinities of the various fossils.

Thanks to J. Murray for enormous support, assistance, encouragement, and constructive criticism of this research and the text. Thanks also to G. M. Narbonne for the invitation to discuss the *Aspidella* controversy over the outcrops in Newfoundland on a field trip in June 2005: the eventual argument over the outcrop with G. M. Narbonne, J. G. Gehling, D. Erwin and M. Laflamme amongst others proved extremely useful in formulating ideas expressed here. Field assistance was provided by L. Flude, E. Bamforth, and R. Martindale. Very constructive reviews of the manuscript by Marc Laflamme and Enrico Savazzi helped greatly improve the paper. BAM is supported by an NUI Galway Postgraduate Fellowship. Partial funding for the Newfoundland trip was provided by an NUI Galway Millennium Research Fund Grant to John Murray. This is a contribution to IGCP Project 493: The Rise and Fall of the Vendian (Ediacaran) Biota.

References

- ALPERT, S. P. 1973. *Bergaueria* Prantl (Cambrian and Ordovician), a probable actinian trace fossil. *Journal of Paleontology*, **47**, 919–924.
- BEKKER, YU. R. 1977. The first palaeontological finds in the Riphean of the Urals. *Izvestiya Akademiyi Nauk SSSR, Seriya Geol.*, **3**, 90–100.
- BEKKER, YU. R. 1990. Vendian Metazoa of the Urals. In: SOKOLOV, B. S. & IWANOWSKI, A. B. (eds) *The Vendian System, Vol. 1: Palaeontology* (English edition), 121–131.
- BERTRAND-SARFATI, J., MOUSSINE-POUCHKINE, A., AMARD, B. & AIT-KACI, A. A. 1995. First Ediacaran fauna found in western Africa and evidence for an Early Cambrian glaciation. *Geology*, **23**, 133–136.
- BILLINGS, E. 1872. Fossils in Huronian rocks. *Canadian Naturalist and Quarterly Journal of Science*, **6**, 478.
- BOYNTON, H. E. & FORD, T. D. 1995. Ediacaran fossils from the Precambrian (Charnian Supergroup) of Charnwood Forest, Leicestershire, England. *Mercian Geologist*, **13**, 165–182.

- CLAPHAM, M. E. & NARBONNE, G. M. 2002. Ediacaran epifaunal tiering. *Geology*, **30**, 627–630.
- CLAPHAM, M. E., NARBONNE, G. M. & GEHLING, J. G. 2003. Paleoecology of the oldest known animal communities: Ediacaran assemblages at Mistaken Point, Newfoundland. *Paleobiology*, **29**, 527–544.
- CLOUD, P. 1960. Gas as a sedimentary and diagenetic agent. *American Journal of Science*, **258-A**, 35–45.
- CLOUD, P. 1973. Pseudofossils: A Plea for Caution. *Geology*, **1**, 123–127.
- COPE, J. C. W. 1977. An Ediacara-type fauna from South Wales. *Nature*, **268**, 624.
- CRIMES, T. P. & GERMS, G. J. B. 1982. Trace fossils from the Nama Group (Precambrian–Cambrian) of southwest Africa (Namibia). *Journal of Paleontology*, **56**, 890–907.
- CRIMES, T. P. & MCILROY, D. 1999. A biota of Ediacaran aspect from lower Cambrian strata on the Digermul Peninsula, Arctic Norway. *Geological Magazine*, **136**, 633–642.
- CRIMES, T. P., INSOLE, A. & WILLIAMS, B. P. J. 1995. A Rigid-Bodied Ediacaran Biota from Upper Cambrian Strata in Co. Wexford, Eire. *Geological Journal*, **30**, 89–109.
- CRUSE, T. & HARRIS, L. B. 1994. Ediacaran fossils from the Stirling Range Formation, Western Australia. *Precambrian Research*, **67**, 1–10.
- DE, C. 2003. Possible organisms similar to Ediacaran forms from the Bhandar Group, Vindhyan Supergroup, Late Neoproterozoic of India. *Journal of Asian Earth Sciences*, **21**, 387–395.
- DE, C. 2006. Ediacara fossil assemblage in the upper Vindhyan of Central India and its significance. *Journal of Asian Earth Sciences*, **27**, 660–683.
- DROSER, M. L., GEHLING, J. G. & JENSEN, S. 2006. Assemblage palaeoecology of the Ediacara biota: The unabridged edition? *Palaeogeography, Palaeoclimatology, Palaeoecology*, **232**, 131–147.
- DROSER, M. L., JENSEN, S. & GEHLING, J. G. 2002. Trace fossils and substrates of the terminal Proterozoic–Cambrian transition: Implications for the record of early bilaterians and sediment mixing. *Proceedings of the National Academy of Sciences of the United States of America*, **99**, 12572–12576.
- FARMER, J., VIDAL, G., MOCZYDLOWSKA, M., STRAUSS, H., AHLBERG, P. & SIEDLECKA, A. 1992. Ediacaran fossils from the Innerelv Member (late Proterozoic) of the Tanafjorden area, northeastern Finnmark. *Geological Magazine*, **129**, 181–195.
- FEDONKIN, M. A. 1978. New locality of nonskeletal Metazoa in Vendian of Winter Shore. *Doklady Akademii Nauk SSSR*, **239**, 1423–1427.
- FEDONKIN, M. A. 1980. New Precambrian Coelenterata in the North of the Russian Platform. *Paleontological Journal*, **1980**(2), 1–10.
- FEDONKIN, M. A. 1981. Belomorskaya biota venda. *Trudy Akademii Nauk SSSR*, **342**, 1–100. [In Russian.]
- FEDONKIN, M. A. 1983. Nonskeletal fauna of the Podolian Pridnyestrovya. In: VELIKANOV, V. A., ASEEVA, E. A. & FEDONKIN, M. A. (eds) *Vend Ukrainy*, 128–139. [In Russian.]
- FEDONKIN, M. A. 1990. Systematic Description of Vendian Metazoa. In: SOKOLOV, B. S. & IWANOWSKI, A. B. (eds) *The Vendian System, Vol. 1: Palaeontology* (English edition), 71–120.
- FEDONKIN, M. A. 2003. The origin of the Metazoa in the light of the Proterozoic fossil record. *Paleontological Research*, **7**, 9–41.
- FERGUSON, C. A. & SIMONY, P. S. 1991. Preliminary report on structural evolution and stratigraphic correlations, northern Cariboo Mountains, British Columbia. *Current Research, Part A, Geological Survey of Canada, Paper*, **91-1A**, 103–110.
- FORD, T. D. 1958. Precambrian fossils from Charnwood Forest. *Proceedings of the Yorkshire Geological Society*, **31**, 211–217.
- FORD, T. D. 1963. The Pre-Cambrian fossils of Charnwood Forest. *Transactions of the Leicester Literary and Philosophical Society*, **57**, 57–62.
- FORD, T. D. 1999. The Precambrian fossils of Charnwood Forest. *Geology Today*, **15**, 230–234.
- FØYN, S. & GLAESSNER, M. F. 1979. *Platysolenites*, Other Animal Fossils, and the Precambrian–Cambrian Transition in Norway. *Norsk Geologisk Tidsskrift*, **59**, 25–46.
- GEHLING, J. G. 1987. Earliest known Echinoderm—a new Ediacaran fossil from the pound subgroup of South-Australia. *Alcheringa*, **11**, 337–345.
- GEHLING, J. G. 1988. A Cnidarian of Actinian-Grade from the Ediacaran Pound Subgroup, South-Australia. *Alcheringa*, **12**, 299–314.
- GEHLING, J. G. 1991. The case for Ediacaran fossil roots to the metazoan tree. *Memoirs of the Geological Society of India*, **20**, 181–224.
- GEHLING, J. G. 1999. Microbial mats in terminal Proterozoic siliciclastics; Ediacaran death masks. *Palaios*, **14**, 40–57.
- GEHLING, J. G. & RIGBY, J. K. 1996. Long expected sponges from the Neoproterozoic Ediacara fauna of South Australia. *Journal of Paleontology*, **70**, 185–195.
- GEHLING, J. G., NARBONNE, G. M. & ANDERSON, M. M. 2000. The first named Ediacaran body fossil, *Aspidella terranovica*. *Palaeontology*, **43**, 427–456.
- GEHLING, J. G., DROSER, M. L., JENSEN, S. & RUNNEGAR, B. N. 2005. Ediacara Organisms: Relating Form to Function. In: BRIGGS, D. E. G. (ed.) *Evolving Form and Function: Fossils and Development: Proceedings of a Symposium Honouring Adolph Seilacher for his Contributions to Paleontology in Celebration of his 80th Birthday*, 43–66. Peabody Museum of Natural History, Yale University, New Haven, Connecticut.
- GERMS, G. J. B. 1972. Thin Concentric Structures of Biologic Origin from the Nama System, South West Africa. *GSA Bulletin*, **83**, 463–466.
- GLAESSNER, M. F. 1959. Precambrian Coelenterata from Australia, Africa and England. *Nature*, **183**, 1472–1473.
- GLAESSNER, M. F. 1969. Trace fossils from the Precambrian and basal Cambrian. *Lethaia*, **2**, 369–393.
- GLAESSNER, M. F. 1984. *The dawn of animal life*. Cambridge University Press, Cambridge.
- GLAESSNER, M. F. & DAILY, B. 1959. The geology and Late Precambrian fauna of the Ediacara fossil reserve. *Records of the South Australian Museum*, **13**, 369–401.
- GLAESSNER, M. F. & WADE, M. 1966. The Late Precambrian fossils from Ediacara, South Australia. *Palaeontology*, **9**, 599–628.
- GRAZHDANKIN, D. V. 2001. Microbial origin of some of the Ediacaran fossils. *Geological Society of America Abstracts with Programs*, **33**, 429.

- GRAZHDANKIN, D. V., MASLOV, A. V., MUSTILL, T. M. R. & KRUPENIN, M. T. 2005. The Ediacaran White Sea biota in the Central Urals. *Doklady Earth Sciences*, **401A**, 382–385.
- GUREEV, Y. A. 1987. Morfologicheskij Analiz i Sistematika Vendiat. *Akademiya Nauk Ukrainskoj SSR, Institut Geologicheskij Nauk.*, Preprint 87–15, 1–53. [In Russian.]
- GÜRICH, G. 1933. Die Kuibis-Fossilien der Nama Formation vom Südwestafrika. *Paläontologische Zeitschrift*, **15**, 137–154.
- HAGADORN, J. W. & BOTTJER, D. J. 1999. Restriction of a late Neoproterozoic biotope; suspect-microbial structures and trace fossils at the Vendian-Cambrian transition. *Palaïos*, **14**, 73–85.
- HAGADORN, J. W., FEDO, C. M. & WAGGONER, B. M. 2000. Early Cambrian Ediacaran-type fossils from California. *Journal of Paleontology*, **74**, 731–740.
- HAGADORN, J. W. & WAGGONER, B. 2000. Ediacaran fossils from the southwestern Great Basin, United States. *Journal of Paleontology*, **74**, 349–359.
- HAHN, G. & PFLUG, H.-D. 1988. Zweischalige Organismus aus dem Jung-Präkambrium (Nama-Gruppe) von Namibia. *Geologica et Palaeontologica*, **19**, 1–19.
- HALVERSON, G. P., HOFFMAN, P. F., SCHRAG, D. P., MALOOF, A. C. & RICE, A. H. N. 2005. Toward a Neoproterozoic composite carbon-isotope record. *Geological Society of America Bulletin*, **117**, 1181–1207.
- HARRINGTON, H. J. & MOORE, R. C. 1956. Part F: Coelenterata. In: IMOORE, R. C. (ed.) *Treatise on Invertebrate Palaeontology*. Geological Society of America and University of Kansas Press: Lawrence, 1–161.
- HOFMANN, H. J. 1971. Precambrian fossils, pseudofossils, and problematica in Canada. *Bulletin of the Geological Survey of Canada*, **189**, 1–146.
- HOFMANN, H. J. 1981. First record of a Late Proterozoic faunal assemblage in the North American Cordillera. *Lethaia*, **14**, 303–310.
- HOFMANN, H. J. & MOUNTJOY, E. W. 2001. *Namacalathus-Cloudina* assemblage in Neoproterozoic Miette Group (Byng Formation), British Columbia: Canada's oldest shelly fossils. *Geology*, **29**, 1091–1094.
- HOFMANN, H. J., FRITZ, W. H. & NARBONNE, G. M. 1983. Ediacaran (Precambrian) Fossils from the Wernecke Mountains, Northwestern Canada. *Science*, **221**, 455–457.
- HOFMANN, H. J., MOUNTJOY, E. W. & TEITZ, M. W. 1985. Ediacaran fossils from the Miette Group, Rocky Mountains, British Columbia, Canada. *Geology*, **13**, 819–821.
- HOFMANN, H. J., MOUNTJOY, E. W. & TEITZ, M. W. 1991. Ediacaran Fossils and Dubiofossils, Miette Group of Mount Fitzwilliam Area, British-Columbia. *Canadian Journal of Earth Sciences*, **28**, 1541–1552.
- HOFMANN, H. J., NARBONNE, G. M. & AITKEN, J. D. 1990. Ediacaran remains from intertillite beds in northwestern Canada. *Geology*, **18**, 1199–1202.
- HOFMANN, H. J., O'BRIEN, S. J. & KING, A. F. 2005. *Hiemalora* and other Ediacaran fossils of Northeastern Newfoundland, and correlations within Avalonia. *Geological Society of America Abstracts with Programs*, **37**, 485.
- IVANTSOV, A. Y. & MALAKHOVSKAYA, Y. E. 2002. Giant traces of Vendian animals. *Doklady Earth Sciences*, **385**, 618–622.
- JENKINS, R. J. F. 1984. Interpreting the oldest fossil cnidarians. *Palaentographica Americana*, **54**, 95–104.
- JENKINS, R. J. F. 1992. Functional and ecological aspects of Ediacaran assemblages. In: LIPPS, J. H. & SIGNOR, P. W. (eds) *Origin and Early Evolution of the Metazoa*. Springer, 131–176.
- JENKINS, R. J. F. & GEHLING, J. G. 1978. A review of frond-like fossils of the Ediacara assemblage. *Records of the South Australian Museum*, **17**, 347–359.
- JENSEN, S., GEHLING, J. G. & DROSER, M. L. 1998. Ediacara-type fossils in Cambrian sediments. *Nature*, **393**, 567–569.
- JENSEN, S., GEHLING, J. G., DROSER, M. L. & GRANT, S. W. F. 2002. A scratch circle origin for the medusoid fossil *Kullingia*. *Lethaia*, **35**, 291–299.
- KNOLL, A. H., WALTER, M. R., NARBONNE, G. M. & CHRISTIE-BLICK, N. 2004. A New Period for the Geologic Time Scale. *Science*, **305**, 621–622.
- LAFLAMME, M., NARBONNE, G. M. & ANDERSON, M. M. 2004. Morphometric analysis of the Ediacaran frond *Charniodiscus* from the Mistaken Point Formation, Newfoundland. *Journal of Paleontology*, **78**, 827–837.
- LAFLAMME, M., NARBONNE, G. M., GREENTREE, C. & ANDERSON, M. M. 2007. Morphology and taphonomy of an Ediacaran frond: *Charnia* from the Avalon Peninsula of Newfoundland. In: VICKERS-RICH, P. & KOMAROWER, P. (eds) *The Rise and Fall of the Ediacaran Biota*. Geological Society, London, Special Publications, **286**, 237–258.
- LEONOV, M. V. 2007. Comparative taphonomy of Vendian genera *Beltanelloides* and *Nemiana*: taxonomy and lifestyle. In: VICKERS-RICH, P. & KOMAROWER, P. (eds) *The Rise and Fall of the Ediacaran Biota*. Geological Society, London, Special Publications, **286**, 259–268.
- MACGABHANN, B. A., MURRAY, J. & NICHOLAS, C. 2007. *Ediacaria booleyi*—weeded from the Garden of Ediacara? In: VICKERS-RICH, P. & KOMAROWER, P. (eds) *The Rise and Fall of the Ediacaran Biota*. Geological Society, London, Special Publications, **286**, 277–296.
- MAPSTONE, B. & MCILROY, D. 2005. The taphonomy of a Neoproterozoic—Cambrian discoidal fauna from the Amadeus Basin, Central Australia; Palaeobiological implications for Ediacaran fossil preservation. *Paleobios*, **25**(2 supp), 79–80.
- MARTIN, M. W., GRAZHDANKIN, D. V., BOWRING, S. A., EVANS, D. A. D., FEDONKIN, M. A. & KIRSCHVINK, J. L. 2000. Age of Neoproterozoic bilaterian body and trace fossils, White Sea, Russia: implications for metazoan evolution. *Science*, **288**, 841–845.
- MCILROY, D., CRIMES, T. P. & PAULEY, J. C. 2005. Fossils and matgrounds from the Neoproterozoic Longmyndian Supergroup, Shropshire, UK. *Geological Magazine*, **142**, 441–455.
- MCMENAMIN, M. A. S. 1996. Ediacaran biota from Sonora, Mexico. *Proceedings of the National Academy of Sciences of the United States of America*, **93**, 4990–4993.

- MISRA, S. B. 1969. Late Precambrian (?) fossils from southeastern Newfoundland. *Geological Society of America Bulletin*, **80**, 2133–2140.
- NARBONNE, G. M. 1994. New Ediacaran fossils from the Mackenzie Mountains, northwestern Canada. *Journal of Paleontology*, **68**, 411–416.
- NARBONNE, G. M. 2004. Modular construction of early Ediacaran complex life forms. *Science*, **305**, 1141–1144.
- NARBONNE, G. M. 2005. The Ediacara biota: Neoproterozoic origin of animals and their ecosystems. *Annual Review of Earth and Planetary Sciences*, **33**, 421–442.
- NARBONNE, G. M. & AITKEN, J. D. 1990. Ediacaran fossils from the Sekwi Brook Area, Mackenzie Mountains, Northwestern Canada. *Palaeontology*, **33**, 945–980.
- NARBONNE, G. M. & GEHLING, J. G. 2003. Life after snowball: the oldest complex Ediacaran fossils. *Geology*, **31**, 27–30.
- NARBONNE, G. M. & HOFMANN, H. J. 1987. Ediacaran biota of the Wernecke Mountains, Yukon, Canada. *Palaeontology*, **30**, 647–676.
- NARBONNE, G. M., SAYLOR, B. Z. & GROTZINGER, J. P. 1997. The youngest Ediacaran fossils from Southern Africa. *Journal of Paleontology*, **71**, 953–967.
- NARBONNE, G. M., MYROLI, P., LANDING, E. & ANDERSON, M. M. 1991. A Chondrophorine (Medusoid Hydrozoan) from the Basal Cambrian (Placentrian) of Newfoundland. *Journal of Paleontology*, **65**, 186–191.
- NORRIS, R. D. 1989. Cnidarian Taphonomy and Affinities of the Ediacara Biota. *Lethaia*, **22**, 381–393.
- O'BRIEN, S. J. & KING, A. F. 2004. Ediacaran fossils from the Bonavista Peninsula (Avalon Zone), Newfoundland: preliminary descriptions and implications for regional correlation. *Current Research, Newfoundland Department of Mines and Energy Geological Survey Report*, **04–1**, 203–212.
- PALIJ, V. M. 1976. Ostatki besskeletnoj fauny i sledy zhiznedeyatelnosti iz otlozhenij verkhnego dokembriya i nizhnego Kembriya Podolii. In: RYABENKO, Y. A. (ed.) *Paleontologiya i Stratigrafiya Verkhnego Kembriya i Nizhnego Paleozoya Yugo-Zapadna Vostochno-Evropejskoj Platformy*, 63–77. [In Russian.]
- PALIJ, V. M., POSTI, E. & FEDONKIN, M. A. 1979. Myagkotelye metazoa i iskopaemye sledy zhivotnykh venda i rannego kembriya. In: KELLER, B. M. & ROZANOV, A. Y. (eds) *Paleontologiya Verkhnedokembrijskikh i Kembrijskikh Otlozhenij Vostochno-Evropejskoj Platformy*, 49–82. [In Russian.]
- PETERSON, K. J. & BUTTERFIELD, N. J. 2005. Origin of the Eumetazoa: testing ecological predictions of molecular clocks against the Proterozoic fossil record. *PNAS*, **102**, 9547–9552.
- PETERSON, K. J., WAGGONER, B. & HAGADORN, J. W. 2003. A fungal analog for Newfoundland Ediacaran fossils? *Integrative and Comparative Biology*, **43**, 127–136.
- PYLE, L. J., NARBONNE, G. M., JAMES, N. P., DALRYMPLE, R. W. & KAUFMAN, A. J. 2004. Integrated Ediacaran chronostratigraphy, Wernecke Mountains, northwestern Canada. *Precambrian Research*, **132**, 1–27.
- RASMUSSEN, B., BENGTSON, S., FLETCHER, I. R. & MCNAUGHTON, N. J. 2002. Discoidal impressions and trace-like fossils more than 1200 million years old. *Science*, **296**, 1112–1115.
- RUNNEGAR, B. N. & FEDONKIN, M. A. 1992. Proterozoic metazoan body fossils. In: SCHOPF, J. W. & KLEIN, C. (eds) *The Proterozoic Biosphere: a Multidisciplinary Study*. Cambridge University Press, Cambridge, 369–388.
- RYABENKO, V. A., ASEEVA, E. A. & FURTES, V. V. 1988. [Biostratigraphy and Palaeogeographic Reconstructions of the Precambrian of the Ukraine]. Kiev, Naukova Dumka. [In Russian.]
- SEILACHER, A. 1984. Late Precambrian and Early Cambrian metazoa: Preservation or real extinctions? In: HOLLAND, H. D. & TRENDALL, A. F. (eds) *Patterns of Change in Earth Evolution*. Springer-Verlag, 159–168.
- SEILACHER, A., GRAZHDANKIN, D. V. & LEGOUTA, A. 2003. Ediacaran Biota: The dawn of animal life in the shadow of giant protists. *Paleontological Research*, **7**, 43–54.
- SEILACHER, A., BUATOIS, L. A. & GABRIELA MANGANO, M. 2005. Trace fossils in the Ediacaran–Cambrian transition: Behavioral diversification, ecological turnover and environmental shift. *Palaeogeography, Palaeoclimatology, Palaeoecology*, **227**, 323–356.
- SEREZHNIKOVA, E. A. 2005. Vendian *Ediacaria* from the Zimmii Bereg locality of the White Sea: New records and new reconstructions. *Paleontological Journal*, **39**, 386–394.
- SEREZHNIKOVA, E. A. 2007. Vendian *Hiemalora* from Arctic Siberia reinterpreted as holdfasts of benthic organisms. In: VICKERS-RICH, P. & KOMAROWER, P. (eds) *The Rise and Fall of the Ediacaran Biota*. Geological Society, London, Special Publications, **286**, 331–338.
- SOKOLOV, B. S. 1972. The Vendian period in Earth history. *Paleontologiya, Doklady Sovetskikh Geologov, Akademiya Nauk SSSR*, **7**, 114–124.
- SOKOLOV, B. S. 1973. Vendian of northern Eurasia. In: PITCHER, M. G. (ed.) *Arctic Geology*. Memoirs of the American Association of Petroleum Geologists, **19**, 204–218.
- SOKOLOV, B. S. & FEDONKIN, M. A. 1984. The Vendian as the Terminal System of the Precambrian. *Episodes*, **7**, 12–19.
- SOUTHCOTT, R. V. 1958. South Australian jellyfish. *South Australian Naturalist*, **32**, 53–61.
- SPELRLING, E., PISANI, D. & PETERSON, K. J. 2007. Poriferan paraphyly and its implications for Precambrian palaeobiology. In: VICKERS-RICH, P. & KOMAROWER, P. (eds) *The Rise and Fall of the Ediacaran Biota*. Geological Society, London, Special Publications, **286**, 355–368.
- SPRIGG, R. C. 1947. Early Cambrian (?) jellyfishes from the Flinders Ranges, South Australia. *Transactions of the Royal Society of South Australia*, **71**, 212–224.
- SPRIGG, R. C. 1948. Jellyfish from the Basal Cambrian in South Australia. *Nature*, **161**, 568–569.
- SPRIGG, R. C. 1949. Early Cambrian 'jellyfishes' of Ediacara, South Australia, and Mount John, Kimberley District, Western Australia. *Transactions of the Royal Society of South Australia*, **73**, 72–99.

- SUN, W.-G. 1986a. Precambrian medusoids: The *Cyclomedusa* plexus and *Cyclomedusa*-like pseudo-fossils. *Precambrian Research*, **31**, 325–360.
- SUN, W.-G. 1986b. Late Precambrian scyphozoan medusa *Mawsonites randellensis* sp. nov. and its significance in the Ediacara metazoan assemblage, South Australia. *Alcheringa*, **10**, 169–181.
- VODANJUK, S. A. 1989. Ostatki besskeletnykh Metazoa iz khatyspytskoi svity Olenëkskogo podniatia. In: KHOMENTOVSKIY, V. & SOVETOV, Y. K. (eds) *Pozdnyy Dokembriy i Ranniy Paleozoi Sibiri. Aktualnyye Voprosy Stratigrafii*, 61–75. [In Russian.]
- WADE, M. 1968. Preservation of soft bodied animals in Precambrian sandstones at Ediacara, South Australia. *Lethaia*, **1**, 238–267.
- WADE, M. 1969. Medusae from uppermost Precambrian or Cambrian sandstones, central Australia. *Palaeontology*, **12**, 351–365.
- WADE, M. 1972. Hydrozoans and Scyphozoans and other medusoids from the Precambrian Ediacara fauna, South Australia. *Palaeontology*, **15**, 197–225.
- WOOD, D. A., DALRYMPLE, R. W., NARBONNE, G. M., GEHLING, J. G. & CLAPHAM, M. E. 2003. Paleoenvironmental analysis of the late Neoproterozoic Mistaken Point and Trepassy formations, southeastern Newfoundland. *Canadian Journal of Earth Sciences*, **40**, 1375–1391.
- ZAIKA-NOVATSKIY, V. S., VELIKANOV, V. A. & KOVAL, A. P. 1968. First Member of the Ediacara Fauna in the Vendian of the Russian Platform (Upper Precambrian). *Paleontological Journal*, **1968**, 269–270.
- ZHOU, C. M., TUCKER, R., XIAO, S. H., PENG, Z. X., YUAN, X. L. & CHEN, Z. 2004. New constraints on the ages of Neoproterozoic glaciations in south China. *Geology*, **32**, 437–440.

Biota in the terminal Proterozoic successions on the Indian subcontinent: a review

P. K. MAITHY¹ & G. KUMAR²

¹Formerly: Birbal Sahni Institute of Palaeobotany, F 2212, Rajaji Puram, Lucknow, 226 017, India

²Formerly: Geological Survey of India, 48 Pandariba, Old Kanpur Road, Lucknow, 226 004, India (e-mail: kumarg@sancharnet.in)

Abstract: On the Indian subcontinent, Late Proterozoic rocks form part of a continuous sequence grading into Cambrian, postdating the Sturtian glaciation (Cryogenian) and terminated by the Xingkaian/Pan African Orogeny (Late Cambrian). These sequences are restricted to the northwestern part of the Indian Shield, are overlain by Cenozoic sediments of the Indo-Gangetic Plain, and rest unconformably on the oldest platform sequences (Meso—Cryogenian) in many parts of the Lesser and Tethys/Higher Himalaya. Of these, the succession in the Krol Belt, Lesser Himalaya, divided into Baliana, Krol and Tal Groups, is fossiliferous. Changes in faunal composition of acritarchs and cyanobacteria are recorded in the upper part of the Baliana Group, as is the appearance and extinction of forms assigned to the Ediacara fauna in the overlying Krol. Such biotic change is accompanied by a significant depletion in $\delta^{13}\text{C}$ values in the 'cap carbonates'. Another $\delta^{13}\text{C}$ depletion is recorded in the upper part of the Krol Group along with appearance of spiny acanthomorphic acritarchs, scaphomorphs and hercomorphs, small shelly fossils, a variety of Early Cambrian trace fossils and trilobites in the overlying Tal Group. A review of biota reported from the oldest platform sediments (Vindhyan Supergroup, Karnool, Bhima Groups) suggests a Meso-Cryogenian (pre-Sturtian glaciation) age.

On the Indian subcontinent, the Late Proterozoic successions grade conformably into the Cambrian, after the major tectono-thermal events associated with Chengjiangian/Cadomian Orogeny in the Cryogenian period and after the Sturtian glaciation. They were deposited in the Palaeotethys-I sea (Shanker *et al.* 2002). Exposures occur in the northwestern part of the Indian Shield, unconformably overlying basement composed of the Malani Igneous Suite (Malani Rhyolite 745 ± 10 Ma; Siwana Granite 731 ± 14 Ma) of the Indian Shield, and are overlain by Cenozoic sediments of the Indus and Ganges plains. These successions extend to the Himalayas, where they rest unconformably on the oldest platform-deposits, referred to as the Salkhala Group, with dated granites (745 ± 50 Ma) or its equivalents the Simla-Jaunsar and Jutogh Groups. These sequences have been examined in detail by participants of IGCP Projects 29 and 303 and IUGS Project on Terminal Proterozoic (Kumar 1995; Kumar *et al.* 1997). In view of the controversies that exist around the identification of fossils ranging in age from Late Proterozoic into Cambrian, other sequences such as the Bhima, Karnool, Chattisgarh and Indravati Groups that occur in detached areas over the basement formed of oldest platform sediments (the Vindhyan or Cuddapah Supergroups over the Archaean—Palaeoproterozoic terrane of the peninsular India),

this material have been reviewed and compared the geology and fossils from the Baliana-Krol-Tal succession. The record of microbiota of Late Proterozoic—Cambrian age from the Buxa or Chilleipam formations, of Arunachal Pradesh, Lesser Himalaya (Tewari 2003) appears to be dubious, as the succession is intruded by granite dated at 1536 ± 60 Ma (Kumar 1997) and hence is, not considered here.

Geological setting

The Indian subcontinent is an assembly of four distinct Archaean—Palaeoproterozoic crustal blocks/terraces, *viz.* Dharwar (DB), Bundelkhand (BB), Trans-Aravalli (TAB) and South Indian—Sri Lankan Granulite (SISLGB). Each has an independent geological history through Archaean and Palaeoproterozoic and are separated by a mobile belt. The first three blocks welded together *c.* 1600 Ma (Zhongyuan/Karelian Orogeny) to form the protocontinent Proterodinia, and the SISLGB welded to DB around *c.* 500 Ma (Xingkaian/Pan-African Orogeny) to form part of Gondwanaland (Shanker *et al.* 2002). Proterodinia formed basement upon which two sequences of platform sediments were deposited during the Precambrian related to two significant marine transgressions of differing magnitude and configuration. These seas are referred to as the Prototethys and Palaeotethys,

each with many cycles related to global tectonothermal events (Shanker *et al.* 2002). Deposition of older sequence took place in the Prototethys commencing in the Mesoproterozoic (*c.* 1500 Ma) and ending with break-up of Rodinia *c.* 750 Ma (Chengjiangian/Cadomian Orogeny) in Cryogenian when sea regressed to the build-up of the Sturtian glaciation. Indicators of other tectonothermal events, *viz.* the Grenvillian (*c.* 1100 Ma) and Jinningian (*c.* 850 Ma) are also present. Relicts of this sequence are presently exposed on Indian shield—the Vindhyan Supergroup and its equivalents Chattisgarh in Central India; the Cuddapah-Karnool, Pakhal/Indravati, and Bhima groups in Southern India (Fig. 1); the Bahraich-Madhubani groups in the Indo-Ganges Plain and are referred to as the Vaikrita/Jutogh and Jaunsar groups in the Himalaya (Shanker *et al.* 1989).

With warming of the climate during the late Cryogenian, sedimentation in the Late Proterozoic commenced (*c.* 650 Ma) in the Palaeotethys-I, giving rise to sequences located on the northwestern Indian Shield and in many parts of the Lesser Himalayan and Higher/Tethys zones (Fig. 2). Such sedimentation was ended by the Xingkaian/Pan-African Orogeny during Late Cambrian

(*c.* 500 Ma). In the Higher/Tethys Himalaya, this sequence is unconformably overlain by Ordovician–Early Carboniferous sediments while parts of the Lesser Himalaya and the Peninsular Shield remained positive areas until the Early Permian marine transgression. Successions located in the Krol Belt, Lesser Himalaya and northwestern part of the Indian Shield are siliciclastic low in the section with the development of thick carbonate–evaporite facies, with or without phosphorite, in upper part, whereas those in the Higher/Tethys Himalaya are dominantly siliciclastic throughout.

The lower and upper boundaries of the Late Proterozoic (Ediacaran) are not precisely defined in the absence of diagnostic fossils or radiometric dates. However, (Knoll *et al.* 2006), the lower boundary of the Ediacaran is defined in the Lesser Himalaya as the base of the top Pink Limestone (Member G) of the Baliana Group. Significant depletion in $\delta^{13}\text{C}$ values is recorded in this pink carbonate (Kumar *et al.* 2000). The upper boundary with the Cambrian cannot be ascertained in terms of the GSSP due to absence of the characteristic Cambrian trace fossil of global Ichno-Zone II (Kumar *et al.* 1997). However, a significant depletion in $\delta^{13}\text{C}$ values has also been recorded in

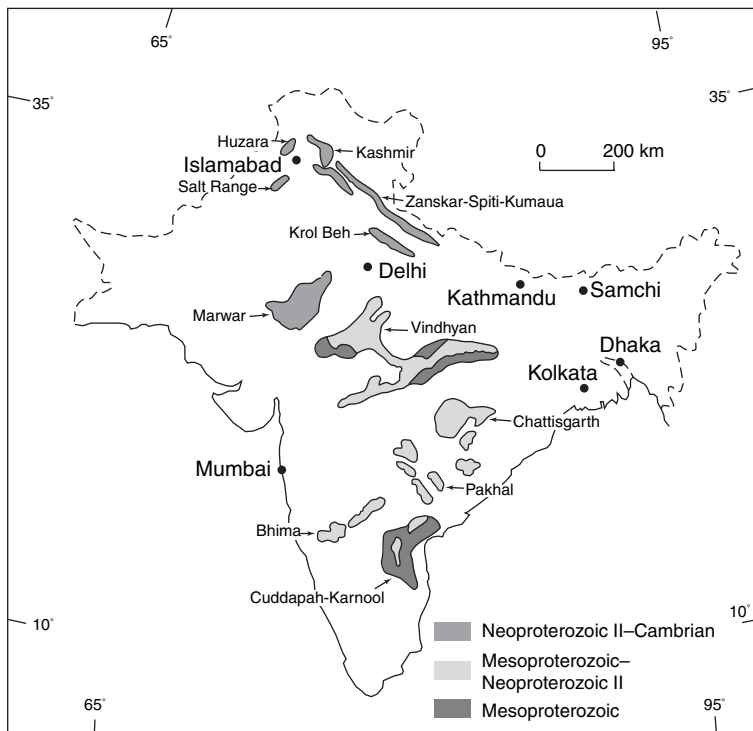


Fig. 1. Map of the Indian subcontinent with location of Mesoproterozoic, Mesoproterozoic Neoproterozoic II and Neoproterozoic II–Cambrian sequences.

Geological Time Scale		Himalaya										Indo-Gangetic Plain	Peninsular Shield					
		Tethys Himalaya					Lesser Himalaya						India	Pakistan	India			
		India			Bhutan (Bhargava 1995)	Pakistan		India			India (Shukla <i>et al.</i> 1994)					Pakistan (Kazmi & Jan 1997)	Northwestern (after Kumar <i>et al.</i> 1997)	
		Kashmir Valley (Kumar <i>et al.</i> 1984)	Zaskar-Spiti (Srikantia & Bhargava 1998)	Kumaun (Kumar 2005)		Arunachal (Kumar 1997)	Hazara (modified after Butt 1989 in Kazmi & Jan 1997)	Jammu Area (Jangpangi <i>et al.</i> 1986)	Kumaun (Krol Belt) (Shanker <i>et al.</i> 1993)									
Neoproterozoic	Ediacaran	Machhal Formation	Lolab Formation	Martoli Group Milam Fm. Lum La Formation		Pele La Group (Maneting Fm.)	Abbottabad Formation Shekhan Bandi Fm. Hazira Fm. Mirpur Mem. Mahhdagali Sangargali Tanaki Mem.	Sinha Fm.	Tal Group Dhaulagiri Fm. Deo Ka Tibba Fm.	Krol Group Kauriyala Fm. Jarashi Fm. Mahi Fm.		Baliara Group Infra Krol Fm. Blaini Fm.	?Karapur Formation	Salt Range Fm. with Khewra Trap at the top	Marwar Supergroup Jutana Fm. Kussak Fm. Khewa Sandstone			Birmanian Formation
		Ramsu Fm.	Kunzam La Fm.		Chekha Fm./Naspe Fm.	Mirpur Mem.					Sinha Fm.					Kauriyala Fm.	Blaini Fm.	
	Cryogenian	Salkhala Group	Salkhala/Vaikrita Group		Central Crystalline (?Archaean-Palaeoproterozoic)	Tanawal Formation					Gamir - Balia - Ramban Fms.					Jaunsar/Vaikrita Group	Bahraich Group; Madhubani Group; (Ujhani-Tilhar-?Karapur Fms.)	
Mesoproterozoic	Tonian																	

Fig. 2. Correlation chart of the Neoproterozoic–Early Cambrian sequences, Indian Subcontinent.

the upper part of carbonate facies of the Krol Group, between horizons yielding Ediacaran fossils and the Early Cambrian phosphorite beds containing small shelly fossils characteristic of the Meischucunian Zone I in the overlying Tal Group. This depletion has also been recorded in the Marwar Supergroup, below a phosphorite bed, and may be correlated with that recorded from Precambrian–Cambrian transition sequence.

Biota and organo-sedimentary structures

Biotic remains are known from the Ediacaran sequences in India, excepting the Marwar Supergroup. Of these Late Proterozoic successions significant biota has been recorded from the Krol Belt, Lesser Himalaya, and Kashmir Higher Himalaya. In Krol Belt (Baliana-Krol-Tal groups), fossil cyanobacteria and acritarchs are present as are fossils reminiscent of Ediacarans: calcareous algae, Conophytonoid and Gymnosolonid stromatolites along with evaporites and phosphate deposits. The sequence is conformably overlain by Early Cambrian Tal Group, which yields trace fossils of the global Ichno-Zone III (Landing 1994), small shelly fossils and stromatolites of the Meischucunian Zone and I & III (Tommotian), redlichid trilobites, microgastropods and inarticulate brachiopods of Qiongzhusian (Atdabanian) and Tsanglangpuian (Botomian) stages (Kumar 1984). Sequences in the Higher/Tethys Himalaya have yielded trace fossils of Ichno-Zone I, II and III, and Early Cambrian (Tommotian) to Middle Cambrian trilobites and brachiopods. Fossils of Late Proterozoic age are rare (Maithy *et al.* 1988) and the diagnostic trace fossils of global Ichno-Zone I are not recorded making precise demarcation of upper boundary of the Late Proterozoic difficult (Raina *et al.* 1983).

Lesser Himalaya: Krol Belt

The Cryogenian to Cambrian succession of this region is divided lithostratigraphically into three groups referred to as the Baliana, Krol and Tal groups. These are exposed in many synclinal outliers, such as the Pachmunda, Nigalidhar, Korgai, Mussoorie, Garhwal and Nainital synclines, in a linear zone stretching over 350 km in the region of the outer Lesser Himalaya (Shanker *et al.* 1993). This sequence rests unconformably on the Jaunsar Group and is transgressively overlapped either by Early Permian or by Late Cretaceous–Paleocene sediments in parts of the Garhwal and Mussoorie synclines.

Baliana Group

Divided into two formations, the Blaini and Infra Krol formations (Fig. 3).

Blaini Formation. Cyanophycean algae *Blainiella*, comparable to extant algal form *Hyella*, has been recorded from the black and bleached shales of the Mussoorie Syncline (Maithy *et al.* 1995). The form is characterized by a linear filament arranged with rectangular cells placed end to end. In extent *Blainiella*, reproduction is by endospore. Thick globular endospores form towards the terminal end of filament and release baeocytes by wall dissolution of endospores. Microbialite *Stratifera unduata* has been reported from the Mussoorie Syncline (Sharma *et al.* 1994).

Infra Krol Formation. Organic walled microfossils (OWM) have been reported from black chert nodules and silicified shale of the topmost litho-unit of the Baliana Group from a unit referred to as the Infra Krol at different locales in the Solon area (Pachmunda, Mussoorie and Nainital Synclines). These microfossils belong to Cyanophycean algae and acritarchs (Tiwari & Azmi 1992; Tiwari & Knoll 1994; Tiwari 1996). Large acanthomorphic acritarchs (*Ericasphaera*, *Echinospaeridium*, *Asterocapsoides*) and Cyanophycean remains similar to *Salome* are dominant forms.

In the Mussoorie Syncline (Prasad *et al.* 1990) and Nainital Syncline (Acharyya *et al.* 1989; Venkatachala *et al.* 1990; Tiwari 1996; Shukla *et al.* 2005) acritarchs included sphaeromorphids, sphaerohystrichomorphids along with vase-shaped microfossils, Synapломorphitae and Nematomorphitae. The age of the Infra Krol has in the past been considered to post-date Marinoan glaciation and thus could predate the diversification of Ediacaran metazoans (Shukla *et al.* 2005).

Krol Group

The Krol Group has been divided into three formations: Mahi (Krol A), Jarashi (Krol B) and Kauriyala (Krol C, D & E) formations in ascending order (Fig. 3). It has yielded rich assemblages of what has been identified as Ediacaran fauna, acritarchs and stromatolites along with calcareous algae (Fig. 3). Prasad *et al.* (1990) assigned the acritarchs to the Sphaeromorphidae from Mussoorie. The acritarch assemblage is characterized by smooth and sculptured-walled forms.

Mahi Formation. Kumar & Rai (1992) noted algal filamentous forms, coccoid acritarchs and spheroid colonies. Subsequently, Gautam & Rai (1997) reported empty sheaths of unbranched filaments, branching filaments resembling eukaryotic forms and a form comparable to Bangiophyceae also known from the Pachmunda Hills in the Solon area. Ediacaran metazoans have been assigned to *Nimbia* cf. *N. oclusa*, recorded from the Mahi Formation (Shanker *et al.* 2004).

BIOTA	Baliana Group						Krol Group					
	Blaini Formation						Kauriyala Formation					
	Member						Infra Krol Fm. (380 m)	Mahi Fm. (254 m)	Jarashi Fm. (54 m)	L. Mem. (Krol C) (134 m)	Mid. Member (Krol D) (636 m)	Upper Member (Krol E) (228 m)
	A (137 m)	B (805 m)	C (452 m)	D (398 m)	E (249 m)	F (55 m)						
Ediacaran:												
<i>Kimberella</i> sp.												
<i>Pteridium</i> sp. cf. <i>P. carolinaense</i>												
<i>Charniodiscus</i> sp. cf. <i>arboreus</i>												
<i>Beltanelliformis</i> sp.												
<i>Medusinites</i> sp.												
<i>Tirasiana</i> sp.												
<i>Cyclomedusa</i> sp.												
<i>Beltanella</i> sp.												
<i>Sekwia</i> sp.												
<i>Irridinitus</i> sp.												
<i>Nimbia</i> sp. cf. <i>N. occlusa</i>												
cf. <i>Dickinsonia</i>												
<i>Conomedusites</i> sp.												
Acritarcha:												
Sphaeromorphida:												
<i>Leiosphaeridia crassa</i>												
<i>L. effusa</i>												
<i>Baltisphaeridium perraum</i>												
<i>Margominuscula simplex</i>												
<i>Granomarginata primitiva</i>												
<i>Gorgonisphaeridium maximum</i>												
<i>Trachyhystrichosphaera vidalii</i>												
<i>Microconcentrica incrustata</i>												
<i>Trachysphaeridium attenuatum</i>												
<i>Saharidia downii</i>												
<i>Protosphaeridium volkovae</i>												
<i>P. densum</i>												
<i>Vavosphaeridium</i> sp.												
<i>Favosphaeridium</i> sp.												
<i>Orymatosphaeridium plicatum</i>												
<i>Symplasoapheridium</i> sp.												
Sphaerohystrichomorphida:												
<i>Ericiasphaera speldnaesii</i>												
<i>Echinospaeridium maximum</i>												
<i>Asterocapsoides</i> sp.												
<i>Micrhystridium echinuatum</i>												
<i>M. tomatum</i>												
<i>Microconcentrica incrustata</i>												
<i>Germinosphaera unispinosa</i>												
<i>Paracrassosphaera dedalea</i>												
<i>Micrhystridium echinuatum</i>												
<i>M. regulare</i>												
<i>M. eatonensis</i>												
<i>Archaeohystrichosphaeridium cellulare</i>												
<i>A. semireticulatum</i>												
Cyanobacteria (Cryptarch):												
Synapломorphitae:												
<i>Blainiella polymorpha</i>												
<i>Globophycus rugosum</i>												
<i>Tetraphycus hebeinsis</i>												
<i>Eomicrocystis malgica</i>												
<i>Bavlinella faveolata</i>												
<i>Satka colonialica</i>												
<i>Palaeoanacystis vulgaris</i>												
<i>Eosphaera</i> sp.												
Nematomorphitae:												
<i>Gunflintia</i> sp. cf. <i>G. minuta</i>												

Fig. 3. Distribution of biota and organo-sedimentary structures in the Baliana-Krol Groups, Krol Belt, Lesser Himalaya.

<i>Eomycetopsis robusta</i>																				
<i>Salome hubeiensis</i>																				
<i>Siphonophycus sepatum</i>																				
<i>S. robustum</i>																				
<i>S. rugosum</i>																				
<i>S.inornatum</i>																				
<i>Eomorphidium orculiformis</i>																				
<i>Satka colonialica</i>																				
<i>Obruchevella</i> sp.																				
Vase-shaped Microfossil:																				
<i>Melanocytrillium hexadiadema</i>																				
Calcareous Algae:																				
<i>Renalcis</i> sp.																				
<i>Epiphyton</i> sp.																				
Stromatolites:																				
<i>Stratifera undata</i>																				
<i>Stratifera irregularis</i>																				
<i>Conophyton garganicus</i>																				
<i>Baicalia baicalia</i>																				
<i>Colonella</i> sp.																				
<i>Paniscollenia</i> sp.																				
<i>Patomia</i> sp.																				
<i>Aldania</i> sp.																				
Algal oolites:																				
Trace Fossils:																				
<i>Gordia</i> sp.																				
<i>Bilimichus biserialis</i>																				
Ichnogenus A																				

Fig. 3. (Continued).

Jarashi Formation. Ediacaran fossils, cf. *Pterinidium carolinaense* (Fig. 4) and cf. *Charnodiscus arborens* (Shanker *et al.* 2004) have been reported from this sequence.

Kauriyala Formation. Consists of the Krol C, Krol D and Krol E members. Fossil content includes the calcareous algae *Renalcis* along with *Oleckmia* from the Krol C (Lower Member) of the Kauriyala Formation of the Nainital Syncline (Gansser 1964).

Ediacaran fossils have also been reported from many locales in the Krol D Member (Fig. 3) (Mathur & Shanker 1989, 1990; Shanker & Mathur 1992; Shanker *et al.* 1997; Mathur & Srivastava 2004). Forms that have been named are *Cyclomedusa* (Fig. 5), *Conomedusites* (Figs 6, 7), *Charniodiscus* (Fig. 8), *Kimberella* sp. cf. *K. quadrata* (Fig. 9), *Dickinsonia* sp. (Fig. 10) and *Beltanella* sp. cf. *B. gilesi* (Fig. 11). The reported *Zolotytsia* is a dubiofossil.

Stromatolites are known from Krol D in the Nainital and Mussoorie synclines (Fuchs & Sinha 1974; Singh & Rai 1977; Tewari 1984). Linked *Conophyton*, *Stratifera*, *Aldania* and *Irregularia* and branching stromatolites are dominant. Calcareous algae similar to *Epiphyton* and *Renalcis* are also known from Krol E Member (Singh & Rai 1983). The reported Archaeocyatha, according to Debrenne *et al.* (1990), is an invalid record.



Fig. 4. *Pteridinium* sp. cf. *P. carolinaense*. GSI No 21129. Scale bar, 5 mm. Repository: Museum, Geological Survey of India, Kolkatta (India). Courtesy: V. K. Mathur, GSI. Reproduced from Mathur & Srivastava (2004).

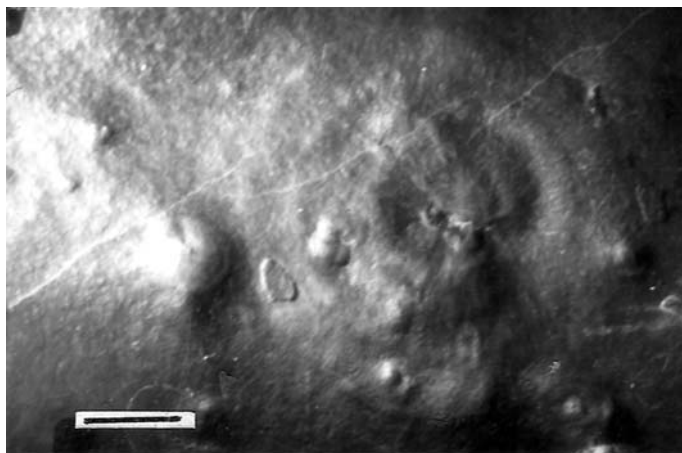


Fig. 5. *Cyclomedusa davidi*. GSI No 20426. Scale bar, 5 mm. Repository: Museum, Geological Survey of India, Kolkatta (India). Courtesy: V. K. Mathur, GSI. Reproduced from Shanker *et al.* (1997).

Higher/Tethys Himalaya, Kashmir

Organic walled microfossils have been described by Kumar *et al.* (1984) and Maithy *et al.* (1988) from the upper 480 m of the Machhal Formation to 580 m of the overlying Razdain Member of the Lolab Formation of the Kashmir Valley. This assemblage contains sphaeromorphida acritarchs, tubular cyanophytes along with globular colonies. This sequence appears to be of Late Proterozoic age as noted by the above authors.

Trace fossils form two assemblages: Assemblage I *Planolites beverleyensis*, *P. reticulatus*

in association with *Skolithos* and *Bergaueria* from the Razdain Member, Lolab Formation, Kashmir (assigned to Late Proterozoic). Assemblage I is older than Assemblage II which yields Early Cambrian forms in the Upper part of the Lolab Formation (Raina *et al.* 1983; Kumar *et al.* 1984).

Indo-Gangetic Plain (Ganges Plain)

The Vindhyan sequence of Central India unconformably overlies the Bundelkhand Gneissic

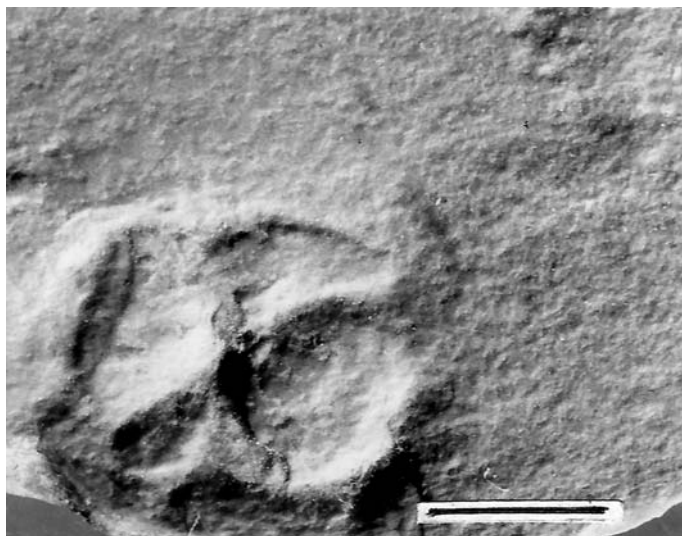


Fig. 6. *Conomedusites* sp. cf. *C. lobatus* (internal mould). GSI No 20429. Scale bar, 5 mm. Repository: Museum, Geological Survey of India, Kolkatta (India). Courtesy: V. K. Mathur, GSI. Reproduced from Shanker *et al.* (1997).

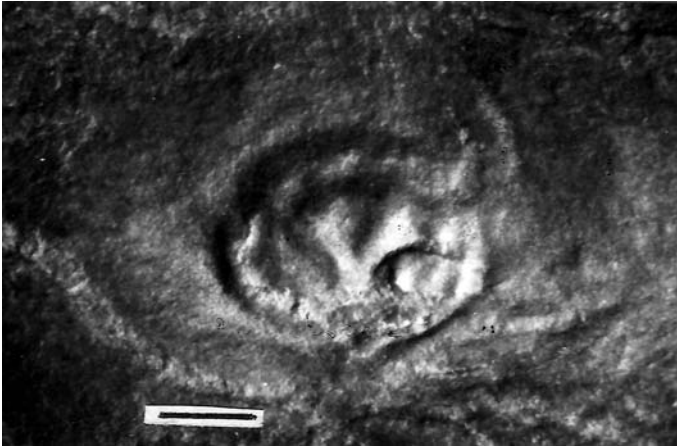


Fig. 7. *Conomedusites* sp. cf. *C. lobatus* (external mould). GSI No 20430. Scale bar, 5 mm. Repository: Museum, Geological Survey of India, Kolkatta (India). Courtesy: V. K. Mathur, GSI. Reproduced from Shanker *et al.* (1997).

Complex in the north and is concealed below Cenozoic sediments. These sediments are divided into the Bahaich and Madhubani groups, the latter further subdivided into the Ujhani, Tilhar and Karanpur formations in ascending order (Shukla *et al.* 1994). Of these, the Bahaich Group has yielded acritarchs belonging to sphaeromorphid Group. The Ujhani Formation contains acritarchs assigned to the genera *Granomarginata*, *Orygmatosphaeridium*, *Vavosphaeridium*, *Kildinella*, *Nucellosphaeridium* along with algae (*Myxococcoides*, *Palaeoanacystis* and *Gunflintia*) (Maithy *et al.* 1983). *Protosphaeridium*

and *Vavosphaeridium* are reported from the Tilhar Formation. *Leiosphaeridia*, *Granomarginata*, *Lophosphaeridium*, *Ellipsaletes* and *Dictyotidium* (Prasad & Asher 2001) have been reported from the Karanpur Formation. The Bahaich and Ujhani groups are considered lateral equivalents of the Semri Group (Mesoproterozoic), while the Tilhar and Karanpur formations are correlated with the Bhandar Group of Mesoproterozoic to Cryogenian (pre-Sturtian glaciation) age. However, Prasad & Asher (2001), considered the Madhubani Group to span from the latest Ediacaran to earliest Devonian on the basis of microbiota

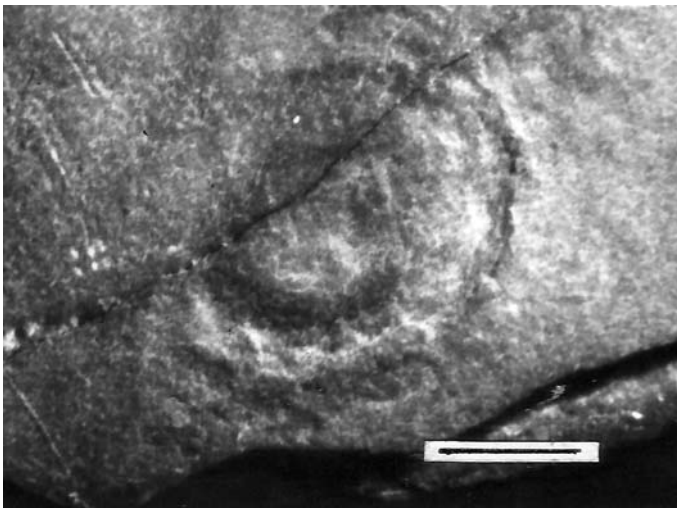


Fig. 8. *Charniodiscus* sp. (holdfast). GSI No 20432. Scale bar, 5 mm. Repository: Museum, Geological Survey of India, Kolkatta (India). Courtesy: V. K. Mathur, GSI. Reproduced from Shanker *et al.* (1997).

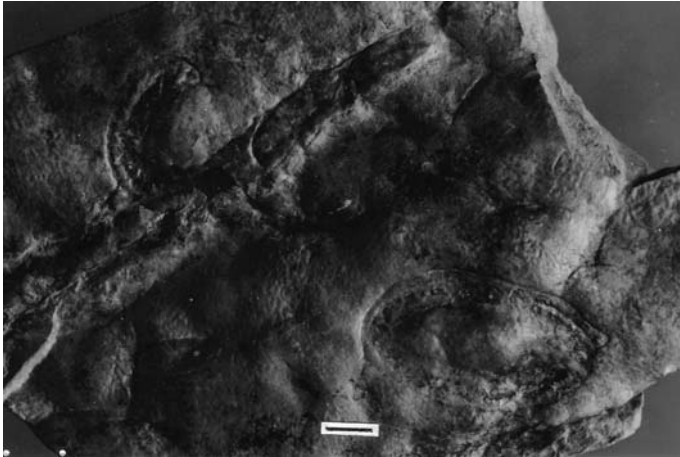


Fig. 9. *Kimberella* sp. cf. *K. quadrata*. GSI No 20399. Scale bar, 5 mm. Repository: Museum, Geological Survey of India, Kolkatta (India). Courtesy: V. K. Mathur, GSI. Reproduced from Shanker & Mathur (1992).

they described. A review of the overall organic walled microfossils indicates that the assemblage is dominated by ornate acritarchs in association with simple ones and Chitinozoa have simple morphologies. In the Silurian and

Devonian, acritarchs with complex spines (branched) and ornamentation are known along with complex Chitinozoa and trilete spores. The absence of these forms in Madhubani Group raises doubts as to the conclusion drawn by Prasad & Asher (2001). The present analysis, however, indicates the youngest of the sediments are only Cambrian. Further detailed collecting from drill-core and careful analysis of the microfossils would help resolve this issue.

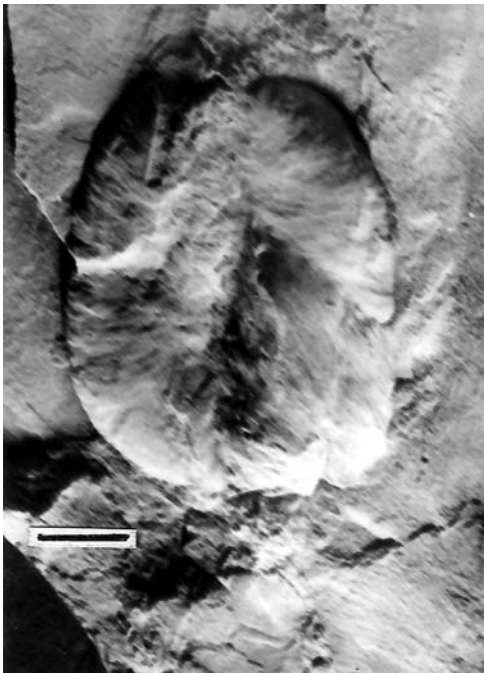


Fig. 10. *Dickinsonia* sp. GSI No 21149. Scale bar, 5 mm. Repository: Museum, Geological Survey of India, Kolkatta (India). Courtesy: V. K. Mathur, GSI. Reproduced from Mathur & Srivastava (2004).

Peninsular India

Sediments of Ediacaran age are lacking from the greater part of the Peninsular India (central and southern India) except in the NW where represented by the Marwar Supergroup. In view of the claims of Ediacaran–Cambrian fossils in the Vindhyan Supergroup and Bhima Group, these successions and others, such as Karnool, Cuddapah and Chhat-tisgarh sequences are also reviewed in Fig. 12.

Marwar Supergroup

The Marwar Supergroup unconformably overlies the Malani Igneous Suite (Malani Rhyolite dated at 745 ± 10 Ma; Siwana Granite 731 ± 14 Ma) or Palaeoproterozoic metasediments. The Marwar Supergroup is divided in ascending order into Jodhpur, the Bilara (Lower Carbonate), the Hanseran Evaporite, and the Nagaur and Birmania (Upper Carbonate) formations. A significant depletion in $\delta^{13}\text{C}$ values occurs in the upper part of the Bilara Formation and a short lived positive excursion of $\delta^{13}\text{C}$ values occurs in the Birmania Formation at the phosphorite levels (Kumar *et al.* 1997).

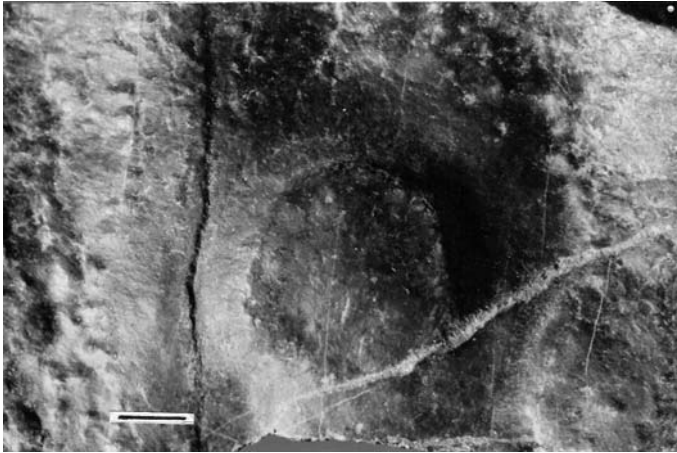


Fig. 11. *Beltanella* sp. cf. *B. gilesi*. GSI No 20311. Scale bar, 5 mm. Repository: Museum, Geological Survey of India, Kolkatta (India). Courtesy: V. K. Mathur, GSI.

Stromatolites *Collenia pseudocolumanaris*, *Collenia* sp., *Concollenia*, *Cryptozoan accidentalis*, *Irregularia* sp. and *Stratifera* are recorded from the Bilara Formation (Burman 1980).

Vindhyan Supergroup

Stromatolites, macro- and microfossils have been reported in abundance from the Vindhyan Supergroup (Fig. 12). Two distinct types of stromatolite assemblages are known. The Semri Group is characterized by an abundance of coniform stromatolites, columnar forms and unnamed, passively branched forms. The assemblage is suggestive of an Early to Middle Riphean age. No stromatolites have been recorded from the Kaimur and Rewa groups, due to absence of carbonates. Stromatolites of the Bhandar Group include *Baicalia* and *Tungusia*, which are assigned a Late Riphean age.

The carbonaceous macrofossils *Chuarua* and *Tawuia* have been reported from the Baghar (Suket) Shale (Semri Group), the Jhiri Shale (Rewa Group), the Sirbu Shale and the Bhavpura (Dholpura) Shale of the Bhandar Group (Maithy 2003). The record of the *Chuarua*–*Tawuia* association in the youngest formation of the Vindhyan indicates that the entire Vindhyan succession was deposited before the Sturtian glaciation. Hofmann (1992) has speculated that *Chuarua* and *Tawuia* may be one and the same taxon, the two forms representing an alternation of generations of a eukaryotic organism. Maithy (2003) noted that *Chuarua* and other discoidal forms are the gametophytic generation and he also suggested that *Tawuia* and other elongated forms represented the sporophytic generation of an extinct alga.

Acritarchs are well known from sediments ranging from youngest strata of the Semri Group:

Bhagwar Shale, Kaimur Group, Rewa Group and Bhandar Group (Maithy 2003). Available data indicate that the Semri, Kaimur and Rewa groups are dominated by Leiosphaeridia *sensu* Jankauskas. In the younger Bhandar Group, the sphaeromorphid acritarchs are present: *Nucellophaeridium* with walls boasting a broad reticulum, *Favosphaeridium* and *Cymatosphaera* with encircling narrow wing-like structure. Additionally, a few acanthomorphid acritarch vesicles are recorded, with simple, short processes: *Baltisphaeridium* and *Michrystridium*. The Neoproterozoic vase-shaped microfossil *Melanocyrrillium* is important (Maithy & Babu 1997). Until now, typical Cambrian acritarch groups Ellipsomorphida, Ooidomorphida and Versimorphida were unknown, thus indicating an absence of Late Proterozoic organisms in the Vindhyan sequence of India.

Azmi (1998) reported a variety of small shelly fossils from the topmost part of the Rohtasgarh Limestone and Shale in the Semri Group in the lower part of the Vindhyan sequence from two areas, Maihar and Rohtas in the Son Valley. He concluded that these sequences represent basal Meischucunian/Tommotian stages (Early Cambrian in age). This has been debated and examined by several workers (Bhatt *et al.* 1999). Most did not agree with the biogenicity of many of the reported ‘fossil’ specimens and considered them produced diagenetically as ‘cone-in cone’ structures with pointed apices which flare outwards and possess undulatory surfaces or perhaps mineral growths or fibrous calcite/secondary calcite veins (Sharma 2003).

Claims of the presence of ichno-fossils in the form of surface trails and tubes have also been made by many workers studying the Semri and Bhandar groups, but most of these reports have

Vindhyan Supergroup (Bhattacharyya 1996)		Chhattisgarh Supergroup (After Murti 1987)		Pakhal Supergroup/ Indravati Group (After Rao 1987; Ramakrishnan 1987)		Cuddapah Supergroup & Karnool Group (After Ramam & Murty 1997)		Bhima Group (After Misra <i>et al.</i> 1987)		Characteristic biota		
Upper Vindhyan sequence	Bhandar Group	Bhavpura				Karnool Group	Nandyal Sh.	Harwal	Carbonaceous remains: <i>Chuarina</i> – <i>Tawuia</i> ; Sponge: <i>Palaeophragmodictaya</i>			
		Balwan Limestone					Koikuntla Limestone.	Katamdevarhalli Limestone.	Algae: <i>Vindhyacapsiopsis</i> , <i>Palaeoglaucocystis</i> ; Acritarchs: <i>Granomarginata</i>			
		Maihar/Shikaoda Sst					Paniam Quartzite					
		Sirbu Shale					Owk Shale	Halkal Shale	Acritarchs: <i>Leiosphaeridia</i> , <i>Granomarginata</i> , <i>Baltisphaeridium</i> , <i>Favosphaeridium</i> ; Cryptarchs: <i>Eomycetopsis</i> , <i>Sphaerocongregus</i> , <i>Obruchevella</i> , <i>Gloecapsomorpha</i> ; Carbonaceous remains: <i>Chuarina circularis</i> – <i>Tawuia dalensis</i> , <i>Sinosabellidites huainanensis</i> , <i>Beltina danai</i> , <i>Protoarenicola baiguashansis</i>			
		Bundi Hill Sst.					Tarenga Formation					
	Reipur Group	Lakheri Limestone	Chandi Formation	Penganga Gp.	Putnur Limestone	Narji Limestone	Shahabad Limestone	Stromatolites: <i>Baicalia</i> , <i>Tungussia</i> and <i>Gymnosolen</i> ; Siliceous sponge spicules; <i>Sekwia excentrica</i> , ?Trace fossils				
		Ganurgarh Shale	Gunderdehi Formation		Takalapalli Arkose	Baganapalli Quartzite	Rabanapalli Conglomerate	Acritarchs: <i>Leiosphaeridia</i> , <i>Orygmatosphaeridium</i> , <i>Granomarginata</i> , <i>Vavosphaeridium</i> , <i>Nucellosphaeridium</i> , <i>Cymatisphaerides</i> , <i>Polytrichoides</i>				
	Rewa Group	Govindgarh Sandstone	Charmuria Formation					Carbonaceous remains: <i>Chuarina circularis</i> , <i>Tawuia dalensis</i>				
		Jhiri Shale										
	Kaimur Group	Asan Sst.										
		Panna Shale										
		Dhaundraul Quartzite										
		Mangesar Formation										
		Bijaiagarh Shale						Acritarchs: <i>Leiosphaeridia</i> , <i>Archaeohystrichosphaeridium</i> , <i>Lophosphaeridium</i>				
		Ghaghar Sandstone										
Susnai Breccia												
Sasaram Fm.												

Fig. 12. Correlation of Mesoproterozoic–Neoproterozoic sequences in Peninsular India, based on organic remains.

Semri Group (Lower Vindhyan)			Rohlas Subgroup				<p>Algae: <i>Myxococcoides</i>, <i>Aphanocapsaopsis</i>, <i>Palaeoscytonema</i>, <i>Oscillatoriaceae</i>; Acritarchs : <i>Granomarginata</i>, <i>Symplastosphaeridium</i>, <i>Orymatosphaeridium</i>, <i>Palaeoanacystis</i>, <i>Vavosphaeridium</i>, <i>Archaeofavosina</i>, <i>Kildenella</i>, <i>Nucellosphaeridium</i>, <i>Zonosphaeridium</i>, <i>Tasmanites</i>, <i>Leiosphaeridia</i>; Carbonaceous: <i>Chuarja circularis</i>, <i>C. minima</i>, <i>Tawuia dalensis</i>, <i>Grypania spiralis</i>, <i>Grypania</i>, <i>Tyrostenia</i>, <i>Daltaenia</i>, <i>Beltenia</i>, <i>Krishnanina</i>, <i>Longfengsahnna choparensis</i></p>
			Rohlasgarh Limestone				
Kheinjua Subgroup			Rampur Formation		Laknavaram / Mulag Shale		
			Salkhan Limestone		Pattipalli/ Mulag Quartzite		
Koldaha (Olive) Shale					Enchencheruvu Dolomite		
			Deonar Fm				
Kajrahat Limestone						Jakram Arcose	
			Arangi Formation			Pandikunta Shale	
Chanderpur Gp. Kansa Pathar Formation							
			Chaporadih Formation			Gunjeda Dolomite/ Kaner Limestone	
Lohardih Formation							
			Deoland Fm				

Fig. 12. (Continued).

Stromatolites: *Conophyton*, *Collenia*, *Colonnella*: Algae: *Obrucevella*, *Myxococcoides*, *Eosynechococcus*, *Sphaerophycus*, *Tetraphycus*, cf. *Palaeopleurocapsa*, *Glenobotrydion*, *Eoentophysalis*, *Gunflintia*, *Huroniospora*, *Siphonophycus*, *Oscillatoriopsis*, *Palaeolyngbya* cf. *Eomicrocoleus*, *Eomycetopsis*, *Bactrophycus*, *Kheinjuaesphaera*, *Coniunctiophycus*, *Archaeoellipsoides*; *Oscillatoripsis*, *Siphonophycus*, *Palaeolyngbya*, cf. *Eomicrocoleus*; Acritarchs: cf. *Trachysphaeridium*, *Leiosphaeridium*

been dismissed as of inorganic in origin (Maithy 2003; Sharma 2003). Recent reports of trace fossils attributed to triploblastic animals from Chorhat Sandstone belonging to Kheinjua Formation (Semri Group) exposed in Madhya Pradesh (Seilacher *et al.* 1998) have also been debated. Knoll & Carroll (1999), and Kumar (1999) have doubted the original 'inorganic' interpretations. However, surface trails in single and paired rows recovered from the Nagod (Lakheri) Limestone near Bankurian in the Rewa district and large diameter burrows collected from the Bundi Hill Sandstone, Bhandar Group from Maihar need careful analysis for their biogenic or abiogenic origin to be assessed (Maithy 2003).

Sekwia, a Neoproterozoic form, reported from Lakheri Limestone, Bhandar Group, has been considered to be 'cocoon' of annelids (Maithy & Babu 1997), and the Neoproterozoic sponge genus *Palaeophragmodictya* was reported from the youngest beds of Vindhyan, Bhavpura Shale, Lakheri, Rajasthan (Shanker *et al.* 2000). The presence of these possible metazoan remains and traces needs detailed investigation. Their possible presence in the Vindhyan sequence is supported by molecular clock estimates suggesting that the divergence of protostome and deuterostome animals took place as early as 1000–1300 Ma (Sharma 2003).

Chhattisgarh Supergroup

This supergroup has been divided into Chanderpur and Raipur groups separated by an unconformity (Fig. 12). There is some disagreement in further subdivision of the Raipur Group: one proposal by Murti (1987) and another by Moitra (1990). However, two distinct stromatolitic zones have been noted (Moitra 2003). The lower zone contains the characteristic forms *Kussiella*, *Conophyton cylindricus*, *Jacutophyton*, *Anabaria* and *Colonella* of Middle Riphean age, comparable to assemblages in the Semri Group (Vindhyan Supergroup). The upper zone hosts *Gymnosolen*, *Tungussia*, *Baicalia*, *Linella*, *Acaleilla* and *Inzeria*, comparable to assemblages in the Bhandar Group of the Vindhyan and assigned to Upper Riphean of Ediacaran age. Organic walled acritarchs have been reported by Moitra (1999) and three distinct zones identified. The lower two zones were assigned an Apebian to Ediacaran age (Vendian) and the upper one an Early Cambrian age. Analysis of the upper zone biota does not support the view of Moitra (1999) who assigned these sequences an early Cambrian age but rather it appears to be from pre-Sturtian glaciation in the Neoproterozoic.

Bhima Group

The Bhima Group unconformably overlies the Cuddapah Supergroup (Fig. 12). Das Sarma *et al.* (1992) reported the presence of the macrofossil *Sabellidites* from the Halkal Formation, Bhima Group and considered the sequence to represent the Late Proterozoic. The *Sabellidites* specimen is strap-shaped with fine transverse partitions. The figured specimen now housed at the Geological Survey of India (Hyderabad) was reexamined in 1994 and fresh collections were made during a field trip under the aegis of IGCP Project 303 (Precambrian–Cambrian event stratigraphy). The flattened ribbon-like compressions or impressions are both straight and curved, but not twisted, with both end rounded, margins entire, surface with fine, closely-spaced transverse thickenings. Transverse thickenings have been formed by compacting packed compressed globular structures. Some specimens preserve carbonaceous matrix but no chitinous material. In overall morphology the original fossil is similar to *Tawuia dalaensis*. Associated with the newly-collected form is *Chuarua circularis* and additional *Tawuia* possessing circular structures at the terminal end, as well as *Beltina* (Maithy & Babu 1996). Similar forms are now well known from Meso-Neoproterozoic sequences of India. These forms are now considered to represent different stages of life cycle of *Chuarua–Tawuia* (Maithy 2003). The acritarch assemblage from the same sediments is dominated by sphaeromorphids; Leiosphaeridia has been recorded from the Halkal Formation (Maithy & Babu 1996). This assemblage compares well with the acritarch assemblage of Suket Shale, which is considered ± 1000 Ma in age. The stable carbon isotope values are in the range ± 1.2 to 3.4 PDB in the Bhima Group (Bhattacharya *et al.* 1996). Based on this data we suggest that the Bhima Group was deposited before the Sturtian glaciation.

Karnool Group

The Karnool Group unconformably overlies the Cuddapah Supergroup (Fig. 12) and a *Chuarua–Tawuia* assemblage has been reported from the Owk Shale in this sequence (Sharma & Shukla 1999).

Discussion

The oldest platform sediments represented in India range in age from Mesoproterozoic to Early Neoproterozoic and seem to have been deposited in an ancient sea, the Prototethys (Shanker *et al.* 2002). Until now, much of the evidence presented indicating the presence of an Ediacaran biota of Late Proterozoic age has proved to be dubious

(Maithy 2003). The presence of *Chuarina–Tawuia* association recovered from the Sirbu and Bhavapura (Dholpur) Shale in the Bhandar Group, Vindhyan Supergroup, from the Halkal Formation, Bhima Group, and the Owk Shale in the Kurnool Group indicate that these rocks are older than the Sturtian glacial sediments. The Halkal Formation was considered by Das Sarma *et al.* (1992) to be Late Proterozoic in age as they reported the presence of Sabellidites. Maithy & Babu (1996) doubted their identifications, as the fossil is a carbonaceous impression with no chitin preserved. The specimen is now identified as *Tawuia*. Furthermore, the sediments are also dominated by a simple acritarch, *Leiosphaeridia*, which are known to occur in the beds ranging age from 1000–900 Ma (Maithy & Babu 1996). Stable carbon isotope values in the Bhima Group are in the range of ± 1.2 to 3.4 PDB. Azmi (1998), based on his finding of brachiopods and small shelly fossils in the Rohtasgarh Formation, Semri Group of the Vindhyan sequence exposed in the Badanpur section (near Maihar, Madhya Pradesh) and in the Ramdhira Quarry section (near Rohtasgarh, Bihar), assigned the sediments to Late Proterozoic–Early Palaeozoic. This finding is questioned here as the reported fossils appear to be of non-biogenic nature (Bhatt *et al.* 1999; Bhatt 2003). The absence of Late Proterozoic sediments is also supported by the organic walled microfossils from the younger succession of Vindhyan Supergroup. The assemblage is dominated by sphaeromorphids, most belonging to the acritarch *Leiosphaeridia*. Ornamented sphaeromorphid acritarchs are extremely rare. However, in the Bhandar Group, *Sphaerocongregus*, *Polytrichoides* and *Obruchevella*, all of Late Proterozoic age, are present. Stromatolites also indicate an older Neoproterozoic age as the typical Vindhyan and Chhattisgarh sequence lack the stromatolite assemblage of *Baicalia–Tungussia–Inzeria*.

Conclusions

An analysis of the organic remains and organosedimentary structures from the Neoproterozoic of the Indian subcontinent suggest that:

1. There is some evidence of organic remains and trace of Late Proterozoic are in sediments of the Lesser Himalaya—in the Krol Belt, Higher/Tethys Himalaya, Kashmir, and possibly in the Karanpur Formation of the Madhubani Group, and the Ganga Plain and Marwar supergroups in the northwestern part of the Indian Shield. Evidence for a Late Proterozoic age of the Vindhyan Supergroup, Chhattisgarh Supergroup, Bhima Group and Kurnool Group

is absent. The stromatolite record suggests a Late Riphean age. The presence of the macroscopic fossil *Chuarina–Tawuia* suggests a date of deposition older than the Sturtian glaciation. This is supported by the acritarch record.

2. Fossil evidence does not support that the Palaeotethys Sea extended south of Son-Narmada Lineament during Late Proterozoic–Cambrian. The lack of sediments of Late Proterozoic age in the greater part of peninsular India is likely due to uplift and thus regression of the Prototethys Sea during Chengjiangian/Cadomian Orogeny (Shanker *et al.* 2002).

Formation detailed work and better quality illustrations are certainly needed to confirm these identifications. A joint trip for IGCP493 is expected to visit critical sites in 2007.

References

- ACHARYYA, S. K., RAHA, P. K., DAS, D. P., MOITRA, A. K., SHUKLA, M. & BANSAL, R. 1989. Late Proterozoic microbiota from the Infra Krol rocks from Nainital Synform, U.P., Himalaya, India. *Indian Journal of Geology*, **61**, 137–147.
- AZMI, R. J. 1998. Discovery of Lower Cambrian small shelly fossils and brachiopods from the Lower Vindhyan of Son valley, central India. *Journal Geological Society India*, **52**, 381–389.
- BHARGAVA, O. N. (ed.) 1995. The Bhutan Himalaya: a geological account. *Geological Survey of India, Special Publications*, **39**.
- BHATT, D. K. 2003. On the report of the small shelly fossils and Brachiopoda from the Vindhyan strata. *Journal Palaeontological Society of India*, **48**, 225–229.
- BHATT, D. K., SINGH, G., GUPTA, S., SONI, M. K., MOITRA, A. K., DAS, D. P. & DE, C. 1999. Fossil report from Semri Group, Lower Vindhyan. *Journal Geological Society of India*, **53**, 717–723.
- BHATTACHARYYA, A. (ed.) 1996. *Recent Advances in Vindhyan Geology*. Geological Society of India, Memoir **36**, iii–viii.
- BHATTACHARYYA, S. K., JANI, R. A., MATHUR, V. K., ABSAR, A., BODAS, M. S., KUMAR, G. & SHANKER, R. 1996. Stable carbon and oxygen isotopic changes across Precambrian–Cambrian Boundary, Lesser Himalaya. In: SHANKER, R. *ET AL.* (eds) *Proceedings Seminar on Recent Advances in Geological Studies in NW Himalaya and Foredeep, Lucknow, February 1995*. *Geological Survey of India, Special Publications*, **21**, 225–231.
- BURMAN, G. 1980. An analysis of the Marwar basin, western Rajasthan in light of stromatolite study. *Geological Survey of India, Miscellaneous Publications*, **44**, 292–297.
- DAS SARMA, D. C., RAHA, P. K., MOITRA, P. K., ASHOK KUMAR, P., ANANTHARAMAN, S., RAMA RAO, V. & SUNDARAM, V. 1992. Discovery of Precambrian–Cambrian transitional fossil Sabellidites from India. *Current Science*, **63**, 40–142.

- DEBRENNE, F., GANGLOFF, R. A. & ZHURAVLEV, A. Y. 1990. Archaeocytha from Krol-Tal succession (Lesser Himalaya), an invalid record. *Geological Magazine*, **127**, 361–362.
- FUCHS, G. R. & SINHA, A. K. 1974. On the geology of Naini Tal (Kumaun Himalaya). *Himalayan Geology*, **4**, 563–580.
- GANSSER, A. 1964. *Geology of Himalayas*. Inter Science Publications, John Wiley & Sons, New York.
- GAUTAM, R. & RAI, V. 1997. Branched microbiota from the bedded black chert of the Krol Formation (Neoproterozoic), Lesser Himalaya, India. *Palaeobotanist*, **46**, 32–40.
- HOFMANN, H. J. 1992. Proterozoic Carbonaceous Films. In: SCHOPF, J. W. & KLEIN, C. (eds) *The Proterozoic Biosphere—a multidisciplinary study*. Cambridge University Press, Cambridge.
- JANGPANGI, B. S., KUMAR, G., RATHORE, D. R. & DUTTA, S. 1986. Geology of the 'Autochthonous Folded Belt', Jammu & Kashmir Himalaya with special reference to the Panjal Thrust. *Journal Palaeontological Society of India*, **31**, 39–51.
- KAZMI, A. H. & JAN, M. Q. 1997. *Geology and Tectonics of Pakistan*. Graphic Publishers, Karachi, Pakistan.
- KNOLL, K. H. & CARROLL, S. B. 1999. Early animal evolution: emerging views from comparative biology and geology. *Science*, **284**, 2129–2137.
- KNOLL, A. H., WALTER, M., NARBONNE, G. & CHRISTIE-BLICK, N. (2006). Ediacaran Period: a new addition to geologic time scale. *Lethaia*, **39**, 13–30.
- KUMAR, G. 1984. The Precambrian–Cambrian boundary beds, northwestern Himalaya, India and boundary problem. In: Proceedings of the 5th Indian Geophytological Conference, Lucknow, Nov. 1983. *Palaeobotanical Society Special Publications*, 89–111.
- KUMAR, G. 1995. The Precambrian–Cambrian biostratigraphy, northwest Himalaya and correlation. In: Proceedings of the International Conference on Global Environments and Diversification of Plants through Geological Time. *Society of Plant Taxonomists*, Allahabad, 159–165.
- KUMAR, G. 1997. *Geology of Arunachal Pradesh*. Geological Society of India, Bangalore.
- KUMAR, G. 2005. *Geology of Uttar Pradesh and Uttaranchal*. Geological Society of India, Bangalore.
- KUMAR, G., RAINA, B. K., BHARGAVA, O. N., MAITHY, P. K. & BABU, R. 1984. The Precambrian–Cambrian Boundary Problem, Northwest Himalaya, India. *Geological Magazine*, **121**, 211–219.
- KUMAR, G., SHANKER, R., MAITHY, P. K., MATHUR, V. K., BHATTACHARYA, S. K. & JANI, R. A. 1997. Late Proterozoic–Cambrian sequences in India: A review with Special reference to Precambrian–Cambrian Boundary. *Palaeobotanist*, **46**, 19–31.
- KUMAR, G., SHANKER, R., MATHUR, V. K. & MAITHY, P. K. 2000. Maldeota Section, Mussoorie Syncline, Krol Belt, Lesser Himalaya, India: A candidate for global stratotype section and point for late Proterozoic system. *Geoscience Journal*, **21**, 1–10.
- KUMAR, S. 1999. Siliceous sponge spicules like forms from Neoproterozoic Bhandar Limestone, Maihar area, Madhya Pradesh. *Journal Palaeontological Society of India*, **44**, 141–148.
- KUMAR, S. & RAI, V. 1992. Organic-walled microfossils from the bedded chert of Krol Formation (Vendian), Solan, Himachal Pradesh, India. *Journal Geological Society of India*, **39**, 229–234.
- LANDING, E. 1994. Precambrian–Cambrian boundary global stereotype ratified and a new perspective of Cambrian time. *Geology*, **22**, 179–182.
- MAITHY, P. K. 2003. Pre-Phanerozoic evidences of life from central India: implication to biostratigraphy and evolution. *Gondwana Geological Magazine, Special Volume 7*, 401–412.
- MAITHY, P. K. & BABU, R. 1996. Carbonaceous macrofossils and organic-walled microfossils from the Halkal Formation, Bhima Group, Karnataka with remarks on age. *Palaeobotanist*, **45**, 1–6.
- MAITHY, P. K. & BABU, R. 1997. Upper Vindhyan biota and Precambrian/Cambrian Boundary. *Palaeobotanist*, **46**, 1–6.
- MAITHY, P. K., VENKATACHALA, B. S. & LELE, K. M. 1983. Microbiota from subsurface of Ganga Basin. *Geophytology*, **13**, 190–194.
- MAITHY, P. K., BABU, R., RAINA, B. K. & KUMAR, G. 1988. Proterozoic microfossils from Machhal and Lolab Formations of Kashmir Himalaya, India. *Neues Jahrbuch für Geologie und Palaeontologie*, **10**, 639–644.
- MAITHY, P. K., BABU, R., KUMAR, G. & MATHUR, V. K. 1995. New Cyanophycean remains from the Blaini Formation (Terminal Neoproterozoic sequence) of Mussoorie Syncline, Lesser Himalaya, India. *Palaeobotanist*, **43**, 39–44.
- MATHUR, V. K. & SHANKER, R. 1989. First record of Ediacaran fossils from the Krol Formation, Nainital Syncline. *Journal Geological Society of India*, **34**, 245–254.
- MATHUR, V. K. & SHANKER, R. 1990. Ediacaran medusoids from the Krol Formation, Nainital Syncline. *Journal Geological Society of India*, **36**, 74–78.
- MATHUR, V. K. & SRIVASTAVA, D. K. 2004. Record of Terminal Neoproterozoic Ediacaran Fossils from Krol Group, Nigalidhar Syncline, Sirmur district, Himachal Pradesh, India. *Journal Geological Society of India*, **64**, 231–232.
- MISRA, N. N., JAYAPRAKASH, A. V., HANS, S. K. & SUNDRAM, V. 1987. Bhima group of Upper Proterozoic—A stratigraphic puzzle. Purana Basins of Peninsular India. *Geological Society of India*, **6**, 227–237.
- MOITRA, A. K. 1990. Chronologic implications of the stromatolites, microbiota and trace fossils of the Chhatisgarh Basin, Madhya Pradesh. Workshop on Precambrian of Central India, Nagpur, India, August 1990. *Geological Survey India, Special Publications*, **28**, 384–399.
- MOITRA, A. K. 1999. Biostratigraphic Studies of Stromatolites and microbiota of the Chhatisgarh basin, M. P. India. *Palaeontologica Indica, Geological Survey of India*, LI.
- MOITRA, A. K. 2003. Stromatolite biostratigraphy in the Chhatisgarh Basin and possible correlation with the Vindhyan Basin. *Journal of the Palaeontological Society of India*, **48**, 215–223.

- MURTI, K. S. 1987. Stratigraphy and sedimentation in Chhattisgarh basin. Purana Basins of Central India. *Geological Society of India, Memoir* **6**, 239–261.
- PRASAD, B. & ASHER, R. 2001. Acritarch biostratigraphy and lithostratigraphic classification of Proterozoic and Lower Paleozoic sediments (pre-unconformity sequence) of Ganga Basin, India. *Paleontographia Indica*, **5**, 151.
- PRASAD, B., MAITHY, P. K., KUMAR, G. & RAINA, B. K. 1990. Precambrian–Cambrian acritarchs from the Blaini-Krol-Tal Sequence of Mussoorie Syncline, Lesser Himalaya, India. *Geological Society of India, Memoir*, **16**, 19–32.
- RAINA, B. K., KUMAR, G., BHARGAVA, O. N. & SHARMA, V. P. 1983. Precambrian–Lower Cambrian ichnofossils from the Lolab Valley, Kashmir Himalaya. *Journal Palaeontological Society of India*, **28**, 91–94.
- RAMAKRISHNAN, M. 1987. Stratigraphy, Sedimentary Environment and Evolution of the Late Proterozoic Indravati Basin, Central India. Purana Basins of Peninsular India. *Geological Society of India*, **6**, 139–160.
- RAMAM, P. K. & MURTY, V. N. 1997. *Geology of Andhra Pradesh*. Geological Society of India, Bangalore.
- RAO, T. S. 1987. Pakhal Basin—a perspective. Purana Basins of peninsular India. *Geological Society of India*, **6**, 161–187.
- SEILACHER, A., BOSE, P. K. & PFLUGER, F. 1998. Triploblastic animals more than 1 Billion Years ago: Trace fossil evidence from India. *Science*, **282**, 80–83.
- SHANKER, R. & MATHUR, V. K. 1992. Precambrian–Cambrian sequence in Krol Belt and Ediacaran fossils. *Geophytology*, **22**, 25–36.
- SHANKER, R., KUMAR, G., SAXENA, S. P. & SINGH, G. 1989. Stratigraphy and sedimentation in Himalaya—A reappraisal. *Geological Survey of India, Special Publication*, **26**, 1–60.
- SHANKER, R., KUMAR, G., MATHUR, V. K. & JOSHI, A. 1993. Stratigraphy of Blaini, Infra Krol, Krol and Tal succession, Krol belt, Lesser Himalaya, India. *Indian Journal of Petroleum Geology*, **2**, 99–36.
- SHANKER, R., MATHUR, V. K., KUMAR, G. & SRIVASTAVA, M. C. 1997. Additional Ediacaran biota from the Krol Group, Lesser Himalaya, India and their significance. *Geoscience Journal*, **XVII**, 79–94.
- SHANKER, R., MAITHY, P. K., SINGH, G. & KUMAR, G. 2000. Palaeogeographic evolution and biotic changes of the Indian Subcontinent from the Late Proterozoic to Early Palaeozoic. Proceedings of International Seminar Precambrian Crust in Eastern and Central India. IGCP Project 368, Bhubaneswar 1998. *Geological Survey of India, Special Publication*, **57**, 34–48.
- SHANKER, R., KUMAR, G. & MAITHY, P. K. 2002. Paleogeographic evolution of India and its implications for hydrocarbon resources: a new approach. In: SWAMY, S. N. & KAPOOR, P. N. Proceedings of Conference on Strategic Challenges and Paradigm Shift in Hydrocarbon Exploration with Special reference to Frontier Basins. 1st Association Petroleum Geology, Conference & Exhibition, 28–29 September 2002, Mussoorie, India, 23–42.
- SHANKER, R., BHATTACHARYA, D. D., PANDE, A. C. & MATHUR, V. K. 2004. Ediacaran biota from the Jarashi (Middle Krol) and Mahi (Lower Krol) Formations, Krol Group, Lesser Himalaya, India. *Journal Geological Society of India*, **63**, 649–654.
- SHARMA, M. 2003. Age of Vindhyan—Palaeobiological evidence: a paradigm shift (?). *Journal Palaeontological Society of India*, **48**, 191–214.
- SHARMA, M. & SHUKLA, M. 1999. Carbonaceous mega remains from the Neoproterozoic Owk Shale Formation of the Kurnool Group, Andhra Pradesh, India. *Current Science*, **79**, 1247–1251.
- SHARMA, M., MATHUR, V. K., SRIVASTAVA, M. C. & SHUKLA, M. 1994. Systematics and significance of microbialite (stromatolite) *Stratifera undata* from Mussoorie Syncline, Lesser Himalaya. *Journal Geological Society of India*, **43**, 705–712.
- SHUKLA, M., BABU, R., MATHUR, V. K. & SRIVASTAVA, D. K. 2005. Additional terminal Proterozoic organic-walled microfossils from the Infra Krol Formation, Nainital syncline, Lesser Himalaya, Uttaranchal, India. *Geological Society of India*, **65**, 197–210.
- SHUKLA, S. N., MUDIAR, B. & MISRA, M. M. 1994. Lithostratigraphy of Ganga basin, India. *Indian Journal of Petroleum Geology*, **3**, 69–90.
- SINGH, I. B. & RAI, V. 1977. On the occurrence of stromatolites in the Krol Formation of Nainital area and its implications on the age of Krol Formation. *Current Science*, **46**, 736–738.
- SINGH, I. B. & RAI, V. 1983. Fauna and biogenic structures in Krol–Tal succession (Vendian–Early Cambrian), Lesser Himalaya; their biostratigraphic and palaeontological significance. *Journal Palaeontological Society of India*, **28**, 69–80.
- SRIKANTIA, S. V. & BHARGAVA, O. N. 1998. *Geology of Himachal Pradesh*. Geological Society of India, Bangalore.
- TEWARI, V. C. 1984. Stromatolite and Precambrian–Lower Cambrian biostratigraphy of Lesser Himalaya, India. In: Proceedings of the V Indian Geophytological Conference, Lucknow, 1983. *Special Publication, The Palaeobotanical Society*, Lucknow, November 71–87.
- TEWARI, V. C. 2003. Sedimentology, palaeobiology and stable isotope chemostratigraphy of the terminal Neoproterozoic Buxa Dolomite, Arunachal Pradesh, NE Lesser Himalaya. *Himalayan Geology*, **24**, 1–18.
- TIWARI, M. 1996. Palaeobiology of Late Proterozoic (Vendian) microbiota: evidences from the Infrakrol Formation of Lesser Himalaya. In: PANDE, J., AZMI, R. J., BHANDARI, A. & DAVE, A. *Contributions to XV Indian Colloquium on Micropalaeontology and Stratigraphy*, K.D. Malviya Institute of Petroleum Exploration, Dehradun, 559–566.
- TIWARI, M. & AZMI, R. J. 1992. Late Proterozoic organic-walled microfossils from the Infrakrol of Solon, Himachal Lesser Himalaya: an additional age constraints in the Krol Belt succession. *Palaeobotanist*, **39**, 387–394.
- TIWARI, M. & KNOLL, A. H. 1994. Large acanthomorphic acritarchs from the Infra Krol Formation of the Lesser Himalaya and their significance. *Himalayan Geology*, **5**, 193–201.
- VENKATACHALA, B. S., SHUKLA, M., BANSAL, R. & ACHARYYA, S. K. 1990. Upper Proterozoic microfossils from the Infra-Krol rocks from Nainital Synform, U. P. Himalaya, India. In: JAIN, K. P. & TIWARI, R. S. (eds) Proceedings Symposium 'Vistas in Indian Palaeobotany', *Palaeobotanist*, **38**, 29–38.

Vendian *Hiemalora* from Arctic Siberia reinterpreted as holdfasts of benthic organisms

E. A. SEREZHNIKOVA

Palaeontological Institute, Russian Academy of Sciences, 123 Profsoyuznaya, Moscow, 117868, Russia (e-mail: serezhnikova@paleo.ru)

Abstract: *Hiemalora* Fedonkin, 1982 is based on cosmopolitan fossils of the late Vendian (Ediacaran) Neoproterozoic sequences. There is no consensus on the nature and systematic position of these organisms. Taphonomic and morphological observations of extensive collections of *Hiemalora pleiomorphus* from Khatyspyt Formation (Arctic Siberia) indicate that this fossil is just a part of an unknown organism. Most probably *Hiemalora* represents a form with a thick-walled body, possessing a cone-like attachment bearing radial processes that resemble sponge root offshoots or algal rhizoids. Originally these structures penetrated the soft sediment and served as anchors as well as a source of symbiotic nutrition. Various imprints of *Hiemalora* could represent different sections of conic-shaped bodies. Probably, there were several organisms referred to as *Hiemalora* that had a similar substrate attachment organ.

Well-preserved material from recently discovered localities have significantly increased our understanding of some Ediacaran taxa and changed views on their reconstructions. More reliable revisions of older reconstructions are obvious when sample size is large and especially when that taxon is from a single fossiliferous bed.

Research history of the genus *Hiemalora*

The genus *Hiemalora* Fedonkin, 1982 (type species: *H. stellaris* = *Pinegia stellaris* Fedonkin, 1980) was first described from the Vendian sequence of the White Sea, Russia. The author allied this new organism with cnidarian polyps or jellyfish with straight tentacles. *Hiemalora* and *Evmiaksia* were then united into the cnidarian Family *Hiemaloriidae* (Fedonkin 1985). *H. pleiomorphus* was discovered in limestones of the Khatyspyt Formation in the Khorbusuonka Group, Arctic Siberia (Vodanjuk 1989). Specimens in the Khatyspyt collection were arranged, depending on the form of the preservation and reconstructed as jellyfish that had fallen on a plastic clay substrate post-mortem (Vodanjuk 1989). In addition to systematic descriptions, there are numerous illustrations and descriptions of fossil forms similar to *Hiemalora* (Gehling *et al.* 2000; Jenkins 1995; De 2003). A star-like form from the Late Proterozoic of Newfoundland was thought to be either an attachment structure or a trace fossil or even the fragment of the body (Anderson & Conway Morris 1982). Several fossil impressions from the Innerelv Member, Late Proterozoic of the NE Finnmark were assigned to *Hiemalora* by Farmer *et al.* (1992). *Hiemalora* is known from the

Mackenzie Mountains of NW Canada (Narbonne 1998). Radial structures of these forms have been interpreted as tentacles of a polyp or the root-like structures of a holdfast (Runnegar 1995; Narbonne 1998). The star-shaped fossils have been compared with modern Protozoan xenophyophores in which the protoplasm has left traces in sediment (Seilacher *et al.* 2003). *Hiemalora* from Arctic Siberia has been regarded as an attachment structure (Dzik 2003). Thus, *Hiemalora* and other star-like fossils are known from many localities of the world, but there is no generally accepted interpretation of the nature and taxonomy of this form.

Material

Numerous imprints of *Hiemalora* were collected by M. A. Fedonkin and A. Y. Ivantsov (PIN RAS) from Arctic Siberia in the 1980–1990s. *Hiemalora* fossils occur in dark grey, thin-bedded limestones of the Khatyspyt Formation in the Khorbusuonka Group, which crops out in the Olenek River Basin, along the Khorbusuonka and Anabyl rivers (Fig. 1). The Khorbusuonka Group can be correlated with Yudomian (Vendian) sediments by use of stromatolites and microphytolites and is dated radiometrically (Sokolov & Fedonkin 1985). Fossils of *Hiemalora* in Siberia are flat to low relief imprints in most cases. Specimens from the sole surface are preserved in negative hyporelief (Fig. 2a), and those from the top surface occur in positive epirelief most often (Fig. 2b). Specimens of *Hiemalora* arranged in preservational rank (Vodanjuk 1989) demonstrate that such assemblages represent one form of a single species, *Hiemalora pleiomorphus* (Fig. 6a–e).

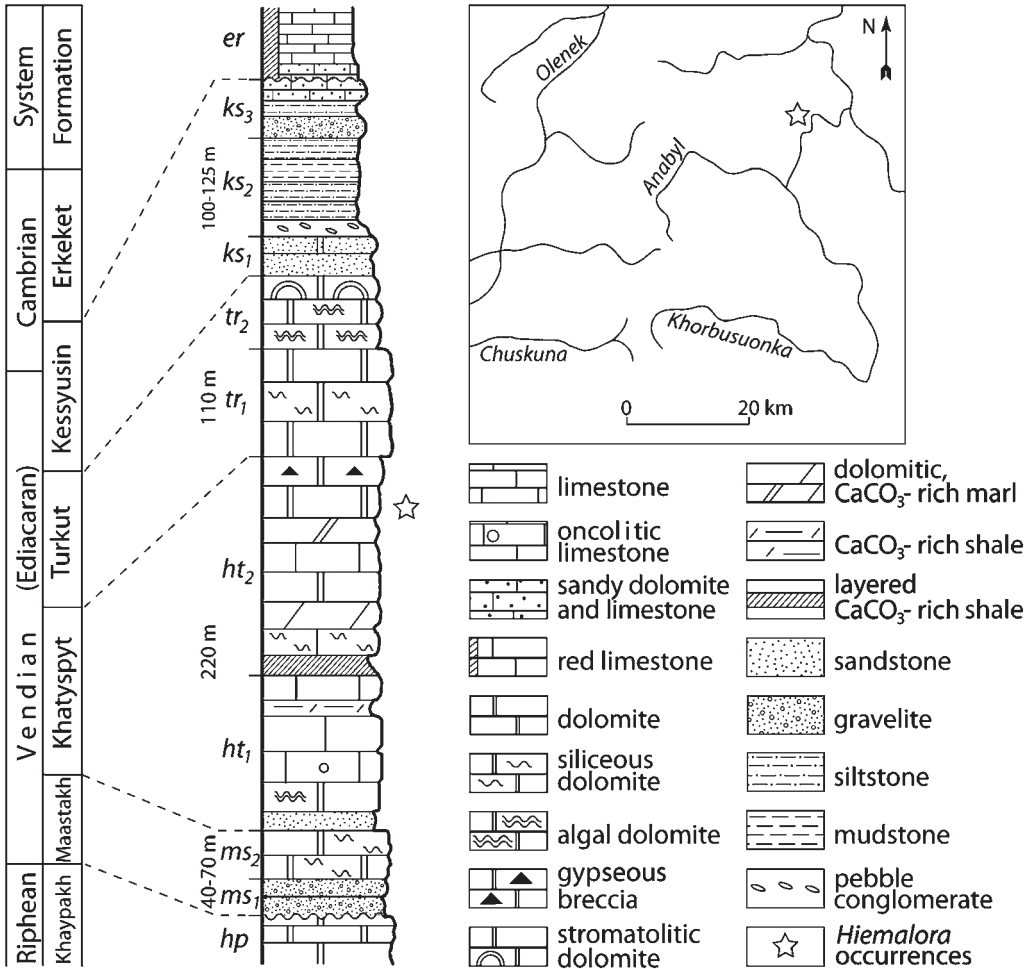


Fig. 1. Generalized stratigraphic section of the Vendian sequence, the Olenek uplift, Arctic Siberia (Vodanjuk 1989).

Fossil structure

Hiemalora imprints have a rounded central part with rod-like radial elements (Fig. 3). The central sections leave a low relief imprint but some forms show higher relief. These higher relief forms could represent remains of: (1) a short column; (2) a small hemisphere; or (3) a broad short cone. Occasionally these fossils are surrounded with a narrow (2–3 mm) ring-shaped border resembling a roll or a furrow (Fig. 3(2)). Fine, sub-parallel grooves interrupt the surface of hemisphere-shaped forms. The space between these grooves is slightly greater in the centre of the casts (Fig. 6a–c) than on the periphery. Small (1–2 mm) impressions (or bumps) are situated randomly on the surface of some specimens (Fig. 3(3)).

Radial elements resembling straight or smoothly curved rods are flat or slightly raised (Fig. 3(4)). In

some cases, these radial elements lie in the shallow isometric depression. Outlines of these elements are smooth and without fissures. There are rare clavate nodules on the endings of these structures. Rod-like radial elements are distributed evenly on the surface of the layer intersecting each other centrally. Some specimens have radial elements which traverse borders of the central parts (Fig. 6d–e) and in other specimens these elements diverge from centres of imprints. The radial structures of the best-preserved specimens diverge from the centre and different points of the periphery resembling a radial network. Some three-dimensional forms resemble stubs with radial elements lying in a ring-like depression.

Hiemalora imprints may be divided into three morphological types (Table 1, Fig. 4): (1) elongate radial elements with a small central part; (2) radial

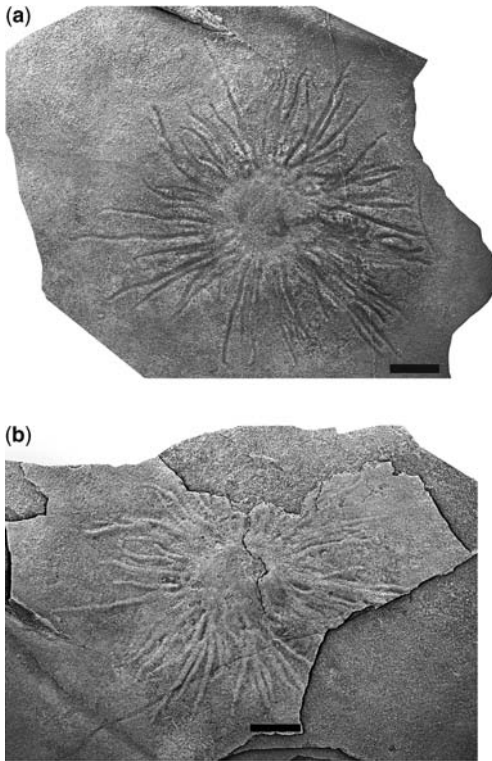


Fig. 2. *Hiemalora pleiomorphus* from the Olenek uplift, Arctic Siberia. (a) PIN, N 3995/251 (from the sole of fossiliferous stratum); (b) PIN, N 3995/251-1 (from the top of fossiliferous stratum layer); scale 1 cm.

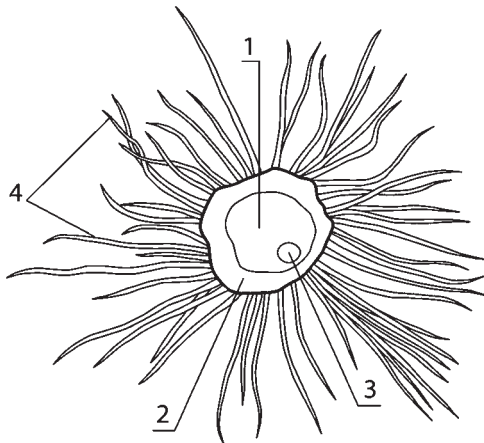


Fig. 3. Schematic drawing of *Hiemalora pleiomorphus* from the Olenek uplift, Arctic Siberia (PIN No. 3995/251): (1) central part; (2) peripheral border; (3) small structure found on central disk; (4) radial elements. See Fig. 4 and Table 1 for size range.

Table 1. Measurements of specimens of *Hiemalora pleiomorphus*

N	D	d	D/d	Q (~)
3995/18	40	15	2.7	
43	20	10	2.0	30
76	5	15	0.3	30
81	9	15	0.6	50
84	30	35	0.9	75
86	12	13	0.9	
91	23	15	1.5	
94	12	15	0.8	
137	28	7	4.0	
251	20	25	0.8	50
252	40	15	2.7	
253	7	5	1.4	25
254-1	08	7	1.1	
254-2	45	15	3.0	
255	10	15	0.7	30
256	50	30	1.7	
257	12	20	0.6	70
258	20	30	0.7	
259	6	15	0.4	40
260	8	15	0.5	
261	11	15	0.7	40
262	40	25	1.6	50
263	25	15	1.7	20
264	50	35	1.4	70
265	17	15	1.1	50
267	13	10	1.3	40
268	15	12	1.3	
269	50	30	1.7	
270	30	10	3.0	
272	8	10	0.8	40
274	10	10	1.0	30
280	9	15	0.6	20
282	20	10	2.0	
283	25	5	5.0	
284-1	20	25	0.8	40
284-2	22	25	0.9	40
285	7	15	0.5	20
286	20	15	1.3	30
287	13	20	0.7	20
288	20	15	1.3	30
289	10	8	1.3	50
290	10	10	1.0	
292	23	15	1.5	
368	22	5	4.4	
397	25	20	1.3	50
512	13	15	0.9	
624	20	25	0.8	

D, diameter of the central part (mm); d, length of radial elements (mm); Q, number of radial elements).

elements approximately equal in length to the central part; and (3) short radial elements with an enlarged central part. There seems to be no relationship between the diameters of the central part and the number of the radial elements. It is doubtful that these morphological types represent different

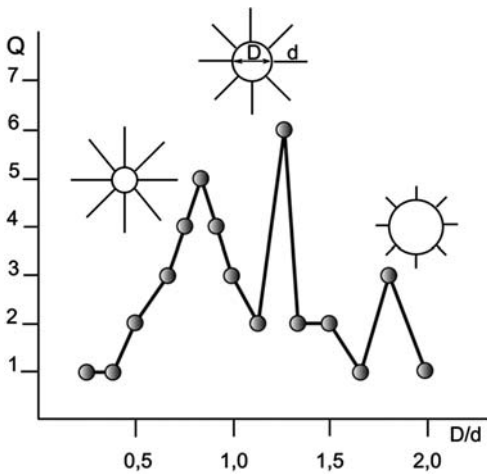


Fig. 4. Histogram of distribution of *Hiemalora pleiomorphus* specimens from the Olenek uplift, Arctic Siberia according to the ratio of D/d . D , diameter of central part (mm); d , length of radial elements (mm); Q , numbers of radical elements. See Table 1 for data.

taxa. This distribution may be related to age differences and/or post-mortem modification in the sediment. Various imprints of *Hiemalora* could also be different sections of a cone-shaped organism.

Interpretation

As there are no signs of transportation or deformation, it appears that this material was preserved *in situ*. The variety of forms of the central part (Figs 5, 6a–e) suggests that the original organism had three-dimensions and was not flat. Since low profile cylindrical-shaped forms suggest that the living organism possessed an internal cavity, sometimes likely filled with the sediment during lifetime or even post mortem. In this case the relief of the central part depends on sediment filling the cavity of the living organism and if so the quantity will determine the degree of relief. A specimen where it could be shown that the central part can be separated from the enclosing sediment would be an indisputable argument for the previous existence of such a hypothetical cavity. The relief can also be explained by collapse of a soft body without a cavity. As it was noted above, some specimens have a ridge or a furrow around the outer border of their central parts, which could be a remnant of a massive body wall. Small, rare, round structures on the surface of the central section could represent holes filled with the sediment, which then were preserved in relief. In collections at the Paleontological Institute there is a single specimen (PIN No. 3995/82) with a sub-oval contour of the central part; if this material were

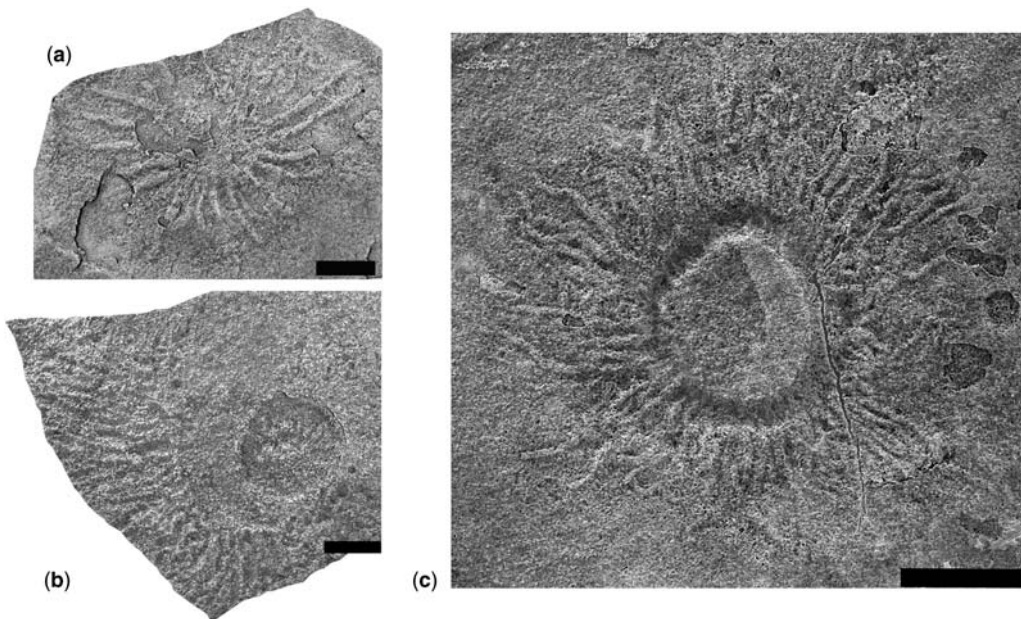


Fig. 5. *Hiemalora pleiomorphus* from the Olenek uplift, Arctic Siberia. (a) PIN, N 3995/287; (b) PIN, No 3995/84; (c) PIN, No 3995/289; scale bar 1 cm.

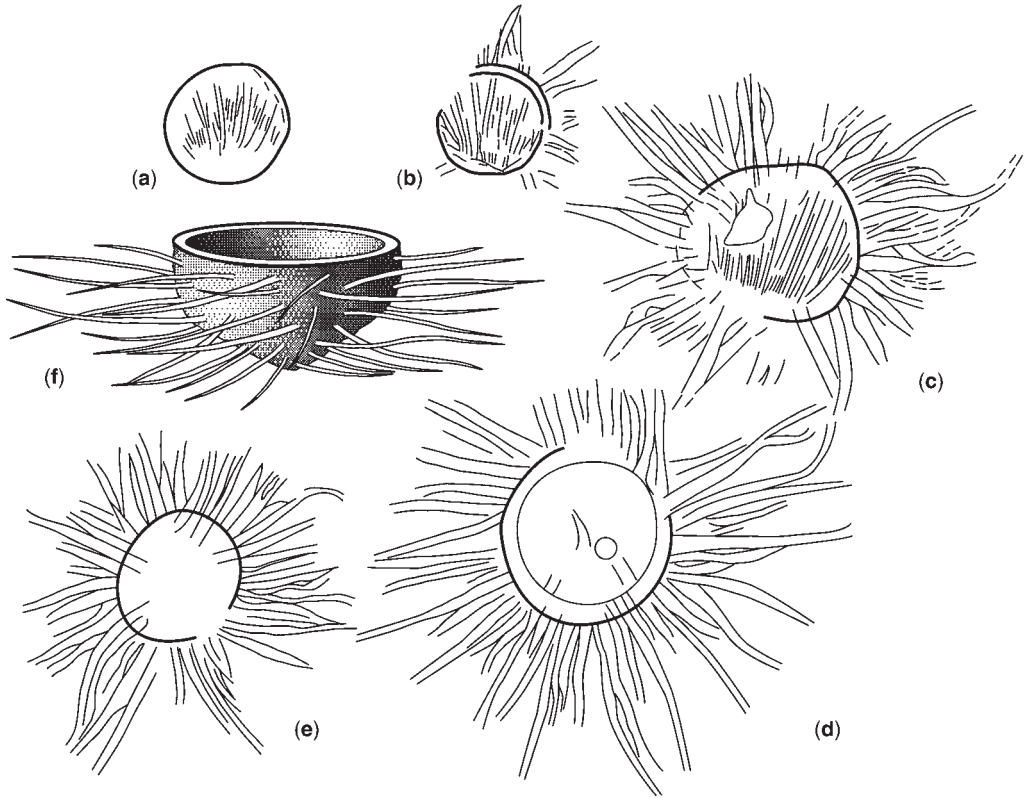


Fig. 6. *Hiemalora pleiomorphus* from the Olenek uplift, Arctic Siberia. (a–e) schematic drawings of a variety of preservational forms, (after Vodanjuk 1989); (f) tentative reconstruction of preserved fossil of *Hiemalora*. See Fig. 4, Table 1 for size range.

more common, one might suggest that *Hiemalora* could divide to form two individuals or clones.

Virtually none of the specimens shows deformation of the radial elements, which are spaced evenly occasionally crossing. This could signal their relative rigidity; moreover only one specimen (N 3995/289) has a broken radial element. There are rare forms where the radial elements are preserved in differing relief, possibly explained by heterogeneity of the tissue.

High-relief specimens can assist in understanding the spatial distribution of radial elements in living organisms. For instance, a low-conical specimen shows radial elements growing from different layers that overlap each other. One can conclude from this, that these radial elements penetrated the sediment randomly rather than lying on the same layer. In other cases, the central part possessed rod-like elements that diverged in many directions and must have had a shape like an upside-down cone. After this collapsed and was affected by sediment compaction, the radial elements from different

layers could have been projected onto one surface. Therefore, these elements seem to be reacting as would the tentacles of a jellyfish or polyp.

A study of a large sample of *Hiemalora* demonstrates that the radial elements are static structures resembling root offshoots of sponges or rhizoids of algae rather than flexible tentacles. During a lifetime of the organisms these structures seem to have penetrated the liquid-rich sediment, and served for anchoring the organism probably, also for nutrition.

Reconstruction

Hiemalora may be reconstructed as an organism with a thick-walled body and a cone-like attachment disc with diverging radial offshoots (Fig. 6f). Reconstruction of *Hiemalora* from fossils is difficult. The fossils have disproportionately elongate offshoots when compared with a small body making it difficult to reconstruct its

lifestyle. *Hiemalora* may be only part of an unknown organism, i.e. basal attachment structure in sediment. This would then explain why the imprints are so diverse, and the offshoots and the main body can be correlated. There may well have been different organisms that are referred to as *Hiemalora* with a similar way of attachment in the substrate. Unfortunately, there are no data on *Hiemalora*'s hypothetical upper-most parts. Considering measurements of these attachment structures which may have anchored an organism to a soft substrate, one would predict that non-preserved upper parts of some specimens may have been of significant size.

Hiemalora's disc-like attachment was likely within the sediment (Fig. 7a) while the body towered above the seabed, therefore explaining the multiple modes of burial of these fragmentary 'animals' (Fig. 7b, c). Burial conditions above the bacterial film and under it would have differed sharply (Gehling 1999). That is the likely explanation why no *Hiemalora*'s upper-most parts would be missing in the fossil record since they were likely to have been destroyed. Disc-like attachments would more likely to have been preserved. The mechanism of the formation of one-sided forms leaving 'leaf-like' imprint, with a

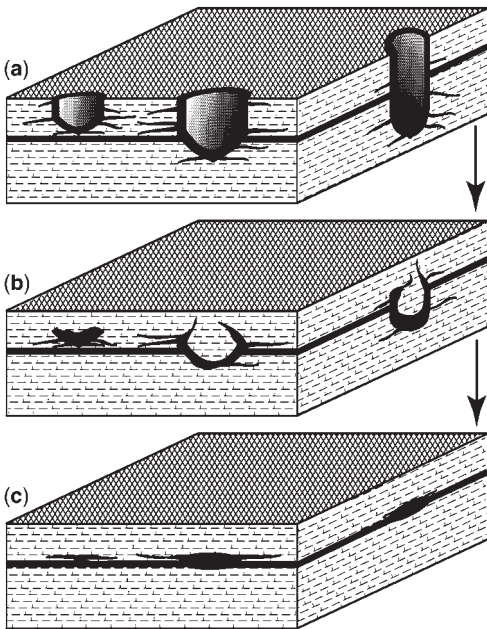


Fig. 7. Suggested patterns of fossilization of *Hiemalora pleiomorphus* from the Olenek uplift, Arctic Siberia. Stages (a) to (c) show gradual development of taphomorph, with (c) being the final stage.

negative imprint of the upper surface of the leaf preserved on bed soles and a positive imprint of the same surface on the top of the underlying layer, was explained by Kryshstofovich (1957). To interpret fossilization of attachments one can use Kryshstofovich's (1957) model, which likens *Hiemalora* structure to the hard capsule around roots of modern plants.

If the fossilization events of *Hiemalora* are reconstructed correctly in this paper, one can suggest that these organisms had a rigid external tissue rather than soft bodies. And with this new reconstruction of *Hiemalora*, the diagnosis of this genus needs to be amended. *Hiemalora* should now be viewed as a problematical benthic organism with the attachments characterized by a monaxonic, heteropolar symmetry of indefinitely high order (terminology after Beklemishev 1964) preserved as low-relief, only rarely as high-relief imprints with a rounded central part associated with a marginal set of the rod-like radial elements.

Taxonomy

The current situation regarding the taxonomy of Ediacaran organisms, particularly rounded ones, is similar to the taxonomy in palaeobotany during the 1980's: '... more than 40% of the genera have to be abolished due to various nomenclature reasons, about 30% are to be revised and re-described and only 40% could more or less safely be used' (Meyen 1990, p. 50). In order to overcome such a situation, it is reasonable to collect specimens of one type from one depositional surface and after that specimens could be viewed in mono-topical assemblages. Harris (1932) pioneered the use of this method of analysis based on his palaeobotanical studies for Triassic/Jurassic sequences of Greenland.

Conclusions

Taphonomic observations on a large sample of fossils from the Khatyspyt Formation of Arctic Siberia demonstrate that *Hiemalora* is a mixed group of fragments of benthic organisms, the basal parts of which were situated within the sediments.

The radial elements of *Hiemalora* were evidently static structures resembling the root offshoots of sponges or rhizoids of algae rather than flexible tentacles, as has been suggested in the past. These structures originally penetrated liquid sediment, served for anchoring within it and, could have been nutrient collectors. *Hiemalora* holdfasts seem to have had a thick body wall with a cone-like attachment disc and diverged radial offshoots.

The study was supported by the Russian Fund for Basic Research (RFBR 02-05-64658) and the Scientific School of Academician Boris S. Sokolov (Grant NSH-1790.3003.5). The author is grateful to M. A. Fedonkin and A. Y. Ivantsov for access to the collections (*Hiemalora*) and the assistance they gave on this study, D. Grazhdankin and M. Leonov for the consultations, O. Panin and D. Serezhnikov for the improving language of the manuscript, A.V. Mazin for the photographs, P. Vickers-Rich for assistance from IGCP Project 493 (UNESCO), of which this study is a part. Thanks are due to the two reviewers: J. Gehling and B. MacGabhann.

References

- ANDERSON, M. M. & CONWAY MORRIS, S. 1982. A review, with description of the soft-bodied fauna of the Conception and St. John's Group (Late Precambrian), Avalon Peninsula, Newfoundland. *Proceedings of the Third North American Paleontological Convention*, **1**, 1–8.
- BEKLEMISHEV, V. N. 1964. *Treatise on Invertebrate Comparative Anatomy: Promorphology*. Nauka, Moscow [in Russian].
- DE, C. 2003. Possible organisms similar to Ediacaran forms from the Bhandar Group, Vindhyan Supergroup, Late Neoproterozoic of India. *Journal of Asian Earth Sciences*, **21**, 387–395.
- DZIK, J. 2003. Anatomical information content in the Ediacaran fossils and their possible zoological affinities. *Integrative & Comparative Biology*, **43**, 114–126.
- FARMER, J., VIDAL, G., MOCZYDLOWSKA, M., STRAUSS, H., AHLBERG, P. & SIEDLECKA, A. 1992. Ediacaran fossils from the Innerelv Member (late Proterozoic) of the Tanafjorden area, northeastern Finnmark. *Geological Magazine*, **129**, 181–195.
- FEDONKIN, M. A. 1980. New Precambrian Coelenterata in the north of the Russian platform. *Paleontologicheskii Zhurnal*, **2**, 7–15 [in Russian].
- FEDONKIN, M. A. 1982. New name of Precambrian Coelenterata]. *Paleontologicheskii Zhurnal*, **2**, 137 [in Russian].
- FEDONKIN, M. A. 1985. Non-skeletal fauna of the Vendian: promorphological analysis. In: SOKOLOV, B. S. & IWANOWSKI, A. B. (eds.) *The Vendian System, vol. 1, Palaeontology* Nauka, Moscow, 10–69. [in Russian].
- GEHLING, J. G. 1999. Microbial mats in terminal Proterozoic siliciclastics: Ediacaran death masks. *Palaaios*, **14**, 40–57.
- GEHLING, J. G., NARBONNE, G. M. & ANDERSON, M. M. 2000. The first named Ediacaran body fossil, *Aspidella terranovica*. *Palaeontology*, **43**, 427–456.
- HARRIS, T. M. 1932. The fossil flora of Scoresby Sound, East Greenland. Description of seed plants *incertae sedis*, together with a discussion of certain cycadophyte cuticles. *Meddelelser om Grønland*, **85**, 1–133.
- JENKINS, R. J. F. 1995. The Problems and Potential of Using Animal Fossils and Trace Fossils in Terminal Proterozoic Biostratigraphy. *Precambrian Research*, **4**, 51–69.
- KRYSHTOFOVICH, A. N. 1957. *Palaeobotany*. Leningrad, Gostoptechizdat [in Russian].
- MEYEN, S. V. 1990. *Theoretical problems of palaeobotany*. Nauka, Moscow. 1–287 [in Russian].
- NARBONNE, G. M. 1998. The Ediacara Biota: A terminal Neoproterozoic experiment in the evolution of life. *GSA Today*, **8**, 1–6.
- RUNNEGAR, B. 1995. Vendobionta or Metazoa? Developments in understanding the Ediacara 'fauna'. *Neues Jahrbuch für Geologie und Palaeontologie, Abhandlungen*, **195**, 303–318.
- SEILACHER, A., GRAZHDANKIN, D. & LEGOUTA, A. 2003. Ediacaran biota: The dawn of animal life in the shadow of giant protists. *Palaeontological Research*, **7**, 43–54.
- SOKOLOV, B. S. & FEDONKIN, M. A. (eds) 1985. *Vendian System: Historical Geological and Palaeontological Substantiation*, **2**, Nauka, Moscow, [in Russian].
- VODANJUK, S. A. 1989. Remains of non-skeletal Metazoa from Khatyspyt formation on the Olenek Uplift. *Pozdnii dokembry and rannii paleozoi Sibiri, Aktualnii voprosi stratigrafii*, 61–75 [in Russian].

A new reconstruction of *Protolyellia* (Early Cambrian psammocoral)

E. SAVAZZI

Hagelgränd 8, 75646 Uppsala, Sweden

*Present address: Kyoto University Museum, Yoshida Honmachi,
Sakyo-ku, 606-8501 Kyoto, Japan (e-mail: enrico5@savazzi.net)*

Abstract: A new reconstruction of *Protolyellia* (psammocoral) from the Mickwitzia sandstone, Early Cambrian of south-central Sweden, is proposed. Observations, conceptual analysis and physical modelling indicate that the distinctive honeycomb or (less frequently) ridge sculpture of the upper side of the sand-button was a wrinkle pattern in a flexible epithelium. Wrinkling was caused by contraction of a subepithelial muscle layer joined to the epithelium by connective tissue. Fine-grained sand particles adhering on, or embedded within, the epithelium preserved its surface relief after the soft parts decomposed. The sand-bearing epithelium covered a subcylindrical structure attached around the periphery of the sand-button and extending upwards. This structure is occasionally preserved felled horizontally near a sand-button, but is more commonly found as isolated shreds. Sudden burial caused the lower portion of this structure to contract and wrinkle against the tissues containing the sand-button. After the soft parts decomposed, sediment compaction pasted the wrinkled layer onto the sand-button, thus producing the typical preservation mode. The wrinkle pattern of *Protolyellia* differs from those of Recent cnidarians, and suggests that *Protolyellia* did not possess mesenteries. *Protolyellia* may be more distantly related to modern cnidarians than previously assumed. In addition, alternative affinities with Ediacaran frond-bearing forms cannot be excluded.

Protolyellia is a discoidal fossil from the Early Cambrian (and possibly also earlier and subsequent ages, see below). Unlike other discoidal fossils of the Late Proterozoic & Early Palaeozoic (e.g. see MacGabhann *et al.* 2007), it consists of a large and thick button of well-sorted, coarse-grained clasts, evidently contained within a soft-bodied organism. This structure is the distinctive feature of psammocorals, a small group of Late Proterozoic–Early Palaeozoic organisms (Seilacher 1992; Seilacher & Goldring 1996).

In the past, *Protolyellia* suffered a fate similar to that of many other discoidal fossils, and was interpreted as a medusan organism, or even an echinoderm (e.g. Torell 1870). It is, at present, thought to have actinian cnidarian affinities (Seilacher 1992, and discussion below). Among the terms proposed in the literature to identify these organisms, I prefer to use ‘psammocorals’ (Seilacher 1992; Seilacher & Goldring 1996) in a morphological sense, rather than as a formal taxon. This paper examines the morphology of *Protolyellia princeps* Torell, 1870 on the basis of material from south-central Sweden, and proposes a reconstruction of its anatomy that differs from earlier ones.

Material

About twenty specimens of *Protolyellia* with diameters varying from approximately 15–150 mm

(the latter inferred from an incomplete specimen) and exhibiting the typical morphology for this genus (see description below) were observed and photographed for this study.

Transverse sections were prepared for one specimen. The side bearing the distinctive relief pattern was coated in a thick layer of epoxy prior to sectioning, to prevent it from detaching.

The studied material was collected from the Mickwitzia Sandstone (File Haidar Formation, Early Cambrian) of Västergötland, south-central Sweden and is housed in the Swedish Museum of Natural History, Stockholm, Sweden (SMNH). When available, inventory numbers are given in figure captions. Most specimens appear to have been collected as loose rubble and several show evident atmospheric wear.

In addition to the above specimens, fragmentary material of atypical aspect, originating from the same localities and stored in the same repository, is identified in this paper as belonging to *Protolyellia*.

Observations

General shape

Typical specimens of *Protolyellia* (Fig. 1) exhibit a discoidal shape with a convex and smooth side (Fig. 1b–c, i), and an opposite side that is flatter, usually bearing a central boss or projection

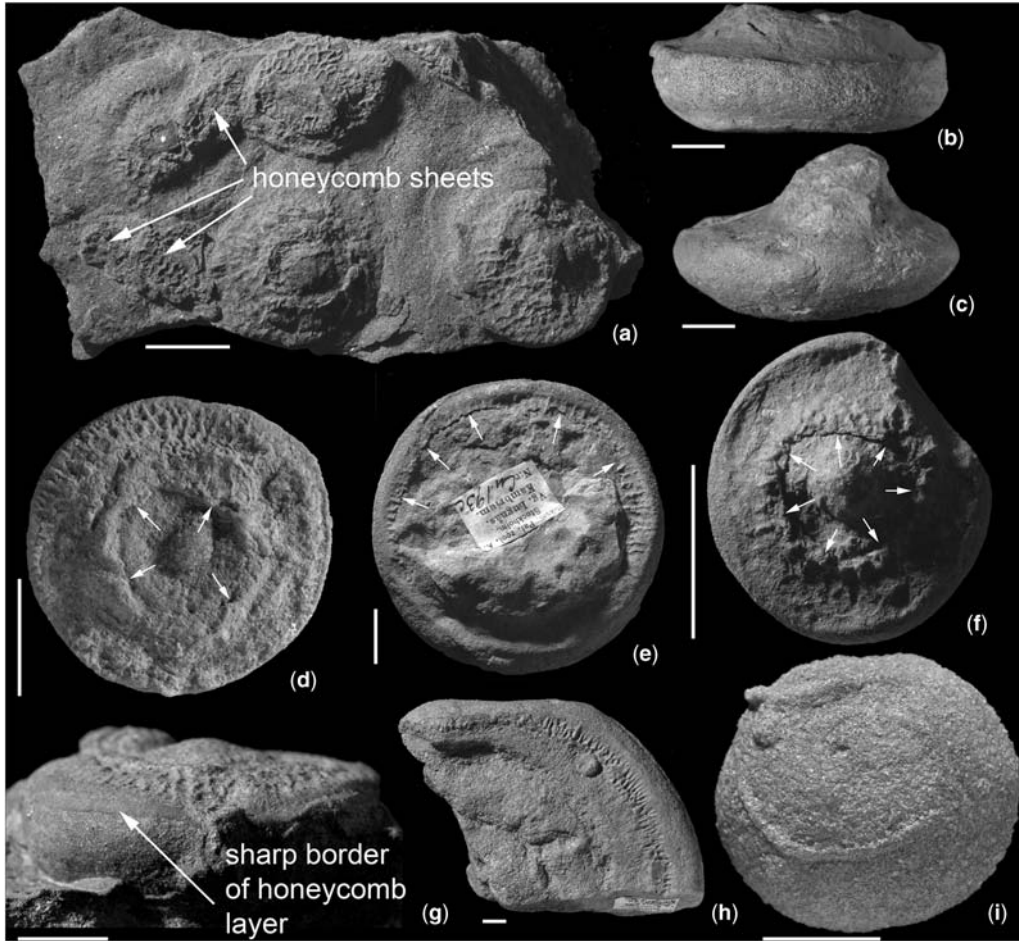


Fig. 1. Typical preservation of *Protolyellia princeps*, Early Cambrian of Sweden. (a) slab containing several specimens (inventory n. SMNH Cn192). (b)–(i). Sand-buttons in side view (b), SMNH Cn218; (c), SMNH Cn194e; (g), SMNH Cn196), upper surface (d), X3087; (e), SMNH Cn193a; (f), lot SMNH Cn193; (h), SMNH Cn32; the last is fragmentary), and lower surface (i) (X3806). Small arrows in (d–f) indicate a structural discontinuity between honeycomb layer and sand-button. Scale bars represent 10 mm.

surrounded by an area bearing a network of ridges. The latter is called herein ‘honeycomb pattern’ because of its tendency to display a somewhat irregular hexagonal arrangement (Fig. 1).

Specimens preserved on the bedding plane, and presumed in life orientation (see below, and Fig. 1a; see also Seilacher 1992; Seilacher & Goldring 1996), have the uniformly convex side positioned lowermost. This side is here referred to as ‘lower’, and the opposite one, bearing the honeycomb pattern, as ‘upper’. Usually, *Protolyellia* is slightly embedded in sediment at the top of bedding planes. Trace fossils are often observed to penetrate *Protolyellia* (Figs 1h–i, 2e), but adjacent individuals of *Protolyellia* never penetrate or indent each other.

The available material varies in shape and apparent mode of preservation. The range of variability is discussed below.

Lower surface

The lower surface is composed of medium-grained, well sorted and well cemented siliceous sand. On first inspection, this sediment appears coarser than the surrounding matrix, which typically is silty sandstone. However, this difference is due to the absence of a silty fraction in the sand-button. In fact, coarser clasts than those present in *Protolyellia* are often present within the surrounding matrix. The lower surface curves evenly upwards

at its periphery, and often blends into the upper surface in correspondence of a distinct shoulder (albeit not a sharp edge) (Fig. 1b–h).

Upper surface

The upper surface usually bears a distinct boss in its centre (Fig. 1a, c–d, f–g), sometimes surrounded by a depression (Fig. 1b–d). The central boss consists of the same material visible on the lower surface. The remaining upper surface usually is covered by a layer of fine-grained material which bears a honeycomb pattern. The material underlying the pattern-bearing layer is similar to the one on the central boss and lower surface. The surface separating the pattern-bearing layer from the coarser material, where visible, is smooth and featureless.

In well-preserved specimens, a sharply distinct border is observed between the fine-grained layer and the underlying material around the periphery of the button, and the best instances display a fine groove between the two layers (Fig. 1g).

A distinct border between the two layers is frequently seen also around the central boss. This border seems to constitute a physical discontinuity, and in several specimens parts of the upper layer appear to have broken off, leaving a sharp edge (white arrows in Fig. 1d–f).

Honeycomb pattern

This pattern typically consists of a somewhat irregular honeycomb of raised ridges (Fig. 1a, d–e, g). Especially around the periphery of the upper surface, the pattern may consist instead of irregular ridges arranged in a radial fashion (Fig. 1d–e, h). This pattern displays a clear negative allometry: larger specimens possess a much higher number of polygonal cells than smaller individuals. However, the absolute size of polygonal cells does increase somewhat during growth.

Atypical preservation

Occasional specimens display no trace of the honeycomb pattern (Fig. 2a). In these instances, it is difficult to detect whether the fine-grained layer is still present. At least in some instances, it appears possible that the honeycomb pattern was not originally present, or that it was subsequently destroyed by taphonomic phenomena within the sediment. In other instances, atmospheric wear after exposure of the fossil may have removed the pattern.

The specimen in Figure 2(b) appears to have a small sand-button at the bottom of a short conical tube that expands upward (assuming the typical orientation for *Protolyellia*). The tube bears the

characteristic honeycomb pattern on its sides. The upper end of the tube is filled with featureless matrix.

A conical structure, without a visible sand-button, is shown in Figure 2(c–d). It displays a honeycomb pattern on its surface, but its polygonal cells, unlike those normally observed on the upper surfaces of sand-buttons, are distinctly compressed along the axis of the cone (Fig. 2d). The orientation of this specimen within the sediment is unknown.

The specimen in Figure 2(e) is penetrated by at least two vertical burrows. Other trace fossils are visible in Figure 1(h–i). Figure 2(f) shows a sand button with a chaotic bottom structure. The sand button in Figure 2(g) is unusual in having a distinctly convex upper surface, a patterned fine-grained layer extending from the periphery almost to the centre of the button, and a pattern consisting largely of radial ridges instead of polygonal cells.

The slab in Figure 3(a) carries a jumble of objects. Most appear to consist of partly cemented sand nodules or sheets, but rock pebbles are also present. One of the nodules (black arrow) displays a finely layered internal lamination that follows a curved profile. It may be a reworked stromatolite, or part of the reworked and eroded sand-skeleton of a psammocoral.

Several of the smaller objects on the same slab (white arrows) display the same honeycomb pattern seen on the upper surface of *Protolyellia* sand-buttons, but their shape indicates that they are not fragments of such buttons. In particular, Figure 3(b–c) (located on a different slab than Figure 3(a)) shows that the polygonal cells of the pattern are distorted, and that the patterned surface was indented by a sharp-edged pebble (which detached from the slab, leaving a depression). Both characteristics indicate that the honeycomb pattern was part of a flexible, soft structure. Figure 3(d–e) show further examples of honeycomb patterns on a cylindrical surface and on an irregularly convex one, respectively. There can be little doubt that these patterned objects represent flexible shreds of *Protolyellia*. The implications of this are discussed below.

A sheet-like object in Figure 3(f) displays a faint honeycomb pattern on part of its surface (especially at centre-left), grading into small irregular wrinkles on other portions. Were it not for this faint hexagonal meshwork, it would not be recognizable as a fragment of *Protolyellia*. The surface of this sheet does not seem to be eroded, because it displays small but sharp creases and spine-like projections. Therefore, the faint honeycomb pattern is a genuine feature, rather than a normal pattern that became worn out. Other featureless sheets that might represent shreds of *Protolyellia* were observed, but they do not display a

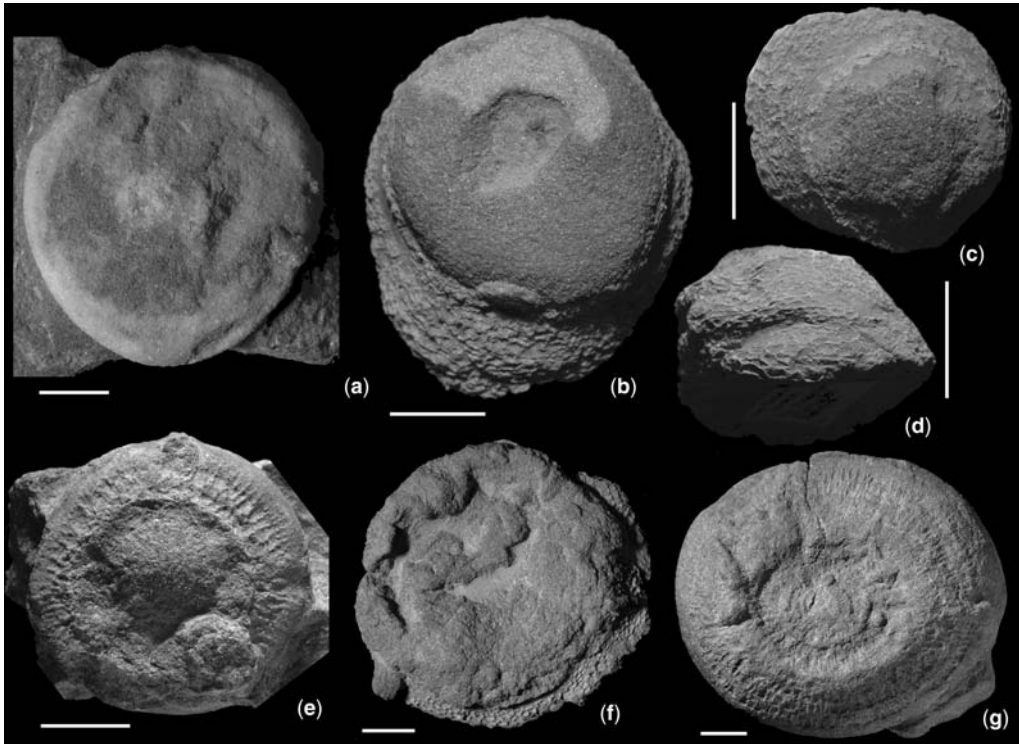


Fig. 2. Atypical preservation of *Protolyellia princeps*, Early Cambrian of Sweden. (a) Sand-button without honeycomb pattern. (b–d) Conical portions of honeycomb layer with a small sand-button (b) and devoid of it (c–d). (e) Sand-button penetrated by vertical burrows (SMNH Cn196). (f) lower surface of sand-button with chaotic structure. (g) Large sand-button with markedly convex surface and honeycomb/wrinkle pattern extending almost to the centre. Scale bars represent 10 mm.

recognizable shape or relief, and cannot be identified conclusively.

Internal structure

Transversal sections of a sand-button (Fig. 4) show that the interior is occupied by cemented siliciclastic sand of the same type and grain-size visible on the lower surface (see above). A meniscus structure parallel to the lower side of the sand-button is barely perceptible, but no true banding or layering. This structure is due to oblong clasts being preferentially oriented with the long axis parallel to the lower surface of *Protolyellia*. A preferential convex-side-up arrangement of irregular clasts can also be observed (see also Jensen 1997, fig. 13b–c).

The honeycomb pattern is a relief on the upper surface of a thin layer of fine-grained siliciclastic sandstone lying directly onto the dorsal side of the coarse-grained structure (Fig. 4c–d). The boundary between the two layers is generally well defined,

although occasional coarse clasts, detached from the underlying layer, are embedded within the fine-grained material (Fig. 4e). No structure is apparent in the fine-grained layer.

Discussion

Life and taphonomic orientation

There is general agreement in the literature (e.g. Seilacher 1992; Seilacher & Goldring 1996) that the upper surface of *Protolyellia* (as defined herein) was oriented uppermost in the life position. The principal reasons are its observed taphonomic occurrence (Seilacher 1992; Seilacher & Goldring 1996; above observations), and the fact that the sand-skeleton is reconstructed as lying lowermost within the organism, with its lower surface in close proximity to the external epithelium, and in this position favoured passive reorientation to the hypothesized life orientation (above references).

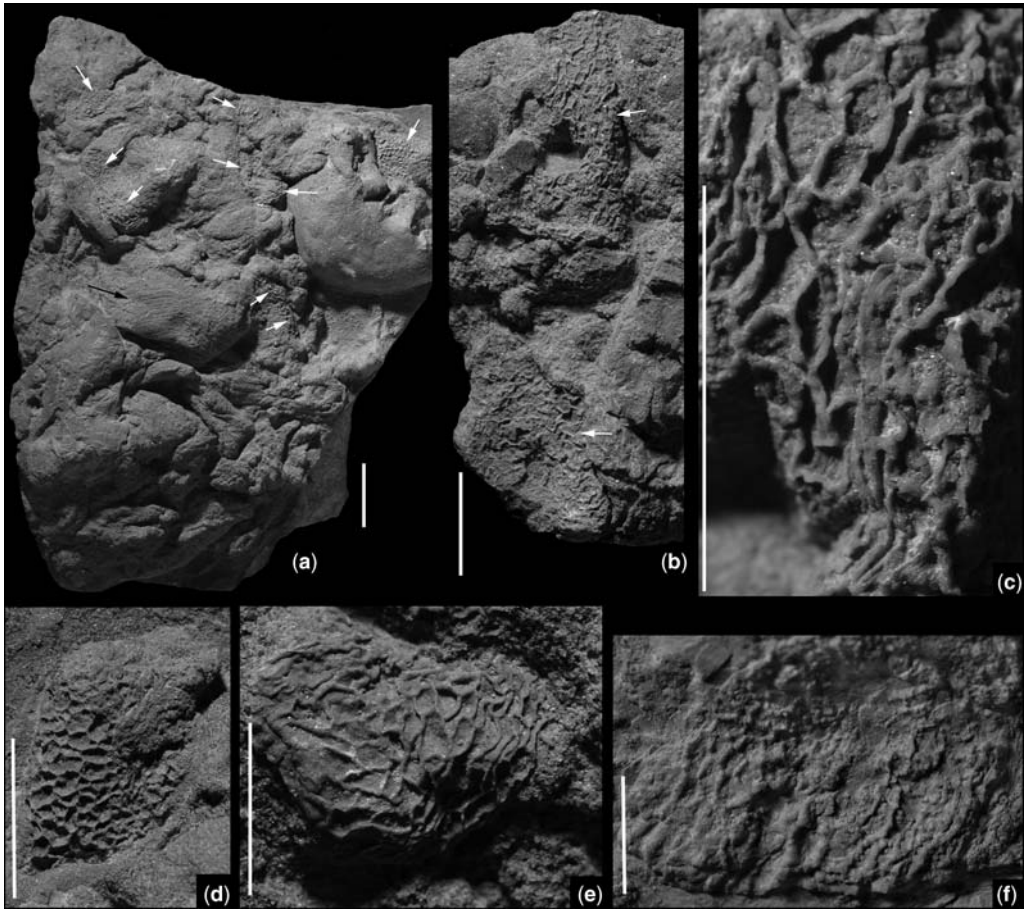


Fig. 3. Isolated fragments of honeycomb layer of *Protolyellia princeps*, Early Cambrian of Sweden. (a) Slab covered with a variety of clasts. White arrows indicate honeycomb patterns. *Black arrow* indicates clast with fine, convex laminated structure. (b–c) Distorted honeycomb patterns (arrows). One of these is indented by a pebble (which detached from the slab, leaving a depression). (d–e) Cylindrical (d) and irregularly convex (e) fragments. (f) Sheet-like fragment displaying a very faint honeycomb pattern in its centre-left portion. Note also the fine creases and spine-like projections in other regions. Scale bars represent 10 mm.

Interpretation of honeycomb pattern

The author proposes that the honeycomb pattern preserves the general morphology of a wrinkled external epithelium, i.e. a soft tissue. In addition, the wrinkled state is not permanent, but originates from the contraction of an underlying muscle layer, probably as a distress reaction caused by sudden burial of the organism. The following sections introduce a variety of theoretical considerations and physical evidence to test this hypothesis.

The variability of the honeycomb pattern (in particular, its ranging from somewhat irregular radial ridges to honeycomb 'cells', even in the same individual) is consistent with a soft-tissue hypothesis.

An immediate cause for the wrinkling of an external epithelium is the contraction of an underlying muscle layer, or the flexing of a portion of the body. This is visible, for instance, in the wrinkles on one's finger knuckles, which all but disappear when the fingers are flexed. This example also demonstrates the basic fact that wrinkles often are perpendicular to the direction of compression of the skin, just like tectonic folds. A difference between skin wrinkles and the honeycomb pattern of *Protolyellia* is that the former wrinkle inward, while the latter folds outward to form ridges (Figs 1–3). The thickness of subcutaneous layers and the presence of pre-determined wrinkling positions are likely involved in this behaviour. The

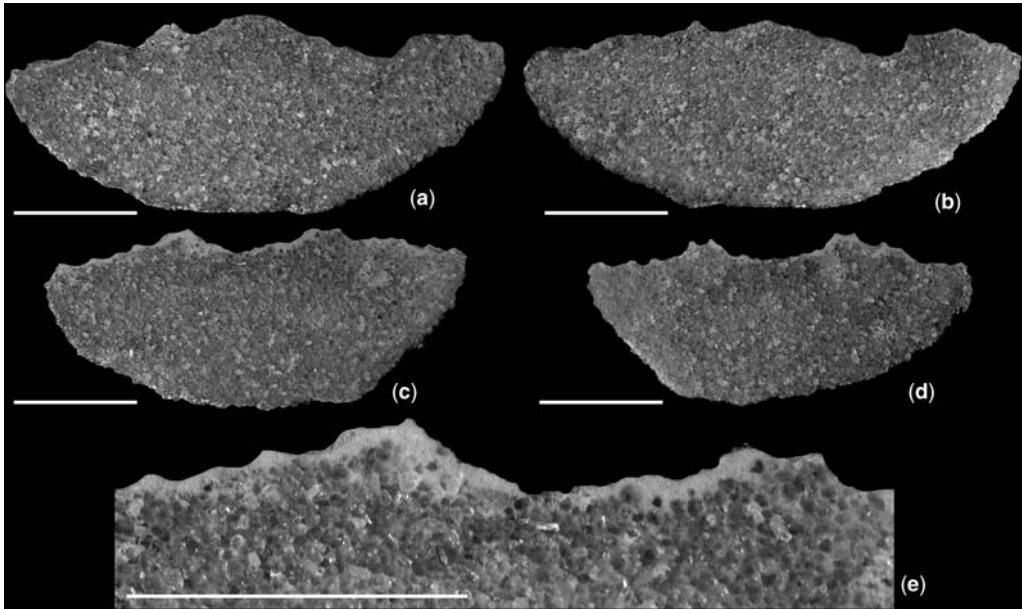


Fig. 4. Transversal sections through a sand-button of *Protolyellia princeps*, Early Cambrian of Sweden. The sections are parallel to each other and range from median (a) to close to the edge (d). The honeycomb layer is visible as a light layer along the top of most sections, including the magnified detail in (e). Scale bars represent 5 mm.

general result (i.e. a shortening of the epithelium in the direction of compression), however, is the same.

In the following discussion, the term ‘paradigm’ is used in a somewhat wider sense than in the paradigm method formalized by Rudwick (1964). In the latter, a paradigm is a conceptual model designed (in an engineering sense) to provide a hypothesized function with maximum efficiency. Herein, a paradigm is an example, or analogue, for the morphology being discussed. This meaning is implicit in the Greek root of the word.

Conceptual paradigm of honeycomb pattern

A conceptual model of epithelium and underlying tissues is shown in Figure 5. In this model, the epithelium is separated from an underlying muscle layer by an intervening layer of connective tissue. Individual collagen fibres in connective tissue are flexible but scarcely elastic (i.e. they bend easily, but their length does not change under tension), and the tissue changes its shape passively due to the fact that the fibres are not normally taut but folded. In actual connective tissue, collagen fibres usually form a three-dimensional latticework, but for the sake of the present discussion, this can be simplified by imagining individual fibres as strings connecting the epithelial and muscle layers and lying within a layer of fluid (Fig. 5a).

In this model, the relaxed muscle layer and epithelium have the same surface (or length, in a two-dimensional model), and collagen fibres are maximally loose in this state (Fig. 5a).

Contraction of the muscle layer reduces its length, causing it to slide underneath the epithelium. As a result, the collagen fibres gradually straighten, until they prevent further reciprocal sliding of the two layers when tightened (left and right extremities of Fig. 5b). At this stage, the epithelium is still unaffected. Further contraction of the muscle layer (Fig. 5c) must result in the formation of an epithelial fold bulging outward. This fold can rise until the collagen fibres underneath its mid-line tighten (Fig. 5c). From this moment onward, further contraction of the muscle causes new folds to appear among existing ones. As mentioned above, whether the epithelium folds outward or inward may depend on several factors. In the present model, folding inward is prevented by the low thickness of the connective layer.

Several factors contribute to a self-organizing character of this pattern. Foremost are the length of fibres and the fact that the epithelium, although pliable, tends to remain as flat as possible, and its surface area does not change. Thus, the smallest possible number of wrinkles appears, and each wrinkle grows to its maximum height. The latter is determined by the length of the fibres.

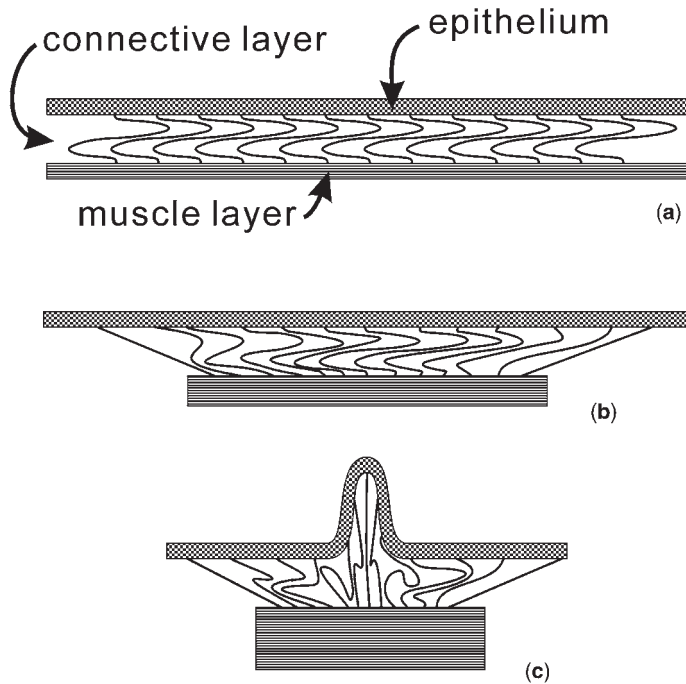


Fig. 5. Conceptual model of epithelial structure. Connective fibres are idealized as ropes joining the muscle to the epithelium. (a) Muscle relaxed. (b) Muscle contracted, tightening the connective fibres at the extremities of the figure. (c) Muscle further contracted, causing an outward wrinkle to form and grow until the fibres located underneath tighten.

In a three-dimensional model, contraction of the muscle layer along one axis produces long parallel folds, perpendicular to the direction of contraction (like on finger knuckles). Contraction along two axes, instead, produces circular domains, or cells, surrounded by a polygonal perimeter of folds. If the properties of this model are homogeneous, cells can be expected to arrange themselves in a hexagonal pattern, which is the two-dimensional packing that best approximates a circular outline of each cell and its lowest ratio of perimeter to area. In practice, small irregularities will cause cells to take somewhat varying sizes and shapes.

The above conceptual paradigm mimics well the basic properties of wrinkles observed on the surface of *Protolyellia* sand-skeletons. However, being qualitative, it cannot be used to visualize a sufficiently large pattern. Implementing this model as a computer program is complex, and requires specialized software. For these reasons, a physical paradigm was developed.

Physical paradigm

A model was built with artificial materials, in order to test whether the properties of the conceptual model and the observed pattern in *Protolyellia* can

be reproduced. Rubber membrane (obtained from party balloons) was used to model both the epithelium and muscle layers. This material is both flexible (although it tends to return to a straight condition, thus reproducing the properties of epithelium) and stretchable. The stretched condition (Fig. 6a) models a relaxed muscle, and allowing a stretched membrane to return to its original size models muscle contraction.

It is difficult to reproduce in an artificial model the properties of connective tissue. Thus, the design of the model was simplified by introducing fixed tie-points between epithelium and muscle. The resulting pattern is not self-organizing, because each tie point occupies a fixed position and determines the centre of a cell, but other basic properties remain similar to those of the conceptual model.

In the physical model, tie-points are implemented as droplets of cyanoacrylate glue deposited on a stretched membrane (Fig. 6b). The epithelial layer (another membrane of the same material, albeit relaxed) is then laid onto the glue (Fig. 6c) and pressed lightly to make it adhere without spreading the glue (which is not always successful).

Once the glue sets, the pins that hold the muscle membrane stretched are repositioned, in order to allow contraction along one axis (Fig. 6d). This

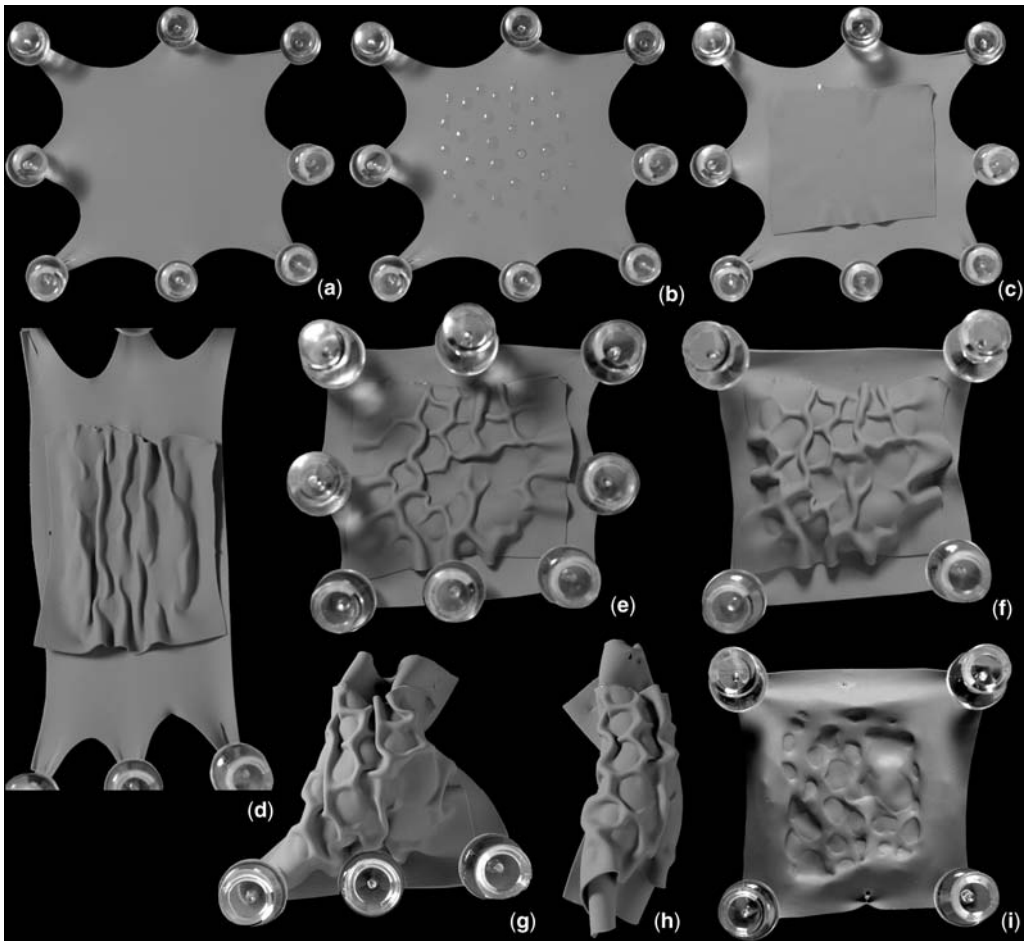


Fig. 6. Physical model of honeycomb pattern. (a) A rubber membrane is stretched. (b) Glue droplets are laid on the membrane. (c) A second, relaxed membrane is placed on top. (d) Relaxing the membrane along one axis causes the formation of straight wrinkles. (e) Relaxing the membrane along both axes causes the formation of a honeycomb pattern of wrinkles. (f–h) Further relaxing the membrane causes it to bulge outward or to roll up. (i) The undersurface of the relaxed membrane displays concave pits in correspondence of the glue droplets.

results in the formation of long, outward bulging folds perpendicular to the direction of contraction, as predicted by the conceptual model. The folds do not run uninterrupted from one edge of the membrane to the opposite one, because the tie-points cannot reposition themselves.

Allowing the membrane to contract to an equal extent along both axes causes the emergence of a distinct polygonal pattern (Fig. 6e), essentially identical to the one observed in *Protolyellia*. Regions in which the glue droplets have spread and touch adjacent ones, of course, cannot fold (mid-right region in Fig. 6e).

Moving the pins closer together causes the double membrane to bulge outward (Fig. 6f). This

is because the epithelial membrane resists folding, thus imparting a stretching force on the nearest surface of the muscle layer. Removing some or all of the pins causes the double membrane to curl itself into an irregular shape (Fig. 6g), or a cylindrical scroll (Fig. 6h).

The inner side of the muscle membrane displays a curious pattern of rounded depressions (Fig. 6i). Such a pattern is not observed in *Protolyellia* sand-buttons, in which the undersurface of the honeycomb layer lies flat against the coarse-grained filling (Fig. 4c–e). A taphonomic explanation for this is discussed below. However, Seilacher (1992; top left of Fig. 6) illustrated a cylindrical object from the Mickwitzia Sandstone of Sweden

displaying such depressions. A reasonable explanation as to why the depressions are on its outer surface is that it represents a fragment of the sub-cylindrical structure of *Protolyellia* (see below) that was broken off by currents (as observed also in the material studied herein, e.g. Figure 2(c–d)) and accidentally turned inside-out like a sock. No comparable situation is observed in the material available for this study.

Inappropriate paradigms

Although the conceptual and physical paradigms discussed above appear appropriate, and reproduce virtually all the observed features of the honeycomb pattern, it is useful to discuss paradigms that are less appropriate, because this provides illuminating insights on features that are essential for the construction of the pattern.

A geometrical construct known as Voronoi (or Dirichlet, or Theissen) tessellation has proven useful in a variety of research fields (e.g. see Boots & Murdoch 1983; <http://www.voronoi.com>, and references therein). A tessellation is a method of covering a plane with adjacent polygons. Therefore, tessellations may help to model features such as the honeycomb pattern of *Protolyellia*. The first step in the construction of a Voronoi tessellation is the selection of a number of points on the plane. Each point will be surrounded by one polygon. Usually (but not necessarily), the distribution of these points is random.

Each point is connected to its neighbours by segments (the method for identifying neighbouring points is crucial, but its description is not relevant here). This stage is known as Delaunay triangulation, because all polygons formed by these segments are triangles (e.g. above references).

For each initial point, lines are drawn through the mid-point of each of its triangulation segments, and perpendicularly to the segment. Each of these lines is truncated where it crosses another line. The result is a convex polygon that surrounds the point. Each side of the polygon is equidistant to the point and to one of its neighbours. The polygons for all initial points cover the entire plane, and constitute the Voronoi tessellation.

Although Voronoi tessellations look superficially similar to the honeycomb pattern of *Protolyellia*, there are important differences if the distribution of the initial points in the Voronoi tessellation is random. Namely, this produces relatively frequent polygons with 3 or 4 sides, polygons with acute angles, and a broad range of polygon sizes (all these features are uncommon or absent in *Protolyellia*). The statistical properties of Voronoi tessellations have been studied extensively (e.g. Boots & Murdoch 1983 and therein; Diggle

1983 and therein; and especially Brakke, unpublished at <http://www.susqu.edu/brakke/aux/downloads/papers/200.pdf> [accessed in 2006], and other reports on the same site), but their discussion is outside the scope of this paper. Suffice it to say that the honeycomb pattern of *Protolyellia* can be approximated by a Voronoi tessellation (with the exception of important details, like the presence of occasional non-convex polygons in the former) only if the initial set of points is non-random. This implies that the wrinkle pattern itself in *Protolyellia* is self-organizing, or that the initial points around which it develops are the result of a self-organizing, or otherwise non-random, pattern.

Another inappropriate paradigm is the wrinkle pattern on the surface of a type of rubber-coated gloves (Fig. 7). This pattern, desirable because it enhances the grip on slippery objects, is self-organizing, and arises when liquid rubber coating a cloth glove begins to solidify. This is because the surface of the rubber solidifies first, and expands while doing so. The increase in surface area forces the outer layer to wrinkle. However, this layer is floating on top of still liquid rubber, and therefore its position relative to the cloth substrate is essentially unconstrained. Thus, wrinkles are free to lengthen and change direction. The result is a pattern of wrinkles that meander in order to continue to grow while avoiding each other, and do not form polygons. This model is inappropriate for *Protolyellia* because it does not include the equivalent of a layer of connective tissue between epithelium and muscle, which is essential to the fabrication of the *Protolyellia* pattern. Other types of patterns on rubber gloves are produced by different, non-self-organizing processes (e.g. moulding) and therefore are not relevant to the present discussion.

Mud-cracks and the columnar fracturing of basalt are also relevant in this context. These patterns are self-organizing, and result from the decrease in volume of a material. If the material is not free to contract uniformly (e.g. contraction of its interior is prevented by a slower loss of humidity or heat), a stress (i.e. a force) is generated within the material. The resulting strain (i.e. change in shape and/or size) of the material causes incipient fractures. Each fracture cancels part of the stress in its immediate neighbourhood and in a direction perpendicular to the crack, thus preventing the formation of subparallel fractures in its vicinity. Therefore, fractures appear at relatively constant reciprocal distances and angles. Because of these characteristics, the resulting pattern is polygonal and often has a clear tendency toward uniform sizes and hexagonal shapes of the cells. In these respects, and in resulting from contraction, mud-cracks and columnar basalt are partly

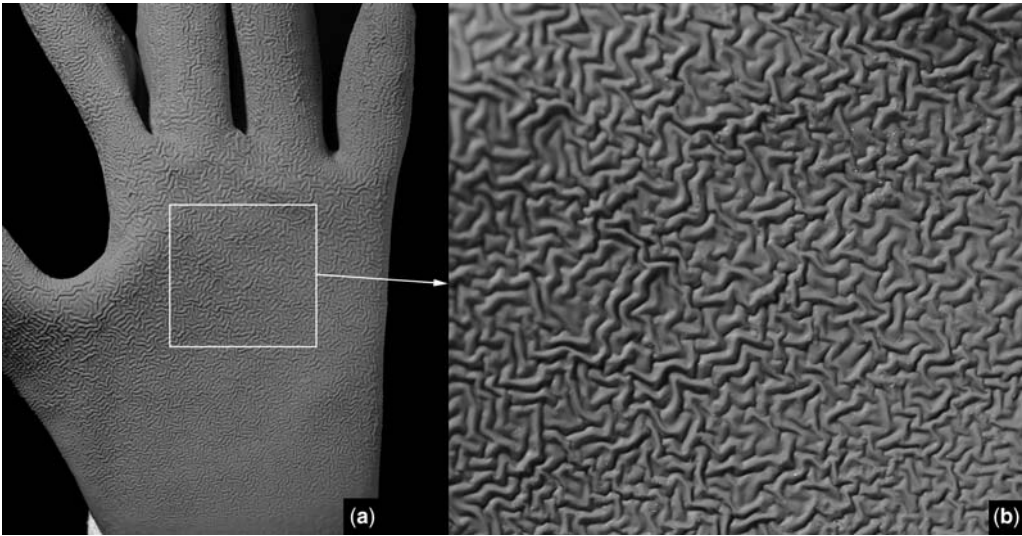


Fig. 7. Inappropriate paradigm for honeycomb pattern. In this rubber-coated glove, the surface wrinkles while solidifying and expanding. Since the solid surface floats on liquid rubber and an equivalent of the connective tissue is absent, wrinkles are free to meander in order to avoid each other, instead of being constrained into a honeycomb pattern.

appropriate paradigms to the *Protolyellia* pattern. They obviously differ in being patterns of cracks, rather than folds, but this is not of fundamental importance. Folds in the *Protolyellia* pattern act in a very similar way to locally reduce stress and prevent the formation of nearby parallel folds.

Significance of the honeycomb pattern

In order to bring the reconstruction of *Protolyellia* one step further, it must be considered that the wrinkled epithelium distends to occupy a much larger surface. Thus, the distended epithelium formed a tube structure both longer and wider than the structure observed on the dorsal surface of *Protolyellia* sand-buttons. This is only possible if the epithelium did not adhere onto the sand-button, and instead extended upwards as a subcylindrical column. This reconstruction differs from Seilacher's (1992) in the fact that the wrinkle pattern is not an internal feature imprinted on the dorsal surface of the sand skeleton, but the surface of an external epithelium. Aside from this, however, the general shape of the organism is essentially the same in both reconstructions, i.e. a suspension-feeding, actinian-like subcylindrical organism with a button of cemented sand located at its bottom and covered by soft tissues.

Around the periphery of the *Protolyellia* skeleton, where the wrinkled epithelium was attached to the tissues containing the skeleton, the wrinkle pattern often consists of radial wrinkles. This indicates that

the tube of soft tissue, in this region, contracted in perimeter, but not lengthwise. The extent of this region of epithelium carrying radial wrinkles varies among individuals. It tends to be wider in morphs with a conical or convex upper surface, and reduced or absent in those with a flat upper surface. This also is consistent with the present model, in that a flat upper surface allows the overlaying soft tissues to slide freely toward the perimeter of the sand button, while a conical or convex surface hinders this movement, thus allowing a circular contraction around the perimeter, but not sliding of the epithelium in a centrifugal direction. Variability in this pattern may also indicate that the sand-skeleton varied in relative diameter (in addition to shape), with respect to the size of the organism.

This reconstruction is supported by the finding of cylindrical or conical portions of wrinkled epithelium preserved without a sand-skeleton (Fig. 2c–d). Presumably, these specimens represent fragments of the soft-tissue column broken off from the rest of the organism. The specimen of Figure 2 (c–d) displays polygonal cells that are significantly compressed in the axial direction of the column. This implies that the column contracted along its axis to a larger extent than along its perimeter.

This specimen also displays coarser polygonal cells on its widest portion (i.e. a lower number of wrinkles per surface unit). This indicates that its narrowest portion is contracted to a larger extent, and, therefore, that the distended shape of this fragment was either cylindrical, or slightly conical.

A qualitative assessment is that its distended size may have been approximately 1.5–2 times its present diameter, and 3–5 times its present length. Thus, this portion of the organism (and therefore the organism as a whole) was significantly taller than its diameter when fully distended.

Construction of the sand-button

The faint concentric fabric in the sand-button of *Protolyellia* indicates that it accreted by the addition of clasts on its lower surface. Seilacher (1992) proposed that clasts entered the digestive system, and subsequently were phagocytised and transported to the lower surface of the sand-button. According to this reconstruction, the sand-button was contained between ectoderm and endoderm (Fig. 8a).

As an alternative, it is also possible that the internal cavity occupied by the sand-button was in direct communication with the cavity of the digestive system, located in the column immediately above the centre of the sand-button (Fig. 8b). In fact, several specimens of *Protolyellia* display a central boss of variable size on the upper surface, which may represent sediment filling to a varying extent the connection between the two cavities. In this model, clasts could have been carried to the ventral surface of the sand-button by ciliary movements of the epithelium lining the button cavity. This was feasible because the honeycomb layer,

in life, was not attached to the upper surface of the button (see also below).

This model also provides an evolutionary pathway leading to a sand-skeleton. The accidental ingestion of sediment may have started this process. Sediment at the bottom of the digestive system, although reducing its efficiency, provided a selective advantage to the organism by stabilizing it (see below for an explanation of the pressing need for stabilization in *Protolyellia*), and the ingestion of sediment became a selected-for behaviour. Initially, sediment accumulated at the bottom of the digestive cavity, and was cemented in place to prevent it from interfering with the digestive functions and from being expelled. Subsequently, a diverticulum evolved at the bottom of the digestive system, with the specific function of containing sediment. In fact, the sand-skeleton of *Spatangopsis*, a coeval psammocoral, filled a central cavity in the organism and was in permanent connection with the external environment through slits in the upper surface of the organism (pers. obs. and Seilacher 1992). This genus may have turned its original digestive system in its entirety into a container for the sand-skeleton, and presumably performed its digestive functions in another way.

Taphonomy

As suggested by Seilacher (1992), *Protolyellia* was likely to have been preserved by quick burial of

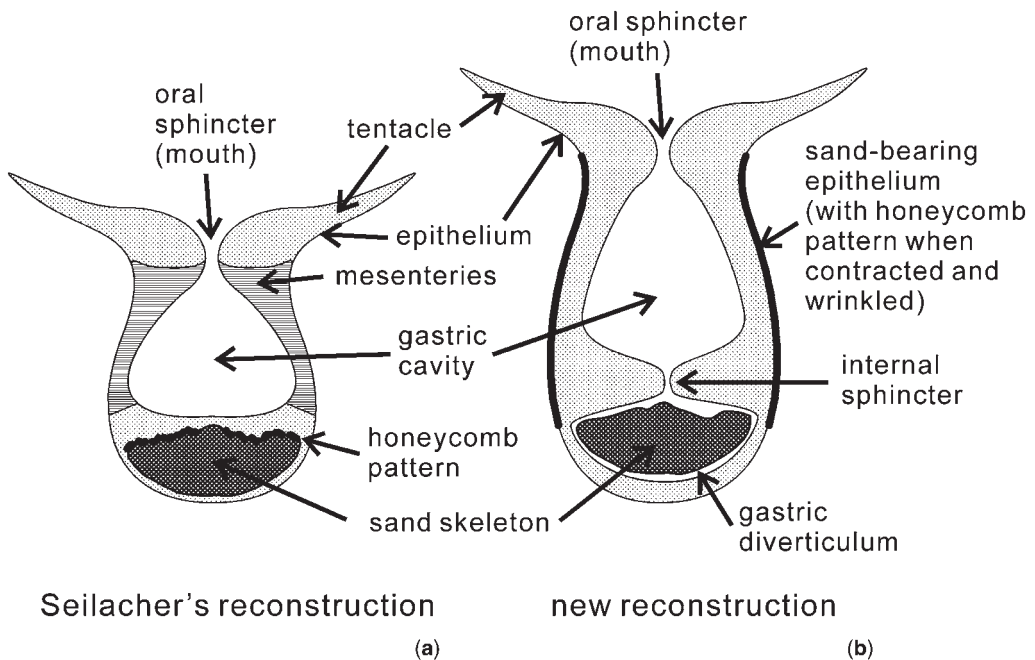


Fig. 8. Reconstruction of anatomy of *Protolyellia* as envisioned by (a) Seilacher (1992) and (b) this paper.

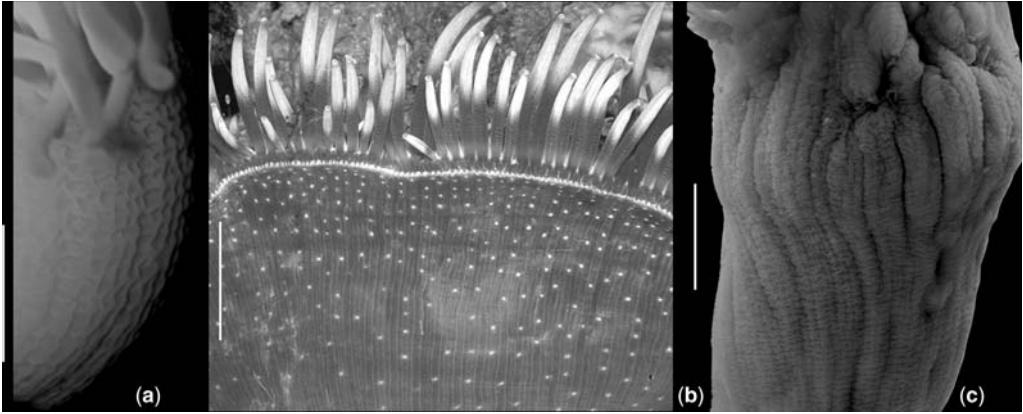


Fig. 9. Wrinkles on the epithelium of living Recent actinians: (a) *Anthenopsis koseriensis* Klunzinger; (b) *Halcurias levis* (Uchida) and preserved pennatulid stalk; (c) *Pteroeides esperi* Herklots). In all three cases, longitudinal mesenteries attached to the inside of the body-wall constrain wrinkles and other surface relief into a pattern with a clear longitudinal alignment. All specimens from the Seto Marine Biology Laboratory. Scale bars represent 10 mm.

living individuals, which allowed the sand-skeleton to keep its original shape, while the soft tissues quickly decomposed afterwards. The preservation mode as envisioned by Seilacher is illustrated in Fig. 10(a–c).

The slab in Fig. 1(a) shows several specimens of *Protolyellia* buried at slightly different levels in a bedding plane. This may represent a storm accumulation or the original life position. An interesting feature of this slab is that two individuals (central part of slab) are flanked, on their left sides, by elongated sheets carrying the distinctive honey-comb pattern. These fragments are of approximately the right size, shape and subparallel

orientation to constitute the remains of a subcylindrical, or stalk-like part of the same individuals, felled onto the sediment by a sudden influx of water-laden sediment, in much the same way as frond-bearing Ediacaran organisms with stalks and holdfasts (e.g. Seilacher 1992, Fig. 2). Contraction of the muscle layer as a result of burial likely snapped these structures away at their ‘necks’ on the sand-button.

Seilacher (1992) described the sand-skeletons of *Protolyellia* and other psammocorals as cemented with an organic matrix that decomposed shortly after burial, together with the soft tissues. As proof of this, he cited the frequent occurrence of

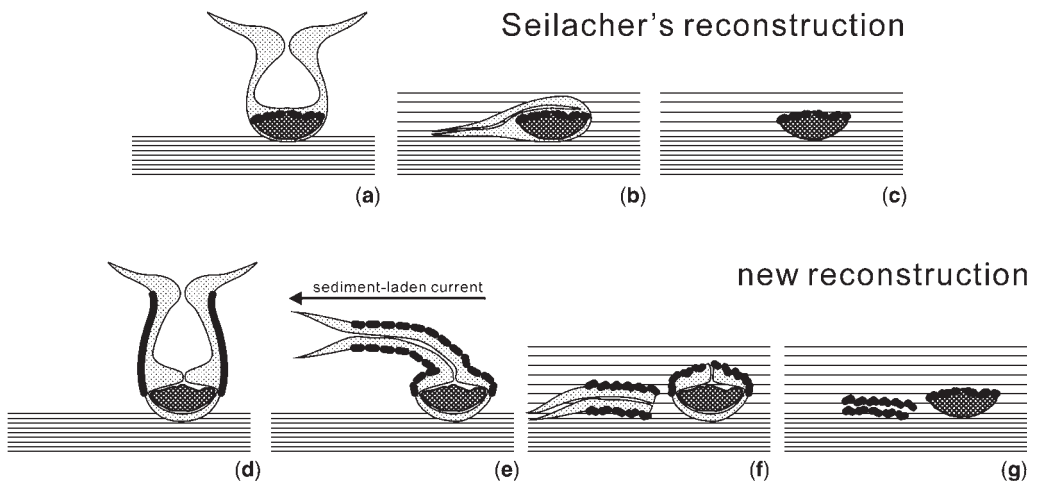


Fig. 10. Preservation mechanism of *Protolyellia*; (a–c) as envisioned by Seilacher (1992) and (d–g) reconstructed in this paper. See the text for details.

trace fossils penetrating sand-skeletons (e.g. Fig. 1i, 2e). In fact, some of the available specimens (Fig. 1i) show galleries that follow the lower surface of the sand-skeleton. This could indicate a foraging behaviour by infaunal organisms or microbes feeding on the decomposed soft tissues that lined this region of the skeleton.

The taphonomy of *Protolyellia* is relevant also in the context of preservation of the honeycomb pattern. The soft tissues of *Protolyellia* (in particular, its suspension-feeding apparatus) are not preserved. On the other hand, the honeycomb pattern is interpreted herein as epithelial wrinkling, i.e. a soft-tissue feature. Thus, it is crucial to the present interpretation to explain why this soft-tissue feature alone is preserved.

The fine-grained particles constituting the wrinkled layer of *Protolyellia* are siliciclasts, like the coarser clasts constituting the sand skeleton, and not the products of biological secretion. Thus, they must have been a layer of sand adhering to the outer surface of the external epithelium, or embedded in it. After burial, decomposition of the epithelium and underlying soft tissues caused the surrounding sediment to compact into the space they occupied, pushing ahead of itself the epithelial sand grains. These grains retained the approximate external relief of the epithelium, while nothing was left of the other soft tissues. Thus, the honeycomb layer is not, properly speaking, a preserved soft tissue, but its imprint.

The typical preservation of *Protolyellia* sand-buttons with honeycomb pattern on their upper surfaces requires three steps:

- (1) Sudden burial of the organism, accompanied by contraction of its column (Fig. 10e). The latter may be partly snapped away by the intruding water, and/or broken off when contracting while immobilised under the weight of the sediment (Fig. 10f). Part of the wrinkled epithelium of the subcylindrical portion likely contracted to a position near the surface of the sand-button, but separated from it by soft tissues (Fig. 10f).
- (2) Decomposition of the soft parts allowed the sediment to compact around the remains of the organism. This caused the layer of fine sand originally located on or in the epithelium, still bearing the original relief of the wrinkle pattern, to be pasted onto the upper surface of the sand-button (Fig. 10(g)).
- (3) Some mixing of the fine and coarse clasts of the two layers, no longer separated by soft tissues or cemented by an organic matrix, could have taken place at the interface between the two layers (Fig. 4e).

Affinities and evolution of *Protolyellia*

All evidence points to *Protolyellia* being a sessile soft-bottom organism, with a weighted basal disc and a columnar body bearing a suspension-feeding structure. Seilacher (1992) regarded *Protolyellia*, together with *Spatangopsis*, as a representative of the Psammocorallia (in the sense of adaptiveness and body-plan, but apparently also taxonomically). An assessment of possible phylogenetic affinities of *Protolyellia* with *Spatangopsis* presupposes a re-examination of the latter taxon, and lies outside the scope of this paper.

While the material observed herein dates from the Early Cambrian, it is possible that the stratigraphic range of *Protolyellia* extends both to earlier and subsequent times (see also Seilacher & Goldring 1996). However, a reassessment of several discoidal fossils is necessary in order to settle this question. A few discoidal fossils of similar age are not related to *Protolyellia*. These include *Eldonia* (Chen *et al.* 1995), *Stellosomites*, *Pararotadiscus* (Zhu *et al.* 2002) and *Rotadiscus* (Dzik *et al.* 1997). These differ from *Protolyellia* in the presence of a U-shaped digestive tract contained within the disc. If such an organ had been present in *Protolyellia* and filled with sediment, its potential for preservation between wrinkled layer and sand-skeleton would have been excellent. Such a structure, however, is absent in *Protolyellia*.

The interpretation of *Protolyellia* as a primitive actinian possessing an internal sand-skeleton (Seilacher 1992) is compatible with the present evidence, and remains in fact the most conservative interpretation. Consequently, this is the morphology chosen for the reconstruction of *Protolyellia* also herein (Fig. 8). Barring the finding of exceptional specimens of *Protolyellia* with additional soft parts (including crucial ones, such as a feeding apparatus), this situation is likely to persist. However, the lack of any trace of mesenteries in the shape of the sand-skeleton and in the wrinkle-pattern of the epithelium raises the question of whether *Protolyellia* did possess the above features. This must be weighted-in when performing an analysis of affinities.

A mesenterial organization is reflected in a prominent longitudinal component of striation and wrinkle pattern of the epithelium of the column of many Recent actinians (Fig. 9a–b), soft coral polyps and even the stalk of pennatulids (Fig. 9c). Among these examples, Figure 9(a) is closest to the wrinkle morphology of *Protolyellia*, but in the Recent example, wrinkles are arranged in longitudinal and transversal rows, and have a subrectangular shape.

If present, mesenterial muscles would likely have produced a recognizable longitudinal pattern

on the epithelium of *Protolyellia*. Although radial wrinkles are observed on *Protolyellia* sand-buttons, they are usually restricted to its periphery, while mesenteries can be expected to run along the entire length of the column. In addition, a longitudinal arrangement of wrinkles is conspicuously absent in isolated fragments bearing the honeycomb pattern. Thus, if *Protolyellia* was an actinian, it probably lacked mesenteries and was either a very primitive form, or a member of an aberrant group, and only distantly related to Recent forms. In this context, Early Cambrian actinian-like cnidarians from the Chengjiang biota (Hou *et al.* 2005) do possess both mesenteries and longitudinal furrows on the column, so these features were already well established at the time in the lineage that likely led to Recent actinians.

As a cautionary note on the affinities of *Protolyellia*, the evidence does not exclude that *Protolyellia* could have been an organism very different from cnidarians, and more similar to Ediacaran frond-bearing forms. In fact, very rare fragments of structures with an apparent quilted structure, comparable in organization to typical Ediacaran forms, do occur in the same beds with *Protolyellia* (pers. obs. and e.g. Seilacher 1992, Fig. 6). With lack of evidence to the contrary, these could conceivably be parts of a suspension-feeding apparatus of *Protolyellia* (as well as entirely distinct organisms).

From the point of view of adaptiveness, it could be asked why *Protolyellia* and other psammocorals, like *Spatangopsis*, evolved sand-skeletons. Seilacher (1992) proposed that this was a way to bypass the limitations imposed by the lack of a rigid skeleton, and represented an early experiment with novel body-plans. An obvious trade-off of this body-plan is that it provided passive stabilization by weighting down the organism and favouring its passive righting by water movements, but at the same time restricted or prevented active movement of the basal disc.

A sand-skeleton provided the above advantages. However, in the Ediacaran period, organisms with large fronds connected to long and slender stalks were able to attach to a soft substrate by using flat, discoidal holdfasts that were neither sand-filled nor deeply buried within the substrate. In several instances, not even the sudden in-rush of sediment-laden water was sufficient to detach the holdfast from the substrate (e.g. see Seilacher 1992, Fig. 2).

The answer to why superficially anchored holdfasts sufficed in the Ediacaran, whereas Early Cambrian organisms required a massively heavy structure to perform the same function, likely lies in the changing nature of the substrate. As discussed by MacGabhann *et al.* (2007), the top layer of

Ediacaran soft sediments typically was cemented by a microbial mat. Thus, neither burying a holdfast under the sediment surface, nor weighting it down was necessary to enhance its performance. On the other hand, the sedimentological signatures of thin microbial mats, almost ubiquitous in the Ediacaran, became scarce after the beginning of the Palaeozoic.

Consequently, the weighted sand-skeleton of psammocorals may reflect an attempt to continue an old mode of life in spite of the changing properties of soft substrates. Rather than being an unsuccessful experiment with early body plans, *Protolyellia* probably should be regarded as a hardy Ediacaran survivor that evolved novel strategies for coping with a changed world.

Conclusions

A new reconstruction of *Protolyellia* (psammocoral) from the Mickwitzia Sandstone, Early Cambrian of south-central Sweden, is proposed. The relief pattern usually present on the upper surface of *Protolyellia* sand-buttons is interpreted as the result of wrinkling of a pliable epithelium attached to a subepithelial muscle layer by an intermediate connective tissue. Conceptual and physical modeling duplicate all essential features of the pattern observed in *Protolyellia*. A honeycomb pattern of outward projecting wrinkles delimiting flat 'cells' was produced by contraction of the muscle layer along perpendicular axes, whereas a pattern of parallel wrinkles resulted from contraction along a single axis.

The relief pattern in *Protolyellia* is not a preserved soft tissue, but an imprint of the relief of the outer surface of the epithelium preserved as a layer of fine-grained siliciclasts. These non-biogenic clasts adhered to, or were embedded in, the epithelium. This explains why there is no trace of other soft-tissue features, like a suspension-feeding apparatus.

Numerous fragments of an originally flexible structure bearing the same honeycomb pattern are found in *Protolyellia*-bearing beds. These fragments have cylindrical, rolled-up or irregularly convex shapes, sometimes deformed by adjacent pebbles. These patterned objects are interpreted as shreds of the epithelium of *Protolyellia*.

A few flat, sheet-like fragments from the same beds display a very faint honeycomb pattern on parts of their surfaces. They are interpreted as relaxed and/or decomposing shreds of *Protolyellia* epithelium.

The sand-bearing epithelium and underlying layers formed a subcylindrical pipe attached around the periphery of the sand-skeleton and

extending upwards. In its relaxed state, the organism was significantly taller than wide. Contraction of the subepithelial muscles following burial by sediment caused the pipe to diminish in length and diameter, and its lower portion to be drawn close to the sand-button. Contraction of the muscles also caused the epithelium to wrinkle. Decomposition of the soft parts shortly after burial resulted in surrounding sediment compacting around the remaining sand-button of the organism, thus pasting the fine-grained sand of the wrinkled layer directly onto the upper surface of the sand-button. This produced the typical preservational mode of *Protolyellia*.

Unlike an earlier interpretation of the honeycomb pattern as an internal feature (i.e. a part of the sand-skeleton) the present reconstruction explains why fragments bearing the honeycomb pattern are frequently found isolated. A few such fragments are preserved adjacent to sand-skeletons in an orientation suggesting that the tubular structure was felled sideways by sediment-laden currents that suddenly buried the organism.

The wrinkle pattern of *Protolyellia* differs from those observed on the epithelium of Recent cnidarians, which display a strong axial component because of the presence of underlying mesenteries. This suggests that *Protolyellia* did not possess a mesenterial organization. While affinities with cnidarians remain a reasonable hypothesis, this points to *Protolyellia* being further removed from modern actinians than previously assumed. However, barring the finding of exceptionally-preserved material with the suspension-feeding apparatus or other key features, the evidence is also insufficient to exclude, as an alternative, affinities with Ediacaran frond-bearing forms.

Ediacaran suspension-feeding organisms with fronds and stalks possessed discoidal holdfasts that were neither weighted by sand, nor deeply buried. The evolution of sand-skeletons in *Protolyellia* (initially as a gastric accumulation of sediment, and later likely placed in a specialized gastric diverticulum) can be explained by the changing nature of soft substrates at the Proterozoic–Palaeozoic border. The ubiquitous, thin microbial mats, which consolidated the uppermost sediment layer throughout the Ediacaran, became scarce in the early Palaeozoic, forcing new anchoring strategies to evolve. The image of *Protolyellia* as a failed early experiment with alternative body-plans probably should be replaced by that of a hardy Ediacaran survivor evolving novel adaptations to the conditions of a changed world.

Research fellowships by the Japan Society for the Promotion of Science and the Swedish Royal Academy of Science at the Kyoto University Museum, Japan, are

gratefully acknowledged. Thanks are due also to the Department of Palaeozoology, Swedish Museum of Natural History, Stockholm, Sweden, for access to the collections, loan of specimens and permission to perform sectioning on this material. Dr S. Kubota facilitated access to living coelenterates at Seto Marine Biological Laboratory, Wakayama, Japan, and identified the specimens displayed in Figure 8. Finally, this study would not have been possible without P. Vickers-Rich, who practically forced me to look at Ediacaran and Early Cambrian organisms and to realize that the methods of functional analysis developed for the study of later, more complex organisms and their skeletal parts are just as applicable to these early forms. This paper was developed as a part of UNESCO IGCP 493. Thanks are also due to the two reviewers, A. Seilacher and S. Jensen.

References

- BOOTS, B. N. & MURDOCH, D. J. 1983. The spatial arrangement of random Voronoi polygons. *Computers and Geoscience*, **9**, 51–365.
- CHEN, J.-Y., ZHU, M.-Y. & ZHOU, G.-Q. 1995. The Early Cambrian discoidal metazoan *Eldonia* from the Chengjiang Lagerstätte. *Acta Palaeontologica Polonica*, **40**, 13–244.
- DIGGLE, P. J. 1983. *Statistical Analysis of Spatial Point Patterns*. Academic Press, New York.
- DZIK, J., ZHAO, Y.-L. & ZHU, M.-Y. 1997. Mode of life of the Middle Cambrian eldoninoid lophophorate *Rotadiscus*. *Palaeontology*, **40**, 385–396.
- HOU, X.-G., STANLEY, JR G. D., ZHAO, J. & MA, X.-Y. 2005. Cambrian anemones with preserved soft tissue from the Chengjiang biota, China. *Lethaia*, **38**, 193–203.
- JENSEN, S. 1997. Trace fossils of the Lower Cambrian Mickwitzia sandstone, south-central Sweden. *Fossils and Strata*, **42**, 1–110.
- MACGABHANN, B. A., MUWAY, J. & NICHOLAS, C. 2007. *Ediacara booleyi*: weeded from the Garden of Ediacara? In: VICKERS-RICH, P. & KOMAROWER, P. (eds) *The Rise and Fall of the Ediacaran Biota*. Geological Society, London, Special Publications, **286**, 277–296.
- RUDWICK, M. J. S. 1964. The inference of function from structure in fossils. *British Journal for the Philosophy of Science*, **15**, 27–40.
- SEILACHER, A. 1992. Vendobionta and Psammocorallia: lost constructions of Precambrian evolution. *Journal of the Geological Society, London*, **149**, 607–613.
- SEILACHER, A. & GOLDRING, R. 1996. Class Psammocorallia (Coelenterata, Vendian—Ordovician): recognition, systematics, and distribution. *Geologiska Föreningens i Stockholm Förhandlingar*, **118**, 207–216.
- TORELL, O. 1870. Petrificata Suecana Formationis Cambriacae. *Lunds Universitets* **6**, Arsskrift, Afdelning, **2**, 1–14.
- ZHU, M.-Y., ZHAO, Y.-L. & CHEN, J.-Y. 2002. Revision of the Cambrian discoidal animals *Stellosomites eumorphus* and *Pararotadiscus guizhouensis* from South China. *Geobios*, **35**, 165–185.

Poriferan paraphyly and its implications for Precambrian palaeobiology

E. A. SPERLING¹, D. PISANI² & K. J. PETERSON³

¹*Department of Geology and Geophysics, Yale University, P.O. Box 208109, New Haven, CT 06520, USA*

²*Laboratory of Evolutionary Biology, The National University of Ireland, Maynooth, County Kildare, Ireland*

³*Department of Biological Sciences, Dartmouth College, Hanover, NH 03755, USA (e-mail: kevin.peterson@dartmouth.edu)*

Abstract: Well-supported molecular phylogenies, combined with knowledge of modern biology, can lead to new inferences about the sequence of character acquisition in early animal evolution, the taxonomic affinity of enigmatic Precambrian and Cambrian fossils, and the Proterozoic Earth system in general. In this paper we demonstrate, in accordance with previous molecular studies, that sponges are paraphyletic, and that calcisponges are more closely related to eumetazoans than they are to demosponges. In addition, our Bayesian analysis finds the Homoscleromorpha, previously grouped with the demosponges, to be even more closely related to eumetazoans than are the calcisponges. Hence there may be at least three separate extant 'poriferan' lineages, each with their own unique skeleton. Because spiculation is convergent within 'Porifera', differences between skeletonization processes in enigmatic Cambrian taxa such as *Chancelloria* and modern sponges does not mean that these Problematica are not organized around a poriferan body plan, namely a benthic, sessile microsuspension feeding organism. The shift from the anoxic and sulphidic deep ocean that characterized the mid-Proterozoic to the well-ventilated Phanerozoic ocean occurs before the evolution of macrozooplankton and nekton, and thus cannot have been caused by the advent of faecal pellets. However, the evolution and ecological dominance of sponges during this time interval provides both a mechanism for the long-term generation of isotopically-light CO₂ that would be recorded in carbon isotopic excursions such as the 'Shuram' event, and an alternative mechanism for the drawdown and sequestration of dissolved organic carbon within the sediment.

The 'explosion' of animals and protist groups near the base of the Cambrian remains one of the most complex and important questions in historical biology. The heart of the debate is focused on timing: Is the fossil record a faithful chronicle of events, with the origin of clades closely predating their appearance, or does the event simply record the appearance of burrowing and biomineralizing organisms whose stocks diverged deep in the Precambrian (Runnegar 1982)? The ancestors of the Cambrian metazoan fauna undoubtedly existed in the Precambrian, and the search for Precambrian ancestors has focused primarily on the soft-bodied Ediacaran faunas of Newfoundland, South Australia, Russia and Namibia (Gehling 1991; Narbonne 1998, 2005). Although these faunas have traditionally been interpreted through direct morphological comparisons with the modern biota, interpretations need to be more tightly constrained by insights gained from both phylogenetic studies of the Metazoa and ecological considerations of modern taxa.

Although a clearer view of triploblast systematics is emerging, the relationships at the base of the

metazoan tree are still largely unknown (Eernisse & Peterson 2004; Halanych 2004). Studies using different markers place sponges, placozoans, cnidarians and ctenophores in almost every conceivable relationship except one: monophyly—all studies (except for some early analyses with limited taxon sampling) unequivocally agree that ctenophores and cnidarians are more closely related to triploblasts than they are to sponges. Recent studies using protein-coding genes from mitochondrial genomes (e.g. Wang and Lavrov 2007, and references therein) recover 'lower' Metazoa as monophyletic, although the authors attribute this to a clear artifact related to rate changes between triploblast and the 'lower' metazoans. Sponges, which are traditionally regarded as the most basal extant metazoans, are always monophyletic in phylogenetic studies based on morphology alone (Zrzavy *et al.* 1998; Peterson & Eernisse 2001). However, analyses of ribosomal data (Cavalier-Smith *et al.* 1996; Collins 1998; Adams *et al.* 1999; Borchiellini *et al.* 2001; Medina *et al.* 2001; Cavalier-Smith & Chao 2003; Manuel *et al.* 2003; Wallberg *et al.* 2004) as well as protein

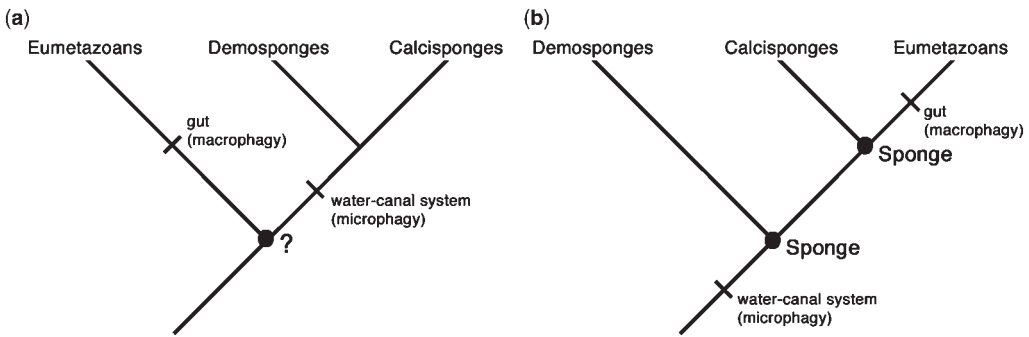


Fig. 1. The importance of paraphyly: if the eumetazoans and poriferans both represent monophyletic groups, each with a unique trophic mode, it is not possible to polarize feeding strategy, given that the outgroups are all non-metazoan (a). However, if calcisponges are more closely related to eumetazoans than demosponges, polarity can be established (b), suggesting the water-canal system is primitive and the gut is derived.

sequence data (Kruse *et al.* 1998; Peterson & Butterfield 2005), suggested that sponges are paraphyletic, with calcisponges more closely related to eumetazoans than to demosponges. The demonstration of poriferan paraphyly represents one of the most important insights that molecular systematics has given palaeontology because paraphyly means that former sponge synapomorphies (shared derived characters, e.g. water canal system [WCS]) are metazoan symplesiomorphies (shared ancestral characters) (Peterson & Butterfield 2005; Peterson *et al.* 2005). Poriferan paraphyly then gives insight into the biology and ecology of the last common ancestor of all living metazoans, because we can now state with confidence that the earliest crown-group metazoans were benthic, sessile, microsuspension feeders that extracted dissolved organic matter and picoplankton out of sea water using the WCS (Fig. 1).

Nonetheless, the importance of poriferan paraphyly extends beyond these palaeoecological insights, as it sheds light on interpreting the phylogenetic affinities of Ediacaran organisms, as well as Cambrian 'Problematica' including *Chancelloria*. In addition, sponges provide an alternative mechanism for the oxidation of the Proterozoic ocean. Here, sponge paraphyly is explored by analysing with Bayesian phylogenetics a concatenated data set consisting of seven protein sequences from 30 eumetazoan and 12 sponge taxa including one homoscleromorph. Paraphyly is again found, with the interesting result that the homoscleromorph *Oscarella* is more closely related to the eumetazoans (cnidarians and triploblasts) than it is to any other sponge lineage. We then explore the palaeobiological implications of this result and argue that poriferan paraphyly gives insight into several disparate areas of Precambrian and Cambrian palaeobiology.

Material and methods

Although the Peterson & Butterfield (2005) tree contained several exemplars of both demosponges and calcisponges, the taxonomic coverage within these groups was not widespread—the two included calcisponges group closely within the Calcarea (Manuel *et al.* 2003), and the three demosponges group in the G4 clade of Borchellini *et al.* (2004: this study found four main demosponge clades, which they labelled G1–G4). Although we were unable to obtain any calcinean calcisponges, we were able to analyse two G1 sponges, *Darwinella mulleri* and *Dysidea camera*, the G2 *Chondria* sp., as well as the putative G3 sponge *Xestospongia* sp. (putative because, although not analysed by Borchellini *et al.* 2004, it groups with the G3 *Haliclona* in Nichols 2005) and the G4 sponge *Halichondria* sp. All were purchased from Gulf Specimens Marine Laboratory (Panacea, Florida); except for *Halichondria*, which was purchased from the Marine Biological Laboratory (Woods Hole, MA). Total RNA from these taxa was prepared from live animals by using a one-step TRIzol method (GIBCO-BRL). Total RNA from the homoscleromorph *Oscarella carmela* was kindly provided by Dr Scott Nichols (University of California, Berkeley). cDNA synthesis was performed with RETROSCRIPT (Ambion, Austin, TX) using 1–2 µg of total RNA.

Partial sequences of seven nuclear-encoded genes were PCR amplified, cloned, and sequenced using standard techniques: aldolase (ALD), ATP synthase beta chain (ATPB), catalase (CAT), elongation factor 1-alpha (EF1a), methionine adenosyltransferase (MAT), phosphofructokinase (PFK), and triose-phosphate isomerase (TPI). Primer sequences are as follows (5'-3'): ALDf: GGGAARGGNATH YTNGCNGC; ALDr: GGGGTNACCATRITNG

GYTT; ATPBf: GTNGAYGT NCARTTYGAYGA; ATPBr: NCCNACCATRTARAANGC; CATf: GAYGARATGDSNCAITTYGAYMG; CATr: CCNARNCKRTGNMDRTGNGTRTC; EF1Af: AAYA TYGTNGTNTATYGGNCAYGT; EF1Ar: ACNGC NACNGTYTGNCACATRTC; MATf: GGNGARG GNCAYCCNGAYAA; MATr: CCNGGNCKIARRTCRAARTT; PFKf: GAYWSNCARGGNA TGAAYGC; PFKr: CCRCARTGNCKNCCCATN ACYTC; TPIf: GGNGGNAAYTGGAARATGAYGG; TPIr: GCNCCNCCNACIARRAANCC. Gene-specific primers (50 pmol) and 2 μ L of cDNA, plus the *Amplitaq* system (using the 10 \times buffer with 15 mM MgCl₂, Applied Biosystems) were mixed and used in a touchdown style PCR. The first touchdown (TD 1) procedure started the annealing temperature at 52°C and then after two cycles dropped one degree for another two cycles, all the way to 40°C, followed by a final ten cycles at 52°C. A second touchdown procedure using 35 cycles at 52°C using 1 μ L of the TD1 as template followed if the genes of interest were not amplified during TD1. PCR fragments of the predicted sizes were excised, purified (Qiagen, Valencia, CA), ligated at 16°C overnight into the pGEM-T-Easy vector according to manufacturer's instructions (Promega, Madison, WI), and electroporated into DH10B cells. Clones containing the correct insert size were sequenced with an ABI373 model sequencer according to manufacturer's instructions (Applied Biosystems, Foster City, CA). We were unable to obtain MAT from *Dysidea* and *Halichondria*, and PFK from *Xestospongia* and *Chondrilla*.

Sequences for the demosponge *Amphimedon queenslandica* (formerly *Reniera*, see Hooper & Van Soest 2006) another putative G3 taxon (again not analysed by Borchiellini *et al.* 2004, but traditionally classified as a chalinid haplosclerid closely related to *Haliclona*), as well as the anthozoan cnidarian *Nematostella vectensis*, the chordates *Branchiostoma floridae* and *Ciona intestinalis*, and the polychaete annelid *Capitella* sp. were downloaded from genomic traces from the NCBI Genbank database. Sequences were edited, translated, and aligned by using MACVECTOR, v. 7.2.3 (Genetics Computer Group). Twelve different sponge lineages plus 30 eumetazoan lineages taken from Peterson *et al.* (2004) and Peterson & Butterfield (2005) and two outgroups were analysed using Bayesian phylogenetics. Bayesian analyses were performed using MrBayes 3.1.2 (Ronquist & Huelsenbeck 2003) under a mixed model, with the parameters of seven unlinked evolutionary models (one for each gene) independently estimated during tree search (including the best fitting amino acid substitution matrix). Two independent runs of four linked MCMC chains

were set up, sampling the chains every 1000 cycles. Convergence was monitored by controlling the standard deviation of the split sequences (Ronquist *et al.* 2005). The results of the two Bayesian runs were summarized by calculating a majority rule consensus of all trees sampled after stationarity was reached.

Results and discussion

Poriferan systematics

A Bayesian analysis was completed for the 12 sponge taxa plus the 30 eumetazoan taxa and the two outgroups (Fig. 2). All expected higher-metazoan relationships (e.g. Metazoa, Eumetazoa, Triploblastica, Protostomia, Ecdysozoa, Spiralia, Deuterostomia, Ambulacraria) (indicated with labelled nodes and the light grey boxes) are recovered, as are the expected internal relationships within phyla (e.g. Cnidaria, Echinodermata, Nemertea, Insecta). The recovery of known external nodes is important in sponge phylogenetics, as hypotheses regarding the phylum are undergoing such flux that there are few internal nodes that can confidently be used as an accuracy check for trees. The posterior probabilities for all nodes are indicated on Figure 2.

The addition of the new sponge taxa does not change the paraphyly of Porifera: calcisponges are more closely related to eumetazoans than they are to demosponges (Fig. 2, dark grey box). And similar to previous molecular studies (Borchiellini *et al.* 2004; Nichols 2005), the G1 clade of keratose sponges (which here includes *Darwinella* and *Dysidea*) is the sister taxon of the G3 + G4 sponges (Fig. 2). Unlike these previous analyses, though, we find strong support for a G1 + G2 (which here includes the taxon *Chondrilla*) clade (Fig. 2). In addition, our analysis does not support the monophyly of the G3 group as *Amphimedon* does not group with *Xestospongia* but instead groups with the two G4 freshwater sponges *Ephydatia* and *Trochospongilla*. Thus, the topology found with ribosomal DNA analyses (Borchiellini *et al.* 2004; Nichols 2005) is partially supported with an independent data set.

Previous molecular studies based on ribosomal data (Borchiellini *et al.* 2004; Nichols 2005) placed the Homoscleromorpha in an unresolved polytomy that included Demospongiae, Calcarea, Ctenophora and Cnidaria. Wang & Lavrov (2007), using sequences from the complete mitochondrial genome of *Oscarella carmela*, recovered this taxon as the sister group of the other sequenced demosponges. As mentioned above, current mitochondrial trees recover a monophyletic 'Lower'

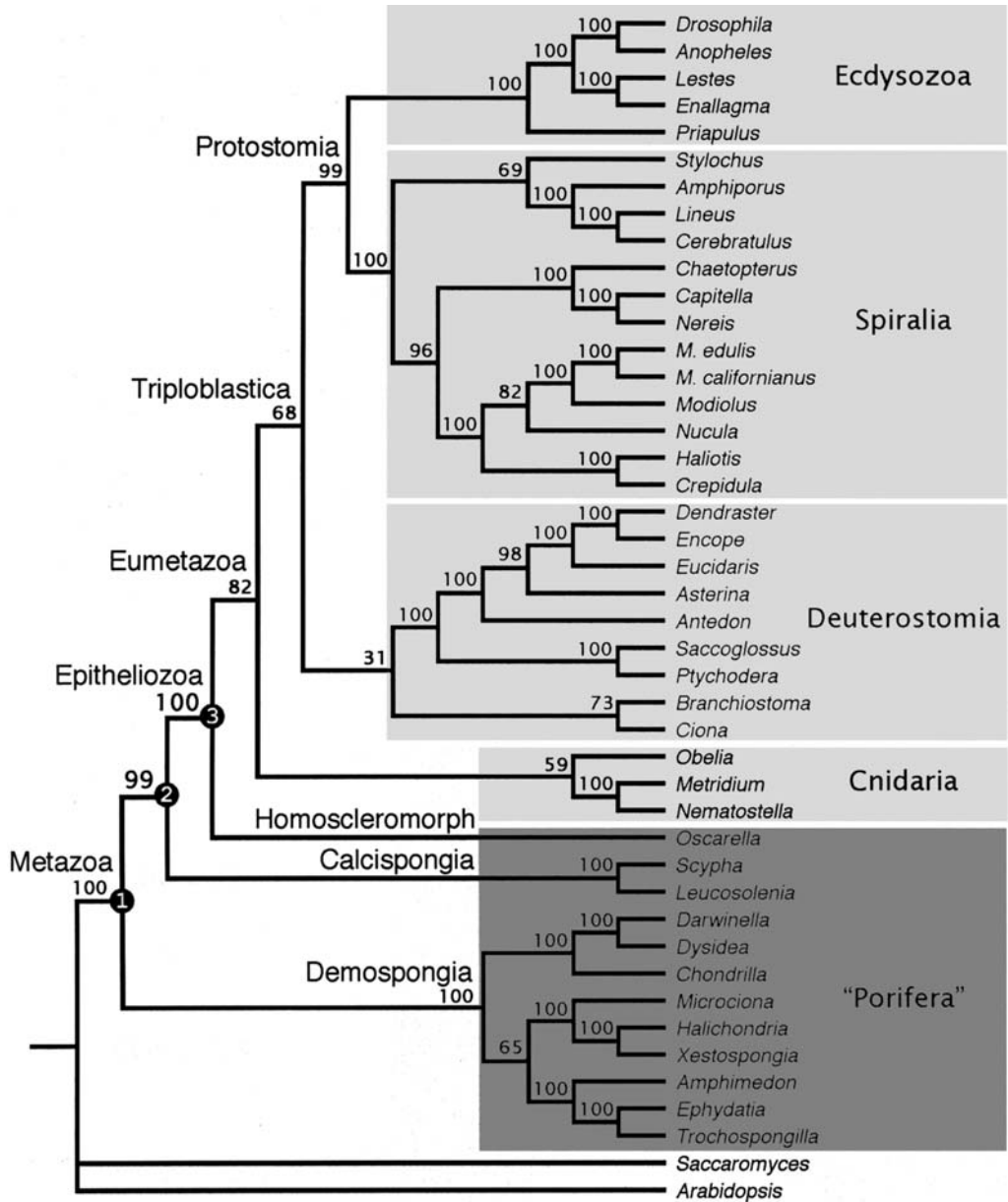


Fig. 2. Bayesian analysis of 30 eumetazoan taxa and 12 ‘sponges’ rooted on the plant *Arabidopsis* and the yeast *Saccaromyces*. Note the paraphyly of ‘Porifera’ (dark grey box) with the homoscleromorph *Oscarella* more closely related to eumetazoans than to other sponges, forming the clade Epitheliozoa (node 3), and the calcisponges more closely related to the epitheliozoans than to demosponges (node 2). In addition, note the division of demosponges into two clades: G1 (*Dysidea*, *Darwinella*) + G2 (*Chondrilla*); and G3 (*Xestospongilla*, *Amphimedon*) + G4 (*Microcionia*, *Halichondria*, *Ephydatia*, and *Trochospongilla*). Major eumetazoan groups are indicated with light grey boxes. *M. edulis* and *californianus* are members of the genus *Mytilus*.

Metazoa, a result that morphological, ribosomal, nuclear protein coding and microRNA (Sempere *et al.* 2006) data sets strongly refute, and it is difficult to evaluate the placement of taxa within an

erroneous topology. The Bayesian tree recovered here places the homoscleromorph *Oscarella* as the sister taxon to Eumetazoa (Cnidaria + Triploblastica). Phyla have both a constructional

and a historical context, and although the homoscleromorph body plan is not exceptionally different from other sponges, this result establishes, in effect, a new phylum-level lineage if further analyses with more homoscleromorph taxa continue to find Homoscleromorpha + Eumetazoa to the exclusion of the other two sponge lineages. This result is not completely unexpected, given that homoscleromorphs are unique among sponges in possessing two eumetazoan characters—true epithelia (Boury-Esnault *et al.* 1984; 2003; Boute *et al.* 1996), and a distinct acrosome (Harrison & De Vos 1991; Boury-Esnault & Jamieson 1999). Although this result must be tested with more taxa, congruence of independent morphological and molecular data sets provides strong support for phylogenetic inferences.

Poriferan paraphyly and character acquisition

Donoghue (2005), in his discussion of plant phylogeny, demonstrated the usefulness of paraphyly in unravelling the sequential evolution of what had once appeared to be a number of phylogenetically coincident character changes. Key changes in plant evolution occurred not at a single node, but were spread along many steps. The demonstration that Porifera is paraphyletic and therefore represents an evolutionary grade has important implications for the polarization of character states and understanding the sequence of character acquisition at the base of Metazoa.

Metazoa (Fig. 2, node 1) is characterized, in part, by the acquisition of multicellularity and the presence of the extracellular matrix, a complex of collagen, proteoglycan, adhesive glycoprotein and integrin, which mediates cell motility and transitions between epithelial and motile cell types (Morris 1993). Because of sponge paraphyly, the WCS with choanocytes (itself a likely plesiomorphic cell type), had also evolved by this point as well. The unnamed clade Calcarea + Epitheliozoa (epitheliozoans are the homoscleromorph + eumetazoans, see below) (Fig. 2, node 2) is potentially characterized by the presence of cross-striated rootlets. Most metazoan ciliated cells have a system of cross-striated rootlets that originates in the ciliary basal body and extends into the cytoplasm. Calcisponge larvae, as well as those of homoscleromorphs, have long, cross-striated cell rootlets (Woollacott & Pinto 1995; Amano & Hori 2001; Boury-Esnault *et al.* 2003) that were perhaps incorporated into adult eumetazoans through neotenous evolution (Maldonado 2004). However, the choanoflagellate *Monosiga*, the placozoan *Trichoplax*, as well as several other

protistan taxa, also have striated rootlets (Nielsen 2001; Boury-Esnault *et al.* 2003) implying that either the rootlets of Calcarea + Epitheliozoa are not homologous with those of choanoflagellates or this trait is plesiomorphic for Metazoa and has been secondarily lost in Hexactinellida and Demospongiae.

The clade Homoscleromorpha + Eumetazoa is herein recognized as Epitheliozoa (Fig. 2, node 3). Ax (1996) defined the clade Epitheliozoa for the clade of epithelial animals, and it is usually considered to include Ctenophora, Cnidaria and triploblasts (e.g. Wallberg *et al.* 2004). The position of the homoscleromorphs as the sister taxa to Eumetazoa, as well as the presence of basal laminae (Boute *et al.* 1996; Boury-Esnault *et al.* 2003), suggests that the Epitheliozoa should include the Homoscleromorpha. A second potential apomorphy of the Epitheliozoa is the presence of an acrosome (Harrison & De Vos 1991; Boury-Esnault & Jamieson 1999). Thus, of the four primary eumetazoan characters—tissues, an acrosome, a nervous system and a gut—the acquisition of tissues and the acrosome antedated the last common ancestor of homoscleromorphs and eumetazoans. The expression of features such as epithelia in the adult, along with the acquisition of these new characters (nervous system and gut), and the loss of the WCS, could be due to a coordinated character change (Jenner 2004) accompanying the neotenous evolution of a non-feeding sponge larva to a predatory eumetazoan. Based on molecular clocks, this coordinated character loss and acquisition accompanying the dramatic change in trophic strategies from sponge to eumetazoan is likely to have occurred sometime during, or soon after, the melting of the Marinoan glaciers *c.* 635 Ma (Peterson & Butterfield 2005), and may be tied to the oligotrophic ocean conditions associated with the Marinoan glaciation.

Poriferan paraphyly and Precambrian palaeobiology

Precambrian fossils are often confusing and contentious and among some of the more enigmatic forms are the rangeomorph fauna, preserved primarily in Ediacaran age strata in the Avalon Zone of Newfoundland. These fossils provide an example of the usefulness of modern systematic studies in constraining the possible phylogenetic hypotheses for Precambrian fossils.

Ediacaran fossils were first discovered in the middle of the 19th century in Newfoundland, but these structures were not recognized as biogenic until very recently (Gehling *et al.* 2000). These fossils were deposited between 575 Ma and 560 Ma (Benus 1988; Bowring *et al.* 2003; Narbonne &

Gehling 2003) in a deep-water setting well beneath the photic zone (Wood *et al.* 2003). The rangeomorphs, or 'fractal vendobionts' (Seilacher *et al.* 2003), which make up more than 85% of specimens in the classic Mistaken Point Formation, are composed of fractally-repeating architectural elements (Narbonne 2004). The organisms grew by pure inflation, with the first-order branches eventually turning into second-order. Fractal or infaltionary systems are a method for increasing the surface area-to-volume ratio, as might be expected for an organism feeding directly from the water-column without orifices. In the presence of a 'soup' of dissolved organic carbon (DOC) that likely existed during the Proterozoic (Rothman *et al.* 2003), rangeomorphs likely fed primarily on this DOC pool using direct absorption. Noting their environmental setting beneath the photic zone, indeterminate growth and lack of movement or taphonomic shrinkage, Peterson *et al.* (2003) suggested that many members of the Newfoundland fauna, such as *Aspidella*, *Charnia* and *Charniodiscus*, resembled Fungi rather than Metazoa. Nonetheless, recent studies have considered the degree of tiering similarity between the Newfoundland Ediacaran ecosystems and both Palaeozoic and Modern ecosystems sufficient to place the rangeomorphs with the Metazoa (Clapham & Narbonne 2002; Clapham *et al.* 2003). The lack of any eumetazoan features such as a gut or mouth, despite the exceptional preservation, prompted Narbonne (2005) to consider the rangeomorphs as an extinct architecture that may lie between poriferans and cnidarians on the metazoan tree, a position first proposed by Buss and Seilacher (1994).

However, in light of the results of sponge paraphyly as discussed above, this phylogenetic placement of the rangeomorphs, while not impossible, does not represent the most likely evolutionary scenario. Given that the last common ancestor of metazoans was something akin to a modern sponge, this implies that a WCS is primitive for Metazoa, and thus must have been lost early in the phylogenetic history of rangeomorphs if the group is apical to sponges. Although eumetazoans must have also lost the WCS, the key difference here is that acquisition of the gut allowed eumetazoans to change trophic modes and feed macrophagously, whereas rangeomorphs would still feed on the abundant DOC in the Proterozoic ocean in a manner analogous to sponges. While evolution is not always a predictable pathway, the loss of the WCS by a sponge-like organism in favour of a fractal construction to feed on the same food source does not represent a parsimonious interpretation of the data. The ecological studies of Clapham and colleagues showing similarity to modern and ancient animal ecosystems is merely sufficient to

demonstrate that they are heterotrophs that partitioned the water column for suspension feeding, but does not necessarily imply that they were, in fact, metazoans. Community tiering to extract nutrients more efficiently from the water column is a simple ecological strategy, likely to be adopted regardless of phylogenetic affinity, as shown by the convergent strategy used by Early Cambrian sponges (Yuan *et al.* 2002). Considering: (1) the deep-water setting which precludes a plant or algal status; (2) the lack of any eumetazoan apomorphies despite exceptional preservation; (3) their fractal organization; (4) the heterotrophic tiering of the community; and (5) the low probability that the WCS would have been lost in favour of a fractal design to feed on the same material, the Newfoundland rangeomorph fauna probably represent members of the opisthokonts (the group defined by the last common ancestor of fungi and animals; Cavalier-Smith 1998), but were not crown-group metazoans. It is worth emphasizing that they still could be stem-group metazoans, but our point is that the most likely explanation of the trophic data is that the last common ancestor of metazoans and rangeomorphs was unicellular, and the fractal and water canal architectures are two different solutions to achieve the same goal, namely feeding upon the abundant DOC available during the Ediacaran.

Poriferan paraphyly and Cambrian 'problematica'

Modern poriferan systematics and biology can also be used to infer the phylogenetic placement of several groups of enigmatic Cambrian fossils, and suggest guidelines for the taxonomy of sponge fossils in general. For example, chancelloriids are a group of early Cambrian spongiform organisms that were originally considered to be sponges but have since been the subject of a long history of taxonomic speculation. They range from the earliest Cambrian to the early Late Cambrian, flourishing in shallow marine environments, often as components of archaeocyathan mounds (Janussen *et al.* 2002). Although they are usually found as dissociated sclerites, complete scleritomes can be found in low-energy depositional environments. The scleritomes show sessile, attached, sac-like fossils that are covered by spiny sclerites. The non-anchored end contains a thick tuft of sclerites that likely surrounded an apical orifice (Bengtson 2005). The sclerites have thin, originally aragonitic walls surrounding a cavity with a restricted basal opening (Bengtson & Missarzhesky 1981). The outer surface was covered by a soft epithelial integument, perhaps indicating the presence of

desmosomal cell junctions (Bengtson & Hou 2001; Janussen *et al.* 2002). Chancelloriids were originally described as poriferans due to their sponge-like body form (Walcott 1920), and some workers still adhere to this position (Butterfield & Nicholas 1996). Nonetheless, in recent years others have suggested possible affinities with ascidians (Mehl 1996), cnidarians (Randall *et al.* 2005), and with the extinct and most likely polyphyletic (Conway Morris & Chapman 1997) Coeloscleritophora (Bengtson & Missarzhevsky 1981). Most arguments against a sponge affinity have focused on the sclerites (Bengtson 2005; Randall *et al.* 2005), and because there are clear differences between the spicules of chancelloriids and sponges, most authors agree that the two are not homologous. We agree. Most workers argue further that if the spicules are not homologous, then chancelloriids are not sponges. We disagree.

First, despite the superficial morphological similarity of spicules, clear structural and developmental differences exist between silicisponges and calcisponges (Harrison & De Vos 1991; Reitner & Mehl 1996; Brusca & Brusca 2002). Silicisponges deposit siliceous spicules intracellularly, first secreting an organic carbon axial filament within an elongated vacuole in a sclerocyte. As the axial filament elongates, hydrated silica is secreted into the vacuole and around the filament. Calcareous sponges, on the other hand, deposit their spicules extracellularly and without an organic axis; each spicule is essentially a single crystal of calcium carbonate. Second, the presence of silicified spicules does not characterize all demosponges. The G1 sponges form their skeleton entirely of spongin fibres and do not secrete a siliceous skeleton. The same is true for most, but not all of the G2s—*Chondrilla* lacks megascleres but possesses aster microscleres that are homoplastic with respect to other demosponges (Borchiellini *et al.* 2004). In fact, if hexactinellids are nested near or within the G3/G4 sponges, as suggested by some rDNA studies (Cavalier-Smith & Chao 2003; Nichols 2005), then this would strongly suggest that siliceous megascleres arose only once; differences between the spicules of hexactinellids and demosponges could be due to the radically different cellular organizations of the two (Leys 2003). And third, the presence of silicified spicules does not characterize all of Homoscleromorpha. Two genera (*Oscarella* and *Pseudocorticium*) are aspiculate (Muricy & Diaz 2002), but whether this is primitive or not is unknown, as the internal phylogeny of Homoscleromorpha remains unexplored by modern molecular means. Therefore, it is clear from the emerging sponge phylogeny that spicules arose at least three times within 'Porifera': at least once within Silicispongia, once within Calcispongia

and once at either at the base or within Homoscleromorpha. Given the clear homoplasy of massive calcareous skeletons within demo- and calcisponges (Chombard *et al.* 1997), convergence of spicule structure as well should not be too surprising.

The inescapable conclusion is that an organism cannot be removed from the poriferan grade based simply on spicule characteristics. An organism is a 'sponge' (taxon in quotes to represent a paraphyletic grade) if it feeds using a WCS, pumping water through a chamber via the power of choanocytes and extracting dissolved organic matter and picoplankton from the current. Fluid physics causes water flow velocities to slow as cross-sectional area increases. Sponges generally have a combined diameter of choanocyte chambers greater than the incurrent pores, and the combined diameters of the excurrent oscula are less than both the choanocyte chambers and incurrent pores (Brusca & Brusca 2002). This causes water to enter at velocity x , slow dramatically over the choanoderm for maximum absorption of nutrients, and then exit the sponge at a velocity far greater than x , sending the water clear of the sponge and avoiding recycling problems. Fossil sponges can be recognized, therefore, as organisms with combined incurrent pores greater in diameter than the combined excurrent openings.

Chancelloriids were sessile, benthic, radially symmetrical organisms constructed with presumed excurrent openings having a lesser diameter than the presumed combined incurrent pores. No specimen shows evidence of a mouth, gut or any other eumetazoan apomorphy, despite their co-occurrence with soft-bodied forms in localities such as Chengjiang (China), the Burgess Shale (Canada) and the Wheeler Shale (USA) that commonly preserve such anatomical features. Finally, the recognition of tissues as a eumetazoan plesiomorphy removes an additional difficulty with a poriferan affinity (Janussen *et al.* 2002) given that, similar to homoscleromorphs, chancelloriids were likely to possess an integument (Bengtson & Hou 2001; Janussen *et al.* 2002).

Archaeocyaths, another Early Cambrian fossil group, provide a historical example of how a focus on skeletal characteristics may incorrectly preclude a group from the poriferan grade. As sessile, conical marine organisms, archaeocyaths were first formally described as possible sponges, but later classified as coelenterates, algae, foraminifera or an extinct phylum or kingdom, with a non-poriferan taxonomic affinity often preferred because their unique double-walled massive calcareous skeleton was unknown in modern sponges (see review in Rowland 2001). However, the discovery of massive, calcareous sponges (sclerosponges and *Vaceletia*) demonstrated that the archaeocyathan

skeleton was not incompatible with a 'sponge' affinity. Studies of archaeocyath ultrastructure (Kruse & Debrenne 1989) and functional morphology (Savarese 1992; Wood *et al.* 1992) further cemented their status as sponges, a point now agreed upon by nearly all archaeocyath and sponge workers (Rowland 2001). The convergent evolution of both spicules and massive skeletons in different 'sponge' lineages suggests the skeletonization process in archaeocyaths and chancelloriids is largely irrelevant to their broad-scale taxonomic position as compared to recognizing the biological constraints afforded by a sessile, radially constructed organism with a probable excurrent osculum and no visible gut or mouth.

Poriferan parphyly and Precambrian oxygenation

Geochemical evidence suggests that the partial pressure of atmospheric oxygen rose substantially circa 2.3 billion years ago (Holland & Beukes 1990; Farquhar *et al.* 2000). While the increase in atmospheric oxygen helped to oxygenate the surficial layers of the ocean, the mid-Proterozoic deep ocean was likely anoxic and sulphidic (Canfield 1998; Anbar & Knoll 2002). Between the mid-Proterozoic and the Phanerozoic there was a transitional period from ancient to modern ocean, the latter characterized by a well-oxygenated mixed or surface layer, a mildly dysoxic to anoxic oxygen-minimum zone from *c.* 200–1000 metres where the mineralization of organic matter descending from surface productivity draws down dissolved oxygen levels, and an oxygenated deep ocean. Evidence from carbon isotope studies indicates that the Proterozoic ocean was a 'soup' of dissolved organic matter (Rothman *et al.* 2003). Logan *et al.* (1995), in their seminal study of sedimentary organic carbon, suggested that hydrocarbons in Proterozoic sediments were derived primarily from bacteria and heterotrophic organisms rather than from photosynthetic organisms as in the modern ocean. Due to the lack of faecal pellets, which increase transport speed to the ocean bottom, the degradation of algal products was unusually complete. Logan *et al.* (1995), therefore, suggested that the slowly sinking algal products were re-mineralized before they could be sequestered in the sediment, and it was the advent of planktonic organisms with faecal pellets that allowed for the drawdown of the organic carbon pool and transition to the Phanerozoic ocean. The timing of this shift as described in Logan *et al.* (1995) is not clear due to the lack of available radiometric dates at that time, occurring at some point between the Late Neoproterozoic and the Early Cambrian (Peterson *et al.* 2005). New

data from carbon and sulphur isotopes in the Huqf Supergroup in Oman suggests that this reorganization and the oxidation of the Proterozoic ocean took place during the 'Shuram' excursion. Chemostratigraphic correlations with other sections worldwide suggest that the Shuram event likely occurred prior to 551 Ma (Condon *et al.* 2005), while detrital zircons from Oman date it younger than 610 Ma (Le Guerroue *et al.* 2006a). The faecal pellets of mesozooplankton do not sink, and only the faecal pellets of macrozooplankton or nekton are capable of rapidly sinking (Peterson *et al.* 2005). Given that the fossil record of planktic predation (Butterfield 1997), and the actual fossil record of the possible predators themselves (Butterfield 1994), indicates that the base of the zooplankton food chain did not exist until after the Tommotian, the evolution of macrozooplankton could not have occurred until significantly after the major oxidation of the dissolved organic carbon reservoir and transition to the Phanerozoic ocean. The origin and diversification of sponges and associated organisms might, however, represent an alternative mechanism for the drawdown of the dissolved organic carbon.

The Shuram negative carbon isotope excursion, preserved in mid-Ediacaran strata in Oman, shows a $\delta^{13}\text{C}_{\text{carb}}$ shift on the order of $>15^{0/00}$ to values of $-12^{0/00}$ (Le Guerroue *et al.* 2006b; Fike *et al.* 2006). It is unique in Earth history in recording long-lasting marine carbonate carbon values with presumed primary signal well below the canonical mantle value of $-6^{0/00}$. Negative excursions of extremely large magnitude, such as those during Snowball Earth episodes (Halverson *et al.* 2005), in the Early Cambrian (Malooof *et al.* 2005) or Early Triassic (Payne *et al.* 2004), which do not show carbonate carbon values below $-6^{0/00}$, can be explained through normal agents such as changes in the fraction of carbon buried as organic carbon and/or changes in isotopic fractionation during photosynthesis. The Shuram excursion, however, demands a fundamentally different explanation for the long-term production of isotopically-light carbonates. Fike *et al.* (2006) suggested that the Shuram excursion was caused by the oxidation of a large dissolved organic carbon (DOC) pool hypothesized to have existed throughout much of the Proterozoic (Rothman *et al.* 2003), but they did not identify any mechanism to account for this event. Here, we posit that the advent of novel modes of heterotrophy, especially the origin and radiation of sponges and rangeomorphs, could account for the Shuram excursion.

According to our hypothesis (Fig. 3), in the early Neoproterozoic, the isotopic composition of marine carbonates is controlled by the normal Phanerozoic paradigm: $\delta^{13}\text{C}_{\text{carb}} = \delta\text{w} - (\Delta\delta\text{x} f \text{org})$ where δw is equal to the isotopic composition of mantle-derived

CO₂ (generally interpreted to be $c. -6^{0/00}$ throughout Earth history), $\Delta\delta$ is the fractionation introduced during photosynthesis, and f_{org} is the fraction converted to organic carbon during photosynthesis. Unlike the Phanerozoic, where $f_{org} \cong$ sedimentary organic matter, a significant percentage of primary production is not buried in the sediment (Logan *et al.* 1995) but is partly degraded in the water column and accumulates as dissolved organic carbon (DOC). By the early- to mid-Ediacaran ('Shuram' time), feeding by sponges and rangeomorphs on DOC led to volumetrically-significant heterotrophic respiration on this DOC pool for the first time in Earth history. Unlike in photosynthesis there is no isotopic fractionation during respiration (oxidation of the DOC), thereby producing large quantities of isotopically-light ($c. -27^{0/00}$) CO₂ that equilibrated with the water and caused a long-lived isotopic excursion below the canonical mantle value. Eventually the DOC reservoir was depleted, leading to a long isotopic recovery and explaining why the Shuram is a singular event in Earth history. The processing of DOC by sponges after the Shuram excursion would still have been important, although the amount of DOC available for feeding would be directly related to production. The evolution of the modern zooplankton food chain with faecal pellets near the base of the Cambrian finally allowed for the direct consumption of algae and the export of carbon to the sediment (Logan *et al.* 1995) without an intermediate DOC step.

This hypothesis is supported by the temporal correlation of the Shuram isotope excursion with the origination and ecological dominance of two unrelated grades of organism, sponges and rangeomorphs. Molecular clocks (Peterson & Butterfield 2005) and the fossil record (McCaffrey *et al.* 1994; Love *et al.* 2006) show that the origin of the sponge-grade is not much older than the Ediacaran, and the first rangeomorphs are dated to $c. 575$ Ma (Narbonne & Gehling 2003). Both were extremely abundant and physiologically well-suited to feed directly on DOC, unlike virtually all other clades of eukaryotes including eumetazoans. The WCS of sponges is extremely efficient at moving water through the body via the power of the choanocytes. For example, a large sponge can filter its own volume of water every 10 to 20 seconds (Brusca & Brusca 2002). *In situ* feeding studies on modern sponges demonstrate that some derive the majority of their food from DOC, and can remove an average of 10% of the DOC in the water in a single pass through the water canal system (Yahel *et al.* 2003). Rangeomorphs, which must also have fed on dissolved organic carbon using a convergent solution based on passive absorption (see above), would also have contributed to the drawdown. The absolute

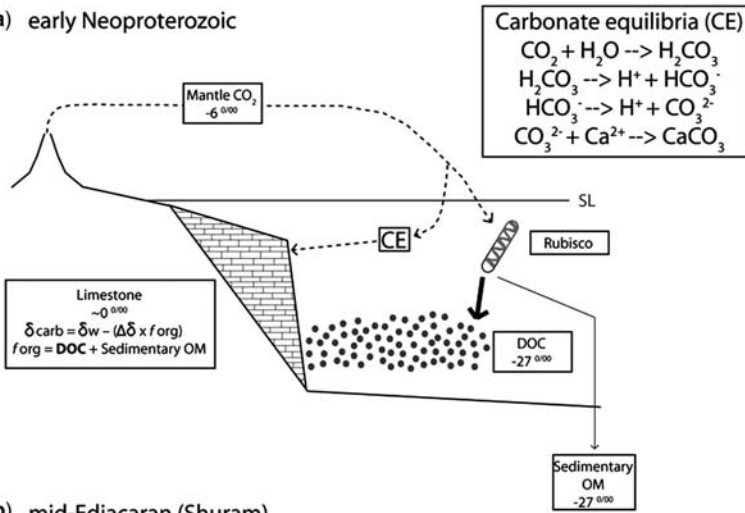
dominance of rangeomorphs in the older ($c. 575$ – 565 Ma) Newfoundland Ediacaran fauna, and their almost complete absence in the younger (and shallower) Ediacara/White Sea (555 Ma) and Namibian ($c. 549$ – 543 Ma) faunas (Narbonne 2005) may be related to their reliance on passive absorption on the disappearing pool of dissolved organic carbon in the deep ocean, whereas sponges, which can essentially bring the ocean through their body with the water-canal system, would have been less affected by a declining reservoir.

Canfield *et al.* (2006) suggested the deep ocean may have become oxygenated around the Gaskiers glaciation, $c. 580$ Ma. Oxidation of the Neoproterozoic DOC pool as discussed above must necessarily have resulted in a *de*-oxygenation of the ocean-atmosphere system, unless a different oxidant is invoked, and so oxygenation and oxidation are not necessarily linked. Nonetheless, the advent of the sponge and rangeomorph body plans allowed DOC to be incorporated into benthic biomass that could be buried and removed as an oxygen sink. Given that algal products could not be buried as faecal pellets until the Cambrian, the reorganization of biogeochemical cycles, as evidenced by the Shuram excursion, could reflect the origin and subsequent radiation of sponges and rangeomorphs.

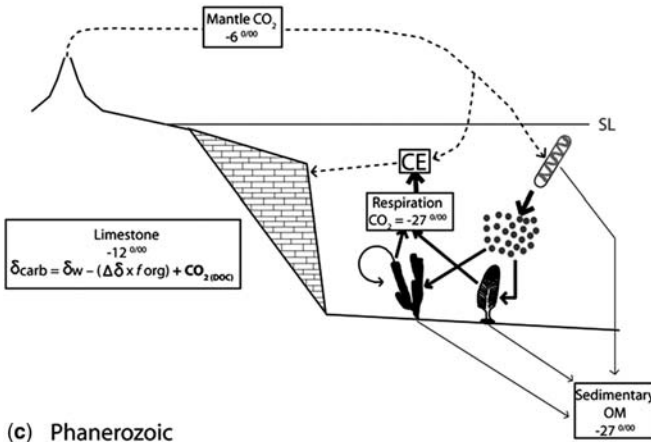
Conclusions

Our molecular results provide further evidence for the paraphyly of Porifera and suggest that there are three 'sponge' phyla: Silicispongia, Calcispongia and Homoscleromorpha. This strengthens the conclusions of Peterson & Butterfield (2005), and previous reports based on ribosomal evidence. Further work is required to test this topology, to provide more concrete evidence for the placement of placozoans and hexactinellids, and to elucidate the internal topology of demosponges and homoscleromorpha. Nevertheless, basal metazoan phylogeny is becoming clearer, and the paraphyly of sponges allows not only for the polarization of character states and an enhanced understanding of the sequence of character acquisition, but sheds much light on the phylogenetic affinities of long-extinct taxa, and provides new insights into global oceanic oxygenation. Finally, the fact that one modern clade of demosponges, the cladorhizids, lost the WCS and feeds macrophagously upon mesozooplankton using a derived mode of extracellular digestion (Vacelet & Boury-Esnault 1995) may shed light on the analogous loss of the WCS in early eumetazoans (Vacelet & Dupont 2004). The concordance between the observations that

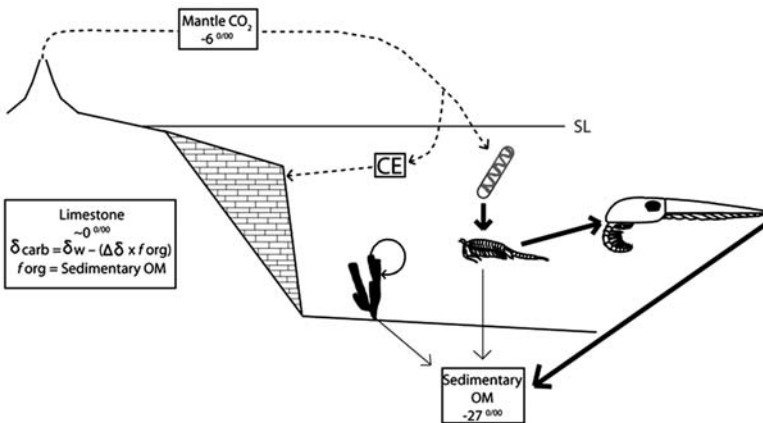
(a) early Neoproterozoic



(b) mid-Ediacaran (Shuram)



(c) Phanerozoic



cladorhizids live in oligotrophic environments, and that eumetazoans arose on the heels of the Marinoan 'snowball Earth', may be of some significance.

We thank S. Nichols for the gift of *Oscarella carmela* total RNA, and E. Dunn, C. Fiove, A. Evans and V. Moy for technical assistance. We also thank G. Love, D. Rothman, L. Buss, D.E.G. Briggs and R. Summons for discussion, and A. Collins and G. Narbonne for formal reviews. KJP is supported by the National Science Foundation, NASA-Ames, and Dartmouth College. EAS was supported by a NASA Planetary Biology Internship grant.

References

- ADAMS, C. L., MCINERNEY, J. O. & KELLY, M. 1999. Indications of relationships between poriferan classes using full-length 18S rRNA gene sequences. *Memoirs of the Queensland Museum*, **44**, 33–43.
- AMANO, S. & HORI, I. 2001. Metamorphosis of coeloblastula performed by multipotential larval flagellated cells in the calcareous sponge *Leucosolenia laxa*. *Biological Bulletin*, **200**, 20–32.
- ANBAR, A. D. & KNOLL, A. H. 2002. Proterozoic ocean chemistry and evolution: a bioinorganic bridge. *Science*, **297**, 1137–1142.
- AX, P. 1996. *Multicellular Animals, Vol. 1. A New Approach to Phylogenetic Order in Nature*. Springer-Verlag, Berlin.
- BENGTSON, S. 2005. Mineralized skeletons and early animal evolution. In: BRIGGS, D. E. G. (ed.) *Evolving Form and Function: Fossils and Development*. Yale Peabody Museum Special Publication.
- BENGTSON, S. & HOU, X. 2001. The integument of Cambrian chancelloriids. *Acta Palaeontologica Polonica*, **46**, 1–22.
- BENGTSON, S. & MISSARZHEVSKY, V. V. 1981. Coelocleritophora—a major group of enigmatic Cambrian metazoans. *U.S. Geological Survey Open-file Report*, 81–743, 19–21.
- BENUS, A. P. 1988. Sedimentological context of a deep-water Ediacaran fauna (Mistaken Point Formation, Avalon Zone, eastern Newfoundland). In: LANDING, E., NARBONNE, G. M. & MYROW, P. M. (eds) *Trace Fossils, Small Shelly Fossils and the Precambrian/Cambrian Boundary*. Bulletin of the New York State Museum, Albany, **463**, 8–9.
- BORCHIELLINI, C., MANUEL, M., ALIVON, E., BOURY-ESNAULT, N., VACELET, J. & LE PARCO, Y. 2001. Sponge parphyly and the origin of Metazoa. *Journal of Evolutionary Biology*, **14**, 171–179.
- BORCHIELLINI, C., CHOMBAR, C., MANUEL, M., ALIVON, E., VACELET, J. & BOURY-ESNAULT, N. 2004. Molecular phylogeny of Demospongiae: implications for classification and scenarios for character evolution. *Molecular Phylogenetics and Evolution*, **32**, 823–837.
- BOURY-ESNAULT, N. & JAMIESON, B. G. M. 1999. Porifera. In: JAMIESON, B. G. M. (ed.) *Progress in Male Gamete Biology*. IBH Publishing Co., New Delhi, 1–20.
- BOURY-ESNAULT, N., DE VOS, L., DONADEY, C. & VACELET, J. 1984. Comparative study of the choanosome of Porifera. I. The Homoscleromorpha. *Journal of Morphology*, **180**, 3–17.
- BOURY-ESNAULT, N., ERESKOVSKY, A., BÉZAC, C. & TOKINA, D. 2003. Larval development in the Homoscleromorpha (Porifera, Demospongiae). *Invertebrate Biology*, **122**, 187–202.
- BOUTE, N., EXPOSITO, J.-Y., BOURY-ESNAULT, N., VACELET, J., NORO, N., MIYAZAKI, K., YOSHIZATO, K. & GARRONE, R. 1996. Type IV collagen in sponges, the missing link in basement membrane ubiquity. *Biological Cell*, **88**, 37–44.
- BOWRING, S., MYROW, P., LANDING, E., RAMEZANI, J. & GROTZINGER, J. 2003. Geochronological constraints on terminal Neoproterozoic events and the rise of metazoans. *Geophysical Research Abstracts*, **5**, 13219.
- BRUSCA, R. C. & BRUSCA, G. J. 2002. *Invertebrates* (2nd edn) Sinauer Associates Inc., Sunderland.
- BUSS, L. W. & SEILACHER, A. 1994. The Phylum Vendobionta: a sister group of the Eumetazoa? *Paleobiology*, **20**, 1–4.
- BUTTERFIELD, N. J. 1994. Burgess Shale-type fossils from a Lower Cambrian shallow-shelf sequence in northwestern Canada. *Nature*, **369**, 477–479.
- BUTTERFIELD, N. J. 1997. Plankton ecology and the Proterozoic–Phanerozoic transition. *Paleobiology*, **23**, 247–262.

Fig. 3. A biological explanation for the Shuram excursion. Bold arrows or font indicate a relatively more important contribution from that source. SL, sea level; CE, carbonate equilibria (CO_2 equilibrates with seawater and combines with ocean Ca^{2+} to form carbonates). (a) In the early Neoproterozoic, the isotopic composition of marine carbonates ($\delta^{13}\text{C}_{\text{carb}}$) is equal to that of mantle-derived CO_2 (δw ; generally interpreted to be $c. -6^{0/00}$ throughout Earth history) minus the fraction converted to organic carbon during photosynthesis (f_{org}), multiplied by the fractionation introduced during the Rubisco cycle ($\Delta\delta$). Unlike the Phanerozoic, where $f_{\text{org}} \cong$ sedimentary organic matter (OM), a significant percentage of primary production is not buried in the sediment but is partly degraded in the water column and accumulates as dissolved organic carbon (DOC). (b) By the early- to mid-Ediacaran, feeding by sponges and rangeomorphs on DOC led to volumetrically-significant heterotrophic respiration on this DOC pool for the first time in Earth history. Unlike in photosynthesis there is no isotopic fractionation during respiration (oxidation of the DOC), thereby producing large quantities of isotopically-light (e.g. $-27^{0/00}$) CO_2 that equilibrated with the water and eventually contributed to a long-lived isotopic excursion below the canonical mantle value. (c) By the Phanerozoic, the carbon isotopic system had achieved its present-day steady state, with a small DOC pool and an isotopic value of marine carbonates controlled primarily by the fraction of carbon buried as organic matter. The evolution of macrozooplankton at the base of the Cambrian finally allowed for the direct processing of algal products and their transport to seafloor as faecal pellets without a DOC intermediate.

- BUTTERFIELD, N. J. & NICHOLAS, C. J. 1996. Burgess Shale-type preservation of both non-mineralizing and 'shelly' Cambrian organisms from the Mackenzie Mountains, northwestern Canada. *Journal of Paleontology*, **70**, 893–899.
- CANFIELD, D. E. 1998. A new model for Proterozoic ocean chemistry. *Nature*, **396**, 450–453.
- CANFIELD, D. E., POULTON, S. W. & NARBONNE, G. M. 2006. Late-Neoproterozoic deep-ocean oxygenation and the rise of animal life. *Science*, **315**, 92–95.
- CAVALIER-SMITH, T. 1998. A revised six-kingdom system of life. *Biological Reviews of the Cambridge Philosophical Society*, **73**, 203–266.
- CAVALIER-SMITH, T. & CHAO, E. E.-Y. 2003. Phylogeny of Choanozoa, Apusozoa, and other Protozoa and early eukaryotic megaevolution. *Journal of Molecular Evolution*, **56**, 540–563.
- CAVALIER-SMITH, T., ALLSOPP, M. T. E. P., CHAO, E. E.-Y., BOURY-ESNAULT, N. & VACELET, J. 1996. Sponge phylogeny, animal monophyly, and the origin of the nervous system: 18S rRNA evidence. *Canadian Journal of Zoology*, **74**, 2031–2045.
- CHOMBARD, C., BOURY-ESNAULT, N., TILLIER, A. & VACELET, J. 1997. Polyphyly of 'sclerosponges' (Porifera, Demospongiae) supported by 28S sequences. *Biological Bulletin*, **193**, 359–367.
- CLAPHAM, M. E. & NARBONNE, G. M. 2002. Ediacaran epifaunal tiering. *Geology*, **30**, 627–630.
- CLAPHAM, M. E., NARBONNE, G. M. & GEHLING, J. G. 2003. Paleocology of the oldest known animal communities: Ediacaran assemblages at Mistaken Point, Newfoundland. *Paleobiology*, **29**, 527–544.
- COLLINS, A. G. 1998. Evaluating multiple alternative hypotheses for the origin of Bilateria: an analysis of 18S rRNA molecular evidence. *Proceedings of the National Academy of Sciences, USA*, **95**, 15458–15463.
- CONDON, D., ZHU, M., BOWRING, S., WANG, W., YANG, A. & JIN, Y. 2005. U–Pb ages from the Neoproterozoic Doushantuo Formation, China. *Science*, **308**, 95–98.
- CONWAY MORRIS, S. & CHAPMAN, A. J. 1997. Lower Cambrian Halkieriids and other Coeloscleritophorans from Aksu-Wushi, Xinjiang, China. *Journal of Paleontology*, **71**, 6–22.
- DONOGHUE, M. J. 2005. Key innovations, convergence, and success: macroevolutionary lessons from plant phylogeny. *Paleobiology*, **31**, Supplement, 77–93.
- EERNISSE, D. J. & PETERSON, K. J. 2004. The history of animals. In: CRACRAFT, J. & DONOGHUE, M. J. (eds) *Assembling the Tree of Life*. Oxford University Press, Oxford, 197–208.
- FARQUHAR, J., BAO, H. M. & THIEMENS, M. 2000. Atmospheric influence of Earth's earliest sulphur cycle. *Science*, **289**, 756–758.
- FIKE, D., GROTZINGER, J., PRATT, L. & SUMMONS, R. 2006. Oxidation of the Ediacaran ocean. *Nature*, **444**, 744–747.
- GEHLING, J. G. 1991. The case for Ediacaran fossil roots to the metazoan tree: *Geological Society of India Memoir*, **20**, 181–224.
- GEHLING, J. G., NARBONNE, G. M. & ANDERSON, M. M. 2000. The first named Ediacaran body fossil, *Aspidella terranovica*. *Palaentology*, **43**, 427–456.
- HALANYCH, K. M. 2004. The new view of animal phylogeny. *Annual Review of Ecology and Systematics*, **35**, 229–256.
- HALVERSON, G. P., HOFFMAN, P. F., SCHRAG, D. P., MALOOF, A. C. & RICE, A. H. N. 2005. Towards a Neoproterozoic composite carbon-isotope record. *Geological Society of America Bulletin*, **117**, 1181–1207.
- HARRISON, F. W. & DE VOS, L. 1991. Porifera. In: HARRISON, F. W. & WESTFALL, J. A. (eds) *Microscopic Anatomy of the Invertebrates. 2: Placozoa, Porifera, Cnidaria, and Ctenophora*. Wiley-Liss, New York, 29–89.
- HOLLAND, H. D. & BEUKES, N. J. 1990. A paleoweathering profile from Griqualand West, South Africa: evidence for a dramatic rise in atmospheric oxygen between 2.2 and 1.8 bybp. *American Journal of Science*, **290-A**, 1–34.
- HOOPER, J. N. A. & VAN SOEST, R. W. M. 2006. A new species of *Amphimedon* (Porifera, Demospongiae, Haplosclerida, Niphathidae) from the Capricorn-Bunker Group of Islands, Great Barrier Reef, Australia: target species for the 'sponge genome project'. *Zootaxa*, **1314**, 31–39.
- JANUSSEN, D., STEINER, M. & MAOYAN, Z. 2002. New well-preserved scleritomes of Chancelloridae from the Early Cambrian Yuanshan Formation (Chengjiang, China) and the Middle Cambrian Wheeler Shale (Utah, USA) and palaeobiological implications. *Journal of Paleontology*, **76**, 596–606.
- JENNER, R. A. 2004. When molecules and morphology clash: reconciling conflicting phylogenies of the Metazoa by considering secondary character loss. *Evolution and Development*, **6**, 372–378.
- KRUSE, M., LEYS, S. P., MÜLLER, I. M. & MÜLLER, W. E. G. 1998. Phylogenetic position of the Hexactinellida within the phylum Porifera based on the amino acid sequence of the protein kinase C from *Rhabdocalypus dawsoni*. *Journal of Molecular Evolution*, **46**, 721–728.
- KRUSE, P. D. & DEBRENNE, F. 1989. Review of archaeocyath microstructure. *Memoirs of the Association of Australasian Palaeontologists*, **8**, 133–141.
- LE GUERROUE, E., ALLEN, P. A., COZZI, A., ETIENNE, J. L. & FANNING, M. 2006a. 50 Myr recover from the largest $\delta^{13}\text{C}$ excursion in the Ediacaran ocean. *Terra Nova*, **18**, 147–153.
- LE GUERROUE, E., ALLEN, P. A. & COZZI, A. 2006b. Chemostratigraphic and sedimentological framework of the largest negative carbon isotope excursion in Earth history: The Neoproterozoic Shuram Formation (Nafun Group, Oman). *Precambrian Research*, **146**, 68–92.
- LEYS, S. P. 2003. Comparative study of spiculogenesis in demosponge and hexactinellid larvae. *Microscopy Research and Technique*, **62**, 300–311.
- LOGAN, G. A., HAYES, J. M., HIESHIMA, G. B. & SUMMONS, R. E. 1995. Terminal Proterozoic reorganization of biogeochemical cycles. *Nature*, **376**, 53–56.
- LOVE, G. D. & FIKE, D. A. ET AL. 2006. Constraining the timing of basal metazoan radiation using molecular biomarkers and U–Pb isotope dating. *Geochimica et Cosmochimica Acta*, **70**, A371.

- MALDONADO, M. 2004. Choanoflagellates, choanocytes, and animal multicellularity. *Invertebrate Biology*, **123**, 1–22.
- MALOOF, A. C., SCHARG, D. P., CROWLEY, J. L. & BROWNING, S. A. 2005. An expanded record of Early Cambrian carbon cycling from the Anti-Atlas Margin, Morocco. *Canadian Journal of Earth Science*, **42**, 2195–2216.
- MANUEL, M., BORCHIPELLINI, C., ALIVON, E., LE PARCO, Y., VACELET, J. & BOURY-ESNAULT, N. 2003. Phylogeny and evolution of calcareous sponges: monophyly of Calcinea and Calcaronea, high level of morphological homoplasy, and the primitive nature of axial symmetry. *Systematic Biology*, **52**, 311–333.
- MCCAFFREY, M. A., MOLDOWAN, J. M., LIPTON, P. A., SUMMONS, R. E., PETERS, K. E., JEGANATHAN, A. & WATT, D. S. 1994. Paleoenvironmental implications of novel C30 steranes in Precambrian to Cenozoic age petroleum and bitumen. *Geochimica et Cosmochimica Acta*, **58**, 529–532.
- MEDINA, M., COLLINS, A. G., SILBERMAN, J. D. & SOGIN, M. L. 2001. Evaluating hypotheses of basal animal phylogeny using complete sequences of large and small subunit rRNA. *Proceedings of the National Academy of Sciences, USA*, **98**, 9707–9712.
- MEHL, D. 1996. Organization and microstructure of the chancellorid skeleton: implications for the biomineralization of the Chancelloridae. *Bulletin de l'Institut Oceanographique de Monaco*, **14**, 377–385.
- MORRIS, P. J. 1993. The developmental role of the extracellular matrix suggests a monophyletic origin of the kingdom Animalia. *Evolution*, **47**, 152–165.
- MURICY, G. & DIAZ, D. 2002. Order Homoscleromorpha Dendy, 1905, Family Plakinidae Schluze, 1880. In: HOOPER, J. N. A. & VAN SOEST, R. W. M. (eds) *Systema Porifera: A Guide to the Classification of Sponges*. Kluwer Academic/Plenum Publishers, New York, 71–82.
- NARBONNE, G. M. 1998. The Ediacara-biota: a terminal Neoproterozoic experiment in the evolution of life. *Geological Society of America Today*, **8**, 1–6.
- NARBONNE, G. M. 2004. Modular construction of early Ediacaran complex life forms. *Science*, **305**, 1141–1144.
- NARBONNE, G. M. 2005. The Ediacara biota: Neoproterozoic origin of animals and their ecosystems. *Annual Review of Earth and Planetary Sciences*, **33**, 421–442.
- NARBONNE, G. M. & GEHLING, J. G. 2003. Life after snowball: the oldest complex Ediacaran fossils. *Geology*, **31**, 27–30.
- NICHOLS, S. A. 2005. An evaluation of support for order-level monophyly and interrelationships within the class Demospongiae using partial data from the large subunit rDNA and cytochrome oxidase subunit I. *Molecular Phylogenetics and Evolution*, **34**, 81–96.
- NIELSEN, C. 2001. *Animal Evolution: Interrelationships of the Living Phyla* (2nd edn). Oxford University Press, Oxford.
- PAYNE, J. L., LEHRMANN, D. J., WEI, J., ORCHARD, M. J., SCHRAG, D. P. & KNOLL, A. H. 2004. Large perturbations of the carbon cycle during recovery from the end-Permian extinction. *Science*, **305**, 506–509.
- PETERSON, K. J. & BUTTERFIELD, N. J. 2005. Origin of the Eumetazoa: Testing ecological predictions of molecular clocks against the Proterozoic fossil record. *Proceedings of the National Academy of Sciences, USA*, **102**, 9547–9552.
- PETERSON, K. J. & EERNISSE, D. J. 2001. Animal phylogeny and the ancestry of bilaterians: inferences from morphology and 18S rDNA gene sequences. *Evolution and Development*, **3**, 170–205.
- PETERSON, K. J., WAGGONER, B. & HAGADORN, J. W. 2003. A fungal analog for Newfoundland Ediacaran fossils. *Integrative and Comparative Biology*, **43**, 127–136.
- PETERSON, K. J., LYONS, J. B., NOWAK, K. S., TAKACS, C. M., WARGO, M. J. & MCPEEK, M. A. 2004. Estimating metazoan divergence times with a molecular clock. *Proceedings of the National Academy of Sciences, USA*, **101**, 6536–6541.
- PETERSON, K. J., MCPEEK, M. A. & EVANS, D. A. D. 2005. Tempo and mode of early animal evolution: inferences from rocks, *Hox*, and molecular clocks. *Paleobiology*, **31**, Supplement, 36–55.
- RANDALL, R. D., LIEBERMAN, B. S., HASIOTIS, S. T. & POPE, M. C. 2005. New chancelloriids from the Early Cambrian Sekwi Formation with a comment on chancelloriid affinities. *Journal of Paleontology*, **79**, 987–996.
- REITNER, J. & MEHL, D. 1996. Monophyly of the Porifera. *Verhandlungen des naturwissenschaftlichen Vereins in Hamburg (Neue Folge)*, **36**, 5–32.
- RONQUIST, F. & HUELSENBECK, J. P. 2003. MrBayes 3: Bayesian phylogenetic inference under mixed models. *Bioinformatics*, **19**, 1572–1574.
- RONQUIST, F., HUELSENBECK, J. P. & VAN DER MARK, P. 2005. MrBayes. Distributed by the authors.
- ROTHMAN, D. H., HAYES, J. M. & SUMMONS, R. E. 2003. Dynamics of the Neoproterozoic carbon cycle. *Proceedings of the National Academy of Sciences, USA*, **100**, 8124–8129.
- ROWLAND, S. M. 2001. Archaeocyaths—a history of phylogenetic interpretation. *Journal of Paleontology*, **75**, 1065–1078.
- RUNNEGAR, B. 1982. The Cambrian explosion: animals or fossils? *Journal of the Geological Society of Australia*, **29**, 395–411.
- SAVARESE, M. 1992. Functional analysis of archaeocyathan skeletal morphology and its palaeobiological implications. *Paleobiology*, **18**, 464–480.
- SEILACHER, A., GRAZHDANKI, D. & LEGOUTA, A. 2003. Ediacaran biota: The dawn of animal life in the shadow of giant protists. *Paleontological Research*, **7**, 43–54.
- SEMPERE, L. F., COLE, C. N., MCPEEK, M. A. & PETERSON, K. J. 2006. The phylogenetic distribution of metazoan microRNAs: insights into evolutionary complexity and constraint. *Journal of Experimental Zoology (Mol Dev Evol)*, **306B**, 576–588.
- VACELET, J. & BOURY-ESNAULT, N. 1995. Carnivorous sponges. *Nature*, **373**, 333–335.
- VACELET, J. & DUPORT, E. 2004. Prey capture and digestion in the carnivorous sponge *Asbestopluma hypogea*

- (Porifera: Demospongiae). *Zoomorphology*, **123**, 179–190.
- WANG, X. & LAVROV, D. V. 2007. Mitochondrial genome of the homoscleromorph *Oscarella carmela* (Porifera, Demospongiae) reveals unexpected complexity in the common ancestor of sponges and other animals. *Molecular Biology and Evolution*, **24**, 363–373.
- WALCOTT, C. D. 1920. Middle Cambrian Spongiae. *Smithsonian Miscellaneous Collections*, **67**, 261–364.
- WALLBERG, A., THOLLESSON, M., FARRIS, J. S. & JONDELIUS, U. 2004. The phylogenetic position of the comb jellies (Ctenophora) and the importance of taxonomic sampling. *Cladistics*, **20**, 558–578.
- WOOD, R. A., ZHURAVLEV, A. Y. & DEBRENNE, F. 1992. Functional biology and ecology of Archaeocyatha. *Palaios*, **7**, 131–156.
- WOOD, D. A., DALRYMPLE, R. W., NARBONNE, G. M., GEHLING, J. G. & CLAPHAM, M. E. 2003. Paleoenvironmental analysis of the late Neoproterozoic Mistaken Point and Trepassay formations, southeastern Newfoundland. *Canadian Journal of Earth Sciences*, **40**, 1375–1391.
- WOOLLACOTT, R. M. & PINTO, R. L. 1995. Flagellar basal apparatus and its utility in phylogenetic analyses of the Porifera. *Journal of Morphology*, **226**, 247–265.
- YAHIEL, G., SHARP, J. H., MARIE, D. & GENIN, A. 2003. *In situ* feeding and element removal in the symbiont-bearing sponge *Theonella swinhoei*: bulk DOC is the major source for carbon. *Limnology and Oceanography*, **48**, 141–149.
- YUAN, X., XIAO, S., PARSLEY, R. L., ZHOU, C., CHEN, Z. & HU, J. 2002. Towering sponges in an Early Cambrian Lagerstätte: disparity between nonbilaterian and bilaterian epifaunal tierers at the Neoproterozoic-Cambrian transition. *Geology*, **30**, 363–366.
- ZRZAVY, J., MIHULKA, S., KEPKA, P., BEZDEK, A. & TIETZ, D. 1998. Phylogeny of the Metazoa based on morphological and 18S ribosomal DNA evidence. *Cladistics*, **14**, 249–285.

Seeing ghosts: Neoproterozoic bilaterian body plans

J. W. VALENTINE

Department of Integrative Biology and Center for Integrative Genomics, University of California, Berkeley CA 94720 USA (e-mail: Jwvsossi@Socrates.Berkeley.edu)

Abstract: Bilaterians originated before 560 Ma. By 520–530 Ma, the fossil record reveals a fauna teeming with bilaterians with highly disparate body plans, in which most living phyla must have been represented. Between these dates, few bilaterian body fossil types have been found, although trace fossils indicate the presence of vermiform animals, small-bodied before the beginning of the Cambrian. The diversity of Cambrian lineages implies a branch-rich phylogenetic tree, yet organisms representing branch nodes of phyla and ancestral alliances of phyla are unknown, and most of the branches are inhabited by ‘ghosts’. The body plans of these ghosts must be precursory to the body plans of crown phyla, and their genomes must be precursory to crown genomes. Bilaterian Hox genes mediate anteroposterior regionation and are usually found in transcriptionally colinear clusters, a feature conserved even when clusters have been broken up during evolution. When body sections mediated by Hox genes are reduced during morphological evolution, the corresponding gene is sometimes deleted. It may be possible to reconstruct the anteroposterior regionation of ghost lineages from Hox clusters modifications. More information on Hox gene assemblages and functions in small-bodied crown phyla, such as acoelomorphs and others, is required to explore this possibility more fully.

The Neoproterozoic has yielded a fascinating, but enigmatic, fauna with marvellous, but mysterious, architectures. Despite indications of the presence of metazoans from *c.* 580 Ma (Xiao *et al.* 1998; Condon *et al.* 2005), it has proven difficult to locate many of the Neoproterozoic fossils on the tree of life. This situation is in contrast to the geologically abrupt appearance of crown phyla during the middle Early Cambrian. Certainly, enigmatic fossils also occur during that ‘Cambrian explosion’ interval, but the Tommotian and especially Atdabanian faunas demonstrate or imply the presence of most crown metazoan phyla, most of which are bilaterians. Clearly there were great radiations of body types following the origin of bilaterians, to produce the many ancestral branches along which the disparate Early Cambrian body plans were assembled. By analogy with radiations that occur when we can trace them in the fossil record, there are likely also to have been many branches arising from those radiations that do not have living or known fossil descendants, and among which the successful branches may actually be in the minority. The Neoproterozoic has not yielded much in the way of bilaterian body fossils. It is certainly possible that *Kimberella* is a stem branch of a lophotrochozoan taxon (Fedonkin & Waggoner 1997) and the sprigginids and vendomiids may have been ecdysozoans (e.g. Fedonkin 1985), but even these forms tell us little about the evolutionary pathways that led to the body plans of crown phyla. Is there any way that we can hope to recover at least

some information about the character of missing Neoproterozoic bilaterian clades in the near absence of a body plan record?

The metazoan tree before the Cambrian explosion

Traditionally, hypotheses of metazoan phylogenies at the phylum and class levels have been based on developmental and morphological similarities, ranging from sperm morphology and cleavage patterns to the gross and microscopic anatomies of adults. As different features have different patterns of resemblance, many different hypotheses were possible, depending on which features were deemed most important—that is, most informative of relationships. For example, the notion that segmentation has arisen once and segmented animals are, therefore, closely related was once widely held, and is still held by some today, although morphologic evidence that segmentation is not homologous among major groups is strong (see Eernisse *et al.* 1992). The molecular phylogenetic tree, although still provisional, also argues against this idea (see below).

As it has become possible to compare DNA sequences among organisms and to erect phylogenetic trees based on mutual sequence similarities of particular genes, such molecular phylogenetics have provided a new dataset with which to evaluate animal relationships that is independent of developmental or morphological data *per se*. However, some genes evolve at different rates than

others, while genes in some animal groups evolve at different rates from those in other groups, and some animal groups evolve at different rates at different times. Such rate variations can result in the same genes in closely related taxa looking rather different

(see Hendy & Penny 1989). Another problem arises if an early radiation is rapid, for those genes not under direct selection for the changes will not evolve many differences, and it may not be possible to resolve the branching pattern (Valentine 2004;

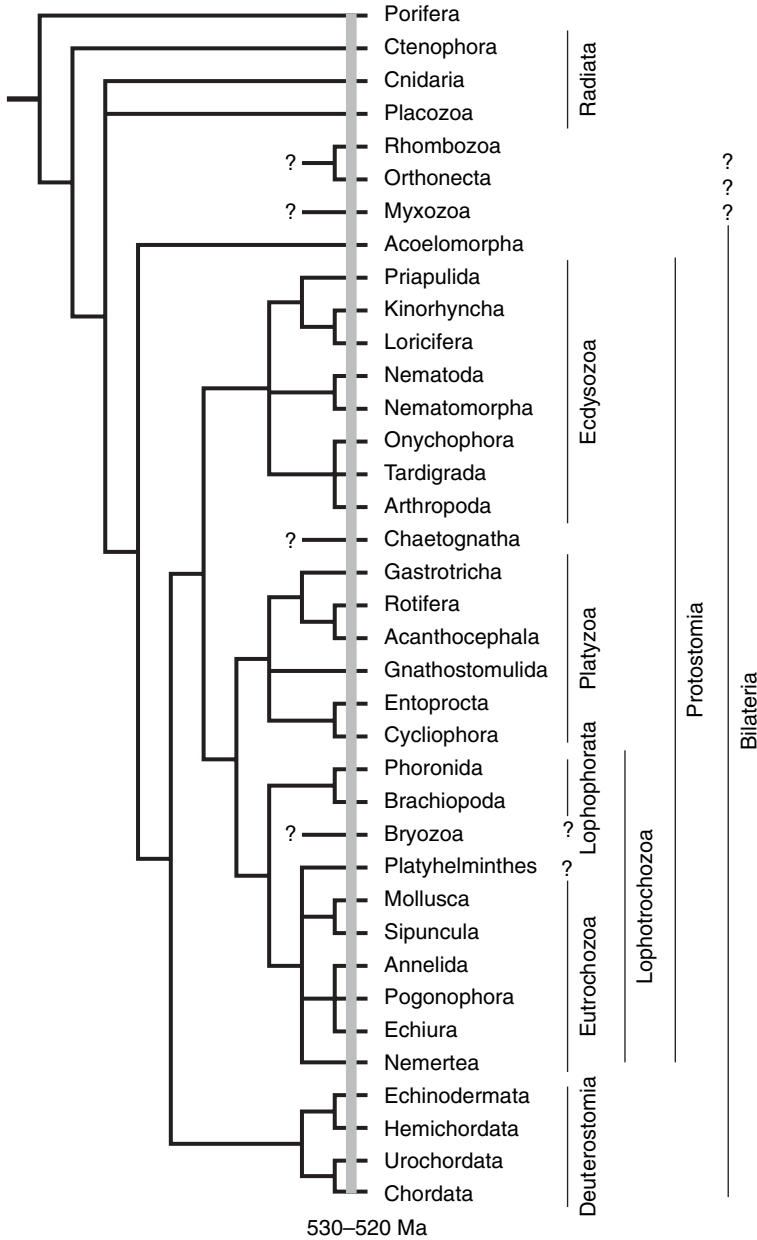


Fig. 1. A provisional hypothesis of the phylogenetic relations among metazoan phyla, based chiefly on the SSU rRNA molecule but supplemented by data from other molecules and, when the often scanty molecular data seem erroneous, on developmental and morphological criteria. The vertical line near the branch tips represents the Cambrian explosion; all of the earlier nodes and most of the risers are occupied by ghosts. After Valentine 2004.

Rokas *et al.* 2005). For these, and somewhat similar reasons, some of the branching patterns of metazoan phyla have not yet been established with certainty from molecular evidence; some of the molecular branchings are likely to be artefacts. However, three major groupings of phyla identified by molecular trees have been supported by numerous studies using varied genes and treeing techniques, and while not thoroughly corroborated, appear presently to be standing the test of time. Some important early contributions to the establishment of these groupings were by Field and others in 1988 (the pioneering study); Lake 1990; Halanych and others 1995; and Aguinaldo and others 1997; important later contributions are far too numerous to list here.

Figure 1 is a tree of metazoan phyla which approximates our knowledge of their interrelationships, based on molecular data but supplemented by developmental and morphological evidence when that seems particularly strong. The grey vertical bar just below the branch tips represents the Cambrian explosion, when body fossils of stem members of many crown phyla first appear. All (or at any rate nearly all) of the nodes representing last common ancestors of major clades occur before we see many body plans—the living phyla are simply represented by a line of distinctive lineages at the crown, and the incredible and unparalleled divergence and branching of the myriad ancestral bilaterian lineages are essentially all ghost lineages. At the base is Acoelomorpha, comprising the formerly flatworm orders Acoela and Nemertodermatida; the acoels appear to be the more basal. Those radiations must have produced large numbers of branches, including stems from the earliest bilaterian radiations, stems from each of the early radiations of the major groupings of phyla, stems from early branchings of sisters within these groupings, and stems from the phyla themselves, some of which we do have from Cambrian faunas. The bilaterian fossils predating the Cambrian explosion must be scattered within the tree, but we are not even sure what nodes they lie between; the possibility that any of them happen to represent any of the nodes in Figure 1 is small indeed.

Neoproterozoic trace fossils

The evidence from much significant work on Neoproterozoic trace fossils indicates the presence of small organisms with the ability to creep on the sea floor or to burrow horizontally, probably just below the sediment surface; some of these organisms could form penetrating burrows, which are minute and rare. The traces first occur *c.* 555–600 Ma. Neoproterozoic trace widths tend to be measured in millimetres (e.g. Crimes 1989; Droser *et al.* 1999),

suggesting the presence of vermiform bodies of perhaps several millimetres or less in length. The lack of significant bioturbation of Neoproterozoic sediments likely indicates that the sea floor was firmer, with less water content in the sediments, thus more likely to preserve traces than is the norm with modern sediments in analogous habitats (Droser *et al.* 2002). Furthermore, some of the trails are likely to have been preserved under algal mats (see Gehling 1999; Dornbos *et al.* 2004). All other things being equal, larger trails and, especially, deeper burrows are more likely to be preserved than small trails and shallow burrows, yet larger traces are the rare ones. Therefore the traces tell us that most benthic ghosts were very small-bodied and most did not burrow or were poor burrowers.

Today, trails that resemble these horizontal Proterozoic traces can be formed by non-coelomate bilaterians using mucociliary locomotory techniques (Collins *et al.* 2000). While organisms with diploblastic body plans are able to produce similar trails, they are not known to do so under normal circumstances, and none of those are yet known that were likely to have been present in the Neoproterozoic. As for the burrows, they could have been formed by small bilaterians via push-pull locomotion, involving anterior and posterior anchors, or via weak forms of peristaltic locomotion. It is well established that the size of traces increased into the centimetre range, and penetrating burrows became more common, at or near the onset of the Early Cambrian (e.g. Crimes 1989; Dzik 2005). The onset of penetrating burrows suggests the presence of fluid skeletons, which could have been either hemocoelic (perhaps something like priapulids) or coelomic (perhaps something like enteropneusts).

Small-bodied crown phyla

The usual way of inferring the body plans of ghosts is to determine the morphological features common to descendant branches that the ghosts must, therefore, have had, although because phyla have such disparate body plans this strategy commonly yields only very general reconstructions at that level. Among living phyla, there is a variety of organisms that might well leave traces similar to those of the Neoproterozoic. However, as there is no record of large bilaterians preceding the earliest Neoproterozoic traces, it is reasonable to eliminate from consideration those small-bodied forms that are descended from benthic ancestors significantly too large to have formed the early traces. Unfortunately, many of the entirely small-bodied phyla have proven difficult to place in the metazoan tree. Some molecular phylogenetic studies have recovered a clade of small-bodied phyla, Platyzoa

(Fig. 1; see Cavalier-Smith 1998; Giribet *et al.* 2000), most members of which were formerly included in the defunct grouping of Aschelminthes. Because Platyzoa originally included acoenelms, which significant evidence now indicates are basal bilaterians, as well as several groups of flatworms, including rhabditophorans, which have the classic cleavage and 4d mesentoblasts of spiralian lophotrochozoans, this grouping seems likely to be an artefact, at least in part. What can be done at present is to examine the architectural features that are widespread among these small-bodied taxa and that can be imputed to have been common among the small-bodied Proterozoic trace-makers.

All of the small-bodied, vermiform bilaterian phyla lack coeloms. These phyla are differentiated along anteroposterior and dorsoventral axes and are triploblastic, with body-wall muscles, usually layered. Some of them are acoenelmate, some pseudocoelomate, and some both, inspiring the term paracoelomate for these forms (Inglis 1985). None of the paracoelomates, even those with pseudocoelms, have blood vascular systems. Most acoenelms do not even have a gut lumen, but most of the paracoelomates do have guts and most guts are entire (the exceptions being obligate parasites that lack guts, and gnathostomulids and flatworm taxa with blind guts). Mucociliary creeping is common, and some paracoelomates can swim, although others are meiofaunal and of these some attach to particles in the substrate. Most paracoelomates have ganglionic brains from which nerve cords run longitudinally, and also proceed to sense organs, but acoenelms do not (Raikova *et al.* 1998). Acoenelms do have a subepidermal nerve plexus, and although many have several longitudinal nerve cords, it is not certain that the cords participate in integrating and coordinating functions. Paracoelomate excretory organs are protonephridia, which however are absent in Acoelomorpha, Gnathostomulida and the parasitic Nematomorpha.

Even among these small-bodied and relatively simple organisms, acoenelms stand out as being simpler. Lacking body cavities and both circulatory and excretory organs, with subepidermal nerve plexuses and 'brains' represented, if at all, by thickened anterior commissures, and with simple reproductive set-ups, acoenelms come close to representing a model stem ancestor for bilaterians. The last common radiate-bilaterian ancestor is likely to have had a subepidermal nerve plexus as a coordinating system, with muscle cells not well developed into muscle (mesodermal) tissues, and may have lacked bilaterian body axes. Presumably the lineage leading to bilaterians developed axial features, a creeping habit, and mesodermal muscles as adaptations to benthic life. Little more is needed to produce an acoenel, which certainly fits

the bill as representing a very early bilaterian body plan.

Inspecting nodes leading to crown phyla (Fig. 1), it is not until the body plans of stem ancestors require hydrostatic coeloms that we can be certain of synapomorphies associated with the last common ancestors of some alliances of phyla. Such a requirement occurs in the annelid/echiuran/pogonophoran stem (schizocoely, and very possibly including the sipunculan stem; the alliances in Figure 1 are, of course, provisional); in the deuterostome stem (enterocoely, pharyngotremy); and perhaps in the phoronid/brachiopod stem (a separate enterocoely?). Perhaps we can squeeze more detail into interpretations of the ghostly early bilaterian architectures if we use genes as well as morphology.

Regulatory genes in early bilaterians

During ontogeny, the gene products that make up parts of a body, such as blood or tissue layers, or that perform physiological processes, such as enzymes, are coded by structural genes. The expression patterns of the structural genes are mediated by regulatory genes, which play the dual roles of architects and skilled artisans in specifying the body plan and insuring that materials are available and correctly assembled during development. It turns out that many of the same regulatory genes are present across a whole array of bilaterian phyla; some are present even in choanoflagellates, more in sponges and many in cnidarians, implying their presence in the last common cnidarian-bilaterian ancestor. The best known and probably most important of the regulatory genes are the Hox genes, a cluster of genes which code for transcription factors that, so far as is known, mediate anteroposterior axial patterning in all Bilateria. As Hox genes are known in Radiata (but not in choanoflagellates or sponges), they were presumably present in the last common ancestor of Radiata and Bilateria (see, for example, Finnerty & Martindale 1999).

A problem in using regulatory genes to interpret morphology is that many have been recruited down through bilaterian history to perform a variety of different functions and thus may affect morphology very differently in different lineages. However, there is a possibility that some aspects of Hox gene expression may prove useful in interpreting Neoproterozoic body plans. Although Hox gene products are certainly used for different developmental functions in different organisms, Hox genes are expressed colinearly when used in anteroposterior axial patterning. That is, they are usually transcribed in the same order that they occur in the cluster, and their domains of expression along the body seem to always be in the same order,

starting anteriorly. Although the Hox clustering is assumed to be the primitive condition—it hardly seems likely that scattered Hox genes would be assembled into a cluster—some of the clusters are broken up, as in the fly *Drosophila*, in which the cluster is in two sections, and in the ascidian *Ciona*, in which the cluster is entirely dispersed. In both these cases, however, the Hox genes remain transcriptionally colinear (Ikuta *et al.* 2004). The reason for this conservation is not resolved.

Not all of the known clusters contain the same Hox genes; in fact, none of the known clusters have the same Hox gene composition in any two phyla, and in the mammals, which have four clusters, each cluster is unique. Some of the differences among phyla are probably owing to paralogy, but some are due to Hox gene loss. In some cases, these losses seem to be correlated with morphology. For example, there is a basic set of 14 Hox genes in chordates, exemplified in the single cluster of *Amphioxus* (Ferrier *et al.* 2000). In *Ciona*, Hox 7, 8 and 9 are missing (Dehal *et al.* 2002). These genes mediate the development of posterior parts of the trunk region in bilaterians and 7 and 8 (presumed orthologs of *abdominal-A* and *Ultrabithorax*) were present in the last common protostome-deuterostome ancestor (de Rosa *et al.* 1999). This region has evidently been lost in ascidians, which certainly display reduced axial differentiation. Further, *abdominal-A* is lost in cirripedes, but is present in other crustaceans, and it has been suggested that this correlates with the reduction in the abdomen of these highly derived creatures (Mouchel-Vielh *et al.* 1998). And finally, the nematode Hox cluster is small, and the genes are scrambled (Kenyon & Wang 1991), yet they remain transcriptionally colinear, and nematode bodies are surely reduced morphologically. Thus in these cases, the loss of Hox genes appears to have a morphological counterpart in the loss of body sections associated with morphological reduction. And, the colinearity of Hox expression domains sometimes enables one to locate the region where the reduction has taken place. This raises the possibility that Hox gene absences in crown bilaterians might yield clues as to the body plans of their Neoproterozoic ancestors.

According to a plausible model of Hox-type gene evolution, the last common radiate-bilaterian ancestor had at least four Hox genes (see Finnerty & Martindale 1999). Three Hox cluster genes are reported in acoels (Baguna *et al.* 2001; Salo *et al.* 2001; Cook *et al.* 2004), representing one anterior, one central, and one posterior Hox type. A *Caudal*-like gene is also present, a Hox-type gene that is, however, not clustered in higher bilaterians. Thus, unless Hox genes have been missed, acoel clusters may have lost at least one, implying that they may be somewhat morphologically reduced from the

stem bilaterian ancestor. The Hox cluster of the last common protostome-deuterostome ancestor (PDA) had at least 7 genes, and possibly more (de Rosa *et al.* 1999), indicating significant growth in the cluster, possibly post-dating the last common acoel-PDA ancestor. During the radiations following the PDA, some Hox genes were lost from the clusters in many phyla.

The timing of these losses is uncertain, but most may have been between the PDA and the rise of crown bilaterian phyla. The reasoning for this notion (Valentine & Jablonski 2003; Valentine 2004) is partly based on the use of the Hox cluster for axial specification, even in cases where axially differentiated organs are absent, as in nematodes. In the relatively simple bodies of early bilaterians, exemplified by acoelomorphs, Hox domains would presumably directly regulate cell or perhaps tissue types along the anteroposterior axis, without an elaborate cascade of regulatory gene expressions following, as there were no appendages or other organs to be built. Deletion of a cell type or some other change in the simple axial pattern would be mediated directly by Hox genes, and thus could involve deletion of the Hox gene itself. So, as the PDA radiated into what was doubtless a wide variety of lineages on, within, and above the Neoproterozoic sea floor, which included subsequent stem ancestors and ancestors at nodes below the stems of living phyla, Hox gene domains were modified as anteroposterior differentiations varied. As those axial patterns were modified in response to the varied requirements of the distinctive marine habitats, some Hox genes were lost, and in different patterns in different lineages. At any rate, these losses had to occur between the PDA, with its cluster, and the crown ancestors of the phyla that display losses in PDA Hox genes. Of course, the addition of Hox genes to some clusters, as may have occurred between the clade ancestor of Rhabditophora and the crown ancestors, further differentiated the Hox gene assemblages.

A major difficulty in further speculation along these lines is that the Hox gene content of the genomes of the small-bodied living phyla is generally unknown, and for such phyla in which Hox genes have been detected, which include rhabditophoran flatworms, the development of the morphologies and functions that they mediate have not been much investigated. Although with the exception of acoelomorphs the living paracoelomates postdate the PDA (Fig. 1), correlation of body-part development with Hox gene function in a variety of paracoelomates could lead to useful models of early body plan differentiation. The comparative study of other key developmental genes in these groups is also likely to greatly improve understanding of the Neoproterozoic evolution of metazoans. Such data are now well within the capacity of molecular

developmental laboratories to acquire; whether these studies will be done at all and soon is simply a matter of priorities.

I thank M. Levine, University of California, for many enlightening discussions of molecular development, and two reviewers, A. Martin and T. Rich, for their comments. University of California Museum of Paleontology contribution no. 1914.

References

- AGUINALDO, A. M. A., TURBEVILLE, J. M., LINDFORD, L. S., RIVERA, M. C., GAREY, J. R., RAFF, R. A. & LAKE, J. A. 1997. Evidence for a clade of nematodes, arthropods, and other moulting animals. *Nature*, **387**, 489–493.
- BAGUNA, J., RUIZ-TRILLO, I., PAPS, J., LOUKOTA, M., RIBERA, C., JONDELIUS, U. & RIUTORT, M. 2001. The first bilaterian organisms: simple or complex? New molecular evidence. *International Journal of Developmental Biology*, **45**, S133–S134.
- CAVALIER-SMITH, T. 1998. A revised six-kingdom system of life. *Biological Reviews*, **73**, 203–266.
- COLLINS, A. G., LIPPS, J. H. & VALENTINE, J. W. 2000. Modern mucociliary creeping trails and the body plans of Neoproterozoic trace-makers. *Paleobiology*, **26**, 47–55.
- CONDON, D., ZHU, M., BOWRING, S., WANG, W., YANG, A. & JIN, Y. 2005. U–Pb ages from the Neoproterozoic Doushantuo formation, China. *Science*, **308**, 95–98.
- COOK, C. E., JIMENEZ, E., AKAM, M. & SALO, E. 2004. The Hox gene complement of acoel flatworms, a basal bilaterian clade. *Evolution and Development*, **8**, 154–163.
- CRIMES, T. P. 1989. Trace fossils. In: COWIE, J. W. & BRASIER, M. D. (eds) *The Precambrian–Cambrian Boundary*. Clarendon Press, Oxford, 166–185.
- DEHAL, P. ET AL. 2002. The draft genome of *Ciona intestinalis*: insights into chordate and vertebrate origins. *Science*, **298**, 2157–2167.
- DE ROSA, R., GRENIER, J. K., ANDREEVA, T., COOK, C. E., ADOUTTE, A., AKAM, M., CARROLL, S. B. & BALAVOINE, G. 1999. *Hox* genes in brachiopods and priapulids and protostome evolution. *Nature*, **399**, 772–776.
- DORNBOS, S. Q., BOTTJER, D. J. & CHEN, J.-Y. 2004. Evidence for seafloor microbial mats and associated metazoan lifestyles in Lower Cambrian phosphorites of southwest China. *Lethaia*, **37**, 127–137.
- DROSER, M. L., GEHLING, J. G. & JENSEN, S. 1999. When the worm turned: concordance of Early Cambrian ichnofabric and trace-fossil record in siliclastic rocks of South Australia. *Geology*, **27**, 625–629.
- DROSER, M. L., JENSEN, S. & GEHLING, J. G. 2002. Trace fossils and substrates of the terminal Proterozoic–Cambrian transition: implications for the record of early bilaterians and sediment mixing. *Proceedings of the National Academy of Sciences USA*, **99**, 12572–12576.
- DZIK, J. 2005. Behavioral and anatomical unity of the earliest burrowing animals and the cause of the ‘Cambrian explosion’. *Paleobiology*, **31**, 503–521.
- EERNISSE, D. J., ALBERT, J. S. & ANDERSON, F. E. 1992. Annelida and Arthropoda are not sister taxa: a phylogenetic analysis of spiralian metazoan morphology. *Systematic Biology*, **41**, 305–330.
- FEDONKIN, M. A. 1985. Systematic descriptions of Vendian Metazoa. In: SOKOLOV, B. S. & IVANOVICH, A. B. (eds) *The Vendian System*, vol. 1. Nauka, Moscow [in Russian; English translation, Springer-Verlag, Berlin, 1990], 70–196.
- FEDONKIN, M. A. & WAGGONER, B. M. 1997. The late Precambrian fossil *Kimberella* is a mollusk-like bilaterian organism. *Nature*, **388**, 68–871.
- FERRIER, D. E. K., MINGUILLON, C., HOLLAND, P. W. H. & GARCIA-FERNANDEZ, J. 2000. The *Amphioxus* Hox cluster: deuterostome posterior flexibility and Hox14. *Evolution and Development*, **2**, 284–293.
- FIELD, K. G., OLSEN, G. J., LANE, D. J., GIOVANNONI, S. J., GHISELIN, M. T., RAFF, E. C., PACE, N. R. & RAFF, R. A. 1988. Molecular phylogeny of the animal kingdom. *Science*, **239**, 748–753.
- FINNERTY, J. R. & MARTINDALE, M. Q. 1999. Ancient origins of axial patterning genes: Hox genes and ParaHox genes in the Cnidaria. *Evolution and Development*, **1**, 16–23.
- GEHLING, J. G. 1999. Microbial mats in terminal Proterozoic siliciclastics: Ediacaran death masks. *Palaios*, **14**, 40–57.
- GIRIBET, G., DISTEL, D. L., POLZ, M., STERRER, W. & WHEELER, W. D. 2000. Triploblastic relationships with emphasis on the acoelomates and the position of Gnathostomulida, Cycliophora, Platyhelminthes, and Chaetognatha: a combined approach of 18S rDNA sequences and morphology. *Systematic Biology*, **49**, 539–562.
- HALANYCH, K. M., BACHELLER, J. D., AGUINALDO, A. M. A., LIVA, S. M., HILLIS, D. M. & LAKE, J. A. 1995. Evidence from 18S ribosomal DNA that the lophophorates are protostome animals. *Science*, **267**, 1641–1643.
- HENDY, M. D. & PENNY, D. 1989. A framework for the quantitative study of evolutionary trees. *Systematic Zoology*, **38**, 297–309.
- IKUTA, T., YOSHIDA, N., SATOH, N. & SAIGA, H. 2004. *Ciona intestinalis* Hox gene cluster: its dispersed structure and residual collinear expression in development. *Proceedings of the National Academy of Sciences USA*, **101**, 15118–15123.
- INGLIS, H. G. 1985. Evolutionary waves: patterns in the origins of animal phyla. *Australian Journal of Zoology*, **33**, 153–178.
- KENYON, C. & WANG, B. 1991. A cluster of *Antennapedia*-class homeobox genes in a nonsegmented animal. *Science*, **253**, 516–517.
- LAKE, J. A. 1990. Origin of the Metazoa. *Proceedings of the National Academy of Sciences USA*, **87**, 763–766.
- MOUCHEL-VIELH, E., RIGOLOTT, C., GIBERT, J.-M. & DEUTSCH, J. S. 1998. Molecules and the body plan:

- the Hox genes of Cirripedes (Crustacea). *Molecular Phylogeny and Evolution*, **9**, 382–389.
- RAIKOVA, O. I., REUTER, M., KOTIKOVA, E. A. & GUSTAFSSON, M. K. S. 1998. A commissural brain! The pattern of 5-HT immunoreactivity in Acoela (Platyhelminthes). *Zoomorphology*, **118**, 69–77.
- ROKAS, A., KRUGER, D. & CARROLL, S. B. 2005. Animal evolution and the molecular signature of radiations compressed in time. *Science*, **310**, 1933–1938.
- SALO, E., TAULE, J., JIMENEZ, E., BAYASCUS, J. R., GONZALES-LINARES, J., GARCIA-FERNANDEZ, J. & BAGUNA, J. 2001. Hox and ParaHox genes in flatworms: characterization and expression. *American Zoologist*, **41**, 652–663.
- VALENTINE, J. W. 2004. *On the Origin of Phyla*. University of Chicago Press, Chicago IL.
- VALENTINE, J. W. & JABLONSKI, D. 2003. Morphological and developmental macroevolution: a paleontological perspective. *International Journal of Developmental Biology*, **47**, 517–522.
- XIAO, S., ZHANG, Y. & KNOLL, A. H. 1998. Three-dimensional preservation of algae and animal embryos in a Neoproterozoic phosphorite. *Nature*, **391**, 553–558.

Towards a morphospace for the Ediacara biota

J. B. ANTCLIFFE & M. D. BRASIER

*Department of Earth Sciences, University of Oxford, Parks Road,
Oxford OX1 3PR, UK (e-mail: jonathan.antcliffe@univ.ox.ac.uk)*

Abstract: The Ediacara biota of the late Neoproterozoic is justly famous as a biological puzzle. Studies of Ediacaran biology have commonly used analogy with living organisms as a cipher for the decoding of biological affinity, and consequently the life mode and habit. Here, we discuss the problems of using such analogous reasoning and put forward our alternative approach, that of using Morphospace Analysis for the study of growth, form and phylogeny. This tool, we suggest, has the potential to be used for testing the unity of an evolutionary clade, such as 'rangeomorphs' and 'dickinsoniomorphs'. Preliminary data from the members of the Ediacara biota do indeed show such a unity within our preliminary morphospace model (all k values are low). This method reveals no clear relationships, between these forms and more recent biological groups such as the sea pens or the Foraminifera.

The problems involved in deducing the biology of long extinct organisms are considerable. Fossils cannot move, reproduce, respire or do any of the things that living organisms do. Their activities can only be inferred from their morphology, from their inferred biological affinities and from the associated environmental information. These difficulties are well illustrated, for example, by the problem of inferring the mode of life in trilobite arthropods (Fortey 1985). As this long extinct group is not thought to be ancestral to any extant arthropod group, their life modes and habits have proved particularly challenging to address. Whereas we can make informed inferences about bivalves from the fossil record because many are alive today (using the principle of uniformity), uniformity cannot be applied directly in the case of a trilobite. There are, of course, living organisms (such as *Limulus*) that are closely related enough to fossil trilobites for us to seek useful *analogies* in both life cycle and behaviour. The study of trilobites is also blessed with detailed biostratigraphic constraints on their fossil record. Even so, the details of trilobite palaeobiology, such as agnostoids, are often moot.

The problems become acute, therefore, when we turn to a group of organisms whose biological affinities are completely uncertain, such as the Ediacara biota of the late Neoproterozoic (Glaessner 1966, 1984). Inferences about the life modes and habits of this biota are not easy to make. One problem here is that the rocks in which they occur are poorly constrained in terms of biostratigraphy and geochronology, so that it is hard to decode their evolutionary history. A second problem arises from the possibility that there were significant differences in the composition of the atmosphere,

hydrosphere, biosphere and lithosphere at the time of the Ediacara biota. Under such circumstances, analogies with modern ecosystems must be fraught with problems.

There are, of course, some things we know about the Ediacara biota that are beyond dispute. First, we have the geological information held within the sediments themselves. This means that we can make useful inferences about the associated facies (and hence make comparisons with modern environments), about sedimentary fabrics and taphonomic processes. Much of this has been done very fruitfully (e.g. Grazhdankin 2000, 2003, 2004), revealing a late Precambrian world that potentially was very different to the Phanerozoic world, which we inhabit. Second, we have the fossils themselves. Unfortunately, the number of analogies drawn between the Ediacaran fossils and living organisms are at least as many as there are authors writing upon the subject. With this methodology, the chosen analogue clearly determines the inference. For example, *Charniodiscus* has been reconstructed as feeding in bottom currents in the manner of modern sea-pens (Jenkins 1992), and *Dickinsonia* has been envisioned as stuck to the sediment surface, drawing in nutrients like a modern deep-sea protist (Seilacher *et al.* 2003).

Such an approach, using analogous reasoning, has a long and respectable history. Fortey (1985), for example, has advocated the use of a closely affiliated, extant organism as an analogue for the functional morphology and behaviour of extinct fossil groups and to increase understanding of their life habits. Unfortunately, we cannot expect the reverse reasoning to be true. That is to say, analogous life modes and habits cannot help to inform

us about taxonomic affinities. Further, no analogue in any situation can actually inform us with regard to the taxonomic position of our problematic fossil. Nor, indeed, can taphonomic studies help us greatly with taxonomic position of an extinct fossil group without the use of arguments themselves based upon analogy. These are real and difficult problems for us because the central question with regard to the Ediacara biota undoubtedly still concerns their taxonomic affinities. Answers to this question will help guide all our other Ediacaran problems.

A new approach

Few features are more useful for distinguishing between the higher taxa, such as classes, phyla and kingdoms, than are their differing modes of growth (see Antcliffe & Brasier 2007). Fortunately, an excellent tool for understanding the growth of long dead organisms is Morphospace Analysis. By this, we mean a graph in which each ordinate has geometric significance, and in which the geometry may be illustrated for selected ordinates at the ordinate point. Hitherto, such morphospace analysis has been undertaken on several groups: molluscs and brachiopods (Raup 1966), foraminiferans (Brasier 1980, 1982), graptolites (Fortey & Bell 1987), bryozoans (Gardiner & Taylor 1980, 1982; McKinney & Raup 1982), higher plants (Honda 1971) and even bird's feathers (Prum & Williamson 2001). Such morphospace studies provide a useful, theoretical structure for the quantification of form, for the accurate discussion of variations in form, and for generating pointed questions about the functional morphology of the group to be posed (such as 'why do these forms exist and not others?'). The most famous morphospace is, of course, that put forward for coiled shell morphology by Raup (1966) based on the logarithmic spiral mode of growth, following the pioneering work of Thompson (1917). This 'Raupian' morphospace was so constructed as to include all mollusc groups, as well as some rhizopod protists and some of the Lophotrochozoa.

Several important conclusions can be drawn from the morphospace of Raup (1966), that are hugely important in evolutionary terms, but which have received scant notice. First, and remarkably, all of the univalved and bivalved molluscs fit into this morphospace. Second, the presence of nearly all molluscs within this morphospace can be taken to imply their unity as a clade. In other words, limited exploitation of morphological possibilities may be taken to imply shared evolutionary constraints from a common ancestry. Those that are absent from this morphospace (for instance the heteromorph ammonoids and vermetid gastropods) are

members that have diverged in their mode of growth from the molluscan 'archetype' described by the Raupian model. It could therefore be argued that the Raupian morphospace provides an incomplete description of the Mollusca. However, it does contain all major molluscan groups—it is only derived subgroups within these that depart from the rules of Raupian morphospace. Third, the mode of growth described in the Raupian morphospace may be representative of the initial conditions for the molluscan growth system.

Morphospace analysis is surely a valuable tool that may yet be shown to have the potential for discrimination between higher taxonomic units. Exceptions that depart from a prescribed morphospace (see above) should not, of course, be taken to imply the formation of new, higher taxa. Like any other feature in phylogenetic analysis, a distinction needs to be made between those situations in which the mode of growth can be considered as a homology, and those in which it would tend to mislead our interpretation of higher taxonomy as a result of homoplasious behaviour. Such a situation is seen, for example, in the heteromorph ammonites and vermetid gastropods previously mentioned. Here, the novel feature of uncoiling is swamped by other homologies (such as embryology, mantle and gills) that clearly imply that these forms are indeed molluscs. Patterson (1982) has helpfully discussed the kinds of criteria needed to establish a given feature as a homology. One criterion is that of 'ontogenetic procedures', notably those of embryonic development, which are likely to be closely linked to the modes of growth. Clearly, the use of homologous growth modes for the determination of higher taxonomic affinities is an interesting, but complex, issue. For the present, we are content to draw attention to the idea that mode of growth is, potentially, a very informative feature for the decoding of long extinct organisms.

There is, of course, little value in developing a morphospace that cannot be easily related to the actual geometry of organisms (McGhee 2001). Thus, the development of a morphospace must be intimately connected to realistic methods for the actual measurement of form. There has been a growing movement over the last decade to quantify morphology in detail. These measurement methodologies have arisen largely in response to the populational approach demanded by evolutionary theory. These methods, termed morphometrics ('measurements of form'), have proven very successful at revealing natural groupings and evolutionary trends (e.g. Hughes 1999). McGee (2001) has discussed the derivation of morphospaces and their integration with morphometric methods to provide what he termed 'a (complete) integrated theoretical morphometry' of the

organism. Although such studies are currently unusual, they clearly point the way forward for palaeobiological research.

Most morphospaces (certainly any biological ones, as opposed to ones quantifying Neolithic axe heads for instance) so far developed make assumptions about the mode of growth. Such morphospaces cannot, however, be directly applied to any group of organisms for which we do not know the mode of growth. We can turn the problem around, however. Rather than using a model of growth to derive a morphospace, we can use a general morphospace (where growth is not an assumed factor) to learn about the mode of growth and thereby make reasoned biological inferences. This is the essential paradigm of our methodology. In such a morphospace, the organisms will 'grow' through the space rather than being confined to a particular point throughout its ontogeny. In this way, the pathways that extinct fossil organisms mark out through their growth may be able to reveal something valuable about the developmental procedures of their group. The greater the number of forms that are parametricised and 'fitted in' to the morphospace, the more robust will be the conclusions that may be drawn.

Formulation—a theoretical morphospace for the Ediacara biota

Here, the formulation of a theoretical morphospace that has general applicability is outlined as is its potential to describe taxa of the Ediacara biota and their possible relatives. The derivation begins with an appreciation of how to define the relationships between points in space.

Mode of line origination (M)

The parameter *M* describes how any given line originates and terminates. This can be best displayed by illustrating *M* as a 'branching tree'. This should not be taken to infer a bifurcating system, though this is allowed by the system. Given a line in space with an origination point and a termination point, then *M* describes how another line in space relates to this line.

In order to do this, we require that there is also another point (termed a node) that lies somewhere on the line defined by the two points. At this node, another line finds its origination point (see Fig. 1b).

After a node, it is necessary to define whether there are additional nodes between node 1 and the termination point on the original line, and whether

there are any nodes on the new line. This is what is formalized by the parameter here called *M*.

In the continual bifurcation, each line originating from the node has another node somewhere along its length before termination. The nature of termination in such bifurcating systems was discussed by Fortey & Bell (1987) with respect to multiramous graptolites, though it should be noted that they did not formalise the line origination in this manner, since they had no need to do so for the purpose of their study.

The inter-point function, F(x, y, z)

In the discussion above, the form of the line between the origination and termination points was assumed to be linear. This form is again shown below, but now with the addition of Cartesian axes. In the general case, $F(x, y, z)$ may be a complex function in three dimensions. That is, it may not entirely lie in the x - y plane. In any case, the form of the inter-point function can be described by a Fourier series, though it may differ as to whether a two- or three-dimensional form is required.

Additionally, it would be possible for the inter-point function to take an ellipsoidal or other closed form (any polygon). This would allow a very accurate description of segmented and septated forms. Again, this could be achieved by Fourier series and effectively incorporates the field of outline analysis (as in studies by Foote 1989; Harper & Owen 1999). The linear form is here taken for the inter-point function. This is a reasonable approximation for most of the forms to be considered, and it is certainly a sensible starting point. However, the natural extension of the work to more complex forms of the inter-point function needs to be noted. Though these will not necessarily alter any of the evolutionary interpretations that can be made, they will make the 'morphospace individuals' look more like real fossil specimens.

The position of the node—the k ratio

The position of the node along the line can now be outlined for the general case. The *k* ratio for a given node is defined as follows:

$$k = \ell/L$$

Where: *L* is the linear distance measured between the two adjacent nodes (or an equivalent termination/origination point) on the line, as shown in Fig. 1e, ℓ is the distance between the node in question and the previous node on the line (or origination point is here called ℓ). Note that by definition, there cannot be another node after the termination point.

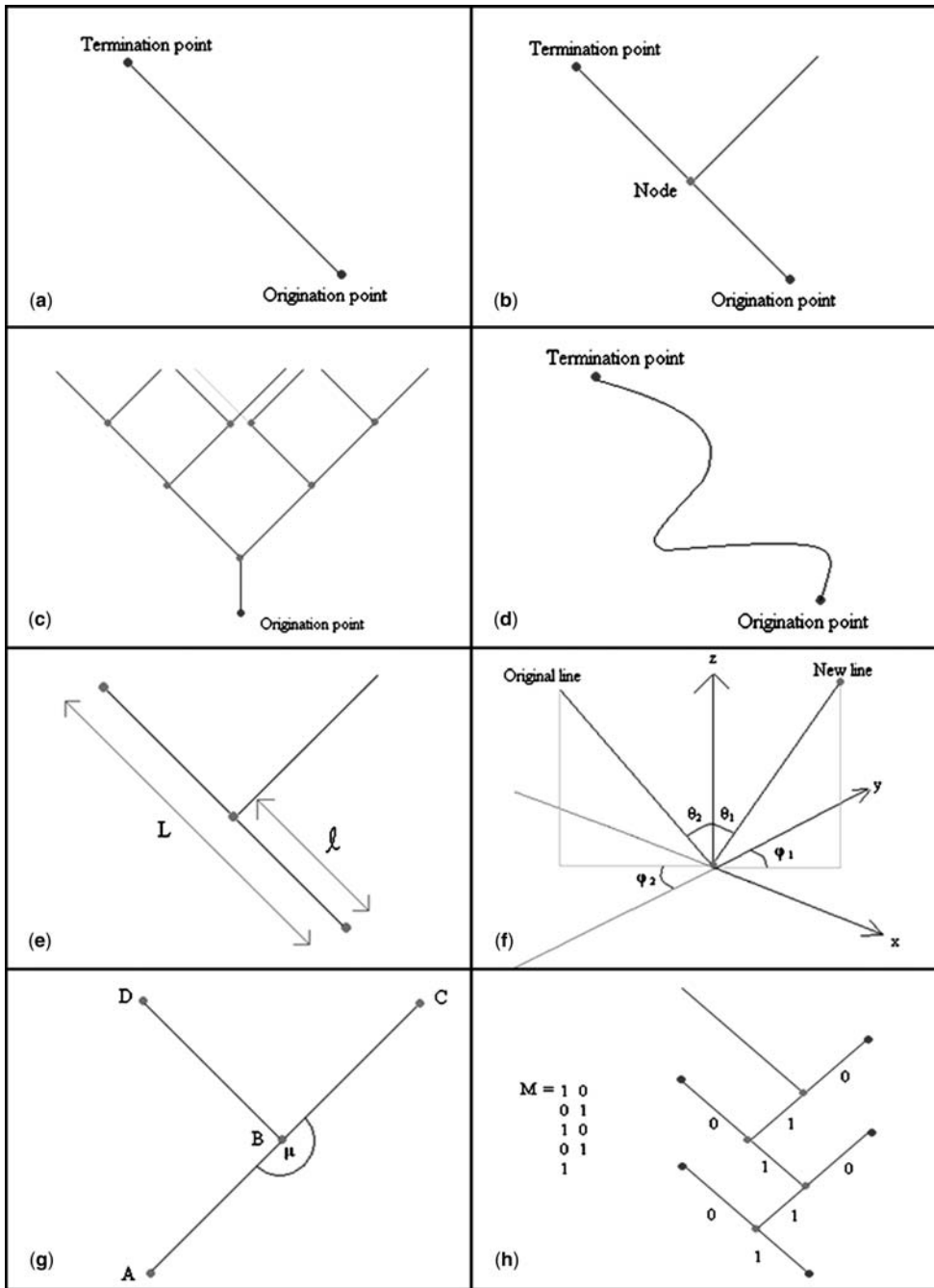


Fig. 1. (a) A line in space defined by an origination point and a termination point. The form of the line between these two points requires another parameter to describe it. (b) The same line in space but with another line originating along its length. (c) The form of M determines the style of line origination and thus influences the overall topology of the form. (d) A more complex form of the inter-point function. (e) Illustrating the measurement of L and l so as to allow the calculation of the parameter k . (f) The angular relations of the two lines. (g) The orientation of the original line after a node must be specified—this is achieved with parameter μ . (h) The statement of M applicable to geometry removes a large range of potential forms from the morphospace—for instance, all bifurcating perpetuating systems (e.g. as in multiramous graptolites, trees).

By taking the ratio of these two lengths, we have produced a dimensionless parameter that will not be altered by the size of the organism *per se* but may vary throughout ontogeny as a result of the mode of growth.

The position of the new line

The new line takes its origination point at a node on the previous line, as described by *k*. We require, however, another point to define this new line uniquely in space. This point is the termination point or the first node on the next line. The position of this line in relation to the previous one can be described uniquely in space by the presence of just four angles (see Fig. 1f).

Note that the origin lies at the node from which the new line originates. The orientation of the *z*-axis is problematic. It could be taken to be the long axis of the organism in question, which would be applicable to many forms. However, the long axis may be obscure in several easily imaginable ways. A slightly more applicable (if less detailed) approach is to assume that ϕ_1 and ϕ_2 are equal (so that the form can be described with only two axes) and that θ_1 and θ_2 are equal (and so we take half the angle between the two lines to get θ values.) This allows a logical extension of the study to understand the nature of the *z*-axis in any forms where it was forced to distort from node to node and through ontogeny.

Orientation of the original line after a node— μ

Consider Fig. 1g. The orientation of the line BD has been determined with respect to the line BC. However this needs to be calibrated by stating the orientation of BC with respect to AB. After all, there is no particular reason that ABD could not be considered the original line and B the node for the origination of the new line BC. By making the following definition, this ambiguity can be removed. The original line is that which continues through the node, with μ closest to 180° . Note that it is not necessary to specify the Cartesian geometry in this case, because for any two lines that share a common point (the node) in space, there is a unique plane that contains both lines— μ is measured in this plane.

A plane for Ediacaran geometry

By taking several particular cases to the treatment above, it is possible to define a plane of the morphospace that will clarify the geometry of many members of the Ediacara biota. It is also possible to define (M) so that is applicable to many

members of the Ediacaran biota, as illustrated is Fig. 1h.

Note that the value of μ is shown to be 180° ; hence this parameter need not be considered further in relation to our Ediacaran geometry. The structure above is planar, so there is also no need to specify values of ϕ (and the associated complexity of determining an appropriate *x-y* plane). We have already stated that the inter-node function, (F), shall not be considered further in this work. Thus, a plane for Ediacaran geometry can be defined with only *k* and θ as variables. It should not be forgotten, of course, that this is a 'morphospace creature' and not a real one. It need not necessarily look exactly like a particular form in any given case. Further, the choice of the origination point, nodes, and terminations points is effectively arbitrary. It is simply required for them to have some consistency across the study, and it is sensible to choose a particular point that can be located on all forms of interest (there is an extensive literature on landmarks as homologies and we refer the reader to Macleod 2001 and Zelditch *et al.* 2001). Thus the line represented by $F(x,y,z)$ does not have to correspond to any given line of actual organism geometry.

It is now essential to relate these parameters to actual organism geometry, by choosing the location of the morphospace nodes using morphometric landmark analysis (*sensu* Bookstein 1991). The example shown is that of *Phyllozoon hanseni* (Fig. 2a, b), which is deliberately chosen because it is a distorted specimen that requires additional treatment before the morphospace, parameters can be extracted. Landmarks are selected that define the geometry of the specimen (Fig. 2b)—consistent with the extraction of the morphospace parameters. An origin for a coordinate system is selected (the top left pixel of the image—this is rather arbitrary and has no effect on results) such that the landmarks can be described by coordinates. The coordinates are then placed into a spreadsheet and viewed without the fossil (Fig. 2c). The approach is comparable to that of Hughes (1999). Regression lines are then fitted to this data to show where the form departs from the ideal (see Fig. 2d). The central axis should be straight; the trend lines quantify how the form departs from the ideal.

The illustrated form departs from ideal by 12° at around $x = 250$. A simple rotational matrix can be used to transform the data set so that no points are in 'incorrect positions'. It should be noted that this kind of work varies specimen-by-specimen and so the method has to be subtly adapted to suit the nature of the deformation. The restored form can be seen in Fig. 2e.

It needs to be stated that while the form still appears to be asymmetric, this cannot be assumed

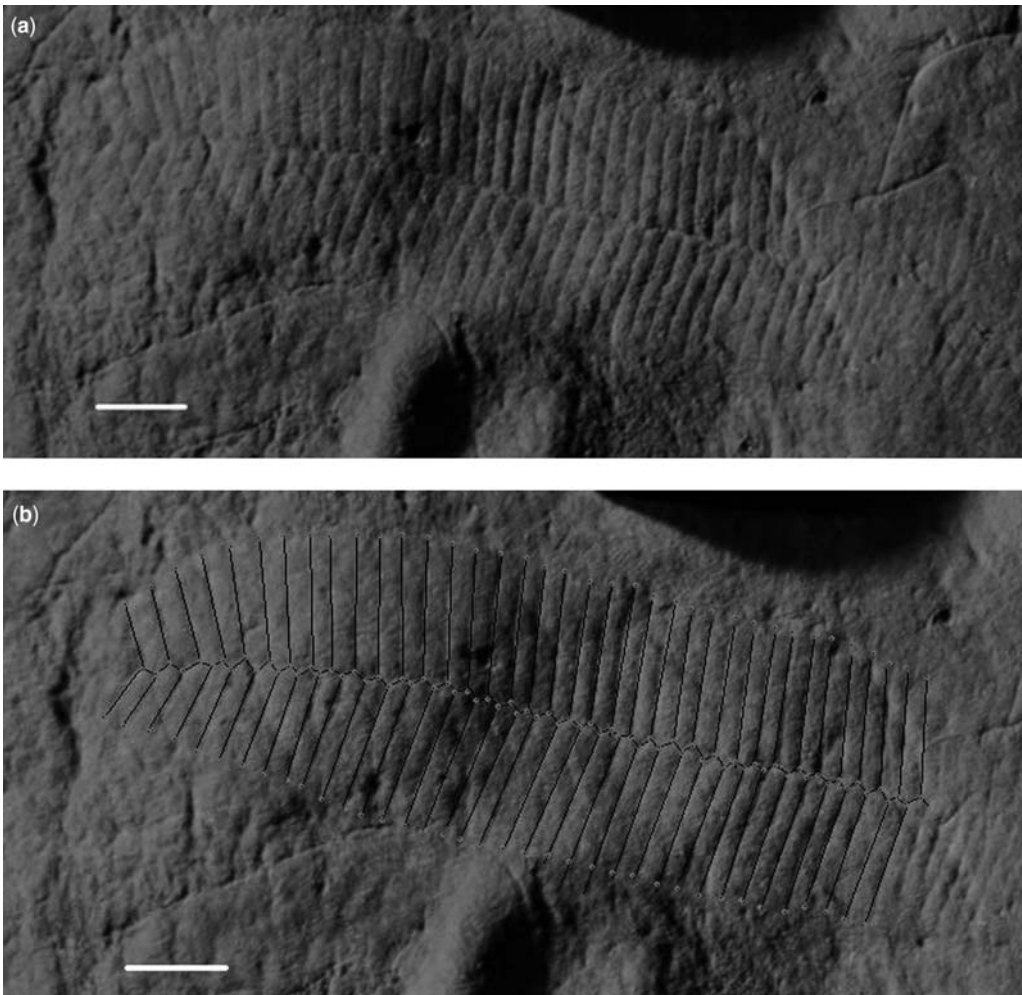


Fig. 2. (a) An image of *Phyllozoon hanseni* from the Flinders Ranges. Photograph: M. D. Brasier. Scale: 1 cm. (b) The same image with morphometric landmarks to define the geometry. Scale: 1 cm. (c) Landmarks are extracted for numerical analysis. (d) Regression analysis of the landmark data. (e) The form after it has been undeformed. It is also a reflection of the image as was previously shown. (f) Illustrating how morphospace parameters are extracted from the restored form.

to be a taphonomic effect because the asymmetry may represent the actual organism geometry. Indeed, Seilacher (1989) and many others have suggested that this asymmetry is a characteristic of Vendobionta construction. From this, the points can be reconnected and the appropriate morphospace parameters extracted. If deformation is not removed, we find that there is little effect upon the morphospace parameters for the majority of the specimens because only those nodes with $x < 250$ have been altered.

For every node, there is a value of k and θ . The orientation of the nodes describes the entire

geometry of the form, thus the k and θ pairs for every node will also describe the whole organism. By plotting k against θ , it is thereby possible to characterize morphology of many Ediacaran organisms.

Results and discussion

Preliminary morphospace results are here presented, (see Fig. 3; plots of k against θ) for taxa in the Ediacaran biota; *Charnia masoni* (holotype), *Phyllozoon hanseni* and *Charniodiscus* sp.

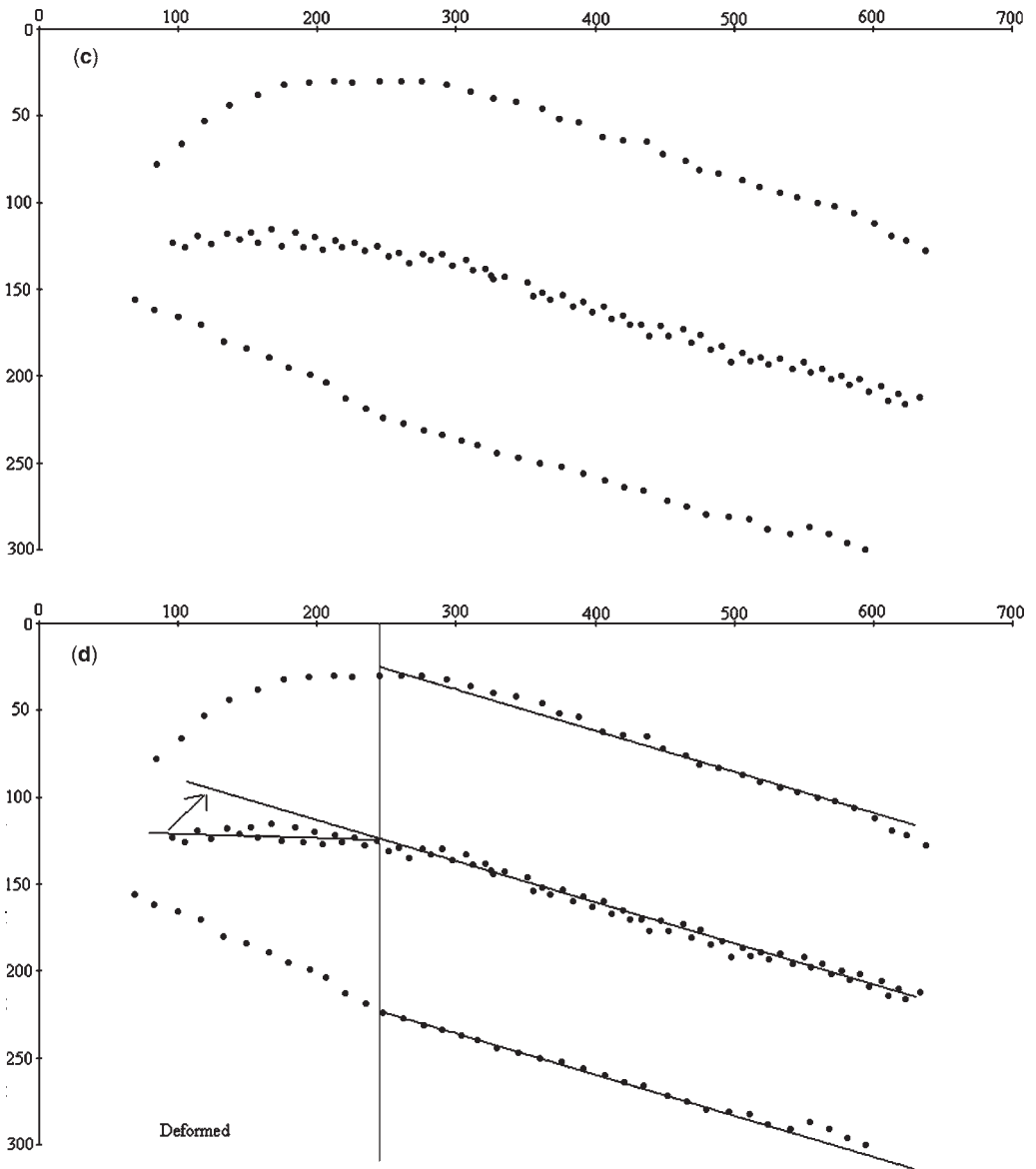


Fig. 2. (Continued).

(holotype). We also plot, for comparison, the plant leaves of living angiosperms *Musa* sp. (banana plant), *Calathea* sp., *Piper* sp., *Alocasia* sp. and *Curculigo* sp. A plot for the biserial foraminiferid *Brizalina* sp. (following the model from Brasier 1982) is also shown. It can be seen from this figure that many disparate Ediacara fossil forms (e.g. *Charnia* sp., *Dickinsonia* sp. and *Phyllozoon* sp.) share fundamentally similar morphospace parameters (k values are all confined to values

between 2 and 5, which is not true for any other group plotted). They are distinguished as a unique group within a morphospace plane and, significantly, they are not closely approached by many putatively similar groups such as the fronds of sea pens, biserial Foraminifera, and plant leaves. The latter show an interesting area of overlap but their total morphospace is much larger. We find that many other groups with suggested affinity to the Ediacara biota,

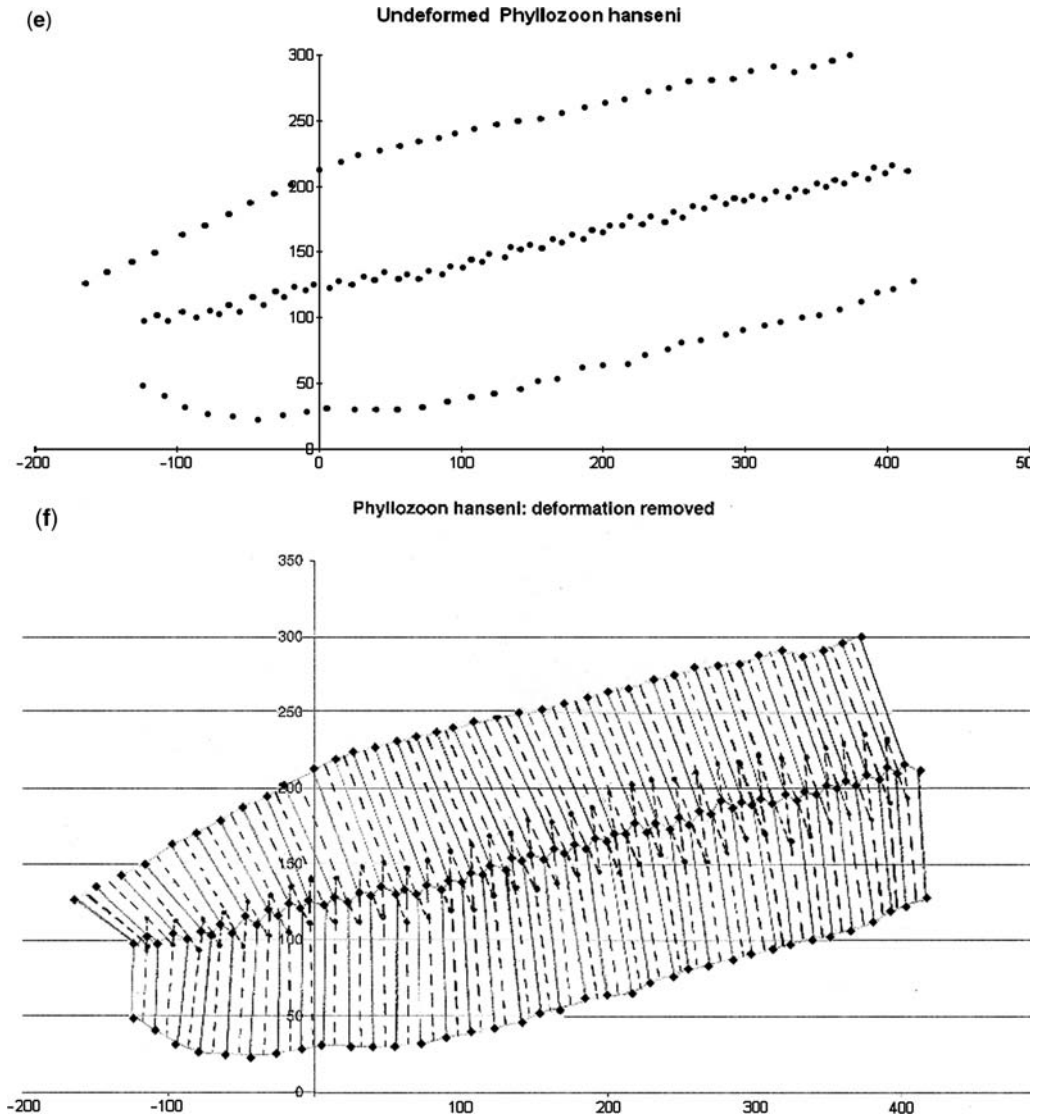


Fig. 2. (Continued).

particularly the xenophyophore foraminiferids (Seilacher *et al.* 2003) require very different parameters to describe them and do not plot in the same morphospace plane (except artificially by parameter projection—like a vector trace). Further morphospace work is required, using the best preserved fossil material, in order to determine the significance of the gaps in morphospace between the extinct Ediacara biota and putatively similar looking groups that are alive today. This should, ultimately, allow us to determine a viable

mode of growth for Ediacaran organisms and, therefore, test the potential higher taxonomic standing of this enigmatic group. At a lower taxonomic level, however, that is within the Ediacara biota, we may now tentatively begin to consider the significance of these early morphospace results. If members of the Ediacara biota are indeed closely related, then there should be a viable evolutionary progression with corresponding alterations in morphospace from the earliest forms to the later ones.

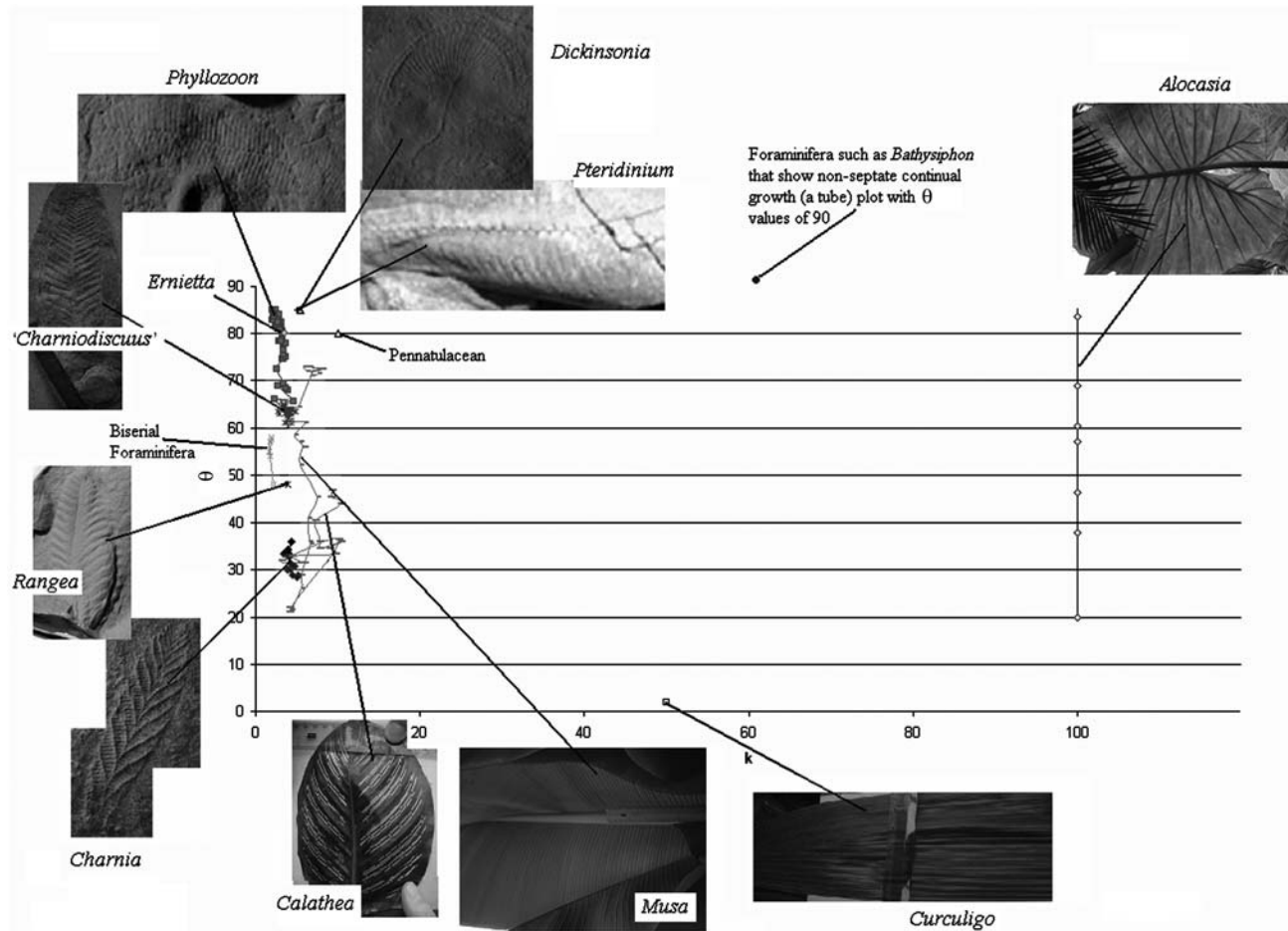


Fig. 3. Illustrates the paths in morphospace required to describe the following forms uniquely: *Charnia masoni* (holotype), *Phyllozoon hansenii* and *Charniodiscus concentricus* (holotype). Plant leaves of the following forms are also shown for geometrical comparison—*Musa* sp. (banana plant), *Calathea* sp., *Piper* sp., *Alocasia* sp. and *Curculigo* sp. A biserial foraminiferid following the model from Brasier (1982) is shown as well. It can be seen that many disparate Ediacara fossil forms (e.g. *Charnia* sp., *Dickinsonia* sp. and *Phyllozoon* sp.) occupy a similar region of the morphospace plane. Further, the interrelationships between members of the Ediacara taxa are only beginning to be understood.

We would like to thank the reviewers S. Jensen and G. Narbonne for their constructive comments. We are also grateful to the editors who have been diligent and tireless in their efforts to improve the manuscript. The research was made possible by a NERC grant awarded to J. B. Antcliffe by the UK government.

References

- ANTCLIFFE, J. B. & BRASIER, M. D. 2007. *Charnia* and sea pens are poles apart. *Journal of the Geological Society of London*, **164**, 49–51.
- BOOKSTEIN, F. L. 1991. *Morphometric tools for Landmark Data: Geometry and Biology*. Cambridge University Press, Cambridge.
- BRASIER, M. D. 1980. *Microfossils*. Chapman and Hall, London.
- BRASIER, M. D. 1982. Architecture and evolution of the foraminiferid test: A theoretical approach. In: BANNER, F. T. & LORDS, A. R. (eds) *Aspects of Micropalaeontology*. Allen and Unwin, London, 1–41.
- FOOTE, M. 1989. Perimeter-based Fourier analysis: a new morphometric method applied to the trilobite cranium. *Journal of Paleontology*, **63**, 880–885.
- FORTEY, R. A. 1985. Pelagic trilobites as an example of deducing the life habits of extinct arthropods. *Transactions of the Royal Society of Edinburgh*, **76**, 219–230.
- FORTEY, R. A. & BELL, A. 1987. Branching geometry and the function of multiramous graptolites. *Paleobiology*, **13**, 1–19.
- GARDINER, A. R. & TAYLOR, P. D. 1980. Computer modelling of colony growth in a uniserial bryozoan. *Journal of the Geological Society, London*, **137**, 107–122.
- GARDINER, A. R. & TAYLOR, P. D. 1982. Computer modelling of branching growth in the bryozoan *Stromatopora*. *Neues Jahrbuch für Geologie und Paläontologie, Abhandlungen*, **163**, 389–416.
- GLAESSNER, M. F. 1966. Precambrian palaeontology. *Earth Science Reviews*, **1**, 29–50.
- GLAESSNER, M. F. 1984. *The Dawn of Animal Life: A Biohistorical Study*. Cambridge University Press, Cambridge.
- GRAZHDANKIN, D. 2000. The Ediacaran genus *Inaria*: a taphonomic/morphodynamic analysis. *Neues Jahrbuch für Geologie und Paläontologie, Abhandlungen*, **216**, 1–34.
- GRAZHDANKIN, D. 2003. Structure and depositional environment of the Vendian Complex in the South-eastern White Sea area. *Stratigraphy and Geological Correlation*, **11**, 313–331.
- GRAZHDANKIN, D. 2004. Patterns of distribution in the Ediacaran biotas: facies versus biogeography and evolution. *Paleobiology*, **30**, 203–221.
- HARPER, D. A. T. & OWEN, A. W. 1999. Quantitative and morphometric methods in Taxonomy. In: HARPER, D. A. T. (ed.) *Numerical Palaeobiology: Computer-based Modelling and Analysis of Fossils and their Distributions*. Wiley, London, 1–40.
- HONDA, H. 1971. Description of the form of trees by the parameters of the tree like body: Effects of the branching angle and the branch length on the shape of the tree like body. *Journal of Theoretical Biology*, **31**, 331–338.
- HUGHES, N. C. 1999. Statistical and imaging methods applied to deformed fossils. In: HARPER, D. A. T. (ed.) *Numerical Palaeobiology: Computer-based Modelling and Analysis of Fossils and their Distributions*. Wiley, London, 127–156.
- JENKINS, R. F. 1992. Functional and ecological aspects of Ediacaran assemblages. In: LIPPS, J. H. & SIGNOR, P. W. (eds) *Origin and Evolution of the Metazoa*. Plenum Press, New York, 131–176.
- MACLEOD, N. 2001. Landmarks, Localization, and the use of morphometrics in phylogenetic analysis. In: ADRAIN, J. M., EDGEcombe, G. D. & LIEBERMAN, B. S. (eds) *Fossils, Phylogeny and Form: An Analytical Approach*. Kluwer/Plenum, New York, 197–234.
- MCGHEE, G. R. 2001. *Theoretical Morphology: The Concept and its Applications*. Columbia University Press, New York.
- MCKINNEY, F. K. & RAUP, D. M. 1982. A turn in the right direction: Simulation of erect spiral growth in the bryozoans *Archimedes* and *Bugula*. *Paleobiology*, **8**, 101–112.
- PATTERSON, C. 1982. Morphological characters and homology. In: JOYSEY, K. A. & FRIDAY, A. E. (eds) *Problems of Phylogenetic Reconstruction*. Academic Press, London, 21–74.
- PRUM, R. O. & WILLIAMSON, S. 2001. Theory of the growth and evolution of feather shape. *Journal of Experimental Zoology*, **291**, 30–57.
- RAUP, D. M. 1966. Geometric analysis of shell coiling. *Journal of Paleontology*, **40**, 1178–1190.
- SEILACHER, A. 1989. Vendozoa: organismic construction in the Proterozoic biosphere. *Lethaia*, **22**, 229–239.
- SEILACHER, A., GRAZHDANKIN, D. & LEGOUTA, A. 2003. Ediacaran biota: The dawn of animal life in the shadow of giant protists. *Paleontological Research*, **7**, 43–54.
- THOMPSON, D. A. W. 1917. *On Growth and Form*. Cambridge University Press, Cambridge.
- ZELDITCH, M. L., SWIDERSKI, D. L. & FINK, W. L. 2001. Homology, characters, and morphometric data. In: ADRAIN, J. M., EDGEcombe, G. D. & LIEBERMAN, B. S. (eds) *Fossils, Phylogeny and Form: An Analytical Approach*. Kluwer/Plenum, New York, 145–196.

The nature of vendobionts

A. SEILACHER

Yale University and Tübingen University (e-mail: geodolf@tuebingen.netsurf.de)

Abstract: The notion that the majority of Ediacaran fossils do not represent stem groups to modern metazoan phyla is now increasingly accepted. Nevertheless, the further claim of the vendobiont hypothesis needs to be elaborated: that these large and seemingly complex organisms were not truly multicellular. Arguments for interpreting vendobionts as an extinct class of rhizopodan Protozoa are: (1) negative allometry of the quilts; (2) presence of a loosely englutinated, but sandy fill skeleton similar to the xenophyophorian *stercomare*; (3) a disparity of designs and lifestyles that would be incompatible with metazoan bauplans and feeding strategies; (4) unusual patterns of regeneration; (5) resting traces of some mobile, epibenthic species.

Undoubted metazoans were certainly present in the later part of the Ediacaran Period; but with regard to size, frequency and diversification they remained in the shadow of what we consider as giant protozoans (vendobionts and xenophyophores). These ‘unicellular dinosaurs’ seem to have dominated shallow-marine sea bottoms before becoming extinct or exiled into deep-sea environments in the Precambrian–Cambrian transition.

Most palaeontologists agree that the benthic biota recorded in Ediacara-type *Konservat-lagerstätten* of the terminal Proterozoic were strange compared to any modern biocoenosis. Firstly, they built on the virtually ubiquitous tough *biomats* (Seilacher & Pflüger 1994; Bottjer *et al.* 2000), which provided the soft-bodied organisms with a firm substrate in life and with a unique kind of fossilization thereafter (‘death masks’; Gehling 1999). Secondly, no macropredation appears to have taken place (‘Garden of Ediacara’; McMenamin 1986). Other differences, such as low oxygen levels, can only be inferred (Rye & Holland 1998).

Still under discussion is the *phyletic* affiliation of the foliate Ediacaran fossils (Vendobionta), which are here considered as an extinct order (or subclass) of rhizopods (Seilacher *et al.* 2003). Their original interpretation as sea-pens or segmented worms (Glaessner 1984) faces functional difficulties. On the other hand, they share a unique foliate construction (quilted pneus; Seilacher 1984) and a flexible, non-agglutinated wall that was not shed, but could expand during growth without moulting. At one time they were even considered an extinct kingdom (Seilacher 1992). Later (Seilacher 1994; Narbonne 2005), some of the Ediacaran fossils were singled out as true animals; but only with the study of mat-living xenophyophores, common in Ediacaran biota (Seilacher *et al.* 2003; fig. 8), was the riddle of the vendobionts, in the author’s view, solved. In the following paper, arguments for their claimed protozoan nature will be reviewed.

Abbreviation: YPM, Yale Peabody Museum, New Haven, Connecticut, USA.

Quilting patterns

In analogy to air mattresses and waterbeds, ‘quilting’ describes a principle, by which a balloon (pneu) is transformed into a flat structure. Functionally it means that the organism can maintain compact shapes that still have a large surface area relative to body volume for interaction with the environment (respiration; nutrient uptake). But quilting also implies that the living content of such a structure is being compartmentalized. In combination with growth, vendobionts likely used two modes to achieve compartmentalization.

In the serial mode (e.g. *Dickinsonia*, *Phyllozoon* and *Pteridinium*), new compartments were added at one or two poles (vegetation points) of the body. In this model, each quilt initially increased its volume by expanding and by growing longer transverse to the body axis; but it usually ceased to grow wider after reaching a certain dimension. *Dickinsonia* and *Yorgia* are bilateral, but without a median seam. *Phyllozoon*, also flat, had such a seam and the ability to introduce new vanes at the margin. In *Namalia* and *Ernietta*, the zigzagged median seam at the base ceased growing at an early stage, and the original two vanes joined into a cylindrical bag, whose quilts continued to grow upward. In older individuals of *Ernietta*, secondary vanes were introduced and grew upward on the outside of this bag at a distance from the primary seams. *Pteridinium* may be either flat (*P. nenoxa* and *P. carolinaensis*) or boat-shaped (*P. simplex*), with a third (median) vane rising from the median seam (Fig. 2b). The fine quilting pattern of *Nasepia* is not clear, because it disappears in the central area of the holotype frond. In principle, it was built like *Ernietta*.

Simple changes in growth programs are probably more adequate than Pflug's (1972) hypothetical reconstructions and terminologies to account for observed morphological disparities.

In the fractal mode, a finite number of primary quilts were initially established in serial succession. As they expanded, secondary and tertiary quilts subdivided the contents from one or both margins.

Members of the Newfoundland biota modified this fractal scheme developing a number of lifestyles: (1) the spindle-shaped form ('*Vendofusus*') was constructed from about 20 pairs of primary quilts, alternately arranged along a median seam. Even after the serial addition of new quilts had stopped, the two equivalent poles maintained their tapering outline; (2) a rarer leaf-shaped species (Seilacher 1992) possessed a similar biserial arrangement of primary quilts, but had a single growth pole. Also, the secondary subdivision of the chevroned primary quilts was asymmetric (they started only from the 'proximal' flanks); (3) in elevated forms (*Charniodiscus*), primary quilts are also chevroned in two series, or vanes, along the axis. Their secondary subdivisions may either cut right across the quilts or begin fractally as oblique chevrons from each side (Narbonne 2004); (4) in the bush-like form (*Bradgatia*), primary quilts form a fan, radiating from a single point. Secondary quilting is again chevroned and symmetrical; (5) the comb-like and fern-like forms are not well enough preserved for such categorization. Except in the upright *Charniodiscus* and an unnamed rangeomorph (Narbonne 2004) all fronds were adhering to biomats and did not become aligned by felling or transport.

In contrast to the erect rangeomorphs from Newfoundland, the Namibian *Rangea* itself may have lived immersed in the sand. Accordingly, it had a three-dimensional structure, with primary quilts rising obliquely from each side of a horizontal axis (see below).

In conclusion, the versatility of quilting patterns and lifestyles is difficult to accommodate with metazoans. On the other hand, allometric compartmentalization of a multinucleate (plasmodial) protoplasm is a common feature also in other oversized rhizopodan protists (Xenophyophoria; larger Foraminifera).

Englutinated fill skeletons

The interpretation of vendobionts as kinds of giant protists is supported by analogy with the Xenophyophoria. These rhizopods appear to have also been common on Ediacaran matgrounds (Seilacher *et al.* 2003); but they also survive on present deep-sea bottoms (Tendal 1972). In contrast to vendobionts,

they have a flexible, but agglutinated and non-expandable wall; otherwise the similarity between the two groups is remarkable. The giant genus *Stannophyllum*, for instance, produces foliate structures that consist of sausage-shaped quilts (here called chambers) and reach up to 25 cm in the adult stage.

What makes xenophyophores even more similar to serially growing vendobionts is the scale of quilting. While the compartments of larger foraminifers have micrometric diameters, they become millimetric in vendobionts and xenophyophores. If compartments must not exceed a certain diameter for metabolic reasons (e.g. diffusion rates), why is this limit not the same in all unicellular organisms?

The answer comes from modern xenophyophores. Their chambers are not simply filled with protoplasm, but contain about 50% of very fine-grained clastic material (*stercomare*; Tendal 1972). The particles have presumably been collected by pseudopodia with the food; but instead of expelling them (as vacuolar faeces), the organism uses this material to build a soft, trabecular fill skeleton. In this way, the actual protoplasm does become subdivided into strands of the right, micrometric, diameters. In addition, the protoplasm contains minute crystals of barite (granellae), perhaps for tissue stiffening.

For applying this model to the quilts of the even more giant vendobionts, a minor preservational detail becomes important. If their quilted hull would have been filled only with fluid protoplasm (or soft tissue), it should have collapsed completely during dewatering and compaction. This is not the case. Actually, quilts may be sand-filled in the lower parts of upright infaunal forms, such as *Ernietta* and *Rangea* (see below). It would be very difficult to get sand into these narrow spaces, which were closed to begin with, by mechanical processes. More likely, this sand was, like the *stercomare*, actively taken up and loosely bound by a process that could be called *englutination* (new term). This fill skeleton would soon after death disintegrate and sink into the lower parts of the quilt chambers.

Versatility in design and lifestyles

Carpet-like recliners

The most basic lifestyle of vendobionts was presumably that of flat recliners. As otherwise soft sediment surfaces were coated by resistant biomats in Proterozoic times, vendobionts could firmly enough adhere to the substrate to resist transport and accumulation by turbidity currents. This can be deduced from their random spacing and lack of alignment, while associated upright forms

have been uniformly felled in downcurrent direction (Mistaken Point, Newfoundland). Nevertheless, corners were occasionally flipped-over like the edge of a carpet (Seilacher 1992). Such specimens show that the lower side had invariably the same quilted pattern as the upper one. So there was no dorso-ventral differentiation, not even in the recliners. Provided the measurements have been retrodeformed to remove the tectonic overprint (Seilacher 1992), these biostratigraphic criteria apply not only to the spindle-shaped, but also to the leaf- and bush-like forms, whose shapes might otherwise have suggested an upright mode of life.

As observed by Jim Gehling (pers. comm. 1994), two carpet-like forms common in the Flinders Ranges, *Dickinsonia* and *Phyllozoon*, show a strange preservational divergence. Whenever they are associated on the same bedding plane (always bed soles), either one or the other has sharp outlines, never both. This reciprocal preservation probably means that the two species were separated in life by the millimetric biomat. Consequently, the contours of either *Dickinsonia* or *Phyllozoon* were pressed through as mere ghost impressions, depending on whether the bedding surface represents the upper or lower side of the mat.

But who lived on top and who below? Like associated epifaunal encrusters (e.g. *Tribrachidium* and *Arkarua*), *Dickinsonia* is always preserved as negative hyporelief (but not its resting trace; see below). *Phyllozoon*, in contrast, forms a positive hyporelief; i.e. its death mask depicts the lower side of the body. It is also commonly associated with elephant-skin structures, which presumably correspond to the lower side of the biomat (Seilacher *et al.* 2003, fig. 5).

On the other hand, the relief criterion does not apply everywhere. In Newfoundland, all vendobionts are preserved as death masks of the lower body surface (positive hyporeliefs relative to the ash layer now weathered away), even though overfolded carpets and the fronds of felled *Charniodiscus* would certainly have been on top of the biomat.

Upright forms

The salient characteristic of forms that were upright in life is a uniform felling direction, with the attachment disc located upcurrent. At Mistaken Point, this disc (which would not have worked on loose sediment) was a voluminous, non-quilted pneu structure, resembling a lifesaver. It never became uprooted; but its consistent elevation above the adjoining bedding plane suggests that it was lifted during felling, together with the adhering mat. In contrast, the stem connecting the disc with the quilted frond always has an opposite relief (negative hyporelief) and indistinct margins. This suggests

that, after having been felled, the stem stayed somewhat aloft from the sediment and that it consisted of a stiffer material, whose belated decomposition caused the underlying bedding surface to bulge up (Seilacher 1992). In Newfoundland, several species of *Charniodiscus* can be distinguished from one another by the shapes and quilting patterns of the fronds (Laflamme *et al.* 2004). In one of them, *C. procerus*, the frond is consistently geniculated at about 45° relative to the stem axis, and always (?) to the same side. Had the environment been shallower, one would relate this 'plant-like' behaviour to photosymbiosis. In any case, the geniculation, as well as the leaf-like construction, contradict the hydrodynamic paradigm of a filter fan, as represented by sea pens.

Among the upright Newfoundland species, there were also a variety of lifestyles (Clapham *et al.* 2003). Their earliest representative (cf. *Paracharnia*) was stemless, flexible and had a meter long, ribbon-shaped frond (Narbonne & Gehling 2003). It likely lived like kelp, attached at the base and floating freely in the current to collect food like flypaper rather than by filtration.

In Namibia, the upright lifestyle is represented by *Swartpuntia*, which has more than three serially quilted vanes. It is preserved flat on bedding planes with uniform felling directions (Narbonne *et al.* 1997).

Infaunal vendobionts

Most unexpected is the lifestyle of vendobionts from the Kuibis Quartzite of Namibia. In this shallow, deltaic environment, where flood events from the rivers dominated sedimentation, serially quilted forms likely lived immersed in the sand (*Pteridinium*, *Ernietta*, *Namalia*, *Rangea*; Grazhdankin & Seilacher 2002). Accordingly, they are three-dimensionally preserved *within* the beds. In this situation, the otherwise flat fronds grew into bowl-, bag-, or boat-like shapes, because the quilts were elongated *upwards* in response to sedimentation. There also may be more than two vanes in the biserially-quilted forms (three in *Pteridinium*, four in *Rangea*).

Serially quilted forms

Occasionally, the Namibian *Pteridinium* communities were partly exhumed during flood events, as shown by tilting of individuals and deformation of the parts exposed by erosion (Grazhdankin & Seilacher 2002). Nevertheless, the bases remained essentially in place, retaining their bulging bag shapes and convex-down orientations. Neither is there an overall current alignment.

In still upright specimens of *Ernietta* (which possessed a median seam, but no median vane), the upper part of the bag commonly appears less turgid than the lower one (Fig. 1). This may indicate that it emerged above the sediment surface in life; but more likely this difference is controlled by a taphonomic overprint, due to the sand of the fill skeleton sinking down within the quilts.

The evolutionary transition from an epi- to an endobenthic lifestyle, or *vice versa*, is well illustrated by two species of *Pteridinium*. In the deep environments of the Albemarle Group in the North Carolina slate belt, *P. carolinaense* (= *P. nenoxa* from the White Sea) has two lateral vanes spreading horizontally on the bedding plane (Fig. 2c). Also, the tips of the quilts are curved and pointed (which led to its original interpretation as a trilobite; St. Jean 1973). The third vane of this epibenthic organism was presumably standing upright in the water column. Narbonne *et al.* (1997) found this species in Namibia strongly current-aligned, another indication of an epibenthic lifestyle.

In the immersed Namibian species (*Pteridinium simplex*; Fig. 2a, b), the quilts of all three vanes

grew eventually upwards, ending commonly along a straight edge, flush with the sediment surface. The same three-dimensional preservation, even less deformed, is found in *Rangea*, although its fractal quilting pattern is more similar to the recently discovered upright and stemmed rangeomorph species from Newfoundland (Narbonne 2004). If fractal versus serial quilting is a synapomorphic character, the incredible morphological and ecological versatility may thus characterize not only Vendobionta as a whole, but also the subgroups.

Rangea

This vendobiont from the Kuibis Quartzite of Namibia has been described many years before the Precambrian age of the Ediacaran biota was recognized. It was first interpreted as a ctenophore (Gürich 1930) and later as an upright filter feeder similar to modern sea-pens (Richter 1955; Glaesner 1984). This idea was based on the presence of an axial structure, flanked on either side by a series of branches that were themselves subdivided into what appeared to be polyps. However, studies

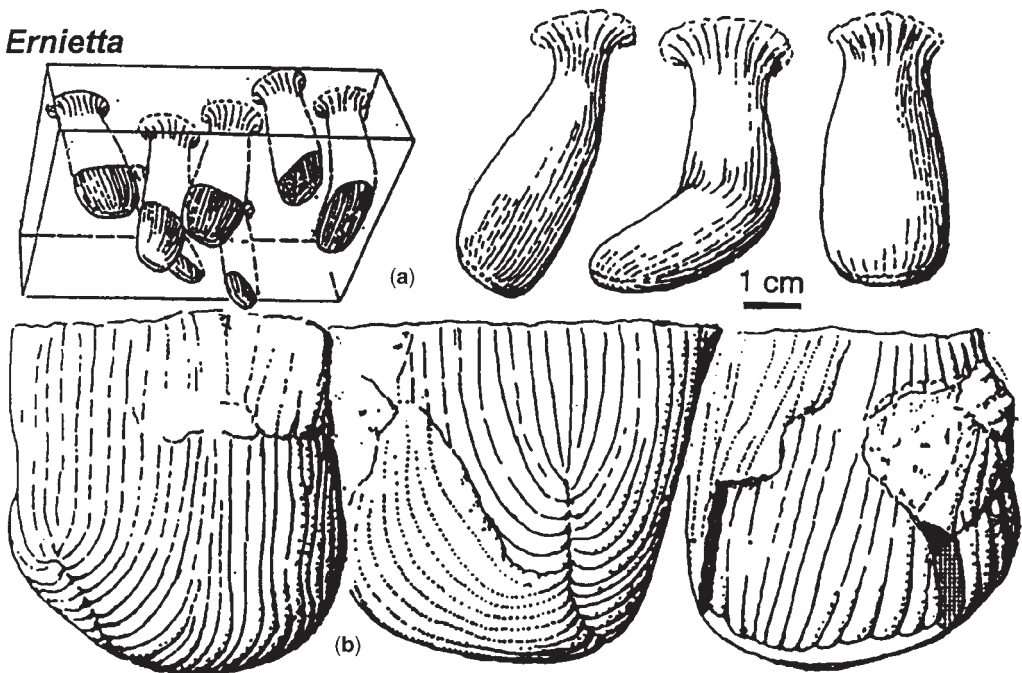
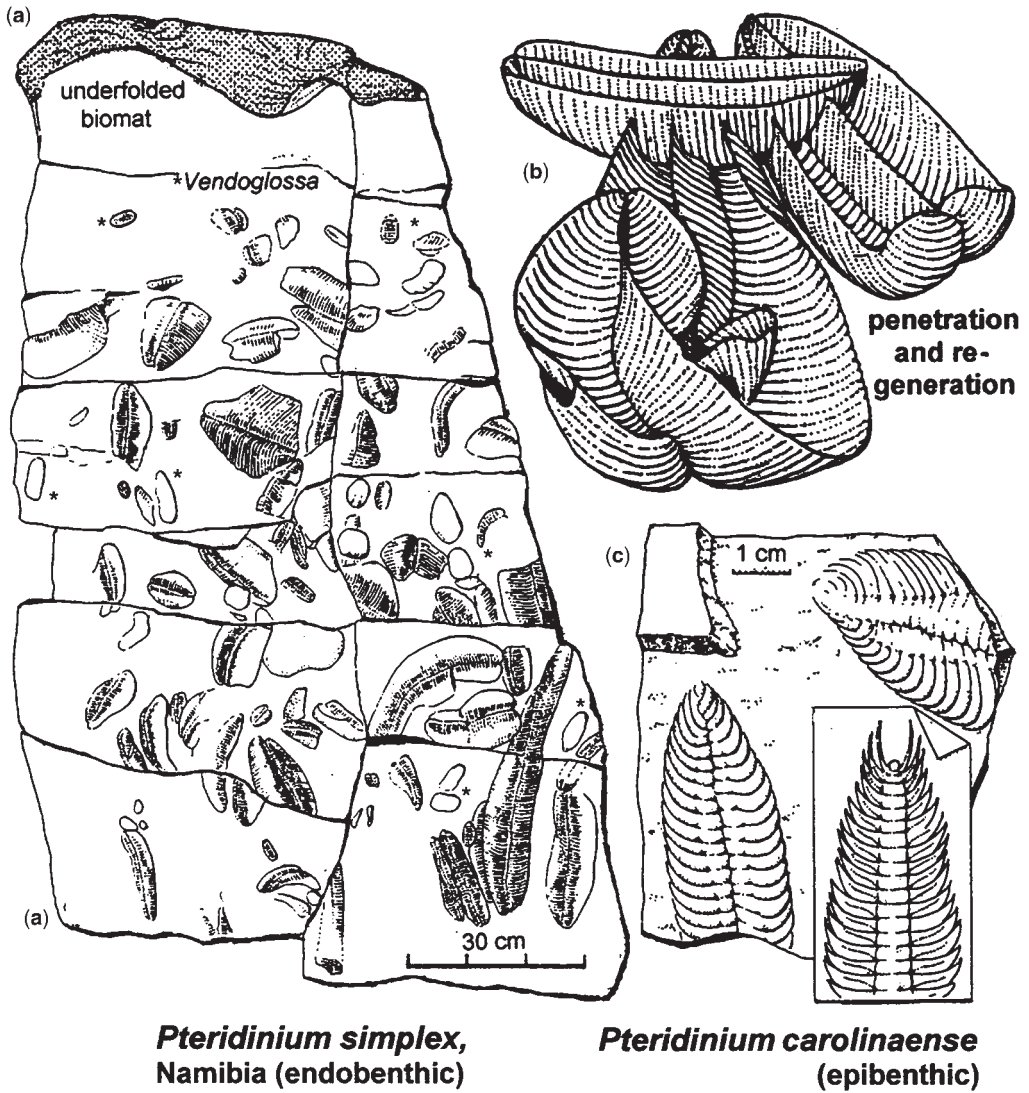


Fig. 1. *Ernietta* initially grew in a biserial mode, similar to *Pteridinium*, but lacked a median vane. The introduction of new segments caused the two vanes to join and quilts grew up with sedimentation, forming a cylindrical bag open at the upper end. Quilts appear less turgid towards the upper margin, probably because englutinated sand sank down within each quilt ((a) cast from Pflug collection, YPM 204 506). In a larger specimen ((b) cast YPM 204 508 in three views) a secondary vane originated from the outside of the bag at a distance from the original seam. Such specimens led to the multifoliate reconstruction by Jenkins (1984). From Seilacher *et al.* 2003, fig. 11.



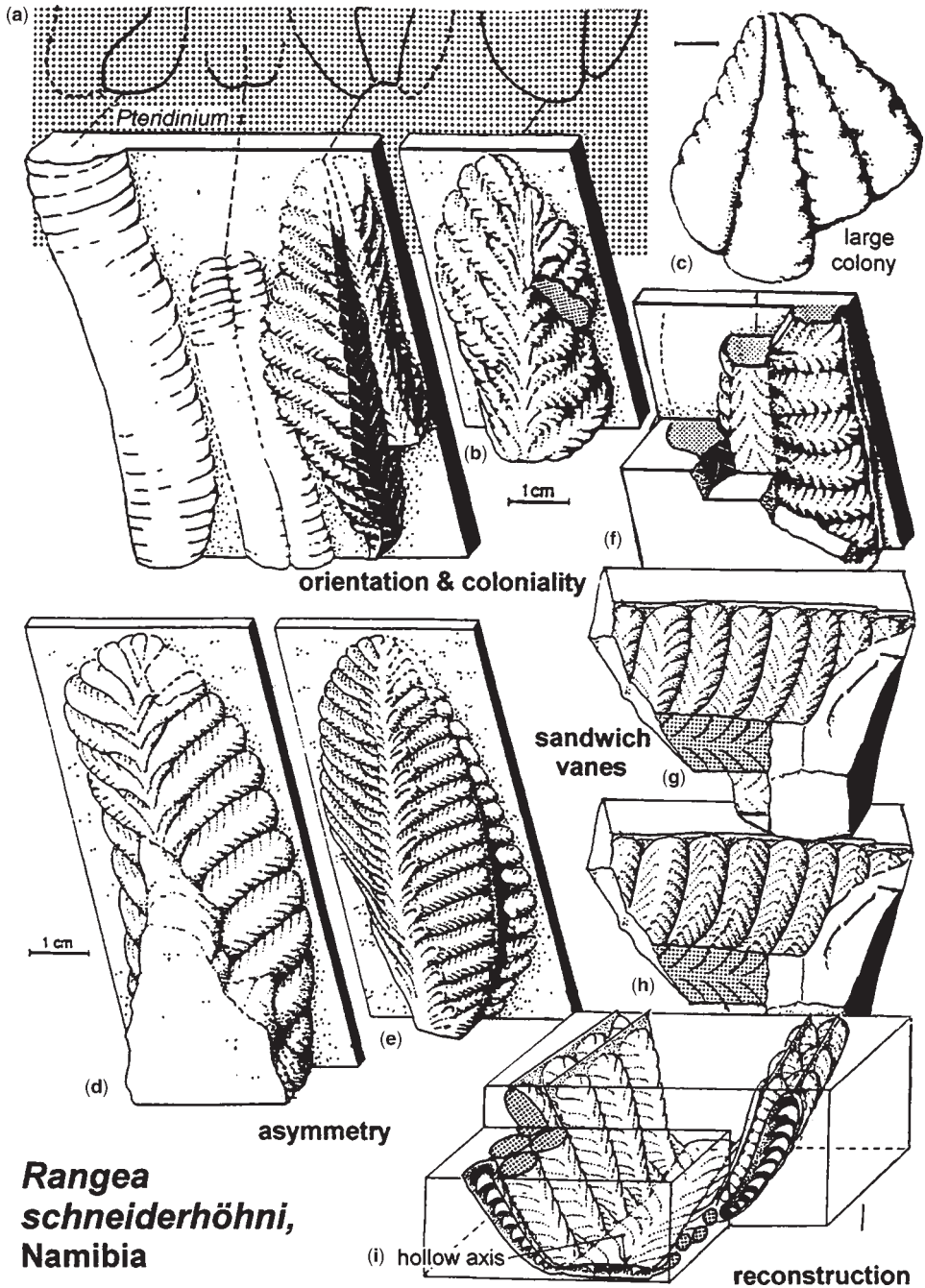
***Pteridinium simplex*,
Namibia (endobenthic)**

***Pteridinium carolinaense*
(epibenthic)**

Fig. 2. *Pteridinium* (a) tiered assemblage of Kuibis Quartzite, (Nama Group, Aar Farm near Aus, Namibia) exposed from below by splitting the rock. Small-scale downhill slumping downwarped the covering biomat (shaded). The top sand accumulating behind it contains only *Vendoglossa* (asterisks), which probably inhabited a higher tier than *Pteridinium* (cast YPM 38277); (b) after having been penetrated by another *Pteridinium* at the bow sides, two individuals switched their 'bow' points to the stern ends, where they grew first upwards with the original convexity. Continued growth in the left specimen re-established the boat shape at a higher level. During this process the convexity reversed, while the right lateral and the median vane of the lower boat switched functions in the upper level (after Grazhdankin & Seilacher 2002, fig. 5f); (c) *Pteridinium carolinaense* (St Jean 1973), originally described as a trilobite (inset), was probably an epibenthic recliner. However, it is uncertain, whether it had a median vane that was free standing in the water column (YPM 201 881 and 882).

of the few available specimens revealed that these branches never separated, because they were quilts in a foliate pneu structure. There is also a continuous marginal seam connecting the tips of the branches (Fig. 3).

Accepting this basic construction, Narbonne recently (2004) erected the taxon Rangeomorpha on the base of a fractal (rather than serial) mode of quilting. In Newfoundland, fractally quilted vendobionts are well represented by recliners



***Rangea*
schneiderhöhni,
Namibia**

Fig. 3. *Rangea* from Kuibis Quartzite, Nama Group, Namibia (a–b) association of two *Pteridinium* in life position, showing that *Rangea* also lived immersed in the sediment with the convex side down (a, b, c, f) multiple fronds (d) single frond with outer branches on one side passing into inner ones on the other (e) single frond with tips of inner vane on right flank (f) multiple frond broken between quilted vanes on right side. Depending on lighting direction, the branches show either their own secondary quilts (as recesses, (g)) or those of the outer branches (as ridges, (h)) i.e. the two vanes were closely appressed with alternating branches. The double number of chevroned quilts on the axial surface (shaded); shows that the impressions do not stem from another frond (i) reconstruction. Note straight edges of vanes in (e) from Germs 1973; all other specimens from Pflug collection; (d–f) (as cast at YPM 38275).

(spindle-, bush-, leaf-, and fern-like forms). In addition, the new feather-like variant (Clapham *et al.* 2003) stood upright on its stem, as documented by uniform felling directions. With this background, the mode of life of the Namibian *Rangaea* gains renewed interest.

All known *Rangaea* specimens from Namibia are preserved three-dimensionally, rather than spreading on a bedding plane. Thus one depends on the accidental course of the rock fracture for reconstructing the complete organism. As published specimens come from float and were largely collected by Bushman shepherds, their original orientation is also unknown.

The latter problem can be solved by associated *Pteridinium simplex*, for which an infaunal lifestyle and the orientation are established (Grazhdankin & Seilacher 2002). They show that the bowl of *Rangaea* stuck concave-up in the sand, as in *Pteridinium* (Fig. 3a).

Another interesting feature of *Rangaea* is the presence of double rows of branches, or vanes, on either side of the axis. They were noted in a specimen (Fig. 3e; Germs 1973), in which the tips of a second row appear along the right margin. An additional row can also be seen in other specimens. This led to the reconstruction of the frond shown in Fig. 3i.

One specimen, originally in the Pflug collection (Fig. 3f; plaster cast YPM 38275) shows other important details:

- (1) The boundaries between branches continue on the axial structure but in a completely flattened relief, rather than bulging.
- (2) In the 'succulent' branches on the left flank, secondary quiltings are arranged as expected, forming an angle opening towards the tip of each quilt (Fig. 3g). If one alters the lighting angle, however, the same branch suddenly appears ratcheted as an arrow tail (Fig. 3h). The now visible subdivisions also form sharp crests rather than reentrants. There is only one explanation to this strange phenomenon: in the rock part chipped away there was a second vane. Its branches were arranged in alternation and so firmly appressed to the ones of the inner row that their secondary quiltings are also seen on the interface. This result has several implications: (1) *Rangaea* was a truly infaunal organism, like the associated *Pteridinium* and like the bag-like *Ernietta* in other beds; (2) the two vanes were only on one flank free to interact with the environment; and (3) as the tips of the quilts are still closed by the straight marginal seam, the sand inside must have been there already in life as an englutinated fill skeleton. The axial part, however,

was not englutinated and therefore collapsed into a flat structure.

But how do we know that there were no more than two rows of branches on either side?

- (1) The flat surface of the axial area mitigates against additional rows above it.
- (2) One poorly preserved specimen in the original Pflug collection (Fig. 3c) shows four *Rangaea* 'individuals' arranged like pieces of a cake. So they were only parts of a larger 'colony', with the partners' growing tips at the centre rather than the circumference. Between them there was no room to accommodate additional branch rows on the outside.

Admittedly, this new picture of *Rangaea* raises additional tantalizing questions regarding lifestyle, growth and nutrition. But certainly it is incompatible with a seapen-style of filtering in the open water, or with that of any other known metazoan animal. If the mode of quilting is indeed a synapomorphic character, the Rangemorphia also show that fractally subdivided vendobionts, like the serial ones, employed a broad variety of lifestyles, ranging from elevators and recliners on matgrounds to being fully immersed in the sand.

Regeneration

In the predator-free Ediacaran environments, vendobionts did not get damaged (at least no 'bitten' specimen has ever been reported). This was different for the endobenthic communities of Namibia, where vendobionts were crowded and could not freely yield to the expansion of a neighbour. So it appears to have happened that individuals of *Pteridinium* became penetrated by others. This interpenetration, unparalleled in metazoans, was probably executed by digestion. It did not kill the victim, but induced a unique reaction.

In a group of *Pteridinium* analysed by Dima Grazhdankin (Grazhdankin & Seilacher 2002), the growing 'bow' of one boat-shaped individual penetrated two others in such a way that they lost their own bows (Fig. 2b). In response, they evidently switched the generation of new quilts to the opposite end (the former stern side). But instead of continuing growth in the direction of the old, horizontal body axis, the regenerating part grew upward and then again horizontal at a level above the old frond. The complex reconstruction of Pflug (1970) was based on such an overturned individual. Alternatively, such specimens might have been explained by mechanical deformation, as in the Newfoundland recliners, had not the overfolded part the same concave-up geometry as the one

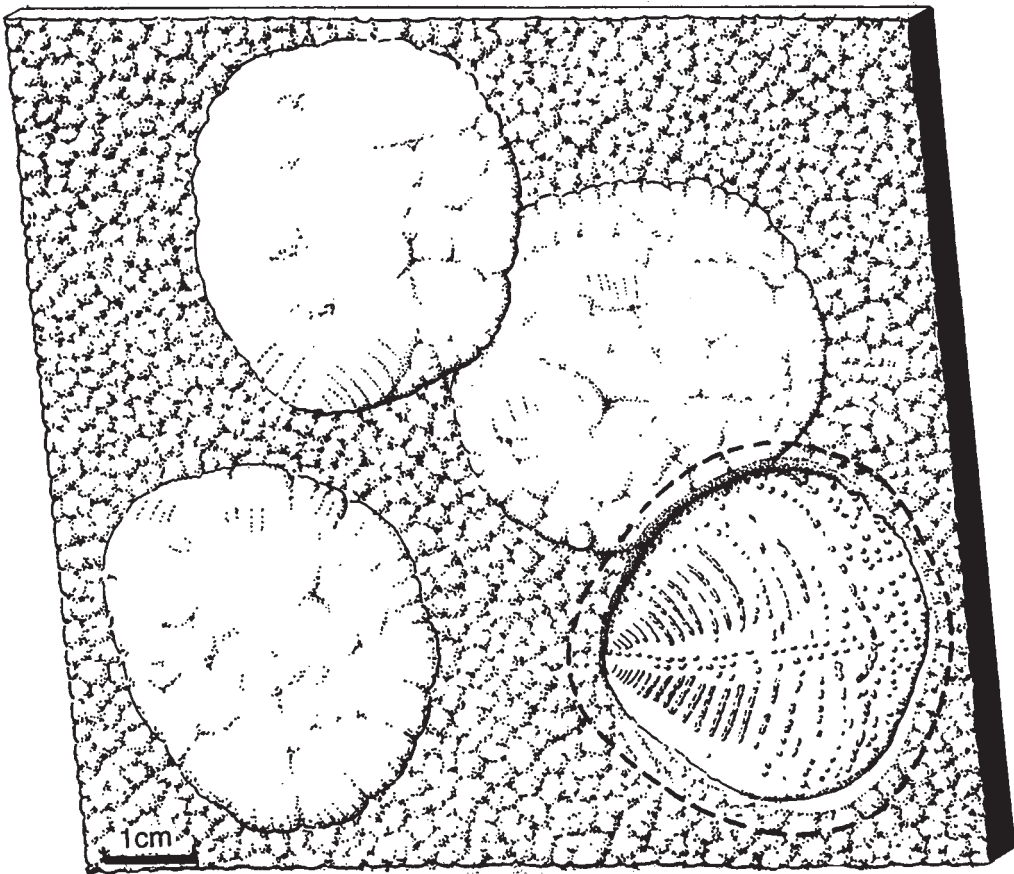
below. Careful observation also demonstrated that vanes swapped functions in the process: one of the lateral vanes from the lower level turned into a median vane in the upper and *vice versa*. So, the differentiation of body parts (bow versus streamlined stern; median versus lateral vanes; dorsal versus ventral side) was not as irrevocable as in triploblastic metazoans.

Resting traces

The sensational discovery (Ivantsov 2001; Fedonkin 2003) of series of resting traces (preserved as positive hyporeliefs) behind death masks (negative hyporeliefs) of *Dickinsonia* and the related *Yorgia* appeared

to be the ultimate proof that vendobionts were metazoans. While the evidence for mobility is undeniable (skip trails would be more aligned), preservational details tell a somewhat different story (Fig. 4):

- (1) The elephant-skin structures on the surrounding bedding plane suggest that it corresponds to a well-developed biomat.
- (2) The resting traces are too deep to have been produced simply by the weight of the organism. In a similar situation, the much heavier early mollusc *Kimberella* did not leave the slightest impression while it grazed the surrounding biomat with its extendible radula (Seilacher *et al.* 2003, fig. 5)



Resting traces of *Yorgia*; White Sea

Fig. 4. (a) Sole surface from the White Sea, Russia, with elephant-skin structure. An epibenthic vendobiont similar to *Dickinsonia* is preserved as a death mask in negative hyporelief. Associated resting traces, probably stemming from the same individual, are somewhat larger and preserved as positive hyporeliefs. Instead of quilt impressions, they show a smooth surface with crease-like reentrants, reflecting external digestion of the biomat. Note that the organism left no trace as it crept from one station to the next, and that it did not move in the direction of the body axis (after Fedonkin 2003, fig. 10).

- (3) Upon leaving, the organism has sometimes left an impression of its quilted underside (Fedonkin 2003, figs 1 & 12). So there can be no doubt about the authorship. Yet the resting traces are mostly smooth with some irregular re-entrant creases. The latter could be due to a process of external digestion or represent incipient elephant-skin structures corresponding to the regeneration of the biomat. This would indicate that the tracks took time to be made.
- (4) More importantly, digging was done without the use of scratching tools. Digestive uptake of individual particles by microscopic pseudopodia would best fit the observed trace morphology.
- (5) After having finished the job, the pseudopodia made the organism glide slowly away, without leaving any trace, in order to make a new resting trace that overlapped little or not at all with the previous one.

Other problematic fossils

Vendobionta are not the only group of Ediacaran fossils whose taxonomic affiliation is, or was, problematic. A large-scale cast made for the travelling

exhibit 'FOSSIL ART' (Seilacher 1997) contains several specimens of a strange fossil (Fig. 2a). It resembles the many associated *Pteridinium* in its mode of preservation, but is much smaller and lacks the quilting typical for vendobionts. Instead there are transverse rows of minute papillae that make it look like a cat's tongue (Fig. 5a). The association with *Pteridinium* in a slightly slumped sand body (Fig. 2a) suggests an infaunal lifestyle. As this fossil is rather common in that locality, but rarely as perfectly preserved as the holotype, a formal description as *Vendoglossa tuberculata* n. gen., n. sp., is given in the appendix.

Another fossil, of which only two specimens have been found at the same locality, resembles a bat's ear (Fig. 5c). In contrast to the folded biomat atop of the large *Pteridinium* slab (Fig. 2a), its margin is sharply defined and its relief pattern does not reflect a dominant stress field. Obviously, one is dealing with a foliate organism of unknown affiliation that increased surface area by local buckling, as some algae do (*Gloeocapsa*).

These two forms are mentioned here only as a reminder that Ediacaran biota contain macroscopic organisms other than metazoans, vendobionts and xenophyophores that remain enigmatic and need further study.

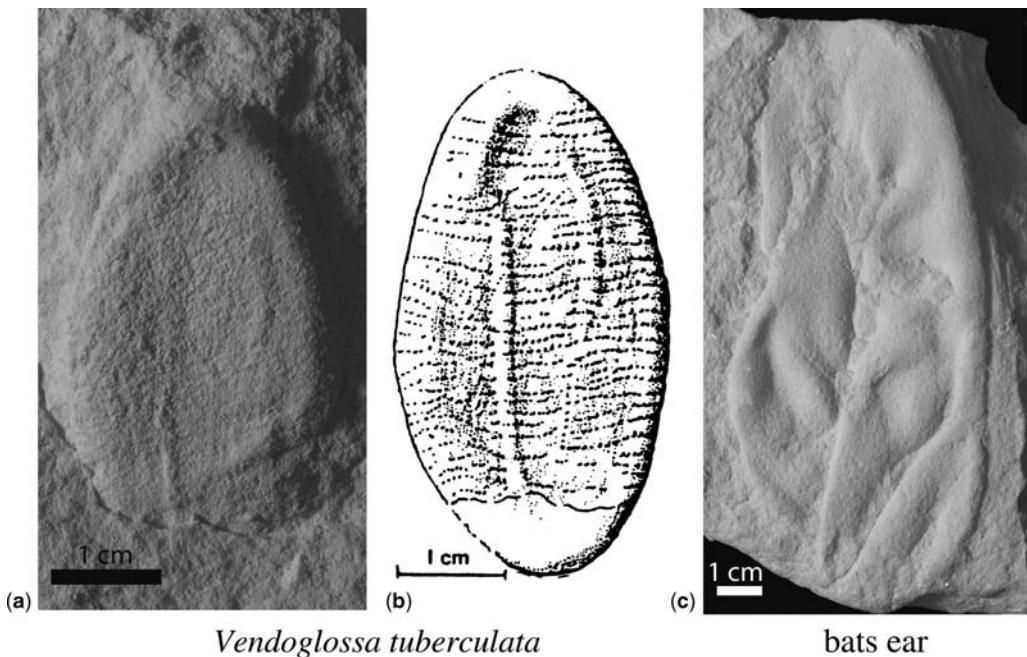


Fig. 5. (a–b) Holotype of *Vendoglossa tuberculata* (cast YPM 204 491 ex 38277); (c) Problematic fossil shaped like a bat's ear (YPM 204 504). Kuibis Quartzite, Aar farm.

Conclusions

The observations listed above are difficult to reconcile with a metazoan nature of the Vendobionta. While their quilted pneu architecture is the chief unifying character, the widely differing lifestyles and geometries would require different modes of feeding and signal different bauplans if these strange organisms had been animals. In spite of their unusual size they are best interpreted as an extinct class of rhizopodan protists, similar to Foraminifera and the similarly large Xenophyophoria.

This does not necessarily mean that the whole organism was a single multinuclear (plasmodial) cell. Different quilts, or quilt complexes, may well have been individualized to allow differentiation (e.g. into attachment discs or stems) in response to morphogenetic signals. Nevertheless, it is suggested here that this was only an analogy to true multicellularity, rather than an ancestral state on the way to metazoan tissues (McMenamin 1986).

That the Vendobionta became practically extinct at the turn to the Cambrian (surviving into the earliest Cambrian (Jensen *et al.* 1998) is a matter of stratigraphic definitions and the nature of *Thaumaptilon* from the Burgess Shale (Conway Morris 1993) remains disputable. How they managed to remain the ecological rulers for tens of millions of years in the presence of true triploblastic animals is another question. Their incumbency resembles that of the dinosaurs in the presence of mammals during the major part of the Mesozoic. Macroevolution does not behave like a global market. The Darwinian fitness game at the level of populations produces innovations all the time. But fitness appears to be balanced by rules operating at the level of ecosystems, which must be responsible for the phenomenon of stasis observed in the fossil record (Eldridge & Gould 1972; Vrba 1993; Brett & Baird 1995). Feedback links between predator and prey species and between parasites and their hosts are suspected to be major balancing factors.

In summary, the Ediacaran biota was not merely a prelude to the Cambrian 'explosion', but represents a singular state in the history of our biosphere—strange as life on another planet, but easier to reach. Ediacaran fossils deserve top priority in future research.

Taxonomic Appendix

Incertae Sedis

Vendoglossa tuberculata n.gen., n.sp.

Holotype: casts of the whole slab in Yale Peabody museum (YPM 382777) and FOSSIL ART (Seilacher 1997, fig. 2a & 5a). Original specimen remains still in the field.

Separate cast YPM 204 491. Type Rock Unit: Kuibis Quartzite (Ediacaran), Nama Group. Type Locality: Aar Farm near Aus (Namibia). Age: Vendian = Russian equivalent of Ediacaran. Basis of name: *glossa* (Greek) = tongue; *tuberculata* (Latin) = pustulate.

Diagnosis: Flat, oval bodies with a rounded edge, whose lower side is ornamented with transverse rows of minute tubercles at regular millimetric intervals. Typical size: 4.3×2.5 cm.

Remarks: An infaunal lifestyle is suggested by the common association with *Pteridinium* in life position. The holotype and the paratype (Fig. 2a) are located behind the front of a small slump, where parts of the surficial biomat became folded-under like a tablecloth. Significantly, *Pteridinium* does not occur in this zone, which may indicate that *Vendoglossa* lived right below the biomat.

Thanks are due to P. Vickers-Rich, M. Fedonkin and J. Gehling for organizing the Prato Symposium, and to all participants for very fruitful discussions. Tim and Theresa Raub (Yale University) critically read an earlier version. A. Rodriguez and E. Seilacher helped with word processing. Critical reviews by M. Brazier, S. Jensen and G. Narbonne are also appreciated.

References

- BOTTJER, D. J., HAGADORN, J. W. & DOMBOS, S. Q. 2000. The Cambrian substrate revolution. *Geological Society of America Today*, **10**, 1–9.
- BRETT, C. E. & BAIRD, G. C. 1995. Coordinated stasis and evolutionary ecology of Silurian to Middle Devonian faunas in the Appalachian Basin. *In*: ERWIN, H. E. & ANSTEY, R. L. (eds) *New Approaches to Speciation in the Fossil Record*. Columbia University Press, New York, 285–315.
- CLAPHAM, M. E., NARBONNE, G. M. & GEHLING, J. G. 2003. Paleocology of the oldest known animal communities; Ediacaran assemblages at Mistaken Point, Newfoundland. *Paleobiology*, **29**, 527–544.
- CONWAY MORRIS, S. 1993. Ediacaran-like fossils in Cambrian Burgess Shale-type faunas of North America. *Palaentology*, **36**, 593–635.
- ELDRIDGE, N. & GOULD, S. J. 1972. Punctuated equilibria: an alternative to phyletic gradualism. *In*: SCHOPF, T. J. M. (ed.) *Models in Paleobiology*. Freeman, Cooper & Co., San Francisco, 82–115.
- FEDONKIN, M. A. 2003. The origin of the Metazoa in the light of the Proterozoic fossil record. *Paleontological Research*, **7**, 9–41.
- GEHLING, J. G. 1999. Microbial mats in terminal Proterozoic siliciclastics: Ediacaran death masks. *Palaos*, **14**, 40–57.
- GERMS, G. J. B. 1973. A reinterpretation of *Rangea schneiderhoehni* and the discovery of a related new fossil from the Namibia group, South West Africa. *Lethaia*, **6**, 1–10.
- GLAESSNER, M. 1984. *The Dawn of Animal Life. A Biohistoric Study*. Cambridge University Press, Cambridge.
- GRAZHDANKIN, D. & SEILACHER, A. 2002. Underground Vendobionta from Namibia. *Palaentology*, **45**, 57–78.

- GÜRICH, G. 1930. Die bislang ältesten Spuren von Organismen in Südafrika. *XV International Congress, Comptes Rendus*, **2**, 670–680.
- IVANTSOV, A. Y. 2001. Traces of active moving of the large late Vendian Metazoa over the sediment surface. In: PONOMARENKO, A. G., ROZANOV, A. Y. & FEDONKIN, M. A. (eds) *Ecosystem Restructure and the Evolution of the Biosphere* **4**. PINRAS, Moscow, 119–120.
- JENKINS, R. J. F. 1984. Interpreting the oldest fossil cnidarians. *Palaeontographica Americana*, **54**, 95–104.
- JENSEN, S., GEHLING, J. G. & DROSER, M. L. 1998. Ediacara-type fossils in Cambrian sediments. *Nature*, **393**, 567–569.
- LAFLAMME, M., NARBONNE, G. M. & ANDERSON, M. M. 2004. Morphometric analysis of the Ediacaran frond *Charniodiscus* from the Mistaken Point Formation, Newfoundland. *Journal of Paleontology*, **78**, 827–837.
- MCMENAMIN, M. A. S. 1986. The garden of Ediacara. *Palaios*, **1**, 178–182.
- NARBONNE, G. M. 2004. Modular construction of early Ediacaran complex life forms. *Science*, **305**, 1141–1143.
- NARBONNE, G. M. 2005. The Ediacara biota: Neoproterozoic origin of animals and their ecosystems. *Annual Reviews of Earth and Planetary Sciences*, **33**, 421–422.
- NARBONNE, G. M. & GEHLING, J. G. 2003. Life after snowball; the oldest complex Ediacaran fossils. *Geology*, **31**, 27–30.
- NARBONNE, G. M., SAYLOR, B. Z. & GROTZINGER, J. P. 1997. The youngest Ediacaran fossils from Southern Africa. *Journal of Paleontology*, **71**, 953–967.
- PFLUG, H. D. 1970. Zur Fauna der Nama-Schichten in Suedwest-Afrika. Teil I, *Pteridinia, Bau und systematische Zugehoerigkeit*. *Palaeontographica*, **A134**(4–6), 226–261.
- PFLUG, H. D. 1972. Systematik der jung-prakambrischen Petalonamae Pflug 1970. *Palaeontologische Zeitschrift*, **46**, 56–67.
- RICHTER, R. 1955. Die ältesten Fossilien Süd-Afrikas. *Senckenbergiana Lethaea*, **36**, 243–289.
- RYE, R. & HOLLAND, H. D. 1998. Paleosols and the evolution of atmospheric oxygen; a critical review. *American Journal of Science*, **298**, 621–672.
- SEILACHER, A. 1984. Late Precambrian and early Cambrian Metazoa: preservational or real extinctions? In: HOLLAND, H. D. & TRENDALL, A. F. (eds) *Patterns of Change in Earth Evolution*. Springer Verlag, Heidelberg, 159–168.
- SEILACHER, A. 1992. Vendobionta and Psammocorallia: lost constructions of Precambrian evolution. *Journal of the Geological Society, London*, **49**, 609–613.
- SEILACHER, A. 1994. Early multicellular life: Late Proterozoic fossils and the Cambrian explosion. In: BENGTON, S. (ed.) *Early Life on Earth*. Columbia University Press, New York, 389–400.
- SEILACHER, A. 1997. *Fossil Art. An Exhibition of the Geologisches Institut Tubingen, University, Germany*. The Royal Tyrell Museum of Palaeontology, Drumheller, Canada.
- SEILACHER, A. & PFLÜGER, F. 1994. From biotopes to benthic agriculture: a biohistoric revolution. In: KRUMBEIN, W. E., PATERSON, D. M. & STAL, L. J. (eds) *Biostabilization of sediments*. Bibliotheks und Informationssystem der Universität Oldenburg, 97–105.
- SEILACHER, A., GRAZHDANKIN, D. & LEGOUTA, A. 2003. Ediacaran biota: the dawn of animal life in the shadow of giant protists. *Paleontological Research*, **7**, 43–54.
- ST. JEAN, J. 1973. A new Cambrian trilobite from the piedmont of North Carolina. *American Journal of Science*, **273**, 196–216.
- TENDAL, O. S. 1972. A monograph of the Xenophyphoria (Rhizopodea, Protozoa). *Galathea Report*, **12**, 7–99.
- VRBA, E. 1993. Turnover-pulses, the Red Queen, and related topics. *American Journal of Science*, **293**-A, 418–452.

Theoretical morphology of quilt structures in Ediacaran fossils

B. TOJO¹, R. SAITO², S. KAWAKAMI¹ & T. OHNO³

¹*Faculty of Education, Gifu University, 1-1 Yanagito, Gifu City 501-1193, Japan
(e-mail: btojo227@cc.gifu-u.ac.jp)*

²*Institut für Palaeontologie der Universität Würzburg, Germany*

³*The Kyoto University Museum, Kyoto University, Japan*

Abstract: Vendobiont type fossils are characterized by possessing ‘gliding symmetry’, in which quilts of the different vanes consisting the body of the Vendobionta meet along the seam with small offset. Because two, three or more vanes are joined along this seam and the quilts of different vanes can be variously offset along the seam, a variety of gliding symmetry exists among Vendobionta. Our theoretical consideration here predicts that the number of possible gliding symmetry is one, two and three for organisms having two, three and four vanes, respectively. We also predict that a special combination of morphological types appear alternatively during the growth of the Vendobionta with two vanes. Further, we were able to identify the existence of two types in gliding symmetry predicted by us for *Pteridinium* specimens with three vanes. Detailed examination of the gliding symmetry of other Vendobionta, therefore, may give important clues in solving riddles veiling the vendobiont relationships.

A considerable number of Ediacaran fossils show ‘gliding symmetry’ and are placed in Vendobionta, on the basis of the existence of this feature. The body of many vendobiont-type fossils consists of vanes that are joined along a seam. The hollow space between the two surface layers defining each vane is separated, by series of more or less parallel walls, into long and narrow quilts. Two, three or more vanes can be joined along the central seam. Quilts of different vanes meet along the seam at nearly a right angle. The quilts meet with an offset shorter than quilt width, leading to the alternation pattern along the central seam (Fig. 1).

Some researchers regard this alternating pattern as merely a variety of bilateral symmetry, whereas others, like Seilacher (1992), regard the pattern as a significant diagnostic feature demanding that the vendobionts be given a high taxonomic rank, one example being as a class of giant rhizopods (Seilacher *et al.* 2003). Rigorous analysis of this feature, however, has seldom been carried out, although a closer look at this ‘gliding symmetry’ may bring a deeper understanding of the true nature of the organisms.

During field surveys on the Neoproterozoic in Namibia, there was the chance to study numerous specimens of *Pteridinium*. This genus has three sheets, or vanes each bearing quilts arranged more or less parallel to each other. The three vanes join along a central axis or seam, along which the quilts meet in an alternating pattern (Pflug 1970; Grazhdankin & Seilacher 2002). This detailed study of *Pteridinium*, reveals two

different ways in which the quilts of three vanes were arranged in this alternating relationship. These observations, together with consideration of another Ediacaran, *Swartpuntia*, which may have had four vanes, leads to the proposal of theoretical models of the alternating quilt patterns in multi-vaned fossils. This paper reports the results of these theoretical considerations.

Quilt arrangement in multi-vaned Vendobionta

The types of alternating quilt arrangements are examined for organisms with two, three and four vanes that join each other along a median seam. The number of vanes is expressed as n ($n = 2, 3$, or 4). For simplicity, we assume that the width of the regularly spaced quilts has a constant value of d . The offset between the quilts of different vanes that meet along the seam is called ‘quilt offset’. When the vane number is two ($n = 2$), the quilt offset of the two different vanes is $d/2$. When the vane number is three ($n = 3$), the value of quilt offset is either $d/3$ or $2d/3$. Therefore, it may be generalized that, for the vane number of n , the minimal quilt offset value is d/n . The vane is assumed to have infinite length to avoid the complication caused when taking the quilt arrangement(s) at both ends of the seam into consideration. The vanes are regarded to consist of an infinite repetition of quilts with uniform widths of d . Each vane is given a number from 1 to n , clockwise. Vanes are then

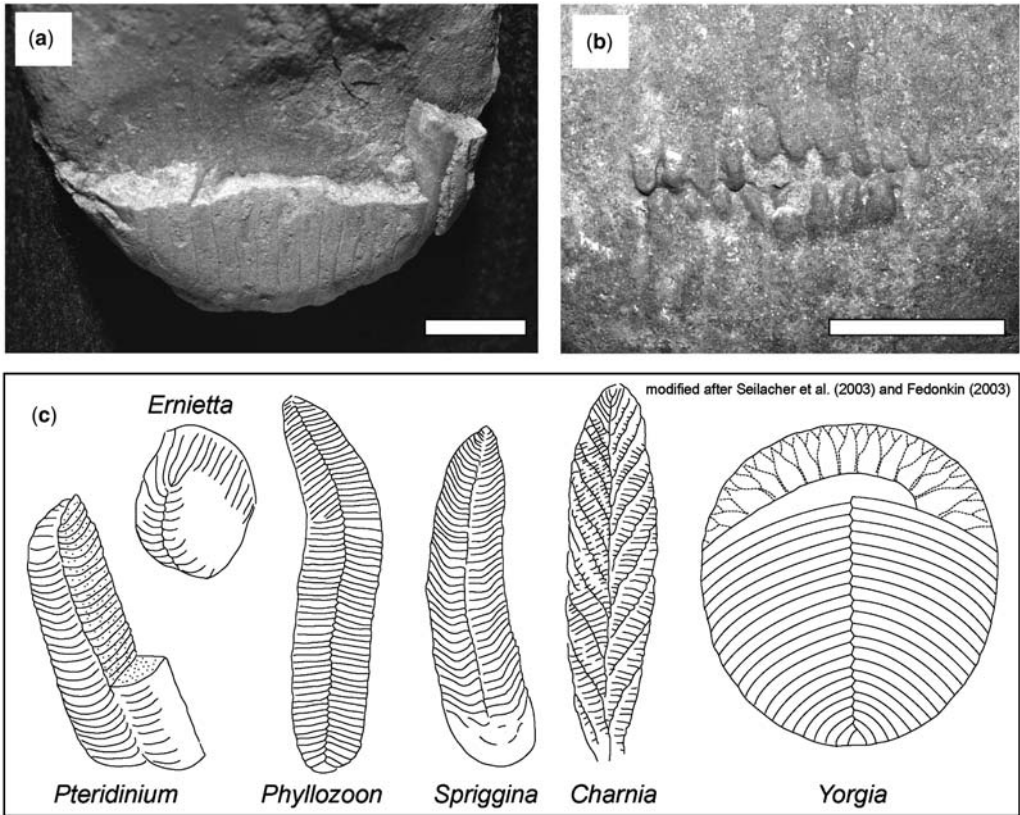


Fig. 1. Quilts in Ediacaran fossils. (a, b) Quilted structures in *Ernietta*. Scale bars are 1 cm long. In the specimen illustrated in (a), quilt structure is broken in the lower half, revealing some of the inner walls separating quilts. Specimen (b) shows the ‘gliding symmetry’ of quilts that meet along the seam located on the bottom of the organism. (c), Various Ediacaran fossils with more or less evenly spaced quilts.

arranged arbitrarily with quilt-offset values of d/n relative to the neighbouring ones along the seam. For vane number n , the number of all possible operations with this rule is $n!$. However, because some operations yield the same results, the number of recognizable arrangements is less than n . Figure 2 summarizes the theoretically possible quilt arrangements for cases with $n = 2, 3$ and 4. In the following text, quilt arrangements for these three cases will be described.

For $n = 2$, the number of possible quilt arrangement is $2! = 2$. Each vane is given a number 1 and 2 clockwise around the axis. Here a symbolic notation for arrangement types will be introduced as follows: a $d/2$ quilt offset of vane 1 ahead of vane 2 will be described as [12], whereas a $1/2d$ quilt offset of vane 2 ahead of the vane 1 will be described as [21]. However, both types can be perfectly overlapped, if one type is shifted $d/2$ along the axis relative to the other. Therefore there is only one quilt arrangement type for $n = 1$.

For $n = 3$, the number of possible quilt arrangements is $3! = 6$. However, [231] and [312] can be overlapped to [123] by shifting operations along the axis. The same can be said for [213] and [321], which can be overlapped to [132]. As a result, there are two quilt arrangement types (Fig. 2). These two cannot be overlapped by shifting and rotational operations along the axis, they are mirror images to each other.

A theoretical description of the shifting operations yielding the above results is as follows. For any numbers a, b , and c ($a \neq b \neq c$) from $\{1, 2, 3\}$, the obtained vane constellation, (for example $[a b c]$) can be overlapped to $[b c a]$ by shifting $d/3$ along the axis and to $[c a b]$ by shifting $2d/3$ along the axis.

For $n = 4$, the number of possible quilt arrangements is $4! = 24$. However, after excluding the identical ones that can be overlapped by shifting operations along the axis, the number of arrangements is reduced to six: [1234], [1243], [1324],

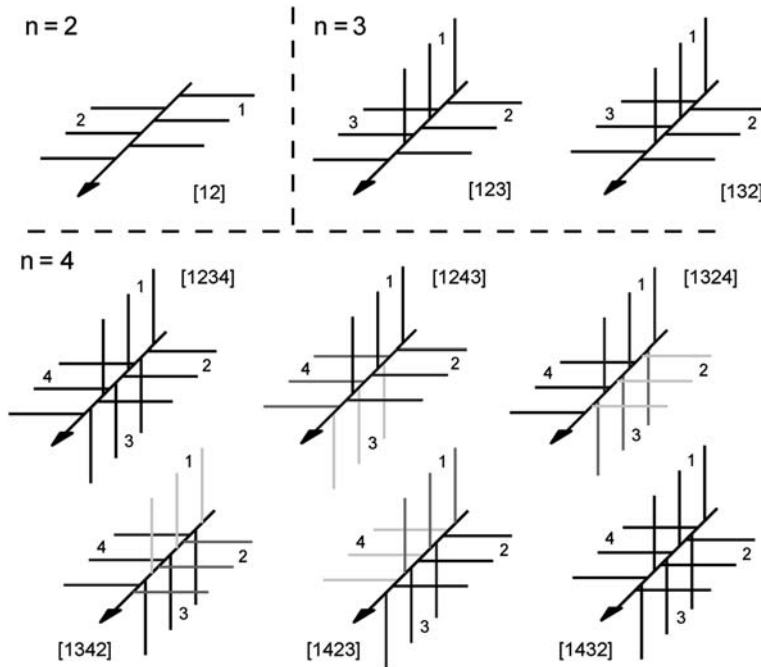


Fig. 2. Theoretical constructs of the quilt arrangement in multi-vaned vendobiont. ‘*n*’ denotes the number of vanes. In the case of *n* = 2, only one type of arrangement is possible. In the case of *n* = 3, there are two types of arrangement possible; these two are mirror images to each other. In the case of *n* = 4, there are three types of arrangement possible: [1234], [1243] and [1432]. [1234] and [1432] are mirror images to each other. For [1243] three equivalent quilt arrangements [1324], [1342] and [1423] are also illustrated. These three can be overlapped with [1243] by rotation along the seam; corresponding vanes of [1243], [1324], [1342] and [1423] are indicated with the same colour.

[1342], [1423] and [1432] (Fig. 2). [1243] can be overlapped to [1324] when the former is rotated by 90° anticlockwise around the axis. In the same way, [1243] and [1423] are equivalent to [1342] after rotation around the seam by 180°, and after rotation by 270°, respectively. Consequently there are only three different arrangement types [1234], [1432] and [1243] (Fig. 2) left for the case *n* = 4. [1234] and [1432] are mirror images to each other. [1243] is the mirror image of itself.

Although the above results are for vanes with infinite length, correlation between them and patterns exhibited by real Vendobionta is easy to carry out, as long as the fossils preserve at least a fragment containing more than one quilt structure on each vane along the seam.

Quilt patterns and mode of growth

Vendobionts have finite lengths defined by the two ends of the seam. The existence of tips introduces more constraints. Here, such constraints are considered for the case with *n* = 2. Quilt arrangement between two tips can be classified into four patterns.

If the total number of quilts in both vanes is odd, and the difference in quilt numbers is minimal between the two vanes, the number of quilts in one vane is by one quilt larger than that of the other vane. According to the condition that odd-numbered quilts are on the left or right vane, there are two types (A and B in Fig. 3). In both cases, the head end of longer quilt sequence is by *d*/2 ahead of the shorter sequence and the tail by *d*/2 behind the even one. If the total number of quilts in the two vanes is even and the difference in quilt number between the two vanes is minimal, both vanes must have the same number of quilts. In this configuration, there are two possible variations: either the quilts on the left or right hand vanes are offset ahead by *d*/2 relative to those on the opposite vanes (C and D in Fig. 3).

This recognition is very important for inferring the mode of growth of those organisms. As an example, we consider the case that the organism grows by adding quilts alternately at one tip and grows in such a manner that the difference between the quilt numbers stays minimal (i.e. one or zero). If the organism of type A is taken as the starting point, the new quilt is added at the right

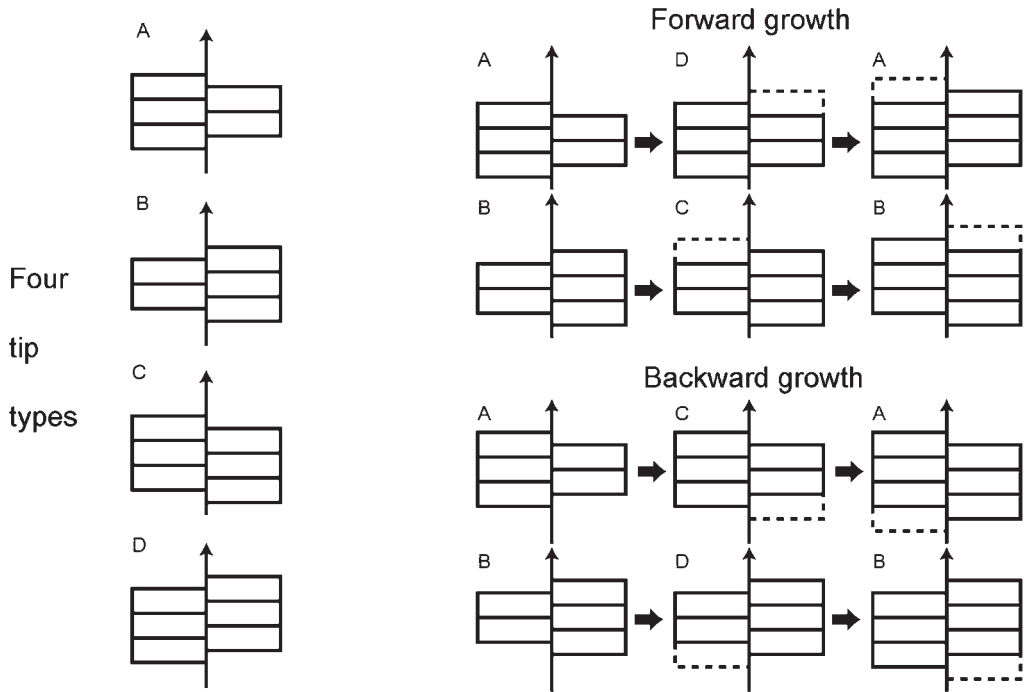


Fig. 3. Quilt patterns at tips and mode of growth. A and B, number of quilts is odd: A, left tip containing one more quilt than the right; B, = right tip containing one more quilt than the left. C and D, number of quilts is even and equal between the two sides: C, the left quilts ahead of the right ones; D, right quilts ahead of the left ones. This theoretical construction predicts that each of different manners of incremental growth at tips yields specific combination of types A to D, which can be recognized among fossil assemblages.

tip, changing the organisms to type D. In this organism of type D, then, the new quilt is added at the left tip, bringing it back to type A. Consequently, in a fossil assemblage with this manner of growth, we can find only the combination of type A and D. Therefore, the distinction of these types in fossils may provide us with the mode of growth of organisms with quilted vanes (see Fig. 3 for other possible growth modes and accompanying occurrence of tip types). This type of analysis may be usefully applied to investigating growth modes of *Yorgia* or *Spriggina* (Fedonkin 2003; Seilacher *et al.* 2003).

Pteridinium specimens from Aar Farm

Pteridinium is a well-known Ediacaran fossil, which has three quilted vanes meeting along a seam. Along the seam, quilts meet each other in an alternating fashion. Previous studies have described in some detail morphological characters of *Pteridinium*. Pflug (1970) reconstructed *Pteridinium* as a complex of vanes connected to form a canoe-shaped body. Grazhdankin & Seilacher (2002) studied

taphonomical and morphological features and described the general morphology of *Pteridinium* as follows. Two sides of the boat (i.e. two lateral vanes) meet along a median seam. Along this seam, the mould can be broken to reveal the impression of the third, median vane. All vanes are patterned by parallel and evenly spaced furrows of quilts, which meet the seam at nearly a right angle.

To test whether or not our simple model can be applied to the morphology of this real Vendobiont, we studied specimens from Aar Farm in Southern Namibia (Fig. 4). Preserving their three-dimensional morphology, they are suitable for this analysis. Normally, quilts within each vane are arched in the same direction (Fig. 4), indicating the polarity of the organism. Here we define the convex side of the arch as anterior facing. Specimen A in Figure 4 is a fragment preserving a lateral vane and a median vane. Figure 4A1 shows the anterior and Figure 4A2 the left side of the median vane of the specimen (see viewing directions for A1 and A2 in the upper left corner of Fig. 4). Figure 4A3 is a line drawing of A2. Specimens B and C are counterparts. Figure 4B2 and

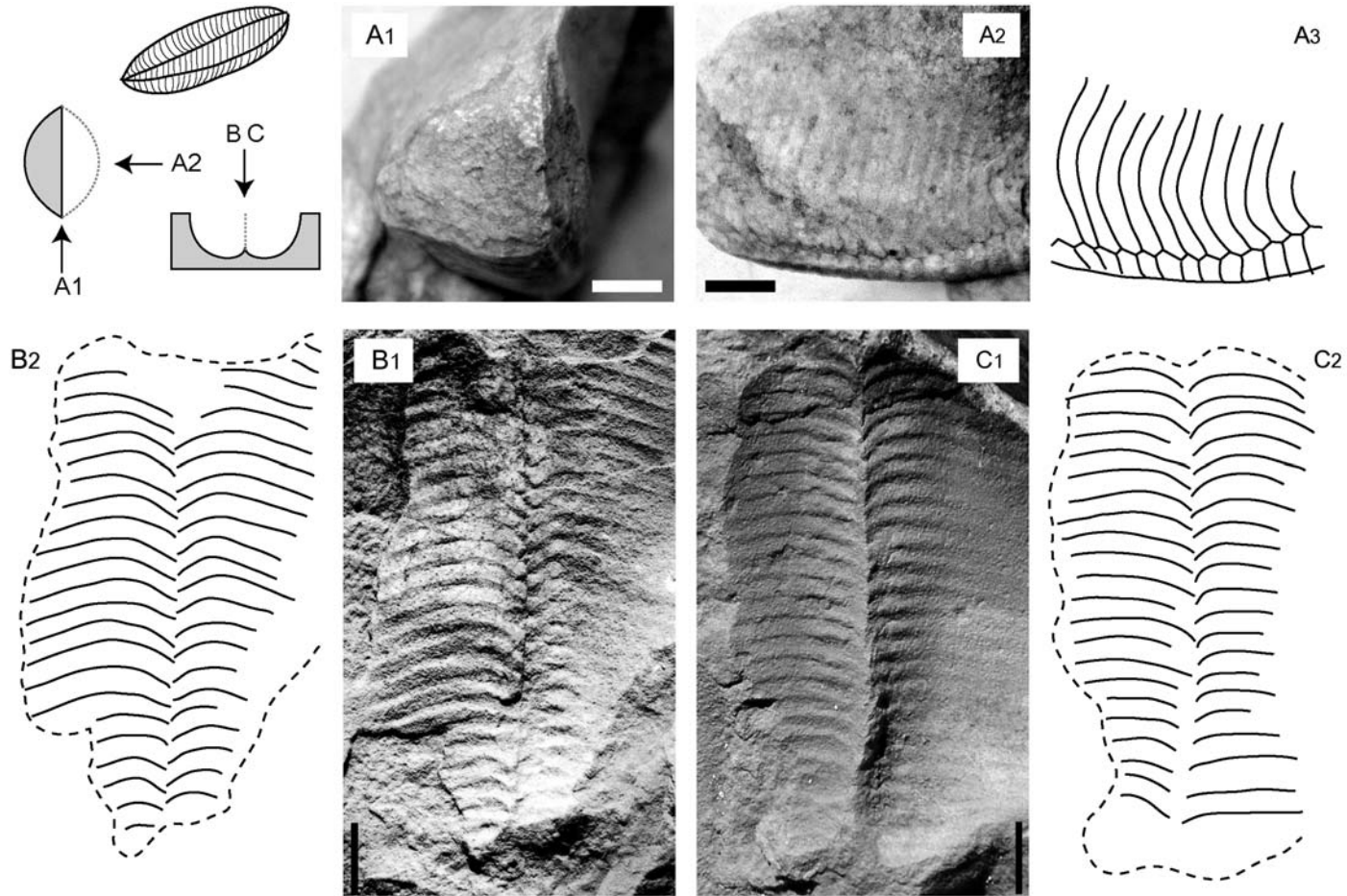


Fig. 4. *Pteridinium* specimens from Aar Farm in southern Namibia. Scale bars are 1 cm long. (A) part preserving a lateral vane and a median vane. (A1) view from the anterior; (A2) lateral view on the median vane (view direction for A1 and A2 pictures are shown on the upper left corner of the figure); (A3), line drawing of A2; (B–C), counter parts; (B1) and (C1), views from the top (viewing directions for these specimens are indicated on the upper left corner of the Figure); (B2) and (C2) line drawings of B1 and C1, respectively.

Figure 4C2 are views from the top for the two specimens (viewing directions in upper left corner). Line drawings for both specimens are also shown (Fig. 4B2 and Fig. 4C2). In about 80 examined specimens, including the three illustrated ones, quilts of the two different vanes meet along the seam in alternating fashion, indicating that in *Pteridinium* the quilts of all three vanes alternate along the seam. Further, the shift between two vanes is about 1/3 of the quilt width. In specimen B of Figure 4, quilts of the right vane shift forward by 1/3 quilt width relative to those on the left side. In the specimen Figure 4C, the quilts of the left vane shift forward by 1/3 quilt width relative to the right vane. The existence of two types of quilt arrangements are predicted for the case where the vane number is three. In fact, the quilt arrangement of the specimen B in Figure 4 corresponds to the [123] type, and the quilt arrangement of the specimen C in Figure 4 to the [132] type. Almost half of the 80 examined specimens shows [123] type and the other half [132] type.

Discussion

Our theoretical consideration predicts that there is a finite number of quilt arrangements along the seam in multi-vane vendobionts, and that the number of possible arrangements increases with the number of vanes. For the case of $n = 3$, we predicted two types ([123] and [132]). The examination on three *Pteridinium* from Aar Farm confirms this prediction.

The two quilt arrangement types observed in the *Pteridinium* are mirror images to each other. In nature there is analogous phenomenon. For example, gastropod shells can coil in sinistral or dextral direction. In gastropods, the chirality (sinistral or dextral of different chirality) is genetically determined. Further, the difficulty of copulation between different chiral individuals of the same species, one of the two would eventually eliminate the other. Thus, the study of the chirality of certain organism, or groups of organisms, can tell demonstrate how genetics and environmental factors influence the evolution of organisms concerned. Further investigation on quilted Vendobionta, by analogy, may provide us with information about the genetic controls on some of the vendobionts.

We do not apply the results of our consideration about the growth of the quilted patterns on all vendobionts. However, at least one tip is preserved as large 'head region' in *Yorgia* and *Spriggina*. Therefore, a statistical study of these forms, might provide clues about their mode of growth, which in turn may shed light on the taxonomic status of vendobionts.

Conclusion

There appears a good match between theoretically predicted quilt arrangements of different vanes meeting together along one seam and a those occurring in the vendobiont *Pteridinium* from Aar Farm, southern Namibia. Nearly half of the 80 specimens examined possessed [123] type and the remainder [132] type. Theoretical considerations predicted that the 'handedness' in quilt arrangement between two tips is determined by the mode of growth, and or what Vendobiont is. Better understanding of the possible genetic control of such growth patterns may in the future assist in determining the true systematic position of vendobionts.

We express our cordial thanks A. Seilacher and R. Jenkins for their useful comments on our study, and G. Schneider (Director of the Geological Survey of Namibia) for her kind permission and support for our research activities in Namibia. We also express our great thanks to Barbara and Bruno Boehm (owners of Aar Farm) for their gracious permission to carry out our research on their land.

References

- FEDONKIN, M. A. 2003. Origin of the Metazoa in the light of the Proterozoic fossil records. *Paleontological Research*, **7**, 9–42.
- GRAZHDANKIN, D. & SEILACHER, A. 2002. Underground Vendobionta from Namibia. *Palaeontology*, **45**, 57–78.
- PFLUG, H. D. 1970. Zur Fauna der Nama-Schichten in Südwest-Africa. I. Pteridinia, Bau and Systematische Zugehörigkeit. *Palaeontographica A*, **134**, 226–262.
- SEILACHER, A. 1992. Vendobionta and Psammocorallia: lost constructions of Precambrian evolution. *Journal of the Geological Society, London*, **149**, 607–613.
- SEILACHER, A., GRAZHDANKIN, D. & LEGOUTA, A. 2003. Ediacara biota: The dawn of animal life in the shadow of giant protests. *Paleontological Research*, **7**, 43–54.

The Verdun Syndrome: simultaneous origin of protective armour and infaunal shelters at the Precambrian–Cambrian transition

J. DZIK

Instytut Paleobiologii PAN, Twarda 51/55, 00–818 Warszawa, and Instytut Zoologii, Uniwersytet Warszawski, Banacha 2, 00–913 Warszawa, Poland
(e-mail: dzik@twarda.pan.pl)

Abstract: All of the structurally identifiable latest Ediacaran and earliest Cambrian infaunal trace fossils represent shelters of animals feeding above the sediment surface. It is the case with the most complete and oldest radiometrically dated Precambrian–Cambrian transition strata along the Khorbusonka River in northern Siberia, in the basal Cambrian succession at Meishucun in southern China, richest in small shelly fossils, as well as in the type succession of the Vendian in Podolia, Ukraine. The oldest traces of feeding within the mud are known from no earlier than the late Tommotian of Siberia, Mongolia, Sweden, and Poland. This suggests that the invention of hydraulic mechanisms of sediment penetration was enforced by predation, not by trophic needs. Various ways to protect the body by secretion of a mineral skeleton or building tubes by collected mineral grains were developed by other animals at the same time. Predation may thus appear to be the triggering mechanism for the ‘Cambrian explosion’. Subsequent increase in the depth of bioturbation resulted in a profound change of taphonomic conditions, artificially enhancing the effects of evolution.

There are two primary sources of evidence on the Precambrian–Cambrian evolution of marine faunas: the ‘Ediacaran biota’ of imprints of soft-bodied organisms in sandstone facies and the ‘small shelly fossils’ assemblages of mostly secondarily phosphatized remains of mineral skeletons in limestone facies. Owing to recent progress in understanding the taphonomy of the Ediacaran fossils, significant anatomical data has rapidly emerged from the long-known fossil collections. Imprints of dorsal surfaces of decaying bodies, fixed by early diagenetic iron sulphide cementation of soft sand (‘Ediacaran death masks’; of Gehling (1999)); may offer information on the distribution and mechanical properties of the internal organs (Dzik 2003). Impressions of animal bodies passively or actively settling on the surface of a microbial mat (‘Shroud of Ediacara’; of Dzik (2003)) inform about the external morphology of Ediacaran animals. Among the minute phosphatic and secondarily phosphatized fossils, easy to extract from limestone samples with organic acids and frequently numerous, there are not only elements of the skeletal armour (scleritomes), but also phosphatized organic tissues or even whole embryos (e.g. Bengtson & Zhao 1997).

These highly valuable sources of palaeontological information have their limitations, however. Early diagenetic phosphatization was a rare phenomenon, except for the Early Cambrian, and gradually

disappeared during the early Palaeozoic, probably the result of increased bioturbation depth in pelagic sediments (Dzik 1994). Fossilization of entirely soft bodies, not easily escaping scavengers and bacterial decay, is even less likely. After their Ediacaran abundance, such fossils became extremely rare. In the Ediacaran White Sea locality Zimmie Gory in northern Russia, the Devonian Bundenbach slates of the Hunsrück Mountains in Germany and the Jurassic Solnhofen lithographic limestone of Bavaria, ‘death tracks’ occur, represented by short (frequently spiral) trace fossils with the carcass of the animal at the end, apparently thrown into a toxic environment. These were thus extreme environments, in the Ediacaran time supporting only bizarre, and probably chemoautotrophic organisms in place (Dzik 2003). Even if the stratigraphic ranges of the Ediacaran biota and small shelly fossils may partially overlap, there is a wide gap in our knowledge of Precambrian–Cambrian organisms in between these two taphonomic windows. The gap exists not only in their time distribution, but also in a range of less unusual environments.

This gap can be filled partially with evidence offered by traces organisms left in their activities, where their bodies had no chance to fossilize. Much data on the latest Precambrian and earliest Cambrian trace fossils has accumulated, but the main difficulty in interpreting this data results

from their lack of precise dating. The situation has improved significantly with the acquisition of diverse and unusually informative trace fossil assemblages from the Mattaia Creek section at Khorbusuonka in northern Siberia (Dzik 2005). These occur primarily below the occurrence of the abundant *Manykodes* (= '*Phycodes*') *pedum*, the appearance of which defines the base of the Cambrian (although it probably also occurs somewhat below in the stratotype section of Newfoundland; Gehling *et al.* 2001), and from above a radiometrically dated volcanic breccia (Bowring *et al.* 1993). All are traces of infaunal activities of animals penetrating the sediment but feeding above it. Their burrows were, thus, protective shelters.

The first skeletal remains of a variety of organisms occur in the same rock unit (Khomentovsky & Karlova 1993), as well as in coeval strata elsewhere. Thus, it is likely that predation forced the latest Ediacaran animals to either seek shelter under the sediment surface or protect themselves with mineral skeletons ('the Verdun Syndrome'; Dzik 2005). Such explanation of the sudden emergence of skeletonized animals at the beginning of the Cambrian was first proposed by Evans (1912).

In the present paper this idea is developed further, with a more specific presentation of the probable anatomy of the earliest producers of infaunal trace fossils. Additional evidence on the succession of specific modes of infaunal penetration, as reflected by trace fossils from Podolia, Ukraine, and the Meishucun locality in Yunnan, China is also presented.

The late Ediacaran infaunal trace makers

The Olenek River region in polar Siberia is among the few sites in the world where the Precambrian–Cambrian transition is documented by radiometric dating (Bowring *et al.* 1993), a stable isotope record (Pelechaty *et al.* 1996; Kouchinsky *et al.* 2001), Ediacaran biotas (Fedonkin 1985), skeletal remains (Khomentovsky & Karlova 1993), and trace fossils (Fedonkin 1985). As in fossiliferous successions elsewhere, traces of infaunal activity are missing in strata with Ediacaran fossils in Siberia. Although Seilacher (1999) suggested that most Ediacaran trace fossil makers fed below the microbial mat, this was falsified by the discovery of intact mats in the Zimmie Gory section (Dzik 2003). Both body and trace fossils occur there on the upper surface of the mat. Only shallow surface burrows are known from deposits of such age elsewhere (Jensen 1995, 2003; Jensen *et al.* 2005). The oldest common traces of deep sediment penetration by worm-like animals have been recovered from the middle part of the Nemakit-Daldynian

(Manykayan) Kessyusa Formation in exposures near the mouth of the Mattaia Creek in the Khorbusuonka River section of the Olenek region.

Many types of trace fossils occur in the Kessyusa Formation. Virtually all bedding plane trace fossils assemblages there are monospecific, and it is difficult to separate results of evolutionary change from changes controlled by purely ecological and environmental factors. Different species seem to be restricted to specific kinds of sediments. Narrow U-shaped, shallow burrows are found in thin layers of dark mudstone intercalated with siltstone and sandstone. The mud was apparently firm, because the burrows remained open during life of their makers, preserving a cylindrical cross-section (Dzik 2005). Synsedimentary faults offer proof that the light-grey quartz mud, in which serial cylindrical burrows of *Manykodes pedum* were dug, was firm in its whole bed volume already before deposition of the overlying pure sand layer. Also, the small trilobate burrows of *Podolodes* were produced in a relatively firm, fine-grained mud. In a softer, but coarser, sediment trace makers tended to dig deeper and make burrows circular in cross-section (Dzik 2005). The horizontal galleries of *Mattaia miettensis* were excavated in green glauconitic sand.

Continuous horizontal galleries in sand

Probably the most bizarre Early Cambrian traces of infaunal activity are those produced by *Psammichnites*. As interpreted by Seilacher (1995) and McIlroy & Heys (1997; referred to as *Plagiognus*), these were made by animals horizontally penetrating sandy sediment at a stable depth. Sediment stripes were left behind as a result of their movement with retrograde peristaltic wave. An organ exposed to the surface was cutting the sediment while the worm moved (Seilacher 1995; Jensen 1997) and collecting food together with the sediment from the surface.

Continuous burrows of *Mattaia miettensis* are similar to those of *Psammichnites*. They occur within the glauconitic sandstone beds in the Mattaia section, as well as in the coeval strata exposed along the Olenek River in the same region of northern Siberia (Fedonkin 1985). Owing to a clear delimitation of particular rock layers by clay-rich laminae (possibly representing remnants of microbial mats), the cross-section of the rock shows the internal structure of the trail (Fig. 1a).

The lack of deformation of layers below the trail indicates that it was not produced by action of any hydraulic pushing mechanism, but the sediment was simply abraded by the organism. The trace itself is filled with two bands of a homogenized sediment, laterally raised and depressed in the centre, where the bands are separated by a vertical fissure filled with clay (cf. Young 1972). The

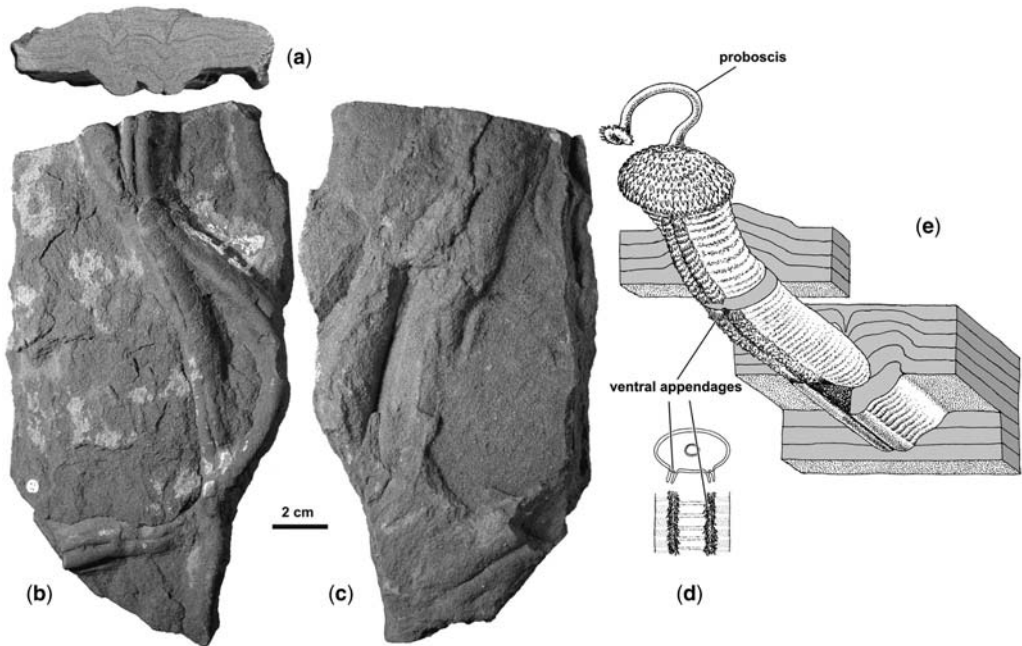


Fig. 1. Reconstruction of *Mattaia miettensis* (Young 1972) from the latest Ediacaran Kessyusa formation at Mattaia Creek, inferred from the structure of its horizontal bilobed galleries. (a–c) Cross-section, lower, and upper surface of a glauconitic sandstone slab with two associated galleries. (d–e). Diagram showing the arrangement of sediment layers while the trail was made. The morphology of the inserted priapulid worm is based on the mid-Cambrian *Louisella* (data from Conway Morris 1977).

volume of these bands corresponds roughly with the volume of sediment removed from the channel. This means that all the material removed mechanically from below was transported behind. The smooth surface of the double ventral furrow at the lower surface of the gallery suggests that this was the route of the sediment transport. In well-preserved specimens the outer lateral bevel consists of series of transverse, slightly oblique folds suggesting that the animal was propelled by retrograde peristaltic wave (Dzik 2005).

The clay laminae above the trail remained intact, but are folded and raised evidently as a result of a gentle hydraulic elevation of sand by the organism. Sediment above the trail first appears to have been pushed upwards to flow on both sides and then collapsed in the middle behind the animal. In the centre of the trail, the laminae dip down to form a vertical zone where the organ exposed to the surface was apparently cutting the sediment while the organism moved, collecting food together with the sediment from the surface (Hofmann & Patel 1989).

In the glauconitic sandstone of the Kessyusa Formation such galleries were dug in so sophisticated a manner that much anatomical information can be extracted from the observed deformations of the sediment layers. Although the inferred body

organization is unlike any living animal and seems strange at a first glance, there were similar organisms in the Cambrian. The Burgess Shale priapulid *Louisella pedunculata*, as restored by Conway Morris (1977), had a long, eversible proboscis, the prosoma armed with hooks, an annulated body and, most interestingly, two ventral strips of minute appendages. Moreover, its cross-section was significantly depressed (Fig. 1d). Using *Louisella* as a prototype, not much transformation would be necessary to have the body organization necessary to produce all those trails (Fig. 1e).

Cylindrical branching burrows

The earliest Cambrian clay-rich sediment surface was probably firm enough that empty burrows in it did not collapse without additional impregnation (Droser *et al.* 2002). These most likely permanently open shelters of a surface detritus feeder subsequently filled with sand (Jensen 1997). That they were empty during life of the producer is convincingly demonstrated by an aggregation of clay-rich faecal pellets at the bottom of burrows of related *Manykodes rectangularis* from the latest Cambrian of the Holy Cross Mountains, Poland (Fig. 2; Orłowski & Żylińska 1996).

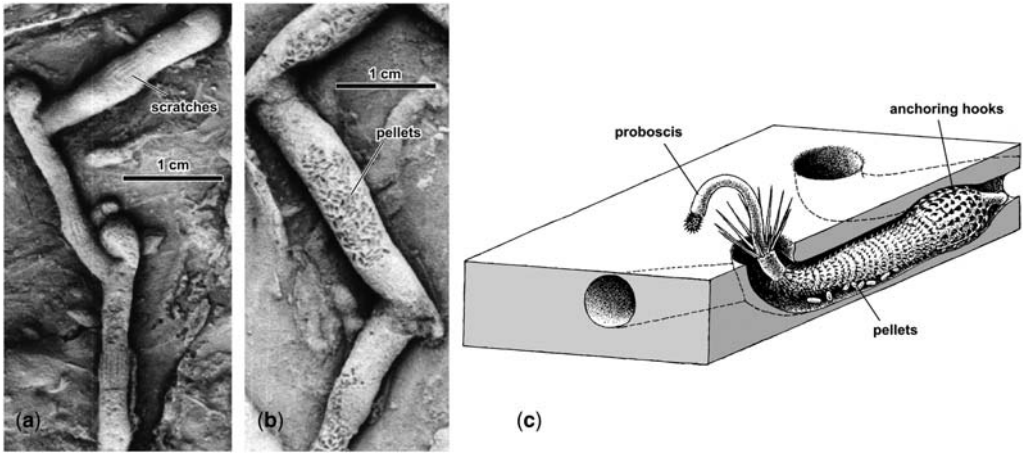


Fig. 2. Biology of *Manykodes rectangularare* (Orłowski & Żylińska 1996) from the latest Cambrian Klonówka Shale at Wiśniówka in the Holy Cross Mountains, Poland, inferred from the morphology of its serial burrows. (a, b) Specimens showing scratches left by hooks covering the animal (a) and faecal pellets at the bottom of chamber (b). Such traces indicate that the burrow was originally empty and that the animal was deposit feeding above the sediment surface (originals of Orłowski & Żylińska 1996). (c) The Early Cambrian priapulid *Corynetis* (data from Huang *et al.* 2004) situated in the burrow of *Manykodes* to demonstrate the correspondence in distribution of scratch marks in the burrow and anchoring hooks in the animal's body.

These Late Cambrian trace fossils provide important information about the anatomy of their makers, which can be extrapolated also to older, earliest Cambrian species. Swollen parts of the burrow are marked with a ring of 15–20 longitudinal striae. Digging was apparently performed with hooks surrounding the body, such as those in the priapulid prosoma. Such swellings developed most probably when the animal retreated to the burrow, contracted and, as a result, widened its body.

The recently published information on the anatomy of the Early Cambrian priapulid *Corynetis* from the Chengjiang Fauna (Huang *et al.* 2004) suggests that it was not necessarily the prosoma, but rather anchoring hooks at the posterior part of the body which were responsible for scratches noted on the burrow wall. The long proboscis of *Corynetis* and the circle of long setae near its base suggest that this trace maker lived in a shelter with only its proboscis and protective setae extending from it, exactly what is suggested by the burrows of *Manykodes*, likely excavated by a related priapulid (Fig. 2c).

First mud eaters

It is commonly argued that internal body cavities originated in connection with hydraulic locomotion and burrowing (Clark 1964) and that it was the search for food which forced early animals to

begin infaunal life. If so, the oldest traces of peristaltic activities of the metazoans should be connected with their infaunal lifestyle. The fossil evidence does not support this.

The geologically oldest evidence of purposeful penetration of sediments for feeding are the horizontal 'rhizocorallium' spreite structures in a marly limestone facies of the late Tommotian (or early Atdabanian) in the Tiktiriktekh section on the Lena River near Yakutsk (Fig. 3a; Dzik 2005). Such feeding traces are known also from roughly coeval sandstones of northern Poland (Paczeńska 1996) and Mongolia (Goldring & Jensen 1996). More sophisticated spreite structures, apparently produced by related organisms in the Atdabanian of Sweden, show a helicoidal organization (Jensen 1997).

In the late Tommotian marly limestone at the Zhurinsky Mys locality along the Lena River section, narrow, linear burrows of probable mud-eaters are restricted to the laminated sediment fill of earlier meandering furrows in the firm ground surfaces, 2–3 cm wide and deep. The already bioturbated sediment was probably softer and easier to penetrate (Fig. 3b–c). It may also have been richer in organic matter, the actual impetus for digging.

Even among the infaunal burrows of the Late Cambrian, those produced by organisms feeding above the sediment surface are the most common (e.g. Orłowski & Żylińska 1996). Not before the

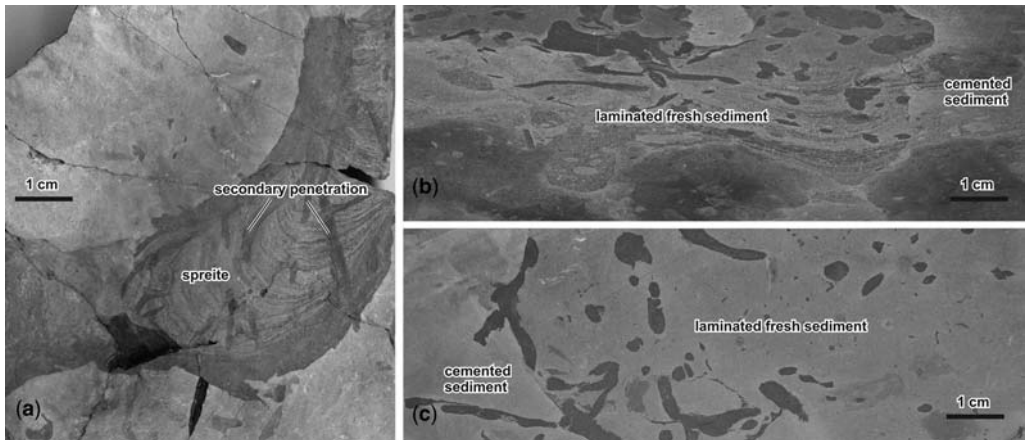


Fig. 3. The oldest infaunal mud-eaters from the Tommotian to earliest Atdabanian Pestrosvetnaya Formation of the Lena River section near Yakutsk. (a) Horizontal spreite structure ('rhizocorallium') from the Tikirikteekh Locality, probably produced by a relative of *Diplocraterion*. Note secondary burrows penetrating the reworked sediment of the spreite. (b, c) Vertical and horizontal section across the sedimentary discontinuity surface at Zhurinsky Mys with minute horizontal burrows preferably penetrating the soft sediment filling the network of older and wider horizontal burrows.

Ordovician do feeding burrows dominate the trace fossils assemblages.

Transitions between various forms of the Ediacaran infaunal behaviour

At first glance, the difference between the short, trilobed and depressed shallow burrows in firm clay, continuous galleries in sand and serial U-shaped cylindrical burrows in firm clay from the latest Ediacaran of the Olenek River region look like a fundamental and abrupt change. However, traces indicative of transitional behaviours are known from other Ediacaran–Cambrian localities.

Intermediates between cylindrical and trilobed burrows

About 15 m above the base of a mudstone series exposed at Khorbusuonka near the mouth of the Mattaia Creek, the lower surface of glauconitic sandstone beds is densely covered with casts of generally shallow burrows in the underlying claystone (referred to *Podolodes tripleurum* in Dzik 2005). The dominant morphology is three-lobed. Similar traces are known also from Namibia (Geyer & Uchman 1995; Jensen *et al.* 2000) and Mongolia (Goldring & Jensen 1996). In profile view, the burrow casts are gently convex, with both ends smoothly disappearing at the bedding plane. Rarely, they are arranged in linear series. On sandstone slabs covering a more sand-rich clay, burrows

have nearly circular cross-section. Similar burrows are known from the Chmielnicki Formation of Podolia, Ukraine, usually exhibiting a medial fissure along their ventral surface and arranged in linear series (Palij *et al.* 1983; Dzik 2005). Sometimes, the fissure splits, giving the ventral surface of the burrow a three-lobate appearance.

The similarity of the three-lobed burrows of *Podolodes* to a branching series of cylindrical burrows of *Manykodes* is highlighted by the plait-like arrangement of alternating series of shallow burrows of *Podolodes triplex* from Podolia (Palij *et al.* 1983; Dzik 2005) and eastern Poland (Paczeńska 1996). In both the specimens from Khorbusuonka and Podolia there is a gradation from three-lobed shallow to fully submerged burrows with a round cross-section and a smooth or bilobed lower surface. They may alternate but may also be arranged linearly (Jensen & Mens 2001).

There is, thus, a gradation of morphologies of trace fossils from shallow U-shaped burrows with circular cross-section to even shallower burrows with a three-lobed ventral surface. Although the burrows do not offer much information about the detailed anatomy of their producers, some inferences can be attempted. Indistinct, transverse wrinkles in the central belt of the trace may reflect a peristaltic wave moving along the body. The clear-cut course of the lateral ridges suggests that they were produced by longitudinally arranged series of appendages. This is not unlike the body plan inferred for *Mattaia*, which is represented by horizontal galleries in sand from the same strata.

Intermediates between bilobed horizontal galleries and trilobed burrows

The collapsing galleries of *Mattaia miettensis* were dug horizontally between sand layers. In this respect they differ rather markedly from other trace fossils recognized in the terminal Ediacaran strata of northern Siberia. However, in the Chmielnicki Formation of Podolia, Ukraine, similar horizontal galleries occur on the sole of sandstone beds covering claystone.

The lower surface of the trails of *Mattaia tirasensis* from Podolia is bilobed (Fig. 4; Palij *et al.* 1983). In places the traces are arranged into series of separate burrows, but in others the burrows are continuous and parallel to the sediment surface. In the short burrows with a three-lobed ventral surface, sometimes developed centrally, the generally irregular appearance of the traces makes observation difficult. These shallow, continuous burrows in clay, possibly produced at the clay-sand interface, demonstrate a transition from the temporary shelters of *Podolodes* to more permanent penetration of sand, resulting in continuous galleries below the sediment surface.

Correlation of earliest infaunal traces and small shelly fossils

There are two reasons to think that the advent of skeletonization was related to the function of the external skeleton, rather than to it resulting simply as a response to the geochemical environment of the Precambrian–Cambrian oceans: (1) skeletons

of calcitic, aragonitic, phosphatic, and siliceous composition emerged virtually simultaneously, although not necessarily in the same environment; (2) amongst the first protective skeletal innovations were agglutinated tubes built of foreign objects by the animals inhabiting them—exemplified by the worm *Onuphionella*, with its collection of mica flakes lining its shelter (Signor & McMenamin 1988). Such particle collecting behaviour required not only anatomical adaptations allowing organisms to pick out and glue together skeletal debris with organic secretions, but also an advanced neural system enabling such sophisticated behaviour.

In order to explain the origin of skeletonization in early animals, it is necessary to establish the chronological relationship between first mineralized armours and the fossil traces of activity of these early ‘arms manufacturers’. The first calcareous tubular fossils occur in strata of similar age to those containing the Ediacaran fauna (Bengtson & Yue 1992), as is also true in the Khorbusuonka section (Khomentovsky & Karlova 1993). However, the metazoan nature of the tubes cannot be established yet. The oldest taxonomically identifiable skeletal fossils of undoubted animal affinity remain the phosphatic small shelly fossils.

In Siberia, the Kessyusa Formation has yielded the oldest record of phosphatic conchs and tubes of unquestionable metazoan affinities. In the section at *Mattaia*, horizons within the dark, laminated mudstone unit containing winnowed concretions have yielded numerous calcareous tubes. In acid-resistant residue, phosphatic internal moulds of their apices with swollen tips demonstrate that these are laterally compressed conchs of a hyolith-like

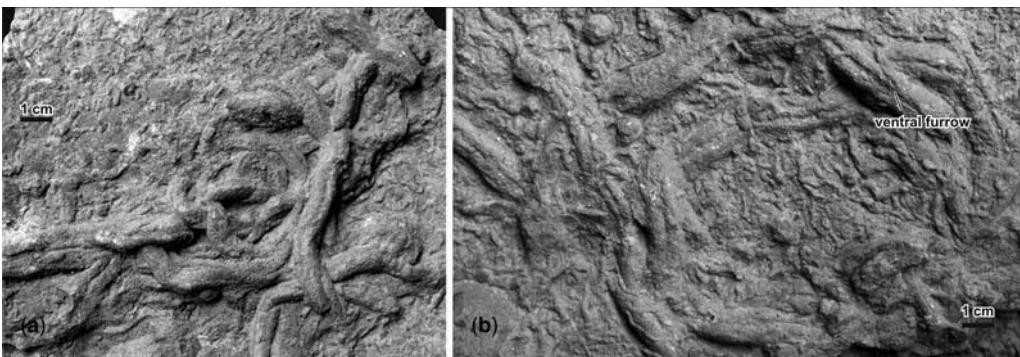


Fig. 4. Burrows of *Mattaia tirasensis* (Palij 1974) from the lower part of the Chmielnicki Formation at the village Subocz on the right bank of the Dniester River, Podolia, Ukraine, dug in clay and morphologically transitional between horizontal bilobed galleries of *Mattaia* and three-lobed series of *Podolodes* (originals of Palij *et al.* 1983 housed at the Geological Institute, Kiev). (a) Sole face of sandstone slab with deep, bilobed burrows tending to develop a separation between ventral furrows, similar to partially three-lobed linearly short burrows of *Podolodes* sp. from the same formation (cf. Dzik 2005, Fig. 3a–b). (b) Slab with shallow burrows more similar to *Mattaia miettensis*; note that in both cases the animal tended to produce short burrows instead of truly continuous galleries.

mollusc—*Ladatheca annae*. Other tubular fossils (enigmatic *Conothecha* and probable anabaritid *Spinulitheca*) are associated (Dzik 2005). In coeval strata exposed along the Olenek River, planispiral conchs of the bellerophonitid mollusc *Latouchella*, the probable sinistral gastropod *Barskovia*, and the low-conical possible monoplacophoran *Purella* occur (Khomentovsky & Karlova 1993). The first infaunal traces of activity in the area are thus coeval with the oldest occurrences of small shelly fossils.

The earliest Cambrian succession at the Meishucun section in Yunnan, China, is the richest in phosphatic fossils. However, its correlation with the Cambrian units of Siberia, is highly controversial. The lowest unit containing skeletal fossils in China is Bed 3 at the base of the Zhongyicun Member of the Dengying Formation (Qian & Bengtson 1989). Qian & Bengtson (1989) recovered small shelly fossils in Beds 3–6, insufficient to assign a precise age correlation with strata elsewhere, but probably about the same age as the Nemakit-Daldynian (Manykayan) strata in Siberia. This is consistent with the occurrence of the first infaunal trace fossils which occur in a phosphate-rich oolite of Bed 3—serially branching circular tubes with openings at the surface (Fig. 5a, b). Most tubes are enveloped in phosphorite, which obliterates details of their morphology. The mode of branching and circular cross-section is similar to *Manykodes*, although diameters (5–7 mm) are larger than in *M. pedum* from Siberia.

Poorly preserved alternating serial burrows similar in size to *M. pedum* occur in Bed 5 of the same rock unit (Fig. 5d), thus it is definitely Cambrian in age (Tommotian according to Jenkins *et al.* 2002). Co-occurring horizontal galleries resemble *Mattaia* in showing a convex ventral surface, but the ventral furrow is not recognizable on the specimen (Fig. 5c). Undoubted *Mattaia* (*Didymaulichnus* in Crimes & Zhiwen 1986) occurs in Bed 7 of the Zhongyicun Member, in which small shelly fossils with a Tommotian aspect occur. In the same bed, the first arthropod resting traces occur (Crimes & Zhiwen 1986), associated with cylindrical U-shaped burrows (Fig. 6a). Although the trilobite nature has not been established, an Atdabanian age of the bed has been suggested. Large horizontal galleries with collapsing roof, representing *Mattaia* or *Psammichnites* (*Taphrhelminthopsis* in Crimes & Zhiwen 1986), emerge in Bed 9 at the base of the Badaowan Member and continue throughout the succession upwards to the Canglangpu Formation (Fig. 6b, c), which is located above the mudstone unit with the Chengjiang fauna, containing fossils of soft-bodied animals. According to Qian & Bengtson (1989), the Badaowan Member small shelly fossils suggest an age not older than Atdabanian, possibly Botomian.

In general, the Meishucun assemblages of trace fossils are similar to those from northern Siberia, although the specimens are not as informative. Their advent is roughly synchronous with the

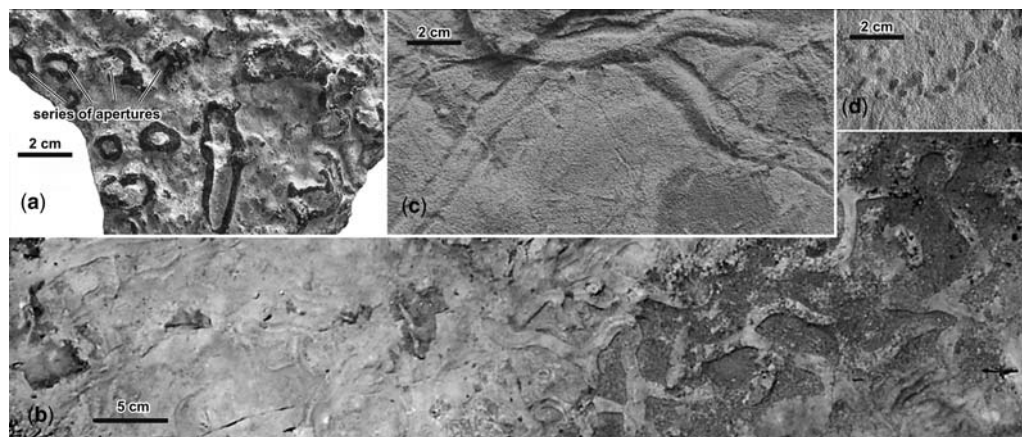


Fig. 5. Trace fossils from the oldest unit containing small shelly fossils (Zhongyicun Member of the Dengying Formation) at Meishucun, Yunnan (specimens collected by Wang Zhongzhi, housed at the Kunyang Phosphorite Mine museum at Kunyang). (a, b) Horizontal cylindrical burrows from Bed 3 remotely resembling *Manykodes*, with serial apertures at the sediment surface; partially weathered out phosphoritic envelopes of the burrows with linearly arranged apertures (a) and branching on an upper bedding plane cut by erosion (b). (c) Horizontal galleries from Bed 3 with convex, possibly bilobed lower surfaces, resembling small-size *Mattaia*. (d) Alternating serial burrows of *Manykodes* from Bed 5.

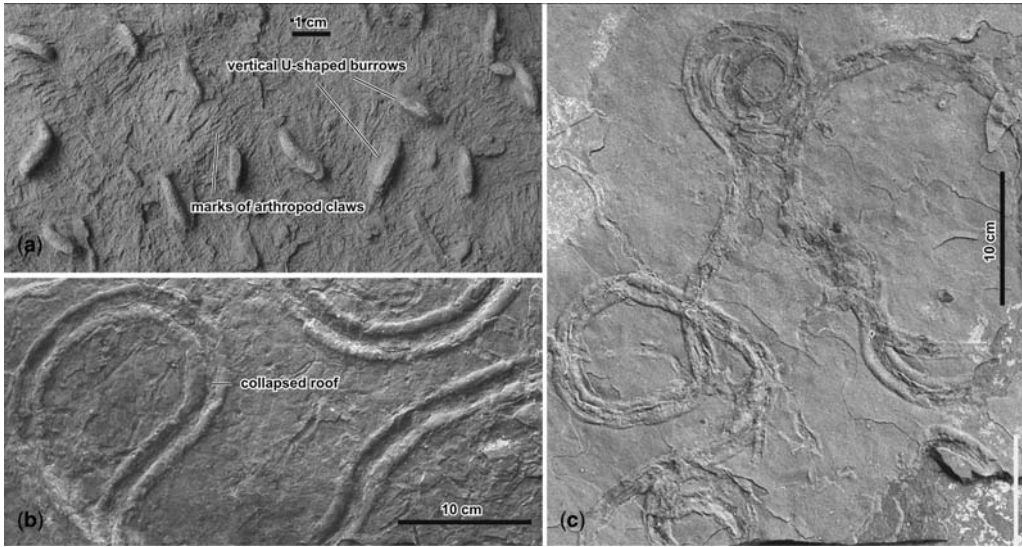


Fig. 6. Trace fossils from the post-Tommotian Early Cambrian of the Meishucun section (specimens collected by Shishan Zhang, housed at the Kunyang Phosphorite Mine museum at Kunyang). (a) Cylindrical U-shaped burrows and marks of arthropod appendages from Bed 7 of the Zhongyicun Member; sole of the bed. (b) Wide horizontal galleries with collapsing roof of *Mattaia* or *Psammichnites* from Bed 12 of the Badaowan Member. (c) Similar but narrower gallery from the Canglangpu Formation.

appearance of phosphatized skeletal remains of unquestionable metazoan affinities. Also in this succession, infaunal feeding traces are unknown in the earliest Cambrian strata. All of the animals producing elaborate chambers and galleries in the sediment seem to have searched for food at the surface.

Conclusion

All interpretable trace fossils from the Ediacaran–Cambrian transition strata of northern Siberia, South China, Ukraine and elsewhere represent shelters of infaunal animals which appear to have been collecting food from above. McIlroy & Heys (1997) found it paradoxical that these animals wasted so much energy in burrowing, while seeking for the organic detritus on the sediment surface. True mud-eaters appeared later (McIlroy & Logan 1999). The synchronicity of the development of various sorts of protective armour with the origin of the infaunal mode of life suggests a similar cause—probably the development of predatory organisms targeting large metazoans. This was the beginning of an ‘arms race’, giving the choice to either shelter behind a strong mineralized skeleton or to hide in the sediment. Eventually, the expansion of infaunal life destroyed the widespread and vast cyanobacterial mats in shallow regions of the sea

(Dzik 2003). Ironically, the profound change in conditions of sedimentation that so strongly biased the fossil record of the animal evolution near the Precambrian–Cambrian transition was at least partially caused by the evolving animals themselves.

I am thankful to A. Y. Ivantsov (Paleontological Institute, Moscow) for providing logistics during the expedition to the Khorbusuonka River section in 2001 (Research Grant 6 PO4D 010 13 from the Polish Committee of Scientific Research); S. Weiguo (Nanjing Institute of Geology and Palaeontology) guided me to the Meishucun section; S. Zhang kindly allowed me to examine and photograph specimens of trace fossils collected by him in the Meishucun Quarry, housed at the Kunyang Phosphorite Mine Museum at Kunyang; many thanks are due to P. Vickers-Rich for invitation to the Prato meeting and inspiration. Two anonymous reviewers significantly improved the text.

References

- BENGTSON, S. & YUE, Z. 1992. Predatorial borings in Late Precambrian mineralized exoskeletons. *Science*, **257**, 367–369.
- BENGTSON, S. & ZHAO, Y. 1997. Fossilized metazoan embryos from the earliest Cambrian. *Science*, **277**, 1645–1648.
- BOWRING, S. A., GROTZINGER, J. P., ISACHSEN, C. E., KNOLL, A. H., PELECHATY, S. M. & KOLOSOV, P.

1993. Calibrating rates of early Cambrian evolution. *Science*, **261**, 1293–1298.
- CLARK, R. B. 1964. *Dynamics in Metazoan Evolution: The Origin of the Coelom and Segments*. Clarendon Press, Oxford.
- CONWAY MORRIS, S. 1977. Fossil priapulid worms. *Special Papers in Palaeontology*, **20**, 1–97.
- CRIMES, P. & ZHIWEN, J. 1986. Trace fossils from the Precambrian–Cambrian boundary candidate at Meishucun, Jinning, Yunnan, China. *Geological Magazine*, **123**, 641–649.
- DROSER, M. L., JENSEN, S. & GEHLING, J. G. 2002. Trace fossils and substrates of the terminal Proterozoic–Cambrian transition: implications for the record of early bilaterians and sediment mixing. *Proceedings of the National Academy of Science of the USA*, **99**, 12572–12576.
- DZIK, J. 1994. Evolution of ‘small shelly fossils’ assemblages of the early Paleozoic. *Acta Palaeontologica Polonica*, **39**, 3, 247–313.
- DZIK, J. 2003. Anatomical information content in the Ediacaran fossils and their possible zoological affinities. *Integrative and Comparative Biology*, **43**, 114–126.
- DZIK, J. 2005. Behavioral and anatomical unity of the earliest burrowing animals and the cause of the ‘Cambrian explosion’. *Paleobiology*, **31**, 507–525.
- EVANS, J. W. 1912. The sudden appearance of the Cambrian fauna. *Report of the Session of the International Geological Congress, Stockholm*, **1910**, 543–546.
- FEDONKIN, M. A. 1985. Paleoikhnologia vendskich Metazoa. *In*: SOKOLOV, B. S. & IVANOVSKY, A. B. (eds) *Vendskaya Sistema. Istoriko-geologicheskoye i paleontologicheskoye obosnovanie. 1 Paleontologia*, 112–117. Nauka, Moscow [in Russian].
- GEHLING, J. G. 1999. Microbial mats in terminal Proterozoic siliciclastics: Ediacaran death masks. *Palaios*, **14**, 40–57.
- GEHLING, J. G., JENSEN, S., DROSER, M. J., MYROW, P. M. & NARBONNE, G. M. 2001. Burrowing below the basal Cambrian GSSP, Fortune Head, Newfoundland. *Geological Magazine*, **138**, 213–218.
- GEYER, G. & UCHMAN, A. 1995. Ichnofossil assemblages from the Nama Group (Neoproterozoic–Lower Cambrian) in Namibia and the Proterozoic–Cambrian boundary problem revisited. *Beringeria Special issue*, **2**, 175–202.
- GOLDRING, R. & JENSEN, S. 1996. Trace fossils and biofabrics at the Precambrian–Cambrian boundary interval in western Mongolia. *Geological Magazine*, **133**, 403–415.
- HOFMANN, H. J. & PATEL, I. M. 1989. Trace fossils from the type ‘Etcheminian Series’ (Lower Cambrian Ratcliffe Brook Formation), Saint John area, New Brunswick, Canada. *Geological Magazine*, **126**, 139–157.
- HUANG, D.-Y., VANNIER, J. & CHEN, J.-Y. 2004. Anatomy and lifestyles of Early Cambrian priapulid worms exemplified by *Corynetis* and *Anningvermis* from the Maotianshan Shale (SW China). *Lethaia*, **37**, 21–33.
- JENKINS, R. J. F. 1995. The problems and potential of using animal fossils and trace fossils in terminal Proterozoic biostratigraphy. *Precambrian Research*, **73**, 51–69.
- JENKINS, R. J. F., COOPER, J. A. & COMPSTON, W. 2002. Age and biostratigraphy of Early Cambrian tuffs from SE Australia and southern China. *Journal of the Geological Society*, **159**, 645–658.
- JENSEN, S. 1997. Trace fossils from the Lower Cambrian Mickwitzia sandstone, south-central Sweden. *Fossils and Strata*, **42**, 1–110.
- JENSEN, S. 2003. The Proterozoic and earliest Cambrian trace fossil record: patterns, problems and perspectives. *Integrative and Comparative Biology*, **43**, 219–228.
- JENSEN, S. & MENS, K. 2001. Trace fossils *Didymaulichnus* cf. *tirasensis* and *Monomorphichnus* isp. from the Estonian Lower Cambrian, with a discussion on the early Cambrian ichnocoenoses of Baltica. *Proceedings of the Estonian Academy of Sciences, Geology*, **50**, 75–85.
- JENSEN, S., SAYLOR, B. Z., GEHLING, J. G. & GERMS, G. J. B. 2000. Complex trace fossils from the terminal Proterozoic of Namibia. *Geology*, **28**, 143–146.
- JENSEN, S., DROSER, M. L. & GEHLING, J. G. 2005. Trace fossil preservation and the early evolution of animals. *Palaeogeography, Palaeoclimatology, Palaeoecology*, **220**, 19–29.
- KHOMENTOVSKY, V. V. & KARLOVA, G. A. 1993. Biostratigraphy of the Vendian–Cambrian beds and the lower Cambrian boundary in Siberia. *Geological Magazine*, **130**, 29–45.
- KOUCHINSKY, A., BENGTON, S., MISSARZHEVSKY, V. V., PELECHATY, S., TORSSANDER, P. & VAL’KOV, A. K. 2001. Carbon isotope stratigraphy and the problem of a pre-Tommotian Stage in Siberia. *Geological Magazine*, **138**, 387–396.
- MCLLROY, D. & HEYS, G. R. 1997. Palaeobiological significance of *Plagiogmus arcuatus* from the lower Cambrian of central Australia. *Alcheringa*, **21**, 167–178.
- MCLLROY, D. & LOGAN, G. A. 1999. The impact of bioturbation on infaunal ecology and evolution during the Proterozoic–Cambrian transition. *Palaios*, **14**, 58–72.
- ORŁOWSKI, S. & ŻYLIŃSKA, A. 1996. Non-arthropod burrows from the Middle and Late Cambrian of the Holy Cross Mountains, Poland. *Acta Palaeontologica Polonica*, **41**, 385–409.
- PACZEŚNA, J. 1996. The Vendian and Cambrian ichnocoenoses from the Polish part of the East-European Platform. *Prace Państwowego Instytutu Geologicznego*, **152**, 1–77.
- PALIJ, V. M. 1974. Bilobate traces from the deposits of the Baltic series in the Dniester Region. *Doklady AN URSR, weirs B (1)*. [in Ukrainian].
- PALIJ, W. M., POSTL, E. & FEDONKIN, M. A. 1983. Soft-bodied Metazoa and animal trace fossils in the Vendian and early Cambrian. *In*: URBANEK, A. & ROZANOV, A. Y. (eds) *Upper Precambrian and Cambrian Palaeontology of the East European Platform*. Wydawnictwa Geologiczne, Warszawa, 56–93.
- PELECHATY, S. M., KAUFMAN, A. J. & GROTZINGER, J. P. H. 1996. Evaluation of $\delta^{13}\text{C}$ chemostratigraphy for intrabasinal correlation: Vendian strata of northeast Siberia. *Geological Society of America Bulletin*, **108**, 992–1003.
- QIAN, Y. & BENGTON, S. 1989. Palaeontology and biostratigraphy of the Early Cambrian Meishucunian Stage

- in Yunnan Province, South China. *Fossils and Strata*, **24**, 1–156.
- SEILACHER, A. 1995. *Fossile Kunst. Albumblätter der Erdgeschichte*. Goldschneck Verlag, Korb.
- SEILACHER, A. 1999. Biomat-related lifestyles in the Precambrian. *Palaios*, **14**, 86–93.
- SIGNOR, P. W. & MCMENAMIN, M. A. S. 1988. The Early Cambrian worm tube *Onuphionella* from California and Nevada. *Journal of Paleontology*, **62**, 233–240.
- YOUNG, F. G. 1972. Early Cambrian and older trace fossils from the southern Cordillera of Canada. *Canadian Journal of Earth Sciences*, **9**, 1–17.

The Cambrian 'basement' of gastropod evolution

P. Y. PARKHAEV

*Paleontological Institute of the Russian Academy of Sciences, Profsoyuznaya 123,
Moscow, 117997, Russia (e-mail: pparkh@paleo.ru)*

Abstract: The oldest gastropods are known from the uppermost Nemakit-Daldynian to lowermost Tommotian deposits. However, to trace ancestry before this time, when most metazoans did not possess shells, is difficult. Study of the oldest gastropods, diagnosed and discussed here, sheds some light on the earliest stages of evolution of major gastropod branches. It appears that the subclass Archaeobranchia served as the base for this early radiation.

Gastropods represent the largest class of the phylum Mollusca: different estimates of diversity vary from 80 000 to 150 000 species. Besides such huge species diversity, gastropods are characterized by several, strikingly different body plans, reaching such variability and ecological success over a long evolutionary history, at least 540 million years of the Phanerozoic.

The earliest fossil gastropods are known from the uppermost Nemakit-Daldynian to the lowermost Tommotian deposits (Khomentovsky *et al.* 1990; Parkhaev 2002a; Fig. 1). But tracing the gastropod family tree back in time to and beyond the Precambrian–Cambrian boundary is difficult, especially in times before true skeletons developed. Little, if anything, is known about 'ancestors' or transitional forms linking other molluscs such as the non-torsioned monoplacophorans.

Nevertheless, the study of the oldest fossil gastropods preserved in Cambrian strata is of special interest as it could shed light on the origin of the class and outline the earliest stages of evolution of its major branches. Molluscs have been studied for more than 150 years. The resulting systematics of the Cambrian molluscs is complicated and contradictory with many opposing opinions (for reviews, see Runnegar 1996; Parkhaev 2002a). Fossil gastropods show few of the features used by modern zoologists in their morphological and systematic analyses. Analysis of the shells in palaeontology is the main approach. Such analyses have been carried out repeatedly (Pojeta & Runnegar 1976; Runnegar & Jell 1976; Runnegar 1981; Peel 1991).

In my own studies on early molluscs (Parkhaev 2000, 2001, 2002a, b, 2004) the emphasis was on morphological structures of shells especially from the Cambrian from a functional viewpoint. Features connected with water current circulation patterns inside the shell (grooves, siphons, sinuses, etc.) and the nature of shell musculature arrangement are of a special importance. As a result, details of

internal anatomy of the Cambrian molluscs have been reconstructed, their ecological peculiarities outlined and, finally, this data used for approaching systematics. This paper focuses on the morphological diversity among the Cambrian univalved molluscs (Fig. 1), and suggests that these are the earliest gastropods, giving a synopsis of the main groups of Cambrian gastropods, including diagnostic characters for each taxon and an estimate of the placement of each group on the gastropod evolutionary tree.

Major groups of Cambrian gastropods

Family Helcionellidae Wenz, 1938

Family includes numerous and diverse forms but with a simple morphology. Shell varies from a low conical to high conical structure with central, subcentral or posteriorly shifted apex. Aperture simple, always lacking grooves or deep sinuses. Posterior or anterior shallow notches occur in some advanced genera. The oldest known taxa occur in terminal Precambrian sediments (uppermost Nemakit-Daldynian). Forms with low shell and marginally-placed apex are very similar to monoplacophorans, which are thought to be helcionellid ancestors. Some monoplacophoran genera may be included in this family since their distinction from the most primitive gastropods is still quite obscure, based as it is on shell characters alone, without data on the internal anatomy. A thorough study of protoconch morphology and microstructure could provide useful input to sort out this current taxonomic enigma.

Exemplary genera. *Scenella* Billings, 1872; *Helcionella* Grabau & Shimer, 1909; *Bemella* Missarzhevsky in Rozanov *et al.*, 1969; *Tannuella* Missarzhevsky in Rozanov *et al.*, 1969; *Obtusoconus* Yu, 1979; *Emarginoconus* Yu, 1979; *Securiconus* Jiang, 1980; *Ilsanella* Missarzhevsky, 1981;

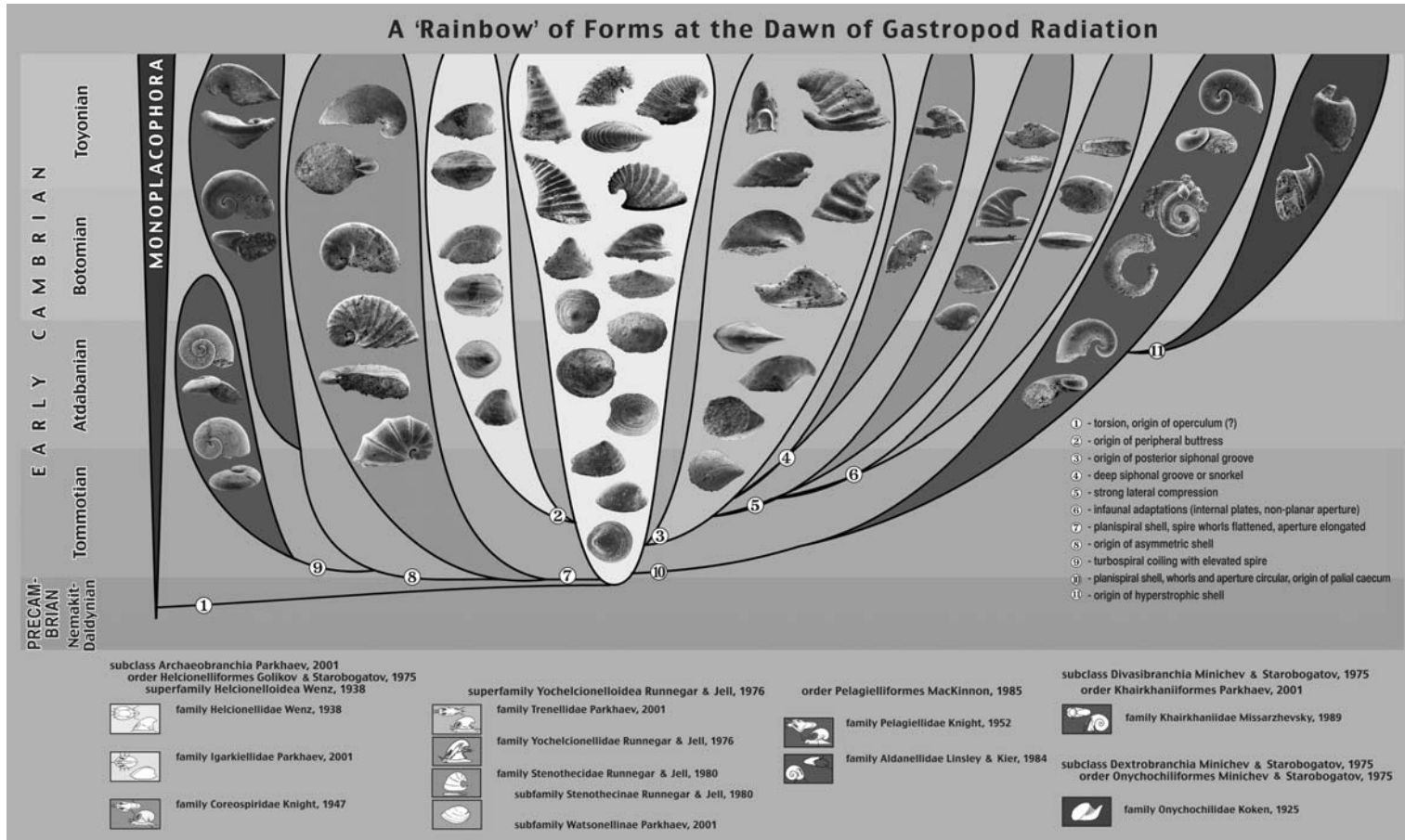


Fig. 1. A 'rainbow' of shell forms at the dawn of gastropod radiation. Numbers in circles indicate the main apomorphies of each group.

Pseudopatella Zhegallo in Esakova & Zhegallo, 1996; *Aequiconus* Parkhaev in Gravestock *et al.*, 2001; *Anuliconus* Parkhaev in Gravestock *et al.*, 2001.

Family Igarkiellidae Parkhaev, 2001

Members of this group have a shell very similar to that of the Helcionellidae in general form. One peculiar, apomorphic feature distinguishes igarkiellids from their helcionellid ancestors. The buttress, running along the anterior field of a cap-like shell from the apex towards the anterior margin of the aperture. The buttress corresponds to a groove on the internal shell surface, which is supposedly a standage, or a water drainage sump in the mantle cavity, which accumulates and expels exhaust water along with excrement from the shell. Earliest members of the family appear in the uppermost Nemakyt-Daldynian. The presence of the peripheral buttress, and hence a similar water circulation pattern, suggests that igarkiellids may be ancestral to Palaeozoic bellerophonitids, but this assumption is still not fully supported by fossils from the Middle–Upper Cambrian interval.

Exemplary genera. *Protoconus* Yu, 1979; *Gonamella* Valkov & Karlova, 1984; *Igarkiella* Vassiljeva, 1998.

Family Coreospiridae Knight, 1947

Family includes genera with planispirally coiled shells. Earliest members occur in sediments of the latest Nemakyt-Daldynian age. Family is likely to be derived from helcionellid ancestors, which include some forms with strongly hooked apices, and hence intermediate between typical cap-shaped helcionellids and coiled coreospirids. A slight deviation from the symmetrical planispiral coiling is noteworthy. Such an initial dextrality or sinistrality of shell, which can simultaneously occur within the same genus and even species (along with normal, bilaterally symmetric specimens) corresponds to the primitive state of coiling, when the advantage of the dextral or sinistral asymmetry of body is not genetically fixed by selection among the most ancient forms (Minichev & Starobogatov 1979).

Main genera included. *Coreospira* Saito, 1936; *Latouchella* Cobbold, 1921; *Oelandiella* Vostokova, 1962; *Cambrospira* Yu, 1979; *Tichkaella* Geyer, 1986; *Kutanjia* Kruse, 1991.

Family Trenellidae Parkhaev, 2001

Members of family characterized by a shell with a parietal train with a groove located on posterior margin of aperture. Groove is supposed to facilitate

water intake. This apomorphic character first appears in gastropods of Early Tommotian age suggesting an origin from helcionellids. Further development of this intake structure takes place in the family, Yochelcionellidae.

Exemplary genera. *Oelandia* Westergård, 1936; *Prosinuites* Poulsen, 1967; *Xianfengella* He & Yang, 1982; *Parailsanella* Zhegallo in Voronina *et al.*, 1987; *Mackinnonia* Runnegar in Bengtson *et al.*, 1990; *Trenella* Parkhaev, 2001.

Family Yochelcionellidae

Runnegar & Jell, 1976

Members of this family have the most striking shell morphology among Cambrian molluscs. Its diagnostic feature is a tubular projection on the posterior shell surface. This siphon (called 'snorkel' after the similarity with a breathing tube) is supposedly homologous with the parietal groove of the trenellids. The transitional condition from the groove to snorkel is present among species in the genus *Eotebena*, which have very deep grooves with merging lower edges but remain divided by a narrow slit. The oldest yochelcionellids appear during the Early Tommotian, but the acme of the family is Botomian to Middle Cambrian.

Genera included. *Yochelcionella* Runnegar & Pojeta, 1974; *Eotebenna* Runnegar & Jell, 1976; *?Enigmaconus* MacKinnon, 1985; *Runnegarella* Parkhaev, 2002.

Family Stenotheceidae

Runnegar & Jell, 1980

The family representatives have trenellid-like shell, but are characterized by strong lateral compression. The oldest members of the family are known from the uppermost Nemakyt-Daldynian and Early Tommotian, but the family was most diverse beginning in the late Atdabanian–Botomian. Strong lateral compression of the shell is supposedly an adaptation to new types of habitats occupied by stenotheceids, i.e. dense algal fields (subfamily Stenotheceinae) or associated with soft-sediments (subfamily Watsonellinae). In addition to lateral compression, adaptation for infaunal living was accompanied by increasing of curvature of the aperture and the origin of internal plates for attachment of strong pedal musculature (in genera *Eurekapegma* and *Watsonella*).

Exemplary genera. *Stenothece* Salter in Hicks, 1872; *Watsonella* Grabau, 1900; *Anabarella* Vostokova, 1962; *Mellopegma* Runnegar & Jell, 1976; *Eurekapegma* Mackinnon, 1985.

Family Pelagiellidae Knight, 1952

This family is characterized by turbospiral, dextrally coiled shells with a somewhat triangular aperture. The basal angulation of the aperture is thought to be a water intake area, and hence homologous with the posterior train of coreospirids, thought to be pelagiellid ancestors. The oldest members of the family appear in the earliest Atdabanian. The Late Atdabanian–Toyonian through to the Middle Cambrian is the acme of the family.

Genera included. *Pelagiella* Matthew, 1895; *Costipelagiella* Horny, 1964; *Tannuspira* Missarzhevsky, 1989.

Family Aldanellidae Linsley & Kier, 1984

Members of the family have turbospiral, most are dextrally coiled with a protruding spire and an elliptical aperture. Morphologically, members of this family can be derived from the pelagiellids, with further development of shell asymmetry resulting in spire protrusion. However, the oldest aldanellids appear in sediments of the basal Tommotian, an interval which still has undescribed pelagiellids. So, the independent origin of the aldanellids from the coreospirids is also possible.

Genera included. *Aldanella* Vostokova, 1962; *Nomgoliella* Missarzhevsky, 1981.

Family Khairkhaniidae Missarzhevsky, 1989

Family is characterized by spirally coiled shell. The planispiral shells, along with slightly dextral or sinistral forms, are included in the family. In contrast to the coreospirids which are characterized by an elongated cross-section of the whorls, khairkhaniids have almost circular cross-section. Thus, the family represents another offspring of the helcionellids, which first appeared in the uppermost Nemakyt-Daldynian, and evidently independently developed a spirally coiled shell. The coiling of a relatively narrow tube in a tight spiral was accompanied by deep transformations inside the palial cavity, resulted in origin of palial caecum (Parkhaev 2002a, fig. 4).

Exemplary genera. *Philoxenella* Vostokova, 1962; *Michniakia* Missarzhevsky, 1966; *Protowenella* Runnegar & Jell, 1976; *Barskovia* Golubev, 1976; *Khairkhania* Missarzhevsky, 1981; *Xinjispira* Yu & Rong, 1987; *Arrossania* Runnegar in Bengtson *et al.*, 1990.

Family Onychochilidae Koken, 1925

Most members of the family are Early Palaeozoic taxa with hyperstrophic shells, but a few forms

from the Earliest Cambrian also belong in this group. Onychochilids are Early Cambrian molluscs that do not belong to the subclass Archaeobranchia, but have been assigned to the Dextrobranchia. Members of the subclass are characterized by a hyperstrophic turbospiral shell, a palial cavity with a palial caecum, which retains only the right part of the palial complex (Starobogatov 1976). Perhaps the khairkhaniids gave rise to the onychochilids. The gradual transition from the nearly planispiral Khairkhaniidae to the hyperstrophic Onychochilidae is clearly visible within the *Protowenella*–*Xinjispira*–*Beshtashella* the lineage.

Exemplary Genera. Besides numerous Early Palaeozoic genera, a single genus occurs in the Early Cambrian, i.e. *Beshtashella* Missarzhevsky in Missarzhevsky & Mambetov, 1981 [= *Yuwenia* Runnegar, 1981].

Discussion

Gastropods appeared in the latest Precambrian (Nemakyt-Daldynian)–Earliest Cambrian (Tommotian). At that time the subclass Archaeobranchia had already formed. It seems to be a monophyletic group including eight families arranged in two orders (see Parkhaev 2001 for further references) (Fig. 1). This subclass was the most diverse in the Cambrian, surviving into the Ordovician (Gubanov & Peel 2001). The most primitive members had a simple, cap-shaped shell with a central or sub-central apex and an apertural margin lacking notches. Two major morphogenetic trends occurred in the archaeobranchian radiation. The first was development of structures which increased water circulation efficiency (special sinuses, grooves, buttresses, and tubes facilitating uptake and/or expulsion of water). A second trend was the development of a spirally coiled shell. Possibly, such developments were not unique, and originated in at least two separate lineages (coreospirids and khairkhaniids). The most advanced coiled archaeobranchians developed an asymmetrical, turbospiral shell (pelagiellids and aldanellids).

The high level systematics and phylogenetic interpretations of gastropod taxa are far from agreed upon (Golikov & Starobogatov 1988; Haszprunar 1988; Ponder & Lindberg 1997, etc.), because most major taxa represent crown-groups of different stems with rather advanced characters, which are difficult to trace through the lengthy record of gastropods and combine into some uniform phylogenetic sequence. It is possible to link at least some major stems by using the oldest and most primitive gastropod group, archaeobranchians, as a reference point. Certainly, it is a very difficult task, since our knowledge on the Cambrian molluscs is far from complete.

Moreover, there is a considerable gap in the fossil record between Cambrian and Ordovician molluscs, most of which already resemble typical modern gastropods and fit within commonly accepted groups more firmly, than the Cambrian univalves do. However, the first attempt to connect archaeobranchians with the recent high-level groups gives some hope for success.

Gastropod systematics for the Russian record was introduced in 1975 by A. N. Golikov and Y. I. Starobogatov, and later improved and amended in a series of subsequent publications (Starobogatov 1976; Minichev & Starobogatov 1979; Golikov & Starobogatov 1988) and their taxonomy works for fossil gastropods. Incorporating a variety of anatomical features, their systematic scheme is based on the general plan of palial complex organization. In contrast to radular type, ctenidian structure and peculiarities of the nervous and digestive systems (features which are extremely important for systematics of recent forms, but inapplicable for fossils), the general organization of the palial complex can be reconstructed using shell morphology. This approach generally allows the definition of eight extant subclasses, and it is possible to trace these groups from the Cambrian archaeobranchians to some modern groups (Fig. 2).

Possibly, the internally asymmetrical forms (Parkhaev 2000; Fig. 3) with turbospiral shell from the order Pelagielliformes gave rise to members of the subclass Scutibranchia, which, in turn, led to the earliest pectinibranchians with a reduced right side of the palial complex. The

position of bellerophonts is of especial interest with respect to the origin of Scutibranchia. Golikov & Starobogatov (1988) included them as a root of, and the most primitive order in, the subclass Scutibranchia, due to the presence of an exhalant anteromedian slit making them intermediate between the pectinibranchians and the Archaeobranchia (Fig. 3).

But the shell slit is present in many different taxa of recent gastropods, where it is considered as convergent and hence the 'shell slit, used alone, is of little phylogenetic importance' (Haszprunar 1988, p. 372). It is better to exclude the order Bellerophontiformes from Scutibranchia, and place it in the subclass Archaeobranchia due to planispiral shell coiling of the bellerophonts (Fig. 2). The bellerophonts can be derived from the family Igarikiellidae, which possesses peripheral buttresses.

Another extant subclass, Dextrobranchia, is supposed to have originated from the family Khairkhaniidae. In Golikov's & Starobogatov's system (Starobogatov 1976), this subclass originates supposedly from the Divasibranchia, which is characterized by having two veins connected by a single auricle. The origin of this state is thought to be a result of the merging of two auricles in primitive ancestor into one (Golikov & Starobogatov 1988). That transformation from a wide conical shell to a shell shaped as a spirally coiled narrow tube likely facilitated the development of ctenida. Hence, it could have facilitated the merging of auricles. Such transformation of the shell also occurs in the lineage leading from the Helcionellidae to the

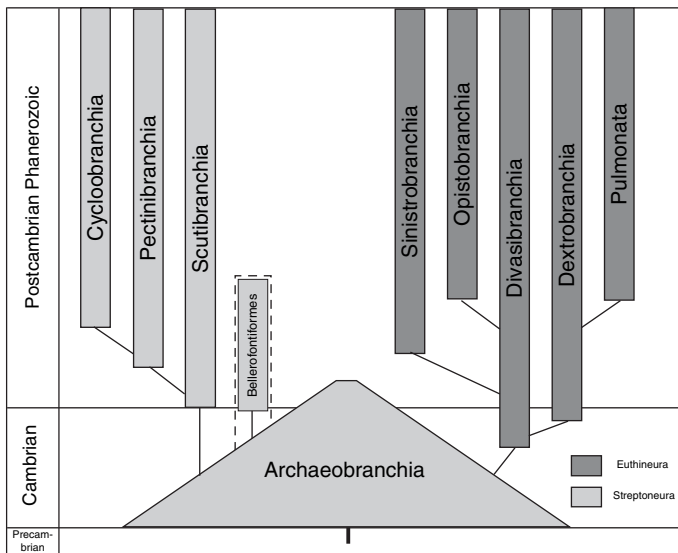


Fig. 2. Supposed phylogenetic relationships of gastropod subclasses.

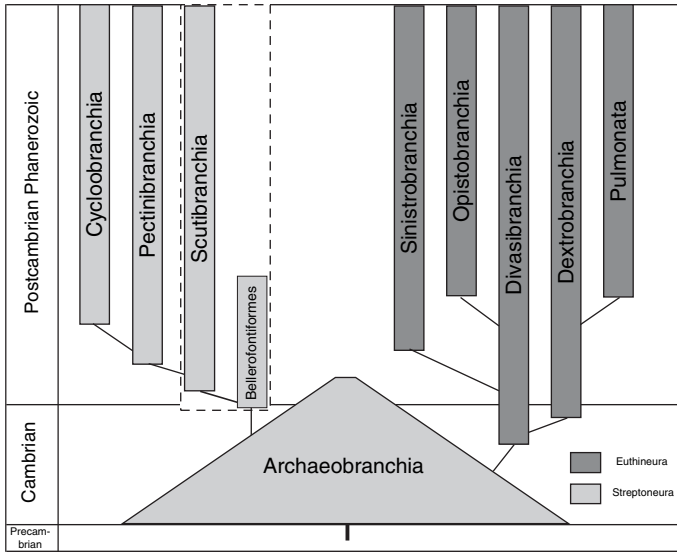


Fig. 3. Supposed phylogenetic relationships of gastropod subclasses. Note the position of bellerophonts between the Archaeobranchia and Scutibranchia, at the base of the latter subclass (compare with Fig. 2).

Khairkhaniidae (Parkhaev 2002a; Fig. 4), so the later family likely represents the state with a single auricle, and consequently falls within the diagnosis of the subclass Divasibranchia.

Archaeobranchians can be connected with representatives of four extant subclasses, the Scutibranchia, Pectinibranchia, Divasibranchia

and Dextrobranchia. Three other euthyneuran subclasses (Sinistrobranchia, Opistobranchia and Pulmonata) are later offshoots of the Divasibranchia and the Dextrobranchia (see Golikov & Starobogatov 1988; Fig. 2). The sole recent subclass without certain relationships with Cambrian archaeobranchians is the Cyclobranchia

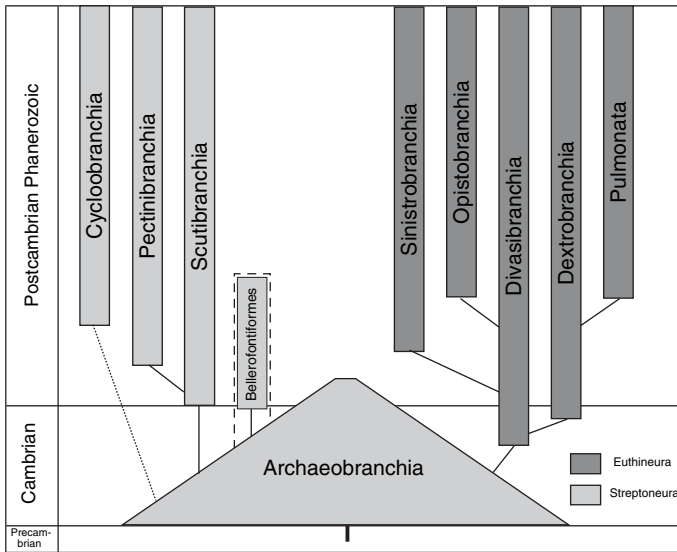


Fig. 4. Supposed phylogenetic relationships of gastropod subclasses. Note the branching of Cyclobranchia from archaeobranchian ancestors, but not pectinibranchians (compare with Fig. 2).

[=Patellogastropoda, Docoglossa]. It is paradoxical that in most studies this group is considered the most primitive, and usually serves as a base of radiation for all other taxa (Golikov & Starobogatov 1975, 1988; Lindberg 1988; Haszprunar 1988; Ponder & Lindberg 1997). There are two theories concerning the evolutionary position of the cyclobranchians. The first is that they are derived from primitive pectinibranchians with coiled shells and have since reduced the right side of palial complex (Fig. 2). If this is the case, the limpet shell is advanced or apomorphic with respect to the pectinibranchians. The second theory is that there is a direct link between cyclobranchians and archaeobranchians (Fig. 4). In this case, the limpet shell is a primitive or plesiomorphic character held over from the Cambrian cap-like ancestors. It is difficult to understand the reasons for the loss of the right part of the palial complex on the pectinibranchians. Probably, further fieldwork and study of Cambrian gastropods, especially concerning their protoconch morphology and shell microstructure will help clarify the taxonomic position of limpets within the gastropods.

Based on Golikov & Starobogatov's studies (1975, 1988) combined with data from Cambrian univalved molluscs, yields the phylogenetic tree shown in Figure 2. The subclass Archaeobranchia in this scheme is considered as basement for radiation of the entire gastropod class.

The study was supported by the Russian Foundation for Basic Researches (project 03-04-48367), The Grants of President of the Russian Federation for Support of Young Russian Scientists and Leading Scientific Schools (projects nos. NSh-974.2003.5 and MK-723.2004.4), and academician programme 'Evolution of the Biosphere'. Thanks to reviewers C. Tassell and A. Braun for comments on the manuscript.

References

- GOLIKOV, A. N. & STAROBOGATOV, Y. I. 1975. Systematics of prosobranch gastropods. *Malacologia*, **15**, 185–232.
- GOLIKOV, A. N. & STAROBOGATOV, Y. I. 1988. Questions of phylogeny and systematics of prosobranchian gastropod mollusc. *Transactions of the Zoological Institute of the Academy of Sciences USSR*, **176**, 4–77 [in Russian].
- GUBANOV, A. P. & PEEL, J. S. 2001. Latest helcionelloid molluscs from the Lower Ordovician of Kazakhstan. *Paleontology*, **44**, 681–694.
- HASZPRUNAR, G. 1988. On the origin and evolution of major gastropod groups, with special reference to the Streptoneura. *Journal of Malacological Studies*, **54**, 367–441.
- KHOMENTOVSKY, V. V., VALKOV, A. K. & KARLOVA, G. A. 1990. New data on the biostratigraphy of the transitional beds in the basin of Aldan River. In: KHOMENTOVSKY, V. V. & GIBBSHER, A. S. (eds) *Late Precambrian and Early Palaeozoic of Siberia: Questions of Regional Stratigraphy*, Novosibirsk, 3–63 [in Russian].
- LINDBERG, D. R. 1988. The Patellogastropoda. In: PONDER, W. F. (ed.) *Prosobranch Phylogeny. Malacological Review Supplement*, **4**, 35–63.
- MINICHEV, Y. S. & STAROBOGATOV, Y. I. 1979. Subclasses of gastropod mollusc and their phylogenetic relationships. *Zoologicheskii Zhurnal*, **58**, 293–305 [in Russian].
- PARKHAEV, P. Y. 2000. Functional morphology of univalved molluscs—helcionellids. 1. *Paleontologicheskii Zhurnal*, **3**, 32–39.
- PARKHAEV, P. Y. 2001. Functional morphology of univalved molluscs—helcionellids. 2. *Paleontologicheskii Zhurnal*, **35**, 20–27.
- PARKHAEV, P. Y. 2002a. Phylogenesis and system of Cambrian univalved molluscs. *Paleontologicheskii Zhurnal*, **36**, 25–36.
- PARKHAEV, P. Y. 2002b. The muscle scars of the Cambrian univalved molluscs and its systematic significance. *Paleontologicheskii Zhurnal*, **36**, 15–19.
- PARKHAEV, P. Y. 2004. New data on the morphology of the shell muscles in Cambrian helcionelloid molluscs. *Paleontologicheskii Zhurnal*, **38**, 27–29.
- PEEL, J. S. 1991. Functional morphology, evolution and systematics of Early Palaeozoic univalved molluscs. *Bulletin of the Groenland Geological Undersøgelse*, **161**, 1–116.
- POJETA, J. JR. & RUNNEGAR, B. 1976. The paleontology of rostroconch molluscs and the early history of the phylum Mollusca. *US Geological Survey Professional Paper*, **968**, 1–88.
- PONDER, W. F. & LINDBERG, D. R. 1997. Towards a phylogeny of gastropod molluscs: an analysis using morphological characters. *Zoological Journal of the Linnean Society*, **119**, 83–265.
- RUNNEGAR, B. 1981. Muscle scars, shell form and torsion in Cambrian and Ordovician univalved molluscs. *Lethaia*, **14**, 311–322.
- RUNNEGAR, B. 1996. Early evolution of the Mollusca: the fossil record. In: TAYLOR, J. (ed.) *Origin and Evolution of the Mollusca*. Oxford University Press, Oxford, 77–87.
- RUNNEGAR, B. & JELL, P. A. 1976. Australian Middle Cambrian molluscs and their bearing on early molluscan evolution. *Alcheringa*, **1**, 109–138.
- STAROBOGATOV, Y. I. 1976. [On the subclasses of gastropod molluscs]. In: SHIMANSKY, V. N., KABANOV, G. K., DMITRIEVA, E. L., STAROBOGATOV, Y. I. & TROFIMOV, B. A. (eds) *Major Problems of Animal Systematics*. Paleontologicheskii Institut AN SSSR, Moscow, 12–16 [in Russian].

Siliceous microfossils and biosiliceous sedimentation in the lowermost Cambrian of China

A. BRAUN¹, J.-Y. CHEN², D. WALOSZEK³ & A. MAAS³

¹*Institute of Palaeontology, University of Bonn, Nussallee 8, D-53115 Bonn, Germany (e-mail: Braun@uni-bonn.de)*

²*Nanjing Institute of Geology and Palaeontology, Chinese Academy of Sciences, Nanjing 210008, China*

³*University of Ulm, Section for Biosystematic Documentation, Helmholtzstrasse 20, D-98081 Ulm, Germany*

Abstract: Clay-rich and siliceous sedimentary rocks of earliest Cambrian age on the Yangtze Platform, China, contain abundant siliceous microfossils. The black cherts and black shales in this sequence, of earliest Cambrian age, contain sponge spicules (both macroscleres and microscleres), derived from lithistid demosponges and hexactinellids. These spicule associations are useful for biostratigraphic correlation, and indicate that Porifera played an important role in the geochemical cycling of silica at the beginning of the Phanerozoic. Phosphatic microfossils also contributed to the deep-sea ecology of this region during the earliest Cambrian.

Clay-rich and siliceous sedimentary rocks of earliest Cambrian age on the Yangtze Platform, China contain abundant siliceous microfossils. Based on their high content of siliceous hard parts these rocks are, in fact, biosiliceous sediments. However, in more clay-rich lithologies, diagenetic dissolution processes caused the removal of siliceous hard parts and led to 'pure mudstones' and silicified claystones, being apparently devoid of siliceous microfossils. Abundant preservation as iron-hydroxide pseudomorphs and in early diagenetic concretions indicates a high biosiliceous content of the original sediments. Rocks investigated belong to the lowermost Cambrian (*Anabarites trisulcatus*–*Protohertzina anabarica* assemblage zone) and come from black chert sequences (Kuanshuanpu, S. -Shaanxi province (Chen *et al.* 2004); Fengkoushao, Yunnan Province) as well as black shales (Nuititang Formation, Songtao Section, Eastern Guizhou Province; Niutitang Formation near the Mengdong train station, Hunan Province). Lighter coloured clay-rich lithologies of a similar age in Guizhou (Taozichong Section (Wang *et al.* 1984)) have similarly yielded abundant siliceous hard parts.

Siliceous microfossils are almost exclusively sponge spicules. Lithologically there seem to be strong similarities with coeval sedimentary rocks in southern Kazakhstan, termed spongiolites by Eganov *et al.* (1986). Among the sponge spicules, there are megascleres as well as microscleres. Both spicule types allow clear identification of which particular sponge groups were present in

the respective depositional environment. Remarkably, some of the solution residues consist exclusively of spicules derived from lithistid demosponges (especially in the lighter coloured, clay-rich facies), whereas others (e.g. most black shale and black chert samples) contain almost exclusively spicules of hexactinellid sponges. Attempting to relate sedimentary facies to the preservation of particular sponge types, it appears that biofacial and ecologic differences were already present by the earliest Cambrian. Quite possibly, sponge spicule associations across the Precambrian–Cambrian boundary (with its predominantly siliceous and clay-rich lithologies on the Yangtze Platform) are suitable for a broadly applicable ecostratigraphic parallelization of rock units, for example in the Mesozoic of the Northern Alps (Mostler 1971). They may also eventually be used for biostratigraphic purposes across the Precambrian–Cambrian boundary.

Rocks rich in siliceous microfossils from the above mentioned occurrences represent sediments deposited on a marine shelf or slope (transitional). In the deeper oceanic basins represented on the Yangtze Platform (the depositional environment of the Hetang Shales, siliceous sponge remains are not common in solution residues. Eventually, the deeper water sea bottoms, being strongly anoxic, had not yet been colonized by sponge faunas in the earliest Cambrian, or were only temporarily occupied during time periods of more favourable ecological conditions. However, these basinal lithologies contain strong petrographical as well

as micropalaeontological signs of extensive phytoplankton blooms occurring in the earliest Cambrian black shale depositional basins.

Somewhat astonishingly, remains of radiolarians are extremely rare in the solution residues. Only one deeper-water sequence (the Hetang Shales in the Xintangwu Section, western Zhejiang Province (Braun & Chen 2003)) yielded a few, very fragmentary specimens. These display strong similarities to spherical radiolarian morphologies found in Palaeozoic rocks younger than Cambrian and Ordovician. However, further conclusions concerning early radiolarian evolution must await additional and more complete discoveries. Micropalaeontological processing of chert successions in the Neoproterozoic and early Cambrian in oceanic basinal facies is expected to yield further data, as they are lithologically very similar to bedded radiolarian cherts of younger Palaeozoic ages.

The significant contribution of biosiliceous particles to early Cambrian sedimentation on the Yangtze platform (as well as to other areas in Kazakhstan and Europe) implies that silica-biomineralizing organisms were playing a significant role in the geochemical cycling of silica in the oceans by the beginning of the Phanerozoic. The abundance of sponge spicules in the sediments indicates that this group (Porifera) played a major ecological role in the early Cambrian. This is supported by findings of complete sponges and spicule clusters on bedding planes of clay-rich sediments and black shales (Reitner 1994; Rigby 1995). But one must be cautious of any statement about the importance of siliceous plankton (radiolarians) by Early Cambrian times until further work is carried out.

Phosphatic microfossils and phosphatic particles from black shales and bedded black cherts contribute to the ecological picture of the oceanic basins as well as to the environments of the anoxic sea bottoms during earliest Cambrian times. The common occurrence of *Protohertzina* (interpreted as chaetognath hooks by Szaniawski (2002)) and microcoprolite-shaped phosphatic particles seems to support suggestions that the 'less anoxic' near surface water masses above shelf and deeper-water

areas, which contained rich phytoplankton, could have served as a food source not only for a rich benthic sponge fauna, but also for metazoan plankton in the earliest Cambrian.

The current joint research project is supported by the Deutsche Forschungsgemeinschaft (grant No. Wa 754/8-1 and Wa 754/8-2) and the National Science Foundation of China (Grant No. 40132010). Financial and organizational help of these institutions is gratefully acknowledged. We thank O. Dülfers (Bonn) for technical support and processing of samples.

References

- BRAUN, A. & CHEN, J.-Y. 2003. Plankton from early Cambrian black shale series on the Yangtze Platform, and its influences on lithologies. *Progress in Natural Science*, **13**, 777–782.
- CHEN, J.-Y., BRAUN, A., WALOSZEK, D., PENG, Q. & MAAS, A. 2004. Lower Cambrian yolk-pyramid embryos from Southern Shaanxi, China. *Progress in Natural Science*, **14**, 167–172.
- EGANOV, E. A., SOVETOV, Y. K. & YANSHIN, A. L. 1986. Proterozoic and Cambrian phosphorite deposits: Karatau, southern Kazakhstan, USSR. In: COOK, P. J. & SHERGOLD, J. H. (eds) *Phosphate Deposits of the World. Vol. 1: Proterozoic and Cambrian Phosphorites*, 175–189.
- MOSTLER, H. 1971. Haeufigkeit und Bedeutung von Schwammspiculae in triassischen Mikrofaunen. *Geologisch-Palaeontologische Mitteilungen Innsbruck*, **1**, 1–19.
- REITNER, J. L. 1994. New phylogenetic and palaeoecological aspects of late Precambrian and early Cambrian sponge communities. In: *Ecological Aspects of the Cambrian Radiation (IGCP 366)*. *Terra Abstracts*, **6**(suppl. 3), 6–7.
- RIGBY, J. K. 1995. Lower Cambrian demosponges and hexactinellid sponges from Yunnan, China. *Journal of Palaeontology*, **69**, 1009–1019.
- SZANIAWSKI, H. 2002. New evidence for the protoconodont origin of chaetognaths. *Acta Palaeontologica Polonica*, **47**, 405–419.
- WANG, Y. *ET AL.* 1984. Stratigraphy of the boundary Sinian-Cambrian in the Yangtzi area of Guizhou. In: WANG, Y., YIN, G., ZHENG, S. & QIAN, Y. (eds) *The Upper Precambrian and Sinian-Cambrian Boundary in Guizhou*, Guiyang.

Fleshing out the Ediacaran period

J. G. GEHLING

South Australian Museum, North Terrace, Adelaide, South Australia 5000, Australia
(e-mail: gehling.jim@saugov.sa.gov.au)

Abstract: The Flinders Ranges Ediacaran succession preserves an apparently primary palaeomagnetic record, distinctive stratigraphic events such as the Acraman ejecta layer, and fossils of the Ediacara biota at three well-separated levels. The fossil assemblage of the Ediacara Member includes both trace fossils and body fossils, and shares at least 65% of its taxa with the White Sea assemblages in northern Russia, suggesting they were coeval. Globally, Ediacaran successions are diverse in their lithostratigraphy but share many characteristics of biota, isotope signatures and events which can be calibrated with radiometric dating. Available radiometric dating of Ediacaran successions supports the concept of distinct Avalon (575 Ma–565 Ma), White Sea (558 Ma–555 Ma) and Nama (549 Ma–543 Ma) associations as a temporal succession rather than being controlled by environment or palaeobiogeography. The challenge to document the tempo and pattern of evolution of early animals and the associated changes in global climate make the subdivision and calibration of the Ediacaran a vital task for the next decade.

The Ediacaran Global Stratotype Section and Point has now been defined at the base of the Nuccaleena Formation in the Flinders Ranges National Park, South Australia. This GSSP marks the end of a major glacial epoch. In the absence of definitive biozones marking the base of the Ediacaran, the utility of this 'cap carbonate' for correlation will depend on the verification of a global fingerprint based on the stratigraphic pattern, stable isotope trends and magnetostratigraphy. Even though the fossil record for the Ediacaran System is relatively sparse, it clearly characterizes this period on all continents except Antarctica. The task facing the Ediacaran Subcommittee of the ICS is the correlation of the GSSP horizon around the globe and to foster biostratigraphic subdivision of the Ediacaran System.

In the Flinders Ranges National Park, the well exposed, structurally uncomplicated, 3.5 km-thick Ediacaran succession is capped with a 2 km-thick, fossiliferous Early Cambrian succession (Fig. 1). The Flinders Ranges Ediacaran succession preserves an apparently primary palaeomagnetic record, distinctive stratigraphic events, and fossils of the Ediacara biota at three well-separated levels.

- The palaeomagnetic record of the Elatina Formation, immediately below the Ediacaran GSSP, indicates that the Adelaide geosyncline experienced a protracted interval of glaciogenic sedimentation when the region was straddling the palaeomagnetic equator (Schmidt & Williams 1995; Sohl *et al.* 1999). New approaches to palaeomagnetic analysis promise a magnetostratigraphy for the Ediacaran succession in the Flinders Ranges.

- Within the lower Ediacaran Bunyeroo Formation, the distinctive Acraman ejecta layer can be traced throughout the Flinders Ranges and in deep bore holes from the coeval Officer Basin 400–600 km NW of the Flinders Ranges. Petrological and geochemical evidence sources the ejecta clasts from Lake Acraman, an eroded impact crater within the 1495 Ma porphyritic rhyolites of the Gawler Craton 300 km west of the Flinders Ranges (Gostin *et al.* 1986). The appearance of large, acanthomorphic acritarchs just above the Acraman ejecta layer, in boreholes from the Officer Basin, suggests a local perturbation on the communities of algal microfossils (Grey *et al.* 2003).
- The Ediacaran succession of the Adelaide Geosyncline consists of at least 6 high order depositional sequences. Three of these sequence boundaries involve 200–1200 m deep submarine valley and canyon incisions that record significant eustatic events (Christie-Blick *et al.* 1990). These may correlate with excursions in the stable isotope and the palaeomagnetic records.
- Although certain claims of very early Ediacara fossils (Glaessner 1968; Dyson 1985) are now discounted, *Palaeopascichnus*, a serial branching body fossil (Haines 2000; Seilacher *et al.* 2003), occurs in dense populations at the top of the Wonoka Formation, and again, 500 m above, within the more diverse Ediacara fossil assemblages of the Rawnsley Quartzite. As yet no radiometric dating is available to constrain the age of the fossiliferous Ediacara Member in the Rawnsley Quartzite. The Ediacara Member, spanning up to 300 m of section,

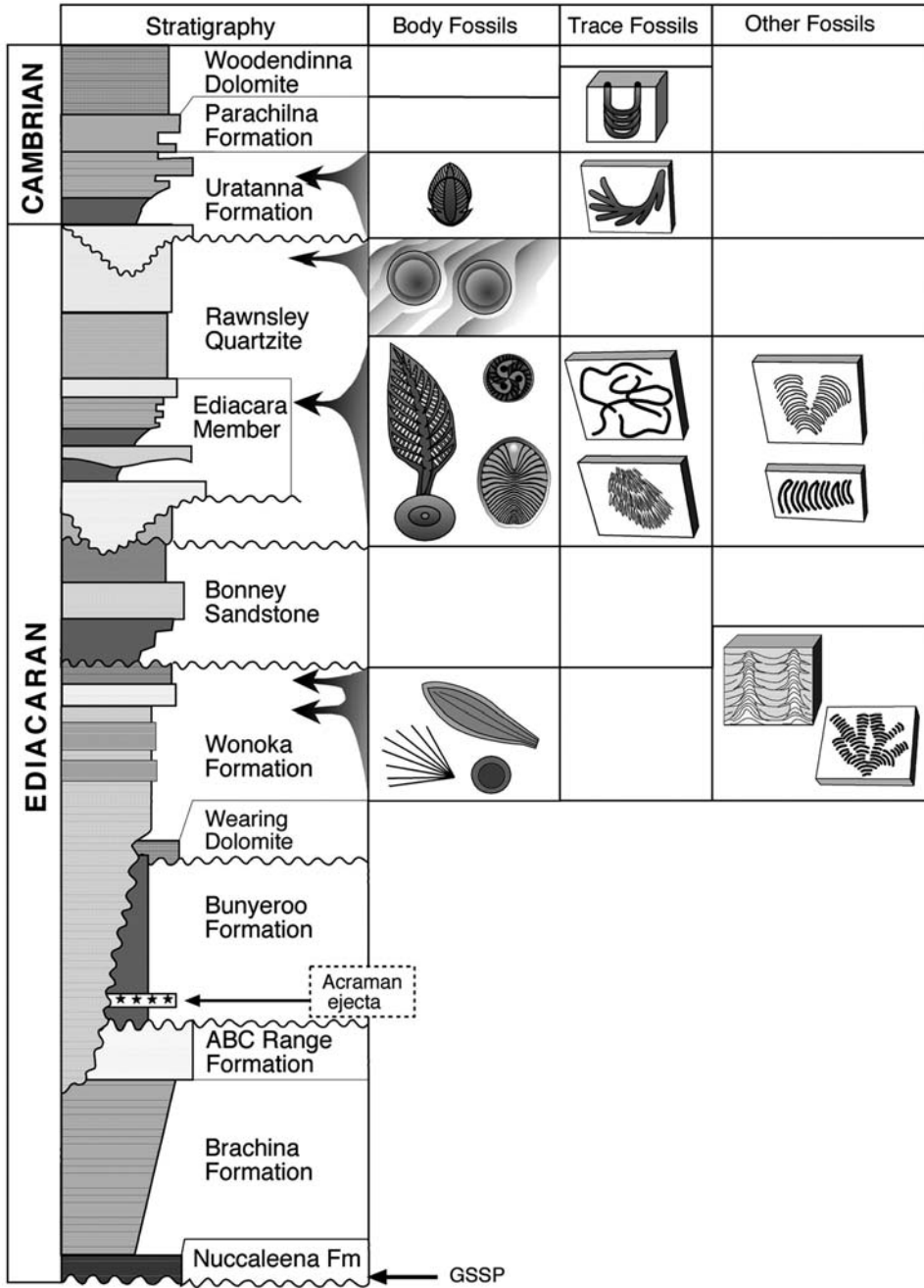


Fig. 1. Generalized stratigraphy and characteristic mega-fossils of successive depositional sequences spanning the Ediacaran–Early Cambrian transition in the Flinders Ranges, South Australia.

consists of 2–5 parasequences, each with fossiliferous facies of slightly differing character (Gehling 2000). The diverse and rich fossil assemblage of the Ediacara Member is notable for the co-occurrence of both trace fossils and body fossils. Since the Ediacara Member shares at least 65% of its described taxa with the White Sea fossil assemblages of northern Russia, it is arguable that they were coeval assemblages. The youngest Ediacara fossil horizon in the Flinders Ranges occurs 300–400 m above the Ediacara Member, just below the regional Ediacaran–Cambrian boundary (Fig. 1). Rippled surfaces bear large rimmed discs preserved much like the Cambrian medusoid fossils described by Hagadorn *et al.* (2002) from the Late Cambrian of Wisconsin.

Globally, Ediacaran successions are diverse in their stratigraphy but share many characteristics of biostratigraphy, chemostratigraphy and event stratigraphy that can be calibrated with radiometric dating.

- Megafossils are unknown from the earliest part of the Ediacaran. In Russia, the Ukraine, China, and in a number of other regions, organic walled microfossils (acritarchs) and algal fossils are important components of Ediacaran successions. A low diversity acritarch assemblage gives way to a more diverse assemblage of large spinous forms, here named the **Sinian association** for the stratigraphic interval preceding the Ediacara biota. The disappearance of the Sinian association in Central and South Australia (Grey *et al.* 2003), just before the appearance of megafossils of the Ediacara biota is not paralleled in southern China where it coincides with a post-Marinoan refrigeration event and the advent of large algal fossils. Close packed compressions of the spherical alga, *Beltanelliformis*, occur in the Sinian association (Xiao *et al.* 2002) and range up into the late Ediacaran. This makes *Beltanelliformis* one of the longest-lived and most widespread megafossils of the Ediacaran. Although the stratigraphic relationships between Ediacara megafossils and organic walled microfossils and algae (e.g. vendotaenids) are still uncertain, biostratigraphy of the Ediacaran will utilize fossils from the Ediacara biota, microfossil and algal associations.
- A parsimony analysis of endemism of 15 megafossil assemblages of the Ediacara biota, produced three clusters (Waggoner 2003), here re-named for the most significant regions. Available radiometric calibration of Ediacaran successions supports the concept of distinct **Avalon**, **White Sea** and **Nama associations** as a temporal succession (Waggoner 2003), rather than simply environmental (Grazhdankin 2004) or palaeobiogeographic assemblages. The fact that the Avalon association is found in deep-water facies in Newfoundland, England and Wales, whereas the more diverse Vendian association is preserved in relatively shallow marine environments, does not exclude a temporal separation. The successions of northwestern Canada, although relatively sparse, show a stratigraphic shift from an Avalon association to a White Sea association, even though the environments represented are outer shelf and slope (Narbonne & Aitken 1995). The Nama association spans diverse environments. The utility of proposed assemblage zones will require a review of taxonomy and assessment of ranges of cosmopolitan Ediacara genera.
- Within the 575–565 Ma time span of the Avalon association in SE Newfoundland, there is a significant stratigraphic increase in taxonomic diversity. No trace fossils or fossils with bilaterian body plans are known from this earliest association. At around 560 Ma, there was a simultaneous appearance of bilaterian body fossils and trace fossils coinciding with a decrease in dominance of fractal-growth or frondose taxa in the White Sea association. The first calcified skeletons appear in the Nama association. These biological events are interpreted as evolutionary stages in the Ediacara biota, rather than simply environmental differences.
- Two of the most significant negative excursions of $\delta^{13}\text{C}_{\text{carb}}$ values, that have ever been recorded, mark the beginning and end of the Ediacaran period (Shields 1999; Walter *et al.* 2000). A less prominent mid-Ediacaran excursion also seems to have coincided with a eustatic fall in sea level (Shields 1999). Considered along with trends in $^{87}\text{Sr}/^{86}\text{Sr}$ ratios and $\delta^{34}\text{S}_{\text{sulfate}}$ values, a first order partitioning of Ediacaran time is possible (Walter *et al.* 2000). The weakening oscillation of $\delta^{13}\text{C}_{\text{carb}}$ values, from the early Cambrian onward, may reflect the geochemical feedback due to biological activities. The first carbonate secreting organisms, and reworking of organic matter at the sediment interface by infaunal burrowers, were key innovations in the ecological revolution that accompanied the rapid Cambrian expansion in number and diversity of metazoans.
- On the Avalon Peninsula of SE Newfoundland, fossils of the Avalon association are bracketed by volcanic ash beds with U–Pb zircons ages of 575.4 ± 0.4 Ma (Bowring *et al.* 2003) and 565 ± 3 Ma (Benus 1988) respectively. The Vendian association of the Ust Peniga Group, White Sea region, Russia, spans volcanic units with U–Pb zircon ages of 558 ± 1 Ma

(Grazhdankin 2004) and 555.3 ± 0.3 Ma (Martin *et al.* 2000). In Namibia, the Nama association ranges from somewhat older than 548.9 ± 1 Ma to a little younger than 543.3 ± 1 Ma (Grotzinger *et al.* 1995).

The challenge to document the tempo and pattern of evolution of early animals and the associated changes in global climate make the subdivision and calibration of the Ediacaran a vital task for the next decade.

References

- BENUS, A. P. 1988. Sedimentological context of a deep-water Ediacaran fauna (Mistaken Point Formation, Avalon Zone, Eastern Newfoundland). In: LANDING, E., NARBONNE, G. M. & MYROW, P. (eds) Trace fossils, small shelly fossils and the Precambrian–Cambrian Boundary. *Bulletin of the New York State Museum*, **463**, 8–9.
- BOWRING, S. A., MYROW, P., LANDING, E. & RAMENZANI, J. 2003. Geochronological constraints on terminal Neoproterozoic events and the rise of metazoans. *NASA Astrobiology Institute General Meeting*, Abstract # **13045**, 113–114.
- CHRISTIE-BLICK, N., VON DER BORSCH, C. C. & DIBONA, P. A. 1990. Working hypotheses for the origin of the Wonoka Canyons (Neoproterozoic), South Australia. *American Journal of Science*, **290**, 295–332.
- DYSON, I. A. 1985. Frond-like fossils from the base of the late Precambrian Wilpena Group, South Australia. *Nature*, **318**, 283–285.
- GEHLING, J. G. 2000. Sequence stratigraphic context of the Ediacara Member, Rawnsley Quartzite, South Australia: a taphonomic window into the Neoproterozoic biosphere. *Precambrian Research*, **100**, 65–95.
- GLAESSNER, M. F. 1968. Trace fossils from the Precambrian and basal Cambrian. *Lethaia*, **2**, 369–393.
- GOSTIN, V. A., HAINES, P. W., JENKINS, R. J. F., COMPSTON, W. & WILLIAMS, I. S. 1986. Impact ejecta horizon within late Precambrian shales, Adelaide Geosyncline, South Australia. *Science*, **233**, 198–200.
- GRAZHDANKIN, D. 2004. Structure and depositional environment of the Vendian complex in the Southeastern White Sea area. *Stratigraphy and Geological Correlation*, **11**, 313–331.
- GREY, K., WALTER, M. R. & CALVER, C. R. 2003. Plankton and isotope changes at the late Neoproterozoic Acraman impact ejecta layer. *Geology*, **31**, 459–462.
- HAGADORN, J. W. & DOTT JR. & R. H., DAMROW, D. 2002. Stranded on a Late Cambrian shoreline: medusae from central Wisconsin. *Geology*, **30**, 147–150.
- HAINES, P. W. 2000. Problematic fossils in the late Neoproterozoic Wonoka Formation South Australia. *Precambrian Research*, **100**, 97–108.
- GROTZINGER, J. P., BOWRING, S. A., SAYLOR, B. Z. & KAUFMAN, A. J. 1995. Biostratigraphic and geochronologic constraints on early animal evolution. *Science*, **270**, 598–604.
- MARTIN, M. W., GRAZHDANKIN, D. V., BOWRING, S. A., EVANS, D. A. D., FEDONKIN, M. A. & KIRSCHVINK, J. L. 2000. Age of Neoproterozoic bilaterian body and trace fossils, White Sea, Russia: Implications for metazoan evolution. *Science*, **288**, 841–845.
- NARBONNE, G. M. & AITKEN, J. D. 1995. Neoproterozoic of the Mackenzie Mountains, northwestern Canada. *Precambrian Research*, **73**, 101–121.
- SCHMIDT, P. W. & WILLIAMS, G. E. 1995. The Neoproterozoic climate paradox: Equatorial palaeolatitude for Marinoan glaciation near sea level in South Australia. *Earth and Planetary Science Letters*, **134**, 107–124.
- SEILACHER, A., GRAZHDANKIN, D. & LEGOUTA, A. 2003. Ediacaran biota: the dawn of animal life in the shadow of giant protists. *Paleontological Research*, **7**, 43–54.
- SHIELDS, G. 1999. Working towards a new stratigraphic calibration scheme for the Neoproterozoic–Cambrian. *Ecologiae Geologicae Helvetiae*, **92**, 221–233.
- SOHL, L. E., CHRISTIE-BLICK, N. & KENT, D. V. 1999. Paleomagnetic polarity reversals in Marinoan (ca. 600 Ma) glacial deposits of Australia: Implications for the duration of low-latitude glaciation in Neoproterozoic time. *Geological Society of America Bulletin*, **111**, 1120–1139.
- WAGGONER, B. 2003. The Ediacaran biotas in time and space. *Integrative and Comparative Biology*, **43**, 104–113.
- WALTER, M. R., VEEVERS, J. J., CALVER, C. R., GORJAN, P. & HILL, A. C. 2000. Dating the 840–544 Ma Neoproterozoic interval by isotopes of strontium, carbon, and sulfur in seawater and some interpretive models. *Precambrian Research*, **100**, 371–433.
- XIAO, S., XUNLAI, Y., STEINER, M. & KNOLL, A. H. 2002. Macroscopic carbonaceous compressions in a terminal Proterozoic shale: a systematic reassessment of the Miaohu biota, South China. *Journal of Paleontology*, **76**, 347–376.

Rugosoopsis: a new group of Upper Riphean animals

T. N. HERMANN & V. N. PODKOYROV

*Institute of Precambrian Geology and Geochronology RAS, St.-Petersburg, 199034,
Russia (e-mail: vpodk@mail.ru)*

Abstract: The Upper Riphean Lakhanda biota (from the Uchur-Mayai region of SE Siberia) contains abundant, well preserved and highly biodiverse microfossil assemblages including *Rugosoopsis* microfossils, characterized by a uniform shape, with prominent closely transversely spaced wrinkles on the outer surface. *Rugosoopsis* are the oldest, microscopic vermiform organisms, with a typical morphology of closely spaced wrinkles on the body's outer surface resembling the Late Vendian–Early Cambrian *Sabellidites*, and even more the smallest representatives in the genus *Sokolovina* Kirjanov, 1968 (Sokolov 1997). Different types of *Rugosoopsis* preservation can be explained by the presence of numerous bacterial microorganisms on the body of *Rugosoopsis* and on organic films. *Rugosoopsis* organisms inhabited the bottom, where they likely existed alongside saprophytic microbes in finely dispersed organic debris. The community of *Rugosoopsis* and bacteria appears to represent a stable trophic system. The exceptional preservation of these microfossils is due to the favourable sedimentary environment in the Lakhanda Basin.

Molecular clocks broadly give evidence of quite deep Mesoproterozoic evolutionary roots for metazoans. The direct evidence of the origin of animal life can be found in the fossils they left, a diverse biota assemblage with a variety of preservational modes.

Abundant, well preserved and highly biodiverse microfossil assemblages are known as the Lakhanda microbiota (from the Upper Riphean, dated at 1025–1010 Ma, in the Uchur-Mayai region of SE Siberia). *Rugosoopsis* microfossils with very long (up to 1 mm, Fig. 1) narrow ribbon-like filaments have been discovered in the Kumakhin Member.

Microfossils assigned to the formal genus *Rugosoopsis* have, as a type species, *R. tenuis*. *Rugosoopsis* has a uniform shape, with prominent closely transversely spaced wrinkles on the outer surface (Timofeev & Hermann 1979, pl. 29, figs 5, 7). Width varies from 25–50 μm , constant throughout the length; some filaments show thick basal terminations.

Abundant *Rugosoopsis* are now known in shales of the Ignikan Formation in the upper part of the Lakhanda Group. Numerous *Rugosoopsis*, with better preservation and greater width (up to 140 μm ; length up to 3 mm), have been preserved on organic sapropel films. Such fragments of these films (0.5 \times 0.5 cm) can preserve up to 20 narrow filamentous and ribbon-like microfossils of *Rugosoopsis*, with varying preservation.

Perhaps *Rugosoopsis* is a kind of cyanobacteria. N. Butterfield demonstrated the double-layer structure of *Rugosoopsis* and the presence on its surface of a *Lyngbya*, like an outer sheath (Butterfield *et al.* 1994; Butterfield 2001; Samuelsson & Butterfield 2001). Butterfield (2001) described this organic material as a 'distinctive inner tabular sheath

surrounded by a less substantial transversely oriented outer sheath, which can sometimes give the (false) impressions of a cellular trichome'. He noted the absence of the outer layer in shale-hosted specimens.

That is correct, but we suggest that *Rugosoopsis* are instead the oldest, microscopic vermiform organisms. *Rugosoopsis* appears to have a multicellular layer of parenchyma, which is covered by a wrinkled layer. Multicellular tissue appears to be composed of small spherical cells (2–3 μm) with narrow intervals between cells, which are arranged in a single layer. We interpret this layer as epithelium—tissue with very little substance between cells, a thin membrane covering the outside and inside of the body. The epithelium can develop into a cuticle—a thin layer of non-cellular material, and in the case of *Rugosoopsis*, may be the outer wrinkled layer. Some peculiar structures observed in *Rugosoopsis* include a system of horizontal, narrow, dense belts, which appear to subdivide the body into several parts. Sometimes, the long body of *Rugosoopsis* is broken across into several short fragments with the development of hemispherical terminations. *Rugosoopsis* may be divided, but does not fall apart and is instead preserved as one elongate vermiform, where fragmented parts of body have rounded terminations. This process resembles parathomia.

Typical morphology of closely spaced wrinkles on the body's outer surface resembles the Late Vendian–Early Cambrian *Sabellidites*, even more the smallest representatives in the genus *Sokolovina* Kirjanov, 1968 (Sokolov 1997). Different types of *Rugosoopsis* preservation can be explained by the presence of numerous bacterial microorganisms on

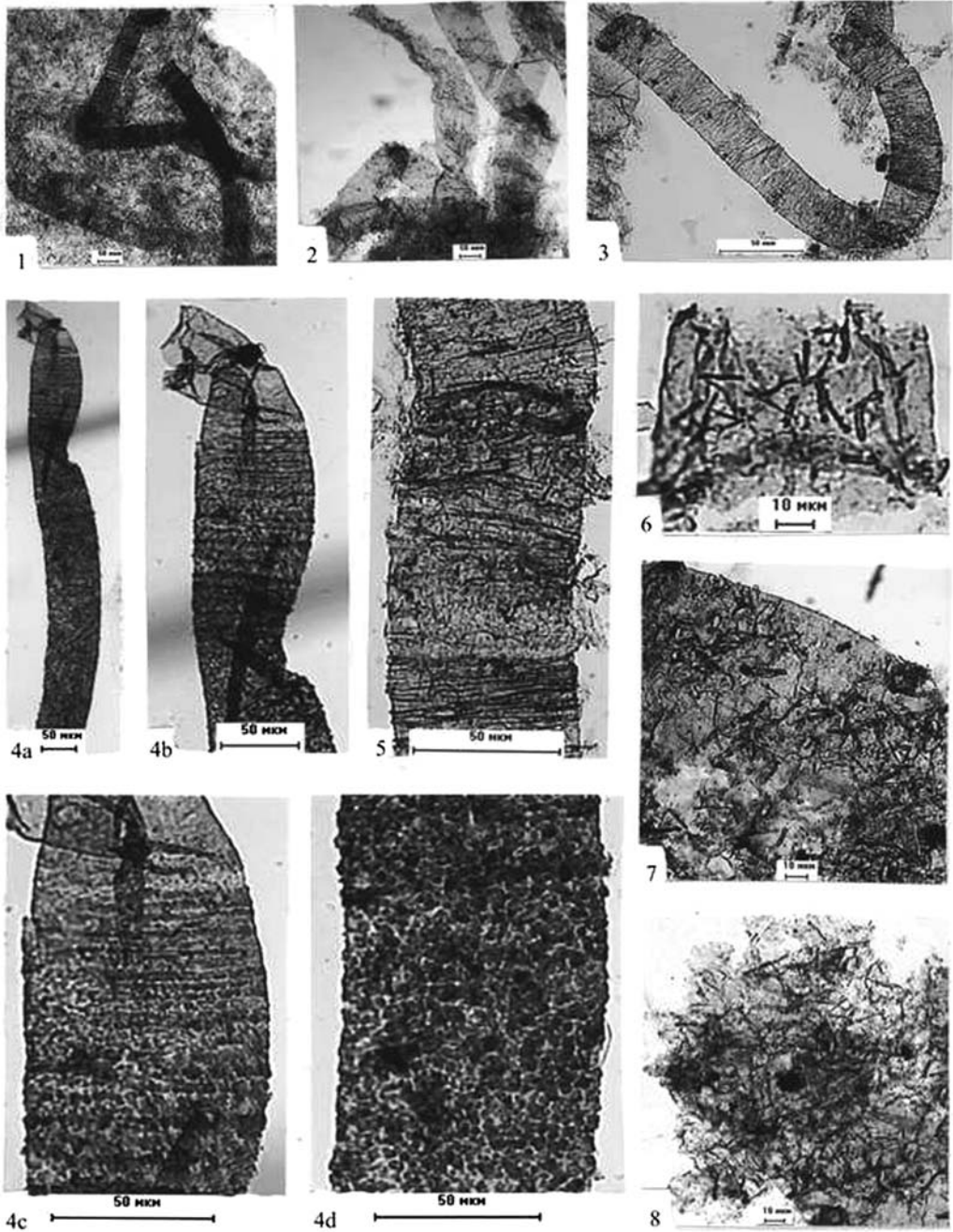


Fig. 1. (1) *Rugosoopsis* subdivided into some fragments with hemispherical terminations, fixed on organic sapropel films. (2) *Rugosoopsis* without typical morphology, degraded by bacterial activity. (3) *R. tenuis*, holotype. (4) Isolated fragment of *Rugosoopsis* with different modes of its preservation: (a) general plane of the filament; (b) magnified view of the central part of a filament; where the upper, curved termination has no wrinkles and appears as a smooth tube; (c) magnified view of the upper part of a filament with a partly preserved outer, transversely wrinkled surface; (d) magnified view of the lower part of the multicellular layer of *Rugosoopsis*. (5) Fragment of *Rugosoopsis* with the peculiar, annular, narrow belt in the upper part of the photo. (6) Bacterial microorganisms similar to *Primoflagella* visible on the smooth termination of *Rugosoopsis*; notice the preserved narrow horizontal belt. (7) Numerous *Primoflagella* on the surface of *Rugosoopsis*. (8) Mat-building *Archaetrichion lacerum*.

the body of *Rugosoopsis* and on organic films. One part of those bacterial remains resembles *Primoflagella*, described by M. B. Gnilovskaya (1979).

Bacteria were developed on the vendotaenia tissue and may be actinomycetes. Morphologically, the body of *Primoflagella* resembles short filaments with the upper part rounded and the lower part narrowed, where branched mycelium invade the vendotaenia tissue. Riphean bacteria do not have such mycelium.

Other bacterial organisms are preserved as mat-building, narrow filaments, described as actinomycetes and attributed to *Archaeotrichion lacerum* Hermann, 1989 (Yankauskas *et al.* 1989). Bacterial activities had a direct influence on the preservation of any organic remains. Sometimes, the outer wrinkled morphology is decayed and filaments have a smooth surface. The thin epithelium membrane in *Rugosoopsis* may be preserved best after grazing of the outer wrinkled layer of cuticle by other organisms. Bacterial remains are seen on *Rugosoopsis* filaments from the material of Lone Land Formation (Samuelsson & Butterfield 2001).

Rugosoopsis organisms inhabited the bottom, where they likely existed alongside saprophytic microbes on finely dispersed organic debris. The community of *Rugosoopsis* and bacterial organisms appears to represent a stable trophic system with expected producers and consumers (Zavarzin 1993). *Rugosoopsis*, in Late Riphean times had developed a tough, non-mineralized cuticle, ornamented by crossed wrinkles in order to protect the inner soft-parts of the body. The exceptional preservation of such non-mineralized organic remains depended on favourable sedimentary environments that are exposed in the Lakhanda Basin, with the biota preserved in fine-grained clays where enzyme interaction with the mineral surface in clay-polymer matrix insured imprinting of fine detail (Butterfield 1990). Microfossils making up the Lakhanda Microbiota are similar in preservation style to fossils in the Burgess Shale—and the microscopic metazoa preserved in the Lakhanda sediments are older than the Ediacara macroscopic metazoans. Among the explanations of early origin and long cryptic evolution of primary

metazoan phyla, which were restricted to spatially limited habitats (relatively cold and well oxygenated basins; Fedonkin 2003), we support the idea of a slow evolution during the Neoproterozoic (moderate concentration of free oxygen and heavy metals, that restrict biological complexity growth and the eukaryotization of biosphere. Rapid Metazoa radiation linked with abrupt geodynamic changes in Vendian (590–540 Ma) ‘can be considered as an evolutionary response to the geochemical deterioration of environment’ (Fedonkin 2003) in conditions of growing concentration of free oxygen that dramatically accelerated biological complexity.

References

- BUTTERFIELD, H. J. 1990. Organic preservation of non-mineralizing organisms and taphonomy of the Burgess Shale. *Paleobiology*, **16**, 272–286.
- BUTTERFIELD, H. J. 2001. Paleobiology of the Late Mesoproterozoic (ca 1200 Ma) Hunting Formation, Somerset Island, Arctic Canada. *Precambrian Research*, **111**, 236–256.
- BUTTERFIELD, H. J., KNOLL, A. H. & SWETT, K. 1994. Paleobiology of the Neoproterozoic Svanbergfjellet Formation, Spitzbergen. *Fossils & Strata*, **34**, 1–85.
- FEDONKIN, M. A. 2003. The origin of Metazoa in light of the Proterozoic fossil record. *Paleontological Research*, **7**, 9–41.
- GNILOVSKAYA, M. B. 1979. The Vendian Metaphyta. *Centre de Recherche Exploration-Production Elf-Aquitaine Bulletin*, **3**, 611–618.
- SAMUELSSON, J. & BUTTERFIELD, N. J. 2001. Neoproterozoic fossils from the Franklin Mountains, Northwestern Canada: Stratigraphic and Paleobiological implications. *Precambrian Research*, **107**, 235–251.
- SOKOLOV, B. S. 1997. *Studies in the Earliest Vendian*. KMK Scientific Press Ltd, Moscow [in Russian].
- TIMOFEEV, B. V. & HERMANN, T. N. 1979. Precambrian microbiota of the Lakhanda Formation. In: *Paleontology of the Precambrian and Early Cambrian*. Nauka, Leningrad, 137–147 [in Russian].
- YANKAUSKAS, T. V., MIKHAILOVA, N. S. & HERMANN, T. N. 1989. *Microfossils of the Precambrian of the USSR*. Nauka, Leningrad [in Russian].
- ZAVARZIN, G. A. 1993. Epicontinental soda lakes as probable relict biotopes of terrestrial biota formation. *Microbiology*, **62**, 473–479.

Microstratigraphy of the Late Ediacaran to the Ordovician in NW Iran (Takab area)

S. M. JAFARI¹, A. SHEMIRANI² & B. HAMDI³

¹*Subsurface Geology Department, Exploration Directorate, Yaghma Alley, Jomhouri St, Tehran, Iran (e-mail: mohieddin300@yahoo.com)*

²*Geoscience Department, Shahid Beheshti University, Evin St, Tehran, Iran*

³*Islamic Azad University, Research and Science Branch, Tehran, Iran*

Abstract: Platform sediments of Iran span the Late Ediacaran and extend into the Palaeozoic. They are primarily clastic and carbonaceous in nature, deposited in coastal and lagoonal settings. They crop out in the Takab area, as the Soltanieh Formation (Late Proterozoic to Atdabanian), the Barut Formation (Early Bottomian), the Zaigun Formation (Middle Bottomian), the Lalun Formation (Late Bottomian) and the Mila Formation (Middle Cambrian to Early Ordovician). A Precambrian–Cambrian assemblage has been identified at the base of Member 3 and the top of Member 2 in the Soltanieh Formation. The Soltanieh Formation consists of shallow marine sediments. Vertical microfacies variation reflects two regressive sequences, the earliest Cambrian System being a regressive cycle. The presence of *Chuarina* and *Vendotaenia* in the Soltanieh Formation allows correlation of Iranian sequences to those elsewhere in the world, indicating a late Neoproterozoic age. Detailed facies analyses of the Soltanieh, Barut, Zaigun, Lalun, and Mila formations allow refined palaeoenvironmental reconstructions to be made for the Ediacaran–Cambrian/Ordovician in Iran.

Platform sediments of Iran and the Middle East span the Late Ediacaran and extend into the Palaeozoic; they are primarily clastic, carbonaceous deposits laid down in coastal and lagoonal settings. In Iran, these sediments are known as the Soltanieh, Barut, Zaigun, Lalun, and Mila formations. Precambrian rocks in Iran show a variety of ages. *Cruziana fasciculata*, from the Lalun Formation, dates it as Early Cambrian, rather than Precambrian. In 1989, Hamdi discovered a Precambrian and Cambrian boundary assemblage at the base of Member 3 and the top of Member 2 in the Soltanieh Formation. There are a variety of palaeoenvironments represented in the Takab area, ranging in age from the Late Ediacaran to Early Cambrian–Ordovician. The Soltanieh Formation, Barut Formation, Zaigun Formation, Lalun Formation and Mila Formation all crop out in the Alborz-Azerbaijan Basin.

Geological setting

Takab lies in the NW of Iran and has been mapped at 1:250 000. The highest elevation is Mt Okuzolon at 2917 m, and the lowest is Mt Ajorlochay at 1400 m. Outcrops represent Precambrian to Recent, and include sedimentary, metamorphic and igneous rocks. Volcanic rocks occur in the Neoproterozoic, Cretaceous, Eocene and Oligo-Miocene; plutonic suites are also present. Major hiatuses exist between sedimentary units: between the

Silurian and Permian, the Early Permian and the Early Jurassic, the Early Cretaceous, Eocene, Oligo-Miocene and Plio-Pleistocene. Shallow epicontinental seas spread across this area during Neoproterozoic to Ordovician times, and again in the Permian to Triassic, and Early Jurassic. Deep-sea deposition began in the Early Jurassic and continued into the Cretaceous, and occurred again in the Miocene. Clastic terrestrial sediments were deposited during the Oligocene, Middle through to Late Miocene and Pliocene.

Petrography and stratigraphy of Upper Ediacaran and Cambrian–Ordovician deposits in the Takab area

Qezel Qeyeh Section

Located 33 km, NW of Shahindezh City, 46° 46' E and 36° 42' N. Erosion, faulting and folding in this area, has left on only the Soltanieh Formation accessible.

Soltanieh Formation. Similar to deposits in the Alborz and Azerbaijan regions. The Bayandor Formation underlies the Soltanieh Formation. In the Takab Quadrangle, the Soltanieh Formation is 803.6 m thick and contains 44 lithological units

and the following 5 lithostratigraphic units, from bottom to top as:

- S1: Lower Dolomite Member:* 58.6 m thick. Dolomite, cherty dolomite and thin-bedded shales.
S2: Lower Shale Member (or Chopoghloo Member): 151.7 m thick. Black shale containing fossils including *Chuarina circularis*, *Tawuia fustiformis*, *Vendotaenia* sp., *Phyllophycos radiatoidalis*. This unit contains phosphatic pellets.
S3: Middle Dolomite Member: 87.3 m thick. Stromatolite-bearing dolomite and grey limestone.
S4: Upper Shale Member: 181 m thick. Grey shale to silty shale.
S5: Upper Dolomite Member: 325 m thick. Stromatolites and cherty dolomites, cyanobacteria present in cherts.

Age: Based on the fossil content of the Soltanieh Formation, the ages of the Soltanieh members are: S1–S2: Late Proterozoic; S3: Manykayian; S4: Tommotian; S5: Atdabanian.

Environments represented: Tidal flat; lagoon; barrier; open marine, with two transgressive sequences.

Kordkandi section

Cambro-Ordovician sediments of the Takab area crop out near Kordkandi Village. Kordkandi is 16 km east of Shahindezh City, its geographical position being 36° 39' N and 46° 44' E. Four formations are known from this area.

Barut Formation. Contains five clastic units, from base to top:

- B1:* 49 m thick. Mudstones and red shales with ripple marks, limestone, dolomite, and stromatolites.
B2: 202 m thick. Greenish grey to red shales, and green sandstone with micaceous shales.
B3: 42 m thick. Micaceous red shales with cross bedding.
B4: 73 m thick. Purple micaceous shales, and silty to sandy shales with cross bedding.
B5: 62 m thick. Micaceous purple shale and grey dolomites.

Age: Stratigraphic correlation of the Barut Formation with other regions of the Alborz Mountains, suggests an age of Early Bottomian.

Environments represented: The litharenites, feldspathic litharenites, chertarenites, arkose and plagioclase arenites are typical of non-marine environments (Tucker 1991). Deltaic to tidal flats.

Zaigun Formation. Overlies the Barut Formation; composed of clastics and can be divided into four units, from base to top:

- Z1: Lower Shale Member:* 24 m thick. Red, micaceous silty shales
Z2: Lower Sandy—Shaly Member: 40 m thick. Red shale and grey mudstones with grey to red sandstones
Z3: Upper Shale Member: 12 m thick. Red to gray micaceous silty shales
Z4: Upper Sandy—Shaly Member: 18 m thick. Pink sandstones, red shales, and siltstones

Age: After stratigraphical correlation of the Zaigun Formation with rocks in other regions of the Alborz Mountains, the age is estimated to be Middle Bottomian.

Environments represented: Tidal flat and shallow marine; tidal channels.

Lalun Formation. 268 m thick. Limestones and sandstones, divided into six units; from bottom to top:

- L1: Lower Red Sandstone:* 15 m thick. Submature red sandstones showing medium sorting.
L2: Lower Pink Sandstone: 30 m thick. Pink to purple pebbly sandstones with ripple marks. Well sorted, mature, fining upward.
L3: Middle red sandstone: 78 m thick, dark red sandstones. Submature, rounded to sub-rounded, fining upward.
L4: Shaly sandstone: 46 m thick. Red sandstones to shaly sandstones. Mature, well sorted.
L5: Upper red sandstone: 81 m thick. Red to pink sandstones, with cross-bedding. Mature to submature.
L6: Shaly: 18 m thick. Red shales with sandy shales, pink to red mature sandstones.

The White Quartzite, previously considered (Stocklin *et al.* 1964) as the upper unit of the Lalun formation, is interpreted here as the lowest unit of the Mila formation, now known as the 'Base Quartzite'.

Age: After correlation of the Lalun Formation with other regions, we consider the age of the Lalun Formation to be Late Bottomian.

Environments represented: Tidal flat and shallow marine; tidal channels.

Mila Formation. Field and microscopic analysis of a distinctive White Quartzite indicates that it belongs to the transgressive base of the Mila Formation. Cambrian-Ordovician deposition seems to have taken place in an epicontinental sea environment, much like the modern Persian Gulf. Previous workers (Stocklin, *et al.* 1964) have divided the Mila Formation into five members, one of which is the White Quartzite. It was previously considered the top part of the Lalun Formation, but our work suggests it is most likely a basal quartzite of the

Mila Formation. These members are from bottom to top:

M1: 120 m thick. Base quartzite (White Quartzite) with dolomitic cement. Supermature.

M2 and *M3*: 231 m thick. Dolomite and cherty dolomites, oolitic limestones, subordinate marl, crinoids and trilobites.

M4: 138 m thick. Cherty limestones, limestones, sandstones and stromatolites.

M5: 52 m thick. Limestones, greenish grey shales and dolomitic limestones.

The Mila Formation is underlain by the shales and sandstones of the Lalun Formation and overlain by the red sandstones of the Doroud Formation (Permian). The Mila Formation is separated from the Doroud Formation by a disconformity.

Age: The age of *M2*, based on trilobites and lithologic correlation to other fossiliferous units, has been set at Middle to Late Middle Cambrian. The age of *M4* appears to be Late Cambrian to Early Ordovician. The age of *M5* of the Mila Formation is Early Ordovician.

Environments represented: Open marine; barrier; lagoon; tidal flat.

Vertical facies variation and transgressive sequences in the Soltanieh Formation

In the Soltanieh Formation, two transgressive episodes occurred in Late Ediacaran to Cambrian. The upper part of the Bayandor Formation, which underlies the Soltanieh Formation, consists of shallow water deposits (siltstones and sandstones), tidal flat mudstones and dolomites (Lower Dolomite, *S1*). After deposition of the Lower Dolomite, the tidal flat environment changed to an open marine setting (*S2*), which persisted until the Ediacaran into the Early Cambrian. Some pelagic fossils, e.g. *Chuarina circularis*, *Vendotaenia* sp. and *Tawuia fusiformis* are preserved in these sediments.

At the beginning of the Cambrian, open marine sedimentation ceased and the 'Stromatolite-bearing Limestone' was deposited as the base of the Middle Dolomite (*S3*) in Manykayan times and continued into the Tommotian. The upper part of the 'Middle Dolomite' is a transgressive sequence. Tommotian-aged sediments are open marine and this environment persists until the Early Atdabanian, followed by a regressive sequence with increasing stromatolites, indicating again a tidal flat environment depositing the Upper Dolomite. Finally, the shallow marine sedimentation of the Soltanieh Formation grades into the tidal flat-deltaic sediments of the Barut Formation.

Vertical facies variation and transgressive sequences in the Mila Formation

The Base Quartzite contains nearshore marine facies at the base of the Mila Formation, grading into deeper marine facies at the top. Sea level rose during deposition of the White Quartzite from the Lalun Formation into the Mila Formation. The first regressive episode in the Mila Formation occurred from *M2* to the Lower *M3* (Middle Cambrian), followed by a transgressive episode from Middle to Late Cambrian. The second regressive episode occurred at the top of *M5* (Early Ordovician) as indicated by the shale and sandstone sequence. After deposition of the Mila Formation, the Caledonian Orogeny brought about a significant hiatus separating the Upper Ordovician and the Lower Permian in the Takab area. Red arenites forming the base of the Doroud Formation (Early Permian) overlie the upper Member 5 of the Mila Formation (Early Ordovician), forming a non-angular disconformity.

Correlation of Late Ediacaran and Cambro-Ordovician deposits of the Takab Area and other regions of Iran

During the Late Neoproterozoic, and after the deposition of the Bayandor Formation, shallow marine environments characterize the north of Iran. Following this, the Lower Dolomite and Lower Shale of the Soltanieh Formation were deposited on top of the Bayandor Formation. At the same time, in central Iran, black shales and green pyritic shales belonging to the Kushk Series, were deposited. Late Ediacaran sediments exposed in the north of Iran contain fossils including *Chuarina circularis* and *Tawuia*. In the north and east of Iran, grey carbonaceous sediments (Tommotian-Atdabanian) were being deposited, while in central Iran, shales (Heshem Formation) and limestones (Aghda Formation) were forming, mirroring shallow marine environments. Above the Soltanieh Formation, in the north and east of Iran, the Barut Formation containing clastic-carbonaceous rocks was deposited after marine regression. In central Iran evaporites accumulated. After this, red muds (now shales) and sands (Zaigun and Lalun formations) were deposited.

During the late Early Cambrian, sea level rose, and the Base Quartzite of the Mila Formation was deposited over most of Iran. These transgressive deposits at the base of the Mila Formation can be correlated with those at the base of the Kuh Banan and Kalshaneh formations in central Iran. Sea level then fell and, in the north of Iran, dolomitic rocks (*M2* of the Mila Formation) were laid down, and

Table 1. Stratigraphic correlation of Upper Ediacaran, Cambro-Ordovician formations, Iran

Global Stratigraphic Chart(1989)			IRAN				
Era	System	Series or Stage	ALBORZ Mount.-AZERBAIJAN		TABAS-KERMAN Area (Central Iran)		
Lower Palaeozoic	Ordovician	Upper	X		X		
		Ashgill					
		Caradoc	X		X		
		Lower	Llandoilo-Llanvirn	Mila Fm	Mbr 5	Shirgesht Fm	
			Arenig				
			Tremadoc				
	Cambrian	Upper	Trempealeuan	Mbr 4	Drenjal Fm		
			Franconian				
			Dresbachian				
		Middle	Mayaian	Mbr 3	Mbr 2		
			Ambaian				
			Toyonian				
	Lower	Bottomian	Mbr 1	Kalshaneh Fm			
		Lalun Fm			Dahu		
		Barut Fm			Desu Aghda		
	Neoproterozoic	Terminal Neoproterozoic	Vendian	Soltanieh Fm		Kushk Series?	
							U. Dolomite
							U. Shale
							M. Dolomite
			L. Shale				
			L. Dolomite				
			Bayandor				

in central Iran the Drenjal Formation formed on top of the Kalshaneh Formation. During the early Middle Cambrian, Member 4 of the Mila Formation represents a transgressive episode in the Takab (North) area, while the Shirgesht Formation was deposited in central Iran. This transgressive episode continued until the Early Ordovician when, in the north of Iran, mud (preserved as shale) and limestones were deposited as M5.

Conclusions

Study of the rock units that crop out in the Takab Area of Iran suggest that during the Neoproterozoic and Cambrian–Ordovician, this area had a history similar to that of the Alborz sedimentary basin. The sedimentary environments represented by the

Soltanieh Formation are shallow marine during the Neoproterozoic and Cambrian–Ordovician. The vertical microfacies variation in the Soltanieh Formation reflects two regressive sequences. The beginning of the Cambrian System is characterized by a regressive episode. The presence of *Chuarina* and *Vendotaenia* in the Soltanieh Formation allows correlation of Iranian sequences to those elsewhere in the world—Newfoundland, Arizona, China and Africa, indicating a late Neoproterozoic age. The Barut Formation was deposited in a delta-tidal flat environment. During the deposition of the Mila Formation, two regressive sequences can be distinguished: one during early Middle Cambrian (M2) and the other during Early Ordovician (M5). The unconformity between the Mila Formation and the overlying Doroud Formation is a result of the Caledonian

Orogeny, which took place during the Late Ordovician, Silurian, Devonian and Carboniferous in the Takab area. Detailed facies analyses of the Soltanieh, Barut, Zaigun, Lalun, and Mila formations allow refined palaeoenvironmental reconstructions to be made for the Ediacaran-Cambrian/Ordovician in Iran.

References

- STOCKLIN, J., RUTTNER, A., NABAVI, M. 1964. New Data on the Lower Paleozoic, North Iran. *Geological Survey of Iran Report*, **1**.
- TUCKER, M. E. 1991. *Sedimentary Petrology. An Introduction to the Origin of Sedimentary Rocks* (2nd edn). Blackwell, New York.

$\delta^{13}\text{C}$ stratigraphy of the Birmania Basin, Rajasthan, India: implications for the Vendian–Cambrian transition

A. MAHESHWARI¹, A. N. SIAL² & S. C. MATHUR³

¹*Department of Geology, University of Rajasthan, Jaipur-4, India
(e-mail: anilm@datainfosys.net)*

²*NEG-LABISE, Department of Geology, C.P. 7852,
Federal University of Pernambuco, Recife, Brazil-50,732-970*

³*Department of Geology, J.N.V. University, Jodhpur, India*

Abstract: The Birmania Basin is an oval-shaped, isolated remnant of the Marwar Basin (Neoproterozoic–Early Palaeozoic), located in the heart of the Thar Desert of western Rajasthan, India. The Birmania Basin comprises a 900 metre-thick sedimentary sequence of siliciclastic, carbonate and phosphorite facies. $\delta^{13}\text{C}$ and $\delta^{18}\text{O}$ -values are presented in this paper, based on samples of phosphorite and carbonate collected at close intervals along two sample lines near Birmania and Kohra in the Birmania Basin, Rajasthan, India. The carbonates of the Birmania Basin sampled have suffered neither deep burial nor alteration and may provide pristine samples of the C-cycle at the time of their deposition. These values can be useful in inter-regional correlation, particularly for unfossiliferous successions. The carbon isotopic pattern observed in the Birmania succession appears to be similar to that observed in well-established Precambrian–Cambrian boundary sections globally. A worldwide phase of phosphogenesis, at or near the Precambrian–Cambrian boundary, supports the inference that biological controls driven by ocean fertility changes influenced the marine carbon reservoir.

The palaeogeographic reconstruction of the late Neoproterozoic assumes a marked significance due to the fact that the interactions between the biosphere, atmosphere, hydrosphere, and geosphere during that time strongly influenced the evolution of life and initiated a remarkable phase of organic evolution, well documented in the rocks of that age. Time-related changes in these carbon reservoirs and processes during the Late Proterozoic have played an important role in the evolution of the environment and of life (Des Marais 1997). Brasier (1992) discussed, at length, various factors which pushed the shallow marine ecosystem of the Late Neoproterozoic–Cambrian towards P-limitation and suggested that nitrate fixation, density stratification and massive removal of P in the sediments were responsible for the formation of phosphatic deposits within this time interval. The East Gondwana assembly of continents provides fine examples of stratigraphic successions in which the ideas related to oceanic stratification, phosphate deposition, enhanced organic production and carbon isotope fluctuations can be verified and correlated from continent to continent (Banerjee & Majumdar 1999).

The Birmania Basin is an oval-shaped, isolated remnant of the Marwar Basin (Neoproterozoic–Early Palaeozoic) located in the heart of the Thar Desert of western Rajasthan, India. It is underlain

by the Malani Igneous Suite of rocks, which range in age from 780 to 680 Ma (Rathore *et al.* 1999). The Birmania Basin comprises a 900 metre-thick sedimentary sequence of siliciclastic, carbonate and phosphorite facies. This sequence is unconformably overlain by the Lathi Conglomerate of Jurassic age on the northern flank of the basin. Global Neoproterozoic glacial activity in western Rajasthan is represented by the Pokaran Boulder Bed, a few kilometres away from the study area. The Pokaran Boulder Bed overlies the Malani Igneous Suite and mainly consists of boulders and angular fragments of igneous rocks belonging to the Malani Suite. The stratigraphic position of this succession is delineated on the basis of regional correlation with rocks of the Salt Range in Pakistan.

$\delta^{13}\text{C}$ - and $\delta^{18}\text{O}$ -values are presented in this paper based on 32 samples of phosphorite and carbonate. They were collected at close intervals along two sample lines near Birmania and Kohra in the Birmania Basin, Rajasthan, India.

Implications of the carbon isotope data for the Late Proterozoic–Cambrian time period

The palaeontological information necessary for characterizing the boundary interval in Birmania

Formation is absent. It is now widely accepted, however, that isotope age curves do provide useful tools for stratigraphic analysis and correlation, particularly for unfossiliferous successions. The primary Birmania Basin carbonates appear to have undergone early fabric-retentive dolomitization, rendering them relatively impermeable. The carbonates of the Birmania Basin sampled for the present study have suffered neither deep burial nor alteration. Consequently, Birmania carbonates may provide pristine samples of the C cycle at the time of their deposition, and these values can be useful in inter-regional correlations.

The base of the Birmania Formation is represented by a stromatolitic phosphorite and is characterized by negative $\delta^{13}\text{C}$ (up to -3.56 PDB ‰). The lower microsparitic dolostone underlying these stromatolitic phosphorites provide negative $\delta^{13}\text{C}$ value on the Kohra block. The middle microsparitic dolostone, lower and upper micritic dolostone and calcrite dolostones overlying the phosphorites all have positive $\delta^{13}\text{C}$ values up to $+3.87$ ‰ PDB. A swing to less positive $\delta^{13}\text{C}$ values is observed in the uppermost carbonates of this sequence. The oxygen isotopic composition of carbonates is very prone to alteration during diagenesis. However, the carbonates of the Birmania succession show a very high oxygen isotopic composition and may be taken to represent close to original values.

Carbon isotope profiles are now available in boundary sections of many parts of world including Siberia, Iran, India, China, Morocco and South Australia (see Brasier *et al.* 1990 for references). There are remarkable similarities in the patterns of $\delta^{13}\text{C}$ variations imprinted in the shallow marine carbonate sequences in spite of their wide geographic distribution. In all cases, the trends show negative-low positive values in the terminal Proterozoic (Vendian) increasing to markedly positive values in the Nemakit-Daldynian, followed by a swing back to negative-less positive values in the early Tommotian (Aharon & Liew 1992; Brasier 1992; Tucker 1992; Ripperdan 1994; Kaufman & Knoll 1995). The pattern of $\delta^{13}\text{C}$ variations in the Birmania Basin is very similar to that observed in different carbonate sequences of the world. Dissimilarities between the $\delta^{13}\text{C}$ records at any one time are likely to be related to the rates of shift, the amplitude of the isotope excursions, and the exact position of the negative $\delta^{13}\text{C}$ offset with respect to the Precambrian/Cambrian boundary.

The carbon isotopic pattern observed in the Birmania succession appears to be similar to that observed in the well-established Precambrian–Cambrian boundary sections of the world (Aharon & Liew 1992;

Kaufman & Knoll 1995; Friedman *et al.* 1997). The Birmania succession is sadly unfossiliferous, resembling the Precambrian–Cambrian boundary succession in Oman, where the strata lack Cambrian body fossils (Burns & Matter 1993). A worldwide phase of phosphogenesis (Cook & Shergold 1984) at or near, the Precambrian–Cambrian boundary supports the inference (Lambert *et al.* 1987; Tucker 1992) that biological controls driven by ocean fertility changes influenced the marine carbon reservoir.

References

- AHARON, P. & LIEW, T. C. 1992. An assessment of the Precambrian/Cambrian transition events on the basis of carbon isotope records. *In*: SCHIDLOWSKI, *ET AL.* (eds) *Early Organic Evolution*. Springer-Verlag, Berlin, 212–213.
- BANERJEE, D. M. & MAZUMDAR, A. 1999. On the late Neoproterozoic–Early Cambrian transition events in parts of east Gondwanaland. *Neoproterozoic*. *In*: ROY, A. B. (ed.) *Special Issue. Neoproterozoic Crustal Evolution and India. Gondwana Linkage. Gondwana Research*, **2**, 199–211.
- BRASIER, M. D. 1992. Global ocean-atmospheric change across the Precambrian–Cambrian transition. *Geological Magazine*, **129**, 161–168.
- BRASIER, M. D. *ET AL.* 1990. The carbon and oxygen isotopic record of the Precambrian–Cambrian boundary interval in China and Iran and their correlation. *Geological Magazine*, **127**, 319–332.
- BURNS, S. J. & MATTER, A. 1993. Carbon isotopic record of the latest Proterozoic from Oman. *Ecologiae Geologicae Helveticae*, **86**, 595–607.
- COOK, P. J. & SHERGOLD, J. H. 1984. Phosphorous, phosphorites and skeletal evolution at the Precambrian–Cambrian boundary. *Nature*, **308**, 231–236.
- DES MARAIS, D. J. 1997. Isotopic evolution of the biogeochemical carbon cycle during the Proterozoic Eon. *Organic Geochemistry*, **27**, 185–193.
- FRIEDMAN, G. M., CHAKRABORTY, C. & KOLKAS, M. 1997. $\delta^{13}\text{C}$ excursion in the end-Proterozoic strata of the Vindhyan basin (central India): Its chronostratigraphic significance. *Carbonates and Evaporites*, **11**, 206–212.
- KAUFMAN, A. J. & KNOLL, A. H., 1995. Neoproterozoic variations in the C-isotopic composition of sea water: stratigraphic and biogeochemical implications. *Precambrian Research*, **73**, 27–49.
- LAMBERT, I. B., WALTER, M. R., WENLONG, Z., ONGNIAN, LU. & GUOGAN, M. A. 1987. Paleoenvironment and carbon isotope stratigraphy of Upper Proterozoic carbonate of Yangtze Platform. *Nature*, **325**, 140–142.
- RATHORE, S. S., VENKATESH, T. R. & SRIVASTAVA, R. K. 1999. Rb–Sr isotope dating of Neoproterozoic (Malani Group) magmatism from Southwest Rajasthan, India: Evidence of younger Pan-African thermal event by ^{40}Ar – ^{39}Ar studies. *In*: ROY, A. B. (ed.) *Neoproterozoic Crustal Evolution and*

- India-Gondwana Linkage. Gondwana Research*, **2**, 271–286.
- RIPPERDAN, R. L. 1994. Global variations in carbon isotope composition during Neoproterozoic and earliest Cambrian. *Annual Review of Earth and Planetary Science Letters*, **22**, 385–417.
- TUCKER, M. E. 1992. The Precambrian–Cambrian boundary: seawater chemistry, ocean circulation and nutrient supply in metazoan evolutions, extinction and bimineralization. *Journal of the Geological Society of London*, **149**, 655–668.

Sprigg, Glaessner and Wade and the discovery and international recognition of the Ediacaran fauna

S. TURNER^{1,2} & P. VICKERS-RICH^{1,3}

¹*School of Geosciences, Box 28E, Monash University, Victoria 3800, Australia*

²*Queensland Museum, Geology & Palaeontology, 122 Gerler Road, Hendra, Queensland 4011, Australia (e-mail: sue.turner@qm.qld.gov.au)*

³*Honorary Research Associate, Laboratory of Precambrian Organisms, Paleontological Institute, Russian Academy of Sciences, 123 Profsoyuznaya, Moscow, Russia 117868*

Abstract: Reg Sprigg was a young geologist when he found Ediacaran fossils in the hills of the western Flinders Ranges of South Australia. At first not taken seriously by his mentors, the reality of his fossils and the true age of his finds were recognized by the late 1940s.

Research on these oldest known metazoans of the time was then carried out by Martin Glaessner and his student, Mary Wade, who first studied Foraminifera. Sprigg was not included in this research but took a different path pursuing a career as an economic geologist and founding Santos. Wade and Glaessner interpreted their Ediacaran fossils as worms and jellyfish, but more recent interpretations have led to very different conclusions.

The first Precambrian fossils in Australia upon which the Ediacaran biota was recognized were found in the Ediacara Hills, Flinders Ranges, South Australia in 1946 by former geology student of the University of Adelaide, Reg C. Sprigg (1919–1994 Fig. 1). Sprigg's mentor, Professor Sir Douglas Mawson, had dampened his enthusiasm over an earlier find because of the perceived difficulties in accepting evidence for Precambrian fossils based on the discredited Tea Tree Gully work of Edgeworth David (Sprigg 1989; Branagan 2005). This meant that Sprigg's original age assessment verged on the cautious side. In giving the first descriptions of many Ediacara fossils—his 'Early Cambrian ['Eocambrian'] jellyfishes', including the iconic *Dickinsonia*, Sprigg (1947, 1949, 1956) chose only local and informal publication. He did acknowledge 'advice' from Curt Teichert. However, the importance and full significance of the fauna was not fully realized internationally until the pivotal series of papers by Professor Martin F. Glaessner (1906–1989; Fig. 2, Cloud 1990; McGowran 1994) and his students, notably Mary J. Wade (1932–2005; Fig. 3; Turner 2005), and colleagues such as Preston Cloud (Cloud & Glaessner 1981).

Sprigg himself had introduced Glaessner to the material at the Perth Australian and New Zealand Association for the Advancement of Science (ANZAAS) Conference in 1947 and had donated most of his finds to the Geology Department in Adelaide, including the iconic type specimen of *Mawsonites* that was actually collected by Sprigg's

business partner Dennis Walter pers. comm., 2004. Glaessner and Wade became directly involved in the late 1950s with another student Brian Daily (1931–1986; Jago & Pledge 1987) after further finds were made by amateurs Hans Mincham and

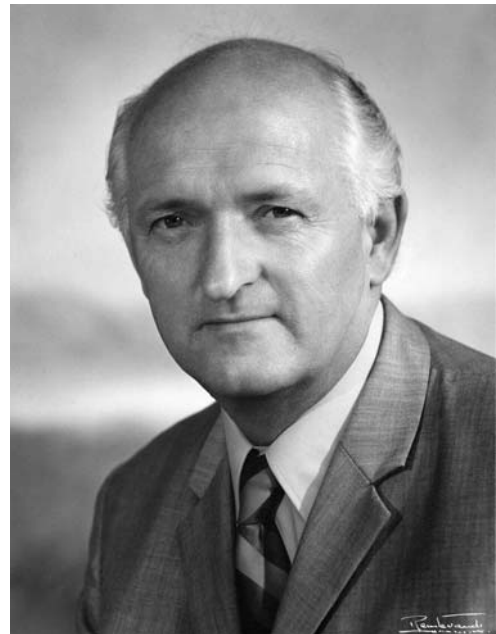


Fig. 1. Reg Sprigg (courtesy of M. & D. Sprigg).



Fig. 2. Martin Glaessner c. 1957, somewhere in Europe during study leave (courtesy of the M. Wade estate).

Ben Flounders with subsequent South Australian Museum and University of Adelaide mounted expeditions (Cloud & Glaessner 1981; Glaessner 1961, 1979, 1984). Glaessner with Daily verified the Precambrian age for the Ediacara horizons (1959). Glaessner's reputation, and his European-training, with long experience of invertebrate palaeontology, seemed to ensure that his espousal of the Precambrian fauna was accepted. Glaessner chose internationally recognized American and



Fig. 3. Mary Wade (second from left) with parents and a friend at her graduation from the University of Adelaide (courtesy of W. J. Wade).

European journals to publicize the fossils (e.g. *Scientific American*, *Palaeontology*, *Geologische Rundschau*). This strategy put the fauna onto the international stage. Sprigg's contribution was 'rewarded' with various named taxa, e.g. *Spriggina*. Despite Sprigg's early efforts, in most people's minds the words 'Ediacaran' and Glaessner & Wade became synonymous.

Wade, one of the few post-World War II women palaeontology students, had chosen to enrol in the department headed by Sir Douglas Mawson at the University of Adelaide in 1947. She took to Geology with gusto and majored in geology and zoology, gaining a demonstratorship, taking six years (1954–1959) to complete her Ph.D. on Tertiary Foraminifera, supervised by Glaessner (Turner 1997, 1998); she then joined him in describing Ediacaran fossils. Wade wrote two major papers with Glaessner and at least seven single-authored works (see Glaessner 1984; Wade 1968, 1969, 1970), which culminated in her contribution on the Scyphozoa to the *Traité de Zoologie* (Grassé 1997).

Sprigg, however, was not involved in this phase of the research, which was a source of regret for him (Sprigg 1989), but his career took a different turn as he continued with the Geological Survey in its search for uranium as part of Cold War paranoia and then later as he set up companies, GeoSurveys and Santos, and finally 'Arkaroola' in the Flinders Ranges as a geological and faunal reserve. As his notes of 29/1/47 state, he was practical about just what one could do in a day: 'A man that cometh to a cross roads must turn his back upon the one way to follow the other' (a quote from *The King's Henchmen* (Millay 1927)). Sprigg, however, being the ever-pragmatic individual, noted (1989) that despite initial doubt being cast on his interpretations of the Ediacaran fauna and its Precambrian age, its preservation and life environment (Wade 1969; Seilacher 1984; Runnegar 1992), his finds were 'epochal'.

Glaessner did not publish his final seminal work *The Dawn of Animal Life* until his last decade and Wade was due to assist with a revised second edition before he died. However, neither he nor Wade were to work further despite remaining staunch advocates of the Ediacarans all belonging to groups with living relatives—jellyfish, annelid worms, arthropods, etc., contrary to the changes in thinking about the phylogenetic and ecological significance of the biota that appeared in the 1980s and beyond (e.g. the 'Vendobiota' of Seilacher 1984), which became the province of other workers.

Family, friends and colleagues of Sprigg, Glaessner and Wade are thanked for their help and candid discussions, especially D. and M. Sprigg, D. Walter, L. Harrington,

H. Mincham and R. Jenkins, and especially the late M. Wade, who has always given us inspiration with her story. The thoughts expressed here are, however, our own. Funding from the Australian IGCP Committee Grant-in-Aid Scheme, which enabled participation of ST in the IGCP 493 Prato meeting, is acknowledged as well as funds from ARC Discovery grant no. DP0453155 to PV-R and ST.

References

- BRANAGAN, D. F. 2005. *T. W. Edgeworth David. A Life. Geologist, Adventurer, Soldier and 'Knight in the Old Brown Hat'*. National Library of Australia, Canberra.
- CLOUD, P. 1990. Obituary. Professor Martin Glaessner 1906–1989. *Precambrian Research*, **47**, 1–2.
- CLOUD, P. & GLAESSNER, M. F. 1981. The Ediacarian Period and System: Metazoa inherit the Earth. *Science*, **218**, 783–792.
- GLAESSNER, M. F. 1959. Precambrian Coelenterata from Australia, Africa and England. *Nature*, **183**, 1472–1473.
- GLAESSNER, M. F. 1961. Precambrian Animals. *Scientific American*, **204**, 72–78.
- GLAESSNER, M. F., 1979. Precambrian. In: ROBINSON, R. A. & TEICHERT, C. (eds) *Treatise on Invertebrate Paleontology. Part A*. Geological Society of America, 79–118.
- GLAESSNER, M. F. 1984. *The Dawn of Animal Life: a Biohistorical Study*. Cambridge University Press.
- GLAESSNER, M. F. & DAILY, B. 1959. The geology and Late Cambrian fauna of the Ediacara Fossil Reserve. *Records of the South Australian Museum*, **13**, 369–401.
- GRASSÉ, P.-P. (ed.) 1997. *Traité de Zoologie: Spongiaires, Cténaïres, Cnidaires*. Tome 3, Volume 2. Dunod, Paris.
- JAGO, J. B. & PLEDGE, N. S. 1987. Obituary Brian Daily 1 April 1931–6 March 1986. *Records of the South Australian Museum*, **21**, 65–68.
- MCGOWRAN, B. 1994. Martin Fritz Glaessner 1906–1989. *Historical Records of Australian Science*, **10**, 61–81.
- MILLAY, E. ST. V. 1927. *The King's Henchman. A Play in Three Acts*. Harper & Brothers Publishers, New York & London.
- RUNNEGAR, B. 1992. Evolution of the earliest animals. In: SCHOPF, J. W. (ed.) *Major Events in the History of Life*. Jones and Bartlett Publishers, Boston, 65–93.
- SEILACHER, A. 1984. Late Precambrian and Early Cambrian Metazoa: Preservation or real extinctions? In: BERNHARD, S. (ed.) *Patterns of Change in Earth Evolution (Dahlem Konferenzen)*. Springer-Verlag, Berlin, 159–168.
- SEILACHER, A. 1989. Vendozoa: Organismic construction in the Proterozoic biosphere. *Lethaia*, **22**, 229–239.
- SPRIGG, R. C. 1947. Early Cambrian (?) jellyfishes from the Flinders Ranges, South Australia. *Transactions of the Royal Society of South Australia*, **71**, 212–224, pls 5–8.
- SPRIGG, R. C. 1949. Early Cambrian 'jellyfishes' of Ediacara, South Australia, and Mount John, Kimberley District, Western Australia. *Transactions of the Royal Society of South Australia*, **73**, 72–99, pls 9–21.
- SPRIGG, R. C. 1956. Fossil jellyfish from the Cambrian of South Australia. *The Australian Amateur Mineralogist*, **2**, 22–24.
- SPRIGG, R. C. 1989. *Geology is Fun (Recollections) or The Anatomy and Confessions of a Geological Addict*. Arkaroola.
- TURNER, S. 1997. Mary Wade. In: MACKAY, J. (ed.) *Brilliant Careers. Women Collectors and Illustrators in Queensland*. Queensland Museum, Brisbane, 75–77, 80.
- TURNER, S. 1998. Women in Paleontology in Australia. In: GOOD, G. A. (ed.) *Sciences of the Earth. An Encyclopedia of Events, People and Phenomena*. Garland Press, New York & London, 848–852.
- TURNER, S. 2005. Obituary Dr Mary Wade. *The Queensland Geologist GSA, Queensland Division Newsletter*, **105**, 4.
- WADE, M. J. 1968. Preservation of soft-bodied animals in Precambrian sandstones at Ediacara, South Australia. *Lethaia*, **1**, 238–267.
- WADE, M. J. 1969. Medusae from uppermost Precambrian or Cambrian sandstones, central Australia. *Palaeontology*, **12**, 351–365.
- WADE, M. J. 1970. The stratigraphic distribution of the Ediacara fauna in Australia. *Transactions of the Royal Society of South Australia*, **94**, 87–104.

Saline giants, cold cradles and global playgrounds of Neoproterozoic Earth: the origin of the Animalia

P. VICKERS-RICH^{1,2}

¹*School of Geosciences, Monash University, Melbourne, Australia*

(e-mail: Pat.Rich@sci.monash.edu.au)

²*Laboratory of Precambrian Organisms, Paleontological Institute, Russian Academy of Sciences, Moscow, Russia*

Abstract: It is still an enigma of just what triggered the development of multicellular animals, the metazoans. The rise of oxygen has commonly been suggested as the cause, which probably had a marked effect. But why do the metazoans seem to appear in the fossil record, with some diversity, in the late Neoproterozoic around 575–580 million years ago? Perhaps the sudden appearance is related to a rapid expansion of metazoans into global oceans as they became markedly less saline with the deposit of saline giants in the Neoproterozoic. Metazoans may well have developed first in ‘cold cradles’ in deltaic and estuarine conditions earlier, when seas were more saline, and with the removal of salts from the global oceans, the seas became their ‘global playgrounds’ and with this invasion the fossil record improved significantly. Such an idea can only be tested with more precise dating of the saline giants themselves.

For much of Earth history, beginning around 2.5 billion years ago, the planet has had a rather mild climate, despite its rather ‘toasty’ beginnings and its current glacial leanings. Thus, the rule of thumb that palaeontologists use in interpreting the past, uniformitarianism (the present is the key to the past), may not always be appropriate. However, during one period of time, from around 700 million to at least 580 million, perhaps it is appropriate—or is it? This was a period of numerous glacial events, some of which were global, and likely much more severe than the glacials of the past two million years on Earth, the Pleistocene. Such severely cold conditions, even at the Equator, and the variability of climate, from cold to warm and back to cold again over more than 180 million years, was the time in Earth history when the first undoubted metazoans appear in the fossil record. They first appear as tiny embryos and adults recorded in China (Xiao *et al.* 1998; Li 2006) and somewhat later as macrofossils known from many places around the globe, most notably from Newfoundland, Australia, Russia and Namibia.

What was so special about this time which fostered such advances in complexity—leading from a world dominated by microbes to one resplendent in complex, often mobile, macro-animals and eventually shelled and skeletonized forms that begin to appear in the latest Neoproterozoic (*Cloudina*)? ‘Weedy environments’ are often sites of innovation—those environments that are new and variable. Neoproterozoic environments were certainly such weedy places—variable in salinity, oxygen

content, temperature and likely saturation of certain minerals needed for construction of hard parts. Knauth (2005) has noted that ocean water salinity could have played an important role in controlling accessibility to global oceans for complex metazoan metabolism. Lower salinity itself favoured metazoan metabolism and also enhanced oxygen saturation. Add to that colder temperature during glacial events, which would have enhanced oxygen concentrations further, and global oceans would have been most inviting to the expansion of metazoans. These metazoans may well have developed elsewhere than in the global hypersaline oceans (perhaps as high as 1.6 to 2 times modern salinities (Land 1995; Knauth 1998, 2005)), prior to massive halite deposition in the late Neoproterozoic and early Phanerozoic, which changed the world’s seas profoundly. Major salt deposition (reflected by ‘saline giants’) is known to have occurred on Earth only a few times in its history, two of those occurring between 500 and 700 million years, with major deposits preserved today in Australia, Oman, Saudi Arabia, Iran and Pakistan. These signal the sequestering of halite on the growing continents, thus significantly lowering salinity in the global oceans. Knauth (2005) has suggested that metazoans might have developed first in fresh waters because of their lower salinity (which would have been accompanied by higher oxygen saturation) during times when the global oceans were too saturated with salts to favour a metazoan presence. Fedonkin (1996) noted that metazoans might have developed in ‘cold cradles’ during the lowered temperatures

of the Neoproterozoic glaciations. This could have happened before the Neoproterozoic glacials in cold, freshwater cradles, or in deltaic areas where inflowing fresh waters lowered the salinity of the open ocean, and in places where lowered temperatures also enhanced oxygen solubility. Then, with deposition of the 'salt giants' on the growing continents, the floodgates to global oceans may have been opened as salinity dropped, oxygen saturation escalated first in the cold oceanic 'playgrounds' that would have been widespread during Neoproterozoic glacial times. Within 4 million years of the meltdown of the final glacial events, the Gaskiers Glaciation dated at around 582 million years (Halverson *et al.* 2005; Bowring & Condon pers. comm., 2006), fully developed, complex metazoans were present. The degree of complexity of these organisms, despite the uncertainty of their relationships with crown groups of today, combined with the data provided by molecular studies (e.g. Blair & Hedges 2004; Hedges *et al.* 2004), in spite of lack of agreement on dates, clearly indicate that complex metazoans were present *before* this date.

Where might one look for the older fossils of the Ediacarans? As mentioned above, Knauth (2005) has echoed a suggestion made before that perhaps metazoans were living in environments not frequently preserved, such as freshwater lakes and rivers—sediments of which need intensive investigation in the future. Such non-salty environments would certainly have provided a more 'inviting' abode for most metazoans and with or without the cold, a place with more oxygen needed to fuel metazoan metabolism. Despite the oceans of the Phanerozoic, including those of today, being ideal environments for the most diverse metazoan communities, this may not have been the case in the Neoproterozoic. Knauth further suggests that the acquisition of shells in the Early and Middle Cambrian may have been the result of changing ocean saturation in calcite, silica and phosphate. Perhaps also related to changing salinity is the erosion of continental shelf sediments exposed during lowered glacial sea levels or even erosion of a lengthy mountain chain in the early Phanerozoic brought about by plate tectonics. Degradation of these highlands would not only have introduced nutrients and new environments (Brasier & Lindsay 2001; Squire *et al.* 2006) but also would have supersaturated the global oceans with the building blocks of hard parts.

And where did the Ediacarans go? Some clearly were stem groups that have relationships to crown groups—*Kimberella* to the Mollusca, as an example. Others may simply have disappeared because their way of life came to an end. With the demise of the vast microbial mats, which so characterized the Neoproterozoic and before, the 'jobs' of

such organisms as *Yorgia* and *Dickinsonia* came to an end. These likely vacuum cleaners or 'cleaning sponges', which may well have absorbed their way into the microbial mats as a way of 'feeding', then moved on to the next 'delicious' spot leaving their long-lasting absorption patterns behind, may simply have run out of food widespread enough to maintain their lifestyle. Just what brought about the demise of the microbial mats and the beginning of deep burrowing and bioturbation, which disrupted these mats forever, may simply have been a change in ocean chemistry and the development of more efficient feeding styles, greater mobility of the newly evolved organisms, including their ability to burrow, at first shallowly and then deeper—forever changing the sea floors of global oceans.

References

- BLAIR, J. E. & HEDGES, S. B. 2004. Molecular clocks do not support the Cambrian explosion. *Molecular Biology and Evolution*, **22**, 387–390.
- BRASIER, M. D. & LINDSAY, J. F. 2001. Did supercontinental amalgamation trigger the "Cambrian Explosion?" In: ZHURAVLEV, A. YU. & RIDING, R. (eds) *The Ecology of the Cambrian Radiation*, Columbia University Press, 69–89.
- FEDONKIN, M. A. 1996. Cold-water cradle of animal life. *Paleontologicheskii Zhurnal (English version)*, **30**, 669–673.
- HALVERSON, G. P., HAFFMAN, P. F., SCHRAG, D. P., MALOOF, A. C. & RICE, A. H. N. 2005. Toward a Neoproterozoic composite carbon-isotope record. *Geological Society of America Bulletin*, **117**, 1181–1207.
- HEDGES, S. B., BLAIR, J. E., VENTURI, M. L. & SHOE, J. L. 2004. A molecular timescale of eukaryote evolution and the rise of complex multicellular life. *BMC Evolutionary Biology*, **4** <http://www.biomedcentral.com/1471-2148/4/2>
- KNAUTH, L. P. 1998. Salinity history of the Earth's early ocean. *Nature*, **395**, 554–555.
- KNAUTH, L. P. 2005. Temperature and salinity history of the Precambrian ocean: implication for the course of microbial evolution. In: NOFFKE, N. (ed) *Geobiology: Objectives, Concepts, Perspectives*. Elsevier, New York, 53–69.
- LAND, L. S. 1995. The role of saline formation water in crustal cycling. *Aquatic Chemistry*, **1**, 137–145.
- LI, C.-W. 2006. Diversity and taphonomy of early metazoan embryos. *IGCP 493 Abstract volume*, IGCP493 Meeting, Kyoto University Museum, Kyoto 27–31 January 2006.
- SQUIRE, R. J., CAMPBELL, A. H., ALLEN, C. M. & WILSON, C. J. L. 2006. Did the Transgondwanan Supermountain trigger the explosive radiation of animals on Earth? *Earth and Planetary Sciences Letters*, **250**(1–2), 116–133.
- XIAO, S., ZHANG, Y. & KNOLL, A. 1998. Three-dimensional preservation of algae and animal embryos in a Neoproterozoic phosphorite. *Nature*, **391**, 553–558.

Index

- Acraman impact ejecta layer 53–4, 117, 123, 126–9, 130–2, 425–7
- acritarchs
- Amadeus and Officer Basins 119
 - biostratigraphy 115–25, 130–2
 - Australian correlations 130–2
 - composite zonation scheme 119, 131, 132
 - India 318–20
 - Ireland 289
 - Spain 232
 - sphaeromorphid 324
- Adelaide, Hallett Cove 68
- Adelaide Rift Complex 115–22, 425
- correlations with Officer Basin 127
 - dating (Sr–Rb) 140
 - generalized time–space diagram, correlations
 - between tectonic units 120
 - location maps 116, 118
 - SE sector cumulative strata thickness 139
 - stratigraphic correlation with Officer Basin 127
 - Stuart Shelf drill holes, correlations 117
 - Sturtian (Umberatana) Group 116, 138
 - Umberatana Group 116, 138
- Africa
- Vendian climatic indicators 17
 - see also* Namibia
- Aldanellidae 418
- algal metaphyta, White Sea Region 271–4
- algal microfossils, White Sea Region 271
- Altenfeld Formation, backarc spreading 44–5, 47–8
- Amadeus Basin
- acritarch zonation 119
 - carbon isotope trends 128
 - generalized time–space diagram, correlations
 - between tectonic units 120
 - location map 118
 - succession 124–5
- Anabarella 230
- Anabarites *tricarinatus* 193
- Anabarites–Protohertzina Zone, Precambrian–Cambrian
- boundary, China 145–7, 423–4
- Andean Basin 1–14
- Andiva 158
- Animalia, origins 447–8
- Appendisphaera *barbata*/Alicosphæridium *medusoidum*/Gyalosphæridium *pulchrum*
- Assemblage Zone 119, 131, 132
- Arabia, Vendian climatic indicators 17
- Archaeobranchia 418–19
- Archaeotrichion *lacerum* 430–1
- Archyfasma 271–4
- Argentina (NW), Puncovicana Formation 1–14
- location map 2
 - stratigraphy 3
- Armorica 36
- armour, and infaunal shelters,
- origins 405–14
- arthropod-type trace fossils, Spain 226–7
- Arumberia *banksi* 285, 290
- Aspidella*
- controversy 300, 301–3, 305
 - ecology 303
 - synonyms 302
- Australia
- Acraman impact ejecta layer 53–4, 117, 123, 126–9, 130–2, 425–7
 - carbon isotope chemostratigraphy 126–9
 - correlations of Ediacaran System and Period 18, 115–35
 - Marinoan glaciation 53–4, 126
- Australia, Ediacaran System and Period
- Bunyeroot–Wonoka Formation transition 137–9, 426
 - Centralian Superbasin 118, 125
 - composite zonation scheme 131
 - correlation methods and results 125–32
 - time–space diagram 120
 - Vendian climatic indicators 17
 - See also* Adelaide Rift Complex; Flinders Ranges
- Avalonian assemblages, Newfoundland 237–57, 303–7, 427
- backarc spreading, Altenfeld Formation 44–5, 47–8
- Baliana–Krol Group, NW Himalaya 319
- Barut Formation, Iran 434
- Bayesian analysis
- eumetazoans 357–9
 - Porifera 357–9
- Belarus, Vendian cyclic structure 21
- Beltanella* 324
- Beltanelliformis*
- Australia 427
 - Russia and Ukraine, comparative taphonomy 259–67
 - Spain 224, 228
- Beltanelloides* 4, 8, 271–4
- Bilateria 369–75
- first appearance 126, 157, 447–8
 - gliding symmetry 399
 - small-bodied crown phyla 371–2
- biosiliceous sedimentation, China, earliest
- Cambrian 146, 423–4
- Birmanian basin, Rajasthan 439–41
- Blaini–Krol–Tal Basin, Lesser Himalaya
- carbon isotope chemostratigraphy 85–91
 - geological map 79
 - global correlations 96
 - trace elements 90
- Blainiella* 318
- Blumenau Shear Zone 37
- Bohemian Massif, Saxo-Thuringian Zone (Cadomian basement) 35–51
- geological map 36–8
- Bonney Sandstone, Flinders Ranges 122, 140, 197, 426
- Brachina Formation 426
- Trezona Bore 65–7, 69–70
- Brachina Gorge, Ediacaran GSSP 196
- Bradgatia* 216

- Breakfast Time Creek Member, Rawnsley Quartzite, Flinders Ranges 197–8
- Bunyerroo Gorge 116
- Bunyerroo–Wonoka Formation transition 121–2, 137–9, 426
- Wearing Dolomite 117, 121–2, 137–9
- Buxa Dolomite, Lesser Himalaya
- carbon isotope chemostratigraphy 91–5
- microfossils 97–8
- Ranjit Window 81, 94
- stromatolite assemblages 93–5
- Cadomian orogeny, Saxo-Thuringian Zone 35–51
- backarc basin 41–4
- Cadomian Unconformity 41
- retroarc basin 45, 47–9
- Cadomian unconformity 35–6, 41
- Cadomian–Avalonian active margin, Peri-Gondwana 46
- calcareous tubular fossils 410
- calcsponges, paraphyly 355–67
- calcite–dolomite cycles, Namibia 103–13
- Cambrian ‘problematica’ 360–2
- cap carbonates
- calcite–dolomite cycles, Namibia 103–13
- carbon isotope chemostratigraphy 126–9
- rhythmic sequences 27–34
- ‘Snowball Earth’ hypothesis 23
- see also* carbonates
- cap dolostone
- magnetics 69–72
- Nuccaleena Formation 54, 59–61, 67–72, 120–1
- carbon isotope chemostratigraphy
- Australia 126–9
- Birman basin, Rajasthan 439–41
- delta $^{13}\text{C}_{\text{carb}}$ values, beginning and end of Ediacaran System and Period 427
- Deoban Group 82, 88
- Lesser Himalaya
- Blaini–Krol–Tal sequence 85–91
- Buxa Dolomite 91–5
- Lameri Limestone, Garhwal 86
- Nemakit–Daldynian 440
- and Precambrian oxygenation 362–3
- Proterozoic ocean 362
- carbonaceous compressions 228–30
- carbonaceous macrofossils, India 324
- carbonaceous microfossils, White Sea Region 269–75
- carbonates
- delta $^{13}\text{C}_{\text{carb}}$ values 27
- Proterozoic ocean 362
- see also* cap carbonates
- Centralian Superbasin
- Australia 118, 125
- location map 118
- Ceratosphaeridium mirabile*/*Distosphaera australica*/*Apodastoides verobturatus*
- Assemblage Zone 119, 131, 132
- Charnia* fronds
- affinities 251
- Australia 210–12
- Avalon peninsula, Newfoundland 237–57
- ecology/life 248–51
- landmark morphometric analysis 240–8
- stratigraphic setting 238
- taphonomy 242
- traditional interpretation of morphology 239
- quiltlike 400
- Charniodiscus* 158, 199, 211–12, 297–8
- affinities 251
- feeding 377
- holdfast 322
- quilting patterns 388
- Chase Quartzite Member, Rawnsley Quartzite 197
- China
- Doushantuo Formation 151–6
- earliest Cambrian 423–4
- Precambrian, ciliated protozoans 151–6
- Precambrian–Cambrian boundary, radiolarian skeletons 143–9, 424
- Vendian climatic indicators 16–17
- Yunnan, Meishucun section 411
- chirodropids, cubozoans, *Kimberella* 157–79
- Chondrophorina 217–18
- Chondroplon* 214, 217
- Chuar*, Iran 435, 436
- Chuar*–*Tawuia* association 324, 328
- Chuosi Formation, cap carbonates, Namibia 27–34, 103–13
- ciliated protozoans, Precambrian, China 151–6
- Ciliophora
- Precambrian, S China 151–6
- systematic palaeontology 155–6
- climatic indicators
- palaeoclimatic and biotic changes 88
- Vendian Period 15–26
- Cloudina*-bearing sediments, Spain 223–4, 230–2
- Cnidaria 218, 355
- Cochlichnus anguineus* 5, 7
- Conomedusites* 320–2
- Coreospiridae 417
- Coryneis* priapulid 408
- crown phyla, small-bodied bilateria 371–2
- ctenophores 355
- cubozoans 157–79
- see also* *Kimberella*
- cyanobacterial films/mats 197, 269–71
- Deoban Chert 78
- Cyclomedusa* 300, 301, 302, 321
- demosponges, paraphyly 355–67
- Deoban Group, carbon isotope chemostratigraphy 82, 88
- Deoban–Gangolihat carbonate belt 78, 88, 95
- Dickinsonia* 158, 198, 199, 292, 323, 443
- carpet-like recliners 389
- feeding 377
- quilting patterns 387–8
- resting traces 394
- Didymaulichnus* *see* *Mattaia*
- Diplocraterion* 409
- discoidal fossils 297–313
- Aspidella* controversy 301–3
- history of research 297–8
- morphology 299–301
- pseudofossils 301

- taphonomy 298–9
 taxonomy 308–9
- dolomite
 calcite–dolomite cycles 103–13
 Gangolihat Dolomite Formation,
 chemostratigraphy 83
 synsedimentary model 110–12
 rip-up clasts 111–12
- Doushantuo Formation, China 151–6
- Eastern Europe, Vendian climatic indicators 16
- Ediacara Member and fauna/assemblage 198–200,
 195, 425–8
 new approach (Morphospace Analysis) 378–9
 preservation 199–204
 Rawnsley Quartzite (Pound Subgroup),
 Flinders Ranges 198–200
- Ediacaran GSSP
 Brachina Gorge 196
 defining 73, 115, 425
 Elatina Formation, rock magnetic experiments 71
 Enorama Creek 54, 55–61, 116
- Ediacaran System and Period
 acritarch biostratigraphy 115–25, 130–2
 composite zonation scheme 131, 132
 correlation with Vendian System, Australia
 18, 115–35
 event stratigraphy 126
 generalized time–space diagram, correlations
 between tectonic units 120
 naming 137–41
 etymology 140
 Waggoner's associations 139, 427
- Ediacaran–Cambrian boundary *see* Precambrian–
 Cambrian boundary
- Ediacaran–Ordovician, stratigraphic
 correlation 435–6
- Ediacaria*, morphology 300
- Ediacaria booleyi*
 five interpretations 291–3
 removal from genus *Ediacaria* 277–95
- Ediacaria flindersi* 279, 291
- Elatina Formation
 correlation with Smalfjord Formation,
 N Norway 139
 dating 140
 palaeomagnetic record 425–8
 rock magnetic experiments 71
- Elatina–Nuccaleena deglaciation 53–76
 Elatina Creek 61–2
 transition, key facies 58
 Trezona Bore 63, 65–7
- Enorama Creek, Ediacaran GSSP 54, 55–61,
 115–16
- Eoholynia* 272, 274
- Eotintinnopsis* (ciliated protozoan)
 Precambrian, China 151–6
 systematic palaeontology 155–6
- Ernietta*
 'colonies' 208, 213
 Namibia, Nama Group 197, 200
 quilting patterns 387–8, 400
 reconstruction 390
- Europe, Eastern, Vendian climatic indicators 16
- Fermeuse-style assemblages 299–307
- Finnmark
 correlations, Flinders Ranges 138
 Vendian climatic indicators 16
- Flinders Ranges 138, 425–8
 correlations with Finnmark, N Norway 138
 Elatina–Nuccaleena deglaciation 53–76
 location map 196
 Pound Subgroup
 Bonney Sandstone 122, 140, 197
 Rawnsley Quartzite 195–9, 426
- Flinders-style assemblages 299
- frondose organisms *see* *Charnia*; *Pambikalbae*
hasenohrae *gen. et sp.*
- Gangolihat Dolomite Formation, Lesser Himalaya,
 chemostratigraphy 83
- Garhwal, Lesser Himalaya,
 chemostratigraphy 79, 82, 84
- gastropod evolution 415–21
 main groups 415–18
 phylogenetic relationships 419–20
 shell forms, radiation 416
- Gawler Craton 425
- genes, regulatory genes in bilateral
 metazoans 372–4
- Georgina Basin
 carbon isotope trends 129
 location map 118
- Germany, Saxo-Thuringian Zone, Cadomian
 basement 35–51
- Glaessner, Martin 443–4
- Glaessnerina* 211, 212
 affinities 251
- gliding symmetry 399
- Glockerichnus* 5, 7
- Gondwana, Cadomian–Avalonian active
 margin 46
- Gymnoblastina* 217
- halite, sequestration as 'saline giants' 447
- Hallett Cove, Adelaide 68
- Helcionellidae 415–17
- Helminthoidichnites tenuis* 5, 7
- Helminthoraphe* 5, 7
- Hetang Formation, radiolarian
 skeletons 143–9
 stratigraphic column 144
 Yangtze Platform 423–4
- Hiemalora* 299, 300, 331–7
 reconstruction 335–6
 research history 331
 stratigraphic section 332
 taxonomy 336
- Himalaya, NW and NE Lesser
 Himalaya 77–101, 318–21
 Garhwal chemostratigraphy 79, 82, 84
 Krol Formation 77–82, 85–91, 318–21
 lithostratigraphy and palaeobiology 80
 Menga (Buxa) Limestone 93–5, 97–8, 81
 Mussoorie Syncline, isotope data 85–92
 Neoproterozoic Transition 88
 palaeoclimatic and biotic changes 88
 Ranjit Window 81

- Hormosiroidea* 226
honeycomb pattern, interpretations 343–9
conceptual paradigm 344–5
physical paradigm 345–7
inappropriate paradigms 347–9
Hox genes, regulatory genes in bilateral metazoans 372–4
Hydroactinidae 217
- Igarkiellidae 417
- Indian subcontinent 77–101, 315–30, 439–41
Birmanian basin, Rajasthan 439–41
carbon isotope stratigraphy 439–41
Higher/Tethys Himalaya: Kashmir 321–2
Indo-Gangetic Plain 322–3
late Proterozoic biota 318–20
correlation charts 317, 325–6
geological setting 315–18
location map 314
Lesser Himalaya 77–101, 315–30, 318–21
Blaini–Krol–Tal Basin 79
Krol Belt 318–21
Mesoproterozoic–Neoproterozoic successions 325–6
NW and NE Lesser Himalaya 77–101
lithostratigraphy 80
palaeoclimatic and biotic changes 88
Peninsular India 323–8
Vendian climatic indicators 17
infaunal trace makers 406–9
continuous horizontal galleries in sand 406–7
correlation with small shelly fossils 410–12
cylindrical branching burrows 407–8
mud eaters 408–9
transitions in infaunal behaviour 409–10
- Inkrylovia* 208, 212
- Iran (Takab area), Ediacaran–Ordovician microstratigraphy 433–7
correlation 435–6
Lalun Formation 434–5
petrography and stratigraphy 433–5
- Ireland, Booley Bay Formation 277–95
age 288–91
location map 278
sedimentological setting 277–85
- isotope data, Mussoorie Syncline, NW and NE Lesser Himalaya 89, 91–2
- Jakutsk, Lena River 408, 409
- Kessyusa Formation, Siberia 406–14
- Khairkhanidae 418
- Khorbusuonka River region, Siberia 406–14
- Kimberella* 157–79, 323, 369
future research directions 181–5
grazing tracks 174–7
morphology 160–74, 184
reconstructions 176, 185
stratigraphic setting 158
taphonomy and ecology 158–60, 182
- King Island/NE Tasmania 129
generalized time–space diagram, correlations between tectonic units 120
- Kotlin–Redkino, Vendian climatic zonation 20
- Krol Formation, NW Himalaya 77–82, 85–91, 318–21
Baliana–Krol Group biota 319
Blaini–Krol–Tal Basin, carbon isotope chemostratigraphy 85–91
late Proterozoic successions 318–21
Mussoorie Syncline
isotope data 89
REE, Y, Sc and Th distribution 91
trace element distribution 90–1, 92
- Kullingia* (swing mark) 301
- Ladatheca annae* 411
- Lakhanda Microbiota 431
- Lalun Formation, Iran 434–5
- Laplendian, Vendian climatic zonation 20–3
- Lausitz Group 41–5
- Leiosphaeridia jacutica*/*L. crassa* Assemblage Zone 117, 119, 131, 132
- Lena River, Jakutsk 408, 409
- Louisella pedunculata* priapulid 407
- Mackenzie, Vendian climatic indicators 16
magnetic susceptibility, temperature dependence 70–2
magnetics
cap dolostone 69–72
hysteresis loops 72
Verwey Transition 66
- Manykodes* (*Phycodes*) *pedum* 406, 411
Manykodes rectangulare 407–8
- Marinoan glaciation
Australia 53, 126
cap carbonates, palaeomagnetism 54
Namibia 104
- Mattaia* 406–12
Mattaia miettensis burrows 406–7, 410
Mattaia tirasensis burrows 410–11
- Mawsonites* 299, 443
- Medusinites* 300
- Menga Dolomite *see* Buxa Dolomite
- metazoans
Bayesian analysis 357–9
before Cambrian explosion 369–71
bilateral 369–75
first appearance 126, 157, 447
regulatory genes 372–4
small-bodied crown phyla 371–2
early radiation 187
first appearance 447–8
origins 178
and origins of Animalia 447–8
paraphyly, eumetazoans and poriferans 356
phylogenetic relations 370
small-bodied crown phyla 371–2
trace fossils 371
- microbial mats
demise 448
Lausitz group, Germany 41, 42
see also Vendobionts
- microfossils
Buxa Dolomite, Lesser Himalaya 97–8
carbonaceous, White Sea Region 269–75
discoidal fossils 297–313
Hetang Formation, China 145–8

- organic-walled, Spain 230–2
- siliceous, China, earliest
 - Cambrian 146, 423–4
- White Sea Region 269–75, 271
 - see also small shelly fossils (SSF)
- Mila Formation, Iran 434, 435
- Mistaken Point, Newfoundland 301–6, 308
- Monomorphichnus lineatus* 5, 7
- Monomorphichnus lineatus*–*Treptichnus pedum* assemblage 232–3
- monoplacophorans, living 183
- Montes de Toledo–Guadalupe, Spain,
 - Precambrian–Cambrian boundary 223–35
- Morphospace Analysis 377–86
 - formulation of morphospace for Ediacara biota 379–82
 - results 382–6
- Mussoorie Syncline
 - Blaini–Krol–Tal Basin, Lesser Himalaya
 - carbon isotope chemostratigraphy 85–91
 - trace elements 90, 91
 - isotope data, Krol Formation 89, 91–2
- Namalia*, quilting patterns 387–8
- Namibia, Nama Group
 - Ernietta* 197, 200, 208, 213, 387–8, 390, 400
 - preservation (taphonomic) processes 200
 - Pteridinium* 402–4
- Namibia, Otavi Group 103–13
 - chemical profiles 108–10
 - Chuos Formation 104
 - location map 105
 - Rasthof Formation cap carbonates 27–34, 104–110
 - thin section data 107–8
- Namibian association 427
- Nantuo Formation, China 151–6
- Nasepia*, quilting patterns 387–8
- Nemakit–Daldynian
 - assemblages, Vendian climatic indicators 17, 18–20
 - carbon isotope chemostratigraphy 440
 - gastropod evolution 415–21
- Nemiana* 9, 158, 300
 - Russia and Ukraine, comparative taphonomy 263–5
- Neonereites biserialis* 5, 7
- Neonereites uniserialis* 5, 7
- Neoproterozoic glacials 447–8
 - ‘Snowball Earth’ hypothesis 21–3
- Neoproterozoic–Early Cambrian transition,
 - Argentina (NW) 1–14
- Nereites saltensis* 5, 7
- Newfoundland
 - Avalon peninsula, *Charnia* fronds 237–57
 - Avalonian assemblages 303–7
 - Mistaken Point 301–6, 308
 - Vendian climatic indicators 16
- Ngalia Basin, location map 118
- Nimbia*
 - Booley Bay Formation 278, 285, 299
 - morphology 300
- Norway
 - Finnmark, Vendian climatic indicators 16
 - Smalfjord Formation, correlation with Elatina Formation, Australia 139
- Stappogiedde Formation, Varanger, discoidal fossils 304–5
- Vestertana Group, and Bunyeroo–Wonoka Formation transition 138
- Nuccaleena Formation cap dolostone 54, 59–61, 67–72, 120–1
 - boundary with Brachina Formation 121
 - dating 140
 - magnetics 69–72
- Officer Basin
 - acritarch zonation 119
 - carbon isotope trends 129
 - correlation with Adelaide Rift Complex 127
 - generalized time–space diagram, correlations between tectonic units 120
 - location map 118
 - sequence stratigraphy and seismic interpretation 126
 - succession 122–4
- Oldhamia curvata* 5, 7
- Oldhamia flabellata* 5, 7
- Oldhamia radiata* 5, 7
- Olenek River region, Siberia 406–14
- Onuphionella*, mica-lined shelter 410
- Onychochilidae 418
- Oraparinna diaphragm 68
- organic-walled microfossils 230–2
- Oscillatoropsis* 269–70
- Otavi Group see Namibia
- Ovatoscutum* 217
- oxygenation
 - and carbon isotope chemostratigraphy 362–3
 - Precambrian era 362–3
 - Shuram excursion 362
 - Precambrian–Cambrian boundary 431
- Palaeolyngbia* 269–70
- palaeopascichnids 262, 425
- Palaeophycus* 5, 7, 8
- Pambikalbae hasenohrae* gen. et sp. 195–222
 - biological relationships 207–18
 - living relatives 214–18
 - morphology 205–7
 - preservation 200–4
 - reconstruction 207, 215
 - systematic palaeontology 205
- paraphyly
 - Cambrian ‘problematica’ 360–2
 - eumetazoans and poriferans 356
 - Precambrian oxygenation 362–3
- pattern interpretations
 - englutinated fill skeletons 388
 - honeycomb 343–9
 - quilting 387–8
- Pelagiellidae 418
- Petalonamae 187–9, 209–18
- ‘petalonamids’ see *Pambikalbae hasenohrae* gen. et sp.
- phosphatic shells see small shelly fossils (SSF)
- phosphogenesis, Precambrian–Cambrian boundary 439
- Phyllozoon*
 - carpet-like recliners 389
 - quilting patterns 387, 400

- Phyllozoon hanseni* 212, 217
 reconstruction 209
 phylogenetics, Bayesian 356
 physonect siphonophores 215
Pilitella 272, 274
 placozoans 355
 plankton communities, early development and
 composition 148
 pneu architecture 387–8
Podolimirus 189
Podolodes burrows 406–11
 Podolodes tripleurum 409, 410
 Podolodes triplex 409
 Poland, Holy Cross mountains 407
 Porifera
 China, earliest Cambrian 424
 paraphyly 355–67
 Bayesian analysis 357–9
 Cambrian ‘problematica’ 360–2
 character acquisition 359–63
 spicules, preservation of radiolarian skeletons 146–8
 Precambrian era, oxygenation 362–3
 Precambrian–Cambrian boundary
 Flinders Ranges 426
 marine phosphogenesis 439
 origin of armour and infaunal shelters 405–14
 radiolarian skeletons 143–9
 Spain 223–35
 preservation (taphonomic) processes
 159, 182, 199–204
 priapulids 407–8
Primoflagella 430–1
Protolyellia 339–53
 affinities 351–2
 interpretation 342–51
 material 339–42
 reconstruction 349
 taphonomy 342, 349–51
 protozoans, Precambrian, China 151–6
Psammichnites 227–8, 406, 411–12
 non-*Psammichnites* 5, 7
 Psammocorallia 293, 339
 see also Protolyellia
Pteridinium carolinaense 198, 200, 208–9, 217, 320
 quilting patterns 387–8, 400
 specimens from Aar Farm, Namibia 402–4
 reconstructions 209, 391
 regeneration 393
 vanes 389
Pteridinium simplex 214
 reconstructions 391
 Puncovicana Formation, Argentina 1–14
 quilt structures, ‘Vendobionta’ 387–8, 399–404
 radiolarian skeletons, Early Cambrian 143–9
 coexistence with sponge spicules 147
 morphology 147–8
Radulichnus 181
 Rajasthan, Birmania basin 439–41
Rangea 210, 216, 390–3
 quilting patterns 388
 reconstructions 392
 vanes 389
 rangeomorphs 359–60
 Ranjit Window, Lesser Himalaya 81, 94
 Rasthof cap carbonates, Namibia 27–34, 103–13
 Rawnsley Quartzite (Pound Subgroup), Flinders
 Ranges 195–200, 426
 Breakfast Time Creek Member 197–8
 Chase Quartzite Member 197
 Ediacara Member 198–200
 Winnowie Member 198
 regulatory genes, bilateral metazoans 372–4
 Rheic Ocean 36
 ‘rhizocorallium’ spreites 408
 rhythmite sequences, cap carbonates 27–34
 Riphean animals 429–31
 Rodinia supercontinent 78
 break-up 78, 82–5
 modern continental outlines 139
Rokopelia spp. 183
 Rothstein Formation, backarc spreading 44–5, 47–8
Rugosoopsis 429–31
 Russia
 Ventogyrus 187–94, 208–14
 see also White Sea region
 sabelliditids 231, 232, 429
 ‘saline giants’ 447
 Saxo-Thuringian Zone (Cadomian basement)
 backarc basin 41–4
 geological map 36–8
 lithosections and geochronological data 38
 retroarc basin 45, 47–9
Sekwia 9, 300, 327
Selkirkia 4, 8
Serebrina 272, 274
 SHRIMP (sensitive high resolution ion microprobe)
 dating 125, 140
 Shuram excursion, oxygenation in Precambrian
 era 362
 Siberia
 Hiemalora 331–7
 Kessyusa Formation 406–14
 Khorbusuonka River region 406–14
 Olenek River region 406–14
 siliceous microfossils, China, earliest Cambrian
 146, 423–4
 Sinian association 437
 siphonophores 215–16, 218
 pneumatophore 216
Siphonophycus 269–70
Skolithos 158
 small shelly fossils (SSF)
 China, Precambrian–Cambrian boundary 143–9
 correlation with infaunal trace makers 410–12
 India 324
 Spain 230
 see also microfossils
 ‘Snowball Earth’ hypothesis 21–3
Sokolovina 429
 Soltanieh Formation, Iran 433–7
 South Africa, Vendian climatic indicators 17
 South American Andean Basin 3–14
 Spain, Precambrian–Cambrian boundary 223–35
 carbonaceous compressions 228–30
 geological setting 223–6

- location map 224
- organic-walled microfossils 230–2
- skeletal fossils 230
- stratigraphic nomenclature 223–6
- trace fossils 226–8
- sphaeromorphid acritarchs 324
- sponges *see* Porifera
- Sprigg, Reg C 443
- Spriggina* 300, 400
- Sr isotope data, Mussoorie Syncline, NW and NE
 - Lesser Himalaya 89, 91–2
- SSU rRNA molecule, phylogenetic relations 370
- Stannophyllum*, englutinated fill skeletons 388
- Stenotheceidae 417
- stromatolite assemblages
 - Australian Ediacaran System 129–30
 - Lesser Himalaya
 - Blaini–Krol–Tal sequence 85–7
 - Deoban–Gangolihat dolomite 78
 - Menga (Buxa) Limestone 93–5
 - Vindhyan Supergroup, India 324
- Stuart Shelf 120–2
 - acritarch zonation 119
- Sturtian glaciation, Namibia 104
- Sturtian (Umberatana) Group, Adelaide Rift Complex 116, 138
- Svalbard, Vendian climatic indicators 16
- Swarpuntia* 189, 200, 208, 212, 213, 217
 - upright form 389
- Sweden, Mickwitzia sandstone, *Protolyellia* 339–53
- Tanarium conoideum*/*Schizofusa risoria*/*Variomargosphaeridium litoschum* Assemblage Zone 119, 131, 132
- Tanarium irregulare*/*Ceratospaeridium glaberosum*/*Multifronsphaeridium pelorum* Assemblage Zone 119, 131, 132
- taphonomic process 159, 182, 199–204
 - comparative taphonomy 259–67
 - Beltanelliformis* 260–2
 - Nemiana* 264
 - discoidal fossils 298–9
 - Ediacaria booleyi* 279
 - Protolyellia* 342, 349–51
- Tasmanadia cachii* 5, 7
- Tasmania, King Island 120, 129
- Tawuia* 435
- Tethys Himalayan sequence 77–8
- Thalassinoides* 5, 9
- Thaumaptilon* 212
- Tirasiana* 259–60, 299
 - morphology 300–1
- trace elements
 - Blaini–Krol–Tal Basin 90
 - Mussoorie Syncline 90–1, 92
- trace fossils 226–7, 371
 - infaunal trace makers 406–9
 - ‘Vendobionta’ 394–5
- Trenellidae 417
- Treptichnus* assemblage 224, 226–7
- Treptichnus cf. aequalternus* 5, 7, 8
- Trezona Bore
 - Brachina Formation 65–7, 69–70
 - Latina–Nuccaleena deglaciation 63, 65–7
- Trilobozoa 192
- Tuberlichnus* 226
- U–Pb aging, Newfoundland 427
- Ukraine
 - Beltanelliformis* 259–67
 - biostratigraphic correlation with White Sea Region 273
- Podolia
 - burrowing infauna 409–10
 - macrophyte algae 271–4
- Umberatana Group, Adelaide Rift Complex 116, 138
- Urals
 - Vendian climatic indicators 16
 - Vendian cyclic structure 22
- Urutanna Formation 426
- Vaizitsinia* 212
- Valdania* 212
- Veleropilina* 183
- Velumbrella* 282
- Vendian System and Period 427
 - climate zonation 20
 - climatic indicators 15–26
 - correlation with Ediacaran System 18
 - correlation of glacial horizons 16–17
 - macrofossil taxa 157
 - Russia
 - Beltanelliformis* 259–67
 - Nemiana* 158, 259–67
 - new data on *Kimberella* 157–79
 - Ventogyrus* 187–94
 - zonality 19
- ‘Vendobionta’ 211, 387–97
 - englutinated fill skeletons 388
 - quilt structures 387–8, 399–404
 - regeneration 393–4
 - resting traces 394–5
 - versatility 388–93
- Vendoconularia* 189
- Vendoglossa* 395, 396
- Vendotaenia*, Iran 435, 436
- Ventogyrus* 187–94, 208–9, 214
 - morphology 188–92, 208–9, 212
 - reconstructions 192–3
 - taxonomy 187–9
- ‘Verdun syndrome’ 405–14
- Vestertana Group, N Norway 138
 - and Bunyeroo–Wonoka Formation transition 138
- Wade, Mary 444
- Wearing Dolomite, Bunyeroo–Wonoka Formation transition 117, 121–2, 137–9
- White Sea Region
 - algal microfossils 271
 - Beltanelliformis* 259–67
 - biostratigraphic correlation with Podolia 273
 - carbonaceous microfossils 269–75
 - new data on *Kimberella* 157–79
 - Ventogyrus* 187–94
 - Verkhova Formation 198
 - Zimney Gory Formation 198, 262, 405
 - see also* Vendian System and Period
- Winnowie Member, Rawnsley Quartzite 198

- Wonoka Formation, Bunyeroo–Wonoka Formation
transition 121–2, 137–9, 426
- Wujiangella* (ciliated protozoan)
Precambrian, China 151–6
systematic palaeontology 155–6
- xenophyophores 387
- XRF analyser, scanning X-ray analytical microscope
(SXAM) 28–32
- Yakutsk, Lena River 408, 409
- Yangtze Plate, China
Hetang Shales 423–4
radiolarian skeletons 143–9
- Yarnemia* 214
- Yocheccionellidae 417
- Yonyangella* (ciliated protozoan)
Precambrian, China 151–6
systematic palaeontology 155–6
- Yorgia* 158, 448
quilting patterns 387–8, 400
resting traces 394
- Zaigun Formation, Iran 434
- Zimney Gory Formation, White Sea region 198, 262,
405–6
- zircons, SHRIMP dating 125, 140